BRITISH COLUMBIA
Ministry of Energy and Mines
Energy and Minerals Division
Geological Survey Branch

GEOLOGICAL FIELDWORK 2000

A Summary of Field Activities and Research

PAPER 2001-1

Energy and Minerals Division
Geological Survey Branch

Schiarizza, P. and Israel, S. (2001): Geology and mineral occurrences of the Nehalliston Plateau, South-Central British Columbia, *B.C. Ministry of Energy and Mines*, Paper 2001-1, p. 1-30.

British Columbia Cataloguing in Publication Data

Main entry under title:

Geological Fieldwork: - 1974 -

Annual.

Issuing body varies

Vols. For 1978-1996 issued in series: Paper / British Columbia. Ministry of Energy, Mines and Petroleum Resources; vols for 1997- 1998, Paper / British Columbia. Ministry of Employment and Investment; vols for 1999- , Paper / British Columbia Ministry of Energy and Mines.

Includes Bibliographical references.

ISSN 0381-243X=Geological Fieldwork

1. Geology - British Columbia - Periodicals. 2. Mines and mineral resources - British Columbia - Periodicals. 3. Geology - Fieldwork - Periodicals. 4. Geology, Economic - British Columbia - Periodicals. 5. British Columbia. Geological Survey Branch - Periodicals. I. British Columbia. Geological Division. II. British Columbia. Geological Survey Branch. III. British Columbia. Geological Survey Branch. IV. British Columbia. Dept. of Mines and Petroleum Resources. V. British Columbia. Ministry of Energy, Mines and Petroleum Resources. VI. British Columbia. Ministry of Employment and Investment. VII. British Columbia Ministry of Energy and Mines. VIII. Series: Paper (British Columbia. Ministry of Energy, Mines and Petroleum Resources). IX. Series: Paper (British Columbia. Ministry of Employment and Investment). X. Series: Paper (British Columbia Ministry of Energy and Mines).

QE187.46 622.1'09711 C76-083084-3 (Rev.)

Cover photo by G. Ray - Quartz vein with dolomite and pyrite on margins, Mosquito Creek mine, Wells, B.C., 2000.

Ministry internet website address:
www.em.gov.bc.ca/geology

VICTORIA
BRITISH COLUMBIA
CANADA

JANUARY 2001

FOREWORD

This is the twenty-sixth edition of Geological Fieldwork: A Summary of Fieldwork and Current Research. This annual publication contains reports summarizing results from the British Columbia Geological Survey projects undertaken during the past year. As well, there are several contributions by associated researchers from industry, Geological Survey of Canada and universities.

The articles in this volume reflect the emphasis of the year 2000 field surveys. The highlights include:

- Reports on the second year activity of the Ancient Pacific Margin NATMAP project, a joint venture with the Geological Survey of Canada.
- Results of geological, geochemical and fluid inclusion studies of gold mineralization in the Wells-Barkerville area, including information on the new Bonanza Ledge discovery.
- An assessment of the potential for volcanogenic massive sulphide deposits hosted by mid-Cretaceous Rocky Ridge volcanics in the Skeena Arch.
- A paper on the Whiterocks Mountain alkaline complex that provides new data about the geological controls of the Dobbin PGE mineralization. A complimentary paper reports on soil geochemistry studies over the PGE mineralized zones.
- A report from a new project within Barkerville Terrane in the Cariboo Lake area. Stratigraphic controls of the recently discovered massive sulphide boulders at Frank Creek are documented.
- Results of mapping in the Ecstall Belt in the Coast Plutonic Complex and a reassessment of volcanogenic massive sulphide potential of the belt.
- Industrial minerals continue to attract more attention in the province. Two papers highlight diatomite and hydro-magnesite occurrences.

The B.C. Geological Survey continued to contribute information on mineral inventory to Land and Resource Management Planning tables. In 2000, field studies focused on documenting the aggregate potential along the Sea to Sky Highway. Mineral occurrence studies and focused regional geochemical sampling were completed in the North Coast planning area.

During 2000 the B.C. Geological Survey initiated a new publication series, delivered exclusively over the Internet, called ***GeoFiles***. These digital products are designed to make information available quickly to clients, and are not necessarily subject to the same editorial standards as hardcopy publications. These products may be downloaded free of charge, through the "*GSB Publications Catalog*" page on the Survey's website.

Our thanks to all the authors whose professional skills in the field and office make this publication possible. The articles have been improved by peer and management review. Special thanks go to Janet Holland and Brian Grant, the Branch's publications staff, who have worked long hours to meet difficult deadlines.

W.R. Smyth
Chief Geologist
B.C. Geological Survey

TABLE OF CONTENTS

Geology and Mineral Occurrences of the Nehalliston Plateau, South-Central British Columbia (92P/7, 8, 9, 10)

By Paul Schiarizza[1] and Steve Israel[2]

KEYWORDS: Nehalliston Plateau, Quesnel Terrane, Nicola Group, Harper Ranch Group, Triassic-Jurassic plutons, skarn, porphyry copper, gold, platinum, dextral strike-slip.

INTRODUCTION

The Bonaparte project is a new multi-year bedrock mapping program of the British Columbia Geological Survey (BCGS) concentrating on Mesozoic arc volcanic and plutonic rocks of the Quesnel Terrane in the northeastern part of the Bonaparte Lake (92P) map sheet (Figure 1). The area encompasses a northwest-trending belt of high mineral potential that includes a number of interesting mineral occurrences, as well as numerous regional geochemical survey and till geochemical anomalies. The project will improve the quality and detail of bedrock maps for the area, which are based primarily on 1:250 000-scale mapping carried out by the Geological Survey of Canada in the 1960s. The mapping will be facilitated by much-improved road access, and will benefit from a more thorough understanding of regional geology and mineral occurrences provided by earlier BCGS projects on the same belt of rocks to the north (Nelson and Bellefontaine, 1996; Panteleyev *et al*., 1996). The new mapping will help attract mineral exploration to the region by providing an improved geologic framework for interpreting the mineral occurrences and geochemical anomalies, and for predicting favourable settings for future discoveries.

Here, we present preliminary results of the first year of mapping for the Bonaparte project. The fieldwork was carried out by the authors in July and August, 2000. The area mapped covers about 700 square kilometres within and adjacent to the informally-named Nehalliston Plateau, which comprises the northeastern tip of the Thompson Plateau of the south-central interior of British Columbia (Holland, 1976). The area is bounded on the east by the North Thompson River, which is followed by Highway 5 and the main line of the Canadian National Railway. It is bisected by Highway 24, which branches westward from Highway 5 at the town of Little Fort, eventually to connect with Highway 97 south of 100 Mile House. Access to most parts of the area is easily attained by an extensive network of logging and Forest Service roads that branch from highways 5 and 24.

The geological interpretations presented here build on the 1:250 000-scale mapping of Campbell and Tipper (1971), whose work incorporated earlier studies along the North Thompson River by Uglow (1922) and Walker (1931). Our work also builds on the study of Preto (1970a) which focused on mineral occurrences in the area north of Eakin Creek. Descriptions of geology and mineralization of a more local nature are found in assessment reports and annual reports of the Ministry of Energy and Mines.

REGIONAL GEOLOGIC SETTING

The Nehalliston Plateau is situated in the eastern Intermontane Belt, which is underlain mainly by Upper Paleozoic to Lower Mesozoic arc volcanic, plutonic and sedimentary rocks of the Quesnel Terrane. Farther west within the Intermontane Belt are coeval Paleozoic and Mesozoic rocks of the oceanic Cache Creek Terrane. At the latitude of the present study area, the boundary between the Cache Creek and Quesnel terranes is hidden beneath a broad area of Tertiary volcanic rocks and unconsolidated Quaternary sediments (Figure 1). Directly east of the Quesnel Terrane are rocks of the Omineca Belt, represented at this latitude by Upper Paleozoic basalt, chert, gabbro and associated rocks of the Slide Mountain Terrane, and Proterozoic and Paleozoic metasedimentary, metavolcanic and metaplutonic rocks of the pericratonic Kootenay Terrane. Jura-Cretaceous granitic rocks, including the Raft and Baldy batholiths, crosscut the boundaries between the Kootenay, Slide Mountain and Quesnel terranes.

The Kootenay Terrane is characterized by a lower Paleozoic succession, represented in part by the Lardeau Group of the Kootenay Arc (Fyles, 1964), that includes graphitic pelite, immature coarse clastic rocks and mafic volcanic rocks. Other distinctive elements include a Devono-Mississippian succession of calc-alkaline to alkaline volcanic rocks and associated granitoid intrusions, found mainly in the Eagle Bay assemblage directly east of the Nehalliston Plateau (Schiarizza and Preto, 1987), and evidence for a pre mid-Mississippian deformation event (Read and Wheeler, 1976; Smith and Gehrels, 1992). This Paleozoic succession differs profoundly from

[1] *British Columbia Ministry of Energy and Mines*
[2] *The University of British Columbia*

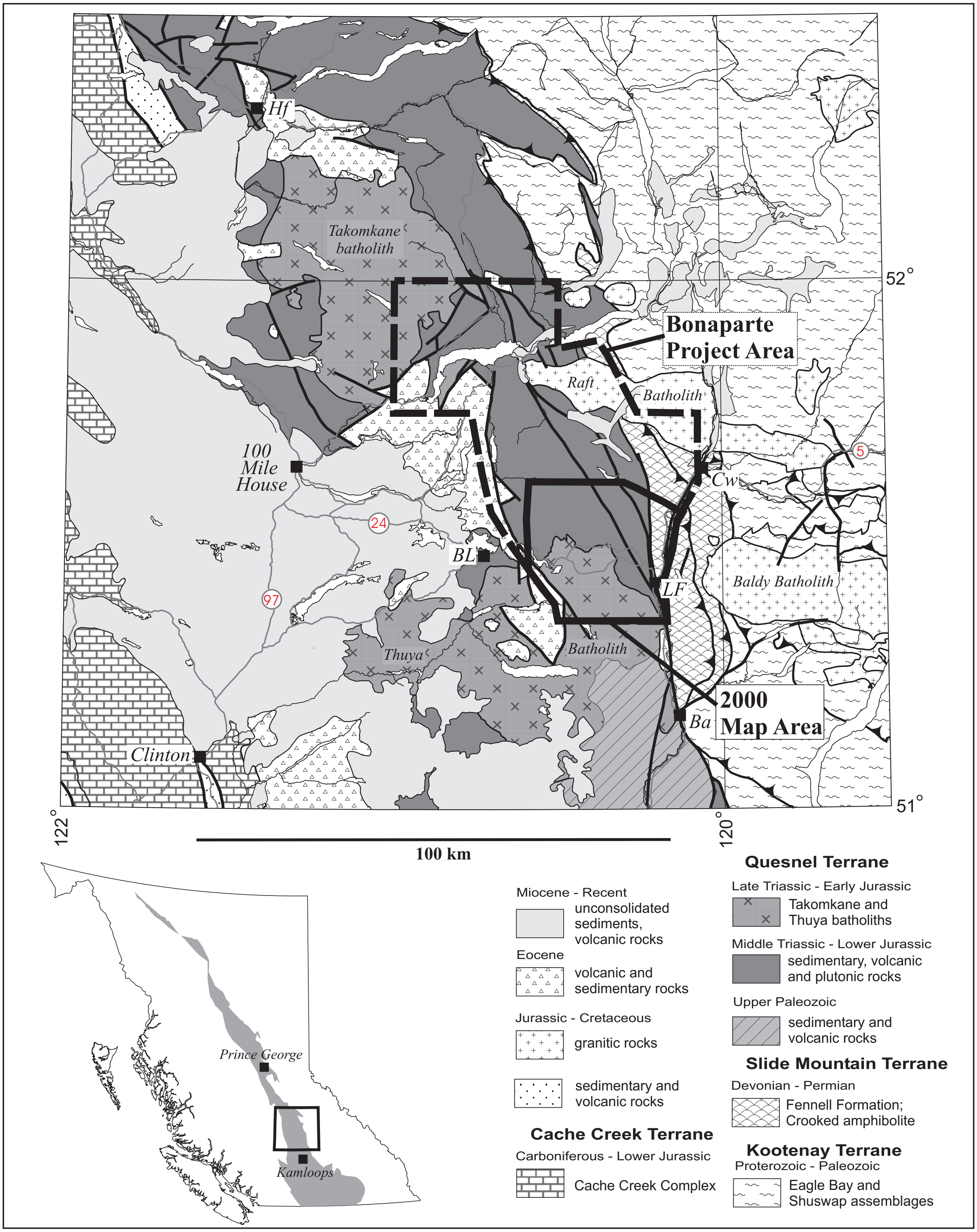

Figure 1. Regional geologic setting of the Bonaparte project area. Abbreviations: Ba, Barriere; BL, Bridge Lake; Cw, Clearwater; Hf, Horsefly; LF, Little Fort. Inset shows location of the map in south-central British Columbia, with distribution of the Quesnel Terrane shown in grey.

homotaxial carbonates and shales of the North American miogeocline, leading to its assignment to a suspect terrane (Monger and Berg, 1984), and the suggestion that it might be part of an allochthon that was thrust eastward over the miogeocline during the Devono-Mississippian Antler orogeny (Smith *et al*., 1993). However, recent work in and near the north end of the Kootenay arc (Colpron and Price, 1995) has confirmed the original stratigraphic interpretations (*eg*. Fyles and Eastwood, 1962; Fyles, 1964) which had this distinctive Paleozoic succession in stratigraphic contact with underlying Lower Cambrian carbonates and mature quartzites that are part of the North American miogeocline. The Kootenay Terrane is therefore, at least in part, a western facies belt of the North American miogeocline rather than an allochthonous terrane. Colpron and Price suggest that the pulses of mafic volcanism and coarse clastic sedimentation that characterize the lower Paleozoic rocks of the Kootenay Terrane reflect intermittent extensional deformation in the outer miogeocline. Younger, Devono-Mississippian volcanic and plutonic rocks may be part of a continental margin arc, reflecting the initiation of east-dipping subduction beneath the North American plate (Schiarizza, 1989).

The Slide Mountain Terrane comprises the most inboard tract of oceanic rocks in the Canadian Cordillera. At the latitude of the Nehalliston Plateau it is represented by the Fennell Formation, a structurally imbricated assemblage of Devonian to Upper Permian rocks that is dominated by chert, basalt, gabbro and diabase (Schiarizza and Preto, 1987). North of the Raft batholith it is represented mainly by a thin unit of amphibolite, greenstone, gabbro and ultramafic rocks, referred to as the Crooked amphibolite, that marks the faulted contact between the Quesnel and Kootenay terranes (Rees, 1987; Bloodgood, 1990). East-directed thrusting of the Quesnel Terrane, and underlying Crooked amphibolite, over the Kootenay Terrane occurred in the Lower Jurassic, and was overprinted by west-vergent folds and thrust faults that formed in Middle Jurassic time (Brown *et al*., 1986; Rees, 1987). A similar scenario, involving post-early Late Permian imbrication and emplacement above Kootenay terrane, followed by west-directed folding and thrust faulting, is documented for the Fennell Formation (Schiarizza, 1983). Schiarizza (1989) suggests, however, that the structural imbrication and emplacement of the Fennell Formation occurred in the late Permian or early Triassic, in an event correlated with the Sonoma orogeny. Although it is allochthonous, the Fennell Formation includes lithologic units, such as Mississippian quartz sandstone and Devonian rhyolite, that may be correlated with rocks in the Kootenay Terrane. Direct or indirect ties with the North American miogeocline are also documented in the Slide Mountain Terrane to the south and north, leading to the common interpretation that it represents the remnants of a marginal or back-arc basin that formed directly outboard of North America (Klepacki and Wheeler, 1985; Schiarizza, 1989; Roback *et al*., 1994; Ferri, 1997)

The Quesnel Terrane is characterized by an Upper Triassic to Lower Jurassic magmatic arc complex that formed above an east-dipping subduction zone (Mortimer, 1987). The Cache Creek Terrane to the west, which locally includes Late Triassic blueschist-facies rocks (Paterson and Harakal, 1974; Ghent *et al*., 1996), is inferred to include the remnants of the associated accretion-subduction complex (Travers, 1977). In southern and central British Columbia the early Mesozoic arc of the Quesnel Terrane is represented mainly by Upper Triassic volcanic and associated sedimentary rocks of the Nicola Group, together with abundant Late Triassic to Early Jurassic calc-alkaline to alkaline intrusions (Schau, 1970; Lefebure, 1976; Preto, 1977, 1979). Lower Jurassic volcanic rocks rest stratigraphically above Triassic arc volcanic rocks in areas north of the Nehalliston Plateau (Panteleyev *et al*., 1996; Nelson and Bellefontaine, 1996), but in southern British Columbia Lower Jurassic arc rocks of the Rossland Group (Hoy and Dunne, 1997) are found well east of the axis of Triassic magmatism.

In southern British Columbia, Mesozoic rocks of the Quesnel Terrane rest stratigraphically above a diverse assemblage of Paleozoic rocks, commonly across an angular unconformity (Read and Okulitch, 1977). Within and south of the Nehalliston Plateau, the Paleozoic part of the Quesnel Terrane comprises the Harper Ranch Group, which is interpreted as part of a late Paleozoic arc complex (Monger, 1977; Smith, 1979; Danner and Orchard, 2000). Elsewhere in southern British Columbia, Mesozoic rocks of the Quesnel Terrane rest stratigraphically above Paleozoic rocks of more oceanic aspect. These include rocks assigned to the Okanagan subterrane by Monger *et al*. (1991), and, along the eastern edge of the Quesnel Terrane, rocks included in the Slide Mountain Terrane (Campbell, 1971; Klepacki and Wheeler, 1985; Rees, 1987). In both southern and central British Columbia there is indirect evidence suggesting that Late Paleozoic arc rocks correlated with the Harper Ranch Group may have formed above a basement with North American affinities (Roback and Walker, 1995; Ferri, 1997). Furthermore, recent mapping just to the south of the Nehalliston Plateau, in the Vernon and Ashcroft map areas, suggests that pericratonic rocks correlative with those in the Kootenay Terrane extend farther west than previously thought, and underlie Permian and Triassic rocks of the Quesnel Terrane across an unconformable stratigraphic contact (Erdmer *et al*., 1999). Some of these complex relationships are explained by models in which the Paleozoic arc rocks of the Quesnel Terrane formed on a fragment of continental crust that rifted away from ancestral North America during back-arc extension that produced the Slide Mountain ocean basin. Subsequent collapse of the Slide Mountain basin in Permo-Triassic time may have formed a diverse, thrust-imbricated basement on which the Triassic-Jurassic arc of the Quesnel Terrane formed (*eg*. Ferri, 1997; Schiarizza, 1989).

LITHOLOGIC UNITS

The Nehalliston Plateau is underlain mainly by Upper Triassic volcanic and sedimentary rocks of the Nicola Group, together with contemporaneous to slightly younger intrusions (Figure 2). These rocks constitute the early Mesozoic magmatic arc that is the most definitive feature of the Quesnel Terrane. Paleozoic sedimentary rocks of the underlying Harper Ranch Group are represented locally, as are Lower Jurassic sedimentary rocks that overlie the Nicola Group. Paleozoic basalt of the adjacent Slide Mountain Terrane, represented by the Fennell Formation, occurs along the eastern edge of the map area. Younger rocks exposed in the area include a small Cretaceous stock that intrudes the Nicola Group northeast of Tintlhohtan Lake, and Eocene sedimentary and volcanic rocks of the Kamloops Group.

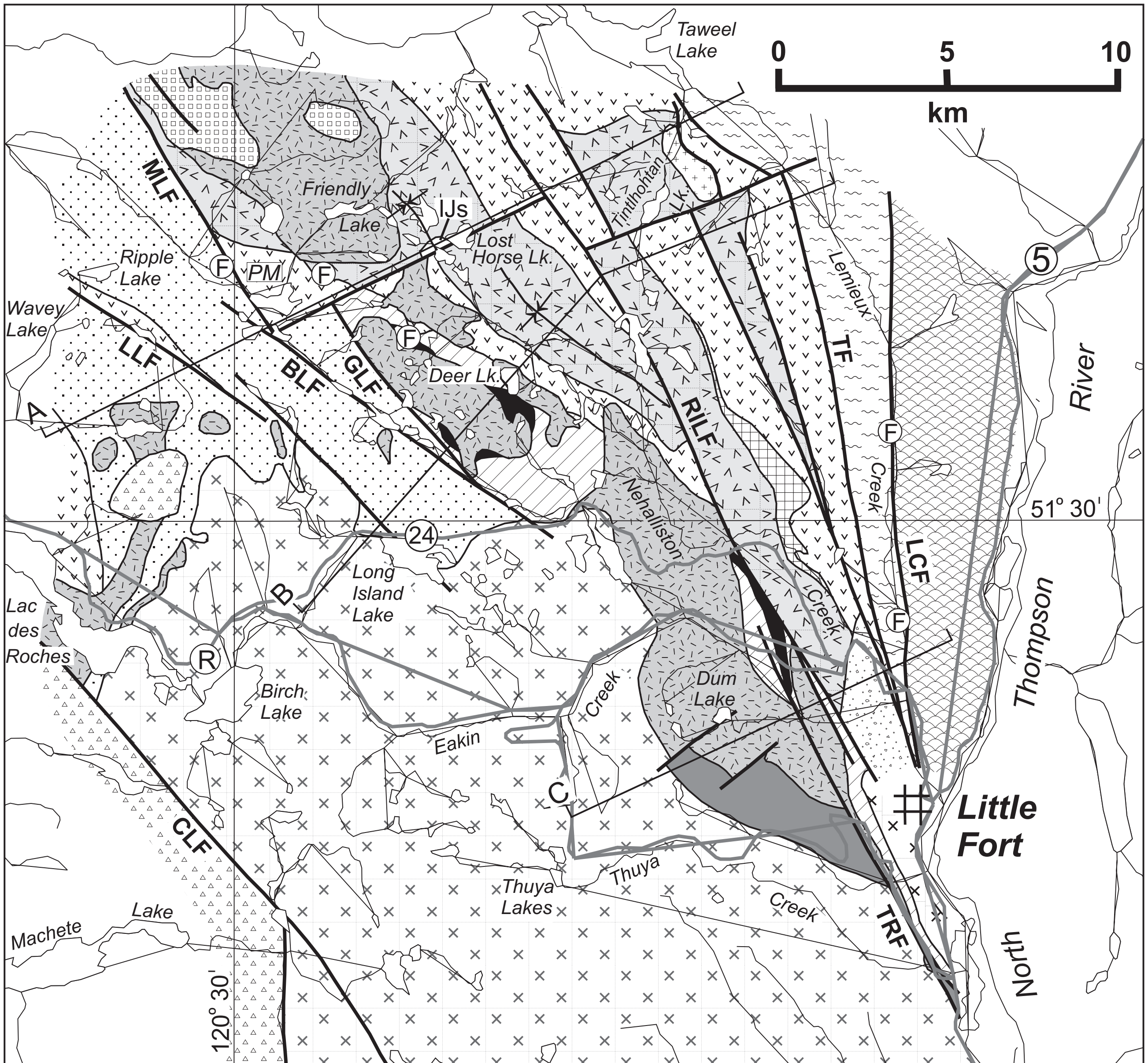

BLF: Blowdown Lake fault; CLF: Caverhill Lake fault; GLF: Gammarus Lake fault; LCF: Lemieux Creek fault; LLF: Long Lake fault; MLF: Monticola Lake fault; RILF: Rock Island Lake fault; TF: Taweel fault; TRF: Thuya Road fault.

F = fossil locality; R =Radiometric date locality PM: Pooytl Mountain

Figure 2a. Generalized geology of the Nehalliston Plateau map area.

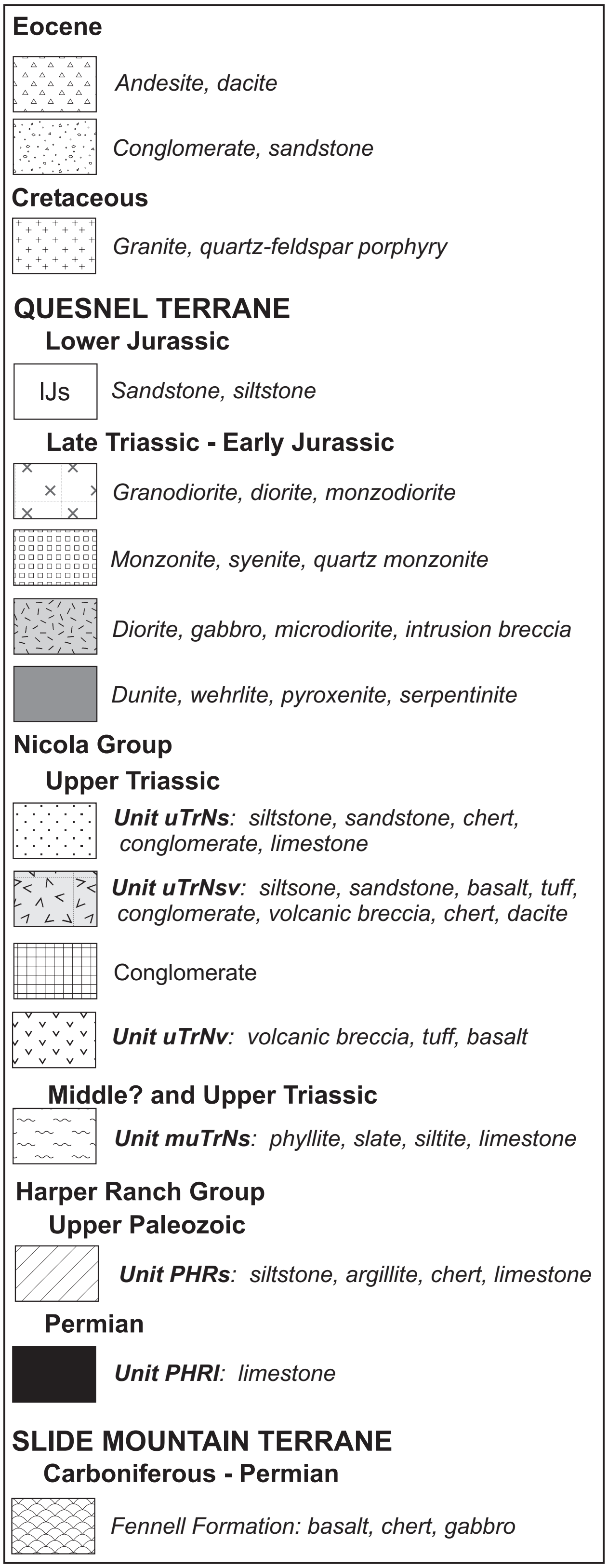

Figure 2b. Legend to accompany Figure 2a.

Fennell Formation

The Fennell Formation was defined by Uglow (1922) to include fine to medium-grained greenstone and associated gabbro and bedded chert which he mapped along the east side of the North Thompson River valley between the Barriere River and Joseph Creek. Campbell and Tipper (1971) traced the Fennell Formation to the north edge of the Bonaparte Lake map sheet, and correlated it with the Antler Formation of the Slide Mountain Group, which crops out 150 kilometres to the north in the Cariboo River area. These rocks, together with apparent correlatives to the north and south, were subsequently assigned to Slide Mountain Terrane, the most inboard oceanic tract within the Canadian Cordillera (Monger *et al*., 1982).

Detailed mapping of the Fennell Formation between the Barriere River and Clearwater by Schiarizza (1983, 1989) established that the formation could be separated into two major divisions. The structurally lower division comprises a heterogeneous assemblage of bedded chert, gabbro, diabase, pillowed basalt, sandstone, quartz-feldspar-porphyry rhyolite and intraformational conglomerate. The upper structural division consists almost entirely of pillowed and massive basalt, together with minor amounts of bedded chert and gabbro. Conodonts extracted from bedded chert range in age from Early Mississippian to early Late Permian (M.J. Orchard *in* Schiarizza and Preto, 1987) and demonstrate that the Fennell Formation comprises an imbricated assemblage and not a simple stratigraphic succession. Internal imbrication occurred in conjunction with emplacement of the Fennell Formation above Mississippian sandstone of Kootenay Terrane across a system of easterly-directed thrust faults. These east-vergent thrusts were subsequently deformed by southwest-vergent synmetamorphic folds and thrust faults, dated regionally as Middle Jurassic (Brown *et al*., 1986; Colpron *et al*., 1996), which comprise the dominant map-scale structures within Kootenay and Slide Mountain terranes in this area (Schiarizza and Preto, 1987).

Within the present map area, the Fennell Formation crops out along a low ridge system, including Mount Olie, Mount Loveway and Skwilatin Mountain, that extends north from Little Fort and separates Lemieux Creek from the North Thompson River. It consists almost entirely of pillowed to massive basalt, with very local intercalations of bedded chert and rare dikes and sills of diabase and gabbro. The basalts form prominent brown-weathered exposures throughout much of the belt, and are well exposed in roadcuts along Highway 5. These rocks belong to the upper structural division of Schiarizza and Preto (1987), which has yielded Pennsylvanian and Permian conodonts to the east and southeast. They are separated from Triassic sedimentary rocks of Quesnel Terrane by a north-striking fault that follows the Lemieux Creek valley.

Harper Ranch Group

Sedimentary rocks of inferred Paleozoic or Precambrian age within the southeastern part of the present map area were assigned to the Badger Creek Formation by Uglow (1922). These rocks were traced to the southern boundary of the Bonaparte Lake sheet by Campell and Tipper (1971) who established their Late Paleozoic age and referred to them as the eastern Cache Creek Group. This followed the usage of Cockfield (1948), Jones (1959) and earlier workers, who had assigned contiguous Paleozoic rocks in the Nicola and Vernon map areas to the Cache Creek Group. This belt of Upper Paleozoic rocks was subsequently recognized to be distinct from those in the type area of the Cache Creek Group to the west (*eg*. Monger, 1977); they were referred to as the Thompson assemblage by Okulitch (1979) and the Harper Ranch Group by Smith (1979). The latter term is currently used, and is derived from good exposures on the Harper family ranch, located east of Kamloops on the north side of the South Thompson River. There, the Harper Ranch Group comprises a Devonian to Upper Permian assemblage of carbonates, siltstones, mudstones, volcaniclastic sandstones and local andesitic volcanic rocks (Smith, 1979; Danner and Orchard, 2000). These rocks are stratigraphically overlain, above an angular unconformity, by Upper Triassic sedimentary and volcanic rocks of the Nicola Group (Danner and Orchard, 2000), and therefore comprise part of the Paleozoic underpinnings of Quesnel Terrane.

Campbell and Tipper (1971) assigned an undated assemblage of sedimentary rocks extending from Highway 5 to north of Eakin Creek to their eastern Cache Creek Group. They also documented an occurrence of fossiliferous Permian limestone located 3 kilometres northwest of Deer Lake. However, they did not map it as a separate unit, but included it as part of a belt of volcanic and sedimentary rocks assigned primarily to the Upper Triassic Nicola Group (their Unit 11). Here, the Permian limestone is mapped separately, as part of the Harper Ranch Group (Unit PHRl), and correlated with several other discontinuous limestone exposures to the southeast near Deer Lake (Figure 2). These limestone units occur within a belt of poorly exposed, fine-grained clastic sedimentary rocks that apparently underlie mafic volcanic rocks included in the Nicola Group. These clastic rocks are also included in the Harper Ranch Group and mapped as Unit PHRs. They are correlated with the undated rocks along Eakin Creek and Highway 5 that Campell and Tipper included in the eastern Cache Creek Group. The belt along Eakin Creek includes a limestone unit that is tentatively correlated with those near Deer Lake (Figure 2).

UNIT PHRL - LIMESTONE

The fossiliferous Permian limestone sampled by Campbell and Tipper (1971) northwest of Deer Lake was located and resampled for both macrofossils and microfossils. It comprises about 10 metres of medium to dark grey, light grey weathered limestone containing a few thin interbeds of dark grey argillite and chert. Parts of the limestone contain abundant bioclastic fragments, up to 3 centimetres in size, together with dark grey, sparry calcite crystals from 2 to 4 millimetres in size. Fossil fragments include corals, brachiopods, crinoids, bryozoans and fusulinids. The fossiliferous limestone is discontinuously exposed along its northwest strike for less than 100 metres, partly on a new logging road just to the northwest of the original locality described by Campbell and Tipper. The limestone is within a belt of sedimentary rocks, assigned mainly to Unit PHRs, that is bounded by a diorite pluton to the southwest, and by mafic volcanic rocks of the Nicola Group and another diorite stock to the northeast. Its relationships to adjacent sedimentary rocks of Unit PHRs is not clear. It may be a discontinuous or poorly exposed layer within them, or it may be part of a more extensive unit that underlies them and has been truncated by the diorite body to the southwest.

Limestone exposures south of Deer Lake are along strike from the fossiliferous Permian unit and are tentatively correlated with it. Where unaltered, the limestone at Deer Lake is typically dark grey, medium to light grey weathered, and locally displays distinct thin beds and laminae. However, much of it is skarn-altered and mineralized. Limestone crops out as scattered exposures over a fairly large area, but diorite and microdiorite dikes are abundant within it, and there is local evidence for folding. Therefore, its actual thickness is difficult to determine.

The limestone exposures directly south of Deer Lake are bounded to the southwest by the same diorite pluton that lies to the southwest of the fossiliferous Permian limestone. Exposures of limestone and skarn-altered limestone also occur along the southwest margin of this pluton, two to three kilometres south-southwest of Deer Lake. These are also tentatively correlated with the Permian unit, and may be on the southwest limb of an anticlinal structure that is largely obscured by the diorite pluton (Figure 3, Section B). Silicified and skarn-altered limestone assigned to Unit PHRl also crops out discontinuously between Eakin and Nehalliston creeks, on the northeast margin of the Dum Lake intrusive complex. It occurs within a belt of fine-grained clastic rocks that is correlated with, and more or less along strike from, the belt that contains the limestone units near Deer Lake (Unit PHRs).

Macrofossils were not observed in any of the limestone units southeast of the fossiliferous exposure described by Campbell and Tipper (1971). Samples have been collected from most of these units, and are being processed for conodont extraction in an attempt to determine their age.

UNIT PHRS - SILTSTONE AND ARGILLITE

Unit PHRs consists mainly of thin-bedded siltstone and siliceous argillite, with local thin interbeds of dark grey limestone and chert. It occurs in two separate belts, one near Deer Lake and the other extending discontinuously from Highway 24 to Highway 5, along the west side of the Rock Island Lake fault. The two belts are more or less along strike from one another, but are separated by intrusive rocks of the Dum Lake complex. Rocks within the two belts are correlated on the basis of this along strike relationship, their lithologic similarity and the presence, within each belt, of mappable limestone units assigned to Unit PHRl. They are inferred to be Late Paleozoic in age because associated limestone of Unit PHRl contains Permian fossils at one locality northwest of Deer Lake.

The most continuous, across-strike exposures of Unit PHRs are found on the Eakin Creek road, although the section is complicated by much faulting, local folding and the presence of gabbro and diorite dikes related to the Dum Lake intrusive complex. There, it comprises a steeply-dipping interval of brown to rusty-weathered, thin-bedded siltstones and slaty siltstones, with local thin interbeds of fine-grained sandstone, chert, or siliceous argillite. The siltstone succession is intruded by gabbroic rocks of the Dum Lake complex to the west, and is in contact with limestone of Unit PHRl to the east. The latter contact is apparently conformable and gradational, marked by about 2 metres of interbedded siltstone and limestone, but the stratigraphic facing direction is unknown. A narrow interval of altered and faulted siltstone also occurs along the east side of Unit PHRl, separating the limestone from gabbro and pyroxenite of the Dum Lake complex. This suggests that the limestone unit is either a conformable layer within the predominantly siltstone succession of Unit PHRs, or that it is folded into Unit PHRs at this locality.

The best exposures of Unit PHRs south of Eakin Creek are found along Highway 5, although these rocks are commonly highly sheared, probably due to their proximity to faults of the Rock Island Lake system. The exposures along Highway 5 comprise thin-bedded siltstones and siliceous argillites with local, thin intervals of limestone and chert. Chloritic schist forms local isolated exposures within or along the belt between Highway 5 and Eakin Creek. These might represent mafic volcanic or volcaniclastic rocks within Unit PHRs, but it is more likely that they were derived from mafic dikes or sills related to the Dum Lake intrusive complex.

The rocks assigned to Unit PHRs in the Deer Lake belt are represented by small, scattered exposures that in-

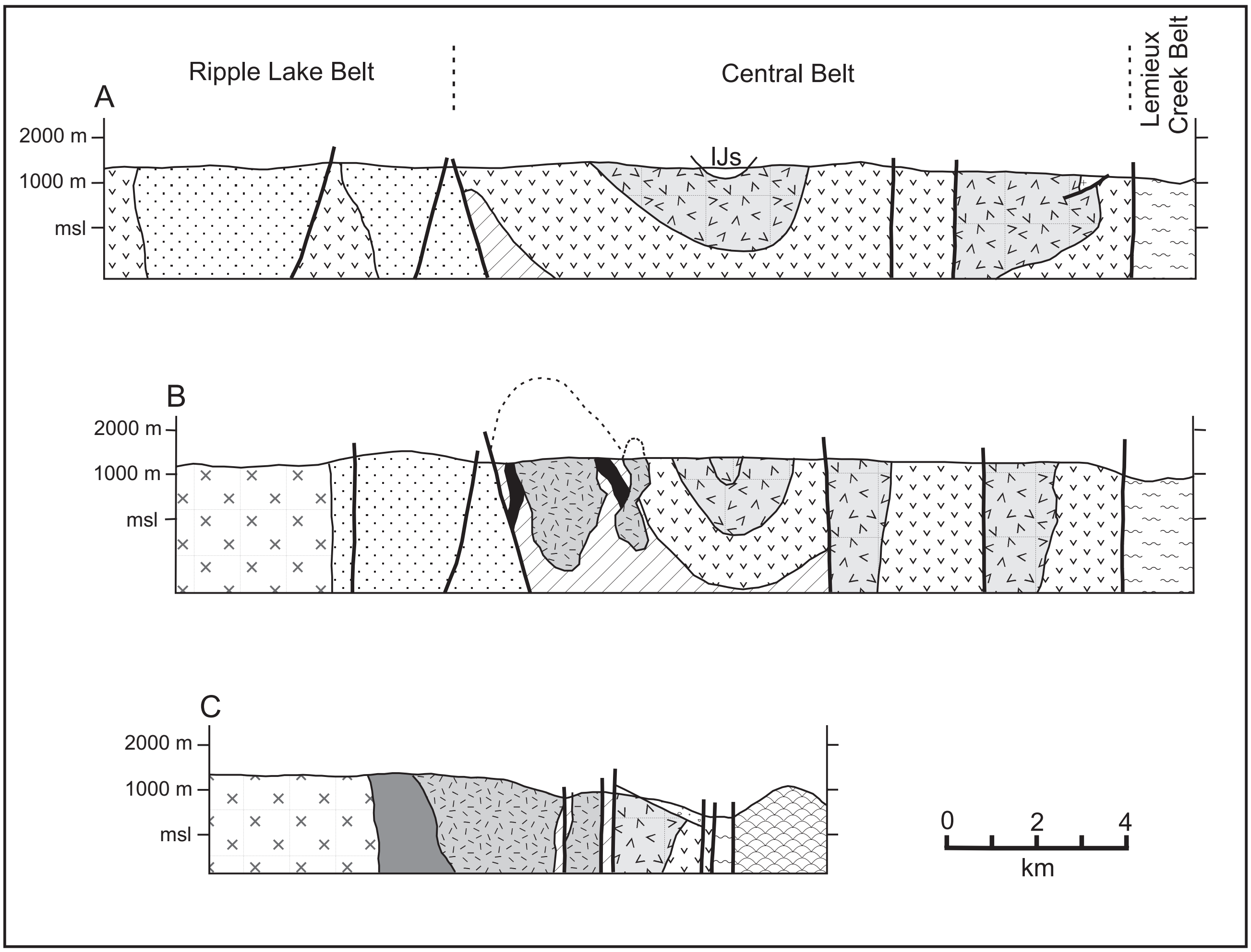

Figure 3. Schematic cross sections across the Nehalliston Plateau. *See* Figure 2a for location of sections and Figure 2b for legend.

clude laminated siltstone, thin-bedded siltstone and argillite, skarn, siliceous hornfels and thinly-interbedded chert, argillite and limestone. The belt also includes a few isolated outcrops of greenstone and pyroxene or hornblende±plagioclase phyric mafic rock. These are thought to be dikes or sills related to the numerous dioritic plutons in the area and/or the overlying volcanic rocks of the Nicola Group.

The rocks assigned to the Harper Ranch Group in the Deer Lake area are intruded by gabbro and diorite of the Dum Lake complex and the three related stocks around Deer Lake. The Paleozoic rocks are bounded by inferred faults to the southwest and northwest, but may be in stratigraphic contact beneath volcanic rocks of the Upper Triassic Nicola Group (Unit uTrNv) to the northeast. However, this contact was not observed and in most places is projected between outcrops of volcanic versus sedimentary rock hundreds of metres apart. Furthermore, the contact projects through areas that are in large part occupied by two dioritic stocks. Therefore, the relationship between the Harper Ranch and Nicola groups is largely unconstrained. The belt of inferred Paleozoic rocks that extends southeastward from Highway 24 provides no additional information, as these rocks are intruded by undated rocks of the Dum Lake complex to the southwest, and bounded by the Rock Island Lake fault to the northeast.

Nicola Group

The term Nicola Series was first used by Dawson (1879) in reference to Triassic volcanic rocks and associated limestone that he described from the south side of Nicola Lake. Later, he expanded his use of the term to encompass a more extensive area of mainly Upper Triassic volcanic and sedimentary rocks in the Kamloops map sheet (Dawson, 1896). The term Nicola Group was retained for these rocks by Cockfield (1948, Nicola map area), and was also used for Upper Triassic rocks in the adjacent Princeton (Rice, 1947), Vernon (Jones, 1959) and Ashcroft (Duffell and McTaggart, 1952) map areas. Collectively, these rocks comprise a diverse assemblage of mainly Upper Triassic volcanic, volcaniclastic and sedimentary rocks that crop out over a broad area in south-central British Columbia, where they are commonly associated with coeval and younger plutons.

Campbell and Tipper (1971) traced the Nicola Group from the Nicola map area into the southern Bonaparte Lake map area via continuous exposures along the Deadman River. They also mapped belts of Nicola Group in the central and northern parts of the map area, where they are separated from each other and the Deadman River exposures by extensive tracts of younger rocks. The Nicola rocks along the north margin of the Bonaparte Lake sheet comprise the south end of a continuous belt of correlative Triassic and associated Lower Jurassic volcanic and sedimentary rocks that extends north-northwest for more than 600 kilometres (Wheeler and McFeely, 1991). These rocks have been given a variety of local names, but are assigned to the Nicola Group in many recent reports (*eg*. Panteleyev *et al*., 1996). Middle to Upper Triassic rocks at the north end of the belt are assigned to the Takla Group (Armstrong, 1949; Nelson and Bellefontaine, 1996).

Campbell and Tipper (1971) assigned the Mesozoic volcanic and sedimentary rocks in the Nehalliston Plateau area to 4 separate map units. Only one of these, their Unit 11, was included in the Nicola Group, and mapped as a belt of volcanic and sedimentary rocks that extended northwestward from the north margin of the Thuya Batholith. Structurally interleaved with their Unit 11 were two map units assigned Lower to Middle Jurassic ages; one of predominantly sedimentary rocks (Unit 15) and the other dominated by volcanic rocks (Unit 16). Their inferred Jurassic age was based, in part, on correlation with a sedimentary section near Windy Mountain, just 5 kilometres north of the northwest corner of the present map area, which yielded fossils of probable Lower Jurassic age. Campbell and Tipper's fourth Mesozoic unit comprised Upper Triassic sedimentary rocks that form a belt along Lemieux Creek (their Unit 10; Unit muTrNs of this report). They did not include Unit 10 in the Nicola Group, and mapped an extensive, fault-bounded belt of Jurassic rocks between it and their Nicola Group to the west.

Preto (1970a) followed the stratigraphic framework of Campbell and Tipper (1971; released in preliminary format as Geological Survey of Canada Map 3-1966) with only slight modifications. He demonstrated the existence of Lower Jurassic rocks in the present map area by finding an ammonite of probable Early Jurassic age a short distance west of Lost Horse Lake.

The interpretation of Mesozoic stratigraphy presented here differs substantially from that of Campbell and Tipper (1971). The belt of Triassic sedimentary rocks along Lemieux Creek remains essentially the same as they show it, but is included in the Nicola Group following more recent assignments along strike to the north, where these rocks are regarded either as the stratigraphic base of the group (Panteleyev *et al*., 1996) or an eastern, sedimentary facies of the group (Struik, 1988). Volcanic and less common sedimentary rocks extending from the Lemieux Creek belt westward to, and partly west of, the Rock Island Lake fault were assigned to the Jurassic by Campbell and Tipper. However, we do not recognize a lithologic distinction between these rocks and those directly to the west that Campbell and Tipper assigned to the Nicola Group on the basis of sparse fossil data. Consequently, we include almost all the Mesozoic rocks west of the Lemieux Creek belt in the Upper Triassic Nicola Group. The exception is a small area of argillite and siltstone near Lost Horse Lake where Preto (1970a) discovered a Jurassic ammonite. These rocks are interpreted as a small, partially fault-bounded outlier of Jurassic rocks (Unit lJs) that rest stratigaphically above the Nicola Group. Campbell and Tipper (1971) also mapped a southeast-tapering, fault-bounded belt of Jurassic sedimentary rocks in the area encompassing Ripple Lake in the northwest part of the present map area. Our mapping shows these rocks to be part of an extensive belt of mainly sedimentary rocks that is faulted against a predominantly volcanic facies of the Nicola Group to the east. The sedimentary belt includes a single Upper Triassic fossil locality, and so is assigned to a predominantly sedimentary facies of the Nicola Group.

In the descriptions that follow, the Nicola Group is discussed in terms of three fault-bounded belts of contrasting lithology and stratigraphy, all of which contain Upper Triassic rocks and therefore may be at least partially coeval. Easternmost is the Lemieux Creek belt, consisting entirely of sedimentary rocks. To the west are the predominantly volcanic facies of the central belt which, in its western part also includes abundant plutonic rocks. This belt may represent the axis of the Nicola magmatic arc at this latitude. The western, Ripple Lake belt consists dominantly of sedimentary rocks, but also includes volcanic rocks that are similar to some of those in the central belt. These belts are similar in some respects to the facies belts of the Nicola Group defined by Preto (1979) in the Merritt - Princeton area, and adopted by Monger and McMillan (1989) throughout the Ashcroft map area, directly south of the Bonaparte Lake area.

LEMIEUX CREEK BELT (Unit muTrNs)

Metasedimentary rocks assigned to Unit muTrNs occur within a single, fault-bounded belt that forms the eastern edge of the Quesnel Terrane north of Little Fort. Within the present map area these rocks are well exposed only along parts of Lemieux Creek. They consist mainly of medium to dark grey slates and slaty siltstones that commonly contain thin beds and lenses of siliceous argillite and quartzose siltite. Locally, in exposures a few kilometres southeast of Taweel Lake, the slaty rocks enclose thin lenticular beds of fine-grained quartzose metasandstone that contain flakes of muscovite and biotite that may be of detrital origin. Limestone is common within exposures of Unit muTrNs for about 10 kilometres north of Highway 24. Dark grey bioclastic limestone forms fractured and brecciated exposures along the Lemieux Creek fault, but also occurs as well-defined thin to medium beds intercalated with slate in exposures to the west of the fault.

Collections of poorly-preserved macrofossils from limestone exposures within Unit muTrNs north of Highway 24, including bivalve, ammonoid and belemnoid fragments, suggest a Late Triassic age (Campbell and Tipper, 1971). Conodonts recovered from limestone within this same belt of rocks, about 50 kilometres northwest of Taweel Lake, also indicate a Late Triassic, probably Carnian age (Okulitch and Cameron, 1976). Still farther to the north, conodonts of both Middle and Late Triassic ages have been recovered from rocks that are probably correlative (Panteleyev *et al.*, 1996). Several collections of limestone made during the 2000 field season are currently being processed for conodont extraction.

Within the Nehalliston Plateau map area, Unit muTrNs is bounded to both the west and east by steeply-dipping faults that are interpreted as components of an Eocene dextral strike-slip system. Farther north, correlative rocks along the eastern edge of the Quesnel Terrane are imbricated, across west-dipping thrust faults, between volcanic rocks of the Nicola Group to the west and the Slide Mountain and Kootenay terranes to the east (Rees, 1987; Struik, 1988). These east-vergent, Lower Jurassic thrust faults are overprinted by Middle Jurassic west-vergent folds and thrust faults (Rees, 1987), possibly including the pre-batholith east-dipping fault defining the east side of the unit north of the Raft batholith (Campbell Tipper, 1971). Okulitch and Cameron (1976) considered the Triassic rocks of this belt to be an eastern, predominantly sedimentary facies of the Nicola Group. This is also the view of Struik (1988), who suggested that this eastern sedimentary facies was separated from the predominantly volcanic facies to the west by a west-dipping thrust fault of regional extent. However, Panteleyev *et al*. (1996) consider these rocks to be the base of the Nicola Group. They recognize the thrust-imbrication in the eastern part of the Quesnel Terrane, but map sedimentary rocks, correlated to the Middle and Upper Triassic sedimentary facies that dominates eastern exposures, stratigraphically beneath volcanic rocks across the full extent of the western volcanic belt.

Preliminary results from the Nehalliston Plateau suggest that stratigraphic and facies relationships among volcanic and sedimentary rocks of the Nicola Group are complex. Unit muTrNs is apparently absent or very thin (and included within the predominantly Paleozoic rocks of Unit PHRs) within the central volcanic belt because pillowed basalt at the base of the Nicola volcanic package crops out only 250 metres away from fossiliferous Permian limestone of the Harper Ranch Group. Sedimentary rocks are prominent in the Ripple Lake belt to the west, but these are stratigraphically above volcanic rocks of uncertain thickness or extent. Relationships within and among the various facies belts will be an ongoing focus of the Bonaparte project.

CENTRAL BELT

On the scale of Figure 2, the central volcanic belt of the Nicola Group can be subdivided into two units: One (Unit uTrNv) consists entirely of mafic volcanic breccias, flows and tuffs, while the other (Unit uTrNsv) comprises similar volcanic and volcaniclastic rocks intercalated with fine to coarse-grained sedimentary rocks. The transition from the entirely volcanic unit to the mixed volcanic-sedimentary unit occurs within each of two west-facing fault panels to the east of the Rock Island Lake fault, and on both limbs of the Nehallison syncline west of the fault. Facing directions from sedimentary structures in each of the two eastern fault panels, and on the western limb of the Nehalliston syncline, show that the mixed volcanic-sedimentary unit stratigraphically overlies the volcanic unit. This is consistent with the map-scale distribution of older and younger units, as the volcanic unit is in contact with Permian rocks on the west limb of the Nehalliston syncline, and Lower Jurassic rocks apparently overlie the mixed unit in the core of the syncline (Figure 3).

Volcanic Unit (uTrNv)

Unit uTrNv consists mainly of mafic volcanic breccias containing clasts of pyroxene-phyric basalt. Also present are massive and pillowed basaltic flows and well-bedded mafic tuffs and volcanic sandstones. Most of the rock types typical of Unit uTrNv are found in a series of good exposures on and around Pooytl Mountain in the northwestern part of the map area (*PM* on Figure 2). It is also well exposed in the northern and central parts of the belt that extends south-southeast from Tintlhohtan Lake, and on ridges north of Lost Horse Lake.

The breccias which dominate the volcanic unit commonly form resistant, blocky, green-brown to rusty-brown weathered outcrops. Fresh surfaces are various shades of medium to dark green. In virtually all exposures the fragments are dominantly or exclusively pyroxene-phyric basalt, although there is commonly considerable textural variation among clasts based on size and abundance of phenocrysts. Feldspar-pyroxene-phyric fragments are also common, and other rock types, including feldspar-phyric andesite or dacite, aphyric greenstone, microdiorite, and hornblende pyroxenite were observed locally. In exposures east of the Rock Island Lake fault, fragments commonly contain amygdules of analcite, calcite, or zeolite minerals.

Pyroxene porphyry fragments within the breccias are typically angular to subangular and unsorted to poorly sorted. The fragments are commonly up to 10 centimetres in size, locally range up to several tens of centimetres, and in places were observed to be more than a metre across. The matrix typically consists of pyroxene plus or minus feldspar crystals and small, commonly pyroxene-bearing lithic grains. In many exposures it is virtually indistinguishable from the fragments, such that the breccia texture is not readily apparent. Stratification, or contacts between different breccia units are generally not evident.

Finer grained, well-bedded tuffs and/or epiclastic rocks are a relatively minor component of the volcanic unit but were observed in all belts where the unit is well exposed. They are most common in the upper part of the unit, and locally form a transition into the overlying mixed sedimentary-volcanic unit. They typically comprise thin to medium beds of volcanic sandstone and siltstone, locally intercalated with thick to very thick beds of volcanic breccia similar to that which characterizes most of the volcanic unit. The volcanic sandstone beds are commonly graded, and scours and load casts may be apparent along their bases. They contain whole and broken crystals of pyroxene and feldspar as well as mafic lithic grains.

Massive basaltic to andesitic flows are locally interspersed with the dominant breccias of the volcanic unit. On Pooytl Mountain one such flow unit consists of 3 to 5 percent pyroxene phenocrysts, 1 to 3 millimetres in size, together with rare calcite amygdules, within a pale to medium green, somewhat chloritized groundmass. Elsewhere, apparently massive pyroxene±feldspar-phyric flows or sills contain a higher proportion of larger phenocrysts, similar to most clasts within the associated breccias. Pillowed flows are common within the belt that passes northeast of Deer Lake, on the southwest limb of the Nehalliston syncline, and were also observed at one locality on the offset northwest extension of this belt, near Pooytl Mountain. The pillows and associated pillow breccias occur within pyroxene±feldspar-phyric basalt. Commonly the pillowed basalts are highly vesicular, and contain abundant calcite as vesicle fillings and pods within inter-pillow spaces.

The volcanic rocks of Unit uTrNv are not directly dated. The belt that passes northeast of Deer Lake apparently lies above sedimentary rocks of units PHRs and PHRl, and pillowed basalt included in the volcanic unit crops out just 250 metres northeast of fossiliferous Permian limestone. East of Pooytl Mountain, this same belt of volcanic rocks is overlain by fossiliferous limestone, near the base of Unit uTrNsv, that has yielded Upper Triassic fossils (Figure 2). Because volcanic rocks similar to those of the volcanic unit continue, stratigraphically upward, to be an important component of Unit uTrNsv, the volcanic unit is allied more closely with the overlying Triassic section and presumed to also be Triassic.

Mixed Volcanic-Sedimentary Unit (uTrNsv)

Unit uTrNsv includes volcanic rocks, mostly similar to those of underlying Unit uTrNv, intercalated with sedimentary rocks that include siltstone, slate, sandstone, conglomerate and minor amounts of chert and limestone. The contact is drawn at the first significant occurrences of sedimentary rocks within the succession. However, the proportions of volcanic versus sedimentary rocks within the unit vary widely from place to place, and many thick sections are dominated by volcanic rocks that are indistinguishable from those of the underlying unit. Unit uTrNsv is well represented by a series of exposures along Highway 24, east of the Rock Island Lake fault.

The most widespread sedimentary rocks within Unit uTrNsv comprise rusty-weathered, thin-bedded intervals of light to medium grey siltstone intercalated with dark grey slate or weakly cleaved argillite. Bedding varies from planar to slighly wavy, and beds are commonly lenticular on the scale of an outcrop. Somewhat thicker, thin to medium beds of grey-green volcanogenic sandstone also occur, and some of these provide facing directions from graded bedding and scoured bases.

The intercalation of fine-grained, thin-bedded sediments, such as those described above, with volcanic sandstones, conglomerates and breccias, is well displayed in roadside exposures just west of the prominent north to west bend in Highway 24, one kilometre east of where it crosses the Rock Island Lake fault. There, grey-green volcanic sandstone or crystal-lithic tuff forms distinct graded beds, between 10 and 100 centimetres thick, intercalated with thin-bedded intervals of black argillite and grey siltstone. The volcanic sandstone units contain pyroxene and feldspar crystals, as well as lithic grains that commonly contain these minerals as phenocrysts. The fine-grained sedimentary intervals between these beds are commonly 10 to 20 centimetres thick, but some are thicker and some are represented only by rip-up clasts incorporated into the bases of amalgamated volcanic sandstone beds. Also present are beds, commonly several metres thick, of poorly sorted breccia containing pyroxene±feldspar-phyric volcanic clasts, and local fragments of argillite/siltstone.

Boulder to pebble conglomerate occurs at several places within Unit uTrNsv, most notably as a locally thick lens along the base of the unit in the panel east of the Rock Island Lake fault, where it is separated out as a mappable unit on Figure 2. The conglomerates are poorly sorted, matrix to clast supported and not conspicuously stratified. Clasts are angular to subrounded, rarely rounded, and occur within a silty to gritty matrix that generally reflects the composition of the clasts. The clast population is typically dominated by pyroxene±feldspar-phyric volcanic rocks. Siltstone, laminated siltstone and argillite clasts are almost invariably present, and clasts of chert (and/or siliceous volcanic rock), aphyric greenstone, arkosic sandstone and limestone were noted in some conglomerate units. This suite of clast types essentially mimics the lithologies found within units uTrNsv and uTrNv, and the conglomerates are inferred to reflect fairly local reworking of these associated rocks.

Thin-bedded to laminated chert was observed within Unit uTrNsv at a few localities west of the Rock Island Lake fault. It is interbedded with siltstone at one locality, in stratigraphic contact with a pyroxene porphyry breccia unit at another, and in contact with mafic rocks that might be sills or flows at other locations. Limestone was observed at only three localities within Unit uTrNsv. It occurs as a narrow bed within black argillite along Highway 24 just east of the Rock Island Lake fault, and occurs near the base of the unit on both limbs of the Nehalliston syncline, south-southwest and north-northeast of Friendly Lake, respectively. The dark grey limestone exposures on the southwest limb of the syncline are interbedded with feldspar-rich volcaniclastic sandstone to small-pebble conglomerate. Macrofossils collected from this area previously were assigned a Late Triassic, probably Late Carnian age (Campbell and Tipper, 1971; fossil locality shown on Figure 2). This is the only age constraint currently available for Unit uTrNsv. However, samples of limestone and chert collected during the 2000 field season are being processed for microfossils.

Volcanic rocks within Unit uTrNsv are mainly pyroxene porphyry breccias and pyroxene±feldspar-phyric basalts or andesites, identical to the dominant volcanic rocks of underlying Unit uTrNv. Pillowed flows are not as common as within the underlying unit, although possible pillow forms were observed at 2 localities, both apparently near the base of the unit. The relatively good exposures provided by Highway 24 roadcuts indicate, in part from local cross-cutting relationships, that some of the massive pyroxene and pyroxene-feldspar-phyric units within the succession are sills and dikes rather than flows. The contacts between sills and enclosing sedimentary rocks commonly occur across complex zones of intermingling that include irregular lobes of mafic rock penetrating the sediments and wispy lenses of argillite within the mafic rock. Locally the contact zones include breccias in which fragments of both pyroxene porphyry and argillite/siltstone occur within either an igneous or fine-grained sedimentary matrix. These may be peperite breccias, suggesting that the sills intruded unconsolidated wet sediments, as would be expected if they are broadly contemporaneous with the lithologically similar flows and fragmental units that are intercalated with the sedimentary rocks.

Felsic volcanic rocks were observed at one locality within Unit uTrNsv, on the southwest limb of the Nehalliston syncline a short distance east of the fossiliferous limestone exposure. Neither the upper nor the lower contact is exposed. The lower part of the interval is a fragmental rock, comprising 95 percent felsic volcanic clasts and 5 percent dark grey argillite fragments in a foliated sericite-chlorite martix. This passes northeastward (presumably up-section) into a massive to weakly foliated aphanitic siliceous volcanic rock. Vague feldspar phenocrysts occur within felsic clasts in the fragmental interval, as well as in the overlying massive volcanic. A single quartz phenocryst was seen in one clast within the fragmental interval.

RIPPLE LAKE BELT

Volcanic Rocks (Unit uTrNv)

Volcanic rocks occur in two areas of limited extent within the Ripple Lake belt. One narrow lens is bounded by the Long Lake fault to the southwest, and is stratigraphically overlain by the predominant sedimentary rocks of the belt to the northeast. The other area is north of Lac des Roches along the western boundary of the map area. It is suspected that these rocks correlate with the lens to the north, and likewise occur stratigraphically beneath the sedimentary rocks that contact them to the north. However, this is not proven as neither the contact nor the stratigraphic facing direction was observed in this area.

The volcanic rocks of the Ripple Lake belt consist mainly of pyroxene porphyry breccias and pyroxene-feldspar-crystal-lithic tuffs that are very similar to rocks found in Unit uTrNv to the east. They are therefore included in Unit uTrNv on Figure 2, although this correlation is only meant in the very general sense that they are a similar volcanic facies within the Upper Triassic Nicola Group. More mapping to the northwest is required to determine if they are part of a major mappable unit that underlies the sedimentary rocks of the Ripple Lake belt, or constitute a volcanic lens within a predominantly sedimentary succession.

Sedimentary Rocks (Unit uTrNs)

The predominantly sedimentary succession of the Ripple Lake belt is assigned to Unit uTrNs on Figure 2. It includes siltstone, slate, argillite, chert, limestone, sandstone and conglomerate. Pyroxene-phyric basaltic rocks occur rarely, but it is not clear if these are intercalated volcanic rocks or sills.

An important reference section for Unit uTrNs occurs between the Long Lake and Monticola Lake faults. This section includes the base of the unit, above volcanic rocks of Unit uTrNv, contains several determinations of stratigraphic facing direction, which consistently indicate that the rocks face to the northeast, away from the volcanic rocks, and the uppermost part of the exposed succession contains the only fossil date presently available for the unit. This fossil locality, on a low ridge west of Pooytl Mountain (Figure 2), comprises Halobiid fragments that were assigned a probable Upper Triassic age (Campbell and Tipper, 1971). The sedimentary succession is truncated by the Monticola Lake fault a short distance to the northeast of the fossil locality, so its stratigraphic top is not defined.

The base of the unit is exposed on an old logging road about 1 kilometre southeast of Long Lake, where pyroxene porphyry breccia and overlying crystal-lithic tuff of the volcanic unit are overlain by dark green, light grey-green weathered, fine to medium-grained volcanic sandstone that is assigned to Unit uTrNs. The sandstone is laminated and locally cross-laminated and includes rare thin interbeds of siltstone. Bedding is near vertical in this area and the northeast facing direction is determined from cross-beds in the sandstone. Similar sandstone forms the dominant rock type over a fairly well exposed interval that extends for about 300 metres to the northeast. Dark green to grey, light grey-weathered, laminated to thin-bedded chert is intercalated with the sandstone over most of this interval and becomes dominant in the upper part. In some exposures the volcaniclastic sandstone forms channels that cut into the chert.

Exposures to the northeast of the volcaniclastic sandstone/chert unit at the base of Unit uTrNs comprise a fairly uniform succession of thin-bedded siltstones intercalated with dark grey argillites and weakly cleaved slates. These lithologies dominate all the way to the Monticola Lake fault. Thin, lenticular beds of fine to medium-grained sandstone, some of which are graded, occur locally. Dark grey micritic limestone and limy argillite are also present, mainly near the northwest corner of the map area and to the north of Long Island Lake. The limestone occurs as thin to thick beds intercalated with siltstone, argillite and, locally (north of Long Island Lake), thin-bedded chert.

Exposures of Unit uTrNs southwest of the Long Lake fault consist largely of fine to medium-grained volcaniclastic sandstone intercalated with thin-bedded chert, argillite and siltstone; lithologies that are very similar to those that define the unit north of the fault. Also present to the south are substantial intervals of pebble to cobble conglomerate containing clasts of mainly sedimentary rock types. The conglomerates are predominantly clast supported, moderately to poorly sorted, and poorly stratified. The subangular to rounded clasts are dominated by laminated siltstone, cherty argillite and argillite, but also include chert, limestone, pyroxene and/or feldspar-phyric volcanic rocks and, locally, hornblende-plagioclase-phyric microdiorite. The matrix commonly varies from a siltstone to a gritty sandstone, and in some conglomerate units is distinctly calcareous.

Conglomerate is also found within Unit uTrNs in the wedge-shaped belt between the Gammarus Lake and Blowdown Lake faults (Figure 2). There, pebble conglomerate occurs locally as layers and lenses up to several metres thick within a succession of mainly thin-bedded cherty argillites and siltstones, that also includes thin to thick beds of green volcanic sandstone. The angular to subrounded pebbles are mainly argillite, chert and siltstone, but also include feldspathic and pyroxene-feldspar-phyric volcanic rocks. The pebbles in most conglomerate units are supported by a silty to siliceous argillite matrix, but conglomerates with tightly packed pebbles and little matrix also occur. Also present are rare limestone-matrix conglomerate units that, in addition to the previously mentioned clast types, also contain limestone and sandstone clasts.

The presence of probable Halobia fossil fragments within Unit uTrNs west of Pooytl Mountain was confirmed during the 2000 field season. Unit uTrNs is thought to be entirely Upper Triassic because this probable Upper Triassic fossil locality is near the top of the section exposed between the Long Lake and Monticola Lake faults, and the basal part of the section overlies volcanic rocks typical of the Upper Triassic Nicola Group. Samples of chert and limestone collected during the 2000 field season are currently being processed for microfossils in order to test this assumption.

Triassic-Jurassic Plutonic Rocks

Calc-alkaline and alkaline plutons of Late Triassic to Early Jurassic age are a prominent feature of the Quesnel Terrane and can host important porphyry Cu (±Au) and skarn deposits. The predominantly granodioritic Thuya batholith, part of which underlies much of the southern half of the map area, has long been recognized as one of these plutons, as has the Takomkane batholith to the north-northwest (Figure 1; Campbell and Tipper, 1971). During the present study, a prominent belt of more mafic plutonic rocks, only partially shown on previous maps, was mapped northwestward from the northeast margin of the Thuya batholith. This belt includes, from southeast to northwest, the Dum Lake ultramafic-mafic intrusive complex, several diorite stocks near Deer Lake, and the Friendly Lake diorite-syenite intrusive complex at the northwest boundary of the map area (Figure 2). These rocks intrude the west side of the central, predominantly volcanic belt of the Nicola Group, as well as underlying Paleozoic rocks of the Harper Ranch Group. It is suspected that they are older than the Thuya batholith and approximately coeval with the associated Nicola Group volcanic rocks. Whiteaker (1996) has documented a similar situation at the Ann porphyry copper property on the east margin of the Takomkane batholith. There, Nicola volcanic rocks, including an andesite that has yielded a U-Pb zircon date of 203.9±4.2 Ma are intruded by a suite of mainly dioritic to monzonitic intrusions, one of which gives a U-Pb titanite age of 203±4 Ma. Granodiorite of the adjacent Takomkane batholith gives a younger, tightly constrained U-Pb zircon date of 193±0.6 Ma.

DUM LAKE INTRUSIVE COMPLEX

The Dum Lake complex comprises ultramafic and mafic plutonic rocks that may be part of an Alaskan-type intrusive body, partially truncated by the Thuya batholith on its southwest side. On the scale of Figure 2 it is subdivided into an ultramafic and a mafic unit. The ultramafic rocks were in part mapped by Campbell and Tipper (1971) as a small lens of serpentinite and serpentinized peridotite along the margin of the Thuya batholith. Some of the associated coarse-grained mafic plutonic rocks were included in the Thuya batholith by Campbell and Tipper, but much of the northeastern part of the complex underlies an area previously mapped as Nicola Group. Campbell and Tipper also mapped a small area of serpentinized peridotite along Highway 5, five and a half kilometres south of Little Fort. These may represent a sliver of the ultramafic portion of the Dum Lake complex, offset along the dextral Thuya Road fault.

The ultramafic portion of the Dum Lake complex includes an assemblage of variably serpentinized, locally carbonate and talc-altered rocks that, from outcrop and hand specimen-scale observations, apparently consists largely of clinopyroxenite, wehrlite and dunite. The proportions and internal distribution of the different rock types are not well known, although clinopyroxenite to clinopyroxene-rich wehrlite seem to dominate along the northeastern margin of the unit. Locally, dikes and veins of clinopyroxenite cut wehrlitic rocks. Elsewhere clinopyroxenite and wehrlite seem to form parallel layers up to several metres thick, but it was not determined if these represent magmatic layering or dikes of one rock type within the other.

The mafic part of the Dum Lake complex is dominated by coarse to medium-grained gabbro and diorite, but locally includes clinopyroxenite, monzogabbro, monzodiorite, microdiorite, and tonalite. The contact between the mafic rocks and the ultramafic unit was observed at one place, 1.5 kilometres southeast of Dum Lake. Clinopyroxenite containing 5 percent disseminated pyrite is in contact with monzogabbro across a sharp, steeply-dippping, northwest-striking contact. An intimate relationship between the two rock types is suggested by relationships within the clinopyroxenite, where identical monzogabbro occurs as isolated patches, up to 10 centimetres in size, that display diffuse contacts with the enclosing clinopyroxenite. Similar patches, of either gabbro or monzogabbro, occur within clinopyroxenite elsewhere along the northeast margin of the ultramafic unit, and clinopyroxenite grading to gabbro was observed at several localities within the mafic part of the complex.

Relationships within the mafic part of the Dum Lake body are very complex, and any given outcrop commonly contains a variety of dioritic to gabbroic phases that show varying degrees of epidote-chlorite alteration and veining, and contact one another across a variety of sharp, diffuse or sheared contacts. Near Dum Lake much of the northeast margin of the complex is an intrusion breccia comprising angular fragments of gabbro, diorite and microdiorite within a matrix (locally more of a mesh-like vein network) of fine to medium-grained leucocratic diorite consisting of plagioclase and two to five percent chloritized hornblende. Associated with these rocks are units of mafic microdiorite that grade into strongly foliated chlorite-hornblende schist. In places, lenses of non-foliated microdiorite are aligned within this foliation, and locally folded around it, whereas other veins and dikelets of leucocratic diorite to tonalite cut the foliation at a high angle. Locally, schistose rocks, similar to the foliated microdiorite, occur as fragments within intrusion breccia that are clearly crosscut by the leucodiorite matrix. Although they are not well understood, these relationships indicate that locally significant ductile strain attended intrusion of the Dum Lake complex.

FRIENDLY LAKE INTRUSIVE COMPLEX

The Friendly Lake intrusive complex comprises two distinct stocks of monzonite, syenite and granite, together with a broad area between and south of these stocks that consists largely of microdiorite, diorite, gabbro, and related intrusion breccias (Figure 2). The monzonitic stocks were mapped by previous workers (Campbell and Tipper, 1971; Preto, 1970a), but the associated dioritic rocks were included in the Nicola Group on previous maps. This may be because they consist mainly of fine-grained microdiorite that is not readily distinguished from an andesitic volcanic rock in isolated exposures. However, the intrusive nature of most of the complex is apparent in several recent logging cuts around Friendly Lake. Exposure is not as good to the north, but scattered outcrops suggest that the same suite of rocks extends to the northern limit of our mapping, in large part encompassing the monzonitic stocks.

Exposures south, west and northwest of Friendly Lake are dominated by medium green, grey-brown to rusty-brown weathered microdiorite. In fine-grained varieties, which are commonly somewhat chloritized, mineral grains and textures may not be apparent, but in many exposures these fine-grained rocks were observed to grade into fine to medium-grained microdiorites and diorites, consisting of randomly oriented, interlocking grains of hornblende±pyroxene and plagioclase. The most definitive evidence of an intrusive origin for these fine-grained green rocks comes from several good exposures south of Friendly Lake, where they comprise distinct dikes, some with chilled margins, that cut through medium-grained diorite and microdiorite-hosted intrusion breccia. Dikes of feldspar porphyry and hornblende-feldspar porphyry were also seen cutting diorite.

Other rock types observed around Friendly Lake include medium to coarse-grained pyroxene gabbro, dark grey pyroxene-feldspar porphyry and intrusion breccia. The pyroxene-feldspar porphyry units typically form tabular bodies, up to a few metres wide, within dioritic rocks. They are suspected to be dikes, although this was not proven. Intrusion breccia was observed in several outcrops south of the west end of Friendly Lake. It comprises tightly packed fragments of diorite, monzodiorite, microdiorite and pyroxene-feldspar porphyry in a sparse matrix of fine-gained microdiorite.

Exposures north of Friendly Lake, around, and directly south of, the monzonitic stocks, include diorite, microdiorite and intrusion breccia that are similar to rocks found in the better-exposed area south of Friendly Lake. Some exposures in this area, however comprise fine-grained greenstone, chloritic schist and skarn-altered rock of uncertain protolith. Furthermore, some intrusion breccias, particularly those near the margins of the largest monzonitic stock, include fragments of siltstone and chert, together with dioritic rocks. It is suspected, therefore, that screens of country rock may form a significant portion of this part of the complex.

The discrete stocks in the northern part of the Friendly Lake complex form resistant pinkish outcrops of medium-grained, leucocratic, porphyritic quartz monzonite to monzonite, locally grading to granite, quartz syenite and syenite. Their contacts are sharp, but dikes and veins of similar composition occur locally in adjacent rocks. Commonly, diorite and greenstone along the margins of the stocks are cut by coarse-grained monomineralic amphibole veins, or by veins with amphibole rims and orthoclase-rich cores. Skarny greenstone along the western margin of the smallest stock is, in part, strongly foliated. Veins of non-foliated monzonite typically cut across the foliation, but some are foliation-parallel and slightly boudinaged. These relationships are somewhat similar to those along the eastern margin of the Dum Lake complex, where the youngest intrusive phases, leucodiorite and tonalite, largely, but not entirely, postdate ductile deformation within associated microdiorite.

OTHER DIORITE PLUTONS

Diorite, locally accompanied by gabbro, microdiorite and intrusion breccia, forms 3 stocks in the Deer Lake area which intrude mainly Paleozoic rocks of the Harper Ranch Group. These stocks define the central portion of the northwest-trending linear belt of intrusions that includes the Dum Lake complex to the southeast and the Friendly Lake complex to the northwest. The plutons around Deer Lake are less varied lithologically than the Friendly Lake and Dum Lake complexes, and are made up of dioritic to gabbroic rocks that are essentially identical to large parts of the adjacent complexes. All of the plutons within this northwest-trending belt are assumed to reflect a common tectonic environment, probably in the roots of the Late Triassic Nicola magmatic arc.

Dioritic rocks also form a number of plugs and small stocks that intrude Nicola Group rocks in the southern part of the Ripple Lake belt, and may represent a more diffuse expression of the magmatism within the central belt to the east. These small intrusions consist mainly of medium-grained, mostly equigranular hornblende diorite, but also include hornblende-plagioclase porphyritic diorite, microdiorite and coarse-grained pyroxene gabbro. The narrow body along the margin of the Thuya batholith, north of Lac des Roches, consists of variably, but locally strongly foliated microdiorite and hornblende-biotite-feldspar schist, that locally contains screens of hornfelsed metasedimentary rock aligned in the foliation. Foliated microdiorite and mafic schist also occur locally along the southeastern margin of the larger, elongate diorite body to the west. On Highway 24, an outcrop on the southeastern margin of this diorite body comprises strongly foliated microdiorite interspersed with skarn lenses. Also present are lenses of fine to medium-grained monzonite that mostly cut across the foliation, but locally seem to be rotated into the folitation. These relationships are not unlike those observed in parts of the Dum Lake and Friendly Lake complexes, where ductile strain localized in some intrusive units largely predates younger intrusive phases.

THUYA BATHOLITH

Granodiorite and related rocks of the Thuya Batholith underlie much of the southern half of the map area. These exposures represent only a relatively small part of the batholith, which extends for a considerable distance to the south and west (Campbell and Tipper, 1971; Figure 1). Along its northwestern margin, the batholith clearly intrudes sedimentary rocks included in Unit uTrNs of the Nicola Group. Along its northeast margin it apparently intrudes ultramafic and mafic rocks of the Dum Lake intrusive complex, but the contact is not well exposed and unequivocal crosscutting relationships were not observed. South of Little Fort the eastern margin of the batholith is defined by the dextral Thuya Road fault. The batholith is also cut by faults in the southwestern part of the map area, where Eocene volcanic rocks of the Skull Hill Formation occur as a down-faulted block within it (Figures 1 and 2).

Within the present map area the Thuya Batholith consists mainly of medium-grained, more or less equigranular and isotropic, hornblende-biotite granodiorite. Mafic phases commonly comprise 10 to 20 percent of the rock, although the ratio of hornblende to biotite seems to vary considerably. Epidote (± chlorite) alteration is ubiquitous, but variable in intensity. Minor, apparently gradational compositional variations to quartz monzodiorite, tonalite and quartz diorite occur locally. However, the northern part of the batholith, particularly that portion northwest of highway 24 between Lac des Roches and Long Island Lake, is more heterogeneous. It consists largely of hornblende-biotite quartz monzonite and quartz monzodiorite, but also includes monzodiorite, diorite and monzonite. Locally within this area, hornblende diorite and hornblende±biotite monzodiorite occur as alternating layers several centimetres thick with diffuse but approximately planar contacts.

Jung (1986) reports K-Ar and Rb-Sr radiometric dates for a sample of hornblende-biotite monzodiorite collected near Highway 24 a short distance east of Lac des Roches (location shown on Figure 2), while Calderwood *et al*. (1990) report a preliminary U-Pb zircon date from the same locality. The K-Ar dates from hornblende and biotite separates are 191±7 Ma and 186±6 Ma, respectively, similar to previous K-Ar dates on unaltered samples from the batholith to the south and west (summarized by Jung, 1986). The Rb-Sr whole rock - mineral isochron date is 183.6±4.4 Ma, with an initial $^{87}Sr/^{86}Sr$ ratio of 0.7042, while the U-Pb zircon upper intercept is 205±9.3 Ma. The relatively large error permits a Late Triassic or Early Jurassic crystallization age for this part of the batholith. A sample of relatively unaltered granodiorite from near Thuya Creek, in the southeastern part of the map area, has been submitted for U-Pb dating in an attempt to further constrain the batholith's age.

Lower Jurassic Sedimentary Rocks

Preto (1970a) collected poorly preserved ammonites of probable Late Sinemurian or Early Pleinsbachian age from argillite in an exploration trench west of Lost Horse Lake. The area was revisited during the present study and an ammonite fragment was collected from the workings excavated from the trench. The fossiliferous rocks occur within a poorly exposed interval of unaltered argillites and siltstones, mapped as Unit lJs on Figure 2, that seeems to be of very limited extent. It is inferred to comprise a small outlier resting stratigraphically above Unit uTrNsv in the core of the Nehalliston syncline, and truncated to the south by the northeast-striking fault that passes through Lost Horse Lake.

The exploration trench that originally yielded the Jurassic ammonites of unit lJs was excavated during an exploration program aimed at evaluating widespread alteration and local base metal sulphide mineralization within and adjacent to the Friendly Lake intrusive complex. An interesting aspect of Unit lJs is its unaltered state when compared to adjacent silicified and chlorite-epidote altered rocks of Unit uTrNsv and the Friendly Lake intrusive complex. Furthermore, fossiliferous Lower Jurassic rocks near Windy Mountain, about 13 kilometres to the northwest, include conglomerates that contain syenite clasts that Campbell and Tipper (1971) specifically relate to the syenitic rocks here included in the Friendly Lake intrusive complex. These observations suggest that mineralization and alteration in this area was closely related to intrusion of the Friendly Lake intrusive complex, which must be of latest Triassic or earliest Jurassic age, and that deposition of the Jurassic rocks followed a period of uplift and erosion that partially unroofed the intrusive complex and its associated alteration-mineralization system. The 2001 field program will cover the Windy Mountain area and, it is hoped, allow us to evaluate more fully the relationship of the Lower Jurassic rocks to the Nicola Group and associated intrusions.

Cretaceous Granite Northeast of Tintlhohtan Lake

A small granitic stock, which hosts the Anticlimax molybdenum-tungsten prospect, occurs within volcanic and sedimentary rocks of the Nicola Group a short distance northeast of Tintlhohtan Lake (Figure 2). The stock consists mainly of medium-grained, leucocratic granite, containing a few percent fresh to chloritized biotite. Associated phases include quartz-feldspar porphyry, pegmatite and aplite (Stevenson, 1940; Preto, 1970b). Soregaroli (1979) obtained a K-Ar date of 102±5 Ma from unaltered magmatic biotite separated from fresh granite within the central part of the stock. Similar mid-Cretaceous K-Ar cooling ages have been obtained from the main body of the Baldy batholith to the southeast (summarized by Jung, 1986), which has also yielded an Early Cretaceous U-Pb (zircon) upper intercept date of 115.9±4.6 Ma (Calderwood, 1990). It is suspected that the Tintlhohtan Lake stock is part of the same suite of late Early Cretaceous plutons.

On its north, west and south sides, the Tintlhohtan Lake stock is in contact with a mixed assemblage of sedimentary and volcanic rocks assigned to Unit uTrNsv. Although the contact was not observed, it is inferred to be intrusive because these country rocks are weakly hornfelsed (Enns, 1980; this study). The stock's eastern contact, with pyroxene porphyry breccias of Unit uTrNv, is mapped as a gently-dipping fault, following Kirkham and Sinclair (1988). Their interpretation was based on diamond drill holes that passed completely through the intrusion, cutting highly sheared and argillically-altered granite before passing into relatively unaltered and unmetamorphosed volcanic breccias. It is consistent with observations made during the present study, as volcanic breccia immediately to the east of the stock is not hornfelsed and is cut by numerous gently-dipping faults.

Eocene Sedimentary and Volcanic Rocks

Eocene rocks in the Bonaparte Lake map area are included in the Kamloops Group, which is further subdivided into the sedimentary Chu Chua Formation and the mainly volcanic Skull Hill Formation (Uglow, 1922; Campbell and Tipper, 1971). Both formations are represented to a limited extent in the Nehalliston Plateau area.

CHU CHUA FORMATION

The Chu Chua Formation is represented by conglomerates and conglomeratic sandstones that occur mainly in a largely fault-bounded, wedge-shaped belt that extends for about 6 km northwestward from Little Fort. Exposures are found mainly in the canyons of Nehalliston and Eakin creeks. A much smaller outlier of the Chu Chua Formation is exposed along the lower reaches of Thuya Creek (Uglow, 1922) but it was not examined during the present study. The Chu Chua Formation northwest of Little Fort is dominated by poorly sorted conglomerate comprising rounded to angular boulders, cobbles and pebbles that grade into a gritty sandstone matrix. Clasts are dominated by dioritic to granodioritic plutonic rocks, but locally include substantial amounts of vein quartz and greenstone of probable mafic volcanic origin. Bedding is not well defined, but a crude stratification is commonly apparent in the conglomerates, and is locally accentuated by thick interbeds of gritty to pebbly sandstone. Where observed, the bedding dips 15 to 25 degrees east.

The eastern contact of the Chu Chua Formation was observed in Nehalliston Creek, where it is a north-northwest striking, steeply-dipping fault that may splay from the Taweel Lake fault to the east. The southwest contact of the formation was not observed, but apparently corresponds to the Rock Island Lake fault. The northwest contact was not observed either, but the orientation of stratification in the conglomerate suggest that this contact is reasonably interpreted as an east-dipping unconformity across which the Chu Chua Formation rests above southwest-dipping volcanic and sedimentary rocks of the Nicola Group (Figure 3, Section C).

The rocks described above as Chu Chua Formation are not dated. However, they are readily correlated, on the basis of lithology and mode of occurrence, with a fault and unconformity-bounded interval of conglomerates and associated finer-grained rocks exposed along the lower reaches of Joseph Creek, 5 kilometres to the east (Schiarizza and Preto, 1987). There, shale and siltstone intercalated with the conglomerates have yielded collections of plant fossils and palynomorphs indicating an Eocene age (Uglow, 1922; Campbell and Tipper, 1971).

SKULL HILL FORMATION

Volcanic rocks of the Skull Hill Formation crop out along the southwest boundary of the map area, south and southeast of Lac des Roches. A volcanic outlier also included in the formation overlies sedimentary rocks of the Nicola Group and an associated dioritic intrusion 3 kilometres north of Lac des Roches (Figure 2). These rocks are markedly less-altered and deformed than the Mesozoic volcanic rocks within the map area. They are assigned to the Skull Hill Formation following Campbell and Tipper (1971), who mapped them as part of a north-northwest trending belt of Eocene volcanic rocks that extends for almost 70 kilometres between Bonaparte and Canim lakes (Figure 1).

Most exposures of Skull Hill Formation observed south and southeast of Lac des Roches consist of friable, rusty-brown-weathered andesite and associated flow breccia, commonly with sparse hornblende phenocrysts and chloritic amygdules. Also present are more competent grey-brown weathered, pyroxene-phyric basalt or andesite flows, and light grey biotite-feldspar-phyric dacite. Sedimentary intervals up to 10 metres thick are locally intercalated with the andesitic flows. These consist of biotite-rich arkosic sandstone containing discontinuous lenses of granule to pebble conglomerate with granitic and volcanic clasts, and thin shale layers containing abundant plant debris.

The volcanic outlier north of Lac des Roches was observed at only one locality near its southern limit, but its aerial extent is readily mapped from air photos. Where seen, it consists of dark grey, brown-weathered basalt containing about 5 percent olivine and pyroxene phenocrysts, 1 to 3 millimetres in size.

Dikes

Dikes of diorite, microdiorite and hornblende-feldspar porphyry are common within sedimentary and volcanic rocks of the Nicola and Harper Ranch groups peripheral to the map-scale dioritic intrusive units that cut these groups west of the Rock Island Lake fault. The dioritic rocks, as well as the adjacent country rocks, are in turn cut by dikes and lenses of tonalite and granodiorite along the north and northwest margins of the Thuya batholith. As discussed previously, some units of massive pyroxene porphyry within the central volcanic belt of the Nicola Group are sills and dikes cutting sedimentary and volcanic rocks, although in many exposures they are difficult to distinguish from flows.

The dikes described above are inferred to be Late Triassic - Early Jurassic in age, and related to the Mesozoic magmatic arc of the Quesnel Terrane. Younger dikes include dark green to grey, fine grained basalt and dark grey, biotite-bearing lamprophyre that are most common within the zone of northwest to north-striking faults east of the Rock Island Lake fault. These dikes are oriented more or less parallel to the faults and, like the faults, are suspected to be Eocene in age. Light grey to pink flow-banded dacite to rhyolite that is intermittently exposed for about 3 kilometres along the splay west of the Taweel fault, 2 to 5 kilometres south of the Tintlhohtan Lake cross fault, may also represent one or more dikes emplaced within this fault system. Dacitic sills or dikes were also observed within sedimentary rocks of the Nicola Group in the western part of the area, where they are spatially associated with, and oriented approximately parallel to, the Long Lake fault.

STRUCTURE

Mesoscopic Structures

Fine-grained Paleozoic and Triassic sedimentary rocks throughout the area commonly display a weak to moderately developed slaty cleavage, whereas associated volcanic and coarse-grained clastic rocks are not generally foliated. As discussed in previous sections, local zones of strong foliation within, or along the margins of, several dioritic plutons appear to be in local zones of high strain that formed during the late stages of intrusion. Steeply-dipping, moderate to intense foliation is also evident in many rocks along fault zones, particularly along faults in the southern part of the Rock Island Lake system.

Mesoscopic folds were noted rarely, generally in thin-bedded siltstone/slate or chert/argillite intervals. The slaty cleavage is axial planar to most folds which, together with bedding/cleavage intersection lineations, plunge to the northwest or southeast. Rarely, folds with similar plunges fold the slaty cleavage. Because they are pervasive, although variably and commonly weakly developed, across the map area, the cleavage and associated folds are inferred to be manifestations of regional contractional deformation accompanied by low-grade metamorphism. They may have formed in Lower to Middle Jurassic time, when compressional tectonic events are well documented elsewhere in the region. More specifically, south-plunging, east-vergent folds associated with west-dipping slaty cleavage within Unit muTrNs may relate to regional, east-directed thrusting that imbricated this unit and placed it above the Kootenay Terrane (Brown *et al*., 1986; Rees, 1987; Struik, 1988; Bloodgood, 1990).

In the Deer Lake area, there were no obvious differences in mesoscopic fabric or metamorphic grade noted between the Paleozoic rocks and nearby Triassic rocks. In contrast, rocks assigned to the Harper Ranch Group in the belt between highways 24 and 5 are commonly strongly foliated, and are locally folded by two generations of folds. These rocks, however, form a narrow belt that is sandwiched between the northeast margin of the Dum Lake intrusive complex, where local zones of strong syn-plutonic deformation are documented, and faults of the Rock Island Lake system. It is suspected, therefore, that the relatively intense mesoscopic-scale deformation within this belt is of more local than regional significance.

Map-Scale Structures

The macroscopic structure of the Nehalliston Plateau is dominated by northwest to north-striking faults. In the eastern part of the area these faults comprise the north to north-northwest trending Rock Island Lake system which cuts rocks as young as Eocene and shows evidence of mainly dextral strike-slip displacement. In the western part of the area, northwest-striking faults also locally cut Eocene rocks and are interpreted as mainly southwest-side-down normal faults. Collectively, these faults, together with associated northeast-striking cross-faults, are part of a system of predominantly Eocene dextral strike-slip and related extensional faults that are well documented throughout much of the Intermontane Belt and adjacent portions of the Canadian Cordillera (Price, 1979; Ewing, 1980; Struik, 1993). The structure within the Nicola volcanic-plutonic belt in the central part of the map area is dominated by a fold system represented mainly by the Nehalliston syncline. The folding apparently affects rocks as young as Lower Jurassic (Figure 3, Section A), but its timing is not well constrained. It might be related to Lower to Middle Jurassic compressional deformation that is well-documented elsewhere in the region (Brown *et al*., 1986; Rees, 1987; Schiarizza and Preto, 1987; Bloodgood, 1990), but could be as young as Eocene. The southeastern boundary of this fold system, and defining the boundary between central volcanic-plutonic belt and the adjacent Ripple Lake belt, is the northwest-striking Monticola Lake - Gammarus Lake fault system. These faults may have a history dating back to the Late Triassic.

ROCK ISLAND LAKE FAULT SYSTEM

The macroscopic structure in the eastern part of the map area is dominated by a system of north-northwest to north-striking faults that are interpreted as part of a Tertiary (probably Eocene) dextral strike-slip system. They are collectively referred to as the Rock Island Lake fault system, after one of the dominant through-going strands within the fault zone. The fault system is almost 10 kilometres wide in the northeastern part of the map area, but individual faults converge southward to a narrow zone confined to the North Thompson River valley south of Little Fort. In the following paragraphs, individual faults are discussed from east to west across the system.

The north-striking Lemieux Creek fault separates Unit muTrNs from the Fennell Formation north of Little Fort. Outcrops near the inferred trace of the fault are commonly brecciated, carbonate-altered, and cut by variably oriented brittle faults. Although the overall trend of the fault is northerly on the scale of Figure 2, on a more detailed scale parts of the system comprise an anastomozing network of north-northeast to north-northwest trending fault strands. These expressions of brittle faulting are suspected to relate to relatively minor amounts of Tertiary displacement on this strand of the Rock Island Lake fault system. Major Tertiary displacement is precluded by the fact that the fault does not apparently cut the Jura-Cretaceous Raft batholith 15 kilometres to the north (Figure 1). There, the contact between the Fennell Formation and Unit muTrNs is mapped as an east-dipping thrust fault of probable Middle Jurassic age (Campbell and Tipper, 1971; Brown *et al*., 1986; Calderwood *et al*., 1990).

The Taweel fault separates Unit muTrNs from volcanic rocks of Unit uTrNv. It trends slightly more westerly than the Lemieux Creek fault, resulting in a widening of the Unit muTrNs outcrop belt northward from Little Fort. The fault zone is exposed along the lower reaches of Nehalliston Creek, where it is marked by close to 100 metres of rusty iron carbonate-quartz-altered rocks cut by a dense network of brittle faults. The faults show a wide variety of orientations, but north to northwest strikes and steep dips are most common. Lenses of black phyllite, siltstone and crystal-lithic tuff occur throughout the zone; some are fault bounded, while others appear to grade into the pervasively quartz-carbonate-altered host across alteration fronts. The eastern limit of the fault zone is not defined in this area. To the west it passes abruptly into well-foliated chlorite schist that locally grades into lenses of massive pyroxene porphyry basalt. About 100 metres of these variably foliated mafic volcanic rocks, part of unit uTrNv, are exposed along the creek. They are bounded to the west by another fault, apparently a splay from the Taweel fault, that juxtaposes them against Eocene conglomerates of the Chu Chua Formation. This fault is marked, from east to west at creek level, by about 5 metres of very friable chlorite schist interleaved with narrow gouge zones, passing into a couple metres of water-saturated clay and then abruptly into unaltered Eocene conglomerate. Individual brittle faults within and adjacent to the fault zone strike slightly west of north and dip steeply. Fault striations and mineral fibres on the fault planes are more or less horizontal and, where movement sense can be inferred from accretion steps, dextral.

The Rock Island Lake fault has been traced from Little Fort to the north boundary of the map area, and is suspected to continue northwestward as the main through-going strand within the system (Figure 1). Its trace is defined mainly by truncations of map-scale features, including the Dum Lake intrusive complex and Chu Chua conglomerate in the south, and the Nehalliston syncline and northeast-striking faults farther north (Figure 2). On highway 24, the inferred trace of the fault is marked by a 200-metre-wide topographic depression that separates intensely faulted and silicified exposures of microdiorite, diorite and skarn-altered sedimentary rocks on the west from chlorite schist and phyllite of Unit uTrNsv to the east (Figure 2). The strong north-northwest striking vertical foliation in the latter rocks is uncharacteristic of most rocks within this unit and is inferred to relate to the faulting. Adjacent outcrops to the east display abundant brittle faults of about the same orientation, and local folds that plunge steeply to the north-northwest. Similar intensely faulted to foliated rocks characterize rocks in proximity to the inferred trace of the fault southeastward to Highway 5, over which distance the fault is fairly well constrained but not actually observed. Brittle faults typically display gently-plunging striations or mineral fibres and dextral movement-sense from accretion steps. There are few bedrock exposures proximal to the fault northwest of Highway 24, where its inferred trace follows a series of linear topographic depressions.

The Thuya road fault is well-defined for about 6 kilometres northwest of Highway 5, where it truncates the Thuya batholith and adjacent ultramafic rocks of the Dum Lake intrusive complex on its western side. The fault zone is marked, at least locally, by rusty-weathered, completely altered carbonate-silica rock. Adjacent granodioritic rocks of the Thuya batholith become strongly fractured, fracture cleaved and locally penetratively foliated as the fault contact is approached. The steeply-dipping foliation strikes up to 20 degrees more westerly than the fault zone, suggesting a dextral sense of shear. Dextral offset of at least 3 to 4 kilometres is also suggested by outcrops of serpentinized ultramafic rock directly east of the fault along Highway 5, which may be displaced from the ultramafic portion of the Dum Lake intrusive complex. At least some of the movement is inferred to be Eocene or younger since the fault apparently bounds exposures of the Chu Chua Formation along Thuya Creek (Uglow, 1922).

The Rock Island Lake fault system follows the North Thompson river valley from the present study area to just south of Barriere, where it apparently continues southeastward as the Louis Creek fault system (Campbell and Tipper, 1971; Okulitch, 1979). The Rock Island Lake fault does not correspond to any faults mapped by previous workers to the northwest, but it is tentatively projected to the east end of Canim Lake, possibly truncating the west end of the Raft batholith (Figure 1). From there it may connect with a system of faults mapped by Campbell and Tipper along the northeast margin of the Takomkane batholith. These ideas will be evaluated as the Bonaparte mapping program continues northward in future years.

NORTHEAST-STRIKING FAULTS

A northeast-striking fault that passes through Lost Horse Lake is inferred from the truncations of several mappable units within the central belt of the Nicola Group (Figure 2). Most truncated units have counterparts on the opposite side of the fault, showing apparent sinistral separations of 600 to 2600 metres. The northeast-striking fault is apparently cut by the Rock Island Lake fault to the east, but a northeast-striking fault passing near the south end of Tintlhohtan Lake is a possible counterpart, showing about 2000 metres of apparent dextral offset along the Rock Island Lake fault. This northeast-striking fault also shows apparent sinistral offsets of mappable units across it.

The northeast striking fault near Tintlhohtan Lake cuts across eastern strands of the Rock Island Lake fault system, but is apparently offset along the main Rock Island Lake fault. This suggests that the northeast-striking structures are broadly contemporaneous with Eocene displacement along the Rock Island Lake fault system. The apparent sinistral offsets are consistent with the interpretation that the northeast-striking structures are antithetic faults within the north-northwest striking dextral strike slip system. An implication of the broadly coeval nature of the two fault sets is that, even if the two northeast-striking strands were once a single fault, the apparent two kilometres of subsequent displacement along the Rock Island Lake fault might measure only a small increment of the total displacement along it.

A pair of northeast-striking faults mapped north of Thuya Creek mark apparent sinistral offsets of the contact separating ultramafic from mafic portions of the Dum Lake intrusive complex. There are no constraints on the actual movement sense along these faults, and their age can only be inferred to be post Late Triassic or Early Jurassic. They may be Tertiary structures, broadly contemporaneous with the northeast-striking faults to the north, or they might be much older, as suggested by the lack of apparent offset of the Thuya Batholith across the northernmost fault (Figure 2).

NEHALLISTON SYNCLINE

The Nehalliston syncline is inferred mainly from relationships in the Friendly Lake area, where right-way-up, northeast-dipping volcanic and volcaniclastic rocks of Unit uTrNv underlying Pooytl Mountain are inferred to be repeated as an interval of lithologically similar volcanic breccias that are exposed on prominent ridges north and northeast of Lost Horse

Lake (Figure 3, Section A). The fold is cored mainly by a mixed volcanic-sedimentary succession assigned to Unit uTrNsv, but the core also includes the small outlier of Lower Jurassic sedimentary rocks exposed southwest of Lost Horse Lake. South of the northeast-striking fault that crosses Lost Horse Lake, the axial trace of the fold is inferred to be within a mixed volcanic-sedimentary succession that is likewise bounded by volcanic rocks of Unit UTrNv to both the northwest and southeast, although there are no facing directions documented within these panels. However, a further symmetry is provided by a unit of volcanic breccias and flows in the core of the fold (not shown on Figure 2, but shown in outline on Figure 3, Section B) that is bounded by lithologically similar conglomerate units to both the northeast and southwest, which are inferred to be repetitions of the same stratigraphic level. As defined in this way, the southern part of the Nehalliston syncline has a more more westerly trend than the Rock Island Lake fault to the east, and is gradually truncated along the fault (Figure 2).

In the Deer Lake area, the Nicola volcanic unit on the southwest limb of the Nehalliston syncline is in contact with, and presumably stratigraphically underlain by, the Harper Ranch Group to the southwest. The internal structure of the Harper Ranch Group is not well understood, but the presence of potentially correlative limestone units on both sides of the diorite stock southwest of Deer Lake suggests that it may be folded into an anticline complimentary to the Nehalliston syncline (Figure 3, Section B).

The Nehalliston syncline apparently formed after depostion of the Lower Jurassic rocks of Unit lJs, (Figure 3, Section A), although relationships are not well enough constrained to be sure that the Lower Jurassic rocks are actually folded into the syncline, rather than unconformably overlying it. The folding occurred before at least some of the movement on the Rock Island Lake fault, which is thought to be mainly Eocene. It is suspected that it formed during the Early to Middle Jurassic compressional deformation documented elsewhere in the region (*eg*. Brown et al., 1986), but it could be older (see next section), and its orientation is permissive for folding, or tightening of a pre-existing fold, during Eocene dextral translation along the Rock Island Lake fault system.

MONTICOLA LAKE - GAMMARUS LAKE FAULT SYSTEM

The Monticola Lake fault is a northwest-striking structure that juxtaposes the Nicola volcanic belt against sedimentary rocks of the Ripple Lake belt in the northwest part of the map area. At its south end it follows a prominent linear depression that corresponds to an abrupt truncation of Unit uTrNv on its northeast side. The Gammarus Lake fault, which places the Harper Ranch Group and an associated diorite stock against the Ripple Lake belt, is inferred to be the southern continuation of the Monticola Lake fault which has been offset across the northeast-striking fault that passes through Lost Horse Lake. The Gammarus Lake fault and the northeast-striking cross-fault are both apparently truncated by the Blowdown Lake fault, which follows a prominent topographic lineament that, at one locality, contains subcrop of highly fractured and brecciated rocks. The Blowdown Lake fault is suspected to be a southwest-side-down Eocene fault, similar to the Long Lake and Caverhill faults to the southwest, which have parallel strikes.

The Monticola Lake - Gammarus Lake fault system forms the boundary between the central volcanic-plutonic belt of the Nicola Group and the adjacent Ripple Lake belt. The specific units juxtaposed across the fault system suggest relative northeast-side-up displacement, whereas the juxtaposition of markedly different facies of the Nicola Group suggests significant lateral telescoping of facies boundaries, and/or syn-Nicola fault activity that may have played a role in localizing the facies belts. Unfortunately, the dip of the fault, and the sense of movement along it, are totally unconstrained. Of note, however, is that the fault system corresponds to little or no apparent displacement of the northeast tip of the Thuya batholith. This suggests pre-Thuya and therefore syn to immediately-post Nicola activity. Corroborating evidence for uplift of the volcanic-plutonic belt at about this time is the presence of syenite clasts, possibly derived from those in the Friendly Lake complex, in Jurassic conglomerate near Windy Mountain (Campbell and Tipper, 1971).

CAVERHILL LAKE AND LONG LAKE FAULTS

The Caverhill Lake fault, first mapped by Campbell and Tipper (1971), passes through the southwest corner of the Nehalliston Plateau map area. The southeastern part of the fault occurs mainly within the Thuya Batholith, but north of Machete Lake it separates the Eocene Skull Hill Formation from Mesozoic rocks to the northeast (Figure 2). The fault was not observed, but its trace is well defined south of Lac des Roches. There, faults observed within the Eocene rocks strike parallel to the inferred trace of the main fault, dip about 70 degrees southwest and show normal-sense offsets. These may reflect the orientation and sense of movement of the main fault.

The Long Lake fault occurs within the Ripple Lake belt of the Nicola Group, east of Wavey Lake, where it is mapped as the southwest boundary of a lens of volcanic rock within the predominantly sedimentary succession. The fault is inferred mainly from the highly fractured nature of the sedimentary rocks that occur locally near its inferred trace, which is approximately parallel to the Caverhill Lake fault. If the volcanic rocks were derived from near the base of the Ripple Lake belt, as is suspected, a southwest-side-down sense of displacemet, similar to Caverhill lake fault, is most likely.

As discussed in the previous section, the Blowdown Lake fault, which apparently cuts the Gammarus Lake fault to the east of the Long Lake fault, is suspected to correlate with the Caverhill and Long Lake faults in terms of age and sense of movement.

MINERAL OCCURRENCES

The Nehalliston Plateau contains a large number of mineral occurrences, but the MINFILE database is incomplete at the present time. Expanding and updating this database will be an important component of the Bonaparte Project. Here, we provide a brief overview of the variety and distribution of known occurrences (Figure 4), and also highlight rock samples collected during 2000 fieldwork that yielded interesting geochemical values (Figure 4 and Table 1).

Most of the known base and precious metal mineral occurrences in the area are concentrated within and adjacent to the belt of ultamafic - mafic - syenitic plutons that defines the western part of the central Nicola belt. Some of these, such as platinum mineralization within ultramafic rocks of the Dum Lake complex, metalliferous skarns adjacent to Deer Lake and Dum Lake dioritic bodies, and porphyry-style copper occurrences in the Friendly Lake complex, are broadly coeval with the plutons. Others concentrated in this belt, such as numerous vein and shear-related gold showings, may be considerably younger than the intrusive rocks. Disseminated copper occurs within and along the margins of the Thuya Batholtih, and in association with dioritic stocks and dikes cutting sedimentary rocks near the northwest margin of the batholith. Mineral occurrences in the northeastern part of the area include molybdenum-tungsten mineralization within the Early Cretaceous Tintlhohtan Lake stock and polymetallic sulphide lenses within sedimentary rocks of Unit muTrNs.

Occurrences Associated with the Dum Lake Intrusive Complex

The rocks within and adjacent to the Dum Lake intrusive complex are host to a variety of mineral occurrences, including skarns, gold-quartz veins, gold in quartz-carbonate-altered fault zones, and platinum in ultramafic rocks. The southern part of the complex is covered by the Golden Loon claim group, which was staked between 1984 and 1986, and has seen several exploration programs directed at gold and platinum since that time. The northern part of the complex includes skarn-related occurrences that were explored on the Cedar claims, and gold-bearing veins that were explored on the "G" claims.

GOLDEN LOON

The Golden Loon property includes several areas of known precious and base metal mineralization within ultramafic and mafic plutonic rocks of the Dum Lake complex; those that are well documented are shown as GL-1 through GL-6 on Figure 4. In addition, several samples collected from this area during our 2000 field program returned anomalous base metal values. The

TABLE 1
GEOCHEMICAL DATA FOR SELECTED ROCK SAMPLES COLLECTED DURING THE 2000 FIELD SEASON
(THE GEOLOGICAL SETTINGS OF INDIVIDUAL SAMPLES ARE DISCUSSED IN THE TEXT)

Element	Mo	Cu	Pb	Zn	Ag	Ni	Co	As	Cd	Sb	Bi	Cr	Ba	W	Hg	Au	Pt	Pd
Units	ppm	ppm	ppm	ppm	ppb	ppm	ppm	ppm	ppm	ppm	ppm	ppm	ppm	ppm	ppb	ppb	ppb	ppb
Method	ARMS	ARMS	ARMS	ARMS	ARMS	ARMS	ARMS	ARMS	ARMS	ARMS	ARMS	ARMS	ARMS	ARMS	ARMS	FA	FA	FA
Lab	ACM	ACM	ACM	ACM	ACM	ACM	ACM	ACM	ACM	ACM	ACM	ACM	ACM	ACM	ACM	ACM	ACM	ACM
Detection	0.01	0.01	0.01	0.1	2	0.1	0.1	0.1	0.01	0.02	0.02	0.5	0.5	0.2	5	2	2	2
Field #																		
00SIS-17	2.89	9.55	9.1	13.4	2198	7.6	7.3	2.6	0.24	0.11	0.08	18.1	87.7	6.5	22	892	3	2
00SIS-23	72.61	1488.46	0.72	42.1	1248	7	41.1	1.9	0.31	0.48	0.05	9.1	30.1	0.3	53	90	10	< 2
00SIS-26	82.14	29.24	33.6	22.2	3250	31	1514.5	66.3	0.49	1.16	17.21	42.5	85.4	101.7	367	845	3	< 2
00SIS-29	2.8	13463.53	3.47	92.9	12590	24	69.1	29.1	0.4	0.52	0.17	5.9	74.9	0.6	65	72	13	62
00SIS-33	1.05	501.39	2.45	75.8	516	11.7	16.5	15.2	0.5	1.1	0.08	4.1	84.6	0.6	114	8	< 2	< 2
00SIS-215	11.11	118.16	30.6	313.4	1253	56.5	15.7	41.4	3.7	10.35	0.07	29.1	21.4	0.7	1071	56	8	4
00SIS-216	5.47	153.97	6.01	15.7	1109	6.2	1.4	9.9	0.14	71.23	0.6	14.4	216.4	5.2	2935	7	3	< 2
00SIS-226	2.56	71.35	195.23	1379.5	18854	92.8	36	2434.4	24.02	1.89	1.49	197.7	81.5	0.6	347	1458	7	10
00SIS-269	6.84	33754.17	198.43	379.7	25434	7.7	10	10.8	32.9	2.9	65.15	6.9	80.2	1.4	263	37	208	149
00SIS-325	2.05	167.95	10.24	86.9	277	12.6	16.1	1.6	0.46	0.63	0.07	23.7	206.3	< .2	15	3	3	3
00SIS-359	11.57	872.32	5.86	58.2	410	29	119.6	53.3	0.15	0.79	0.32	27.2	48.1	6.5	34	14	2	4
00PSC-14-2	1.85	1826.08	569.07	8.3	15104	5.6	2.1	11.8	0.13	0.24	2.78	24.1	27	7.6	33	704	< 2	4
00PSC-76	0.43	16.24	12.25	10.3	101	409.6	68.6	9.8	0.15	1.35	0.08	458.7	28.9	0.5	44	5	65	3
00PSC-124	16.35	871.09	7.98	70.7	929	332.5	340.2	8	0.28	0.57	0.17	85.2	45.7	1.1	23	199	9	22
00PSC-283	90.91	96.98	21.78	25.8	557	23.7	12.5	250.8	0.04	1.78	1.48	33.2	156	8	68	693	5	4
00PSC-334	11.14	227.29	4.49	252.7	803	58.4	13.4	8.1	0.98	0.87	0.8	70.6	78.2	2	27	26	3	9
00PSC-337	13.41	262.53	2.24	56.2	341	67.1	99.4	22.1	0.02	0.67	0.18	35.4	65.2	1.3	9	10	< 2	4

Analysis of steel-milled samples prepared by ACME analytical Ltd.
ARMS = Aqua regia digestion - ICPMS
FA = Lead fire assay-ICP finish
ACM = ACME Analytical, Vancouver

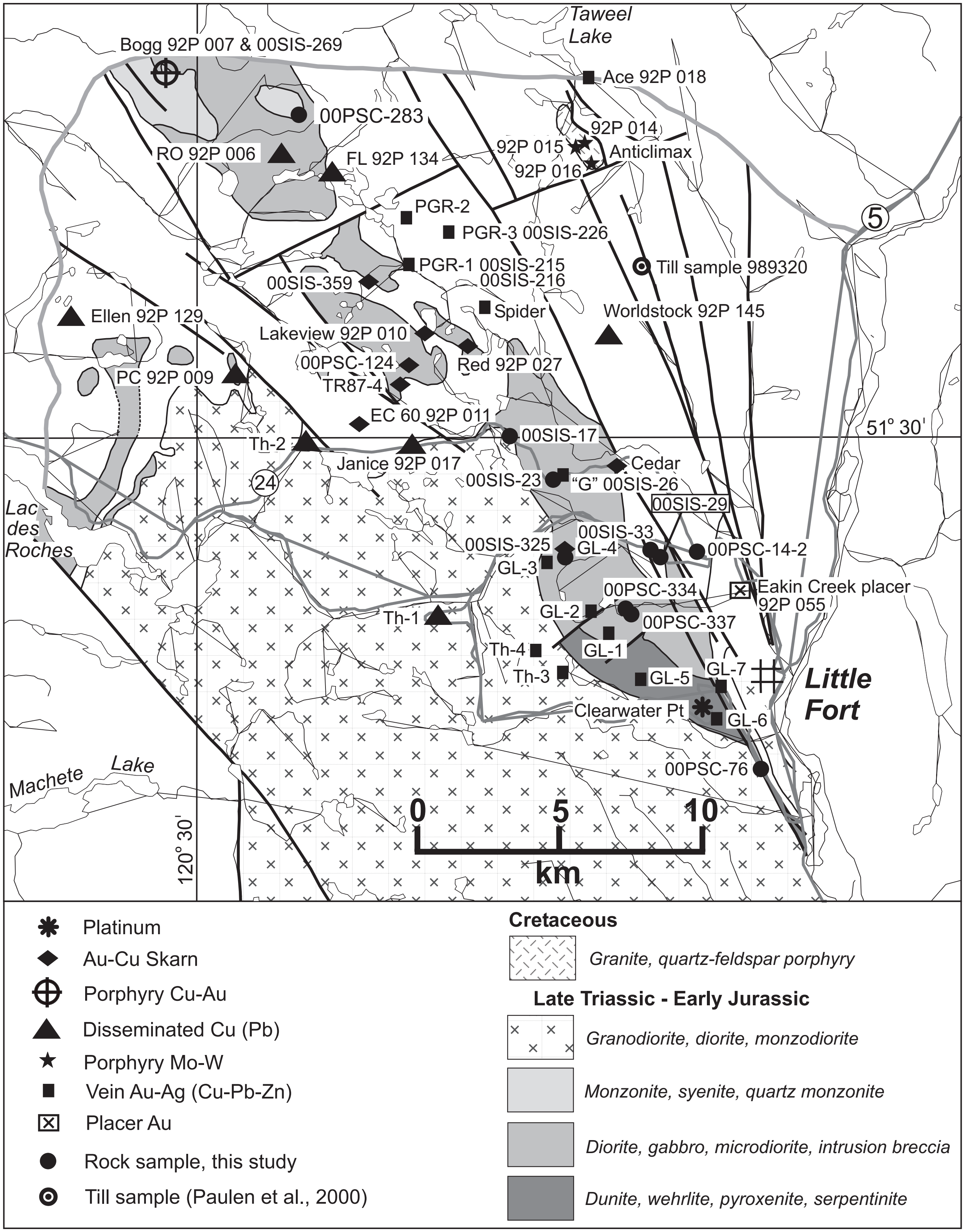

Figure 4. Locations of some of the precious and base metal mineral occurrences in the Nehalliston Plateau. Base map is derived from Figure 2, with only plutonic rocks and faults shown. The occurrences are discussed in the text.

Clearwater platinum prospect and occurrences associated with the Thuya Road fault are also on the Golden Loon claim group, but are discussed separately.

At GL-1, known as the “high grade zone”, a narrow quartz vein, dipping 50 degrees west and containing scattered pyrite, sphalerite, chalcopyrite and galena has been traced for about 50 metres (Dawson, 1977). Mineralized float continues along strike to the north, and a trench about 400 metres to the north exposes a quartz vein, 10 to 40 centimetres wide, which assayed up to 5.6 g/t Au and 75.6 g/t Ag. Drilling beneath the “high grade zone” in 1997 intersected a number of narrow quartz veins but gold grades were low (Dawson, 1997).

GL-2, known as the “low grade zone”, is described as a northwest-trending carbonate-silica-altered shear zone that is exposed along strike for about 150 metres (Dawson, 1997). A trench within the zone exposed more than 6 metres of pervasive silicification containing disseminated and fracture controlled specularite and pyrite. In a 1990 private report to Corona Corporation quoted by Dawson (1997), R.C. Wells and J.R. Bellamy state that “gold values in the 0.5 to 2.5 g/t range occur throughout the trench and average 1.17 g/t for all samples”. Gold values were also encountered in shallow drill holes bored beneath the “low grade zone”, with the best intersection being 2.67 g/t Au over 10.4 metres. About 100 metres along strike to the southeast of GL-2, a north-trending vein up to 70 centimetres wide contains up to 8.3 g/t Au and 66.7 g/t Ag. The wall rock, a bleached and silicified intrusive rock, returned values up to 2.0 g/t Au.

At GL-3 silicified diorite with quartz vein stockwork and 5 percent pyrite contained 736 ppb Au (sample 11941 of Wells and Metail, 1993). Approximately 1 kilometre to the northeast, at GL-4, strongly sheared fine-grained hornfels and skarn contain galena, sphalerite, pyrite and chalcopyrite in north-trending fractures. A sample of this mineralized material returned 476 ppm Cu, 544 ppm Pb, 8870 ppm Zn and 3195 ppm As (sample 11940 of Wells and Metail, 1993). In this same area, chlorite-epidote-altered gabbro locally contains disseminated pyrrhotite and chalcopyrite, with small splotches of malachite stain. A sample of this material (00SIS-325) returned 168 ppm Cu.

Skarn alteration was also observed within the Dum Lake intrusive complex over an 800 metre stretch along a deactivated logging road a short distance southeast of Dum Lake. There, a zone of strongly foliated microdiorite, grading to feldspar-epidote-chlorite schist, contains local lenses of pyrrhotite-pyrite skarn and silicified pyritic epidote-chlorite schist. One sample of silicified, pyritic schist (00PSC-334) returned 227 ppm Cu, 253 ppm Zn and 0.8 ppm Ag. Another (Sample 00PSC-337) returned 263 ppm Cu.

At GL-5, a 10 centimetre-wide quartz vein within the ultramafic portion of the Dum Lake intrusive complex returned .085 oz/T Au, 29.1 ppm Ag and 3764 ppm Pb (sample ZED 4 of Wells, 1988). Three kilometres to the southeast, a series of old trenches expose brecciated, silicified and chalcedony-veined ultramafic rock with sparse pyrite and galena. Wells (1988) reports that a sample of this mineralized material returned 270 ppb Au and 2.5 ppm Ag (location GL-6 on Figure 4).

THUYA ROAD FAULT

The Thuya Road fault was recognized during the early stages of exploration on the Golden Loon property, and malachite staining was reported along the Thuya Creek logging road where it follows the fault (Wells, 1988). In addition, there were a number of small quartz veins noted directly east of the fault, over a strike length of about 1.5 kilometres, which returned anomalous gold values. Location GL-7, at the north end of this zone, represents the best assay reported by Wells (1988, sample EDF 10); this pyrite-galena-chalcopyrite-mineralized vein returned 355 ppb Au, 25.3 ppm Ag, 26 ppm Cu and 2700 ppm Pb.

Several samples were collected from carbonate-silica-altered rock along the southern part of the Thuya Road fault during the 2000 field season, but none yielded significantly anomalous Au or Ag values. One sample (00PSC-76), however, returned 65 ppb Pt.

CLEARWATER PLATINUM

In the late summer of 1999, 150 rock samples collected from the ultramafic portion of the Dum Lake complex were analysed for platinum, paladium and gold (McDougall, 1999). Twenty of the samples were anomalous in Pt, including three which exceeded 100 ppb Pt. One of these, a football-sized sample of highly oxidized ultramafic material cut by thin chromite stringers, contained 13 798 ppb Pt, 25 ppb Pd and 23 ppb Au (McDougall, 1999, Sample 165509; this sample site shown as Clearwater Pt occurrence on Figure 4). A second highly anomalous sample was collected about 1 kilometre to the north. It comprised dark peridotite with chromite veins and yielded assays of 483 ppb Pt, 10 ppb Pd and 2 ppb Au. The property (Golden Loon claim group) was subsequently optioned, and an exploration program for platinum group elements, referred to as the Clearwater Platinum Project, was initiated in the summer of 2000. The results of this exploration program were not known at the time of writing this report.

CEDAR

The Cedar claims were staked in December and January of 1983 and 1984 to cover mineralization exposed in a roadcut on Highway 24. The roadcut exposes highly faulted and skarn-altered limestones and associated silicified sedimentary rocks, here asssigned to the Harper Ranch Group, enveloped by diorite, microdiorite and silicified greenstone of the Dum Lake intrusive complex. The highly faulted nature of the outcop reflects its location just 100 metres west of the inferred trace of the Rock Island Lake fault.

The most significant mineralization occurs near the eastern end of the outcrop, where two separate sulphide zones, each approximately 1 metre wide, occur within silicified microdiorite and greenstone. The two zones contain about 35 and 20 percent sulphides, respectively, comprising veins, lenses and disseminations of pyrite, pyrrhotite and chalcopyrite (Yorston and Ikona, 1985). A one metre sample across the most sulphide-rich zone contained 7328 ppm Cu, 4.5 ppm Ag and 580 ppb Au, and a sample of the same width across the other sulphide zone contained 6154 ppm Cu, 4.2 ppm Ag and 160 ppb Au. Yorston and Ikona also report that a sample of the best sulphide material available yielded 11 475 ppm Cu, 9.1 ppm Ag and 1460 ppb Au.

The altered limestone exposed in the Highway 24 roadcut locally contains narrow lenses of heavily disseminated pyrrhotite-pyrite, with traces of chalcopyprite and molybdenite (Dom, 1989), in association with garnetiferous skarn. The limestone can be traced northward to Nehalliston Creek and southward to Eakin Creek and is sparsely mineralized with chalcopyrite, and locally galena, in a few places within this belt (Yorston and Ikona, 1985). Associated diorite also locally contains disseminated pyrite with traces of chalcopyrite. On the Eakin Creek road, faulted, silicified and skarn-altered limestone correlated with this unit crops out near the eastern side of the belt of rocks mapped as Harper Ranch Group. It is bounded by a section of siltstones to the west, and by pyroxenite and gabbro of the Dum Lake intrusive complex to the east. A sample of silicified limestone with up to 5 percent disseminated pyrite from the western part of the limestone unit contained 501 ppm Cu and 0.5 ppm Ag (Sample 00SIS-33). A sample from a narrow shear zone containing pyrite, chalcopyrite and malachite near the eastern edge of the limestone unit contained 13 463 ppm Cu, 12.6 ppm Ag, 72 ppb Au, 13 ppb Pt and 62 ppb Pd (Sample 00SIS-29).

G OCCURRENCE

The G claims were staked in 1988 to cover an outcrop containing mineralized veins on Highway 24, 1.5 kilometres west of the Cedar occurrence. The outcrop, referred to as the Discovery Zone, includes variably oriented chlorite-calcite-quartz veins, 1 to 3 centimetres wide, within complexly veined and faulted diorite and gabbro of the Dum Lake intrusive complex. The veins are mineralized with pyrite and local traces of galena. They were explored for their precious metal content, and yielded assays of up to 3.15 g/t Au and 36.9 g/t Ag over 3.0 m (Dom, 1989). Along Nehalliston Creek, 500 metres to the northeast, a series of planar, moderately west-dipping quartz veins, averaging about 20 centimetres in width, cut microdiorite of the Dum Lake complex. These veins contain up to 2 percent pyrite and traces of galena. The best result out of a series of rock chip samples collected from these veins returned 450 ppb Au and 13.7 ppm Ag (Dom, 1989).

In 1991, investigation of soil geochemical anomalies for gold led to the discovery of abundant float of altered and mineralized intrusive rock extending for almost 1 kilometre south of the Discovery Zone. The float fragments commonly contain 3 to 5 percent disseminated pyrite and many are silicified and display breccia and stockwork textures (Gruenwald, 1992). Precious metal values range up to 0.121 oz/ton Au and 2.60 oz/ton Ag.

During the present study, a sample of pyritic rock from a narrow shear zone within the Discovery Zone outcrop yielded 82 ppm Mo, 29 ppm Cu, 3.3 ppm Ag and 845 ppb Au (sample 00SIS-26), whereas a sample of gabbro containing heavily disseminated pyrite from a separate outcrop along the highway, 400 metres to the west, contained 73 ppm Mo, 1488 ppm Cu, 1.2 ppm Ag, 90 ppb Au and 10 ppb Pt (sample 00SIS-23).

Skarn Occurrences near Deer Lake

Skarn mineralization in the Deer Lake area occurs where limestone of the Harper Ranch Group is cut by Triassic-Jurassic dioritic rocks. The most significant is the Lakeview (MINFILE 92P 010) Fe-Cu-Au skarn occurrence, located near the southwest corner of Deer Lake (Figure 4). The mineralization was discovered in 1930 (Nichols, 1931) and continues to receive considerable attention, in part because of its high gold content. The skarn-alteration and mineralization at the main Lakeview prospect is well exposed in a series of trenches, pits and small adits. The area contains very little natural bedrock exposure, but local outcrops and trenches indicate that similar alteration and mineralization occurs, at least locally, for several hundred metres to the south and north, defining a northerly-trending belt more than one kilometre long (Bruland, 1990).

At the Lakeview occurrence, garnet-pyroxene exoskarn and endoskarn is developed where dioritic dikes, presumably related to larger stocks mapped a short distance to the northeast and southwest, intrude limestone of Unit PHRl. Mineralization associated with the skarn includes massive to semi-massive lenses, pods and veins of magnetite or pyrrhotite, containing variable amounts of pyrite and chalcopyrite. Westerman (1987) reports high gold values in an old open cut above the main adit. The gold occurs within a silicified and pyritized skarn unit, 3.9 metres wide, located between two massive pyrrhotite units, each about one metre wide. He chip-sampled the entire 3.9 metre width of the silicified skarn zone and obtained an average value of 6.61 g/t Au. Chip samples of the bounding pyrrhotite skarn units returned assays of 2.84 g/t and 2.20 g/t Au, respectively, across one metre widths.

The Lakeview occurrence is bounded to the south by a large diorite stock. Limestone and skarn are also exposed at two locations along the southeastern margin of this stock. In one of these areas, Westerman (1987) reports that a pyritic zone between limestone and skarn near the diorite contact assayed 1.01 g/t Au across one metre (location TR87-4 on Figure 4). A zone of skarn-alteration within the diorite pluton, between the Lakeview occurrence and location TR87-4, was sampled during our 2000 mapping program and returned values of 871 ppm Cu and 199 ppb Au (sample 00PSC-124).

The Red (MINFILE 92P 027) occurrence is located within the eastern part of the diorite stock that bounds the Lakeview prospect to the northeast (Figure 4). According to Naylor and White (1972) it is marked by two old adits that cut magnetite-pyrrhotite-chalcopyrite mineralization within fractured and epidote-carbonate altered diorite. Bruland (1990) reports that samples of locally-derived pyrite-chalcopyrite altered dioritic float from near the south margin of the stock, directly south of the Red occurrence, returned assay values of up to 0.71 percent Cu.

Several kilometres northwest of the Lakeview prospect, thin-bedded, locally skarn-altered, sedimentary rocks of Unit PHRs are separated from the diorite stock to the northeast by a poorly-exposed lens of massive pyrrhotite-pyrite, with traces of chalcopyrite. A sample from this sulphide lens returned 872 ppm Cu and 14 ppb Au (sample 00SIS-359).

Gold Prospects North and East of Deer Lake

The PGR claim group, north of Deer Lake, includes a number of mineralized veins and alteration zones that have seen recent exploration directed mainly at their gold content. Three of the more prominent vein systems are shown on Figure 4 as locations PGR-1 throught PGR-3. Numerous other occurrences in the same area are shown on maps by Wells and Evans (1992) and Belik (1997).

The PGR-1 (Road zone) and PGR-2 (Zone A) occurrences are near the south and north ends, respectively, of an area containing several north-northwest trending quartz±carbonate vein systems and silicified stockwork/breccia zones cutting volcanic and sedimentary rocks of Unit uTrNsv (Belik, 1997). The vein systems are reported to have weak to moderately strong Au-Ag-Mo-Pb-Zn-Cu mineralization (Belik, 1997). Wells (2000) reports that assay samples from the road zone (PGR-1) returned up to 62.8 g/t Au, and that polymetallic veins at PGR-2 yielded values in the 1 to 5 g/t Au and 12 to 118 g/t Ag ranges. During the present study, a vuggy, pyritic quartz vein containing traces of chalcopyrite and malachite was sampled from the road zone (sample 00SIS-216) along with the silicified and pyritized wallrock (sample 00SIS-215) of uncertain protolith. The samples returned only moderately anomalous copper and silver values, but were very high in antimony and mercury (Table 1).

Location PGR-3 comprises a system of northerly-striking, polymetallic quartz-carbonate veins that contain up to 10 percent sulphides as blebs, stringers, disseminations and massive pods (Belik, 1997). The sulphide minerals include pyrite, galena, sphalerite, tetrahedrite and chalcopyrite. This vein system is referred to as the Silver Lake zone by Belik (1997), who states that the veins commonly return high silver values, but generally contain less gold than the vein and stockwork systems directly to the west. The veins occur mainly in sedimentary rocks of Unit uTrNsv, but cut volcanic rocks in the southern part of the system. A sample of silicified volcanic rock cut by quartz stockwork, and containing heavily disseminated pyrite with traces of chalcopyrite and malachite, was sampled during the present study (sample 00SIS-226). In addition to high base metal values, this sample returned 18.85 ppm Ag, 2434 ppm As and 1458 ppb Au.

The Spider occurrence, east of Deer Lake (Figure 4), comprises a northeast-trending zone of sulphide-bearing quartz-carbonate veins and stockwork that resembles some of the mineralization on the PGR claims to the north (Watt, 1999). Sulphide minerals include pyrite, chalcopyrite and galena.

Occurrences Associated with the Friendly Lake Intrusive Complex

The Bogg (MINFILE 92P 007) occurrence comprises porphyry-style copper mineralization within and along the northeast margin of the largest monzonite-syenite stock within the Friendly Lake intrusive complex (Figure 4). Disseminated and fracture-controlled pyrite, chalcopyrite and bornite occur within both the syenitic rocks and adjacent greenstone, microdiorite and intrusion breccia. Edwards (1991) reports that pyroxene-potassium feldspar-calcite veinlets, interpreted to have formed in the late stages of intrusion of the syenite body, locally contain chalcopyrite and galena. Disseminated and fracture-controlled pyrite-chalcopyrite mineralization also occurs farther west, within a steeply-dipping, northwest-striking quartz-carbonate altered fault zone that cuts through the southwestern part of the monzonite-syenite stock. This zone is up to 300 metres wide and comprises silicified fragments of syenite, microdiorite, greenstone and altered sedimentary rocks cut be several episodes of quartz and carbonate veins.

Sample 00SIS-269 is from pyrite-chalcopyrite-bornite-rich intrusion(?) breccia in the main mineralized area of the Bogg occurrence. It returned 33 754 ppm Cu, 25 ppm Ag and, of particular interest, 208 ppb Pt and 149 ppb Pd (Table 1).

The smaller monzonite stock within the eastern part of the Friendly Lake complex is not apparently mineralized. However, a narrow zone of heavily disseminated pyrite was noted at one place along the southeast margin of the stock, where microdiorite is cut by abundant veins of monzonite, orthoclase-amphibole and carbonate. A sample of the pyritic rock (00PSC-283) returned 693 ppb Au.

Mineralization at the RO occurrence (MINFILE 92P 006), north of Friendly Lake, comprises disseminated galena, pyrite and chalcopyrite in fine-grained andesitic rock (microdiorite?) that is stongly altered to bluish antigorite, pyroxene, chorite and calcite (Preto, 1970a). Similar mineralization and alteration occurs to the east, near the eastern margin of he Friendly Lake complex (Preto, 1970a), and to the northwest, between the two monzonite-syenite stocks (Gamble and Farmer, 1986).

The FL occurrence (MINFILE 92P 134) is located near the east end of Friendly Lake, along the eastern margin of the Friendly lake intrusive complex. The mineralization is hosted by brecciated and carbonate-sericite-chlorite altered biotite hornfels derived from a mafic volcanic protolith (Rebagliati, 1987). It comprises disseminated fine-grained pyrite, with trace amounts of chalcopyrite, galena, sphalerite, molybdenite and arsenopyrite, within the breccia fragments and, to a lesser extent, the matrix (Rebagliati, 1987).

Mineral Occurrences in the Southwestern Part of the Map Area

OCCURENCES IN THE THUYA BATHOLITH

Disseminated copper occurs locally within and along the margins of the Thuya Batholith. The eastern part of the batholith also hosts auriferous quartz veins on and near the Golden Loon claim group, which are similar to veins within the Dum Lake complex to the east.

Sparse occurrences of chalcopyrite within granodiorite and related rocks of the Thuya Batholith, between Eakin Creek and Thuya Lakes, are described by Preto (1970a), and were confirmed during our 2000 fieldwork (Location Th-1 on Figure 4). Preto also described disseminated pyrite and chalcopyrite in hornfels near the northern contact of the batholith, northwest of Long Island Lake (Location Th-2). The Janice occurrence (MINFILE 92P 017) comprises similar disseminated pyrite and chalcopyrite in silicified and hornfelsed sedimentary rocks on the margin of the batholith northeast of Long Island Lake.

On the Golden Loon property, at location Th-3 on Figure 4, a quartz vein containing galena and pyrite returned assay values of .088 oz/T Au, 23.2 ppm Ag, 85 ppm Cu and 495 ppm Pb (Wells, 1988). At location Th-4, 1400 metres to the northwest, silicified granodiorite is cut by numerous quartz veins, commonly with pyrite, chalcopyrite and galena, many of which yield anomalous gold values (Wells and Metail, 1993). The best assay reported from this area returned 2080 ppb Au, 27.4 ppm Ag, 1106 ppm Cu and 5628 ppm Pb (sample 3808 of Wells and Metail, 1993). On Highway 24, an outcrop of epidote-altered hornblende diorite along the northeast margin of the Thuya Batholith is cut by a narrow, mineralized quartz vein that dips gently to the west. A sample of mineralized vein material (00SIS-17), which contains pyrite and traces of chalcopyrite, returned 2.2 ppm Ag and 892 ppb Au.

EC 60 (92P 011)

The EC 60 occurrence is within calcareous shale, siltstone and chert of the Ripple Lake belt, about 800 metres north of Long Island Lake and the north contact of the Thuya Batholith (Figure 4). According to Preto (1970a) the mineralization comprises small sulphide lenses in a zone of skarny alteration 15 to 18 metres wide, that parallels bedding in the enclosing sedimentary rocks. Bedding dips steeply west to west-southwest, and is intruded by a 10-metre-wide sill of sericitized and weakly mineralized quartz-feldspar porphyry directly east of the mineralized zone. The sulphides include pyrrhotite, pyrite and galena, locally accompanied by minor amounts of chalcopyrite and sphalerite (Preto, 1970a; Bruland, 1990).

OCCURRENCES ASSOCIATED WITH DIORITE NORTHWEST OF THE THUYA BATHOLITH

At the PC (MINFILE 92P 009) and Ellen (MINFILE 92P 129) occurrences (Figure 4), minor amounts of disseminated chalcopyrite occur within dioritic plugs, dikes and sills, or within adjacent pyritic hornfels of Unit uTrNs (Preto, 1970a; Wares and MacDonald, 1972). Wares and MacDonald also report minor amounts of molybdenite within diorite at the Ellen occurrence.

Occurrences East of the Rock Island Lake Fault

ACE (MINFILE 92P 018)

The Ace occurrence is along upper Lemieux Creek, a little more than 100 m downstream from the outlet of Taweel Lake. The mineralization was briefly mentioned by Davis (1925, p. B152), who reported that a sample submitted by a local prospector assayed 0.04 ounces gold per ton, 2.05 ounces silver per ton, 0.2 percent copper and 20 percent lead. Subsequent work is not well documented, but included the sinking of a shallow shaft on the southwest bank of Lemieux Creek, some trenching and some diamond drilling. Most of this work occurred in the early to mid 1900s, although three shallow diamond drill holes were drilled in 1988 (Steiner, 1988).

The Ace prospect is hosted by metasedimentary rocks of Unit muTrNs. The mineralization at the old shaft along Lemieux Creek consists of lenses of massive pyrrhotite-pyrite-arsenopyrite with minor chalcopyrite. Individual sulphide lenses are up to several tens of centimetres wide, and are hosted in dark grey phyllite containing contorted layers and fragments of lighter grey siltite and fine-grained quartzose metasandstone. Jenks (1999) reports that massive sulphide lenses, including sphalerite, galena, chalcopyrite and pyrite, also occur in trenches located about 600 metres northeast of the Lemieux Creek shaft, where they are hosted by similar brecciated metasedimentary rocks. He states that both zones have a significant gold content.

ANTICLIMAX (MINFILE 92P 014, 015, 016)

The Anticlimax showing comprises molybdenum-tungsten mineralization within the Cretaceous granitic stock northeast of Tintlhohtan Lake. The mineralization was discovered in 1938, and since that time the property has been explored intermittently by several companies. The original workings were described by Stevenson (1940), and the results of subsequent exploration are summarized by McCammon (1962), Preto (1970b) and Kirkham and Sinclair (1988). The occurrence is currently listed in MINFILE as three separate showings, corresponding to three areas of mineralization described as “A”, “B”, and “C” by McCammon (1962), in the central, west-central and southern parts of the stock.

Stevenson (1940) reported that the highest grade molybdenum mineralization was in a gently-dipping lens, measuring about 2.5 metres in diameter and 65 centimetres wide, near the western margin of the stock (area “B” of McCammon, 1962). The lens (largely removed at the time of Stevenson’s inspection) comprised heavily disseminated molybdenite associated with patches of quartz-felspar pegmatite within aplite and quartz-feldspar porphyry. Elsewhere, mineralization typically occurs in narrow quartz veins containing variable amounts of pyrite, molybdenite, bismuthinite, pyrrhotite, wolframite and fluorite (Preto, 1970b). Although widespread, and within all phases of the stock, the known mineralization is sporadic and below economic grade.

As discussed previously, a biotite separate from unaltered granite of the Tintlhohtan Lake stock yielded a K-Ar date of 102±5 Ma. Soregaroli (1979) also dated sericite from an alteration envelope bordering a mineralized vein and obtained a date of 90.7±3.3 Ma, concluding that the alteration and associated molybdenum-tungsten mineralization was genetically related to the host stock. These dates suggest that the Tintlhohtan Lake stock is part of the mid-Cretaceous Bayonne suite of intrusions, which is widespread in southeastern British Columbia and currently the focus of a study to assess its potential for plutonic-related gold mineralization (Logan, 2000).

WORLDSTOCK (MINFILE 92P 145)

The Worldstock showing comprises an isolated outcrop of iron carbonate-chlorite-pyrite-silica-altered rock with traces of chalcopyrite. It was discovered in 1997, in a landing along a logging road, and returned 0.78 % copper over a 4 metre by 3 metre panel sample (Wells, 2000). The showing is located along or near the contact between pyroxene porphyry and volcanic breccia of Unit uTrNv and overlying conglomerate of Unit uTrNsv, although the actual protolith to the altered rock is uncertain. A pyrite-silica-altered rock exposed about 800 metres to the NW, however, appears to have been derived from a feldspar-phyric intrusive rock, consistent with the suggestion that the Worldstock showing may represent part of a porphyry system (Wells, 2000). A sample collected from the altered intrusive rock during the present study did not yield anomalous base or precious metal values.

TILL GEOCHEMICAL ANOMALY SOUTHEAST OF TINTLHOHTAN LAKE

The BCGS till geochemistry program described by Paulen *et al*. (2000) yielded several interesting anomalies within the Nehalliston plateau map area. One of these (sample 989320) is a multi-element anomaly for zinc, copper, cadmium, molybdenum, nickel, cobalt and antimony in an area of poor bedrock exposure about 4 kilometres southeast of Tintlhohtan Lake. This anomalous sample is within a linear, north-northwest trending belt of till and soil geochemical anomalies that local prospectors traced for more than 10 kilometres in 1998 and 1999 (Figure 4; Mike Cathro, personal communication, 2000). The detailed geochemical exploration in this belt has yielded highly anomalous values for zinc, cadmium, copper, antimony, arsenic, barium and mercury. The linear anomaly appears to be along or near the contact between volcanic rocks of Unit uTrNv and overlying sedimentary rocks at the base of Unit uTrNsv, althouth the contact is locally marked by faults of the Rock Island Lake system. This geological setting suggests the possiblility of either an Eskay Creek-style VMS occurrence or a younger epithermal environment localized along the Rock Island Lake fault system. The area was further explored in the summer of 2000, but the results of this program were not known at the time of writing this report.

MINERALIZED QUARTZ VEIN ALONG HIGHWAY 24

A ribboned quartz vein exposed along Highway 24 about 5 km NNW of Little Fort contains selvages of chlorite and rusty carbonate, and local malachite and azurite together with tiny grains of chalcopyrite and a grey sulphide of uncertain composition. The vein cuts a microdiorite sill that intrudes fine-grained sedimentary rocks of Unit uTrNsv. It is 1 metre wide, dips about 60 degrees to the west and was traced for 10 metres. A sample of mineralized vein material (00PSC-14-2) yielded 1826 ppm Cu, 569 ppm Pb, 15 ppm Ag and 704 ppb Au. Similar quartz veins occur elsewhere in the outcrop, but are not visibly mineralized.

EAKIN CREEK PLACER (MINFILE 92P 055)

Placer gold was recovered from gravels in the lower reaches of Eakin Creek (referred to as Threemile Creek in early reports) periodically from the early 1920s through the early 1930s (Uglow, 1922; Nichols, 1926, 1932). There are no records as to the amount of gold recovered, but Nichols (1932) reports that some of the gold was quite coarse, and good nuggets were obtained locally from the gravel/bedrock interface. Uglow suggested that the placer gold might have been derived from a resistant conglomerate unit within the Chu Chua Formation, which formed a gorge directly above the original workings. Nichols (1926) did not consider such a local source probable, pointing to the fact that placer gold had subsequently been found above the gorge cutting through the conglomerate. As shown on Figure 4, numerous small gold occurrences are now known from within and around the drainage basin of Eakin Creek.

SUMMARY OF MAIN CONCLUSIONS

Mesozoic volcanic and sedimentary rocks underlying the Nehalliston Plateau were subdivided into Triassic and Jurassic units by Campbell and Tipper (1971), but are here considered to be almost entirely Upper Triassic and part of the Nicola Group. Within the map area, the Nicola Group occurs in three fault-bounded belts of contrasting lithology which are thought to be at least partially coeval. The central belt consists mainly of volcanic rocks, and is flanked by entirely sedimentary rocks to the east, and by sedimentary and local volcanic rocks to the west. Paleozoic limestone and associated argillite and siltstone of the Harper Ranch Group underlie Triassic volcanic rocks of the central belt and are more widespread than previously thought.

A prominent belt of ultramafic - mafic - syenitic plutonic rocks, only partially shown on previous maps, extends northwestward from the northeast margin of the Thuya batholith. These rocks intrude the central, predominantly volcanic belt of the Nicola Group, as well as underlying Paleozoic rocks of the Harper Ranch Group. It is suspected that they are slightly older than the Thuya batholith and approximately coeval with the associated Nicola Group volcanic rocks. This northwest-trending plutonic belt apparently defines a prominent axis of magmatism within the Nicola arc.

Base and precious metal mineral occurrences are concentrated within and adjacent to the belt of ultamafic - mafic - syenitic plutons that defines the western part of the central Nicola belt. Some of these, such as platinum mineralization within ultramafic rocks of the Dum Lake complex, skarn occurrences adjacent to Deer Lake and Dum Lake dioritic bodies, and porphyry-style copper in the Friendly Lake complex, are broadly coeval with the plutons. Others, such as numerous vein and shear-related gold showings, although concentrated in this belt, may in part be considerably younger.

A limited amount of data suggests that a period of uplift and erosion affected the Nicola volcanic belt and associated alkalic intrusions prior to the deposition of Lower Jurassic sedimentary rocks. The Monticoa Lake - Gammarus Lake fault system, which defines the southwest boundary of the Nicola volcanic belt, may have a history of movement dating back to this time. The 2001 field season will encompass Jurassic rocks that may allow this idea to be more fully evaluated.

The structure of the Nehalliston Plateau is dominated by systems of mainly northwest-striking Eocene faults. Some faults in the western part of the area show southwest-side-down normal displacement, but a prominent system of dextral strike-slip faults, referred to as the Rock Island Lake fault system, dominates the structure in the eastern part of the area. The latter faults may be part of a significant dextral strike-slip system that has not been well documented in this part of the cordillera.

ACKNOWLEDGMENTS

We are indebted to Vic Preto, formerly of the Geological Survey Branch, for sharing his insights into the geology of the region and providing us with data collected during his 1970 fieldwork in the area. We also thank Mike Cathro of the Kamloops regional office for touring us through some of the geology and mineralization in the area, and Dave Lefebure, who visited us in the field and shared his knowledge of Nicola Group stratigraphy and related volcanic processes. We are grateful to Gerry Ray and Ian Webster for explaining some aspects of skarn mineralization during a visit to the Lakeview occurrence. Thanks are also extended to Shawn Ling, along with his family and staff at Peaceful Cove Resort, for their hospitality during fieldwork. Dave Lefebure reviewed an earlier version of the manuscript and suggested improvements. We thank Janet Holland for formatting the final version of the manuscript.

REFERENCES

Armstrong, J.E. (1949): Fort St. James map-area, Cassiar and Coast districts, British Columbia; *Geological Survey of Canada*, Memoir 252, 210 pages.

Belik, G.D. (1997): Drilling report on the PGR claim group; *British Columbia Ministry of Energy and Mines*, Assessment Report 24 827, 28 pages.

Bloodgood, M.A. (1990): Geology of the Eureka Peak and Spanish Lake map areas, British Columbia; *British Columbia Ministry of Energy, Mines and Petroleum Resources*, Paper 1990-3, 36 pages.

Brown, R.L., Journeay, J.M., Lane, L.S., Murphy, D.C. and Rees, C.J. (1986): Obduction, backfolding and piggyback thrusting in the metamorphic hinterland of the southeastern Canadian Cordillera; *Journal of Structural Geology*, Volume 8, pages 255-268.

Bruland, T. (1990): Assessment report of the 1989 and 1990 geological geophysical and geochemical programs on the Haida property; *British Columbia Ministry of Energy, Mines and Petroleum Resources*, Assessment Report 20 014, 27 pages.

Calderwood, A.R., van der Heyden, P. and Armstrong, R.L. (1990): Geochronometry of the Thuya, Takomkane, Raft and Baldy batholiths, south-central British Columbia; *Geological Association of Canada - Mineralogical Association of Canada*, Annual Meeting, Vancouver. B.C., Program with Abstracts, Volume 15, page A19.

Campbell, K.V. (1971): Metamorphic petrology and structural geology of the Crooked Lake area, Cariboo Mountains, British Columbia; unpublished Ph.D. thesis, *The University of Washington*, 192 pages.

Campbell, R.B. and Tipper, H.W. (1971): Bonaparte Lake map area, British Columbia; *Geological Survey of Canada*, Memoir 363, 100 pages.

Cockfield, W.E. (1948): Geology and mineral deposits of Nicola map area, British Columbia; *Geological Survey of Canada*, Memoir 249, 164 pages.

Colpron, M. and Price, R.A. (1995): Tectonic significance of the Kootenay terrane, southeastern Canadian Cordillera: An alternative model; *Geology*, Volume 23, pages 25-28.

Colpron, M., Price, R.A., Archibald, D.A. and Carmichael, D.M. (1996): Middle Jurassic exhumation along the western flank of the Selkirk fan structure: Thermobarometric and thermochronometric constraints from the Illecillewaet synclinorium, southeastern British Columbia; *Geological Society of America,* Bulletin, Volume 108, pages 1372-1392.

Danner, W.R. and Orchard, M.J. (2000): Paleontology of the Cache Creek and Quesnellia terranes, southwestern British Columbia; *in* Guidebook for geological field trips in southwestern British Columbia and northern Washington, edited by G.J. Woodsworth, L.E. Jackson, Jr., J.L. Nelson and B.C. Ward, published by the Cordilleran Section, *Geological Association of Canada*, for the Geological Society of America, Cordilleran Section 2000 Annual Meeting, Vancouver, B.C., pages 117-173.

Davis, A.W. (1925): Central Mineral Survey District (No. 3); *in* Annual Report of the Minister of Mines for 1924, *British Columbia Bureau of Mines*, pages B134-B158.

Dawson, G.M. (1879): Preliminary report on the physical and geological features of the southern portion of the interior of British Columbia; *in* Report of Progress, 1877-1878, Part B, *Geological Survey of Canada*, pages 1B-187B.

Dawson, G.M. (1896): Report on the area of the Kamloops map-sheet, British Columbia; in Annual Report (new series), Volume V11, 1894, Geological Survey of Canada, pages 1B-427B.

Dawson, J.M. (1997): Diamond drilling report on the Golden Loon property; *British Columbia Ministry of Energy and Mines*, Assessment Report 25431, 10 pages.

Dom, K. (1989): 1988 assessment report on the G claims; *British Columbia Ministry of Energy, Mines and Petroleum Resources*, Assessment Report 18 597, 26 pages.

Duffell, S. and McTaggart, K.C. (1952): Ashcroft map area, British Columbia; *Geological Survey of Canada*, Memoir 262, 122 pages.

Edwards, K. (1991): Geochemical and geological assessment report for the Bogg 1-4, 7-20, CC 1-8, Wind 3*; British Columbia Ministry of Energy, Mines and Petroleum Resources*, Assessment Report 21 776, 23 pages.

Enns, S.G. (1980): Anticlimax Property; *British Columbia Ministry of Energy, Mines and Petroleum Resources*, Assessment Report 8492, 8 pages.

Erdmer, P., Thompson, R.I. and Daughtry, K.L. (1999): Pericratonic Paleozoic succession in Vernon and Ashcroft map areas, British Columbia; *in* Current Research 1999-A, *Geological Survey of Canada*, pages 205-213.

Ewing, T.E. (1980): Paleogene tectonic evolution of the Pacific Northwest; *Journal of Geology*, Volume 88, pages 619-638.

Ferri, F. (1997): Nina Creek Group and Lay Range Assemblage, north-central British Columbia: Remnants of late Paleozoic oceanic and arc terranes; *Canadian Journal of Earth Sciences*, Volume 34, pages 854-874.

Fyles, J.T. (1964): Geology of the Duncan Lake area, Lardeau District, British Columbia; *British Columbia Ministry of Energy, Mines and Petroleum Resources*, Bulletin 49, 87 pages.

Fyles, J.T. and Eastwood, G.E.P. (1962): Geology of the Ferguson area, Lardeau District, British Columbia; *British Columbia Ministry of Energy, Mines and Petroleum Resources*, Bulletin 45, 92 pages.

Gamble, A.P.D. and Farmer, R. (1986): 1985 summary exploration report: Geological surey, soil and lithogeochemical surveys, induced polarization geophysical survey and trenching on the Ta Hoola project; *British Columbia Ministry of Energy, Mines and Petroleum Resources,* Assessment Report 15 221, 76 pages.

Ghent, E.D., Erdmer, P., Archibald, D.A. and Stout, M.Z. (1996): Pressure - temperature and tectonic evolution of Triassic lawsonite - aragonite blueschists from Pinchi Lake, British Columbia; *Canadian Journal of Earth Sciences,* Volume 33, pages 800-810.

Gruenwald, W. (1992): Geochemical, geophysical and geological report on the "G" claims; *British Columbia Ministry of Energy, Mines and Petroleum Resources*, Assessment Report 22 183, 21 pages.

Paterson, I.A. and Harakal, J.E. (1974): Potassium-argon dating of blueschists from Pinchi Lake, central British Columbia; *Canadian Journal of Earth Sciences*, Volume 11, pages 1007-1011.

Holland, S.S. (1976): Landforms of British Columbia, a physiographic outline; *British Columbia Department of Mines and Petroleum Resources*, Bulletin 48, 138 pages.

Hoy, T. and Dunne, K.P.E. (1997): Early Jurassic Rossland Group, southern British Columbia: Part I - stratigraphy and tectonics, *British Columbia Ministry of Employment and Investment*, Bulletin 102, 123 pages.

Jenks, J. (1999): Assessment Report, Geological Mapping and Prospecting, Lem 1-3 Mineral Claims; *B.C. Ministry of Energy and Mines*, Assessment Report 25 939, 16 pages.

Jones, A.G. (1959): Vernon map area, British Columbia; *Geological Survey of Canada*, Memoir 296, 186 pages.

Jung, A. (1986): Geochronometry and geochemistry of the Thuya, Takomkane, Raft and Baldy batholiths, west of the Shuswap metamorphic complex, south-central British Columbia; unpublished B.Sc. thesis, *The University of British Columbia*, 140 pages.

Kirkham, R.V. and Sinclair, W.D. (1988): Comb quartz layers in felsic intrusions and their relationship to porphyry deposits; *in* Recent Advances in the geology of granite-related mineral deposits, edited by R.P. Taylor and D.F. Strong, *The Canadian Institute of Mining and Metallurgy*, Special Volume 39, pages 50-71.

Klepacki, D.W. and Wheeler, J.O. (1985): Stratigraphic and structural relations of the Milford, Kaslo and Slocan groups, Goat Range, Lardeau and Nelson map areas, British Columbia; *in* Report of Activities, Part A, *Geological Survey of Canada*, Paper 85-1A, pages 277-286.

Lefebure, D.V. (1976): Geology of the Nicola Group in the Fairweather Hills, British Columbia; unpublished M.Sc. thesis, *Queens's University*, 179 pages.

Logan, J.M. (2000): Plutonic-related gold-quartz veins in southern British Columbia; *in* Geological Fieldwork 1999, *British Columbia Ministry of Energy and Mines*, Paper 2000-1, pages 193-206.

McCammon, J.W. (1962): Tintlhohtan Lake (Calder Molybdenum Company Limited); in Annual Report of the Minister of Mines and Petroleum Resources for 1961, *British Columbia Ministry of Mines and Petroleum Resources*, pages 49-51.

McDougall, J.J. (1999): Geochemical report (bedrock sampling) on Golden Loon I, Golden Loon II, Golden Loon III and Golden Loon VIII of the Golden Loon Group mineral claims; *British Columbia Ministry of Energy and Mines*, Assessment Report 26 100, 17 pages.

Monger, J.W.H. (1977): Upper Paleozoic rocks of the Canadian Cordillera and their bearing on cordilleran evolution; *Canadian Journal of Earth Sciences*, Volume 14, pages 1832-1859.

Monger, J.W.H., Price, R.A., and Tempelman-Kluit, D.J. (1982): Tectonic accretion and the origin of the two major metamorphic and plutonic welts in the Canadian Cordillera; *Geology*, Volume 10, pages 70-75.

Monger, J.W.H. and Berg, H.C. (1984): Part B: Lithotectonic terrane map of western Canada and southeastern Alaska; *in* Lithotectonic terrane maps of the North American cordillera, edited by N.J. Silberling and D.L. Jones, *United States Geological Survey*, Open-file Report 84-523.

Monger, J.W.H. and McMillan, W.J. (1989): Geology, Ashcroft, British Columbia (92I); G*eological Survey of Canada*, Map 42-1989, sheet 1, scale 1:250 000.

Monger, J.W.H., Wheeler, J.O., Tipper, H.W., Gabrielse, H., Harms, T., Struik, L.C., Campbell, R.B., Dodds, C.J., Gehrels, G.E. and O'Brien, J. (1991): Part B. Cordilleran Terranes, in Upper Devonian to Middle Jurassic assemblages, Chapter 8 of Geology of the Cordilleran Orogen in Canada, edited by H. Gabrielse and C.J. Yorath, *Geological Survey of Canada*, Geology of Canada, No. 4, pages 281-327.

Mortimer, N. (1987): The Nicola Group: Late Triassic and Early Jurassic subduction-related volcanism in British Columbia; *Canadian Journal of Earth Sciences,* Volume 24, pages 2521-2536.

Naylor, H. and White, L.G. (1972): Geological and geophysical report, Deer Lake area; *British Columbia Ministry of Energy, Mines and Petroleum Resources*, Assessment Report 3945, 9 pages.

Nelson, J.L. and Bellefontaine, K.A. (1996): The geology and mineral deposits of north-central Quesnellia; Tezzeron Lake to Discovery Creek, central British Columbia; *British Columbia Ministry of Employment and Investment*, Bulletin 99, 112 pages.

Nichols, H.G. (1926): Central Mineral Survey District (No. 3); *in* Annual Report of the Minister of Mines for 1925, *British Columbia Bureau of Mines*, pages A163-A189.

Nichols, H.G. (1931): Central Mineral Survey District (No. 3); *in* Annual Report of the Minister of Mines for 1930, *British Columbia Bureau of Mines*, pages A179-A208.

Nichols, H.G. (1932): Central Mineral Survey District (No. 3); *in* Annual Report of the Minister of Mines for 1931, *British Columbia Bureau of Mines*, pages A102-A116.

Okulitch, A.V. (1979): Lithology, stratigraphy, structure and mineral occurrences of the Thompson-Shuswap-Okanagan area, British Columbia; *Geological Survey of Canada*, Open File 637.

Okulitch, A.V. and Cameron, B.E.B. (1976): Stratigraphic revisions of the Nicola, Cache Creek, and Mount Ida groups, based on conodont collections from the western margin of the Shuswap metamorphic complex, south-central British Columbia; *Canadian Journal Earth Sciences*, Volume 13, pages 44-53.

Panteleyev, A., Bailey, D.G., Bloodgood, M.A. and Hancock, K.D. (1996): Geology and mineral deposits of the Quesnel River - Horsefly map area, central Quesnel Trough, British Columbia; *British Columbia Ministry of Employment and Investment*, Bulletin 97, 155 pages.

Paterson, I.A. and Harakal, J.E. (1974): Potassium-argon dating of blueschists from Pinchi Lake, central British Columbia; *Canadian Journal of Earth Sciences*, Volume 11, pages 1007-1011.

Paulen, R.C., Bobrowsky, P.T., Lett, R.E., Jackaman, W., Bichler, A.J. and Wingerter, C. (2000): Till geochemistry of the Chu Chua - Clearwater area, B.C. (parts of NTS 92P/8 and 92P/9); *British Columbia Ministry of Energy and Mines*, Open File 2000-17, 233 pages.

Preto, V.A.G. (1970a): Geology of the area between Eakin Creek and Windy Mountain; *in* Geology, Exploration and Mining in British Columbia, *British Columbia Department of Mines and Petroleum Resources*, pages 307-312.

Preto, V.A.G. (1970b): Anticlimax (Mo); *in* Geology, Exploration and Mining in British Columbia, *British Columbia Department of Mines and Petroleum Resources*, pages 304-307.

Preto, V.A. (1977); The Nicola Group: Mesozoic volcanism related to rifting in southern British Columbia; *in* Volcanic regimes in Canada, edited by W.R.A. Baragar, L.C. Coleman and J.M. Hall, *The Geological Association of Canada*, Special Paper 16, pages 39-57.

Preto, V.A. (1979): Geology of the Nicola Group between Merritt and Princeton; *British Columbia Ministry of Energy, Mines and Petroleum Resources*, Bulletin 69, 90 pages.

Price, R.A. (1979): Intracontinental ductile crustal spreading linking the Fraser River and Northern Rocky Mountain Trench transform fault zones, south-central British Columbia and northeast Washington; *Geological Society of America*, Abstracts with Programs, Volume 11, page 499.

Read, P.B. and Okulitch, A.V. (1977): The Triassic unconformity of south-central British Columbia; *Canadian Journal of Earth Sciences*, Volume 14, pages 606-638.

Read, P.B. and Wheeler, J.O. (1976): Geology, Lardeau west half, British Columbia; *Geological Survey of Canada*, Open File 432.

Rebagliati, C.M. (1987): Ta Hoola property assessment report; *British Columbia Ministry of Energy, Mines and Petroleum Resources*, Assessment Report 16 462, 13 pages.

Rees, C.J. (1987): The Intermontane-Omineca belt boundary in the Quesnel Lake area, east-central British Columbia: tectonic implications based on geology, structure and paleomagnetism; unpublished Ph.D. thesis, *Carleton University*, 421 pages.

Rice, H.M.A. (1947): Geology and mineral deposits of the Princeton map-area, British Columbia; *Geological Survey of Canada*, Memoir 243, 136 pages.

Roback, R.C., Sevigny, J.H. and Walker, N.W. (1994): Tectonic setting of the Slide Mountain terrane, southern British Columbia; *Tectonics*, Volume 13, pages 1242-1258.

Roback, R.C. and Walker, N.W. (1995): Provenance, detrital zircon U-Pb geochronometry, and tectonic significance of Permian to Lower Triassic sandstone in southeastern Quenellia, British Columbia and Washington; *Geological Society of America*, Bulletin, Volume 107, pages 665-675.

Schau, M.P. (1970): Stratigraphy and structure of the type area of the Upper Triassic Nicola Group in south-central British Columbia; *in* Structure of the southern Canadian Cordillera, edited by J.O. Wheeler, The Geological Association of Canada, Special Paper 6, pages 123-135.

Schiarizza, P. (1983): Geology of the Barriere River-Clearwater area; *British Columbia Ministry of Energy, Mines and Petroleum Resources*, Preliminary Map 53.

Schiarizza, P. (1989): Structural and stratigraphic relationships between the Fennell Formation and Eagle Bay Assemblage, western Omineca Belt, south-central British Columbia: Implications for Paleozoic tectonics along the paleocontinental margin of western North America; unpublished M.Sc. thesis, *University of Calgary*, 343 pages.

Schiarizza, P. and Preto, V.A. (1987): Geology of the Adams Plateau-Clearwater-Vavenby area; *British Columbia Ministry of Energy, Mines and Petroleum Resources*, Paper 1987-2, 88 pages.

Smith, R.B. (1979): Geology of the Harper Ranch Group (Carboniferous-Permian) and Nicola Group (Upper Triassic) northeast of Kamloops, British Columbia; unpublished M.Sc. thesis, *The University of British Columbia*, 211 pages.

Smith, M.T. and Gehrels, G.E. (1992): Structural geology of the Lardeau Group near Trout Lake, British Columbia: Implications for the structural evolution of the Kootenay Arc; *Canadian Journal of Earth Sciences*, Volume 29, pages 1305-1319.

Smith, M.T., Dickinson, W.R., and Gehrels, G.E. (1993): Contractional nature of Devonian-Mississippian Antler tectonism along the North American continental margin; *Geology*, Volume 21, pages 21-24.

Soregaroli, A.E. (1979): K-Ar radiometric dates, Anticlimax molybdenum prospect; *in* Age determinations and geological studies, K-Ar isotopic ages, Report 14, by R.K. Wanless, R.D. Stevens, G.R. Lachance and R.N. Delabio, *Geological Survey of Canada*, Paper 79-2, page 17.

Stevenson, J.S. (1940): Molybdenum deposits of British Columbia; *British Columbia Department of Mines*, Bulletin 9, 96 pages.

Struik, L.C. (1988): Regional imbrication within Quesnel Terrane, central British Columbia, as suggested by conodont ages; *Canadian Journal of Earth Sciences*, Volume 25, pages 1608-1617.

Struik, L.C. (1993): Intersecting intracontinental Tertiary transform fault systems in the North American Cordillera; *Canadian Journal of Earth Sciences*, Volume 30, pages 1262-1274.

Travers, W.B. (1977): Overturned Nicola and Ashcroft strata and their relations to the Cache Creek Group, southwestern

Intermontane Belt, British Columbia; *Canadian Journal of Earth Sciences*, Volume 15, pages 99-116.

Uglow, W.L. (1922): Geology of the North Thompson Valley map area, British Columbia; *in* Summary Report, 1921, Part A, *Geological Survey of Canada*, pages 72A-106A.

Walker, J.F. (1931): Clearwater River and Foghorn Creek map-area, Kamloops District, British Columbia; *in* Summary Report, 1930, Part A, *Geological Survey of Canada*, pages 125A-153A.

Wares, R. and MacDonald, A.L.J. (1972): Geological, geochemical and geophysical report on the Ellen-Gizelle claims, 92P/10E; *British Columbia Department of Mines and Petroleum Resources*, Assessment Report 4365, 21 pages.

Watt, P.S. (1999): Prospecting and geological report on the Spider claim group; *British Columbia Ministry of Energy and Mines*, Assessment Report 25 894, 17 pages.

Wells, R.C. (1988): Geochemical report on the Golden Loon claim group; *British Columbia Ministry of Energy, Mines and Petroleum Resources*, Assessment Report 17 342, 20 pages.

Wells, R.C. (2000): Soil geochemical and prospecting report for the Worldstock copper-gold target; *British Columbia Ministry of Energy and Mines*, Assessment Report 26 180.

Wells, R.C. and Evans, G.W. (1992): Geological and prospecting report on the PGR claim group; *British Columbia Ministry of Energy, Mines and Petroleum Resources*, Assessment Report 22 180, 36 pages.

Wells, R.C. and Metail, J-F (1993): Geological and geochemical assessment report for the Golden Loon claim group; *British Columbia Ministry of Energy, Mines and Petroleum Resources*, Assessment Report 22 818, 16 pages.

Westerman, C.J. (1987): Geological, geochemical and geophysical report on the Haida gold property; *British Columbia Ministry of Energy, Mines and Petroleum Resources*, Assessment Report 16 223, 23 pages.

Wheeler, J.O. and McFeely, P. (1991): Tectonic Assemblage map of the Canadian cordillera and adjacent parts of the United States of America; *Geological Survey of Canada*, Map 1712A, 1:2 000 000-scale.

Whiteaker, R.J. (1996): The geology, geochronology and mineralization of the Ann property: An Early Jurassic alkalic porphyry system near Lac La Hache, B.C.; unpublished B.Sc. thesis, *The University of British Columbia*, 65 pages.

Yorston, R. and Ikona, C.K. (1985): Geological Report on the Cedar I to VI mineral claims; *British Columbia Ministry of Energy, Mines and Petroleum Resourcess*, Assessment Report 13 519, 10 pages.

Geological Setting of the Frank Creek Massive Sulphide Occurrence near Cariboo Lake, East-Central British Columbia (93A/11, 14)

By Filippo Ferri

KEYWORDS: Volcanogenic massive sulphide (VMS), besshi, Snowshoe Group, Barkerville Subterrane, Cariboo Subterrane, Kootenay Terrane, Keithley, Harveys Ridge, Agnes conglomerate, Goose Peak quartzite, Downey, Frank Creek volcanics, geochemistry, Frank Creek, Ace, Big Gulp, Sellers North.

INTRODUCTION

The recent discoveries of the Frank Creek and Ace showings within the Snowshoe Group of the Cariboo Lake area has underlined the potential for these rocks to host volcanogenic massive sulphide (VMS) mineral occurrences. This should not have been a surprise considering that the Snowshoe Group represents the northern continuation of the Kootenay Terrane which, to the south, hosts important sedex and VMS occurrences in rocks of Cambrian and Devonian age. These include the Spar, Mosquito King and Homestake occurrences of the Eagle Bay Assemblage and the Goldstream deposit found within rocks of the Lardeau Group.

Except for the Downey succession, the dearth of volcanic rocks shown on existing maps of the Snowshoe Group has resulted in this area being little considered for hosting VMS occurrences. A cursory description of the metavolcanics in the Frank Creek area was produced by Martin (1989); however the presence of these volcanics is not widely known and their compositional and tectonic significance is not understood. In addition, Höy and Ferri (1998) proposed, based on correlation with lithologies in the southern Kootenay Terrane, that Snowshoe stratigraphy as defined by Struik (1986, 1988), may in part be inverted implying different ages (and mineral potential) for the various units.

In 2000 the B.C. Geological Survey Branch initiated a new mapping program which would provide: 1) a better understanding of the geological setting of the Frank Creek and Ace mineral occurrences; 2) information on the regional extent, nature and significance of metavolcanic rocks at the Frank Creek showing; 3) evaluation of the nature and significance of metavolcanic rocks within the Downey succession and 4) test a model suggesting the inversion of Snowshoe stratigraphy.

The following article summarizes preliminary results of this mapping program. Although mapping commenced in the Frank Creek area, detailed mapping only reached the alpine areas of Mount Barker during the summer of 2000 and no mapping was carried out in the immediate vicinity of the Ace property. Therefore the subsequent summary deals primarily with the geological setting of the Frank Creek showing.

A total of 60 days were spent in the field from the middle of June to the end of August. A base was set up in Likely, which represents the nearest community to the Frank Creek area that contains basic services. This small centre is reached by paved road from a turn-off some 20 kilometres south of Williams Lake on Highway 97 (Figure 1). Logging roads extend from Likely westward and cover a large portion of the southern, northern and western parts of the sub-alpine regions of the map area.

The project area lies within the Goose Range of the Quesnel Highlands and is bounded to the north by the Little River, the west by Cariboo Lake and River, the south by Sellers Creek and to the east by Grain and Barker Creeks (Figure 1). The Goose Range is located south of the Snowshoe Plateau, across the Cariboo River valley. These mountains represent the first high peaks as one leaves the interior plateau and before entering the rugged Cariboo Mountains to the east. Relief is moderate with peaks reaching 2100 metres and alpine occurring at approximately 1700 metres.

In light of the economic significance of the Wells - Barkerville area, the region immediately north of the present map area has been examined by many workers over the years (*see* Struik, 1988 for a listing). Mapping within the present project area has been carried out on a regional scale by Campbell (1978) and at a more detailed level by Struik (1983a, b; 1988). Panteleyev *et al*. (1996) examined Quesnel Terrane rocks to the west and also gives a good account of regional geology. Rees (1987), as part of a Ph.D. dissertation, examined in considerable detail the boundary between the Quesnel and Barkerville terranes between Cariboo Lake and Mount Brew.

The present study is linked to the Ancient Pacific Margin NATMAP program and is part of a multi- disciplinary effort by the B.C. Geological Survey Branch within the region. Ray *et al*. (2001) and Dunne *et al.* (2001) are conducting a detailed examination of gold mineralization at the newly discovered Bonanza Ledge zone in the Wells area. Bichler and Bobrowsky (2001) have carried out a till orientation survey in the vicinity of the Ace property and a regional till survey around the Lottie massive sulphide showing northwest of Wells.

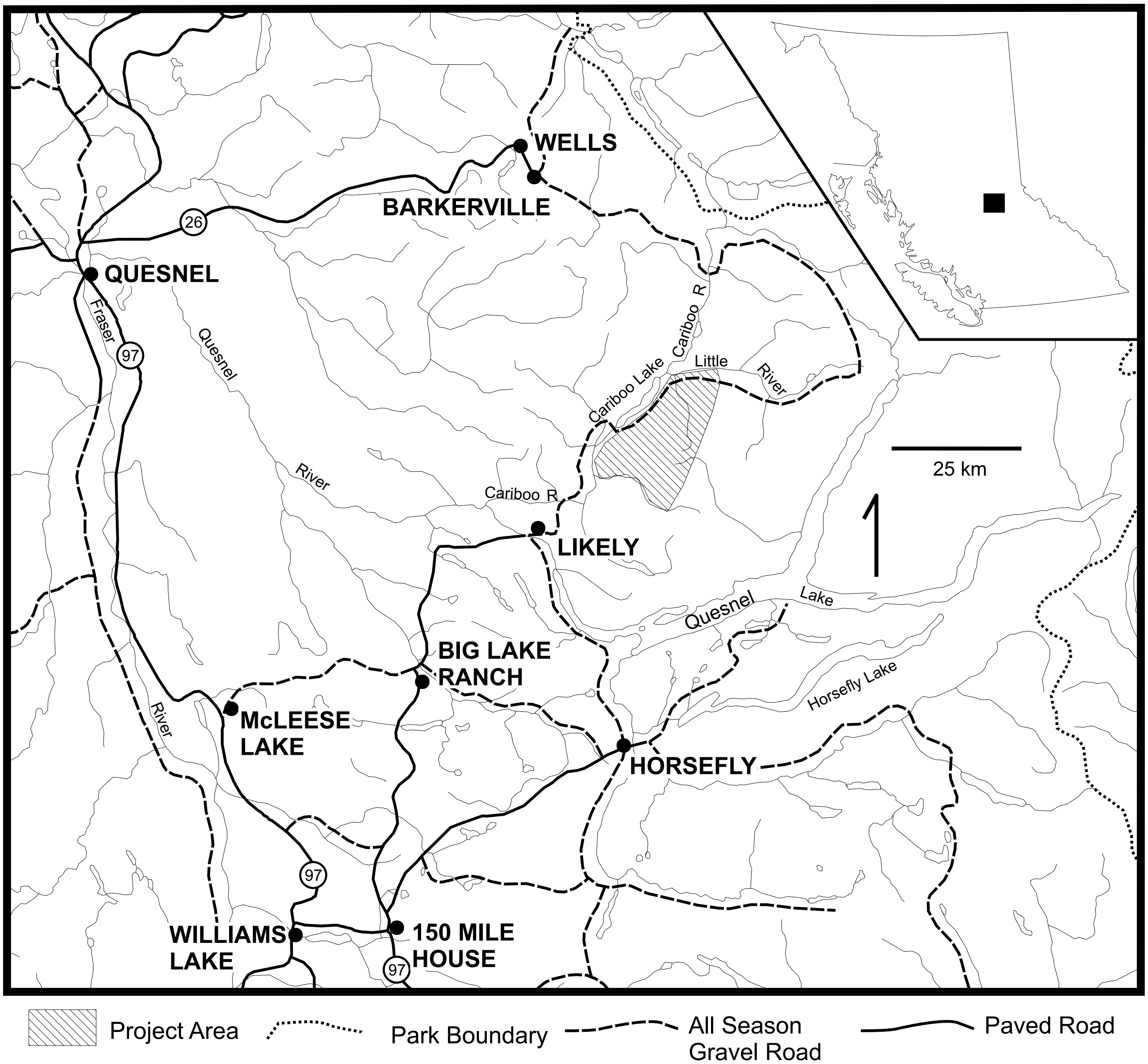

Figure 1. Location diagram centered on the map area showing main access routes and drainages.

REGIONAL SETTING

The Late Proterozoic to Paleozoic Snowshoe Group is a dominantly siliciclastic package of continental derivation and most likely represents the distal western edge of Ancestral North America. This fault-bounded sequence is stratigraphically distinct from other packages around it and as such has been called the Barkerville Subterrane, a subset of the Kootenay Terrane, with which it shares many similarities (Struik, 1986, 1988). To the east of the Snowshoe Group, across the westerly-verging Pleasant Valley Thrust, are rocks of the Kaza, Cariboo and Black Stuart groups which also contain an abundance of siliciclastics, but with facies that suggest a more proximal continental shelf setting. Many of these units can be correlated with similar stratigraphy within Ancestral North American rocks. These rocks are placed within the Cariboo Subterrane, representing, like the Cassiar Terrane to which it belongs, a displaced piece of Ancestral North America (Struik, 1986, 1988). The west flank of the Snowshoe Group is occupied by the Quesnel Terrane, a composite volcanic-arc sequence dominated by Mesozoic mafic to intermediate volcanic rocks. It is separated from the Snowshoe Group by the easterly-directed Eureka thrust fault along which are found slivers of mafic and ultramafic rocks assigned to the Crooked Amphibolite. These latter rocks have been correlated with rocks of the Slide Mountain Terrane, a package of ocean floor volcanics and sediments which structurally straddle the Barkerville and Cariboo terrane lithologies along the Pundata Thrust north of Wells (Figure 2).

Although the Snowshoe Group has an overall stratigraphic sequence which is distinct from that of the Cariboo Subterrane, there are similarities between the two, particularly with rocks of the Cariboo Group (Figure 3). This resulted in early workers taking stratigraphic terminology developed within the Snowshoe Plateau and extending it eastward into rocks of Cariboo Mountains (see Struik, 1988). This led to stratigraphic problems and it was not until Campbell *et al*. (1973) realized that the two sequences were quite distinct, requiring redefinition and new type sections. As a result Struik (1988) formally reassigned rocks within the Snowshoe Plateau to the Snowshoe Group.

The present structural interleaving of the various terranes and dominant structural fabrics resulted from deformation which began in early Middle Jurassic time, although there may be earlier events of Permo-Triassic or Devono-Mississippian age. The latter is supported by the presence of the Early Mississippian Quesnel Lake Gneiss, possibly related to arc volcanism (Ferri *et al.*, 1999). This deformation resulted from the easterly thrusting of Quesnel and Slide Mountain terrane rocks on to the Snowshoe Group along Eureka and Pundata thrusts. There are three sets of cross-cutting structural features within the map area with metamorphism reaching amphibolite grade during the second period of deformation.

The Snowshoe Group has been subdivided into several informal units or successions by Struik (1988; Figure 3). It is dominated by siliciclastic rocks with lesser carbonate and volcanic sequences. Due to the penetrative fabric, together with lack of suitable lithologies for geochronology and preservation of fossils, there are few age constraints for this package. Regional correlations and scant trace fossils indicate a Late Proterozoic to Late Paleozoic age (Figure 3). The lower to middle Snowshoe Group is broadly correlative with the Kaza and lower to middle Cariboo Group (Figure 3, Struik, 1986). The coarse clastics of the Goose Peak quartzite, in conjunction with the volcanics of the Downey and inferred Late Paleozoic age for the Bralco Limestone have no direct correlatives within rocks of the Cariboo Subterrane. This would be resolved, in part, if the Bralco Limestone correlates with the Mural Formation, a suggestion indirectly inferred by Struik (1988) who correlates the Bralco with the Archaeocyathid-bearing Tshinakin limestone of the Eagle Bay Formation (Schiarizza and Preto, 1987) implying it is age equivalent to the Mural Formation.

STRATIGRAPHY

Mapping this past summer encountered units from the middle part of the Snowshoe Group and include rocks of the Keithley, Harveys Ridge, and possibly Downey successions together with the Goose Peak quartzite and Agnes conglomerate. Marble along the north side of Sellers Creek may be part of the Kee Khan marble although it is presently assigned to the Keithley succession. These rocks are intruded by several bodies of the Early Mississippian Quesnel Lake Gneiss and post-deformation mafic dikes or plugs. Geologically, the southern part of the map area is structurally bounded by mafic to ultramafic rocks of the Crooked Amphibolite and dark grey phyllites and siltstones of Late Triassic age which belong to the basal Nicola Group (as per Panteleyev *et al*., 1996) and have been informally termed the "Black Phyllite" (Rees, 1987).

The light coloured, relatively thin, orthoquartzite at the top of the Keithley succession serves as an excellent marker within the map area and facilitated in the delineation of major fold structures shown in Figure 5. Although poorly exposed in sub-alpine areas, this unit can be used in conjunction with the contrasting lithologies of the Keithley schists and sandstones, and dark phyllites and sandstones of the Harveys Ridge, to establish overall map patterns.

Late Mafic Intrusions

Numerous small mafic intrusions are present within Snowshoe Group lithologies. They are typically less than 10 metres in size and it is commonly difficult to ascertain if they are dikes or small plugs. These are undeformed, compositionally quite variable and are typically porphyritic containing up to 30 per cent hornblende and feldspar phenocrysts, although others are accompanied by biotite and pyroxene. One intrusive body south of Goose Peak is noteworthy in that it contains rounded xenoliths of granite, gneiss and sediments up to 30 centimetres in size.

Quesnel Lake Gneiss

Several deformed granitic bodies of Early Mississippian age are found within the map area and are collectively termed the Quesnel Lake Gneiss (see Ferri *et al*., 1999). These large sill-like bodies have been subdivided into a megacrystic, peraluminous western suite and metaluminous eastern suite. Only the Western Quesnel Lake Gneiss was encountered within the current map area. The unit invariably displays a strong flattening fabric and lineation, the latter amplified by the alignment of potassium feldspar megacrysts. Although the extreme flattening displayed by many outcrops of this unit leads to the use of the term "orthogneiss" in its description, some outcrops exhibit less deformation and should be simply described as deformed granite.

Lithologically, the Quesnel Lake Gneiss is characterized by megacrysts of potassium feldspar from 1 to over 5 centimetres in length, which can comprise up to 30 per cent of the rock. These are commonly broken parallel to lineation with fractures healed by quartz. Quartz can form recrystallized masses up to 0.5 centimetre in diameter, although these are typically flattened and can form "ribbons" several centimetres long. These porphyroclasts are set in a coarsely crystalline matrix composed of quartz, plagioclase, potassic feldspar, muscovite, biotite

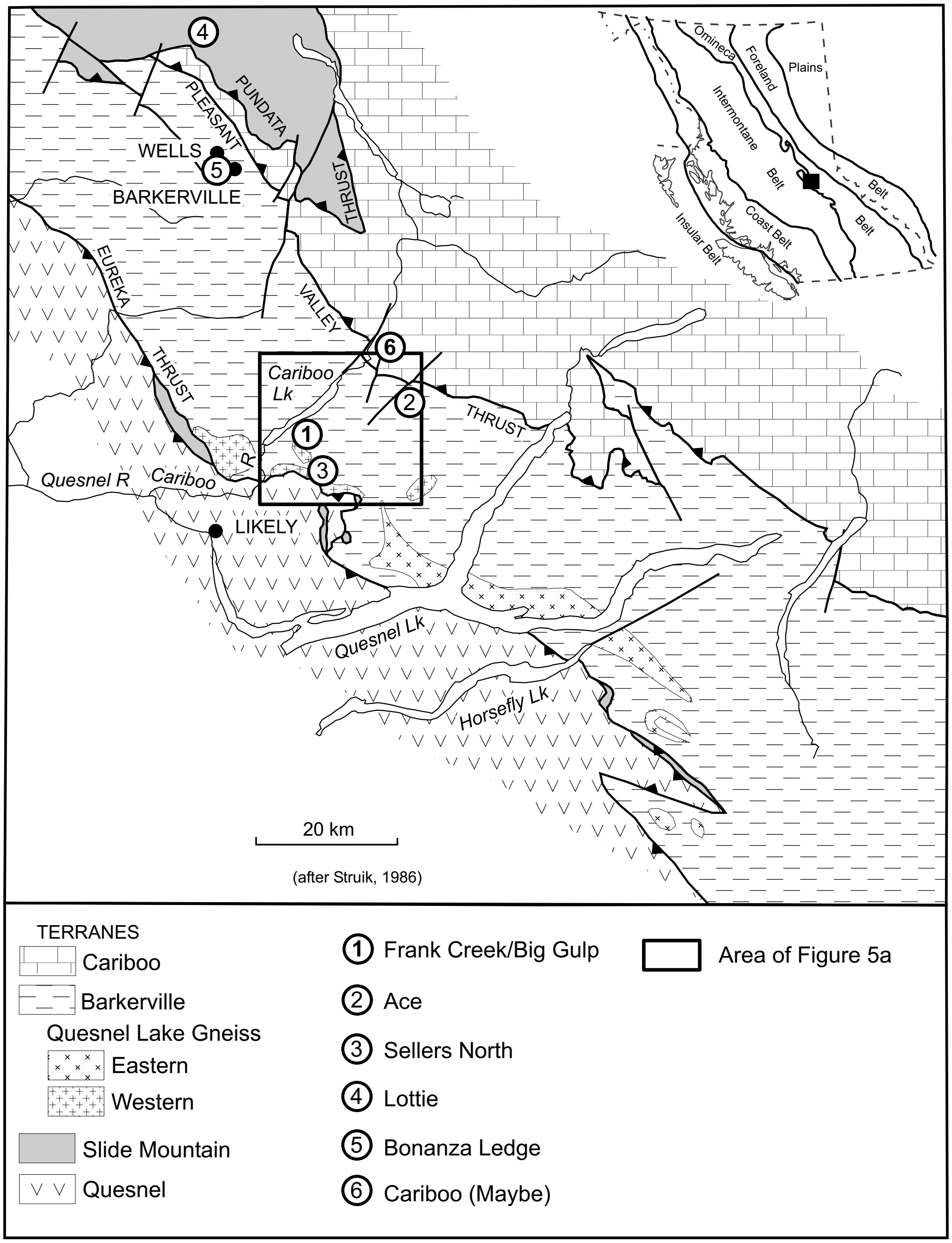

Figure 2. General geology in the vicinity of the project area showing the major geologic elements and selected mineral occurrences.

(chloritized) and locally garnet. Feldspar is typically altered to muscovite.

The contact of the Quesnel Lake Gneiss with the Snowshoe Group is exposed along a logging road-cut southeast of Browntop Mountain where it intrudes a package of interlayered schist and marble. A small finger of the Quesnel Lake Gneiss is mapped at this locality and it appears that the body intruded along bedding supporting the interpretation that they are sills.

The significance of the Quesnel Lake Gneiss has been the subject of much debate. Ferri *et al.*, (1999) suggests these bodies are related to Late Devonian to Early Mississippian arc volcanism whereas others (Montgomery and Ross, 1989) propose that the alkaline geochemistry found within parts of the Eastern Quesnel Lake Gneiss may imply intrusion in an extensional regime.

Black Phyllite

The Black phyllite unit was only encountered along the north slopes of Sellers Creek. Where seen, it consists of rusty-weathering dark grey to blue grey or silvery

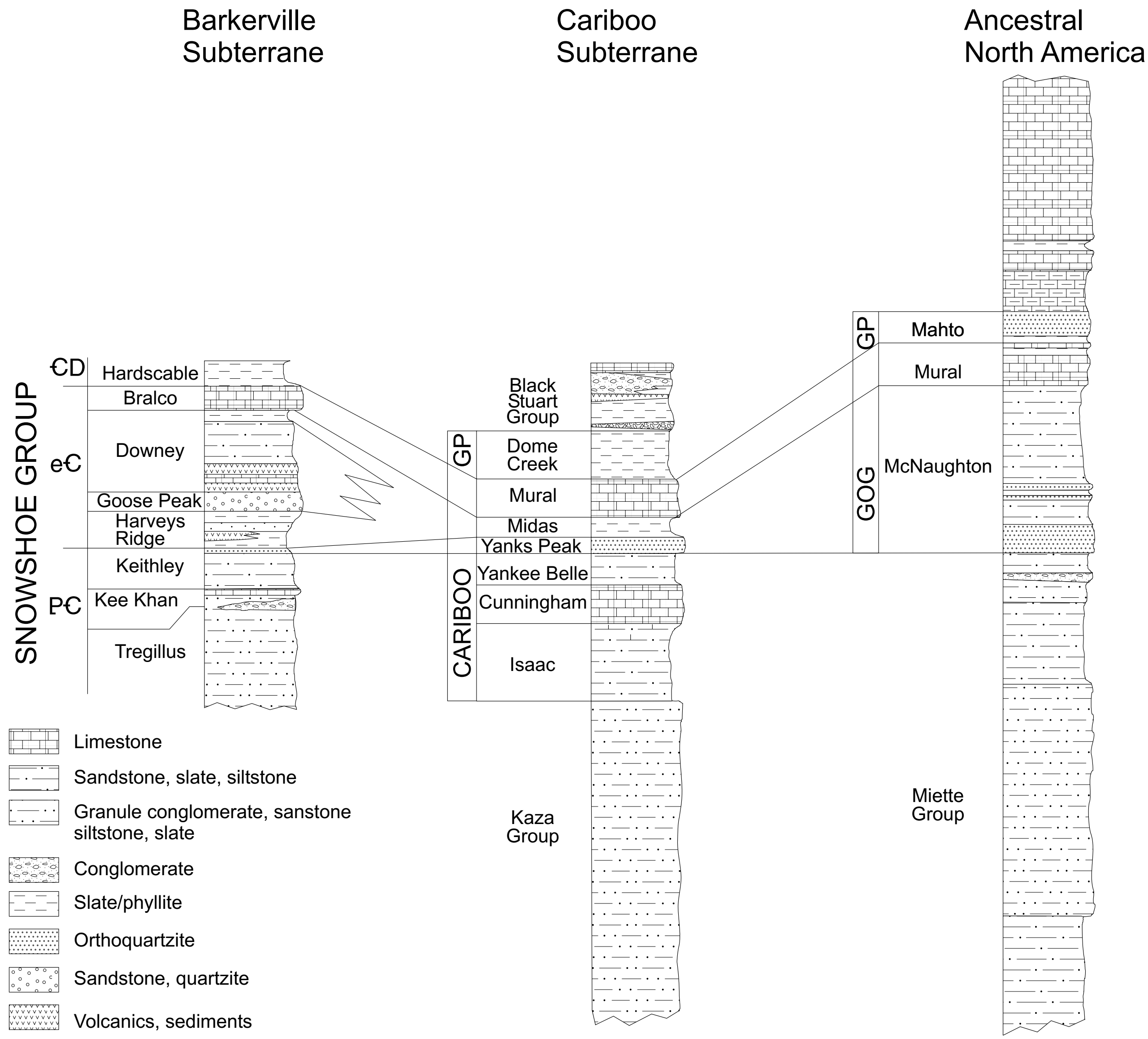

Figure 3. Generalized stratigraphic columns of the Barkerville and Cariboo subterranes and Ancestral North American rocks showing possible correlations of Snowshoe Group stratigraphy [modified from Struik (1986)].

phyllite. It contains thin horizons or bands of siltstone and may have argillaceous partings. Some of the siltstone beds are up to 5 centimetres thick and locally grade into very fine-grained sandstone. It is usually quite friable in comparison to the denser and more indurated Harveys Ridge phyllites and siltstones, and commonly displays a crenulation cleavage near its contact with the Snowshoe Group.

These rocks are believed to be Late Triassic in age (see Panteleyev *et al*., 1996) and form basement to the Nicola arc to the west. Western exposures of the Black phyllite contain sections of mafic tuffaceous sediments which interfinger with volcanic rocks typical of the Nicola Group (Panteleyev *et al., ibid.*)

Crooked Amphibolite

Outcrops of Crooked amphibolite are found south of Browntop Mountain and Badger Peak. These commonly consist of chlorite schist and amphibolite (actinolite) which display a strong fabric. Talc schist, with large porphyroblasts of iron-carbonate, are present in a few localities and is commonly associated with serpentinite.

The Crooked amphibolite is a thin, mafic to ultramafic unit which is intermittently found at the contact between the basal Nicola and Snowshoe groups. Its chemistry suggests ocean floor affinities (Rees, 1987; Figure 6) and it can be traced periodically southwards into the Black Riders Complex, a klippe of oceanic lithosphere (Radloff, 1989), and further south into rocks of the Fennell Formation, all of which infers it is correlative with the Late Paleozoic Slide Mountain Terrane.

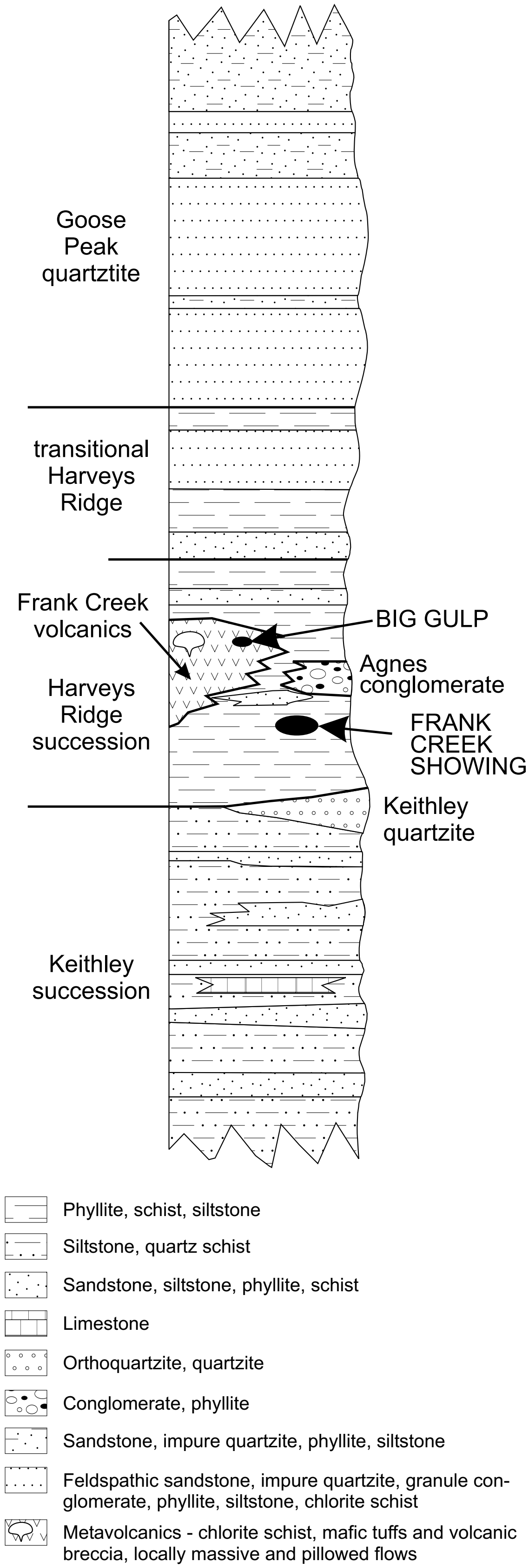

Figure 4. Generalized stratigraphic column of main rock units found within the map area.

Snowshoe Group

KEITHLEY SUCCESSION

The bulk of the Keithley succession consists of thin to medium bedded and interlayered light green to grey micaceous quartz sandstone to siltstone and green to grey phyllite to schist. These rocks are also characterized by being brown to rusty brown weathering, probably a reflection of the abundant pyrite porphyroblasts found throughout most exposures. This unit is commonly capped by a quartzite to orthoquartzite. Sandstone can be beige to white in places, up to 30 centimetres thick and approaching a quartzite in composition. Grading is present locally and white, chalky feldspar can constitute several per cent of the thicker sandstone beds. Thin interlayers of brown-weathering grey limestone were also seen in the Sellers Creek area. The thickness of the unit is difficult to determine as the base was not seen and it is only poorly exposed along the low ground west of Browntop Mountain. Struik (1988) states that the unit is less than 300 metres in thickness.

Orthoquartzite at the top of the Keithley succession is quite distinct within the map area. It is usually light coloured, being white, cream, beige, pink or purplish and when pure forms massive outcrops in which bedding is not discernible. Commonly there are micaceous partings between thin to thick quartzite beds and the quartzite can be impure with several per cent mica and white feldspar grains. It is typically less than 10 metres in thickness, although massive outcrops in excess of 100 metres are found in the valley north of Browntop Mountain which may represent thickening in the core of second phase folds. This horizon can be traced to the southeast where the unit is only several metres thick in the saddle. Although the unit is typically found at the very top of the Keithley, there are areas, such as near Browntop Mountain, where orthoquartzite occurs up to 10 metres below the transition into dark Harveys Ridge lithologies. Locally (*e.g.* north of Mount Borland and west of Browntop Mountain) the orthoquartzite is not present. Typically, if one crosses into Harveys Ridge lithologies without initially finding the quartzite, a few moments of searching will usually uncover thin to thick lenses of light coloured orthoquartzite. These lenses probably resulted from tectonic thinning of the quartzite along the limbs of second phase folds.

The upper contact of the orthoquartzite with siltstones and phyllites of the Harveys Ridge is quite abrupt and it is not possible to discern if it is conformable. Where the orthoquartzite is missing, greenish phyllites or schists and sandstones of the Keithley grade abruptly into dark lithologies of the Harveys Ridge suggesting a conformable contact.

Southwest of Browntop Mountain, along a logging road cut, is a section of rusty-weathering chloritic schists, green micaceous sandstones, beige to white quartzite and beige to brown weathering, grey to white banded marble. These are intruded along the western part of the exposure by the Quesnel Lake Gneiss. The marble is found in two

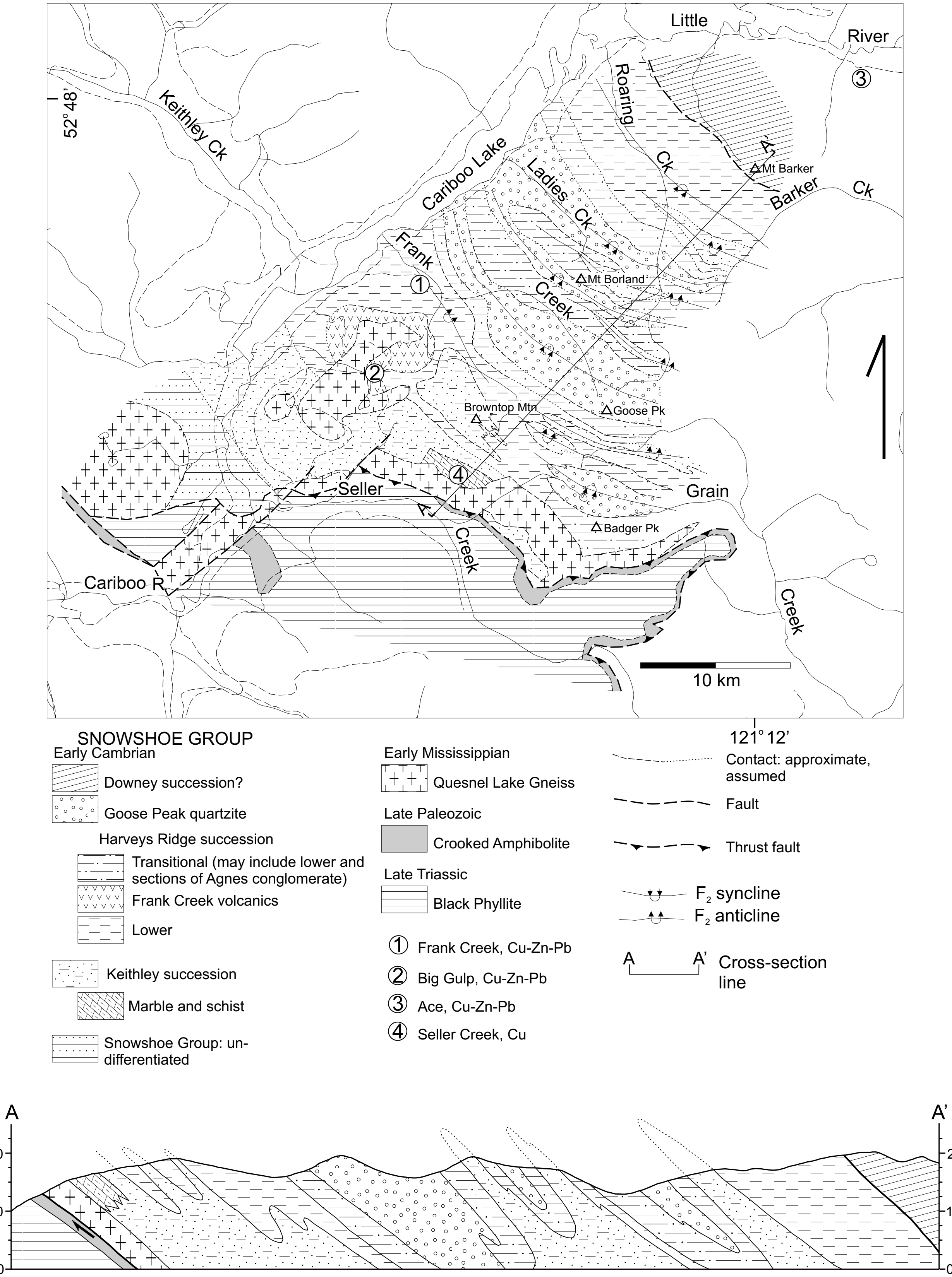

(a)

(b)

Figure 5. (a) Simplified geologic map of the project area. Geology of the southwestern boundary from Struik (1983a). (b) Structural cross-section across the map area. Location is shown in Figure 5a.

sections, both 50 to 75 metres thick. They are interpreted as different horizons since second phase vergence structures suggests they are on the same overturned fold structure. The overall aspect of the schists are similar to those of the Keithley succession. They are quite chloritic in places and suggest a volcanic origin. The quartzite is notable as it contains disseminations of chalcopyrite, sphalerite and galena.

HARVEYS RIDGE SUCCESSION

The Harveys Ridge succession is characterized by grey to dark grey or black phyllite, schist, siltstone, sandstone to impure quartzite and mafic volcanics. Dark grey to black phyllite and siltstone predominate and are found near the base of the unit. Pyrite porphyroblasts can be an important constituent, comprising up to 15 per cent of the unit and leading to a rusty to brown-weathering surface. These sections are monotonous and commonly lack discernible bedding. Phyllite and schist are characterized by millimetre-thin, discontinuous layers of white siltstone to fine sandstone which constitute less than 30 per cent of the rock. Dark grey to black siltstone along the ridge west of Browntop Mountain is pure and massive, essentially composed of fine grained, dark grey to black vitreous quartz. Thin to thick interbeds of blocky to platy dark grey to grey sandstone is seen up section in several localities and is characterized by floating grains of dark to black, vitreous quartz. Isolated outcrops of these coarser lithologies can sometimes be confused with those of the Keithley succession. Generally, coarser grained sections of Harveys Ridge lithologies tend to be planar bedded and are darker in colour than those of the Keithley succession.

The upper contact of the Harveys Ridge is gradational with both the Agnes conglomerate and Goose Peak quartzite. Matrix to much of the Agnes conglomerate is a black to dark grey phyllite or siltstone like the Harveys Ridge. As well, sections of phyllite and siltstone of the Harveys Ridge contain sections of Agnes conglomerate in the upper parts.

The top of the Harveys Ridge succession is characterized by an influx of coarse grained feldspathic sandstones very and wackes similar to those of the Goose Peak quartzite (Photo 1). These beds are thin to thickly bedded and comprise less than 50 per cent of the section. They commonly display a darker colour than typical Goose Peak lithologies and together with the abundance of darker Harveys Ridge rock types, these sections have an overall darker appearance on weathered surfaces than sections of the Goose Peak quartzite or Keithley succession. The contact with the Goose Peak quartzite is placed at the first thick section of clean, feldspathic quartz sandstone to quartzite. Grey to beige feldspathic and micaceous sandstone, like that of the Goose Peak or the transitional unit, is found near the Frank Creek massive sulphide showing.

The thickness of the Harveys Ridge unit is quite variable. It is over 500 metres in the Frank Creek area and in excess of 1000 metres south of Mount Barker, in the core of a second phase fold. Along the alpine ridges north of Badger Peak it can be less than a few hundred metres in thickness. In some areas, such as near Mount Borland, the basal dark grey to black phyllite and siltstone unit is not developed and one only sees the upper transitional sandstone/siltstone sequence.

In the Frank Creek area, dark phyllites of the Harveys Ridge interfinger with mafic volcanics here informally referred to as the Frank Creek volcanics. These metavolcanics cover an area of some 5 to 6 square kilometres and are intruded by a northeast-trending prong of Quesnel Lake Gneiss. They are typically well foliated, chlorite-actinolite schists and typically have no primary depositional features preserved. Two varieties are discernible in the field: 1) a more siliceous, lighter green to green package within which layered tuffs or lapilli tuffs and volcanic breccia are sometimes preserved (Photo 2) and 2) a darker green, chloritic schist which locally contains pillowed to massive porphyritic volcanics (Photo 3). The latter are poorly represented and are well exposed along the high ground between the Big Gulp and Frank

Photo 1. Transitional Harveys Ridge succession. This is in the core of an F_2 fold. Lighter coloured quartz and feldspathic quartz sandstones, similar to those of the Goose Peak quartzite, can be seen interfingered with dark grey to grey siltstones, wackes, sandstones and phyllites of the Harveys Ridge suc-

Photo 2. Fragmental volcanics within the Frank Creek volcanics. These volcanics are more siliceous than the pillows shown in Photo 3 and may reflect an original intermediate or basaltic-andesite composition.

Photo 3. Pillowed mafic (basalt) volcanics of the Frank Creek volcanics, located approximately 1.25 kilometres southwest of the Frank Creek massive sulphide showing. The chemical signature of these volcanics suggests an alkaline affinity.

Creek showings and display alkaline basalt compositions. Phenocrysts are altered and consist of 5 to 10 per cent pseudomorphs of actinolite, after pyroxene, up to 1 centimetre in size, and 5 to 10 per cent sericitized carbonatized laths of feldspar. The more siliceous varieties are more widespread and range into andesitic compositions with possible calc-alkaline affinities. Abundant iron-carbonate porphyroblasts and a light green mica (mariposite?) are locally present within the metavolcanics.

South of Badger Peak is a section of chlorite schist, mafic gneiss and meta-gabbro within rocks tentatively assigned to the upper transitional unit of the Harveys Ridge succession. Rees (1987) assigned these meta-volcanics to the Crooked Amphibolite. They form two distinct packages in the Badger Peak area and are separated by sediments of the Snowshoe Group. Placing these volcanics with the Crooked amphibolite would require imbrication and/or folding of the basal thrust carrying the Crooked Amphibolite prior to second phase deformation. The presence of quartz clastics within sections of chlorite schist, together with geochemical analysis, suggests that these meta-volcanics are probably part of the Snowshoe stratigraphic sequence.

Badger Peak metavolcanics consist of nondescript crenulated chlorite-actinolite-clinozoisite-feldspar ± carbonate schists and contain a strong fabric. Sections are differentiated into mafic and felsic-rich bands and appear gneissic. Schist and sandstone up to 100 metres in thickness separate two horizons of meta-volcanics.

AGNES CONGLOMERATE

Rocks which have been mapped as the Agnes conglomerate by Struik (1988, 1983a) are found north and south of the lower part of Frank Creek and along the main logging road south of Cariboo Lake (Struik (1983) originally called these rocks the Pine Creek conglomerate). This unit occurs in the upper part of the Harveys Ridge succession, within a section that is transitional into the Goose Peak Quartzite. Regional mapping by Struik (1988) has shown that this unit is probably a lateral equivalent of the Goose Peak quartzite. The mapping here supports this in that it places the conglomerate within the upper transitional unit of the Harveys Ridge which contains lithologies found within the Goose Peak quartzite.

The occurrence of the Agnes conglomerate is quite restricted within the map area. It was encountered along the lower parts of Frank Creek, occurring within the upper limb of a large second phase structure. It can be traced southeast, along strike, at the same structural and stratigraphic level and is recognized as far south as the Goose Peak area. This unit was not seen in any other panel of Harveys Ridge succession or Goose Peak quartzite.

The Agnes conglomerate consists of clasts of quartzite to feldspathic quartzite very similar in appearance to quartzite of the Goose Peak. Clasts are poorly sorted and range from granule to boulder in size. Clasts are commonly matrix-supported with the matrix typically being dark grey phyllite (Photo 4a), although a few localities in the Frank Creek area consist of quartzite clasts in a quartzite matrix (Photo 4b). Phyllite supported conglomerate usually has less than 50 per cent clasts whereas the quartzite-matrix conglomerate is clast-rich. Clasts are commonly elongate due to deformation. Along the southwest flank of the ridge containing Goose Peak, the conglomerate consists of 10 to 20 per cent cobbles of grey-green feldspathic sandstone and grey micaceous sandstone to siltstone set in a dark grey phyllite to siltstone typical of the Harveys Ridge succession.

The presence of Goose Peak-like clasts of feldspathic sandstone within the Agnes conglomerate suggests that it and the Goose Peak are, in part, a lateral equivalent of the Harveys Ridge succession. This inference is supported by the transitional nature of the Harveys Ridge succession and Goose Peak quartzite.

The thickness of the Agnes conglomerate is quite variable. It is lest than 1 metre thick south of Goose Peak and is estimated to be between 10 and 20 metres thick in the Frank Creek area. Struik (1988) states that it is generally less than 30 metres thick and up to 60 metres locally. The sporadic nature of this unit suggests it may form lenses within the upper part of the Harveys Ridge succession.

GOOSE PEAK QUARTZITE

The Goose Peak quartzite is characterized by thick to massive beds of greenish-grey to grey micaceous and feldspathic sandstone to quartzite and contains minor amounts of grey to dark grey phyllite or schist, siltstone wacke and chlorite schist (metavolcanics). This resistive unit forms the tops of many of the higher ridges within the map area, including near Badger Peak, the ridge containing Goose Peak and in the Mount Borland area. The lower part of the unit is transitional into the Harveys Ridge succession.

Massive to thick bedded quartzite with a "limestone grey" colour is also distinguishing feature of Goose Peak sections. Thin interbeds or partings of dark grey to grey

Photo 4. Agnes conglomerate. (a) Clasts of quartz sandstone (some feldspathic) “floating” in dark grey to black phyllite or siltstone. This locality is found immediately south of the Frank Creek massive sulphide showing and is surrounded by lithologies typical of the Harveys Ridge succession. Quartz sandstone clasts are similar in appearance to sandstone within the Goose Peak quartzite. (b) Quartzite clast conglomerate the matrix of which is also quartz sand giving an almost intraformational appearance to the unit. This exposure is also found very close to the Frank Creek massive sulphide occurrence.

4b

phyllite to siltstone are common. Sections or beds of quartzite are commonly over 2 metres in thickness and some were seen to be in excess of 5 metres. Mica can form up to 5 or 10 per cent of the rock. White Feldspar grains are broken and commonly sericitized. They are typically composed of plagioclase and lesser microcline, and can comprise up to 10 per cent of the section. Sandstone is commonly coarse grained and locally grades into granule conglomerate. Thin section examination shows that some of the coarser quartz grains can be polycrystalline. Chlorite schist was seen at several localities within Goose Peak sections and are believed to represent metavolcanics.

The thickness of this unit is quite variable due to deformation. It ranges from several hundred metres to over 1 kilometre within the core of the syncline along Goose Peak. Struik (1988) estimates the Goose Peak quartzite is 250 metres in thickness and is lensoidal on a regional scale.

DOWNEY SUCCESSION?

Schist, sandstone, carbonate and metavolcanics along Mount Barker have been assigned to the Downey succession by Struik (1988, 1983a). Work this past summer suggests that these rocks may be part of the Keithley succession. The mapping of Harveys Ridge rocks northward towards Mount Barker has shown that they form the core of a large southwesterly verging, second phase syncline. A 10 metre section of white, beige to purplish pink orthoquartzite was found on the upper, overturned limb of this structure at the change from Harveys Ridge lithologies into those presently assigned to the Downey succession. This quartzite appears very similar to that at the top of the Keithley succession and is found structurally and stratigraphically at the proper position with respect to the Harveys Ridge. Furthermore, top indicators suggest that the volcanics found along the peak containing Mount Barker are overturned and sit stratigraphically below the orthoquartzite section.

Assignment of these rocks along Mount Barker to the Keithley raises regional stratigraphic problems. These metavolcanics and metasediments can be traced northwestward into sections of typical Downey lithologies (Struik, 1988). As such, until more information can be obtained about the true stratigraphic setting of these units, they will remain as part of the Downey succession, albeit with a cautionary note.

Structurally above the orthoquartzite, southwest of Mount Barker, is a 200 metre section of interlayered dark grey to grey or green-grey schist and beige to grey-green micaceous quartz sandstone beds up to 1 metre thick, all of which are not unlike parts of the Keithley succession. These rocks contain a 50 metre thick section of dark grey magnetite-bearing chloritic schist in the upper part. Parts of this chlorite schist appear to be tuffaceous, although this interpretation is tenuous due to deformation.

The above rocks are followed by a thick (approximately 500 metres) section of mafic metavolcanics consisting primarily of crystal to lithic tuff. These tuffs are commonly massive and can contain lenses of orange weathering carbonate alteration up to 1 by 5 centimetres in size. In some areas relict crystals of feldspar and pyroxene are seen (now altered to chlorite - actinolite - sericite ± clinozoisite and carbonate) within the tuff forming overturned, graded beds up to 15 centimetres thick. Sections of coarse to very coarse-grained meta-gabbro up to 5 or 10 metres thick were encountered within this section and may represent co-magmatic subvolcanic intrusions. A 50 to 75 metre thick section of rusty weathering, greenish grey to grey muscovite schist is found in the lower part of this unit and may represent felsic meta- volcanics.

A mixed sequence of red-brown weathering, light grey schist, dark grey to black banded limestone, orange to honey weathering, grey to cream limestone, dark grey to black phyllite and cream, unevenly bedded quartzite are found intermixed with mafic metavolcanics in a succession some 200 metres thick northeast of Mount Barker. These metasediments form sequences in excess of 30 metres thick with individual sections of phyllite, quartzite or limestone ranging from 1 to 10 metres.

Although metavolcanics and sediments can be traced onto the ridge running east from Mount Barker, they become thinner and sections of massive to thickly bedded, greenish grey micaceous and feldspathic quartz sandstones, similar to those of the Goose Peak quartzite, are found suggesting either a facies change or a late fault as suggested by Struik (1988).

Mafic metavolcanics are encountered on the lower, north facing slope of Mount Barker and are also found with meta-gabbro and greenish micaceous sandstone. Keithley-like metasediments and light coloured quartzite occur west of Clair Creek and between metasediments of the Harveys Ridge and chlorite schists (metavolcanics) similar to those on Mount Barker.

Preliminary Geochemistry of Igneous Rocks

Major and partial trace element geochemistry was obtained for selected metavolcanics of the Snowshoe Group and Crooked amphibolite (Table 1). Some of these will then be analyzed for rare-earth-element geochemistry in hopes of further characterizing the various units. Major element concentrations should be used with caution due to probable mobilization during upper greenschist to lower amphibolite metamorphic conditions and high loss on ignition (LOI) values. In light of this, the classification and comparison of the chemical signatures of the various volcanic packages will be based on trace element abundances which are believed to be less affected by these metamorphic conditions (see Rollinson, 1993).

Three main packages of volcanics were analyzed within the Snowshoe Group: the Frank Creek volcanics, volcanics in the Badger Peak area and volcanics presently assigned to the Downey succession. In addition several samples of the Crooked Amphibolite were analyzed for comparative purposes. Metavolcanics in the Badger Peak region have been correlated with the Crooked Amphibolite by Rees (1987), although mapping this summer suggests they are part of the Snowshoe Group. It was hoped that chemical analysis would help determine the affinity of these metavolcanics.

A cursory examination of major element concentrations reveals compositional trends also reflected by the trace element data (Table 1, Figure 6a). Based strictly on SiO_2 contents, Downey, Badger Peak and many of the Frank Creek volcanics are basaltic, with some of the Frank Creek volcanics ranging from basaltic andesite to andesite (Table 1). Most of the basalts fall within the alkaline field or are transitional on the SiO_2 versus total alkali plot (Figure 6a). Only the more siliceous varieties of the Frank Creek volcanics display sub-alkaline trends and these are calc-alkaline based on their position within the AFM plot (not shown).

The broad classification of these rocks based on $Zr/Ti0_2$ versus Nb/Y indicates that most were originally alkaline basalts in composition, although some analyses fall within the sub-alkaline basalt field and some of the Frank Creek volcanics trend into andesitic compositions (Figure 6b). Chemical analyses suggests that Badger Peak volcanics are not part of the Crooked Amphibolite. This is based on their alkaline nature, the within-plate signature displayed by data plotted in diagrams in Figures 6c, e and f, and on the comparison of trace element abundances with those of the Crooked Amphibolite as shown in Figures 6b to f.

Both the Frank Creek and Downey volcanics display alkaline to subalkaline compositions (Figure 6a, b). Furthermore there is also a subdivision of this data which corresponds to broad lithologic characteristics displayed by these rocks. The darker, more mafic (*i.e.* lower SiO_2 content) and commonly porphyritic Frank Creek volcanics have lower Zr/TiO_2 ratios in Figure 6a than the more silicic, lighter coloured fragmental metavolcanics which also plot closer to the andesite and trachyandesite field. The more mafic Frank Creek volcanics are similar in composition to those in the Badger Peak area. Downey volcanics also show two clusters: coarser, gabbroic samples display subalkaline compositions whereas finer chloritic schists are alkaline in nature (Figure 6a, b).

These lithologic and chemical similarities are also evident within the other discrimination diagrams shown in Figures 6c to f. The overall trace element concentrations within these volcanics suggests within-plate alkali and tholeiitic basalt, and E-type MORB characteristics (Figure 6c). Subalkaline, gabbroic volcanics of the Downey together with the subalkaline sample of the mafic Frank Creek volcanics all plot within the E-type MORB field. The clustering of data is much more evident when examining the levels of Ti and V in comparison to some of the other trace elements.

Relative levels of Ti are lower within the lighter coloured, more silicic Frank Creek volcanics and gabbroic Downey volcanics such that they plot within the calc-alkalic basalt field of the Ti versus Zr plot of Figure 6e. A similar pattern is also displayed within the Ti-Zr-Y

TABLE 1
MAJOR AND PARTIAL TRACE ELEMENT GEOCHEMISTRY OF SNOWSHOE GROUP AND CROOKED AMPHIBOLITE METAVOLCANICS

	00FFE-15-9	00FFE-22-1	00FFE-22-2	00FFE-24-2	00FFE-23-5	00FFE-23-6	00FFE-24-6	00FFE-6-1	00FFE-34-4	00FFE-34-6	00FFE-34-8	00FFE-34-5
	CA	CA	CA	CA	BP	BP	BP	DV	DV	DV	DV	DVg
Easting	610828	614272	614538	616084	616125	616164	616791	618855	621228	621300	621325	621233
Northing	5839105	5835709	5835485	5836461	5837760	5837567	5837284	5852940	5849252	5849441	5849754	5849302
SiO_2	48.15	52.13	48.72	48.84	41.11	41.59	45.27	42.88	46.79	48.86	42.70	46.52
TiO_2	0.99	1.37	2.19	1.72	2.20	1.23	1.75	1.27	0.79	1.57	2.27	0.89
Al_2O_3	14.97	14.57	14.56	14.39	17.20	12.03	15.47	9.10	15.02	16.27	12.47	14.82
Fe_2O_3	9.57	10.67	12.59	12.17	13.96	9.80	10.86	14.10	11.67	14.07	10.57	12.23
MnO	0.11	0.07	0.15	0.17	0.25	0.12	0.11	0.15	0.17	0.09	0.18	0.18
MgO	7.28	8.22	6.21	4.21	9.64	14.22	11.21	17.71	4.59	4.53	5.42	5.11
CaO	6.13	5.96	6.84	6.55	8.02	11.43	7.21	8.90	7.11	3.46	12.69	7.73
Na_2O	3.89	2.90	4.65	4.88	1.12	1.35	2.66	0.07	4.42	4.94	3.79	3.54
K_2O	0.05	0.23	0.05	0.21	0.14	0.18	0.31	0.02	0.27	0.52	0.17	0.15
P_2O_5	0.11	0.14	0.18	0.14	0.41	0.09	0.37	0.10	0.21	0.28	0.33	0.25
LOI	8.35	3.44	3.50	6.34	5.69	7.57	4.38	4.84	8.65	5.13	8.68	8.07
SUM	99.61	99.72	99.65	99.63	99.75	99.62	99.62	99.15	99.71	99.79	99.28	99.5
Zr	53	94	135	106	156	58	138	79	77	121	158	83
Y	21	34	43	38	29	15	23	8	21	18	31	20
Sr	242	231	185	157	421	211	272	24	449	243	464	431
Nb	3	9	9	4	38	14	31	16	7	15	24	9
Th	4	<3	3	6	<3	<3	9	<3	<3	15	3	7
Ta	<3	<3	12	<3	4	<3	<3	5	<3	5	<3	<3
V	320	320	369	307	257	207	228	228	291	322	288	272
La	7	11	4	9	28	8	27	22	23	27	13	18
Ce	36	6	20	53	100	26	52	53	45	31	55	32
Ba	49	177	69	28	114	105	175	19	188	730	59	39
Rb	10	10	<3	20	11	9	15	4	14	19	10	10

	00FFE-35-2	00FFE-36-7	00FFE-4-14	00FFE -9-7	00FFE-8-10	00FFE-8-11	00FFE-4-1	00FFE-4-7	00FFE-4-11	00FFE-8-2	00FFE-38-1
	DVg	DVg	FCm	FCm	FCm	FCm	FC	FC	FC	FC	FC
Easting	621817	620252	609712	608683	610179	610090	607352	608730	609883	608248	609864
Northing	5849596	5851854	5842941	5842293	5844196	5844241	5844008	5843209	5843781	5844719	5841876
SiO_2	48.20	45.43	43.81	49.77	45.36	46.47	52.49	59.13	54.91	53.90	51.06
TiO_2	0.77	0.87	2.00	1.55	1.66	1.97	0.61	0.64	0.58	0.62	0.79
Al_2O_3	16.60	15.73	13.86	15.40	19.32	14.59	16.54	17.12	16.94	17.22	15.31
Fe_2O_3	12.30	11.82	11.50	11.26	9.71	10.26	6.23	6.21	5.94	5.65	6.23
MnO	0.14	0.15	0.07	0.14	0.10	0.12	0.10	0.05	0.05	0.07	0.07
MgO	7.17	5.09	7.61	5.90	6.82	6.73	4.78	3.97	4.76	5.59	4.00
CaO	5.21	7.01	5.51	8.38	3.22	9.02	10.43	3.58	9.92	8.11	7.90
Na_2O	4.84	4.40	3.50	3.80	2.95	3.58	2.96	2.67	0.69	3.48	1.66
K_2O	0.10	0.25	0.76	0.40	2.60	0.05	1.65	2.31	2.76	2.43	2.66
P_2O_5	0.23	0.25	0.33	0.14	0.20	0.25	0.10	0.07	0.07	0.15	0.14
LOI	4.25	8.77	10.28	2.52	5.86	6.42	2.68	3.39	2.35	1.82	9.30
SUM	99.82	99.8	99.37	99.39	98.93	99.7	99.04	99.39	99.21	99.25	99.46
Zr	70	80	131	100	104	130	92	114	99	100	151
Y	22	25	17	34	6	10	11	11	15	13	24
Sr	477	290	181	532	128	489	848	474	557	520	262
Nb	10	8	23	10	23	22	17	12	13	16	15
Th	14	<3	9	<3	5	13	18	19	6	11	19
Ta	<3	7	<3	5	<5	<3	3	3	<3	<3	11
V	246	271	263	353	261	275	78	82	114	104	121
La	26	20	63	14	7	15	37	50	50	39	37
Ce	43	50	32	6	10	10	10	55	14	48	<3
Ba	83	285	1444	1253	11286	2389	4698	2455	2436	2071	3395
Rb	9	8	20	16	45	3	51	71	92	85	87

NOTES

Steel mill grinding at the B.C. Geological Survey Branch. Chemical analysis at Cominco Research Laboratories, Vancouver, B.C.

Major oxides determined by fused disc - X-ray fluorescence and reported in per cent (%). Trace elements determined by pressed pellet - X-ray fluorescence and reported in parts per million (ppm).

LOI = loss on ignition @ 1100^{o}C. SUM = sum of oxides. CAL = calculated sum.

CA: Crooked Amphibolite; BP: Badger Peak volcanics; DV: Downey volcanics, g - gabbro; FC: Frank Creek volcanics, m - mafic;

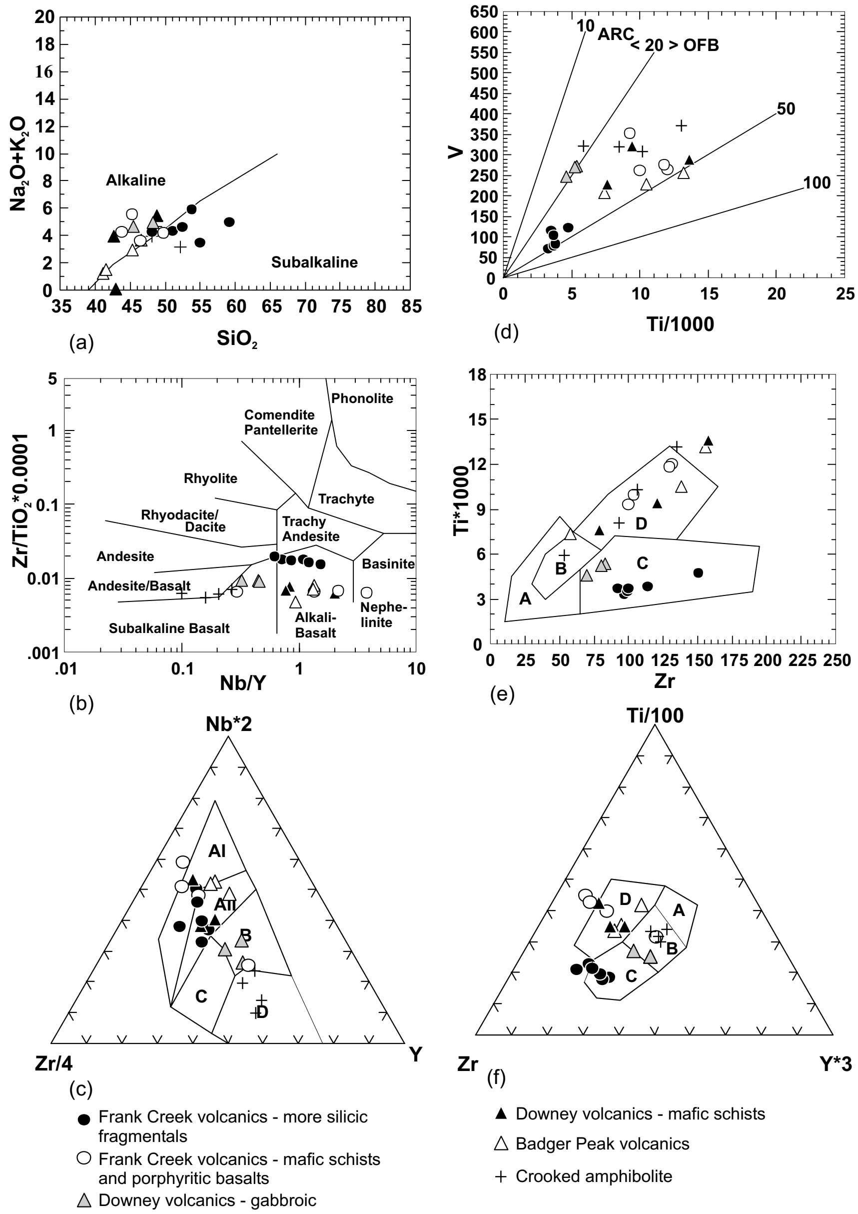

Figure 6. Major and trace element geochemical plots for selected volcanics from the project area. (a) Silica versus K_2O+Na_2O showing the separation between alkaline and subalkaline igneous rocks (Irvine and Baragar, 1971) (b) Zr/TiO_2*0.0001 versus Nb/Y (Winchester and Floyd (1977). (c) Nb*2 - Zr/4 - Y (Meschede, 1986); AI - within-plate alkali basalts; AII - within-plate alkali basalts and within-plate tholeiites; B - E-type MORB(mid-ocean ridge basalt) ; C - within-plate tholeiites and volcanic-arc basalts; D - N-type MORB and volcanic-arc basalts. (d) V versus Ti/1000 (Shervais, 1982); ARC - volcanic arc basalts; OFB - ocean floor basalts. (e) Ti*1000 versus Zr (Pearce and Cann, 1973); A - island-arc tholeiites; B - MORB, calc-alkali basalts and island-arc tholeiites; C - calc-alkali basalt; D - MORB. (f) Ti/100 Zr - Y*3 (Pearce and Cann, 1973); A - island-arc tholeiites; B - MORB, island-arc tholeiites and calc-alkali-basalts; C - calc-alkali basalts; D - within-plate basalts.

diagram of Figure 6f. The clustering of data is even more evident when comparing Ti versus V (Figure 6d) where the more silicic Frank Creek volcanics have a relatively low concentration of V. Gabbroic Downey volcanics, although higher in V, cluster away from the other volcanics due to their low Ti values.

Preliminary analyses suggest that the alkalinity displayed by the bulk of the volcanics record eruption within an extensional environment. The significance of the chemical variation, particularly the low Ti concentrations, is not fully understood. Do they reflect other tectonic processes (*i.e.* nearby volcanic arc) which are influencing the chemical composition of these within-plate volcanics? Clearly further chemical and field data is needed.

Regional Correlations

Struik (1988 and 1986) correlated the Keithley quartzite with the Early Cambrian Yanks Peak Formation of the Cariboo Subterrane. Struik (1988) also suggested that the Bralco limestone may be correlative with the Early Cambrian Tshinakin limestone of the Eagle Bay Formation. This latter unit, based on age and composition, has been correlated with the Badshot Formation in the Kootenay Arc (Schiarizza and Preto, 1987). The Badshot, and underlying Hamill Formation, have been equated eastward with the Mural and McNaughton formations, respectively, of the Gog Group within Ancestral North American stratigraphy. This circuitous correlation would suggest that the Bralco limestone is also correlative with the Mural Formation of the Cariboo Subterrane and would make all units between the Bralco limestone and Keithley quartzite (Harveys Ridge, Agnes conglomerate, Goose Peak quartzite, Eaglenest succession and Downey succession) Early Cambrian in age (Figure 3) and correlative to the Midas Formation (Figure 3).

Parts of the Midas Formation have similarities to the dark grey to black phyllite and siltstone of the Harveys Ridge succession together with parts of the overlying transitional unit (Struik, 1988). There are no direct equivalents within Midas sections for lithologies contained within the Goose Peak quartzite, Agnes conglomerate or Eaglenest succession. The only coarse, distinctive unit within the Midas Formation is the Vic Sandstone (Struik, 1988) and correlating rocks of the Goose Peak, Agnes and Eaglenest (all facies correlatives) would suggest a profound facies change. If this is the case, clearly the depositional basin now represented by the Barkerville Subterrane was closer to a higher energy source which was unroofing rocks of igneous composition and was also experiencing igneous activity not seen further east.

Based on the above arguments, the sequence encompassing the Keithley, Harveys Ridge, Agnes, Goose Peak, Eaglenest, Downey and Bralco limestone is broadly correlative with Early Cambrian units EBQ, EBH and EBG of the Eagle Bay Assemblage (Schiarizza and Preto, 1987). Units EBQ and EBH have similarities to the Keithley succession whereas schists and limestone of unit EBG are similar to those of the Harveys Ridge, Downey and Bralco limestone. The coarse clastics of the Goose Peak quartzite, Agnes conglomerate and Eaglenest succession have no correlatives within Cambrian rocks of the Eagle Bay Assemblage or elsewhere within the Kootenay Terrane and are, as Struik (1988) points out, unique to the Snowshoe Group.

The above relationships led Höy and Ferri (1998) to suggest re-assignment of ages to various units within the Snowshoe Group. They suggested that the Downey correlate with the Lardeau Group and the Ramos with Devono-Mississippian rocks that elsewhere contain a felsic volcanic component. Subsequent U-Pb dating of zircons from possible felsic tuff in the Ramos succession is inconclusive (unpublished data). All recovered zircons were detrital and Proterozoic in age suggesting the "tuff" was probably sedimentary in origin. Work this summer could not resolve this question as no rocks of Ramos age were encountered. Correlation of the Downey succession with the basal Lardeau was also not resolvable due to incomplete data; Downey rocks were only briefly encountered. As a result, I will adhere to Struik's (1986, 1988) designation until further mapping helps resolve these proposed correlations.

STRUCTURE AND METAMORPHISM

Structurally the map area is complex due to the presence of multiple periods of deformation. Overprinting relationships between structural elements at the outcrop scale indicate that strata within the map area have been affected by at least three episodes of penetrative deformation. In addition, a regional, prograde metamorphic event, which reached lower amphibolite grade in the map area, accompanied the second phase of folding. Although this would suggest a protracted structural history, stratigraphic and structural relationships together with geochronological data presented by Rees (1987) and Struik (1988) suggests that this deformation was probably initiated in the late Early Jurassic in response to eastward overthrusting of Quesnel rocks and that folding related to the last period of deformation was over in late Middle Jurassic times.

The first period of deformation (D_1) is manifested by a layer-parallel fabric which is subsequently crenulated by later folding events (Figure 7a). This can be observed along pelitic horizons within the core of second phase folds. This fabric is strongest along the contact between Quesnel and Barkerville rocks, forming a well developed mylonitic fabric within rocks of the Quesnel Lake Gneiss. Although outcrop scale rootless F_1 folds are sometimes seen, no large-scale structures have been attributed to this period of folding. This deformation is believed to be eastward verging based on analysis of meso and microscopic structural elements (rotated feldspar megacrysts, shear bands, etc.) within the mylonitic fabric developed at the terrane boundary (Ferri, 1982; Rees and Ferri, 1983).

The well developed mineral lineation within the Quesnel Lake Gneiss has been attributed to D_1 deformation (Figure 7b; Rees, 1987). It is interesting that the two bodies of gneiss within the map area display very different orientations for this lineation. The easiest explanation for this is folding about F_2 and/or F_3 fold axis, which are very close in orientation to the required rotation axis.

Stretched-pebbles or grains within Snowshoe sediments have orientations parallel to F_2 fold axes or S_0 /S_2 intersection lineations (Figure 7g and h). This fold axis-parallel stretching is a common feature within folds of this generation within the cordillera.

The second phase of deformation (D_2) is southwest verging and has produced megascopic folds which essentially control the distribution of map patterns within the area (Figure 5). The trace of the Eureka Thrust fault, and the Crooked Amphibolite, reflect F_2 folding. In the Sellers Creek area this fault is on the overturned limb of

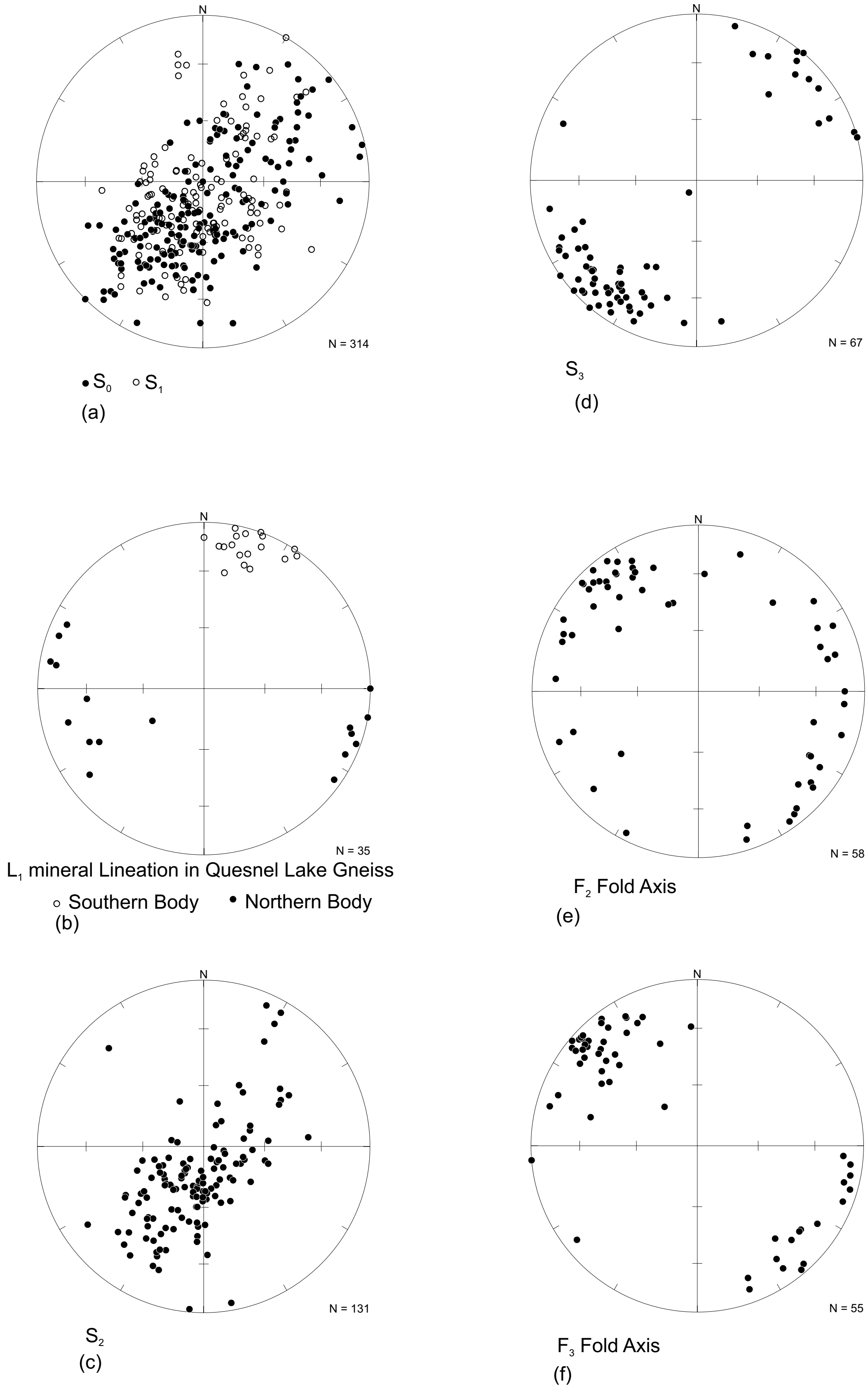

Figure 7. Equal area plots of structural data collected within the map area. (a) S_0 and S_1 foliations. (b) L_1 mineral lineations within the Quesnel Lake Gneiss. (c) S_2 foliations. (d) S_3 foliations. (e) F_2 fold axes. (f) F_3 fold axes. (g) L_2 stretching lineations in Snowshoe sediments. (h) S_0/S_2 intersection lineations.

an F_2 anticline. These folds are quite large, some traceable across the map area (greater than 10 kilometres in length) and having wavelengths several kilometres in size. Axial planes, in accordance with the mean dip of S_2 foliation (Figure 7c), dip moderately to the northeast. Although S_2 foliation is commonly parallel to sub-parallel with compositional layering (and S_1 foliation) on the limbs of F_2 folds, small scale folds structures and bedding cleavage relationships, together with delineation of key stratigraphic units, has allowed the delineation of F_2 fold structures seen in Figure 5. On outcrop scale these folds display a similar style suggesting ductile conditions during their formation. This is consistent with their production concurrent with the peak of regional metamorphism.

A vertical to steeply southeast dipping crenulation affects both S_1 and S_2 foliations within the map area (Figure 7e and f). Commonly this crenulation cleavage is parallel with open to moderately tight folds that contain hinges without appreciable thickening. Map-scale F_3 structures have only been delineated in the Frank Creek area where S_2 foliation is broadly folded across several kilometres.

Most of the map area occurs within middle to upper greenschist grade metamorphism. Typically chlorite and muscovite are the only metamorphic minerals developed within the metasediments. Metavolcanics contain mostly chlorite, although actinolite is not uncommon within many of the outcrops in the Frank Creek area. Metamorphic grade increases to the southeast resulting in the consistent appearance of biotite and then garnet porphyroblasts. Textural relationships between porphyroblasts suggest that growth occurred after D_1 fabrics were developed (as seen by inclusion trails in garnet) and during D_2 deformation. The latter inference is supported by the growth of biotite flakes sub-parallel with S_2 foliation and the concurrent flattening of this fabric around these porphyroblasts. Chlorite and muscovite porphyroblasts are sometimes seen growing parallel to S_3 crenulation planes indicating, as Rees (1987) suggested, that D_3 deformation occurred near the end of metamorphism. Although the above relationships are consistent throughout most of the map area, immediately east of Badger Peak one locality contains idiomorphic garnet porphyroblasts that are post-D_2 or show little or no deflection of S_2 foliation. Rees (1987) also noted that the timing between peak metamorphic conditions and D_2 deformation varied in a similar fashion between Mount Brew and Cariboo Lake and suggested that either metamorphism or D_2 deformation propagated at different rates. The age of this metamorphism is believed to be Middle Jurassic based on the U-Pb dating of metamorphic sphene recovered from the Quesnel Lake Gneiss in the Isosceles Mountain area (Mortensen *et al*., 1987).

MINERAL OCCURRENCES

Rocks of the Snowshoe Group have produced an abundance of lode and placer gold from the Wells - Barkerville area. Lode gold production has been primarily from veins and replacement bodies within metasediments of the Downey succession. Nearby placer deposits are believed to be weathering by-products of these deposits. Similar mineralization has been traced southward to the Cariboo Lake area; however, no substantial placer production or vein mineralization has been documented south of the lake.

Although the search for VMS targets within Snowshoe Group lithologies has gone on intermittently since the early 1980s, the Ace and Frank Creek properties represent the first significant showings of this type within these rocks (Lane and MacDonald, 2000). Massive sulphide mineralization was first discovered in the map area by Louis Doyle (now of Barker Minerals Ltd.) who found mineralized boulders within till along the south side of the Little River. This led to the discovery of the Ace property (093A 142), which possibly represents a sheared, besshi-style system within meta-sediments and volcanics of the Downey succession (Höy and Ferri, 1998; Payne, 1998, 1999 and Lammle, 1995; Lane and MacDonald, 2000). In light of this, Barker Minerals Ltd. carried out further exploration within the region leading to the discovery of the Big Gulp (093A 143) and Frank Creek (093A 152) sulphide showings within the Harveys Ridge succession. Exploration efforts in the Frank Creek area benefited from work carried out by exploration companies and prospectors in the 1980s who were led to the area by the discovery of massive sulphide boulders by placer gold prospectors along the lower parts of Frank Creek (*see* Lane and MacDonald, 2000 and Barkerminerals.com for a more detailed account of early exploration in this area). The other newly discovered mineral occurrence of note is the Sellers Creek showing (093A 131) consisting of Cu-Pb-Zn disseminations within quartz sandstone. The following descriptions will deal with the Big Gulp, Frank Creek and Sellers Creek occurrences.

The mixed volcanic and sedimentary succession, together with the Cu-Zn-Pb mineralogy of the Frank Creek and Big Gulp occurrences indicate that these are besshi-type sulphide showings. The relatively high Pb content simply reflects the influence of continental crust in their formation. Furthermore, the stratigraphic position of these occurrences above the Keithley quartzite, which has been correlated with the basal lower Cambrian Yanks Peak Formation (a correlative of the lower Hamill Formation found further south) suggests that these occurrences may be age equivalent to deposits such as the Mosquito King, Lucky Coon, Elsie and King Tut of the Eagle Bay Formation (Höy, 2000), although these are SEDEX in nature.

Big Gulp (093A 143)

The Big Gulp occurrence is located on the “C” logging road approximately 3 kilometres due east of the south end of Cariboo Lake (Figure 5). This occurrence was discovered by Barker Minerals Ltd. in 1996 and consists of disseminations and thin layers (several centimetre thick and 2 to 5 centimetres long) of sphalerite, chalcopyrite and pyrite (4.5 and 0.06 per cent Zn and Cu, respectively from a grab sample; Höy and Ferri, 1998) within mafic tuffs now assigned to the Frank Creek volcanics, a unit of the Harveys Ridge succession. Mineralization is found sporadically along the outcrop immediately north of the main logging road. Brown to orange-weathering carbonate and muscovite are associated with sulphide mineralization and may reflect primary alteration features. Mineralization is also found within quartz stringers which are now parallel to S_1 foliation and can be elongate parallel to the strong D_2 mineral lineation. Although deformation has virtually obliterated primary depositional features, relic structures in several areas suggests these volcanics were originally fine to coarse tuffs and possibly lapilli tuffs. These volcanics are part of the more siliceous fragmentals which display mafic to intermediate compositions.

Frank Creek (093A 152)

The Frank Creek Cu-Zn-Pb-Ag massive sulphide occurrence was discovered by Barker Minerals Ltd. in 1999 following a program tracing massive sulphide float and stream sediment geochemical anomalies. It is located on the "D" logging road 2 kilometres southeast of the mouth of Frank Creek (Figure 5). The main showing consists of a 1 metre thick massive sulphide horizon in dark grey to black phyllites of the Harveys Ridge succession. Extensive drift cover has masked the three dimensional configuration of the massive sulphide body. Massive pyrite-chalcopyrite pods several 10s of centimetres in length were also seen within the dark phyllites (Lane and MacDonald, 2000). Grab sample analyses by Lane and MacDonald (2000) indicate values up to 0.65 per cent Cu, 0.12 per cent Pb, 0.10 per cent Zn, 0.14 grams per tonne Au and 69 grams per tonne Ag. Average grab samples analysis reported by Barker Minerals Ltd. Are 2.13 percent Cu, 1.06 percent Zn, 0.16 percent Pb, 129.4 grams per tonne Ag and 215 ppb Au. A few hundred metres below the main showing, and also along the D road, is a thin zone of disseminated sulphides (pyrite and chalcopyrite) also within dark grey phyllites of the Harveys Ridge succession. Grab sample analysis of this stringer zone shows values up to 4.7 per cent Cu, 0.5 per cent Pb, .6 per cent Zn and 194 grams Ag (Barkerminerals.com).

Although a few top indicators in the vicinity are present (*i.e.* pillows) showing overturned bedding, the overall sequence youngs to the west in the immediate area of the showings. The Frank Creek volcanics sit stratigraphically above the dark grey phyllites hosting the massive sulphide mineralization. Southeast of these, one can trace orthoquartzite and metasediments of the Keithley succession from along Browntop Mountain and show that they plunge below the volcanics and associated dark lithologies of the Harveys Ridge succession. Furthermore, structural and stratigraphic data suggest mineralization together with the Frank Creek volcanics are within the core of a F_2 fold which is modified by F_3 folding. This latter warping has folded S_1 and S_2 foliations into west dipping attitudes around the deposit, opposite to their regional easterly dip.

Agnes conglomerate is found several hundred metres south and east of the Frank Creek showing. This conglomerate is found immediately down slope (stratigraphically below) an unknown thickness of light coloured feldspathic sandstone which can be traced for several hundred metres. It is locally characterized by the presence of large (up to 1 centimetre) dark grey and lesser opalescence blue quartz clasts. It appears to sit above the Frank Creek showing, within dark grey phyllite of the Harveys Ridge succession and is very similar in appearance to sandstones within the Goose Peak quartzite. A similar sandstone is faulted against dark grey phyllite of the Harveys Ridge succession just north of the disseminated sulphide occurrence found down slope from the main Frank Creek showing. The sandstone has been described as a felsic tuff by Barker Minerals Ltd. although the author believes it displays characteristics consistent with a sedimentary origin (*i.e.* dominantly detrital quartz grains, many of larger are polygonal, lack of embayment features on quartz and lack of preservation of crystal faces on quartz and feldspar grains). Frank Creek mafic metavolcanics are found up slope (and stratigraphically up section) from the Frank Creek showing, across a thickness of several hundred metres of dark grey to black phyllite and siltstone of the Harveys Ridge succession.

Sellers Creek (093A 131)

The Sellers Creek showing was also discovered by Barker Minerals Ltd. in 1999 and occurs towards the end of the "C" logging road, approximately 2 kilometres south of Browntop Mountain. This showing consists of disseminated chalcopyrite, galena and sphalerite found within a quartz sandstone immediately adjacent to white and grey banded marble and can be traced for several hundred metres. Reported grab sample values are: 0.39 per cent Cu, 0.19 per cent Pb and 0.1 per cent Zn (Lane and MacDonald, 2000). The sandstone horizon is from 2 to 3 metres thick and locally contains a calcareous cement. The banded marble, sandstone and chloritic schists have been tentatively assigned to the Keithley succession although the marble may be older or younger (*i.e.* Kee Khan marble or Downey succession). Malachite staining was also observed within chloritic schists, at their contact with marble.

CONCLUSIONS

Mapping in the Frank Creek area encompasses units assigned to the Snowshoe Group and includes lithologies of the Keithley, Harveys Ridge and possibly Downey successions together with rocks of the Goose Peak quartzite and Agnes conglomerate.

Massive sulphide mineralization at the Frank Creek showing occurs within black shales of the Harveys Ridge succession and are spatially associated with mafic to intermediate volcanics of alkaline composition. This, in conjunction with the Cu-Zn-Pb sulphide mineralogy suggests a besshi-type VMS setting.

Although three periods of deformation are evident within the rocks of the map area, second phase fold structures dominate the megascopic map patterns. The peak of regional metamorphism occurred during second phase deformation.

Testing of the stratigraphic correlations put forth by Höy and Ferri (1998) was not possible due to incomplete data.

ACKNOWLEDGEMENTS

I would like to thank Pat Johnstone for his competent, thoughtful and cheerful assistance this past summer. His ability to repair any damaged mechanical device with duct tape and baling wire would put Red Green to shame. I would also like to thank Barker Minerals Ltd., especially Louis Doyle, for providing us with logistical and technical support during part of the summer. I also benefited from numerous discussions with John Payne on the geology of the Frank Creek showing.

I would also like to thank Bert Struik of the Geological Survey of Canada for providing information and guidance during the initial stages of the project. Bert provided his original field data for this area and also took me a tour of the stratigraphic sequence during the last week of June. This is greatly appreciated as it quickly gave me an understanding of the overall stratigraphy and saved me quite a bit of time on the "learning curve".

The excellent hospitality and service at Neilsen's Lakeshore Cabins and the Highland Motel made our stay in Likely much more enjoyable. Flycamps were located and supported through the help of Tom Arduini of Arduini Helicopters and demobilized by Highland Helicopters.

I would like to thank Dave Lefebure and Trygve Höy for reading early versions of this manuscript and for providing useful and constructive criticism.

REFERENCES

Bichler, A. and Bobrowsky, P. T. (2001): Barkerville Project: regional till geochemistry (93H/4, 5) and orientation (93A/14) studies; *in* Geological Fieldwork 2000, *B.C. Ministry of Energy and Mines*, Paper 2001-1.

Campbell, R.B., Mountjoy, E.W., and Young, F.G. (1973): Geology of the McBride map area, British Columbia; *Geological Survey of Canada*, Paper 72-35.

Campbell, R.B. (1978): Quesnel Lake, British Columbia; *Geological Survey of Canada,* Open File 574.

Dunne, K.P.E., Ray, G.E. and Webster, I.C.L. (2001): Preliminary fluid inclusion study of quartz vein and massive banded stringer pyrite mineralization in the Barkerville gold camp, east-central British Columbia; *in* Geologic Fieldwork 2000, *B.C. Ministry of Energy and Mines*, Paper 2001-1.

Ferri, F. (1982): Examination of a shear zone on the boundary between the Intermontane Belt and Omineca Crystalline Belt near Quesnel Lake, British Columbia; Unpublished B.Sc. thesis, *Carleton University*, Ottawa, Ontario, 50 pages.

Ferri, F., Höy, T. and Friedman, R.M. (1999): Description, U-PB age and tectonic setting of the Quesnel Lake Gneiss, east-central British Columbia; *in* Geological Fieldwork 1998, *B.C. Ministry of Energy and Mines*, Paper 1999-1, pages 69-80.

Höy, T. and Ferri, F. (1998): Zn-Pb deposits in the Cariboo Subterrane, central British Columbia (93A/NW); *in* Geological Fieldwork 1997, *B.C. Ministry of Employment and Investment*, Paper 1998-1, pages 13-1 - 13-12.

Irvine, T.N., and Baragar, W.R.A. (1971): A guide to the chemical classification of the common volcanic rocks; *Canadian Journal of Earth Sciences*, Volume 8 pages 523-548.

Lammle, C.A.R(1995): Prospecting, line cutting, geochemistry, geophysics and geology - Mount Barker Project, Ace Property; *B.C. Ministry of Energy and Mines*; Assessment Report 24286.

Lane, B. and MacDonald, K. (2000): Volcanogenic massive sulphide potential in the Slide Mountain and Barkerville terranes, Cariboo Mountains; *B.C. Ministry of Energy and Mines*, Exploration and Mining in British Columbia - 1999, pages 65 to 78.

Martin, L.S. (1989): Geological, geochemical and geophysical report on the Mass Property; *B.C. Ministry of Energy, Mines and Petroleum Resources*, Assessment Report 19345.

Meschede, M. (1986): A method of discriminating between different types of mid-ocean ridge basalts and continental tholeiites with the Nb-Zr-Y diagram; *Chemical Geology*, Volume 56, pages 207 - 218.

Montgomery, J.R., and Ross, J.V. (1989): A note on the Quesnel Lake Gneiss, Cariboo Mountains, British Columbia; *Canadian Journal of Earth Sciences*, Volume 26, pages 1503-1508.

Mortensen, J.K., Montgomery, J.M. and Fillipone, J. (1987): U-Pb zircon, monazite, and sphene ages for granitic orthogneiss of the Barkerville Terrane, east-central British Columbia; *Canadian Journal of Earth Sciences*, Volume 24, pages 1261-1266.

Panteleyev, A, Bailey, D.G., Bloodgood, M.A. and Hancock, K.D. (1996): Geology and mineral deposits of the Quesnel River-Horsefly map area, central Quesnel Trough, British Columbia; *Ministry of Employment and Investment*, Bulletin 97, 156 pages.

Payne, J. (1998): Geological, geochemical and geophysical report on the Ace and peripheral properties; *B.C. Ministry of Energy and Mines*, Assessment Report 25437.

Payne, J. (1999): Geological, geochemical and geophysical report on the Ace property, *B.C. Ministry of Energy and Mines*, Assessment Report 25904.

Pearce, J.A. and Cann, J.R. (1973): Tectonic setting of basic volcanic rocks determined using trace element analysis; *Earth and Planetary Science Letters*, Volume 19, pages 290 - 300.

Radloff, J.K. (1989): Origin and obduction of the ophiolitic Redfern Complex on the Omineca - Intermontane belts boundary, western Cariboo Mountains, British Columbia; Unpublished M.Sc. thesis, *University of British Columbia*, Vancouver, British Columbia, 178 pages.

Ray, G.E., Webster, I.C.L., Ross, K. and Hall, R. (2001): Geochemistry of auriferous pyrite minealization at the Bonanza Ledge, Mosquito Creek mine and other properties in the Wells-Barkerville area, British Columbia; *in* Geological Fieldwork 2000, *B.C. Ministry of Energy and Mines*, Paper 2001-1, this volume.

Rees, C.J. (1987): The Intermontane - Omineca Belt boundary in the Quesnel Lake area, east-central British Columbia: Tectonic implications based on geology, structure and paleomagnetism; Ph.D. Thesis; *Carleton University*, Ottawa, Ontario, 421 pages.

Rees, C.J. and Ferri, F. (1983): A kinematic study of mylonitic rocks in the Omineca-Intermontane Belt tectonic boundary in east-central British Columbia, *in* Report of Activities, *Geological Survey of Canada* Paper 83-1B, pages 121-125.

Schiarizza, P. and Preto, V.A. (1987): Geology of the Adams Plateau-Clearwater-Vavenby Area; *B.C. Ministry of Energy, Mines and Petroleum Resources*, Paper 1987-2, 88 pages.

Shervais, J.W. (1982): Ti - V plots and the petrogenesis of modern and ophiolitic lavas; *Earth and Planetary Science Letters*, Volume 59, pages 101 - 118.

Struik, L.C. (1983a): Bedrock geology of Spanish Lake (93A/11) and parts of adjoining map areas, central British Columbia; *Geological Survey of Canada*, Open File 920.

Struik, L.C. (1983b): Bedrock geology of Quesnel Lake (93A/10) and part of Mitchell Lake (93A/15) map areas, central British Columbia; *Geological Survey of Canada*, Open File 962.

Struik, L.C. (1986): Imbricated terranes of the Cariboo Gold belt with correlations and implications for tectonics in southeastern British Columbia; *Canadian Journal of Earth Sciences*, Volume 23, pages 1047-1061.

Struik, L.C. (1988): Structural geology of the Cariboo Gold Mining District, east-central British Columbia; *Geological Survey of Canada*, Memoir 421, 100 pages.

Winchester, J.A. and Floyd, P.A. (1977): Geological discrimination of different magma series and their differentiation products using immobile elements; *Chemical Geology*, Volume 20, pages 325-342.

British Columbia Geological Survey
Geological Fieldwork 2000

Geology of North-Central Jennings River Area (104O/14E, 15)

By JoAnne Nelson

KEYWORDS: Mississippian, Dorsey Terrane, Yukon Tanana Terrane, northern British Columbia, volcanogenic massive sulphides.

INTRODUCTION

The goal of this project is to trace into central northern B.C. stratigraphy known to host Mississippian volcanogenic massive sulphide deposits such as Kudz Ze Kayah, Wolverine, and Fyre Lake, which lie within the Yukon Tanana Terrane in the Finlayson Lake belt of central Yukon. It is part of the Jennings River/Wolf Lake component of the Ancient Pacific Margin NATMAP project, a cooperative effort with the Geological Survey of Canada that aims to decipher the stratigraphically and structurally complex late Paleozoic pericratonic sequences along the B.C.-Yukon border near Swift River.

The present map area, 104O/14E and 15, is centrally located between other areas covered by the Jennings/Wolf project, and thus provides geological linkages between them. It abuts both the Big Salmon Complex to the west (Mihalynuk *et al.*, 1998, 2000), and the southwestern Wolf Lake map area to the north (Roots *et al.*, 2000, Roots and Heaman, 2001; Figure 1), and is separated from the southern Dorsey Terrane area (Nelson , 1999*,* 2000; Nelson *et al.*, 2000) by the Early Jurassic Nome Lake batholith.

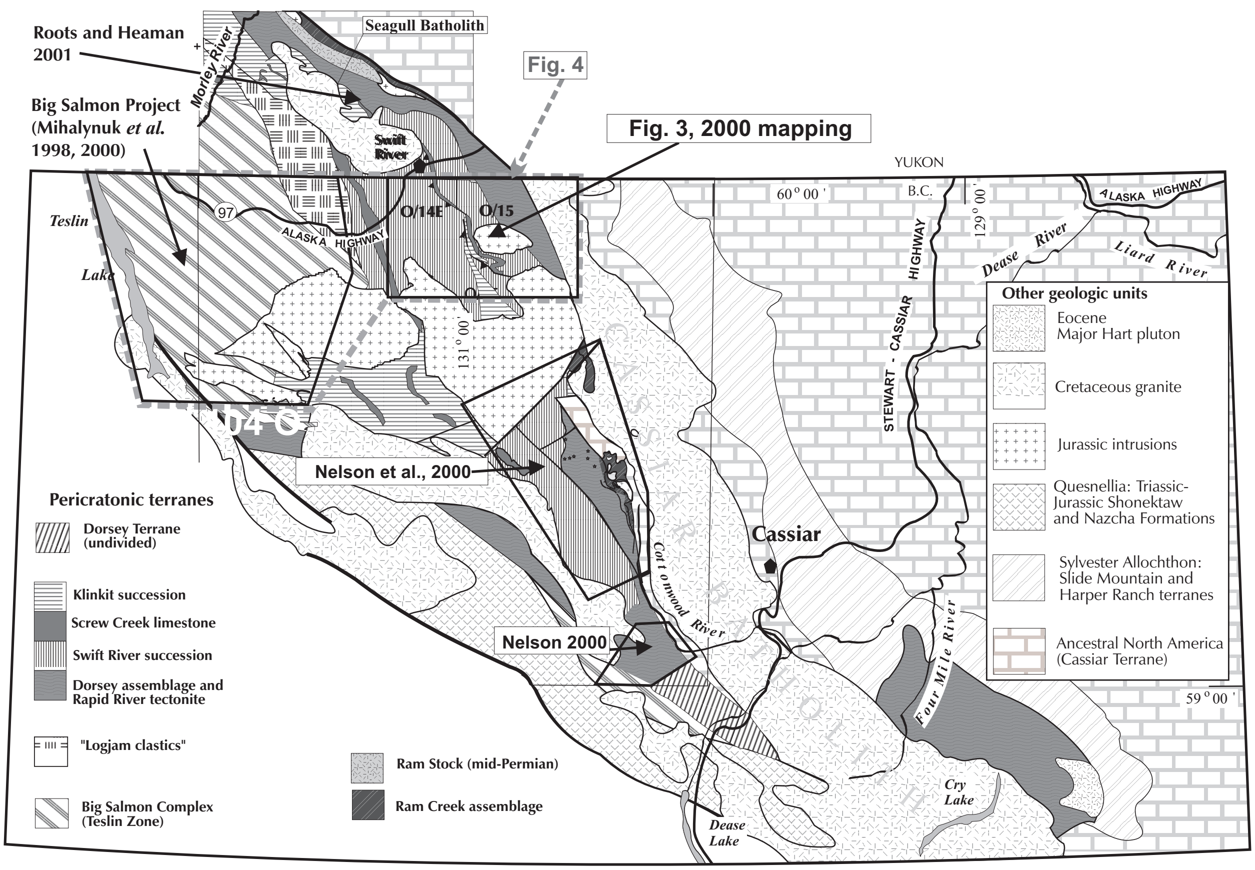

Figure 1. Location and tectonic setting of 104O/14E and 15 in the context of the Wolf-Jennings project. Regional geology from Gabrielse (1963, 1969, 1994), Stevens and Harms (1995), Mihalynuk *et al*., 2000, and Nelson *et al*., 2000.

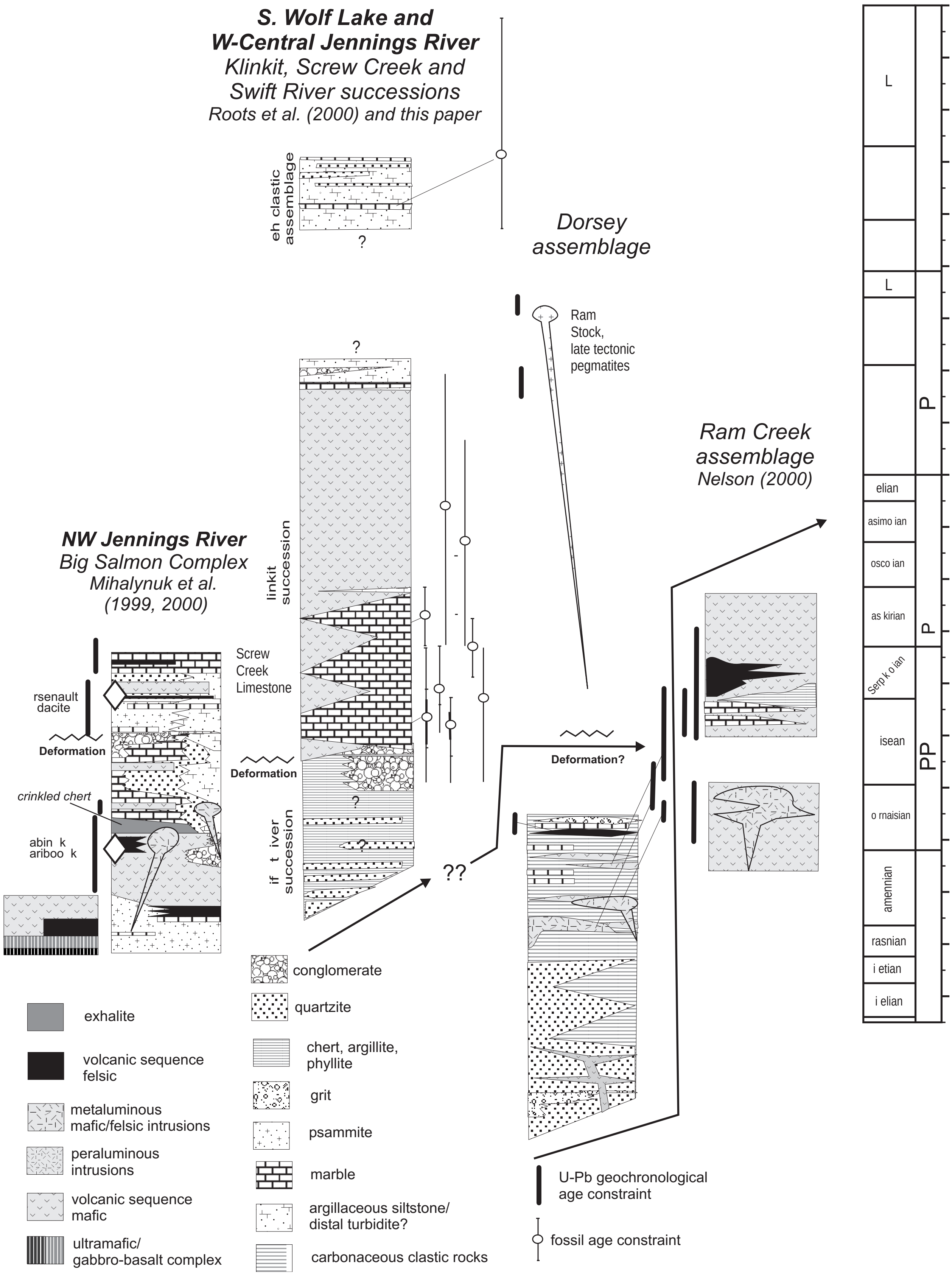

Figure 2. Stratigraphic columns for units of the Dorsey Terrane and Big Salmon Complex. Data sources for fossil and radiometric constraints: 1. E.W. Bamber (personal communication 1998): this paper Table 1. 2. E.W. Bamber (personal communication 2000) 3. Stevens and Harms (2000) 4. Roots and Heaman (2001) 5. Nelson *et al*. (2000).

Mapping results from this year's program are available at 1:50,000 scale (Nelson *et al*., 2001). Field work focused on the Dorsey Terrane, a complex pericratonic entity that outcrops west of the Cretaceous Cassiar batholith. Harms and Stevens (1996) divided the eastern and central Dorsey Terrane into four assemblages (Figure 2). From most easterly and structurally lowest they are: the Ram Creek, Dorsey, Swift River and Klinkit assemblages. It should be noted that the Dorsey assemblage is a sub-unit of the Dorsey Terrane. The Jennings/Wolf project has further subdivided these assemblages into regionally mappable subunits and has provided age control by uranium-lead dating. It has also explored relationships between the various assemblages; and between them and the Big Salmon Complex, now recognized as the southeastern extension of the Yukon Tanana Terrane in the Teslin and Wolf Lake map areas (Mihalynuk *et al*., 1998, 2000).

Coverage includes the Plate Lake (104O/15) and eastern half of Swan Lake (104O/14E) map areas. The Alaska Highway, which locally follows the Swift River and crosses into B.C. east of McNaughton Creek, offers access to a small part of it. Most access is by helicopter. In this region, isolated mountains and ridges are separated by broad, flat, outwash and till-filled valleys; bedrock exposure accordingly varies from excellent to non-existent.

LOCAL GEOLOGY

The map area straddles two terranes, the allochthonous, pericratonic Dorsey and the para-autochthonous, miogeoclinal Cassiar terrane, which here are separated by the Cassiar Fault (Figure 3, Figure 3-legend). The Cassiar Fault is a dextral transcurrent fault of regional extent, with K-Ar evidence for mid-Cretaceous displacement (Gabrielse, 1985). Lower Paleozoic Cassiar Terrane strata only occur within an embayment in the Cassiar batholith in northeastern 104O/15. They are contiguous with extensive miogeoclinal exposures located farther east in 104O/16 (Nelson and Bradford, 1987).

The Dorsey Terrane consists of stratified and metamorphic rocks intruded by several large Early Jurassic plutons, the Simpson Peak and Nome Lake batholiths and the Plate Creek Stock. The structurally lowest, regionally metamorphosed rocks in the Dorsey Terrane are assigned to the Dorsey assemblage, based on their correlation with along-strike exposures in southern Yukon (Stevens and Harms, 2000) and south of the Nome Lake Batholith (Nelson, 2000). Structurally overlying the Dorsey Assemblage, and dominating the central and western parts of the map area, are stratified rocks of the Swift River succession, Mississippian to Pennsylvanian Screw Creek limestone, and Klinkit succession (Figure 2). [The term "succession" is introduced here in preference to "assemblage" in naming these stratified units, because they exhibit clear sedimentary and volcanic protolith textures, stratigraphic continuity, and depositional contacts, in spite of considerable penetrative deformation.] The stratigraphically lowest Swift River succession overlies the Dorsey assemblage along faulted contacts. It is dominated by cherts and argillites with lesser siliclastic components. A local accumulation of grits and quartzites interbedded with chert, argillite and dust-tuff occurs at its top in northern 104O/14E (Figure 3). It is unconformably overlain by the Screw Creek limestone. The Klinkit succession, which overlies and also interfingers with the Screw Creek limestone, is dominated by volcaniclastic/epiclastic rocks with lesser siliciclastic components.

The northern margins of the Early Jurassic Nome Lake and Simpson Peak batholiths are exposed in the southern part of the map area. They are post-tectonic, cutting all units and structures in the Dorsey Terrane, including the Dorsey assemblage/Swift River succession contact and a set of northerly-striking normal faults with west-side down displacement.

Dorsey Terrane

DORSEY ASSEMBLAGE

The Dorsey assemblage forms a narrow strip along the eastern margin of the Dorsey Terrane, lying structurally above the Ram Creek assemblage and below the Swift River succession/Screw Creek limestone/Klinkit succession (Figure 1). In 104O/15, the Ram Creek assemblage is cut out by the Cassiar Fault and the Dorsey assemblage is juxtaposed directly against the Cassiar Batholith. The Dorsey assemblage here is divisible into two units, upper and lower. Unlike the other stratified units except the base of the Swift River succession, it has undergone regional metamorphism to garnet grade. In 104O/15, its lower part is a thick (probably structurally repeated) sequence of metamorphosed quartz-plagioclase grit, greywacke, quartzite, and phyllite. Its upper part is more variable, with magnetite-porphyroblastic biotite-sericite-chlorite schist and quartz-sericite schist representing intermediate and felsic meta-tuffs respectively, interlayered with meta-chert, quartzite, phyllite, meta-grit and meta-tonalite. The two units are now juxtaposed across northerly normal faults. The upper/lower distinction within the Dorsey assemblage here does not directly correspond to that defined farther south, which is based on the presence of abundant metabasites in the lower unit (Nelson *et al*., 1999; 2000). Metabasites are notably missing in this area, although in other respects, such as the mixed siliciclastic/basinal/distal volcanic protoliths, degree of metamorphism and intensity of deformation, the Dorsey assemblage in 104O/15 strongly resembles localities to the north and south.

Although minor grits occur near the top of the Dorsey assemblage in the Yukon (Roots *et al.*, 2000; author's field observations near Munson Lake), the thick sequence of coarse siliciclastics in the lower Dorsey assemblage in 104O/15 is unusual. Its closest parallel is in 104O/1, in the southeastern Jennings River area near the Cottonwood River, where a thick sequence of metamorphosed quartzose clastics is intruded by pre-metamorphic ultra-

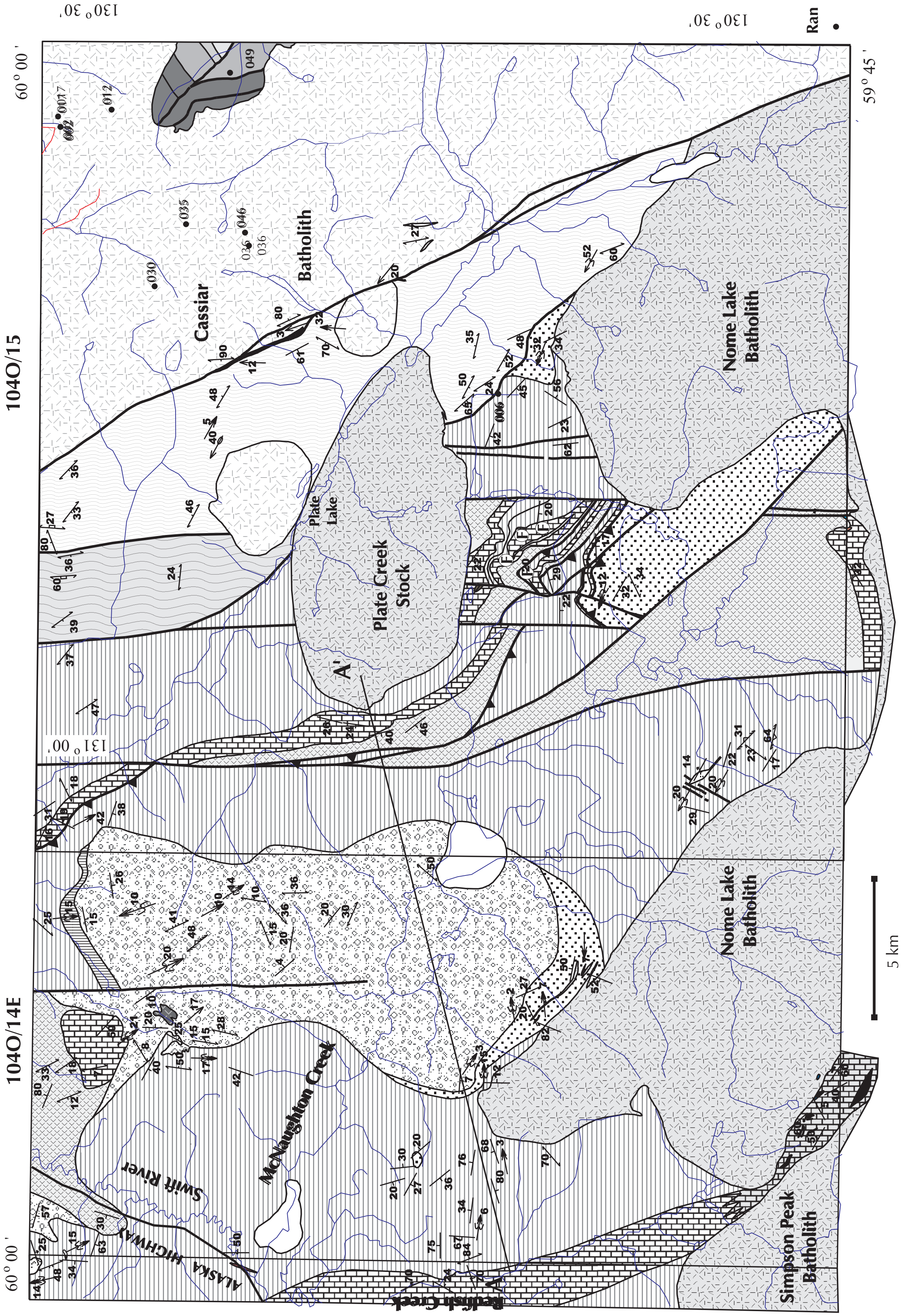

Figure 3. Geology of 104O/14E and 15.

LEGEND FOR FIGURE 3

POST-ACCRETIONARY UNITS
QUATERNARY

Tuya basalt: valley-filling basalt flows

EARLY CRETACEOUS (circa 110 Ma)
Granite, granodiorite, quartz monzonite, diorite; granite protomylonite and mylonite along Cassiar Fault

DORSEY TERRANE
EARLY JURASSIC (circa 188 Ma)
Simpson Peak and Nome Lake batholiths: coarse grained granodiorite, diorite, granite;
Plate Creek Stock: medium grained hornblende diorite, coarse grained gabbro, granodiorite

UPPER PALEOZOIC
KLINKIT SUCCESSION

Andesite flow or sill

Epiclastic and pyroclastic rocks, predominantly medium green lapilli tuff and tuffaceous siltstone;
maroon and green tuffaceous phyllite, green to grey well-bedded chert, argillite and quartz arenite

MISSISSIPPIAN-PENNSYLVANIAN
SCREW CREEK LIMESTONE

Grey limestone, locally silicified, locally fossiliferous; maroon and green phyllite; green well-bedded chert,
limestone-matrix and phyllite-matrix volcanic and/or chert-clast conglomerate

Calc-silicate hornfels, marble, metasandstone, metasiltstone, metavolcanic hornfels

White marble

UPPER PALEOZOIC
SWIFT RIVER SUCCESSION

Greywacke, quartz-plagioclase grit, quartz arenite , chert, grey to green-grey phyllite,
minor thin limestone beds, maroon and green phyllite, pebble conglomerate

Black, grey, grey-green thick to thin-bedded chert, argillite with prominent grey to white quartzite beds

Green phyllite, fine grained, thin-bedded tuff

Black, grey, grey-green thick to thin-bedded chert, argillite, local clean grey to white quartz arenite;
quartzite-clast conglomerate and chert-clast greywacke near top

PALEOZOIC (AND OLDER?)
DORSEY ASSEMBLAGE

Upper Dorsey assemblage: green phyllite with magnetite porphyroblasts, chlorite schist, mafic schist,
quartz-sericite schist, metachert, quartzite, highly foliated metaplutonic rocks

Lower Dorsey assemblage: quartz-plagioclase grit, quartzite, quartz-feldspathic schist, phyllite, pelitic schist

CASSIAR TERRANE
SILURIAN-DEVONIAN
RAMHORN FORMATION

Dolomitic quartz arenite, quartzite, dolostone, limestone

ORDOVICIAN-SILURIAN
ROAD RIVER GROUP

Black, commonly limy slate, locally graptolitic; argillaceous limestone
OSRR?:Road River Group?: Black slate in sliver along Cassiar Fault zone (could be Earn Group)

CAMBRIAN-ORDOVICIAN
KECHIKA GROUP

Pale-coloured calcareous slate, siltstone, limestone, calc-silicate and biotite hornfels

LOWER CAMBRIAN
ROSELLA FORMATION

Limestone, dolostone, marble, thin-bedded calcsilicate hornfels mafic and mafic sills (Nelson, 2000). The tuffaceous protoliths in the upper part of the Dorsey assemblage in 104O/15 are like those in the upper Dorsey south of the Nome Lake batholith (Nelson, 1999, 2000) and in the Yukon (Roots and Heaman, 2001). In the Yukon, one quartz-phyric metatuff yielded a 355 Ma zircon age (Roots and Heaman, 2001), identical to that of a dated intrusion within the Dorsey assemblage near the Cottonwood River (R. Friedman personal communication, in Nelson, 1999). These dates on representative bodies of an extensive metavolcanic and metaplutonic suite constrain the Dorsey assemblage to be early Mississippian and older, and suggest that it represents both the thin volcanic carapace and pericratonic substrate of an early Mississippian arc.

SWIFT RIVER SUCCESSION

The Swift River succession overlies the Dorsey assemblage on a sheared contact south of Plate Lake. It is unconformably overlain by the Screw Creek limestone at numerous localities throughout the map area. It exhibits two depositional themes: hemipelagic, deep-water sedimentation that gave rise to thick successions of dark-coloured chert and argillite; and sporadic siliciclastic influx, represented by quartzite/phyllite sequences near its base, local units of quartz wacke, grit, argillite and phyllite, particularily near its top in northern 104O/14, and isolated beds of clean quartzite within otherwise monotonous chert-argillite piles. Swift River cherts are thin to thick ribbon-bedded (2-20 centimetre beds). They are predominantly black, also grey and greenish to olive grey: this attests to their deposition in deep, anoxic waters, in contrast with the bright maroon and green colours within the overlying Screw Creek limestone and Klinkit succession. The thickness of the Swift River succession cannot be determined within the present area, as no intact, unfaulted top to bottom sections are present. In the southern Yukon its structural thickness is of the order of 3.5 kilometres, of which over 95% is chert and argillite.

In places near the top of the unit, chert-chip breccias (sharpstone conglomerates) occur interbedded with chert. Black to grey angular chert clasts are identical to the bedded cherts around them, and so could be derived intraformationally. A particularily spectacular example of coarse clastics occurs around the Northwest Tel repeater tower located between Screw and Partidge Creeks, 3 kilometres west of the map area, where boulder conglomerates with chert and quartzite clasts are interbedded with the uppermost chert and argillite of the Swift River succession east of and stratigraphically below the base of the Screw Creek limestone. All of the clasts represent units found within the Swift River succession. In contrast with the smaller breccia occurrences, some of the clasts are rounded, indicating subareal, stream or beach transport prior to incorporation in submarine debris flows. Perhaps the sharpstone beds represent the development of seafloor relief (through faulting?), while the “Repeater Tower conglomerate” represents actual erosion into parts of the Swift River succession. There is no direct age control on the Swift River, other than that it predates the late Mississippian-early Pennsylvanian Screw Creek limestone.

In easternmost 104O/14 and western 104O/15, the highest Swift River unit is in part an unusual, undated siliciclastic sequence, uPSRgw, which contains elements that show a disturbing resemblance to the Klinkit or even the Dorsey assemblage. This enigmatic unit was previously assigned to the lower Jurassic by Gabrielse (1969), based on its coarse and immature clastic character. Most of its exposures are on the crest of a flat, bifurcating ridge crest in northeastern 104O/14E. There, it consists of strongly deformed quartzite, quartz- plagioclase-microcline grit, quartz wacke, phyllite, chert, argillite and minor calcareous layers. Colours are monotonous greys, grey-buffs, greenish greys. However, stratigraphically lower, nearer its basal contact above the Swift River succession, green tuffaceous phyllite and siltstone and maroon and green phyllite form part of the sequence. These suggest an affinity with the Klinkit succession. The base of the unit rests abruptly on top of Swift River black chert and argillite. This contact is well exposed on the low, forested ridge 7 kilometres east of the Swift River, and on the B.C.-Yukon border at the northwestern corner of 104O/14E, east of Partidge Creek. At the first locality, the two units are interfolded to form a series of recumbent secondary folds on the eastern limb of a westerly-overturned anticline (Figure 3). Here, the grit unit is overlain by two distinct units: on top of the ridge, by an andesite flow or sill with green tuffaceous siltstones at its base; and at the north end of the ridge by maroon and green tuffaceous phyllite that interfinger with a grey limestone assigned to the Screw Creek. Near Partridge Creek, Screw Creek-like limestone is missing altogether and monotonous black chert of the Swift River succession is overlain along strike either by grit, greywacke and phyllite or by green siltstone, tuff, and well-bedded sea-green chert of the lowest Klinkit. Such abrupt changes could be explained as the result of multiple unconformities and local volcanic, clastic and limestone facies development in a tectonically active arc.

In thin section, grits of this unit are dominated by clasts of coarse, monocrystalline quartz and plagioclase with minor microcline and muscovite and traces of biotite, muscovite schist, tourmaline and zircon. A predominantly plutonic and subordinate metamorphic source is indicated. This source could be the Dorsey assemblage, in which case it was exposed and undergoing erosion by late Mississippian time.

SCREW CREEK LIMESTONE

Named for Screw Creek in 104O/14W, where it is extensively exposed, the Screw Creek limestone provides an excellent marker that is structurally repeated throughout the present map area as well as in adjacent parts of the Yukon (Figure 1). An important mapping result from this season was to trace the previously-known outcropping belt of the limestone from north of the Alaska Highway southwards for over 15 kilometres into the valley of Redfish Creek. It is inferred to extend farther south into marble/calcsilicate hornfels exposures that separate the Simpson Peak and Nome Lake batholiths in the southeastern corner of the map area. Along Redfish as well as Screw Creek north of the Alaska highway, the Screw Creek limestone occupies the core of a southwesterly-overturned syncline, with Swift River succession chert, argillite and siliciclastics exposed both to the east and west (Figures 1 and 3). This outrcrop belt extends from west of the Seagull Batholith to the narrow inlier between the Simpson Peak and Nome Lake batholiths, a distance of over 30 kilometres. In a second, more easterly area of exposure, the Screw Creek limestone, overlain by Klinkit succession volcaniclastic epiclastic strata, outcrops patchily in a much broader synclinal keel that runs from near the Swift River truck stop through the southern reaches of McNaughton Creek. A third group of exposures lies northeast of a thrust fault west of Plate Creek, which splays into a set of thrust faults that repeat the limestone on a set of ridges south of the Plate Creek Stock. Our mapping corroborates the suggestion of Gabrielse (1969) that other limestone bodies in the area, mapped by him as 12b, 12c, are in fact correlatives of the Screw Creek limestone.

The Screw Creek limestone exhibits considerable internal variation in all of its exposures, consistent with its probable development in an active arc or arc-marginal location. It includes grey limestone that ranges from barren to richly fossiliferous, green tuffaceous limestone, red and green chert-clast conglomerate interbeds, green and maroon phyllite, sea-green chert, and local green volcaniclastic accumulations. Fossils include crinoids, corals and brachiopods. Only a few have been observed in growth position; most occur in debris beds that suggest down-slope transport. Ages of separate fossil collections from the main Screw Creek limestone range from late Mississippian to early Pennsylvanian (M.J. Orchard, in Stevens and Harms 2000; W. Bamber personal communication 2000). The limestones south of the Plate Creek Stock yielded four collections, two of which are late Mississippian and one of which is early Pennsylvanian to Early Permian (W. Bamber, personal communication 1998; Table 1). A Pennsylvanian-Early Permian conodont age was obtained from the extension of this belt of limestone north of Swift River (M.J. Orchard, in Stevens and Harms 2000). These ages show that the Screw Creek limestone was deposited over a considerable time interval, at least from late Mississippian through early Pennsylvanian and perhaps into the Permian. The presence of volcaniclastic and epiclastic debris in it suggests that it interfingers with the volcanogenic Klinkit succession.

Klinkit Succession

The Klinkit succession in 104O/14E and 15 is characterized by its volcanic and epiclastic rocks. It also contains quartz clastics, and interfingers with the Screw Creek limestone. Its green and locally bright maroon palette contrasts sharply with the monotonous dark tones of the main Swift River succession. A 5-20 metre thick unit of maroon and green chert marks its base above the Screw Creek limestone in thrust imbricates south of the Plate Creek stock. Typical rock types throughout the Klinkit succession are green heterolithic lapilli tuff, volcanic sandstone and tuffaceous siltstone, accompanied by green tuffaceous phyllite, green chert, quartzite, and local conglomerates. The lapilli tuff contains chloritic ash lapilli and lesser lithic clasts of intermediate composition, including epidote-rich (altered?) fragments. Flow rocks are rare in this area. One andesite flow or sill occurs on a brushy summit 7 kilometres east of the Swift River. Fine fragmental units with a mixture of volcanic and sedimentary clastic material are common in the Klinkit succession. On the south side of the Alaska Highway, 3 kilometres east of the Swift River truck stop and 2 kilometres north of the Yukon border, volcanic-matrix conglomerate contains abundant large white limestone clasts. Just south of this outcrop, blocks of quartzite occur in a green

TABLE 1
MACROFOSSIL IDENTIFICATIONS FROM SCREW CREEK LIMESTONE IN CENTRAL 104O/15

Station	UTM East	UTM North	Fauna	Age
96JN38-4	397841.1	6632433.8	*Siphonodendron lisburnensis* Armstrong?	Early Carboniferous (Late Visean or Serpukhovian)
96JN38-8	397135.7	6632688.2	*Petalaxis* ? Spec. indet.	?Early Carboniferous to Early Permian (Asselian)
96JN38-10	399102.1	6636283.1	*Stelechophyllum* sp. cf. S. mclareni	Early Carboniferous (Late Visean or Serpukhovian)
96JN38-12	399366.1	6635738	*Paraheritschoides?* sp.	Bashkirian? to Early Permian (Asselian)

Identifications from E.W. Bamber, Geological Survey of Canada, Paleontological Report 1-EWB-1998 epiclastic sandstone “greenwacke” matrix. The blocks appear to represent pieces of a single, slumped bed. Polylithic conglomerate occurs a half-kilometer south of the Yukon border and 2.5 kilometres southeast of the limestone-clast highway exposure. It contains clasts of quartzite, chert, argillite and greenstone in a chloritic matrix. It is interbedded with green quartz-plagioclase grit, and occurs near green pyroclastic breccia with abundant subangular to subrounded andesitic clasts in the 1-5 centimetre range. This mixing of siliciclastic and volcanogenic units is a local microcosm of the Klinkit succession as a whole: it documents the development of discrete, mainly intermediate, volcanic centres in a pericratonic environment. The Klinkit succession in this area has a distal volcanic character, in contrast with the thick piles of flows and coarse fragmentals seen elsewhere, for instance south of Munson Lake in the southern Yukon, and near Teh Creek in west-central Jennings River area.

INTRUSIVE BODIES

Early Jurassic Suite

The Nome Lake and Simpson Peak batholiths outcrop in the southern part of the area. They are essentially the same body, divided by a narrow screen of calc-silicate and hornfels in the headwaters of Redfish Creek. The Nome Lake batholith southwest of McNaughton Creek is a uniform, coarse-grained equigranular hornblende-biotite granodiorite characterized by large, round, equant quartz “raisins” .5 centimetres in diameter, and scattered mafic inclusions. The abundance (roughly 20%) and prominent shapes of the quartz grains in this phase are unusual in the Early Jurassic intrusive bodies, which tend to contain only minor, interstitial quartz except in uncommon granite phases. The eastern margin of the Simpson Peak body is exposed in the southwestern corner of the map area. It consists of coarse grained biotite-hornblende tonalite and granite. The multiphase Plate Creek Stock crops out in the centre of the map area. Its areal extent is smaller in our interpretation than that of Gabrielse (1969), restricted to the area southwest of the Plate Creek valley. It is a highly variable body, as is typical of the Early Jurassic suite. Near its western margin it has two compositional variants: medium grained equigranular granodiorite to diorite with 20 to 25% mafic minerals, hornblende > biotite; and coarse grained granodiorite with 10-15% biotite and scarce hornblende. Along its southern margin a mafic to ultramafic border phase shows extreme variation in grain size, from medium grained to pegmatitic, and in percentage of mafic minerals, from 40% in medium grained diorite to over 80% in hornblende pegmatites.

Hornblende-phyric dikes occur sporadically throughout the terrane. Typically, they are andesitic to trachyandesitic in composition, with acicular hornblende and subordinate lath-shaped plagioclase phenocrysts. Small mafic inclusions are a typical, though not universal feature. Like the larger Early Jurassic bodies, these dikes are unfoliated, and in some cases cut faults and shear zones. They are assumed to be part of the Early Jurassic intrusive suite.

Mid-Cretaceous? Intrusions

Two separate, texturally and compositionally distinctive bodies intrude the Dorsey assemblage northeast of Plate Creek. Previously included within the Plate Creek stock (Gabrielse, 1969), these have been distinguished in our mapping (Figure 3). The more northerly body is a Kspar-megacrystic granite cut by aplite and pegmatite dikes, which strongly resembles the nearby Cassiar Batholith. The more southerly body is a coarse grained, equigranular granite dominated by equant plagioclase and globular quartz. The interstitial mafic minerals in it, biotite and hornblende, are completely chloritized. It cuts strongly deformed and metamorphosed lower Dorsey assemblage schists, but is itself unfoliated. A zircon age determination is in progress.

Cassiar Terrane

STRATIFIED UNITS

Lower Paleozoic Cassiar Terrane strata are exposed in an embayment in the Cassiar batholith in the northeastern corner of the map area. They include the Lower Cambrian Boya and Rosella formations and the Kechika and Road River groups. Geology in this area is continuous with more extensive exposures to the east (104O/16; Nelson and Bradford, 1987).

CASSIAR BATHOLITH

The mid-Cretaceous Cassiar Batholith outcrops in the highest ranges of the Cassiar Mountains on both sides of Tootsee Lake. It is predominantly granitic, ranging from coarse grained equigranular to Kspar-megacrystic, and granodioritic in areas of higher hornblende-biotite concentration. Aplites and pegmatites cut the main phases.

Structure

The map area can be seen as four structural zones, with different phases of deformation dominating in each (Figure 3). East of the Cassiar Fault, the relatively undeformed Cassiar batholith intrudes folded and block-faulted strata of the Cassiar Terrane. Although farther south the Dorsey and Cassiar terranes are juxtaposed across a gently-dipping thrust fault (Nelson, 2000; Nelson *et al*., 2000) in this area the post-accretionary Cassiar Fault forms the terrane boundary. The fault is expressed as anastomosing mylonite zones at the western edge of the Cassiar Batholith in the high country northeast of Plate Lake and in the headwaters of Carlick Creek. From the Cassiar Fault westwards to McNaughton Creek in the south, and to the eastern margin on 104O/14 in the north, the stratified rocks of the Dorsey Terrane dip moderately southwestward, forming a homocline with the lower Dorsey assemblage exposed at its northeastern base, overlain sequentially by the Swift River succession, Screw Creek limestone and, in places, Klinkit volcanics. This central panel is bounded to the southwest by a thrust fault, or set of thrust faults, that repeat the upper Paleozoic stratigraphy. Southwest of the thrust faults, in the fourth structural zone, the stratified rocks dip very gently, except for the steep to overturned Screw Creek limestone along Redfish Creek on the western boder of 104O/14E. The structure of this western area is interpreted as a series of southwesterly-vergent recumbent folds involving the Swift River, Screw Creek and Klinkit successions.

At least five phases of deformation are recognized in the Dorsey Terrane stratified rocks (Figure 4). All of them predate the Early Jurassic intrusions. The earliest phase (D1) involved the development of a foliation in all units, which was affected by subsequent folding events. The issue of whether the metamorphic Dorsey assemblage underwent deformation that did not affect the other units, cannot be resolved from current data in this area. South of the Nome Lake Batholith, a strong east-west quartz stretching lineation is restricted to the Dorsey assemblage and lowermost part of the Swift River succession (Nelson, 2000).

In the current map area, the first recognizable folding event (D2) created minor and outcrop-scale recumbent folds in the Swift River succession southwest of McNaughton Creek. Their trends, roughly easterly, are sharply discordant with those of the major north-northwesterly D3 recumbent folds; they may represent an event that only affected the Swift River and not the overlying Screw Creek limestone and Klinkit succession.

The best example of a regional D3 fold is the overturned, southwesterly-verging syncline that involves the Screw Creek limestone in the valleys of Screw and Redfish creeks. It trends north-northwest over more than 30 kilometres. The axis of a D3 anticline is interpreted in the Swift River succession just southwest of McNaughton Creek; farther to the northeast, overlying Klinkit and Screw Creek strata reappear. Thrust faults (D4) east of McNaughton Creek truncate the southwesterly verging fold pattern: this suggests that they are younger. They dip southwest, and are inferred to have northeasterly displacement. Thus, in the Dorsey Terrane, southwesterly-verging ductile deformation (D3) was succeeded by brittle northeasterly-vergent thrusts (D4). Northeasterly-vergent minor chevron folds form part of this late episode. The thrust faults are truncated by a series of north-trending, generally west-side-down normal faults (D5). The top of the Dorsey assemblage between the Nome Lake Batholith and Plate Creek stock is a more gently southwest-dipping, layer-parallel shear zone with Swift River succession in its hanging wall. The normal sense on this contact is shown by shear bands and upward decrease of metamorphic grade. Both the Dorsey assemblage/Swift River succession contact and the high angle faults are cut off by the Early Jurassic intrusions.

D1

Foliation parallel to layering is developed in all of the Dorsey Terrane units in the map area, from the basal Dorsey assemblage to the uppermost Klinkit volcaniclastics. Particularily in the upper units, foliation development is variable. This may largely reflect compositional control. Metatuffs and phyllites with abundant platey minerals - sericite, chlorite, and biotite - more readily acquire a foliation than cherts, quartzites, or limestones. Foliation development in clastic rocks is dependant on the amount and nature of the matrix, whether phyllitic or quartz-rich.

D2

The D2 event involved recumbent folding in the Swift River succession around axes that average 257/24 (Figure 4), now shown in concentrations of minor folds and local modification of gently dipping contacts. The D2 fold axes are geometrically very distinct from the north-northwesterly trends of D3. This early episode does not have the regional expression of D3; no map-scale F2 folds have been identified. Although D2 minor folds are prevalent between Redfish McNaughton Creeks, the basal surface of the Screw Creek limestone along Redfish Creek has not been modified by east-northeasterly folding: for this reason, D2 is considered to predate deposition of the limestone.

D3

This episode of north-northwest-trending recumbent folding produced the major map patterns in the western part of the map area (Figure 3). The character of D3 deformation is shown in the cross section in Figure 4. To the west along Redfish Creek, the Screw Creek limestone forms a tight, westerly-verging synclinal closure. This outcrop belt is separated from gently-dipping Screw Creek and Klinkit units to the east by a recumbent anticline cored by Swift River chert, argillite and siliciclastics. Along Redfish Creek, the Screw Creek limestone is nearly vertical. Bedding facing directions in the uppermost Swift River there show tops to the west. Northeast of the anticlinal axis, the S3 cleavage dips somewhat more steeply to the northeast than do major unit contacts: this is seen clearly on the flat ridge 10 kilometres east of the Swift River. Minor fold axes (F3) associated with this event average 151/15 (Figure 4). Some of these measurements come from mountain-side exposures in northern 104O/14E, where the contact between Swift River cherts and the highest Swift River clastic unit is intricately interfolded on the northeastern limb of the regional anticline.

D4

Just northeast of McNaughton Creek in the south, and at the eastern margin of 104O/14 in the north, the stratified rocks tilt southwestwards and are cut by at least one northwesterly-striking, southwesterly-dipping thrust

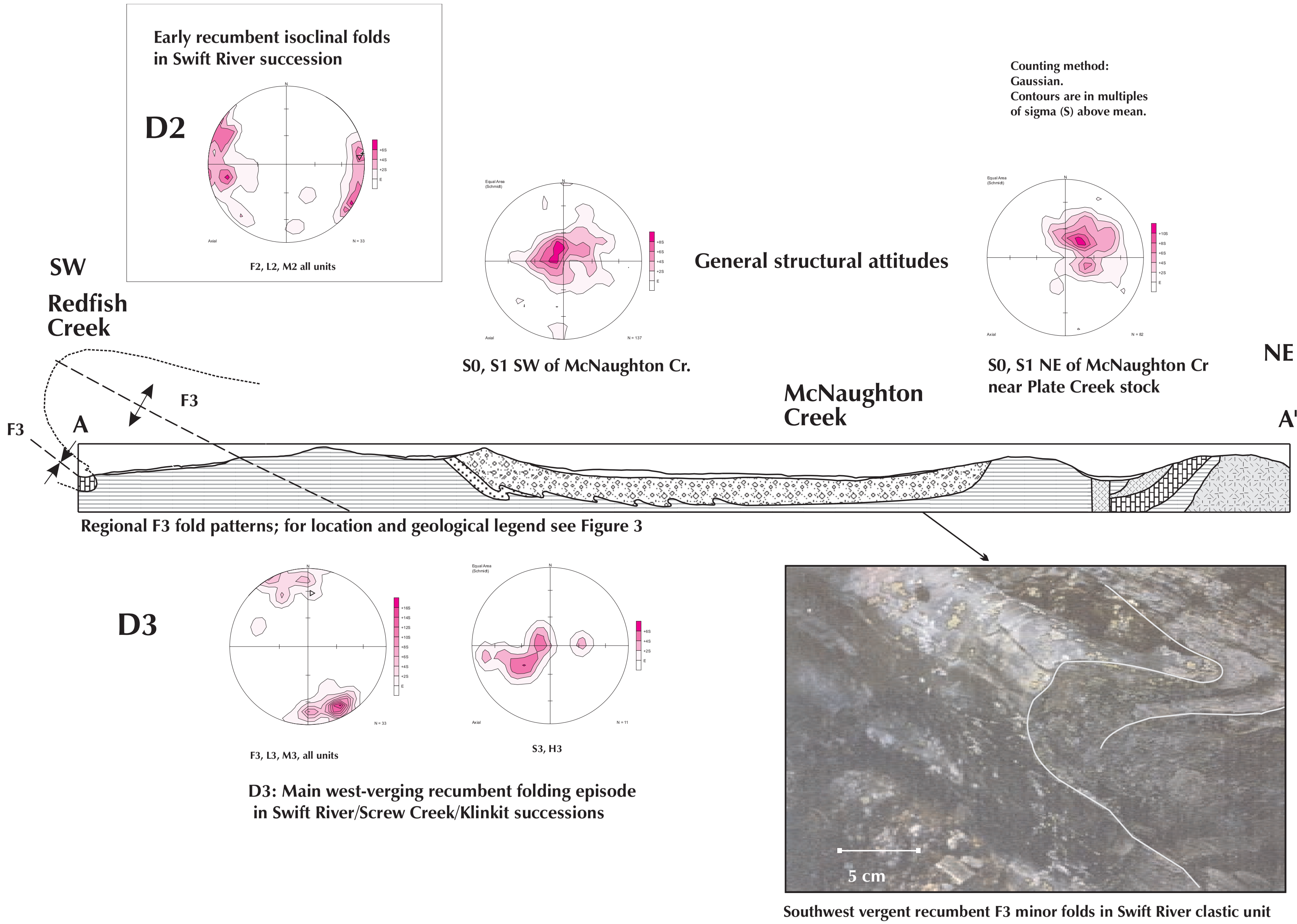
Early recumbent isoclinal folds
in Swift River succession
D2
F2, L2, M2 all units
SW
Redfish
Creek
S0, S1 SW of McNaughton Cr.
General structural attitudes
Counting method:
Gaussian.
Contours are in multiples
of sigma (S) above mean.
S0, S1 NE of McNaughton Cr
near Plate Creek stock
NE
McNaughton
Creek
A
A'
F3
F3
Regional F3 fold patterns; for location and geological legend see Figure 3
D3
F3, L3, M3, all units
S3, H3
D3: Main west-verging recumbent folding episode
in Swift River/Screw Creek/Klinkit successions
5 cm
Southwest vergent recumbent F3 minor folds in Swift River clastic unit

Figure 4.

Late events

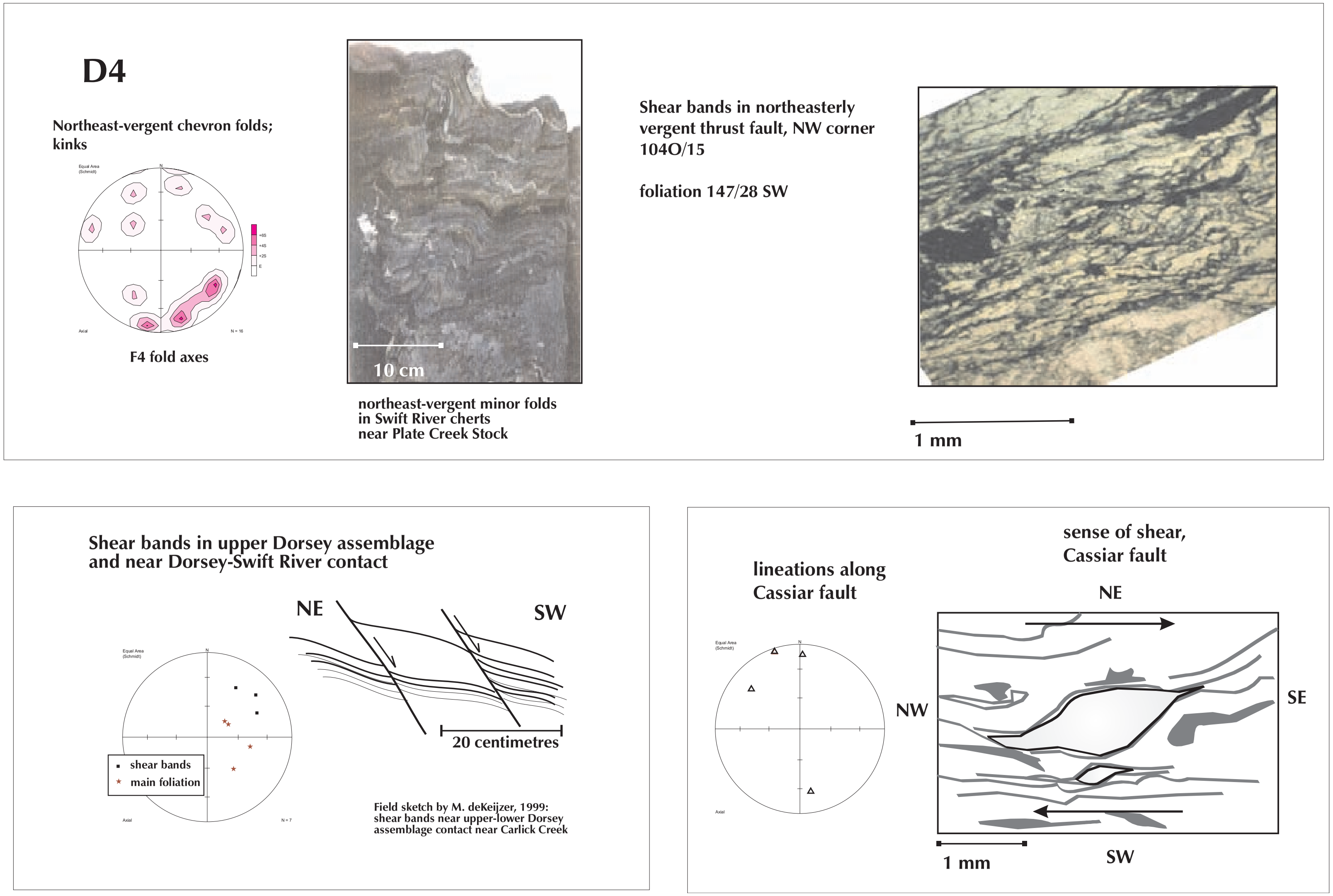

Figure 4. Deformational events and styles in the 1040O/14E, 15 map area.

fault. In the complex of thrust panels south of the Plate Creek stock, two fossil collections from the Screw Creek limestone show an older-over-younger relationship, with late Mississippian corals in the overlying, and Pennsylvanian in the lower panel. A shear zone related to this fault episode, located 2 kilometres west of Plate Creek near the northern boundary of the map area, shows top to the northeast shear bands (Figure 4). It is cut by an undeformed hornblende porphyry dike. Northwesterly-trending chevron folds (F4, Figure 4), many with northeasterly vergence, are best developed near the zone of thrusting.

NORMAL FAULTS

A set of steep north-stiking, west-side down normal faults cut the Dorsey assemblage and stratified units of the Dorsey Terrane in the central part of the map area. Such a fault is inferred to juxtapose upper and lower Dorsey assemblage in the Carlick Creek drainage. Well-developed shear bands in the upper Dorsey assemblage near it show top-down-to-southwest displacement. Another fault in this set juxtaposes thrust-imbricated Klinkit, Screw Creek and Swift River succession with Swift River between the Plate Creek stock and Nome Lake Batholith. On the ridges immediately east, parallel strands within the Swift River succession are expressed as zones of iron staining, high fracture density, and Fe-oxide-cemented breccias.

None of these faults appear the offset the Early Jurassic intrusions; and the two exposed strands described above are clearly truncated by the Plate Creek stock.

The southwest-dipping top of the Dorsey assemblage is well-exposed in a gully 4 kilometres south of Plate Lake. There, a lithologic transition occurs up-section over 200 metres of outcrop. At the base of the section, but above the highest Dorsey grits, a thin and highly variable upper Dorsey assemblage - garnetiferous and magnetite-bearing green biotite-sericite-chlorite schist, quartzite, amphibolite, black phyllite, and quartz-sericite schist - passes into monotonous black chert and phyllite/argillite of the lower Swift River succession. In the uppermost Dorsey assemblage, garnet-bearing schist occurs as nodules within retrograde magnetite-porphyroblastic biotite schist. There is not an appreciable metamorphic grade diifference between this retrograde assemblage, and biotite-bearing assemblages developed in Swift River phyllites immediately above the contact. The area of the contact is strongly sheared throughout. Lensoid bodies of intact rock are separated by distinct, anastomosing brittle shear zones that contain fault breccia and cataclasite. A tonalite dyke, texturally similar to the nearby Nome Lake Batholith and Plate Creek stock, cuts across the shear zone and is neither displaced nor deformed.

Field observations showed shear bands and minor faults that dip more steeply to the southwest than the overall foliation. A thin section of black biotite phyllite from near the base of the Swift River succession indicates top-to-the-southwest shear sense in sigma-shaped composite biotite porphyroblasts. These features suggest that the last motion to occur near the Dorsey/Swift River contact was of normal sense. Similar observations were made at this contact south of the Nome Lake batholith (Nelson, 2000).

THE CASSIAR FAULT

Within the map area, the Dorsey and Cassiar terranes are juxtaposed across the Cassiar Fault. Farther south, this fault truncates an earlier thrust-faulted accretionary boundary (Nelson *et al.*, 2000). The Cassiar Fault strikes north-northwesterly and is essentially vertical. Protomylonite is developed along fault splays in the Cassiar Batholith up to 4 kilometres east of the main strand of the fault in the southeastern corner of the map area. Along the fault itself, mylonite development is intense: dark grey sugary mylonite stringers cut through protomylonitized Kspar-megacrystic granite. Field and thin section observations confirmed the dextral sense of motion on the fault (Figure 4).

In an area 3 kilometres northeast of Plate Lake, weakly deformed muscovite pegmatites, presumably a late phase of the Cassiar Batholith, cut across previously protomylonitized granite and are not displaced. Textures in these pegmatites - kinking of muscovite plates and mortar texture in quartz - suggest that they are late synkinematic to the mylonite-forming event. If they are late melts of the Cassiar batholith, this suggests that most of the motion on the Cassiar fault took place after overall cooling of the batholith, but before its final solidification.

MINERAL DEPOSITS AND MINERAL POTENTIAL

The known mineral occurrences in the map area are of three types: silver-lead-zinc veins within the Cassiar Batholith, one skarn and one instance of stibnite (epithermal?) veining near the Plate Creek stock.

POLYMETALLIC VEINS

The Holliday-Discovery (104O-001), Holliday-Shipment (104O-002), Lake (104O-012), and Pit (104O-017) are groups of narrow but high-grade veins hosted by Cassiar batholith granite in the headwaters of Freer and Alan Creeks. Narrow, decimetre-scale galena-sphalerite-pyrite veins are surrounded by thin selvages of sericitic alteration. A 14 tonne combined shipment from the Discovery and Pit zones in 1979 assayed 1.3 g/tonne Au, 532 g/tonne Ag, 29.1% Pb and 13.9% Zn (DIAND, 1983), and in 1983 the George Cross Newsletter reported inferred ore in the Discovery-Shipment-Pit veins at 36, 287 tonnes with 427.2 g/tonne Ag, 14.95% Pb and 20.78% Zn (cited in MINFILE). Lead isotopic signatures from the Lucky vein of this group plot in a cluster with other local polymetallic occurrences of known mid-Cretaceous (Silverknife) through Eocene (YP) age (Bradford, 1988). Abbott (1984) has related the veins and replacements of the Rancheria district to small granites that post-date the main Cassiar Batholith.

SKARNS

The Bear showing (104O-049) is a garnet-diopside skarn in the Kechika Group that contains scheelite, molybdenite, powellite and minor galena (MINFILE). It is located in the embayment in the Cassiar batholith in far eastern 104O/15, where granite probably underlies the strongly hornfelsed metasedimentary rocks at fairly shallow depths (Bradford, 1988). Trenching has exposed two stratabound skarn bodies up to 1 metre wide (MINFILE).

During fieldwork this year, malachite stains were noted in rusty calcsilicates in the inlier between the Nome Lake and Simpson Peak batholiths, suggesting the possibility of skarn-type mineralization. The new stream-sediment geochemical release (Jackaman, 2000) identified two highly anomalous Au values in Redfish Creek of 500 and 51 ppb (785930, 785931) 10 kilometres downstream from this area. Other elements such as As, Sb, Ag and base metals are low, suggesting that these may be placer gold accumulations; however the possibility of a local bedrock source remains.

FAULT-RELATED STIBNITE AND POLYMETALLIC? VEINS

At the Tan showing (104O-006), a 20 centimetre-wide quartz vein in the Dorsey assemblage contains stibnite and pyrite (MINFILE). It is located within an area of normal faulting. Some of the faults in the vicinity display zones of alteration, brecciation and Fe-staining. Iron oxide boulders occur in talus over the trace of one of the faults. The boulders, probably of fault breccia, consist of small, angular chert fragments in a rusty limonitic matrix. The fragments are much more angular and more regular in size than the surface talus, evidence that these are not parts of a dismembered ferrocrete deposit. Two grab samples from nearby gossanous zones are anomalous in Ba (Table 2). The area is characterized by anomalous stream-sediment results as well: the sample in the drainage containing the Tan showing, 785740, is statistically rated as 3rd highest in total base metal content, and 8th highest in total precious metals plus indicators (Au, Ag, Sb, As) for the whole sample suite in the Jennings River map area (Jackaman, 2000). The regional geochemical survey shows it as part of a northwesterly trend of high base metal as well as Au values As and Sb in stream sediments, that parallels Plate Creek for a distance of over 10 kilometres. The highest Au analysis in this trend is 206 pbb (sample 785735), is from a creek that drains northest into Plate Creek, 10 kilometres northwest of the Tan showing.

INTRUSION-RELATED GOLD

The Ran (104O/037), located in the southwestern corner of 104O/16 adjacent to the present map area, is an areally extensive area of sericitic alteration and quartz veining within protomylonitized granite of the Cassiar

TABLE 2
GEOCHEMICAL ANALYSES OF
PROSPECTING SAMPLES FROM MAP AREA

Element				Mo	Cu	Pb	Zn	Ag	Ni	Co	Mn	Fe	As	Au	Sb	Bi	Ba	Hg	Se
Units				ppm	ppm	ppm	ppm	ppb	ppm	ppm	ppm	%	ppm	ppb	ppm	ppm	ppm	ppb	ppm
Method				ARMS	ARMS	ARMS	ARMS	ARMS	ARMS	ARMS	ARMS	ARMS	ARMS	ARMS	ARMS	ARMS	ARMS	ARMS	ARMS
Field Number	**UTM-east**	**UTM-north**	**Description**																
00JN-2-4	403095.2	6634800.5	rusty feldspar porphyry cuts metachert	0.39	46.97	4.44	27.2	86	18.7	3.5	69	1.38	10.7	2.7	6.35	0.23	847.8	23	0.3
00JN-2-7	402097.5	6636811.8	rusty fault zone with Fe-ox cemented bx	0.38	90.8	2.74	49.9	317	4.5	0.6	27	2.98	0.9	1.7	1.41	0.22	2379	15	0.8
00JN-3-5	405643.1	6635648	rusty, bleached zone in siliceous argillite	1.37	20.58	4.43	15.9	79	5.7	0.7	96	0.86	7.2	0.3	4.69	0.23	92	< 5	0.4
00JN-4-7.5	403936	6637299.2	rusty qtzt near qss with pyrite streaks	11.98	20.24	2.65	9.7	48	7.3	1.2	137	1.07	0.6	0.4	2.91	0.21	43.9	< 5	0.5
00JN-21-6	382232.5	6646402.7	waxy pale green rhyolite or dacite w/pyrite	1.02	3.77	10.64	5	256	4.7	1	43	1.86	82.3	54	0.88	0.19	96.9	19	0.1
ACME Q/C				32.45	19.18	11.58	9.1	113	2.4	0.4	47	0.85	6.1	9.6	0.24	0.35	79.6	5	5
Std. Red Dog				12.73	159	7.13	48.3	70	11.2	9.8	415	3.79	5.3	34.1	0.24	0.49	53.3	17	3.3
ACME Q/C				13.69	125.3	32.51	150.9	245	33.7	11	792	2.97	61.6	193	9.59	10.55	150.6	223	2.1
NOTES																			
Analysis of steel milled crushed rock prepared by ACME Analytical																			
ARMS = Aqua regia digestion - ICPMS																			
ACM = ACME Analytical, Vancouver																			
ELEMENT				Mo	Cu	Pb	Zn	Ag	Ni	Co	Mn	Fe	As	Au	Sb	Bi	Ba	Hg	Se
Mean+2SD				15.5	177.3	7.816	53.306	92.29	13.8	12.64	470.1	4.285	6.81	88.28	0.215	0.547	60.61	30	4.029
Mean-2SD				10.9	160	6.284	47.894	81.71	11.14	9.829	431.2	3.822	5.524	-11.48	0.192	0.486	52.12	26	2.971
Std. Red Dog				12.73	159	7.13	48.3	70	11.2	9.8	415	3.79	5.3	34.1	0.24	0.49	53.3	17	3.3

Batholith (Nelson and Bradford 1987). The veins contain pyrite, galena, bismuthinite, argentite, sphalerite, chalcopyrite and molybdenite (MINFILE). Grab samples of the veins collected this summer show a pattern of strongly anomalous bismuth (1000-3000 ppm) as well as very high values of Ag and Pb; although gold and associated elements (As, Sb) are low (P. Wodjak, unpublished data). Nevertheless, the style of alteration and mineralization at the Ran, as well as the high Bi values, encourage further thought about the existence of intrusion-hosted gold deposits in the Cassiar Batholith.

VOLCANOGENIC MASSIVE SULPHIDE POTENTIAL

On the eastern slope of the forested ridge 7 kilometres east of the Swift River in northern 104O/14E, pyritic quartz-sericite schist with quartz eyes occurs in an area of poor outcrop within unit uPSRgw, the dominantly siliciclastic, uppermost unit of the Swift River succession. It resembles metarhyolite tuffs in the Ram Creek assemblage, Big Salmon complex, and upper Dorsey assemblage, and suggests that the Swift River succession, like them, may have potential for hosting volcanogenic deposits. A grab sample from this zone contains 82 ppm As (Table 2).

Tectonics

Mapping of the stratified Swift River succession, Screw Creek limestone and Klinkit succession has aided in reconstructing the tectonic history of the central Dorsey Terrane. Their integrity as a depositional sequence sheds light on its late Paleozoic history; their subsequent deformation helps to chronicle late Paleozoic to early Mesozoic (pre-Early Jurassic) tectonic events.

The lower Swift River succession in northern Jennings River area represents a deep basin with sources of siliciclastic and minor plutonic, but not volcanogenic debris. Its upper age limit is provided by the unconformably overlying Screw Creek limestone, which ranges down to probable late Visean age (late Mississippian, 340-333 Ma). Its oldest age is unknown, because it rests structurally on the Dorsey assemblage. If this is a modified depositional contact, then its base can be no older than 357 Ma (early Mississippian), the age of a metamorphosed tuff in the upper Dorsey assemblage in the Yukon (Roots and Heaman, 2001); and probably no older than 340 Ma, the age of the youngest dated intrusion in the southern Dorsey assemblage (Nelson *et al*., 2000). The entire Swift River succession must then have been deposited over a time duration of between 0 and 25 million years. This short interval is difficult to reconcile with the 3.5 kilometre section of mainly chert and argillite in the southern Yukon, even given the likelihood of structural thickening. If, on the other hand, the contact represents tectonic juxtaposition, then the Swift River succession could range to considerably older ages; moreover, if it does, then the complete absence in it of rocks representing the Early Mississippian igneous event displayed in the Dorsey assemblage would suggest considerable separation between them at that time. By contrast, the highest siliciclastic unit in the Swift River succession represents erosion of a plutonic/metamorphic source terrane, possibly the Dorsey assemblage.

The Screw Creek limestone and volcanic/clastic Klinkit succession are intimately associated. Using only the most tightly constrained available fossil ages, Screw Creek limestone ranges from late Mississippian to early Pennsylvanian (probable late Visean; late Visean-Serpukhovian; late Serpukhovian-early Bashkirian; Bashkirian; 340-333; 340-323; 327 (approx.) - 316 (approx.); 323-310 Ma). It is generally the lowest unit overlying the Swift River succession, but farther north in the Teslin map area, multiple limestone bodies occur at different levels within Klinkit volcaniclastics (units Mv and Ml; Gordey and Stevens 1994). The interfingering of volcanic, carbonate and quartz clastic facies suggests a late Mississippian to Early Permian volcanic arc with continental or pericontinental basement, within which limestone banks developed in favorable settings. This pericratonic arc environment is demonstrably of regional extent: the Klinkit succession and affiliated limestones are exposed at least from Teslin map area in the north (units Mv and Ml, Gordey and Stevens, 1994) to central Jennings River area in the south (Harms and Stevens, 1996), a distance of over 200 kilometres.

The age range of the Screw Creek limestone overlaps the interval of time in which at least the upper, siliciclastic-felsic tuff unit of the Big Salmon Complex was being deposited, based on a 325 Ma U/Pb zircon age (Mihalynuk *et al*., 1999; *see* Figure 2). Present time constraints are permissive of lithostratigraphic correlation with the fossiliferous limestone unit in the Big Salmon, which like the Screw Creek limestone contains crinoids, horn corals and at least one colonial coral. However the Big Salmon greenstone unit, instead of being equivalent to the overlying Klinkit volcanics, appears to stratigraphically underlie the limestone (Mihalynuk *et al*., 2000). Ongoing petrochemical and geochronological comparisons between the Big Salmon and Klinkit volcanics, part of an M.Sc. thesis by Renée-Luce Simard of St. Mary's University and an undergraduate project by Fionnulla Devine at the University of British Columbia, may help to clarify this apparent paradox.

The D3 folding event, which produced regional, north-northwest-trending, west-verging recumbent folds in the late Paleozoic sequence, is probably not confined to 104O/14 and 15. In northwestern Jennings River area, Mihalynuk *et al.* (1998) recognized a west-verging, post-peak-metamorphic, recumbent folding episode (also D3 in their sequence) that produced the major map patterns in stratified units of the Big Salmon Complex. Southwesterly-vergent recumbent folds affect the Klinkit succession south of the Simpson Peak batholith in 104O/11 and 12 (Mihalynuk *et al*., 2000). The Triassic Teh clastics are involved in this episode (T. Harms, personal communication, 2000), which predated the Early Jurassic intrusions.

The Dorsey Terrane has been correlated with the multi-phase arc terrane Quesnellia further south (Harms *et al*., 1997; Nelson 1997). Points of similarity can be adduced from rocks ranging from the oldest to the youngest in each. Both terranes have at least partial pericratonic basement with a Devonian-Mississippian igneous component (Roback and Walker, 1995, Simony 1979). The Swift River-Screw Creek-Klinkit sequence has close parallels in the late Paleozoic Lay Range Assemblage of central British Columbia (Nelson, 1997). Although, unlike Quesnellia, there is little evidence for a Late Triassic igneous episode in the Dorsey Terrane, it contains abundant Early Jurassic intrusions that are coeval with parts of the Hogem batholith and other Quesnellian bodies. A suite of andesitic to trachyandesitic dykes in the Dorsey Terrane resembles Jurassic volcanic and hypabyssal rocks of central Quesnellia, in terms of age, textures and shoshonitic petrochemistry.

In this context, the D3 folding event stands out as a significant divergence between the history of the Dorsey Terrane and that of central and southern Quesnellia. Although there is a minor unconformity between the Triassic and Jurassic successions in central Quesnellia (Nelson and Bellefontaine, 1996), major deformation is not inferred. The earliest evidence of ductile deformation is coeval with the 186-Ma Polaris body along the eastern margin of Quesnellia; it is associated with easterly tectonic transport (Nixon *et al*., 1993). Southwesterly-verging folding of the eastern margin of Quesnellia did not begin until after its accretion to North America, in mid-Toarcian to Aalenian time or about 180-174 Ma (Murphy *et al*., 1995). Completion of the preaccretionary D3 event predates this by at least 10 million years. It must be the result of collisions among the offshore arc elements, prior to the impingement of the continent on the pericratonic collage. Northern Stikinia fits the profile of the hypothetical collider: its tectonic history underwent a rapid shift from arc volcanism to coarse clastic sedimentation and rapid local uplift at about the Triassic-Jurassic boundary.

CONCLUSIONS

Mapping of 104O/14E and 15 in 2000 contributes to a growing geologic corpus in Jennings River and Wolf Lake map areas, facilitated by the Ancient Pacific Margin Natmap project. This area features well exposed late Paleozoic stratified rocks, whose stratigraphy and structure enable further understanding of the Dorsey Terrane, the southern continuation of the Yukon Tanana Terrane in the Finlayson Lake and Teslin belts. A major advance in this field season was the recognition that the Swift River succession, Screw Creek limestone and Klinkit succession are not separate assemblages, but constitute a single stratigraphic sequence. This has implications for the internal geological coherency of a large part of the allochthonous Dorsey Terrane.

Our studies have confirmed the possibility that equivalents of the early Mississippian arc strata that host VMS deposits near Finlayson Lake can also be found within the Dorsey Terrane. As well, extensive late Mississippian silica (-manganese-iron) exhalites have been documented in the Big Salmon Complex, located just to the west. The Screw Creek limestone and Klinkit succession, the upper two stratified units, may correlate with parts of the Big Salmon Complex.

Two prospecting discoveries were made this summer, malachite staining in calcsilicates between the Nome Lake and Simpson Peak batholiths, and pyritic quartz-sericite schist in the upper clastic unit of the Swift River succession. A re-release of regional geochemical survey data (Jackaman, 2000), including key new elements such as Au, As, and Sb, offers intriguing and unexplained anomalies for future follow-up.

ACKNOWLEDGEMENTS

Significant contributions to mapping and understanding of this area were made by Tekla Harms, Charlie Roots, Martin deKeijzer, and Richard Friedman. Dave Lefebure's review improved the manuscript. Norm Graham and Jeff Reed of Discovery Helicopters delivered highly professional service. I thank Sarah Laxton for cheerful assistance in the field.

REFERENCES

Abbott, J.G. (1984): Silver-bearing veins and replacement deposits of the Rancheria district: *in* Yukon Exploration and Geology 1983, *Exploration and Geological Services Division, Indian and Northern Affairs Canada*, pages 34-44.

Bradford, JA. (1988): Geology and genesis of the Midway silver-lead-zinc deposit, north-central British Columbia: M.Sc. thesis, University of British Columbia, 280 pages.

Gabrielse, H. (1969): Geology of Jennings River map area, British Columbia (104/O); *Geological Survey of Canada*, Paper 68-55.

Gabrielse, H. (1985): Major dextral transcurrent displacements along the Northern Rocky Mountain Trench and related lineaments in north-central British Columbia; *Geological Society of America Bulletin*, Volume 96, pages 1-14.

Gordey, S.P. and Stevens, R.A. (1994): Preliminary interpretation of the bedrock geology of the Teslin area (105C), southern Yukon; *Geological Survey of Canada*, Open File 2886 (uncoloured map, scale 1:250 000).

Harms, T.A. and Stevens, R.A. (1996): Assemblage analysis of the Dorsey Terrane; Slave-Northern Cordillera Lithospheric Evolution (SNORCLE) and Cordilleran Tectonics Workshop, Report of the 1996 Combined Meeting; pages 199-201.

Harms, T.A., Stevens, R.A., and Creaser, R.A. (1997) Assemblage analysis and tectonostratigraphic affinity of Dorsey Terrane and adjacent areas - northern BC and southern Yukon: GAC-MAC Annual Meeting Abstracts Volume, Volume 22, page A-64.

Jackaman, Wayne (2000): British Columbia Regional Geochemical Survey; NTS 104O - Jennings River: Stream sediment and water geochemical map booklet; BC RGS 52, B.C. Ministry of Energy and Mines.

Mihalynuk, M. Nelson, J.L. and Friedman, R.M. (1998): Regional geology and mineralization of the Big Salmon Complex (104N NE and 104O NW), in Geological Fieldwork 1997, *B.C. Ministry of Employment and Investment*, Geological Survey Branch, Paper 1998-1, pages 6-1 - 6-20.

Mihalynuk, M.G., Nelson, J., Roots, C.F. and Friedman, R.M. (2000): Ancient Pacific Margin part III: Regional geology and mineralization of the Big Salmon Complex (104N/9,10 & 104O/12,13,14W); *in* Geological Fieldwork 1999, *B.C. Ministry of Energy and Mines*, Geological Survey Branch, Paper 2000-1,pages 27-46.

Nelson, J. (1997): The Dorsey Terrane: Quesnellia north? in Slave-Northern Cordillera Lithospheric Evolution (SNORCLE) and Cordilleran Tectonics Workshop, Report of the 1997 Combined Meeting; pages 230-232.

Nelson, J.L. (2000): Ancient Pacific Margins Part VI: Still heading south: Potential VMS hosts in the eastern Dorsey Terrane, Jennings River(104O/1; 7,8,9,10) *in* Geological Fieldwork, 1999, *British Columbia Ministry of Employment and Investment*, Geological Survey Branch, Paper 2000-1, pages 107-126.

Nelson, J.L. and Bellefontaine, K.A. (1996): The Geology and Mineral Deposits of North-Central Quesnellia; Tezzeron Lake to Discovery Creek, Central British Columbia; *B.C. Ministry of Energy, Mines and Petroleum Resources*, Bulletin 99.

Nelson, J. and Bradford, J. (1987): Geology of the area around the Midway Deposit, Northern British Columbia (104O/16), *B.C. Ministry of Energy, Mines and Petroleum Resources*, Geological Fieldwork 1986, Paper 1987-1, pages 181-192.

Nelson, J., Harms, T.A., Zantvoort, W., Gleeson, T. and Wahl, K. (2000): Geology of the southeastern Dorsey Terrrane, 104O/7, 8, 9, 10; *B.C. Ministry of Energy and Mines,* Geological Survey Branch, Open File 2000-4.

Nelson, J.L., Harms, T.A., Roots, C.F., Friedman, R. and deKeijzer, M. (2001): Geology of north-central Jennings River map area, 104O/14E, 15; *B.C. Ministry of Energy and Mines*, Geological Survey Branch, Open File 2001-6.

Murphy, D.C., M. Gerasimoff, P. van der Heyden, R.R., Parrish, D.W. Klepacki, W.R. McMillan, L.C. Struik, and J. Gabites, 1995, Constraints on Jurassic deformation of the western edge of North America, southeastern Canadian Cordillera, *in* Miller, J.M., ed., Jurassic Magmatism and Tectonics of the North American Cordillera, *Geol. Soc. Am Spec. Paper 299*, pages 159-171.

Nixon, G.T., Archibald, D.A. and Heaman, L.M. (1993): 40Ar-39Ar and U-Pb geochronometry of the Polaris Alaskan-type complex, British Columbia: Precise timing of Quesnellia-North America interaction; *Geological Association of Canada*, Abstracts with Programs, Volume 18, page A76.

Roots, C.F., de Keijzer, M., Nelson, J.L., and Mihalynuk, M.G. (2000): Revision mapping of the Yukon-Tanana and equivalent terranes in northern B.C. and southern Yukon between 131^{o} and 132^{o} W; *in* Current Research 2000-A; *Geological Survey of Canada*, in press.

Roback, R.C. and Walker, N.W. (1995): Provenance, detrital zircon U-Pb geochronometry, and tectonic significance of Permian to Lower Triassic sandstone in southeastern Quesnellia, British Columbia and Washington; *Geological Society of America* Bulletin, Volume 107, pages 665-675.

Roots, C.F. and Heaman, L.M. (2001): Mississippian U-Pb dates from Dorsey terrane assemblages in the upper Swift River area, southern Yukon; *in* Current Research 2001-A; *Geological Survey of Canada*, in press.

Simony, P.S. (1979): Pre-Carboniferous basement near Trail, British Columbia; *Canadian Journal of Earth Sciences*, Volume 16, pages 1-11.

Stevens, R.A. and Harms, T.A. (2000): Bedrock geology of the Dorsey Range, south Yukon Territory and Northern British Columbia; *Geological Survey of Canada,* Open File 3926, scale 1:100 000.

Geologic Setting of Paleozoic Strata and Mineral Occurrences in the Mount Tod Region, South-Central British Columbia

By Shannon L. Acton[1], Suzanne Paradis[2], and Stephen T. Johnston[1]

KEYWORDS: Kootenay Terrane, Quesnel Terrane, Silver Creek Formation, Eagle Bay Assemblage, Nicola Group, skarn alteration, massive sulphide deposits, disseminated sulphide mineral occurrences, Steep, Serpent, Chase Silica.

INTRODUCTION

The correlation and extent of pericratonic strata deposited on the western distal margin of ancient North America in south-central British Columbia is problematic. Within the Thompson-Okanagan-Shuswap and Adams Lake regions, strata included within the pericratonic Kootenay Terrane are poorly exposed, obscured by intense deformation, and mapped only at reconnaissance scale (Figure 1; Wheeler and McFeely, 1991). As a result, the boundary between pericratonic rocks of the Kootenay Terrane and rocks of the allochthonous Quesnel Terrane is a subject of debate. This boundary has been interpreted as a large scale, complex thrust zone (Monger *et al*., 1972, 1982; Wheeler and McFeely 1991). Alternatively, Mesozoic volcanic and volcaniclastic rocks of Quesnel Terrane may stratigraphically overlie and be linked to pericratonic strata of the Kootenay Terrane (Thompson and Daughtry, 1997).

Rocks of the Eagle Bay Assemblage in the Adams Plateau – Clearwater – Vavenby area, and the Sicamous, Tsalkom and Silver Creek formations in the Thompson – Okanagan – Shuswap region are included within the pericratonic Kootenay Terrane (Jones, 1959; Okulitch, 1979; Schiarizza and Preto, 1987). Volcanic and volcaniclastic rocks of the Late Triassic Nicola Group and arc-related rocks of the Devonian to Late Permian Harper Ranch Group characterize Quesnel Terrane in the Thompson – Okanagan – Shuswap area (Monger *et al*., 1982; Wheeler and McFeely 1991). The relationship of strata in the Mount Tod – Adams Lake area to assemblages of the Kootenay and Quesnel terranes is uncertain. These rocks are of significant economic interest since they are host to several polymetallic massive sulphide deposits. However, the distribution, setting, and age of most of these deposits is not well established (Höy, 1999).

[1] *University of Victoria*

[2] *Geological Survey of Canada*

Mapping of the area west of Adams Lake to Mount Tod was undertaken as part of the Ancient Pacific Margin NATMAP Project in an attempt to address these problems (Figures 2, 3 and 4). Particularly, reconnaissance and de-

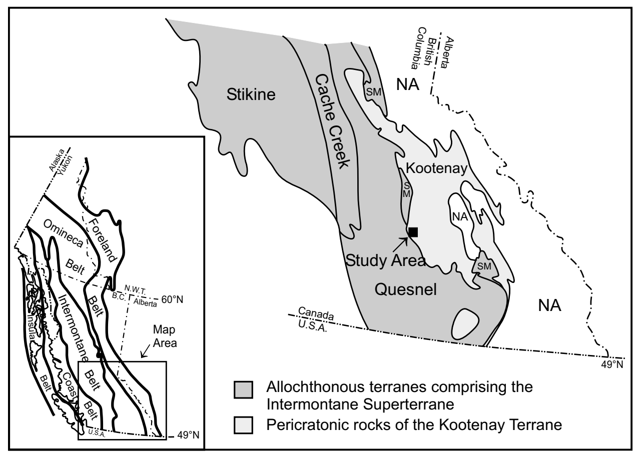

Figure 1. Location of the study area and the pericratonic Kootenay Terrane in southern British Columbia. SM = Slide Mountain Terrane, NA = North America.

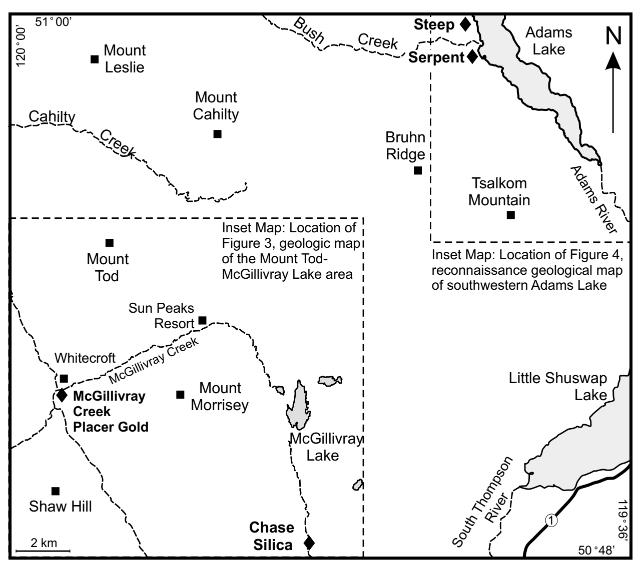

Figure 2. Location of the Mount Tod and Adams Lake study areas and limit of preliminary mapping.

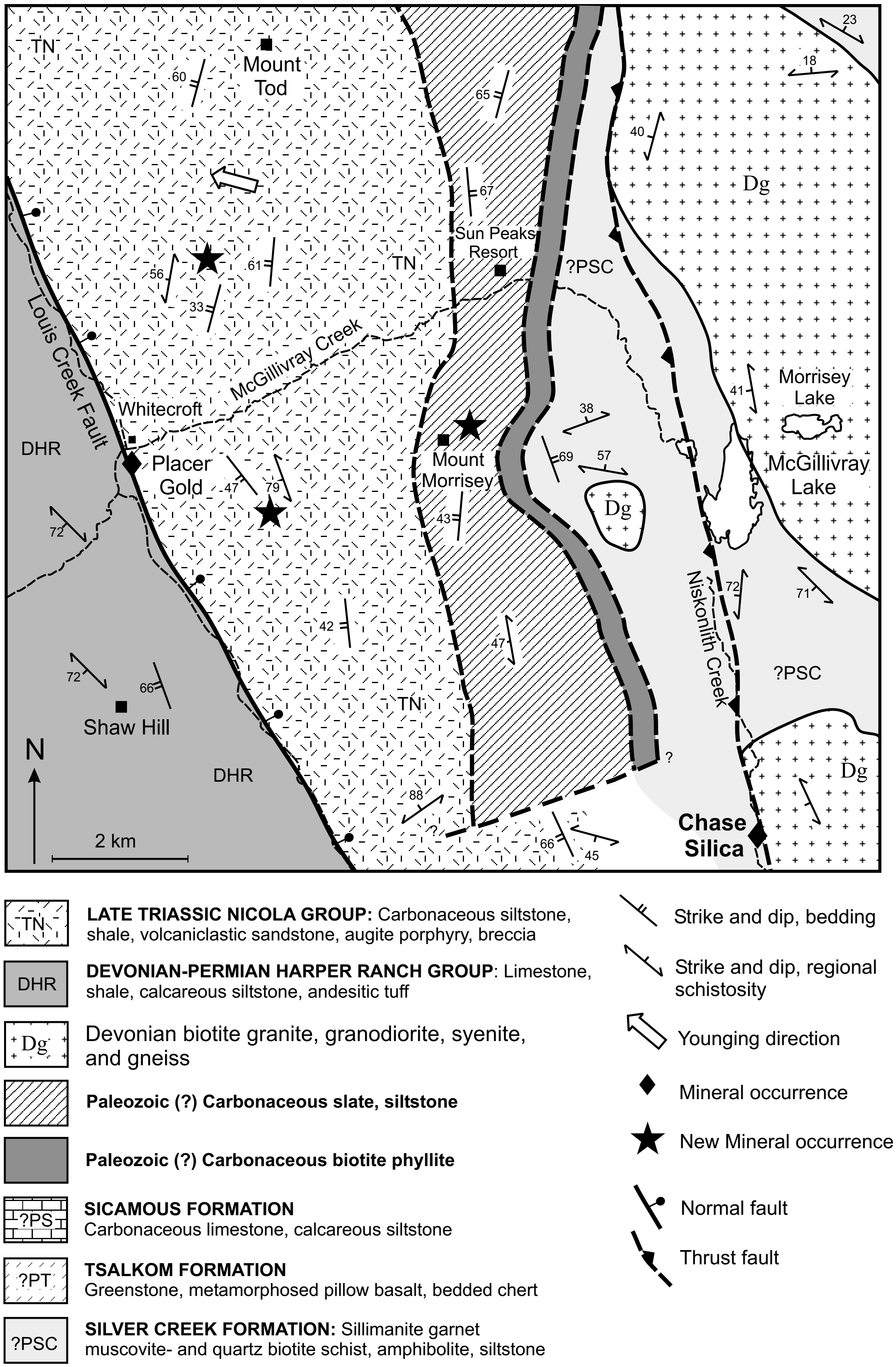

Figure 3. Simplified geologic map of the Mount Tod – McGillivray Lake area.

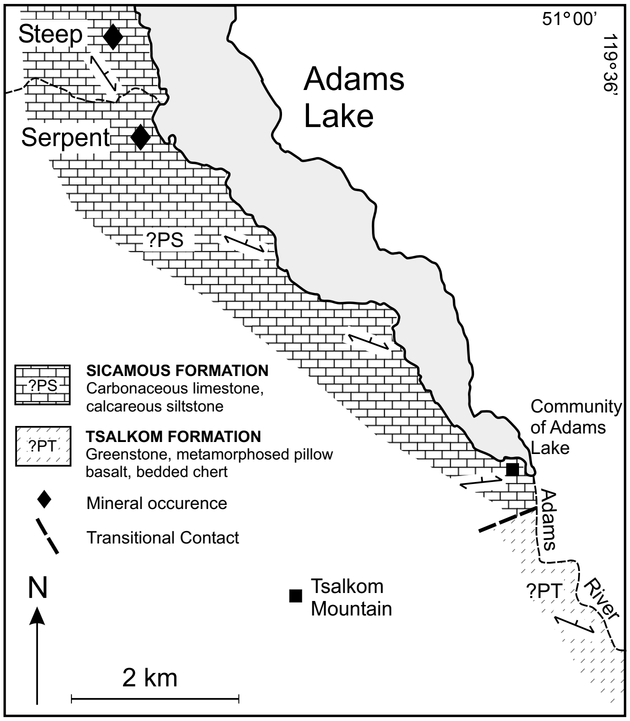

Figure 4. Reconnaissance geologic map of the shore of southwestern Adams Lake. Refer to Figure 3 for complete legend.

tailed field work focused on the following: 1) the relationship of rocks of the Early Cambrian to Mississippian Eagle Bay Assemblage in the Adams Lake-Clearwater region, and the Paleozoic Tsalkom and Sicamous formations mapped to the west and south of Adams Lake to rocks in the Mount Tod area; 2) the structural and tectonic relationships of pericratonic rocks in the Adams Lake – Mount Tod region; and 3) the distribution and setting of mineral deposits within the Mount Tod-Adams Lake region. This paper summarizes the initial findings of 9 weeks of fieldwork completed during the summer 2000 season.

REGIONAL GEOLOGY

Volcanic and clastic sedimentary rocks comprising the Devonian to Permian Fennell Formation of the oceanic Slide Mountain Terrane structurally overlie the Early Cambrian to Mississippian Eagle Bay Assemblage in the Adams Plateau – Clearwater – Vavenby area (Schiarizza and Preto, 1987; Roback *et al*. 1995). The Eagle Bay Assemblage consists of a complex succession of metasedimentary and metavolcanic rocks that are intruded by Late Devonian orthogneiss (Jones, 1959; Okulitch, 1979, 1989; Schiarizza and Preto, 1987). The basal part of the Eagle Bay Assemblage consists of quartzite and schist (Units EBQ and EBH) overlain by mafic metavolcanic rocks (Unit EBG) intercalated with Early Cambrian Tshinakin limestone. These lithologies are overlain by undated phyllite, carbonate, and metavolcanics (Unit EGS), metamorphosed basalt, chert and quartzite (Unit EBM), and carbonaceous phyllite and limestone (Unit EBL). The upper part of the Eagle Bay Assemblage consists of felsic to intermediate metavolcanic and metasedimentary rocks (Units EBA and EBP; Schiarizza and Preto, 1987).

Phyllite and limestone of the Sicamous Formation overlie mafic metavolcanic rocks of the Tsalkom Formation and quartzite, schist and marble of the Silver Creek Formation in the Thompson – Okanagan – Shuswap region (Jones, 1959; Okulitch, 1979, 1989; Roback *et al*., 1995). The ages of these formations are unknown due to a lack of microfossils and minerals suitable for radiometric age analysis. Jones (1959) proposed that the Silver Creek, Tsalkom, and Sicamous formations were “Archean or younger”. Okulitch (1979) revised the geology of the Shuswap region, and assigned a Late Triassic age to the Sicamous Formation based on similarities to the Slocan Group in the Kootenay Arc. Okulitch (1989) modified this interpretation, and suggested that the Tsalkom and Sicamous formations may correlate with the Cambrian to Ordovician Jowett and Index formations within the Kootenay Arc based on lithological comparisons.

Volcanic and volcaniclastic rocks of the Late Triassic Nicola Group unconformably overlie unmetamorphosed sedimentary and volcanic rocks of the Devonian to Late Permian Harper Ranch Group in the Thompson – Okanagan – Shuswap area (Monger *et al*., 1982; Wheeler and McFeely 1991; Roback *et al*., 1995). The Nicola and Harper Ranch groups are the main stratigraphic elements of the island-arc Quesnel Terrane in this region.

GEOLOGY OF THE MOUNT TOD REGION

Silver Creek Formation

The Silver Creek Formation is a deformed and metamorphosed assemblage of pelitic schist, gneiss, amphibolite, siltstone, carbonaceous phyllite, aplite and pegmatite. These rocks have been metamorphosed to sillimanite grade and deformed into a series of tight polydeformed folds. The age of the Silver Creek Formation is unknown, but may be Late Proterozoic, to as young as Middle to Late Paleozoic (Okulitch, 1979, 1989; Thompson and Daughtry, 1997; Thompson, pers. comm. 2000). The upper contact of the Silver Creek Formation may be transitional with the basal portion of the Tsalkom and / or Sicamous Formation in the Okanagan-Shuswap region (Thompson and Daughtry, 1997).

The Silver Creek Formation is characterized by sillimanite-garnet-muscovite and quartz- plagioclase-biotite schist in the region immediately east of McGillivray Lake (Figure 3). Almandine garnet porphyroblasts are 0.5-2.0 cm in diameter, and are rotated relative to the enclosing fabric. Fine-grained crystals of pink-brown, fibrous sillimanite overprint and crosscut fine- to medium-grained metamorphic biotite. Schistosity is defined by the parallel alignment of coarse-grained flakes of biotite and muscovite up to 3 cm in diameter. Thin layers of dark grey-green actinolite-biotite schist and amphibolite occur locally in the McGillivray Lake area. These strata represent metamorphosed rocks of the Silver Creek Formation within the contact aureole of a Devonian (?) granitic body. West of McGillivray Lake, tightly folded, thinly bedded medium grey quartzite and siltstone metamorphosed to biotite grade are the dominant lithologies.

The metamorphic grade of the Silver Creek Formation decreases from sillimanite grade to chlorite-biotite grade eastwards from McGillivray Lake to the Tsalkom Mountain area (Figure 3). In the Tsalkom Mountain area, beds of rusty to brown weathering carbonaceous phyllite, slate and siltstone are interbedded with fine-grained quartz-biotite schist.

Sills of orthogneiss and sills and dikes of leucogranitic aplite and pegmatite are present throughout the Silver Creek Formation. The aplite and pegmatite sills and dikes are undeformed to weakly strained and 1-10 m in thickness. These sills and dikes may be intrusions related to the Devonian (?) granitic body near McGillivray Lake.

Carbonaceous Phyllite-Slate-Siltstone

A package of rocks consisting predominantly of carbonaceous phyllite and slate can be distinguished between the Silver Creek Formation and Nicola Group in the Mount Morrisey - McGillivray Creek area (Figure 3). Rusty weathering carbonaceous phyllites and slate are highly recessive, strongly deformed and metamorphosed to biotite-garnet grade near the peak of Mount Morrisey. Porphyroblasts of biotite are pervasive and occur as resistant-weathering books 2-4 mm in diameter. Biotite porphyroblasts are preferentially aligned along phyllitic surfaces that crosscut an older bedding-parallel foliation. Phyllites and slate are interbedded with thin beds of carbonaceous siltstone 0.5 to 1.5 m thick. Carbonaceous siltstones are rusty weathering, poorly indurated, and contain minor amounts of disseminated pyrite.

The carbonaceous phyllite-slate-siltstone unit may correlate with an assemblage of schist, marble, and quartzite separating the Silver Creek Formation from Triassic rocks correlative with the Nicola Group in the Vernon area (Thompson and Daughtry, 1997, 1998; Underschutz *et al*., 1999). This assemblage is interpreted as a stratigraphic transition zone, implying that rocks assigned to Quesnel Terrane are stratigraphically linked with pericratonic rocks of the Kootenay Terrane. Alternatively, these rocks may be metamorphosed sediments at the base of the Nicola Group, or a Sicamous Formation equivalent (Jones, 1959; Okulitch, 1979).

Devonian – Permian Harper Ranch Group

Limestone, slate, and calcareous and carbonaceous siltstone of the Harper Ranch Group are exposed in a northwest trending belt west of Louis Creek (Figure 3). These units are intercalated with thin layers of crystal-lithic andesitic tuff and ash tuff. Rocks of the Harper Ranch Group have been folded during chlorite- biotite-grade metamorphism, resulting in the development of a penetrative slatey cleavage. Mississippian to Permian limestones in the Shaw Hill area can be correlated with similar carbonaceous and calcareous siltstones to the northwest (Ray and Webster, 2000).

Carbonaceous siltstones of the Harper Ranch Group are brown to rusty weathering, silty and recessive. Two penetrative, intersecting cleavages are present. Beds of carbonaceous siltstone grade into thinly bedded light to medium grey calcareous siltstone up-section. Thin interbeds of limestone and veinlets of calcite (1-5 mm thick) are present throughout the siltstone unit. These rocks are overlain by dark brown weathering, massive, dark grey argillaceous limestone. Beds of argillaceous limestone are foliated and 5 to 20 m thick. The contact between these lithologies is poorly exposed, and is interpreted as being transitional. Carbonaceous siltstones and argillaceous limestones of the Harper Ranch Group are metamorphosed to chlorite grade.

Sedimentary rocks of the Harper Ranch Group are intercalated with layers of light to medium grey-green augite crystal-lithic andesitic tuff and chlorite ankerite ash tuff. These rocks are brown to rusty weathering, massive and friable. Contacts between tuffaceous and sedimentary units are sharp.

Triassic Nicola Group

Carbonaceous siltstone and slate, volcaniclastic sandstone and siltstone, augite crystal tuff, and augite porphyry flows and breccia characterize the Late Triassic Nicola Group in the area surrounding Mount Tod. These lithologies are well exposed, and deformed and metamorphosed to chlorite-biotite grade. Proximal to Louis Creek, west of Mount Tod, slate, siltstone and volcanic rocks of the Nicola Group are well-cleaved and metamorphosed to chlorite-biotite grade (Figure 3).

Carbonaceous siltstone and slate of the Nicola Group are rusty weathering and recessive, and consist of mud to silt-sized grains of quartz, feldspar, carbonaceous material and minor disseminated pyrite. Beds of slate and siltstone are 0.1 to 1.5 m thick and exhibit a phyllitic sheen on some bedding surfaces.

Massive beds of tuff and volcaniclastic sandstone are intercalated with carbonaceous siltstone and slate. Layers of medium grey, homogenous augite crystal and crystal-lithic tuff are 0.2 to 2.0 m thick with sharp basal contacts. Sandstone beds are rusty weathering, medium grey, fine to medium-grained, finely laminated and competent. Contacts between the sandstone and finer-grained units are undulating and sharp. Clasts of undeformed shale and siltstone (0.2-2.5 cm in diameter), cross-bedding, scours and graded bedding occur within the volcaniclastic sandstone. Facing directions are consistently up to the west and south, indicating that the units are upright.

Augite porphyry and augite porphyry breccia form resistant ridges and knobs throughout the study area. Ridges of augite porphyry comprise Mount Tod, which is the highest topographical feature in the region. Phenocrysts of euhedral black and pale green augite 2-4 mm in diameter are dispersed within an aphanitic matrix of andesitic composition. Breccia consists of sub-rounded to sub-angular clasts of augite porphyry 5 to 40 cm in diameter within a matrix of augite crystal-lithic tuff. All flows are 10 to 40 m in thickness, and 10 to 100 m in length along strike.

INTRUSIVE ROCKS

A poorly exposed body of massive biotite granite, granodiorite, syenite and gneiss intrudes metasedimentary rocks of the Silver Creek Formation in the McGillivray-Morrisey Lakes area (Figure 3). Equigranular, medium to coarse-grained granites and granodiorites consist of quartz, plagioclase, potassium feldspar, biotite and muscovite. These rocks are undeformed except in rare zones of intense deformation and strain in which biotite gneiss is developed.

Biotite granite and granodiorite in the McGillivray lake region has been previously interpreted to be Jurassic-Cretaceous in age (Jones, 1959). However, based on lithologic similarities to granitic intrusions such as the Ordovician (?) Little Shuswap Gneiss in the Thompson-Okanagan-Shuswap region and unit "Dgn" near Adams Lake, this granitoid may be of Ordovician to Devonian age (Okulitch, 1979, 1989; Schiarizza and Preto, 1987).

STRUCTURE

Deformation of the Silver Creek Formation and "carbonaceous phyllite-slate" unit in the Mount Tod region is dominated by a series of broad, northwest trending, west verging folds. Associated with the folds is a penetrative cleavage defined by the parallel alignment of micaceous minerals within slatey and pelitic rocks of the Nicola Group and Silver Creek Formation. This style of deformation is similar to the folding of strata of the Eagle Bay Assemblage in the Adams Lake-Johnson Lake region. Folds in the Johnson Lake region are northwest trending, shallowly dipping, and approximately parallel to a series of northwest trending thrust faults (Schiarizza and Preto, 1987; Bailey *et al*., 2000).

Rocks in the Mount Tod-Adams Lake region record at least two phases of folding. Two intersecting cleavage surfaces are evident within incompetent shale and slate sequences of the Harper Ranch and Nicola Groups. In these examples, a bedding-parallel cleavage is intersected by a second cleavage at an acute angle. Also, parasitic folds on limbs of tightly folded siltstones and quartzites of the Silver Creek Formation are common.

Volcanic and volcaniclastic rocks of the Nicola Group near Mount Tod are separated from rocks of the Harper Ranch Group in the Shaw Hill area by the Louis Creek Fault (Figure 3). Displacement across the Louis Creek Fault, a northwest-southeast trending, east-dipping normal fault, is estimated at 1 to 2 km. A west-dipping, north-south trending thrust fault separates rocks of the Silver Creek Formation from unit "Dg" in the Chase Silica quarry region (Figure 3). Rocks of the Silver Creek Formation are present in both the hangingwall and footwall north of the Chase Silica quarry, suggesting that displacement along the fault is minor. However, the original extent of the Silver Creek Formation is unknown, and the displacement across this fault is uncertain.

STRATIGRAPHY SOUTHWEST OF ADAMS LAKE

Tsalkom and Sicamous Formations

Exposures of the Tsalkom and Sicamous formations were examined during reconnaissance field trips along the western perimeter of Adams Lake (Figure 4). The Tsalkom Formation consists of laterally discontinuous massive greenstone, metamorphosed pillow basalt and bedded chert along the Adams Lake West Road south of the community of Adams Lake (Figure 4). The greenstones consist of massive, olive green, and foliated chlorite biotite schist. Altered chilled margins of remnant pillows can be identified within the metamorphosed basalts. Layers of well-bedded chert are intercalated with the greenstones and pillow basalts. Individual chert beds are white to light grey and 0.2 to 2.0 cm thick; each intercalated package of bedded chert is 1 to 10 m thick.

Massive outcrops of carbonaceous limestone and calcareous siltstone of the Sicamous Formation are present along the Adams Lake West Road proximal to the town of Adams Lake. Randomly oriented white calcite veins 2-6 cm thick crosscut the medium to dark grey limestone and siltstone. These rocks have been correlated with limestone and calcareous phyllite (unit EBL of Schiarizza and Preto, 1987) of the Eagle Bay Assemblage mapped in the Adams Lake-Clearwater region (Schiarizza and Preto, 1987; Schiarizza, pers. comm. 2000).

The contact between the Tsalkom and overlying Sicamous formation has been interpreted as gradational in the Adams Lake – Shuswap region (Thompson and Daughtry, 1997, 1998). Within the contact zone, which is 10 to 40 m thick, massive foliated greenstone of the Tsalkom Formation is interlayered with calcareous siltstone of the Sicamous Formation (Figure 4). The Sicamous Formation directly overlies rocks of the Silver Creek Formation in the area northeast of Adams Lake where the Tsalkom Formation is absent due to either non-deposition or structural disruption.

MINERALIZATION

Paleozoic rocks in the Mount Tod – Adams Lake region are host to several polymetallic massive sulphide, disseminated sulphide and silica deposits. The Steep / Eve (BC Minfile 082LNW052), Serpent / Eve (BC Minfile 082LNW051), and Chase Silica (BC Minfile 082LNW031) prospects were examined during the summer 2000 field season (Figures 2 and 4). As well, previously unrecognized and undescribed sulphide mineralization within the Nicola Group and carbonaceous phyllite-slate map unit near Mount Morrisey and the village of Whitecroft was investigated.

The Steep Pb-Zn skarn showing is located within altered and mineralized argillaceous limestone and calcareous phyllite of the Sicamous Formation. These rocks are overlain by quartz-sericite schist of the Eagle Bay Assemblage (Unit EBK), which are intruded by Late Devonian orthogneiss (Unit Dgn; Schiarizza and Preto, 1987). A concordant zone of skarn alteration is traceable for at least 10 km along strike and includes phyllitic calc-silicate and massive garnet-rich skarn (Ettlinger and Ray, 1989; Miller, 1989). The calc-silicate skarn is 50 to 140 m thick and includes actinolite, plagioclase, chlorite, epidote, pyroxene and quartz, whereas the garnet-rich skarn is greater than 50 m thick and comprises garnet, calcite, epidote, actinolite, chlorite, quartz, potassium feldspar, plagioclase and apatite. Mineralization is dominated by disseminated (5% average) to massive pyrrhotite, with lesser disseminated and massive pyrite, chalcopyrite, magnetite and rare sphalerite and galena. Trace amounts of gold associated with bismuth occurs with the pyrrhotite in some samples. Maximum assay values from drillhole intersections range from 1.68 to 5.8 grams per tonne gold, 4.6 ppm silver, 694 to 3830 ppm copper, 256 to 6910 ppm lead, and 400 ppm zinc (Ettlinger and Ray, 1989; Miller, 1989). It is uncertain whether the Steep property is an intrusion-related, epigenetic skarn deposit, or a syngenetic, exhalitive stratiform skarn deposit (Ettlinger and Ray, 1989).

The Serpent Cu-Pb-Zn massive sulphide showing occurs within the transitional contact zone between limestone and calcareous phyllite of the Sicamous Formation and quartz-sericite schist of the overlying Eagle Bay Assemblage (unit EBK of Schiarizza and Preto, 1987). The Serpent showing is located 2-3 km south of the Steep showing along the western shoreline of Adams Lake, proximal to a Devonian orthogneiss intrusion (Dgn of Schiarizza and Preto, 1987). Fine-grained and massive to disseminated pyrite, sphalerite, galena and chalcopyrite occurs within siliceous phyllite, graphitic schist, calcareous slate and limestone of both formations. The origin of the mineralization may be similar to the Steep property skarn deposit, yet remains uncertain.

Deposits in metasedimentary rocks of the Silver Creek Formation are located within altered and strained zones proximal to intrusive contacts. For example, the Chase Silica quarry is characterized by the occurrence of a 7 to 15 m thick white quartz vein located near the contact between pelitic schist and amphibolite of the Silver Creek Formation and Devonian (?) granite (Minfile 082LNW031). Within the quarry, located on Niskonlith Creek south of McGillivray Lake, the Silver Creek Formation is host to an extensive quartz vein stockwork system and exhibits pervasive quartz- sericite-fuchsite-pyrite alteration (Figure 3). Mineralization includes disseminated pyrite (2 to 7%), chalcopyrite (2 to 6%), pyrrhotite (2 to 5%), sphalerite, galena, scheelite and tungstenite.

Volcanic and volcaniclastic rocks of the Nicola Group and the carbonaceous phyllite-slate map unit are host to previously unrecognized showings of sulphide mineralization. Disseminated pyrite (2 to 8%), chalcopyrite (2 to 5%), and minor galena (< 2%) occur within metamorphosed augite crystal-lithic andesitic tuff and volcaniclastic sandstone and siltstone of the Triassic Nicola Group. Mineralized zones are 5 to 10 m thick and laterally discontinuous. The two main zones of mineralization are located west of Mount Morrisey and north of McGillivray Creek on the western flank of Mount Tod (Figure 3).

The carbonaceous-phyllite-slate unit is host to abundant disseminated sulphides. Fine-grained disseminated pyrite and chalcopyrite (2 to 5%) occurs within thin (0.5 to 1.5 m thick), rusty weathering beds of carbonaceous siltstone interbedded with phyllite and slate. Mineralized zones are laterally discontinuous, and extend 5 to 20 m along strike. Mineralization is constrained to the Mount Morrisey area. The age and origin of mineralization within rocks of the Nicola Group and carbonaceous phyllite-slate map unit is unknown.

SUMMARY

Preliminary mapping has resulted in two important observations pertaining to the the Mount Tod – Adams Lake area.

1) A sequence of carbonaceous phyllite and slate separate the Silver Creek Formation and Nicola Group in the Mount Morrisey - McGillivray Creek area. This package of rocks may represent a previously unrecognized sequence, a Sicamous Formation equivalent, or a package of metamorphosed sediments at the base of the Nicola Group.
2) Previously unrecognized disseminated pyrite, chalcopyrite, and galena mineralization occurs within reworked tuff of the Nicola Group, and within the carbonaceous phyllite-slate-siltstone map unit near Mount Morrisey and Mount Tod. Two zones of mineralization within rocks of the Nicola Group are recognized near Mount Morrisey and McGillivray Creek. Disseminate pyrite and chalcopyrite within the carbonaceous phyllite-slate-siltstone map unit is restricted to the Mount Morrisey area.

Establishing the stratigraphic and structural relationships of the Paleozoic rocks in the Adams Lake region is important for understanding the genesis of massive sulphide deposits and tectonic setting of the ancient distal margin of North America. Additional fieldwork is planned in the Mount Tod region, including detailed and regional mapping near Cahilty and Tsalkom Mountain, and sampling for paleontological and geochronological analyses.

ACKNOWLEDGMENTS

Particular thanks are given to Ken Daughtry, Bob Thompson, Mike Cathro, Paul Schiarizza, Trygve Höy, and Andrew Okulitch who provided field guidance, maps and sections, karma, and helpful discussions regarding the geology of the area. Thanks are given to Morgan Soley for his efficient field and technical assistance. Paul Schiarizza provided a critical review of the manuscript.

REFERENCES

Bailey, S.L., Paradis, P., and Johnston, S.T. (2000): Geological setting of the Samatosum and Rea massive-sulphide deposits, Eagle Bay Assemblage, south-central British Columbia; *Geological Survey of Canada*, Current Research 2000-A15, 10 pages.

Ettlinger, A.D. and Ray, G.E. (1989): Precious Metal Enriched Skarns in British Columbia: An overview and geological study; *British Columbia Ministry of Energy and Mines,* Paper 1989-3, 120 pages.

Höy, T. (1999): Massive Sulphide deposits of the Eagle Bay Assemblage, Adams Plateau, South-Central British Columbia (082 M/3, 4); *in* Geological Fieldwork 1998, *British Columbia Ministry of Energy and Mines*, Paper 1999-1, pages 223-245.

Jones, A.G. (1959): Vernon map-area, British Columbia; *Geological Survey of Canada,* Memoir 296, 186 pages.

Miller, D.C. (1989): Geological and Geochemical Report: Steep 1, 3, 4 and 5 Claims; *Discovery Consultants*, Vernon / Kamloops, B.C., 14 pages.

Monger, J.W.H., Souther, J.G. and Gabrielse, H. (1972): Evolution of the Canadian Cordillera; a plate tectonic model; *American Journal of Science*, volume 272, pages 577-602.

Monger, J.W.H., Price, R.A. and Templeman-Kluit, D.J. (1982): Tectonic accretion and the origin of the two major metamorphic and plutonic welts in the Canadian Cordillera; *Geology*, volume 10, pages 70-75.

Okulitch, A.V. (1979): Lithology, stratigraphy, structure and mineral occurrences of the Thompson-Shuswap-Okanagan area, British Columbia; *Geological Survey of Canada*, Open File 637.

Okulitch, A.V. (1989): Revised stratigraphy and structure in the Thompson-Shuswap-Okanagan map area, southern British Columbia; in Current Research, Part E, *Geological Survey of Canada*, Paper 89-1E, pages 51-60.

Ray, G.E. and Webster, I.C.L. (2000): Geology of the Heffley Lake Area, South-central British Columbia; *British Columbia Ministry of Energy and Mines*, Open File 2000-10.

Roback, R.C., Schiarizza, P., Nelson, J., Fyles, J., Ferri, F., Höy, T., Ash, C. and Danner, W.R. (1995): Late Paleozoic Arc and Oceanic Terranes and their external relationships, southern Quesnellia; *GAC/MAC Annual General Meeting 1995*, Field Trip Guidebook B2, Victoria, British Columbia, 79 pages.

Schiarizza, P. and Preto, V.A. (1987): Geology of the Adams Plateau-Clearwater-Vavenby area; *British Columbia Ministry of Energy, Mines and Petroleum Resources*, Paper 1987-1, 88 pages.

Thompson, R.I. and Daughtry, K.L. (1997): Anatomy of the Neoproterozoic-Paleozoic continental margin, Vernon map area, British Columbia; in Current Research 1997-A; *Geological Survey of Canada*, pages 145-150.

Thompson, R.I. and Daughtry, K.L. (1998): Stratigraphic linkages across Vernon map area, British Columbia; in Current Research 1998-A; *Geological Survey of Canada*, pages 181-187.

Wheeler, J.O. and McFeely, P. (comp.) (1991): Tectonic Assemblage Map of the Canadian Cordillera and adjacent parts of the United States of America; *Geological Survey of Canada*, Map 1712A, scale 1:2 000 000.

Geology of the Area Between the Sustut Copper Deposit and the Day Porphyry Copper Prospect

By Andrew Legun

KEYWORDS: Takla Group, Moosevale Formation, Savage Mountain Formation, Upper Triassic, Lower Jurassic, Hazleton Group, Sustut copper deposit, Day prospect, volcanic redbed copper, Willow showing.

INTRODUCTION

The area of study lies within the headwaters of the Sustut River drainage about 350 kilometres north of Prince George, covering portions of NTS 94D/7 and D/10. The Omineca Mining Road lies just to the east of the area. To the northeast, across the Moosevale valley, lies the southern McConnell Range mapped by the writer in 1997 (Figure 1).

The Kemess mine is forty-five kilometres to the north. Elevations range from 1200 metres to 2300 metres with the tree line at about 1650 metres. In the summer of 2000 helicopters were stationed either at the Kemess mine or a trailer camp at kilometre 400 of the Omineca Mining Road.

The writer spent 20 days in the field assisted by Brent Carbno, a recent M.Sc. graduate from the University of Victoria. Traverses were based from three fly camps. The report here references information from a larger area than shown in figure 1.

OBJECTIVES

The principal objectives of the project were:

1. To determine the distribution of various copper-bearing sedimentary subunits of the Moosevale Formation.
2. To map the broad band of geology from the Sustut deposit southward to the Day prospect.
3. To relate the economic stratigraphy at Sustut to similar stratigraphy in the southern McConnell Range.

PREVIOUS WORK

The region was covered by 1:250 000 mapping by the Geological Survey of Canada during the mid 1940s (Lord, 1948). A number of showings were found. One of these, the Marmot, was the focus of the first modern exploration (1960s) in the general area. At the same time there was significant exploration activity for porphyry copper and molybdenum mineralization in the intrusive belt running north and south through the McConnell Range. A large gossan was discovered in 1966 at the present site of the Kemess North prospect and led to similar exploration on nearby ground. Falconbridge Nickel Ltd., during a reconnaissance helicopter flight in 1971, discovered a malachite-stained bed in the Sustut drainage that was traceable for over 2500 feet. Their assessment suggested a replacement copper deposit hosted by volcaniclastic rocks in the upper part of the Takla Group. Numerous junior and major resource companies acquired ground in the area. In 1972 copper was found on the Willow cliffs on the opposite side of the Sustut River and a porphyry style target was identified at the Day. In 1973 the B.C. Geological Survey conducted a mineral deposit study of the Sustut copper area (Church, 1974a). The Geological Survey of Canada returned to pursue general and detailed studies within the McConnell sheet (Richards 1976, and Monger 1977). Monger and Church (1976) revised the stratigraphic nomenclature based on breaks and lithological changes in the volcanic succession supported by fossil data and field observations. In 1983, follow up of a gold-copper-molybdenum soil anomaly led to the discovery of the Kemess South porphyry deposit.

Site-specific work continued in the 1980s and 1990s on various properties. In 1996 a regional geochemical survey of the McConnell map sheet resulted in numerous multi-element precious and base metal anomalies within the general area of interest (Jackaman, 1997). Diakow mapped the northern part of the nearby McConnell Range in 1997 (Diakow, 1998) and this writer pursued studies at its south end (Legun, 1998).

In late 1999 Doublestar Resources Ltd. purchased all of Falconbridge Nickel's properties in British Columbia, including Sustut Copper. Doublestar's 2000 exploration program at Sustut consisted of fill-in drilling (20 holes for 5865 feet) in the higher grade Southeast Zone. Since their work program was helicopter-supported, the British Columbia Geological Survey field crew were able to use the same aircraft for their field work at much reduced cost.

REGIONAL GEOLOGIC SETTING

The area is underlain by volcanic rocks of the Asitka, Takla and Hazleton Groups (Figure 2).

Regionally the Takla Group lies disconformably to unconformably above cherts and siliceous mudstone of

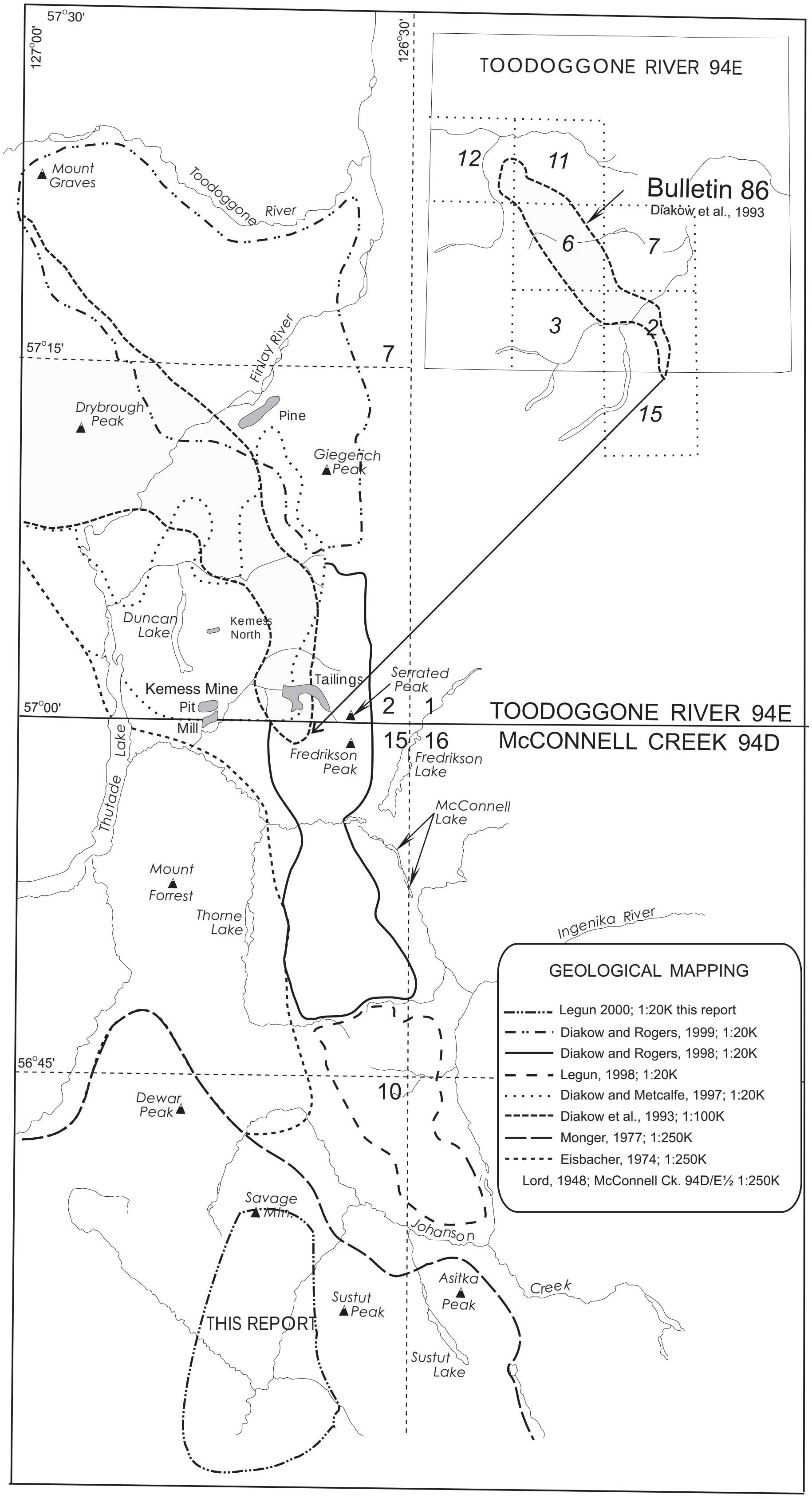

Figure 1. Location of recent and previous mapping in the northeastern McConnell Creek (94D) and southern Toodoggone River (94E) map areas. Modified after Diakow (1998).

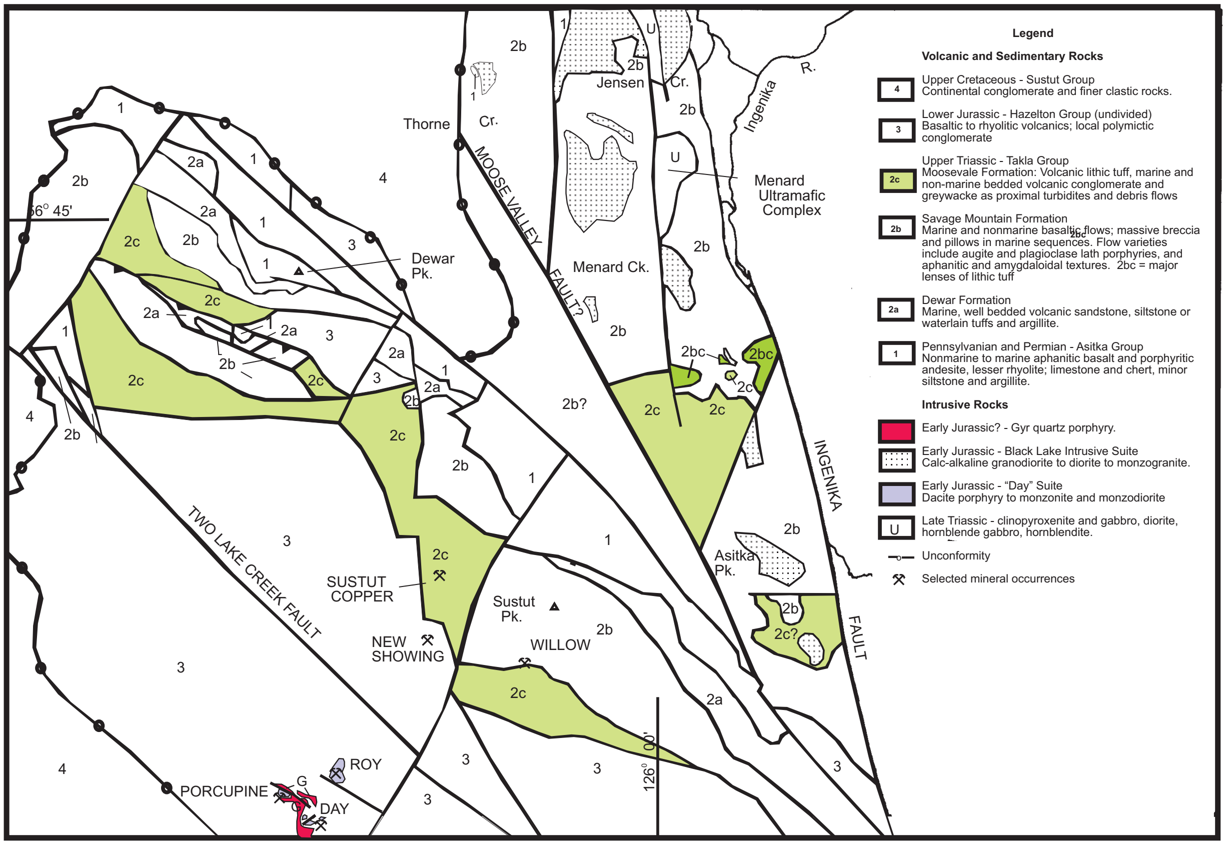

Figure 2. Schematic geology of the McConnell Range and Sustut-Day areas showing major lithostratigraphic divisions and plutonic rocks. Geology after Monger (1976), Legun (1998), Diakow (1998) and unpublished maps of Falconbridge Nickel Mines Ltd.

the early Permian Asitka Group, a volcano-sedimentary package that includes rhyolites and limestone as well as mafic volcanics, shale and chert. Diakow (1998) places the base of the Takla at the first occurrence of Halobia-bearing shale above cherts. The Asitka is confined to the slopes facing Moosevale valley and was not examined.

The Dewar Formation, forming the base of the Takla succession, is regionally the most extensive facies of the Takla, but is thin in the area of study, consisting of 300-400 metres of siltstone, crystal-rich sandstone, and interbedded argillite. It thickens to the southeast and is up to 1600 metres thick in the Sikanni Range. It thins to a feather edge in the northern McConnell Range where Diakow recognises only a few metres below Savage volcanics and above the Asitka (Diakow 1998, Figure 8.3).

The Savage Mountain and Moosevale Formations dominate the Takla in the area of study. Augite-bearing pillowed flows and minor breccias constitute the Savage (1600 metres) which passes laterally to Dewar facies toward the Sikanni Range. Overlying the Savage is a sequence, 1400 metres thick, dominated by breccias. The breccias are disorganised in the lower part of the sequence but stratified in its upper. This is the Moosevale Formation that hosts the Sustut deposit. In the Sikanni Range it rests directly on the Dewar Formation.

Fossil data shows the Dewar and Savage are upper Carnian to lower Norian (Late Triassic), while the Moosevale may be restricted to the lower Norian.

A few kilometres south of Sustut the upper contact of the Takla Group is marked by a transition to polymictic conglomerate. The contact here appears gradational over 5 metres or so but regionally it is an unconformity. The conglomerate comprises the base of the Hazelton Group, a volcano-sedimentary package of more calc-alkaline affinity than the Takla. Monger suggested the polymictic conglomerate was probably of Lower Jurassic Sinnemurian age based on correlation with similar rocks in the area of Mt. Iktlaki, 16 kilometres to the south (Monger and Church, 1976).

Strata of the Takla Group are regionally metamorphosed to zeolite (prehnite-pumpellyite) facies grade. This contrasts with generally higher greenschist to amphibolite grades found east of the Ingenika fault.

STRATIGRAPHY

Takla Group

SAVAGE MOUNTAIN FORMATION

The Savage Mountain Formation is characterized by pyroxene basalt porphyry, pyroxene-feldspar porphyry and massive basalt. Work by the author in the Southern McConnell Range showed a clear upward change in composition. Pyroxene porphyries dominated the lower sequence while coarse feldspar lath porphyries approaching andesite composition cap the sequence.

These compositional changes are not apparent in the Savage Mountain Formation at Sustut. At Sustut the Savage Mountain Formation is dominated by pillow lavas that are pyroxene porphyries. The top of the sequence shows some development of spherulites, is locally carbonated and massive. Interbeds between pillow sequences at Sustut show gradations to pillow breccia, and beds of nodular debris with greenish cherty bands. The pillow breccia perhaps originates as spalling material from submarine flows on appreciable slopes.

Across the Sustut River at the Willow showing Church (1974b) and Burns (1974) show the upper sequence is dominated by thin aphanitic and amygdaloidal flows. However, the writer noted at one location a clear pillow sequence at the very top of the Savage Formation.

In southern McConnell Range the upper Savage consist of a series of flows with reddish oxidised tops. As well there are large mappable intercalations or wedges of tuff breccia. This is not apparent at Sustut.

In the Dewar-Sustut-Willow area the Savage Formation thus appears to have formed broad submarine edifices while in the McConnell Range shield volcanoes emerged above sea level. The rapid thickening northward of lath porphyry flows and wedges of tuff breccia is evidence for those subaerial edifices.

MOOSEVALE FORMATION

The Moosevale Formation is a volcaniclastic unit that lies abruptly on the Savage Mountain Formation. In this study area the subdivisions of Harper (1977) were found to be useful, but the writer has given decriptive names to the subdivisions 3a,3b,3c,3d. These are a basal marine shale, a lower division breccia facies called the “chaotic breccia” in this article, a middle sandy unit, and an upper semi-stratified breccia and matrix-supported conglomerates with graded beds. The lower and upper breccias correspond to the lower and upper members of the Moosevale described by Monger and Church (1976) and the sandy unit is not formally known outside the area.

Most clasts in the Moosevale can be ascribed to the Savage Formation but not from immediate sources. For example, coarse feldspar lath porphyry is unknown in the Savage Formation at the Sustut copper property. Similarly clasts in the Moosevale at Sustut carry no vestiges of pillows rinds.

Feldspar porphyries and pyroxene-hornblende feldspar porphyries are common as clast types in the Moosevale Formation. Pyroxene (without feldspar) porphyry clasts are less common in contrast to their abundance in the Savage. Monger (1977) suggested in an AFM diagram that Moosevale clasts lay in a field between Hazleton and Savage compositions.

Basal Shale and Siltstone Band

This marine shale unit is described by Monger and Church (1976) as transgressive as it occasionally overlaps volcanic flows interpreted to be subaerial.

The shale band is best developed at Willow Ridge where up to 60 metres of Halobia-bearing black shales and argillites are present (Burns, 1974). The shale thins rapidly along strike and within a few hundred metres to the east is only about 10 metres thick. At that location it lies abruptly on reddish limestone that caps pillowed lava of the Savage Mountain Formation. The shale probably drapes a preserved submarine topography. The shale is missing on the ridge to the east (cut out by a volcaniclastic wedge?), but reappears further east where Burns notes 30 metres of fossiliferous brown to black shale near a showing called the Sit.

West of Willow Ridge the shale band is offset at the Sustut River fault and reappears as a band of greenish cherty siltstones at the base of cliffs north of the Sustut deposit. The band is visible in a gully where large peels of siltstone are found in sandy turbidite interbeds and it is offset and truncated in a succession of faults.

To the northeast in the southern McConnell Range (Legun, 1998) a possible equivalent is present in a sandy lens at the base of the chaotic breccia unit of the Moosevale. The lens is about 50 metres thick and a few hundred metres wide. It comprises thick beds of calcareous and lithic tuffaceous sandstones (with crossbeds and mud chips), stratified grit and conglomerate, minor red and green siltstone, calcareous argillite and laminated chert.

The stratified sediments are overlain by at least 800 metres of lithic tuffs, massive tuffs, slump facies with red siltstones, graded conglomerates, and tuffaceous breccias cut by occasional sills of megacrystic augite porphyry. The breccias are similar to that of the lower Moosevale seen elsewhere. The minor presence of quartz in the lens is however atypical.

To the northwest the basal shale unit has not been formally recognized in the area of Dewar Peak; however, the entire Moosevale Formation is described as marine (Monger, 1977). Therefore, it is probably masked by coarse influx from a proximal sediment source.

The marine shale or its equivalent may be present to the southeast in a fault block panel between the Asitka and Sustut rivers. Monger (1977) notes fossiliferous grey argillite and siltstone interbedded with conglomerate near the base of the formation.

Chaotic Breccia

A thick sequence of breccias, which belong to the lower division breccia facies, overlie the basal sediments. Bedding attitudes are difficult to discern in these chaotic breccias. There are two main lithotypes.

One, lithic tuff breccias with similar volcanic material in the matrix and clasts. Clasts are subrounded to subangular, the matrix has fragmented and sparse crystals of feldspar. The clasts are dominated by pyroxene-feldspar porphyries.

Two, complex breccias which contain large blocks up to 2 metres or more in a matrix of variable composition. The matrix may be irregular masses of bedded sediment, often siltstone, and lensoid masses of stratified conglomerate. Some armoured clasts seem to be present.

Sandy Unit

The sandy unit at Sustut is present at the northern base of the cliffs of the "mesa". The same unit was mapped half a kilometre southwest of Savage peak. The unit includes minor mudstones. Some beds have detached isoclinal folds suggesting slumps, others are full of large blocky chips of red siltstone, one distinct bed comprises a sharp based graded tuffaceous sandstone with crescent and oval-shaped inclusions of mudstone. Monger (1977) retrieved Halobia fossils from this unit (sample H and I on map), probably from the mudstones. The sandy unit represents a shallower marine environment than that represented by the basal marine band. It may have been occasionally emergent as evidenced by mudcracks.

UPPER SEMI-STRATIFIED BRECCIA AND CONGLOMERATE

At Sustut the sandy unit is overlain by thick beds of semi-stratified breccia. Semi-stratified breccia bodies include matrix-supported conglomerates and significant lenses and interbeds of stratified and graded beds with mudstone rip-ups. In contrast to the chaotic breccia, strike and dip bedding surfaces are discernible in intercalated sediments. The semi-stratified breccia still includes a considerable portion of slump and "tuff breccia" similar to the lower unit.

The tuff breccia includes monomictic breccias with embayed and very irregular shaped volcanic clasts in a slightly darker matrix. They may be peperites, formed by interaction of magma with wet sediments. Other tuff breccia variants include clasts with alteration rims and clasts "etched" against altered matrix. These may be subaqueous eruption breccias.

The upper part of semi-stratified breccia is dominated by sandy, matrix-supported conglomerates. Harper noted that the upper 365 metres (1200 feet) of the upper division was rather reddish with a more lime-rich matrix than the red and green beds immediately below.

EXTENT AND THICKNESS OF MOOSEVALE

It is apparent that the structural basin of deposition underwent changes in the Lower Jurassic. For example on the ridge network east-southeast of Willow Ridge the Hazleton cuts down into the Savage Mountain Formation in stepwise fashion. A tilting fault block is probable. Monger also reports dramatic local thickness changes in the Moosevale Formation at Mt. Dewar related to downcutting channels at the base of the Hazleton.

It is clear that the Moosevale, once of wider extent, is preserved in a remnant structural basin by earliest Jurassic time. The remnant basin appears to preserve the thicker deposits of the original basin.

Hazleton Group

POLYMICTIC CONGLOMERATE

On the ridge immediately south of the Sustut highland the transition to a polymictic conglomerate is marked by the appearance of chert clasts within matrix supported conglomerates of the Moosevale and their increase up section. The transition interval varies from a few metres to perhaps ten metres of section. The polymictic conglomerate is clast to matrix-supported, with clast support more evident in the upper beds. Generally it has less matrix than Moosevale breccias and the clasts are more closely packed. The matrix is more of a wacke with mudstone matrix rather than the tuffaceous, broken crystal-rich matrix common to the Moosevale. Clasts include pale volcanic feldspar porphyries, red siltstones, chert and limestone (up to 50 centimetres diameter). Some limestones are fossiliferous and carry ammonites. The clasts reflect erosion of Asitka lithologies but with some component of Takla volcanics.

Regionally the contact with the Takla Group varies from faulted to erosional channel fills or conformable transitions. It appears alluvial fans from an eroding source prograded into the area but local conditions varied from subaerial to subaqueous. Richards reports (in Monger 1976) bedding current directions indicating sources from north and east.

Lower Hazleton Group

On the ridge network a kilometre south of the Sustut mesa the lithologies immediately above the polymictic conglomerate comprise matrix-supported conglomerates with finer grained, sandy, reddish tops. Clasts are pale andesitic to dacitic feldspar porphyries. The lack of Takla Group clasts suggests the landscape was buried under renewed volcanism in the early Jurassic. Richards (1976) mapped this area on the north side of Two Lake Creek fault as part of a northwest trending half graben fill of volcaniclastics (unit 6a). Conglomerate and breccia passes upward to reddish lithic tuffs, tuffaceous sandstone, lapilli tuff and reddish andestic flows of clear subaerial character.

On the south side of Two Lake Creek fault massive greenish grey andesitic volcanics dominate. These do not have pillow features and belong to an extensive volcanic unit (unit 6 of Richards 1976) probably overlying the volcaniclastics. The volcanics are faulted and mantled by tuffs and subaerial flows in well bedded sequences.

A well exposed sequence overlies massive andesites in the drainage of Harper Creek. It includes welded tuffs, columnar jointed tuffs, lapilli tuff, rubbly subaerial breccias and very vesicular flows (with chalcedonic "thunder eggs"). The columnar jointed tuff, possibly the ignimbrite described by Church (1983), fills a paleochannel, probably cut in a volcanic slope. Some flows abut earlier andesites marking an unconformity or fault. The volcanic topography must have evolved in a rather complex manner. In the Day area dacitic ignimbrites represent evolving felsic magmatism. Their source may be the Gyr porphyry (Church, personal communication).

DACITE PORPHYRY AND MONZODIORITE PLUGS

South of Two Lake Creek a suite of intrusive plugs of common character extend southeast to northwest across the Sustut River. Only those on the west side near the Day, Roy and Birch minfile showings were examined. These are plugs of dacite porphyry/monzodiorite with varying development of pyritic and silicic alteration and bearing local concentrations of copper mineralization. Locally they carry abundant magnetite as an accessory mineral. The Day "granodiorite" is the best known example. Others include an intrusive at the Roy showing (minfile 94D 078), a dacite porphyry near the Birch (minfile 94D 077). Two other plugs of modest size are noted on old Falconbridge maps west of the Day (one of which was drilled). The bodies have been listed under a rather confusing variety of names in individual reports, perhaps due to textural variations from porphyritic to equigranular. However, an unpublished compilation map of Falconbridge Ltd., refers to them all as unit 11 "diorites". To the east, across Sustut River other intrusives may be part of the suite (eg. one is informally known as the Pat intrusive). In two areas there have been anomalous zinc values at sample sites near these intrusives (eg Gyr and Brown, 1973) but no clear association shown. The Day and Pat have been dated to a metallogenetically significant period (185 m. yrs for Lorraine, Mt. Milligan deposits.). By association these other plugs are also of some interest and constitute a theme for some reassessment of the area. The minfile showings are described in more detail in the Economic Geology section.

GYR PORPHYRY

The Gyr porphyry has an aphanitic, occasionally flow banded matrix and is reddish to orange on the fresh surface with sparse feldspar phenocrysts. It contains a few per cent quartz eyes which clearly distinguish it from the dacite porphyry/monzodiorites. Its age relationship to the latter is unclear. Church (1983) showed the rock was rhyolitic in composition and described it as "a sinuous assemblage of small felsic stocks, dikes, and sill-like bodies". More detailed mapping in the area of interest suggests the main body is a large sill. Many contacts are shallow, concordant with regional bedding.

ECONOMIC GEOLOGY

Sustut Copper Deposit

The best defined mineral resource in the area of study is the Sustut Copper deposit, located south of Savage Mountain. It has an inferred resource of 20.1 million tonnes at an indicated grade of 1.17% copper, including the Southeast zone which contains 7.6 million tonnes grading 1.64% copper (George Cross News Letter, September 20, 2000). The deposit consists of fine grains of hematite, pyrite, chalcocite, bornite, chalcopyrite and native copper (in decreasing abundance) dispersed in matrix and clasts of volcaniclastic rocks in the Moosevale Formation. Alteration minerals include epidote, quartz, prehnite and carbonates. The main mineralized zone is partially concordant with bedding, and lies within the semi-stratified breccia, 250 metres above the sandy unit (Harper, 1977). This places it 400 metres below the polymictic conglomerate. Harper (ibid) noted that the upper 365 metres (1200 feet) of the semi-stratified breccia was rather reddish with a more lime rich matrix than the red and green beds immediately below. Interestingly the lime rich band would then lie just above the main Sustut band of mineralization.

Willow Showing

A thin grey-black lapilli tuff unit at the top of the basal shale of the Moosevale contains limestone as well as volcanic clasts. This unit contains irregularly distributed chalcopyrite and chalcocite mineralization. Church (1974b) described the mineralization as fine grained disseminations (less than a mm) constituting up to 30% by weight of some samples. The best showing is a lens 25 by 10 feet. A grab sample assayed 8.06 % copper (Burns, 1974). Most other assays over 5 foot intervals in this unit returned much lower values (0.25% Cu or less). Mineralized shears in the unit assayed up to 2.18% Cu over 5 feet. Drilling did not intersect the main surface showing at depth. However minor base metal values were intersected in the shale (maximum 10 foot assay of 0.11% oz/T Ag, 0.05% Zn, 0.08% Pb, 0.02% Cu). Burns traced this unit some 3000 metres to the east.

New Showing

A new showing was found during the field season on the ridge immediately south of Sustut highland. The showing comprises a set of malachite/bornite/chalcocite veins and shears extending over a width of about 10 metres and extending perhaps 10-15 metres vertically within the basal polymictic conglomerate close to its contact with Hazleton volcaniclastics. Epidote and calcite line the wallrock of the main vein which is 10-15 centimetres wide. The mineralization is near an inferred fault. Though clearly cross-cutting and non-stratiform, the mineralogy of the vein is similar to the sulphides and alteration phases found at Sustut.

DAY PORPHYRY COPPER PROSPECT

At the main showing altered dacite porphyry intrusive is well mineralized with bornite and chalcopyrite associated with a rusty quartz-ribboned outcrop knob. Quartz ribbons are apparently late fissure fills of silica with a central, dark seam of unknown material. Chalcopyrite is the main ore mineral, pyrite is also abundant in massive knots. There is a bit of chalcocite and abundant malachite stain on the rusty outcrop. Molybdenite has been identified in drill core. At the main showing the intrusive is highly altered and carbonated, but accessory magnetite is intact. Church (1983) showed through chemical analysis that the altered rock was enriched in potassium and carbon dioxide. The fresh intrusive is quartz poor, carries abundant feldspar plates, and up to 10% amphibole. Fracturing is well developed with chalcopyrite abundant on surfaces. Chalcopyrite is also disseminated and forms stringers and clots. The mineralization is clearly associated with the quartz flooding. Late thin calcite veins cut the quartz veins. Epidote is lacking. In more extensive exposures to the east the intrusive is relatively unaltered amd mineralization is restricted to a few fracture coatings with malachite and chalcopyrite.

The Day intrusive is cut off on the north side by a fault and a separate small intrusive body lies to the north. Another body of uncertain size lies to the east. Limited drilling of the main mass suggests it may be a sill or laccolith. Existing data could also be interpreted as a series of elongate dike-like bodies, conceivably related to a larger underlying body.

Roy Showing

The Roy showing is hosted in a weakly zoned intrusive body varying from dacite porphyry near margins to monzodiorite and monzonite in the core. In hand specimen the intrusive is similar to the Day “granodiorite”, consisting of abundant sodic plagioclase, some potassium feldspar and hornblende, remnant chloritised pyroxenes and up to 10% quartz, most of which is believed to be secondary. Petrographic work suggests weak to moderate propylitic and sericitic alteration.

The contact with andesite porphyry wallrock is rather subtle, the intrusive rock characterized by a paler matrix and more abundant feldspar phenocrysts. To date the boundaries of the intrusive have not been completely defined though a magnetic high provides the basic shape. The writer defined its southern border. The intrusive exhibits fairly widespread pyritic alteration and local silicic alteration, possibly related to shears. A pyritic halo extends into the wallrock on its southeast side. The northwest margin shows some peculiar breccias of greenish blocks within a pinkish matrix that may be an alteration effect rather than primary.

At the showing a series of trenches have been cut into the monzonitic phase of the intrusive. The trenches expose a sporadically mineralised belt of quartz shears and stockworks with chalcopyrite, malachite and magnetite trending west northwest (Fox, 1991). Best results are a weighted average of 0.121 % copper and 0.016 oz/ton gold over 62 metres (Fox, ibid). There was apparently some undocumented drilling in 1997 on the property.

Though the Roy appears to fall short of the mark in porphyry grade, it appears to be a larger body with a broader alteration zone than the Day.

Cisco-Porcupine Showing

A series of trenches were examined along a creek in this claim group. Successive trenches show similar massive silica-pyrite banded masses. The host rock to the extensive alteration zone is unclear, but Aussant (1991) reported altered dacite. A map by Falconbrige indicates an intrusive “diorite”. The sulphide is essentially stringers and pods of massive pyrite within quartz, some magnetite and local chalcopyrite. Though banding is somewhat variable in orientation there does seem to be a northwest trend. This is roughly parallel to a fault margin of an elongate body of Gyr porphyry immediately to the east. The quartz zone may thus plug the fault at the contact of Gyr porphyry and dacite. Sampling returned some anomalous gold values and to 2.4% copper over 0.9 metres in one trench. Aussant (ibid) suggested a volcanogenic massive sulphide target but the writer believes these quartz-pyrite-magnetite zones are related to dacite porphyries as at the Roy showing.

COMMENTS PERTINENT TO REGIONAL EXPLORATION

Potential exists for Sustut targets in areas underlain by the Moosevale Formation at lower elevations. For example, work in the 1970s in the Willow area appeared to end with some showings found at or just below tree line. Low elevation areas at Willow Creek, southern McConnell Range, and Asitka peak are prospective though exposures may be limited. The area at Willow Creek is unfortunately within a designated park.

The polymictic conglomerate at the base of the Hazleton Group is prospective for a Sustut target. The new showing found this summer raises the potential of this unit. Burns reports the Horseshoe copper showing which is also hosted in this conglomerate (Burns, 1974 page 26). As well there is at least one report of mineralized transported clasts in this unit (Monger, 1976).

The potential to discover small intrusive porphyry bodies west of the Day area is high, particularly at lower elevations. Some assessment of them as a suite may be useful. Magnetic highs are indicative of their presence, though in highly altered zones this signature is missing.

The origin of large silica-pyrite zones with anomalous values including copper, west of Day is unclear. It does not appear to be a volcanogenic massive sulphide target as suggested in some reports. It may be related to Gyr porphyry bodies or silica altered dacite porphyries with modest copper-gold potential.

REFERENCES

Aussant, Claude H. (1991): Geological and Geochemical Sampling Report on the Cisco 1-7 Claims, Omineca Mining Division; Ministry of Energy, Mines and Petroleum Resources, Mineral assessment report 21857, 49 pages.

Burns, P.J. (1974): Report of Progress During 1973 on the Willow-Will-Asitka Claims, Omineca Mining Division; Internal Report for Falconbridge, 29 pages.

Church, B.N. (1974a): Sustut Copper; in Geology, Exploration and Mining in British Columbia, 1973; B.C. Ministry of Energy, Mines and Petroleum Resources, pages 417-432.

Church, B.N. (1974b): Willow; in Geology, Exploration and Mining in British Columbia 1973; B.C. Ministry of Energy, Mines and Petroleum Resources, pages 432-433.

Church, B.N. (1983): Geology of the Day Porphyry Copper Prospect; in Geology in British Columbia 1976, B.C. Ministry of Energy, Mines and Petroleum Resources, pages 110-119

Diakow, L.J. (1998): Toodoggone-McConnell Project: Geology of the McConnell Range-Serrated Peak to Jensen Creek, Parts of NTS 94E/2 and 94D/15; in Geological Fieldwork 1997, B.C. Ministry of Employment and Investment, Paper 1998-1, pages 8a-1 to 8a-13.

Fox, M. (1991): Geological and Geochemical Report and Review of Geochemical and Geophysical Data, Sus 1 to 4 Claims; Ministry of Energy, Mines and Petroleum Resources, Mineral assessment report 4784, 3 15 pages.

Gyr,T., and Brown, D.H. (1973): Geochemical Report on the Pat Group of Claims; Ministry of Energy, Mines and Petroleum Resources, Mineral assessment report 4784, 3 pages.

Harper, G. (1977): Geology of the Sustut Copper Deposit in B.C.; The Canadian Institute of Mining and Metallurgy Bulletin, Volume 70, Number 777, pages 97-104.

Jackaman, W.J. (1997): British Columbia Regional Geochemical Survey, NTS 94D - McConnell Creek; B.C. Ministry of Employment and Investment, BCRGS 45.

Legun, A.S. (1998): Toodoggone-McConnell Project: Geology of the McConnell Range-Jensen Creek to Johanson Creek, Parts of NTS 94D/9,10,15,16; in Geological Fieldwork 1997, B.C. Ministry of Employment and Investment, Paper 1998-1, pages 8b-1 to 8b-10.

Lord, C.S (1948): McConnell Creek Map-Area, Cassiar District, British Columbia; Geological Survey of Canada, Memoir 251, 72 pages.

Monger, J.W.H. (1976) Lower Mesozoic rocks in McConnell Creek map-area (94D) British Columbia; in Report of Activities, Part-A, Geol. Survey of Canada, Paper 76-1A. pages 51-55.

Monger, J.W.H. (1977): The Triassic Takla Group in McConnell Creek Map-Area, North-Central British Columbia; Geological Survey of Canada, Paper 76-29, 45 pages.

Monger, J.W.H. and Church, B.N. (1976): Revised Stratigraphy of the Takla Group, North-Central British Columbia; Canadian Journal of Earth Sciences, Volume 14, pages 318-326.

Richards, T.A. (1976): McConnell Creek map-area (94D east-half), British Columbia; Geological Survey of Canada, Open File 342.

Wilton, D.H. and Sinclair, A.J. (1988): Ore Petrology and Genesis of a Strata-Bound Disseminated Copper Deposit at Sustut, British Columbia; Economic Geology, Volume 83, pages 30-45.

British Columbia Geological Survey
Geological Fieldwork 2000

A Hydrothermal Origin for "Crinkle Chert" of the Big Salmon Complex

By Mitchell G. Mihalynuk[1] and Jan M. Peter[2]

KEYWORDS: Economic geology; Big Salmon Complex, volcanogenic massive sulphide, mineralization, chert geochemistry, exhalite, Yukon-Tanana Terrane, Kootenay Terrane, Jennings River.

A key focus of fieldwork in the Big Salmon Complex in 2000 was further investigation of a manganiferous metachert marker horizon referred to as the "crinkle chert" (Mihalynuk *et al.*, 1998). The crinkle chert forms a regional sedimentary layer that extends over 80 kilometres in northern British Columbia (Figure 1), and it is similar to a unit known from the Little Salmon area (Colpron and Reinecke, 2000), 250 km to the north. However, at this latter locality, the oldest age of the manganiferous chert is constrained as Late Mississippian, the oldest age limit of fossils in underlying strata (ibid.); whereas the Big Salmon Complex crinkle chert is older than Middle Mississippian based on dikes that cut overlying strata (Mihalynuk *et al.*, 2000).

The crinkle chert could be interpreted as a pure meta-siltstone, however microscopic analyses fail to reveal clear evidence of clastic sedimentary textures from anywhere except near the upper contact where it is locally overlain by impure quartzite. An alternate explanation is that it is a metamorphosed radiolarian chert, as such cherts can contain elevated Mn, and to a lesser extent Ba. Greenschist metamorphism and the highly strained nature of these rocks precludes the recognition of radiolarian microfossils, if present, which would unequivocally establish a biogenic origin for the crinkle chert.

Field investigations in 2000 revealed stratiform magnetite layers up to a decimetre thick within, and near the top of the crinkle chert unit (Figure 1). These layers are difficult to explain other than by a hydrothermal origin, as originally suggested by Nelson (1997), based on the presence of trace to minor barium, copper and manganese. Our evaluation of five existing geochemical analyses of the crinkle chert (Cook and Pass, 2000) indicates a hydrothermal, not hydrogenous origin (e.g., Figure 2). The recognition of seafloor hydrothermal origin for the crinkle chert unit points to the possible presence of undiscovered volcanogenic massive sulphide (VMS) mineralization in the area. Explorationists can consider the crin-

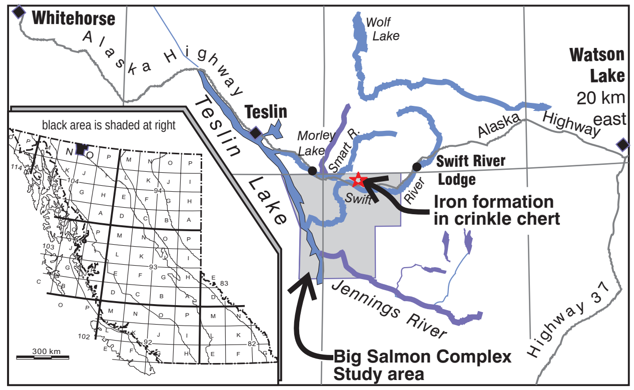

Figure 1. Location of the Big Salmon Project area. The star denotes the locality where iron formation has been observed within the crinkle chert unit. For the regional distribution of the crinkle chert unit in northern British Columbia *see* Mihalynuk *et al.* (2000).

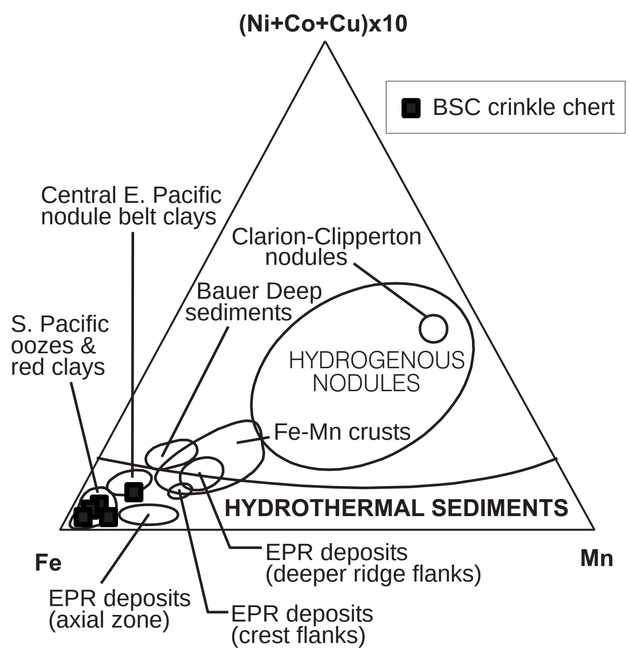

Figure 2. (Ni+Co+Cu)*10-Fe-Mn ternary plot for Big Salmon Complex crinkle chert (Cook and Pass, 2000). Also shown are the general fields for hydrothermal sediments and hydrogenous nodules (Bonatti et al., 1972), Fe-Mn crusts (Toth, 1980), for Bauer Deep sediments (Sayles and Bischoff, 1973), East Pacific Rise deposits (axial zone, crest flanks, and deeper ridge flanks) (Germain-Fournier, 1986), South Pacific biogenous oozes and red clays, siliceous clays from the Central East Pacific nodule belt, and Clarion-Clipperton zone associated Mn nodules (Karpoff *et al.*, 1988).

[1]*British Columbia Ministry of Energy and Mines*
[2]*Geological Survey of Canada*

kle chert as a time-stratigraphic marker for hydrothermal activity.

REFERENCES CITED

Bonatti, E., Kraemer, T. and Rydell, H. (1972): Classification and genesis of iron-manganese deposits, in Ferro-manganese Deposits on the Ocean Floor, edited by D.R. Horn, New York, *Harriman, Arden House and Lamont-Doherty Geological Observatory*, pages 149-166.

Colpron, M. and Reinecke, M. (2000): Glenlyon Project: Coherent stratigraphic succession from Little Salmon Range (Yukon-Tanana Terrane), and its potential for volcanic-hosted massive sulphide deposits; *in* Yukon Exploration and Geology 1999, edited by D. S. Emond and L. H. Weston, Exploration and Geological Services Division, Yukon, *Indian and Northern Affairs Canada*, pages 87-100.

Cook, S.J. and Pass, H.E. (2000): Ancient Pacific Margin Part V: Preliminary Results of Geochemical Studies for VMS Deposits in the Big Salmon Complex, Northern British Columbia; *in* Geological Fieldwork 1999, *B.C. Ministry of Energy and Mines*, Paper 2000-1, pages 71-106.

Germain-Fournier, B. (1986): Les sédiments métallifères océaniques actuels et anciens: caractérisation, comparaisons: Unpublished Ph.D. thesis, University Bretagne Occidentale, France.

Karpoff, A. M., Walter, A.-V. and Pflumio, C. (1988): Metalliferous sediments within lava sequences of the Sumail ophiolite (Oman): Mineralogical and geochemical characterization, origin and evolution; *Tectonophysics*, Volume 151, pages 223-245.

Mihalynuk, M.G., Nelson, J. and Friedman, R.M. (1998): Regional Geology and Mineralization of the Big Salmon Complex (104N NE and 104O NW) *in* Geological Fieldwork 1997, *B.C. Ministry of Employment and Investment*, Paper 1998-1, pages 157-170.

Mihalynuk, M.G., Nelson, J.L., Roots, C.F., Friedman, R.M. and de Keijzer, M. (2000): Ancient Pacific Margin Part III: Regional Geology and Mineralization of the Big Salmon Complex (NTS 104N/9E,16 & 104O/12,13,14W), *in* Geological Fieldwork 1999, *B.C. Ministry of Energy and Mines*, Paper 2000-1, pages 27-46.

Nelson, J.(1997): Last Seen Heading South: Extensions of the Yukon-Tanana Terrane into Northern British Columbia; *in* Geological Fieldwork 1996, *B.C. Ministry of Employment and Investment*, Paper 1997-1, pages 145-156.

Sayles, F. L. and Bischoff, J. L. (1973): Ferromanganese sediments in the equatorial east Pacific; *Earth and Planetary Science Letters*, Volume 19, pages 330-336.

Toth, J. R. (1980): Deposition of submarine crusts rich in manganese and iron; *Geological Society of America Bulletin*, Volume 91, pages 44-54.

Sedex and Broken Hill-Type Deposits, Northern Monashee Mountains, Southern British Columbia

By Trygve Höy

KEYWORDS: Sedex, Broken Hill, Monashee complex, Paleoproterozoic, Cottonbelt, Ruddock Creek, Kneb, Jordan River.

INTRODUCTION

The existence of a number of stratabound zinc-lead-silver deposits has long been known within high grade metamorphic rocks in the Monashee Mountains of southern British Columbia (Figure 1). A number of these, including Big Ledge south of Revelstoke, and Jordan River, Cottonbelt and Ruddock Creek to the north, have been moderately explored, but none have had any production. The deposits typically comprise thin layers of massive to semi-massive sulphides that have strike lengths of several kilometres. They are intensely deformed and metamorphosed and locally invaded by extensive zones of pegmatite.

The purpose of this paper is to describe a number of these deposits within the northern Monashee Mountains north of Revelstoke and to compare them with both Broken Hill-type and classical sedex deposits. Age constraints on these deposits are also reviewed. Four weeks were spent in the field, mapping the Kneb and eastern exposures of Ruddock Creek. Several days were spent at both Cottonbelt and Jordan River examining the host stratigraphy in order to attempt detailed correlations and to identify key assemblages or units that are characteristic of Broken Hill successions elsewhere.

The Broken Hill-type deposit (BHT) is named after Broken Hill, a large lead-zinc-silver massive sulphide deposit in highly metamorphosed metasedimentary rocks of Paleoproterozoic age in New South Wales, Australia. As it is the largest and best studied of this type of deposit, it is described below.

BROKEN HILL-TYPE DEPOSITS

Many authors regard Broken Hill-type deposits as metamorphosed equivalents of more classical sedex deposits (cf. Gustafson and Williams, 1981; Sangster, 1990). Others, however, argue that they represent a distinct class of sediment-hosted massive sulphides containing unique chemistry and occurring within distinct sequences (Plimer, 1986; Walters, 1995; Parr, 1994; Parr and Plimer, 1993).

Broken Hill-type deposits are stratiform base metal orebodies hosted by thick accumulations of clastic and minor volcanic rocks that typically have undergone multiphase deformation and high grade regional metamorphism. The best known examples are within Proterozoic rocks, and include the world-class Broken Hill deposit in New South Wales, Australia, the Aggeneys and Gamsberg deposits in South Africa (Rozendal, 1986; Ryan et al, 1986) and deposits of the Bergslagen district, Sweden (Hedström *et al.*, 1989).

Broken Hill, New South Wales

The Broken Hill deposits in southeastern Australia contain approximately 300 million tonnes of ore extending over a strike length of 7 kilometres. They are within the Willyama Supergroup, a sequence of deformed Paleoproterozoic schists and gneisses, unconformably overlain by Neoproterozoic sedimentary rocks and minor basalt. Due to generally intense deformation and metamorphism, the protoliths to some of the metamorphic rocks of the Willyama Supergroup have been and continue to be the focus of considerable debate. However, it is generally agreed that they represent mainly metasedimentary rocks, some possible rhyodacitic volcanics, a minor component of mafic volcanics, and migmatites derived from partial melting of these rocks. Calcsilicates, banded iron formations and "lode" rocks - quartz-gahnite and garnet quartzite - are minor components.

The Willyama Supergroup has been interpreted to have been deposited as a rift, rift fill and cover sequence, developed on continental crust (Willis *et al.*, 1983; Stevens *et al.*, 1988). The Broken Hill and underlying Thackaringa groups host most of the main Broken Hill-type massive sulphide bodies, some stratabound tourmaline-rich rocks, stratabound scheelite occurrences, and the banded iron formations and other "lode" rock types. These groups are interpreted to record a rift stage, overlain by rift fill of the Sundown Group and platformal deposits of the Paragon Group.

The age of the Willyama Supergroup and contained sulphide deposits is now well known due to recent zircon U-Pb SHRIMP geochronological studies. A maximum age is afforded by 1710-1700 Ma detrital zircons within the Thackaringa Group while a date of 1704±4 Ma on the intrusive Alma Gneiss provides a minimum age (Page *et al.*, 2000). Gneisses within the Broken Hill Group, in-

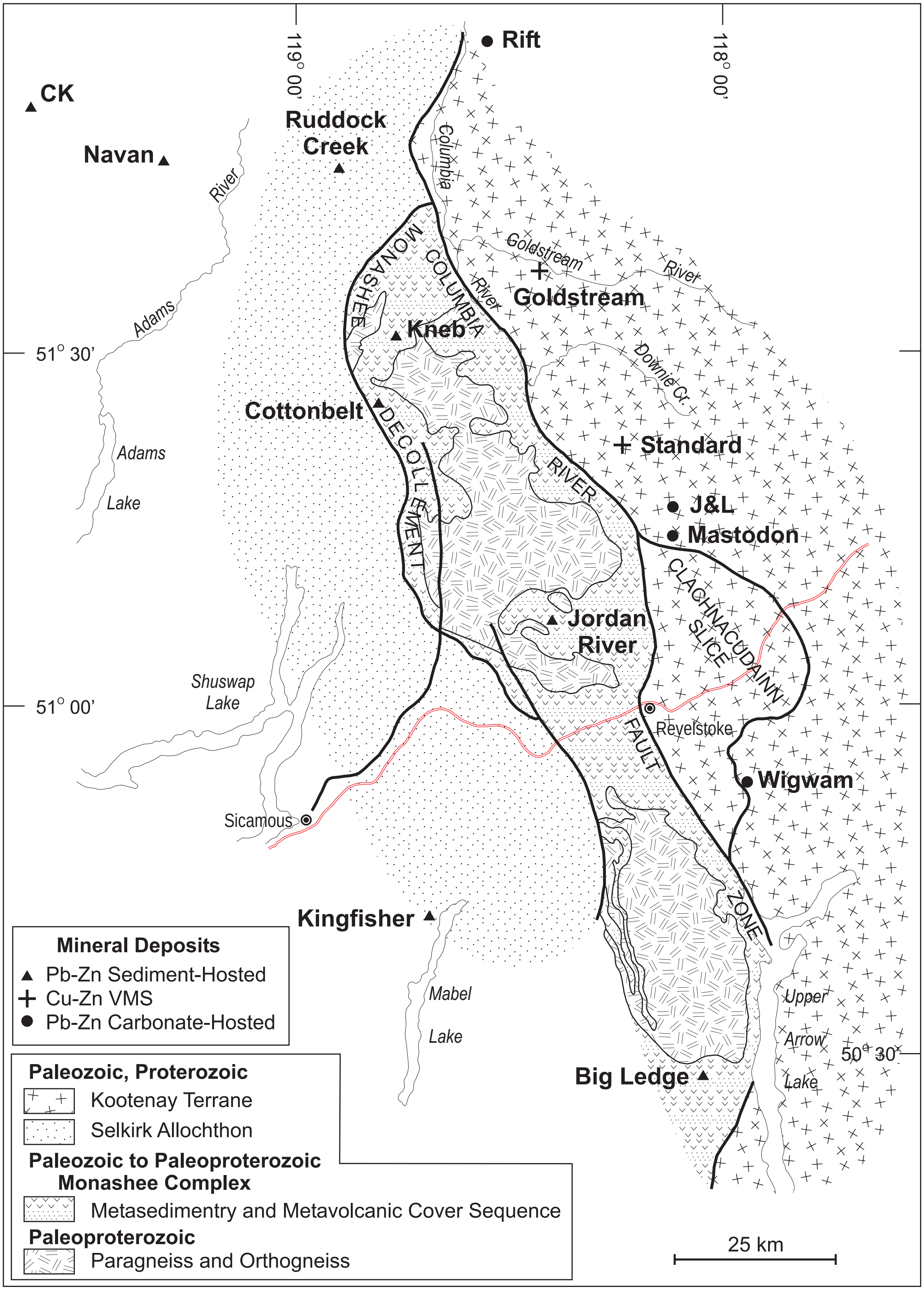

Figure 1. Setting of stratabound massive lead-zinc deposits of the Monashee Complex, southern British Columbia.

cluding the Potosi and Hores gneisses, have been interpreted to be felsic volcaniclastics and intrusive rocks. These have yielded dates of 1693±5 to 1686±3 Ma and therefore provide depositional ages for the Broken Hill deposit host rocks (Page and Laing, 1992; Page *et al.*, 2000). The overlying Sundown Group contain detrital zircons as young as 1690-1700 Ma, but most are derived from ca. 1790 and 1820-1860 Ma terrains. Tuffaceous siltstones in the Paragon Group, the upper part of the Willyama Supergroup, have yielded 1656±5 Ma zircons that are interpreted to be a depositional age. In summary, the rift sequence of the Willyama Supergroup was deposited in a relatively short time span, from ca. 1710 to 1690 Ma; overlying platformal cover rocks continued deposition until ca. 1642 Ma.

The Broken Hill orebodies occur in the upper portions of the Hores gneiss at the top of the Broken Hill Group. They are described by numerous workers; the following is largely summarized from Parr and Plimer (1995) and Walters (1995). The deposits are zoned on a regional scale with more zinc-rich lodes occurring at lower stratigraphic levels and in more southern exposures. Host rocks are variable, reflecting both sedimentary deposition and alteration. The siliceous zinc-rich deposits are within quartz-rich psammopelitic metasedimentary rocks that contain variable but minor amounts of gahnite, spessartine, orthoclase, sulphides, sillimanite and biotite; individual orebodies are typically separated by blue quartz, quartz-spessartine and quartz-gahnite rocks. The lead lodes are more carbonate or calcsilicate rich, and may be enveloped by quartz, garnet, or plagioclase-rich rocks. Sulphide-silicate contacts are usually sharp.

The garnet-rich lithologies are conspicuous units within, adjacent to or as strike equivalents to the lead lodes. Garnetites, comprising greater than 80 percent spessartine grains, are considered to be original manganiferous chemical sediments (Spry and Wonder, 1989). Quartz-garnet rock, containing minor gahnite and sulphides, commonly surrounds lead lodes and may be a hydrothermal alteration envelope. Spessartine-quartz rich envelopes, containing variable but minor sericite, plagioclase, fluorapatite, fluorite and sulphides, are more common where host rocks are pelitic or psammopelitic.

Broken Hill deposits are commonly characterized by close association with a number of unusual lithologies, mainly dominated by Si-Fe-Mn-Ca, and generally regarded as exhalites or possibly alteration zones (Plimer, 1986). The most conspicuous of these are the various iron formations, dominated by either sulphide or magnetite phases, quartz-rich zones with minor spessartine or gahnite, the gahnite-quartz layers, barite, calcareous units that may appear as skarn-like assemblages and quartz-tourmalinites.

These "enrichment" zones are important exploration guides. With closer proximity to deposits or camps, the diversity and number of these zones increase. Furthermore, the enrichment of Fe, Si, Mn, Ca, P, F, K and carbonate not only signifies closer proximity to deposits or camps, but may also characterize deposits size or grade. Walters (1995) concludes that the extreme Ca-Mn-F enrichments, or calcsilicate associations, are restricted to significant, proximal zones of larger, "more evolved" systems more likely to be associated with high-grade mineralization whereas Fe-Si-(Mn) dominant systems characterize the majority of "less evolved" proximal systems associated with numerous smaller occurrences in BHT districts.

In summary, some significant regional features of Broken Hill deposits include (after Walters, 1995):

- association with diverse suites of generally thin exhalite marker units such as quartzites, quartz-gahnites, tourmalinites or banded iron formations
- numerous, small, base metal occurrences
- diversity of other deposit types, including veins and skarns.

Camp or deposit-scale features include:

- rapid lensing and stacking of exhalite lenses
- association with significant magnetite in some lenses
- wallrock alteration involving silicification, magnetite, garnet, K-feldspar and sillimanite
- dominant galena-sphalerite mineralization, with low pyrite or pyrrhotite
- strong zoning from siliceous Zn-rich to carbonate-calcsilicate Pb-Ag rich
- low S:base metal ratios, with lead-zinc enrichment in numerous silicate and oxide facies
- association with minor elements, Cu, Au, Bi, Sb, W, Co and As
- "skarn-like" mineralogies, involving carbonates, fluorite, apatite, garnets, pyroxenes, and pyroxenoids
- high levels of manganese.

Many of these features are also common to more classical sedex deposits (Goodfellow *et al.*, 1993). However, differences include the abundance of a variety of forms of exhalite mineralization, possible association with volcanic rocks, and in deposits themselves, occurrence of magnetite and unusual chemistry that includes high F, Mn, P, Ca and Mg and low iron sulphide content.

Other features are common to sedex deposits, or to their metamorphosed equivalents. The following descriptions of some of the massive sulphide deposits of the Northern Monashee Mountains emphasize features in common with Broken Hill-type deposits. Some, such as Cottonbelt, are unusual and share many similarities while others, such as Jordan River, appear to be more similar to metamorphosed sedex deposits.

MASSIVE SULPHIDE DEPOSITS OF THE NORTHERN MONASHEE MOUNTAINS

Introduction

The deposits of the Monashee Mountains (Figure 1) are within the Monashee Complex, a 2-3 kilometre thick succession of mainly platformal rocks that unconformably overlies crystalline basement. This basement is exposed in two structural culminations, the Frenchman Cap dome in the north (Wheeler, 1965; Höy and Brown, 1980) and Thor-Odin dome in the south (Reesor and Moore, 1971; Read, 1980). Granitic orthogneiss in these basement exposures range in age from ca. 1.87 Ga to 2.27 Ga (Armstrong *et al.*, 1991; Parkinson, 1991; Crowley, 1997). However, the age of the overlying Monashee Complex, and contained deposits, is known with less certainty, and may range from Paleoproterozoic to Paleozoic.

The northern Monashee Mountains are located west of the Columbia River and north of the Trans Canada Highway. The Jordan River, Cottonbelt, Kneb and Ruddock Creek deposits are all above timberline in relatively rugged terrane; however, traversing by foot on most of the showings is relatively easy. They are accessible by helicopter from a base at Revelstoke.

Regional Geology

The Jordan River deposit is located within the Monashee complex in a large structural embayment on the southern margin of Frenchman Cap dome (Figure 2). Cottonbelt and Kneb are on the northwestern and northern margin of the dome. The complex is exposed within a tectonic window beneath a crustal-scale thrust fault, the Monashee decollement (Read and Brown, 1981; Brown *et al.*, 1986). The Monashee complex comprises basement gneisses, referred to as the core gneisses, and an unconformably overlying succession of mainly metasedimentary rocks, termed the cover sequence.

Core Gneiss

Core gneisses in the northern Frenchman Cap area have been subdivided into three structural units (Journeay, 1986). The lowest consists of intercalated biotite paragneiss, pelitic schist and quartzofeldspathic gneiss that is intruded by K-feldspar augen gneiss. A middle orthogneiss complex, structurally above the paragneiss, includes feldspar augen gneiss, overlain by well layered amphibolites, syenitic gneisses, and homogeneous biotite quartzofeldspathic gneisses. It is in turn overlain by a heterogeneous paragneiss succession that includes quartz-feldspar schist, biotite schist, hornblende gneiss, amphibolite and feldspar gneiss with variable orthogneiss and granitic intrusive component (Höy, 1987).

Age Constraints: Core Gneisses

The age of the core gneisses is reasonably well constrained. Armstrong *et al.* (1991) summarize and present Rb-Sr model dates that suggest core gneiss ages of ca. 2200 Ma. In the Thor-Odin dome, 1.93 and 1.86 Ga U-Pb dates have been obtained from orthogneisses (Parkinson, 1991) and in the Malton Complex near Valemont north of Frenchman Cap dome, ages of 1.87, 1.99 and ca. 2.1 Ga are reported (McDonough and Parrish, 1991). Paleoproterozoic intrusive ages for orthogneisses in Frenchman Cap dome, summarized in Table 1, range from ca. 1862±1 Ma (Crowley, 1997) to 2103±16 Ma (Armstrong *et al.*, op. cit.). The older intrusive age from within the lower core gneiss unit (Unit 1) restricts the paragneiss component of that succession to pre 2.1 Ga.

Detrital zircon data from the basal part of the overlying cover sequence (Unit 3, Figure 3) are also summarized in Table 1. These dates, 1.99-2.00 Ga (n=12), 2.02 Ga (n=1), 2.17 Ga (n=1) and 2.04-2.05 Ga (n=2) (Crowley, 1997; Ross and Parrish, 1991) suggest that the core complex, including Unit 2, is older than 1.99 Ga; younger detrital zircon dates (<1.99 Ga) only occur in units higher in the Monashee cover sequence (Table 1, Figure 3). The undeformed, postkinematic nature of the 1951±8 Ma granite (Table 1, Figure 3) indicates that, at least in the central and eastern part of the dome, the most intense deformation is PreCambrian in age, with only "modest disturbance during Late Cretaceous-Eocene time" (Parrish, op. cit., p. 1628). Hence it is probable that a ca. 1.9 Ga metamorphism that is recorded in the core gneisses (Armstrong *et al.*, 1991; Crowley and Schaubs, 1994; Parrish, 1995) may record a metamorphic-tectonic event separating core gneiss Unit 2 from the cover sequence.

In summary, paragneisses in the lower structural unit within the core gneiss complex (Unit 1) are older than 2.1 Ga and the overlying, dominantly paragneiss succession of Unit 2 is probably older than 1.99 Ga. The hiatus between core gneisses and the overlying cover sequence may be a regional tectonic event that is recorded by the 1.9 Ga metamorphic and 1.95 Ga intrusive dates (Figure 4). A number of zircons with Archean ages (2.88 Ga; 2.95-2.94 Ga: Crowley, 1997) indicate an Archean source terrane for at least part of the cover sequence, and lend support to the conclusion of Duncan (1984) that basement gneiss, at least in Thor-Odin dome, may contain an Archean component.

Monashee Cover Sequence

The Monashee cover sequence is a succession of dominantly metasedimentary rocks that unconformably overlies the core gneisses. The cover sequence of Frenchman Cap also includes a number of thin amphibolite layers interpreted to be mafic volcanics or intrusions, and a regionally extensive carbonatite tuff, the Mount Grace carbonatite (McMillan, 1973; McMillan and Moore, 1974; Höy and Kwong, 1986; Höy and Pell, 1986). It also hosts the Jordan River, Cottonbelt and Kneb deposits. It is intruded by a variety of meta-igneous rocks, including

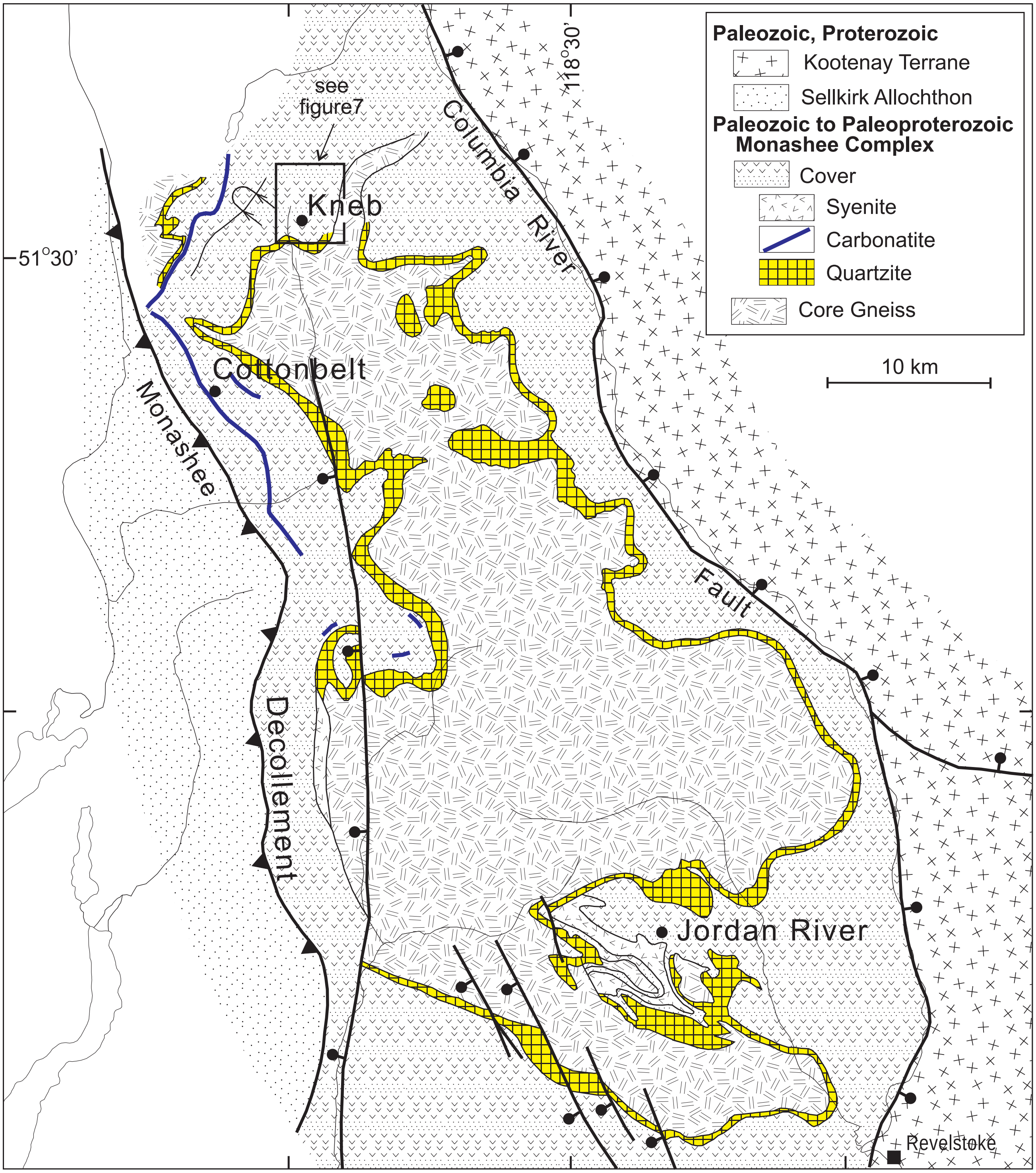

Figure 2. Geological map of Frenchman Cap dome showing distribution of tectonic elements, main lithologic units, dated intrusions, and massive lead-zinc deposits (from Höy and Brown, 1981, and references therein).

TABLE 1
SUMMARY OF U-PB DETRITAL AND MAGMATIC ZIRCON DATA, NORTHERN MONASHEE MOUNTAINS

Reference	*Field No.*	*Source*	*Description*	*Date(s)*	*Note*
1	RS-4	Parrish, 1995	amphibolite	541 ± 11 Ma (magmatic) 57 + 1 Ma (metamorphic)	adjacent to mafic pyroclastic unit, unit 6, cover sequence
2	207	Crowley, 1997	Mt. Grace syenitic orthogneiss	724 + 5 Ma (magmatic)	intrudes unit 4, cover sequence
3	341	Crowley, 1997	deformed pegmatite	1852 + 4 Ma (magmatic)	intrudes lower part of unit 4, cover sequence
4	180	Crowley, 1997	metamorphosed leucogranite	1762 + 6 Ma (magmatic)	intrudes ? unit 4 ?, cover sequence
5	WN-474	Parrish & Scammel, 1988; Okulitch et al, 1981	Mt. Copeland syenite gneiss	740 ± 36 Ma (magmatic) 59 + 1 Ma (metamorphic)	intrudes unit 4, cover sequence in Jordan River area
6	locality 9	Parrish, 1995	syenite	670 + 96 Ma (magmatic) - 93 Ma (magmatic)	intrudes top of unit 2, core paragneiss
7	187	Crowley, 1997	Kirbyville granodiorite orthogneiss	1862 + 1 Ma (magmatic)	intrudes unit 2, core paragneiss in Kirbyville anticline
8	R212	Armstrong et al, 1991	dyke	2103 + 16 Ma (magmatic)	Dyke intruding unit 1, core orthogneiss
9	R244	Armstrong et al, 1991	core orthogneiss	2066 + 8 Ma (magmatic)	core orthogneiss of unit 1
10	R245	Armstrong et al, 1991	orthogneiss	2010 + 7 Ma (magmatic)	orthogneiss within unit 2, core gneiss
11	PCA-3058-83	Armstrong et al, 1991	post-kinematic granitic intrusion	1951 ± 8 Ma (magmatic ?), or metamorphic ?)	intrudes unit 1 (?), core gneiss
12	257	Crowley, 1997	semipelitic schist	2.95 - 2.94 Ga (n=2) 2.88 Ga (n=1) 1.85 - 1.81 Ga (n=4) 1.75 Ga (n=1) 1.21 Ga (n=1)	derital zircons in unit 6, cover sequence
13	300	Crowley, 1997	pelitic schist	2.86 Ga (n=1) 1.84 - 1.81 Ga (n=4)	detrital zircons in unit 6, cover sequence
14	335	Crowley, 1997	quartzite	2.05 - 2.04 Ga (n=2) 2.02 Ga (n=1) 2.00 - 1.99 Ga (n=5)	detrital zircons in unit 3, cover sequence
15	S85-6	Ross & Parrish, 1991	quartz pebble conglomerate	2.166 Ga (n=1) 2.00 - 1.99 Ga (n=7)	detrital zircons at base of unit 3, cover sequence

syenitic to granitic orthogneisses and intrusive carbonatites. These orthogneisses help constrain the age of this succession (Crowley, 1997).

Description

The stratigraphic succession for the cover sequence along the northwestern margin of Frenchman Cap dome is shown in Figure 3. It comprises approximately 1 km of metamorphosed rocks that are exposed in the core of the Mount Grace syncline (Figure 5). Correlations to the south along the margins of the dome suggest that this represents approximately half the known cover sequence of Frenchman cap dome.

A basal quartzite (Unit 3) overlies core gneisses throughout the margins of the dome. In the Kneb-Cottonbelt area, it thickens from a few metres at its most northern exposures to several hundred meters southeast of Cottonbelt (Figure 5). It comprises a number of generally fining-upward sequences. The basal unit typically consists of coarse-grained feldspathic and micaceous quartzite, overlain by an orthoquartzite that commonly grades upward to a micaceous quartzite, and is capped by a quartz-rich micaceous schist. Thick-bedded, generally massive orthoquartzite grading up into thin-bedded, fine-grained micaceous quartzite and capped by a few metres of micaceous schist, forms the top of Unit 3 east of Cottonbelt (Figure 5).

Unit 4 is a sequence of dominantly calcareous and pelitic schists between Unit 3 and the regionally extensive crystalline marble of Unit 5. Calcareous and pelitic rocks interfinger extensively and grade laterally into each other. The top of Unit 4 is thinner bedded and more heterogeneous, and includes impure marble layers, quartzite, amphibolite, and the Mount Grace carbonatite tuff (described below). Calcsilicate layers within Unit 4 consist largely of granular quartz, plagioclase, microcline and diopside, with variable phlogopite, muscovite, actinolite, calcite and garnet. Coarse quartz-feldspar-mica sweats are common, and late tourmaline-bearing pegmatites locally crosscut foliation.

A grey-weathering calcite marble (Unit 5) is also a prominent marker in the cover sequence. It is commonly underlain by a white orthoquartzite or by the orthoquartzite and a few metres of intervening calcsilicate gneiss.

A succession of calcsilicate gneiss and pelitic schist of Unit 6 overlies Unit 5. The basal part is calcareous and includes the Cottonbelt and Jordan River sulphide layers. The upper part (Unit 6b) is mainly micaceous schist and gneiss with occasional thin amphibolite, quartzite and quartz-pebble conglomerate layers. The conglomerates consist of large flattened and elongated clasts of

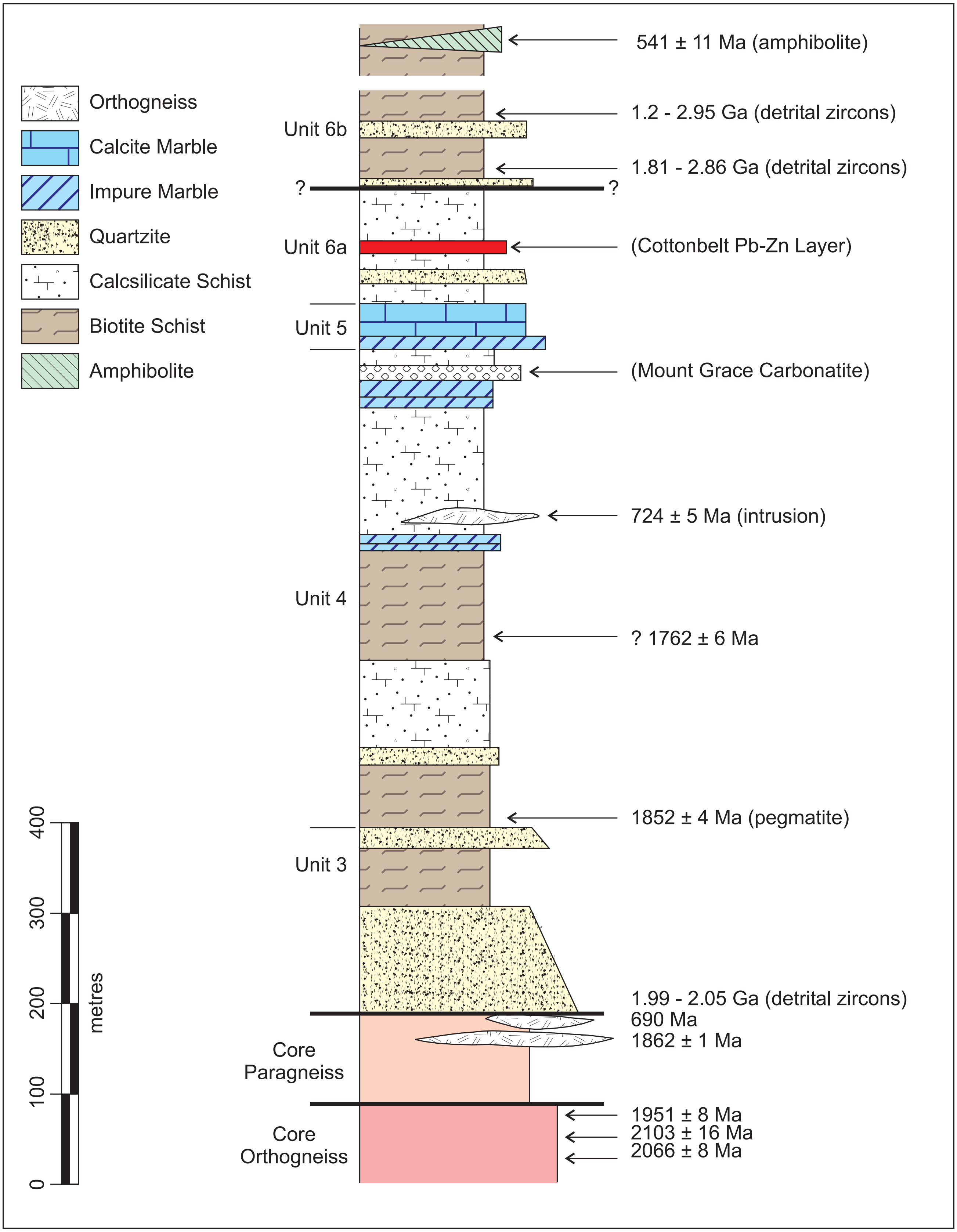

Figure 3. Stratigraphic succession in the Mount Grace - Kirbyville Creek area (from Höy, 1987 and Scammel and Brown, 1990); U-Pb data is from Crowley (1997), Parrish (1995), Armstrong *et al.* (1991) and Ross and Parrish (1991). *See* table 1 for summary of U-Pb data.

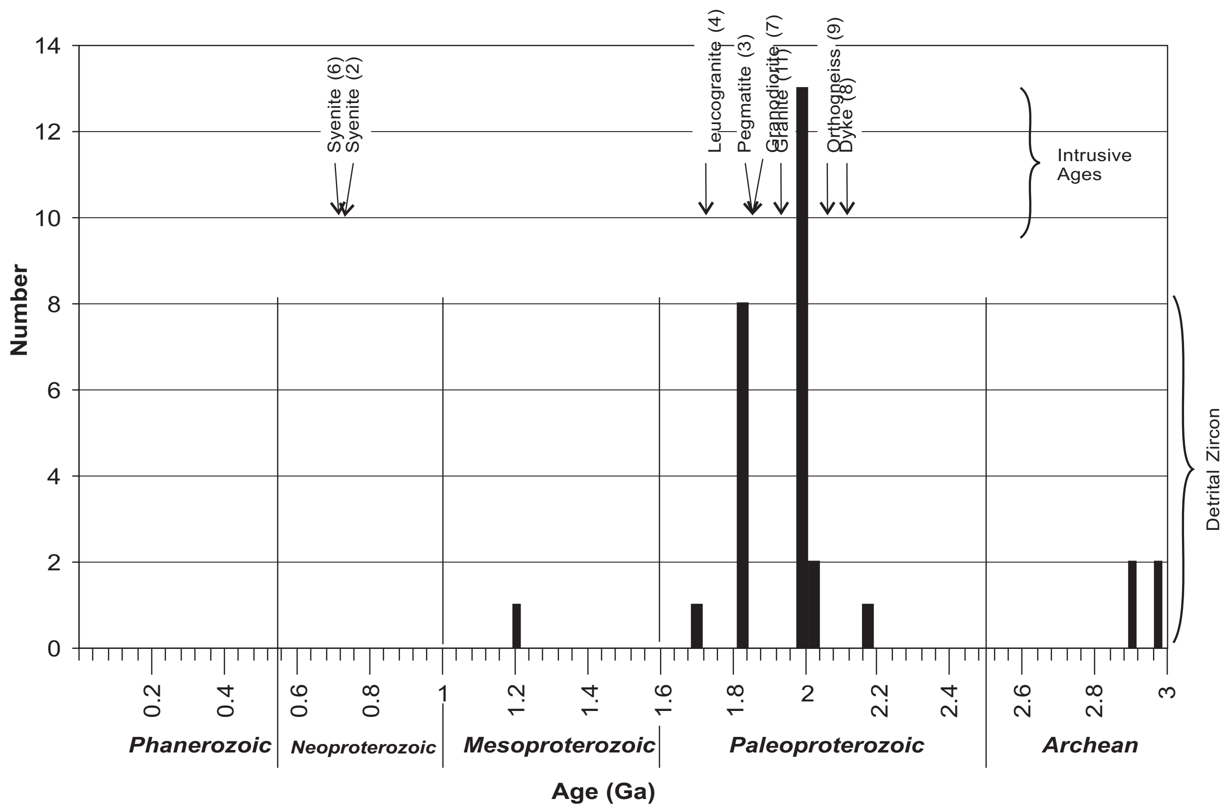

Figure 4. Bar graph showing distribution of U-Pb detrital and intrusive ages, Frenchman Cap dome (*see* Table 1 for data sources).

orthoquartzite in a granular quartz-feldspar-mica matrix. They may be graded with coarse grained feldspathic quartzite ("grit") at the top.

Farther north in the Kirbyville Creek area, several hundred metres of cover sequence apparently overlie Unit 6 (Scammel and Brown, 1990). This overlying succession includes considerable quartzite and arkosic rocks, amphibolite, schist and gneiss, but considerably fewer calcareous units than in the underlying succession.

Correlations of the Monashee cover sequence in Frenchman Cap dome are shown below (Figure 8). The most distinctive marker units are the basal quartzite (Unit 3), the prominent white marble (Unit 5) and the Mount Grace carbonatite. In particular, the succession including the carbonatite, an impure marble, thin quartzite, amphibolite and white marble, comprises a marker succession that occurs at both the Cottonbelt and Jordan River deposits.

Mount Grace Carbonatite

The Mount Grace carbonatite has been extensively studied (McMillan and Moore, 1974; Höy, 1987; Höy and Kwong, 1986; Höy and Pell, 1986). It is the most prominent marker unit along the western margin of Frenchman cap dome, extending more than 60 kilometres from Jordan River in the south to north of Kneb occurrence (Figure 2).

The carbonatite commonly comprises a blocky tephra layer associated with a number of thin, laterally persistent, finer grained tuff layers. In the field it is recognized and characterized by an unusual pale to medium-brown weathering colour. Grains of dark brown phlogopite, colourless apatite and needles of amphibole weather in relief. Pyrrhotite, pyrochlore and zircon are locally developed accessory minerals. The blocky tephra layers contain three distinctive types of matrix-supported clasts: small granular albite clasts up to 3 cm in diameter, "syenite" clasts to approximately 10 cm in diameter, and large rounded to subrounded heterolithic clasts. The albitite and "syenite" clasts are interpreted to be pieces of fenite, whereas the lithic clasts were derived primarily from underlying core gneisses (Höy, 1987).

Analyses of the Mount Grace carbonatite, presented in Höy (op. cit.) indicate that it is mainly a sövite or calcite carbonatite. It is highly enriched in strontium (ave. 4460 ppm), barium (2300 ppm) and manganese (3100 ppm). Total rare earth element concentrations range from approximately 600 ppm to greater than 8000 ppm, with average values of 1000 to 2000 ppm.

Age Constraints: Cover Sequence

Estimates of the depositional ages for the cover sequence have ranged from Mesoproterozoic to Paleozoic. These ages were based initially on lithological correlations with Kootenay terrane and North American rocks to

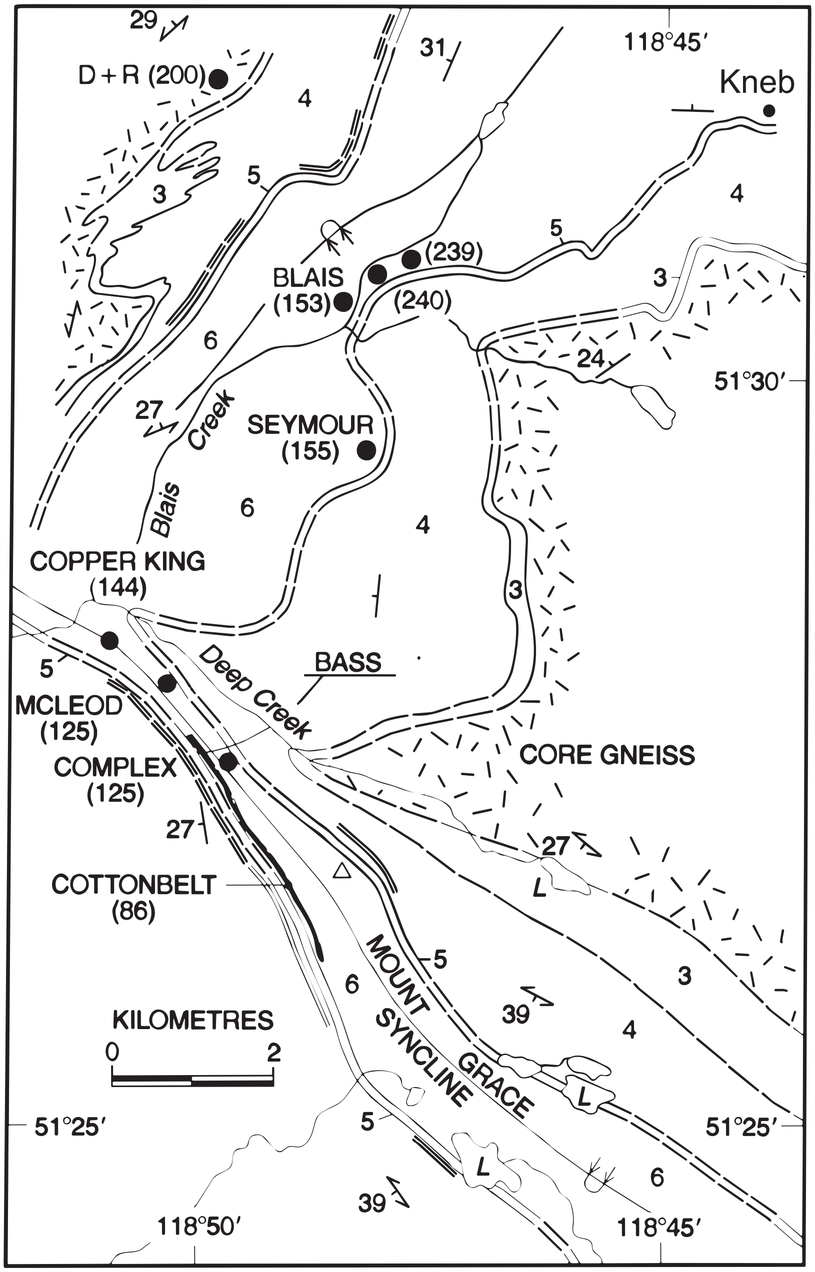

Figure 5. Geology and mineral occurrences of the Mount Grace area, northern Frenchman Cap dome (after Höy, 1987). Numbers in brackets are BC Minfile numbers.

the east. The platformal nature of the Monashee cover succession, and the 740 Ma intrusive age for the Mount Copeland syenite in the lower part of the sequence (Okulitch *et al.*, 1981; Parrish and Scammel, 1988), supported a Neoproterozoic to Paleozoic age. A Pb-Pb Cambrian model age for the Cottonbelt deposit (Höy and Godwin, 1988) supported these regional correlations.

Better constraints on the age of the cover sequence, based on dates of detrital zircons and intrusions, have been determined by Crowley (1997); detrital zircons provide a maximum age for the host unit, and intrusive dates, a minimum age. The youngest detrital zircons in Unit 3 at the base of the cover sequence (Ross and Parrish, 1991; Crowley, op. cit.) indicate that the depositional age is less than 1.99 Ga (Table 1, Figure 3). A pegmatite that intrudes overlying rocks of Unit 4 is dated at 1852±4 Ma, thereby restricting deposition of the basal succession to between 1.99 Ga and 1.85 Ga. As suggested above (Age constraints: core gneisses) this depositional age range is probably further restricted to post 1.95 Ga. A second intrusion, higher in the succession but still below the Cottonbelt sulphide layer, has a 1762±6 Ma date, confirming the Paleoproterozoic age for this part of the succession (Crowley, 1997).

Attempts to date the Mount Grace carbonatite have not been successful. Zircons collected from a carbonatite sample from near the headwaters of Kirbyville Creek were mainly composite, "being composed of mainly 55-60 Ma metamorphic crystals surrounding rare and very small Precambrian zircons of mainly detrital origin" (sample RS-3, Parrish, 1995, p. 1641).

Maximum age constraints on the overlying part of the cover sequence are restricted by 1.2 Ga detrital zircons in Unit 6b (Crowley, 1995; Table 1). These are from a semipelitic schist in the core of the Mount Grace syncline, several hundred metres stratigraphically above Cottonbelt (Figure 3). An amphibolite from the Kirbyville Creek area north of Cottonbelt has also been dated (Parrish, 1995) at 541±11 Ma. The amphibolite is interpreted to be stratigraphically above the section exposed in the core of the Mount Grace syncline (Scammel and Brown, 1990). As it is not known whether this amphibolite is intrusive or extrusive, this date only provides a minimum age for the host succession. However, it is within a package that includes mafic pyroclastics and it is therefore likely that even if it is intrusive, it is a subvolcanic sill or dyke and therefore provides a depositional age.

In summary, the basal part of the cover sequence, below the Cottonbelt sulphide layer, is between 1.95 and 1.85 Ga. The top of the sequence, at the stratigraphic level of the amphibolite complex, is probably 540 Ma or Early Cambrian in age. This tremendous age span suggests that there are one or more unconformities in the cover sequence. Along the western and southern margin of the dome, the succession below the Cottonbelt and Jordan River sulphide layers appears to be continuous with no recognized unconformity. It is therefore probable that the sulphide layers are within a Paleoproterozoic stratigraphic succession. However, conglomerates in the succession overlying the sulphide layers may record an unconformity as is shown on Figure 3.

COTTONBELT (082M 086)

Introduction

The geology of the Cottonbelt deposit is described in considerable detail in Höy (1987) and is only reviewed briefly here. Cottonbelt is an unusual lead-zinc-magnetite layer in calcsilicate gneisses near the base of Unit 6. It has been traced or projected on surface for approximately 2.5 kilometres strike length. Geological reserves are estimated at approximately 750,000 tonnes containing 6 percent lead, 5 percent zinc and 50 g/tonne silver. Other mineral showings in the Mount Grace area include widely scattered occurrences of galena, chalcopyrite, pyrrhotite and magnetite in calcsilicate gneisses, marbles and quartzites north of Cottonbelt; perhaps the most important of these is Kneb, described below.

Cottonbelt was first staked in 1905 by Cotton Belt Mines Ltd. Surface stripping and trenching, bulk sampling and driving of a number of shafts and tunnels was done on Cottonbelt and immediately adjacent properties up until 1911. By 1922, shafts of 12 metres had been sunk on the Bass showing, 45 metres on Copper King and 75 metres on Cottonbelt (Figure 5). By 1927, 15 buildings had been constructed in the Cottonbelt area and approximately 500 metres of underground development completed. Sixteen short diamond-drill holes in 1926 intersected almost continuous mineralization along a strike length of approximately 2 kilometres, at depths of 82 to 112 metres. Underground work continued through 1927-1928, but was eventually suspended due to the remoteness of the area, difficult access and narrow widths of the mineralized layer.

Work resumed in the 1970s with surface mapping, trenching and geophysical surveys by Great Northern Petroleum and Mines Ltd. Between 1976 and 1978, Metallgesellschaft Canada Ltd. in a joint venture with United Minerals Ltd. carried out considerable mapping, sampling and geophysical surveys, and drilled two holes totaling 517 metres in an attempt to intersect possibly structurally thickened mineralization in the core of the Mount Grace syncline.

In 1995, with Explore B.C. Program support, CanQuest Resources Corporation completed geological and geophysical surveys and 1937 metres of diamond drilling in 27 holes, confirming the great lateral extent but limited and variable thickness of the deposit (Gibson, 1996). Resources were estimated at 725,000 tonnes containing 11 percent combined lead and zinc and 58.3 grams per tonne silver (Information Circular 1996-1, p. 23-25).

The Mount Grace area, and north to the headwaters of Ratchford Creek, were mapped by the author in 1978 (Höy, 1979; Höy and McMillan, 1979) and by M. Journeay as part of a Ph.D. thesis (Journeay, 1986). The area was revisited in 1986 as part of a regional study of alkaline rocks of the Canadian Cordillera (Höy and Pell, 1986; Höy and Kwong, 1986) and then again this past summer. The latest work focused on regional correlations and evaluation of Cottonbelt as a Broken Hill-type deposit.

Host Succession

Cottonbelt is within a highly metamorphosed, calcareous succession near the base of Unit 6 in the cover sequence of Frenchman Cap dome (Figure 2) As described above, the cover sequence comprises a thick basal quartzite (Unit 3), a sequence of calcareous and pelitic schists (Unit 4) that includes the Mount Grace carbonatite, and a grey-weathering crystalline marble (Unit 5).

The structure of the Cottonbelt area is dominated by the Mount Grace syncline, an isoclinal, recumbent fold that is draped around the northwestern margin of Frenchman Cap dome (Figure 5). Core gneisses are exposed in both its limbs and the youngest rocks in the area, Unit 6, in its core. Since Cottonbelt occurs on the western overturned limb of the Mount Grace syncline, it and its host stratigraphy are inverted, with older rocks occurring in the hangingwall and younger in the footwall.

A detailed, right-way-up section through Cottonbelt is illustrated in Figure 6. The Mount Grace carbonatite is generally underlain by an impure, siliceous marble up to a few metres thick, and stratigraphically overlain by 5 to 10 metres of calcsilicate gneiss that may contain one or two thin quartzite layers and minor amphibolite near the top. Elsewhere, such as in the Kneb deposit area, the quartzites and amphibolites are up to several metres in thickness. The calcsilicate unit is overlain by marble of Unit 5 followed by dominantly calcsilicates at the base of Unit 6a. Unit 6a includes scapolite-bearing calcsilicate gneiss, sillimanite and kyanite schist layers and a crumbly, grey to light brown-weathering impure dolomitic marble referred to as the "camp marble".

The Cottonbelt layer has sharp contacts with host rocks. The stratigraphic footwall varies from calcsilicate schist to well-layered garnet-sillimanite-muscovite schist or garnet-biotite schist. Garnet content in these layers is commonly up to 50 percent. The immediate base of the sulphide layer is typically a calcsilicate with locally minor dispersed galena. Garnet-sillimanite-muscovite schist interlayered with garnet-biotite schist also occurs just above the sulphide layer. However, analyses of these garnet-rich schist layers in the immediate footwall (CB2000-1a) and hangingwall (CB2000-1b) do not show manganese enrichment (Table 2).

The top of Unit 6a is mainly a calcsilicate schist with thin garnet-sillimanite or garnet-kyanite layers, quartzites and metavolcanic amphibolites. The quartzites locally contain minor dispersed garnet or muscovite. Interlayered sillimanite schist, quartz-feldspar gneiss, biotite schist and thin quartzites of Unit 6b overlie Unit 6a.

Mineralization

Cottonbelt is a sulphide-oxide layer comprising variable amounts of sphalerite, galena and magnetite, minor pyrrhotite and traces of chalcopyrite, pyrite, tetrahedrite and molybdenite. Gangue mineralogy is dominated by a massive to crudely banded manganiferous calcsilicate olivine-pyroxene-amphibole assemblage. Sulphides are only occasionally finely laminated. In general, massive sulphides are restricted to a single layer; however, thin layers can occur in the immediate footwall or hangingwall, and disseminated galena is locally noted in stratigraphic footwall calcsilicates or marbles. Some of these different styles of mineralization are shown in Photo 1 (a-c).

A common and distinguishing feature of the sulphide layer is the high MnO content. Analyses of 14 mineralized samples showed that MnO content ranged from 1.4 to 13.28 percent, with an average of greater than 8 percent (Höy, 1987).

Gangue minerals are unusual as they reflect the high manganese content and the overprint of regional metamorphism to upper amphibolite facies. Silicate minerals include varying proportions of knebelite (a manganiferous olivine), actinolite and manganiferous cummingtonite, pyroxenes, spessartine, biotite and minor accessory chlorite. Pyroxenes include diopside, hedenbergite, kanoite (a manganese-rich magnesium pyroxene) and less commonly eulite (a manganiferous orthopyroxene). Ankerite is the dominant carbonate, but minor calcite and kutnahorite (a calcium-manganese carbonate) have been identified (Höy and Kwong, 1986). Accessory minerals include epidote, plagioclase, graphite, gahnite and hematite.

Discussion

Cottonbelt is assumed to be a metamorphosed sulphide layer, initially deposited in a shallow marine platformal environment (Höy, 1987). The abundance of scapolite in some layers has been attributed to metamorphism of sedimentary layers containing evaporitic minerals, and thin quartzites are inferred to represent chert layers (Höy, 1987). Mafic volcanics in the succession, and a change from platformal carbonate deposition to possibly deeper water shales (now preserved as micaceous schists) suggest regional extension in a possible rift environment.

Evidence of a synsedimentary origin for the sulphide layer includes its layer-like form, crude to locally well-developed layering, premetamorphic formation, association with layers of probable exhalite origin and, perhaps most important, the occurrence of widespread mineralization at this discrete horizon. Mineralization at this level occurs on the east limb of the Mount Grace syncline at the McCleod and Complex showings, widely dispersed over several metres strike length approximately 6 kilometres farther north, and at Kneb, 11 kilometres northeast of Cottonbelt (Figure 5). As well, detailed stratigraphic correlations with the Jordan River deposit indicates that it also is at the same stratigraphic level (*see* Figure 8).

A number of layers within the stratigraphic succession are believed to have exhalite origin. These include some of the thin, fine-grained quartzite and rare garnet quartzite layers that occur immediately overlying the sulphide layer. A thin quartzite layer containing minor gahnite (a zinc spinel) discovered approximately 6 kilometres northeast of Cottonbelt, is also assumed to be a metamorphosed distal exhalite.

Alteration assemblages around the margins of Cottonbelt are not well developed or preserved probably due, at least in part, to extreme attenuation on the limb of the recumbent Mount Grace syncline. Sulphide gangue is enriched in manganese, with up to 13 percent MnO in some samples. It is also possible that the high calcium and magnesium content in the gangue, with development of calcsilicates during regional metamorphism, may reflect an original exhalite or alteration chemistry, rather than exclusively a sedimentary protolith. Silica content is typically low, with generally little free quartz. Locally, high sillimanite content in some adjacent layers may reflect local aluminum enrichment. The virtual total lack of iron sulphides in adjacent layers is noteworthy. There is no rusty-weathering envelope or footwall to the Cottonbelt layer.

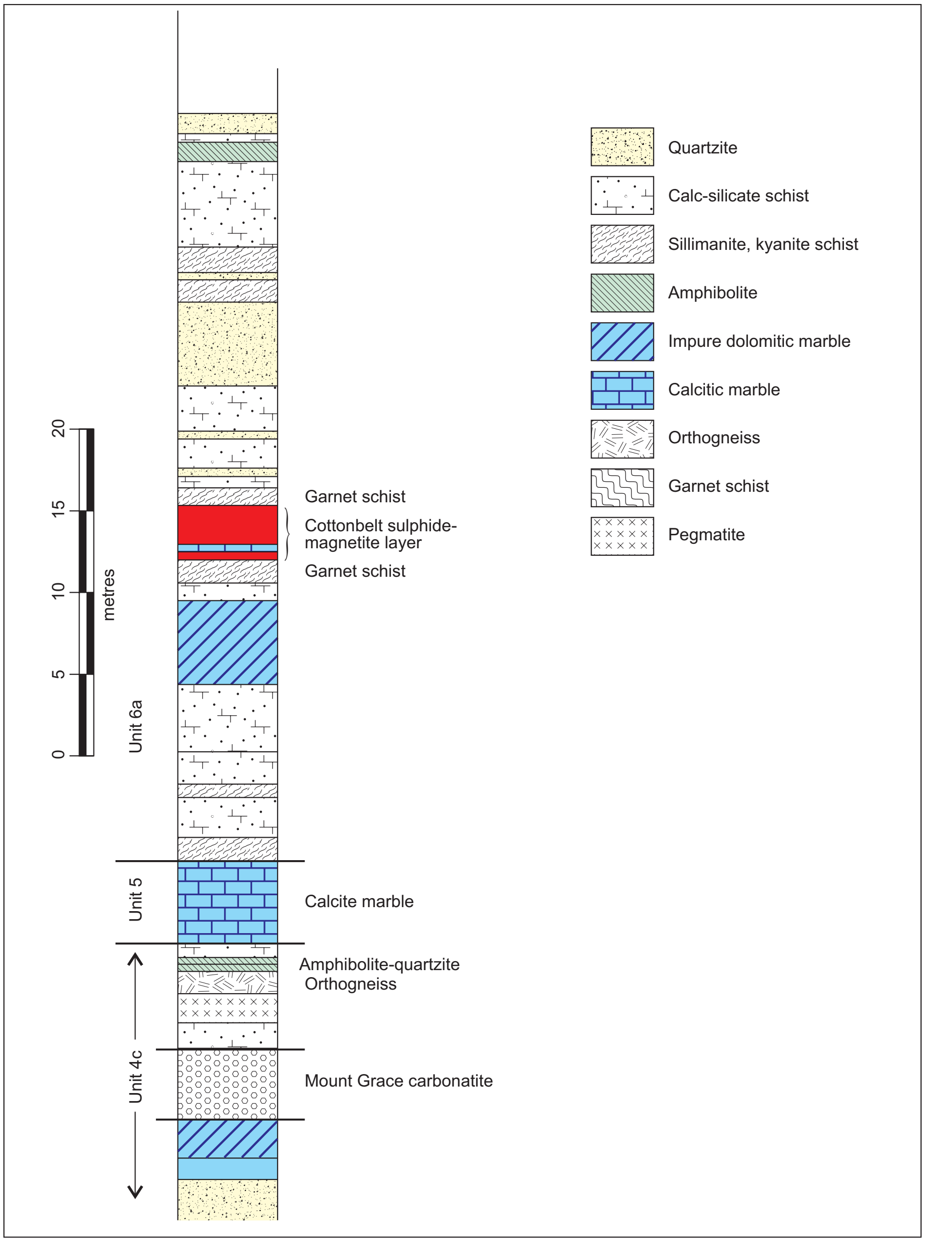

Figure 6. Detailed section through the mineralized interval, Cottonbelt deposit.

Metavolcanic rocks occur in the Cottonbelt stratigraphic succession. The Mount Grace carbonatite tuff occurs stratigraphically below the Cottonbelt sulphide layer and massive amphibolites occur above and below the layer. The Mount Grace carbonatite records extreme alkalic volcanism prior to formation of the Cottonbelt sulphide layer. Felsic volcanic protoliths have not been recognized, possibly because they do not exist in the immediate stratigraphic succession or perhaps because subsequent high grade metamorphism and intense deformation have made it difficult to identify them.

Deposit Classification

The Cottonbelt deposit is a massive lead-zinc layer in an original sedimentary succession, a feature common to both sedex and Broken Hill-type deposits. It probably occurs in a rift setting as it is associated with both alkalic and tholeiitic volcanism and occurs near a transition from shallow water platformal to deeper water?, more pelagic environments.

However, a number of features of the deposit and host succession are more typical of Broken Hill-type deposits. These include the unusual skarn-like mineralogy, a result of a calcareous gangue, an unusually high Mn content, and the abundance of magnetite rather than the more com-

TABLE 2
WHOLE ROCK ANALYSES OF SELECTED LITHOLOGICAL HAND SAMPLES FROM THE COTTONBELT, KNEB, JORDAN RIVER AND RUDDOCK CREEK DEPOSIT AREAS

Lab No.	Field no.	Note	UTM east	UTM north	SiO2	TiO2	Al2O3	Fe2O3	MnO	MgO	CaO	Na2O	K2O	P2O5	Ba*	LOI	SUM	Rb	Sr	Zr	Nb	Y	V
					%	%	%	%	%	%	%	%	%	%	%	%	%	ppm	ppm	ppm	ppm	ppm	ppm
Ruddock Creek area																							
55570	RC-1	amphibolite	368866	5737800	49.11	0.93	17.39	9.05	0.2	7.98	10.93	1.1	1.29	0.03	0.03	1.17	99.21	75	279	62	11	24	184
55571	RC-5	bi amphibolite	368951	5738370	48.11	2.8	14.97	14.38	0.2	6.13	8.05	2.05	1.89	0.31	0.03	0.75	99.67	144	316	160	23	27	337
55572	RC-9	calcsilicate	369392	5788193	40.88	1.13	26.95	6.05	0.1	0.46	22.28	0.25	0.05	0.07	0.01	1	99.23	7	755	236	53	57	121
55573	RC-26A	marble, M zone	368212	5738744	36.06	0.5	9.48	2.41	0.02	0.64	27.29	0.67	2.41	0.12	0.18	16.77	96.55	81	1340	95	13	24	48
55574	RC-37	serpentinite	368301	5737704	40.68	0.01	0.46	8.43	0.1	40.81	0.03	0.01	0.17	0.01	0.01	7.46	98.18	24	<3	7	4	<3	20
55575	RC-39	amphibolite	368234	5737720	48.33	1.3	13.43	14.18	0.2	7.23	11.6	1.96	0.4	0.11	0.01	0.8	99.55	16	148	72	3	32	342
55576	RC-41	amphibolite	368157	5737993	49.72	1.58	14.07	13.76	0.23	6.86	10.43	1.7	0.6	0.1	0.01	0.77	99.83	13	214	87	11	34	374
55577	RC-52	impure quartzite	368798	5737741	65.52	0.01	14.02	4.34	1.14	0.68	1.88	4.53	2.85	0.01	0.22	4.23	99.43	94	227	41	7	31	11
55578	RC-57a	gn quartzite	369274	5737086	69.19	0.1	14.05	3.82	0.07	0.01	11.46	0.17	0.01	0.01	0.01	0.67	99.57	4	414	35	6	19	33
55579	RC-61a	marble	368505	5737940	24.25	0.37	8.22	3.56	0.05	1.23	35.02	0.7	1.72	0.09	0.02	23.06	98.29	56	2844	52	12	20	32
55580	RC-61b	marble	368505	5737940	29.4	0.43	10.1	3.84	0.03	1.42	31.48	0.77	1.83	0.1	0.02	18.85	98.27	59	2562	66	15	17	34
55581	RC-63	hb gneiss	368567	5737620	42.95	0.87	6.32	13.84	0.18	25.45	6.69	0.66	0.2	0.15	0.01	1.96	99.28	13	96	55	17	18	131
Kneb area																							
55582	Kneb-30a	footwall calcsilicate	379532	5710319	71.33	0.01	0.55	5.32	0.36	6.44	12.43	0.01	0.1	0.01	0.01	2.57	99.14	8	109	12	<3	6	16
55583	Kneb-30b	gangue	379532	5710319	68.16	0.01	0.28	6.21	0.38	6.96	14.05	0.01	0.02	0.01	0.01	3.05	99.15	7	134	3	<3	12	18
Jordan River area																							
55586	JR-1	carbonatite	401149	5665434	21.09	0.25	5.8	4.57	0.41	6.13	31.14	2.29	1.02	0.58	0.29	24.35	97.92	33	5796	6	146	34	32
55587	JR-5	carbonatite	401592	5665022	25.53	0.33	8.14	5.17	0.33	5.28	27.73	2.89	0.99	0.36	0.21	21.59	98.55	40	2956	7	119	37	30
55588	JR-8	impure marble	401758	5664821	3.65	0.01	0.28	1.13	0.09	1.95	51.25	0.11	0.07	0.03	0.05	41.06	99.68	11	345	10	<3	20	9
55589	JR-10	impure marble	401675	5664907	1.98	0.01	0.23	1.37	0.14	2.27	51.16	0.69	0.02	0.01	0.01	41.84	99.73	6	295	11	6	13	4
55590	JR-11a	carbonatite	401461	5665168	21.17	0.3	8.52	3.65	0.1	4.13	30.2	3.66	1.78	0.21	0.19	25.23	99.14	75	2078	40	62	22	42
55591	JR-11b	carbonatite (?)	401461	5665168	17.45	0.21	7.01	2.75	0.07	2.69	36.22	2.07	0.87	0.05	0.1	29.88	99.37	43	761	35	10	19	37
55592	JR-12a	carbonatite (?)	401366	5665310	23.53	0.3	9.93	2.71	0.01	3.29	30.3	2.79	1.41	0.05	0.12	24.71	99.15	55	646	37	7	14	53
55593	JR-12b	carbonatite (?)	401366	5665310	10.39	0.05	1.14	1.13	0.05	3.44	47.58	0.15	0.07	0.03	0.01	35.49	99.53	12	331	32	6	8	4
55594	JR-13a	bi amphibolite	401366	5665310	66.94	0.89	13.38	5.88	0.14	3.92	3.34	0.56	3.09	0.11	0.03	1.02	99.3	157	116	269	37	38	108
55595	JR-13b	bi amphibolite	401366	5665310	64.13	0.87	13.82	6.59	0.2	4.8	3.46	0.46	3.59	0.12	0.03	1.19	99.26	195	93	237	26	28	126
Cottonbelt area																							
55597	CB2000-1a	gn-si schist, hangingwall	373588	5700806	60.06	0.82	20.64	7.88	0.11	1.55	1.27	0.37	4.42	0.12	0.13	1.9	99.27	164	115	182	20	29	99
55598	CB2000-1b	gn-si schist, footwall	373588	5700806	50.49	0.75	21.57	16.26	0.28	3.18	0.37	0.2	5.28	0.11	0.14	1.15	99.78	195	59	110	19	26	101
55599	CB2000-2	amphibolite	373644	5700821	43.93	1.98	14.27	12.4	0.23	9.65	12.21	2.14	0.62	0.56	0.03	1.36	99.38	16	608	135	46	24	264
55600	CB2000-3	ky schist	373709	5700825	41.5	1.04	22.95	15.19	0.07	10.23	0.4	1.73	2.29	0.12	0.03	4.34	99.89	105	38	228	17	20	136
55601	CB2000-4a	gn-si schist, hangingwall	373743	5700547	51.65	0.79	22.47	13.89	0.3	2.61	0.57	0.28	5.55	0.09	0.15	1.37	99.72	200	73	114	20	23	95
55602	CB2000-5b	gn schist	373760	5700411	58.15	0.87	22.19	8.98	0.15	1.99	0.61	0.27	4.63	0.09	0.1	1.78	99.81	179	81	195	20	20	83
55603	CB2000-7	amphibolite	373475	5701034	45	3.45	14.88	13.93	0.2	6.48	9.35	3.35	1.25	1.07	0.13	0.73	99.82	43	388	165	44	28	313
55604	CB2000-9	amphibolite	373455	5701051	44.9	2.98	15.77	14.06	0.23	5.71	11.06	3.27	0.31	0.52	0.01	0.72	99.54	9	520	158	46	24	386

Notes

Steel mill grinding @ Cominco; Lab: Cominco Research Lab

Method: oxides - fused disc, X-ray fluorescence

Method - trace elements: Pressed pellet X-ray fluorescence

Ba* = Fused disc analysis for XRF calibration. Values should be used with CAUTION.

Photo 1. (1a). Exposure of the Cottonbelt sulphide-magnetite layer enclosed in light-coloured garnet-sillimanite schist and calcsilicate gneiss.

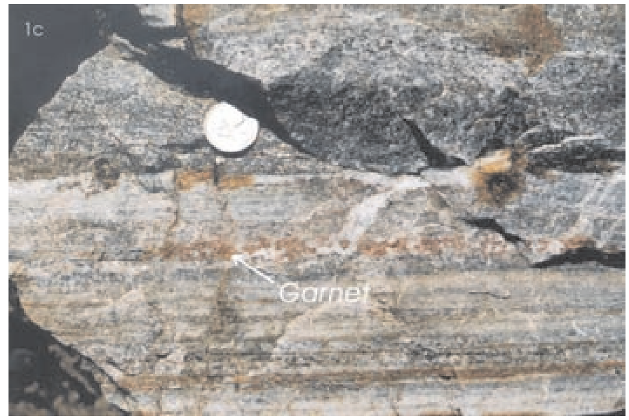

Photo 1c. Semi-massive sulphide-magnetite mineralization (top) in quartz-rich gangue, enclosed in spessartine garnet-calcareous quartzite host.

Photo 1b. Massive to semi-massive magnetite, sphalerite and galena mineralization in manganiferous calcsilicate gangue, in contact with siliceous marble with minor dispersed sulphide and magnetite (top).

mon iron sulphide phases. Immediate host rocks have abundant garnet and sillimanite, similar to Broken Hill host rocks. Thin quartzite and garnet quartzite layers that occur stratigraphically above Cottonbelt are similar to some of the exhalite facies that characterize Broken Hill stratigraphy as is an occurrence of gahnite with quartz located 6 kilometres northeast of Cottonbelt.

KNEB (082M 241)

Introduction

The Kneb occurrence was discovered during regional mapping by the author in 1980 and described briefly in a bulletin released in 1987 (Höy, 1987). It is located at an elevation of approximately 2150 metres at the headwaters of Ratchford Creek, 11 kilometres north-northwest of Cottonbelt (Figure 5). It is within the cover sequence of the Monashee Complex, at approximately the same stratigraphic level as Cottonbelt. A number of other unnamed showings of both Pb-Zn and Cu occur at this level southwest of Kneb.

Cominco Ltd. staked Kneb in 1998, and in 1999 conducted a geophysical program that comprised 24.7 km of electromagnetic and 19.2 km of magnetic surveys (Holyroyd, 1999). This survey concentrated on the showing and its projected extension beneath the glacier to the east. As the showing is not conductive and only weakly magnetic, it was difficult to trace. However, a small magnetic high located beneath glacier ice is a possible source of newly-discovered, high grade lead-zinc boulders (Holyroyd, 1999).

Host Succession

The Kneb occurrence is in Unit 6a, a dominantly calcsilicate assemblage above the white marble of Unit 5. Footwall rocks to Kneb were only poorly exposed, due to snow and moraine cover. However, several hundred metres of hangingwall rocks are exposed just north of Kneb in the east limb of the Mount Grace syncline (Figure 7).

Kneb occurs at the top of a tan weathering, massive to layered dolomitic marble approximately 15 metres thick. The marble contains minor knebelite, pyroxene and amphibole and trace chalcopyrite and pyrrhotite. Immediate

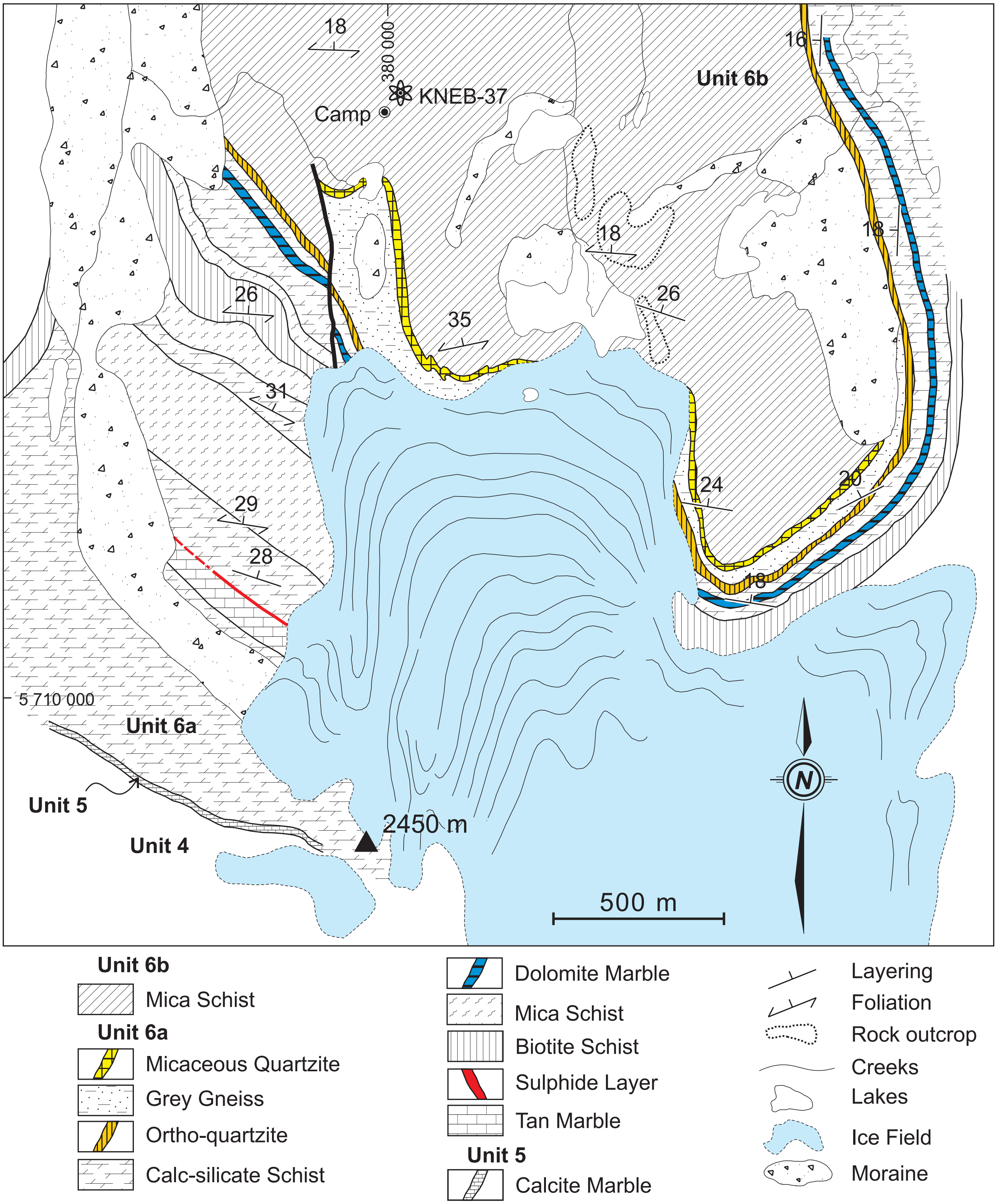

Figure 7. Geology of the Kneb deposit area.

hangingwall rocks comprise diopside rich calcsilicate schists interlayered with minor garnet-muscovite schist. Approximately 100 metres of mixed micaceous schists, calcsilicate schists and granular quartz-feldspar mica schists overlie these hangingwall rocks. This is overlain by a prominent, rusty-weathering coarse-grained biotite schist, with minor dispersed pyrrhotite, and thin interlayers of calcite marble and calcsilicate schist. The top of Unit 6a (Figure 7) comprises silver-coloured garnet-muscovite schist, calcsilicate gneisses, a thin well-bedded dolomitic marble and massive to layered quartzite (Photo 2). Thin amphibolite layers that occur just above the quartzite may correlate with amphibolite layers that occur above Cottonbelt, or with amphibolites farther north in the Kirbyville Creek area.

Unit 6b comprises mainly grey quartz-feldspar orthogneisses (?) and micaceous schist. The grey gneisses are commonly massive to foliated, swirled, and contain numerous coarser quartz-feldspar augens. One of these (located on Figure 7) has been submitted for zircon extraction and U-Pb dating in an attempt to provide a minimum age for the underlying Kneb and Cottonbelt deposits. Within the orthogneisses are well-layered and foliated micaceous schists and gneisses. These paragneisses are commonly rusty-weathering muscovite-biotite-garnet schists that are locally associated with impure quartzite layers or with thin hornblende schist layers.

Mineralization

Kneb is a thin, semi-massive to massive sulphide layer in marble and calcsilicate schist. It comprises mainly chalcopyrite with variable amounts of sphalerite, galena and pyrrhotite. To the northeast, massive sulphide boulders that appear to originate beneath glacier ice are mainly galena and sphalerite.

Mineralization occurs at the top of a tan dolomitic marble and is overlain by diopside-rich calcsilicate schist (Photo 3). It is within a thin siliceous zone comprising mainly quartz with minor dispersed garnet and sulphides. This siliceous zone grades out to an envelope of diopside “skarn-like” rock that contains minor dispersed pyrrhotite, chalcopyrite, dolomite, amphibole, quartz, knebelite and garnet. These alteration assemblages are better developed in the footwall, with widths up to several metres. Although the silica and skarn zoning are crudely developed as described above, in detail they interfinger considerably. The hangingwall alteration is thinner, comprising mainly quartz with minor dispersed sulphides and silicates that grade outward to calcsilicate schists.

The sulphide-silica layer is up to several metres thick and comprises mainly quartz with variable chalcopyrite, galena, sphalerite and pyrrhotite. A thin chalcopyrite-rich layer occurs near the top of the sulphide zone. Gangue minerals include diopside and an amphibole, and generally minor carbonate, knebelite and garnet. The sulphides, quartz and a thin dolomite are crudely layered.

Analyses of the Kneb sulphide layer (Table 3) show the high copper content, generally low zinc and only very

Photo 2. Well-bedded sequence of micaceous schist, quartzite, marble, and calcsilicate gneiss near the top of Unit 6a, Kneb prop-

Photo 3. Kneb sulphide layer (top) enclosed within calcareous quartzite and underlain by tan-coloured dolomitic marble.

minor lead. Manganese is high, with two samples containing 6536 and 4736 ppm Mn. Gold and silver contents are low, but cobalt and nickel range up to several hundred ppm.

Discussion

Kneb has many similarities to a Besshi deposit. It is a semi-massive copper-zinc deposit within a metasedimentary succession that contains minor mafic metavolocanics. However, as only a limited extent of the sulphide layer is exposed, and as massive sulphide boulders that may be sourced along strike are lead-zinc rich, it is possible that Kneb is a zoned sedex or BHT deposit with only the more proximal, copper-rich portion exposed.

JORDAN RIVER (082M 001)

Introduction

The Jordan River property, also know as the King Fissure, is located on the steep north slopes of a ridge between Copeland and Hiren creeks (Photo 4). Access is by helicopter from Revelstoke, 20 kilometres to the southeast. A number of other showings and deposit types are

TABLE 3
ANALYSES OF SELECTED MINERALIZED HAND SAMPLES OF THE KNEB, JORDAN RIVER AND RUDDOCK CREEK DEPOSITS

Lab No.	Field No.	Deposit	UTM East	UTM North	Mo ppm	Cu ppm	Pb ppm	Zn ppm	Ag ppm	Ni ppm	Co ppm	Mn ppm	Fe %	As ppm	U ppm	Au ppm	Th ppm	Sr ppm	Cd ppm	Sb ppm	Bi ppm	V ppm
Ruddock Creek																						
52265	H96RC-1	E zone	368900	573700	1	459	31116	99999	4	119	34	668	14.83	8	< 5	< 2	< 2	74	312.1	2	21	27
52266	H96RC-2	E zone	368900	573700	< 1	13	29239	99999	5.7	3	14	336	5.14	< 2	< 5	< 2	< 2	81	379.2	< 2	28	9
52267	H96RC-3a	E zone	368900	573700	15	88	16623	46858	1.3	16	4	232	1.02	2	9	< 2	< 2	723	58.6	12	< 2	9
52268	H96RC-4	E zone	368900	573700	1	17	32060	7494	8.6	2	< 1	17	0.09	< 2	< 5	< 2	< 2	170	33.5	71	2	< 1
52269	H96RC-8	M zone	368207	5738758	< 1	215	34011	99999	3.2	71	36	877	10.73	8	< 5	< 2	< 2	134	251.5	5	27	23
52270	H96RC-9	M zone	368207	5738758	142	228	9718	43515	2	52	11	130	4.41	< 2	< 5	< 2	< 2	107	59.5	16	6	12
55605	RC-11b	F zone	368532	5737545	10	25	38931	99999	10.6	51	24	443	5.38	5	< 10	< 4	< 2	97	237.2	< 5	41	40
55606	12b	F zone	368537	5737520	9	190	37463	99999	7.7	105	26	454	14.49	< 5	< 10	< 4	2	144	292.7	14	15	35
55607	13	F zone	368508	5737526	18	532	7745	21826	6.9	381	42	114	23.64	< 5	< 10	< 4	9	99	28.5	< 5	110	87
55608	14a	F zone	368379	5737418	6	9	853	5161	< .5	19	4	188	1.13	< 5	< 10	< 4	10	202	4.9	< 5	< 5	79
55609	14b	F zone	368379	5737418	12	616	35216	99999	5.4	185	49	500	16.96	< 5	< 10	< 4	4	78	179.1	12	10	50
55610	14c	F zone	368379	5737418	22	128	493	2100	< .5	58	9	314	4.23	< 5	< 10	< 4	8	107	0.4	< 5	< 5	175
55611	17	lower G	368335	2737675	8	19	41058	99999	9.9	< 2	38	454	6.88	5	< 10	< 4	< 2	52	413.6	11	22	12
55612	18	lower G	368320	5737730	12	55	35502	99999	6.5	7	26	93	5.93	5	< 10	< 4	< 2	44	340.1	15	< 5	49
55613	23	upper G	368350	5738000	22	46	42666	99999	3.8	17	28	313	6.78	< 5	< 10	< 4	2	60	302.9	10	< 5	45
55614	26b	M zone	368207	5738758	26	206	38198	99999	4.6	75	25	1400	9.12	< 5	< 10	< 4	< 2	96	256.2	19	6	118
55615	26c	M zone	368207	5738758	10	242	3990	54475	0.9	90	15	428	7.19	< 5	< 10	< 4	5	153	66	< 5	6	149
55616	26d	M zone	368207	5738758	5	30	3834	40371	3	9	2	168	1.13	< 5	20	< 4	< 2	796	48.8	14	20	7
55617	26e	M zone	368178	5738764	22	20	21503	99999	3.8	6	10	626	3.83	5	< 10	< 4	< 2	420	255.1	23	8	8
55618	43a	upper G	368234	5738087	19	553	25157	99999	9.3	235	55	649	14.98	< 5	< 10	< 4	< 2	57	313.7	5	66	198
55619	43b	upper G	368234	5738087	28	8	8303	2227	5.9	17	2	1485	5.31	< 5	12	< 4	6	123	4.8	7	72	162
55620	43c	upper G	368234	5738087	20	283	170	20319	< .5	151	27	235	4.68	< 5	24	< 4	2	16	44.9	< 5	< 5	10
55621	47a	F zone	368200	5738485	31	651	10961	58146	2.1	402	54	282	23.48	5	< 10	< 4	5	61	71.5	7	8	332
55622	47b	F zone	368200	5738485	35	53	34697	99999	18.5	12	8	441	3.2	< 5	< 10	< 4	< 2	301	377.3	49	20	4
55623	56		369239	5738022	8	49	235	876	< .5	27	8	797	2.61	< 5	< 10	< 4	10	175	< .4	< 5	< 5	92
55624	36	upper G	368384	5738063	15	150	30883	99999	4.3	110	33	389	10.09	< 5	< 10	< 4	2	77	191.9	9	16	89
Jordan River																						
55626	JR-3a		401084	5665420	3	935	32364	62411	164.3	85	19	10653	8.87	< 5	< 10	< 4	12	109	243.3	167	< 5	63
55627	3b		401084	5665420	7	211	30083	79625	151.1	15	9	8174	5.93	< 5	< 10	< 4	9	152	325	148	< 5	49
55628	4		401038	5665433	5	58	29792	78508	115.5	20	8	5755	3.76	6	< 10	< 4	9	191	336.7	139	< 5	47
55629	6		401889	5664688	< 2	378	31465	668	65.9	8	2	140	0.97	10	< 10	< 4	< 2	2218	7.8	228	< 5	< 2
55630	7		401767	5664784	18	128	1675	36061	1.5	75	15	519	27.43	< 5	< 10	< 4	3	9	18.3	19	< 5	15
55631	9		401680	5664864	34	244	21855	99999	38.5	27	16	4451	17.27	5	< 10	< 4	9	65	555.8	46	6	140
Kneb																						
55633	Kneb-30c		379532	5710319	4	9325	371	1000	10.3	48	23	2719	12.27	< 5	< 10	< 4	2	130	3	< 5	< 5	9
55634	Kneb-30d		379532	5710319	< 2	6182	2752	865	15.7	10	7	4968	7.52	< 5	< 10	< 4	< 2	111	3.8	16	38	27
54962	KNEB 5		379532	5710319	< 2	2624	37	139	1.7	106	46	6536	30.44	11	15	< 4	< 2	144	5.6	< 5	< 5	2
54963	KNEB 6		379532	5710319	< 2	14294	42	806	12.4	32	20	4736	13.78	< 5	< 10	< 4	< 2	108	2.1	< 5	< 5	11
54964	KNEB 7		379532	5710319	3	1483	16	66	1.4	188	103	807	39.62	< 5	< 10	< 4	3	5	< .4	< 5	< 5	2
54965	KNEB 8		379532	5710319	6	1477	8	19	1.3	216	111	493	49.56	< 5	< 10	< 4	3	2	< .4	8	< 5	< 2

TABLE 3 CONTINUED
ANALYSES OF SELECTED MINERALIZED HAND SAMPLES OF THE KNEB, JORDAN RIVER AND RUDDOCK CREEK DEPOSITS

Lab No.	Field no.	Deposit	UTM East	UTM North	Ca %	P %	La ppm	Cr ppm	Mg %	Ba ppm	Ti %	Al %	Na %	K %	W ppm	Zr ppm	Sn ppm	Y ppm	Nb ppm	Be ppm	Sc ppm	Au** ppb	Pt** ppb	Pd** ppb
Ruddock Creek																								
52265	H96RC-1	E zone	368900	573700	5.3	0.024	1	35	< .01	11	0.05	0.64	0.06	0.15	< 2									
52266	H96RC-2	E zone	368900	573700	6.5	0.013	1	45	< .01	21	0.02	0.46	0.14	0.11	< 2									
52267	H96RC-3a	E zone	368900	573700	26	0.124	3	52	0.02	76	0.01	0.63	0.01	0.02	< 2									
52268	H96RC-4	E zone	368900	573700	14	0.007	2	46	0.01	56	< .01	0.33	0.43	0.2	< 2									
52269	H96RC-8	M zone	368207	5738758	8.1	0.068	3	36	0.06	19	0.07	1.12	0.07	0.11	< 2									
52270	H96RC-9	M zone	368207	5738758	6.8	0.044	< 1	107	< .01	19	0.01	0.48	0.13	0.1	< 2									
55605	RC-11b	F zone	368532	5737545	4.4	0.07	3	118	0.05	144	0.04	0.93	0.08	0.18	< 4	4	5	6	7	2	1	< 2	< 2	< 2
55606	12b	F zone	368537	5737520	3.3	0.024	< 2	113	0.07	161	0.08	1.04	0.06	0.22	< 4	2	7	6	4	1	2	< 2	5	8
55607	13	F zone	368508	5737526	2	0.139	14	75	0.05	157	0.24	1.98	0.05	0.52	< 4	10	35	13	18	< 1	5	< 2	2	22
55608	14a	F zone	368379	5737418	3.7	0.033	27	61	0.37	424	0.22	3.79	0.51	0.14	< 4	5	2	10	11	5	7	< 2	< 2	2
55609	14b	F zone	368379	5737418	5.1	0.068	5	99	0.12	184	0.11	1.55	0.1	0.24	< 4	2	7	8	5	2	3	4	< 2	< 2
55610	14c	F zone	368379	5737418	3.6	0.213	25	75	0.24	60	0.36	3.24	0.43	0.07	< 4	5	2	15	19	1	7	< 2	5	3
55611	17	lower G	368335	2737675	8.6	0.01	< 2	145	0.01	156	0.01	0.37	0.02	0.01	< 4	2	10	5	< 2	< 1	1	2	2	3
55612	18	lower G	368320	5737730	6.3	0.053	< 2	135	< .01	113	0.01	0.24	0.03	0.14	< 4	< 2	2	3	< 2	< 1	1	< 2	< 2	< 2
55613	23	upper G	368350	5738000	3.4	0.051	< 2	137	0.05	182	0.03	0.39	0.05	0.14	< 4	< 2	4	4	< 2	< 1	1	< 2	2	< 2
55614	26b	M zone	368207	5738758	3.5	0.076	4	145	0.08	173	0.06	0.73	0.05	0.31	< 4	< 2	4	9	2	1	2	< 2	7	5
55615	26c	M zone	368207	5738758	2.9	0.215	16	112	0.17	124	0.12	1.85	0.26	0.93	< 4	3	< 2	11	4	3	4	< 2	8	7
55616	26d	M zone	368207	5738758	27	0.058	< 2	32	0.02	345	0.01	0.12	0.02	0.02	< 4	2	< 2	7	< 2	< 1	1	< 2	4	3
55617	26e	M zone	368178	5738764	18	0.033	5	85	0.08	240	0.01	0.4	0.02	0.07	< 4	< 2	3	10	< 2	< 1	1	< 2	3	< 2
55618	43a	upper G	368234	5738087	1.3	0.207	5	144	0.11	224	0.09	1.25	0.15	0.43	< 4	2	7	13	4	2	3	< 2	3	24
55619	43b	upper G	368234	5738087	16	0.054	23	71	0.45	135	0.33	6.52	0.06	0.02	< 4	11	9	19	24	11	8	3	< 2	< 2
55620	43c	upper G	368234	5738087	0.8	0.2	2	54	0.03	303	0.01	0.12	0.02	0.02	< 4	< 2	< 2	4	< 2	< 1	1	< 2	3	6
55621	47a	F zone	368200	5738485	1.4	0.195	8	127	0.18	115	0.11	1.99	0.18	1.05	< 4	2	2	16	4	2	5	< 2	3	5
55622	47b	F zone	368200	5738485	11	0.028	2	105	0.06	162	< .01	0.45	0.04	0.14	< 4	< 2	7	5	< 2	1	1	2	< 2	< 2
55623	56		369239	5738022	3.7	0.15	29	57	1.14	292	0.2	4.31	0.61	1.16	8	4	2	19	11	1	7	< 2	4	4
55624	36	upper G	368384	5738063	3.4	0.093	4	106	0.08	159	0.07	1.07	0.06	0.31	< 4	< 2	4	7	3	1	2	3	< 2	< 2
Jordan River																								
55626	JR-3a		401084	5665420	2	0.035	38	92	2.25	197	0.28	6.23	0.07	2.13	9	2	2	15	8	1	10	94	< 2	< 2
55627	3b		401084	5665420	3.2	0.025	22	104	1.27	111	0.22	4.51	0.11	1.64	< 4	2	3	10	6	1	7	73	< 2	< 2
55628	4		401038	5665433	3.8	0.03	22	97	1.38	110	0.22	4.65	0.1	1.89	< 4	2	3	11	7	2	7	53	< 2	< 2
55629	6		401889	5664688	0.1	< .002	< 2	3	0.02	144	< .01	0.07	0.01	0.02	< 4	< 2	< 2	< 2	< 2	< 1	< 1	33	3	< 2
55630	7		401767	5664784	0.1	< .002	2	46	0.05	128	0.01	0.34	0.03	0.09	5	< 2	2	< 2	< 2	< 1	< 1	26	3	2
55631	9		401680	5664864	1.6	0.023	14	128	1.26	219	0.14	2.94	0.06	1.22	< 4	3	3	8	5	1	5	813	< 2	< 2
Kneb																								
55633	Kneb-30c		379532	5710319	7.2	0.005	< 2	18	2.79	46	< .01	0.05	0.03	0.01	< 4	< 2	< 2	< 2	< 2	< 1	1	76	< 2	< 2
55634	Kneb-30d		379532	5710319	13	0.027	5	12	6.01	109	0.04	0.63	0.07	0.2	< 4	< 2	2	4	< 2	< 1	3	130	< 2	< 2
54962	KNEB 5		379532	5710319	8.4	0.005	< 2	6	2.23	11	< .01	0.03	0.01	0.01	< 4	3	< 2	2	< 2	< 1	< 1	13		
54963	KNEB 6		379532	5710319	11	0.008	< 2	25	5.42	4	< .01	0.12	0.04	< .01	< 4	2	< 2	< 2	< 2	< 1	1	45		
54964	KNEB 7		379532	5710319	0.8	< .002	< 2	57	0.37	15	< .01	0.05	0.01	0.01	< 4	< 2	< 2	< 2	< 2	< 1	< 1	3		
54965	KNEB 8		379532	5710319	0.2	< .002	< 2	57	0.1	9	< .01	0.05	0.01	0.01	< 4	< 2	< 2	< 2	< 2	1	< 1	2		

Notes

Samples milled by ACME in a Cr-Steel mill. Possible Fe & Cr contamination from grinding

Method: HCLO4-HNO3-HCl-HF digestion - inductively coupled plasma emission spectroscopy

Lab: ACME Analytical

**FAA = Fire assay-ICP finish

99999: greater than 9.9 per cent

Photo 4. Steep slopes on the north side of Copeland ridge, showing the location of the Jordan River sulphide layer in the northeast limb of the Copeland syncline. The core of the syncline is located just south (right) of the sulphide layer, and underlying rocks of Units 4 and 5 are exposed to the north.

known in the immediate area, probably the most important being the Mount Copeland molybdenite deposit located along the margins of a syenite gneiss complex approximately 300 metres west of the Jordan River deposit. Mount Copeland (082M 002) was mined from 1970 to 1974 by King Resources Ltd., producing 1,191 tonnes of molybdenum from 169,729 tonnes of ore. Its geology is described in considerable detail by Fyles (1970) and summarized in BC Minfile.

The Jordan River deposit was reportedly discovered in the late 1800s by prospectors following up on the discovery of placer gold in Jordan River (Riley, 1961). Systematic exploration began on the property in the 1950s after it was optioned by Consolidated Standard Mines Ltd. Work included mapping, sampling and drilling by this company and Bunker Hill Exploration Ltd., and continued in the 1960s under Bralorne Pioneer Mines Ltd.

Exploration in the Jordan River area continued in the 1990s for Equinox Resources on the behalf of the owner, First Standard Mines Ltd. (MacGillivray and Laird, 1990). This work resulted in the recognition that a buff-weathering marble mapped by Fyles (1970) was the Mount Grace carbonatite of the Cottonbelt area, supporting a regional structural reinterpretation of the Jordan River area proposed by Höy and McMillan (1979) and Höy and Brown (1981). Subsequent work led to the discovery of several occurrences of gem-quality crystals, including emerald-green gahnite, almandine garnet and black tourmaline (Laird, 1997).

The current project concentrated on confirming the correlation of the Jordan River stratigraphy with that at Cottonbelt and evaluating Jordan River as a Broken Hill-type deposit. This report relies considerably on the regional and property-scale mapping by Fyles (1970) and more detailed work, including considerable sampling, by MacGillivray and Laird (1990) and Laird (1997).

Regional Geology

Fyles (1970) established a stratigraphic succession in the Jordan River area but conceded that above the Bews Creek fault, in the Jordan River deposit area, stratigraphic tops were not known. Höy and McMillan (1979) correlated Unit 10 of Fyles (op. cit.) with the core gneisses, thereby extending these gneisses well to the south as well as inverting the stratigraphy in the embayment of cover rocks of the deposit area. This revision of facing directions allowed correlation with similar successions to the south (Read, 1980) and to the north in the Perry River, Cottonbelt and Kirbyville Creek areas (Höy and Brown, 1981; Höy, 1987; Scammel and Brown, 1990). Detailed work corroborated these structural and stratigraphic revisions with the recognition of the marker Mount Grace carbonatite in the footwall of the Jordan River deposit (MacGillivray and Laird, 1990).

The revised stratigraphic succession of the Jordan River area is shown in Figure 8. The nomenclature follows that established at Cottonbelt. Unit 3 comprises mainly white quartzite with rare interlayers of micaceous schist and calcsilicate gneiss. Unit 4 includes a thick succession of calcsilicate gneisses, marbles, micaceous schists and a relatively thick quartzite (Unit 7 of Fyles, 1990). The top of Unit 4, the “grey-green gneiss” of Fyles, comprises mainly quartz-biotite-hornblende gneiss with lesser amounts of calcsilicate gneiss, fine-grained mica schist, a few thin, well-defined quartzite layers and the carbonatite tuff. Unit 5 is a distinctive white calcite marble that is recognized throughout the margins of Frenchman Cap dome. It is overlain by a calcsilicate-quartzite succession and the sulphide layer and, in the core of the Copeland syncline, sillimanite-biotite schists of Unit 6a (Figure 9).

The carbonatite on the northeast limb of the Copeland syncline is a tan to brown-coloured calcite marble layer that is interlayered with white to buff-coloured marble, and commonly underlain by a 30 cm thick, layered white marble. It is overlain by a mixed calcsilicate-im-

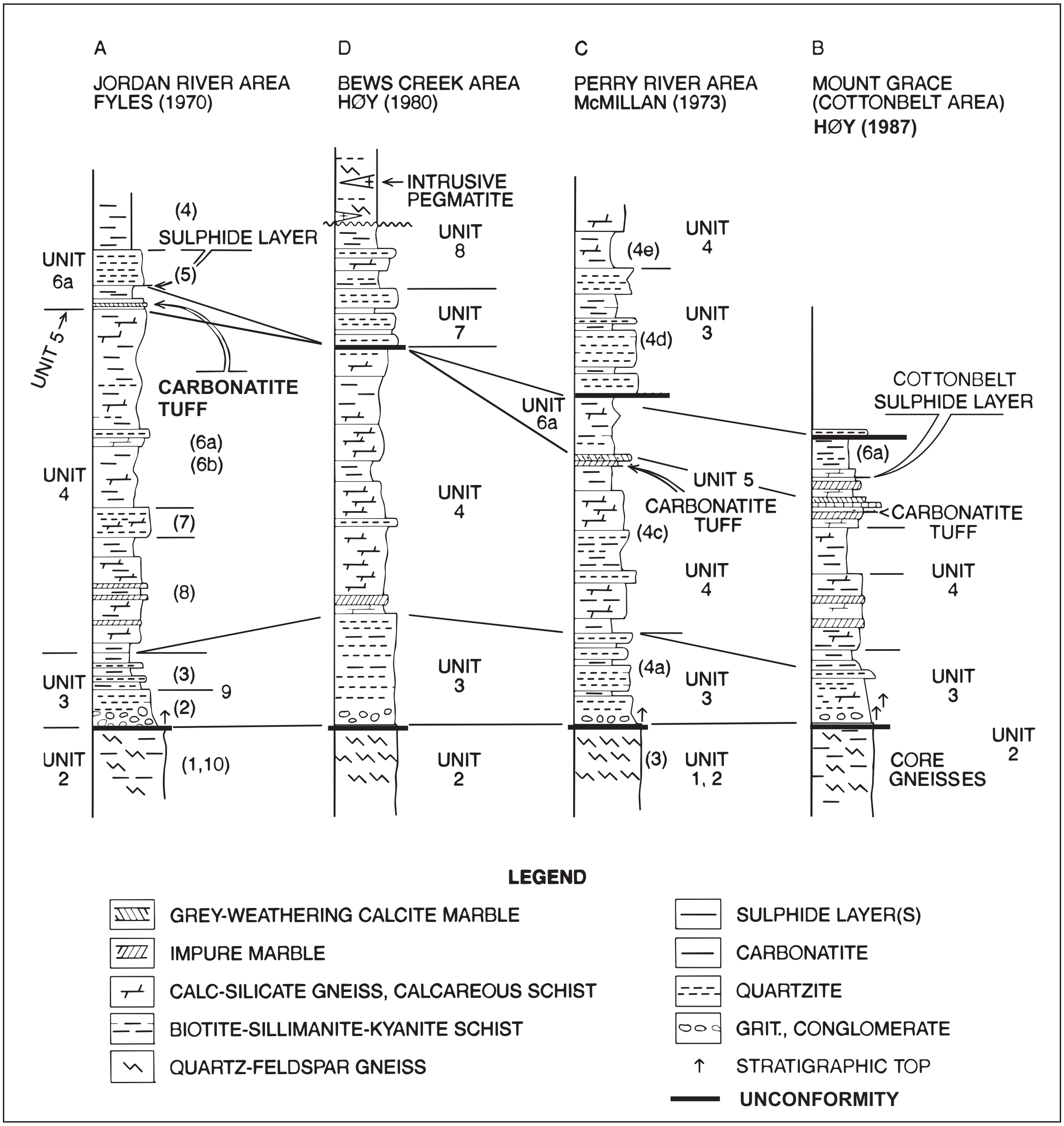

Figure 8. Composite cover sequence section, Jordan River deposit area, and correlation with sections along the west and north margin of Frenchman Cap dome; note numbers in brackets in the Jordan River section refer to unit designations of Fyles (1970); after Fyles (1970), Höy (1980), McMillan (1973) and Höy (1987).

pure marble succession, several metres thick, and the grey-weathering calcite marble of Unit 5. It is recognized in the field by its distinctive colour, numerous dispersed grains of brown mica and, less commonly, amphibole and abundant small clasts of granular, white albite. Analyses of the carbonatite (JR-1, JR-5, JR-11a; Table 2) shows that it contains up to 5800 ppm Sr, 146 ppm Nb, 0.58 percent P2O5, 0.29 percent Ba and 0.41 percent Mn. Rare earth element concentrations in two samples reported by Laird (1990) are also highly anomalous, with up to 608 ppm La, 1108 ppm Nd and 731 ppm Ce. Analyses of samples of buff to white marbles immediately adjacent to the carbonatite (Table 2) have trace and rare earth element concentrations that are comparable to marbles with sedimentary protoliths, as summarized in Höy (1997).

An orthogneiss, the Mount Copeland syenite, is exposed south of the Jordan River deposit area (Figure 9). It is a medium-grained, grey nepheline-feldspar-biotite gneiss that appears to have been involved in all deformation phases (Fyles, 1970). Lenses of coarse-grained K-feldspar pegmatites are common within it. The Mount Copeland syenite has been dated 740 ± 36 Ma (Parrish and Scammel, 1988), a similar age as the Mount Grace syenitic orthogneiss in the Cottonbelt area (Table 1; Crowley, 1997).

The structure of the deposit area is dominated by the Phase 2 Copeland syncline (Fyles, 1970). Its hinge and limbs are clearly outlined by Unit 5 and the sulphide layer. In the western part of the deposit area (Figure 9), the syncline plunges 30 degrees towards 150 degrees with an axial plane that dips south 45 degrees (Fyles, op. cit.). To the east, the fold becomes very tight and the plunge decreases through the horizontal to a low westerly plunge, resulting in the banana-shaped outcrop pattern. In the west, a syncline-anticline pair, folds E and F, warp the south limb of the Copeland syncline, and extend beyond the area mapped by Fyles, a distance of over 8 kilometres. The hinges of these Phase 2 folds are generally open and concentric with little appreciable thickening of the sulphide sequence (Photo 5).

Phase 1 folds are small recumbent isoclines with axial planes essentially parallel to layering. Fold axes are outlined by a penetrative mineral lineation which, throughout the deposit area, generally plunge to the southwest.

Mineralization

The Jordan River deposit comprises a sequence of one or more sulphide layers, with lenses of quartz and locally barite, in a calcsilicate gneiss succession that totals up to 10 metres in thickness (Fyles, 1970). Measured reserves reported by Riley (1961) total 2.6 million tonnes containing 5.6 percent Zn, 5.1 percent Pb and 37.7 g/tonne silver.

The sulphide layers are massive to crudely banded. They comprise mainly fine-grained pyrrhotite, sphalerite and galena with scattered grains of pyrite in a gangue of quartz, barite, calcite, plagioclase, garnet and some calcsilicate minerals. Barite content ranges from isolated grains within the sulphides to massive layers that contain variable amounts of sulphides.

Analyses of a number of hand samples of the sulphide layer in the northeast limb (Figure 9) are given in Table 3. A number of the samples contain considerable manganese, ranging up to 10653 ppm Mn, and relatively high cadmium and antimony. Silver content is higher than in other stratiform sulphide layers in the Northern Monashees, with three of the six samples containing more than 115 ppm Ag. These values are comparable to or somewhat lower than those reported by MacGillivray and Laird (1990) but much higher than in the measured reserves of Riley (1961). Gold content is also relatively high with one zinc-rich sample assaying 813 ppb Au (Table 3).

Discussion

The only age constraints on the Jordan River succession is the 740 Ma Copeland syenite that intrudes Unit 4 below the Jordan River deposit. However, the recognition of the carbonatite tuff and white calcite marble just below the Jordan River sulphide layer allows direct correlation with the Cottonbelt succession. Both sulphide deposits are stratabound layers at approximately the same stratigraphic level and, based on arguments from the Cottonbelt area, the Jordan River host succession may therefore be as old as 1.85 billion years. As in the Cottonbelt area, no unconformities have been recognized in the cover sequence below the Jordan River deposit.

Jordan River has many features that are typical of metamorphosed sedex deposits. Diagnostic features of Broken Hill-type deposits, such as siliceous or manganese rich envelopes, unusual chemistry, abundance of recognized exhalite facies in surrounding stratigraphy, or magnetite within ore lenses are not apparent. However, slightly elevated manganese, copper and antimony, and high gold and silver content, are typical of BHT deposits. It is probable that Jordan River represents a metamorphosed stratiform sulphide deposit that is closer to the sedex end of a BHT-sedex spectrum.

RUDDOCK CREEK

Introduction

The Ruddock Creek deposit was discovered in 1960 by prospectors under the supervision of Earl Dodson of Falconbridge Nickel Mines Ltd. The property was mapped in detail by H.R. Morris of Falconbridge in the summers of 1961 to 1963 and by J. T. Fyles in 1968 (Fyles, 1970). The writer spent one week on the property in late August of this year, mapping in detail the eastern part of the Ruddock Creek property. Exploration on Ruddock Creek included considerable drilling by Falconbridge from 1961 to 1963. Cominco Ltd. optioned the property in 1976, and during the late 1970s conducted extensive exploration that included considerable drilling,

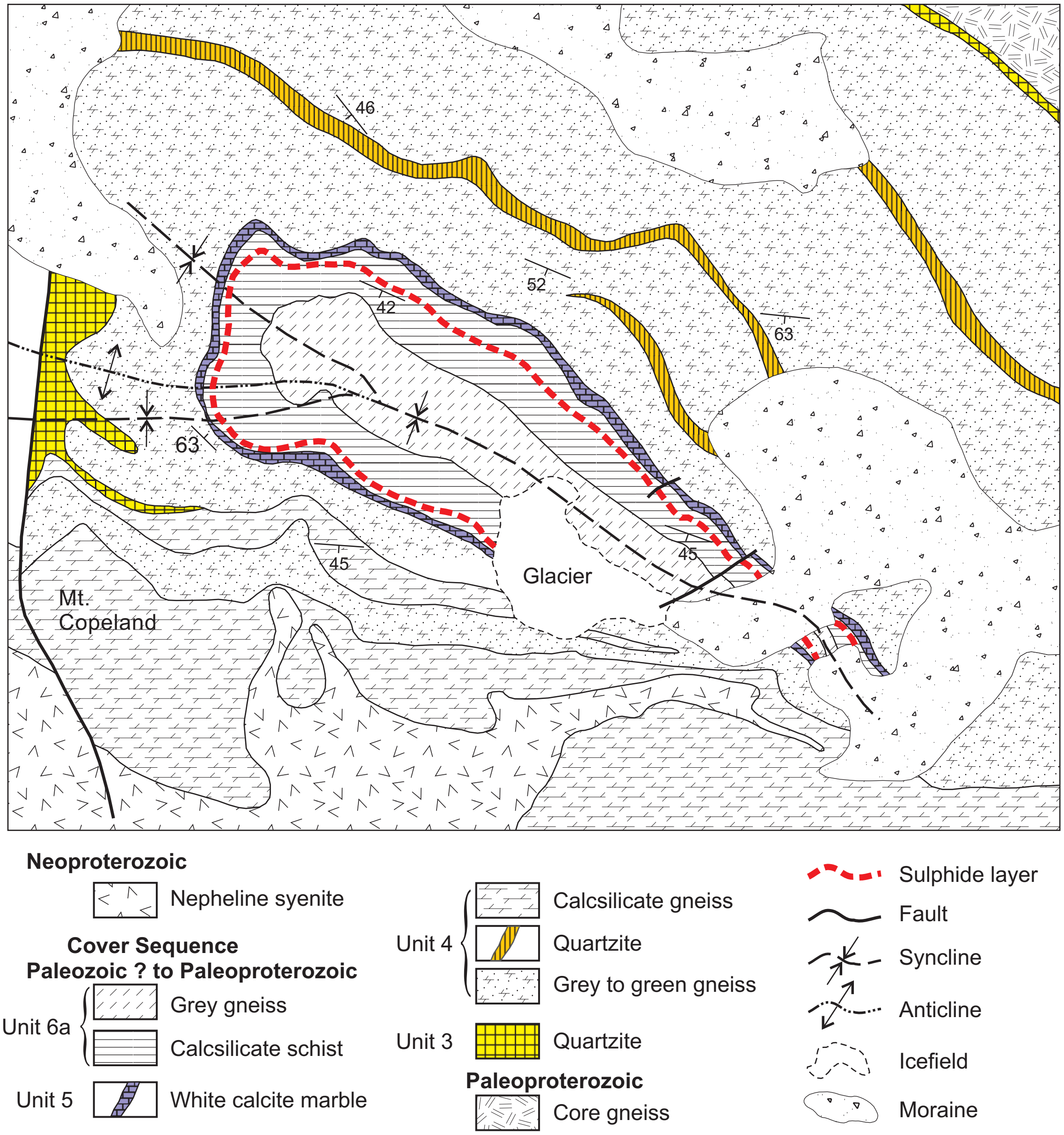

Figure 9. Geology of the Jordan River deposit area (after Fyles, 1970).

more detailed mapping, sampling and geophysical surveys. A considerable part of this work was directed towards defining the closure of the tight fold that forms the E zone. Double Star Resources Inc. obtained the Ruddock Creek claims in 1999 and this past summer began a program that consisted mainly of structural mapping and sampling. This report draws extensively on previous work; it describes main geological features, presents some new geochemical data and attempts correlations with units at other Monashee massive sulphide deposits to the south.

Ruddock Creek is located in the Script Ranges, nearly 100 kilometres north of Revelstoke (Figure 1). It is accessible by helicopter from both Revelstoke or Blue River, 50 km to the northwest. Ruddock Creek is a thin massive sulphide layer that can be traced or extrapolated through a distance of nearly 13 kilometres on south facing slopes near the headwaters of Ruddock Creek and a small tributary of Oliver Creek (Figure 10). Although most showings are above treeline and exposure is excellent, the steep topography on north facing slopes, together with glacier and snow cover, and very extensive “pegmatite” and “granite” tend to obscure this horizon.

Host Succession

As noted by previous workers, it is difficult to develop a composite section due to the pervasive “granite” and “pegmatite”, and structural complexity. Much of this granitic material contains remnant metasedimentary lay-

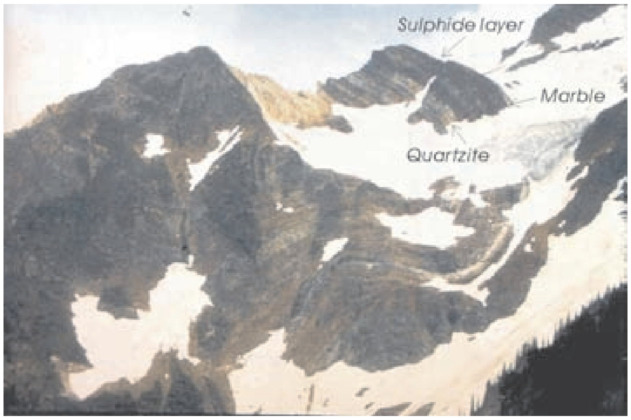

Photo 5. The Copeland syncline, viewed to the east, outlined by marble of Unit 5 and quartzites of Unit 6.

ers, only a few of which are shown on Figure 11. In some places, only the sulphide layer remains, entirely enclosed in granitic rock. However, a general succession, as noted by Fyles (1970), comprises a structurally lower calcareous section with the sulphide layer near the top, and an upper non-calcareous section. More detailed descriptions (below) are mainly from exposures on the slopes above the E zone and just west of the camp and E zone fault. As both of these exposure areas are on the upper limb of a tight, overturned syncline, they are interpreted to be inverted (Fyles, 1970).

The lower calcareous section comprises a mixture of calcsilicate gneisses, micaceous schist, pure to impure marble and minor amphibolites and thin quartzites. Calcsilicates are typically pale green with abundant diopside and variable garnet, quartz, feldspar and amphibole. They range in composition into impure quartzites with dispersed diopside and other calcareous minerals. At least two grey-weathering, white calcite marbles are recognized, separated by several hundred metres of mixed calcsilicates and schists. The lower grey marble, exposed northwest of camp (Figure 11) is structurally underlain by a tan to buff-coloured impure diopsidic marble and overlain by calcsilicate gneisses. Rusty-weathering biotite ± sillimanite schist layers are common within the calcareous section, particularly directly below the sulphide layer. Quartzites are not common, although a number of thin layers with minor diopside or garnet occur within a few hundred metres above and below the sulphide layer. Other thin quartzite layers that contain dispersed pyrrhotite and less commonly sphalerite occur in the section below the sulphide layer east of the E showing. They are interpreted to be recrystallized siliceous exhalite units. Some that contain only dispersed garnet may also be exhalative in origin, similar to those described at Broken Hill. Analyses of two of these quartzites (RC-52 and RC-57a, Table 2) show values fairly typical of impure sedimentary quartzites; however, slightly elevated Mn in one sample may reflect an exhalative origin.

The tan weathering marble described above was analyzed with the possibility that it is a carbonatite, even though it did not contain lithic clasts nor dispersed biotite characteristic of carbonatites at Jordan River and Cottonbelt. Analyses (RC-61a and RC-61b, Table 2) indi-

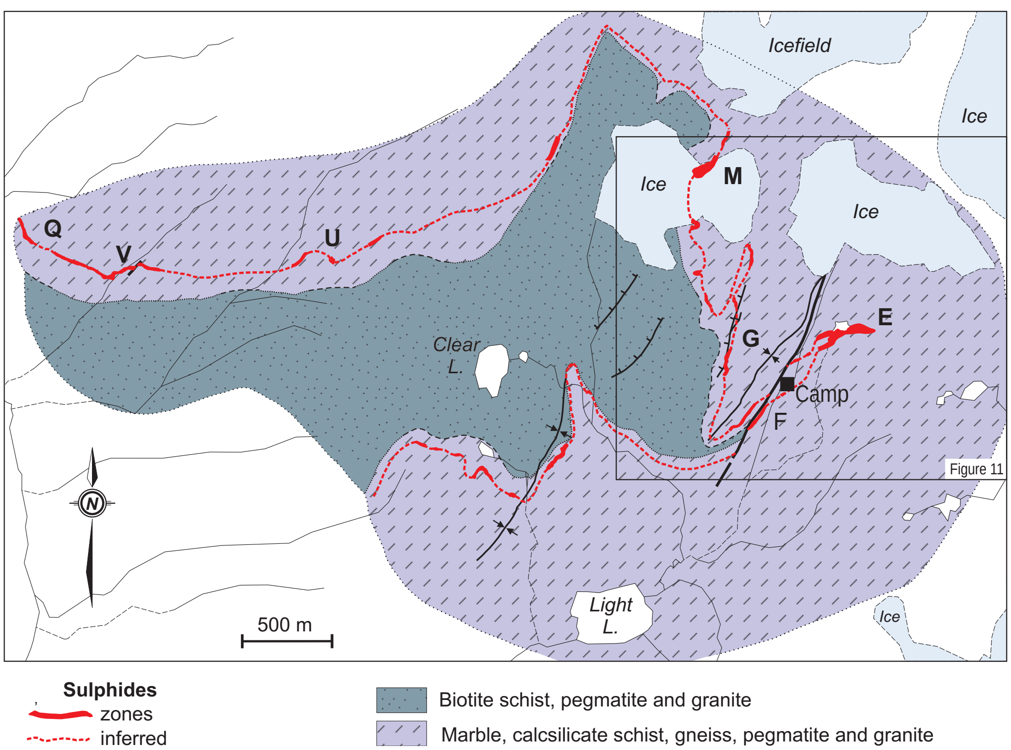

Figure 10. Geology of the Ruddock Creek deposit area (after Fyles, 1970).

cate it is mainly a calcitic marble with Ba and Mn contents typical of sedimentary limestones. Only Sr is anomalously high, but is still within the upper range of marble with a sedimentary protolith.

The upper non-calcareous section is only exposed as remnant brown-weathering biotite schist layers enclosed in pegmatite and granite in the western part of the map area (Figure 11). Fyles (1970) estimated that it may have a total stratigraphic thickness of 300 to 400 metres.

"PEGMATITE" AND "GRANITE"

These rocks include a wide variety of textures and grain sizes, ranging from coarse-grained unfoliated pegmatite, through medium-grained, massive to foliated quartz-feldspar "granite", to aplite and aplitic gneiss. They occur throughout the map area, typically covering more than 50 percent of the outcrop area (Figure 11). As described by Fyles (1970), they can form thick, essentially continuous sheets with only minor remnant metasedimentary layers to thin cross-cutting dykes. Contacts with metasediments are typically sharp whereas contacts between the granitic phases range from sharp to gradational. Most granitic bodies are foliated, although many appear to be massive and discordant. They were emplaced prior to, during and after penetrative deformation.

Structure

The structure of the Ruddock Creek area has been described in considerable detail by Fyles (1970) and Marshall (1978) and is reviewed only briefly here. It is dominated by the E fold, a tight Phase 1(?) synform with a hinge zone exposed at the E showing. The fold plunges 27 degrees towards 285 degrees, with an axial plane that dips 45 degrees to the north (Fyles op. cit.).

Phase 2 folds are recumbent with west-dipping axial surfaces. Their hinge zones range from tight to relatively open. On the slopes just west of the E fault, a Phase 2 synform (the FG synform of Fyles, op. cit.) plunges west and trends to the north-northeast (Figure 11). Layering in its eastern limb, including the F zone, strikes northeast and dips to the northwest, while layering in the west limb strikes more northerly, with a steep west dip. The apparent thickening of the Lower G zone is probably due to structural repetition by minor folds on the west limb of the FG synform.

Faults include north-trending mylonite zones and late northeast-trending faults that commonly form prominent air-photo lineaments. One of these, the E zone fault, has been studied in considerable detail as it offsets the mineralized hinge zone of the E fold. The mylonites are most conspicuous in sulphides in the Lower G zone and the M zone.

Mineralization

The distribution of the Ruddock Creek sulphide layer is shown in Figures 10 and 11. Zones of thickened mineralization, due either to structural complexity or possibly original sedimentary thickening, are also labeled. Between these zones, the sulphide layer is typically not recognized due to extensive granite, or may be marked by slight rusting in granite or a very thin sulphide layers in calcsilicates.

E ZONE

The E zone is well exposed at an elevation of 2230 metres, adjacent to a small lake (Photo 6). It is a thickened and structurally repeated sulphide zone in the hinge of the Phase 1 syncline. Mineralization in both limbs trends westward to the E fault where they are offset approximately 250 metres down to the west, measured in the plane of the fault (Fyles, 1970). The total exposed length of mineralization in the E zone is nearly 300 metres, with a width of 18 metres across strike in the east and 70 metres across the limbs in the west (Mawer, 1976). Drilling has extended the known plunge length of the hinge zone to approximately 200 metres, for a geological reserve of 1.4 million tonnes containing 10 percent Zn + Pb with a Zn to Pb ratio of 5:1 (Mawer, op. cit.).

The zone comprises a number of individual sulphide layers, comprising mainly sphalerite and galena with pyrrhotite. They are separated by rusty-weathering quartzite with disseminated pyrrhotite and sphalerite, thin calcsilicate schist, and thin marble that contains sulphides and thin discontinuous laminations of fluorite (Photo 7). Fyles noted that the zone comprises two structurally repeated and thickened sulphide layers. However, a number of thin sulphide layers, as well as disseminated sulphides, occur throughout the rusty-weathering zone below the main sulphide layers. Marshall (1978) also recognized two additional layers and suggested that the E zone represents an original thicker portion of the Ruddock Creek horizon. He further argued that there appears to be little thickening of individual layers as they are traced around the hinge of the E fold. The conclusion that this zone represents an originally thicker mineralized interval seems to be reasonable in light of the thickness and extent of the alteration here, the number of sulphide layers, and the number of thin mineralized quartzite layers in the immediate underlying stratigraphy.

Mineralization comprises dark sphalerite and less galena, pyrrhotite, minor pyrite and trace chalcopyrite, in a rusty-weathering calcareous quartzite gangue. Gangue minerals include quartz, calcite, fluorite, feldspar, muscovite, brown mica, and minor amphiboles, pyroxene (diopside?) and barite.

Analyses of selected hand sample of the E zone are given in Table 3. Analyses of the mineralized quartzite layers in the section below the sulphide zone are also given in Tables 2 and 3. As described above, one of these layers has slightly elevated manganese content (compared to sedimentary quartzites) and sample RC-56 (Table 3) has elevated Pb, Zn, Mn, Ba and W suggesting that these may be exhalite horizons.

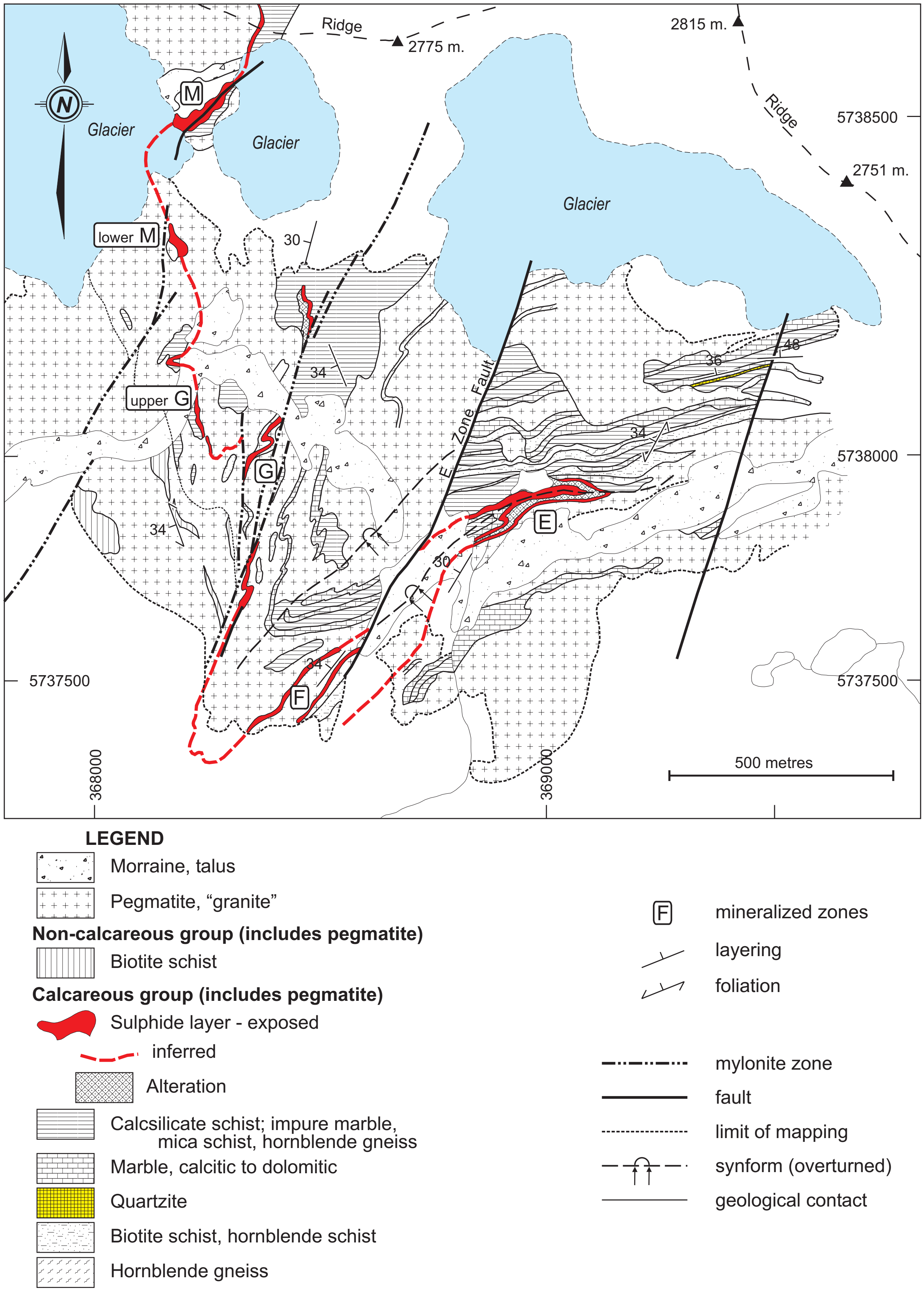

Figure 11. Detailed geology of the eastern part of the Ruddock Creek deposit area. UTM Nad 83 grid.

Photo 6. View to the southeast of the E zone in the core of the E zone syncline. The syncline closes to the east (left). Note abundant pegmatite in foreground.

F ZONE

The F zone is exposed as a number of sulphide lenses located southwest of the camp (Figure 11). One of these lenses (RC-11) is enclosed by pegmatite and has a pegmatite lens within it. The sulphide lens is exposed for 20 metres along a cliff face and is up to 2 metres thick. It comprises massive, fine-grained sphalerite, pyrrhotite and galena with minor to abundant clear quartz, feldspar and pyroxene? grains. Towards the margins of the lens, quartz content increases until it comprises a mineralized quartzite with dispersed sulphides.

RC-12 is a sulphide pod approximately 10 metres in length and 3 metres thick. It varies from massive pyrrhotite, sphalerite and galena with a quartz gangue to quartzite with disseminated sulphides.

RC-13 is a thin sulphide exposure, comprising mainly massive pyrrhotite with sphalerite and galena, on strike southwest of RC-11. It is immediately underlain by streaked, fine-grained quartzite with disseminated sulphides. The sulphide and siliceous envelope are within diopside-plagioclase calcsilicates. The analyzed sample (Table 3) is a quartz-diopside rock containing pyrrhotite, sphalerite and galena.

RC-14 is exposed at the top of a high steep cliff farther to the southwest. The massive sulphide layer (RC-14b; Table 3) is approximately one metre thick, and contains numerous small rounded quartz grains. Quartzite in its immediate footwall (RC-14a) and hangingwall (RC-14c) contains disseminated pyrrhotite, sphalerite and galena, pyroxene? and rare garnet and calcsilicate minerals. The sulphide zone is underlain by a thin impure marble layer that grades upward to calcsilicate just beneath the footwall quartzite, then granular biotite-quartz-feldspar gneiss, and finally calcsilicate gneiss.

G ZONE

The G zone includes a number of discrete sulphide zones on the inverted western limb of the FG synform.

Photo 7. Fluorite layers in calcite marble in footwall rocks at the E zone.

Shearing, probably related to east-directed thrusting, has both attenuated sulphide layers of the G zone and repeated them farther northwest as the upper G zone. The mineralized layers are exposed discontinuously along a strike length of approximately 400 metres. Although relatively thin or poorly exposed at surface, drilling (DDH ED-4) intersected a true thickness of 16 metres at the upper G zone containing 6.12 percent Zn and 0.79 percent Pb (Mawer, 1976). This interval included barren pegmatite as well as a number of higher grade sulphide layers. Eight X-ray holes drilled in 1977 also intersected mineralization, with the one 2-metre interval in DDH UG 77-4 containing 1.79 % Pb and 11.08 % Zn within a zone 28 metres thick that contained 0.32 % Pb and 2.28 % Zn (Nichols, 1978). The lower G was also tested by six X-ray drill holes with one intersection of 5 metres grading 2.59 % Pb and 11.91 % Zn (Nichols, op. cit.).

The lower G zone (Figure 11) comprises a contorted massive sulphide layer that is intermixed with remnants of impure marble and calcsilicate gneiss layers. It is stratigraphically underlain by impure tan to white calcite (with minor fluorite) marble and calcsilicate and overlain by quartzite with disseminated sulphides and rare emerald green gahnite? grains. Open to relatively tight macroscopic folds, with similar vergence as the FG synform, repeat the sulphide layer. North-striking mylonites cut both sulphides and host rocks. Analyses of a number of selected hand samples of the lower G zone (RC-17, RC-18 and RC-23) are given in Table 3. They are similar to those of the E and F zones, with high Zn and Pb values and low silver content.

The upper G zone is exposed on both sides of a moraine northwest of the lower G zone. A small exposure (partially snow covered) just south of the moraine comprises a 1-metre thick, medium-grained black, sphalerite-pyrrhotite-galena layer with quartz and minor calcite and garnet gangue. It is underlain by dark quartz that contains disseminated sulphides and garnet, and locally overlain by massive coarse-grained garnet-pyroxene skarn that contains variable quartz and sulphides. Analyses of a sample of the sulphide layer (RC-43a) is shown in Table 3. High manganese content of the garnet-rich skarn (RC-43b) indicates that the garnet is mainly spessartine. The high zinc content of the quartzite in the footwall (RC-43c) suggests that it is an alteration assemblage.

M ZONE

The M zone comprises a number of exposures, largely enclosed by glacier ice, at elevations ranging from 2450 metres to 2675 metres. The largest of these (RC-26; Figure 11) includes several sulphide layers that are structurally repeated by tight, west-plunging recumbent folds. The lower exposure of the M zone is 260 metres downslope to the south from the main showing, and the highest exposure is located on the ridge to the north of the main showing.

Sulphide layers at the main M showing comprise mainly sphalerite, pyrrhotite and galena with quartz and minor calcite and fluorite gangue. Sulphides (sample RC-26b, Table 3) are generally massive with clear quartz eyes, but also are locally layered or mylonitized. They are within a siliceous, tan-weathering calcite marble that contains streaks of fluorite, minor barite and occasional to relatively abundant sulphides (RC-26a, 26d). In some places, a siliceous, quartz-sulphide envelope (RC-26e) surrounds the sulphide layers, or occurs below them. The sulphide layers and host rocks are stacked due to a series of recumbent Phase 2? folds with rounded hinge zones that plunge at variable angles to the west and northwest. These folds are broadly warped by south plunging Phase 3 folds.

The lower M zone was only partially exposed within glacier ice and snow. The exposed sulphide layer has a thickness of 2 metres; it comprises mainly pyrrhotite and sphalerite and minor galena with a quartz-rich gangue (sample RC-47a). It is structurally underlain by “pegmatite” and overlain by a very silicified zone comprising mixed quartzites, calcsilicates and marbles.

The quartzite, commonly in contact with the sulphide layer, ranges from pure to containing variable amounts of garnet and diopside and randomly dispersed grains of gahnite(?) or sulphides. It is overlain by a pale green to tan siliceous calcsilicate or skarn assemblage, comprising mainly diopside, quartz, minor garnet and some dispersed sulphides. Lenses of swirled sphalerite, galena, quartz and calcite, but virtually no iron sulphide, occur within the calcsilicate zone. One of these lenses (RC-47b) contains the highest silver content (18.5 g/tonne) of any sample analyzed from the Ruddock Creek area. Other lenses in the calcsilicate unit include quartz-garnet, quartz-garnet + diopside and quartz - pyrrhotite units. Farther removed from the massive sulphides, the calcsilicate zone is less quartz rich, comprising mainly diopside or garnet, or a diopside - garnet ± quartz assemblage. This alteration zonation appears to reflect decreasing silica and increasing manganese with distance above the sulphide layer.

DISCUSSION

Ruddock Creek comprises a number of sulphide layers within a thin (less than 20 metre thick) stratigraphic package. These can be traced or extrapolated through a strike length of approximately 13 kilometres. Locally, they are structurally repeated or thickened by folding and possibly thrust faulting. The E zone may be structurally thickened, but it is also possible that it comprises an originally thicker sedimentary succession that localized the tight E syncline.

The sulphide layers are commonly enclosed, overlain or underlain by a zone of intense silicification, now occurring as a quartzite with variable garnet, sulphide and calcsilicate mineral content. This zone typically grades outward to a magnesium-rich calcsilicate zone or manganiferous garnet “skarn” assemblage. Dispersed sulphides, commonly with higher lead/zinc ratios occur in the alteration envelope.

A number of thin quartzite layers in the underlying succession are interpreted to be exhalite units. They may contain disseminated sulphides, mainly pyrrhotite and minor sphalerite, garnet, and rarely gahnite.

It is difficult to correlate the Ruddock Creek stratigraphy with that at Cottonbelt and Jordan River as there are no distinctive marker units other than the sulphide layer itself; carbonatites were not clearly identified at Ruddock Creek, although a tan-weathering marble in the underlying stratigraphy superficially resembles the Mount Grace carbonatite. Despite this, it is possible that Ruddock Creek is in the same package as other stratabound sulphide occurrences as most appear to be at a similar stratigraphic level. As well, the broad subdivision between a lower calcareous and an upper noncalcareous section is common to all occurrences. This, however, may simply reflect a similar change in depositional environment at all occurrences, from more shallow to deeper water environments that reflects extensional tectonics and basin deepening.

Ruddock Creek has some features diagnostic of Broken Hill-type deposits. The relatively high base metal/iron sulphide ratio, high fluorine and the calcareous host typify BHT deposits. As well, the pronounced quartz and spessartine alteration envelope around sulphide layers is characteristic of these deposits. Finally, the numerous sulphide-quartzite layers in the footwall stratigraphy, and occasional gahnite-quartzite and garnet-quartzite layers, are similar to the exhalite horizons around BHT deposits.

SUMMARY

A number of stratabound zinc-lead-silver deposits occur in highly metamorphosed and deformed metasedimentary rocks in the Monashee Mountains in southeastern British Columbia. Some of these, including Big Ledge and Kingfisher south of Revelstoke and Jordan River, Cottonbelt and Ruddock Creek to the north, have been fairly extensively explored, but none have had any production. The deposits are thin layers of massive to semi-massive sulphides that have strike lengths of several kilometers and widths of generally less than a few meters. They are intensively deformed and metamorphosed and locally invaded by extensive zones of pegmatite and granite.

The deposits are within the Monashee Complex, a succession of mainly platformal rocks, referred to as the cover sequence, that unconformably overlies crystalline basement of the core complex. The core complexes are exposed in two structural culminations, the Frenchman Cap dome in the north and Thor-Odin in the south. The age of the core complex is reasonably well constrained by Paleoproterozoic granitic orthogneisses that range in age from ca. 1.87 to 2.27 Ga.

The age of the cover sequence, particularly that part of the succession hosting the sulphide layers, is not as well known. Estimates based mainly on lithologic correlations with Kootenay terrane and North American rocks to the east have ranged from Mesoproterozoic to Paleozoic. Recent dating of detrital zircons and intrusions, however, indicate that deposition of the basal part of the cover sequence occurred between ca. 1.95 and 1.85 Ga (Crowley, 1997). The sulphide layers occur only a few hundred meters above this basal part of the sequence. A maximum age for rocks considerably higher in the succession, above the sulfide layers, is provided by 1.2 Ga detrital zircons, and a minimum age by a 541 Ma magmatic amphibolite. These ages are compatible with a Cambrian Pb-Pb galena date on Cottonbelt. However, if the sulphide layers are Cambrian, then the thin interval separating them from the basal part of the sequence requires a major unconformity, recording a hiatus of ca. 1.3 billion years. As this unconformity is not recognized in the field, either by omission of units or distinctive lithologies, the suggestion that the sulphide layers themselves are Paleoproterozoic must be considered. This requires reevaluation of the lead isotopic systematics of Cottonbelt.

A number of features of some of the deposits, and of the host successions, are typical of a class of deposits referred to as the Broken Hill-type. These include skarn-like mineralogy, a result of a calcareous gangue, locally high Mn content, and the abundance of magnetite (at Cottonbelt) rather than iron sulphide phases more common in typical sedex deposits. Immediate host rocks may contain fluorite and have abundant garnet and sillimanite, similar to Broken Hill host rocks. As well, thin quartzite, garnet-quartzite and sulphide-quartzite layers are similar to some of the exhalite facies that characterize Broken Hill stratigraphy, as is the local occurrence of gahnite in some of these layers.

ACKNOWLEDGEMENTS

I would like to thank Fil Ferri and Nick Massey for their constructive review of this paper. Discussions with Jim Fyles, Peter Lewis and Paul Gray helped in understanding the geology of the Ruddock Creek area and G. Derrick, the Broken Hill deposit. Mike Fournier is thanked for drafting the diagrams and Ray Lett, for expediting samples for geochemical analyses, and J. Holland for layout and formatting. Finally, I would like to thank Gloria DeFields and Lorraine Höy for their support and help in the field.

REFERENCES

Armstrong, R.L., Parrish, R.R., van der Heyden, P., Scott, K., Runkle, D. and Brown, R.L. (1991): Early Proterozoic basement exposures in the southern Canadian Cordillera: core gneiss of Frenchman Cap, Unit 1 of the Grand Forks Gneiss, and Vaseaux Formation; *Canadian Journal of Earth Sciences*, volume 28, pages 1169-1201.

Brown, R.L., Journeay, J.M., Lane, L.S., Murphy, D.C. and Rees, C.J. (1986): Obduction, backfolding and piggyback thrusting in the metamorphic hinterland of the southeastern Canadian Cordillera; *Journal of Structural Geology,* volume 8, pages 225-268.

Crowley, J.L. (1997): U-Pb geochronologic constraints on the cover sequence of the Monashee complex, Canadian Cordillera: Paleoproterozoic deposition on basement; *Canadian Journal of Earth Sciences*, volume 34, pages 1008-1022.

Crowley, J. and Schaubs, P.M. (1994): Field evidence for early Proterozoic tectonism in core gneisses of Frenchman Cap dome, southern Canadian Cordillera; *in* Current Research, 1994-A, *Geological Survey of Canada*, Paper 94-1A, pages 131-141.

Duncan, I.J. (1984): Structural evolution of the Thor-Odin gneiss dome; *Tectonophysics*, volume 101, pages 87-130.

Fyles, J.T. (1970): The Jordan River area near Revelstoke, British Columbia; *B.C. Department of Mines and Petroleum Resources*, Bulletin 57, 64 pages.

Gibson, G. (1996): Geological, geophysical and drilling report on the Cottonbelt property, Kamloops Mining Division; *B.C. Ministry of Energy and Mines*, Assessment report 24367.

Goodfellow, W.D., Lydon, J.W. and Turner, R. (1993): Geology and genesis of stratiform sediment-hosted (SEDEX) zinc-lead-silver sulphide deposits, *in* Kirkham, R.V., Sinclair, W.D., Thorpe, R.I. and Duke, J.M., eds., Minerals Deposit Modeling: *Geological Association of Canada*, Special Paper 40, pages 201-251.

Gustafson, L.B. and Williams, N. (1981): Sediment-hosted stratiform deposits of copper, lead and zinc; *Economic Geology*, 75th Anniversary Volume, pages 139-178.

Hedström, P., Simeonov, A. and Malmstrom, L., (1989): The Zinkgruvan ore deposit, south-central Sweden: A Proterozoic proximal Zn-Pb-Ag deposit in distal volcanic facies; Economic Geology, volume 84, pages 1235-1261.

Holyroyd, R.W. (1999): 1999 Assessment report, Kneb property, reconnaissance ground geophysical surveys (utem/mag), Revelstoke Mining Division; *B.C. Ministry of Energy and Mines,* Assessment report 26090.

Höy, T. (1980): Geology of the Bews Creek area, southwest margin of Frenchman Cap gneiss dome; *B.C. Ministry of Energy, Mines and Petroleum Resources,* Geological Fieldwork 1979, Paper 1980-1, pages 17-22.

Höy, T. (1987): Geology of the Cottonbelt lead-zinc-magnetite layer, carbonatites and alkalic rocks in the Mount Grace area, Frenchman cap dome, southeastern British Columbia; *B.C. Ministry of Energy, Mines and Petroleum Resources*, Bulletin 80, 99 pages.

Höy, T. and Brown, R.L. (1980): Geology of the eastern margin of the Shuswap Complex, Frenchman Cap area; *B.C. Ministry of Energy, Mines and Petroleum Resources*, Preliminary map 43.

Höy, T. and Godwin, C.I. (1988): Significance of a Cambrian date from galena lead-isotope data for the stratiform Cottonbelt deposit in the Monashee Complex, southeastern British Columbia; *Canadian Journal of Earth Sciences*, volume 25, pages 1534-1541.

Höy, T. and Kwong, Y.T.J. (1986): The Mount Grace carbonatite - an Nb and light rare earth element enriched marble of probable pyroclastic origin in the Shuswap Complex, southeastern British Columbia; *Economic Geology,* volume 81, pages 1374-1386.

Höy, T. and McMillan, W.J. (1979): Geology in the vicinity of Frenchman Cap dome; *B.C. Ministry of Energy, Mines and Petroleum Resources,* Geological Fieldwork 1978; Paper 1979-1, pages 25-30.

Höy, T. and Pell, J. (1986): Carbonatites and associated alkalic rocks, Perry River and Mount Grace areas, southeastern British Columbia; *B.C. Ministry of Energy, Mines and Petroleum Resources*, Geological Fieldwork 1985, Paper 1986-1, pages 69-87.

Journeay, J.M. (1986): Stratigraphy, internal strain, and thermo-tectonic evolution of northern Frenchman cap dome, an exhumed basement duplex structure, Omineca hinterland, southeastern Canadian Cordillera; Ph.D. thesis, Queens University, Kingston, Ontario.

Laird, J.W. (1997): Assessment report on the Riley mineral claims, Revelstoke Mining Division; *B.C. Ministry of Energy and Mines*, Assessment report 25173, 13 pages.

McDonough, M.R. and Parrish, R.R. (1991): Proterozoic gneisses of the Malton Complex, near Valemont, British Columbia: U-Pb ages and Nd isotopic signatures; *Canadian Journal of Earth Sciences*. volume 28, pages 1202-1216.

MacGillivray, R.G. and Laird, J. (1990): A geological report on the Jordan River deposit, Revelstoke Mining Division, British Columbia; *B.C. Ministry of Energy and Mines,* Assessment report 20513.

McMillan, W.J. (1973): Petrology and structure of the west flank, Frenchman's Cap dome, near Revelstoke, British Columbia; *Geological Survey of Canada*, Paper 71-29.

McMillan, W.J. and Moore, J.M. (1974): Gneissic alkalic rocks and carbonatites in Frenchman's Cap gneiss dome, Shuswap Complex, British Columbia; *Canadian Journal of Earth Sciences*, Paper 71-29, 87 pages.

Marshall, B. (1978): Structural investigations of the Ruddock Creek property; unpublished internal Cominco report, 18 pages.

Mawer, A.B. (1976): Geological report, Ruddock Creek property (It, In claims), Revelstoke area, southern B.C.; unpublished internal Cominco report, 8 pages.

Nichols, R.F. (1978): Ruddock Creek; 1977 termination report; unpublished internal Cominco report, 14 pages.

Okulitch, A.V., Loveridge, W.D. and Sullivan, R.W. (1981): Preliminary radiometric analyses of zircons from the Mount Copeland syenite gneiss, Shuswap Metamorphic Complex, British Columbia; in Current Research, Part A; *Geological Survey of Canada*, Paper 81-1A, pages 33-36.

Page, R.W. and Laing, W.P. (1992): Felsic metavolcanic rocks related to the Broken Hill Pb-Zn-Ag orebody, Australia; *Economic Geology*, volume 87, pages 2138-2168.

Page, R.W., Stevens, B.P.J. and Gibson, G.M. (2000): New Shrimp zircon results from Broken Hill: towards robust stratigraphic and event timing; abstract *in* Geological Society of Australia, *15th Australia Geological Convention*, Sidney, Australia.

Parkinson, D. (1991): Age and isotopic character of Early Proterozoic basement gneisses in the southern Monashee complex, southeastern British Columbia; *Canadian Journal of Earth Sciences*, volume 28, pages 1159-1168.

Parr, J.M. (1994): The geology of the Broken Hill-type Pinnacles Pb-Zn-Ag deposit, Western New South Wales, Australia; *Economic Geology*, volume 89, pages 778-790.

Parr and Plimer (1993): Models for Broken Hill-type lead-zinc-silver deposits, in Kirkham, R.V., Sinclair, W.D., Thorpe, R.I. and Duke, J.M., eds., Mineral Deposit Modeling; *Geological Association of Canada*, Special Paper 40, pages 253-288.

Parrish, R.R. (1995): Thermal evolution of the southeastern Canadian Cordillera; *Canadian Journal of Earth Sciences*, volume 32, pages 1618-1642.

Parrish, R.R. and Scammel, R.J. (1988): The age of the Mount Copeland syenite gneiss and its metamorphic zircons, Monashee Complex; in Radiogenic Age and Isotopic Studies, Part 2; *Geological Survey of Canada*, Paper 88-2; pages 21-28.

Plimer, I.R., (1986): Sediment-hosted exhalative Pb-Zn deposits - Products of contrasting ensialic rifting; *Geological Society of South Africa*, Transactions, volume 89, pages 57-73.

Read, P.B. (1980): Stratigraphy and structure: Thor-Odin to Frenchman cap "domes", Vernon east-half map area, southern British Columbia; *in* Current Research, part A; *Geological Survey of Canada*, Paper 80-1A, pages 19-25.

Read, P.B. and Brown, R.L. (1981): Columbia River fault zone: southeastern margin of the Shuswap and Monashee complexes, southern British Columbia; *Canadian Journal of Earth Sciences*, volume 18, pages 1127-1145.

Reesor, J.E. and Moore, J.M. (1971): Petrology and structure of Thor-Odin gneiss dome, Shuswap metamorphic complex; *Geological Survey of Canada*, Bulletin 195.

Riley, C. (1961): The River Jordan lead-zinc deposit, Revelstoke Mining Division, B.C.; *Canadian Institute of Mining and Metallurgy*, Transactions, volume 64, pages 268-272.

Ross, G.M. and Parrish, R.R. (1991): Detrital zircon geochronology of metasedimentary rocks in the southern Omineca Belt, Canadian Cordillera; *Canadian Journal of Earth Sciences*, volume 28, pages 1254-1270.

Rozendal, A., (1986): The Gamsberg zinc deposit, Namaqualand district, in Anhaeusser, C. R. and Maske, S., eds., Mineral Deposits of Southern Africa; *Geological Society of South Africa*, pages 1477-1488.

Ryan, P.J., Lawrence, A.L., Lipson, R.D., Moore, J.M., Paterson, A., Stedman, D.P. and Van Zyl, D. (1986): The Aggeneys base metal sulphide deposits, Namaqualand district, *in* Anhaeusser, C.R. and Maske, S., eds., Mineral Deposits of

Southern Africa; *Geological Society of South Africa,* pages 1447-1473.

Sangster, D.F. (1990): Mississippi Valley-type and SEDEX lead-zinc deposits; *Institute of Mining and Metallurgy*, Transactions, volume 99, pages B21-B42.

Scammel, R.J. and Brown, R.L. (1990): Cover gneisses of the Monashee Terrane: a record of synsedimentary rifting in the North American Cordillera; *Canadian Journal of Earth Sciences,* volume 27, pages 712-726.

Spry, P.G. and Wonder, J.D. (1989): Manganese-rich garnet rocks associated with the Broken Hill lead-zinc-silver deposit, New South Wales, Australia; *The Canadian Mineralogist*, volume 27, pages 275-292.

Stevens, B.P.J., Barnes, R.G., Brown, R.E., Stroud, W.J. and Willis, I.L. (1988): The Willyama Supergroup in the Broken Hill and Euriowie blocks, New South Wales; *Precambrian Research*, volume 40/41, pages 297-327.

Walters, S. (1995): Broken Hill-type Pb-Zn-Ag deposits - geological characteristics and exploration models; Mineral Deposit Research Unit, T*he University of British Columbia*, Short course #19, Metallogeny of Proterozoic Basins, 56 pages

Wheeler, J.O. (1965): Big Bend map-area, British Columbia (82N east half); *Geological Survey of Canada*, Paper 64-32.

Willis, I.L., Brown, R.E., Stroud, W.J. and Stevens, B.P.J. (1983): The Early Proterozoic Willyama Supergroup: Stratigraphic subdivision and interpretation of high to low-grade metamorphic rocks in the Broken Hill Block, New South Wales; *Journal of the Geological Society of Australia*, volume 30, pages 195-224.

Soft Sediment Carbonate Vein Networks in the Belt Purcell Rocks of Southeastern BC: A New Mode of Formation

Dan Marshall[1] and C.D. Anglin[2]

KEYWORDS: Belt Purcell, Molar-Tooth Structures, Paleo-atmospheric CO_2, Gas-hydrates, Clathrates, Sub-marine seismic activity.

INTRODUCTION

The Belt Purcell Supergroup rocks extend from the Western United States into Southern British Columbia and Alberta. Soft sediment carbonate vein networks occur within various formations of the Belt Purcell rocks. These vein networks outcrop in various localities, however, this paper is limited to a description of the outcrops of the Kitchener Formation, west of Moyie Lake (Figure 1) in Southeastern British Columbia. These vein networks in the Purcell Range have been named Molar Tooth Structures (MTS) by Smith (1968) and that terminology is adopted here. This paper presents a hypothesis that the formation of MTS is the result of clathrate (gas-hydrate) destabilization. As gas hydrates destabilize, often explosively, they release considerable quantities of CO_2 gas and may also release abundant seismic energy. This model does not preclude the formation of MTS in a clathrate-poor environment, but proposes a geological environment that is consistent with both the gas bubble and seismic models of MTS formation. This model is also consistent with postulated Proterozoic atmospheric compositions and the observed absence of MTS in the Phanerozoic.

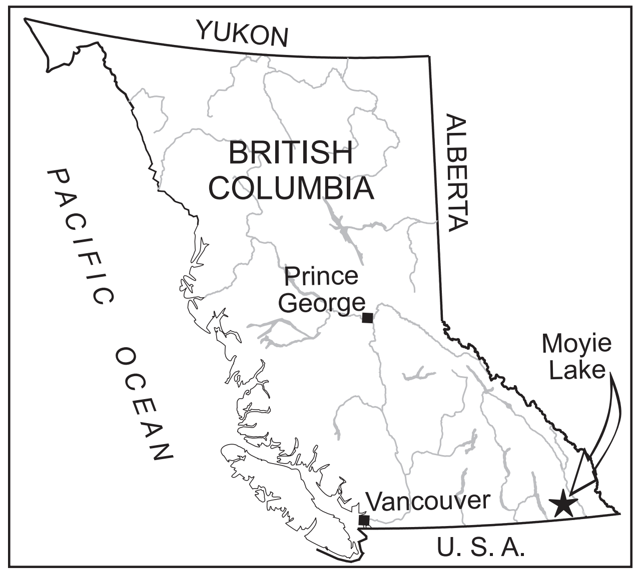

Figure 1. Index map showing the location of the MTS structures at Moyie Lake.

DESCRIPTION

At Moyie Lake, the MTS are best observed on the weathered surface, where they tend to weather recessively relative to the host carbonates. The MTS develop a whitish-grey weathered surface that contrasts with the tan coloured weathering of the host rocks (Photo 1). Both the MTS and the host carbonates have a similar medium grey colour on fresh surfaces. The dominant fill in the MTS are carbonates, which are generally authigenic and rarely clastic in origin (James *et al*., 1998). Authigenic pyrite and feldspar are found as accessory minerals within the MTS, attesting to fluid flow along these structures after initial infill by carbonate. Generally, the MTS are stratabound thin sinuous and/or linear vein-like structures occurring perpendicular to bedding, ranging up to a few centimetres in width which tend to pinch and swell. The MTS often appear to be folded, however, upon closer inspection, these fold-like structures are the result of syn-sedimentary deformation or a reflection of the complicated geometry of these interconnected MTS networks, or both (Photo 1).

FORMATION OF MOLAR TOOTH STRUCTURES

The origin of carbonate MTS has long been an enigma in the geological community. These interconnected networks of carbonate veins are hosted within platformal Proterozoic carbonate rocks. Detailed studies by a number of workers have proposed two modes of formation for MTS. Some studies (Furniss *et al*., 1998; Frank and Lyons, 1998) have shown that gas bubble expansion is a viable explanation for the formation of these

[1]*Simon Fraser University*

[2]*Geological Survey of Canada, Contribution #2000198*

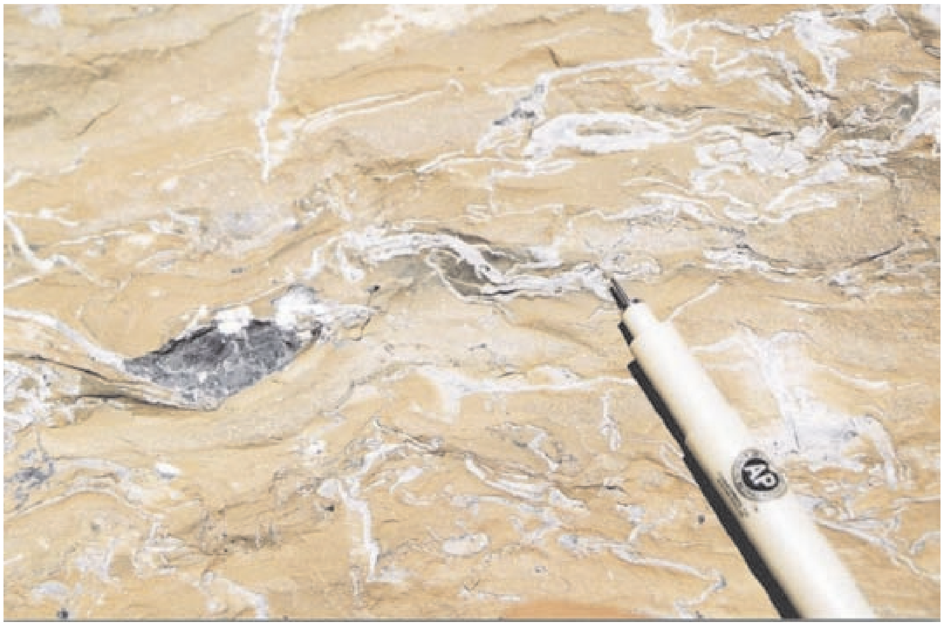

Photo 1. Molar Tooth Structure from the Belt Purcell Proterozoic carbonates at Moyie Lake, BC. The MTS is greyish-white on the weathered surface and a medium grey colour on the fresh surface (middle left of photo). The host carbonates weather a buff-tan colour. The tip of the pen points to an authogenic pyrite grain within the MTS.

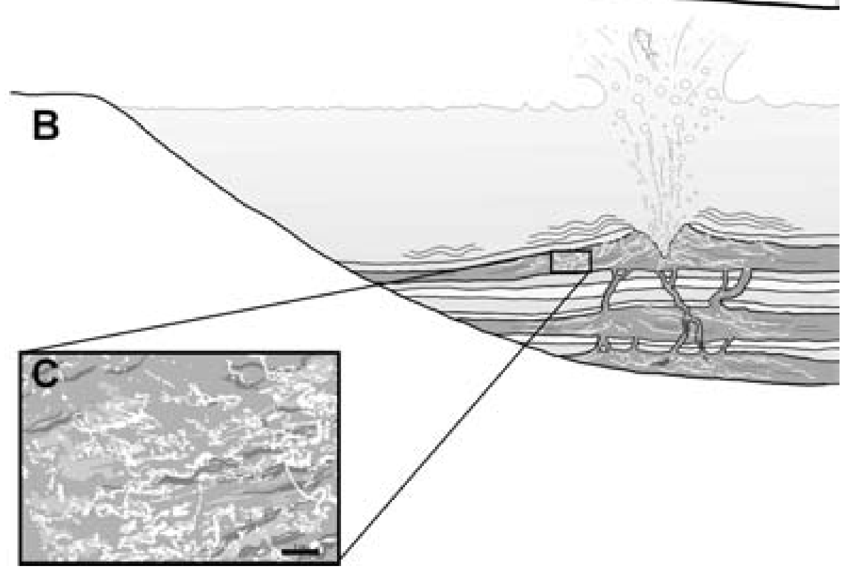

Figure 2. An idealized model of molar tooth formation via clathrate destabilization. A: a typical continental slope environment where clathrates can accumulate as part of the sedimentary column. B: destabilization of the clathrates leading to explosive conditions with volatile charged water and sediment columns in regions of abundant clathrate with more typical MTS found in the sediments with lesser clathrate concentrations. C: Idealized trace of MTS from outcrop similar to Photo 1. Actual MTS shown in white, bedding and structure within the Belt-Purcell carbonate are shown with greys.

structures, whereas other research (James *et al*., 1998; Pratt, 1998) on MTS worldwide has shown that MTS are limited to ramp and shallow platformal environments and formed during some sort of "seismic basinal event" accompanied, to varying degrees, by liquifaction and dewatering. In addition these studies have noted that MTS are limited in geologic time and occur exclusively in Proterozoic and older rocks.

Two major questions emerge from previous research: 1) is there a single geological environment that can readily produce the necessary conditions for both postulated modes of MTS formation, and 2) is there a reason why this geological environment existed during the Proterozoic and not since that time. This paper attempts to answer these questions by proposing that the MTS observed in Proterozoic platformal carbonate rocks are the result of the destabilzation of CO_2-clathrate contained within the platformal sediments and atmospheric changes from the Proterozoic to the Phanerozoic were less favourable to CO_2-clathrate stability.

Clathrates are solid solutions of H_2O and common gases, generally CO_2, CH_4, N_2, C_2H_6, O_2 Ar, NH_3 and H_2S (Bakker, 1998). There are two lattice forms of clathrate in which an expanded ice lattice traps gases in cage-like structures. One lattice type contains 46 H_2O molecules while the other has 136. These structures contain 8 and 24 gas cages respectively. Hydrates occur in many places on the Earth's surface, predominantly on the continental slopes, polar ice caps and permafrost areas. Their pressure-temperature stability fields vary depending upon composition, with the CH_4 and CO_2 clathrates being stable at the temperatures and pressures found on the continental slopes (Lerche and Bagirov, 1998; Booth *et al*., 1998). These clathrates occur as finely disseminated grains in sediment, nodules, thin layers and blocks. CO_2 clathrates have a more limited stability field than methane clathrates with destabilization occurring above 10 and 31°C respectively.

During the Proterozoic, Earth experienced its greatest change in atmospheric chemistry. The early Proterozoic atmosphere is thought to have contained predominantly CO_2, CO, H_2O and N_2 (Abelson, 1966) or possibly was a CH_4 dominant atmosphere (Oparin, 1953), whereas by the Cambrian Period, atmospheric compositions more closely resembled those found today (Kasting, 1993). Proterozoic atmospheric CO_2 concentrations were approximately 3 orders of magnitude higher than today (Kasting, 1993). This increased CO2 fugacity in the atmosphere would have resulted in increased CO_2 activity in the oceans as well.

In a simple system, in which two CO_2 bearing solids (clathrates and carbonates) compete for CO_2 in seawater, the precipitation of carbonate is represented by the reaction

$$Ca^{+2} + 2CO_3^{-2} \Leftrightarrow CaCO_3$$

This reaction is dependent upon pH as the production of the bicarbonate ion is related to the dissociation of carbonic acid (H_2CO_3),

$$H_2CO_3 \Leftrightarrow HCO_3\text{-} + H^+ \text{ and } HCO_3\text{-} \Leftrightarrow CO3^{-2} + H^+$$

with carbonic acid produced via the reaction

$$CO_2 + H_2O \Leftrightarrow H_2CO_3$$

The increased CO_2 content of the early atmosphere would have resulted in locally increased carbonic acid concentrations (and activities) near the atmosphere-seawater interface relative to today's conditions. This decreased pH (increased acidity) would lower the stability of calcite.

The formation of the CO_2 hydrate ($CO_2.5.75H_2O$) is not pH dependent and is based solely upon the availability of H_2O and CO_2, temperatures of less than 10°C, and pressures easily obtained below tens of metres of water or sediment. These pressure-temperature conditions are consistent with the James *et al*. (1998) depositional environment for MTS at or above storm wave-base. Thus it is conceivable that Proterozoic atmospheric conditions may have favoured the precipitation of clathrate as well as calcite.

The destabilization of clathrate is accompanied by a large volume increase and a corresponding energy release. Explosive destabilization of clathrate has been envoked to explain a large number of phenomena occurring on continental slopes, including: mud volcanoes; the disappearance of ships and aircraft in the Bermuda triangle; 350 meter diameter conical pockmarks on continental slopes, giant submarine landslides (USDOE, 1998), tsunamis (Discover, 2000) and "mistpouffers" which are distant explosion like sounds sporadically heard along the continental slopes of Europe and Atlantic Canada (USDOE, 1998).

A column of sediment with finely disseminated grains of clathrate could provide the necessary gas bubbles to form the MTS via the gas bubble formation model (Furniss *et al*, 1998). Sedimentary columns with larger amounts of destabilized clathrate would produce sufficient seismic energy to produce MTS (Figure 2) via the seismic MTS model (James *et al*., 1998; Pratt, 1998). Additionally, the presence of abundant CO_2 gas from clathrate destabilization could react with Ca and Mg in seawater to quickly form the carbonate infills commonly observed in MTS. This relatively rapid precipitation of calcite within the veins and the outflow of gas from the destabilized clathrate would inhibit clastic material from entering any of the cracks open to the sediment water interface and is consistent with the lack of clastic material within MTS. The limited appearance of MTS in the geological record (Figure 3) is also consistent with a clathrate destabilization model, as CO_2 was more abundant in the Earth's atmosphere up until the end of the Proterozoic.

The apparent peak in MTS formation near the end of the Proterozoic may be due to favourable CO_2 clathrate stability conditions associated with the specific CO_2/O_2 atmospheric ratio, the reduced development of continental slopes associated with supercontinent formation during the early Archean, or may be a function of younger rocks being preferentially preserved relative to older rocks.

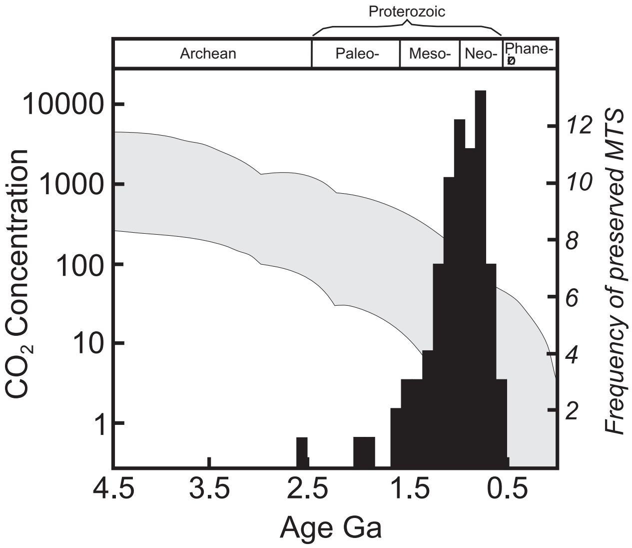

Figure 3. Histogram showing the frequency MTS occurrence (James *et al.,* 1998) vs. age (black) overlaying a plot of atmospheric CO_2 concentration (Kasting 1993) relative to present day atmosphere.

The clathrate model of MTS formation also offers some insight into the discussion of a CH_4 or CO_2 dominant atmosphere prior to the Cambrian. The clathrate model presented here is consistent with the model for a CO_2 dominant Proterozoic atmosphere, because a CH_4 dominant atmosphere would be more likely to precipitate methane clathrates on the continental slopes similar to modern day clathrate deposits. The abundance of CH_4 and lesser concentration of CO_2 would inhibit the precipitation of calcite and therefore not favour the formation of MTS.

CONCLUSIONS

Two models of Molar Tooth Structures are crack formation by gas bubble expansion and seismic shaking in platformal Proterozoic carbonate successions. This paper presents a model for MTS formation based on clathrate (CO_2-hydrate) destabilization that is consistent with the geological data for MTS and unites the two existing models into one geological environment. This model does not preclude the seismic or gas bubble models for MTS formation. It offers a possible mode of formation for MTS that is consistent with the seismic or gas bubble models, but does not preclude either model of MTS formation in the absence of clathrates. This model is also consistent with a pre-Phanerozoic CO_2 rich atmosphere.

ACKNOWLEDGEMENTS

Trygve Höy and Dave Lefebure from the B.C. Geological Survey Branch are thanked for their introduction to the MTS rocks at Moyie Lake. The enthusiastic help of Danae Voormeij for field assistance and drafting is gratefully acknowledged.

REFERENCES

Furniss, G.J., Rittel, J.F. and Winston, D., 1998, Gas bubble and expansion crack origin of "Molar-Tooth" calcite structures in the middle Proterozoic Belt supergroup, Western Montana; *Journal of Sedimentary Research,* v. 68, pages 104-114.

Frank, T.D and Lyons, T.W., 1998, "Molar-tooth" structures: A geochemical perspective on a Proterozoic enigma; Geology, v. 26, pages 683-686.

Bakker, R.J., 1998, Improvements in clathrate modelling II: the H_2O-CO_2-CH_4-N_2-C_2H_6 fluid system; Geological Society of London, Special Publication. v. 137, pages 75-105.

Booth, J.S., Winters, W.J., Dillon, W.P., Clennell, M.B. and Rowe, M.M., 1998, Gas Hydrate Reservoirs; *Geological Society of London,* Special Publication. v. 137, pages 113-127.

James, N.P., Narbonne, G.M. and Sherman, A.G., 1998, Molar-tooth carbonates: Shallow subtidal facies of the mid- to late Proterozoic; *Journal of Sedimentary Research*, v. 68, no.5, Part A, pages 716-722.

Lerche, I. and Bagirov, E., 1998, Guide to gas hydrate stability in various geological settings; *Marine and Petroleum Geology*, v 15, pages 427-437.

Pratt, B., 1998, Gas bubble and expansion crack origin of molar tooth calcite structures; *Journal of Sedimentary Research*, v. 69, pages 1136-1140.

Abelson, P.H., 1966, Chemical events on the primitive earth; *Proceedings of the National Academy of Sciences of the United States of America*, v. 55; 6, pages 1365-1372.

Oparin, A.I., 1953, The origin of life; *Dover Publications Inc*., New York. 270 pages.

Kasting, J.F., 1993, Earth's early atmosphere; *Science*, v. 259, pages 920-926.

USDOE (United States Department of Environment) Energy Information Administration, 1998, Energy Information Administration, *International Energy Outlook,* Natural Gas 1998: Issues and Trends; Future supply potential of natural gas hydtrates. pages 73-90.

Discover Magazine, 2000, Thar she blows; October issue, page 18.

Smith, A.G. The origin and deformation of some "Molar-Tooth" structures in the Precambrian Belt-Purcell Supergroup; *Journal of Geology*, v. 76, pages 426-443.

Geology of the Gibraltar Copper-Molybdenite Deposit, East-Central British Columbia (93B/9)

By Chris H. Ash [1] and Claudia P. Riveros[2]

KEYWORDS: Gibraltar Mine, Granite Mountain Batholith, copper-molybdenite deposit.

INTRODUCTION

During its 25 years of production from 1972 to 1998, the Gibraltar Cu-Mo mine in east-central British Columbia (Figure 1) milled a total of 324 million tons of ore containing an average 0.351% Cu from four open pits. Fieldwork during 2000 involved just over two weeks of detailed pit mapping at the mine. Results of this work and several earlier intervals of pit mapping conducted in 1998 and 1999 are summarized below. This detailed examination of the deposit followed an evaluation of its regional geological setting in 1998 (Ash *et al*., 1999a, b) which built on early work by Panteleyev (1977 and unpublished data).

This paper documents controls copper and molybdenite mineralization at the Gibraltar mine. Detailed results of recently obtained isotopic ages for magmatism (U-Pb), mineralization (Re-Os), and alteration (Ar-Ar), as well as a detailed analysis of structural data will be presented elsewhere (Ash *et al*., in preparation).

PREVIOUS WORK

Initial published descriptions of the Gibraltar Mine geology and related mineralization (Sutherland Brown, 1966; Eastwood, 1970) occurred during the period of increased exploration preceding mine development. Simpson (1970) described the mineralogical and textural character of host plutonic rocks in the mine area. Publications detailing deposit geology during the active mine life include those of Drummond *et al*, (1973, 1976), Sutherland-Brown (1974) and Bysouth *et al*., (1995). Recently, Raffel (1999) completed a study of element mobility associated with a localized hydrothermally altered shear zone at the Gibraltar and Pollyanna pits.

GEOLOGICAL SETTING

The Gibraltar Cu-Mo deposit is hosted within the Granite Mountain Batholith. This is a Late Triassic (215±0.8 Ma; Ash *et al*., in preparation), medium to very coarse-grained quartz diorite to tonalite intrusion that has been variably deformed, metamorphosed and hydrothermally altered. Primary compositional and textural changes are mappable within the batholith (Figure 2). These are indicated by a progressive increase northward across the batholith in quartz content (15-20% to 35-40%) and grain size (2-3mm up to 1 cm), accompanied by a reduction in the mafic mineral content (35 to 10%) (Figure 2). A late, volumetrically minor leucocratic dike phase with minimal mafic minerals (1-2%) intrudes the batholith in the mine area.

Primary contact relationships of the batholith with surrounding lithologies are poorly constrained. To the east and west it is most likely bordered by faults which juxtapose it with Late Paleozoic oceanic Cache Creek rocks. These rocks consist of disrupted chert argillite deposits that range from broken formation to mélange with blocks or lenses of limestone and mafic basalt. Eight samples of chert from several variants of the chert-argillite unit were processed and evaluated for radiolarians, but were unproductive due thermal recrystallization (Fabrice Cordey, personal communication, 1999). Samples from

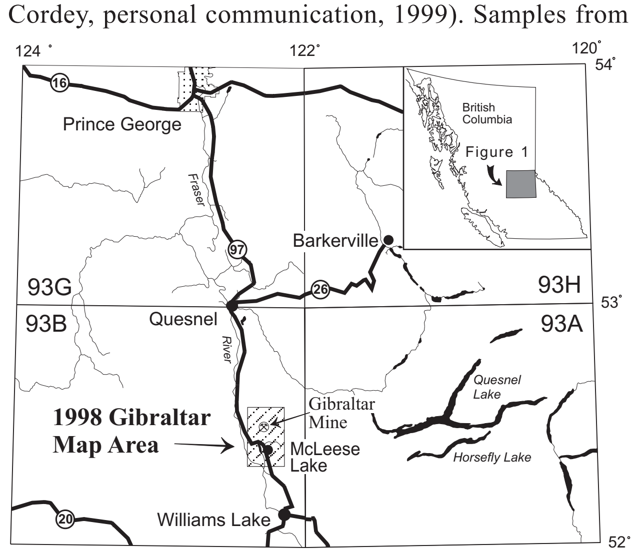

Figure 1. Location of the Gibraltar map area.

[1] *British Columbia Ministry of Energy and Mines*
[2] *Riveros Geological Services*

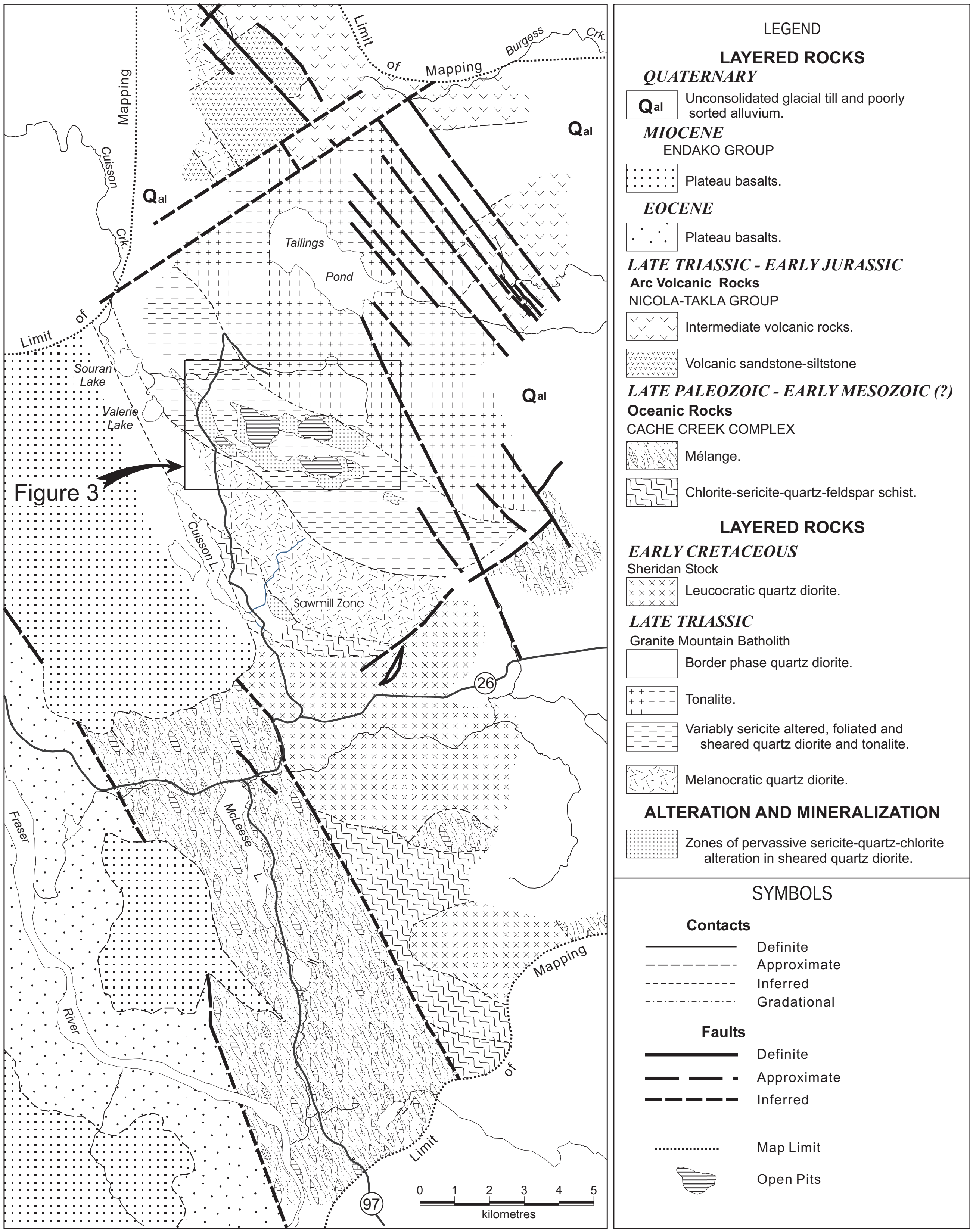

Figure 2. Regional geological setting of the Gibraltar mine (modified after Ash *et al*., 1999).

three limestone blocks in Cache Creek mélange were examined for conodonts but no diagnostic fauna were identified (Orchard, 2000).

The southern margin of the batholith is in part faulted against and in part separated from the Late Cretaceous Sheridan stock along a broad, low-angle, north-dipping shear zone. The Sheridan stock is a 108.1±0.6 Ma (Ash *et al*, in preparation) medium-grained, massive to locally strongly foliated, predominantly leucocratic quartz diorite. The shear zone is dominated by chlorite-rich schists with mylonitic fabrics that are locally well developed. A characteristic feature of this unit is veining from several centimetres up to a metre in thickness, consisting of quartz, chlorite, carbonate or epidote, or some combination of these minerals. Protoliths are interpreted to include both melanocratic phases of the Granite Mountain Batholith and most likely basaltic volcanics from the Cache Creek terrane.

To the north, the pluton is juxtaposed against a variably deformed succession of epiclastic and volcaniclastic rocks (Figure 2). These have been interpreted as Quesnellia, arc-derived clastic rocks and correlated with the latest Early Jurassic Hall Formation (Wheeler and McFeely, 1991). The nature of the contact is unknown.

GIBRALTAR MINE GEOLOGY

The geology of the Gibraltar mine is exposed in four open pits that include Gibraltar West, Gibraltar East, Pollyanna and Granite Lake (Figure 3). These all occur between 900 and 1200 metres elevation (above sea level) on the west-facing slope of Granite Mountain and extend from 100 to 300 metres below the surface, the deepest being Gibraltar East.

Pit mapping, conducted at 1:2000 scale was limited by an inability to safely access the majority of the pit walls. Mapping focused mainly on the western and northwest wall of the Gibraltar East pit where the haulage road provided access to a large vertical and lateral section. Conveniently, it is oriented at a high angle to the dominant northwest-trending structural fabric and is also centered on a section of high-grade Cu ore. Mapping was also conducted in lesser detail throughout safely accessible areas of the Pollyanna and Gibraltar West pits. The Granite

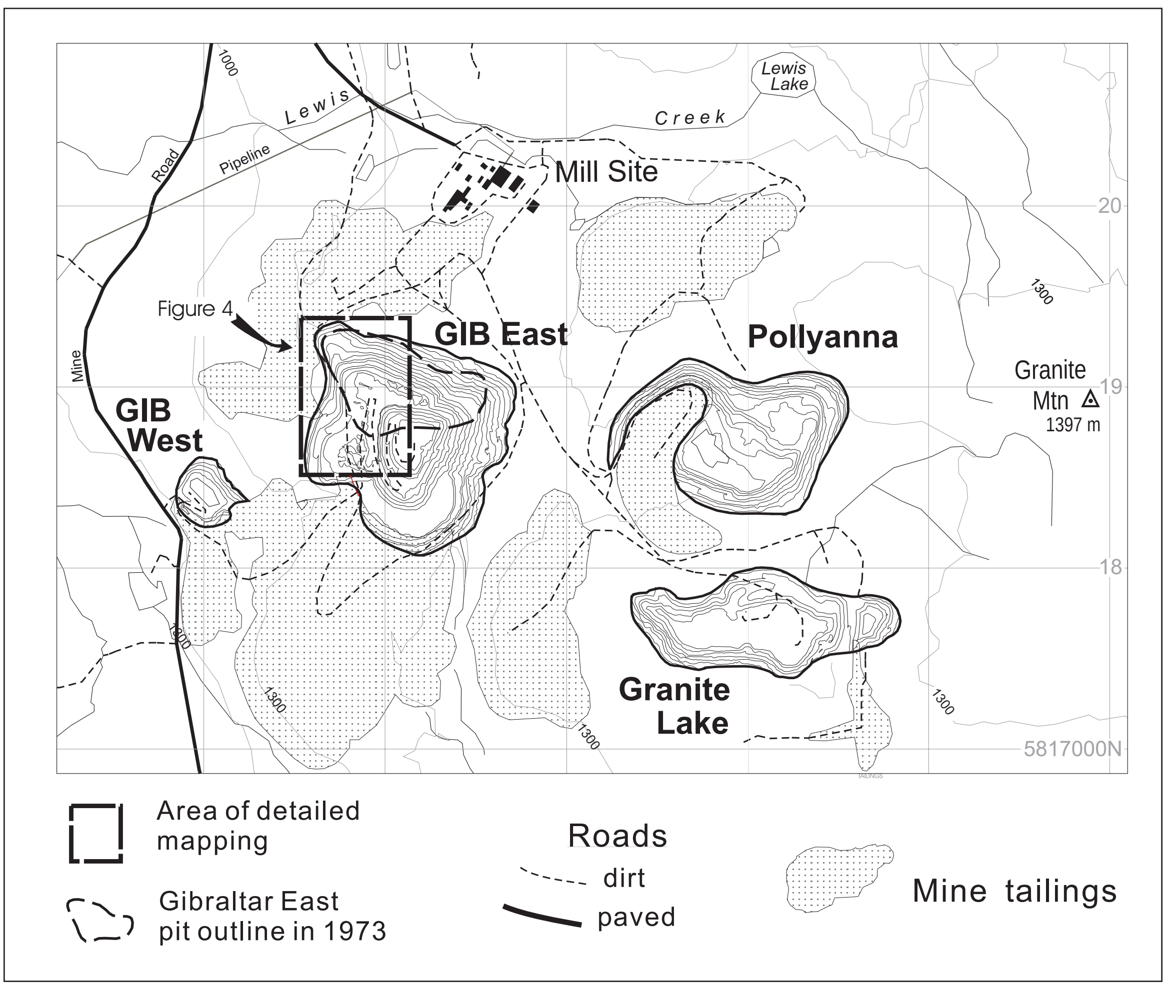

Figure 3. Detailed location map of the Gibraltar Mine area.

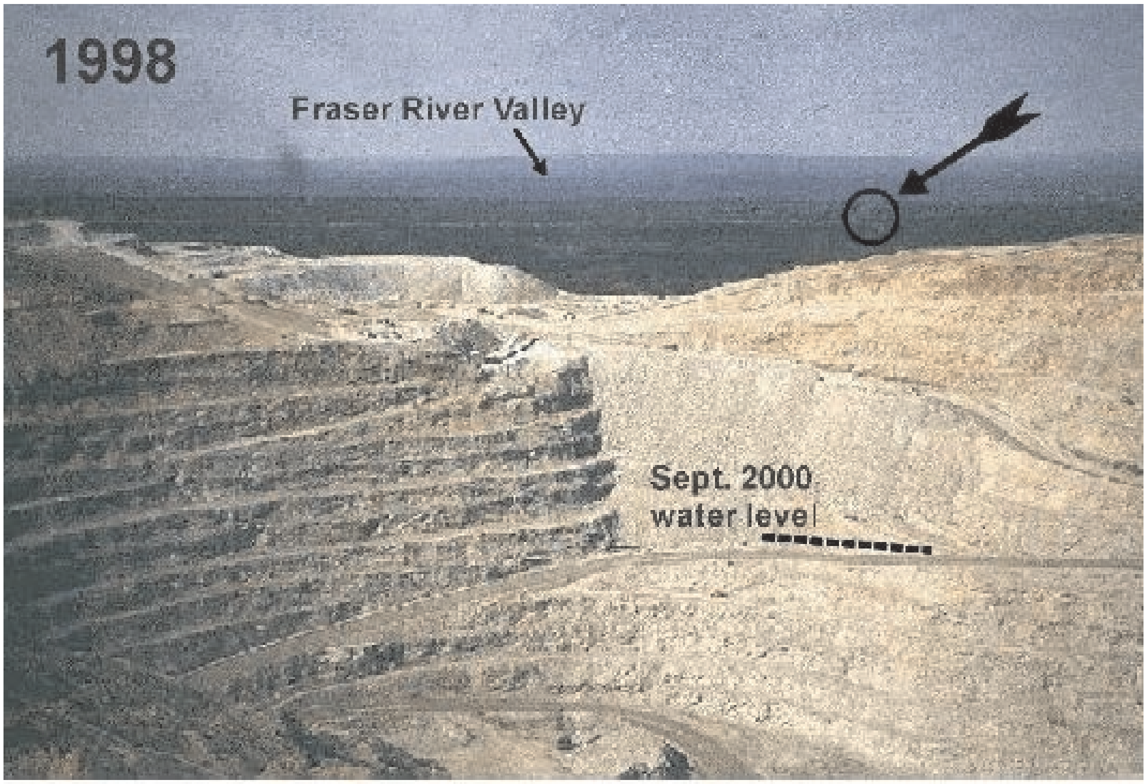

Photo 1. View of the Gibraltar East pit, looking west just prior to mine closure on the 2640 ft bench level in 1998 (top photo) compared to mining a year after start-up on the 3365 ft bench level in 1973 (bottom photo, Plate IV of Sutherland Brown, 1974). Circled area in background gives an idea of relative scale and position of the individual photos. Position of the pit in 1973 relative to that of the current pit outline is illustrated in Figure 3.

Lake pit was not mapped during this study. In many instances the other areas examined are either vertically or laterally restrictive but provided sufficient information to characterized mine scale relationships. Mapping and sampling of this pit was timely as pumping of water into it from the tailings pond was started in February, 1999, and deeper levels are becoming progressively flooded. As this was the initial startup pit in 1972 and also where mining ended in 1998 (Photo 1), significant superficial variation in the appearance of similar rock units has resulted from varying periods of surface oxidation, which diminishes with pit depth.

The four pits lie in a zone of pervasively greenschist metamorphosed, variably hydrothermally altered and veined, deformed and recrystallized tonalite referred to as the 'mine phase tonalite' (Bysouth *et al*., 1995). Where undeformed it is medium to coarse-grained, equigranular rock (Photo 2) and displays a relatively uniform grain size and mineralogical composition throughout the mine area. All primary minerals excluding quartz, are partially to completely replaced by alteration assemblages reflecting greenschist grade metamorphism which is characteristic of the batholith as a whole. It consists of 35-40% (relict) plagioclase, 25-30% quartz, 20-25% epidote and zoisite, 15-20% chlorite, 5-10% sericite and trace amounts of sphene, zircon, apatite, iron oxides, carbonate and ±sulphides. Weathered surfaces are light grey to buff white and commonly display a distinctive splash of disseminated pistachio-green epidote.

Map Units

Throughout the pit area variations in the appearance of the Mine Phase tonalite result from either differences in the style and type of veining or superimposed deformation and associated hydrothermal alteration. Veining is prevalent throughout the mine area and varies in type and intensity (vein density). In contrast, hydrothermally-altered and deformed rocks are restricted to discrete planar zones where the tonalite is converted to schists and phyllonites.

Three primary mappable variations of the Mine Phase tonalite are distinguished on the basis of vein morphology, structural style and alteration. These include from oldest to youngest (1) stockwork tonalite, (2) sheeted tonalite and (3) schistose tonalite. The early quartz stockwork tonalite is restricted in occurrence to the Pollyanna pit and has no visible mineralization. In contrast, the later types are prominent throughout the mine area and constitute the subdivision of individual mine units mapped in the Gibraltar East pit (Figures 4a, b). Sheeted tonalite includes two distinct types of prominent heterogeneously developed, sub-parallel planar vein sets that are designated as 'sheeted veins' and 'sheeted veinlets'. Both sheeted vein sets are locally cut by and deformed where marginal to later, hydrothermally altered, phyllosilicate-rich, high-strain zones. Two distinct ages of later high-strain schistose tonalite zones are recognized. An older sequence of several stacked, sub-horizontal, undulating zones is openly, upright folded against a younger northwest trending sub-vertical zone of highly crenulated schistose rock (Figures 4a, b).

STOCKWORK TONALITE

This earliest style of veined tonalite was identified only in the southwest wall of the Pollyanna pit. Stockwork tonalite is characterized by randomly oriented quartz stockwork veining in medium-grained massive tonalite (Photo 3a and b). Veins range from 0.5 to 1 centimetre in width and consist of fine-grained white quartz. Although in general the veining is random, it locally contains planar vein sets that dip at intermediate angles to the southwest (Photo 3c).

Dikes of white aphanitic to medium-grained tonalite from several centimetres to several tens of centimetres wide display multiple intrusive relationships with the quartz stockwork veins. Quartz veins are in places cut by the leucocratic tonalite dikes as illustrated in the bottom right portion of Photo 2a. In other areas quartz veins of similar character cut these tonalite dikes.

The leucocratic tonalite phase is best represented along the opposite, north wall of the Pollyanna pit where several large, 2 to 6 metre wide northeasterly dipping dikes intrude the more mafic host tonalite (Photos 4.a, b). The age of these dikes has been interpreted from U-Pb dating at 212±0.4 Ma (Ash *et al*., in preparation) which is 2 to 3 million years younger than the magmatic age of the host batholith, at 215±0.8 Ma. On the basis of the multiple intrusive character and relative age relationships the stockwork veins are considered to be late syn-magmatic. Stockwork tonalite is affected by all subsequent styles of veined and/or deformed tonalite described below.

SHEETED TONALITE

Sheeted tonalite is characterized by the presence of two distinct sub-parallel planar vein sets including both 'veins' and 'veinlets'. Both are generally openly S-folded with moderate to steep dips to the southwest except where folded adjacent to later shear zones. Sheeted veins are thicker, more widely spaced and compositionally distinct

Photo 2. Typical textural character of undeformed mine phase tonalite from the west wall, Gibraltar East pit.

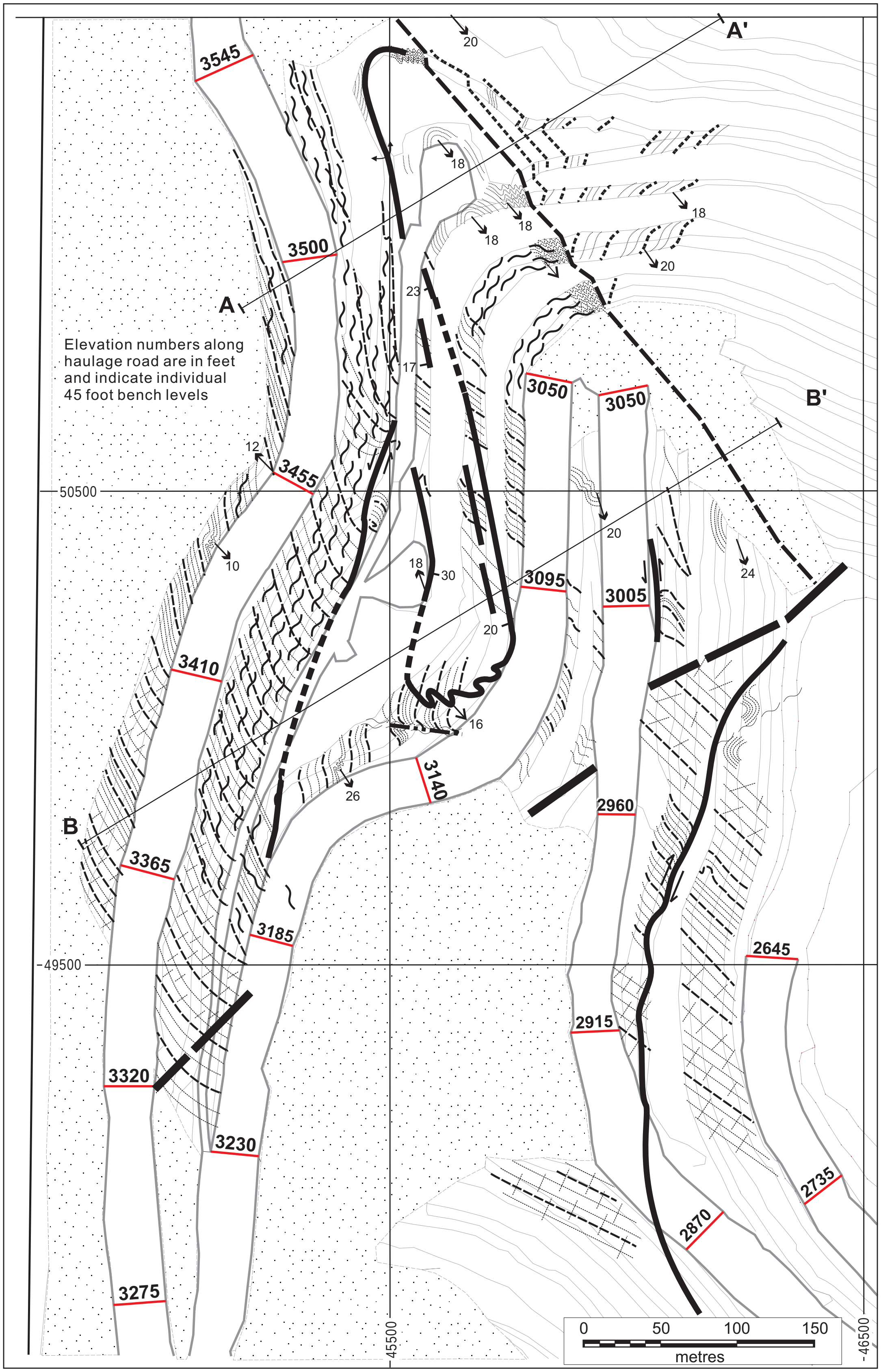

Figure 4a. Generalized geology of the northwest portion of the Gibraltar East pit. Location of map area indicated in Figure 3.

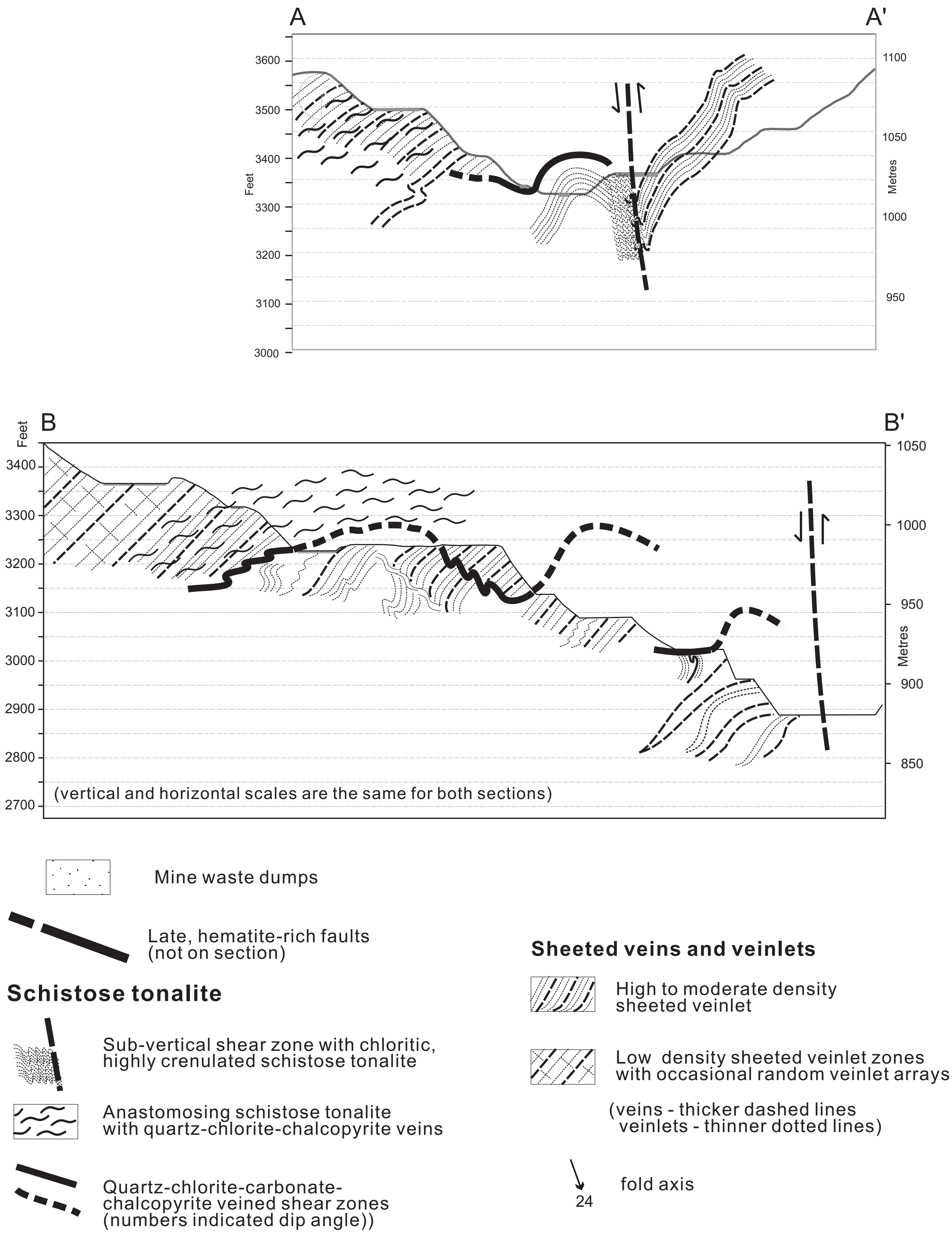

Figure 4b. Generalized cross-sections through of the northwest wall of Gibraltar East pit. Line of section located in Figure 4a.

Photo 3a. Quartz stockwork veining in tonalite along the 3750 foot bench, southeast wall of the Pollyanna pit.

Photo 3b. Detailed character of quartz-stockwork veined massive equigranular tonalite.

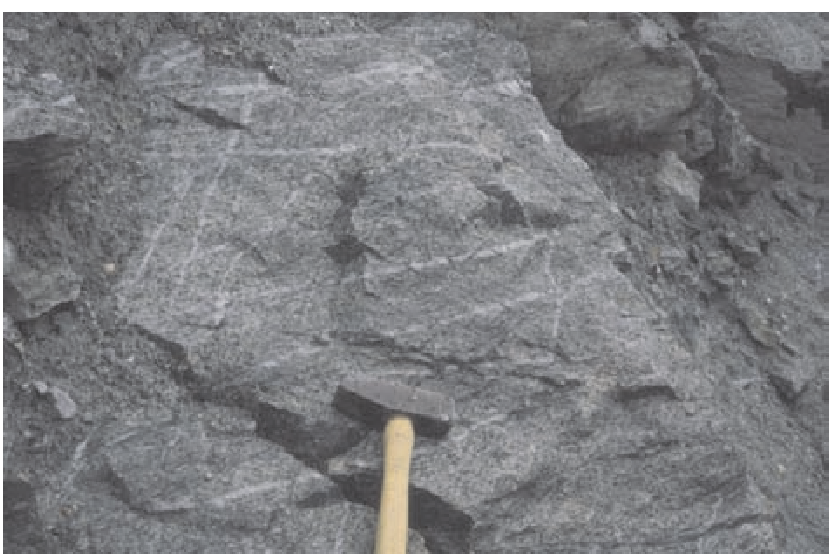

Photo 3c. Local development of planar quartz veins in the stockwork tonalite.

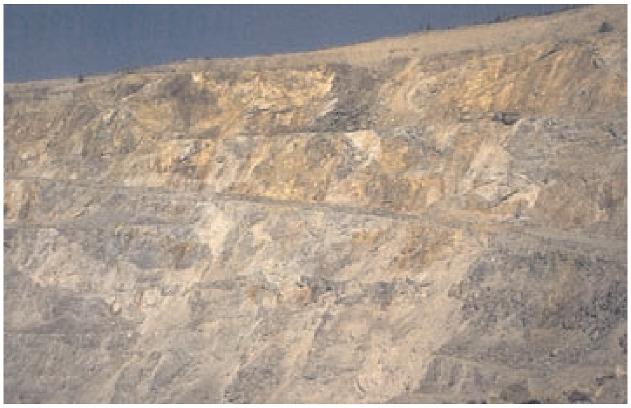

Photo 4a. White leucocratic tonalite dikes intruding lighter grey tonalite along the north wall of the Pollyanna pit.

Photo 4b. Detailed intrusive relationship along the upper margin of one of the dikes shown in photo 4a. Field of view is approximately 4 meters.

from the thinner sub-parallel sheeted veinlets (Photo 5). In general, sheeted veins are thicker and more numerous in zones of high-density sheeted veinlets.

Sheeted Veins

Sheeted veins are characterized by high sulphide content and well-developed sericitic vein envelopes. These veins are the most prominent features throughout the pits due to their high Fe-sulphide content and distinctive rusty-brown weathering colour. They occur over intervals of three to five metres and typically range from 5 to 25 centimetres in width but may be up to 60 centimetres wide. Sericitic vein envelopes range from several to 15 centimetres in width and are usually strongly sheared. The veins are dominated by quartz and sulphides, mainly pyrite which comprises from 30 to greater than 50% of the vein material (Photos 6a,b). Pyrite is well banded and sometimes associated with thinner bands of molybdenite. Pyrite also occurs as disseminations throughout the quartz veins and in the sericitic vein envelopes where it also occurs within deformed quartz-sulfide stringers. In

Photo 5.Typical appearance of well developed sheeted veinlets with more widely spaced rusty-brown weathering sheeted veins along the west wall of the Gibraltar East pit between the 278 and 3050 foot intervals (individual benched are spaced at 45 foot intervals).

Photo 6a.Exceptionally wide banded sulphide-rich quartz vein with well developed sericitic envelopes. 3320 foot level, northwest

Photo 6b. Banded sulphide-rich quartz vein with both pyrite and molybdenite. 3140 foot bench, west wall Pollyanna pit.

addition to the dominant pyrite and lesser, molybdenite these veins have also been noted (Drummond *et al.*, 1973, 1976) to contain minor amounts of pyrrhotite, magnetite and chalcopyrite.

Petrographic examination of the sheeted vein envelopes indicates that they consist of two alteration types, one dominated by sericite the other by quartz. Sericite-rich envelopes consist of strongly flattened and stretched, very fine-grained, anastamosing and strongly fissile zones of sericite (70-90%), quartz (10-20%), epidote (5-10%), chlorite (1-5%) and trace to several percent sulphides. These zones bound flattened, augen-shaped, discontinuous aggregates of deformed, fine-grained quartz (85%), epidote (7-10%), sericite (5-10%) chlorite (5%) and sulphides (1-10%). These quartz-rich components of the vein envelopes may represent deformed and hydrothermally altered portions of the surrounding sheeted veinlets. Very fine-grained, recrystallized quartz and subhedral to euhedral fine-grained epidote aggregates form in the pressure shadows of the augen-shaped aggregates which may suggest that there was an episode of epidote formation during the time of deformation of the sheeted vein envelopes.

Sericite-rich envelopes of the sheeted veins commonly display well-developed S-C fabrics commonly suggesting an apparent dextral sense of shear. The ‘c’ fabric is defined by fine-grained sericite and quartz-rich laminae that are slightly discordant to and wrapped around flattened, augen quartz-rich aggregates of fine-grained quartz, chlorite and epidote, which locally contain sulphides. These augen of quartz-rich aggregates define the ‘s’ fabric. This schistosity usually dissipates within a short distance from the sheeted veins. Intervening panels of relatively massive tonalite with sheeted quartz-sulfide veinlets may develop a weak parallel foliation proximal to the vein defined by the flattening and alignment of chlorite. A regionally consistent counter-clockwise oblique angle of about 10º between the vein-marginal schistosity (mean of 135/25) and the sericite-rich quartz-sulfide sheeted veins (mean of 145/45) further implies an apparent dextral sense of shear along these deformed sheeted veins. A conspicuous mineral stretching lineation defined by the alignment of stretched sulphides, sericite and chlorite grains is developed on these sheared surfaces. Millimetre-scale crenulations are also locally developed in the schistose margins of these sericite-rich sheeted veins. Stretching mineral lineations and fold axes are slightly scattered with a weak cluster that plunges sub-horizontally towards 155^o, while the stretching mineral lineations show a cluster with a mean plunge of 50^o towards 140^o. In a few instances, the fold axes and stretching lineations are parallel, which may imply localized high strain, intense shearing and development of sheath folds.

Sheeted Veinlets

Sheeted veinlets are the dominant planar feature throughout the mine and are characterized by semi-continuous, sub-parallel 1 to 3 millimetre wide veins. Variability in vein density is a notable feature throughout the pits. Zones of sheeted veinlets with vein spacing from 1 to 10 centimetres (Photo 5), form panels usually on the order of several tens of metres in thickness between broad intervals with more widely spaced veinlets. In these intervening panels of relatively massive tonalite veinlets are present but spacing is significantly increased, generally on the order of several tens of centimetres or greater. There are also areas containing several vein sets (2 to 4 in number) with varying orientations in contrast to the consistent and uniform orientation of the higher density sheeted zones.

Sheeted veinlets show some degree of variability in terms of vein morphology. Most often they are dominated by grey quartz (Photo 7) but in some areas, usually where closely associated with sulphide-rich sheeted veins, the sheeted veinlets are often dominated by pyrite. In other areas these sheeted features are defined by highly chloritic slip surfaces with little vein material. Dominant quartz veinlets consist of fine-grained, recrystallized smoky-gray quartz (65-70%), subhedral to anhedral chlorite (15-20%), epidote (5-10%), pyrite and chalcopyrite (5-10%), sericite (1-5%) and iron oxides (trace - 1%). Chlorite and epidote in sheeted veinlets produce the dark green colour in the veins.

Microscopic observations suggest sulphides in quartz-rich sheeted veinlets are commonly associated with quartz-chlorite-epidote aggregates and form as inclusions in chlorite and epidote. Inclusions of epidote, chlorite, quartz, sericite and iron oxides are also common in sulphides. Chalcopyrite forms in the interstices of epidote-epidote and epidote-quartz grains and may be flattened sub-parallel to the vein walls. Chalcopyrite partially and completely replaces pyrite cubes forming pyrite pseudomorphs. Pyrite may have chalcopyrite inclusions and iron oxide replacement rims. Quartz is recrystallized along chlorite-chlorite contacts as well as in the rest of the vein. Sericite replaces chlorite in the sheeted veinlets. Veinlet compositional variations which include magnetite, molybdenite and pyrrhotite are less common.

Photo 7. Detailed character of sheeted veinlets.

Sheeted quartz veinlets commonly develop micaceous envelopes in proximity to later hydrothermally altered shear zones. Where envelopes are not developed, discrete sericite-rich fissile zones, which are parallel to the foliation in the rock, cross cut relatively uniform sheeted veinlets at oblique angles. Where envelopes are developed, sericite-rich envelopes wrap around augen-shaped and boudinaged sheeted veins. Envelopes comprise very fine grained, flattened and stretched sericite (50-55%), quartz (30-35%), epidote (10-15%), chlorite (2-5%) and trace amounts of sulphides.

SCHISTOSE TONALITE

Schistose tonalite is locally developed along hydrothermally-altered, high-strain zones within the Gibraltar mine. On the basis of structural relationships two distinct ages of schistose tonalite are recognized. These include an earlier series of undulating, sub-horizontal shear zones and a later, sub-vertical, high-strain zone. Both are associated with high-grade Cu ore at the Gibraltar mine. The earlier sub-horizontal shear zones cause folding and shearing of the sheeted veins and their intervening host rocks. The later, sub-vertical zone causes shearing and folding of the older sheeted veins and early sub-horizontal shear zones (Figure 4b).

Early Sub-Horizontal Shear Zones

Sub-horizontal shear zones are manifest in two forms, occurring as several discrete zones and as a broad, roughly 100 metre wide zone with numerous thinner discontinuous anastomosing shears. The most prominent type consists of relatively continuous, discrete, 1 to 2 metre wide, strongly foliated, fissile, phyllosilicate-rich, carbonate-altered shear zones. These high strain zones deform all previously described vein types. At least three and possibly four distinct, shallow to sub-horizontal continuous shear zones are recognized in the Gibraltar East pit and are repeated vertically at roughly 100 metre intervals. Rocks within the zone vary from schistose tonalite to a phyllonitic schist and are characterized by penetrative zones of sericite-rich, anastamosing laminations that wrap around flattened, augen-shaped quartz-rich aggregates. Discontinuous white, bull quartz veins with locally concentrated coarse-grained aggregates of chlorite, carbonate and Cu-sulphide minerals are a characteristic feature of these zones (Photos 8 and 9). Quartz-chlorite-carbonate-Cu veins are deformed in the schistosity of this unit and also crosscut the schistosity in these shear zones.

These shear zones are also typified by pervasive iron-carbonate alteration, which is largely restricted to the schistose tonalite between the well-defined bounding surfaces of the shear zones (Photo 10). This addition of iron-carbonate results in a distinctive orange-brown weathering colour. Iron-carbonate forms in the interstices of quartz, relict plagioclase and chlorite grains, in quartz-chlorite aggregates, and in ribbons in quartz grains. These carbonate ribbons are crosscut by phyllosilicate-rich fissile zones. These carbonate-altered zones are also characterized by penetrative, centimetre-scale crenulations and a crenulation cleavage. Proximal to the footwall of these shallow shear zones, sheeted veins are commonly openly to tightly S-asym-

Photo 8. Discontinuous bull-white quartz vein in shallow westerly dipping shear zone between the 3150 and 3225 levels, west wall, Gibraltar East pit. Quartz veined shear zone goes from bottom left to top right.

Photo 9 Detail of coarse-grained aggregates of chalcopyrite and chlorite in quartz vein shown in sub-horizontal shear zone. 3320 foot bench level, west wall Gibraltar East pit.

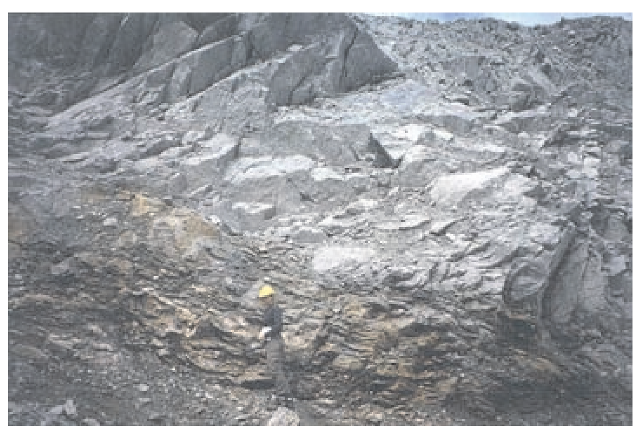

Photo 10. Sub-horizontal carbonate altered and quartz-carbonate veined shear zone cross cutting sheeted veinlets. 2870 foot bench, west wall Gibraltar East pit.

metrically folded, with axial planes that have consistent moderate dips to the east. In the hanging wall of these shear zones the sulphide-rich sheeted veins are mechanically rotated into the shear zone. Geometric relationships most often suggest an apparent sinistral sense of shear along these high-strain zones, but this is not everywhere consistent. Eastwood (1970) indicates that the original Pollyanna showing, referred to as the Pollyanna shear zone, consisted of quartz lenses and copper minerals in a quartz-muscovite schist zone trending 055 degrees.

Less conspicuous, though economically significant is a broader zone with numerous 2 to 10 centimetre-wide shears spaced over several tens of centimetres that contain discontinuous quartz-chlorite-Cu sulphide veins (Photo 11). The general trend of this broad zone, as well as the individual shears, conforms to the same general trend of the underlying discrete continuous shear zone (Figure 4b). Iron-carbonate is less conspicuous in quartz veins and sheared tonalite throughout this zone of anastomosing shears.

The nature of the Cu-sulphide minerals present in these white bull-quartz veins varies as a function of depth in the Gibraltar East pit. Chalcopyrite dominates. However above the 3140-foot pit level it is partially to completely replaced by a fine-grained, dark-gray to black mineral, possibly covellite and/or chalcocite, which imparts a distinctive indigo-blue colour on oxidized surfaces.

The transition from relatively massive to schistose tonalite involves an increase in the intensity of schistosity (Photo 12) and by increased amounts of sericite and quartz (Figure 5). Increased amounts of sericite are concentrated along discrete to penetrative, anastamosing, fissile zones of mainly stretched sericite (70-90%) with lesser fine-grained, stretched quartz, epidote and chlorite. Fine sericite also partially (30-60%) to completely replaces relict plagioclase laths. An increase in the content of secondary quartz is demonstrated by quartz occurring as impregnations in the interstices of quartz and relict plagioclase grains, in addition to quartz replacing chlorite, sericite and altered plagioclase. Deformed anhedral grains to subhedral cubes of pyrite are associ-

Photo 11. Discontinuous anastomosing shear zones (for scale the individual benched 45 feet high).

Photo 12. Flattening fabric in schistose tonalite.

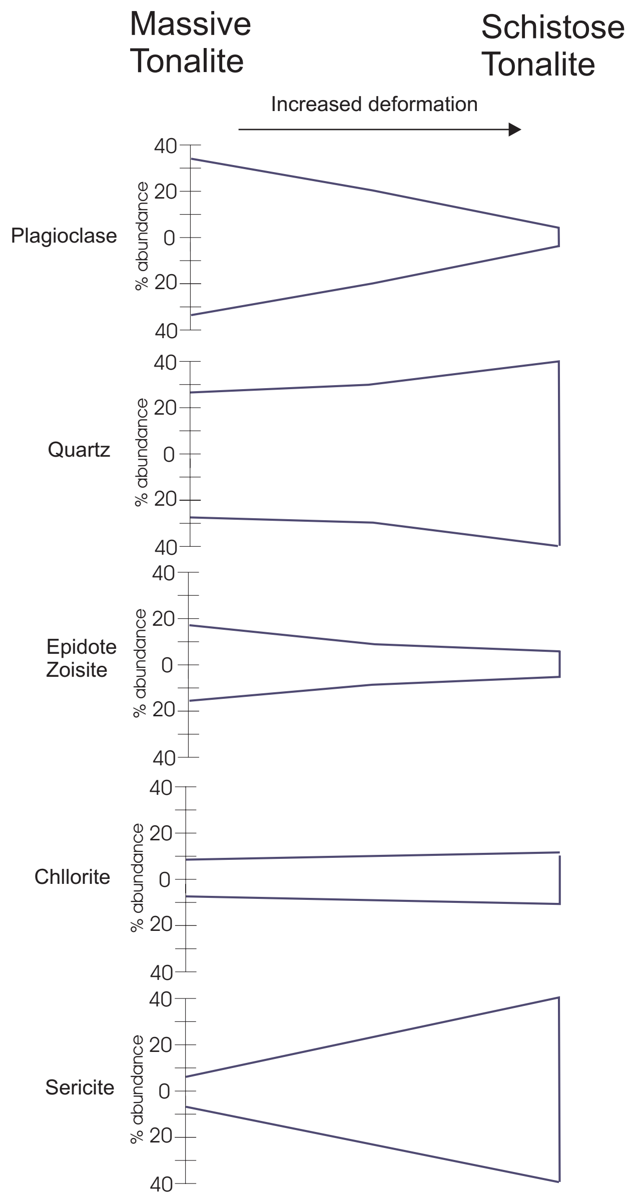

Figure 5. Relative mineralogical variation in mine phase tonalite as a function of progressive deformation, going from least deformed massive tonalite to schist.

ated with moderately flattened augen-shaped aggregates of quartz, epidote and chlorite. Anhedral chalcopyrite grains are concentrated along the phyllosilicate-rich zones, while very fine (recrystallized) subhedral pyrite is disseminated throughout the unit. Anhedral to subhedral pyrite also forms inclusions in and replaces the margins of chalcopyrite.

Sub-Vertical Schistose Tonalite Zone

A major, sub-vertical high deformation zone, several metres wide, cuts the northwest portion of the Gibraltar East pit (Figure 4). Towards this zone, sheeted veins and veinlets, low-angle shear zones and contained veins become progressively deformed, from openly folded to tightly crenulated (Photo 13a,b) to transposed. All major and minor fold axes plunge at shallow angles (5-20^{o}) to the southeast. Clockwise rotation of planar features on the southwest side of this zone combined with asymmetrical Z-folding of steeply southwesterly dipping sheeted veins where entering this zone on the northeast side (Photo 14) indicate relative movement on this structure (Figure 4b). Strongly sheared rocks within the zone are chlorite-rich and dark in colour and are associated with pervasive sericite and carbonate alteration. Copper sulphide minerals are significantly enriched and are typically smeared out along chloritic slip surfaces within the schistosity.

Photo 13a. Open folding of sheeted veins and veinlets along the southwest side of the Sub-vertical shear zone.

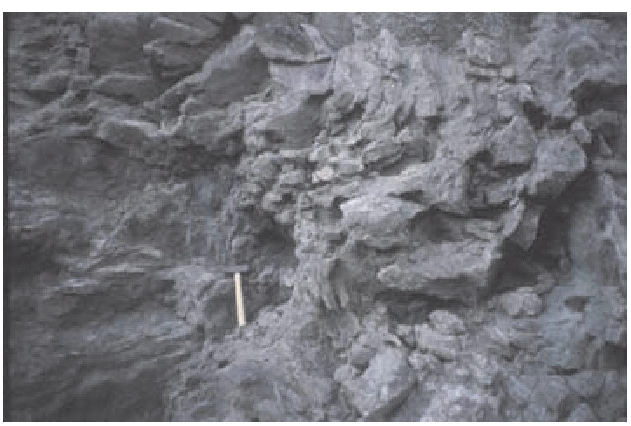

Photo 13b. Nature of folded, chloritic, Cu-rich schistose tonalite within the sub-vertical shear zone.

Photo 14. Asymetrically z-folded, Fe-sulphide-rich sheeted vein on northeast side of sub-vertical shear zone.

Structure

Deformation of the Gibraltar mine was localized along discrete high-strain zones in a relatively massive and unfoliated tonalite. No extensive or pervasive foliations were recognized in the mine. The intensity of folding of veins and planar fabrics generally varies as a function of scale. On the regional scale, folds are open warps. At the local scale, in particular in proximity to discrete high deformation zones, folds are tight to transposed. The majority of folds plunge shallowly to the southeast (Figure 4). The orientation of mineral stretching lineations on foliation and shear surfaces varies from shallowly to moderately plunging to the southeast. A detailed synopsis and kinematic interpretation of the structural data from the Gibraltar mine will be given elsewhere (Ash *et al*., in preparation).

LATE BRITTLE FAULTING

A late, major northeast-trending steeply northwest dipping brittle fault cuts across the Gibraltar East pit through the middle of the area mapped (Figure 4a). It is characterized by a distinctive purplish-red stain and it cross-cuts all previously described map units and consists of hematite-rich incoherent clay gouge zones from 5 to 15 centimetres wide. Zones of hematite-rich alteration and minor hematite-stained fractures and faults marginal to the main gouge zones range from several decimetres to over a metre wide. Fault surfaces have horizontal to obliquely-plunging slickensides, which suggest strike-slip to oblique-slip movement on the faults. Although no obvious offsets were observed there is a subtle change in character in the rocks on either side of the fault. In the hanging wall, strongly deformed and sericite-altered rocks appear to be more prevalent than in the footwall. Sutherland Brown (1974) interpreted these faults to cause pit-wall instability and groundwater movement. He observed displacements of less than 10 metres along the faults in the Gibraltar East pit. Drummond and others (1976) suggest regional-scale, late, steep north to northeast-trending faults that cut the Gibraltar area have a net throw of 300 m.

SUMMARY

On the basis of structural style, morphology and relative age relationships, three generations of veining are recognized at the Gibraltar Mine. The earliest are random stockwork to weakly planar quartz veins that are locally restrictive and largely unmineralized. The second generation includes two types of heterogeneously developed sub-parallel, sheeted veins and veinlets that pervade the mine area. The thicker sericite-enveloped, Fe-sulphide-rich, banded quartz veins contain concentrations of molybdenite. Cu-sulphide minerals are less conspicuous. Both of these generations of veins appear to be prekynematic and formed prior to development of any penetrative foliation fabrics within the batholith. The sericite enveloped, sheeted veins have accommodated significant amounts of later shearing but this is also largely non-penetrative and restricted to vein marginal shears.

The third generation of veining is compositionally distinct for earlier vein types containing quartz, chlorite, carbonate, and abundant Cu-sulphide minerals. These are syn to late kynematic and associated with and developed along high-strain deformation zones. No molybdenite mineralization was noted in these veins. The general schistose character of high-grade copper ore at the Gibraltar mine resulted in its ease of crushing and milling or low work index.

Regional Considerations

The syn kinematic high-strain, sub-vertical shear zone controls the overall geometry and setting of copper ore in the Gibraltar East pit. It is mimicked on the mine and regional scale. The shear zone which localizes high-grade ore in the northwestern portion of the Gibraltar East pit is also well defined at the western end of the Pollyanna pit. Towards the southeast, this northwesterly-trending shear zone bends to the east and is consistent with a comparable change in orientation of all planar (sheeted veins) and linear (fold hinges and mineral stetching lineations) structural elements at both the mine and regional scale (Ash *et al.*, 1999a).

Two distinct sub-vertical parallel zones are attributed to ore control, a northerly zone related to ore at the Gibraltar East and Pollyanna pits and a southern zone controlling mineralization at the Gibraltar West and Granite Lake pits (Figure 6). A similarly oriented shear zone with asso-

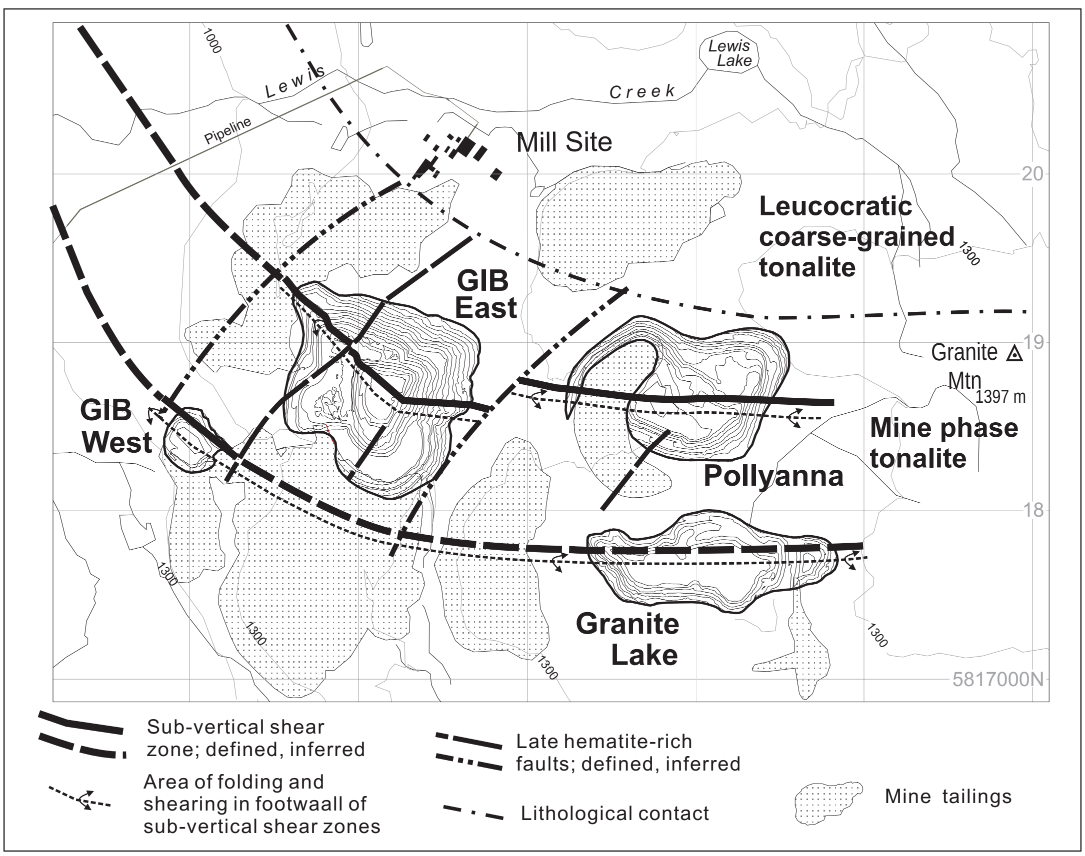

Figure 6. Mine scale distribution of sub-vertical high-stain shear zones relative to the position of Cu-ore at Gibraltar.

ciated schistose quartz diorite and tonalite along the southern margin of the Granite Mountain Batholith is associated with Cu-mineralization at the Sawmill Zone (Figure 2). The overall trend of these zones is also consistent with the orientation of contacts between specific phases of the pluton.

A series of 28 soil samples were collected by Sutherland Brown (1966) at roughly 150-meter intervals in a general east-northeasterly direction from across the Gibraltar Mine area and mercury concentrations were determined. It is significant that samples collected above the major sub-vertical, mineralized shear zones have elevated mercury concentrations that are 2 to 3 times background values. These data, although limited, suggest that mercury concentrations in soils may be useful in identifying similarly mineralized shear zones. No mercury analysis were undertaken in this study.

CONCLUSIONS

Copper ore at the Gibraltar mine is structurally controlled. Ore grade mineralization is localized along high-strain shear zones that are associated with significant sericite enrichment.

Two major parallel northwest to east-trending sub-vertical shear zones control the distribution of copper mineralization at the mine. Regionally smilar parallel zones appear to control occurrences of anomalous Cu mineralization.

ACKNOWLEDGMENTS

Enthusiastic and capable assistance provided by Kris Raffle and Jennifer Dicus during 1999 pit mapping was greatly appreciated. For insights and contributions to pit mapping by Allan Galley with Geological Survey of Canada in 1999 we are thankful. The cooperation and assistance of the Gibraltar Mine staff has been instrumental in completing this work. We are specifically indebted to Murray Rydman and George Barker. The warm hospitality of Gerry and Henry Funk and staff of the Oasis Motel is graciously acknowledged. This report has been improved from reviews by Nick Massey, Derek Brown, Brian Grant and Ron Smyth. Mike Fournier with the British Columbia Geological Survey assisted in generating the figures.

REFERENCES

Ash, C.H., Panteleyev, A., MacLennan, K.L Payne, C.W. and Rydman, M.O. (1999a): Geology of the Gibraltar mine area (93B/8&9); *B.C. Ministry of Energ and, Mines*, Open File 1999-7, 1:50 000 scale map.

Ash, C. H., Rydman, M.O., Payne, C.W., Panteleyev, A. (1999b) Geological setting of the Gibraltar mine south central British Columbia (93B/8, 9), *B.C. Ministry of Energy and Mines*, Exploration and Mining in British Columbia, pages A1-A15.

Ash, C.H., Riveros, C.P., Friedman, R.M., Reynolds, P.H., Stein, H.J. and Creaser, R.A. (in preparation): Structural setting & age constraints of copper-molybdenite mineralization, Gibraltar Mine, east-central British Columbia.

Bysouth, G.D., Campbell, K.V., Barker, G.E. and Gagnier, G.K. (1995): Tonalite-trondhjemite fractionation of peraluminous magma and the formation of syntectonic porphyry copper mineralization, Gibraltar mine, central British Columbia; *in* Porphyry Deposits of the Northwestern Cordillera of North America, T.G. Schroeter, Editor, *Canadian Institute of Mining and Metallurgy*, Special Volume 46, pages 201-213.

Drummond, A.D., Tennant, S.J. and Young, R.J. (1973): The interrelationship of regional metamorphism, hydrothermal alteration and mineralization at the Gibraltar mines copper deposit in BC; *Canadian Institute of Mining and Metallurgy*, Bulletin 66, No. 730, pages 48-55.

Drummond, A.D., Sutherland Brown, A., Young, R.J. and Tennant, S.J. (1976): Gibraltar - regional metamorphism, mineralization, hydrothermal alteration and structural development; *in* Porphyry Deposits of the Northwestern Cordillera of North America, A. Sutherland Brown, Editor, *The Canadian Institute of Mining and Metallurgy*, Special Volume 15, pages 195-205.

Eastwood, G.E.P. (1970): McLeese Lake, geology of the Granite Mountain Stock; *in* Geology, Exploration and Mining in British Columbia 1969, *B.C. Ministry of Energy, Mines and Petroleum Resources*, pages 162-172.

Orchard, M.J. (2000): Report on conodonts and other microfossils, Quesnel (93B); *Geological Survey of Canada*, Internal Report No. MJO-2000-9, 2 pages.

Panteleyev, A. (1977): Granite Mountain project; *In* Geological Fieldwork, 1976, *British Columbia Ministry of Mines and Petroleum Resources*, pages 39-42.

Raffel (1999): Structure, deformation and element mobility of the Gibraltar Mine, south central British Columbia; *unpublished B.Sc. Thesis*, University of British Columbia, 70 pages.

Simpson, R.Y. (1970): Geology of the Gibraltar – Pollyanna copper deposit; unpublished B.Sc. thesis, *The University of British Columbia,* 43 pages.

Sutherland Brown, A. (1957): Williams Lake, McLeese-Cuisson lakes area, *British Columbia Minister of Mines,* Annual Report 1957, pages 14-16.

Sutherland Brown, A. (1966): Geology of the Granite Mountain-Cuisson lakes area, *in* Minister of Mines Annual Report 1966, *B.C. Ministry of Energy, Mines and Petroleum Resources*, pages 121-125.

Sutherland Brown, A. (1974): Gibraltar Mine (93B-12, 13), Geology, exploration and mining in British Columbia 1973, *B.C. Department of Mines and Petroleum Resources*, pages 299-318.

Wheeler, J.O. and McFeely, P (1991): Tectonic assemblage map of the Canadian cordillera and adjacent parts of the United States of America: *Geological Survey of Canada*, Map 1712A, scale 1:2 000 000.

Geochemistry of Auriferous Pyrite Mineralization at the Bonanza Ledge, Mosquito Creek Mine and Other Properties in the Wells-Barkerville Area, British Columbia

By Gerry Ray[1], Ian Webster[1], Kika Ross[2] and Richard Hall[3]

KEYWORDS: Gold, Wells, Barkerville, Mosquito Creek Mine, Island Mountain Mine, Cariboo Gold Quartz Mine, Bonanza Ledge, Pyrite, Quartz veins, Geochemistry, Exploration, Economic Geology.

INTRODUCTION AND LOCATION

The 30 km-long, northwest trending Wells-Barkerville Gold Belt lies approximately 65 km east of Quesnel in east-central British Columbia. It has had a 140 year-long mining history, having produced over 75 tonnes of gold from placer sources and a further 38.3 tonnes by underground mining. The belt contains numerous small pits and adits that were commonly driven on auriferous quartz veins; examples of these are at the Warspite, Proserpine, Canusa, Blackbull, Hardscrabble and BC veins, as well as at the Perkins and Standard Location properties situated southwest of the main belt and east of Stanley townsite (Figure 1). Most of the belts' production, however, came from four larger underground properties, the Mosquito Creek, Island Mountain (Aurum), and Cariboo Gold Quartz mines at the northwest end of the belt (Figures 1 and 2) and the Cariboo-Hudson further southeast. Apart from minor amounts of coarse visible free gold in quartz (Skerl, 1948), most gold occurs as micron-sized particles intimately associated with crystalline pyrite (Rhys and Ross, 2000).

There are two main styles of pyritic gold mineralization: (1) auriferous pyrite that lies in or adjacent to generally barren quartz ± carbonate ± sericite veins, and (2) massive to semi-massive banded and stringer pyrite that form small tabular and lenticular "replacement" bodies (Photos 1 and 2). Both types of mineralization are present at the Mosquito Creek, Island Mountain and Cariboo Gold Quartz mines. However, quartz-vein-related pyrite was the main ore mined at Cariboo Gold Quartz and it was also significant at the Island Mountain Mine (Skerl, 1948). Massive to semi-massive replacement and pyrite stringer ore bodies were the main economic focus at the Mosquito Creek Mine (Alldrick, 1983), and were also important at the Island Mountain Mine (Hanson, 1935; Benedict, 1945; Sutherland Brown, 1957).

The replacement bodies are mineralogically and chemically zoned (Alldrick, 1983). Their central portions are marked by fine grained, highly auriferous pyrite with a dolomite and quartz gangue; laterally, they grade out to coarser grained barren pyrite with arsenopyrite and minor galena, sphalerite and rare pyrrhotite. Outboard, the pyrite bodies are enveloped by silicified or sericitized limestone or sericite schist (Alldrick, 1983).

Exploration in the belt was recently revitalized by the discovery of the Bonanza Ledge Gold Zone by International Wayside Gold Mines Ltd. This property is located approximately 3 km southeast of the Wells townsite and the former Cariboo Gold Quartz mine (Figures 1 and 2). A staking rush took place after the announcement of several spectacular drill intersections, including 24.65 g/t Au over 25.8 m in hole BC-2K-10. As a result of this discovery, the B.C. Geological Survey, in co-operation with International Wayside and its contractors, began a program to examine the Bonanza Ledge and other pyritic gold properties in the belt.

This paper presents major and trace element geochemical data concerning the different styles of gold mineralization and their associated alteration. In addition, samples of quartz in the veins and massive pyritic replacements were subjected to fluid inclusion analysis, the results of which are summarized by Dunne and Ray (2001, this volume). Preliminary data suggests significant variations in the mineralogy and chemistry of the auriferous pyrite, as well as some chemical differences of fluids in the quartz veins throughout the belt. It is not yet known whether these variations reflect district-scale chemical zoning and temperature differences, but the distinctive chemical signatures noted in the Bonanza Ledge mineralization could be used to locate other pyritic gold zones of this type.

PREVIOUS WORK

Some of the earliest published work in the district includes the superb geology and placer maps of Bowman (1889, 1895). Since that time there have been numerous government and company geologists working in the district; these have produced a wealth of data concerning the

[1] *British Columbia Ministry of Energy and Mines*
[2] *Panterra Geoservices Inc.*
[3] *Consulting Geologist*

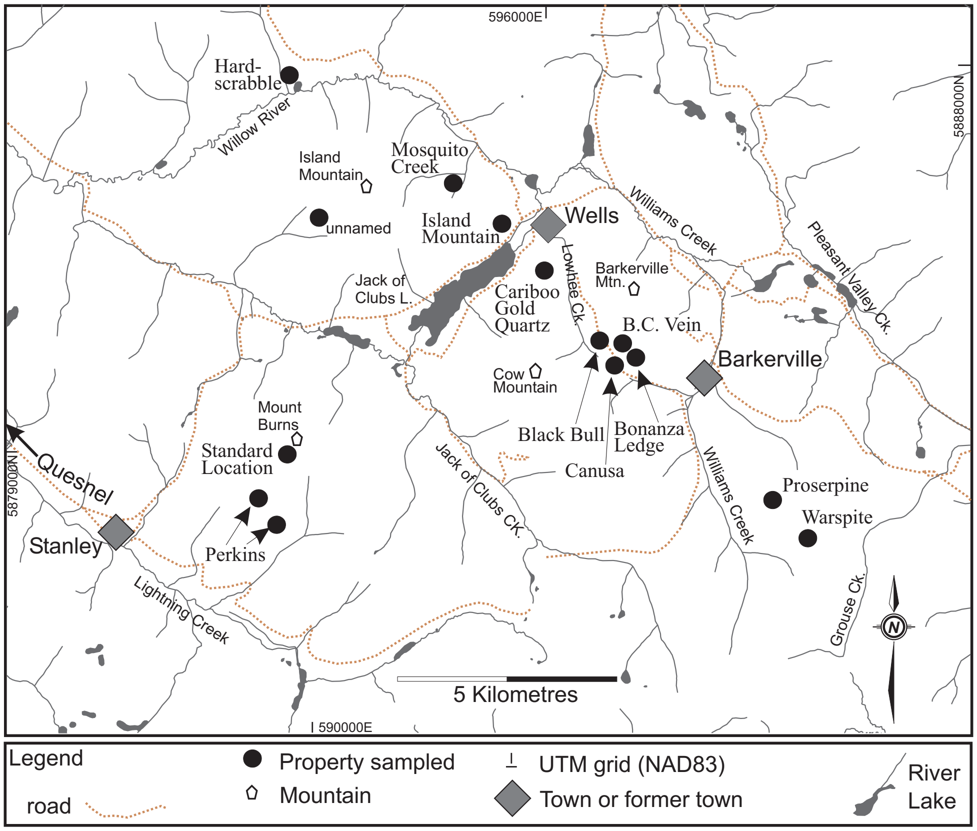

Figure 1. The NW part of the Wells-Barkerville Gold Belt showing the location of the gold mines and occurrences mentioned in this paper.

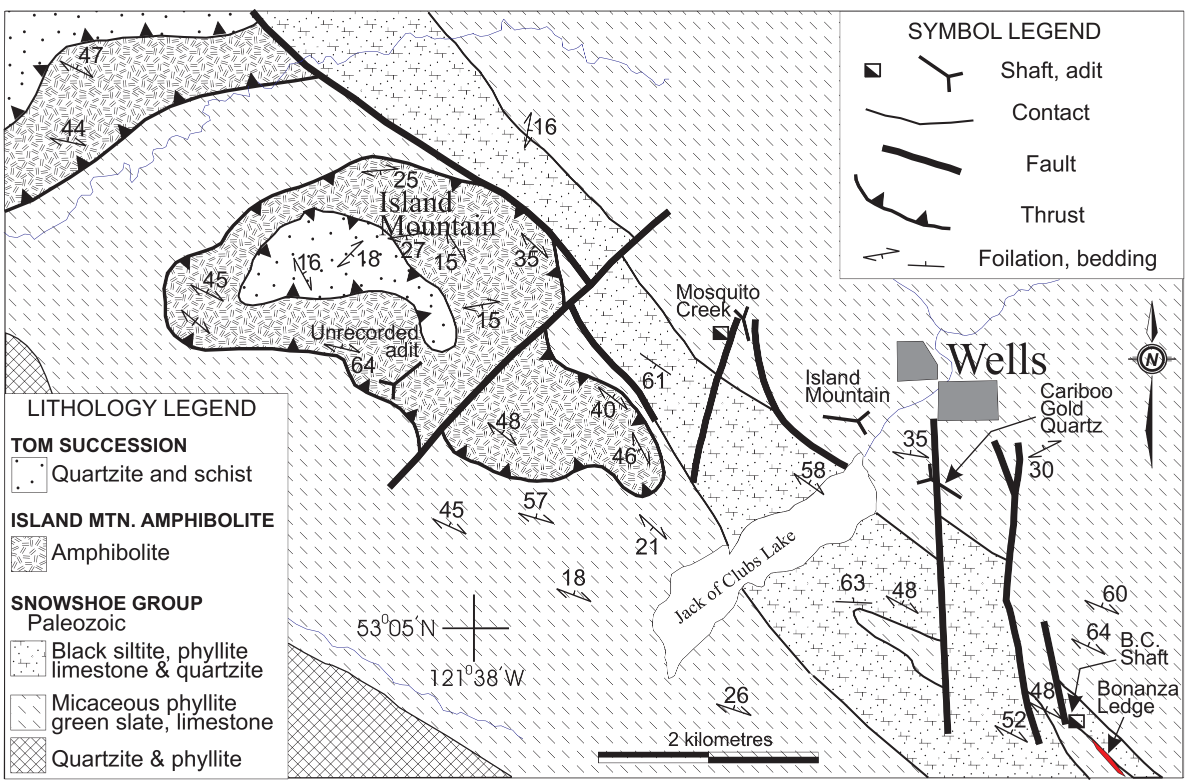

Figure 2. Simplified geology of the Wells area (adapted after Alldrick, 1983 and Struik, 1988b).

Photo 1. NNE-trending white quartz vein with dolomite and pyrite-rich margins and sigmoidal satellite quartz veinlets. Exposure in the Number 1 underground level (4400 feet), Mosquito Creek Gold Mine.

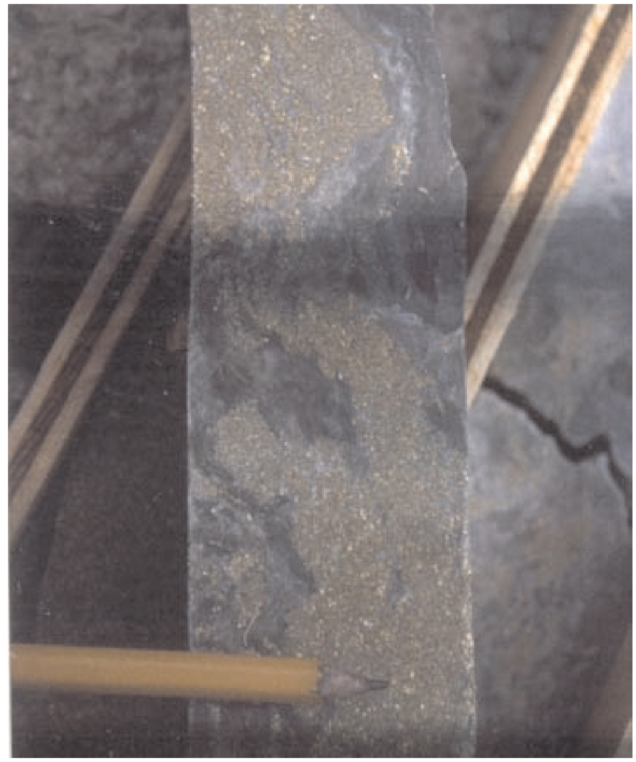

Photo 2. Gold-bearing semi-massive pyrite mineralization in drill core at the Bonanza Ledge Gold Zone. Drill hole BC-2K-19 at 310 feet.

placer and lode gold in the area, although some is unfortunately unpublished. Information on the placers is given by Uglow and Johnson (1923), Johnson and Uglow (1926), Clague (1989), McTaggart and Knight (1993), and Levson and Giles (1993).

Bedrock mapping includes work by Hanson (1934, 1935), Holland (1948, 1950, 1954), Sutherland Brown (1957, 1963) and more recently by Struik (1988a and 1988b). More detailed work on the deposits has been completed by Bacon (1939), Benedict (1945), Skerl (1948), Runkle (1950), Alldrick (1983), and Robert and Taylor (1989). Recent summaries of the camp have been completed by Hall (1999) and of the Bonanza Ledge Gold Zone by Rhys and Ross (2000) and Rhys (2000). The preliminary results concerning the fluid inclusion characteristics of some mineralized veins and replacements in the district are presented by Dunne and Ray (2001, this volume). Observations on the possible regional controls between the Wells-Barkerville Au mineralization and listwanite-altered ophiolitic rocks in the district are presented by Ash (in press).

GEOLOGY AND STRUCTURE

The Wells-Barkerville Gold Belt lies in the Proterozoic to Paleozoic Barkerville subterrane. The subterrane in this area comprises metamorphosed grits, quartzites, phyllitic argillites and schists with lesser carbonates, tuffs and mafic volcanic rocks. Many of the argillites are dark and organic-rich except where they have been bleached during metamorphism (Sutherland Brown, 1957).

In the immediate Wells-Barkerville vicinity, the succession belongs to the Paleozoic Snowshoe Group (Struik, 1988a, 1988b). However, Paleozoic or older rocks represented by the Island Mountain Amphibolite and the structurally overlying Tom succession occupy the summit of Island Mountain (Figure 2). The structural relationship between these two latter packages is uncertain, and Alldrick (1983) and Struik (1988a, 1988b) suggest they occupy klippes that structurally overlie the Snowshoe Group rocks. The stratigraphic relationship of the foliated and banded mafic rocks in the Island Mountain Amphibolite is also controversial; the unit may represent an unusual facies of the Snowshoe Group or thrust slices derived either from the Slide Mountain Terrane to the northeast or the Crooked Amphibolite unit further southwest (Struik, 1988a, 1988b) .

Both the pyritic quartz-vein and replacement mineralization in the belt are mainly hosted by lower greenschist facies phyllitic Snowshoe Group rocks and are generally confined to a stratigraphic interval in the upper part of the succession (Sutherland Brown, 1957, 1963; Alldrick, 1983; Robert and Taylor, 1989). These rocks display moderate to high strain; bedding is locally preserved (Alldrick, 1983; Robert and Taylor, 1989), but in many parts it is undetectable or has been intensely transposed. The positive identification of mappable stratigraphic units throughout the district is difficult for a number of reasons: the lack of widespread marker horizons and fossils (Struik, 1988a), the rarity of reliable bedding-cleavage intersections and the bleaching effects caused by hydrothermal or metamorphic overprinting (Photo 3; Sutherland Brown, 1957).

At least three major deformational events are recognized (Struik, 1988a, 1988b; Robert and Taylor, 1989) resulting in various fold styles and the formation of three sets of foliations and cleavages. The earliest foliation corresponds to layering of possible tectonic origin in the metasedimentary rocks, together with boudinage, ductile shearing and the formation of small scale isoclinal rootless folds (Struik, 1988a, 1988b; Robert and Taylor 1989).

The second period of ductile folding (F2) appears to have been the dominant structural event in the Wells-Barkerville area. It resulted in isoclinal to tight asymmetric folds (Photo 4), together with axial planar S2 fabrics that vary from a penetrative, intense sericite-muscovite cleavage and schistosity to a more widely spaced, less strong fracture cleavage.

The S2 foliations strike northwest to west and mostly have a moderate to gentle northeast dip. The F2 event was associated with the development of a strong mineral lineation and elongate rodding or mullion structures; these plunge gently to moderately northwest, parallel to the F2 fold axes (Alldrick, 1983; Struik, 1988a, 1988b; Robert and Taylor, 1989). The massive pyritic ore bodies at the Mosquito Creek mine also plunge sub-parallel to the F2 linear structures (Alldrick, 1983) and the margins of some quartz veins (*e.g.* the BC Vein) exhibit similar northwest plunging rodding structures. Likewise, recent work demonstrates that the Bonanza Ledge mineralization is folded by F2 structures (Rhys, personal communication, 2000). This is evidence that introduction of the older replacement pyritic bodies and many of the slightly younger quartz veins occurred before the F2 deformation had ceased. Thus, the mineralization may well have accompanied, and been controlled by, this regional structural-metamorphic event.

The third deformation (F3) was possibly related to a broad anticlinorium that developed west of the Wells area (Struik, 1988a; Robert and Taylor, 1989). This resulted in open folds, formation of both miceaceous planar and crenulation strain-slip cleavages, and brittle faulting.

SAMPLING

Sampling was mainly confined to the northwest part of the Wells-Barkerville Belt (Figure 1). This area includes three of the major underground mines (Mosquito Creek, Island Mountain and Cariboo Gold Quartz) as well as the Bonanza Ledge mineralization. In addition, samples were taken from the Perkins-Standard Location veins in the southwest, and from mineralization in the Warspite-Grouse Creek area to the southeast (Figure 1).

Photo 3: Blue-grey phyllite that is partially bleached by fluids of presumed metamorphic or igneous hydrothermal origin. Snowshoe Group metasediments, 2.5 km NW of the Hardscrabble occurrence, UTM 588465E; 5890076N.

Photo 4. Tight to isoclinal F2 folding in an interbedded carbonate-phyllite unit. Underground exposure, Island Mountain Mine.

The following rock types were sampled and assayed:

1. Massive to semi-massive pyritic and stringer "replacement" mineralization from the Bonanza Ledge Zone (Photo 2) and the Mosquito Creek and Island Mountain mines. The mine samples were taken mostly from underground workings although some mineralized float specimens on the mine dumps were also included. The pyritic Bonanza Ledge samples were selected from two drill holes (BC-2K-19 and BC-2K-29) and were analysed for major and trace elements (Tables 1A and 2B).
2. Barren footwall and hanging-wall alteration adjacent to the auriferous pyrite in the above two drill-holes at the Bonanza Ledge Zone. These samples were analysed for major and trace elements (Table 1A).
3. Massive to semi-massive pyrite within or adjacent to quartz veins at the Mosquito Creek and Cariboo Gold Quartz mines (Photo 1). These samples were taken from underground exposures and mineralized float on the mine dumps; they were assayed for their trace element content (Table 2A).
4. Pyrite-poor quartz veins, some of which contain minor quantities of galena and sphalerite. These includes samples from the BC, Proserpine, Warspite, Canusa, Black Bull, Standard Location and Perkins veins, as well as from some other unnamed vein occurrences. This outcrop and mine dump material was sampled and assayed for trace elements (Table 3A).
5. Igneous rocks: these are rare in the district. However, samples were taken from presumed metavolcanics of the Island Mountain Amphibolites southwest of Island Mountain (Figure 1) as well as from some altered intrusions recently intersected by drilling in the Mosquito Creek mine area. These samples were analysed for major and some trace elements to determine their composition and possible origin. The data will be published in full at a later date, but discrimination plots suggest that the Island Mountain Amphibolite rocks compositionally resemble tholeiitic ocean floor basalts while the intrusive rocks intersected in the drilling at Mosquito Creek are alkalic diorites.
6. Miscellaneous samples collected due to either their distinctive alteration (*e.g.* the presence of possible fuchsite-mariposite) or unusual sulphide content (*e.g.* massive galena from the Mosquito Creek mine dump). This data is presented in Table 3A.

In addition to the above, a heavy mineral pan concentrate sample collected by placer miner Mr. Wilfred Frederick from Lowhee Creek, southeast of Wells (Figure 1), was assayed. The results are presented in Table 4.

BONANZA LEDGE ZONE

Geology and Mineralogy

This newly discovered pyritic gold zone has been traced for over 130 m along strike and reaches widths up to 30 m. It is hosted by an overturned, northeast-dipping, predominantly clastic meta-turbidite sequence that possibly includes some highly altered carbonates and tuffaceous rocks. The sequence has been overprinted by muscovite-sericite, greenschist facies metamorphic assemblages and was affected by several episodes of ductile-brittle folding and later brittle fracturing (Rhys and Ross, 2000). The mineralization lies in structurally deformed and transposed footwall rocks below the northwest-trending BC quartz vein. This vein exceeds 700 m in length and reaches more than 15 m in width (Sutherland Brown, 1957). Most of the vein quartz is barren, but pyrite-rich pockets in the vein and sporadic pods and lenses along its margins have been historically mined for gold. The Bonanza Ledge Zone was discovered during a drilling program to test the BC Vein, and the generalized sequence as logged by the staff of International Wayside and Panterra Geoservices Inc. is as follows (Figures 3A and 3B; Rhys and Ross, 2000; Rhys, 2000):

1. Pale muscovite phyllite in the structural hangingwall with porphyroblasts of magnetite and lesser carbonate. This unit may form part of the Rainbow Member of Hanson (1935) and Hardscrabble Mountain Succession of Struik (1988a, 1988b).
2. White B.C. quartz vein. The vein margins are often marked by graphitic shears and the vein is locally cut out by brittle faulting.
3. Black carbonaceous phyllite with silty interbeds. This sequence is believed to belong to the BC Member of Hanson (1935).
4. Pale, well-laminated muscovitic pelites and phyllites with areas containing Fe-Mg carbonate (?dolomite) that occurs as laminae and pervasive, tan-colored zones. These rocks and the remaining footwall section are thought to belong to the Lowhee Member of Hanson (1935) (D. Rhys, personal communication, 2000). These unit 4 rocks in part host the auriferous Bonanza Ledge pyrite zones (Photos 5 to 9). Much of the dolomitic alteration is probably related to the mineralizing event, although some may be derived from original carbonate sediments.
5. The drilled footwall of the sequence comprises altered and sheared sedimentary phyllites and meta-turbidites that are locally well laminated with transposed bedding. The upper parts may host auriferous Bonanza Ledge pyrite mineralization. Locally, this unit and unit 4 above are altered and quartz-rich ("watery quartzite") with abundant parallel thin slivers of white and blue-grey quartz, some cross-cutting quartz and dolomitic veinlets, muscovite and trace rutile. Lower in the section there are sporadic disseminations and bands of pyrite and pyrrhotite, both of which tend to be barren.

The auriferous zones at Bonanza Ledge comprise between 5 and 75 percent fine to medium-grained pyrite that forms euhedral to subhedral crystals (Photos 5 to 9). These pyrite crystals reach up to 8 mm in diameter, but are mostly < 1.5 mm. Pyrite forms semi-massive layers up to 0.75 m thick, as well as thinner pods, stringers and folded veins. It can be fine grained and disseminated (Photo 5) or be concentrated in bands that follow either transposed

TABLE 1A
GEOCHEMICAL DATA OF SAMPLES FROM DRILLHOLES BC-2K-19&29
BONANZA LEDGE GOLD ZONE, WELLS-BARKERVILLE, B.C.
(FOR SAMPLE DESCRIPTION *SEE* TABLE 1B)

	Depth	Au	Au	As	Hg	Sb	Ba	Be	Bi	Cd	Ca	Ce	Cs	Cr	Co	Cu	Ga	Ge	La	Pb	Li	Mo	Ni	Nb	P	Rb
	in feet	ppb	g/tonne	ppm	ppb	ppm	ppm	ppm	ppm	ppm	%	ppm	ppm	ppm	ppm	ppm	ppm	ppm	ppm	ppm	ppm	ppm	ppm	ppm	ppm	ppm
Hole BC-2K-19																										
2K-19-1	58	<5	-----	7	<10	0.9	1210	2.7	1.4	0.12	0.36	102.5	11.25	86	22.8	<1	26.6	2.1	49	414	125.5	<0.2	37.4	3.8	680	182
2K-19-2	87	120	-----	228	<10	7	500	3.4	0.4	0.24	0.93	41.9	7.05	98	20.8	45	24.1	2.1	19.5	84.5	12.6	<0.2	39.8	2.8	510	210
2K-19-3	115	<5	-----	1	<10	0.3	1090	2.05	0.13	0.06	0.8	86.2	14.7	79	24.2	104	21.9	1.9	38.5	26.5	90.2	1	38.6	5	590	120
2K-19-4	135	255	-----	459	<10	1.2	190	2.3	0.85	0.18	7.57	36.6	9.75	107	19.4	1	21.9	1.3	17	19	13.2	9	76.8	2	2980	187.5
2K-19-5	141	20	-----	236	<10	0.6	960	2.35	0.11	0.26	11.75	73.6	5.75	300	35.6	<1	17.7	1	32.5	14.5	11.8	1.8	79.8	9.2	3350	149
2K-19-6	177	<5	-----	324	<10	0.7	1180	1.3	0.19	0.24	13.3	22	2.9	458	31.6	<1	12.9	0.6	10.5	12	5.8	0.2	139	2.6	790	96.2
2K-19-7	208	15	-----	303	<10	2	370	1.4	0.89	0.06	9.32	16.55	3.9	285	34.8	15	12	1	7.5	28	6.8	0.8	165.5	2.4	580	114.5
2K-19-8	230	20	-----	120	110	1.6	130	1.5	0.25	0.18	4.27	29.8	4.15	180	36.6	89	20.2	1.3	12.5	21.5	6.8	0.4	92.1	9.2	1500	146
2K-19-9	246	80	-----	598	<10	1.6	960	2.3	0.33	0.24	5.94	67.2	4.9	478	55.6	26	22.2	1.4	29	14	6.4	2.2	272	10	2350	189
2K-19-10	249	20	-----	96	<10	0.4	1210	1.9	0.14	0.08	0.32	73.5	4.1	62	11	14	18.1	1.9	33	14	6	0.4	29.6	2.8	400	134.5
2K-19-20	294	25000	25	876	2370	1.4	1720	3.9	5.15	0.16	2.74	32.6	7.4	44	91.7	7	29.5	1.9	14.5	39.5	8.2	0.8	152.5	12.6	1790	246
2K-19-21	323	8300	-----	953	1110	0.8	2360	3.35	7.56	<0.02	1.62	87.8	7.45	77	78.2	8	32.4	1.8	39.5	43.5	11.6	0.8	159.5	2.6	570	257
2K-19-22	318	1505	-----	729	270	0.7	2600	4.1	7.06	0.02	0.53	87.5	8	111	89.2	4	35.9	2.1	39	20.5	13	1	154	2.4	600	300
2K-19-23	309	31800	31.8	845	4350	5.2	1180	3.1	7.22	0.04	0.34	47.7	6.9	68	36.2	16	27.7	1.5	19.5	61	9.2	1	88.4	1.4	380	238
2K-19-11	333	<5	-----	26	<10	0.4	3210	3.2	0.07	0.24	6.69	55.5	6.95	46	8.2	19	30.1	1.8	23.5	13.5	13.4	0.8	15.6	17.8	1670	232
2K-19-12	350	10	-----	293	20	0.7	580	1.3	0.13	0.2	3.55	21.8	4.15	170	43	83	17.8	1.5	9.5	8.5	6.2	<0.2	80.5	5.4	970	134.5
2K-19-13	365	4740	-----	708	6610	2.8	1670	2.1	12.85	0.1	1.82	58.5	5.05	57	36.8	13	17.9	1.2	25.5	45.5	6.6	2	71	1	960	149
2K-19-14	393	545	-----	240	3670	2.2	1170	3.9	11.5	0.18	0.35	109	8.3	118	31.8	15	35.5	2.1	45.5	21.5	11.6	0.8	69.5	2	680	276
2K-19-15	398	475	-----	146	1750	1.1	1300	4.25	6.43	0.18	0.22	118.5	8.8	139	29.2	17	38.2	2.3	48.5	19.5	13.8	0.6	57.3	2.4	760	315
2K-19-16	426	10	-----	83	110	2.2	110	2.05	0.18	0.24	0.47	24.3	5.4	904	90.6	94	25.1	2	10	13	6.8	1.6	419	5.6	1940	187
2K-19-17	453	5	-----	8	<10	0.4	1280	1.7	0.2	0.12	0.15	81.5	4.6	70	12.8	28	22.6	1.9	37.5	33	8.6	1.8	24.4	4.4	420	162.5
2K-19-18	465	10	-----	24	<10	0.5	330	1.55	0.63	0.08	0.29	65.2	4.65	64	18.2	28	20.2	1.8	28.5	17.5	9.2	1	29.2	2.2	450	149
2K-19-19	498	5	-----	5	<10	0.1	670	1.3	0.25	<0.02	0.31	76.8	3.3	49	10	18	15.9	1.7	34.5	15.5	9.6	0.6	21.4	2.4	280	115
Hole BC-2K-29																										
2K-29-1	55	70	-----	57	10	6.2	1320	2.35	0.17	0.06	0.34	100.5	9.8	93	27.6	15	27.6	2.3	43.5	9	17	<0.2	43.8	5.2	670	247
2K-29-2	78	180	-----	105	<10	1.8	1460	2.2	0.38	0.5	6.66	58	6.2	96	15.4	18	16.3	1.6	28	96	72.6	1.6	41	4.4	840	123.5
2K-29-3	89	75	-----	34	<10	0.6	40	<0.05	1.15	0.02	0.22	1.92	0.35	16	1.8	5	0.5	3.4	0.5	8	11.6	0.2	6.6	<0.2	130	4
2K-29-4	116	20	-----	228	<10	1.6	1040	1.55	0.1	0.2	6.6	43.3	3.4	294	34.6	65	18.2	1.3	19.5	8	9.6	1	81.6	9.8	1200	153
2K-29-5	166	80	-----	116	450	2.5	230	1.15	0.22	0.24	2.57	33.2	3.2	40	44	70	22.6	1.2	13.5	8	5.8	3.4	47.2	13.6	1830	183
2K-29-6	215	4210	-----	847	3660	1.8	1710	3.25	11.4	0.12	1.7	34.7	5.85	71	82.6	<1	29.4	1.7	13.5	19	10.6	2.2	175	8.2	3070	184
2K-29-19	219	100	-----	139	4590	2.3	1990	2.05	0.74	0.16	0.91	31.4	4.65	60	44	33	22.1	1.9	12	9	9	5.4	59.5	11.6	2810	138.5
2K-29-18	225	405	-----	121	2510	1.8	530	2.95	3.47	0.12	1.34	34	5.6	58	43.8	8	24.8	2	13	13	12	3.4	66.5	11.4	2960	171
2K-29-17	235	14000	14	1180	3230	1.5	1280	2.6	5.36	0.1	0.89	45.4	4.6	29	110	26	27.3	1.5	18	86.5	7	0.8	309	12	2510	198
2K-29-20	243	24800	24.8	1295	2030	1.1	530	1.65	11.2	0.24	1.98	35.1	3.9	58	63.2	42	18.9	1.2	14	129.5	5	1.4	170	5.2	1010	132.5
2K-29-7	271	20	-----	44	440	0.7	1630	0.9	0.16	0.14	0.7	59.9	3.5	41	37.6	229	28.3	1.8	26.5	5.5	4.2	0.4	57.4	24.2	2320	97.2
2K-29-8	294	20	-----	182	1700	5.5	230	1	0.03	0.18	1.38	20.6	4.1	93	59.4	113	22.5	1.7	8	5.5	6.2	1	96.3	8.6	1220	172
2K-29-9	327	15	-----	75	5100	2.7	250	0.9	0.03	0.18	0.84	23.5	4.1	33	45.8	146	23.1	1.5	7.5	6.5	6.2	1.6	47.4	12.4	1960	104
2K-29-10	344	15	-----	103	1160	3	340	1.55	0.05	0.1	0.78	28.3	4.95	58	26.6	44	21.6	1.6	11.5	4	8.2	0.8	27	12.4	2970	123.5
2K-29-11	371	5	-----	119	80	0.9	1630	1.45	0.01	0.06	0.95	56.4	4.5	40	32.2	99	27.9	1.8	25	3	6.2	0.4	48	22.6	2420	130
2K-29-12	390	10	-----	131	320	0.4	2370	1.8	0.06	0.12	3.52	21.5	5.3	181	24.8	18	19.5	1.5	10	3	7.4	<0.2	60.5	7.2	600	152.5
2K-29-13	410	5	-----	80	30	0.5	2130	1.75	0.01	0.16	2.54	46.7	3.9	37	22	97	19.7	1.3	21	3	6	0.2	24.6	16	1280	104
2K-29-14	430	45	-----	170	930	0.7	260	1.75	0.42	0.1	0.89	37.5	4	48	28.2	85	20.9	1.6	14	5	6.6	0.4	41.2	12.6	1860	114.5
2K-29-15	451	<5	-----	30	<10	0.2	2630	5.25	0.02	<0.02	0.47	227	8.7	117	2.8	<1	47.1	2.2	99	8	10.8	0.2	7.2	6.2	830	357
2K-29-16	480	40	-----	75	<10	0.1	620	1.35	0.09	0.04	0.08	60	2.35	39	7.2	19	11.8	1.7	25	5.5	4.2	0.2	14.6	1.8	300	96.4

TABLE 1A CONTINUED
GEOCHEMICAL DATA OF SAMPLES FROM DRILLHOLES BC-2K-19&29
BONANZA LEDGE GOLD ZONE, WELLS-BARKERVILLE, B.C.

SAMPLE	Depth in feet	Ag ppm	Sr ppm	Ta ppm	Te ppm	Tl ppm	Th ppm	W ppm	U ppm	V ppm	Y ppm	Zn ppm	Al2O3 %	CaO %	Cr2O3 %	Fe2O3 %	K2O %	MgO %	MnO %	Na2O %	P2O5 %	SiO2 %	TiO2 %	LOI %	TOTAL %
Hole BC-2K-19																									
2K-19-1	58	1.35	128.5	0.25	<0.05	0.82	13.4	0.6	1.6	119	7	112	18.68	0.51	<0.01	9.12	4.25	2.01	0.11	1.24	0.18	54.84	1.30	6.76	99.00
2K-19-2	87	0.4	109	0.15	<0.05	0.88	9.2	1.9	1.8	143	5.9	60	17.84	1.35	<0.01	7.58	5.08	1.66	0.16	0.37	0.14	56.48	1.32	6.84	98.82
2K-19-3	115	0.4	89.5	0.3	<0.05	0.6	11.6	0.8	2	111	6.6	112	15.17	1.16	<0.01	7.97	2.90	2.09	0.20	0.82	0.17	59.02	1.29	8.27	99.06
2K-19-4	135	0.3	591	0.1	<0.05	1.14	7.4	5.6	2.6	377	19.7	36	16.27	11.15	<0.01	10.40	4.57	5.34	0.22	0.20	0.74	26.22	0.69	17.05	92.85
2K-19-5	141	0.2	628	0.45	<0.05	0.78	4.4	11.2	1.4	218	21.7	36	10.07	16.60	0.02	9.36	2.90	6.41	0.28	0.16	0.79	24.47	2.58	21.18	94.82
2K-19-6	177	0.05	450	0.1	<0.05	0.48	1.2	4.2	0.8	200	9.6	56	8.96	18.66	0.04	8.41	2.60	9.11	0.19	0.18	0.20	21.16	1.42	23.21	94.14
2K-19-7	208	0.3	300	0.05	<0.05	0.74	1.2	4.4	0.8	169	5.7	52	11.38	13.28	0.04	8.46	3.33	5.62	0.19	0.14	0.17	34.35	0.76	14.53	92.25
2K-19-8	230	0.25	270	0.5	<0.05	1.34	2.4	4.5	0.2	228	6.8	92	14.02	6.18	0.02	11.36	3.69	4.14	0.13	0.83	0.37	42.13	2.59	13.03	98.49
2K-19-9	246	0.3	403	0.6	0.05	1.48	4.2	8.8	2.4	253	14.5	82	15.16	8.84	0.06	12.17	4.68	6.39	0.25	0.24	0.60	24.89	3.51	16.01	92.80
2K-19-10	249	0.15	68.7	0.2	0.1	1.3	17.4	1.6	2.6	64	7.1	46	12.70	0.46	<0.01	4.55	3.57	1.44	0.04	0.23	0.12	70.48	0.59	5.10	99.28
2K-19-20	294	1.75	248	0.75	0.05	4.74	3.8	14.2	0.8	280	11.8	22	20.03	4.09	<0.01	19.42	6.43	1.98	0.09	0.24	0.49	25.87	4.02	15.94	98.60
2K-19-21	323	1.2	179	0.2	<0.05	5.02	15.2	4.1	3.4	128	10.1	10	22.31	2.25	<0.01	19.52	6.50	1.58	0.07	0.37	0.16	30.26	0.99	14.76	98.77
2K-19-22	318	0.65	117.5	0.15	0.15	4.66	15	5.1	4	157	9.5	10	25.77	0.71	<0.01	15.15	7.69	0.92	0.02	0.36	0.17	34.20	1.29	11.86	98.14
2K-19-23	309	8.55	77	0.05	0.05	7.54	15	3.3	3.6	128	8.4	16	20.57	0.51	<0.01	26.41	6.55	0.73	0.01	0.29	0.12	26.07	1.09	16.22	98.57
2K-19-11	333	0.35	559	0.95	<0.05	3.52	4.4	9.7	0.8	329	22.1	32	21.47	10.07	<0.01	5.41	6.36	4.66	0.26	0.45	0.41	27.33	3.30	14.13	93.85
2K-19-12	350	0.2	193	0.3	0.1	1.84	1.6	4.1	0.2	215	4.2	56	14.35	5.23	0.01	10.53	4.17	3.53	0.20	0.21	0.25	47.04	1.86	11.11	98.49
2K-19-13	365	1.15	162	0.05	0.3	6.14	8.6	2	1.8	91	8.6	12	13.74	2.60	<0.01	35.72	4.11	1.36	0.06	0.15	0.22	17.65	0.71	22.28	98.60
2K-19-14	393	0.4	84.5	0.15	0.2	13.6	19.4	4	5.2	143	8.6	50	27.44	0.48	<0.01	13.28	8.03	0.83	0.01	0.33	0.21	36.38	1.16	11.11	99.26
2K-19-15	398	0.25	90.3	0.2	0.05	9.02	20.8	3.3	4.6	143	8.8	64	27.30	0.27	0.04	13.05	8.11	0.70	<0.01	0.40	0.20	36.64	1.29	10.71	98.71
2K-19-16	426	0.2	100.5	0.3	<0.05	4.44	2	2.7	3.2	307	5.9	98	18.99	0.67	0.20	11.16	5.39	0.96	0.03	0.43	0.48	47.65	3.71	8.98	98.65
2K-19-17	453	0.2	84.1	0.3	<0.05	2.42	13.8	1.5	3.2	91	5.8	66	15.92	0.20	0.08	3.74	3.59	0.85	0.01	0.26	0.10	68.88	0.70	4.64	98.97
2K-19-18	465	0.15	96.9	0.15	0.05	1.94	12.2	2.4	3.4	75	5.5	76	15.09	0.38	0.09	5.50	3.57	1.13	0.01	0.37	0.11	66.34	0.62	5.81	99.02
2K-19-19	498	0.05	77.4	0.15	<0.05	1.24	17.4	0.7	3.8	53	6.3	62	11.12	0.42	0.04	5.08	2.79	1.51	0.04	0.32	0.08	71.80	0.50	5.25	98.95
Hole BC-2K-29																									
2K-29-1	55	0.25	91.8	0.3	<0.05	1.32	14	1.7	2	150	7.1	118	18.17	0.49	<0.01	9.25	5.21	2.29	0.11	0.38	0.17	52.54	1.39	8.38	98.38
2K-29-2	78	0.35	267	0.2	<0.05	0.7	9.6	6.1	1.6	127	9.2	72	11.37	8.85	<0.01	5.68	2.94	3.80	0.13	0.18	0.20	53.21	0.55	11.70	98.61
2K-29-3	89	0.15	12.2	<0.05	<0.05	0.02	0.2	0.7	0.2	9	0.9	2	0.88	0.25	<0.01	0.82	0.12	0.07	0.01	<0.01	0.06	96.10	0.03	0.82	99.16
2K-29-4	116	0.2	253	0.35	<0.05	0.66	3.6	6	2	218	8.7	44	12.46	9.81	<0.01	7.67	3.72	4.96	0.20	0.09	0.30	44.08	1.98	13.44	98.71
2K-29-5	166	0.3	116	0.7	<0.05	1.44	2.6	5.3	1	267	7.1	90	14.22	3.62	<0.01	13.82	4.59	2.31	0.14	0.15	0.44	43.60	3.07	12.70	98.66
2K-29-6	215	0.7	103.5	0.45	0.5	6.08	2	8.3	0.6	240	11	30	21.02	2.39	<0.01	20.32	6.78	1.19	0.09	0.30	0.77	27.72	3.38	14.40	98.36
2K-29-19	219	0.3	97.4	0.6	<0.05	4.78	2	4.9	0.2	206	6.6	50	17.21	1.22	<0.01	12.49	5.26	1.19	0.04	0.26	0.66	48.12	2.61	9.72	98.78
2K-29-18	225	0.35	110.5	0.75	0.05	4.3	3.2	7.6	1.6	189	9.2	52	18.24	1.94	<0.01	9.51	5.55	1.02	0.05	0.23	0.73	50.36	2.72	8.16	98.51
2K-29-17	235	1.8	64.6	0.65	0.05	2.38	3.4	12.4	1	340	9	22	19.39	1.32	<0.01	25.03	6.36	0.56	0.04	0.20	0.61	24.97	4.53	15.54	98.55
2K-29-20	243	3.25	92.8	0.25	<0.05	2.46	2.8	7.8	0.6	227	6.3	42	12.40	3.10	<0.01	35.92	3.92	1.33	0.12	0.04	0.27	15.87	3.09	22.46	98.52
2K-29-7	271	0.5	115	1.25	<0.05	2.26	4.4	0.7	<0.2	289	6.8	80	18.48	1.05	<0.01	9.68	3.12	1.30	0.15	4.55	0.63	48.60	4.10	7.41	99.07
2K-29-8	294	0.2	100.5	0.5	<0.05	7.2	1.6	1.5	<0.2	224	4.2	138	16.06	2.02	<0.01	14.96	3.88	2.26	0.16	1.12	0.31	43.20	2.46	12.30	98.73
2K-29-9	327	0.25	72.5	0.65	<0.05	8.66	1.8	1.3	0.2	269	5.9	84	13.97	1.18	<0.01	19.25	3.28	1.04	0.08	2.18	0.50	41.51	3.35	12.29	98.63
2K-29-10	344	0.2	102	0.7	<0.05	5.2	2	3.9	<0.2	202	7.4	60	17.80	1.08	<0.01	11.43	4.44	1.76	0.14	2.02	0.73	47.60	2.75	9.09	98.84
2K-29-11	371	0.3	121.5	1.2	<0.05	2.8	4	4.1	<0.2	336	7.3	94	17.82	1.45	<0.01	10.07	3.52	2.10	0.12	3.51	0.57	46.91	4.06	8.51	98.64
2K-29-12	390	0.1	181.5	0.35	<0.05	2.62	1.6	3.8	<0.2	155	3.9	38	14.77	5.16	<0.01	8.71	3.98	3.67	0.13	0.91	0.16	48.04	1.85	11.10	98.48
2K-29-13	410	0.2	168	0.8	<0.05	3.08	3	5.2	<0.2	238	4.9	96	15.53	3.93	<0.01	12.60	3.36	3.69	0.22	1.66	0.35	42.15	2.99	12.91	99.39
2K-29-14	430	0.25	105	0.6	<0.05	5.82	2.2	3.6	0.2	180	5.9	62	12.86	1.25	<0.01	12.49	3.65	2.26	0.16	0.26	0.47	52.18	2.79	10.23	98.60
2K-29-15	451	0.1	112.5	0.4	<0.05	3.8	36.4	4.3	6.8	131	12	14	34.33	0.65	<0.01	1.15	10.43	0.91	0.02	0.49	0.25	44.36	1.22	4.88	98.69
2K-29-16	480	0.15	36.4	0.1	<0.05	1.02	13.8	1	2	39	5.4	36	9.87	0.12	<0.01	4.14	2.76	1.15	0.05	0.10	0.08	76.17	0.44	4.13	99.01

All sample analysed by ALS Chemex, Aurora Laboratory Services Ltd., 212 Brookbank Ave, Vancouver, BC, V7J 2C1
Methods used for all data in this table: Major oxides = XRF.
Au = Fire assay and AA finish; As = AAS; Hg by cold vapour with ICP-MS rechecks. Other elements = ICP-MS

TABLE 1B
DESCRIPTION OF SAMPLES FROM HOLES BC-2K-19 & 29
BONANZA LEDGE GOLD ZONE, WELLS-BARKERVILLE
(*SEE* TABLE 1A)

Hole BC-2K-19 Sample	Depth in feet	DESCRIPTION
2K-19-1	58	Light tan hangingwall phyllite with disseminated magnetite porhyroblasts
2K-19-2	87	Light tan hangingwall phyllite with dolomite veins & minor magnetite porphyroblasts
2K-19-3	115	Light tan hangingwall phyllite without magnetite porphyroblasts
2K-19-4	135	Black graphitic sheared phyllite with disseminated pyrite & dolomitic porphyroblasts
2K-19-5	141	Tan dolomitic metasediment with dolomite veins & disseminated pyrite cubes
2K-19-6	177	Gritty dolomitic metasediment with pyrite porphyroblasts & fuchsite along shears
2K-19-7	208	Gritty dolomitic metasediment with fuchsite & disseminated pyrite cubes
2K-19-8	230	Gritty dolomitic metasediment with dolomite porphyroblasts & trace rutile
2K-19-9	246	Blue-grey "watery quartzite" unit with disseminated coarse pyrite cubes & dolomite veins
2K-19-10	249	Blue-grey "watery quartzite" unit with coarse pyrite cubes
2K-19-20	294	Semi-massive to stringer pyrite with sericite, carbonate and minor rutile
2K-19-21	323	Semi-massive to stringer pyrite with sericite
2K-19-22	318	Semi-massive to stringer pyrite with sericite
2K-19-23	309	Massive to semi-massive pyrite with sericite, dolomite and trace tourmaline & rutile
2K-19-11	333	Tan phyllite with dolomite and calcite veinlets
2K-19-12	350	Laminated tan phyllite with pyrite layers and quartz veinlets
2K-19-13	365	Tan, sericitic phyllite with blebs & veins of pyrite
2K-19-14	393	Dark muscovitic phyllite with disseminated pyrite
2K-19-15	398	Dark muscovitic phyllite with disseminated pyrite
2K-19-16	426	Brown-tan mottled metasediment with pyrite stringers and fuchsite-shears
2K-19-17	453	Dark, folded phyllite with disseminated coarse pyrite cubes
2K-19-18	465	Black, folded phyllite with pyrite cubes
2K-19-19	498	Pale layered gritty metasediment with pyrite cubes
Hole BC-2K-29		
2K-29-1	55	Bleached hangingwall sericitic phyllites with disseminated magnetite porphyroblasts
2K-29-2	78	Black graphitic phyllite close to hangingwall contact of the BC quartz vein
2K-29-3	89	White BC quartz vein with minor dolomite, pyrite & graphite
2K-29-4	116	Tan, dolomitic and fractured phyllite with fuchsite along shears
2K-29-5	166	Tan & blue-grey sericitic metasediment with disseminated pyrite cubes
2K-29-6	215	Tan sericitic metasediment with pyrite stringers and disseminated dolomite & pyrite porphyroblasts
2K-29-19	219	Sericitic phyllite with stringer and blebs of pyrite
2K-29-18	225	Semi-massive and stringer pyrite with quartz & abundant sericite
2K-29-17	235	Semi-massive pyrite with abundant muscovite-sericite & trace rutile
2K-29-20	243	Massive to semi-massive pyrite with sericite & trace rutile
2K-29-7	271	Grey to tan, thinly laminated sericitic metasediment with dolomitic and albitic veinlets
2K-29-8	294	Light grey laminated metasediment with dolomite veinlets & fuchsite on shears
2K-29-9	327	Grey, laminated and thin bedded metasediment with layers rich in pyrite, quartz and feldspar
2K-29-10	344	Light grey, weakly foliated sericitic metasediment with disseminated pyrite & mottled brown carbonate
2K-29-11	371	Light grey, weakly foliated metasediment with disseminated pyrite & carbonate, albite & trace rutile
2K-29-12	390	Light grey to purple, weakly foliated metasediment with mottled yellow-brown dolomite
2K-29-13	410	Light grey to purple, weakly foliated metasediment with mottled yellow-brown dolomite
2K-29-14	430	Grey-purple metasediment with thin pyrite & dolomite layers
2K-29-15	451	Light grey, talcose & micaceous phyllite
2K-29-16	480	Light grey quartz-muscovitic phyllite

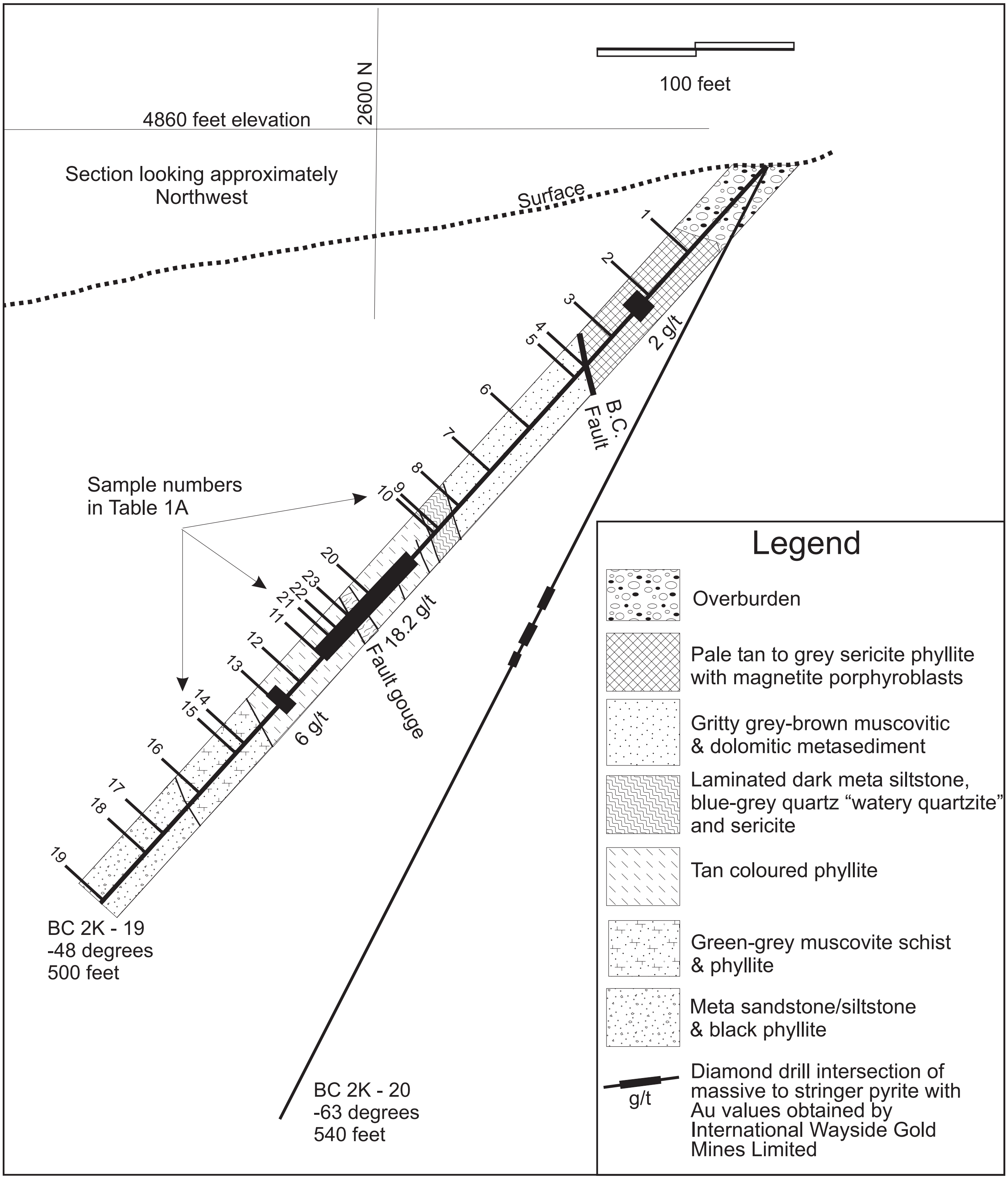

Figure 3A. Simplified drill logs of hole BC-2K-19, Bonanza Ledge Gold Zone, showing location of the sample data presented in Tables 1A and 1B. Logging by K. Ross, Panterra Geoservices Inc.

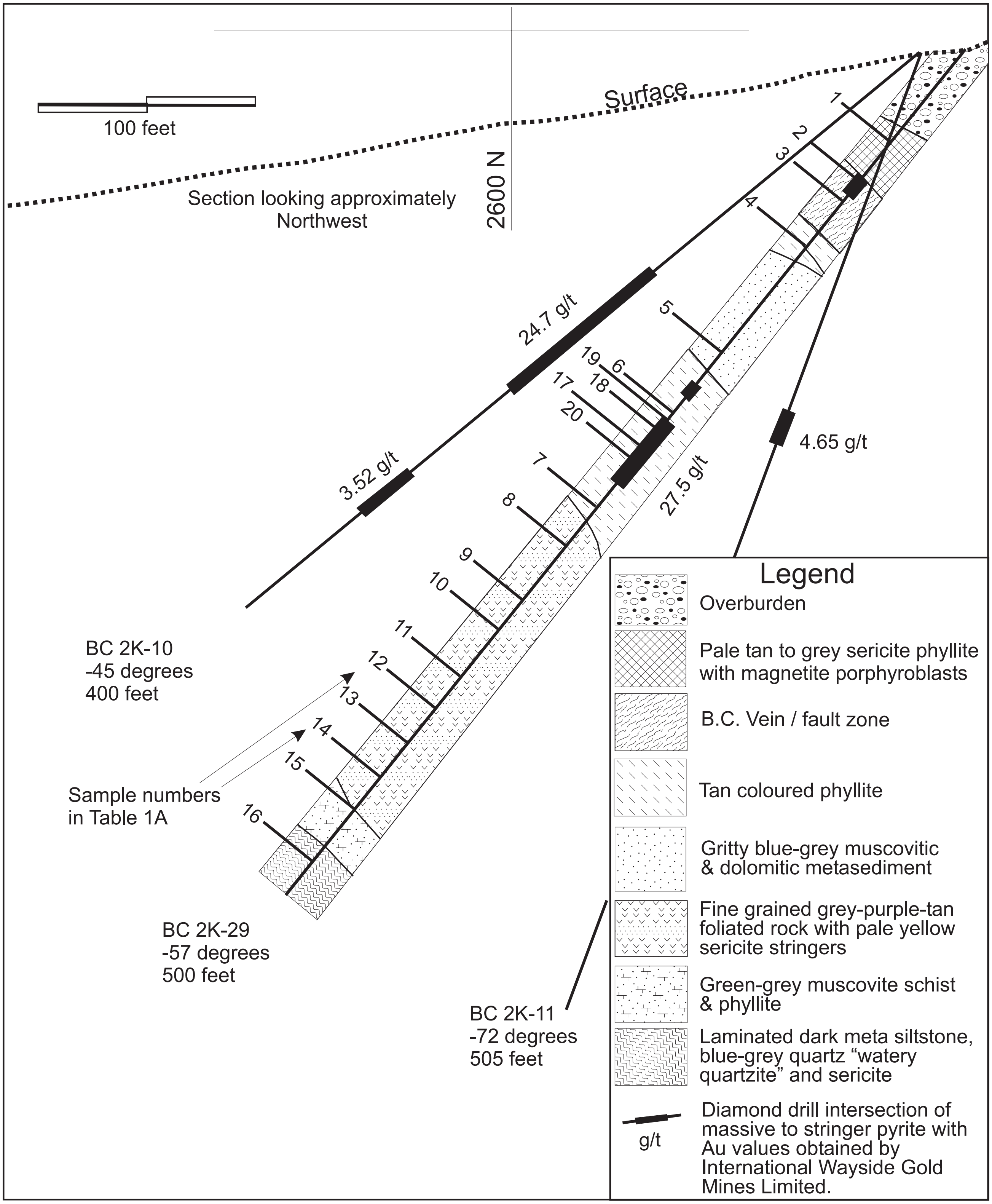

Figure 3B. Simplified drill logs of hole BC-2K-29, Bonanza Ledge Gold Zone, showing location of the sample data presented in Tables 1A and 1B. Logging by K. Ross, Panterra Geoservices Inc.

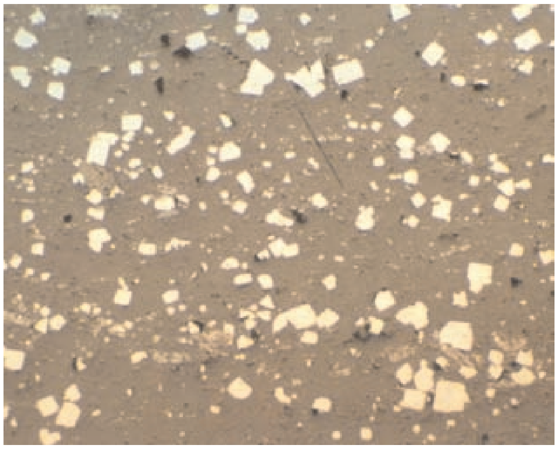

Photo 5. Small euhedral crystals of disseminated pyrite in a schistose gangue dominated by sericite, carbonate and accessory rutile, Bonanza Ledge Zone. Sample BC-2K-19-20 assaying 25 g/t Au, from drill hole BC-2K-19 at 294 feet. Photomicrograph, reflected light, uncrossed polars, and long field of view is 2 mm.

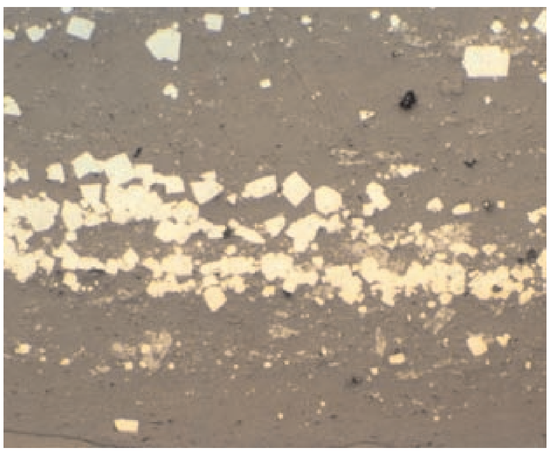

Photo 6. Trails of small euhedral pyrite crystals growing along phyllitic cleavages, Bonanza Ledge Zone. Sample BC-2K-19-20, drill hole BC-2K-19 at 294 feet. Photomicrograph, reflected light, uncrossed polars, and long field of view is 2 mm.

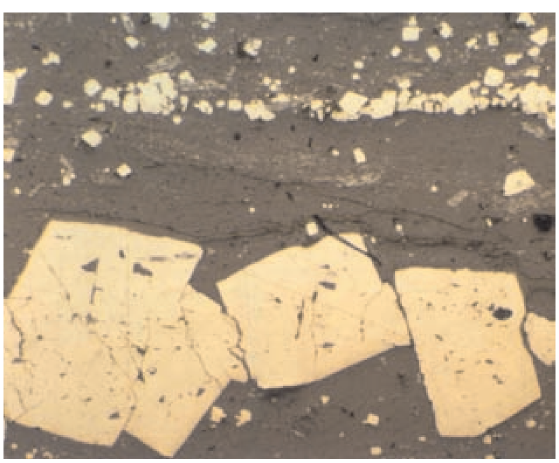

Photo 7. Trails of coarse and fine grained euhedral pyrite crystals growing along phyllitic cleavages, Bonanza Ledge Zone. Sample BC-2K-19-20, drill hole BC-2K-19 at 294 feet. Photomicrograph, reflected light, uncrossed polars, and long field of view is 2 mm.

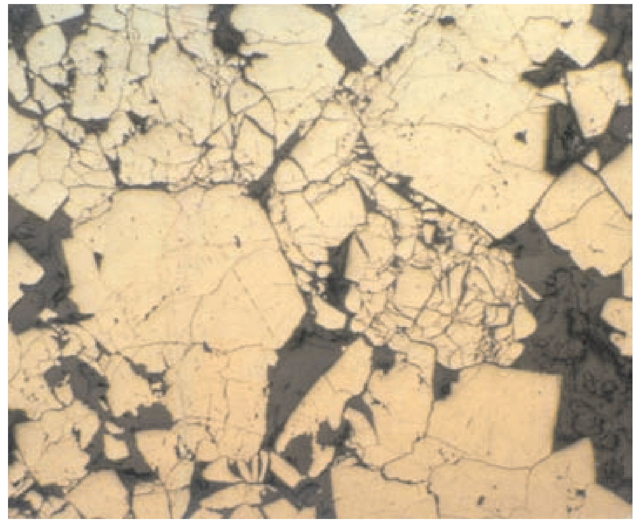

Photo 8. Coarse grained and weakly brecciated subhedral pyrite crystals, Bonanza Ledge Zone. Sample BC-2K-19-23 assaying 31.8 g/t Au, drill hole BC-2K-19 at 309 feet. Photomicrograph, reflected light, crossed polars, and long field of view is 1.5 mm.

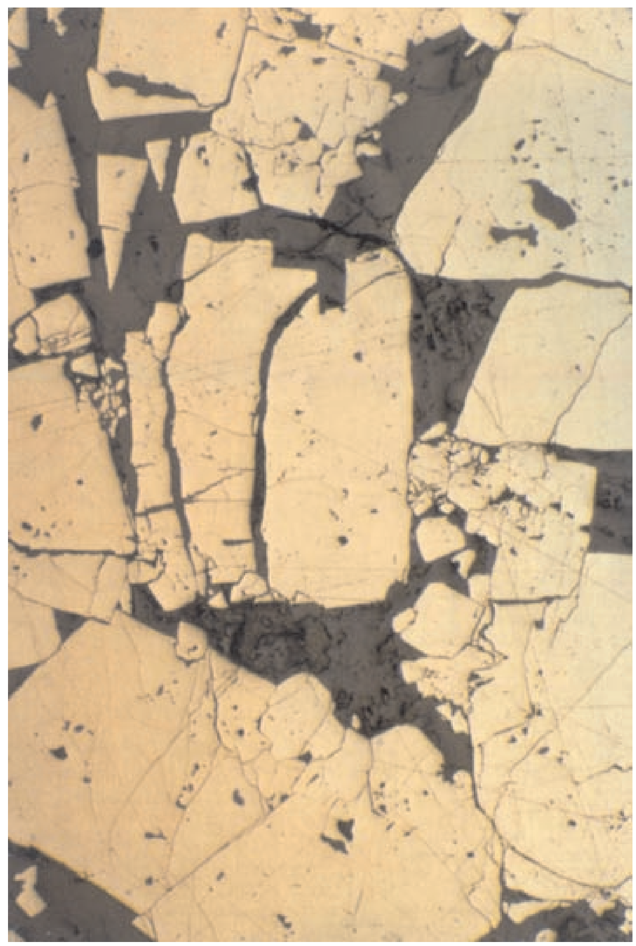

Photo 9. Coarse grained, shattered and subhedral pyrite crystals in a carbonate-sericite gangue, Bonanza Ledge Zone. Sample BC-2K-19-23, drill hole BC-2K-19 at 309 feet. Photomicrograph, reflected light, crossed polars, and long field of view is 2.5 mm.

bedding or the S2 phyllitic foliation (Photos 6 and 7). Some of the larger pyrite crystals have undergone moderate brecciation (Photos 8 and 9). On the small scale, much of the pyrite appears to be concordant to the transposed bedding, although cross-cutting veins and stringers are common. On a larger scale, however, the auriferous pyrite zones and the BC Vein are discordant to the stratigraphy (D. Rhys, personal communication, 2000). Locally, the pyritic rock may be schistose and comprise thin (0.5 cm) layers of disseminated pyrite that alternate with layers containing over 70 percent white mica and carbonate. Grades commonly range up to 40 g/t Au although some pyritic intersections contain up to 80 g/t Au. Gold forms 2.5 to 60 µm native grains that occur either: (1) along pyrite crystal boundaries (2) along microfractures in the pyrite, or (3) as micron-sized particles encapsulated in the Fe sulphides (Rhys and Ross, 2000; Rhys, 2000). These authors also report that the Au may be associated with chalcopyrite and galena, although the mineralization only averages 14.6 ppm Cu and 55 ppm Pb (Tables 1A and 2B) .

The gangue includes abundant muscovite-sericite, Fe-Mg carbonate and quartz, together with rutile and sporadic trace tourmaline. In some samples, rutile makes up to 2 percent by volume, forming dark brown, subhedral crystals up to 0.15 mm long or brown euhedra less than 25 microns in length. In some microshears, it may be intergrown with abundant, fine sericite and tourmaline. The latter mineral forms small euhedral prisms up to 0.1 mm in length. The cores of some crystals have a dark colour zoning, with a khaki-green pleochroism suggesting an intermediate dravite-schorl composition (C. Leitch, personal communication, 2000). The auriferous pyritic zones are enveloped by pale and barren alteration that has bleached and overprinted some of the originally dark, organic-rich phyllitic units. This includes some pervasive sericite-carbonate assemblages and zones of blue-grey "watery quartz" veinlet alteration that marks silicificification (Figures 3A and 3B, Rhys and Ross, 2000). Micaeous shear zones both in and outside the pyritic zones are locally marked by green fuchsite-mariposite alteration that contains weakly elevated values of Cr (up to 904 ppm Cr; Tables 1A and 1B).

Chemistry of the Bonanza Ledge Mineralization and its Alteration Envelope

To test the chemistry of the auriferous pyrite horizons and the adjacent altered wallrocks, 43 samples were collected from drillholes BC-2K-19 and BC-2K-29 that intersect well-mineralized portions of the Bonanza Ledge Zone (Figures 3A and 3B). Samples were taken not only from the pyrite, but also from the other altered and barren units in the hanging and footwall parts of the holes (Figures 3A and 3B).

The samples were analysed for their major oxide and trace element contents and the data, together with the downhole depth of each sample are presented in Tables 1A and 1B and in Figures 4 and 5. Both holes intersected two gold-bearing pyrite zones that are separated by barren interlayers (Figures 4A and 4C). The auriferous pyritic zones are characterized by higher quantities of Fe (between 13 and 36 percent Fe_2O_3 as total iron), K_2O and Al_2O_3 reflecting the abundance of pyrite and sericite-muscovite. They also coincide with increased amounts of Hg, Bi, As, and Pb, and lower quantities of Zn, Cu, CaO, MgO and SiO_2 (Figure 4). Elevated Hg values (up to 6610 ppb) occur not only in the aurifeous pyrite, but may extend well down into the barren footwall rocks (Table 1A; Figures 4C and 5B). Higher Hg values coincide with core intersections containing > 13 percent Fe_2O_3 as total iron. This suggests that the Hg is hosted by pyrite, whether or not the sulphide is auriferous or barren.

Some parts of both holes contain > 4 percent TiO_2 which represent intersections particularly rich in rutile (Figure 4A). However, TiO_2 enrichment is generally absent in the auriferous horizons but occurs sporadically in the footwall and hanging wall rocks. Dolomitic alteration, marking either original sedimentary carbonate or the results of overprinting is best developed in the hanging wall where it is associated with increased MgO and CaO values (Figure 4B).

Comparative binary plots of the geochemistry in the two Bonanza Ledge drill holes are presented in Figures 5A and 5B. These, together with Figures 4A to 4C, further demonstrate the moderate to strong positive correlations that exist between Au and some other elements such as Fe, As, Bi, Pb, Ag, K_2O and Al_2O_3, and the negative relationship between Au and Zn and Au and Cu. The negative association between Cu and Ag and positive correlation between Au and Ag (Figure 5A) suggests that Ag is hosted in the Au.

To summarize, data in Tables 1A, 2B and 2D indicate that, compared to the Mosquito Creek replacement ore, the Bonanza Ledge mineralization contains higher quantities of Cu and Hg and lower amounts of Ag, As, Sb, Bi, Pb and W. At Bonanza Ledge, strong correlations between Au:Bi, Au:As, Au:Ag and Au:K_2O are noted, and poor correlations exist between Au:Zn and Au:Cu. The Au/Ag ratios of our mineralized Bonanza Ledge samples average 6.6; by contrast, Au/Ag ratios in the Mosquito Creek replacement ore averages 3.1 (Table 2D).

COMPARATIVE CHEMISTRY AND MINERALOGY OF THE BONANZA LEDGE, MOSQUITO CREEK AND CARIBOO GOLD QUARTZ MINERALIZATION

The Mosquito Creek, Island Mountain and Cariboo Gold Quartz deposits all contain two types of auriferous pyrite: massive pyrite in replacement ore and pyrite associated with quartz veins (Hanson, 1935; Skerl, 1948; Runkle, 1950; Sutherland Brown, 1957, 1963; Alldrick, 1983; Robert and Taylor, 1989).

For this study, material representing both pyritic quartz veins and massive replacements were collected from the Mosquito Creek and Cariboo Gold Quartz underground mine workings and the mine dumps. The analytical data of these samples together with data for the pyritic mineralization from the Bonanza Ledge drill holes (Figures 3A and 3B) are presented in Tables 1 and 2.

Superficially, the pyrite in and along the margins of the quartz veins appears to be similar in all the mines and occurrences. However, the analytical data for the quartz vein pyrite reveal some geochemical differences between samples from veins at the Mosquito Creek and Cariboo Gold Quartz mines (Table 2A and 2D). Although the quartz vein pyrite in both mines has a similar Fe content (avg. 20-24 percent Fe) and Au grade (avg. 27-28 g/t Au, Tables 2A and 2D), the pyrite in the Mosquito Creek quartz veins has higher quantities of Ag, As, Sb, Pb, Zn, Al and W. It also contains higher averages of elements such as Ce, La, Li, Mn, Te and Ga, as well as having higher As/Au ratios than pyrite in veins at the Cariboo Gold Quartz mine. Although Skerl (1948) reports chalcopyrite in the Cariboo Gold Quartz Mine, all our pyritic vein samples from this deposit and from Mosquito Creek have a very low Cu content, averaging 1.3 and 3.6 ppm Cu at Mosquito Creek and Cariboo Gold Quartz respectively (Tables 2A and 2D). The Cariboo Gold Quartz vein pyrite is also distinguished from the Mosquito Creek ore in having higher Au/Ag ratios (avg. 9.7 versus 2.4).

To the naked eye, the massive replacement pyrite bodies at Mosquito Creek, Island Mountain and Bonanza Ledge appear similar in many of their features. However, there are a number of notable differences between the mineralization at Bonanza Ledge on the one hand and the Mosquito Creek and the Island Mountain mineralization on the other. These differences include:

1. Size: the replacement pyritic ore bodies at Mosquito Creek and Island Mountain tend to be smaller, reaching up to 3 m in thickness, 6 m in width and 30 to several hundred metres in down-plunge length (Alldrick, 1983). By contrast the Bonanza Ledge mineralized zone reaches 30 m in width and 130 m in strike length.
2. Pyrite textures: from the limited polished thin sections examined, pyrite at Bonanza Ledge appears to have been more brecciated (Photos 8 and 9). At Mosquito Creek and Island Mountain, the pyrite includes crystals that are highly euhedral (Photo 10), as well as others with textures suggesting recrystallization and replacement. In some cases, large euhedral crystals appear to have partially overgrown and replaced an earlier generation of smaller, possibly brecciated pyrite crystals (Photos 11 and 12). The outer parts of some coarse pyrite crystals at Mosquito Creek contain growth zones marked by or trails of fine grained silicate inclusions (Photo 13; C. Leitch, personal communication, 2000).
3. Structural and stratigraphic position: the Mosquito Creek, Island Mountain and Bonanza Ledge mineralization all lie on the western, overturned limb of an F2 fold (Sutherland Brown, 1957; Alldrick, 1983; Struik, 1988a, 1988b; D. Rhys, personal communication, 2000). However, the Mosquito Creek orebodies are hosted by carbonate-bearing rocks of the Baker Member but tend to occur within 25 m of the contact between this member and the structurally underlying Rainbow Member (Alldrick, 1983). By contrast, the Bonanza Ledge mineralization and its alteration envelope appear to be spatially related to, but cut by, the BC Vein structure. Recent work (Rhys and Ross, 2000; Rhys, 2000) indicates the mineralization is folded and hosted by organic-rich argillites of the Lowhee Member of Hanson (1935). These hostrocks lie approximately 200 to 300 m below the Rainbow-Baker stratigraphic contact (Hanson, 1935; Sutherland Brown, 1957).
4. Host lithologies: the replacement-style mineralization at both the Mosquito Creek and Cariboo Gold Quartz mines tends to be hosted by limestones and thin bedded clastic sediments (Skerl, 1948; Sutherland Brown, 1957; Alldrick, 1983) while carbonaceous phyllites, with possible altered carbonates, are important host for the Bonanza Ledge pyritic mineralization (Rhys and Ross, 2000; Rhys, 2000).
5. Gangue mineralogies: different hostrock lithologies result in different gangue mineralogies at the various properties. Replacement pyritic mineralization at the Bonanza Ledge, Mosquito Creek and Island Mountain is marked by a gangue containing variable proportions of Fe-Mg carbonate, quartz and sericite, with trace rutile and some fracture-controlled trace fuchsite-mariposite. However, rutile is far more abundant at Bonanza Ledge, which also contains more sericite-muscovite and trace quantities of tourmaline.
6. Chemistry: the analytical data presented below demonstrates there are significant chemical differences between the replacement mineralization at Mosquito Creek and Bonanza Ledge (Table 2, Figures 6A to 6C).

The data presented in Table 2B show that, on average, the Bonanza Ledge samples contain less total Fe than Mosquito Creek (avg. 24.6 percent Fe_2O_3 as total iron versus 43 percent at Mosquito Creek). This reflects the more massive pyritic nature of the Mosquito Creek samples and probably accounts for their higher average Au grade (34 g/t Au versus 14 g/t at Bonanza Ledge; Table 2B). It may also partly explain why the Bonanza Ledge mineralization averages less Ag, Bi, As, Pb, Te and W (Tables 2B and 2D).

However, despite the lower pyrite and Au content of our Bonanza Ledge samples, the mineralization contains noticeably higher quantities of Al, K, Si, P and Ti, which mark the greater abundance of sericite-quartz-rutile alteration assemblages. Also, in contrast to the Mosquito Creek pyritic ore, the Bonanza Ledge mineralization contains greater amounts of Co, Cu, Ni, and Hg, as well as more elevated quantities of elements such as Ba, Be, Ce, Cs, Ga, Ge, La, Li, Y, Th, V, Tl, Nb, Rb, Sr and Ta. Some, but not all of the chemical differences between the Mosquito Creek and Bonanza Ledge mineralization (Tables 1 and 2) probably reflect the contrasting host-rock lithologies at these two properties.

TABLE 2A
COMPARATIVE ANALYTICAL DATA OF PYRITE-RICH SAMPLES FROM QUARTZ VEINS: MOSQUITO CREEK & CARIBOO GOLD QUARTZ DEPOSITS
(FOR SAMPLE DESCRIPTION *SEE* TABLE 2C)

Mosquito Creek Deposit: pyrite in or adjacent to quartz veins

	Au	Ag	As	Hg	Al	Sb	Ba	Be	Bi	Cd	Ca	Ce	Cs	Cr	Co	Cu	Ga	Ge	Fe	La	Pb	Li	Mg
	g/tonne	ppm	ppm	ppb	%	ppm	ppm	ppm	ppm	ppm	%	ppm	ppm	ppm	ppm	ppm	ppm	ppm	%	ppm	ppm	ppm	%
Sample																							
MC1	3.9	57.2	2580	10	0.24	9.7	10	0.1	182	0.48	0.39	2.9	0.1	198	80.8	1.0	0.7	0.7	25.0	1.5	2110.0	1.8	0.06
MC5	12.6	3.2	1970	<10	5.46	2.6	210	1.6	10	0.02	1.75	56.7	1.4	117	26.0	1.0	13.9	1.3	19.8	29.5	275.0	10.2	0.31
MC7	30.1	28.0	10000	<10	0.26	26.0	10	0.5	346	0.5	4.61	13.0	0.5	82	44.0	3.0	<1	2.0	25.0	5.0	856.0	2.0	1.53
MC8	46.9	8.0	2530	<10	1.32	4.5	10	0.5	17	0.02	0.06	15.0	0.7	131	28.4	1.0	3.7	1.3	21.0	7.5	157.0	13.8	0.04
MC9	95.7	17.2	7860	<10	1.14	30.0	10	0.3	26	0.02	0.06	11.3	0.7	172	90.0	1.0	3.0	0.9	25.0	6.0	1010.0	18.6	0.03
GR00-31	6.6	50.6	1060	<10	0.01	4.7	5	0.1	215	0.34	0.01	0.6	0.1	239	619.0	1.0	0.3	0.7	25.0	0.5	2110.0	0.6	0.01
GR00-32	1.4	10.5	993	<10	0.07	10.1	5	0.1	54	0.14	0.05	0.9	0.1	306	319.0	1.0	0.4	0.7	25.0	0.5	482.0	1.2	0.01
Avg (n = 7)	**28.2**	**25.0**	**3856**	**6**	**1.21**	**10.3**	**37**	**0.4**	**121**	**0.22**	**0.99**	**14.5**	**0.5**	**178**	**172.5**	**1.3**	**3.7**	**0.9**	**23.7**	**7.6**	**1000.0**	**7.7**	**0.28**
Max	95.7	57.2	10000	10	5.5	30.0	210	1.6	346	0.5	4.6	56.7	1.4	306	619.0	3.0	13.9	1.3	25.0	29.5	2110.0	18.6	1.53
Min	1.4	3.2	993	<10	0.0	2.6	5	0.1	10	0.0	0.0	0.6	0.1	82	26.0	1.0	0.3	0.7	19.8	0.5	157.0	0.6	0.01
Std. Dev	34.0	21.4	3576	2	1.9	10.1	76	0.5	129	0.2	1.7	21.5	0.5	77	221.7	0.8	5.2	0.3	2.3	11.1	815.4	7.6	0.56

Cariboo Gold Quartz Deposit: pyrite in or adjacent to quartz veins

Sample	Au	Ag	As	Hg	Al	Sb	Ba	Be	Bi	Cd	Ca	Ce	Cs	Cr	Co	Cu	Ga	Ge	Fe	La	Pb	Li	Mg
CGQ1	21.3	5.3	1480	<10	0.09	12.2	5	0.1	970	0.48	0.01	0.9	0.1	246	143.5	7.0	0.3	1.1	21.4	0.5	409.0	0.6	0.01
CGQ2	29.4	3.1	786	<10	0.02	0.7	5	0.1	23	0.06	0.01	0.1	0.1	212	40.6	8.0	0.1	1.2	14.9	0.5	173.0	0.8	0.01
CGQ3	36.4	2.7	778	10	0.05	1.0	5	0.1	20	0.02	0.01	0.3	0.1	297	63.9	1.0	0.2	0.9	25.0	0.5	60.0	1.0	0.01
CGQ4	11.6	8.9	620	<10	1.75	5.8	50	0.4	263	0.26	1.19	17.4	0.6	262	131.5	6.0	4.4	1.1	16.8	8.0	421.0	2.4	0.17
CGQ5	21.8	1.8	2910	10	0.75	0.5	30	0.2	8	0.02	0.03	8.5	0.2	175	214.0	1.0	2.2	0.7	25.0	4.5	13.0	1.2	0.02
CGQ6	16.6	4.7	1375	<10	0.83	5.8	60	0.3	149	0.22	1.72	9.5	0.3	178	47.6	4.0	2.1	1.1	19.8	5.0	231.0	1.2	0.49
CGQ7	72.0	2.7	331	40	0.27	1.0	20	0.1	34	0.06	0.05	2.8	0.1	311	199.5	1.0	0.8	0.7	25.0	1.5	76.5	0.8	0.01
CGQ8	8.4	1.3	603	<10	0.27	10.0	30	0.1	15	0.02	0.38	3.0	0.1	247	46.2	1.0	0.8	1.2	16.7	2.0	19.0	0.6	0.04
Avg (n = 8)	**27.2**	**3.8**	**1110**	**11**	**0.5**	**4.6**	**26**	**0.1**	**185**	**0.1**	**0.4**	**5.3**	**0.2**	**241**	**110.9**	**3.6**	**1.4**	**1.0**	**20.6**	**2.8**	**175.3**	**1.1**	**0.10**
Max	72.0	8.9	2910	40	1.8	12.2	60	0.4	970	0.5	1.7	17.4	0.6	311	214.0	8.0	4.4	1.2	25.0	8.0	421.0	2.4	0.49
Min	8.4	1.3	331	<10	0.0	0.5	5	0.1	8	0.0	0.0	0.1	0.1	175	40.6	1.0	0.1	0.7	14.9	0.5	13.0	0.6	0.01
Std. Dev	20.2	2.5	825	12	0.6	4.6	21	0.1	329	0.2	0.7	6.1	0.2	50	71.0	3.0	1.5	0.2	4.2	2.8	165.6	0.6	0.17

TABLE 2A CONTINUED
COMPARATIVE ANALYTICAL DATA OF PYRITE-RICH SAMPLES FROM QUARTZ VEINS: MOSQUITO CREEK & CARIBOO GOLD QUARTZ DEPOSITS
(FOR SAMPLE DESCRIPTION *SEE* TABLE 2C)

Mosquito Creek Deposit: pyrite in or adjacent to quartz veins

Sample	Mn ppm	Mo ppm	Ni ppm	Nb ppm	P ppm	K %	Rb ppm	Na %	Sr ppm	Ta ppm	Te ppm	Tl ppm	Th ppm	Ti %	W ppm	U ppm	V ppm	Y ppm	Zn ppm	Cu/Au	Au/Ag	As/Au	Bi/Au
MC1	250	1.0	58	0.2	50	0.09	4	0.01	6	0.05	4.8	0.08	0.6	0.01	1.3	0.2	5.0	0.7	8.0	0.254	0.1	656.5	46.2
MC5	870	0.2	40	1.8	260	2.33	88	0.21	58	0.05	0.3	0.48	8.6	0.08	13.8	1.4	64.0	4.4	10.0	0.079	3.9	156.3	0.8
MC7	7310	1.0	88	1.0	150	0.11	8	0.07	132	0.05	4.5	0.1	12	0.01	<10	1.0	9.0	11.0	32.0	0.100	1.1	332.2	11.5
MC8	45	0.6	35	0.2	40	0.56	24	0.02	4	0.05	0.8	0.18	3	0.01	1.7	0.6	13.0	1.3	2.0	0.021	5.9	53.9	0.4
MC9	10	1.6	53	0.4	80	0.45	18	0.01	5	0.05	5.05	0.22	2.2	0.01	1.6	0.2	11.0	0.8	2.0	0.010	5.6	82.1	0.3
GR00-31	30	5.8	92	0.2	10	0.01	0	0.01	2	0.05	5.15	0.06	0.4	0.01	0.7	0.2	1.0	0.4	1.0	0.152	0.1	160.8	32.6
GR00-32	25	0.8	118	0.2	5	0.01	1	0.01	3	0.05	1.4	0.18	0.1	0.01	0.8	0.2	3.0	0.1	1.0	0.730	0.1	724.8	39.6
Avg (n = 7)	**1220**	**1.6**	**69**	**0.5**	**85**	**0.51**	**23**	**0.05**	**30**	**0.05**	**2.9**	**0.2**	**2.5**	**0.02**	**3.6**	**0.5**	**15.1**	**1.3**	**8**	**0.192**	**2.4**	**309.5**	**18.8**
Max	7310	5.8	118	1.8	260	2.33	88	0.21	132	0.05	5.2	0.5	8.6	0.08	13.8	1.4	64.0	4.4	32.0	0.730	5.9	724.8	46.2
Min	10	0.2	35	0.2	5	0.01	0	0.01	2	0.05	0.3	0.1	0.1	0.01	0.7	0.2	1.0	0.1	1.0	0.010	0.1	53.9	0.3
Std. Dev	2703	1.9	31	0.6	91	0.83	33	0.07	49	0.00	2.3	0.2	3.2	0.03	5.2	0.5	22.0	1.6	11.2	0.251	2.6	275.7	20.1

Cariboo Gold Quartz Deposit: pyrite in or adjacent to quartz veins

Sample	Mn ppm	Mo ppm	Ni ppm	Nb ppm	P ppm	K %	Rb ppm	Na %	Sr ppm	Ta ppm	Te ppm	Tl ppm	Th ppm	Ti %	W ppm	U ppm	V ppm	Y ppm	Zn ppm	Cu/Au	Au/Ag	As/Au	Bi/Au
CGQ1	20	2.0	36	0.2	10	0.04	2	0.01	1	0.05	2	0.02	0.2	0.01	1.1	0.2	1.0	0.1	2.0	0.329	4.0	69.5	45.5
CGQ2	25	0.2	44	0.2	50	0.01	0	0.01	2	0.05	0.25	0.02	0.2	0.01	0.3	0.2	1.0	0.1	4.0	0.272	9.6	26.7	0.8
CGQ3	15	0.6	182	0.2	50	0.01	0	0.01	1	0.05	0.45	0.02	0.2	0.01	0.3	0.2	3.0	0.1	1.0	0.027	13.7	21.4	0.5
CGQ4	235	0.4	22	0.2	170	0.76	29	0.05	31	0.05	0.85	0.18	2.8	0.02	0.9	0.2	17.0	1.7	6.0	0.517	1.3	53.4	22.7
CGQ5	5	0.8	58	0.2	50	0.33	13	0.01	3	0.05	0.65	0.06	1.8	0.01	0.9	0.2	10.0	0.8	1.0	0.046	12.1	133.5	0.4
CGQ6	960	0.2	55	0.2	300	0.36	15	0.02	53	0.05	0.9	0.1	2	0.01	0.6	0.8	7.0	2.5	16.0	0.241	3.5	82.8	8.9
CGQ7	15	1.6	90	0.2	50	0.11	5	0.01	2	0.05	0.45	0.02	0.6	0.01	0.8	0.2	4.0	0.3	1.0	0.014	27.2	4.6	0.5
CGQ8	70	0.6	86	0.2	90	0.11	5	0.01	8	0.05	0.5	0.08	1	0.01	0.4	0.6	4.0	0.4	2.0	0.119	6.5	71.7	1.8
Avg (n = 8)	**168**	**0.8**	**72**	**0.2**	**96**	**0.22**	**9**	**0.02**	**13**	**0.05**	**0.8**	**0.1**	**1.1**	**0.01**	**0.7**	**0.3**	**5.9**	**0.8**	**4.1**	**0.196**	**9.7**	**58.0**	**10.1**
Max	960	2.0	182	0.2	300	0.76	29	0.05	53	0.05	2.0	0.2	2.8	0.02	1.1	0.8	17.0	2.5	16.0	0.517	27.2	133.5	45.5
Min	5	0.2	22	0.2	10	0.01	0	0.01	1	0.05	0.3	0.0	0.2	0.01	0.3	0.2	1.0	0.1	1.0	0.014	1.3	4.6	0.4
Std. Dev	329	0.7	50	0.0	95	0.26	10	0.01	19	0.00	0.5	0.1	1.0	0.00	0.3	0.2	5.4	0.9	5.1	0.177	8.3	41.1	16.3

Note: when assay values are below detection, then half the detection limit was used to calculate the averages etc.
All sample analysed by ALS Chemex, Aurora Laboratory Services Ltd., 212 Brookbank Ave, Vancouver, BC, V7J 2C1
Methods used for all data in this table:
Au = Fire assay and AA finish; As = AAS; Hg by cold vapour with ICP-MS rechecks. Other elements = ICP-MS

TABLE 2B

COMPARATIVE ANALYTICAL DATA OF PYRITE-RICH SAMPLES FROM MASSIVE REPLACEMENT MINERALIZATION: MOSQUITO CREEK DEPOSIT & THE BONAZA LEDGE GOLD ZONE

(FOR SAMPLE DESCRIPTION *SEE* TABLE 2C)

Mosquito Creek Deposit: pyrite in replacement ore

Sample	Au	Ag	As	Hg	Al	Sb	Ba	Be	Bi	Cd	Ca	Ce	Cs	Cr	Co	Cu	Ga	Ge	Fe	La	Pb	Li	Mg	Mn	Mo	Ni	Nb	P
	g/tonne	ppm	ppm	ppb	%	ppm	ppm	ppm	ppm	ppm	%	ppm	ppm	ppm	ppm	ppm	ppm	ppm	%	ppm	ppm	ppm	%	ppm	ppm	ppm	ppm	ppm
GR00-34	25.27	8.0	2740	<10	0.98	1.5	40	0.3	40	0.04	0.21	9.2	0.4	243	5.0	1.0	3.5	0.9	25.0	5.5	121.0	1.0	0.04	155	5.8	9	0.6	350
GR00-39	63.42	19.5	2750	<10	0.23	620.0	10	0.1	137	0.34	3.81	1.4	0.1	124	1.4	3.0	1.0	0.4	25.0	0.5	280.0	0.6	0.48	3700	0.4	5	0.2	140
MC2	37.10	27.5	2650	<10	0.58	3.3	30	0.2	226	0.28	3.46	4.2	0.2	119	29.0	1.0	1.6	0.5	25.0	2.0	324.0	1.4	0.49	3040	0.6	30	0.2	390
MC3	39.00	8.3	3010	10	0.84	1.6	40	0.3	89	0.36	5.59	9.3	0.2	92	8.2	2.0	2.3	0.5	21.9	3.5	102.0	2.0	1.55	8640	0.2	11	0.2	470
MC4	7.48	3.2	1995	40	0.68	3.0	40	0.3	28	0.5	6.82	7.1	0.2	39	13.0	1.0	1.0	3.0	25.0	5.0	60.0	1.0	1.80	10000	1.0	13	1.0	360
MC6	16.40	5.8	10000	<10	1.37	6.0	30	0.3	20	0.5	3.18	12.8	0.5	61	20.0	1.0	2.0	3.0	25.0	5.0	170.0	1.0	1.44	7860	1.0	18	1.0	390
MC10	51.00	11.9	3520	<10	0.96	10.9	30	0.9	68	0.08	0.60	3.8	0.5	102	6.6	1.0	2.8	0.9	25.0	2.0	389.0	2.0	0.11	820	0.6	16	0.2	170
Avg (n = 7)	**34.2**	**12.0**	**3809**	**11**	**0.81**	**127.5**	**31**	**0.3**	**87**	**0.3**	**3.38**	**5.6**	**0.3**	**111**	**11.9**	**1.4**	**2.2**	**0.6**	**24.6**	**2.7**	**206.6**	**1.4**	**0.84**	**4888**	**1.4**	**15**	**0.3**	**324**
Max	63.4	27.5	10000	40	1.37	620.0	40	0.9	226	0.5	6.82	9.3	0.5	243	29.0	3.0	3.5	0.9	25.0	5.5	389.0	2.0	1.80	10000	5.8	30	0.6	470
Min	7.5	3.2	1995	<10	0.23	1.5	10	0.1	20	0.04	0.21	1.4	0.1	39	1.4	1.0	1.0	0.4	21.9	0.5	60.0	0.6	0.04	155	0.2	5	0.2	140
Std. Dev	19.5	8.6	2767	13	0.4	275.4	11	0.3	73	0.2	2.4	3.5	0.2	66	9.7	0.8	1.0	0.2	1.2	1.9	124.9	0.6	0.73	3933	2.0	8	0.2	122

Bonanza Ledge: pyrite in replacement ore

Sample	Au	Ag	As	Hg	Al	Sb	Ba	Be	Bi	Cd	Ca	Ce	Cs	Cr	Co	Cu	Ga	Ge	Fe	La	Pb	Li	Mg	Mn	Mo	Ni	Nb	P
	g/tonne	ppm	ppm	ppb	%	ppm	ppm	ppm	ppm	ppm	%	ppm	ppm	ppm	ppm	ppm	ppm	ppm	%	ppm	ppm	ppm	%	%	ppm	ppm	ppm	ppm
2K-19-20	25.0	1.8	876	2370	10.3	1.4	1720	3.9	5	0.16	2.74	32.6	7.4	44	91.7	7.0	29.5	1.9	10.9	14.5	39.5	8.2	1.07	690	0.8	153	12.6	1790
2K-19-21	8.3	1.2	953	1110	11.85	0.8	2360	3.4	8	0.01	1.62	87.8	7.5	77	78.2	8.0	32.4	1.8	11.8	39.5	43.5	11.6	0.83	485	0.8	160	2.6	570
2K-19-22	1.5	0.7	729	270	13.05	0.7	2600	4.1	7	0.02	0.53	87.5	8.0	111	89.2	4.0	35.9	2.1	9.5	39.0	20.5	13.0	0.44	140	1	154	2.4	600
2K-19-23	31.8	8.6	845	4350	11.05	5.2	1180	3.1	7	0.04	0.34	47.7	6.9	68	36.2	16.0	27.7	1.5	16.2	19.5	61.0	9.2	0.35	85	1	88	1.4	380
2K-19-13	4.7	1.2	708	6610	7.49	2.8	1670	2.1	13	0.1	1.82	58.5	5.1	57	36.8	13.0	17.9	1.2	21.1	25.5	45.5	6.6	0.74	475	2	71	1.0	960
2K-29-6	4.2	0.7	847	3660	11.25	1.8	1710	3.3	11	0.12	1.7	34.7	5.9	71	82.6	1.0	29.4	1.7	12.5	13.5	19.0	10.6	0.63	630	2.2	175	8.2	3070
2K-29-17	14.0	1.8	1180	3230	10.2	1.5	1280	2.6	5	0.1	0.89	45.4	4.6	29	110.0	26.0	27.3	1.5	15.0	18.0	86.5	7.0	0.33	290	0.8	309	12.0	2510
2K-29-20	24.8	3.3	1295	2030	7.01	1.1	530	1.7	11	0.24	1.98	35.1	3.9	58	63.2	42.0	18.9	1.2	21.1	14.0	129.5	5.0	0.77	935	1.4	170	5.2	1010
Avg (n = 8)	**14.3**	**2.4**	**929**	**2954**	**10.275**	**1.9**	**1631**	**3.0**	**8**	**0.11**	**1.45**	**53.7**	**6.1**	**64**	**73.5**	**14.6**	**27.4**	**1.6**	**14.7**	**22.9**	**55.6**	**8.9**	**0.65**	**466**	**1.25**	**160**	**5.7**	**1361**
Max	31.8	8.6	1295	6610	13.1	5.2	2600	4.1	13	0.2	2.7	87.8	8.0	111	110.0	42.0	35.9	2.1	21.1	39.5	129.5	13.0	1.1	935	2.2	309	12.6	3070
Min	1.5	0.7	708	270	7.0	0.7	530	1.7	5	0.0	0.3	32.6	3.9	29	36.2	1.0	17.9	1.2	9.5	13.5	19.0	5.0	0.3	85	0.8	71	1.0	380
Std. Dev	11.5	2.6	208	1989	2.1	1.5	657	0.8	3	0.1	0.8	22.6	1.5	24	26.3	13.5	6.2	0.3	4.5	10.8	36.9	2.7	0.3	288	0.6	71	4.7	991

TABLE 2B CONTINUED
COMPARATIVE ANALYTICAL DATA OF PYRITE-RICH SAMPLES FROM MASSIVE REPLACEMENT MINERALIZATION: MOSQUITO CREEK DEPOSIT & THE BONAZA LEDGE GOLD ZONE
(FOR SAMPLE DESCRIPTION *SEE* TABLE 2C)

Mosquito Creek Deposit: pyrite in replacement ore

Sample	K	Rb	Na	Sr	Ta	Te	Tl	Th	Ti	W	U	V	Y	Zn	Cu/Au	Au/Ag	As/Au	Bi/Au	Al_2O_3	CaO	Fe_2O_3	K_2O	MgO	MnO	Na_2O	P_2O_5	SiO_2	TiO_2	LOI	TOTAL
	%	ppm	%	ppm	ppm	ppm	ppm	ppm	%	ppm	ppm	ppm	ppm	ppm					%	%	%	%	%	%	%	%	%	%	%	%
GR00-34	0.44	21	0.01	8	0.05	1.05	0.22	2.8	0.01	1.2	0.6	10.0	1.0	1.0	0.040	3.2	108.4	1.6	1.70	0.26	41.00	0.54	0.06	0.06	0.26	0.14	30.40	0.06	24.36	98.84
GR00-39	0.10	5	0.01	40	0.05	2.2	2.92	0.8	0.01	0.5	1.2	4.0	2.3	8.0	0.047	3.3	43.4	2.2	0.48	5.38	53.00	0.18	0.72	0.46	0.24	<0.01	2.48	<0.01	32.48	95.42
MC2	0.25	9	0.05	32	0.05	4.1	0.08	1.2	0.01	1.1	0.8	8.0	4.0	12.0	0.027	1.3	71.4	6.1	0.98	5.26	48.70	0.34	0.74	0.36	0.26	0.04	7.30	0.02	30.37	94.37
MC3	0.36	12	0.08	70	0.05	0.8	0.06	1	0.01	48.3	1.2	12.0	9.1	24.0	0.051	4.7	77.2	2.3	1.48	14.02	31.50	0.48	2.36	1.20	0.28	0.08	14.82	0.06	20.57	86.85
MC4	0.29	10	0.12	109	0.05	0.25	0.1	4	0.01	5.0	1.0	7.0	7.0	36.0	0.134	2.3	266.7	3.7	1.06	9.84	39.60	0.38	2.76	1.74	0.26	0.02	11.16	0.04	25.11	91.97
MC6	0.60	24	0.08	66	0.05	0.5	0.1	6	0.01	5.0	1.0	15.0	10.0	18.0	0.061	2.8	609.8	1.2	2.42	11.64	36.00	0.80	2.28	1.02	0.28	0.06	8.86	0.06	25.82	89.24
MC10	0.38	15	0.03	9	0.05	1.35	0.1	1.4	0.01	70.2	1.0	12.0	2.4	28.0	0.020	4.3	69.0	1.3	1.52	1.16	52.20	0.50	0.18	0.14	0.28	<0.01	14.46	0.04	27.73	98.21
Avg (n = 7)	**0.35**	**13**	**0.05**	**48**	**0.05**	**1.9**	**0.68**	**1.44**	**0.01**	**18.8**	**1.0**	**9.7**	**3.8**	**18.1**	**0.054**	**3.1**	**178.0**	**2.6**	**1.38**	**6.79**	**43.14**	**0.46**	**1.30**	**0.71**	**0.27**	**0.07**	**12.8**	**0.05**	**26.6**	**93.6**
Max	0.60	21	0.12	109	0.05	4.1	2.92	2.8	0.01	70.2	1.2	15.0	9.1	36.0	0.134	4.7	609.8	6.1	2.42	14.02	53.00	0.80	2.76	1.74	0.28	0.14	30.40	0.06	32.48	98.84
Min	0.10	5	0.01	8	0.05	0.8	0.06	0.8	0.01	0.5	0.6	4.0	1.0	1.0	0.020	1.3	43.4	1.2	0.48	0.26	31.50	0.18	0.06	0.06	0.24	0.02	2.48	0.02	20.57	86.85
Std. Dev	0.16	6	0.04	36	0.00	1.3	1.3	0.8	0.00	28.4	0.3	3.7	3.2	12.1	0.038	1.1	204.4	1.8	0.62	5.22	8.30	0.19	1.13	0.62	0.02	0.05	8.87	0.02	3.96	4.47

Bonanza Ledge: pyrite in replacement ore

Sample	K	Rb	Na	Sr	Ta	Te	Tl	Th	Ti	W	U	V	Y	Zn	Cu/Au	Au/Ag	As/Au	Bi/Au	Al_2O_3	CaO	Fe_2O_3	K_2O	MgO	MnO	Na_2O	P_2O_5	SiO_2	TiO_2	LOI	TOTAL
	%	ppm	%	ppm	ppm	ppm	ppm	ppm	%	ppm	ppm	ppm	ppm	ppm					%	%	%	%	%	%	%	%	%	%	%	%
2K-19-20	4.48	246	0.42	248	0.75	0.05	4.74	3.8	0.50	14.2	0.8	280.0	11.8	22	0.280	14.3	35.0	0.2	20.03	4.09	19.42	6.43	1.98	0.09	0.24	0.49	25.87	4.02	15.94	98.60
2K-19-21	5.11	257	0.53	179	0.20	0.05	5.02	15.2	0.12	4.1	3.4	128.0	10.1	10	0.964	6.9	114.8	0.9	22.31	2.25	19.52	6.50	1.58	0.07	0.37	0.16	30.26	0.99	14.76	98.77
2K-19-22	5.63	300	0.55	118	0.15	0.15	4.66	15	0.14	5.1	4.0	157.0	9.5	10	2.667	2.3	486.0	4.7	25.77	0.71	15.15	7.69	0.92	0.02	0.36	0.17	34.20	1.29	11.86	98.14
2K-19-23	4.78	238	0.44	77	0.05	0.05	7.54	15	0.09	3.3	3.6	128.0	8.4	16	0.503	3.7	26.6	0.2	20.57	0.51	26.41	6.55	0.73	0.01	0.29	0.12	26.07	1.09	16.22	98.57
2K-19-13	3.17	149	0.29	162	0.05	0.3	6.14	8.6	0.07	2	1.8	91.0	8.6	12	2.766	4.1	150.6	2.7	13.74	2.60	35.72	4.11	1.36	0.06	0.15	0.22	17.65	0.71	22.28	98.60
2K-29-6	4.95	184	0.43	104	0.45	0.5	6.08	2	0.36	8.3	0.6	240.0	11	30	0.238	6.0	201.7	2.7	21.02	2.39	20.32	6.78	1.19	0.09	0.30	0.77	27.72	3.38	14.40	98.36
2K-29-17	4.67	198	0.31	65	0.65	0.05	2.38	3.4	0.51	12.4	1.0	340.0	9	22	1.857	7.8	84.3	0.4	19.39	1.32	25.03	6.36	0.56	0.04	0.20	0.61	24.97	4.53	15.54	98.55
2K-29-20	3.06	133	0.23	93	0.25	0.05	2.46	2.8	0.24	7.8	0.6	227.0	6.3	42	1.694	7.6	52.2	0.5	12.40	3.10	35.92	3.92	1.33	0.12	0.04	0.27	15.87	3.09	22.46	98.52
Avg (n = 8)	**4.48**	**213**	**0.40**	**131**	**0.32**	**0.15**	**4.88**	**8.23**	**0.25**	**7.15**	**2.0**	**198.9**	**9.3**	**20.5**	**1.371**	**6.6**	**143.9**	**1.5**	**19.40**	**2.12**	**24.69**	**6.04**	**1.21**	**0.06**	**0.24**	**0.35**	**25.33**	**2.39**	**16.68**	**98.51**
Max	5.6	300	0.6	248	0.8	0.5	7.5	15.2	0.5	14.2	4.0	340.0	11.8	42.0	2.766	14.3	486.0	4.7	25.8	4.1	35.9	7.7	2.0	0.1	0.4	0.8	34.2	4.5	22.5	98.8
Min	3.1	133	0.2	65	0.1	0.1	2.4	2.0	0.1	2.0	0.6	91.0	6.3	10.0	0.238	2.3	26.6	0.2	12.4	0.5	15.2	3.9	0.6	0.0	0.0	0.1	15.9	0.7	11.9	98.1
Std. Dev	0.9	57	0.1	62	0.3	0.2	1.8	6.0	0.2	4.4	1.5	86.5	1.7	11.1	1.025	3.7	150.6	1.7	4.4	1.2	7.7	1.3	0.5	0.0	0.1	0.2	6.1	1.5	3.8	0.2

Note: when assay values are below detection, then half the detection limit was used to calculate the averages etc.
All sample analysed by ALS Chemex, Aurora Laboratory Services Ltd., 212 Brookbank Ave, Vancouver, BC, V7J 2C1
Methods used for all data in this table: Major oxides = XRF.
Au = Fire assay and AA finish; As = AAS; Hg by cold vapour with ICP-MS rechecks. Other elements = ICP-MS

TABLE 2C
DESCRIPTION OF PYRITE-RICH SAMPLES LISTED IN TABLES 2A & 2B
MOSQUITO CREEK & CARIBOO GOLD QUARTZ DEPOSITS AND THE BONANZA LEDGE GOLD ZONE

Sample No.	Description
	MOSQUITO CREEK DEPOSIT
	Pyrite in or adjacent to quartz veins
MC1	Underground; 10 cm wide, steeply dipping vein that strikes 120 degrees
MC5	Underground; 0.4m wide quartz vein
MC7	Underground; 15cm wide vein that strikes 350 and dips 70E
MC8	Underground; 1.3m thick quartz vein that strikes 070 degrees & dips 60NE
MC9	Underground; 1.3m wide vein that strikes 070 and dips 60NE
GR00-31	No.1 adit mine dump; float of coarse pyrite in a quartz vein
GR00-32	Surface outcrop near No. 1 adit; massive pyrite on margins of quartz vein
	CARIBOO GOLD QUARTZ DEPOSIT
	Pyrite in or adjacent to quartz veins, 1200 level workings.
CGQ1	Underground; fine grained pyrite in white quartz vein
CGQ2	Underground; pyrite in a 0.6m wide quartz vein
CGQ3	Underground; massive pyrite in centre of a 7cm quartz vein
CGQ4	Underground; 10 cm-wide, steeply dipping quartz vein that strikes 020 degrees
CGQ5	Underground; coarse grained pyrite from a 15cm wide, steeply dipping vein that strikes 360
CGQ6	Underground; pyrite in 3cm wide, steeply dipping quartz vein that strikes 040
CGQ7	Underground; coarse pyrite in 1m wide quartz vein that strikes 040
CGQ8	0.2m wide quartz vein near the 1200 level adit.
	MOSQUITO CREEK DEPOSIT
	Pyrite in massive replacement ore
GR00-34	No. 1 adit mine dump; float of massive, fine grained pyrite.
GR00-39	No. 1 adit mine dump; float of massive, fine grained pyrite.
MC2	Underground; massive pyrite
MC3	Underground; coarse grained massive to semi-massive pyrite
MC4	Underground; coarse grained massive to semi-massive pyrite
MC6	Underground; coarse grained massive to semi-massive pyrite
MC10	Underground; coarse grained massive to semi-massive pyrite
	BONANZA LEDGE GOLD ZONE; Drillholes BC-2K-19 & 29
	Semi-massive to stringer pyrite mineralization
2K-19-20	Semi-massive to stringer pyrite with sericite, carbonate & minor rutile @ 294 feet
2K-19-21	Semi-massive to stringer pyrite with sericite @ 323 feet
2K-19-22	Semi-massive to stringer pyrite with sericite @ 318 feet
2K-19-23	Massive to semi-massive pyrite with sericite, dolomite & trace tourmaline & rutile @ 309 feet
2K-19-13	Tan, sericitic phyllite with blebs & veins of pyrite @ 365 feet
2K-29-6	Tan sericitic metasediment with pyrite stringers and disseminated dolomite & pyrite porphyroblasts @ 215 feet
2K-29-17	Semi-massive pyrite with abundant muscovite-sericite & trace rutile @ 235 feet
2K-29-20	Massive to semi-massive pyrite with sericite & trace rutile @ 243 feet

TABLE 2D
AVERAGE CHEMICAL VALUES OF AURIFEROUS PYRITE SAMPLES, MOSQUITO CREEK & CARIBOO GOLD QUARTZ MINES & THE BONANZA LEDGE GOLD ZONE
(DATA FROM TABLES 2A & 2B)

	Au	Ag	As	Hg	Cu	Sb	Ba	Bi	Pb	P	Nb	Ce	Cs	Ga	La	Al	K	Au/Ag	Cu/Au
VEINS	g/t	ppm	ppm	ppb	ppm	ppm	ppm	ppm	ppm	ppm	ppm	ppm	ppm	ppm	ppm	%	%		
Mosquito Creek Mine n=7	28.2	25.0	3856	6	1.3	10.3	37	121	1000.0	85	0.5	14.5	0.5	3.7	7.6	1.21	0.51	2.4	0.19
Cariboo Gold Quartz Mine n=8	27.2	3.8	1110	11	3.6	4.6	26	185	175.3	96	0.2	5.3	0.2	1.4	2.8	0.50	0.22	9.7	0.19
REPLACEMENTS																			
Mosquito Creek Mine n=7	34.2	12.0	3809	11	1.4	127.5	31	87	206.6	324	0.3	5.6	0.3	2.2	2.7	0.81	0.35	3.1	0.05
Bonanza Ledge n=8	14.3	2.4	929	2954	14.6	1.9	1631	8	55.6	1361	5.7	53.7	6.1	27.4	22.9	10.28	4.48	6.6	1.37

TABLE 3A
GEOCHEMISTRY OF MISCELLANEOUS SAMPLES COLLECTED IN THE WELLS-BARKERVILLE AREA

	Au	Au	As	Hg	Al	Sb	Ba	Be	Bi	Cd	Ca	Ce	Cs	Cr	Co	Cu	Ga	Ge	Fe	La	Pb	Pb	Li
Sample	ppb	g/tonne	ppm	ppb	%	ppm	ppm	ppm	ppm	ppm	%	ppm	ppm	ppm	ppm	ppm	ppm	ppm	%	ppm	ppm	%	ppm
IWE-00-4	<5	-----	<1	80	7.24	1.5	4560	1.9	0.32	0.16	0.14	83	7.85	111	8.4	33	19.8	2.2	3.56	43	6.5		65.6
IWE-00-5	<5	-----	20	100	0.49	2.7	5340	0.05	0.03	0.06	0.01	4.49	0.2	19	<0.2	34	0.9	0.3	0.56	3.5	10		1.6
IWE-00-6	1545	-----	1240	<10	0.56	0.9	60	0.4	0.13	0.1	0.34	3.75	0.3	19	9.8	9	1.6	2	8.92	2	270		2.4
IWE-00-8	<5	-----	4	<10	2.22	0.2	270	0.4	<0.01	0.02	0.55	21.9	1.1	60	7.8	45	6.7	1.2	2.12	9.5	5		19.4
GR-00-50	<5	-----	3	<10	2.63	0.1	100	0.35	0.19	0.08	1.44	24.5	0.8	25	4.2	19	5.7	1.1	1.69	11.5	20.5		12.4
GR-00-51	<5	-----	4	<10	1.69	<0.1	10	0.05	0.08	0.04	0.98	18.75	0.15	18	1.4	1	1.3	1.1	0.76	8	13.5		0.8
GR-00-52	10	-----	13	<10	0.64	0.2	30	0.05	4.24	0.16	1.44	3.73	0.25	21	9.2	23	1.2	1.1	1.43	1.5	90		1.4
GR-00-53	<5	-----	<1	<10	0.95	<0.1	40	0.3	0.06	0.02	0.08	3.55	0.35	19	2.6	7	2.2	1.5	1.34	1.5	7.5		9.6
GR-00-54	5880	-----	5	<10	0.08	13	60	<0.50	68	5	0.03	3.5	<.5	12	3	2	<1	3	0.84	<5	>10000	3.49	4
GR-00-55	1885	-----	92	<10	0.28	1.3	20	<0.05	4.16	0.08	0.02	1.67	0.15	21	11.2	4	0.6	1.3	2.32	0.5	412		1.6
GR-00-57	2390	-----	575	<10	1	17.8	70	0.25	0.29	0.16	<0.01	15.95	0.5	71	1.2	60	2.7	2.5	2.54	7.5	84.5		1.6
GR-00-58	>10000	83.18	20	10	0.54	0.4	40	<0.05	0.15	0.14	<0.01	5.43	0.3	26	0.8	1	1.2	1.6	0.84	2.5	198.5		0.6
GR-00-59	15	-----	18	<10	0.04	0.4	<10	<0.05	0.02	<0.02	<0.01	0.22	0.05	18	<0.2	1	<0.1	1.1	0.05	<0.5	11		0.2
GR-00-61	165	-----	75	<10	0.38	0.1	130	0.15	0.18	<0.02	0.01	1.56	0.2	21	1.4	<1	0.9	1.3	0.95	0.5	3.5		1.4
GR-00-64	7220	-----	498	<10	10.3	0.5	50	4.3	2.63	<0.02	0.06	101.5	4.2	91	23.2	<1	27.6	1.5	7.2	45	71.5		12.4
GR-00-65	7680	-----	1010	30	0.11	1.6	10	0.05	11	0.8	0.99	5.94	0.05	4	61.4	<1	0.3	0.8	>25.0	1.5	91		0.8
GR-00-66	15	-----	108	<10	3.98	0.4	1290	0.6	0.14	0.12	9.03	19.55	3.85	1460	73.2	96	10.5	0.9	3.67	9	5.5		8.4
GR-00-72	>10000	29.59	2450	<10	1.64	2	30	0.4	95.9	0.04	0.64	9.67	0.4	16	34.6	<1	4.6	1	22.2	5	79		1
GR-00-74	125	-----	1075	10	0.48	8.7	40	0.15	4.43	0.14	0.84	61	0.3	21	39.2	348	1.2	1	6.1	33.5	253		0.6
GR-00-75	575	-----	239	<10	1.66	0.1	440	0.35	0.23	<0.02	0.05	18.9	0.7	19	1.6	1	3.6	1.3	1.69	9	9.5		1.8
GR-00-78	805	-----	205	<10	1.27	0.3	100	0.45	0.85	0.02	0.3	154	0.75	23	6	8	3.1	1.4	2.97	87	71		1.4
GR-00-82	2540	-----	7230	10	0.06	120	10	<0.50	156	19	0.01	1.3	<.5	11	1	3	<1	4	0.66	<5	>10000	13.6	<2
GR-00-83	4370	-----	1835	<10	0.32	1.9	20	<0.05	0.55	0.06	0.08	1.9	0.2	16	17.8	<1	0.8	1.6	7.79	1	445		1.4
GR-00-86	>10000	49.97	2150	<10	1.41	2.3	20	0.5	65.9	0.12	1.88	15.9	0.3	6	139.5	<1	3.9	0.6	>25.0	8	91		1.2
GR-00-87	5760	-----	523	<10	0.1	1.7	<10	<0.05	5.46	<0.02	0.03	1.06	0.1	9	63.8	87	0.3	1.4	13.45	0.5	42.5		0.4
GR-00-93	85	-----	<1	50	2.93	2.9	20	0.6	1.35	1.8	11.5	30.8	0.75	28	29	263	4.9	0.5	19.55	15	2250		3.6
GR-00-95	20	-----	1	<10	3.21	1.8	10	0.35	1.25	0.16	1.28	9.72	0.05	18	21.8	362	5.8	1.2	5.52	5	341		5.8
GR-00-96	40	-----	590	<10	4.85	1.7	10	0.2	0.15	0.02	0.11	21.5	0.15	10	21	1	6.9	1.1	11.15	10.5	25.5		0.6
GR-00-97	<5	-----	3	<10	8.54	0.3	870	1.25	0.12	0.14	3.71	28	0.8	12	40	17	15.9	1.5	8.2	13.5	46.5		58.4
GR-00-98	20	-----	1	<10	0.05	38.7	10	<0.05	54	10.7	0.01	0.73	0.05	20	1.4	16	0.1	1.2	0.82	<0.5	>10000	3.53	0.2
GR-00-99	5	-----	8	40	7.45	0.8	620	2.55	0.68	0.08	9.33	159.5	4.15	1	30.6	<1	22.3	1.6	7.69	74.5	165		112
GR-00-100	<5	-----	<1	<10	0.27	0.3	20	0.05	0.14	0.02	0.06	2.57	0.1	20	1.6	9	0.7	0.7	0.33	0.5	110.5		2
GR-00-101	<5	-----	3	<10	3.55	0.4	630	1.15	0.09	0.02	0.32	23.7	2.25	51	2.8	37	9.8	1.3	1.98	14	17.5		20.2
GR-00-102	<5	-----	52	31200	3.97	13.1	330	0.95	0.25	0.02	0.01	45.4	2.25	30	3.2	9	9.1	1.9	4.88	22	18		16.4
GR-00-103	<5	-----	<1	<10	0.05	0.4	<10	<0.05	0.15	<0.02	<0.01	0.63	0.05	18	<0.2	1	<0.1	3.3	0.06	<0.5	8.5		2.4
GR-00-104	30	-----	26	1460	4.06	1.3	260	0.7	2.76	5.3	0.04	15.45	0.85	8	2.6	59	7.7	1	0.94	8.5	592		3.6
GR-00-105	<5	-----	1270	<10	7.98	2.9	920	0.8	0.17	0.5	8.18	25	2.4	2410	115.5	5	20.7	1.2	8.72	14	22.5		43.4
GR-00-106	1920	-----	2130	10	0.81	0.5	40	0.4	6.73	0.1	5.09	3.75	0.25	24	8.8	<1	2.1	1.2	9.44	2	29.5		0.6
GR-00-107	880	-----	62	<10	0.03	831	<10	<0.50	2490	137	0.16	5.7	<.5	4	<1.0	37	<1	2	0.3	5	>10000	79.3	<2

TABLE 3A CONTINUED
GEOCHEMISTRY OF MISCELLANEOUS SAMPLES COLLECTED IN THE WELLS-BARKERVILLE AREA

Sample	Mg %	Mn ppm	Mo ppm	Ni ppm	Nb ppm	P ppm	K %	Rb ppm	Ag ppm	Na %	Sr ppm	Ta ppm	Te ppm	Tl ppm	Th ppm	Ti %	W ppm	U ppm	V ppm	Y ppm	Zn ppm
IWE-00-4	1.13	230	1.4	33.4	9.8	450	2.26	128	0.55	0.05	33.2	0.6	0.05	0.68	14.2	0.28	1.3	2	143	7.4	86
IWE-00-5	0.01	5	1.6	1.4	<0.2	80	0.13	4.4	0.7	<0.01	15.4	<0.05	<0.05	0.02	<0.2	0.01	<0.1	0.2	9	1.3	12
IWE-00-6	0.14	180	<0.2	42.4	<0.2	200	0.23	13.8	0.75	0.01	18.2	<0.05	<0.05	0.06	0.4	<0.01	2	0.2	5	2.4	26
IWE-00-8	0.82	385	0.2	18.2	2.2	190	0.61	34.6	0.15	<0.01	20.8	<0.05	<0.05	0.18	2.6	0.18	0.7	0.6	65	4.8	48
GR-00-50	0.92	735	<0.2	8	1	150	0.52	29	0.25	0.68	83	<0.05	<0.05	0.14	3.4	0.05	0.1	0.8	17	3.2	44
GR-00-51	0.39	380	0.2	3.6	0.2	120	0.04	2	0.1	0.96	64.3	<0.05	<0.05	<0.02	1.6	0.01	0.1	0.4	1	1.6	4
GR-00-52	0.55	980	<0.2	19.4	<0.2	200	0.17	9	0.95	0.15	88.1	<0.05	0.25	0.04	0.2	<0.01	<0.1	0.2	4	2.7	10
GR-00-53	0.13	130	<0.2	5.8	<0.2	100	0.18	10.2	0.05	0.07	28.2	<0.05	<0.05	0.06	1.6	<0.01	<0.1	0.2	6	1.4	34
GR-00-54	0.07	205	<1.0	3	<2	<10	0.01	<2	47	<0.01	<1.0	<.5	3	<.2	<2	<0.01	<10.0	<2	<1	1	48
GR-00-55	0.07	45	<0.2	7	<0.2	40	0.07	3.8	5.95	0.01	3.6	<0.05	0.25	<0.02	<0.2	0.02	<0.1	0.2	6	0.6	52
GR-00-57	0.02	35	0.8	4.6	2.6	90	0.35	21.6	2.1	0.05	14.6	<0.05	0.05	0.12	1	0.09	3.6	1	22	1.4	152
GR-00-58	0.01	190	<0.2	2	<0.2	10	0.19	9.6	0.55	0.02	6.4	<0.05	<0.05	0.04	<0.2	0.01	0.1	0.2	5	0.9	18
GR-00-59	<0.01	5	<0.2	1	<0.2	<10	0.01	0.6	0.15	<0.01	1.8	<0.05	<0.05	<0.02	<0.2	<0.01	<0.1	<0.2	<1	<0.1	<2
GR-00-61	0.01	30	<0.2	3.6	<0.2	<10	0.17	7.2	0.05	<0.01	4.8	<0.05	<0.05	0.02	<0.2	<0.01	0.6	<0.2	3	0.1	<2
GR-00-64	0.23	30	<0.2	34.8	5.8	130	3.46	209	0.9	0.31	34.6	0.25	0.05	1.02	14	0.18	9.4	1.8	135	6	12
GR-00-65	0.37	600	<0.2	242	<0.2	350	0.04	1.8	3.25	<0.01	31.2	<0.05	0.6	0.06	0.6	<0.01	6.2	<0.2	2	3.3	104
GR-00-66	3.09	990	0.2	160.5	1.8	160	1.54	62.2	0.2	0.18	294	0.05	<0.05	0.4	1	0.14	0.7	0.2	147	5.2	30
GR-00-72	0.1	395	<0.2	41.6	0.8	350	0.73	33.2	14.15	0.01	11	<0.05	1.4	0.12	4	0.03	1.1	1	12	1.3	<2
GR-00-74	0.34	940	0.2	154	0.2	170	0.2	9.2	2.3	0.01	29.2	<0.05	0.15	0.6	1.8	0.01	0.5	0.6	6	2.4	14
GR-00-75	0.05	25	<0.2	3.8	0.6	30	0.64	32.8	0.35	0.04	9.4	<0.05	<0.05	0.16	3.8	0.03	1.3	0.6	11	1.2	2
GR-00-78	0.12	230	0.6	29.6	0.2	110	0.5	25.4	0.8	0.03	23.8	<0.05	<0.05	0.14	3.4	0.01	1	0.8	13	3.6	2
GR-00-82	<0.01	<5	<1.0	<1.0	<2	50	0.03	<2	228.0	<0.01	9	<.5	2.5	<.2	<2	<0.01	<10.0	6	<1	<1	26
GR-00-83	0.1	200	<0.2	17.8	<0.2	40	0.13	6.8	1.1	<0.01	4.2	<0.05	<0.05	0.02	1	<0.01	1.2	<0.2	3	0.8	6
GR-00-86	0.44	1640	0.6	145.5	0.6	230	0.64	30.4	10.45	0.01	24.4	<0.05	1.15	0.14	5.4	0.03	1	1	12	3.1	<2
GR-00-87	0.01	30	<0.2	53.8	<0.2	<10	0.04	2.2	1.05	<0.01	2.6	<0.05	0.15	0.02	0.2	<0.01	0.2	<0.2	1	0.3	<2
GR-00-93	0.26	980	0.4	119.5	1	150	0.63	30	4.25	1.09	535	<0.05	<0.05	0.3	7	0.03	0.4	2.4	22	10.5	416
GR-00-95	0.45	535	1.4	34	0.2	70	0.04	1.4	1.8	2.35	114	<0.05	0.15	0.18	2	0.01	1.3	0.6	6	2.1	14
GR-00-96	0.03	20	<0.2	79.6	0.2	30	0.04	1.4	0.15	3.77	89.1	<0.05	0.05	0.06	6	<0.01	0.6	0.6	1	1.6	<2
GR-00-97	1.02	1535	<0.2	12.4	0.6	1220	0.42	17.8	0.15	3.09	777	<0.05	<0.05	0.08	4.6	0.09	0.6	0.8	256	5.2	100
GR-00-98	0.01	30	<0.2	2.2	<0.2	50	0.06	1.2	76.4	0.01	5.2	<0.05	3	0.02	<0.2	<0.01	0.1	<0.2	2	0.1	716
GR-00-99	2.35	915	2.8	5.2	21.8	6800	1.87	74.8	0.65	1.01	1015	1	<0.05	0.3	8.4	0.91	0.7	1.2	181	24.7	156
GR-00-100	0.1	60	<0.2	5.2	<0.2	50	0.06	2.8	0.35	<0.01	6.2	<0.05	<0.05	<0.02	<0.2	0.02	<0.1	<0.2	9	0.8	8
GR-00-101	0.66	225	0.8	6.8	7.6	620	1.3	69.2	0.2	0.01	15.6	0.4	<0.05	0.36	4.2	0.36	1	1.2	109	7.6	50
GR-00-102	0.1	10	2.4	8.8	2	80	1.31	65.8	0.75	0.21	57	0.1	<0.05	7.32	9.8	0.06	0.5	2	28	4	26
GR-00-103	<0.01	<5	<0.2	0.6	<0.2	<10	0.01	0.8	0.05	<0.01	2.4	<0.05	<0.05	0.08	<0.2	<0.01	<0.1	<0.2	<1	<0.1	<2
GR-00-104	0.08	5	<0.2	2.2	6.2	110	0.93	49	1.65	1.77	43.8	0.5	0.1	0.22	4.8	<0.01	0.5	1.2	<1	1.1	2800
GR-00-105	4.3	1235	1.6	945	2.2	500	1.72	85.4	0.15	1.16	469	0.1	<0.05	0.48	4.4	0.11	1.8	1.4	193	9.7	234
GR-00-106	0.32	2120	<0.2	11.4	<0.2	590	0.37	16	0.7	0.01	66.4	<0.05	0.85	0.06	0.8	0.01	0.6	1.4	10	3.7	10
GR-00-107	0.03	100	<1.0	1	<2	10	<0.01	<2	1935.0	<0.01	26	<.5	30	1.6	<2	<0.01	<10.0	<2	1	3	6

All sample analysed by ALS Chemex, Aurora Laboratory Services Ltd., 212 Brookbank Ave, Vancouver, BC, V7J 2C1
Methods used for all data in this table:
Au = Fire assay and AA finish; As = AAS; Hg by cold vapour with ICP-MS rechecks. Other elements = ICP-MS

TABLE 3B
DECRIPTION & LOCATION OF MISCELLANEOUS SAMPLES COLLECTED IN THE WELLS-BARKERVILLE AREA

Sample	Description	UTM (E)	UTM (N)
IWE-00-4	Pyritic grey phyllite with ankerite & quartz veins	588858	5891008
IWE-00-5	Float of quartz vein in black phyllite; trench near Mt Tom	588121	5889542
IWE-00-6	Quartz vein at Prosperpine adit: hosted in silicified quartzite	602167	5876126
IWE-00-8	Quartz vein cutting Island Mt Amphibolite, Adit at head of Coulter Creek, west side of Island Mt.	590677	5884954
GR-00-50	Float of quartz vein with malachite, trace pyrite, sericite & ankerite, Lower Perkins adit	589076	5877469
GR-00-51	Float of white quartz vein with disseminated pyrite. Lower Perkins adit dump.	589076	5877469
GR-00-52	Float of white quartz vein with sericite & ankerite. Lower Perkins adit dump.	589076	5877469
GR-00-53	Float of rusty quartz vien with pyrite & sericite. South end of Perkins trench.	588743	5877799
GR-00-54	Flloat of quartz vein with pyrite & galena. Middle part of Perkins trench	588721	5877885
GR-00-55	Float of rusty quartz vein with pyrite & sericite. North end of Perkins trench	588742	5877973
GR-00-57	Vuggy, 1.5 m wide quartz vein with disseminated pyrite. Shaft at Standard Location vein.	589559	5879180
GR-00-58	Narrow quartz vein with coarse pyrite. Trench below Standard Location veins	588990	5878244
GR-00-59	Black Bull quartz vein with sericite but no pyrite	596891	5881398
GR-00-61	Float of white quartz vein & abundant pyrite. Canusa mine dump.	597330	5881044
GR-00-64	Coarse pyrite in wallrock near brecciated quartz vein, Lowhee Creek	596403	5882475
GR-00-65	Coarse massive pyrite in quartz vein. Lowhee Creek	596403	5882475
GR-00-66	Brown phyllite with shears & mariposite-fuchsite. Lowhee Creek	596485	5882190
GR-00-72	Massive pyrite replacement ore outcropping near Mosquito Creek mine headframe.	593640	5885105
GR-00-74	Float of white quartz vein with pyrite, sericite & graphite. Lower Warspite adit dump	601406	5877003
GR-00-75	Float of grey quartz vein with coarse disseminated pyrite. Lower Warspite adit dump	601406	5877003
GR-00-78	Float white quartz vein with coarse pyrite & graphite. Lower Warspite adit dump,	601406	5877003
GR-00-82	Float of white quartz vein with pyrite, arsenopyrite & galena. Upper Warspite adit dump.	602178	5876111
GR-00-83	Float of white quartz vein with pyrite, arsenopyrite & galena. Upper Warspite adit dump.	602178	5876111
GR-00-86	Float of massive pyrite replacement ore, Island Mountain mine dump.	595138	5884383
GR-00-87	Float of white quartz vein with pyrite. Island Mountain mine dump	595138	5884383
GR-00-93	Underground outcrop, 8 cm wide pyrite-pyrrhotite layer. Island Mountain mine.	-	-
GR-00-95	Pyrite in 0.25m wide quartz vein trending 145/43NE. Dukes adit, Mosquito Creek area.	-	-
GR-00-96	Underground, Pyrite on margins of a 15 cm wide quartz vein trendind 040/SV, Island Mt mine.	-	-
GR-00-97	Outcrop of altered tuff with disseminated pyrite. Grouse Creek area.	603584	5877659
GR-00-98	Float of white quartz vein with galena, pyrite & sericite. Grouse Creek.	602801	5875660
GR-00-99	Altered, orange phyllite with pyrite-pyrrhotite veinlets. Coulter Creek area.	589942	5882889
GR-00-100	Quartz vein cutting Island Mt Amphibolite. Adit entrance, head of Coulter Creek	590672	5884944
GR-00-101	2 m-wide boulder float of rusty vuggy quartz vein above adit, head of Coulter Creek	590708	5884961
GR-00-102	Float of pyritic altered metasediment, dump outside old adit below the BC shaft	597043	5881343
GR-00-103	White quartz vein from south side of BC vein	597278	5981356
GR-00-104	Cleaved, sugary quartzite, Lightning Creek, Castle Minerals sample site 114547	589642	5874917
GR-00-105	Listwanitic, fuchsite-rich boulder float. Frank Nestles placer camp	598939	5889465
GR-00-106	Massive pyrite replacement. Outcrop near Mosquito Creek adit.	593706	5885133
GR-00-107	Float of galena-quartz sample. Mosquito Creek mine adit dump	593700	5885120

Binary plots comparing the chemistry of the Mosquito Creek deposit replacement ore and the Bonanza Ledge auriferous pyrite are presented in Figures 6A, 6B and 6C. These illustrate some of the chemical differences described above and also show that in both deposits there is a positive correlation between Au:Ag, Au:Pb, Au:Bi and Au:As. However, the Mosquito Creek ore tends to be more Ag-rich and Cu-poor than the Bonanza Ledge mineralization (Table 2D).

One of the most surprising findings of this study was the discovery of elevated Hg in the Bonanza Ledge mineralization and its alteration envelope. Apart from two notable exceptions (Table 3A), no Hg-enrichment is seen in any other samples collected throughout the district. However, Hg-rich Au placers are reported in a few creeks in the district (McTaggart and Knight, 1993) which raises possibilities that these streams drain areas containing unexposed Bonanza Ledge-type Au deposits.

OTHER MISCELLANEOUS SAMPLES COLLECTED FROM THE WELLS-BARKERVILLE AREA

In addition to the samples already described above, a number of altered or mineralized samples were collected from throughout the Wells-Barkerville area during this project. The assay data, description and location of these samples are presented in Tables 3A and 3B. They include samples from Mosquito Creek and Island Mountain mines that were taken too late to include in our comparative database listed in Tables 2A and 2B. The Perkins and Standard Location veins in the Mount Burns area were also sampled, as were the Warspite and Prosperpine veins south of Barkerville, and the Canusa, BC and Black Bull quartz veins in the Bonanza Ledge area (Figure 1).

The data in Table 3A reveals large variations in the Au, Ag, As, Pb and Zn contents of the samples, although all have low to very low quantities of Cu and W. Very high Au assays are seen in some of the Perkins and Standard Locations veins, with one sample (GR-00-58) con-

TABLE 4
ASSAY OF STREAM SEDIMENT PAN CONCENTRATE TAKEN FROM LOWHEE CREEK, WELLS-BARKERVILLE (SAMPLE GR-00-63)

		Sample GR-00-63			Sample GR-00-63
Au	g/t	380	Li	ppm	9.8
Pt	g/t	<0.07	Mg	%	0.14
Pd	g/t	<0.07	Mn	ppm	870
Rh	g/t	<0.03	Mo	ppm	3.6
As	ppm	297	Ni	ppm	128.5
Hg	ppb	10	Nb	ppm	1.2
Al	%	1.84	P	ppm	1200
Sb	ppm	6.7	K	%	0.6
Ba	ppm	190	Rb	ppm	34.6
Be	ppm	0.95	Ag	ppm	6.6
Bi	ppm	80	Na	%	0.11
Cd	ppm	0.46	Sr	ppm	80
Ca	%	0.33	Ta	ppm	<0.05
Ce	ppm	>500	Te	ppm	1.4
Cs	ppm	1.25	Tl	ppm	0.22
Cr	ppm	85	Th	ppm	153.5
Co	ppm	105.5	Ti	%	0.68
Cu	ppm	102	W	ppm	5000
Ga	ppm	11	U	ppm	10.6
Ge	ppm	2.4	V	ppm	193
Fe	%	>25.0	Y	ppm	40.3
La	ppm	>500	Zn	ppm	106
Pb	ppm	1010			

Sample collected on Lowhee Creek (UTM 596384E; 5882421N) by placer miner, Wilf Frederick
Methods: Au = Fire assay and AA finish; As = AAS; Hg by cold vapour with ICP-MS rechecks.
Pt, Pd & Rh = Fire assay-ICP. Other elements = ICP-MS
Sample description:
stream sediment pan concentrate with abundant, fine grained black magnetite, quartz and some coarse grains of scheelite

taining 83 g/t Au. The other highly Au-rich samples represent massive replacement ore at the Mosquito Creek and Island Mountain mines.

Galena ± arsenopyrite are present in some of the Perkins and Warspite veins which accounts for the sporadically high Pb and As values. A galena-rich sample (GR-00-107) from the Mosquito Creek Mine adit dump is very Ag-rich (1935 ppm) and contains elevated amounts of Au, Bi and Cd.

Apart from two notable exceptions, all the samples listed in Table 3A have a very low Hg content. One Hg-rich sample (GR-00-102) comprises barren pyritic meta-sedimentary float collected from a dump (UTM 597043E; 5881343N) near an old adit that lies immediately below the BC shaft and the BC Vein, approximately 300 m northwest of the Bonanza Ledge Zone. This sample assayed > 31 000 ppb Hg and suggests that a Hg-rich zone could extend parallel to the BC Vein for some distance northwest of Bonanza Ledge. Another sample (GR-00-104 containing 1460 ppb Hg) was taken from a cleaved, sugary quartzitic metasediment in Lightning Creek at UTM 589642E; 5874917N. It suggests this vicinity should be checked for possible Bonanza Ledge-type mineralization.

One quartz vein sampled at the head of Coulter Creek on Island Mountain (Figures 1 and 2; UTM 590672E; 5884944N) deserves mention because it may be important regarding the timing of the quartz veins in relation to the structural emplacement of the Island Mountain Amphibolite. This unnamed, east to east-southeast-trending vein was not recorded in the BC MINFILE. It has been explored underground along a 2 m high adit for at least 50 m. The 7 m thick quartz vein cuts sheared and chloritic rocks of the mafic Island Mountain Amphibolite. Slickenslides in the wallrock indicate that the structure controlling the vein has undergone late subhorizontal sinistral movement. The vein largely comprises both white and clear quartz. Locally, along its margins, it splits and interdigitates with the hostrocks. The vein includes both massive and annealed brecciated textures that are similar to the brittle textures seen in other veins in the structurally underlying Snowshoe Group, including the BC Vein and those at the Mosquito Creek Mine. The small dump close to the portal contains float of rusty quartz with coarse brown carbonate, some muscovite and trace quantities of fine grained disseminated pyrite. Samples taken from the vein and dump were barren (Table 3A). Despite the absence of Au however, this vein closely resembles parts of the BC Vein; if it belong to the same generation then it implies that the auriferous quartz veining in the district occurred after the structural emplacement of the Island Mountain Amphibolite klippe (Figure 2).

The assay data of a heavy mineral pan concentrate sample collected from Lowhee Creek (UTM 596384E;

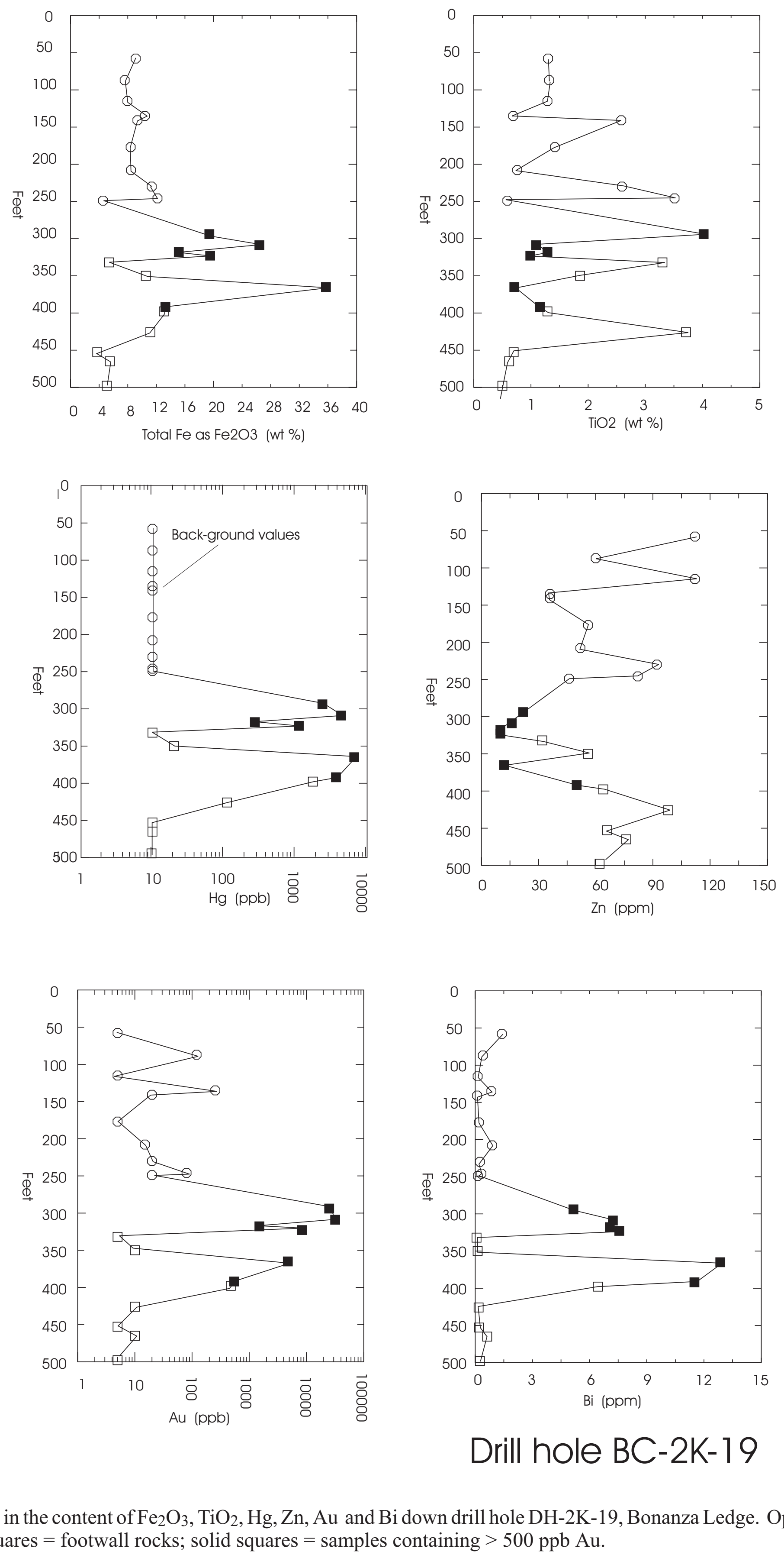

Figure 4A. Changes in the content of Fe_2O_3, TiO_2, Hg, Zn, Au and Bi down drill hole DH-2K-19, Bonanza Ledge. Open circles = hanging wall rocks; open squares = footwall rocks; solid squares = samples containing > 500 ppb Au.

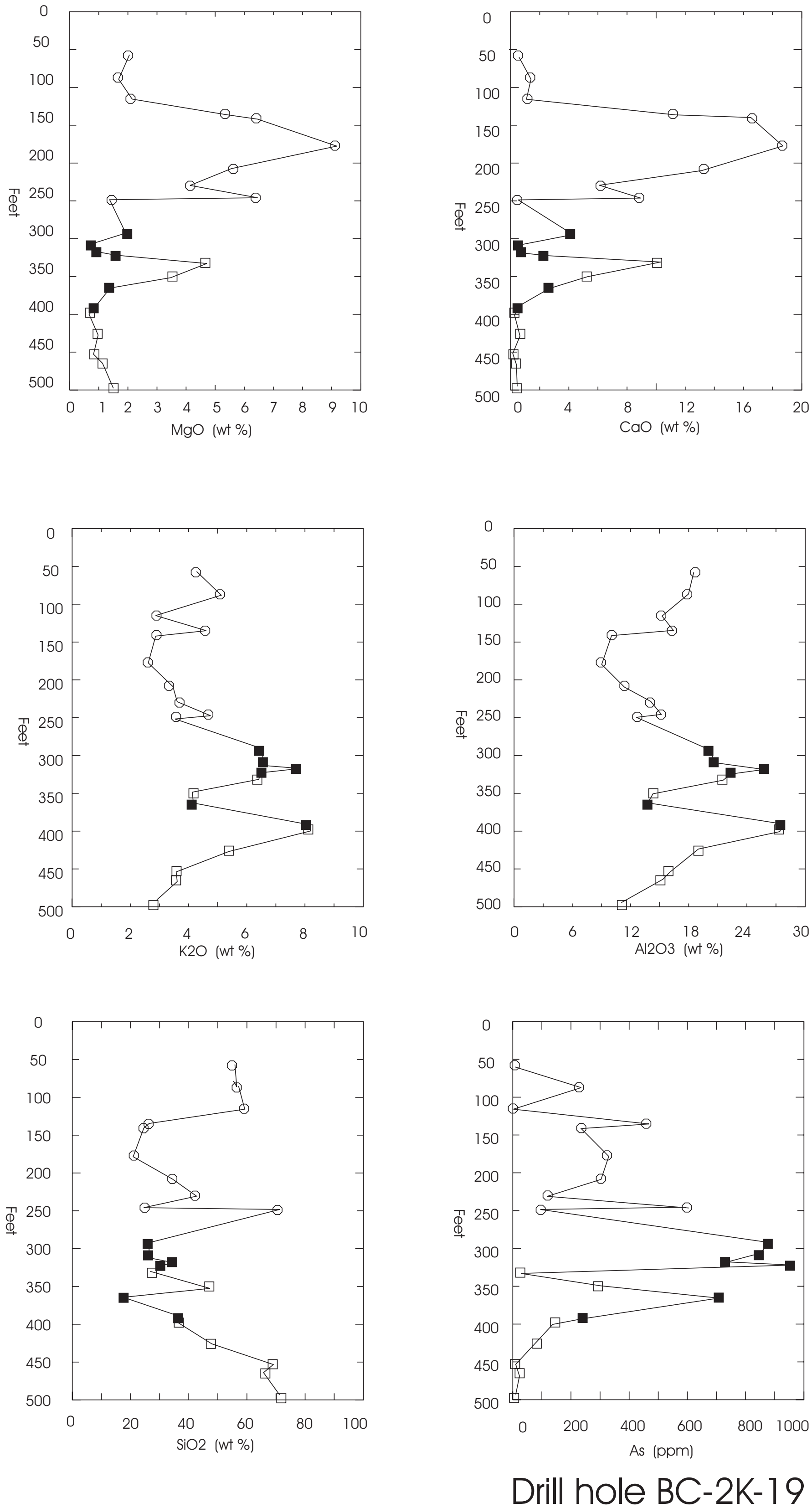

Figure 4B. Changes in the content of MgO, CaO, K_2O, Al_2O_3, SiO_2 and As down drill hole DH-2K-19, Bonanza Ledge. Open circles = hanging wall rocks; open squares = footwall rocks; solid squares = samples containing > 500 ppb Au.

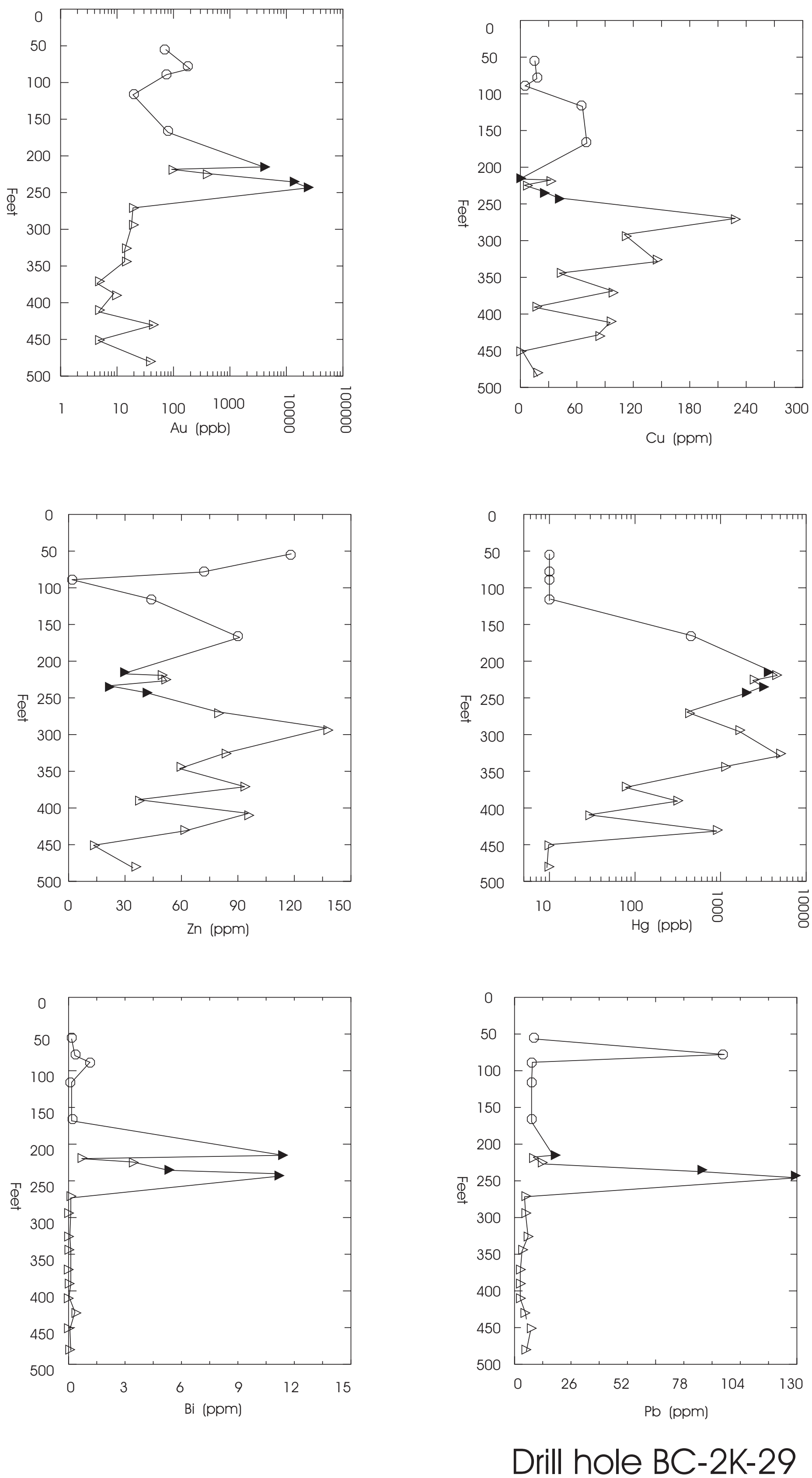

Figure 4C. Changes in the content of Au, Cu, Zn, Hg, Bi and Pb down drill hole DH-2K-29, Bonanza Ledge. Open circles = hanging wall rocks; open triangles = footwall rocks; solid triangles = samples containing > 500 ppb Au.

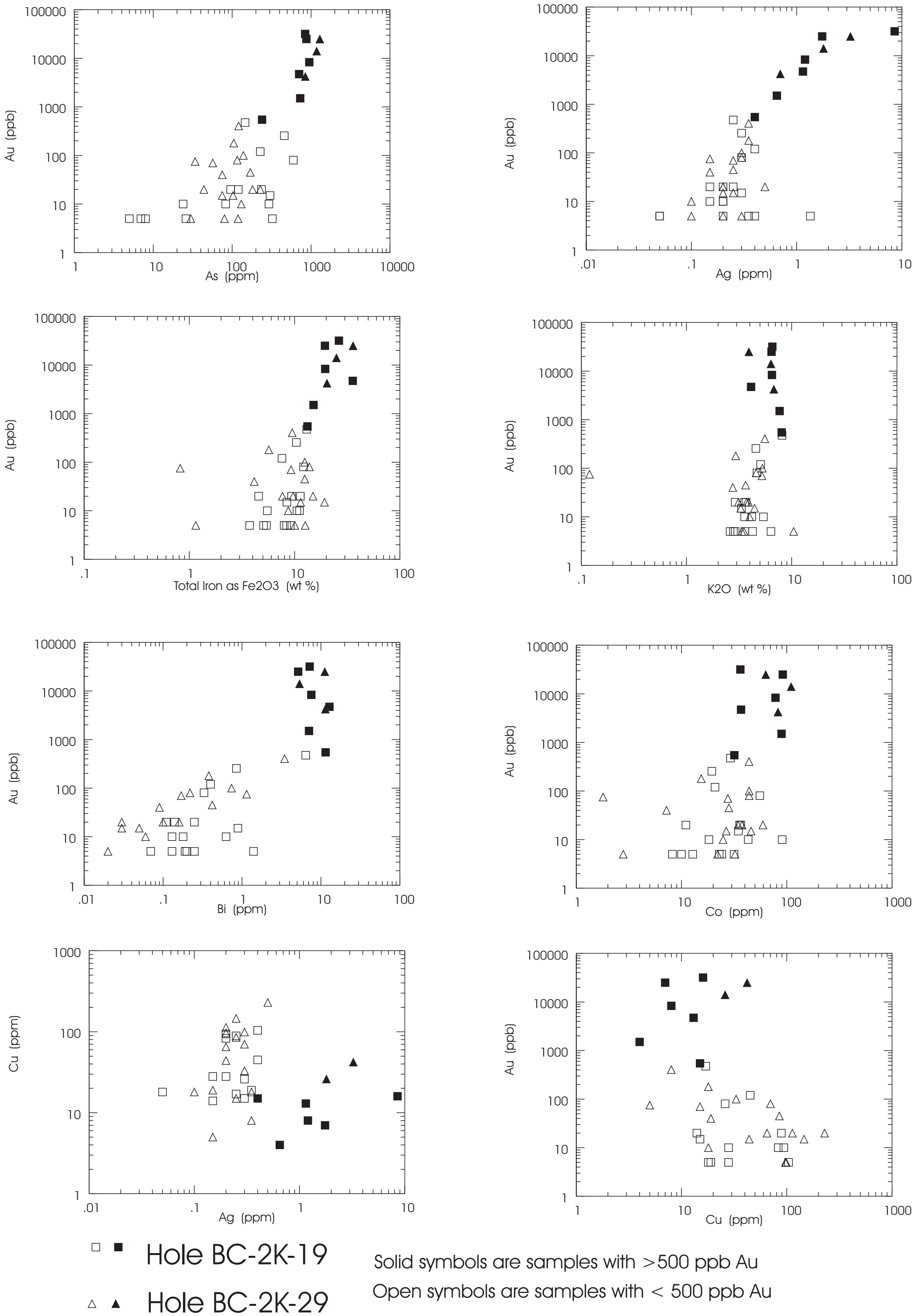

Figure 5A. Binary plots of geochemical data listed in Table 1A for drill holes BC-2K-19 & 29, Bonanza Ledge Gold Zone.

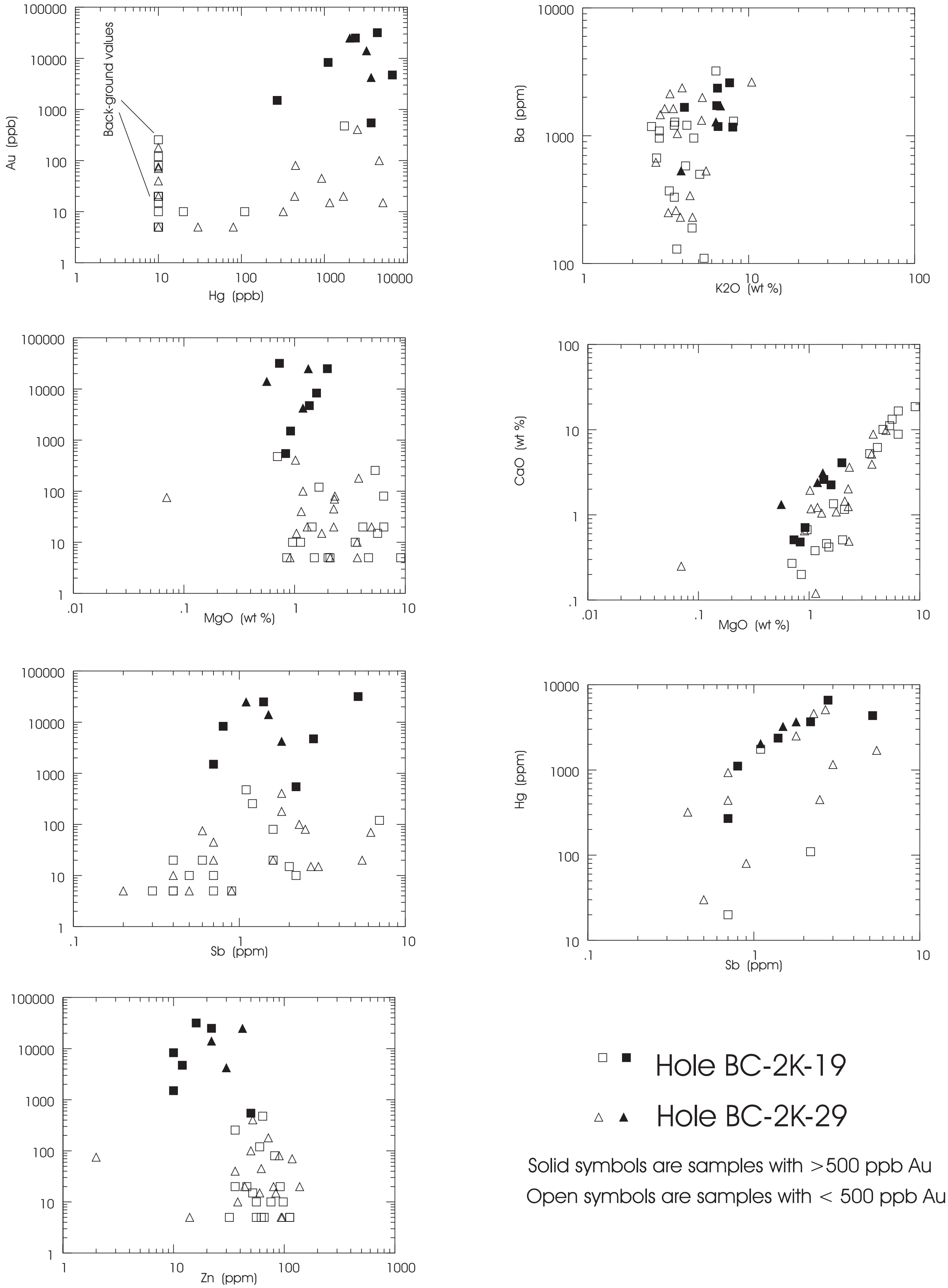

Figure 5B. Binary plots of geochemical data listed in Table 1A for holes BC-19 & 29, Bonanza Ledge Gold Zone.

5882421N) by placer miner Wilf Frederick is presented in Table 4. This sample was taken from a 0.75 kg composite of heavy mineral material collected over a period of time during Mr. Fredericks' placer operation. It contained abundant, fine grained magnetite and quartz, some very fine grained gold and larger fragments of scheelite up to 0.4 cm in diameter. Due to the sporadic presence of fuchsite-mariposite in the Wells-Barkerville district, this Lowhee Creek sediment sample was assayed to specifically test for ultramafic-related elements such as Cr, Pd, Pt and Ni. The data in Table 4 shows no enrichment in these elements, although enhanced quantities of Au, As, Bi, Co, Pb and W are present. The abundance of REE's such as La and Ce may indicate the presence of apatite or monazite. Although Lowhee Creek drains part of the area underlain by the BC Vein (Figure 1), the sample has a very low Hg content (10 ppb), suggesting that the element is relatively immobile in this area.

SUMMARY AND CONCLUSIONS

This preliminary study has involved the collection of relatively few samples. Consequently, our conclusions are tentative, although the following points can be made:

- As noted by many previous workers, the Wells-Barkerville district contains two types of auriferous pyrite mineralization: (1) pyrite that is intimately associated with at least four different sets of quartz veins and (2) pyrite in massive to semi-massive "replacement" bodies that mostly plunge gently northwest parallel to the axes of tight, ductile F2 folds. The newly discovered Bonanza Ledge Zone is thought to represent the latter type.
- For a number of reasons, Bonanza Ledge represents an exciting and significant new gold discovery: it occurs some distance from other known deposits, it lies in a different structural, stratigraphic and lithological setting to the massive replacement mineralization at the Mosquito Creek and Island Mountain mines (Rhys, 2000), and it has a different chemistry and gangue mineralogy. Thus it probably represents a newly recognized sub-type of the auriferous replacement pyrite mineralization in the district.
- Although the massive to semi-massive auriferous pyrite bodies at the Mosquito Creek and Island Mountain mines resemble the Bonanza Ledge mineralization, the latter is characterized by a gangue containing abundant sericite-muscovite, more quartz and rutile, and trace amounts of tourmaline.
- Despite the presence of sporadic chalcopyrite, both types of auriferous pyrite mineralization throughout the district generally have very low Cu contents, ranging from 1 to 8 ppm Cu in the veins and 1 to 42 ppm Cu in the replacements (Tables 2A and 2B).
- The average Au grades in our samples of vein-related pyrite from the Mosquito Creek and Cariboo Gold Quartz mines show little overall difference in grade to the massive pyrite replacement at the Mosquito Creek mine (avg. 27-28 g/t Au in the veins and 34 g/t Au in the Mosquito Creek replacement ore; Table 2D).
- There are chemical differences between the quartz-vein pyrite at Mosquito Creek and the quartz vein pyrite at the Cariboo Gold Quartz mine, despite their similar Au grades. The vein-associated pyrite at Mosquito Creek has higher quantities of Ag, As, Sb, Pb, Zn, W and As and lower Au/Ag ratios (2.4 versus 9.7; Table 2D).
- The replacement auriferous pyrite at the Mosquito Creek mine is chemically different to the similar looking mineralization at the Bonanza Ledge. The latter contains higher quantities of Al, K, Si and Ti, reflecting the greater abundances of quartz, sericite and rutile at Bonanza Ledge. It also has, on average, higher quantities of Cu, Co and Hg, as well as having more Ba, Be, Ce, Cs, Ga, Ge, Hg, La, Li, Nb, Ni, Sr, Th, Ta, Rb, V and Y. By contrast, the replacement mineralization at Mosquito Creek has higher quantities of As, Pb, W, Te, Bi and Cr. Some, but not all of these geochemical differences noted above probably reflect the contrasting sedimentary hostrock lithologies at the various properties.
- At Bonanza Ledge, there are strong correlations between Au:Bi, Au:As, Au:Pb, Au:K_2O and Au:Al_2O_3. By contrast, the correlations between Au:Zn and Au:Cu are poor to negative.
- One of the most distinctive geochemical differences between the replacement mineralization at Mosquito Creek and Bonanza Ledge is the latters' higher Hg content. Elevated Hg values occur not only in the Bonanza Ledge auriferous pyritic horizons but extends down into the barren footwall rocks (Figures 4A and 4C).
- The source, significance, nature, and host mineral of the Hg enrichment at Bonanza Ledge are unknown. However, the strong correlation between Fe and Hg and the poor to moderate correlation between Au and Hg suggests that the latter element is hosted by both barren and auriferous pyrite.
- There are at least three possible reasons for the apparent Hg enhancement at Bonanza Ledge, namely: (1) it is temporally and genetically related to the pyritic Au mineralization, (2) it represents a chemical overprint related to younger hydrothermal fluids that were channeled along the BC vein-fault system, or (3) it accumulated syngenetically during deposition of the organic-rich sediments and is thus an inherited feature of the rocks now hosting the Bonanza Ledge.
- The lack of intrusive rocks in the district, the low Cu and W contents of the auriferous pyrite and its development during the F2-related metamorphism, and findings of the recent fluid inclusion study (Dunne and Ray, 2001, this volume) are supportive evidence that the fluids responsible for the Wells-Barkerville Au were metamorphic in origin, rather than magmatic-hydrothermal.
- The potential for other Bonanza Ledge-type bodies in the district is high, given that large parts of the area are covered by glacial till. Exploration criteria would include looking for: (1) BC Vein-type structures, (2) hostrocks that include carbonates and organic-rich argillites, (3) magnetite porphyroblasts

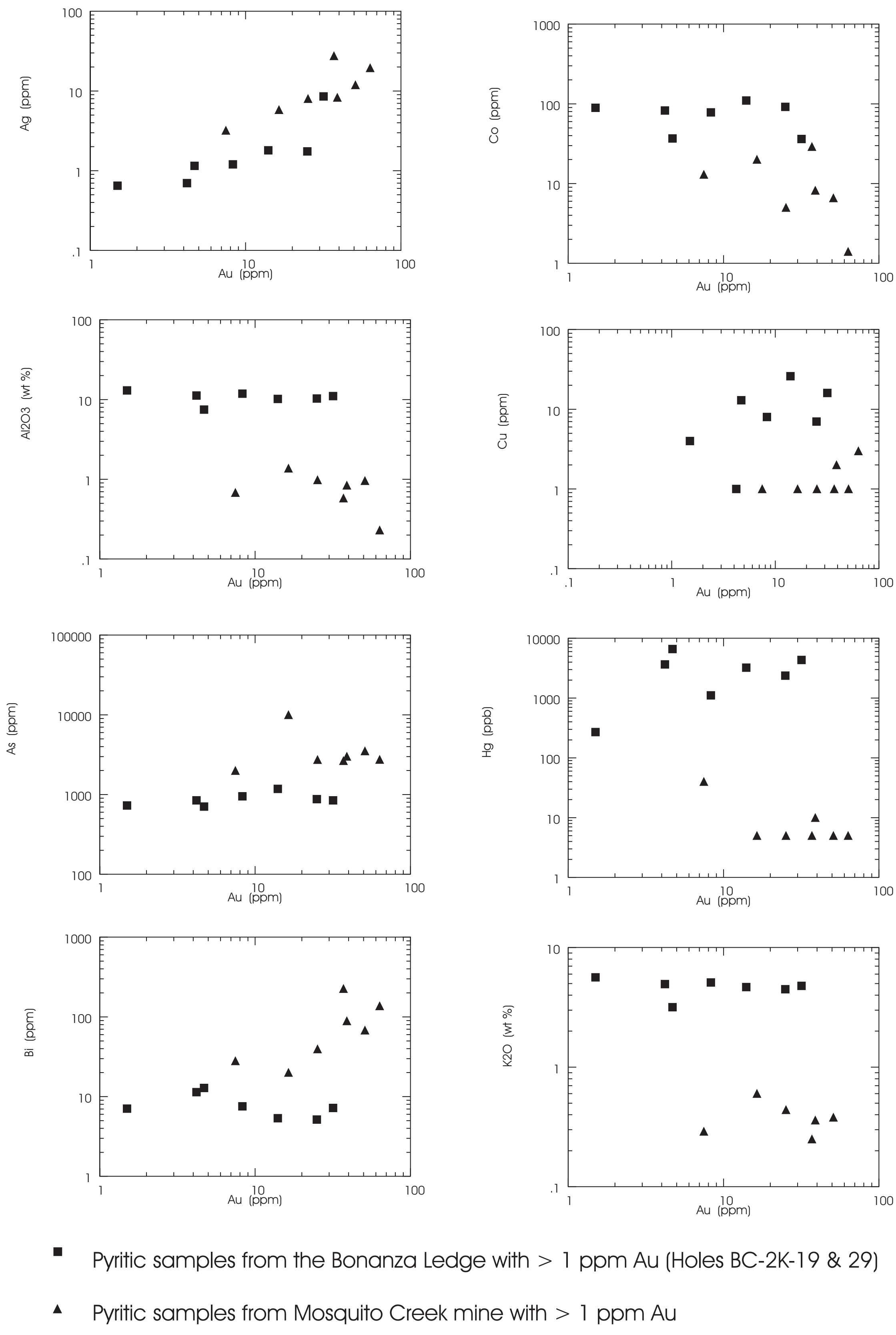

Figure 6A. Binary plots of data listed in Table 2B comparing the chemistry of the auriferous replacement pyrite at Bonanza Ledge and Mosquito Creek.

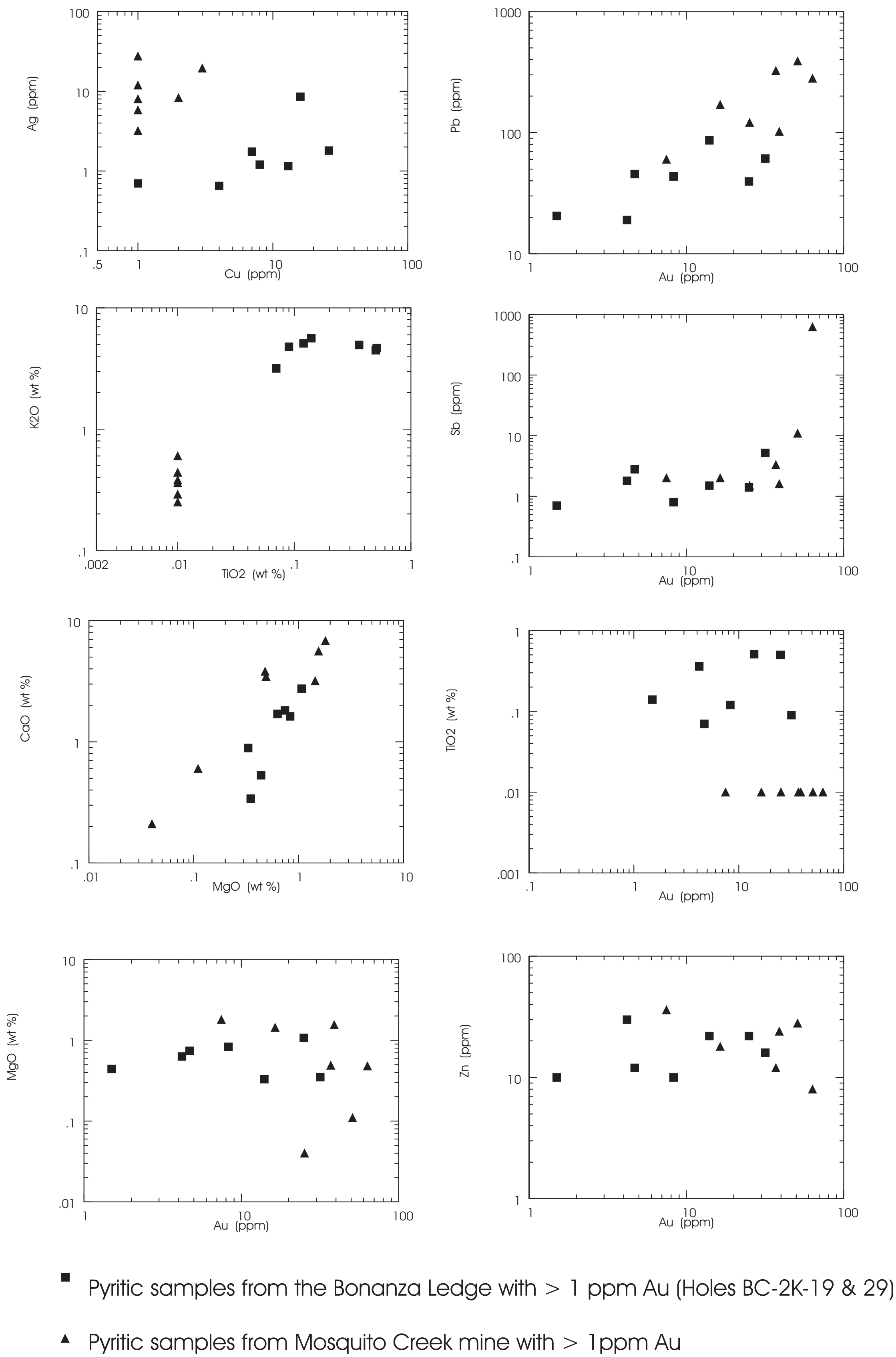

Figure 6B. Binary plots of data listed in Table 2B comparing the chemistry of the auriferous replacement pyrite at Bonanza Ledge and Mosquito Creek.

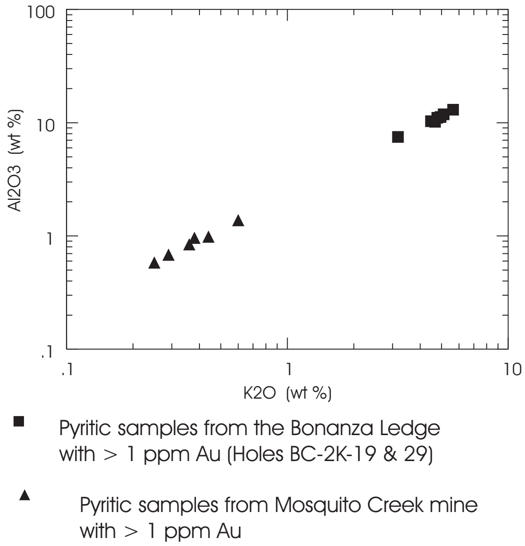

Figure 6C. Binary plot of data listed in Table 2B comparing the chemistry of the auriferous replacement pyrite at Bonanza Ledge and Mosquito Creek.

Photo 10. Replacement pyrite ore at the Island Mountain Mine. Coarse auriferous pyrite cubes in a gangue dominated by quartz, lesser sericite and trace rutile. Sample GR-00-86 assaying 49.9 g/t Au. Pyritic float sample taken from the Island Mountain Mine dump. Photomicrograph, reflected light, crossed polars, and long field of view is 2.5 mm.

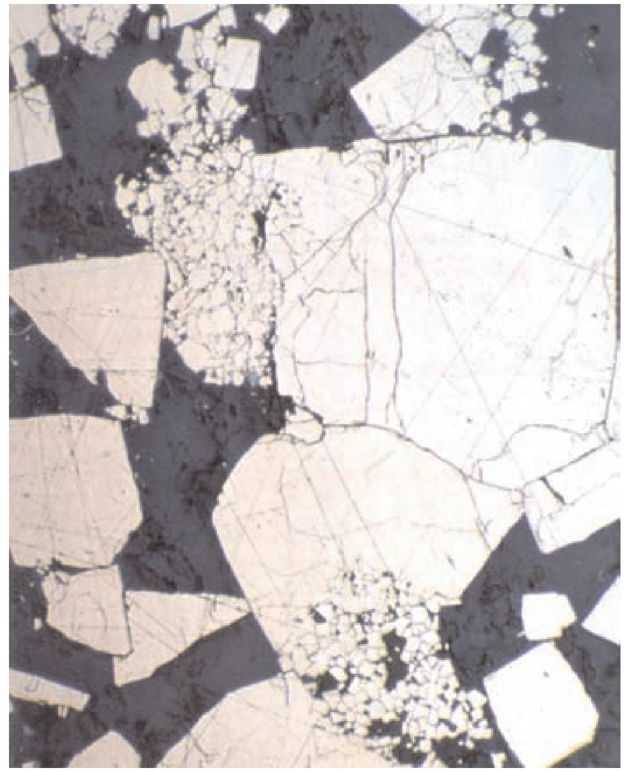

Photos 11 and 12. Replacement pyrite ore at the Island Mountain Mine. ?Early fine grained pyrite being replaced and overgrown by coarse pyrite. Sample GR-00-86. Photomicrograph, reflected light, crossed polars, and long field of view is 2.5 mm.

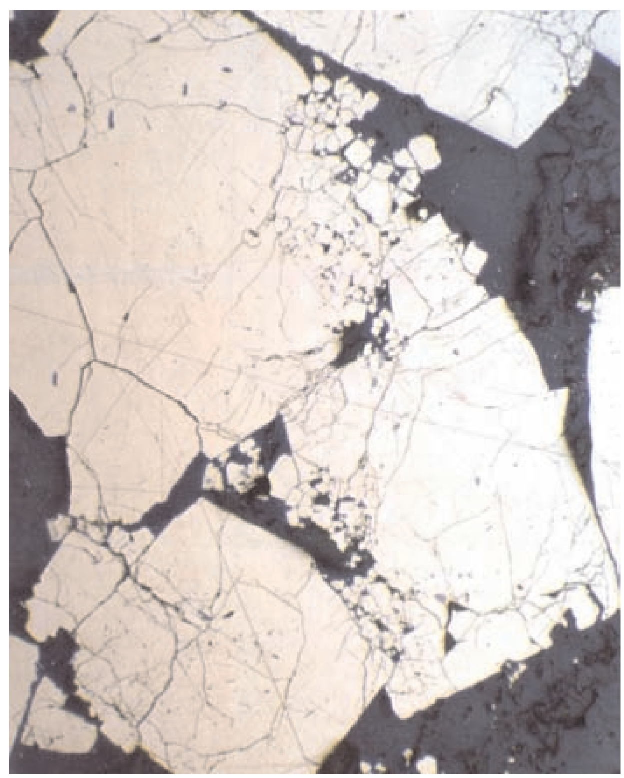

Photo 12.

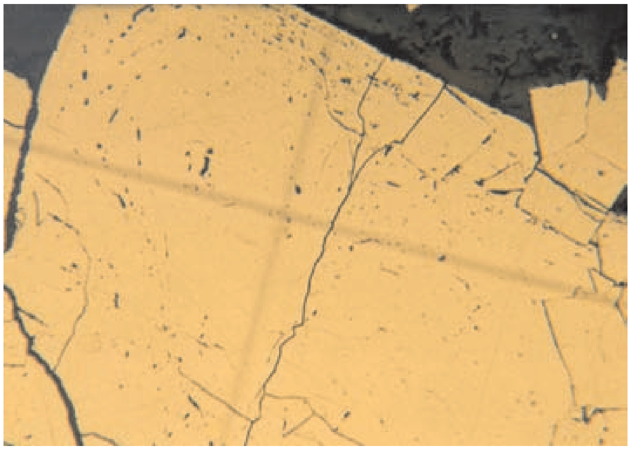

Photo 13. Replacement pyrite ore at the Mosquito Creek Gold Mine. Coarse, euhedral pyrite crystals with margins containing growth zones marked by trails of small silicate inclusions. Sample GR-00-34 assaying 25.2 g/t Au. Pyritic float from the No. 1 adit mine dump. Photomicrograph, reflected plane light, and long field of view is 2 mm.

and pervasive sericite-dolomite-pyrite-albite ± rutile ± tourmaline alteration, and (4) Au-Bi-As-Ti-Hg geochemical anomalies. In addition, Rhys (personal communication, 2000) reports a strong association between replacement Au mineralization and enhanced Pb values.

- Besides conventional geophysical and geochemical soil-sediment surveys, biogeochemical sampling for certain pathfinder element could be a useful tool to locate other Bonanza Ledge-type bodies in the till-covered areas.
- To summarize, the two most important recent findings regarding exploration in the Wells-Barkerville area are: (1) the recognition (Rhys and Ross, 2000; Rhys, 2000) that replacement mineralization can be hosted by a variety of metasedimentary lithologies and is not necessarily confined to the Rainbow-Baker members, and (2) that two types of replacement mineralization may exist in the district, as represented by Mosquito Creek on the one hand and Bonanza Ledge on the other. Elements such as Au, Bi, As, Pb and Hg could be useful pathfinder element to locate Bonanza Ledge-type orebodies. McTaggart and Knight (1993) note that several streams in the district have Hg-rich gold placers derived from unknown bedrock sources. These authors conclude that in most cases the Hg is primary and not due to human contamination. Drainages with Hg-rich placers in the Wells-Barkerville region include those along Mary (Toop), Frye, Jerry, Sugar, Dragon, Montgomery and Nelson creeks as well as in the Quesnel Canyon (McTaggart and Knight, 1993). These streams warrant exploration for Bonanza Ledge-type replacement Au mineralization.

Photo 14. Replacement pyrite ore at the Mosquito Creek Gold Mine. Coarse pyrite crystal with embayed margins in a quartz-carbonate rich gangue. Sample GR-00-34. Pyritic float from the No. 1 adit mine dump. Photomicrograph, reflected light, crossed polars, and long field of view is 2 mm.

ACKNOWLEDGMENTS

This study was made possible by the encouragement and help of Frank Callaghan, president of International Wayside Gold Mines Ltd., and thanks are given to him and his staff at the Wells exploration office. In addition, we thank the following for informative geological discussions in the field or office: Robert (Ned) Reid, Dave Rhys, Craig Leitch, Geoff Goodall, Wilf Frederick, Bob Lane, Gary Polischuck, Dani Alldrick, Bert Struik, Kathryn Dunne, Derek Brown, Fil Ferri, Dave Lefebure, Tom Schroeter and Ken Lord. Particular thanks are given to Claude Blagdon and Mike Mulholland who assisted in the underground sampling at the Mosquito Creek, Island Mountain and Cariboo Gold Quartz mines. We also thank Nick Massey for his editorial comments.

REFERENCES

Alldrick, D. J. (1983): The Mosquito Creek Mine, Cariboo Gold Belt (93H/4); *British Columbia Ministry of Energy, Mines and Petroleum Resources*, Geological Fieldwork 1982, Paper 1983-1, pages 99-112.

Ash, C.H. (in press): Ophiolite related gold quartz veins in the North American Cordillera; *British Columbia Ministry of Energy and Mines,* Bulletin 108.

Bacon, W.R. (1939): A mineralographic study of ore specimens from Island Mountain Mine, British Columbia; unpublished report, The University of British Columbia, 10 pages.

Benedict, P.C. 1945: Structure at Island Mountain Mine, Wells, B.C.; Canadian Institute of Mining and Metallurgy, Transactions, V. 48, p. 755-770.

Bowman, A. (1889): Report on the mining district of Cariboo, Geological Survey of Canada, Annual Report, 1887-1888, Volume III, Part 1, Part C.

Bowman, A. (1895): Maps of the Principal Auriferous Creeks in the Cariboo, Geological Survey of Canada, Maps 364-372, 1895.

Clague, J.J. (1989): Placer gold in the Cariboo District, British Columbia; *Geological Survey of Canada*, Paper 89-1E, pages 243-250.

Dunne, K.P.E., and Ray, G.E. (2001, this volume): Preliminary Fluid Inclusion Study of Quartz Vein and Massive-Banded-Stringer Pyrite Mineralization in the Wells-Barkerville Gold Belt, East-Central British Columbia *British Columbia Ministry of Energy, Mines and Petroleum Resources*, Geological Fieldwork 2001, Paper 2001-1, this volume.

Hall, R. (1999): Cariboo Gold project at Wells, British Columbia; prepared for *International Wayside Gold Mines Limited* at http://www.wayside-gold.com/i/pdf/RHall_report.pdf, 52 pages.

Hanson, G. (1934): Willow River Map Area, Cariboo District, British Columbia: general geology and lode deposits; *Geological Survey of Canada*, Summary Report, 1933, Part A, pages 30A-48A.

Hanson, G. (1935): Barkerville Gold Belt, Cariboo District, British Columbia; *Geological Survey of Canada*, Memoir 181, 42 pages.

Holland, S.S. (1954): Geology of the Yanks Peak - Roundtop Mountain Area, Cariboo District, British Columbia; *British Columbia Department of Mines*, Bulletin No. 34, 102 pages.

Holland, S.S. (1950): Placer Gold Production of British Columbia; *British Columbia Department of Mines*, Bulletin No. 28, 89 pages.

Holland, S.S. (1948): Report on the Stanley Area, Cariboo Mining Division; *British Columbia Department of Mines*, Bulletin No. 26, 66 pages.

Johnson, W.A. and Uglow, W.L. (1926): Placer and vein gold deposits of Barkerville, Cariboo District, British Columbia; *Geological Survey of Canada*, Memoir 149, 246 pages.

Levson. V.M. and Giles, T.R. (1993): Geology of Tertiary and Quaternary gold-bearing placers in the Cariboo Region, British Columbia (93A, B, G, H); *British Columbia Ministry of Energy, Mines and Petroleum Resources*, Bulletin 89, 202 pages.

McTaggart, K.C. and Knight, J. (1993): Geochemistry of Lode and Placer Gold of The Cariboo District, B.C.; *British Columbia Ministry of Energy, Mines and Petroleum Resources*, Open File 1993-30, 26 pages.

Rhys, D.A.E. (2000): The Cariboo Gold Project of International Wayside Gold Mines; *Vancouver Mineral Exploration Group*, Abstract, November 29, 2000, 2 pages.

Rhys, D.A.E. and Ross, K.V. (2000): Report on petrography, check sampling and geological interpretation of drill core at the Bonanza Ledge zone, Cariboo Gold Quartz property, British Columbia; Prepared for International Wayside Gold Mines Ltd. by Panterra Geoservices Inc. *at* http://www.wayside-gold.com/i/pdf/PanterraGeoReport_new.pdf, 77 pages.

Robert, F. and Taylor, B.E. (1989): Structure and mineralization at the Mosquito Creek Gold Mine, Cariboo District, B.C.; *in* Short Course Number 14, *Geological Association of Canada, Cordilleran Section*, pages 25-41.

Runkle, J.D. (1950): Mineralography of the Island Mountain ore; unpublished report, Department of Geology, *The University of British Columbia*, 16 pages.

Skerl, A.C. (1948): Geology of the Cariboo Gold Quartz Mine, Wells B.C.; *Economic Geology*, Volume 43, pages 571-597.

Sutherland Brown, A. (1957): Geology of the Antler Creek Area, Cariboo District, British Columbia; *British Columbia Department of Mines*, Bulletin number 38, 105 pages.

Sutherland Brown, A. (1963): Geology of the Cariboo River Area, British Columbia; *British Columbia Department of Mines and Petroleum Resources*, Bulletin number 47, 60 pages.

Struik, L.C. (1988a): Structural geology of the Cariboo gold mining district, East-central British Columbia; *Geological Survey of Canada*, Memoir 421, 100 pages.

Struik, L.C. (1988b): Geology, Wells, Cariboo Land District, British Columbia; *Geological Survey of Canada*, Map 1635A, scale 1:50 000.

Uglow, W.L. and Johnson, W.A. (1923): Origin of the placer gold of the Barkerville Area, Cariboo District, British Columbia, Canada; *Economic Geology*, Volume 18, pages 541-561.

Preliminary Fluid Inclusion Study of Quartz Vein and Massive-Banded-Stringer Pyrite Mineralization in the Wells-Barkerville Gold Belt, East-Central British Columbia

By Kathryn P.E. Dunne[1] and Gerry E. Ray[2]

KEYWORDS: Economic geology, quartz veins, massive-banded-stringer pyrite ore, gold, fluid inclusions, salinity, homogenization temperature, Wells, Barkerville, Island Mountain mine, Mosquito Creek mine, Cariboo Gold Quartz mine, Bonanza Ledge zone.

INTRODUCTION

The Wells-Barkerville Gold Belt lies approximately 65 km east of Quesnel, in the Cariboo Mining Division, British Columbia. Gold in this area is hosted by two types of mineralization: quartz-pyrite vein and massive-banded-stringer pyrite ore. Both types are hosted by a lower greenschist facies stratigraphic interval within clastic metasedimentary rocks of the Barkerville subterrane.

This paper is the first publication of fluid inclusion data from the belt. The objectives of this study are to:

- document fluid inclusion characteristics (i.e. temperature, composition) in quartz from both vein and 'massive' pyritic mineralization at the Mosquito Creek and Island Mountain mines, and from quartz vein mineralization at the Cariboo Gold Quartz mine, and the BC, Warspite and Perkins vein occurrences (Figure 1).
- compare fluid inclusion characteristics of vein and massive-banded-stringer ore within and between deposits in the belt.
- compare fluid inclusion data from the Wells-Barkerville Belt with data from other gold districts hosted in low metamorphic-grade rocks.
- discuss the use of fluid inclusion data as a tool to determine the depositional environment of deposits in the Wells-Barkerville Belt.

GEOLOGICAL SETTING

The Wells-Barkerville Belt is within the Barkerville subterrane of the Late Proterozoic and Paleozoic Kootenay Terrane. The Barkerville subterrane comprises metamorphosed grit, quartzite, phyllite, lesser limestone and volcaniclastic rocks of the Snowshoe Group (Struik, 1988). Quartz-pyrite vein and massive, banded and stringer pyritic mineralization in the Wells-Barkerville Belt are confined to a lower greenschist facies stratigraphic interval within the upper Snowshoe Group variably termed the 'Baker and Rainbow Members" (Hansen, 1935), Snowshoe Formation (Sutherland-Brown, 1957) and Downey and Hardscrabble successions (Struik, 1988).

Isoclinal to tight folds and shear zones record conditions of early ductile flow in the Barkerville Subterrane (Struik *et al.,* in Gabrielse, 1991). Open folds and faults characteristic of brittle conditions are superimposed on the ductile structures (Struik op. cit.). A progressive sequence of veining at the Cariboo Gold Quartz, Island Mountain and Mosquito mines spans early veins formed during the dominant phase of ductile deformation and later least strained veins that contain most of the gold (Rhys and Ross, 2000; Rhys, 2000).

MINERAL DEPOSITS

Two types of gold-bearing ore occur in the Wells-Barkerville Belt: quartz-pyrite veins and massive-banded-stringer pyrite (Johnson and Uglow, 1926; Hanson, 1935; Benedict, 1945; Skerl, 1948; Richards, 1948; Sutherland-Brown, 1957; Alldrick, 1983; Robert and Taylor, 1989). McTaggart and Knight (1993) suggest that gold from the 'massive' pyritic ore at Island Mountain and Mosquito Creek mines (average fineness of 870) differs from gold in quartz veins at the Cariboo Gold Quartz mine (fineness of 945). Production figures from the Island Mountain mine indicate that gold grades in the 'massive' ore are higher than grades in the 'vein' ore (Benedict, 1945).

Vein ore typically comprises dominantly massive, white to translucent quartz, lesser dolomite/ankerite, muscovite (as sericite) and pyrite and rarely minor arsenopyrite, galena, sphalerite and/or scheelite (cf. Skerl, 1948). Pyrrhotite and chalcopyrite have been reported as accessory minerals (Skerl, op. cit.; International Wayside Gold Mines Ltd., 2000). Wide veins, such as the BC Vein, can be greater than 15 metres in width and may have sheared graphitic margins. Sericite from quartz veins in the Cariboo Gold Quartz mine, Mosquito Creek Gold mine and Cariboo Hudson mine have been dated using the

[1] *Consulting Geologist*

[2] *British Columbia Ministry of Energy and Mines*

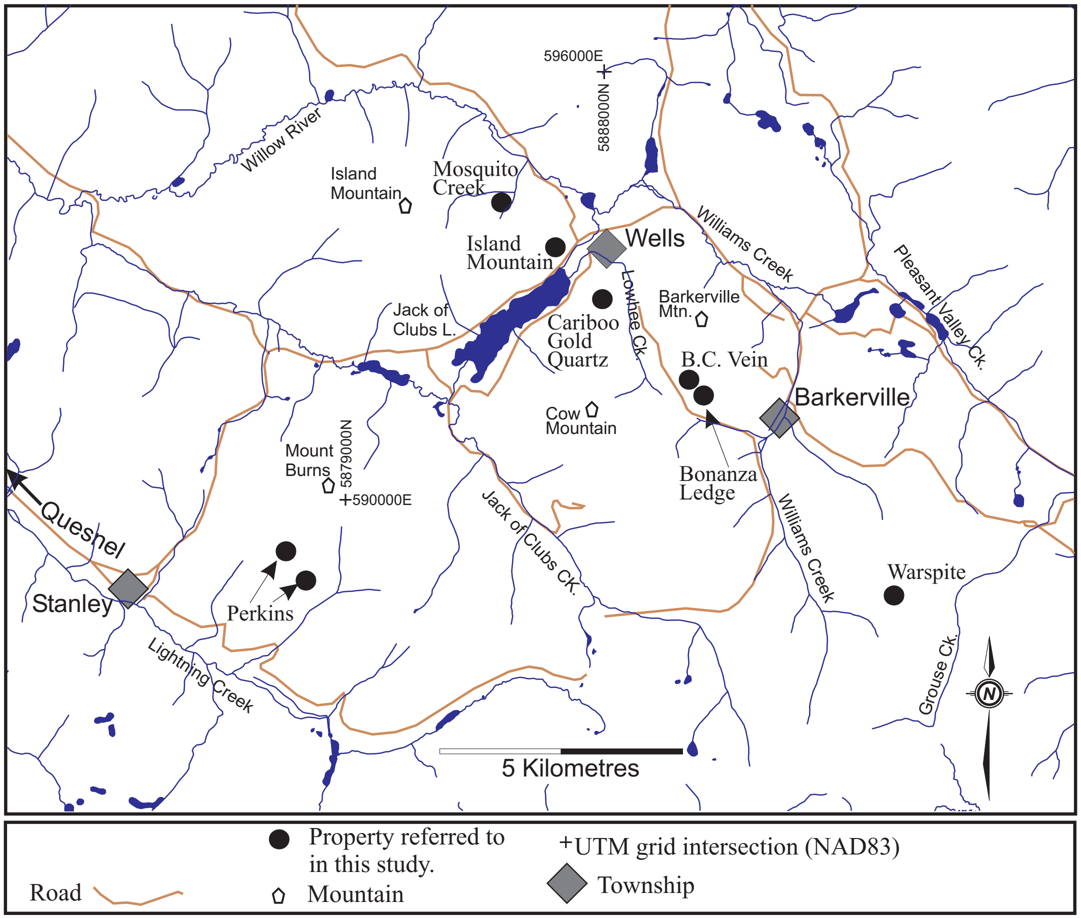

Figure 1. Location map of properties sampled and referred to in this study, Wells-Barkerville area.

K-Ar method at 140 Ma (International Wayside Gold Mines Ltd., 2000).

Vein textures in the Wells-Barkerville Belt are highly variable. Massive, white to translucent 'bull' quartz veins comprise subhedral to anhedral crystals from less than 0.5 mm to approximately 2 mm in size. Sutured grain boundaries have been noted in some samples. Many of the massive veins are highly fractured (Photo 1) and in some cases the abundance of microfractures results in a texture described by Reynolds (1991) as 'wispy quartz' (Photo 2). Reynolds (op. cit.) suggests that this texture is characteristic of deep vein environments (> 4km and possibly > 8 km). In contrast, breccia textures indicative of brittle crushing reflecting higher level emplacement are observed in other veins (Photos 3 and 4). Skerl (1948) reports that approximately 1 percent of the veins at the Cariboo Gold Quartz deposit have vugs containing well terminated quartz crystals. These vugs indicate open-space filling late in the vein history. They have been noted in veins elsewhere in the Wells-Barkerville Belt (*eg*. Mosquito Creek, Warspite, Perkins). The quartz crystal terminations are typically translucent whereas most of the massive quartz is white due to abundant fluid inclusions along microfractures. Even fractured and wispy quartz veins have vugs (*cf*. Photo 2 - centre). Differences in temperature and composition between the late (?), open-space fill quartz and the earlier massive quartz are described below.

Four distinct, structurally-controlled vein orientations occur in the Wells-Barkerville Belt: strike, bedding-parallel veins (NW-SE/45-70NE), northerly (N-S/40-70E), orthogonal (030-040/70SE) and diagonal (070-090/subvertical) (Hanson, 1935; Benedict, 1945; Richards, 1948; Skerl, 1948; Robert and Taylor, 1989). Orthogonal veins are most abundant and these contain the highest concentrations of gold (Benedict, 1945, Robert and Taylor, 1989, International Wayside Gold Mines Ltd., 2000).

Two distinct styles of pyritic ore mineralization are evident in the belt. At Mosquito Creek and Island Mountain mines the pyritic orebodies occur within or adjacent to limestone units (Benedict, 1945; Alldrick, 1983), but at Bonanza Ledge in carbonaceous metasedimentary units and limestone (Rhys and Ross, 2000; Rhys, 2000). Pyrite orebodies at Mosquito Creek and Island Mountain mines tend to be commonly associated with fold hinges. Stope dimensions for these orebodies in fold hinges are commonly less than 10 metres thick and several hundred metres in the down plunge direction (Benedict, 1945, Robert and Taylor, op. cit.). Pyrite lenses at Mosquito

Photo 1. Highly fractured 'bull' quartz vein, Cariboo Gold Quartz deposit. Note open vug lined with quartz crystals top right of photo. Sample CGQ-FI-3. Transmitted plane light. Width of photo 2mm.

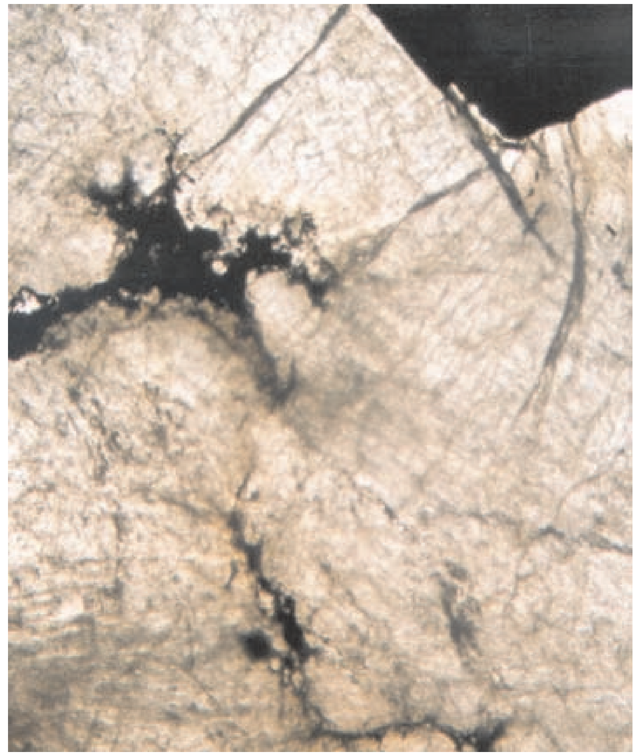

Photo 2. Abundant 'sweeping' microfractures giving appearance of wispy quartz texture in quartz-pyrite-sphalerite vein, Warspite occurrence. Note large vug left of centre. Sample GR-00-81. Transmitted plane light. Width of photo 2mm.

Photo 3. Quartz breccia with angular fragments from 0.5 to 2 cm provides evidence of brittle deformation near footwall of BC Vein above Bonanza Ledge. Open-space filling with clear euhedral quartz crystals is noted in this sample. Sample GR-00-46. Transmitted plane light. Width of photo 18.5 mm.

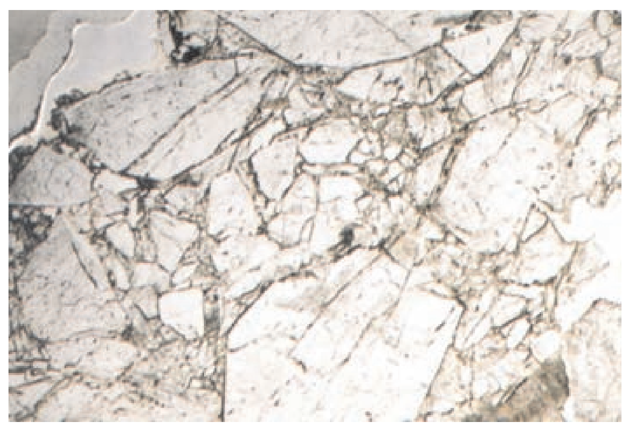

Photo 4. Quartz breccia with angular fragments of clear euhedral quartz from open vugs, Mosquito Creek deposit. Sample GR-00-73. Transmitted plane light. Width of photo 18.5 mm.

Creek can either be parallel to the strong foliation or parallel to the bedding (Robert and Taylor, 1989). At the Bonanza Ledge zone, Rhys (2000) describes folded high-grade pyrite mineralization that is discordant to stratigraphy and locally more than 30 metres thick over a strike length of 130 metres.

Pyritic ore at Bonanza Ledge comprises veinlets, concordant laminations and massive bands of pyrite, often with trace chalcopyrite and galena, in a gangue of muscovite, dolomite/ankerite and quartz (Rhys and Ross, 2000; Rhys, 2000). Pyrite orebodies at Mosquito Creek typically comprise fine to medium-grained crystalline pyrite forming individual or stacked lenses (Robert and Taylor, 1989). At the Cariboo Gold Quartz mine, massive crystalline pyrite orebodies contain little or no quartz but grey and white carbonates, galena, sphalerite and scheelite are reported around the margins of the ore (Skerl, 1948). Examples of the massive and banded pyrite ore from the Island Mountain mine in a gangue of fine-grained quartz, sericite and minor carbonate are in Photos 5 and 6.

Quartz in the massive pyritic Bonanza Ledge ore occurs as subhedral to anhedral crystals from about 0.25 mm to 1.5 mm in size, or as finer-grained, possibly recrystallized crystals that are mostly < 0.15 mm in diameter, with sutured grain boundaries (C. Leitch, written communication to G.E. Ray, October 2000). Undulose extinction indicative of strain is common in the larger crystals (C. Leitch, op. cit.). Similar quartz textures are evident in a limited number of samples collected from Mosquito Creek and Island Mountain deposits.

Most workers in the Wells-Barkerville Belt (Hanson, 1935; Benedict, 1945; Skerl, 1948; Sutherland-Brown, 1957; Alldrick, 1983; Rhys and Ross, 2000; Rhys, 2000) believe that the pyrite lenses formed by replacement of carbonate units. A syn-sedimentary origin has also been proposed by Robert and Taylor (1989).

FLUID INCLUSION DATA

This preliminary paper describes fluid inclusions in quartz in the quartz-pyrite veins and in the massive-banded-stringer pyrite. Samples were examined from the Warspite, Cariboo Gold Quartz, Island Mountain, Mosquito Creek, and Perkins properties (Figure 1). The former Cariboo Gold Quartz, Island Mountain and Mosquito Creek mines were the principal lode gold producers in the belt. Description of the geology of the deposits have been given by Hanson (1935), Benedict (1945), Holland (1948), Johnson and Uglow (1926), Skerl (1948), Richards (1948) and Sutherland-Brown (1957). Where possible, samples were taken from surface outcrops, underground exposures and drillcore. However, as some mine workings are inaccessible, a number of samples were collected from dumps adjacent to portals. Over 30 'quick plates' were prepared for fluid inclusion petrography. Quick plates are thick sections, 80 to 100 microns thick, mounted on glass slides with epoxy and polished on the top surface only. Of these, 12 samples, 2 from each of the 5 properties listed above and 2 from the BC Vein were selected for fluid inclusion microthermometry and re-prepared as doubly-polished sections. Samples were selected to give broad representation of both types of mineralization and, for veins, to give representation of some of the four vein orientations (Table 1).

Quartz was used for microthermometry because it has high tensile strength and is relatively translucent. Sphalerite is another high tensile strength mineral and is preferable to quartz because it is a sulphide mineral. Sphalerite is present in the BC Vein in the hanging-wall of the Bonanza Ledge zone (Ray *et al.*, 2001, this volume) but unfortunately the mineral in the sample (GR-00-91) is too opaque for fluid inclusion study. Future work in the belt should focus on the potential of sphalerite and scheelite for fluid inclusion microthermometry.

Fluid inclusions were evaluated using the concept of fluid inclusion assemblages (FIA's). This ensures that the data was not biased by samples containing large numbers of fluid inclusions and helps to eliminate inconsistent data caused by changes in mass, volume or shape of inclusions after entrapment (i.e. eliminate non-representative inclusions that are the result of diffusion, stretching, or necking-down processes). A fluid inclusion assemblage (FIA) is a petrographically-associated group of inclusions such as those aligned along primary growth zones or secondary fracture planes. One representative data point, rather than several data points is used for each FIA.

Petrography

Fluid inclusions in quartz from both vein and 'massive' ore in our Wells-Barkerville samples are typically less than 15 microns in longest dimension with inclusions in 'massive' ore usually less than 6 microns in longest dimension. Inclusions in some vein samples reach 30 microns in longest dimension. They vary in shape from irregular to smooth and in some cases they mimic the host crystal form and are 'negative-crystal'-shaped.

Fluid inclusions in our vein samples are classified as secondary or indeterminate. Secondary inclusions are aligned along fractures that crosscut grain boundaries

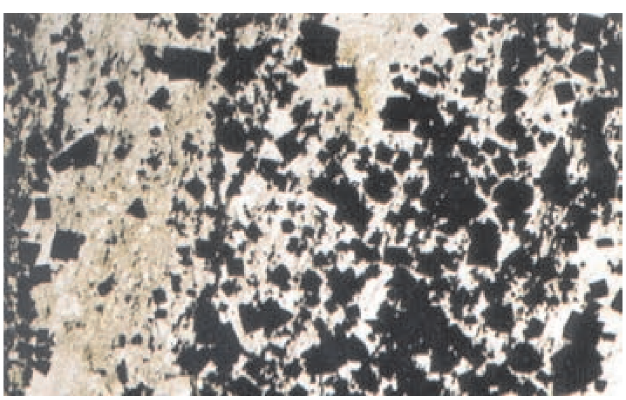

Photo 5. Medium-grained crystalline pyrite (black), quartz and minor fine-grained sericite representative of 'massive' ore, Island Mountain deposit. Sample GR-00-85. Transmitted plane light. Width of photo 18.5 mm.

Photo 6. Fine and medium-grained crystalline pyrite (black), quartz, minor sericite and carbonate representative of 'banded' ore, Island Mountain deposit. Sample GR-00-88. Transmitted plane light. Width of photo 18.5 mm.

TABLE 1
SUMMARY DESCRIPTIONS OF SAMPLES USED FOR FLUID INCLUSION MICROTHERMOMETRIC ANALYSES, WELLS-BARKERVILLE GOLD BELT

DEPOSIT NAME	SAMPLE NUMBER	ORE TYPE	STRUCTURE TYPE	LOCATION IN VEIN	VEIN TEXTURES	MINERALS[1]
Cariboo Gold	CGQ-FI-3	vein	orthogonal?	?	bull qz	qz
Quartz (mine)	CGQ-FI-4	vein	?	whole vein	bull qz	qz
BC Vein	GR-00-91	vein	strike	footwall	massive	sph
(Bonanza Ledge)						qz
BC Vein	GR-00-46	vein	strike	margin	bx, vugs	qz
Island Mountain	GR-00-85	massive			massive/banded	py,qz,ser
(mine)	GR-00-94	vein	diagonal	?	recry. qz	gal,qz
					bull qz	
Mosquito Creek	GR-00-67	vein	strike	centre of 1 m	vugs	qz
(mine)	GR-00-68	massive		thick vein	banded/stringer	py, qz
					recry. qz	
Warspite (veins)	GR-00-81	vein	dump	?	bull qz	py, sph, qz
	GR-00-82	vein	dump	?	bull qz	gal, qz
Perkins (veins)	GR-00-49	vein	dump	?	vugs	qz
	GR-00-56	vein	orthogonal?	?	vugs	qz

1. Mineral abbreviations: qz=quartz, py=pyrite, sph=sphalerite, gal=galena, ser=sericite

(Roedder, 1984). Interpretation of secondary fluid inclusion data reflects the conditions of formation of post-crystal formation fluids trapped in fractures after crystal growth ceased. No gold particles were seen with any fluid inclusions in this study but gold is reported to be directly associated with secondary fluid inclusions in quartz veins at the Sigma Mine in Quebec (Robert and Kelly, 1987). Further detailed petrographic work is required to evaluate the occurrence of gold with respect to fluid inclusion chronology in the quartz veins of the Wells-Barkerville Belt.

The fluid inclusions noted in our 'massive' pyrite ore samples are classified as primary, secondary, pseudosecondary or indeterminate, based on the criteria of Roedder (1984) and Bodnar *et al.* (1985). Primary fluid inclusions are aligned along growth zones in quartz proximal to sulphide grains in 'massive' ore from the Mosquito Creek deposit (Photos 7 and 8). Unfortunately, these primary inclusions are less than 1-2 microns long and are too small for heating-freezing work. However, slightly larger primary and pseudosecondary fluid inclusions trapped in quartz in recrystallized zones around pyrite in 'massive' ore from the Island Mountain and Mosquito Creek deposits have been observed and measured (Photos 5, 9, 10 and 11). Pseudosecondary fluid inclusions (Photos 11 & 12) are aligned along fractures that do not crosscut grain boundaries and are presumed to represent fluids trapped in fractures at the time the crystal was growing (Roedder, 1984).

The occurrence of primary and pseudosecondary fluid inclusions in our samples is unusual because typically, in deposits hosted by metamorphosed and deformed rocks, significant deformation of quartz leads to recrystallization and expulsion of inclusions as well as cracking and trapping of secondaries, which may be subsequently annealed out (*cf.* Yardley, 1999). However, some studies report that the quartz grains are not completely recrystallized. For example, Garba and Akande (1992) document primary fluid inclusions in vein quartz hosted by metasediments in the Zuru Schist Belt of northwestern Nigeria. Primary fluid inclusions have also been documented in euhedral quartz encapsulated in sulphide grains at the Sigma mine in Quebec (Guha *et al.*, 1991).

The primary and pseudosecondary fluid inclusions documented in this study have relatively consistent liquid-to-vapour ratios but moderately variable homogenization temperatures. The variability in homogenization temperature data may be due to thermal re-equilibration as suggested by Smith and Yardley (1999), undetectable necking down (post-entrapment change in inclusion shape) or real variability in the FIA's. Further petrographic work on additional 'massive' ore samples at a number of deposits in the Wells-Barkerville Belt is required to assess whether the primary inclusions represent fluids formed syn-crystallization or whether the primary inclusions show the effects of leakage or decrepitation.

In the Wells-Barkerville Belt, four compositional types of fluid inclusions have been identified in quartz from both vein and 'massive' ore in the Wells-Barkerville Belt through observation of phases present and volume percent of phases at room temperature. For each measured fluid inclusion type within a fluid inclusion assem-

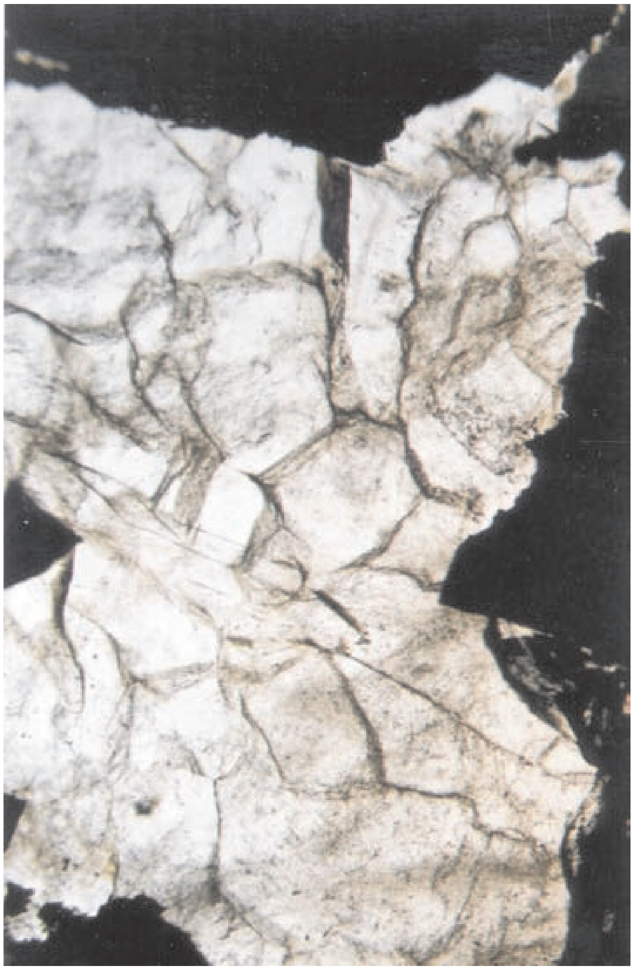

Photo 7. Subhedral to anhedral quartz crystals adjacent to medium-grained crystalline pyrite (black) in 'massive' ore, Mosquito Creek deposit. Evidence of quartz recrystallization? seen as fine-grained quartz crystals with 120°C grain boundaries at top right of photo. Note area of enlargement for Photo 8 is top right of photo 7. Sample GR-00-68. Transmitted plane light. Width of photo 2mm.

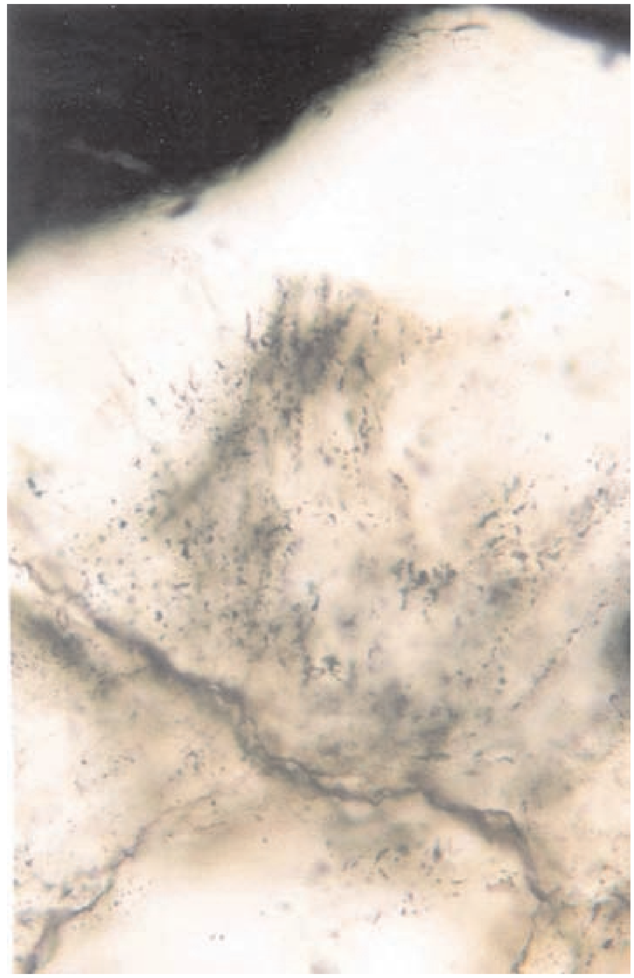

Photo 8. Tiny (<1 micrometre) primary fluid inclusions aligned along growth zones in quartz proximal to medium-grained pyrite in 'massive' ore, Mosquito Creek deposit. This photo is an enlargement of top right of Photo 7. Sample GR-00-68. Transmitted plane light. Width of photo 400 µm.

blage (FIA), the liquid-to-vapour ratios were relatively consistent (±20 volume percent vapour). The compositional types, based on phases present at room temperature (20°C), modified from the nomenclature of Nash (1976) are: two-phase aqueous liquid-rich (Type I), multiphase (Type III), two and three-phase mixed aqueous and CO_2-rich (Type IV) and monophase vapour CO_2-CH_4 (Type V).

Type I fluid inclusions are characterised by 2 aqueous phases, liquid and vapour (Photo 12). The vapour phase typically comprises approximately 5 volume percent of the inclusion but rarely 10, 20 and 30 volume percent vapour have been observed. Type I fluid inclusions have been noted in all samples except in quartz from the Perkins occurrence.

Type III inclusions comprise a liquid brine, vapour and one or more solid phases (Photo 13). The vapour phase typically comprises approximately 10 to 30 volume percent of the inclusion. Many of the solid phases are dominantly translucent and cubic and therefore are presumed to be salts. Confirmation of the identity of the solid phases as salts has not been possible as fluid inclusions containing these phases decrepitate prior to solid phase dissolution. In some cases, secondary planes of type III inclusions with comparable phases present have been observed, although some 'isolated' type III inclusions may have formed by accidental trapping of the solid phases or post-entrapment changes in the inclusions. Type III inclusions have been noted in quartz veins from the Cariboo Gold Quartz, BC Vein and Perkins mineral occurrences and in quartz associated with 'massive' ore at the Mosquito Creek deposit. Limited freezing and subsequent melting behaviour of type III fluid inclusions in quartz from the Perkins occurrence indicates a CO_2-bearing vapour phase (*see* below).

Type IV inclusions consist of 2 or 3 phases at room temperature. These are either an aqueous liquid and CO_2-bearing liquid (Photo 14) or an outer aqueous liquid, inner CO_2-bearing liquid and a CO_2-bearing vapour (Photo 15). The CO_2 volumetric proportions of Type IV

Photo 9. Recrystallized quartz zone, approximately 0.5 mm wide, with virtually no fluid inclusions, around medium-grained pyrite (black) in massive ore, Mosquito Creek deposit. Note area of enlargement for Photo 11 is right of centre of Photo 9. Sample GR-00-68. Transmitted plane light. Width of photo 2mm.

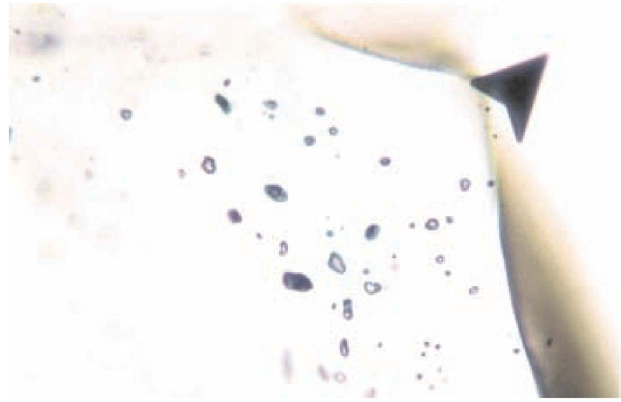

Photo 11. Pseudosecondary fluid inclusions aligned along fractures in recrystallized quartz proximal to pyrite crystals (black), 'massive' ore, Mosquito Creek deposit. Note occurrence of 2 phase liquid-rich and monophase vapour-rich fluid inclusions trapped in the same healed fracture. This photo is an enlargement of area right of centre of Photo 9. Sample GR-00-68. Transmitted plane light. Width of photo 300 µm.

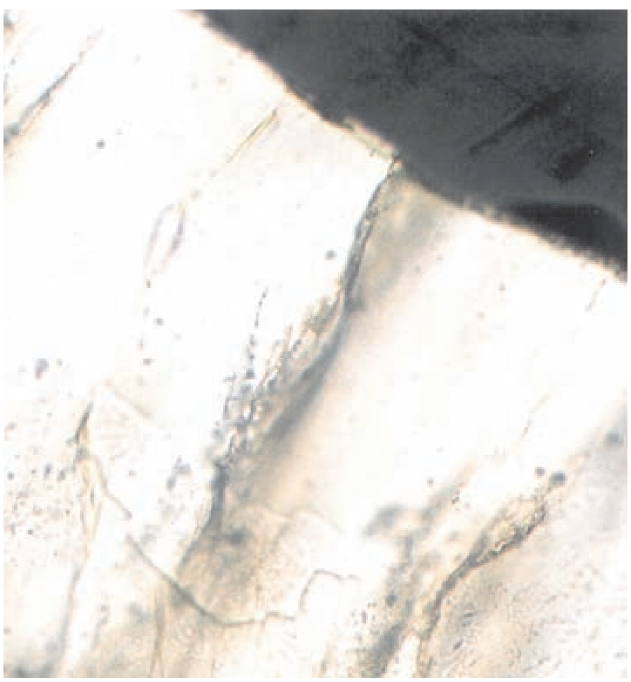

Photo 10. Recrystallized quartz zone, approximately 0.3 mm wide, around medium-grained crystalline pyrite (black) in 'massive' ore, Island Mountain deposit. Recrystallized zone comprises less than one percent tiny fluid inclusions. Sample GR-00-85. Transmitted plane light. Width of photo 340 µm.

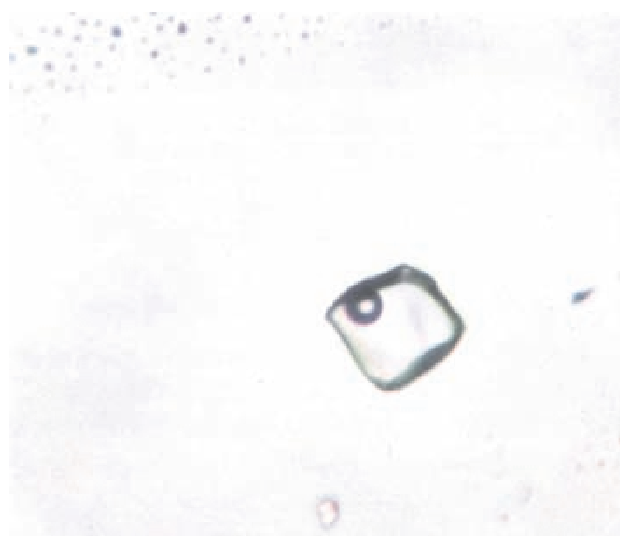

Photo 12. Negative crystal - shaped Type I fluid inclusions characterized by 2 aqueous phases: liquid and vapour in vein quartz, Mosquito Creek deposit. Sample GR-00-67. Transmitted plane light. Width of photo 160 µm.

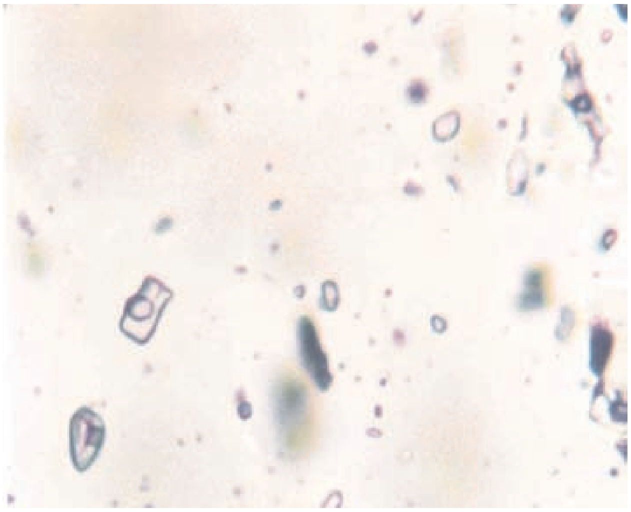

Photo 13. Smooth to negative crystal - shaped Type III fluid inclusions in a massive 'bull' quartz vein, Cariboo Gold Quartz deposit. Note solid 'daughter' crystals in the fluid inclusions left of centre and far right. Sample CGQ-FI-4. Transmitted plane light. Width of photo 160 µm.

inclusions range from 5 percent to 90 percent with 20 to 30 percent most typical. Type IV inclusions have been noted in all samples except GR-00-91(BC Vein) and GR-00-94 (Island Mountain vein).

Type V inclusions are typically very dark and consist of a single vapour phase at room temperature (Photo 14). Freezing and subsequent melting behaviour of these inclusions indicate the presence of CO_2-CH_4±N_2 phases. Type V fluid inclusions in quartz have been noted in all samples except in 'massive' pyritic ore from the Island Mountain mine and in veins from the Perkins occurrence.

Two phase liquid-rich Type IV inclusions are coeval with monophase vapour-rich Type V inclusions in secondary and pseudosecondary fracture planes in quartz from both vein and massive ore (Photos 11and 14). The coexistance of CO_2-bearing liquid-rich inclusions with variable liquid-to-vapour ratios and vapour-rich inclusions in the same fracture plane indicates that local effervescence occurred.

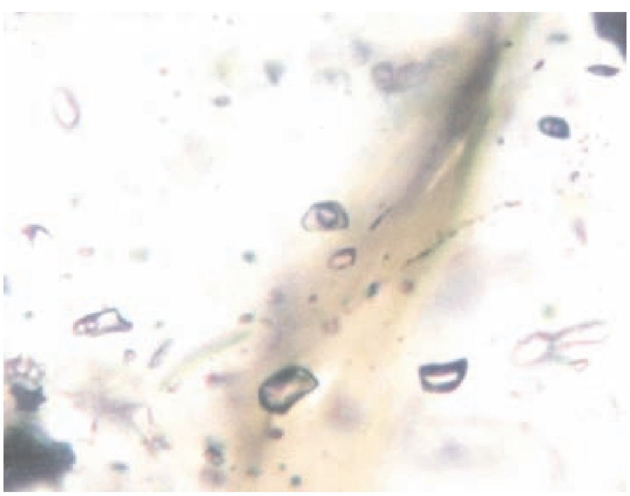

Photo 14. Coexisting monophase vapour-rich Type V inclusions and two phase liquid-rich Type IV inclusions aligned along a secondary fracture plane in quartz from a massive 'bull' quartz vein, Cariboo Gold Quartz deposit. Sample CGQ-FI-3. Transmitted plane light. Width of photo 160 µm.

Microthermometric Data

Microthermometric data were obtained using a Fluid Inc. adapted USGS gas-flow heating-freezing stage housed at the Mineral Deposit Research Unit, Department of Earth and Ocean Sciences, University of British Columbia. Calibration of the stage was achieved using commercial Syn Flinc synthetic fluid inclusions and ice with the following accuracies: at -56.6±0.2°C, 374.1±0.6°C and 0.0±0.1°C. Temperatures of phase changes are presented for each fluid inclusion type from lowest to highest. Variation in final aqueous homogenization temperature with respect to fluid inclusion origin, deposit type and comparison between deposits are illustrated.

TYPE I FLUID INCLUSIONS

Temperatures of first melting were obtained on 15 fluid inclusions from 4 samples representing both vein and 'massive' styles of mineralization (Figure 2). First melting temperatures range from -28.6°C to -20.0°C, with an average of -23.1°C. No systematic differences were

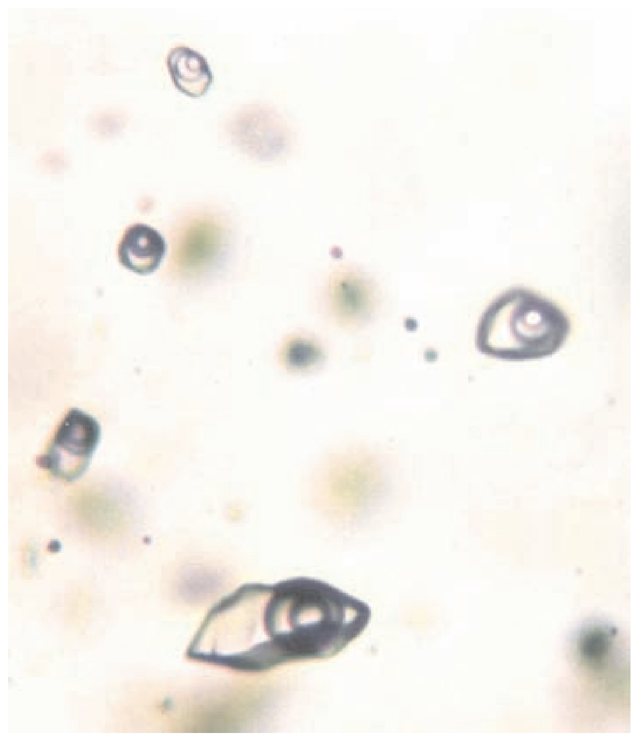

Photo 15. Smooth to negative - crystal shaped Type IV fluid inclusions in quartz from a quartz vein, Mosquito Creek deposit. Note the three CO_2 and H_2O phases present at room temperature (20°C). Sample GR-00-67. Transmitted plane light. Width of photo 160 µm.

noted between vein and 'massive' styles of mineralization.

First melting temperature approximates the eutectic temperature of the salt-water mixtures. The observation of first melting below -21.2°C, the stable NaCl-H_2O eutectic, indicates the addition of small concentrations of K+, Ca_2+, Mg_2+ or other ions to an H_2O-NaCl fluid. For the purposes of this preliminary study, the type I fluid is modelled as an NaCl brine partly because most formational fluids are NaCl-dominant (Goldstein and Reynolds, 1994) and because comparison of the cotectic surfaces where ice melts for various systems (Figure 6, from Crawford, 1981) shows only relatively small variations (< 5 wt.% change).

Temperatures of final ice melting were obtained from 30 fluid inclusions from the same and additional samples as the first melting temperatures (Figure 2). Final melting temperatures range from -9.2°C to -0.2°C, with an average of -3.3°C. Salinities calculated from final melting temperatures and the equation of Bodnar (1993) range from 0.4 to 13.1 weight percent NaCl equivalent (wt. percent NaCl equiv.) and average 5.4 wt. percent NaCl equiv. No systematic differences were noted between vein and 'massive' styles of mineralization. Metastable hydrate melting (possible hydrohalite) is observed from 0 to 10°C after ice melting.

Final homogenization temperatures of the inclusions, always to the liquid phase, were obtained on 39 Type I fluid inclusions from the same samples and some additional samples as the freezing data (above). Homogenization temperatures range from 101.1 to 298.8°C and average 168.9°C (Figure 3). Five fluid inclusions in quartz vein samples from the Cariboo Gold Quartz mine and BC Vein exhibited decrepitation of fluid inclusions prior to homogenization at temperatures between 150 and 300°C

TYPE III FLUID INCLUSIONS

Limited data (4 data points) on freezing and subsequent melting behaviours of Type III fluid inclusions in quartz from the Perkins vein parallel the behaviour of CO_2-bearing Type IV fluid inclusions (see below). On heating, the solid phases do not melt prior to decrepitation (leakage) of the fluid inclusions at temperatures ranging from 220 to 258°C. Homogenization of one type III inclusion was achieved at 224°C, within the range for Type IV fluid inclusions (*see* below), prior to inclusion decrepitation at 250°C.

It is not known whether the Type III inclusions contain minerals that are true 'daughter' minerals or if the minerals are trapped accidental solids or are the result of 'necking down'. If the solids are salts and true 'daughter' minerals, this combination of salt-saturated and CO_2-bearing fluids trapped within inclusions in quartz veins at the Perkins veins has rarely been documented in fluid inclusion literature.

TYPE IV FLUID INCLUSIONS

On freezing of the inclusions, phase separation of the vapour bubble into CO_2-liquid and CO_2-vapour phases occurred at about +5 to + 25°C. Further cooling resulted in freezing of the H_2O phase at about -35 to -50°C and the CO_2 phase at about -90 to -95°C. Temperatures of CO_2 melting were obtained on 50 fluid inclusions from both vein and 'massive' styles of mineralization. Carbon dioxide melting temperatures typically range from -61.4 to -56.6°C with an average of -57.5°C (Figure 4). The average CO_2 melt temperature of -57.5°C indicates that < 4 mole percent or virtually no CH_4 or N_2 is dissolved in the CO_2. Type IV fluid inclusions can therefore be modelled using an H_2O-CO_2-NaCl system. Carbon dioxide-melting temperatures in quartz from the Perkins veins are much lower (Figure 3). These inclusions comprise from 0 to 20 mole percent CH_4 dissolved in the CO_2 using VX diagrams of Thiery *et al.* (1994).

Temperatures of clathrate (gas hydrate) melting were obtained on 47 fluid inclusions from the same samples as the CO_2-melting temperatures. Clathrate melting, which occurs after ice melting, varies from 0.2 to 9.8°C with an average of 6.6°C (Figure 4). Clathrate melting temperatures less than +10°C are another indication of very low CH_4 or N_2 presence in Type IV inclusions. Clathrate melting temperatures in excess of + 10°C are related to CH_4 impurities (Burruss, 1981). Salinities calculated from clathrate melting using the MacFlincor computer program (Brown and Hagemann, 1994) range from 1.4 to 15.7 wt. percent NaCl equiv.

Homogenization temperatures of CO_2 liquid and vapour were obtained from 45 fluid inclusions from the same samples as CO_2-melting and clathrate melting temperatures. Homogenization of the inclusions (always to the liquid phase) ranges from 5.6 to 30.5°C with an average of 19.7°C (Figure 4) which combined with volume estimates indicate a range in density of 0.54 to 0.84 grams per cubic centimetre for the CO_2 component of the inclusions.

Final homogenization temperatures of the inclusions, again always to the aqueous phase, were obtained on 36 Type IV fluid inclusions from the same samples as the freezing data (above). Homogenization temperatures range from 124.7 to 341.9°C and average 241.1°C (Figure 3). A large proportion, approximately one-third, of all Type IV inclusions decrepitate at temperatures ranging from 150 to 300°C prior to homogenization. This large proportion occurred irrespective of reasonable heating rates which were reduced to 5 degrees per minute in an attempt to lower the number of failed homogenization temperatures. Figure 3 shows that overall, Type IV fluid inclusions homogenize at significantly higher temperatures than Type I fluid inclusions for data evaluated in this study.

TYPE V FLUID INCLUSIONS

On freezing the monophase Type V inclusions, phase separation of the vapour bubble into CO_2-bearing liquid

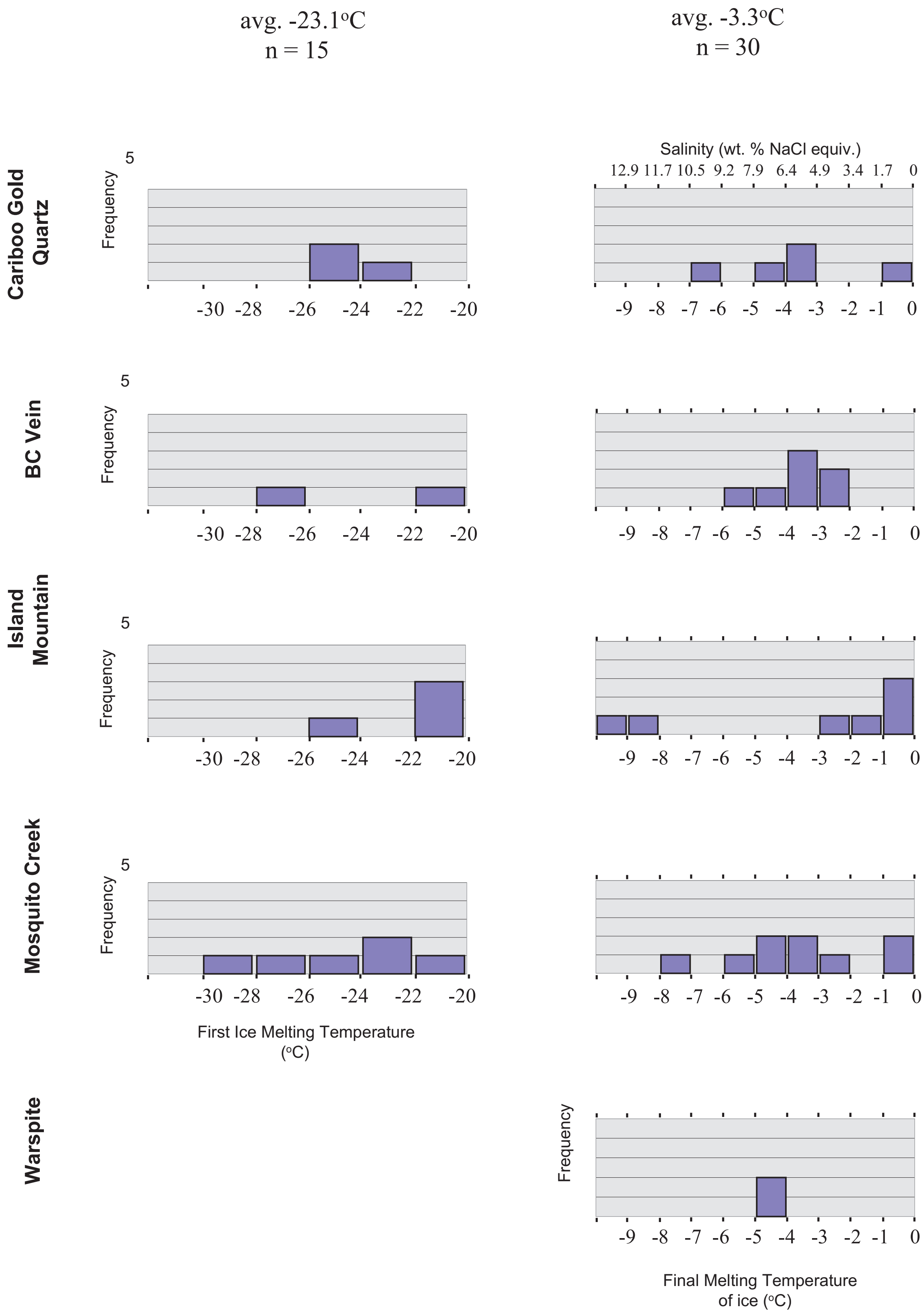

Figure 2. Temperatures of first melt and final melt of Type I (aqueous) fluid inclusions from the Cariboo Gold Quartz, Island Mountain, Mosquito Creek mines and BC and Warspite veins, respectively. The first melt approximates the eutectic temperatures of the fluid inclusions. The final melt is used to calculate the equivalent salinity. Note the diagrams share common x axes.

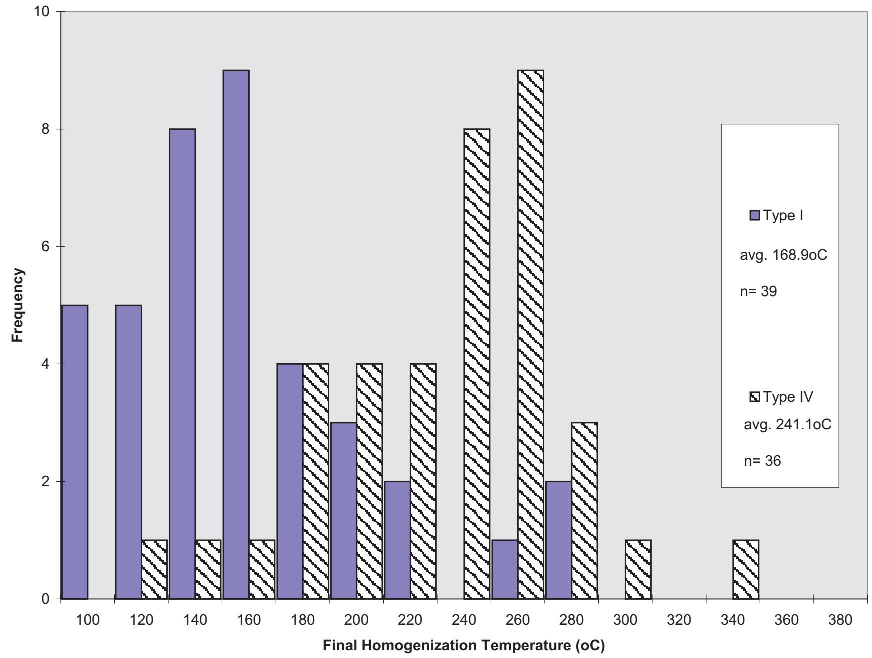

Figure 3. Type I (aqueous) versus Type IV (CO_2-bearing) fluid inclusion final homogenization temperatures, to the aqueous phase, in quartz from all vein and massive pyrite samples evaluated in this study.

and CO_2-bearing vapour phases occurred at temperatures below 20°C, often below 0°C. Further cooling resulted in freezing of the CO_2 phase at about -90 to -95°C. Rarely, the segregation of a second CO_2-rich liquid occurs at temperatures just below the freezing point. Up to 3 different stable phase transitions and rarely one metastable phase transition are observed on warming to just above room temperature ~22°C. The phase transitions observed were: initial melting (occasionally), final melting, metastable partial liquid homogenization (rarely) and final homogenization.

The first observed melting event is incipient or first melting, termed 'initial melting' by Kerkhof and Thiery (1994), which occurs as the formation of a liquid on melting solid CO_2 (but not complete melting of solid CO_2). This melt event which ranges from -94 to -69°C is observed in 6 fluid inclusions in as many samples.

The second observed melting event, observed in 25 fluid inclusions in quartz, is final melting of solid CO_2. Carbon-dioxide melting temperatures typically range from -84 to -56.6°C with an average of -61.1°C (Figure 5) which is significantly lower than the range and average observed for CO_2 melting of Type IV fluid inclusions (Figure 4). Some CO_2-melting temperatures in quartz from the BC Vein and Island Mountain mine are much lower than the average temperature (Figure 5).

Metastable partial liquid homogenization of fluid inclusions that have segregated a second CO_2-rich liquid has been observed in 2 fluid inclusions from separate samples in the BC Vein. This phase transition involves disappearance of the outer meniscus between the two CO_2-rich liquid phases. Fluid inclusions from the BC Vein show metastable partial liquid homogenization at -56.6 and-63.9°C respectively.

Final homogenization temperatures of CO_2 liquid and vapour were obtained from 22 fluid inclusions from the same samples as CO_2-melting temperatures. Homogenization of the inclusions (always to the liquid phase) ranges from -62.8 to 21.3°C with an average of -6.9°C (Figure 5). Final homogenization temperatures in quartz from the BC Vein and Island Mountain mine are much lower than the average temperature (Figure 5) as is the case for CO_2-melting temperatures (*see* above).

The measured CO_2 melt and homogenization temperatures are used to calculate fluid molar volumes (or the density) and composition of Type V fluid inclusions using VX diagrams of Thiery *et al.* (1994). The average CO_2 melt temperature of -61.1°C and average CO_2 homogenization temperature of -6.9°C indicates an average molar volume of 51 cubic centimetres per mol and on average < 16 mole percent CH_4 dissolved in the CO_2 (Thiery *et al.*, op. cit.). Some CO_2-melting and homogenization temperatures in quartz from the BC Vein and Island Mountain occurrences are much lower than the above calculated averages. These inclusions have molar volumes in the range of 51 to >100 cubic centimetres per mol and comprise from 33 to possibly > 90 mole percent CH_4 dissolved in the CO_2 (Thiery *et al.*, op cit.). The high CH_4 in the Type V fluid inclusions from the BC Vein and Island Mountain occurrences indicate that they are CH_4-dominant and represent CH_4-CO_2 fluids. When the CH_4-CO_2 fluid inclusions are removed from fluid inclusions used in the the

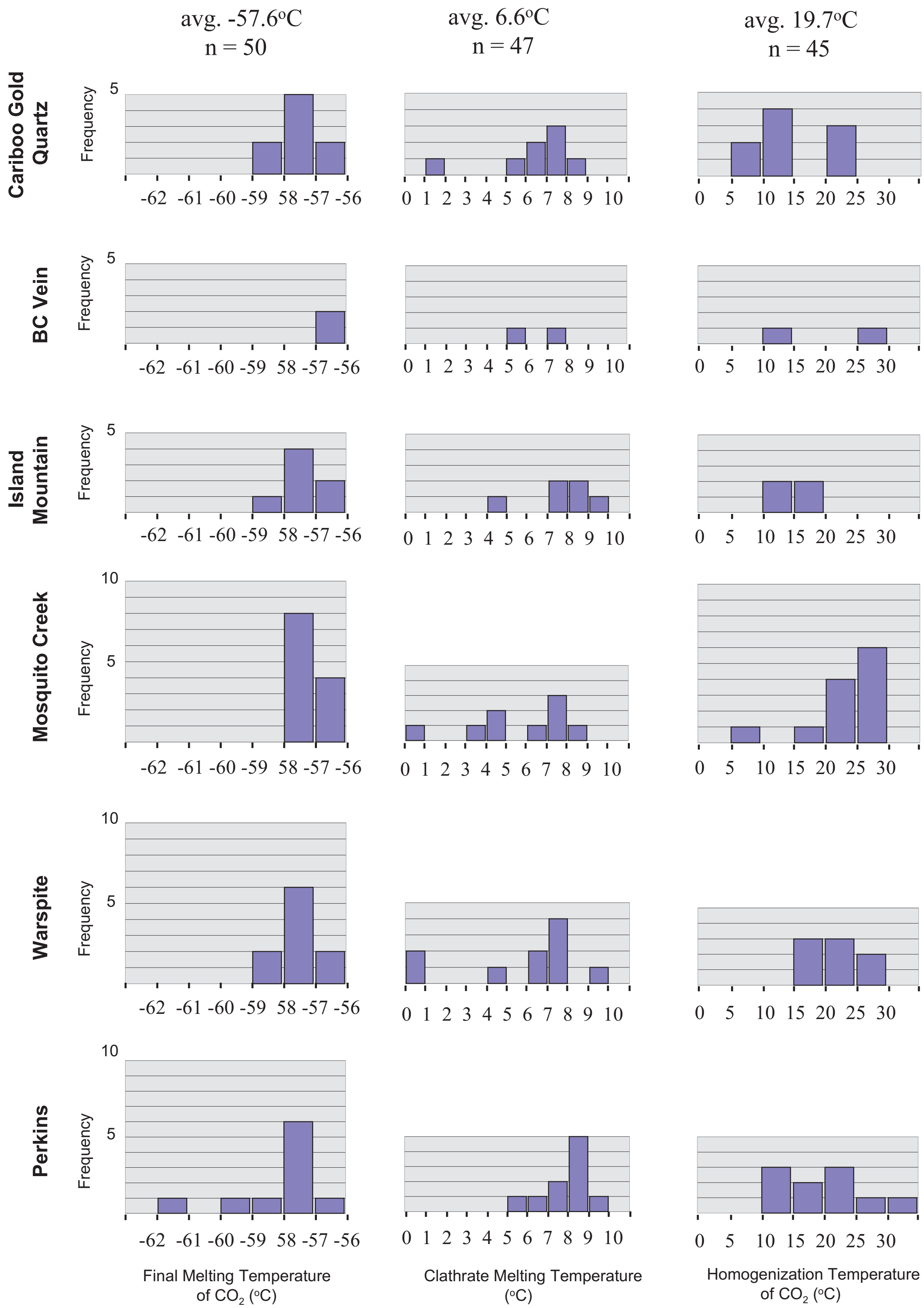

Figure 4. Temperatures of final CO_2 melt, clathrate melt and homogenization of CO_2 phases of Type IV (CO_2-bearing) fluid inclusions from the Cariboo Gold Quartz, Island Mountain, Mosquito Creek mines and BC, Warspite and Perkins veins, respectively. The final CO_2 melt temperature is used approximate the proportion of CH_4, N_2 or other volatile phases trapped in the fluid inclusions. The clathrate melt is used to calculated the equivalent salinity. The homogenization temperature of CO_2 is used to calculate the CO_2 density. Note the diagrams share common x axes.

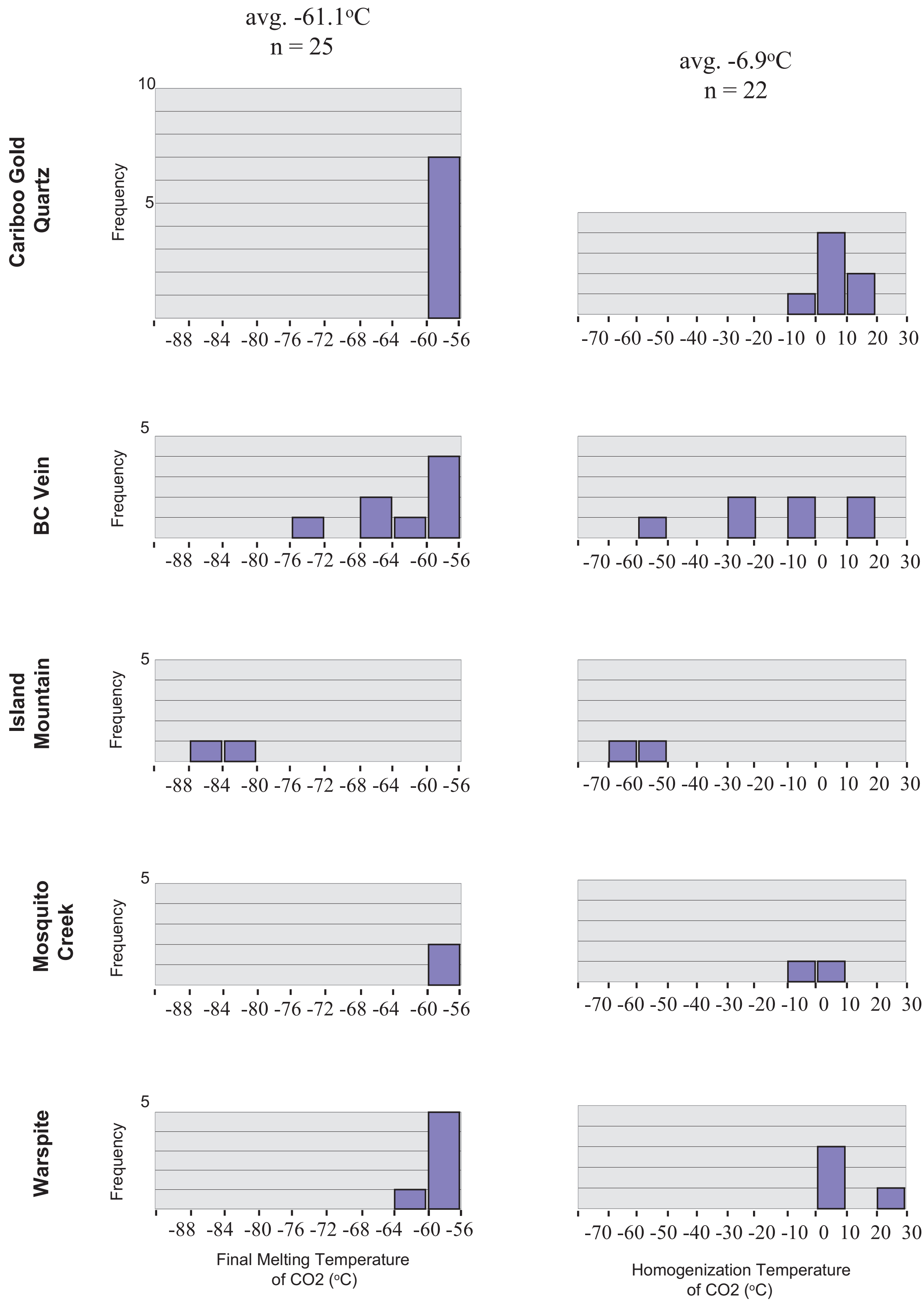

Figure 5. Temperatures of final CO_2 melt and CO_2 homogenization of Type V (CO_2-CH_4±N_2) fluid inclusions.

average calculation of fluid molar volume and composition for Type V fluid inclusions, the average molar volume and composition of dominantly CO_2-CH_4 fluid inclusions is 50 cubic centimetres per mol and 4 mole percent CH_4.

Variation in Final Homogenization Temperature

Fluid inclusion final homogenization temperatures to the aqueous liquid phase for 75 Type I and IV fluid inclusions in quartz collected from quartz veins and massive pyrite mineralization in the 6 mineralized zones studied show virtually no difference between fluid inclusions of primary versus secondary origin (Figure 6). A wide spread in homogenization temperatures for both fluid inclusion origins range from 120 to 300°C. Fluid inclusions of indeterminate origin display a similar homogenization temperature range.

Preliminary comparison of the homogenization temperatures and composition of fluid inclusions in late (?), open-space fill quartz vugs and the earlier massive quartz were evaluated on 8 and 6 fluid inclusions from 2 quartz veins at the Mosquito Creek and Perkins deposits respectively. Types I and IV fluid inclusions in massive 'cloudy' quartz from a vein at Mosquito Creek (GR-00-67) showed salinities between 3.5 and 7.6 wt. percent equivalent NaCl and homogenization temperatures ranging from 162 to 258°C. Types I and IV fluid inclusions in 'clear' quartz from the same vein showed salinities between 2.8 and 5.1 wt. percent equivalent NaCl and homogenization temperatures ranging from 155 to 289°C. Type IV fluid inclusions in massive 'cloudy' quartz from the Perkins vein (GR-00-56) showed salinities between 2.4 and 3.9 wt. percent equivalent NaCl and homogenization temperatures ranging from 274 to 279°C. Type IV fluid inclusions in 'clear' quartz from the same vein showed salinities between 1.4 and 3.9 wt. percent equivalent NaCl and homogenization temperatures ranging from 224 to 270°C. The results of the preliminary comparison are inconclusive due to the limited data. Further detailed microthermometric work on more fluid inclusions in quartz vugs and massive quartz from a number of vein samples is needed to determine the temperature and compositional differences between these two vein textures.

Fluid inclusion final homogenization temperatures to the aqueous liquid phase for 73 Type I and IV fluid inclusions in quartz from vein and 'massive' styles of mineralization are compared in Figure 7. This figure includes homogenization temperatures from primary, secondary, pseudosecondary and intermediate fluid inclusions based on the premise that virtually no difference exists between the homogenization temperatures of fluid inclusions of primary versus secondary origin (Figure 6). The homogenization temperature range (approximately 100 to 300°C)

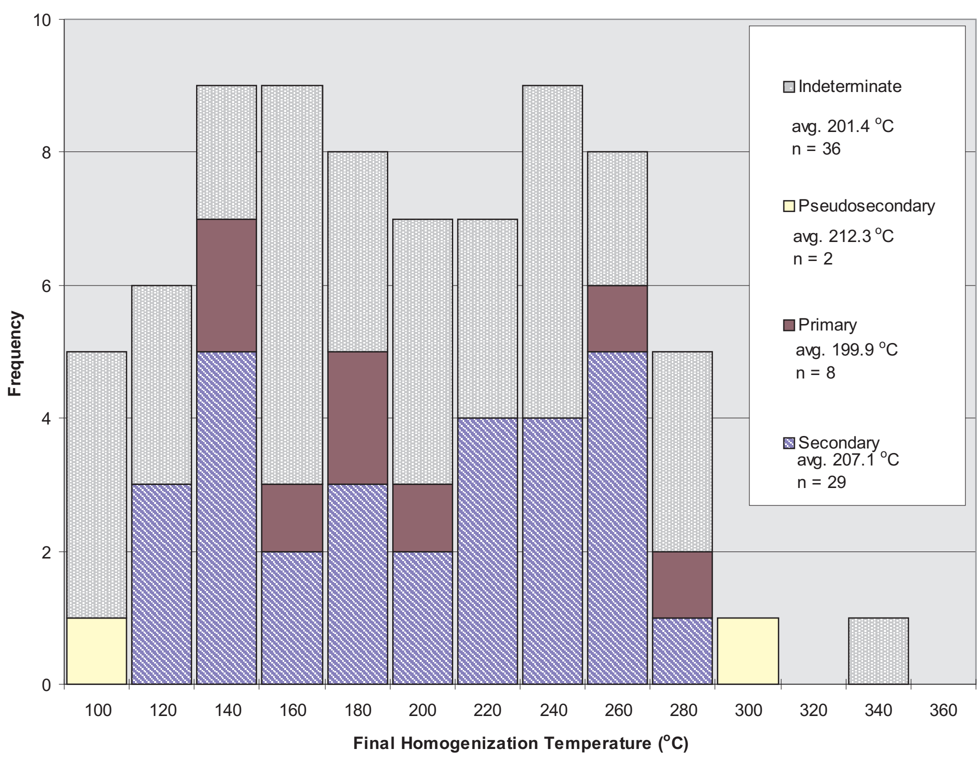

Figure 6. Distribution of primary, pseudo-secondary, secondary and indeterminate fluid inclusion origins with respect to final homogenization temperatures, to the aqueous phase, for Type I and IV fluid inclusions in quartz collected from quartz vein and massive pyrite samples from the Cariboo Gold Quartz, Island Mountain, Mosquito Creek mines and BC, Warspite and Perkins veins, respectively.

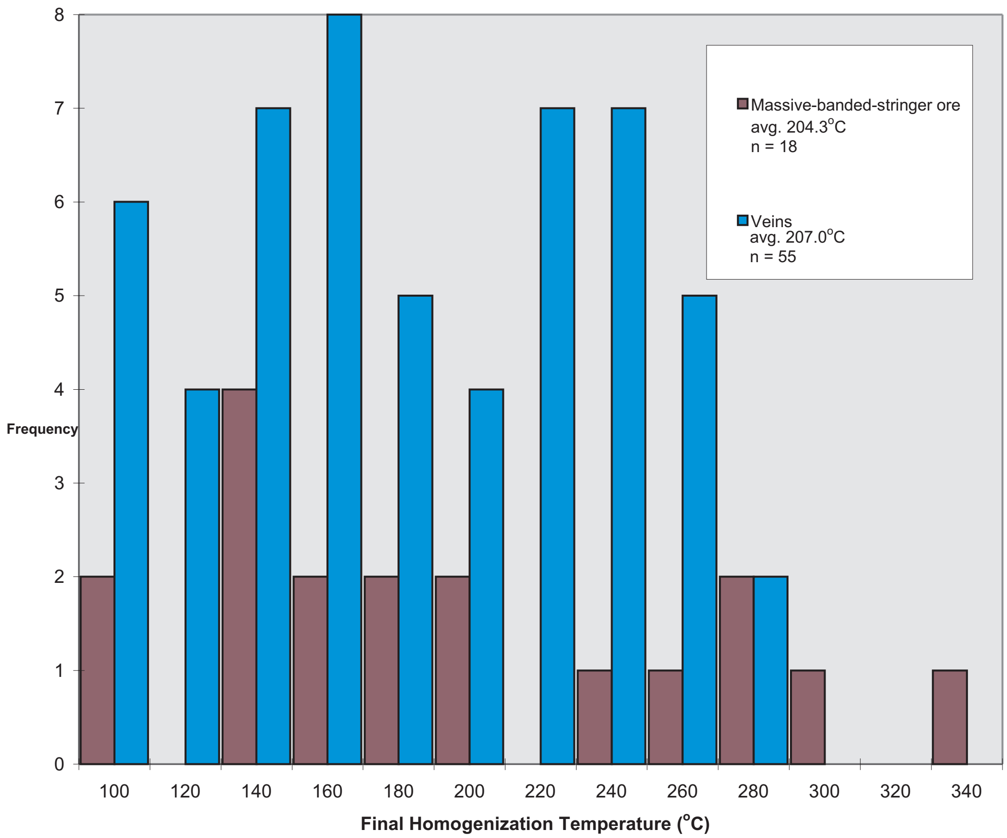

Figure 7. Distribution of final homogenization temperatures, to the aqueous phase, for Type I and IV fluid inclusions in quartz veins from the Cariboo Gold Quartz, Island Mountain, Mosquito Creek mines and BC, Warspite and Perkins veins, respectively, versus in quartz from massive-banded-stringer ore at the Island Mountain and Mosquito Creek mines.

is the same for vein and 'massive' styles of mineralization as are the homogenization temperature averages: 207 and 204°C, respectively (Figure 7). Additional analyses and comparison of homogenization temperatures for each fluid inclusion Type and direct comparison of secondary fluid inclusion origins are recommended to verify the above preliminary results.

Preliminary comparison of fluid inclusion final homogenization temperatures to the aqueous liquid phase for 75 Type I and IV fluid inclusions in quartz from samples from vein and 'massive' styles of mineralization at the Cariboo Gold Quartz, Island Mountain, and Mosquito Creek mines and the Warspite, Perkins, and BC veins are in Figure 8. Vein mineralization is indicated by fluid inclusion homogenization data represented by white and striped columns, 'massive' pyrite style mineralization by black columns. This figure includes homogenization temperatures from primary, secondary, pseudosecondary and intermediate fluid inclusions based on the premise that virtually no difference exists between the homogenization temperatures of fluid inclusions of primary versus secondary origin (Figure 6). There is virtually no difference in the homogenization temperature range of the vein and 'massive' styles of mineralization at the Island Mountain and Mosquito Creek mines (Figure 8). Both styles at Mosquito Creek show two distinct populations (100 to 180°C and 240 to 360°C). that may reflect differences due to homogenization temperatures of lower temperature Type I versus higher temperature Type IV fluid inclusions (Figure 3).

Homogenization temperatures from both the vein and 'massive' styles of mineralization are averaged in Figure 8 based on the premise that virtually no difference exists between homogenization temperatures from both styles of mineralization (Figure 7). The homogenization temperatures for the Cariboo Gold Quartz and Island Mountain mines and BC vein show remarkably consistent averages (between 180 and 192°C) although the range of homogenization temperatures are similar (approximately 120 to 300°C). Average homogenization temperatures from the Mosquito Creek mine and Warspite veins are considerably higher at 212 and 217°C respectively. Quartz in the Perkins veins have the highest average homogenization temperatures (avg. 253°C). This may reflect the absence of generally lower temperature Type I fluid inclusions (Figure 3) in quartz at the Perkins veins.

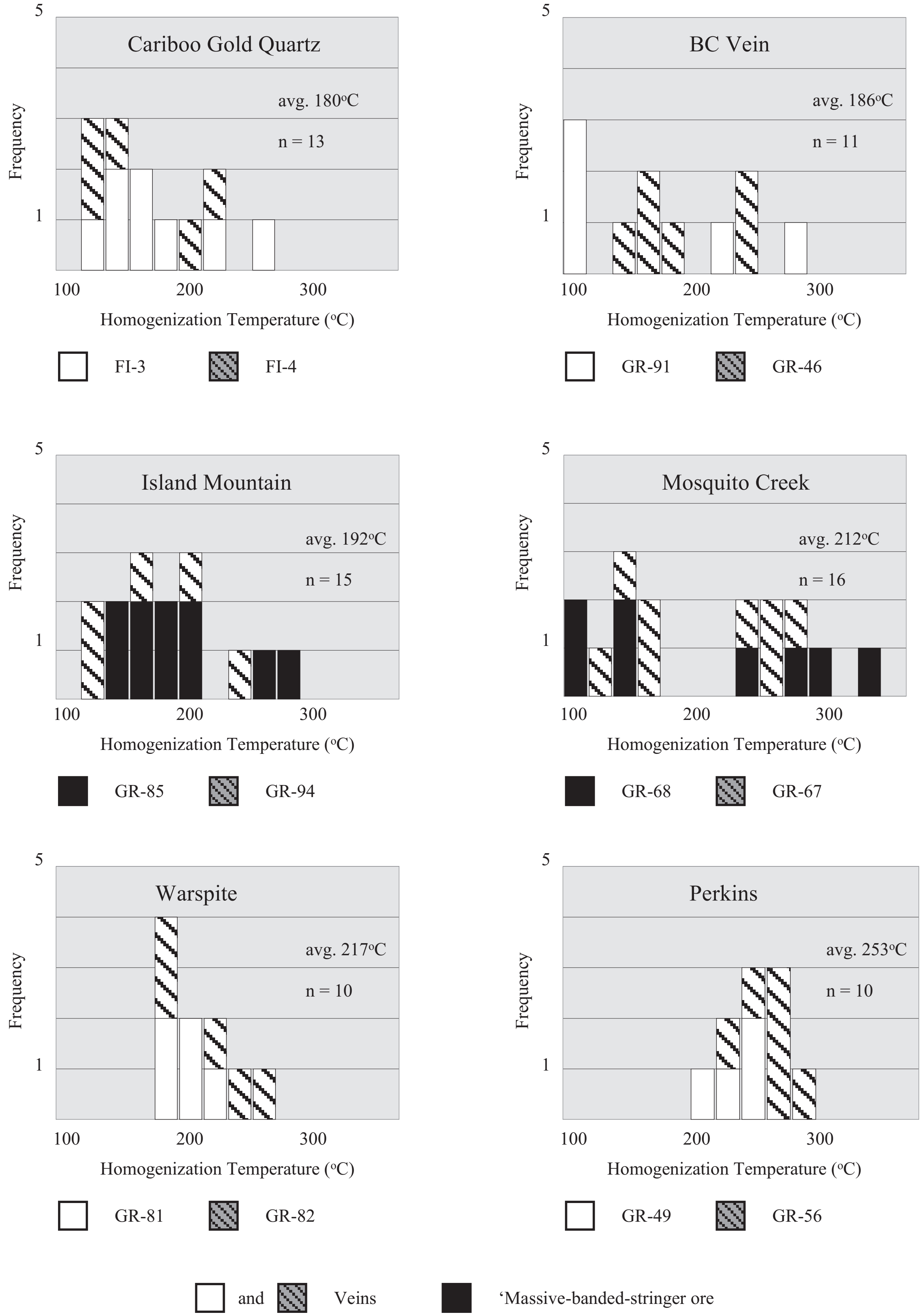

Figure 8. Final fluid inclusion homogenization temperatures (range, average and number), to the aqueous phase, for Type I and IV fluid inclusions from the Cariboo Gold Quartz, Island Mountain, Mosquito Creek mines and BC and Warspite veins, respectively. Note the diagrams share common x axes.

DISCUSSION

This discussion focuses on the following: (1) estimated fluid properties of inclusions in quartz from both vein and 'massive' ore in the Wells-Barkerville Belt, (2) the relationship of fluid inclusions to metamorphism and the introduction of metals in these types of mineral deposits and (3) proposed analogues to the Wells-Barkerville mineralization from a fluid inclusion standpoint.

Fluid Properties

Petrographic and microthermometric data on primary, pseudosecondary and secondary fluid inclusions in quartz from vein and 'massive' ore in the belt indicates there are four compositional types of fluid inclusions. These were identified through observation of phases present and volume percent of phases at room temperature: two-phase aqueous liquid-rich (Type I), multiphase (Type III), two and three-phase mixed aqueous and CO_2-rich (Type IV) and monophase CO_2- CH_4 (Type V). Estimates of average composition, salinity and final homogenization temperature for each fluid inclusion type are in Table 2.

COMPOSITION AND SALINITY

Type I fluid inclusions are H_2O-dominant with low average homogenization temperatures (169^{o}C) compared with Type IV fluid inclusions (241^{o}C). Salinities of Type I fluid inclusions are low averaging 5.4 wt. percent NaCl equiv. This type of inclusion is commonly found in submetamorphic to subgreenschist facies metamorphic rocks (Marshall *et al.*, 2000). Marshall (op. cit.) notes that H_2O dominates in the uppermost continental crust but is progressively diluted by CH_4 and then CO_2 during prograde metamorphism and that CO_2±CH_4±N_2 is typical in inclusions from the lower crust and mantle. Low temperature (< 200^{o}C) aqueous fluid inclusions with H_2O-NaCl-$CaCl_2$ composition in gold-bearing quartz vein deposits from the southeastern Abitibi Subprovince, Quebec, represent late, post-mineralizing, fresh meteoric waters that percolate downward mixing with brines (Boullier *et al.*, 1998). These deposits may be analogues to gold-bearing veins in the Wells-Barkerville Belt (*see* below).

Multiphase Type III fluid inclusions appear to be H_2O-dominant and some inclusions contain CO_2 (based on freezing behaviour). At least some of the solid phases appear to be salts which would indicated salt-saturation and minimum salinities of 26.3 wt. percent NaCl equiv. Calculations based on ice melting temperatures give approximate average salinities of 11.8 wt. percent NaCl equiv. Further work using additional analytical techniques is required to resolve the composition of this type of inclusion.

Type IV fluid inclusions fall in the category of High XH_2O (Low XCO_2) compositional type based on compositions in Table 2 (Diamond, 1994). This type is typical of CO_2-H_2O fluid inclusions found in low to medium grade metamorphic rocks and mesothermal to hypothermal ore deposits (Diamond, op. cit.). Marshall *et al.* (2000) suggests that H_2O-dominant fluid inclusions with only minor

TABLE 2
SUMMARY OF FLUID INCLUSION CHARACTERISTICS FOR FLUID TYPES PRESENT IN VEINS AND MASSIVE-BANDED-STRINGER ORE IN THE WELLS-BARKERVILLE BELT

FI TYPE (see text)	ORIGIN[1]	BULK INCLUSION COMPOSITION (AVERAGE)	SALINITY[2] wt. percent NaCl equiv.	HOMOGENIZATION TEMPERATURE, to the aqueous phase, RANGE AND (AVERAGE)[3] in ^{O}C	ESTIMATED MINIMUM PRESSURE RANGE[4] (bars)
I	P, S	(H2O 0.98, NaCl 0.02)	5.4 n=30	101.1 to 299 (169) n = 39	
III	S	(H2O 0.96, NaCl 0.04? , CO2?)	11.8 n = 3 or > 26.3?	224 n = 1	
IV	S (all quartz veins)	(H2O 0.85, CO2 0.13, NaCl 0.02)	6.2 n = 17	178 to 277 (242) n = 11	1628 to 3081 n = 11
	P (massive pyrite from IMm)	(H2O 0.93, CO2 0.05, NaCl 0.02)	4.2 n = 3	189 to 292 (249) n = 3	1910 to 3412 n = 3
V	S	(CO2 0.96 , CH4 0.04) and(CH4 0.7, CO2 0.3)		0	

1. Fluid inclusion origins: P = primary, S = secondary (see text for explanation)
2. Salinity given as weight percent NaCl equivalent, n = number of analyses
3. Number of analyses for average = n
4. Number of analyses for range = n

CO_2 are predominant in greenschist facies metamorphic rocks.

Type V inclusions in this study are classified as homogenization or H-type inclusions (Kerkhof and Thiery, 1994) because the last phase transition observed is characterized by liquid-gas homogenization (always to the liquid phase) rather than solid-gas or solid-liquid homogenization. Type V inclusions are further subdivided into H_3 and H_2 types based on the observed differences in phase behaviour. Fluid inclusions that exhibit initial melting, final melting and final homogenization of CO_2-rich phases are classified as H_3-type (Kerkhof and Thiery, op. cit.); inclusions exhibiting final melting plus or minus metastable phase transitions followed by final homogenization of CO_2-rich phases are classified as H_2-type (Kerkhof and Thiery, op. cit.). Type H_2 behaviour is typical for CO_2-CH_4 mixtures and type H_3 behaviour is typical for CO_2-rich compositions (Kerkhof and Thiery, op. cit.). Fluid inclusions in this study are dominantly H_2-type. Based on the dominance of H_2-type inclusions, the CO_2-CH_4 model system, rather than the CO_2-N_2 model system, is used for Type V inclusions in this study.

The composition of type V inclusions falls in two distinct ranges: high CO_2 - low CH_4 and low CO_2-high CH_4 (Table 2). The latter high CH_4 composition has only been noted in secondary fluid inclusions at the BC Vein and in a vein from the Island Mountain mine.

MINIMUM PRESSURE ESTIMATES

Minimum pressure estimates have been calculated for Type IV fluid inclusions using bulk density estimates for the carbonic portion of the inclusions, and projecting isochores calculated using the equation of Kerrick and Jacobs (1981) and the FLINCOR program of Brown and Hagemann (1994) to temperatures of homogenization (minimum trapping temperature estimates). Although this technique assumes binary CO_2-H_2O mixtures, it can be applied to CO_2-H_2O mixtures with the addition of up to 15 wt. percent NaCl equiv. (Diamond, 1994). The range in density for the CO_2 component of the inclusions is 0.54 to 0.84 grams per cubic centimetre (Thiery *et al.*, 1994).

The range of minimum pressures of entrapment for secondary Type IV (H_2O-CO_2-NaCl) fluid inclusions in quartz veins in the belt are 1628 to 3081 bars (Table 2). Entrapment pressures for primary Type IV fluid inclusions in quartz from massive pyritic ore at the Island Mountain mine, are 1910 to 3412 bars (Table 2). Minimum depths of formation for the secondary inclusions in quartz veins are conservatively estimated at about 6 to 12 km. Minimum depths of formation for the primary inclusions in 'massive' pyrite at the Island Mountain mine are conservatively estimated at about 7 to 13 km. Both minimum pressure estimates assume lithostatic pressure (greater depths would be inferred for hydrostatic conditions).

Genetic Models

As intrusive rocks are extremely rare in the Wells-Barkerville Belt, a magmatic-hydrothermal source for the gold seems unlikely. However, two alternative models have been proposed for mineralization: (1) a synmetamorphic model involving the introduction of metals. In the case of the massive pyritic ore this involved replacement during or just after prograde regional metamorphism (Benedict, 1945, Skerl, 1948, Alldrick, 1983), and (2) a syn-sedimentary model involving metamorphic overprinting of sedimentary-exhalative ore (Robert and Taylor, 1989). As part of their argument, these authors suggest that Wells-Barkerville gold differs from typical mesothermal deposits because they are hosted by a dominantly sedimentary sequence and lack any spatial association with major faults or recognized shear zones.

Relationship of Fluid Inclusions to Metamorphism

Petrographic observation indicates that primary and pseudosecondary fluid inclusions with relatively consistent liquid-to-vapour ratios but moderately variable homogenization temperatures formed in recrystallized zones around pyrite in massive-banded-stringer ore at the Mosquito Creek and Island Mountain deposits. The variability in homogenization temperature data may be due to thermal reequilibration, undetectable necking down or real variability in the FIA's. The cause of the variability is difficult to assess given the limited data available. Assuming the real variability in the FIA's and noting that the pyrite also appears to be recrystallized, it is possible that the primary and pseudosecondary inclusions may trap fluids that record metamorphic conditions during or just after peak metamorphism when the sulphides and gold were introduced as massive-banded-stringer ore.

Marshall *et al.* (2000) suggest that fluid inclusion studies of ores that are potentially metamorphosed or synmetamorphic require identification of: (1) preserved premetamorphic fluid inclusions, (2) inclusions relating to peak metamorphic conditions, and (3) inclusions relating to retrograde remobilization of ore or mineralization overprinting. Such detailed work requires evaluation of structural and metamorphic parageneses in combination with fluid inclusion paragenesis, preferably from a number of gangue and sulphide phases, to derive a fluid history. Ideally, future fluid inclusion work should examine fluid inclusions in sphalerite, scheelite and quartz in each vein set as well as the two styles of 'massive' pyritic ore in the belt.

A question to be answered is the relationship of secondary fluid inclusions in the quartz veins in the belt to the synmetamorphic introduction of metals. The similarity in composition, salinity and homogenization temperature range of primary and pseudosecondary fluid inclusions in the 'massive' style mineralization and secondary fluid inclusions in the Island Mountain and Mosquito Creek veins may be preliminary evidence that the two fluid inclusion types did trap similar metamorphic fluids. Or, perhaps the secondary inclusions record microfracture histories that postdate the main vein-filling and mineralizing fluid events. Detailed work as described above is required to resolve this question. McKeag and Craw (1989) report no significant statistical difference between the primary and secondary inclusions at the Macraes shear zone-related gold vein in the Otago Schist Belt of New Zealand. They consider the two fluid inclusion origins to have formed contemporaneously.

Criteria for local effervescence, or unmixing of a primary, homogeneous CO_2-H_2O fluid phase, have been observed in pseudosecondary fluid inclusions in quartz from 'massive' ore at the Mosquito Creek deposit and in secondary fluid inclusions from a vein at the Cariboo Gold Quartz deposit. This mechanism coupled with evidence of gold precipitation in secondary fluid inclusion filled fractures is cited as the cause of gold mineralization in veins at the Sigma Mine in Quebec (Robert and Kelly, 1987).

Analogues

Gold-bearing mineralization in the Wells-Barkerville Belt is not spatially associated with any plutonic rocks but is hosted by greenschist facies phyllite supracrustal rocks that have undergone early ductile and subsequent brittle deformation. Both the veins and the massive pyrite ore probably formed late in the F_2 ductile deformation history (Ray *et al.*, 2001, this volume).

Veins in the Mosquito Creek and Cariboo Gold Quartz deposits, specifically, have been classified as 'Au-Quartz veins' by Ash and Alldrick (1996). This broad classification includes "mesothermal" veins associated with major faults or shear zones such as the Mother Lode district in California (Weir and Kerrick, 1987), the Bralorne-Pioneer system west of Lillooet in British Columbia (Leitch *et al.*, 1988) and Archean lode gold deposits in Ontario and Quebec, for example, at the Sigma mine (Robert and Kelly, 1987).

The Otago Schist Belt of New Zealand includes two types of W-and Au-mineralized veins: (1) 'syn-metamorphic' foliation-parallel veins that formed close to the peak metamorphic temperature and post peak-pressure conditions and (2) 'post-peak metamorphic' veins which are typically hosted in extension structures (Smith and Yardley, 1999). The main difference in fluid inclusion composition between the two vein types is the presence of CO_2 as a major component in the post-metamorphic vein inclusions and absence of detectable CO_2 in the syn-metamorphic veins (Smith and Yardley, op. cit.). Post-metamorphic veins also tend to have higher salinities (up to > 9 wt. percent NaCl equiv.) rather than salinities equivalent to sea-water or less (< 3.3 wt. percent NaCl equiv.) which were recorded for syn-metamorphic veins (McKeag and Craw, 1989, Smith and Yardley, op. cit.). Fluid inclusions from all the Wells-Barkerville Belt quartz veins evaluated in this study have readily detectable CO_2 and salinities comparable to 'post-metamorphic lodes' (Henley *et al.*, 1976) of the Otago Schist Belt in New Zealand. Other potential analogues for Wells-Barkerville Belt veins include the 'mesothermal' veins in the Klondike District, Yukon (Rushton *et al.*, 1993), Meguma Terrane, Nova Scotia (Kontak *et al.*, 1988) and the Bendigo Gold Fields, Central Victoria, Australia (Jia *et al.*, 2000).

SUMMARY

This preliminary study of fluid inclusions in quartz from vein and 'massive' styles of pyritic mineralization provides the following information concerning the nature of fluids that may relate to metamorphism, deformation and deposition of gold and/or late tectonic overprinting in the Wells-Barkerville Gold Belt:

- Some veins in the belt exhibit wispy quartz textures indicating deep (> 4 km) environments and other veins exhibit breccia and open-space filling textures indicating (later?) deposition at more shallow levels (< 1-3 km?) environments. In some veins, both deep and shallow textures are observed.
- Quartz in the quartz-pyrite veins contain fluid inclusions of mostly secondary origin. It is not clear whether some secondary inclusions have trapped metamorphic fluids or whether they record microfracture histories that postdate the main vein-filling and mineralizing fluid events.
- Quartz in the massive-banded-stringer pyrite ore includes variable proportions of very fine-grained, possibly recrystallized or highly strained quartz that contains primary and pseudosecondary fluid inclusions. These fluid inclusions may trap fluids that record synmetamorphic conditions at the time of sulphide and gold deposition.
- The following four compositional types of fluid inclusions are identified in the vein and 'massive' styles of mineralization based on phases present at room temperature and microthermometric data: Type I: 'Aqueous' H_2O-NaCl, Type III: 'Multiphase' H_2O-NaCl ($\pm CO_2$), Type IV: 'CO_2-bearing' H_2O-CO_2-NaCl and Type V: 'CO_2-CH_4' CO_2-CH_4 ($\pm N_2$) or 'CH_4>CO_2'.
- The dominant fluid inclusion types in both the vein and 'massive' mineralization are Type I and Type IV.
- Type I inclusions have average bulk composition (mole percent) of approximately 98% H_2O and 2% NaCl.
- Type IV secondary inclusions from veins have an average bulk composition (mole percent) of about 85% H_2O, 13% CO_2 and 2% NaCl.
- Type IV primary inclusions from 'massive' mineralization at the Island Mountain mine have average bulk composition (mole percent) of approximately 93% H_2O, 5% CO_2 and 2% NaCl. This composition is significantly different from the composition of Type IV secondary fluid inclusions in veins.
- Overall, Type IV fluid inclusions homogenize at significantly higher final temperatures (avg. 241^{o}C) than Type I fluid inclusions (avg. 169^{o}C).

- No significant differences are seen between primary and secondary fluid inclusion final homogenization temperatures for Type I and Type IV fluid inclusions.
- No significant differences are seen in final homogenization temperature in the vein and 'massive' styles of mineralization, either in the same deposits or between deposits.
- Quartz in the Perkins veins has different fluid inclusion characteristics from other veins in the belt. It is characterized by Type III and IV fluid inclusions that homogenize at significantly higher temperatures (avg. 253^{o}C) than the other vein deposits studied which average < 220^{o}C. Type I and V fluid inclusions are notably absent in the Perkins veins.
- The range of minimum pressures of entrapment for secondary Type IV (H_2O-CO_2-NaCl) fluid inclusions in veins from the Cariboo Gold Quartz mine and BC, Warspite and Perkins veins are 1628 to 3081 bars. Minimum depths of formation are conservatively estimated at about 6 to 13 km, assuming lithostatic pressure
- The range of minimum pressures of entrapment for primary Type IV (H_2O-CO_2-NaCl) fluid inclusions in massive ore from the Island Mountain mine are 1910 to 3412 bars. Minimum depths of formation are conservatively estimated at about 7 to 12 km, assuming lithostatic pressure
- This fluid inclusion study suggests that the Wells-Barkerville gold-bearing veins are analogues to the 'post-metamorphic' gold-bearing veins in the Otago Schist Belt of New Zealand.

ACKNOWLEDGMENTS

International Wayside Gold Mines Ltd. are thanked for permission to collect samples at the BC Vein, Cariboo Gold Quartz, Island Mountain and Mosquito Creek deposits. In particular, Richard Hall is thanked for field discussions concerning the Mosquito Creek deposit and providing access to underground workings at the Island Mountain Mine. We appreciate the help of Claude Blagdon who led us underground at the Island Mountain Mine to collect samples. Kika Ross of Panterra Geoservices Inc. is thanked for providing the sphalerite-bearing drill-core sample GR-00-91 from the BC Vein. We appreciate the editorial reviews by Nick Massey and Ian Webster; the latter is also thanked for geological discussions and help with the drafting .

REFERENCES

Alldrick, D.J. (1983): The Mosquito Creek Mine, Cariboo Gold Belt, B.C.; in Geological Fieldwork 1982, *British Columbia Ministry of Energy, Mines and Petroleum Resources*, Paper 83-1, pages 98-112.

Ash, C. and Alldrick, D. (1996): Au-quartz Veins; in Selected British Columbia Mineral Deposit Profiles, Volume 2 - Metallic Deposits, Lefebure, D.V. and Höy, T., Editors, *British Columbia Ministry of Employment and Investment*, Open File 1996-13, pages 53-56.

Benedict, P.C. (1945): Structure at Island Mountain Mine, Wells, B.C.; *Canadian Institute of Mining and Metallurgy*, Transactions, Volume 48, pages 755-770.

Bodnar, R.J. (1993): Revised equation and table for determining the freezing point depression of H2O-NaCl solutions; *Geochimica et Cosmochimica Acta*, Volume 57, pages 683-684.

Bodnar, R.J., Reynolds, T.J. and Kuehn, C.A. (1985): Fluid-Inclusion Systematics in Epithermal Systems; in Geology and Geochemistry of Epithermal Systems, Berger, B.R. and Bethke, P.M., Editors, *Mineralogical Society of America*, Reviews in Economic Geology, Volume 2, pages 73-97.

Boullier, A-M., Firdaous, K. and Robert, F. (1998): On the Significance of Aqueous Fluid Inclusions in Gold-Bearing Quartz Vein Deposits from the Southeastern Abitibi Subprovince (Quebec, Canada); *Economic Geology*, Volume 93, pages 216-223.

Brown, P.E. and Hagemann, S.G. (1994): MacFlincor: a computer program for fluid inclusion data reduction and manipulation; in Fluid Inclusions in Minerals: Methods and Applications, Short Course of the Working Group (IMA) "Inclusions in Minerals", De Vivo, B. and Frezzotti, M.L., Editors, *Virginia Polytechnic Institute and State University*, pages 231-250.

Brown P.E. and Lamb W.M. (1989): P-V-T properties of fluids in the system H_2O-CO_2-NaCl: New graphical presentations and implications for fluid inclusion studies; *Geochimica et Cosmochimica Acta*, Volume 53, 1209-1221.

Burruss, R.C. (1981): Analysis of Phase Equilibrium in C-O-H-S fluid inclusions; in Short Course in Fluid Inclusions: Applications to Petrology, Hollister, L.S. and Crawford, M.L., Editors, *Mineralogical Association of Canada*, Volume 16, pages 39-74.

Diamond, L.W. (1994): Introduction to phase relations of CO2-H2O fluid inclusions; in Fluid Inclusions in Minerals: Methods and Applications, Short Course of the Working Group (IMA) "Inclusions in Minerals", De Vivo, B. and Frezzotti, M.L., Editors, *Virginia Polytechnic Institute and State University*, pages 131-158.

Gabrielse, H. (Comp.) (1991): Structural styles, Chapter 17; in Geology of the Cordilleran Orogen in Canada; Gabrielse, H. and Yorath, C.J., Editors, *Geological Survey of Canada*, Geology of Canada, Number 4, pages 571-675.

Garba, I. and Akande, S.O. (1992): The Origin and Significance of Non-Aqueous CO2 Fluid Inclusions in the Auriferous Veins of Bin Yauri, northwestern Nigeria; *Mineralium Deposita*, Volume 27, pages 249-255.

Giles, A.D. and Marshall, B. (1994): Fluid-inclusion studies on a multiply deformed, metamorphosed volcanic-associated sulfide deposit, Joma mine, Norway; *Economic Geology*, Volume 89, p. 803-819.

Goldstein, R.H. and Reynolds, T.J. (1994): Systematics of Fluid Inclusions in Diagenetic Minerals; *Society for Sedimentary Geology*, Short Course 31, 199 pages.

Guha, J., Lu, H-Z., Dube, B., Robert, F. and Gagnon, M. (1991): Fluid Characteristics of Vein and Altered Wall Rock in Archean Mesothermal Gold Deposits; *Economic Geology*, Volume 86, pages 667-684.

Hanson, G. (1935): Barkerville Gold Belt, Cariboo District, British Columbia; *Geological Survey of Canada*, Memoir 181, 42 pages.

Henley, R.W., Norris, R.J. and Paterson, C.J. (1976): Multistage Ore Genesis in the New Zealand Geosyncline A History of Post-Metamorphic Lode Emplacement; *Mineralium Deposita*, Volume 11, pages 180-196.

Holland, S.S. (1948): Report on the Stanley Area Cariboo Mining Division; *British Columbia Department of Mines*, Bulletin 26, 66 pages.

International Wayside Gold Mines Ltd. (2000): Cariboo Gold Project Application to British Columbia Ministry of Energy and Mines under Environmental Assessment Act.

Jia, Y., Li, X. and Kerrich, R. (2000): A Fluid Inclusion Study of Au-Bearing Quartz Vein Systems in the Central and North Deborah Deposits of the Bendigo Gold Field, Central Victoria, Australia; *Economic Geology*, Volume 95, pages 467-494.

Johnson, W.A. and Uglow, W.L. (1926): Placer and Vein Gold Deposits of Barkerville, Cariboo District, British Columbia; *Geological Survey of Canada*, Memoir 149, 246 pages.

Kerkhof, F. van den and Thiery, R. (1994): Phase Transitions and Density Calculation in the CO2-CH_4-N_2 System; in Fluid Inclusions in Minerals: Methods and Applications, Short Course of the Working Group (IMA) "Inclusions in Minerals", De Vivo, B. and Frezzotti, M.L., Editors, *Virginia Polytechnic Institute and State University,* pages 171-190.

Kerrick D.M. and Jacobs G.K. (1981): A modified Redlich-Kwong equation for H_2O, CO_2 and H_2O-CO_2 mixtures at elevated pressures and temperatures; *American Journal of Science*, Volume 281, pages 735-767.

Kontak, D.J., MacDonald, D. and Smith, P.K. (1988): Fluid Inclusion Study of the Beaver Dam Gold Deposit, Meguma Terrane, Nova Scotia; in Report of Activities 1988, Part A, *Nova Scotia Mines and Minerals Branch*, Report 88-3, pages 63-69.

Leitch, C.H.B., Godwin, C.I. and Brown, T.H. (1989): Characteristics of Mineralizing Fluids in the Bralorne-Pioneer Mesothermal Gold Vein Deposit: Results of a Fluid Inclusion, Stable Isotope, and Thermodynamic Study; in Geological Fieldwork 1988, *British Columbia Ministry of Energy, Mines and Petroleum Resources*, Paper 1989-1, pages 365-375.

Marshall, B., Giles, A.D. and Hagemann, S.G. (2000): Fluid Inclusions in Metamorphosed and Synmetamorphic (Including Metamorphogenic) Base and Precious Metal Deposits: Indicators of Ore-Forming Conditions and/or Ore-Modifying Histories?; in Metamorphosed and Metamorphogenic Ore Deposits, Spry, P.G., Marshall, B. and Vokes, F.M., Editors, *Mineralogical Society of America*, Reviews in Economic Geology, Volume 11, pages 119-148.

McKeag, S.A. and Craw, D. (1989): Contrasting Fluids in Gold-Bearing Quartz Vein Systems Formed Progressively in a Rising Metamorphic Belt: Otago Schist, New Zealand; *Economic Geology*, Volume 84, pages 22-33.

McTaggart, K.C. and Knight, J. (1993): Geochemistry of Lode and Placer Gold of the Cariboo District, B.C.; *British Columbia Ministry of Energy, Mines and Petroleum Resources*, Open File 1993-30, 26 pages.

Ray, G.E., Webster, I.C.L., Lane, R., Ross, K. and Hall, R. (2000): Geochemistry of auriferous pyrite mineralization at the Bonanza Ledge, Mosquito Creek Mine and other properties in the Wells-Barkerville area, British Columbia; *British Columbia Ministry of Energy and Mines*, Geological Fieldwork 2000, Paper 2001-1, this volume.

Reynolds, T.J., (1991): Short Course on Fluid Inclusions; *Mineral Deposit Research Unit*, Short Course 6.

Richards, F. (1948): Cariboo Gold Quartz Mine; in Structural Geology of Canadian Ore Deposits, *Canadian Institute of Mining and Metallurgy*, pages 162-168.

Robert, F. and Kelly, W.C. (1987): Ore-forming fluids in Archean gold-bearing quartz veins at the Sigma mine, Abitibi Greenstone Belt, Quebec, Canada; *Economic Geology*, Volume 82, pages 1464-1482.

Robert, F. and Taylor, B.E. (1989): Structure and Mineralization at the Mosquito Creek Gold Mine, Cariboo District, B.C.; in Structural Environment and Gold in the Canadian Cordillera, *Geological Association of Canada*, Cordilleran Section, Short Course 14, 174 pages.

Roedder E. (1984): Fluid Inclusions; *Mineralogical Society of America*, Reviews in Mineralogy, Vol. 12, Bookcrafters Inc., Chelsea, Michigan, 644 pages.

Rushton, R.W., Nesbitt, B.E., Muehlenbachs, K. and Mortensen, J.K. (1993): A Fluid Inclusion and Stable Isotope Study of Au Quartz Veins in the Klondike District, Yukon Territory, Canada: A Section through a Mesothermal Vein System; *Economic Geology*, Volume 88, pages 647-678.

Rhys, D. (2000): The Cariboo Gold Project of International Wayside Gold Mines; *Vancouver Mineral Exploration Group*, Abstract, November 29, 2000, 2 pages.

Rhys, D.A.E. and Ross, K.V. (2000): Report on Petrography, Check Sampling and Geological Interpretation of Drill Core at the Bonanza Ledge Zone, Cariboo Gold Quartz Property, British Columbia; Prepared for International Wayside Gold Mines Ltd. by *Panterra Geoservices Inc*. at *http://www.wayside-gold.com/i/pdf/PanterraGeoReport_new.pdf,* 77 pages.

Skerl, A.C. (1948): Geology of the Cariboo Gold Quartz Mine, Wells, B.C.; *Economic Geology*, Volume 43, pages 571-597.

Smith, M.P. and Yardley, B.W.D. (1999): Fluid Evolution during Metamorphism of the Otago Schist, New Zealand: (I) Evidence from fluid inclusions; *Journal of Metamorphic Geology*, Volume 17, pages 173-186.

Struik, L.C. (1988): Structural Geology of the Cariboo Gold Mining District, East-Central British Columbia; *Geological Survey of Canada*, Memoir 421, 100 pages.

Sutherland-Brown, A. (1957): Geology of the Antler Creek Area, Cariboo District, British Columbia; *British Columbia Department of Mines*, Bulletin 38, 105 pages.

Thiery, R., van den Kerkhof, A.M. and Debussy, J. (1994): VX Properties of CH_4-CO_2 and CO_2-N_2 fluid inclusions; Modelling for T<31 degrees C and P< 400 bars; European Journal of Mineralogy, Volume 6, Number 6, pages 753-771.

Weir, R.H. Jr. and Kerrick, D.M. (1987): Mineralogic, Fluid Inclusion, and Stable Isotope Studies of Several Gold Mines in the Mother Lode, Tuolumne and Mariposa Counties, California; *Economic Geology*, Volume 82, p. 328-344.

Yardley, B. (1999): Discussion of inclusion survival in sheared quartz; FI Discussion Archives at http://www.geology.wisc.edu/%7Epbrown/fi.html

Whiterocks Mountain Alkaline Complex, South-Central British Columbia: Geology and Platinum-Group-Element Mineralization

By Graham T. Nixon and Brent Carbno

KEYWORDS: Platinum-group-elements, Whiterocks Mountain, alkaline complex, sulfides, mineralogy, electron-microprobe analysis.

INTRODUCTION

The recent increase in the price of platinum-group elements (PGE) in world markets has sparked renewed interest in exploration for these metals. Although world-class deposits of PGE such as those associated with tholeiitic or komatiitic flood-basalt provinces (*e.g.* Noril'sk–Talnakh, Russia, and Kambalda, Western Australia) and large layered intrusions (*e.g.* Bushveld, South Africa) have yet to be discovered in the Cordillera, there are other prospective geological environments specific to the supra-subduction zone setting which characterizes much of Cordilleran evolution. For example, placer and lode occurrences associated with Alaskan-type ultramafic-mafic intrusive complexes are known to host PGE as a primary commodity (*e.g.* Tulameen, southern British Columbia, *cf*. Nixon *et al.*, 1997 for a summary relevant to British Columbia). In addition, there are other predominantly sulfide-bearing environments where the PGE occur as a subsidiary component of certain base- and precious-metal (Cu±Au±Ag) deposit types which are common in the Cordillera such as porphyry environments (*e.g.* Copper Mountain-Ingerbelle) and Cu-PGE (±Au±Ag) mineralization associated with alkalic intrusive complexes (*e.g.* Maple Leaf showing in the Franklin Camp (Averill Complex); and the Sappho prospect, southern British Columbia). The latter style of mineralization has been informally referred to as "Coryell-type" after the alkaline rocks of the Tertiary (Eocene) Coryell Batholith in southern British Columbia (Hurlbert *et al.* 1988). Clearly, given current metal prices, even the typically low tenor of PGE in these latter deposit types has the potential to attract exploitation of an otherwise subeconomic base- and precious-metal resource.

In an effort to promote further exploration for PGE in British Columbia, a new mapping and sampling program was undertaken to examine PGE-bearing sulfide environments in the Cordillera. Fieldwork this past summer focused on the Whiterocks Mountain alkaline intrusive complex in south-central British Columbia where previous work by industry has revealed anomalous concentrations of PGE associated with Cu-Fe sulfides in a "Coryell-type" intrusive setting. The results of recent geological mapping together with lithogeochemical and mineral analyses are reported below. In addition, a companion contribution (Dunn *et al.*, this volume) presents preliminary results for a soil survey employing new techniques which are capable of detecting Pt at ultra-low concentrations (~0.1 ppb).

LOCATION AND ACCESS

The Whiterocks Mountain alkaline plutonic complex is named for Whiterocks Mountain (50.01°N, 119.75°W; 1873 m) which is situated west of Okanagan Lake approximately 25 kilometres northwest of Kelowna (Figure 1). The map area straddles the boundary between two 50 000-scale topographic sheets (NTS 82L/4 and 82E/13)

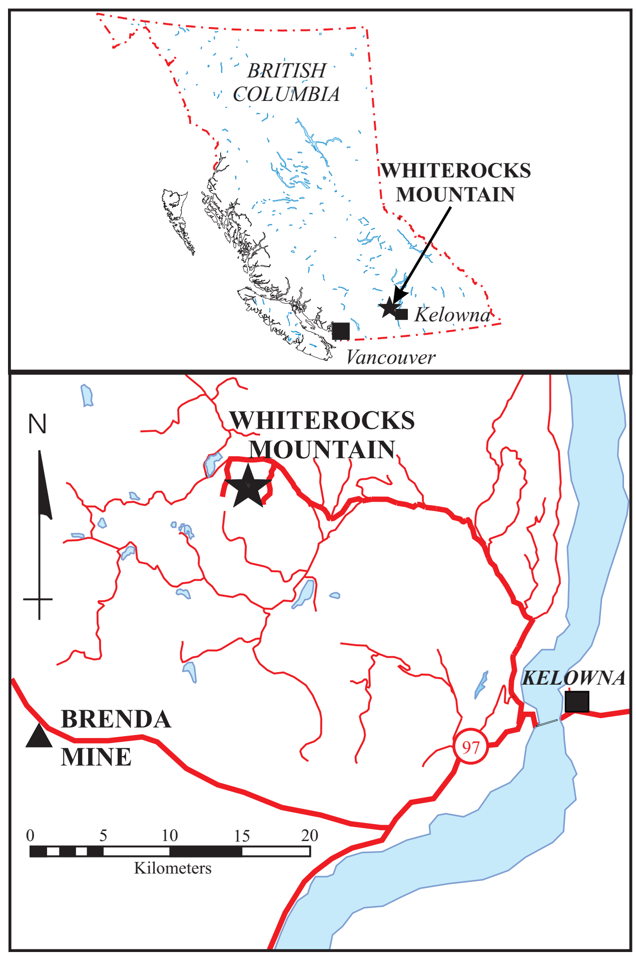

Figure 1. Location of the Whiterocks Mountain area, south-central British Columbia.

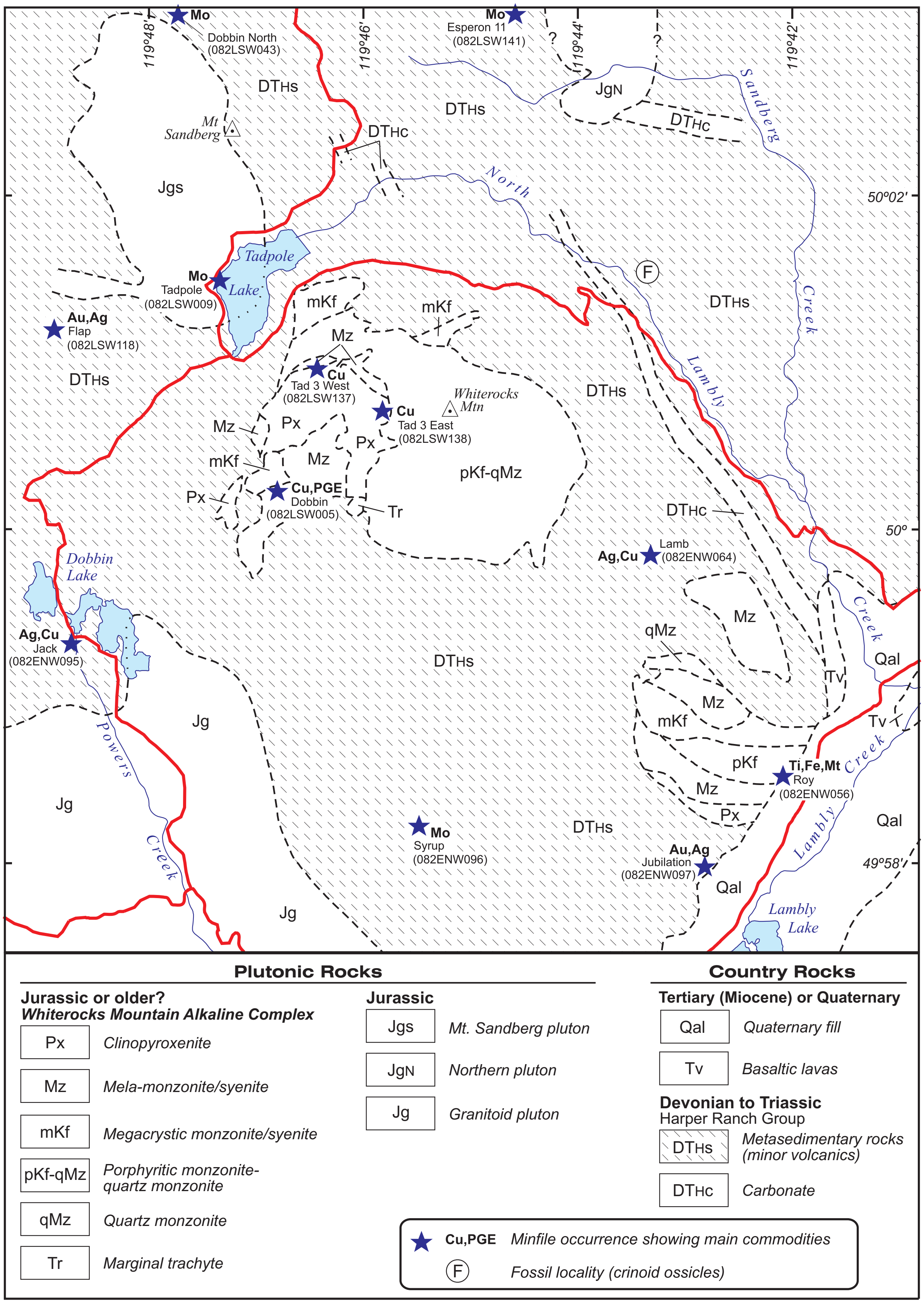

Figure 2. Generalized geological map of the Whiterocks Mountain area showing MINFILE occurrences. The star for the Dobbin Cu-PGE prospect marks the location of the 1997 drill program referred to in the text.

near the eastern margin of the Thompson Plateau. Road access is via the Bear Main Forest Services road which leaves West Okanagan Lake Road on the west shore of Okanagan Lake just north of Bear Creek Provincial Park. The Whiterocks Main logging road leaves Bear Main at Kilometre 17 for the Tadpole Lake area where a system of spur roads maintained by Riverside Forest Products of Kelowna provide excellent access to the map area. The hilly topography is well forested with pine and spruce and generally covered by a thin veneer of glacial drift.

MINERAL OCCURRENCES AND EXPLORATION HISTORY

The MINFILE occurrences for base- and precious-metals in the region are numerous. The most notable is the former Brenda Mine which is located about 24 kilometres southwest of Whiterocks Mountain (Figure 1). This Cu-Mo porphyry deposit produced approximately 272 000 tonnes of copper, 65 000 tonnes of molybdenum, 113 000 kg of silver and 1800 kg of gold over its 20-year mine life (1970-1990; Weeks *et al.* 1995). Figure 2 shows the MINFILE occurrences in the project area. The two principal prospects in the vicinity of Whiterocks Mountain are the Dobbin Cu-Pd-Pt (MINFILE 082LSW005) and Tadpole Mo (082LSW009) occurrences. The main (Dobbin) copper anomaly in the area was named for Dobbin Lake. The Tadpole Mo showing, located on the west shore of Tadpole Lake, is partially submerged beneath the waters of the enlarged reservoir. The Dobbin and Tadpole showings are currently covered by claims owned by joint venture partners Verdstone Gold Corporation and Molycor Gold Corporation.

The first prospectors to enter the area arrived at the beginning of the 20th century or earlier. Intermittent exploration activity ensued until the late 1960s and early 1970s when a succession of exploration companies following copper and molydenum stream-silt anomalies in the area around Whiterocks Mountain performed considerable work involving geological mapping, trenching, soil and rock-chip geochemistry, magnetometer and induced-polarization surveys, and percussion and diamond drilling (details are given in the British Columbia Ministry of Energy and Mines Assessment Reports). It was this work that established and first tested the molybdenum anomaly at Tadpole Lake and the main copper anomaly at the Dobbin property. Grades encountered in drilling ranged 0.1-0.4 % Cu and up to 0.017 % Mo with Ag ~3.4 g/t over intersections of up to 44.8 m.

Following this activity, Cominco Limited acquired the ground in 1977 and through to 1980 performed extensive work which further delineated mineralization, produced detailed geological maps and supported an M.Sc. thesis (Osatenko, 1978, 1979a, 1979b, 1980; Mehner, 1982). According to this work, mineralization at the Tadpole showing is related to a porphyry Mo system with the most intense mineralization centered on a quartz stockwork zone (1.5 x 1 km) which is focused at the southwestern margin of the granitoid stock. The best drill intersection gave 0.061 % Mo over 180 ft. Rock-chip samples collected at the main Dobbin copper anomaly yielded grades similar to previous results (0.014-0.017 % Mo; 0.2-0.4 % Cu). During the course of this work, Cominco geologists apparently were the first to analyze for PGE. Rock chip samples from the main copper anomaly returned maximum abundances of 390 ppb Pt and 265 ppb Pd (fire assay) combined with low Au and Ag (40 ppb and 2 ppm, respectively). It was noted that the PGE appear to be preferentially associated with disseminated sulfides (pyrite-chalcopyrite-bornite) in hornblende pyroxenites of the Whiterocks Mountain complex and cross-cutting epidote-albite veins, and the style of mineralization was related to an alkaline porphyry deposit type.

Almost a decade later, Chevron Canada Resources Ltd. conducted several prospecting surveys on the northwest flank of Whiterocks Mountain about 1.5 kilometres northeast of the main Dobbin copper anomaly (MINFILE 082LSW137). Soil and rock-chip samples indicated anomalous metal concentrations of ~2000 ppm Cu, 240 ppb Pt, 80 ppb Pd and 29 ppb Au.

In 1997, Verdstone/Molycor, the current owners of the Dobbin property, conducted soil and lithogeochemical sampling of the “central” (main) Dobbin copper anomaly, and 22 diamond drill holes (4689 m) were completed and logged. The best drill intersection yielded 0.19 % Cu, 0.41 g/t Pt and 0.35 g/t Pd over 111 m (288-399 m depth), which includes a 15 m zone of 0.54 % Cu, 1.32 g/t Pt and 0.95 g/t Pd (333-348 m; Makepeace, 2000). The core from this intersection was resampled and analyzed during the course of this study. The new results confirm the anomalously high concentrations of PGE in the core (discussed below).

PREVIOUS WORK AND REGIONAL GEOLOGY

The map area straddles the boundary (50° N) between original 250 000-scale mapping done by the Geological Survey of Canada. The northern part of the area lies within the Vernon sheet (Jones, 1959) and the southern portion is covered by the Kettle River west half sheet (Cairnes, 1940; Little, 1961). A 250 000-scale compilation of the Thompson-Shushwap-Okanagan region by Okulitch (1979) covers the entire Whiterocks Mountain area and draws heavily on previous mapping (Okulitch, personal communication, 2000); and Okulitch (1989) subsequently published a revision of parts of the geology. A compilation by Templeman-Kluit (1989) at the same scale covers the southern part of the map area. In addition, both the Vernon and Penticton (NTS 82E) sheets were re-compiled at 250 000-scale during the Provincial Mineral Potential Project .

The Whiterocks Mountain alkaline complex was the subject of a M.Sc. thesis by Mehner (1982) who produced a geological map (5000-scale) and the first detailed petrographic and geochemical descriptions. Although details differ, his geology is basically the same as the Cominco property map provided by Osatenko (1979a) who also produced a detailed map of the stock west of Tadpole Lake.

In terms of its regional stratigraphic setting, the Whiterocks Mountain area lies near the eastern margin of the Intermontane Belt within the Quesnellia tectonostratigraphic terrane (Harper Ranch subterrane). The oldest rocks in the region belong to the Paleozoic Chapperon Group which lies just outside the map area to the west and north. Ultramafic bodies within the Chapperon Group, known as the Old Dave "intrusions", are probably remnants of an obducted sliver of oceanic crust presumably emplaced within a Paleozoic subduction complex off to the west. The hostrocks of the Whiterocks Mountain alkaline complex comprise a series of deformed and metamorphosed, Paleozoic volcanic and sedimentary rocks including limestone, argillite, chert and conglomerate (Figure 2). In the most recent compilation (Provincial Mineral Potential Project), these rocks have been assigned to the Devonian to Triassic Harper Ranch Group. The youngest stratigraphic units in the surrounding region include Tertiary (Eocene) volcanic flows and sedimentary sequences of the Kamloops Group, basaltic lavas of the Chilcotin Group (Miocene and younger) and Quaternary valley basalt. Plutonism in the vicinity of the map area, including the Whiterocks Mountain complex, has been assigned to the Late Jurassic (Okulitch, 1989). The region as a whole has been subjected to a Tertiary (Eocene) extensional and thermal event which occurred contemporaneous with the emplacement of alkalic plutons of the Coryell Suite.

WHITEROCKS MOUNTAIN ALKALINE COMPLEX

The Whiterocks Mountain stock was originally subdivided by Osatenko and Mehner into a quartz-deficient alkalic complex underlying Whiterocks Mountain, which is the focus of this study, and a quartz-enriched calc-alkaline complex extending north-northwesterly from Tadpole Lake, referenced herein as the Mt. Sandberg pluton (Figure 2). Based on their contrasting petrography, geochemistry and styles of mineralization, both authors considered the alkaline and calc-alkaline complexes to be genetically unrelated. The contact between these intrusive bodies is not exposed and they appear to be separated by a screen of country rock about 700m wide at surface. In this report, the Mt. Sandberg pluton is treated as a completely separate entity and is considered to be genetically distinct from the alkaline stock at Whiterocks Mountain.

The age of the Whiterocks Mountain alkaline complex (Whiterocks complex) is poorly determined. Biotite mineral separates from a biotite clinopyroxenite have yielded a two-point Rb-Sr isochron age of 149 ± 22 Ma (R. L.Armstrong *in* Mehner, 1982). Whole-rock plus mineral isochrons (biotite, hornblende, and potassium feldspar separates) for a porphyritic monzonite and leucocratic quartz monzonite have produced Rb-Sr isochron ages of 291 ± 38 Ma and 338 ± 37 Ma, respectively (Wilkins, 1981). On the other hand, conventional K-Ar dating of porphyritic monzonite and hornblende clinopyroxenite gave isotopic ages of 169 ± 6 Ma and 174 ± 6 Ma (Wilkins, 1981). In addition, calc-alkaline quartz diorite dikes which cut the alkaline rocks have yielded K-Ar dates of 147 ± 5 Ma and 145 ± 5 Ma, and a concordant Rb-Sr isochron age of 154 ± 6 Ma. Taken as a whole, these data indicate that the alkaline complex is Mesozoic or Paleozoic in age, and evidently much too old to be correlative with Eocene alkaline rocks of the Coryell batholith.

As previously mapped, the Whiterocks complex occupied an area of about 9 km^2 and its contact east of Whiterocks Mountain was poorly defined. New mapping on recently constructed logging roads has better delineated the eastern contact and recognized a sizeable (~4 km^2) extension of the complex to the southeast near Lambly Creek. An area of sparse outcrop (1.5 km in width), which represents a relatively thin carapace of country rock, divides the Whiterocks Mountain stock into a northern and southern cupola. The northern cupola occupies a subcircular outcrop area of approximately 3.5 km maximum diameter centered just west of Whiterocks Mountain. The mafic and ultramafic rocks are restricted to the western half of the stock and have a north-northeasterly distribution. The more leucocratic, quartz-bearing monzonites forming the eastern half of the intrusion have a northwesterly elongation and at their northern extremity transect the melanocratic rocks. The southern cupola comprises a northwesterly trending intrusion at least 2 kilometres in length which disappears to the southeast beneath thick Quaternary alluvial deposits occupying the Lambly Creek drainage. A smaller satellitic body of monzonite crops out 300 m beyond the northeastern contact with the country rocks. As discussed below, the southern cupola embodies all of the major rocks types found to the north and is similarly characterized by a well-defined high on the aeromagnetic map (Geological Survey of Canada, 1968). Interestingly, this body is also coincident with a Ti-Fe (-magnetite) occurrence in the MINFILE database (Figure 2).

The principal rock types of the Whiterocks complex comprise a diverse suite of porphyritic to non-porphyritic ultramafic, mafic and felsic plutonic rocks and related minor intrusions. The map units shown in Figure 2 essentially correspond to lithologies identified by Mehner (1982). They include biotite- and hornblende-bearing clinopyroxenites and their feldspar-bearing variants, clinopyroxene- and hornblende-bearing melanocratic monzonites and syenites, porphyritic and megacrystic monzonites and syenites with conspicuously large crystals of potassium feldspar, and leucocratic quartz monzonites; minor lithologies include hornblendite and hornblende gabbro/diorite, leuco-syenite and rare trachyte.

Many of the rocks exhibit textures which may be described in terms of classical cumulate terminology. This does not necessarily imply that these lithologies were formed by gravitative settling of crystals, although this is considered as a likely concentration mechanism for the crystal cumulates which form the clinopyroxenites and hornblende gabbro/diorites.

The mineralogical descriptions which follow make frequent reference to "biotite" and "hornblende" ; these terms are used a generic sense to indicate ferromagnesian mica and calcic amphibole, respectively. Electron-microprobe analyses of these minerals allow for a more specific nomenclature which is discussed below. Although quartz appears in the more leucocratic rocks, feldspathoids appear to be completely lacking. Of note, however, is the presence of igneous garnet in a number of monzonitic samples.

Clinopyroxenite and Hornblendite

The best exposures of the ultramafic lithologies are found due west of Whiterocks Mountain summit. Dark greenish grey to almost black, medium-grained clinopyroxenites generally contain both hornblende and biotite in variable proportions, accessory magnetite and apatite, and may carry small amounts of disseminated sulfide. Locally, hornblende forms large (≤3 cm) poikilitic crystals enclosing pyroxene. Outcrops are strongly magnetic and commonly cut by planar veins of hornblendite or hornblende+feldspar (partially epidotized) from several millimetres to centimetres in width. Anastomizing, virtually monomineralic veins and irregular clots of coarse-grained to pegmatitic biotite crystals (5 mm to 2 cm) are a conspicuous feature of many outcrops, although not nearly as prevalent as the hornblendite veins. Clinopyroxenites and hornblendites with subequal proportions of amphibole and pyroxene occur on the margins of the mappable clinopyroxenite bodies near contacts with melanocratic monzonite-syenite. They commonly contain small amounts of feldspar and are observed to grade over narrow intervals into gabbro/diorite and melanocratic monzonite.

In thin section, subhedral to anhedral, colourless to very pale green and weakly pleochroic clinopyroxenes (≤5 mm) have cumulus textures and may exhibit rare schillered features and a weak preferred orientation. Some clinopyroxenites contain oscillatory zoned, and rarely, sector zoned crystals. Inclusions of euhedral biotite, magnetite and apatite have been observed but not primary amphibole. Pyroxenes in hornblende-bearing rocks are usually flecked with patchy to vermicular amphibole whose optical properties are similar to the igneous amphiboles and quite distinct from secondary, uralitic green amphibole which partially replaces some grains. Euhedral to anhedral, cumulus to intercumulus biotite, (≤3 mm) is strongly pleochroic from colourless to reddish brown or very dark brown and locally exhibits incipient bleaching (green biotite) and chloritic alteration. Inclusions of biotite have been observed in pyroxene and hornblende, and in some rocks, exsolution of acicular rutile, probably caused by subsolidus oxidation, has produced a sagenitic texture. Anhedral, intercumulus poikilitic hornblende (typically ≤5 mm) shows olive-green to dark green or brown pleochroism and is locally altered to secondary actinolitic amphibole. In the more hornblende-rich clinopyroxenites, amphibole joins pyroxene as a cumulus phase. Euhedral to anhedral magnetite (≤0.5 mm) and apatite (≤1.3 mm) occur as ubiquitous cumulus and intercumulus grains whose modal abundances reach about 8 and 4 vol. %, respectively. In particular, apatite locally forms disrupted monomineralic cumulate layers several millimetres thick and over a centimetre in length. Anhedral, patchy zoned plagioclase partially altered to sericite, epidote and clay minerals forms a minor (trace to 5 vol. %) intercumulus phase in feldspathic clinopyroxenites and hornblendites. The feldspathic hornblendites may also contain trace amounts of subhedral to anhedral brownish sphene as an intercumulus phase. In addition, disseminations and veins of sulfides, predominantly pyrite and chalcopyrite, occur as trace or minor constituents and are discussed further below in reference to the mineralization.

Melanocratic Monzonite-Syenite

Scattered outcrops of melanocratic monzonite-syenite (mela-monzonite) are found in the northern cupola north and south of the main pyroxenite body, and in the southern cupola, along the northern margin of the clinopyroxenite as well as further north (Figure 2). Medium grey-brown to greenish brown-weathering, mela-monzonites contain essential plagioclase and potassium feldspar, as well as hornblende and typically clinopyroxene, and accessory magnetite, apatite and sphene; other minor phases include garnet and biotite. In addition, one fine-grained, more leucocratic specimen collected at the contact of this map unit with metasedimentary country rocks contains minor quartz (~4 vol. %). In general, the mela-monzonites are equigranular, medium- to coarse-grained rocks with plagioclase:potassium feldspar ratios in the range 3:2 to 1:3 and modal proportions of mafic minerals averaging 20-40 vol. % (Mehner, 1982). Modal layering is commonly observed near contacts with clinopyroxenites. Locally, the layering exhibits a well-defined igneous lamination marked by a preferred orientation of prismatic hornblende crystals (≤1.5 cm) and tabular feldspars (usually potassium feldspar ≤3 cm). Some outcrops exhibit intercalated layers of feldspathic clinopyroxenite and rounded xenoliths of biotite-hornblende clinopyroxenite. Locally, the mela-monzonites are cut by an irregular network of leucocratic feldspathic dikes (≤10 cm in width) and veins of feldspathic hornblendite and hornblende gabbro/diorite. Rusty-weathering outcrops betray the presence of minor amounts of disseminated sulfides.

In thin section, textures range from equigranular to pseudoporphyritic, and the majority of mela-monzonites exhibit a pronounced igneous lamination. The rocks are usually only weakly altered to epidote, sericite, carbonate and clay minerals. Sodic plagioclase (≤5 mm) occurs as subequant to prismatic, subhedral crystals with cumulate textures and commonly displays patchy-zoned cores and oscillatory-zoned mantles. Colourless to very pale brownish green clinopyroxene (≤3 mm) forms anhedral to subhedral grains, many of which have reacted to form hornblende or occur as relicts enclosed in amphibole. Clinopyroxene-rich mela-monzonites contain subhedral cumulate pyroxene. Brownish green to dark brown hornblende (≤5 mm) generally occurs as anhedral grains poikilitically enclosing feldspar, clinopyroxene, magnetite and apatite through adcumulus growth. Some rocks, however, also contain subhedral cumulus hornblende. Potassium feldspar typically occurs as anhedral interstitial grains or, more rarely, subhedral prismatic crystals. Euhedral microcline with well-developed tartan twinning is found in the porphyritic variants. Pale pinkish brown garnet generally occurs as anhedral poikilitic crystals partially to completely enclosing plagioclase, microcline, clinopyroxene, hornblende and apatite, textures which indicate a magmatic origin. Some grains exhibit a weak colour zoning, and in one sample submitted for electron-probe microanalysis (discussed below) birefringent garnets display fine oscillatory zoning. Euhedral to subhedral apatite, magnetite and pale brownish sphene are ubiquitous accessory phases (trace to 1 vol. %).

Megacrystic Monzonite-Syenite

Excellent exposures of megacrystic monzonite-syenite (megacrystic monzonites) are found in a logging slash at the western extremity of the northern cupola just north of the main Dobbin copper anomaly. Locally, outcrops are stained with hematite and limonite and carry traces of sulfides. The buff-weathering monzonites contain megacrysts of pale grey potassium feldspar (>2.5<15 cm and typically 3-6 cm) set in a medium-grained melanocratic feldspathic groundmass averaging about 25-30 vol. % mafic minerals. Megacryst habits vary from blocky (*e.g.* 5 x 5 cm) to subequant (*e.g.* 12 x 5 cm) to tabular (*e.g.* 10 x 2.5 cm) and typically exhibit a strong trachytic texture (Photo 1). The distribution of megacrysts is non-uniform such that crowded megacryst zones pass gradationally into zones with relatively few megacrysts, and locally, the larger crystals occur in disoriented aggregates. Rare modal layering is defined by thin (<5 mm) laminae of hornblende crystals oriented parallel to the megacryst fabric and traceable for up to 5 metres over the outcrop (Photo 2). The northern megacrystic monzonites are cut by thin (≤10 cm) dikes of feldspathic hornblende clinopyroxenite. Some of these dikes have curvilinear margins and taper out along strike indicating that the host was hot and plastic at the time of intrusion. Sporadic clinopyroxenite or mela-monzonite xenoliths (≤10 cm) with irregular shapes may represent early remobilized dikes. Megacrystic monzonites in the southern cupola are cut by mela-monzonite dikes with pseudoporphyritic textures involving hornblende, clinopyroxene and plagioclase.

Mineralogical differences exist between megacrystic monzonites in the northern cupola, which contain clinopyroxene and hornblende, and those in the southern cupola which carry only biotite. In thin section, the rocks exhibit weak to moderate alteration to sericite, clay minerals and minor epidote. Microcline megacrysts exhibit distinctive cross-hatched twinning and patchy perthite development, and may contain zonally-arranged inclusions of plagioclase and very fine-scale oscillatory zoning. The northern megacrystic monzonites are more melanocratic with about 30 vol. % mafic minerals in the groundmass. Pale brown to deep olive-green hornblende (≤2 mm) forms subequant to prismatic crystals in a fine- to medium-grained groundmass. Subhedral to anhedral, very pale green clinopyroxene (≤1 mm) has reacted with the melt to form hornblende. Accessory phases, predominantly apatite and magnetite, form up to 1-2 vol. % of the rock. The southern, more leucocratic counterparts contain pale brown to almost black pleochroic biotite (≤1.5 mm; ~15 vol. %) as an interstitial, late-crystallizing phase, and magnetite and apatite in trace amounts.

Photo 1. Microcline-megacrystic monzonite-syenite exhibiting a well-developed igneous flow lamination, western margin of northern cupola, Whiterocks complex. (Knife is 25 cm in length.)

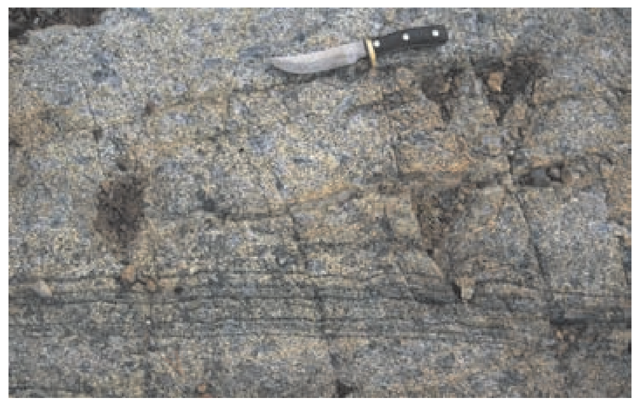

Photo 2. Delicate, hornblende-rich layering (lower part of photograph) in microcline-megacrystic monzonite-syenite, western margin of northern cupola, Whiterocks complex. (Knife is 25 cm in length.)

Porphyritic Monzonite and Quartz Monzonite

Porphyritic monzonites with potassium-feldspar crystals generally measuring 1-2 centimetres in length, and rarely 3-5 centimetres, are found as minor lithologies associated with the main melanocratic monzonite-syenite unit in the southwestern part of the northern cupola, and form a small body in the central part of the southern cupola (Figure 2). In addition, this rock type forms the western part of the composite porphyritic monzonite-quartz monzonite unit underlying the summit region of Whiterocks Mountain and passes into more leucocratic, quartz-bearing lithologies to the east. Mehner (1982) included these quartz-bearing monzonites in the alkaline complex whereas Osatenko (1979a) considered them as belonging to a separate calc-alkaline suite. These authors placed the porphyritic monzonite – leuco-monzonite contact in radically different locations on their maps. As indicated in Figure 2, these lithologies appear to comprise a single mappable unit in which rocks with porphyritic textures grade into quartz-bearing monzonites lacking potassium feldspar phenocrysts. A small body of quartz monzonite also occurs as a marginal phase of melanocratic monzonite-syenite at the northern edge of the southern cupola.

Buff to pale grey-weathering outcrops of porphyritic monzonite in the northwestern part of the northern cupola near the mela-monzonite contact are locally stained with hematite and limonite and commonly exhibit rusty patches due to disseminated sulfides (largely pyrite). A weak to moderate igneous flow lamination is locally highly variable in strike over 20-30 m of continuous outcrop but dips remain steep. A finer-grained phase with sparse potassium feldspar phenocrysts occurs near the contact with medium to coarse-grained mela-monzonite and locally carries angular to subangular xenoliths (≤1 m) and larger rafts of metasediments and mela-monzonite. Dikes of porphyritic monzonite with sharp contacts are observed cutting mela-monzonite and hornblende clinopyroxenite.

Porphyritic monzonites west of Whiterocks Mountain summit near the clinopyroxenite contact are weakly to strongly laminated and locally intercalated with thin (5-20 cm) layers of melanocratic hornblende diorite or monzodiorite and hornblende-porphyritic mela-monzonite. In the coarser layers prismatic hornblende crystals and tabular potassium feldspars reach 2.5 and 3 centimeters in length, respectively, and some trachytic-textured zones are crowded with feldspar. Xenoliths of hornblende-poor clinopyroxenite with diffuse margins have also been observed. These diverse lithologies pass westward into relatively uniform porphyritic monzonite and non-porphyritic, leucocratic quartz-bearing monzonite which commonly lack a distinct igneous fabric.

The medium to coarse-grained leucocratic quartz monzonites near the eastern margin of the intrusion are typically non-porphyritic and contain 5-10 vol. % mafics minerals and up to 19 vol. % quartz, although most appear to have less (5-10 vol. %; Mehner, 1982). Xenolith trains of hornfelsed metasedimentary rocks, some with well-developed reacton rims involving coarse-grained intergrowths of hornblende and feldspar, occur locally near the contact (Photo 3). Two samples of slightly more melanocratic monzonite (15 vol. % mafic minerals), one collected near the southern contact of the composite body, and the other from the southern cupola, contain igneous garnet.

Mineralogically, the porphyritic monzonites and quartz monzonites contain plagioclase and potassium feldspar in subequal proportions, hornblende ± biotite ± quartz and accessory magnetite, apatite and sphene. In general, the rocks are weakly altered to an assemblage of epidote + sericite + clay ± chlorite ± carbonate. Sodic plagioclase (≤4 mm) occurs as subhedral crystals with patchy and fine-scale oscillatory zoning. Euhedral to subhedral, well-twinned microcline phenocrysts exhibit patch and string perthite textures and some crystals show very fine oscillatory zoning. Potassium feldspar also forms small laths and anhedral grains in the groundmass.

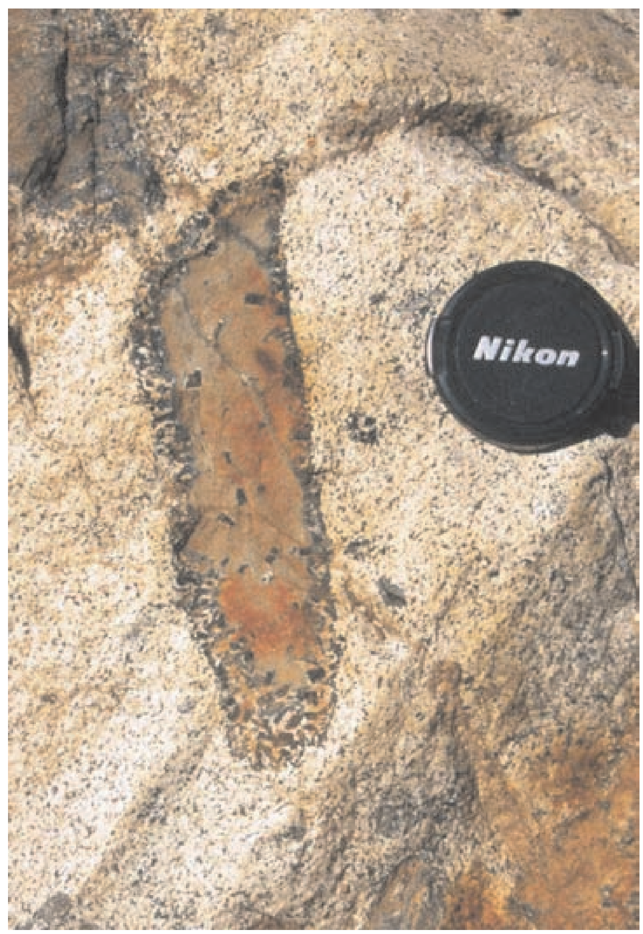

Photo 3. Metasedimentary xenolith in leucocratic quartz monzonite displaying a reaction rim of coarsely crystalline hornblende and feldspar, eastern margin of composite porphyritic monzonite – quartz monzonite unit, northern cupola, Whiterocks complex. (Pencil magnet is 13 cm in length.)

Subhedral to anhedral, pale brown to dark green pleochroic hornblende (≤4 mm) may enclose biotite and rare relict clinopyroxene, and in the more leucocratic rocks is commonly partially altered to epidote and chlorite. Quartz and colourless to pale brown biotite in the latter rocks occur in fine-grained intergrowths with feldspar. Pale pinkish brown poikilitic garnet (≤5 mm) is found in quartz-free monzonite and contains inclusions of euhedral plagioclase, microcline and apatite. Brownish subhedral sphene (≤0.7 mm), apatite and magnetite combined form less than 1 vol. % of the leucocratic rocks but are two to three times as abundant in the more melanocratic porphyritic monzonites.

Marginal Trachyte

A tan-weathering, aphanitic felsic volcanic rock, pale grey on fresh surfaces, is exposed in an area of low scattered outcrops at the southwestern margin of the northern cupola (Figure 2). The rock has a marked flow lamination and contains large (≤6 cm) vesicles lined with clay minerals and flattened parallel to the plane of flowage. This unit can be traced a short distance laterally almost to its contact with the porphyritic monzonite and clinopyroxenite where it has been hornfelsed to a pinkish grey rock with a sugary texture. Xenoliths of the hornfelsed trachyte have been observed in the porphyritic monzonite. Contacts with metasedimentary host rocks to the south appear to be hidden beneath a thin cover of glacial drift.

In thin section, a relict flow fabric is preserved amidst areas of recrystallization. Microphenocrysts of subhedral clinopyroxene (≤0.3 mm) are set in a finely crystalline groundmass of potassium feldspar, plagioclase and minor brown pleochroic hornblende. Within the contact aureole, the rock is converted to an assemblage of granular clinopyroxene, quartz and feldspar (mainly plagioclase), and has areas rich in fine-grained epidote and diffuse veins of feldspar and quartz. The rock is classified as a trachyte based on its chemical composition (presented below). It is interpreted to represent a chilled facies of the Whiterocks alkaline suite which was probably intruded as a dike, and was later subject to intrusion by the plutonic members of the suite.

Minor Intrusions

Dikes and veins observed cutting the Whiterocks complex and mineralogically similar to the main lithologies described above include hornblendite and hornblende gabbro/diorite, melanocratic monzonite, megacrystic and porphyritic monzonite-syenite, and leucocratic quartz monzonite. Other related varieties include medium to coarse-grained leuco-syenite dikes and feldspathic veins, biotitite veins (only found in clinopyroxenite), and plagioclase-clinopyroxene-hornblende porphyritic dikes. A microcline-megacrystic dike cutting clinopyroxenite contains small (<1 mm) euhedral to subhedral crystals of pinkish brown igneous garnet. A pegmatitic segregation vein in porphyritic monzonite contains muscovite with hematite lamellae along cleavage traces which indicate that it is most likely pseudomorphous after biotite, a common phase in the hostrock.

Emplacement History

The emplacement history of the Whiterocks alkaline suite has been deduced from the nature of contacts, xenoliths and crosscutting relationships. The earliest members of the suite are the clinopyroxenites, which formed by crystal accumulation, and the melanocratic monzonites. Interlayering of clinopyroxenite, hornblendite, hornblende gabbro/diorite and melanocratic monzonite on the scale of the outcrop, mutual inclusions of plastically deformed clinopyroxenite and mela-monzonite xenoliths near the contacts of map units, and the presence of mappable bodies of clinopyroxenite within mela-monzonite (Mehner, 1982; Osatenko, 1979a; not differentiated in Figure 2) indicate that there was more than one period of clinopyroxenite and mela-monzonite crystallization. At least some of the megacrystic monzonite also appears to have formed during the crystallization of mela-monzonite since composite dikes cutting clinopyroxenite in the northern cupola exhibit an early melanocratic monzonite margin and late megacrystic monzonite core (Photo 4). In the southern cupola, however, mela-monzonite intrudes megacrystic monzonite-syenite. The latter contacts are diffuse and evidently formed while the megacrystic monzonite was hot and plastic. Also, potassium feldspar megacrysts are rarely encountered in laminar zones within the mela-monzonite, and dikes of the latter are found cutting megacrystic monzonite in the northern cupola.

The porphyritic and quartz-bearing monzonites, and associated leucocratic dikes, are considered to be the youngest members of the suite. The contact of the clinopyroxenite with the large porphyritic monzonite – quartz monzonite unit in the northern cupola was originally mapped by Mehner (1982) as a foliated "gneissic"

Photo 4. Microcline-megacrystic monzonite-syenite dike containing platy xenoliths of mela-monzonite peeled off the dike margin and angular inclusions of clinopyroxenite, western margin of northern cupola, Whiterocks complex. The dike is cut by a late leuco-syenite vein (left of hammer).

hybrid zone, some 5 to 80 metres in width, incorporating coarse to medium-grained monzonite, monzodiorite, hornblende gabbro/diorite and hornblendite. According to Mehner, this zone originated by the interaction of fluids from a partially liquid porphyritic monzonite with solid pyroxenite. This zone has been re-interpreted herein to represent a transitional contact where these lithologies primarily reflect crystallization from rapidly changing parental melt compositions within the magma chamber. Locally, lithologies which comprise this zone may have experienced remobilization shortly after their deposition. As noted above, the monzonite progressively loses its porphyritic texture and becomes more leucocratic and quartz-bearing to the east, ultimately becoming a leucocratic quartz monzonite near its eastern margin with no obvious intrusive contact between the two lithologies. At the northwestern extremity of this map unit, the nature of the contact between a leucocratic sparsely porphyritic monzonite and the clinopyroxenite and mela-monzonite units to the south is quite different. Here, dikes of the porphyritic monzonite cut sharply through the more mafic units and the margin of the intrusion is locally fine-grained (aplitic). If, indeed, the porphyritic and leucocratic monzonites form a single composite intrusion, as suggested above, the clinopyroxenites and mela-monzonites on the western margin of the northern cupola must be older than equivalent rock types to the east.

MT. SANDBERG PLUTON AND OTHER INTRUSIONS

The Mt. Sandberg pluton is an elongate stock (3.5 x 1.5 km) which lies on the same north-northwesterly oriented trend as the alkaline intrusions (Photo 5). According to Rb-Sr whole-rock isochron systematics, the Mt. Sandberg pluton has an isotopic age of 147 ± 6 Ma (R. L. Armstrong *in* Mehner, 1982). Osatenko (1979a) subdivided the stock into a number of rock types including quartz porphyry, quartz monzonite, diorite and leucocratic quartz diorite (not differentiated in Figure 2).

The main lithology is a quartz- and potassium feldspar-porphyritic biotite monzogranite. Rounded quartz crystals (≤6 mm) and sparse, subhedral potassium feldspars (≤5 mm) are set in an equigranuilar, biotite-bearing (~8 vol. %) quartzofeldspathic groundmass. Locally, the cores of plagioclase crystals are partially altered to clay and sericite, and biotite is weakly chloritized. The rock is cut locally by a stockwork of quartz veins which are known to be associated with trace amounts of molybdenite mineralization (Osatenko, 1979a). Other subordinate rock types include weakly saussuritized, medium-grained, hornblende-bearing biotite quartz monzonite and dikes of sericitized biotite granodiorite and aplite.

East of Mt. Sandberg, a stock at the northern limit of the map area, informally referred to as the northern pluton, is associated with weak garnet-epidote skarn development in carbonate hostrocks with traces of pyrite, and chalcopyrite, and malachite staining. Texturally, the intrusion varies from equigranular and medium-grained biotite-quartz monzonite to a rock with similar mineralogy but carrying pink, euhedral-subhedral potassium feldspar-megacrysts (4 x 1 cm), rounded quartz crystals (≤6 mm), and flakes of biotite (≤3 mm; 10-15 vol. %). The rock appears to lack an internal primary fabric but exhibits a strong flow foliation at its margin where it entrains metasedimentary xenoliths.

A diverse suite of sills and dikes are observed cutting hostrocks of the Harper Ranch Group in the map area and include hornblende-biotite quartz monzonite, biotite-plagioclase porphyries and medium-grained, equigranular clinopyroxene-bearing diorite. The majority of these minor intrusions are probably Jurassic in age,

Photo 5. View of Mt. Sandberg across Tadpole Lake looking northwest from the Dobbin property.

the exception being the diorite which may be older (Upper Paleozoic?). In addition, Mehner (1982) mapped a suite of leucocratic quartz diorite dikes which postdate the alkaline rocks of the Whiterocks complex and, as noted above, yield uppermost Jurassic isotopic ages.

HARPER RANCH GROUP

Country rocks of the Harper Ranch Group in the map area comprise mainly interbedded metamorphosed sedimentary rocks including black to grey-green, calcareous to non-calcareous pelites (slates and phyllites), siliceous siltstones and volcaniclastic wackes, dark grey to brownish cherts and argillaceous to relatively pure carbonate units variably tranformed to marble, especially near intrusive contacts (Figure 2). The regional grade of metamorphism appears to be mid-greenschist facies but may reach upper greenschist to lowermost amphibolite grade in the vicinity of intrusive contacts. At the scale of mapping, one argillaceous limestone – marble unit in the eastern part of the map area can be traced along strike for over 5 kilometres and may be the same unit as that transected by the eastern margin of the northern pluton. In this part of the map area, thinner carbonate horizons are commonly found interbedded with the fine-grained siliciclastic rocks, and one such unit contains abundant transported crinoid ossicles (Photo 6 and Figure 2). Throughout the map area, sedimentary structures are relatively scarce. However, well-developed load-and-flame structures have been observed in a sequence of thinly bedded feldspathic wackes and siltstones near the eastern margin of the northern cupola of the Whiterocks Mountain stock where they indicate that the beds are overturned to the east (Photo 7).

Photo 6. Well-preserved crinoid ossicles in thin carbonate unit, Harper Ranch Group. Fossil locality shown in Figure 2.

Photo 7. Well-developed load-and-flame structures in metasandstone-siltstone beds of the Harper Ranch Group indicating tops to the right (northeast), eastern margin of northern cupola of the Whiterocks complex. (Pencil magnet is 14 cm in length).

STRUCTURE

The principal structural features of the Whiterocks Mountain area are shown in Figure 3 and plotted in stereonets and rose diagrams in Figure 4. The stratigraphy of the Harper Ranch Group strikes north-northwesterly, parallel to the trend of the Whiterocks Mountain – Mt. Sandberg stocks, and dips moderately to steeply westward. A strong penetrative foliation lies parallel or subparallel to bedding planes and is a transposed fabric locally containing dismembered minor fold limbs, rootless fold hinges and local mylonitic shear zones, especially within the more ductile carbonate units. Kinematic indicators, specifically C-S fabrics, indicate eastward tectonic transport (Photo 8). The foliation has been arbitrarily designated S1, although earlier fabrics may well exist. The similar attitude of bedding and foliation, the identification of beds locally overturned to the east, and eastward-directed tectonic transport in some ductile shear zones, are consistent with a northeasterly-directed compressional event involving isoclinal folding on a regional scale prior to pluton emplacement.

In contrast to the attitudes of bedding and foliation, primary igneous laminations in the Whiterocks Mountain

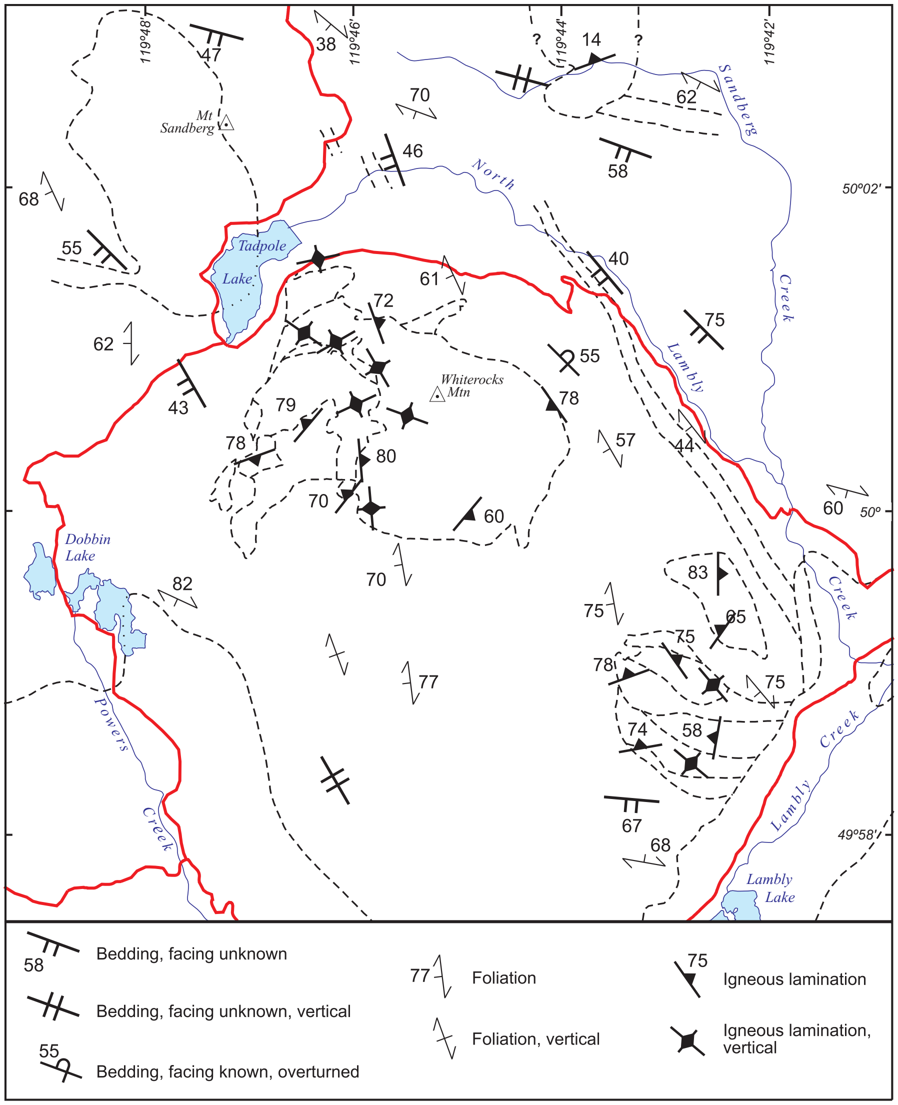

Figure 3. Generalized map of structural features in the Whiterocks Mountain area showing attitude of bedding (S0), the main foliation (S1) and igneous flow laminations within the alkaline complex.

alkaline complex show no such consistency, at least on a regional scale. The lamination, which is predominantly observed in, but not restricted to, the feldspathic rocks, has been formed by the deposition of crystals during viscous flowage and reflects the activity of convection currents in alkaline magma chambers. Locally, it may permit the reconstruction of igneous stratigraphy which would be an asset in the event that controls on sulfide mineralization are magmatic in part (discussed below).

MINERAL CHEMISTRY

A small suite of ultramafic and feldspathic rocks were selected for mineral analysis. Mineral compositions were determined by wavelength-dispersive analysis using a CAMECA SX-50 electron-microprobe at the University of British Columbia. Mineral grains were analyzed at an accelerating voltage of 15 kV and 20 nA beam current with a minimum peak-counting time of 20 s for both major and minor elements. Instrument calibration was performed on documented natural standards and standard ZAF corrections were applied to all analyses. A minimum of two spot analyses per grain were used to determine homogeneity on both a mineral and thin-section scale. Estimates of within-run accuracy and precision were determined by bracketing analyses of unknowns with analyses of international mineral standards (Table A1, Appendix).

Pyroxene

Representative analyses of pyroxenes from clinopyroxenites and hornblendites are presented in Table 1 and plotted in Figures 5 and 6 in accordance with the classification scheme of Morimoto (1989). The ferric iron content was estimated by charge balance according to stoichiometric constraints.

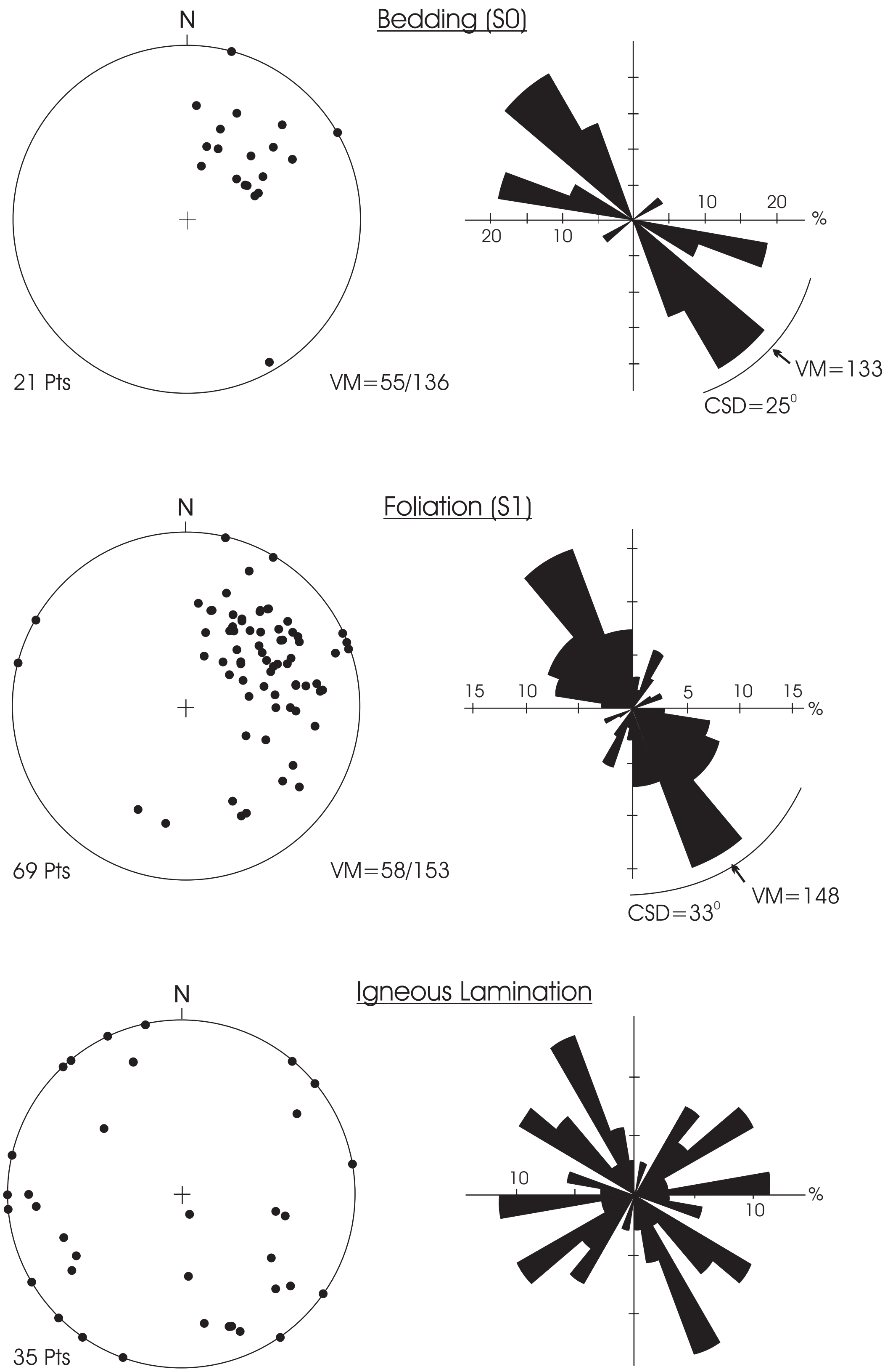

Figure 4. Equal-angle (Wulf) stereonet plots (lower hemisphere, pole to planes) and azimuth-frequency rose diagrams for structural elements in the Whiterocks Mountain area. VM, vector mean orientation; CSD, circular standard deviation. Note the concordance of bedding and foliation in the country rocks, and the lack of any preferred regional orientation for flow fabrics within the Whiterocks complex.

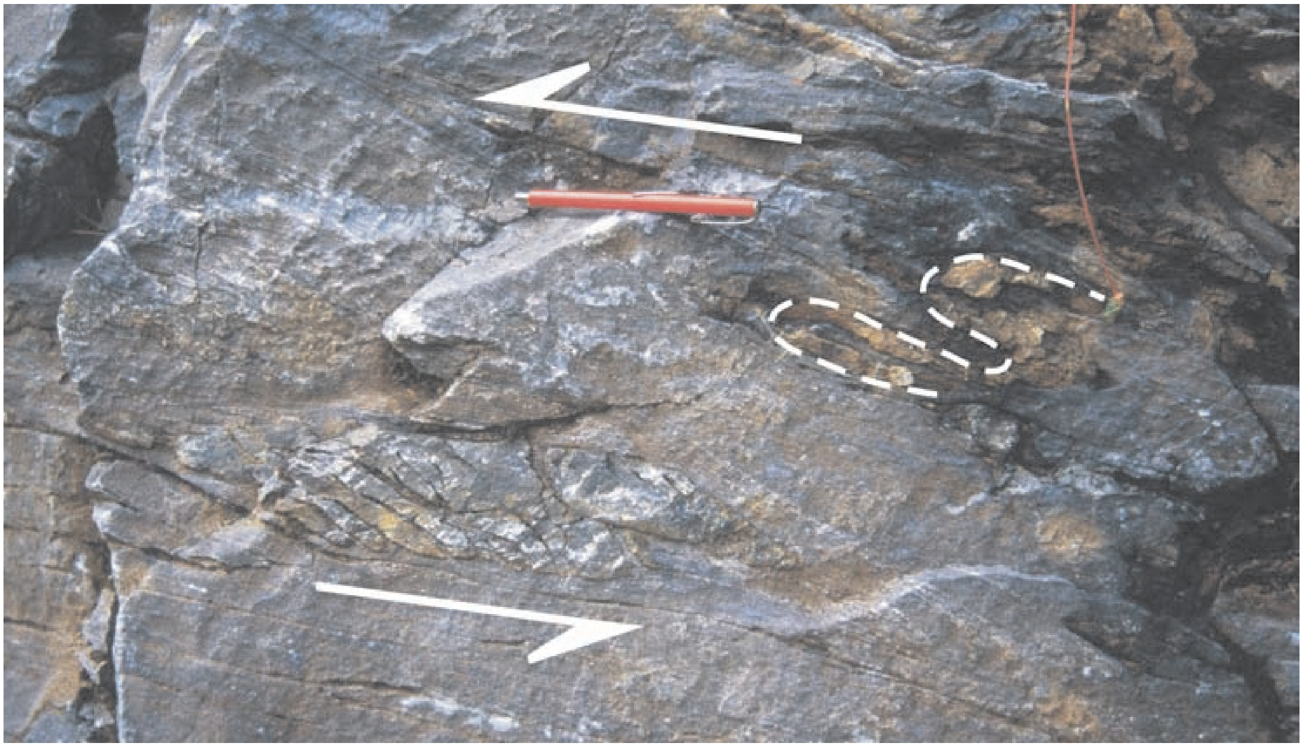

Photo 8. Rootless minor fold hinges (right of 14 cm pencil magnet) and C-S fabrics (left and lower left of magnet) in thin carbonate unit, Harper Ranch Group (unit lies structurally beneath 5 km-long carbonate layer shown in Figure 2 beyond the eastern margin of the Whiterocks complex). Both features indicate tops to the left (northeast).

All analyzed pyroxenes are high-calcium clinopyroxenes with CaO contents of 22 to 25 wt. % and Mg-numbers (100Mg/(Mg+Fe^{2+}+Fe^{3+}))ranging from 57 to 77. Molecular percentages of end-members (WEF) range Wo_{48-50} En_{28-40} Fs_{10-24}. As shown in Figures 5 and 6, the pyroxenes are diopsidic and plot well within the Ca-Mg-Fe quadrilateral (Quad or Q) field on the Q-J(=2Na) and WEF-Jd(jadeite)-Ae(aegirine) diagrams. The latter diagram reveals that some pyroxenes contain small amounts of the aegirine end-member but all have low Na (0.16-1.0 wt. % Na_2O). The highest Mg-numbers (~76) are found in biotite-hornblende clinopyroxenite and the lowest occur in an altered hornblende clinopyroxenite which hosts Cu-PGE sulfides and was recovered from drill core at the main Dobbin copper anomaly (DDH97-21). Significant zoning on the scale of the thin section is apparent in some samples (*e.g.* 6-4-1) though intra-grain core to rim zoning appears weak.

Amphibole

The results of the amphibole analyses in a wide range of rock types are presented in Table 2 and plotted in Figure 7. The distribution of ferrous and ferric iron has been determined using the method of Robinson *et al.* (1981) for calcic amphiboles.

According to the classification scheme of Leake *et al.* (1997), the majority of the amphiboles are either pargasite to ferropargasite ($^{VI}Al>Fe^{3+}$) in composition (Figure 7A); or magnesiohastingsite and hastingsite ($^{VI}Al<Fe^{3+}$) in composition (Figure 7B), depending on the accuracy of the Fe^{3+} recalculation. Using X-ray diffraction methods, Mehner (1982) determined that the am-

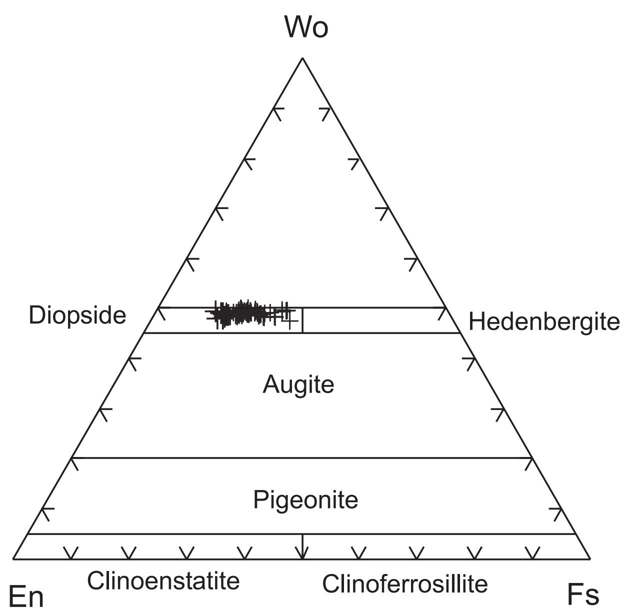

Figure 5. Wo-En-Fs (Ca-Mg-Fe) plot (mol. %) of pyroxene compositions in clinopyroxenites and hornblendites from the Whiterocks complex showing the classification scheme of Morimoto (1989). All pyroxenes fall within the diopside field.

TABLE 1
REPRESENTATIVE ELECTRON-MICROPROBE ANALYSES OF PYROXENE

Rock Type	Bi-Hb cpxite		Fs Cpx hbite		Fs Cpx hbite*		Bi-Hb cpxite		Bi cpxite	
Sample	13-5-3	13-5-3	16-2-2	16-2-2	DDH97-21-57-1		6-4-1	6-4-1	6-5-1	6-5-1
SiO_2	50.54	50.61	49.38	50.85	50.39	52.28	52.64	48.15	49.72	49.41
TiO_2	0.41	0.51	0.58	0.39	0.12	0.01	0.02	0.63	0.54	0.51
Al_2O_3	2.73	3.05	4.55	3.26	1.93	0.43	0.89	5.53	3.87	3.91
FeO	7.46	7.70	9.46	8.08	12.76	11.38	7.58	10.08	8.72	8.84
Cr_2O_3	0.02	0.00	0.03	0.01	0.00	0.06	0.03	0.00	0.00	0.00
MnO	0.25	0.17	0.34	0.38	0.44	0.57	0.29	0.37	0.32	0.38
MgO	13.84	13.55	11.40	12.76	9.64	11.07	13.60	11.38	12.57	12.55
CaO	23.34	23.68	23.18	23.42	23.57	23.66	24.50	23.31	23.77	23.95
Na_2O	0.34	0.35	0.89	0.84	0.59	0.56	0.53	0.59	0.50	0.44
Total	98.93	99.63	99.81	99.98	99.43	100.02	100.08	100.02	100.01	99.98
TSi	1.89	1.88	1.85	1.89	1.93	1.98	1.95	1.80	1.85	1.84
TAl	0.11	0.12	0.15	0.11	0.07	0.02	0.04	0.20	0.15	0.16
TFe^{3+}	0.00	0.00	0.00	0.00	0.00	0.00	0.01	0.00	0.00	0.00
M1Al	0.01	0.02	0.05	0.03	0.02	0.00	0.00	0.04	0.02	0.01
M1Ti	0.01	0.01	0.02	0.01	0.00	0.00	0.00	0.02	0.02	0.01
$M1Fe^{3+}$	0.10	0.09	0.14	0.12	0.09	0.06	0.08	0.16	0.13	0.15
$M1Fe^{2+}$	0.11	0.12	0.16	0.13	0.32	0.29	0.14	0.14	0.13	0.13
M1Cr	0.00	0.00	0.00	0.00	0.00	0.00	0.00	0.00	0.00	0.00
M1Mg	0.77	0.75	0.64	0.71	0.55	0.62	0.75	0.63	0.70	0.70
M2Mg	0.00	0.00	0.00	0.00	0.00	0.00	0.00	0.00	0.00	0.00
$M2Fe^{2+}$	0.03	0.03	0.00	0.00	0.00	0.00	0.00	0.01	0.01	0.00
M2Mn	0.01	0.01	0.01	0.01	0.01	0.02	0.01	0.01	0.01	0.01
M2Ca	0.94	0.95	0.93	0.93	0.97	0.96	0.97	0.93	0.95	0.96
M2Na	0.03	0.03	0.07	0.06	0.04	0.04	0.04	0.04	0.04	0.03
Total Cations	4.00	4.00	4.00	4.00	4.00	4.00	4.00	4.00	4.00	4.00
Mg #	76.8	75.8	68.2	73.8	57.4	63.4	76.1	66.7	72.0	71.6
Q**	1.85	1.84	1.72	1.77	1.83	1.88	1.87	1.72	1.79	1.78
J***	0.05	0.05	0.13	0.12	0.09	0.08	0.08	0.09	0.07	0.06
WO	48.01	48.65	49.63	49.02	49.84	48.88	49.42	49.28	49.20	49.26
EN	39.61	38.74	33.98	37.16	28.36	31.84	38.17	33.48	36.20	35.92
FS	12.37	12.62	16.39	13.82	21.80	19.28	12.41	17.24	14.61	14.81

Sample prefix: 00GNX. Oxides in weight percent. Number of cations calculated on the basis of 6 oxygens.
Mg# = 100Mg/(Mg+Fe2++Fe3+) Ferric iron content estimated by charge balance according to stoichiometric constraints.
* relict Cpx in sheared Bi-Act hbite. **Q = Ca+Mg+Fe^{2+} ***J = 2Na
Abbreviations: Bi, biotite; Hb, hornblende; Cpx, calcic clinopyroxene; Fs, feldspathic; Act, actinolite; cpxite, clinopyroxenite; hbite, hornblendite.

phiboles in most rocks are "ferrohastingsite". One sample, a leuco-quartz monzonite dike (16-4-1) near the summit of Whiterocks Mountain contains amphiboles zoned to edenite compositions. In general, Mg-numbers decrease from clinopyroxenites (62) through hornblendites (42) to the mela-monzonites (23-31) consistent with trends expected of rocks related by fractional crystallization. Rim and core analyses on most grains show no significant compositional zonation.

Mica

Analytical results for Fe-Mg micas in several clinopyroxenites and a biotitite pegmatitic vein are given in Table 3 and plotted in Figure 8. Mica analyses were recalculated on an anhydrous basis assuming that all iron is present as ferrous iron.

Mica compositions show a limited range of variation in Mg/(Mg+Fe) (0.75-0.50) across the boundary which formerly separated the biotite-phlogopite fields (Figure 8). The most magnesian biotites (6-5-1) exhibit a large variation in tetrahedral aluminum towards an "eastonitic" component (Figure 8). It is noteworthy that mica analyses from the biotite pegmatites have similar compositions to cumulus and intercumulus biotites occurring in host clinopyroxenites (Table 3). This indicates that the biotitite veins are igneous in origin and not hydrothermal as previously proposed by Mehner (1982). Analyses at the cores and rims of mica grainss failed to show any significant zoning.

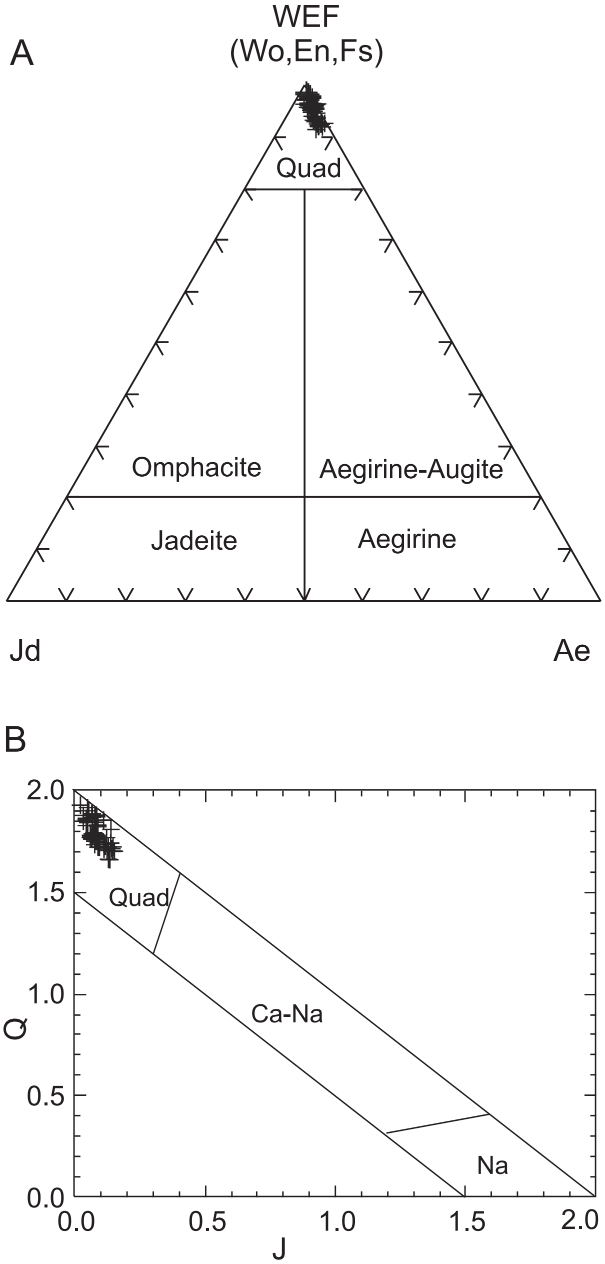

Figure 6. Classification of components other than quadrilateral constituents ("Others") in clinopyroxenes of the Whiterocks complex (after Morimoto, 1989). A, WEF-Jd-Ae and B, Q (Ca+Mg+Fe^{2+}) – J (2Na) plots (atoms per formula unit) showing the incorporation of small amounts of the aegirine end-member.

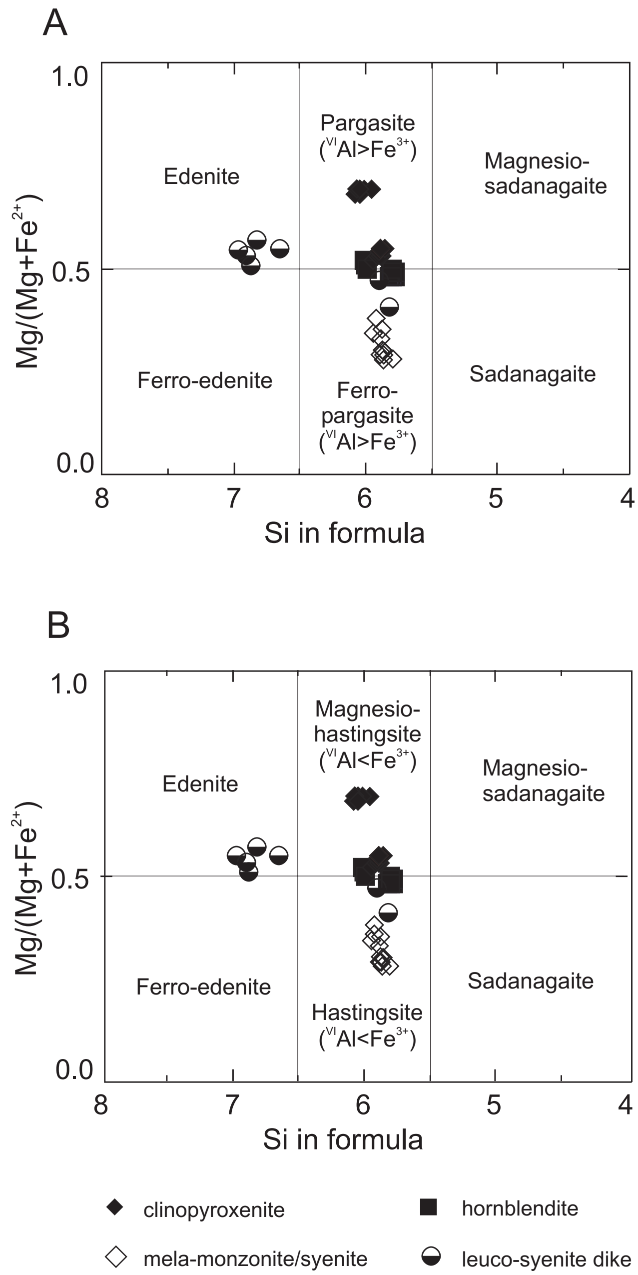

Figure 7. Classification of calcic amphiboles with CaB>1.50, (Na+K)A>0.50, and Ti<0.50 (atoms per formula unit) in selected rocks from the Whiterocks complex showing the effect of uncertainty in the amount of ferric iron (calculated after Robinson *et al.*, 1981) on the nomenclature. A, octahedral alumina is greater than ferric iron; B, octahedral alumina is less than ferric iron. Note the zoning towards edenitic compositions in the leuco-syenite dike.

Garnet

The first occurrence of garnet in the Whiterocks complex was noted by J. F. Harris in a petrographic report prepared for Verdstone/Molycor (Kikauka, 1997). The garnet was found in a leucocratic syenite vein cutting clinopyroxenite in drill core DDH97-2 (23.5 m) which was recovered from the main Dobbin copper anomaly. This sample was obtained for analysis and the results are given in Table 4. The partitioning of ferrous and ferric

TABLE 2
REPRESENTATIVE ELECTRON-MICROPROBE ANALYSES OF AMPHIBOLE

Rock Type	Bi-Hb cpxite		mKf(Gt)-Hb mmz/sy		Cpx hbite	Fspo lqmz dyke		Bi-Hb cpxite	
Sample	13-5-3	13-5-3	13-9-2	13-9-2	16-2-2	16-4-1	16-4-1	6-4-1	6-4-1
SiO_2	40.25	40.63	37.81	36.65	37.45	37.08	45.83	38.76	38.62
TiO_2	1.76	1.78	2.03	1.53	1.98	2.10	0.26	1.99	2.06
Al_2O_3	13.33	13.20	13.66	13.60	13.99	13.41	6.65	12.89	13.58
FeO	13.61	13.58	23.20	25.59	19.87	20.96	18.52	18.40	17.90
Cr_2O_3	0.01	0.06	0.00	0.00	0.02	0.05	0.00	0.00	0.03
MnO	0.13	0.15	0.70	0.89	0.51	1.53	2.48	0.40	0.32
MgO	12.38	12.42	5.76	4.38	8.17	6.55	9.89	9.38	9.79
CaO	12.28	12.17	11.22	10.96	11.40	11.29	11.24	11.48	11.66
Na_2O	1.86	1.90	1.36	1.56	1.88	1.52	1.06	2.18	2.11
K_2O	1.56	1.50	2.36	2.34	2.53	2.22	1.01	2.16	2.21
F	0.23	0.27	0.07	0.15	0.22	0.62	0.59	0.12	0.23
Cl	0.08	0.11	0.21	0.12	0.08	0.15	0.04	0.09	0.13
Total	97.47	97.71	98.38	97.77	98.09	97.43	97.57	97.85	98.60
TSi	6.01	6.05	5.88	5.80	5.77	5.82	6.96	5.94	5.86
TAl	1.99	1.96	2.12	2.20	2.23	2.18	1.05	2.06	2.14
CAl	0.35	0.36	0.38	0.34	0.31	0.30	0.14	0.27	0.28
CCr	0.00	0.01	0.00	0.00	0.00	0.01	0.00	0.00	0.00
*CFe^{3+}	0.45	0.42	0.53	0.69	0.52	0.57	0.52	0.38	0.45
CTi	0.20	0.20	0.24	0.18	0.23	0.25	0.03	0.23	0.24
CMg	2.75	2.75	1.34	1.03	1.88	1.53	2.24	2.14	2.21
CFe^{2+}	1.24	1.25	2.47	2.70	2.03	2.18	1.83	1.95	1.79
CMn	0.01	0.01	0.05	0.06	0.03	0.16	0.24	0.03	0.02
CCl	0.02	0.03	0.05	0.03	0.02	0.04	0.01	0.02	0.03
CF	0.11	0.13	0.03	0.07	0.11	0.31	0.29	0.06	0.11
BFe^{2+}	0.01	0.02	0.02	0.01	0.02	0.00	0.00	0.03	0.03
BMn	0.01	0.01	0.05	0.06	0.03	0.05	0.08	0.03	0.02
BCa	1.96	1.94	1.87	1.86	1.88	1.90	1.83	1.89	1.90
BNa	0.02	0.03	0.07	0.08	0.06	0.05	0.09	0.06	0.06
ANa	0.52	0.52	0.34	0.40	0.50	0.41	0.22	0.59	0.56
AK	0.30	0.29	0.47	0.47	0.50	0.45	0.20	0.42	0.43
Total Cations	15.82	15.80	15.81	15.88	16.00	15.86	15.42	16.01	15.99
Mg #	61.9	62.0	30.7	23.4	42.3	35.8	48.8	47.6	49.4

Sample prefix: 00GNX. Oxides in weight percent. Number of cations based on 23 oxygens. $Mg\# = 100Mg/(Mg+Fe^{2+}+Fe^{3+})$

*Ferric iron recalculated on an anhydrous basis by method of Robinson (1981).

Abbreviations: Bi, biotite; Hb, hornblende; Cpx, calcic clinopyroxene; Fs, feldspar; Gt, garnet; mKf, megacrystic (>2.5 cm) potassium feldspar; m, melanocratic; l, leucocratic; cpxite, clinopyroxenite; mz, monzonite; qmz, quartz monzonite; sy, syenite; po, porphyritic.

iron in garnet was handled by the empirical formulation of Knowles (1987).

The analyzed garnets are pinkish brown, subhedral to euhedral crystals with broad birefringent rims which possess fine-scale oscillatory zoning. Compositions are andradite and andradite-grossular solid solutions, with 65-81 mol. % andradite, 15-32 mol. % grossular and <3 mol. % each of almandine, spessartine, and pyrope components (Table 4). Of note are the TiO_2 contents of these garnets which range from 0.43-1.8 wt. % and thus become melanitic (TiO_2 >1 wt. %). The high-Ti compositions are predominantly core analyses and appear to correlate with elevated abundances of MnO (>1 wt. %). Except for their birefringent, oscillatory-zoned mantles, which may be related to late carbonate-epidote alteration in this sample, these crystals appear optically similar to igneous garnets encountered elsewhere in the suite.

Feldspar

Several monzonitic samples from the suite were analyzed for plagioclase and potassium feldspar. The results are given in Table 5 and plotted in Figure 9. Most of the feldspars analyzed have cumulus and intercumulus textures, and large cumulus grains generally show oscillatory zoning. Such zoning in these crystals, however, appears to be weak since core to rim microprobe traverses did not detect appreciable compositional variation.

The alkali feldspar compositions are all microcline, and the majority of plagioclase compositions range from sodic oligoclase to sodic andesine, with minor albite.

TABLE 3
REPRESENTATIVE ELECTRON-MICROPROBE ANALYSES OF MICA

Rock Type	Biotitite vein in Bi-Hb cpxite		Bi-Hb cpxite		Biotitite vein in Bi-Hb cpxite		Bi cpxite	
Sample	13-5-3	13-5-3	6-4-1	6-4-1	6-4-2	6-4-2	6-5-1	6-5-1
SiO_2	36.06	36.21	35.91	35.94	35.74	36.16	36.86	34.89
TiO_2	2.11	1.81	1.54	0.00	2.07	1.89	2.27	3.95
Al_2O_3	15.55	14.87	14.94	15.70	14.71	14.93	16.15	17.09
FeO	10.92	14.18	19.30	22.09	16.28	15.23	10.94	13.18
Cr_2O_3	0.00	0.04	0.01	0.00	0.10	0.10	0.00	0.02
MnO	0.19	0.11	0.32	0.00	0.25	0.20	0.22	0.38
MgO	18.44	16.82	12.46	12.27	14.25	14.94	17.70	16.81
CaO	0.14	0.06	0.03	0.02	0.03	0.00	0.00	0.04
Na_2O	0.25	0.26	0.16	0.12	0.16	0.20	0.20	0.21
K_2O	9.38	9.55	9.77	10.05	9.90	9.86	9.70	9.30
F	0.50	0.43	0.12	0.00	0.38	0.23	0.25	0.34
Cl	0.05	0.07	0.03	0.00	0.01	0.02	0.02	0.04
Total	93.59	94.41	94.58	96.20	93.88	93.77	94.31	96.24
Si	5.44	5.50	5.57	5.53	5.53	5.55	5.49	5.17
Al^{IV}	2.57	2.50	2.44	2.47	2.47	2.45	2.51	2.83
Al^{VI}	0.20	0.16	0.29	0.38	0.21	0.25	0.32	0.15
Ti	0.24	0.21	0.18	0.00	0.24	0.22	0.25	0.44
$*Fe^{2+}$	1.38	1.80	2.50	2.84	2.11	1.95	1.36	1.63
Cr	0.00	0.01	0.00	0.00	0.01	0.01	0.00	0.00
Mn	0.02	0.01	0.04	0.00	0.03	0.03	0.03	0.05
Mg	4.14	3.81	2.88	2.81	3.28	3.42	3.93	3.71
Ba	0.00	0.00	0.00	0.00	0.00	0.00	0.00	0.00
Ca	0.02	0.01	0.01	0.00	0.01	0.00	0.00	0.01
Na	0.07	0.08	0.05	0.04	0.05	0.06	0.06	0.06
K	1.80	1.85	1.93	1.97	1.95	1.93	1.84	1.76
Cations	15.88	15.92	15.88	16.05	15.89	15.87	15.79	15.81
CF	0.47	0.41	0.12	0.00	0.38	0.23	0.23	0.32
CCl	0.03	0.04	0.02	0.00	0.01	0.01	0.01	0.02
Fe^{2+}/Mg	0.33	0.47	0.87	1.01	0.64	0.57	0.35	0.44
Mg #	0.75	0.68	0.54	0.50	0.61	0.64	0.74	0.69
X	1.90	1.94	1.99	2.01	2.01	1.99	1.90	1.82
Y	5.72	5.76	5.67	6.03	5.59	5.62	5.61	5.49
Z	8.00	8.00	8.00	8.00	8.00	8.00	8.00	8.00

Sample prefix: 00GNX. Oxides in weight percent. Number of cations based on 22 oxygens.
X = K+Na+Ca, Y = $Mg+Fe^{2+}+Al^{VI}$, Z = $Si+Al^{IV}$ Mg # = $Mg/(Mg+Fe^{2+})$
Abbreviations: Hb, hornblende; Bi, biotite; cpxite, clinopyroxenite.

There is a range of coexisting feldspar compositions for each rock type. In the leuco-quartz monzonite (10-4-1), potassium feldspar compositions of Or_{87}-Or_{96} coexist with plagioclase of Ab_{78}-Ab_{96}. A porphyritic garnet-bearing mela-monzonite (13-9-2) has potassium feldspar compositions of Or_{82}-Or_{95} coexisting with plagioclase of Ab_{61}-Ab_{81}; and a leuco-monzonite dike (16-4-1) contains potassium feldspar compositions of Or_{91}-Or_{97} and coexisting plagioclase of Ab_{70}-Ab_{96}.

Summary of Electron-Microprobe Results

The electron-microprobe analyses permit for a quantitative characterization of the mineralogy of the Whiterocks complex. All pyroxenes are high-Ca clinopyroxenes of diopsidic composition as opposed to aegirine augite (Mehner, 1982). Amphibole compositions are pargasite to ferro-pargasite, or magnesio-hastingsite to hastingsite depending on the accuracy of the ferric iron recalculation. Ferromagnesian micas straddle the boundary which formerly defined phlogopite-biotite compositions; the compositions of pegmatitic mica in biotitite veins in clinopyroxenite, together with inclusions of euhedral apatite and relict clinopyroxene, indicate that the biotitites are magmatic as opposed to hydrothermal in origin and unrelated to the mineralization. Megacrysts of alkali feldspar in monzonitic rocks are low-temperature microclines. The textural relationships and melanitic composition of garnet in monzonitic rocks of the complex confirm an igneous origin for the garnet.

TABLE 4
REPRESENTATIVE ELECTRON-MICROPROBE ANALYSES OF GARNET

Rock Type			Syenite vein in Hb cpxite			
Sample			DDH97-2 (23.5 m)			
SiO_2	35.25	35.49	35.54	35.91	35.53	35.50
TiO_2	1.04	0.82	0.93	0.43	0.67	0.64
Al_2O_3	4.92	5.67	7.78	8.21	7.72	7.90
FeO	22.13	22.25	19.75	20.42	20.50	20.36
Cr_2O_3	0.06	0.05	0.02	0.00	0.00	0.00
MnO	1.23	1.30	0.26	0.32	0.23	0.24
MgO	0.07	0.09	0.03	0.04	0.02	0.04
CaO	32.84	32.63	34.14	33.94	33.93	33.54
Na_2O	0.00	0.02	0.00	0.03	0.01	0.00
Total	97.54	98.33	98.46	99.29	98.61	98.23
*FeO(calc)	1.11	1.11	0.99	1.02	1.03	1.02
*Fe_2O_3(calc)	23.36	23.49	20.85	21.55	21.64	21.49
Total(calc)	99.82	100.62	100.52	101.44	100.77	100.38
TSi	2.92	2.91	2.88	2.88	2.88	2.88
TAl	0.08	0.09	0.12	0.12	0.13	0.12
Al^{VI}	0.40	0.46	0.62	0.66	0.61	0.64
Fe^{3+}	1.45	1.45	1.27	1.30	1.32	1.31
Ti	0.07	0.05	0.06	0.03	0.04	0.04
Cr	0.00	0.00	0.00	0.00	0.00	0.00
Fe^{2+}	0.08	0.08	0.07	0.07	0.07	0.07
Mg	0.01	0.01	0.00	0.00	0.00	0.01
Mn	0.09	0.09	0.02	0.02	0.02	0.02
Ca	2.91	2.86	2.96	2.92	2.94	2.92
Na	0.00	0.00	0.00	0.01	0.00	0.00
Total Cations	8.00	8.00	8.00	8.00	8.00	8.00
Alm	2.48	2.50	2.19	2.27	2.29	2.30
And	75.79	74.00	65.15	65.54	66.88	65.92
Gross	18.43	19.88	31.87	31.18	30.18	31.07
Pyrope	0.28	0.36	0.12	0.14	0.09	0.16
Spess	2.80	2.97	0.58	0.71	0.51	0.56
Uvaro	0.20	0.18	0.08	0.00	0.00	0.00
XCa	0.64	0.64	0.69	0.68	0.68	0.68
XFe	0.34	0.34	0.31	0.32	0.32	0.32
XMg	0.00	0.00	0.00	0.00	0.00	0.00

Sample prefix: 00GNX. Oxides in weight percent. Number of cations based on 12 oxygens.
*Ferrous and ferric iron recalculated after Knowles (1987).
$XCa=Ca/(Ca+Mg+Fe^{2+}+Fe^{3+}+Mn)$; $XFe=(Fe^{2+}+Fe^{3+})/(Ca+Mg+Fe^{2+}+Fe^{3+}+Mn)$;
$XMg=Mg/(Ca+Mg+Fe^{2+}+Fe^{3+}+Mn)$

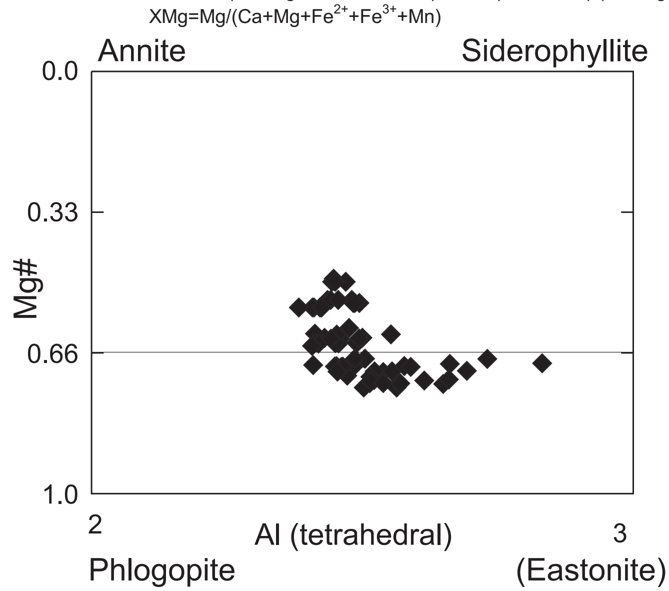

Figure 8. Mg# [Mg/(Mg+Fe)] versus tetrahedral Al plot (atoms per formula unit) for Fe-Mg mica compositions in clinopyroxenites of the Whiterocks complex. The horizontal line represents the former division (obsolete) between the compositional fields of phlogopite and biotite.

TABLE 5
REPRESENTATIVE ELECTRON-MICROPROBE ANALYSES OF FELDSPAR

Rock Type	Kfpo (Hb) lqmz		mKf(Gt)-Hb mmz/sy				Fspo lmz	
Sample	10-4-1	10-4-1	13-9-2	13-9-2	13-9-2	13-9-2	16-4-1	16-4-1
Mineral	Kf	Pl	Pl	Pl	Kf	Kf	Kf	Pl
SiO_2	65.02	63.65	59.02	64.43	64.61	64.36	65.33	64.32
Al_2O_3	18.39	23.11	26.30	22.88	18.59	19.25	18.38	22.63
FeO	0.04	0.14	0.01	0.05	0.01	0.12	0.10	0.39
MgO	0.00	0.00	0.00	0.00	0.00	0.00	0.00	0.00
CaO	0.00	4.07	7.96	3.86	0.02	0.49	0.01	3.52
Na_2O	0.62	9.17	6.84	9.43	0.60	1.71	1.00	9.32
K_2O	16.29	0.13	0.08	0.13	16.22	13.84	15.62	0.23
Total	100.37	100.27	100.22	100.79	100.05	99.78	100.43	100.42
Si	11.99	11.22	10.51	11.28	11.95	11.85	12.00	11.31
Al	3.99	4.80	5.51	4.72	4.05	4.17	3.98	4.69
Fe	0.01	0.02	0.00	0.01	0.00	0.02	0.02	0.06
Mg	0.00	0.00	0.00	0.00	0.00	0.00	0.00	0.00
Ca	0.00	0.77	1.52	0.72	0.00	0.10	0.00	0.66
Na	0.22	3.13	2.36	3.20	0.22	0.61	0.36	3.18
K	3.83	0.03	0.02	0.03	3.83	3.25	3.66	0.05
Total Cations	20.04	19.96	19.92	19.97	20.04	19.99	20.01	19.95
Ab	5.50	79.70	60.60	81.00	5.30	15.40	8.80	81.60
An	0.00	19.60	38.90	18.30	0.10	2.50	0.00	17.10
Or	94.50	0.80	0.50	0.80	94.60	82.10	91.10	1.30

Sample prefix: 00GNX. Oxides in weight percent. Number of cations based on 32 oxygens.
Abbreviations: Hb, hornblende; Gt, garnet; Fs, feldspar; Pl, plagioclase; mKf, megacrystic (>2.5 cm) potassium feldspar; Kfpo, porphyritic (<2.5 cm) potassium feldspar; m, melanocratic; l, leucocratic mz, monzonite; qmz, quartz monzonite; sy, syenite; po, porphyritic.

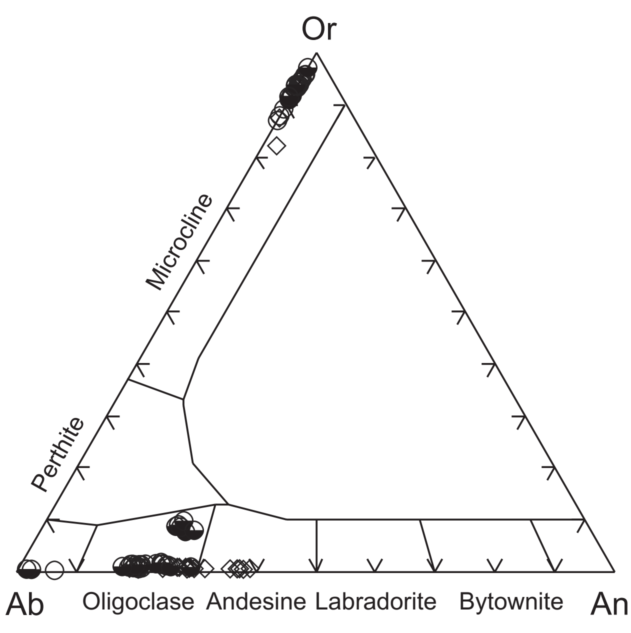

Figure 9. Or-Ab-An plot (mol. %) of potassium feldspar and plagioclase compositions in selected feldspathic lithologies of the Whiterocks complex. Open circles are leuco-quartz monzonite 10-4-1 (Table 5); other symbols as in Figure 7.

WHOLE-ROCK GEOCHEMISTRY

A suite of 58 rock samples representing a broad range of rock types from the Whiterocks Mountain alkaline complex, the Mt Sandberg pluton, and associated minor intrusions were analyzed for major elements by X-ray fluorescence at the Cominco Research Laboratory, Vancouver. Rocks were crushed in a hardened-steel jaw crusher and selected chips were reduced to <150 mesh powder in a tungsten carbide swingmill. A quartz sand wash was done between samples to prevent cross-contamination. Rock powders were dissolved in a lithium tetraborate fusion mixture using standard calibration and data reduction procedures. Accuracy and precision were monitored by international standards included in the run. The analytical results are listed according to map unit in Table 6 which also provides a summary of pertinent petrographic features for the analyzed rocks. The classification of rock types given in Table 6 were derived from visual estimates of mineral abundances using the modal classification scheme of Le Maitre *et al.* (1989). The CIPW-normative compositions of the analyzed rocks are plotted in Figure 10 and sample locations are shown in Figure 11.

Feldspathic Rocks

The QAP ternary diagram in Figure 10 provides a more quantitative and systematic basis for classifying and comparing the various petrographic groupings. Since

TABLE 6
WHOLE-ROCK MAJOR ELEMENT ANALYSES OF THE WHITEROCKS MOUNTAIN ALKALINE COMPLEX AND OTHER IGNEOUS ROCKS

ID	Sample	Rock Type	NAD 1983 Easting	NAD 1983 Northing	SiO_2	TiO_2	Al_2O_3	Fe_2O_3t	MnO	MgO	CaO	Na_2O	K_2O	P_2O_5	LOI	Total
Whiterocks Mountain Alkaline Complex																
Clinopyroxenite																
34	00GNX-1-1-1	Bi-Hb cpxite (Ap≤0.4)	301595	5542706	42.00	1.04	7.50	16.51	0.28	10.73	17.62	0.73	1.17	0.94	0.93	99.45
16	00GNX-16-1-1	fBi-Hb cpxite (Ap≤0.3)	301897	5543695	40.29	1.25	9.81	17.90	0.30	9.14	16.82	0.77	1.44	0.92	0.60	99.24
56	00GNX-13-8-1	Hb-Bi cpxite (Ap≤0.4)	305006	5539428	40.04	1.41	6.00	19.71	0.27	11.10	17.34	0.44	1.41	1.24	0.40	99.36
22	00GNX-16-2-8	Bi-Hb cpxite (Ap≤0.6)	301945	5543412	39.40	1.17	6.07	20.87	0.33	9.98	17.47	0.47	1.50	1.61	0.33	99.20
58	00GNX-13-5-1	Bi-Hb cpxite (Ap≤0.5)	305525	5539076	39.17	1.38	6.96	20.80	0.33	9.74	16.31	0.82	1.64	1.51	0.61	99.27
33	00GNX-21-1050	fHb cpxite (Ap≤1.2)	300762	5542803	38.31	1.42	6.96	21.80	0.31	8.21	19.26	0.47	0.55	1.69	0.49	99.47
29	00GNX-1-5-1	fHb cpxite (Ap≤1.3)	301968	5542895	37.58	1.75	9.71	22.76	0.55	7.26	15.25	1.49	1.29	1.39	0.82	99.85
21	00GNX-6-4-1	Bi-Hb cpxite (Ap≤0.7)	301252	5543441	37.33	1.30	6.32	23.86	0.31	9.60	15.72	0.66	1.67	1.70	0.60	99.07
18	00GNX-6-5-1	Bi cpxite (Ap≤0.7)	301284	5543472	37.00	1.47	5.26	24.71	0.28	10.55	17.51	0.41	0.93	1.20	0.15	99.47
Hornblendite																
23	00GNX-16-2-5	Cpx hbite (Ap≤0.8)	301945	5543412	39.79	1.13	7.17	20.40	0.41	8.52	18.20	0.93	0.85	1.53	0.31	99.24
24	00GNX-16-2-1	fCpx hbite (Ap≤0.8)	301945	5543412	36.74	1.57	9.34	25.21	0.47	7.13	14.78	1.11	1.14	0.87	0.82	99.18
Melanocratic Monzonite-Syenite																
44	00GNX-12-3-1	Hb mz	306325	5540518	56.86	0.68	17.95	6.44	0.17	1.91	6.55	4.07	3.58	0.27	0.75	99.23
52	00GNX-13-9-2	mKf (Gt)-Hb mmz/sy	304861	5539524	56.77	0.34	20.03	4.61	0.12	0.87	5.82	4.80	4.40	0.15	0.85	98.76
14	00GNX-7-15-2	(Cpx)-Hb mz	301440	5544241	56.15	0.61	14.84	7.82	0.14	3.16	6.53	3.01	5.80	0.38	0.54	98.98
53	00GNX-13-9-3	(Cpx)-(Gt)-Hb mz	304861	5539524	55.31	0.40	20.62	5.34	0.15	0.92	7.53	5.26	2.75	0.18	1.01	99.47
27	00GNX-6-1-1	Gt-Hb-Cpx mmz	301149	5543349	53.56	0.60	16.90	8.15	0.18	2.45	6.98	3.65	5.71	0.43	0.68	99.29
57	00GNX-13-3-1	(Cpx)-Bi-Gt-Hb mmz	305515	5539246	53.13	0.56	17.04	8.09	0.18	2.51	6.55	4.05	5.67	0.44	1.25	99.47
13	00GNX-7-5-1	Hb-Cpx mmz	301865	5544269	52.00	0.75	16.25	9.96	0.18	3.23	8.25	3.42	4.28	0.50	0.41	99.23
54	00GNX-13-9-1	mKf (Gt)-Hb mmz/sy	304863	5539522	49.90	0.88	16.85	11.01	0.34	2.31	8.61	3.49	3.99	0.37	1.35	99.10
45	00GNX-11-17-1	Cpx-Hb mmz	305416	5540484	48.25	0.76	15.72	11.81	0.27	3.54	10.43	2.98	3.27	0.70	1.30	99.03
Kf-Megacrystic Monzonite/Syenite																
47	00GNX-11-15-2	mKf Bi mz/sy	304813	5540468	60.62	0.22	19.66	2.64	0.10	0.44	2.08	5.26	7.37	0.07	1.15	99.61
48	00GNX-11-15-6	mKf Bi mz/sy	304813	5540468	58.36	0.27	19.23	3.97	0.10	0.82	3.25	4.61	7.03	0.15	1.63	99.42
49	00GNX-11-15-1	mKf Bi mz/sy	304813	5540468	57.45	0.42	18.97	5.40	0.19	0.86	3.14	4.56	7.13	0.18	1.23	99.53
32	00GNX-17-3-1	mKf Cpx-Hb mmz	300661	5542831	51.09	0.93	17.19	10.56	0.20	2.55	9.64	3.34	3.29	0.56	0.44	99.79
30	00GNX-17-2-1	mKf Cpx-Hb mmz	300661	5542870	49.45	0.82	17.87	10.43	0.20	2.93	10.25	2.71	3.44	0.50	0.75	99.35
Kf-Porphyritic Monzonite/Quartz Monzonite																
41	00GNX-10-3-1	Kfpo Hb lqmz	303472	5542038	68.70	0.14	16.63	1.49	0.05	0.17	1.74	4.92	4.75	0.01	0.62	99.22
28	00GNX-10-4-1	Kfpo (Hb) lqmz	303774	5543018	67.44	0.15	17.45	1.50	0.05	0.18	2.23	5.00	5.07	0.02	0.37	99.46
25	00GNX-10-5-2	Hb lmz/qmz	304024	5543374	64.51	0.25	17.77	2.65	0.08	0.42	3.06	4.96	5.01	0.06	0.69	99.46
12	00GNX-7-4-1	Kfpo Hb lmz	301917	5544337	62.00	0.31	18.88	3.00	0.10	0.46	3.79	5.23	4.71	0.07	0.92	99.47
11	00GNX-7-12-1	Kfpo Hb lmz	301487	5544347	61.22	0.33	19.17	3.26	0.12	0.44	4.28	5.32	4.80	0.07	0.61	99.62
39	00GNX-2-1-1	Kfpo Hb mz	302005	5542321	58.29	0.37	19.52	4.80	0.15	1.10	4.76	5.23	4.73	0.18	0.56	99.69
40	00GNX-10-2-1	(Bi)-Gt-Hb mz	303093	5542176	55.43	0.43	19.23	5.88	0.18	1.52	6.44	4.76	4.32	0.28	0.60	99.07
35	00GNX-2-5-1	Kfpo Hb mz	301801	5542632	55.05	0.56	18.79	6.60	0.20	1.40	6.53	3.55	5.63	0.25	0.63	99.19
51	00GNX-13-1-1	Kfpo Gt-Bi mz	305753	5539563	54.83	0.51	18.30	6.57	0.20	1.24	6.46	4.17	5.96	0.23	0.98	99.45
Quartz-monzonite																
42	00GNX-11-19-1	Bi lqmz	305349	5540779	64.12	0.28	18.39	2.90	0.07	0.57	1.98	5.00	4.78	0.07	1.23	99.39
43	00GNX-11-18-1	Hb lqmz	305365	5540610	63.45	0.25	17.80	3.00	0.10	0.50	3.07	4.90	5.40	0.05	0.88	99.40
Marginal Trachyte																
36	00GNX-2-4-1	Cpx hornfels in trachyte	301754	5542623	69.48	0.41	11.43	3.60	0.03	1.64	8.17	2.85	1.34	0.09	0.18	99.22
37	00GNX-2-2-1	trachyte	301628	5542502	63.13	0.75	13.85	4.25	0.02	2.18	4.21	3.07	6.57	0.14	1.00	99.17

TABLE 6 CONTINUED
WHOLE-ROCK MAJOR ELEMENT ANALYSES OF THE WHITEROCKS MOUNTAIN ALKALINE COMPLEX AND OTHER IGNEOUS ROCKS

ID	Sample	Rock Type	NAD 1983 Easting	NAD 1983 Northing	SiO_2	TiO_2	Al_2O_3	Fe_2O_3t	MnO	MgO	CaO	Na_2O	K_2O	P_2O_5	LOI	Total
Minor Intrusions in the Whiterocks Complex																
17	00GNX-16-4-1	Fspo lqmz dyke	302588	5543533	68.33	0.11	16.87	1.40	0.05	0.18	2.27	5.07	4.67	0.01	0.49	99.45
46	00GNX-11-17-2	lsy dyke	305416	5540484	63.38	0.10	18.70	1.25	0.03	0.38	1.37	4.59	8.77	0.05	0.77	99.39
55	00GNX-13-2-1	Ms sy pegmatitic vein	305937	5539450	62.31	0.05	21.56	0.63	0.01	0.05	0.66	5.21	8.36	0.01	0.86	99.71
6	00GNX-9-10-1	Kfpo Hb mz dyke	301121	5545016	59.61	0.41	18.50	4.61	0.11	0.83	4.46	4.88	5.01	0.14	0.76	99.32
15	00GNX-6-9-1	mKf (Cpx)-Gt-Hb mz dyke	301369	5543867	54.02	0.56	18.29	7.25	0.23	1.59	6.61	3.50	6.09	0.25	0.69	99.08
31	00GNX-17-2-3	(Cpx)-Bi-Hb mmz dyke	300661	5542870	50.22	0.86	13.92	12.11	0.23	5.55	9.63	2.92	2.72	0.61	0.87	99.64
20	00GNX-16-6-1	Hb mdi/mmzdi dyke?	301838	5543463	48.95	0.82	14.97	11.82	0.25	4.34	10.55	2.73	3.60	0.66	0.46	99.15
50	00GNX-11-15-3	Plpo Cpx-Hb mmz dyke	304813	5540468	47.47	0.91	15.90	12.47	0.30	3.64	10.47	3.39	2.82	0.66	1.00	99.03
19	00GNX-16-5-1	Cpx-Hb-Pl po dyke	301885	5543465	45.11	0.56	19.50	11.05	0.21	2.97	12.31	2.64	2.07	0.47	2.14	99.03
Mt Sandberg Pluton																
8	00GNX-3-17-5	aplite dyke	298672	5544978	76.61	0.05	13.48	0.55	0.01	0.05	0.83	5.67	1.16	0.01	1.03	99.45
4	00GNX-8-8-1	Qzpo Bi mzg	300410	5545630	71.47	0.25	14.71	2.00	0.03	0.62	2.05	4.07	3.59	0.09	0.67	99.55
5	00GNX-8-10-1	Kfpo Bi mzg	299416	5545520	69.66	0.25	15.35	2.47	0.07	0.85	2.41	4.46	2.93	0.11	1.05	99.61
7	00GNX-3-17-6	Bi gd dyke*	298671	5544978	69.19	0.31	16.21	2.18	0.03	0.79	2.11	4.92	2.22	0.10	1.40	99.46
2	00GNX-4-8-1	(Hb)-Bi mzg	299117	5546771	67.47	0.34	16.04	3.17	0.07	1.00	2.90	4.75	2.55	0.18	1.04	99.51
Minor Intrusions																
38	00GNX-1-8-1	Hb-Bi qmz dyke/sill	301181	5542444	69.65	0.28	15.56	2.31	0.03	0.70	2.74	4.57	2.54	0.09	1.07	99.54
10	00GNX-11-1-2	Bi-Pl po dyke	304367	5544850	68.66	0.31	15.84	2.50	0.05	1.05	3.02	4.73	2.38	0.10	0.94	99.58
3	00GNX-9-5-1	Bi-Pl po sill	302346	5546104	63.88	0.58	15.77	4.84	0.10	1.67	4.40	3.00	3.25	0.23	1.36	99.08
9	00GNX-9-12-1	Cpx di sill**	303749	5544891	50.36	0.86	15.85	9.35	0.14	9.18	6.40	4.07	0.85	0.20	1.94	99.20
Northern Pluton																
1	00GNX-5-9-1	Bi mzg	304496	5547973	70.01	0.33	15.18	2.66	0.05	0.79	2.65	3.54	3.64	0.11	0.81	99.77
Xenolith																
26	00GNX-10-5-1	recrystallized xenolith	304024	5543373	54.08	0.97	14.69	9.38	0.21	4.26	5.07	2.81	5.92	0.25	1.08	98.72
	Standard MRG-1	(in house)			39.04	3.77	8.39	17.95	0.15	13.52	14.73	0.75	0.17	0.07	1.39	99.93
	Rec. value***				39.32	3.69	8.5	17.82	0.17	13.49	14.77	0.71	0.18	0.06		
	Standard SY-3	(in house)			59.56	0.14	11.64	6.48	0.31	2.67	8.26	4.05	4.15	0.54	1.23	99.03
	Standard SY-3	(in house)			59.68	0.15	11.68	6.48	0.31	2.68	8.27	4.07	4.15	0.52	1.17	99.16
	Standard SY-3	(hidden)			59.56	0.15	11.67	6.46	0.31	2.65	8.26	4.07	4.15	0.52	1.25	99.05
	Standard SY-3	Average			59.60	0.15	11.67	6.47	0.31	2.67	8.26	4.06	4.15	0.53	1.22	99.09
	Rec. value***				59.68	0.15	11.80	6.42	0.32	2.67	8.26	4.15	4.20	0.54		

Fe_2O_3t = total Fe as Fe_2O_3 * sericitized ** sericite-actinolite alteration *** anhydrous basis (Abbey, 1979) ID, samples located on Figure 11

Abbreviations: Hb, hornblende; Bi, biotite; Cpx, calcic clinopyroxene; Gt, garnet; Qz, quartz; Ap, apatite (apatite grain size given in millimetres); mKf, megacrystic (>2.5 cm) potassium feldspar; Kfpo, porphyritic (<2.5 cm) potassium feldspar; Pl, plagioclase; f, feldspathic; m, melanocratic (mela-); l, leucocratic (leuco-); cpxite, clinopyroxenite; hbite, hornblendite; di, diorite; mz, monzonite; mzdi, monzodiorite; qmz, quartz monzonite; gd, granodiorite; sy, syenite; mzg, monzogranite; po, porphyry or porphyritic. Brackets indicate mineral present in low (trace-1 vol. %) modal proportions.

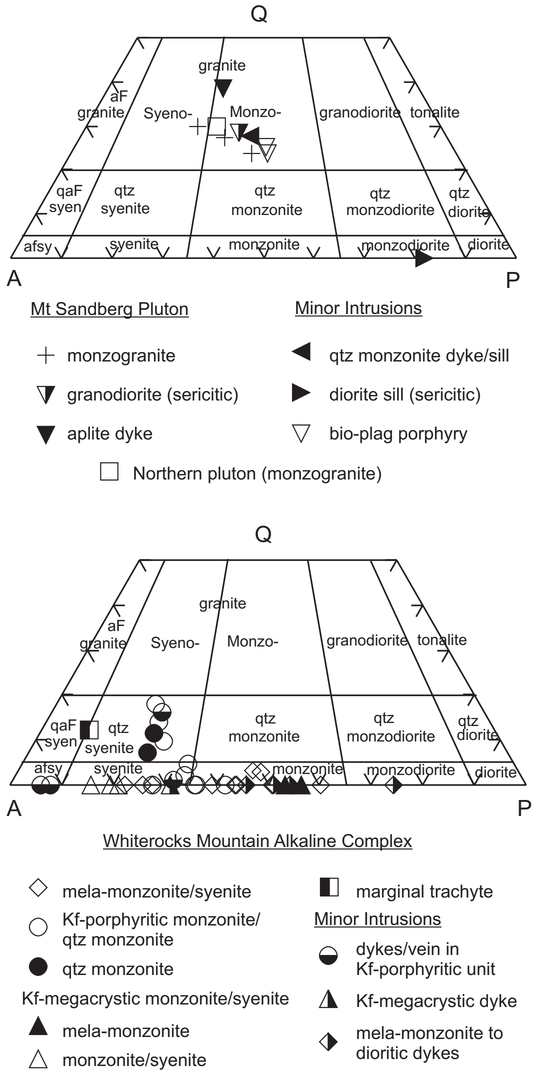

Figure 10. CIPW-normative compositions (wt. %) of plutonic rocks from the Whiterocks complex and other intrusions in the area projected into the QAP classification scheme of Le Maitre *et al.* (1989).

no modal felspathoid minerals are present, the foid-equivalent part of this classification scheme has been ignored. Accordingly, rocks that have normative *ne* (all Kf-megacrystic rocks, practically all mela-monzonites/syenites and the least siliceous Kf-porphyritic rocks of the Whiterocks complex) are forced to plot on the A-P join. This permits a rigourous comparison between modal and normative mineralogy in these feldspathoid-free rocks, particularly with respect to alkali feldspar:plagioclase (A:P) ratios.

As shown in Figure 10, the Whiterocks Mountain alkaline suite is quite distinct from granitoid rocks of the Mt. Sandberg pluton, as well as practically all minor intrusions not associated with the Whiterocks suite, all of which are enriched in normative *qz* at equivalent A:P ratios. The Whiterocks fractionation trend forms a linear array away from the P apex and exhibits a marked bifurcation towards Q-rich and A-rich components for the most differentiated members of the suite (Figure 10). The melanocratic monzonite-syenite rocks extend from alkali-poor monzonite to syenite, and microcline-megacrystic rocks form two distinct groups of monzonites and syenites, all in good agreement with their modal mineralogy. Microcline-porphyritic rocks extend from the monzonite field through syenite to quartz syenite, and together with the non-porphyritic quartz monzonite, are displaced to higher A:P ratios than in the equivalent modal classification scheme. Minor intrusions associated with the Whiterocks aklkaline suite extend the range of rock types from monzodiorite (plagioclase-pophyritic dike) to alkali-feldspar syenite (leuco-syenite dike and a pegmatitic segregation vein), and the marginal trachyte phase lies on the quartz syenite - quartz alkali-feldspar syenite boundary. The displacement of the more differentiated CIPW-normative compositions to higher A:P ratios relative to the modal scheme stems mainly from the inability of the normative calculation to represent important fractionating hydrous minerals (amphibole, biotite) which contain significant amounts of alkalies. A contributing factor may have been a systematic understimation of the modal abundance of potassium feldspar either in the fine-grained groundmasses of minor intrusions or in rocks with a non-uniform distribution of potassium feldspar megacrysts/phenocrysts.

The normative compositions of rocks belonging to the Mt. Sandberg pluton, a granitoid intrusion at the northern edge of the map area and biotite-plagioclase porphyry dikes north of the Whiterocks complex are classified as monzogranites (Figure 10), which is consistent with their mineralogy. The single exception is a biotite-bearing quartz porphyry which falls just within the syenogranite field. Sericitic alteration may account for the monzogranite classification of a granodiorite dike, and likewise, a clinopyroxene-phyric diorite sill which falls within the monzodiorite field.

In an alkalies-silica diagram (Figure 12), the granitoid rocks are distinctly subalkaline except for the monzodiorite sill which is transitional. In an alkalies-iron-magnesia plot (Figure 13), these rocks are calc-alkaline. In contrast (Figure 12), early melanocratic fractionates of the Whiterocks complex together with associated minor intrusions form a differentiation trend within the alkaline field which diverges for more felsic magmas into a pronounced alkaline lineage and a well-defined offshoot which crosses the discriminant boundary into the subalkaline field, and reflects the increasingly *qz*-normative nature of these rocks. The dichotomous bahaviour of these felsic differentiates indicates that more than one fractionation process has governed the evolution of the Whiterocks Mountain alkaline suite. The trend towards subalkaline compositions crosses the low-pressure thermal divide (approximately coincident with the discriminant boundary given in Figure 12) which separates alkaline and subalkaline rock series at pressures below about 5 kb in *anhydrous* systems (Yoder and Tilley, 1962). As discussed previously, the vesicular nature of the marginal trachyte phase implies that, given reasonable volatile concentrations, the Whiterocks alkaline

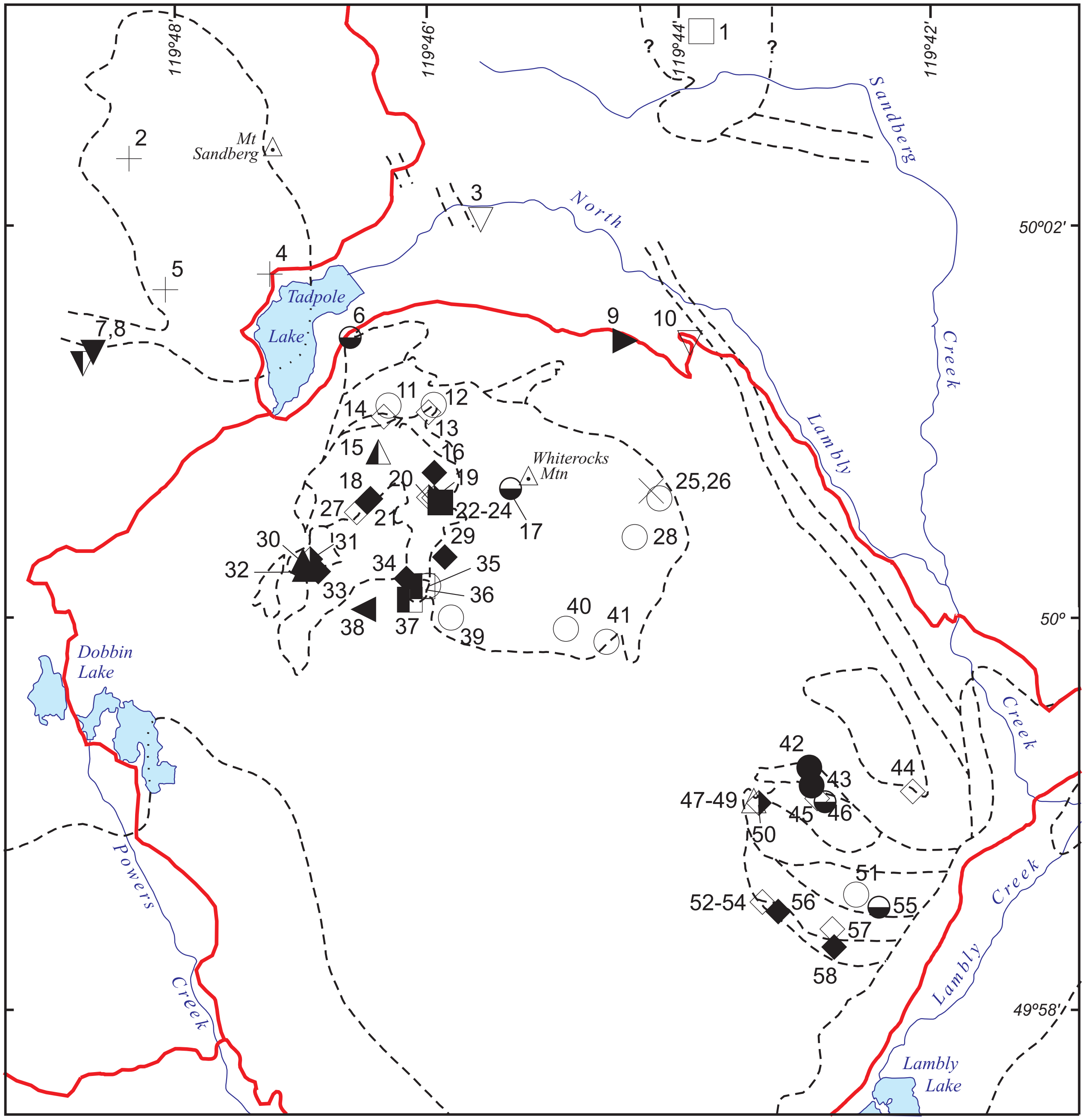

Figure 11. Location of sample sites for whole-rock major element analyses given in Table 6 and plotted in Figure 10. Symbols correspond to those shown in Figure 10 except for a reconstituted xenolith (X).

suite was emplaced at low pressures, probably within several kilometres of the paleosurface. The quartz-normative offshoot from the Whiterocks alkaline trend, therefore, indicates that either the fractionation of hydrous minerals such as biotite and hornblende played an important role in driving these magmas across the thermal divide, or open-system fractionation processes prevailed in the form of crustal contamination of alkaline magmas with *qz*-normative country rocks, or possibly both mechanisms were operating concurrently.

Ultramafic Rocks

The clinopyroxenites and hornblendites are characterized by relatively low alumina (5-10 wt. %) and MgO (7-11 wt. %), moderate TiO_2 (1-1.8 wt. %) and high FeOt (20-25 wt. %), CaO (15-19 wt. %), K_2O (0.5-1.7 wt. %) and P_2O_5 (0.9-1.7 wt. %). Their compositions reflect the accumulation of major silicate liquidus or near-liquidus phases such as high-Ca clinopyroxene, biotite and hornblende, together with accessory phases such as magnetite and apatite. Their relatively low Mg-numbers (100Mg/(0.85Fe+Mg) = 40-61) and cumulate mineral

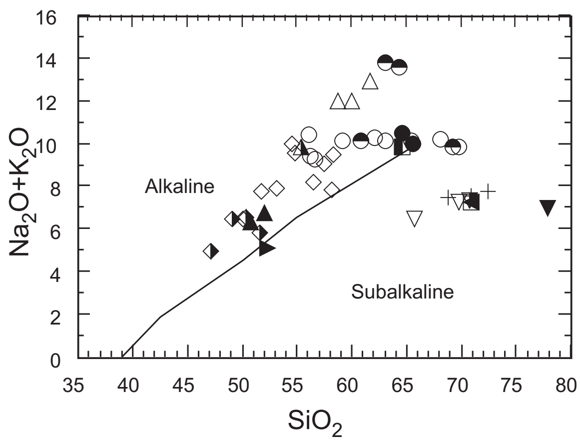

Figure 12. Alkalies versus silica plot (wt. %) for the Whiterocks Mountain alkaline suite and other intrusions within the map area showing the discriminant of Irvine and Baragar (1971) between alkaline and subalkaline fields.

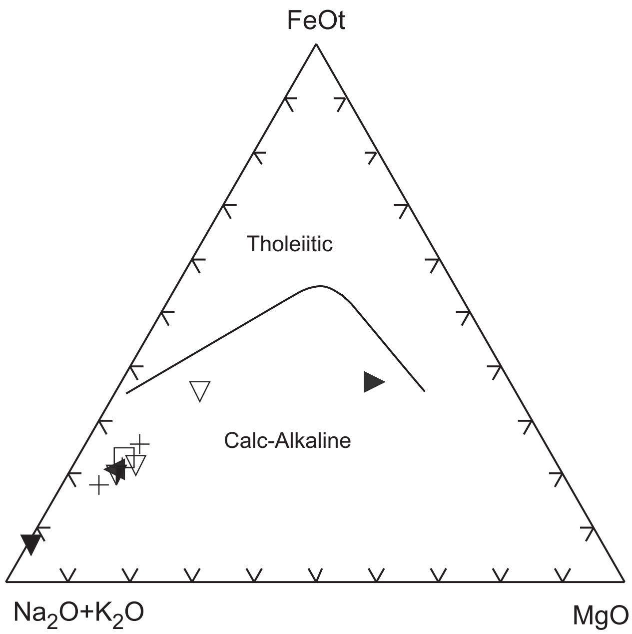

Figure 13. Alkalies-total iron-magnesia plot (wt. %) for calc-alkaline granitoid rocks in the area showing the discriminant of Irvine and Baragar (1971) between the calc-alkaline and tholeiitic fields.

compositions indicate that magmas parental to these ultramafic rocks were not primitive mantle-equilibrated melts but rather evolved, Fe-enriched compositions. In particular, apatite and magnetite are important modal constituents of these rocks (~3-4 and 7-8 vol. %, respectively) and attest to the relatively early saturation of these phases in Fe-enriched, alkaline mafic magmas.. In particular, cumulate apatite is present in anomalous abundances in certain PGE-enriched rocks containing disseminated and partially remobilized sulfides which may be magmatic in origin. The strong positive correlation between P_2O_5 and FeOt in the Whiterocks alkaline suite as a whole indicates that apatite and magnetite were co-crystallizing throughout the entire magmatic evolution (Figure 14).

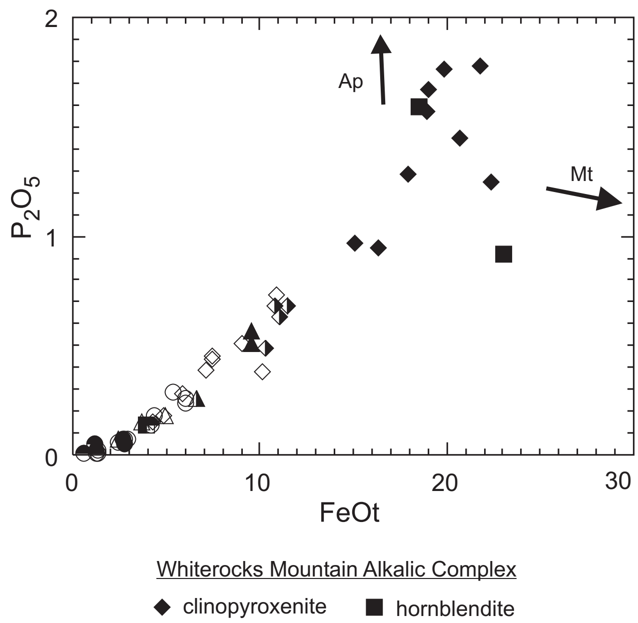

Figure 14. Plot of P_2O_5 versus FeO as total iron (wt. %) for the Whiterocks Mountain alkaline suite showing the high phosphorus and iron contents of clinopyroxenite and hornblendite cumulates. Arrows indicate the effects of accumulation of apatite (Ap) and magnetite (Mt). Symbols for the feldspathic rocks are those of Figure 10.

LITHOGEOCHEMICAL ASSAYS

Mineralized and unmineralized rock samples were prepared using the same crushing and grinding techniques as those employed for the whole-rock samples. Mineralized samples were analyzed by Acme Analytical Laboratories Ltd., Vancouver, for major and minor elements (including sulphur) and a suite of 42 trace elements including base and precious metals and PGE (Pt and Pd). Rock powders (1 g) were digested in aqua regia which is generally expected to yield “near-total” recovery of base and precious metals, and acts as a partial leach for rock-forming (lithophile) elements. Solutions were analyzed by inductively-coupled-plasma mass spectrometry (ICP-MS) and emission spectroscopy. The results are given in Table 7.

A hidden sulfide standard (SU-1a) included in the ICP-MS run (Table 7) yielded base metal concentrations (Ni, Co and Cu) slightly lower than the values recommended by Steger and Bowman (1980). However, the relatively high metal concentrations for Ni and Cu in the standard exceed or lie just below the maximum concentration of the analytical method (10 000 ppm). The results for precious metals (Ag and Au) also appear low, and the PGE show diverse behaviour with Pd in excellent agreement with the standard whereas Pt is anomalously low. It would appear that the acid digest provides “near-total” extraction for base metals, and also Pd in this sulfide-bearing standard, whereas Ag, Pt and possibly Au are problematic. The single duplicate analysis of an unknown shows excellent agreement for all elements except Au.

TABLE 7
LITHOGEOCHEMICAL ANALYSES OF MINERALIZED PLUTONIC AND COUNTRY ROCKS

				wt. %									ppm			
Sample	Depth (ft)	Rock Type	Alteration/Mineralization	Ti	Al	Fe	Mg	Ca	Na	K	P	S	Li	Be	B	Cs
00GNX 3-1-1	outcrop	metasediment	silicified, pyritic, sericitic	0.011	0.29	2.43	0.16	0.04	0.040	0.15	0.033	1.20	6.5	0.3	2	0.57
00GNX 3-17-4	outcrop	aplite dyke	pyritic	0.028	0.48	0.90	0.20	0.21	0.057	0.13	0.027	0.29	4.1	0.2	1	0.75
00GNX 4-9-1	outcrop	metasediment (calc-silicate)	silicified, dissem. S	0.179	0.64	3.92	0.25	0.76	0.099	0.14	0.071	2.39	4.9	0.1	2	0.63
00GNX 5-8-1	outcrop	calc-silicate skarn	trace S	0.147	3.61	4.34	0.60	4.20	0.180	0.29	0.025	2.48	18.9	0.8	4	1.52
00GNX 5-8-2	outcrop	calc-silicate skarn	trace S	0.150	1.07	3.69	0.14	6.00	0.003	0.01	0.017	1.90	1.6	0.1	1	0.18
00GNX 5-8-3	outcrop	calc-silicate skarn	trace S	0.139	0.90	3.42	0.14	4.69	0.005	0.01	0.022	1.72	1.6	0.1	1	0.18
00GNX 8-7-1	outcrop	hornfelsed metasediment	pyritic	0.164	0.63	3.30	0.22	0.88	0.054	0.05	0.119	1.78	9.1	0.5	1	1.2
00GNX 9-9-1	outcrop	Hb monzonite	pyritic	0.115	0.88	2.90	0.18	0.88	0.119	0.07	0.119	1.90	7.3	0.3	1	1.22
00GNX 10-1-1	outcrop	Qz vein	dissem. S	0.049	0.38	1.16	0.30	0.11	0.011	0.24	0.037	0.22	17.9	0.1	1	5.45
00GNX 10-4-2	outcrop	Qz vein	pyritic	0.021	0.27	1.62	0.10	0.61	0.055	0.13	0.010	1.09	13.8	0.1	1	0.85
00GNX 13-5-2	outcrop	Bi cpxite (Ap≤0.5)	dissem. Mt	0.147	0.52	13.46	0.69	0.57	0.023	0.18	0.037	0.02	3.2	0.1	1	0.31
00GNX 16-1-1	outcrop	fBi-Hb cpxite (Ap≤0.3)	dissem. Mt	0.157	2.04	5.87	1.69	3.27	0.292	0.71	0.381	0.04	9.0	0.5	1	0.38
00GNX 16-2-1	outcrop	fCpx hbite (Ap≤0.8)	dissem. Mt	0.180	1.71	9.12	1.24	3.33	0.315	0.43	0.293	0.05	14.2	0.9	1	0.16
00GNX 16-2-5	outcrop	fCpx hbite (Ap≤0.8)	dissem. Mt	0.077	1.74	7.37	1.44	4.13	0.376	0.47	0.632	0.02	6.3	0.6	2	0.17
00GNX 16-2-8	outcrop	Bi-Hb cpxite (Ap≤0.6)	dissem. Mt	0.065	1.75	8.13	1.87	3.02	0.142	1.18	0.621	0.02	24.5	0.1	1	1.44
DDH97-7																
00GNX 30-1	560	fine grained Bi hbite	Mt+Ep veins & patches, Act	0.320	2.23	12.54	2.38	2.23	0.119	1.41	0.349	7.24	18.4	0.3	1	15.03
DDH97-21																
00GNX 53-1	993	fHb cpxite (Ap≤1.3)	Ep+Ser+clay+Act, dissem. S	0.046	1.17	9.76	0.94	4.70	0.170	0.23	0.936	0.27	5.8	0.4	1	0.43
00GNX 53-2	1004	Hb cpxite/Cpx hbite (Ap≤1.3)	Ep+Ab+S veins, Act+Ep, dissem. S	0.086	1.30	9.30	1.11	3.76	0.127	0.45	0.697	5.02	7.5	0.5	1	10.51
00GNX 53-2r	1004	Hb cpxite/Cpx hbite (Ap≤1.3)	Ep+Ab+S veins, Act+Ep, dissem. S	0.086	1.28	9.18	1.09	3.71	0.125	0.45	0.678	4.73	8.1	0.7	2	10.73
00GNX 55-2	1043	Bi-Hb cpxite/Bi-Cpx hbite (Ap≤1.8)	Ep+Cc+S veins, Act	0.088	1.72	9.76	1.64	3.39	0.115	1.05	0.608	3.74	17.8	0.5	2	19.36
00GNX 56-1	1051	fBi-Hb cpxite/fBi-Cpx hbite (Ap≤1.1)	Ep+Cc+S veins, Act, dissem. S	0.081	1.34	8.29	1.17	3.57	0.112	0.64	0.597	2.77	11.9	0.4	2	10.52
00GNX 56-2	1055	fine grained Bi hbite	Ep+Cc veins & patches, Act, dissem. S	0.329	2.37	6.58	2.24	3.51	0.405	0.84	0.179	0.58	20.0	0.4	1	5.04
00GNX 57-1	1070	cpxite	Bi+Act+Ep+S+Mt+Hm veins	0.067	1.33	10.72	1.30	4.43	0.234	0.33	0.653	1.54	7.4	0.8	1	3.89
00GNX 57-2	1075	Hb cpxite/Cpx hbite (Ap≤0.7)	Bi+Act+Ep+S veins & patches, dissem. S	0.092	1.04	6.30	0.92	2.53	0.087	0.43	0.515	2.39	7.0	0.3	2	7.73
00GNX 58-1	1089	Hb cpxite/Cpx hbite	Bi+Ep+Kf+Ms veins & patches, dissem. S	0.439	3.93	7.46	4.27	1.20	0.160	3.37	0.066	0.62	94.6	0.3	2	30.81
00GNX 58-2	1100	Hb cpxite/Cpx hbite (Ap≤0.6)	Ep+Cc+S veins, Act, dissem. S	0.123	0.89	7.99	0.67	2.63	0.116	0.14	0.406	2.05	4.2	0.3	2	0.76
00GNX 60-1	1131	fHb cpxite (Ap≤1.4)	Ep+Cc+S veins, Ep+Ser, dissem. S	0.122	0.75	9.08	0.61	2.90	0.081	0.10	0.389	1.06	4.8	0.3	1	0.47
00GNX 60-2	1137	Hb cpxite (Ap≤0.8)	Act	0.059	0.73	9.19	0.59	3.47	0.089	0.08	0.647	0.40	4.2	0.2	2	0.14
00GNX 61-1	1150	Hb cpxite (Ap≤1.4)	Ep veins, dissem. S	0.127	0.89	7.73	0.78	3.04	0.113	0.23	0.412	1.51	5.0	0.4	2	3.18
00GNX 61-2	1160	Hb cpxite (Ap≤1.3)	Ep veins	0.133	0.84	8.16	0.71	2.74	0.100	0.10	0.348	0.81	4.7	0.3	1	0.23
Std SU1a				0.106	1.61	14.75	1.16	0.58	0.066	0.51	0.051	6.49	15.2	0.2	2	1.65
Rec. Value*																
Std DS2				0.098	1.83	3.16	0.63	0.57	0.035	0.17	0.102	0.03	14.8	0.6	3	3.05
Rec. Value**				0.096	1.69	3.07	0.59	0.52	0.029	0.16	0.090	0.03	14.7	0.6	2	0.52
RSD %***				3.700	2.90	2.10	2.40	3.80	6.500	5.60	3.200	26.90	3.2	16.0	39	3.8
DTL****				0.001	0.01	0.01	0.01	0.01	0.001	0.01	0.001	0.02	0.1	0.1	1	0.1

TABLE 7 CONTINUED
LITHOGEOCHEMICAL ANALYSES OF MINERALIZED PLUTONIC AND COUNTRY ROCKS

	ppm																			
Sample	Rb	Sr	Ba	Y	Zr	Hf	Nb	Th	U	La	Ce	Mn	Sc	V	Cr	Ni	Co	Cu	Mo	Pb	Zn
00GNX 3-1-1	9.3	20.8	130.8	2.77	20.5	0.53	0.02	2.2	1.9	10.5	14.6	43	3.4	198	35.1	29.1	7.5	17.1	28.6	28.5	40.0
00GNX 3-17-4	6.0	7.4	64.0	3.20	22.4	1.18	0.33	12.4	7.2	6.4	9.8	171	1.2	19	17.1	2.1	2.8	17.7	4.0	3.3	6.9
00GNX 4-9-1	6.2	31.8	23.2	7.06	2.5	0.08	0.27	0.6	0.2	2.5	4.4	104	2.0	45	18.5	17.8	14.1	262.8	26.5	11.3	25.0
00GNX 5-8-1	12.4	123.1	23.3	13.83	7.5	0.22	0.15	0.8	2.3	6.5	8.8	126	3.6	74	29.7	12.4	13.0	63.2	10.6	2.2	36.2
00GNX 5-8-2	0.4	30.9	5.3	27.99	11.2	0.30	0.46	0.6	1.7	9.5	11.2	267	2.3	35	29.8	15.8	12.2	42.0	48.1	3.0	19.9
00GNX 5-8-3	0.4	33.5	8.7	26.07	8.3	0.28	0.49	0.6	1.9	8.3	9.6	195	1.9	29	20.1	11.4	12.5	38.1	25.4	2.0	22.0
00GNX 8-7-1	2.7	20.7	64.9	11.59	5.1	0.21	0.33	2.3	0.6	9.8	17.2	284	3.4	50	15.4	11.1	11.3	119.4	7.9	5.4	55.3
00GNX 9-9-1	2.7	57.1	49.6	7.93	3.9	0.19	0.40	1.8	0.6	8.7	14.5	125	0.8	23	16.4	12.9	10.8	166.2	35.3	3.1	15.3
00GNX 10-1-1	20.1	7.6	48.7	1.70	3.7	0.10	0.15	0.7	0.8	1.0	2.0	213	1.4	37	25.5	9.4	2.7	7.4	5.2	2.3	17.5
00GNX 10-4-2	7.0	30.7	27.9	3.44	1.5	0.05	0.22	1.4	0.4	3.7	6.1	581	0.6	8	17.1	1.2	1.8	2.8	2.7	2.3	9.1
00GNX 13-5-2	7.5	15.2	73.2	1.19	2.5	0.10	0.02	0.1	0.1	0.7	1.7	278	5.9	663	45.0	48.2	45.9	7.1	1.6	1.1	18.8
00GNX 16-1-1	14.7	359.6	431.8	13.29	1.9	0.02	0.02	1.1	0.2	16.2	32.4	841	10.6	251	71.4	25.5	30.2	148.2	0.8	0.9	62.7
00GNX 16-2-1	3.8	200.9	108.9	15.19	3.8	0.04	0.04	1.5	0.3	14.8	30.7	1413	8.5	357	29.8	13.7	26.2	71.3	1.6	5.3	157.3
00GNX 16-2-5	5.2	222.2	113.1	21.67	1.3	0.02	0.02	1.9	0.5	25.2	50.5	1383	10.1	310	17.1	10.2	25.3	182.8	0.5	1.4	94.9
00GNX 16-2-8	49.1	289.9	631.2	19.58	0.4	0.02	0.02	1.4	0.4	23.9	47.6	1038	7.1	369	33.4	18.3	34.9	182.8	1.4	1.5	95.2
DDH97-7																					
00GNX 30-1	65.3	29.3	36.2	8.56	5.0	0.14	0.04	0.3	0.1	2.9	8.6	1014	11.6	320	8.3	41.7	142.0	7068.9	1.2	1.7	97.6
DDH97-21																					
00GNX 53-1	4.4	129.1	37.6	21.32	0.5	0.02	0.02	1.7	0.3	13.8	31.9	842	7.7	675	14.2	23.1	28.2	1938.0	1.0	1.6	81.5
00GNX 53-2	33.5	86.2	24.5	13.01	1.0	0.02	0.02	1.0	0.2	6.2	14.4	730	8.6	348	10.8	21.7	72.7	1385.7	0.9	4.9	79.4
00GNX 53-2r	33.5	85.2	24.2	12.72	1.1	0.02	0.02	1.0	0.2	6.3	15.0	720	8.3	341	12.9	21.6	69.0	1364.1	0.8	5.0	78.0
00GNX 55-2	95.1	73.1	64.6	14.19	0.3	0.02	0.02	0.8	0.2	6.9	16.5	805	7.1	359	16.1	24.3	59.2	1050.0	1.5	4.2	106.6
00GNX 56-1	59.6	108.6	28.7	13.93	0.7	0.02	0.02	0.8	0.2	7.0	16.6	654	5.3	383	12.7	17.4	59.8	452.0	0.9	4.8	63.8
00GNX 56-2	23.7	109.0	135.1	10.07	10.8	0.40	0.02	0.2	0.1	2.6	7.3	902	21.4	370	5.8	20.6	39.5	2360.8	0.5	2.0	72.9
00GNX 57-1	10.6	123.0	42.6	13.43	0.5	0.02	0.02	0.7	0.1	6.1	15.6	920	11.5	546	11.5	24.6	53.7	1475.3	0.9	3.4	83.1
00GNX 57-2	27.2	106.9	56.0	11.41	0.5	0.02	0.02	0.6	0.1	6.1	13.7	485	6.1	254	14.9	27.2	42.5	5535.5	0.8	2.7	160.9
00GNX 58-1	197.3	27.7	426.4	7.77	3.8	0.13	0.02	0.1	0.1	0.8	2.5	946	11.4	326	75.8	57.3	59.4	3588.0	2.5	1.5	125.1
00GNX 58-2	2.6	54.1	14.9	9.69	2.4	0.04	0.02	0.7	0.1	4.6	11.1	499	5.4	361	18.0	47.7	56.8	20481.3	1.0	2.5	178.5
00GNX 60-1	2.6	58.6	12.2	9.15	1.9	0.03	0.03	0.5	0.1	5.3	12.1	528	4.2	600	24.0	33.6	39.1	12254.4	0.5	0.9	137.1
00GNX 60-2	1.2	67.6	9.4	13.07	0.9	0.02	0.02	0.7	0.1	8.8	19.5	523	5.1	659	15.1	30.9	29.6	3911.7	1.0	1.8	98.6
00GNX 61-1	14.1	56.4	12.3	9.79	2.0	0.04	0.03	0.4	0.1	4.4	10.5	561	6.2	458	28.1	22.6	33.4	3849.1	0.7	1.3	102.5
00GNX 61-2	1.7	64.1	19.3	9.08	2.2	0.04	0.02	0.4	0.1	4.8	11.3	519	6.0	568	27.3	26.2	35.0	6233.9	1.1	2.2	113.7
Std SU1a	23.8	21.8	55.2	4.51	2.0	0.08	0.18	3.3	1.8	12.8	26.2	414	1.7	52	141.2	10981.1	331.7	8315.5	1.2	59.9	133.1
Rec. Value*																12330.0	410.0	9670.0			
Std DS2	13.1	28.0	165.7	7.66	3.2	0.03	1.32	3.6	18.9	15.6	30.5	844	3.0	78	172.5	37.2	11.5	130.3	14.5	32.7	163.1
Rec. Value**	12.6	27.7	146.5	7.70	2.9	0.05	1.25	3.7	19.0	15.6	30.0	815	2.9	76	158.4	35.0	11.9	128.0	13.9	32.0	160.0
RSD %***	9.6	4.3	2.7	2.60	7.7	19.50	6.50	4.1	4.9	4.4	3.1	2.2	4.7	2.4	3.2	3.8	3.6	2.1	2.7	3.7	2.5
DTL****	0.1	0.5	0.5	0.10	0.1	0.02	0.02	0.1	0.1	0.5	0.0	1	0.1	2	0.5	0.1	0.1	0.01	0.01	0.01	0.1

TABLE 7 CONTINUED
LITHOGEOCHEMICAL ANALYSES OF MINERALIZED PLUTONIC AND COUNTRY ROCKS

	ppm											ppb					
Sample	As	Sb	Bi	Tl	Ga	Ge	Cd	In	Sn	Se	Te	Re	Hg	Ag	Au	Pt	Pd
00GNX 3-1-1	15.4	1.63	0.55	0.10	1.4	0.1	0.06	0.04	0.3	7.1	0.13	28	9	282	0.4	3	10
00GNX 3-17-4	0.8	0.03	0.28	0.06	2.3	0.1	0.05	0.02	0.3	0.2	0.12	1	5	59	1.1	2	10
00GNX 4-9-1	0.4	0.05	6.86	0.06	2.5	0.1	0.51	0.02	0.6	3.5	0.78	17	5	629	2.0	2	10
00GNX 5-8-1	0.1	0.04	0.22	0.06	7.7	0.1	0.39	0.02	0.4	1.3	0.20	16	5	304	2.2	2	11
00GNX 5-8-2	0.1	0.09	0.15	0.02	2.9	0.1	0.23	0.03	0.7	1.2	0.07	39	5	202	1.1	2	10
00GNX 5-8-3	0.1	0.07	0.18	0.02	2.4	0.1	0.26	0.03	0.4	1.2	0.14	23	5	332	0.8	2	10
00GNX 8-7-1	0.7	0.10	1.75	0.04	2.5	0.2	1.54	0.06	1.1	1.6	0.11	3	6	285	1.4	2	10
00GNX 9-9-1	1.3	0.06	0.54	0.04	2.0	0.1	0.10	0.04	0.4	2.0	0.18	47	5	263	1.2	2	10
00GNX 10-1-1	6.5	0.16	0.17	0.11	2.2	0.1	0.01	0.04	1.6	0.2	0.03	1	5	72	0.5	2	10
00GNX 10-4-2	3.9	0.07	1.18	0.04	1.1	0.1	0.06	0.05	0.3	0.3	0.10	1	5	104	1.3	2	10
00GNX 13-5-2	0.1	0.02	0.02	0.02	7.4	0.1	0.04	0.07	0.7	0.1	0.02	2	6	12	0.8	2	10
00GNX 16-1-1	0.1	0.02	0.02	0.02	6.7	0.2	0.08	0.08	0.7	0.1	0.02	1	5	103	6.6	2	24
00GNX 16-2-1	1.0	3.39	0.10	0.02	8.2	0.2	0.19	0.11	1.4	0.1	0.04	1	6	102	2.4	3	17
00GNX 16-2-5	0.6	0.05	0.02	0.02	7.8	0.2	0.12	0.11	1.1	0.1	0.02	1	5	119	6.6	2	34
00GNX 16-2-8	0.1	0.03	0.02	0.06	9.0	0.2	0.09	0.09	0.8	0.1	0.02	1	6	151	12.1	2	38
DDH97-7																	
00GNX 30-1	0.8	0.04	2.30	0.31	7.0	0.3	0.67	0.14	0.5	7.2	0.31	13	9	2686	72.7	56	77
DDH97-21																	
00GNX 53-1	1.3	0.31	0.54	0.02	7.9	0.2	0.73	0.11	1.0	0.9	0.16	2	7	1163	28.0	299	893
00GNX 53-2	3.2	0.14	3.13	0.21	7.1	0.3	0.71	0.10	1.0	3.5	0.31	1	5	810	75.6	437	375
00GNX 53-2r	3.3	0.14	3.24	0.22	6.8	0.3	0.72	0.10	0.8	3.5	0.32	1	5	815	101.1	443	353
00GNX 55-2	1.5	0.10	2.50	0.56	8.8	0.3	0.95	0.08	0.9	2.6	0.35	1	9	1100	3.3	397	299
00GNX 56-1	2.1	0.11	2.36	0.30	7.0	0.3	0.43	0.08	0.9	1.9	0.16	1	5	434	1.9	295	185
00GNX 56-2	0.1	0.06	0.75	0.11	7.8	0.2	1.63	0.11	1.2	0.8	0.08	1	5	2246	14.1	27	60
00GNX 57-1	13.2	2.99	2.07	0.08	7.3	0.3	1.99	0.09	0.9	1.2	0.52	1	5	1812	1.9	493	882
00GNX 57-2	0.7	0.26	3.19	0.24	5.0	0.2	18.02	0.09	0.7	1.7	1.17	1	9	10148	12.3	1141	1512
00GNX 58-1	0.1	0.04	2.45	0.89	11.5	0.2	2.90	0.07	0.4	1.2	2.20	9	5	4731	9.8	1880	442
00GNX 58-2	1.2	0.20	7.06	0.07	5.0	0.2	5.53	0.14	0.9	10.2	1.56	1	18	22911	83.6	1763	2034
00GNX 60-1	0.9	0.89	1.40	0.02	6.8	0.2	3.37	0.09	0.7	7.5	0.60	1	5	6432	67.3	1790	3018
00GNX 60-2	0.5	0.12	1.07	0.02	7.4	0.1	0.85	0.04	0.8	1.6	0.33	2	6	2546	30.4	1050	585
00GNX 61-1	0.8	0.16	1.31	0.12	6.4	0.2	5.09	0.05	0.8	2.0	0.15	1	5	3523	13.3	271	549
00GNX 61-2	0.6	0.51	1.13	0.02	6.6	0.1	1.39	0.05	0.9	3.0	0.28	1	7	2792	54.2	999	2289
Std SU1a	27.0	2.97	3.86	0.37	5.1	0.3	1.64	0.18	3.7	23.6	1.65	25	5	2852	100.9	134	363
Rec. Value*														4300	150.0	410	370
Std DS2	59.5	9.38	11.22	1.87	6.2	0.1	10.19	5.09	25.1	2.3	1.86	2	235	257	193.9	2	10
Rec. Value**	58.0	9.50	10.92	1.87	6.0	0.0	10.45	5.25	25.2	2.3	1.90	1.5	239	258	208.4		
RSD %***	4.1	3.40	3.50	2.90	3.6	0.0	2.90	6.20	3.5	4.3	3.80	46.9	4.5	3.0	10.0		
DTL****	0.1	0.02	0.02	0.02	0.0	0.1	0.01	0.02	0.0	0.1	0.02	1	5	2	0.2	2	10

Analytical method: 1g sample powder (-150 mesh, W-carbide mill) dissolved in 6 ml HCl-HNO3-H2O (2:2:2) at 95°C and diluted to 20 ml prior to ICP-MS/ES analysis.
Sample locations given in Table A2 (Appendix). "Near-total" leach: Au, Ag, As, Bi, Cd, Co, Cu, Ni, Mo, Pb, Sb, Se, Te, Tl, Zn, Hg, Ge, Re, Sn, Pt, Pd.
Partial loss due to volatilization: As, Sb. Partial leach for remaining elements.
Abbreviations: Hb, hornblende; Bi, biotite; Cpx, calcic clinopyroxene; Qz, quartz; Ap, apatite; Mt, magnetite; Hm, hematite; S, sulphide; Ep, epidote; Ab, albite; Kf, potassium feldspar; Ms, muscovite; Ser, sericite; Act, actinolite-tremolite; f, feldspathic; cpxite, clinopyroxenite; hbite, hornblendite; apatite grain size given in millimetres. r = replicate analysis.
* Steger and Bowman (1980) except Au **In-house standard, Acme Analytical Laboratories *** Relative standard deviation **** Detection limit
ppm, parts per million ppb, parts per billion

TABLE 8
LITHOGEOCHEMICAL ASSAYS FOR PLATINUM-GROUP ELEMENTS IN DIAMOND DRILL HOLE 97-21, DOBBIN MAIN COPPER ANOMALY

		ppb								g
Sample	Method*	Os	Ir	Ru	Rh	Pt	Pd	Au	Re	Mass
00GNX53-2	INAA	19	1.9	<5	2.6	424	282	63	<5	50
00GNX 53-2	FA				<5	411	321			15
00GNX 53-2	ICP-MS					437	375	76	1	1
00GNX 53-2dup	ICP-MS					443	353	101	1	1
00GNX55-2	INAA	6	0.7	<5	1.4	379	201	4.4	<5	50
00GNX 55-2	FA				<5	397	264			15
00GNX 55-2	ICP-MS					397	299	3	1	1
00GNX 56-1	FA				<5	233	131			15
00GNX 56-1	ICP-MS					295	185	2	1	1
00GNX56-2	INAA	<2	<0.1	<5	0.3	39	40	3.9	<5	50
00GNX 56-2	FA				<5	15	41			15
00GNX 56-2	ICP-MS					27	60	14	1	1
00GNX 57-1	FA				5	628	881			15
00GNX 57-1	ICP-MS					493	882	2	1	1
Standards										
SARM-7	INAA	63	73	430	235	3710	1500	310	<5	10
SARM-7dup	INAA	65	73	420	245	3750	1550	310	<5	10
Rec. Value**		63	74	430	240	3740	1540	310		
INAA DTL		2	0.1	5	0.2	5	2	0.5	5	

		ppb								g
Method*	Sample	Os	Ir	Ru	Rh	Pt	Pd	Au	Re	Mass
INAA	00GNX57-2	15	1.8	<5	4	1150	929	67	<5	50
FA	00GNX 57-2				<5	1185	1647			15
FA	00GNX 57-2dup				<5	1205	1345			15
ICP-MS	00GNX 57-2					1141	1512	12	1	1
FA	00GNX 58-1				<5	1922	353			15
ICP-MS	00GNX 58-1					1880	442		9	1
INAA	00GNX58-2	560	7.3	<5	7	2550	1378	91	<5	50
FA	00GNX 58-2				13	2648	1928			15
ICP-MS	00GNX 58-2					1763	2034	84	1	1
FA	00GNX 60-1				17	3319	2650			15
ICP-MS	00GNX 60-1					1790	3018	67	1	1
FA	00GNX 60-2				5	1789	588			15
ICP-MS	00GNX 60-2					1050	585	30	2	1
	Standards									
FA	FA-10R				103	480	498			15
	Rec. Value***				100	500	500			
	FA DTL				5	1	1			
ICP-MS	SU1a					134	363	101		1
	Rec. Value****					410	370	150		
	ICP-MS DTL					2	10	0.2		

* INAA, Instrumental Neutron Activation Analysis using NiS fire assay preconcentration, Activation Laboratories Ltd., Ancaster, Ontario; FA, fire assay preconcentration using Au inquart and Inductively-coupled plasma (ICP) finish, Acme Analytical Laboratories Ltd., Vancouver; ICP-MS, ICP mass spectrometry and emission spectroscopy analysis using an aqua regia digest, Acme Analytical Laboratories Ltd., Vancouver. ppb, parts per billion dup, duplicate analysis
** Steele *et al.* (1975) *** In-House standard **** Steger and Bowman (1980) except Au DTL, Detection limit

Notwithstanding the reservations outlined above, the results for surface samples reveal some interesting trends. In general, the highest overall abundances of sulphur (1.2-2.5 wt. %), Mo (8-48 ppm), Re (3-47 ppb) and Ag (202-629 ppb), and the highest abundance of Cu (263 ppm), Pb (28 ppm) and As (15 ppm) in any one sample are found in altered sulfide-bearing metasedimentary rocks and calc-silicate skarns near the contacts of the calc-alkaline Mt. Sandberg and northern plutons, and a related monzonitic dike at Tadpole Lake which intrudes the Harper Ranch Group near the northern margin of the alkaline complex. Pt and Pd in all these rocks are near or below detection limits and pyritic quartz veins cutting Whiterocks leucocratic quartz monzonite are metal poor. Interestingly, despite low abundances of sulphur (~200-500 ppm), clinopyroxenites and hornblendites from the northern cupola (*i.e.* excluding biotite clinopyroxenite sample 00GNX-13-5-2 from the southern cupola) have weak but anomalous enrichments in Cu (71-183 ppm), Zn (63-157 ppm), Pd (17-38 ppb) and Au (2.4-12 ppb), and low abundances of Mo and Re, and also have relatively low Ag. It is important to note that these rocks are among the freshest samples collected and seem to be free of hydrothermal veining. Thus, the metal signatures in the surface lithogeochemistry, though subtle, appear to indicate contrasting elemental associations: a Cu-Pd (-Zn±Au) association which appears to be a primary magmatic fingerprint related to ultramafic lithologies of the alkaline complex; and a Mo-Re (-Ag±Cu±Pb±As) association related to the calc-alkaline stocks.

Comparison of Platinum-Group-Element Assays

In addition to ICP-MS analysis, a subset of sulfide-enriched samples from drill core was selected for analysis by fire assay for Pt, Pd and Rh using a 15g sample aliquot and Au inquart (Acme Analytical Laboratories Ltd.), and by neutron activation (Activation Laboratories, Ancaster, Ontario) using nickel sulfide preconcentration for PGE, Re and Au . In particular, hole DDH97-21, which consistently yielded anomalous abundances of Pd (0.41 g/t) and Pt (0.35 g/t) over 111 m, was re-sampled. The analyzed samples represent small widths of core (~10 cm) with relatively abundant disseminated and veins of sulfide in a fairly uniform host (biotite- and hornblende-bearing clinopyroxenite ± feldspar). The analytical results are given in Table 8 and sample locations are listed in the Appendix (Table A2).

It is evident that the various analytical techniques appear to give reasonable reproducibility for Pt and Pd at lower concentrations, but are notably erratic for samples enriched in PGE (>1000 ppb) with three out of five samples yielding anomalously low Pt abundances by acid digestion relative to fire assay. All samples, however, are distinctly enriched in PGE with the highest assays in any one sample (00GNX60-1) reaching 3.3 g/t Pt, 2.6 g/t Pd and 17 ppb Rh. Another sample (00GNX58-2) has highly anomalous Os (560 ppb) and 7 ppb Ir. The abundances of Au are low (<101 ppb) and Re is at or below the detection limit (except 00GNX58-1 with 9 ppb). These results confirm the highly anomalous concentrations of Pt and Pd reported by Verdstone/Molycor from hole DDH97-21 over a substantial width (>100 m) of ultramafic hostrock, and are particularly encouraging with respect to the potential for identifying platinum-group minerals.

MINERALIZATION

Mineralization in the Whiterocks complex occurs in the form of chalcopyrite, magnetite, pyrite, and minor bornite and is primarily hosted by hornblende-bearing clinopyroxenite with scattered sulfide showings in biotite clinopyroxenite and melanocratic monzonite-syenite. As noted previously, the most significant metal-rich area is the "main copper anomaly" near the southwestern margin of the northern cupola (Figure 2).

Mehner (1982) observed that the copper mineralization occurs as both disseminated sulfides and in stringers and fractures associated with epidote and, less commonly, amphibole and minor chlorite. He noted a strong association between magnetite and sulfides in the pyroxenites, and pointed out that grains of magnetite, chalcopyrite and pyrite were commonly found interstitial to clinopyroxene and as inclusions within poikilitic amphibole ("ferrohastingsite") which replaces clinopyroxene. These textural observations, among others, lead Mehner to conclude that the mineralization was related to the intrusion of a sulphur- and copper-enriched "evolved" melt composition which crystallized amphibole (replacing pyroxene), plagioclase, potassium feldspar and sulfides. Sulfide veins and stringers cutting biotite clinopyroxenite and melanocratic monzonite-syenite were related to this intrusive event, which occurred after the crystallization of clinopyroxene but prior to the emplacement of porphyritic monzonite. The conditions under which mineralization occurred were considered to be late magmatic or deuteric and coincident with the crystallization of "ferrohastingsite", hornblende and epidote. It appears that all of these observations have since been reconciled with an alkalic porphyry deposit model (MINFILE 082LSW005; *cf.* Panteleyev, 1995; Osatenko, 1979a).

Origin of the PGE: Hydrothermal or Magmatic?

Evidence for a hydrothermal overprint on the ultramafic and melanocratic feldspathic rocks, at least, is strong. But how does this event bear on the origin of the Cu-PGE mineralization?

There are abundant hydrothermal veins and stringers containing pyrite and lesser chalcopyrite±bornite in drill core recovered from the central copper anomaly (Kikauka, 1997). Our own observations in clinopyroxenites and feldspathic hornblendites in core from DDH97-21 have noted sulfide-bearing veins locally associated with epidote, carbonate, quartz, potassium feldspar, biotite, sericite, chlorite, magnetite, and rare hematite and garnet; and Kikauka (*ibid.*) also noticed rare traces of molybdenite in minor shear zones. Most of the vein-hosted sulfides appear to be preferentially associated with epidote, and some of the thicker veins contain a sulfide-rich core surrounded by euhedral epidote at their margins. In addition, geochemical aspects of this hydrothermal signature in the soils over this zone include interelement correlations among Cs, Cu, Mo and Ag (Dunn *et al.* this volume). Interestingly, this signature is very similar to the Mo-Re (-Ag±Cu±Pb±As) signature of hydrothermal systems related to the calc-alkaline stocks in the area, especially the Mt. Sandberg porphyry Mo prospect at Tadpole Lake. The implication is that hydrothermal alteration at the main Dobbin copper anomaly is genetically related to a *calc-alkaline* rather than an alkaline magmatic source.

Despite the strong evidence for hydrothermal alteration, certain aspects of the mineralization are not well explained by purely considering such an origin, not the least of which is the tenor of the PGE over such a large interval (>100m) in DDH97-21, for example, and the close association between sulfides and ultramafic lithologies. On this point, it appears possible to reconcile many of Mehner's observations, and our new results, with a magmatic origin for the Cu-PGE-bearing sulfides, albeit remobilized to variable extents by subsequent hydrothermal activity.

We have a different view of the origin of the hornblende clinopyroxenite which appears to be the most important host for the Cu-PGE mineralization. The evolution of the alkaline magma chamber progressed from the crystallization of clinopyroxene cumulates through hornblende-rich feldspathic cumulates to melanocratic monzonites. Because of the intercalated nature of these lithologies, at least locally, evolution of the magma chamber was evidently punctuated by fresh incursions of more primitive parental magma. The large poikilitic crystals of hornblende in this rock were formed by adcumulus growth of amphibole as calcic clinopyroxene reacted with the liquid at *high* (magmatic) temperatures. Textural evidence for the latter reaction includes the subhedral to rounded and resorbed habit of cumulus pyroxene and the patchy to vermicular replacement by amphibole. Furthermore, it is this reaction that is ultimately responsible for the elimination of clinopyroxene (except as a relict phase) in the more differentiated rocks. Cumulus hornblende crystallized in the melt prior to the disappearance of clinopyroxene and formed the minor hornblendite and hornblende gabbro/diorite lithologies encountered near the clinopyroxenite – melanocratic monzonite transition. Accessory phases such as apatite and magnetite attain their maximum grain sizes and modal abundances in hornblende clinopyroxenites and clinopyroxene hornblendites, and occur as both cumulus and intercumulus minerals; whereas plagioclase in feldspathic variants is only observed as an intercumulus phase and is considered to represent crystallization of trapped residual melt. Both magnetite and apatite are intimately associated with Cu-PGE mineralization in DDH97-21.

As originally described by Mehner (1982), disseminated Cu-PGE sulfides in the clinopyroxenites are commonly enclosed by hornblende and also occur as interstitial grains accompanied by magnetite and apatite. Although not conclusive, such textures are consistent with those commonly attributed to sulfide immiscibility in silicate melts. If one accepts the textural evidence as indicative of a magmatic heritage, an explanation is required for the composition of the sulfides, which are copper-rich as opposed to nickeliferous. In this regard, the most important control on sulfide composition at the onset of immiscibility is the composition of the coexisting silicate melt.

Although accumulative in origin, the pyroxenites are depleted in MgO, as well as Ni and Cr (Table 6 and Mehner, 1982), and, therefore, crystallized from a fractionated mafic parental melt already depleted in these highly compatible elements. The fact that Ni is compatible in early crystallizing silicate minerals and Cu is relatively incompatible has been a fundamental tenet of modern interpretation in igneous petrology. The behaviour of PGE with respect to mafic silicates has been controversial, but interpretations do exist which indicate that Pd is also incompatible in early crystallizing silicates (*e.g.* Barnes and Naldrett, 1986). Thus, a magma evolving by crystal fractionation would be expected to concentrate Cu, and potentially Pd, in mafic residual liquids up to the point of sulfide immiscibility. Since Whiterocks clinopyroxenites are the predominant host of disseminated sulfides and have the highest copper abundances (6-357 and averaging 142 ppm Cu for biotite clinopyroxenites; 129-5550 ppm and averaging 853 ppm Cu in hornblende clinopyroxenites; Mehner, 1982), melts that crystallized the clinopyroxenites must also have achieved sulfide saturation.

It is also possible to explain the tenor of PGE in these sulfides by appealing to igneous processes of the type which were evidently operating in these alkaline magma chambers. Given the evidence cited above for magma chamber replenishment early in the evolution of the alkaline suite, and the widespread indications of convective activity in the form of igneous laminations, including rare examples in the pyroxenites where recognition of such textures usually requires thin-section examination, it is evident that the Whiterocks alkaline rocks evolved in dynamic magma chambers. Under these conditions, small amounts of immiscible sulfide droplets would have been well distributed throughout the magma chamber and exposed to many times their own mass of silicate melt, and in addition, would have come into contact with new batches of metal-enriched, more primitive magma. Such an environment would have been conducive for increasing the tenor of PGE in the sulfide droplets, especially the anomalous abundances of Pt which accompany Pd, given the extremely high partitioning of PGE into sulfide melts.

In conclusion, it is emphasized here that the inferences given above regarding a magmatic origin for Cu-PGE mineralization in the Whiterocks alkaline complex represent a working hypothesis only. Whether or not in fact PGE enrichment actually relates to such an origin remains to be adequately tested by detailed study of the textures and compositions of coexisting oxides, sulfides and silicates, as well as any platinum-group minerals that may be present. If a magmatic heritage for the Cu-PGE association is ultimately considered more likely than a purely hydrothermal origin, there are important implications not only for local controls on mineralization (*i.e.* lithologic and potentially stratigraphic rather than structural) but also for similar base-metal - PGE associations in other alkaline complexes in British Columbia and elsewhere.

ACKNOWLEDGMENTS

We would like to extend our appreciation to the directors of Verdstone Gold Corporation and Molycor Gold Corporation, in particular John Fisher, Larry Reaugh and John Chapman, for freely sharing information on the geology of the Whiterocks complex and allowing us to sample drill core. Sincere thanks to Andris Kikauka for providing geological data and samples of drill core, and for many discussions concerning the Dobbin property. Dave Lefebure and Colin Dunn are thanked for their interest and field visits, and Dave Lefebure for his constructive and timely review of the manuscript.

REFERENCES

Abbey, S. (1979): Reference materials – rock samples SY-2, SY-3, MRG-1; *CANMET* Report 79-35, 66 pages.

Naldrett, A.J. and Barnes, S..J. (1986): The behaviour of platinum-group-elements during fractional crystallization and partial melting with special reference to the composition of magmatic sulfide ores; *Fortschritte der Mineralogie*, Volume 64, pages 113-133.

Cairnes, C. E. (1940): Kettle River (west half) map sheet; *Geological Survey of Canada,* Map 538A.

Geological Survey of Canada (1968): Aeromagnetic map of Shorts Creek, British Columbia; *Geological Survey of Canada,* Map 5207G.

Hulbert, L.J. Duke, M.J., Eckstrand, O.R., Lydon, J.W. Scoates, R.F.J., Cabri, L.J. and Irvine, T.N. (1988): Geological environments of the platinum-group elements; *Geological Association of Canada*, Cordilleran Section Workshop, Vancouver, 151 pages.

Jones, A. G., (1959): Vernon map area, British Columbia; *Geological Survey of Canada*, Memoir 296, 186 pages.

Kikauka, A. (1997): Geological, geochemical and diamond drilling report on the Dobbin claim group, Whiterocks Mountain, Kelowna, B.C; *British Columbia Ministry of Energy and Mines*, Assessment Report 25290.

Knowles, C. R. (1987): A basic program to recast garnet end-members; *Computers and Geosciences*, Volume 13, pages 655-658.

Leake B.E., Woolley, A.R., Arps, C.E.S., Birch, W.D., Gilbert, M.C., Grice, J.D.,Hawthorne, F.C., Kato, A., Kisch, H.J., Krivovichev, V.G., Linthout, K., Laird, J., Mandarino, J.A., Maresch, W.V., Nickel, E.H., Schumacher, J.C., Smith, D.C., Stephenson, N.C.N., Ungaretti, L., Whittaker, E.J.W., and Youzhi, G. (1997): Nomenclature of amphiboles: report of the subcommittee on amphiboles of the International Mineralogical Association, Commission on New Minerals and Mineral Names; *Canadian Mineralogist*, Volume 35, pages 219-246.

Little, H. W. (1961): Kettle River, west half map area; *Geological Survey of Canada*, Map 15-1961.

Makepeace, D. K. (2000): Summary review of the Dobbin property, Tadpole Lake area, Vernon and Nicola Mining Divisions, British Columbia, Canada; Internal Report for Verdstone/Molycor Gold Corporations, Surrey, British Columbia, 48 pages.

Mehner, D. T. (1982): Geology of the Whiterocks Mountain alkalic complex, South-central British Columbia; unpublished M.Sc. thesis, *University of Manitoba*, 89 pages.

Morimoto, N. (1989): Nomenclature of pyroxenes; *Canadian Mineralogist*, Volume 27, pages 143-156.

Nixon, G.T. Hammack, J.L., Ash., C.H., Cabri, L.J., Case, G., Connelly, J.N. Heaman, L.M., Laflamme, J.H.G., Nuttall, C., Paterson, W.P.E. And Wong, R.H. (1997): Geology and platinum- group-element mineralization of Alaskan-type ultramafic-mafic complexes in British Columbia; *Ministry of Energy and Mines*, Bulletin 93, 142 pages.

Okulitch, A.V. (1979): Geology and mineral occurrences of the Thompson-Shushwap-Okanagan region, south-central British Columbia.

Okulitch, A.V. (1989): Revised stratigraphy and structure in the Thompson-Shuswap-Okanagan map area, southern British Columbia; *Geological Survey of Canada*, Paper 89-1E, pages 51–60.

Osatenko, M.J. (1978): Geological; stream silt, rock and soil geochemical and ground magnetics work on the Dobbin property (Tad 1-6); *British Columbia Ministry of Energy and Mines*, Assessment Report 6732.

Osatenko, M.J. (1979a): Geological; ground magnetics, I.P.; rock and silt geochemical and percussion drilling work on the Dobbin property (Tad 1-6); *British Columbia Ministry of Energy and Mines*, Assessment Report 7269-1.

Osatenko, M.J. (1979b): Assessment report of geology, soil geochemisty, percussion and diamond drilling on the Dobbin property (Tad 1-3, Tad 5-12, Tad 14, Tad 19 and Esperon 11 claims), Tadpole Lake, Vernon and Nicola M. D.; *British Columbia Ministry of Energy and Mines*, Assessment Report 7596.

Osatenko, M.J. (1980): Assessment Report of Percussion Drilling on the Dobbin Property (Tad 1-12, Tad 14, Tad 19-22 claims), Tadpole Lake Area, Vernon and Nicola M. D., B.C.; *British Columbia Ministry of Energy and Mines*, Assessment Report 8456.

Panteleyev, A. (1995): Porphyry Cu-Au alkalic (L03); in Selected British Columbia Mineral Deposit Profiles Volume 1 – Metallics and Coal, Lefebure, D.V. and Ray, G.E., editors, *B.C. Ministry of Energy and Mines*, Paper 1995-20, pages 83-86.

Robinson, P., Spear, F.S., Schumacher, J.C., Laird, J., Klein, C., Evans, B.W. and Doolan, B.L. (1981): Phase relations of metamorphic amphiboles: natural occurrence and theory; *Mineralogical Society of America* Reviews in Mineralogy, Volume 9B, pages 1-228.

Steger, H.F. and Bowman, W.S. (1980): SU1a: a certified nickel-copper-cobalt reference ore; *CANMET* Report 80-9E, 25 pages.

Steele, T.W. (1975): Preparation and certification of a reference sample of a precious metal ore; *National Institute for Metallurgy* (South Africa), Report 1696-1975, 50 pages.

Weeks, R.M., Bradburn, R.G., Flintoff, B.C., Harris, G.R. and Malcolm, G. (1995): The Brenda Mine: the life of a low-cost porphyry copper-molybdenum producer (1970-1990), southern British Columbia; *in* Porphyry Copper Deposits of the Canadian Cordillera, *Canadian Institute of Mining* Special Volume 46, pages 192-200.

Wilkins, A.L. (1981): K-Ar and Rb-Sr dating of the Whiterocks Mountain alkalic complex in the Intermontane Belt west of Okanagan Lake, south-central British Columbia; unpublished B.Sc. thesis, *The University of British Columbia*.

Yoder, H.S. and Tilley, C.E. (1962): Origin of basaltic magmas: an experimental study of natural and synthetic rock systems; *Journal of Petrology*, Volume 3, pages 342-532.

APPENDIX TABLE A1
WITHIN-RUN ELECTRON-MICROPROBE ANALYSES OF INTERNATIONAL STANDARDS

	Diopside			Albite		
Oxide (wt%)	s439nom (accepted)	s439 avg (measured)	% rel dev (2σ)	s430nom (accepted)	s430avg (measured)	% rel dev (2σ)
Na_2O	0.38	0.39	19.56	11.46	11.43	3.743
MgO	17.94	17.83	2.36	-	-	-
Al_2O_3	0.43	0.6	12.07	19.77	19.69	1.814
SiO_2	55.19	55.32	1.33	68.14	69.11	1.224
K_2O	-	-	-	0.23	0.12	51.999
CaO	25.18	25.38	2.64	0.38	0.08	76.64
TiO_2	0.03	0.03	-	-	-	-
Cr_2O_3		0.05	-	-	-	-
MnO	0.06	0.06	-	-	-	-
FeO	0.89	0.86	21.65	0.01	0.01	-
BaO	-	-	-	-	-	-
Total	100.10	100.49		99.99	100.43	

	Orthoclase			Anorthite		
Oxide (wt%)	s438nom (accepted)	s438avg (measured)	% rel dev (2σ)	t101nom (accepted)	t101avg (measured)	% rel dev (2σ)
Na_2O	0.91	0.95	10.929	0.03	0.07	77.477
MgO	-	0.01	-	-	-	-
Al_2O_3	16.74	16.36	1.907	36.5	36.49	1.494
SiO_2	64.8	65.24	1.227	43.3	43.62	1.406
K_2O	15.49	15.44	3.468	-	0.01	-
CaO	-	-	-	20.3	20.25	2.952
TiO_2	-	-	-	-	-	-
Cr_2O_3	-	-	-	-	-	-
MnO	-	-	-	-	-	-
FeO	2.01	1.96	13.519		0.05	-
BaO	0.05	-	-	-	-	-
Total	100.00	99.96		100.13	100.48	

s439 natural diopside standard; s430 natural albite standard; and s438 natural orthoclase standard all supplied by C.M. Taylor Company, Amelia, Virginia, U.S.A.
t101 synthetic anorthite standard, Jun Ito (pure $CaAl_2Si_2O_8$)

APPENDIX TABLE A2
SAMPLE LOCATIONS FOR ICP-MS ANALYSES

	NAD 1983	
Sample	Easting	Northing
00GNX 3-1-1	299477	5544098
00GNX 3-17-4	298672	5544979
00GNX 4-9-1	300417	5547915
00GNX 5-8-1	304359	5547277
00GNX 5-8-2	304360	5547275
00GNX 5-8-3	304360	5547276
00GNX 8-7-1	300802	5545658
00GNX 9-9-1	301170	5545058
00GNX 10-1-1	302714	5542409
00GNX 10-4-2	303773	5543018
00GNX 13-5-2	305525	5539076
00GNX 16-1-1	301897	5543695
00GNX 16-2-1	301945	5543412
00GNX 16-2-5	301945	5543412
00GNX 16-2-8	301945	5543412

	NAD 1983	
Sample	Easting	Northing
DDH97-7		
00GNX 30-1	300773	5542803
DDH97-21		
00GNX 53-1	300762	5542803
00GNX 53-2	300762	5542803
00GNX 53-2r	300762	5542803
00GNX 55-2	300762	5542803
00GNX 56-1	300762	5542803
00GNX 56-2	300762	5542803
00GNX 57-1	300762	5542803
00GNX 57-2	300762	5542803
00GNX 58-1	300762	5542803
00GNX 58-2	300762	5542803
00GNX 60-1	300762	5542803
00GNX 60-2	300762	5542803
00GNX 61-1	300762	5542803
00GNX 61-2	300762	5542803

Orientation Study of Surface Geochemical Methods to Assist in the Exploration for Platinum Group Metals in the Whiterocks Mountain Alkalic Complex, Near Kelowna, British Columbia (82L/4)

By Colin E. Dunn[1], Gwendy E.M. Hall[1] and Graham Nixon[2]

KEYWORDS: Platinum, palladium, soils, multi-element selective leach, vegetation analysis.

INTRODUCTION

The surface geochemical response to bedrock containing elevated levels of the platinum group elements (PGE) is commonly so subtle that standard geochemical methods are insufficiently sensitive to assist the exploration geologist. At the Geological Survey of Canada, recent research on analytical methods by one of us (GEMH) has been directed toward the development of a selective leach of soils and sediments that will provide improved methodology for the detection of precious metals.

Along with soils, vegetation samples were collected for analysis. In effect, trees and shrubs perform a natural selective leach of elements contained within the substrate by absorbing through their root systems the elements that they require for healthy growth, while passively tolerating certain other elements and permitting their entry into cell structures. Thus, from a study of the chemical element content of common plant species it becomes possible to map zones of mineralization that are concealed by overburden.

To these ends an orientation study was undertaken to collect soil and vegetation from the vicinity of known PGE enrichment on the Dobbin property in south-central British Columbia, to further develop the use of surficial materials in the exploration for minerals. All data presented here should be considered 'preliminary', since method development is continuing. Data from the analysis of the plant tissues are pending. The study was undertaken in conjunction with a mapping program by the third author to evaluate the geological setting of the PGE mineralization.

WHITEROCKS MOUNTAIN AREA

Location, Climate and Vegetation Cover

The survey area is located 2 kilometres west-southwest of Whiterocks Mountain, in the south central part of NTS 82L/4 (Shorts Creek), at an elevation of approximately 1750 metres, within the West Okanagan Provincial Forest. Soils are poorly developed with a thin humic layer overlying an oxidized B horizon. According to the classification of Valentine *et al*. (1978), the soils at this locality are generally humo-ferric podzols. The high-elevation forests that cover the plateaus of this region are dominated by subalpine fir (*Abies lasiocarpa),* Engelmann spruce *(Picea engelmannii)* and a few lodgepole pine *(Pinus contorta)*. Common shrubs are rhododendron (*Rhododendron albiflorum)* and blueberry *(Vaccinium spp.)*. Climate is severe with cool, short growing seasons and long, cold winters.

Local Geology

Within the small survey region the dominant rocks are biotite- and hornblende-bearing clinopyroxenites, melanocratic monzonites and microcline-porphyritic (<2.5 cm) to megacrystic (<15 cm) monzonites of the Jurassic(?) Whiterocks Mountain alkaline complex (Figure 1: lithologies 5, 4A, 4B, 3A, 3B). The geology of this part of the intrusion has been mapped in detail by Mehner (1982) and the results of new mapping elsewhere in the complex and surrounding region are presented by Nixon and Carbno (this volume). The host rocks of the intrusion are predominantly fine-grained, siliciclastic sediments with lesser carbonate and minor volcanic/volcaniclastic rocks which form part of the Devonian-Mississippian Harper Ranch Group (Figure 1: lithology 1). The PGE-enriched sulphide mineralization appears to be preferentially associated with the clinopyroxenites and with epidote albite carbonate veins that cut the ultramafic rocks. Previous workers (MINFILE 082LSW005) have related the Cu-Fe-PGE sulphides to an alkaline porphyry style of mineralization.

Mineralization and Exploration History

Mineral exploration in the Whiterocks Mountain area has been active intermittently since the beginning of the 20th century. Between 1968 and 1980, geological surveys and silt, soil and bedrock geochemical sampling conducted on the western flanks of Whiterocks Mountain successfully delineated the main copper anomalies, including the "central" Dobbin Cu-PGE anomaly

[1]*Geological Survey of Canada*
[2]*British Columbia Ministry of Energy and Mines*

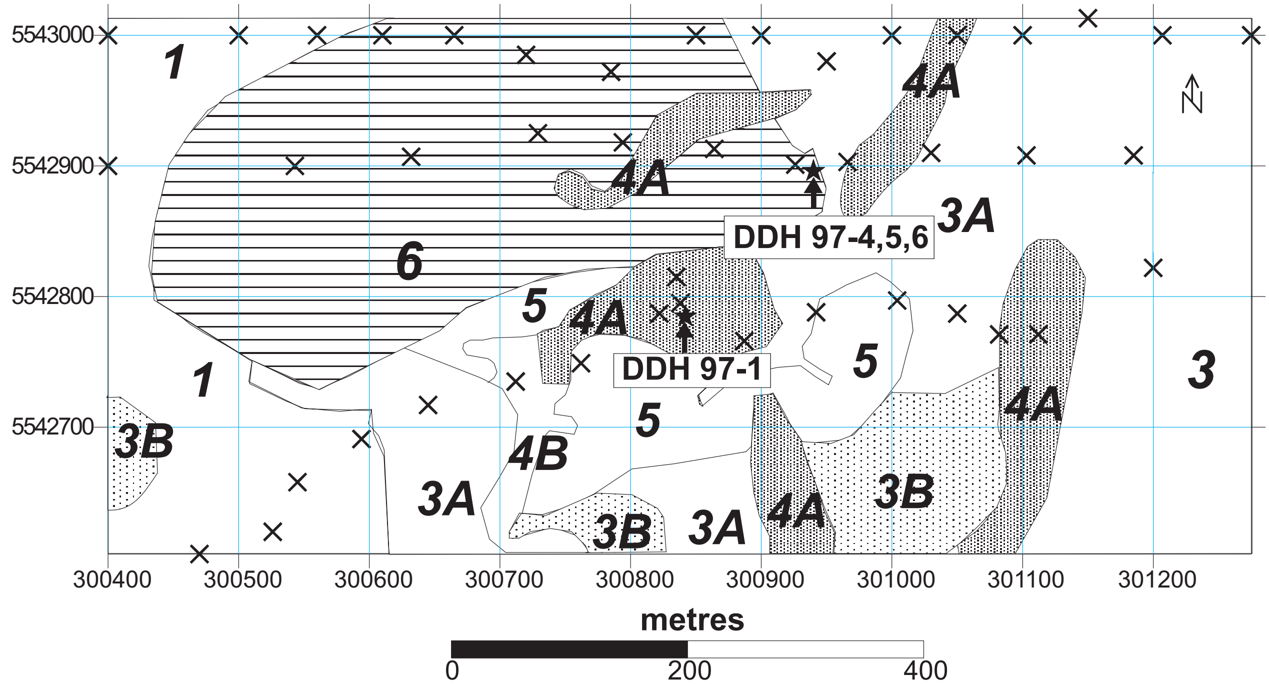

Figure 1. Geology of the Dobbin property showing selected recent drill holes and soil sample sites. Geological units modified after Osatenko (1979) and Mehner (1982): 6, porphyritic (megacrystic) monzonite (Kspar>2 cm); 5, porphyritic monzonite (Kspar <2 cm); 4A, hornblende pyroxenite; 4B, biotite pyroxenite; 3A, B, mafic monzonite and hornblende gabbro/diorite; 1, metasedimentary and metavolcanic rocks (Harper Ranch Group).

(MINFILE 082LSW005) which is the prime target of this study. Recent work by joint venture partners Verdstone Gold Corporation and Molycor Gold Corporation has established a northerly-trending zone (250 x 600 m) of Cu-enriched soils underlain by bedrock containing disseminated Cu-Fe sulphides (pyrite-chalcopyrite-bornite), which carry anomalous concentrations of PGE. Chip samples of outcrops in this zone have yielded maximum concentrations of 0.73 % Cu, 0.20 g/t Pt and 0.35 g/t Pd over widths of about 1 metre (Kikauka, 1997). Drilling that took place in 1997 encountered mineralization in diamond drill hole (DDH) 97-1, a few metres from mineralized outcrop, from 0-3 metres grading 0.21% Cu, 0.41 g/t Pt and 0.21 g/t Pd. Approximately 150 m to the northeast DDH 97-4, 5, and 6 were drilled within a few metres of each other. Hole #4 yielded grades of 0.08% Cu, 0.05 g/t Pt and 0.05 g/t Pd from depths of 3-6 m, with higher grades at greater depth. Further details of the exploration history may be found in Nixon and Carbno (this volume) and the B.C. Ministry of Energy and Mines assessment reports.

SCOPE OF SAMPLING PROGRAM

The principal intent of this orientation program was to collect approximately 50 soil samples. A total of 43 samples were collected from the vicinity of known PGE mineralization, and an additional 7 samples from 'background' sites over parts of the Whiterocks Complex considered remote (several kilometers) from known mineralization. The 43 samples were from the Dobbin claims, currently held by Verdstone Gold Corporation of Whiterock, B.C.

At each sample site a small pit was dug with a shovel, and a stainless steel trowel was used to collect sufficient B horizon soil (depth of about 20 cm) to fill a standard 'kraft' soil bag. At selected sites, 50-70 g of outer bark from Engelmann spruce was collected with a hardened-steel paint scraper and placed into a second kraft bag. In addition, at a few sites samples of twigs were snipped from subalpine fir, rhododendron and blueberry, following the collection protocols developed and described in Dunn (1999 and in press).

SAMPLE PREPARATION AND ANALYSIS

Soils

Soil samples were oven-dried at 60^{o}C, and then screened through a –80 mesh stainless steel Tyler sieve (mesh aperture of 177µm). A bulk sample of soil from a site close to subcropping mineralization was also dried, sieved, and used as a guide to analytical precision and accuracy by interspersing several portions at random through the sequence of samples. Several soil samples were split to obtain an estimate of sample precision, and the laboratory staff at the GSC inserted additional analytical quality control samples of known composition to monitor the accuracy.

Details of the selective leach that is being developed at the GSC are confidential at the present time. In general, samples are digested in an acidic leach of sufficient strength to selectively target elements associated with both hydrous Mn and Fe oxide phases, and adsorbed, exchangeable and carbonate-bound fractions. The pH of each solution is carefully controlled. Elements structurally incorporated in crystal lattices are not released. The methodology is being developed specifically to extract and stabilize the precious metals Au, Pt and Pd in the leachate for measurement at low detection limits. For this orientation phase of the work, 1 g of soil was accurately weighed, the elements extracted, and the solution analysed for 57 elements by inductively coupled plasma mass spectrometry (ICP-MS).

Vegetation

Samples were dried in an oven for 12 hours at 90°C. Foliage was then removed from twigs, and the twigs and bark were reduced to ash by controlled ignition at 470°C for approximately 12 hours. After the insertion of appropriate quality control samples, they were submitted to Activation Laboratories Ltd (Ancaster, Ontario) for digestion in aqua regia followed by analysis by ICP-MS to provide data for 60 elements. The data are pending, and will be compared with the soil selective leach data to assess which method is the more suitable and informative for PGE exploration in this environment. By comparison with previous studies of PGEs in vegetation tissues from the vicinities of PGE mineralization in British Columbia, a modest response might be expected (Dunn, 1992).

PRELIMINARY RESULTS

Table 1 shows summary statistics for the 43 soil samples from three transects that extended from background sites, across subcropping PGE mineralization, and back into background. The last column to the right shows average values from seven background sites several kilometres from the survey area. In general, the median values from the survey area are similar to the mean values from the seven background sites, indicating that samples from many of the survey sites were from unmineralized ground. Exceptions are higher Cu, Cs, Br and I from survey area suggesting that these elements were associated with the mineralizing event and might be of value as pathfinder elements. At background sites, levels of Ca, Mg, Rb, Sr, Mn and the rare earth elements (REE) are higher, presumably reflecting the typically more elevated levels of these elements in the more felsic lithologies that predominate within the region.

The three 700–800 metre long transects (43 sites) were designed to sample at intervals of approximately 50 metres across zones known to contain Pt and Pd. A sketch of soil sample sites (Figure 1) shows the geology and the locations of drill holes that have intersected significant mineralization.

Elements that show the greatest anomaly to background contrast near known zones of mineralization are Pt, Bi, Ag, Cu, Mo. Dots proportional in size to concentrations of Pt, Bi and Ag (Figure 2) and Cu, Mo and Pb (Figure 3) are superimposed on data that have been contoured, using a natural neighbour plotting method ('Surfer' software), at percentile intervals of 50, 70, 80 and 90. Comparison of the dot patterns with the sample sites that are shown on Figure 1 permits the relationship of element concentrations to underlying lithology to be observed.

Element concentrations are lower than those that typically occur in analyses of soils by an aqua regia leach, because the method employed for this study is selective in its attack on the soil particles. The leach extracts only that portion of an element that is readily released (details above). Figure 2 shows that the highest Pt concentration, although only 2.5 ppb, occurs close to DDH97-1 (center of the map, and see Figure 1). The contoured plot of Pt indicates that the zone with values greater than the 80th percentile occurs to the north and northwest from this site that includes an area that has not been drill tested. Distribution patterns of Bi and Ag also show relatively high concentrations close to DDH97-1, with modest enrichment northeastward from DDH97-4, 5 and 6. Figure 3 shows that most of the highest concentrations of Cu, Mo and Pb occur in the northeast part of the survey area, east of DDH 97-4, 5 and 6. Lead values are highest close to the drill hole locations. Elements commonly associated with PGE enrichment in ultramafic rocks include Ni, Co, Cr, and Mg, but none of these exhibit relative enrichment in the leachates of soils from these sites. Therefore, for this style of mineralization, they are of limited use as pathfinders for PGE by this analytical method. A brief review of the distribution patterns of the other elements indicates that, with the exception of Cs, none are of obvious value as pathfinders for the PGEs. Cesium, however, exhibits a similar distribution pattern to the other elements shown in Figures 2 and 3, and especially to those of Cu, Mo and Ag. As stated above, the analytical methodology, especially data for Pd, needs refining before conclusions are drawn as to its value in delineating enrichments of PGE in the substrate. Preliminary indications are encouraging.

CONCLUSIONS

The analytical methodology currently under development, especially the analysis for Pd, needs refining before conclusions are drawn as to its value in delineating enrichments of PGE in the substrate. Preliminary indications from the Dobbin property in south-central British Columbia are encouraging. Compared to background sites, there is a general slight enrichment of Br and I in soil samples from the Dobbin property. Subtle enrichments of Bi, Ag, Mo, Cu, Pb and Cs appear to be associated with known Cu-PGE mineralization, thereby providing a multi-element signature that may assist in delineating mineralized zones concealed by overburden.

TABLE 1
SELECTIVE LEACH OF SOILS – STATISTICS

	D.L.	Mean	Std. Dev.	Minimum	Percentiles					Maximum	*Mean Bkgrd-7 sites*
					25	*50*	*70*	*80*	*90*		
Pd ppb*	*2*	2.07	1.57	1	1	1	2.96	3.52	4.56	7	*1.00*
Pt ppb	*0.1*	0.715	0.394	0.2	0.52	0.61	0.80	0.92	1.25	2.5	*0.57*
Au ppb	*0.1*	0.641	0.304	0.3	0.42	0.59	0.75	0.934	1.06	1.7	*0.52*
Ag ppb	*2*	179	121	46	98	139	200	263	305	553	*122*
As ppb	*40*	421	200	204	286	375	465	543	627	1331	*337*
Be ppb	*2*	201	64	68	171	185	208	242	302	407	*164*
Bi ppb	*4*	153	149	47	86	116	145	182	273	914	*247*
Br ppb	*1600*	2589	1618	800	800	2235	3161	3972	4780	7551	*1320*
Cd ppb	*8*	129	122	39	63	91	125	155	257	603	*73*
Ce ppb	*4*	6271	2970	1493	3938	5511	8675	10042	10465	13218	*9750*
Cs ppb	*4*	584	744	28	164	234	567	808	1798	3277	*167*
Dy ppb	*2*	454	272	91	248	378	539	670	787	1403	*666*
Er ppb	*2*	231	157	40	107	183	292	362	417	852	*323*
Eu ppb	*2*	141	87	35	75	112	169	210	253	413	*231*
Gd ppb	*2*	609	400	123	308	458	741	949	1108	2001	*990*
Ho ppb	*2*	82	54	14	43	66	103	126	145	282	*117*
I ppb	*600*	3480	1488	300	2650	3493	4119	4528	5304	7945	*2036*
In ppb	*4*	9	2	6	8	9	10	10	10	15	*9*
La ppb	*4*	3111	2196	779	1666	2326	3310	3991	7126	10413	*4161*
Li ppb	*2*	293	353	96	143	176	240	296	670	2134	*278*
Lu ppb	*2*	24	19	3	10	18	30	36	45	109	*30*
Mo ppb	*20*	128	191	10	36	74	110	159	255	1157	*116*
Nd ppb	*2*	2821	1939	573	1403	2122	3293	4139	5683	9420	*4503*
Pb ppb	*4*	3500	1113	1389	2799	3362	3859	4185	4798	7610	*3185*
Pr ppb	*2*	719	486	151	365	530	827	1074	1487	2424	*1068*
Rb ppb	*20*	2232	1034	701	1414	1878	2763	3190	2232	4595	*3134*
Re ppb	*2*	1	0	1	1	1	1	1	1	1	*1*
Sb ppb	*4*	17	7	4	12	17	20	21	26	33	*13*
Se ppb	*400*	220	105	200	200	200	200	200	200	864	*228*
Sm ppb	*2*	559	357	111	301	441	666	837	1012	1751	*966*
Tb ppb	*2*	91	55	17	50	70	112	142	163	275	*142*
Th ppb	*2*	83	55	1	49	70	107	122	145	269	*120*
Tl ppb	*2*	18	11	5	12	17	20	24	28	74	*13*
Tm ppb	*2*	29	20	4	13	23	38	43	54	108	*36*
U ppb	*2*	248	104	91	179	214	272	323	391	621	*259*
Y ppb	*4*	2142	1763	324	917	1560	2696	3350	3974	10321	*2810*
Yb ppb	*2*	173	124	25	80	146	218	249	321	696	*223*
Al ppm	*4*	7141	2401	2623	5650	6896	8342	9237	9929	14889	*5976*
B ppm	*0.1*	0.6	0.3	0.4	0.5	0.6	0.7	0.9	1	1.5	*0.4*
Ba ppm	*0.2*	47	29	17	29	40	52	60	87	157	*69*
Ca ppm	*4*	1858	2115	86	364	958	2031	3381	5362	8874	*3022*
Co ppm	*0.02*	3	4.7	0.2	0.9	2	2.8	3.9	5.5	31	*2.7*
Cr ppm	*0.02*	1.9	0.6	1	1.4	1.8	2.2	2.4	2.8	3.4	*2*
Cu ppm	*0.04*	43	116	3	5	12	25	40	69	707	*6*
Fe ppm	*1*	4086	1140	2329	3154	3925	4664	4987	5953	6642	*3470*
K ppm	*2*	165	76	71	102	150	195	235	266	372	*173*
Mg ppm	*1*	221	438	17	55	92	173	257	478	2825	*271*
Mn ppm	*1.0*	199	147	12	77	160	273	294	427	657	*207*
Na ppm	*1*	22	6	11	19	22	24	25	29	43	*20*
Ni ppm	*0.04*	1.1	1.2	0.2	0.5	0.9	1.1	1.4	2.1	7.8	*0.8*
P ppm	*10*	510	476	110	217	343	551	710	1122	2382	*1198*
Sc ppm	*0.02*	0.02	0.01	0.01	0.01	0.01	0.02	0.03	0.04	0.05	*0.10*
Si ppm	*4*	1459	796	328	922	1338	1732	2002	2429	3933	*1411*
Sr ppm	*0.02*	9	10	1	2	5	10	15	22	43	*24*
Ti ppm	*0.4*	34	14	20	26	31	37	40	47	107	*39*
V ppm	*0.04*	11	5	5	8	10	13	14	18	26	*9*
Zn ppm	*0.1*	8.2	5.4	1.8	4.1	7	10	11	18	24	*5*

**Data for Pd are preliminary and subject to modification. DL= detection limit: for computational purposes values below DL were taken at half DL. Data for Pd and Pt are shown first, followed by elements with concentrations in ppb then elements in ppm.*

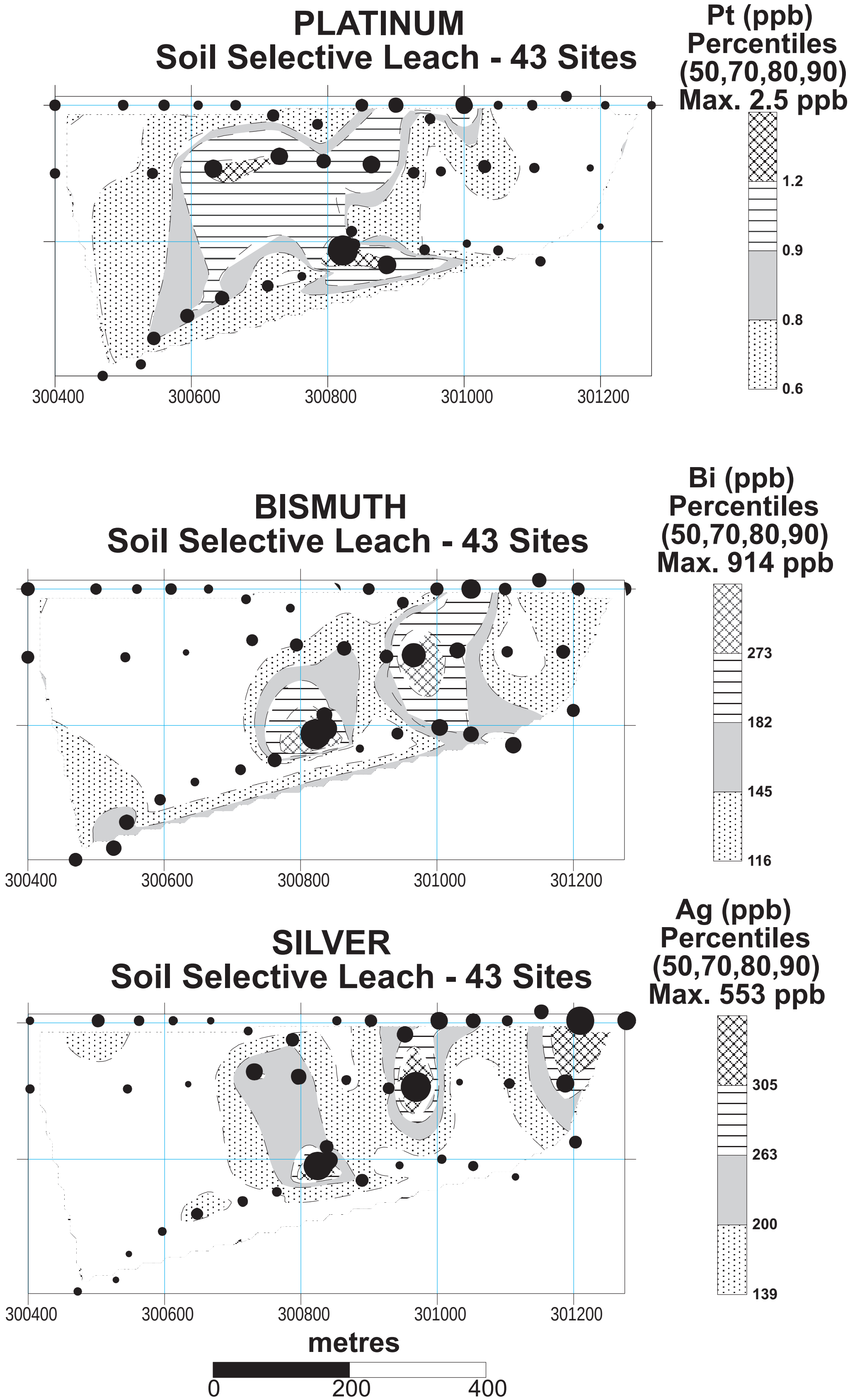

Figure 2. Platinum, bismuth and silver values derived from a selective leach of soils. Values contoured as percentiles and overlain with dots proportional to concentrations.

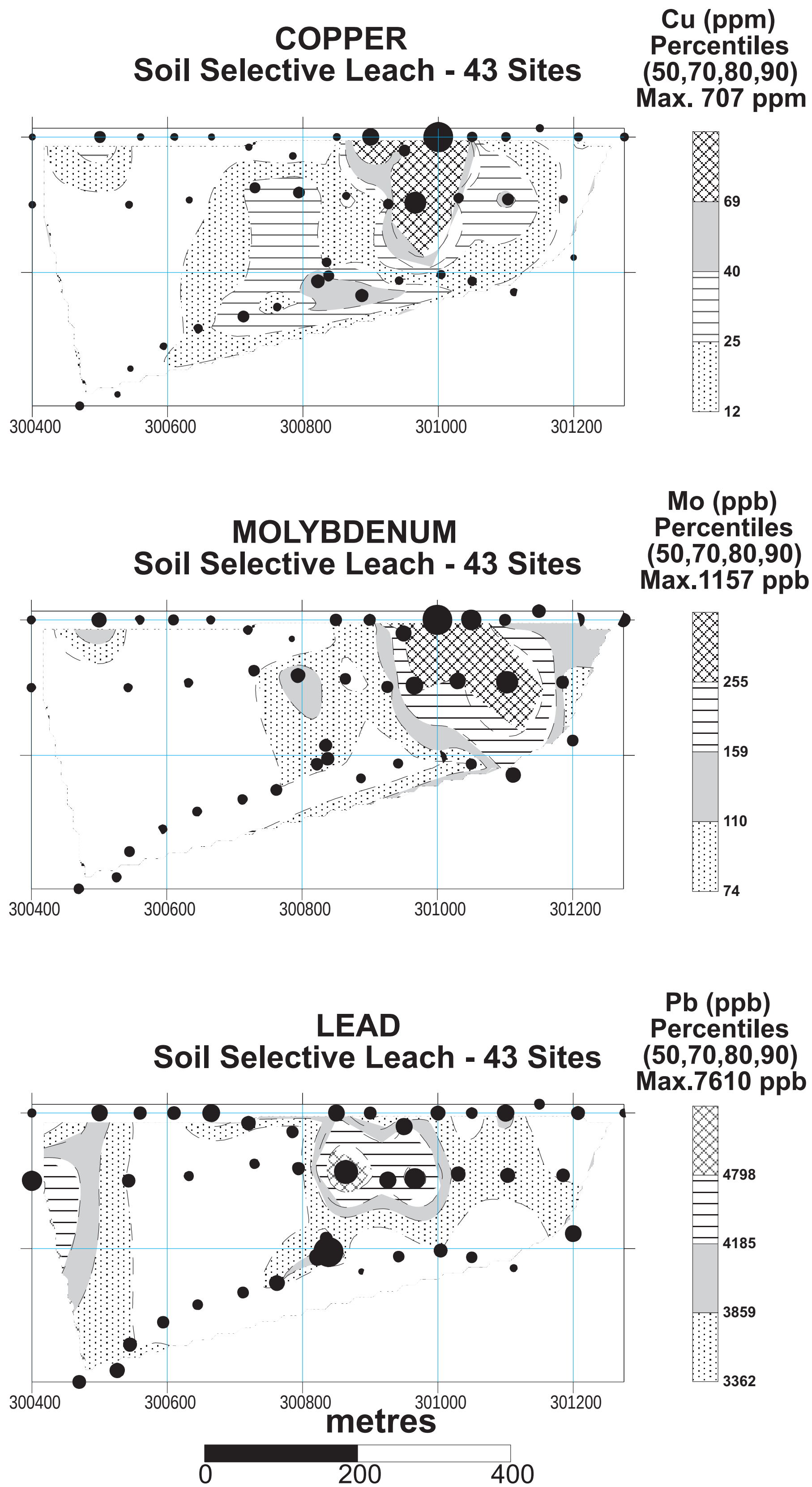

Figure 3. Copper, molybdenum and lead values derived from a selective leach of soils. Values contoured as percentiles and overlain with dots proportional to concentrations.

REFERENCES

Dunn, C.E., (1992). Biogeochemical exploration for deposits of the noble metals. Chapter 3 in: Noble Metals and Biological Systems (Ed. R.R. Brooks), *CRC Press,* Boca Raton, FL, pages 47-89.

Dunn, C.E., (999). Biogeochemical exploration methods in the Canadian Shield and Cordillera. 19th International Geochemical Exploration Symposium, Vancouver, *Association of Exploration Geochemists*, Short Course Notes.

Dunn, C.E. (in press). Biogeochemical exploration methods in the Canadian Shield and Cordillera. *Geochemistry: Exploration, Environment, Analysis*.

Kikauka, A. (1997): Geological, geochemical and diamond drilling report on the Dobbin Claim Group, Whiterocks Mountain, Kelowna, B.C; *British Columbia Ministry of Energy and Mines*, Assessment Report 25290.

Makepeace, D. K. (2000): Summary review of the Dobbin Property, Tadpole Lake Area, Vernon and Nicola Mining Divisions, British Columbia, Canada; Internal Report for Verdstone/Molycor Gold Corporations, Surrey, British Columbia, 48 pages.

Mehner, D. T. (1982): Geology of the Whiterocks Mountain Alkalic Complex, South-central British Columbia; unpublished M.Sc. thesis, *University of Manitoba,* 89 pages.

Valentine, K.V., Sprout, P.N., Baker, T.E. and Lavkulich, L.M., (1978): The soil landscapes of British Columbia, *B.C. Ministry of Environment*, Resource Analysis Branch, 197 pages.

Prospective Areas for Intrusion-Related Gold-Quartz Veins in Southern British Columbia

By James M. Logan

INTRODUCTION

Cretaceous granitic rocks can be traced the length of the northern Cordillera and are known for their association with tungsten and tin mineralization. In Alaska and Yukon the mid-Cretaceous Tombstone Suite intrusions are also associated with base metal-poor, gold-bismuth mineralization, including the Fort Knox (127.5 x 10^6 g Au), Dublin Gulch (35.7 x 10^6 g Au) and Brewery Creek deposits (28.7 x 10^6 g Au) (Figure 1). Similar, smaller intrusion-related gold-quartz vein occurrences (*i.e.* Valparaiso and Cam-Gloria) are located in southern British Columbia associated with the mid-Cretaceous Bayonne Suite (Logan, 2000). In contrast with the metaluminous, subalkalic, reduced I-type Tombstone Suite, the Bayonne suite consists of mostly peraluminous, subalkalic hornblende-biotite granodiorite and highly fractionated 2-mica granites, aplites and pegmatites. These, like there northern counterparts, are emplaced into miogeoclinal rocks of ancestral North America and the Shuswap and Kootenay terrane pericratonic rocks.

The first year's field studies focused on two intrusion-hosted gold-quartz systems in southern BC, the Cam-Gloria and Valparaiso. The former is now known to be hosted in a Middle Jurassic intrusion located 7.5 km from (peripheral to) the causative Cretaceous intrusion/mineralizing system. This summer, fieldwork continued mapping and deposit studies in the southern Omineca belt and attempted to assess gold-bismuth±tungsten±copper systems hosted in mid to high-grade metamorphic rocks located peripheral or proximal to mid-Cretaceous intrusions. Fieldwork was carried out east of the Columbia River Fault in the Selkirk Mountains and north of Shuswap Lake between Baldy Batholith and the Monashee décollement. These two areas were selected for follow-up from a subset of prospective areas recognized as favorable to host intrusion-related gold-tungsten-bismuth veins by Lefebure *et al.* (1999).

In the Selkirk Mountains, Au-W quartz veins (Orphan Boy, Stanmack mineral occurrences) located on the southern flank of the northwest-trending Windy Range metamorphic culmination (Read and Brown, 1981) were visited and sampled. Tungsten-skarn, tin and molybdenum mineral occurrences in and around the Battle Range Batholith, were examined, in our ongoing effort to characterize and assess the intrusion-related gold potential of Cretaceous plutons. This multi-phase batholith, located southeast of Revelstoke, occurs at the centre of the arcuate magmatic belt of Cretaceous rocks. It links those bodies which intrude ancestral North American strata at the southeastern end (Bayonne, Mount Skelly Pluton) with

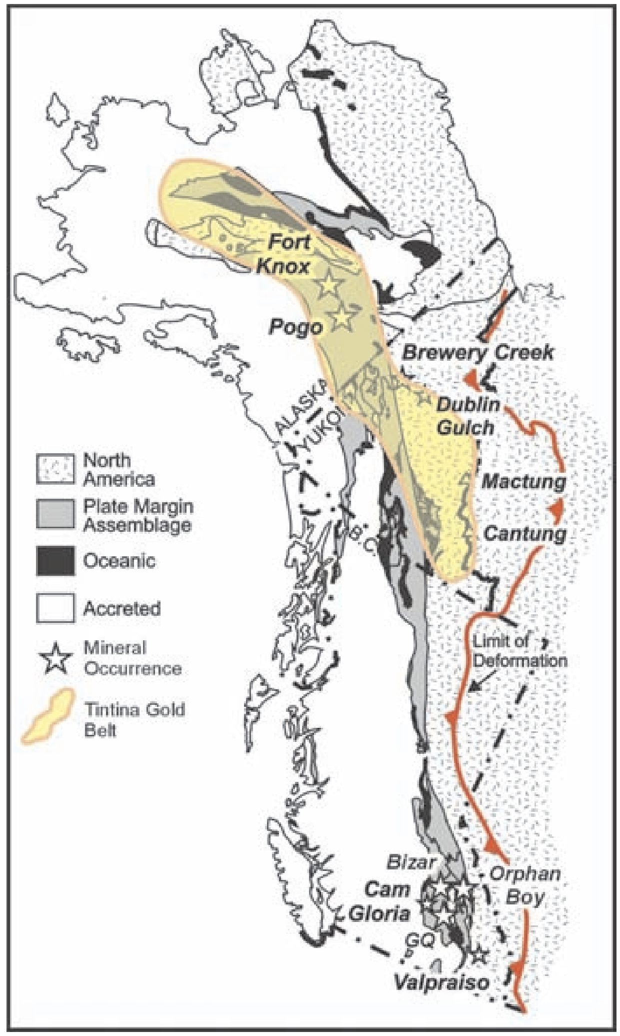

Figure 1. Tectonic assemblage map, after Wheeler and McFeely (1991) showing the distribution of North American, plate margin, oceanic and accreted rocks of the Canadian and Alaskan Cordillera, the location of the Tintina Gold belt and select gold occurrences.

those plutons intruding Kootenay terrane strata at the northwestern termination (Baldy/Shuswap area).

The Shuswap component comprised follow-up of anomalous samples from last years work in the Baldy Batholith area (Logan and Mann, 2000) and continues sampling and lithogeochemical characterization of plutonic rocks in the area east of Adams Lake. In addition, the high grade metamorphic "Pogo-like" setting of the Shuswap complex-hosted Bizar-Goldstrike and GQ mineral prospects (Cathro and Lefebure, 2000) were mapped and sampled.

INTRUSION-RELATED MODEL

The principal features of intrusion-related deposits are reviewed in recent publications, by McCoy *et al.* (1997), Poulsen *et al.* (1997) and Thompson *et al.* (1999). The major deposits in the Yukon and Alaska comprise diverse styles of gold mineralization that can be describe with respect to their spatial relationship to the causative intrusion (Figure 2):

- the intrusion-hosted low grade, large tonnage sheeted and stockwork low sulphide vein systems at Fort Knox (Bakke, 1995; Bakke *et al.*,1998), Dublin Gulch and Clear Creek,
- and the skarn, replacement and vein systems that occur in country rocks proximal, peripheral and distal - to the granitoid intrusions, such as on the Dublin Gulch property, at Brewery Creek and True North.

SELKIRK REGION

Battle Range Batholith

The Battle Range Batholith (BRB) is an elliptical, northwest-trending, mid- to Late Cretaceous post accretionary intrusive, and one of a group of intrusions which comprise the Bayonne Granitic Suite. It extends from Duncan River west to the head of Albert Creek and covers an area of approximately 800 km^2 (Figure 3).

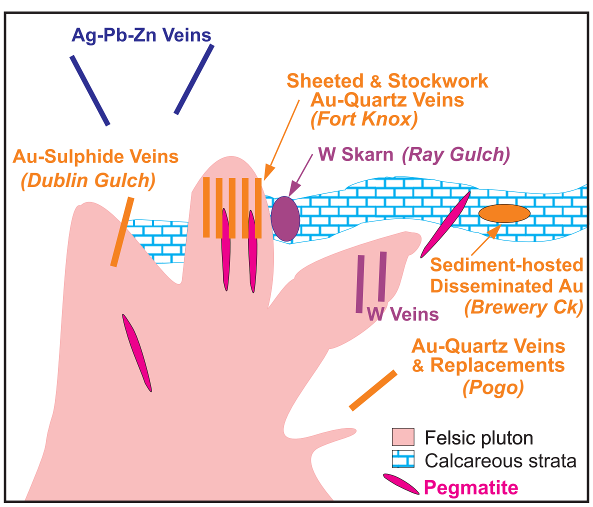

Figure 2. Schematic model of plutonic-related mineral deposits, showing different styles and zonation of intermediate to felsic "reduced"plutons intruded into a continental margin setting.

GEOLOGY

The BRB discordantly intrudes Late Proterozoic to Early Paleozoic metasedimentary and metavolcanic rocks of the Hamill to Lardeau Groups. Northwest-trending, southwest-verging regional fold and faults structures control the distribution of these units and characterize the southwestern Illecillewaet Synclinorium. Late northwest-trending subvertical crenulation cleavage is superposed on an early north-striking, compositional layering parallel schistosity. The early structures dip east, and plunge north. The southwest-verging deformation accompanied peak regional metamorphism which occurred at metamorphic conditions of 6-7 kbar in the Middle Jurassic (Colpron, 1996). Chlorite, biotite and garnet mineral zones of regional metamorphism are overprinted by chlorite, biotite, andalusite, sillimanite and sillimanite-orthoclase zones of contact metamorphism in the aureole around the Albert Stock and Battle Range Batholith (Sears, 1979). The contact metamorphic assemblage sillimanite-andalusite-staurolite-garnet-biotite-muscovite-quartz constrains the pressure between bathozone 2 and 3, approximately 3.5 kbar (Sears, 1979).

The batholith is a composite body consisting of three subalkalic, weakly peraluminous intrusive phases differentiated on mineralogy, texture, grain size and magnetic signature (Read and Wheeler, 1976). From oldest to youngest, these include a biotite-hornblende quartz monzonite (sodic andesine), a muscovite-biotite granodiorite (calcic oligoclase), and pyritiferous alaskite (Read and Wheeler, 1976). Hamill, Badshot and Lardeau Group metasedimentary strata comprise re-entrants in the north and south parts of the batholith. North of the northern re-entrant, the intrusion is comprised mostly of porphyritic biotite granite and equigranular biotite-muscovite granite. These phases are gradational from one to the other. The porphyritic variety is coarser grained and characterized by up to 2.5 cm phenocrysts of potassium feldspar. Dikes of pyritic aplite, muscovite pegmatite and sheeted quartz-sulphide veins are common features in the area north of Freeze Creek. Mean magnetic susceptibility measurements are low (0.34, n=10). The main body of the intrusion south of the metasedimentary screen comprises a potassium feldspar porphyritic biotite granite to granodiorite (Figure 4). Mean magnetic susceptibility measurements are also low (0.31, n=9). South of the headwaters of Houston Creek and encircled on its western end by metasedimentary rocks of the southern re-entrant is a biotite-hornblende granodiorite phase of the batholith (Figure 3). In contrast to the calcic oligoclase of the two-mica granite, this phase is characterized by sodic andesine (Read and Wheeler, 1976). As anticipated for the more mafic hornblende-bearing phase, the mean magnetic susceptibility measurements are higher (6.87, n=12).

Read and Wheeler (1976) recognized a third and youngest phase of the Batholith. It consists of a small (3 km^2) pyritiferous aplite centered on Pequod Glacier, approximately just east of the center of the Batholith (Figure 3). In addition, fine to medium-grained, quartz-feldspar-garnet aplite dikes, quartz veins and less commonly coarse-grained pegmatite dikes occur primarily near the margins of all the intrusive phases.

Recalculated K-Ar dates for two of three samples collected from Freeze Creek cirque (Figure 3), in the northern part of the Battle Range Batholith give uniform mid-Cretaceous cooling ages. The ages on a biotite-muscovite pair from a fine-grained monzogranite (GSC 62-21 and -20), yield 93.4 Ma and 94.2 Ma respectively and a biotite separate from coarse quartz monzonite with potassium feldspar megacrysts, yield an age of 96.5 Ma (Leech *et al.*, 1963). The third sample, a combined aplite and pegmatite vein which crosscuts the former two rock types gave an unexpected older age of 122.6 Ma (Leech *et al.*, 1963). Late Cretaceous to Paleocene mica cooling ages in the Clachnacudainn complex suggest a protracted thermal evolution at lower structural levels, and anatextic generation of leucogranite and pegmatite along its western margin (Colpron *et al.*, 1999).

Sampling in the Freeze Creek cirque area and south of Houston Creek has been completed for Ar-Ar and U-Pb, zircon dating to establish the crystallization ages of these separate phases of BRB.

MINERALIZATION

A number of magmatic-hydrothermal styles of mineralization occur associated with the Battle Range Batholith. These include those hosted within (molybdenum greisen veins, tin pegmatites and tungsten veins) and those located adjacent to the batholith in metasedimentary and metavolcanic rocks (Au quartz veins, W ± Mo skarns and polymetallic base metal ± Au veins). The only record of gold mineralization for the area is located 8 to 15 kilometres east of the eastern margin of the batholith. Past production of gold, with scheelite values is recorded from mainly silver-rich base metal workings at McMurdo Creek and the Ruth-Vermont deposit (Figure 3).

Mad

The Mad (82K-167) showing is a porphyry Mo occurrence located below Pequod Glacier in the headwaters of Butters Creek. Molybdenite occurs as disseminations

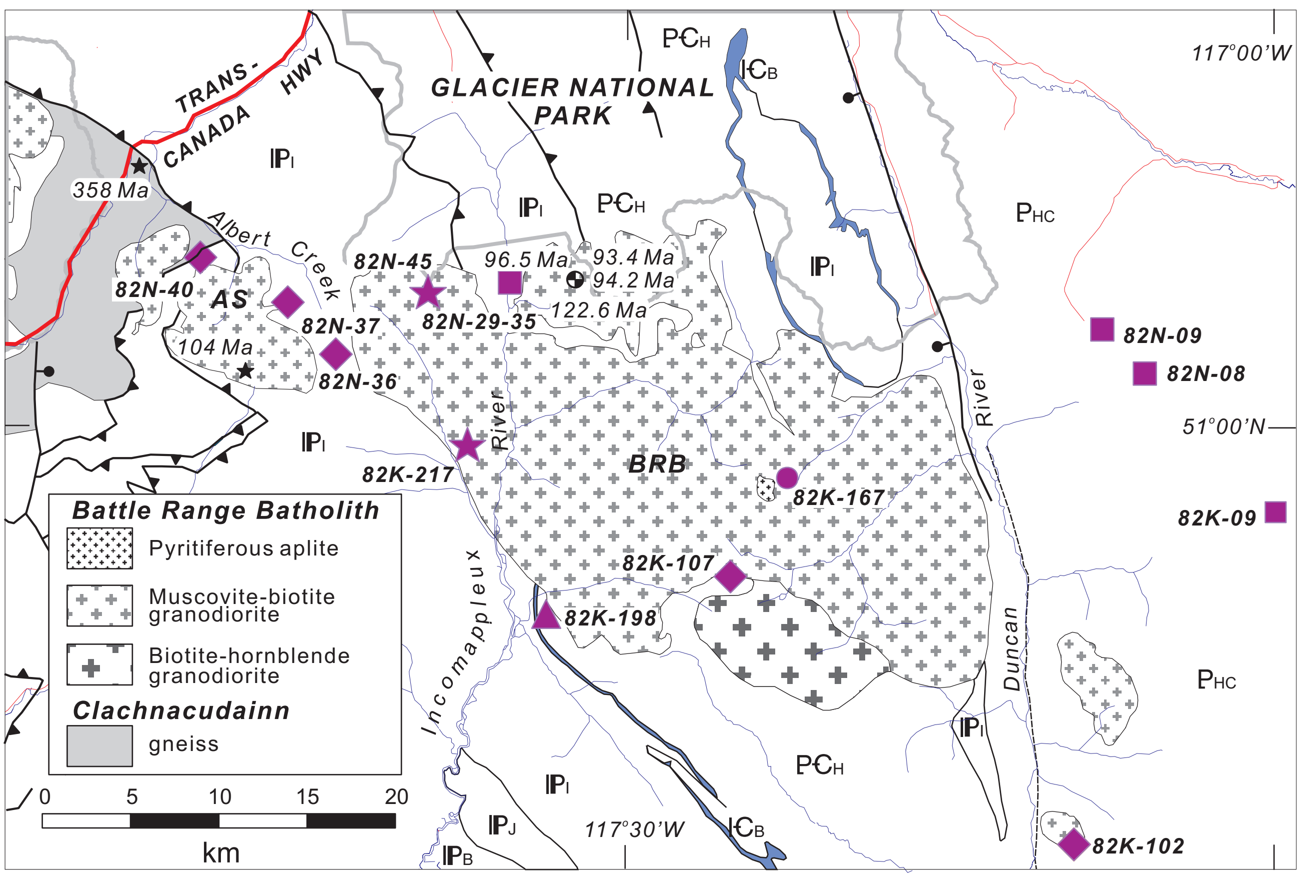

Figure 3. Regional Geology of Battle Range Batholith showing three magmatic phases; biotite hornblende granodiorite, muscovite-biotite granite and pyritiferous aplite phases, modified after Read and Wheeler (1976). In addition are location and ages of K-Ar analyses (Leech *et al.*, 1963), zircon dates for Albert stock (AS) (Crowley and Brown, 1994) and Clachnacudainn gneiss (Parrish, 1992). MINFILE occurrence symbols include tin (star), molybdenum (circle), tungsten-molybdenum (diamond) and lead-siver-zinc±gold veins (square).

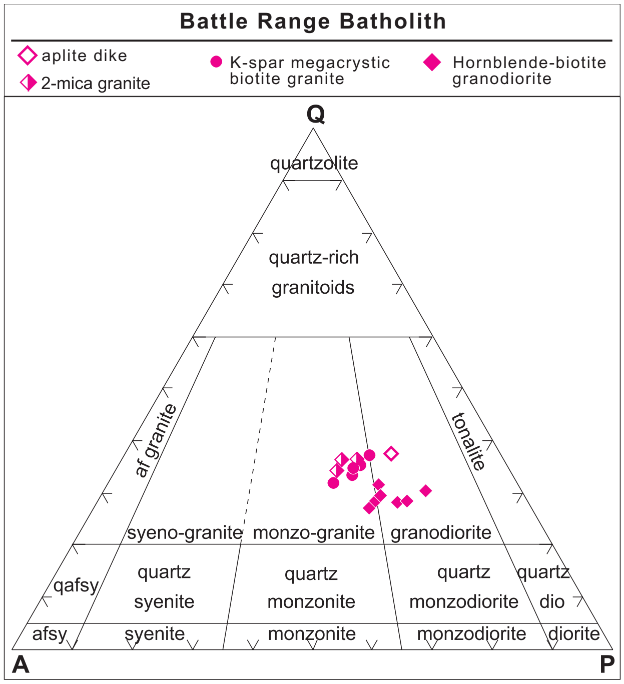

Figure 4. Modal quartz-alkali feldspar-plagioclase feldspar plot for Battle Range Batholith. Fields from LeMaitre (1989).

and quartz-sericite greisen veins within a pyritiferous alaskite porphyry stock which intrudes the coarse grained potassium feldspar megacrystic biotite granite of the main phase of the Battle Range Batholith.

Wrong Glacier

A series of narrow, en echelon, north-striking quartz-filled fractures and joint planes forms the Wrong Glacier occurrence. It is located 1.5 km southeast of Oasis Lake in biotite-hornblende granodiorite near the southern end of the batholith. The 1-3cm wide veinlets contain quartz, muscovite, pyrite and acicular tourmaline needles. The veins are enveloped by a bleached alteration zone comprised of sericite, pyrite and dolomite extending 1-5 cm into the potassium-feldspar megacrystic, granodiorite host. Grab samples from two sulphide and tourmaline bearing quartz veinlets returned below detection values for gold with slightly elevated tungsten values (Table 1).

McBean

North of Freeze Creek near the northern margin of the batholith, the biotite-muscovite granite is cut by pink weathering aplite dikes and numerous sheeted, sulphide-bearing quartz veins (Figure 3). The veins are commonly 6 to 10 cm wide and spaced 2 or 3 per metre. The predominant sulphide is pyrite. Alteration is restricted to narrow greisen-style envelopes of sericite and quartz (Photo 1). Two grab samples of the vein material returned below detection values for gold, although one (JLO31-271-2) contained anomalous values of bismuth and tungsten and elevated lead values (Table 1).

Ice, Ex90

The Ice (82N-36) and Ex90 (82N-37) occurrences are located at the head of Albert Creek. Mineralization was first discovered and assessed by the Union Carbide Exploration Company in 1971. The Ice claims (Westervelt, 1972) were staked to cover anomalous tungsten stream geochemical values located in the Albert Creek valley. Follow-up work located a stratabound horizon of disseminated scheelite mineralization and discordant tungsten-bearing quartz veins. In addition, a 10 to 15m wide, north-trending sulphidized-breccia zone was recognized. The north-trending zone of stratabound scheelite was defined by night lamping to be 425 m long and between 3-12 m in width (Westervelt, 1972). C. Graf (1986) spent a day prospecting and sampling the head of Albert Creek to evaluate the extent of the stratabound tungsten mineralization. Rock sampling (n=9) indicated ranges of WO3 values from .03% WO3 to 0.64% WO3 and anomalous values for fluorine, bismuth and copper (Graf, 1986).

The mineral occurrences occupy a narrow belt of Early Paleozoic Lardeau, Index Formation metasedimentary rocks (Sears, 1979) that separate the mid-Cretaceous Albert Stock in the west from the Battle

Photo 1. Sheeted sulphide-bearing quartz veins (10 cm wide) and greisen alteration in biotite-muscovite granite, south of Mount McBean.

TABLE 1
SELECTED GEOCHEMICAL ANALYSES, SELKIRK MOUNTAINS AREA, BATTLE RANGE BATHOLITH AND GROUNDHOG BASIN

Field Number	Au	Ag	As	Bi	Cu	Mo	Pb	Sb	W	Zn	DESCRIPTION
Battle Range-Wrong Glacier											
00JLO-30-270	-2	-5	<1	0.24	1	1.2	9	-0.1	74.3	26	Qtz-tourmaline veinlets
00MZA-30-165	-2	-5	1	0.09	8	1.2	14	0.5	28.1	24	Qtz-tourmaline veinlets
Battle Range-Ice, EX90											
00JLO-24-212	-2	-5	4	0.17	45	1.2	18.5	-0.1	1.7	72	grab hornfels metapelite, pyrrhotite
00JLO-24-215	-2	-5	1	0.2	25	0.6	15.5	0.3	0.6	82	grab pyrrhotitic hornfels quartzite
00JLO-24-220	-2	-5	<1	0.16	74	3.6	7.5	-0.1	2.3	132	grab calcsilicate, diss pyrrhotite
00JLO-24-220-2	-2	-5	1	0.15	137	7.8	24.5	-0.1	1.7	140	grab pyrrhotitic hornfels quartzite
00JLO-25-224	-2	-5	**46**	0.75	64	1	4	0.3	3.1	6	Sulphidized, silicified breccia, float
00JLO-25-225	-2	-5	**63**	1.8	56	1	6.5	0.2	5.9	6	Sulphidized, silicified breccia, grab
00JLO-25-226	17	-5	**208**	**45.5**	8	2.8	45.5	1.7	5.9	16	2 m chip pyrite+silica fault zone
00JLO-25-228	6	-5	<1	**26.6**	8	1	3	0.1	2	4	30 cm chip qtz vein, x-cutting
00JLO-25-231	-2	-5	<1	**32.1**	4	3.8	13	0.3	2.6	4	grab of 75 cm qtz vein, x-cutting
00JLO-25-232	-2	-5	<1	0.89	2	0.8	1	-0.1	2.3	2	grab of 3 qtz veins, x-cutting
00JLO-26-235	-2	-5	3	0.12	22	1.2	13	-0.1	61.6	8	aplite dike
00JLO-27-244	-2	-5	<1	**22.8**	4	1	2	0.2	**410**	<2	grab of qtz vein, x-cutting
00JLO-27-245	3	-5	7	**35.8**	15	5	2.5	-0.1	14.8	6	1.25 m chip qtz vein, x-cutting
00JLO-27-247	-2	-5	17	0.74	10	1.2	26	0.2	7.1	12	grab tourmaline-pegmatite
Battle Range-Escalade											
00JLO-28-253	-2	-5	7	6.91	114	**431**	12.5	0.2	**144**	246	pyrrhotite-Mo skarn
00JLO-28-253	-2	-5	14	7.67	98	**667**	15	0.4	**137.5**	254	pyrrhotite-Mo skarn
00JLO-28-254	-2	-5	2	0.34	104	33	19	2.2	4.5	278	grab hornfels metapelite, pyrrhotite
00JLO-29-261-2	-2	-5	6	0.1	21	1.6	20	0.2	2	16	aplite dike
00JLO-29-262	-2	-5	7	0.15	<1	1	4.5	-0.1	1.8	102	calcsilicate
Battle Range-McBean											
00JLO-31-271-2	-2	-5	2	**62.5**	65	7.8	111.5	0.1	**798**	98	pyritic sheeted qtz veins
00JLO-31-271-4	-2	-5	13	1.41	137	15.6	11.5	-0.1	26.9	52	pyritic sheeted qtz veins
Battle Range-McMurdo											
00JLO-32-285	**1250**	48	**955**	**30**	85	1	**>2.43%**	91.9	<10.0	524	grab 30 cm qtz-carbonate vein
00JLO-32-285-2	**835**	7	**3200**	3.93	74	1.8	3290	13	**802**	3900	grab 20 cm qtz vein, Sn//
00JLO-32-286	-2	-5	7	0.07	10	1.6	16	0.3	22.5	44	grab, 1.0 m qtz vein (axial planar)
00JLO-32-287	**5130**	-5	**3360**	0.26	3	1.6	10.5	-0.3	10.8	6	1 m chip qtz vein + pyritic Hw zone
00JLO-32-287-2	**32500**	-5	**1410**	3.72	3	4.4	9.5	-0.2	4.8	2	1 m chip qtz vein + pyritic Fw zone
00JLO-32-287-3	**16200**	-5	**>10000**	1.94	3	1.8	20.5	2.1	5.4	<2	grab, pyrite-rich Fw+Hw zones
Battle Range-Ruth/Vermont											
00JLO-33-288	**4060**	**381**	**>10000**	2	**4630**	<1.0	**19.40%**	**4160**	<10.0	5.49%	dump sample mineralized vein
00JLO-33-288-3	-2	7	**95**	0.18	19	1.8	2620	53.3	**1130**	472	50 cm chip,So // qtz vein
00JLO-33-288-4	**1800**	34	**>10000**	0.41	380	1.6	404	**308**	1.9	486	grab, 20 cm qtz vein (axial planar)
Groundhog basin-Ole Bull											
00JLO-20-183	-2	-5	9	0.39	3	0.6	8.5	-0.1	**209**	<2	30 cm chip qtz vein, NE-trending
00JLO-20-183-2	4	-5	4	0.11	5	0.6	5.5	-0.1	3.4	2	48 cm chip qtz vein, NE-trending
00JLO-20-184	**25**	-5	9	**4.17**	10	1	105.5	-0.1	5.4	6	1 m chip, qtz vein + pyritic phyllite
00JLO-22-195	8	-5	10	0.04	3	0.4	2.5	0.1	0.3	2	50 cm chip qtz vein, NE-trending
00JLO-22-195-2	**5950**	-5	12	0.05	96	0.6	5.5	0.2	0.7	2	grab, sulphide-rich vein material
Groundhog basin-Aurun											
00JLO-20-185	**38**	-5	12	**5.27**	3	0.6	390	-0.1	0.7	2	40 cm chip qtz vein, NE-trending
Groundhog basin-Lund											
00JLO-20-186	**85**	-5	6	0.52	15	0.6	70.5	0.9	0.7	30	25 cm grab, qtz+pyrrhotite zone
Groundhog basin-Orphan Boy											
00JLO-20-187	7	5	6	**11.4**	10	0.6	303	-0.1	0.9	2	60 cm chip qtz vein, NE-trending
Groundhog basin-regional											
00JLO-21-189	-2	-5	5	0.04	5	0.6	6	-0.1	0.3	22	qtz vein float
00JLO-21-191	-2	-5	21	0.37	34	1	19	-0.1	0.5	12	grab, 5 cm qtz vein, N-trending
00JLO-21-193	-2	-5	7	<0.01	3	0.6	1.5	-0.1	0.3	2	grab, 25-10 cm qtz vein, Sn //
00JLO-22-196	**85**	-5	11	0.1	7	0.6	9.5	-0.1	0.5	2	grab, pyrrhotite-rich qtz vein float
00JLO-22-197	14	-5	9	0.1	10	0.4	11	-0.1	0.3	40	grab 25cm qtz-CO_3 vein, NE-trending
00JLO-22-199	-2	-5	<1	0.06	1	0.6	4	-0.1	0.5	2	grab, 18 cm qtz vein, NW-trending
00JLO-22-200	-2	-5	6	0.76	25	1.2	6	0.2	0.4	4	grab, 20 cm qtz vein, Sn //
00JLO-22-201	2	-5	7	0.29	130	0.6	20.5	-0.1	0.8	54	grab, pyrrhotitic graphitic lmsn
00JLO-22-202	-2	-5	2	0.02	2	0.6	1	-0.1	0.2	<2	grab 35cm qtz vein, NE-trending
00JLO-22-203	-2	-5	18	0.03	6	0.6	2.5	-0.1	0.3	6	grab, 50cm qtz-CO_3 vein, S_{n+1} //

Au, As and Sb by INA; other elements by total digestion-ICP

Au in ppb, rest in ppm

Sample locations *see* Figures 3 and 6.

Range Batholith to the east (Figure 3). In this area, the Index Formation consists of a mixed and interbedded package of grey and dark green phyllite, micaceous quartzites and phyllitic grits. The strata trend-northerly, dip-easterly and are folded into southwesterly overturned folds that characterize the western flank of the Selkirk Fan. The contact metamorphic aureole from the two mid-Cretaceous magmatic bodies, overprints syntectonic, lower greenschist facies regional metamorphism. Semi-pelite and micaceous quartzite units are characterized by large andalusite porphyroblasts retrograded to muscovite, chlorite and quartz assemblages. A narrow, less than 1 km wide sillimanite zone, with sillimanite-biotite-muscovite-andalusite-garnet-quartz-plagioclase metamorphic mineral assemblage occurs adjacent to Albert Stock and western contact of the BRB.

Prospecting and sampling along the eastern contact zone of the Albert Stock, in the area of the Ex90 tungsten-molybdenum skarn, did not locate any anomalous precious or base metal mineralization. Four grab-samples (2-pyritic semipelite, 1-micaceous quartzite and 1-calcsilicate, Table 1) all returned low metal values.

Mapping and sampling on the east side of Albert Creek was directed to test the gold potential of known mineralization at the Ice prospect. Scheelite occupies north-trending fractures as coarse 1-1.5cm masses, and as fine disseminations with minor wolframite distributed through the quartzite host-rock. For the most part the fracture density in the quartzite averages 1 per 0.5 m. Orthogonal to the stratabound mineralization, are narrow, 30cm rarely up to 100 cm wide, east-trending quartz-pyrite-muscovite veins that contain disseminated scheelite. The east-trending (260-300°Azimuth) quartz veins contain an envelope of coarse intergrown muscovite and vuggy quartz, with a narrow, sericite alteration selvage that extends several centimeters into the country rock. Five samples of this type of quartz vein show consistently elevated Bi, and erratic but elevated Au and W values (Table 1). The north-trending, sulphidized-breccia zone can be traced for approximately 800m. It is a 10 to 15m wide steep west-dipping zone, comprised of separate metre-scale silicified and sulphidized breccia zones. Pyrite forms the matrix to breccia clasts, fine disseminations and coarse cubes in open-space fillings and variably replaces clasts. Pyrrhotite occupies tight, cross cutting fractures. The zone was sampled at three locations. Grab samples contain anomalous arsenic and elevated bismuth and gold values (Table 1).

Escalade

A small tungsten mineralized skarn zone, the Escalade occurrence (82K-107) is developed in a belt of interbedded limestone and rusty pelite which forms a reentrant of Lower Cambrian metasediments near the southern margin of the batholith. The area straddles the headwaters of Houston and Kellie creeks. Read and Wheeler (1976) show the re-entrant to be comprised of quartzite, phyllitic quartzite and black phyllite of the Marsh Adams Formation and limestone with green and grey calcareous phyllite of the Mohican Formation. Strata is folded into a northeast plunging antiformal syncline with younger thin layered Mohican Formation limestone and rusty phyllite occupying the core of the fold (Read and Wheeler, 1976). The Escalade showing includes a number of small tungsten and molybdenum mineralized, skarned-carbonate and rusty pelite developed adjacent to the northerly-trending contact of potassium feldspar megacrystic, biotite±hornblende granite of the BRB. Grab samples from the divide between Houston and Kellie creeks returned elevated molybdenum and tungsten and minor bismuth, but like other sulphidic-phyllite and calcsilicate samples from east of Stygian Lake, no gold values (Table 1).

McMurdo and Ruth Vermont

The Crown Point (MINFILE 82N-09) property is located at the head of McMurdo Creek, about 10 km northeast of the Battle Range Batholith and the Ruth Vermont (MINFILE 82K-09) about 17 km east of the batholith. Both are past producers. The Ruth-Vermont operated sporadically between 1892 and 1970. The majority of the production of 17,248 kg of Ag, 9.4 kg of Au, 23,137 kg of Cd, 55,693 kg of Cu, 3,253,956 kg of Pb and 5,947,422 kg of Zn occurred between 1970 and 1981. The Crown Point produced 8,211 g of Ag and 3,808 kg of Pb from 5 tonnes mined prior to 1930. Mineralization is chiefly silver-rich, Pb-Zn vein and replacement deposits hosted in Late Proterozoic Horsethief Creek Group phyllite, argillaceous limestone, quartzite, grit and pebble conglomerate. The units are folded into regional northwest-trending, westerly-verging folds with mineralized veins occupying oblique, transverse and bedding parallel fracture sets related to fold geometries. The quartz-carbonate veins consist of pyrite, galena, sphalerite, arsenopyrite and silver-rich copper-antimony sulphosalts. Gold is generally associated with arsenopyrite and pyrite and scheelite occurs in late stage quartz veins. Where the density of veins crosscutting limestone beds is high, silicification and fine-grained sulphide replacement has taken place.

Several narrow, less than one metre wide axial planer auriferous quartz veins comprise the “Gold showing” at the Crown Point past producer. The veins are north to northwest-striking and dip steeply northeast. They cut micaceous quartzites and quartz grits in the hinge-zone of a NW-trending anticline. The veins are mainly quartz and carbonate, locally vuggy with euhedral quartz crystals and contain pyrite, minor galena, sphalerite and trace chalcopyrite. Three samples (JLO32-287, -2, -3) across a 2 metre wide quartz vein from this area returned anomalous Au and As (Table 1). The 20 to 25 cm wide hangingwall and footwall zones to the vein contain approximately 30 % coarsely crystalline cubic pyrite. A number of other 20 to 30 cm wide bedding parallel and orthogonal quartz-carbonate veins occur in the immediate area. These contain minor pyrite, galena and sphalerite and anomalous Au, As and locally tungsten values (Table 1).

GOLD POTENTIAL OF BATTLE RANGE BATHOLITH

Field studies of the Battle Range Batholith confirmed the presence of several styles of mineralization commonly found associated with mid-Cretaceous intrusion-related gold mineralization in Alaska and the Yukon. Unfortunately, the limited number of samples didn't turn up any new gold mineralization and there are no RGS data to show the prospective nature of the region for gold. The results of these studies suggest the northwestern end of the batholith was emplaced at about 10 km depth in the upper crust. This is deeper than most of the Yukon and Alaska intrusion-related deposits. The Au-As-Sb association with PB-Zn-Ag veins at the Crown Point and Ruth Vermont has some analogies with distal intrusion-related deposits in Alaska (Dolphin?, True North).

Groundhog Basin

The Orphan Boy (82M-167) and Stanmack (82M-80) showings standout as potential intrusion-related gold systems in the Lefebure *et al.* (1999) province-wide evaluation of MINFILE occurrences. The showings are drained by creeks with placer gold production and the auriferous quartz veins contain low (1-2%) total sulphide content, consisting of pyrite, pyrrhotite, tungsten, minor galena and chalcopyrite. The showings occupy the Groundhog basin, which lies in the Goldstream River area, east of the Columbia River and approximately 90 km north of Revelstoke (Figure 5).

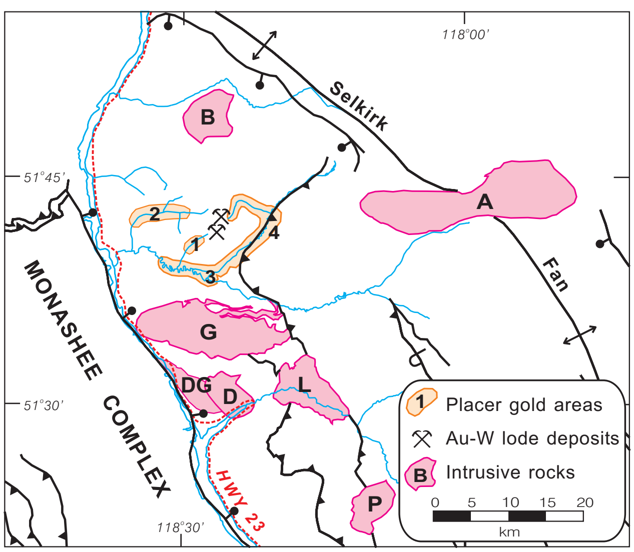

Figure 5. Location of the Orphan Boy and Stanmack Au-quartz vein occurrences on the western flank of the Selkirk fan structure, within the Columbia River Fault hangingwall rocks of the Selkirk allochthon. Shows placer gold creeks; McCulloch (1), Old Camp (2), Goldstream (3) and French (4) and the distribution of granitic rocks; Early Mississippian Downie gneiss (DG), Middle Jurassic Pass Creek (P) and Adamant (A), Late Jurassic Bigmouth (B), mid-Cretaceous Goldstream (G) and Long Creek (L) and Late Cretaceous Downie (D).

HISTORY

Placer gold was first discovered on Goldstream, French and McCulloch creeks as early as 1865. Although large amounts of gold are know to have been recovered from them during those early years, there is no record of production until 1886. In 1906, H. Carmichael, the Provincial Assayer, referred to some \$3,000,000 of gold taken during the 1865-6 season, this included a \$375 nugget from French Creek. The total recorded production of 6240 ounces or 194,064 grams (Holland, 1980) was derived primarily from French Creek (86.6%). Lode gold was discovered in the late 1890's in the Groundhog Basin and by 1896 development was underway on the Ole Bull and Orphan Boy claims (Gunning, 1929; Wheeler, 1965).

The majority of the exploration work to date has concentrated on the Crown Grants that contain the known quartz vein structures. A number of exploration programs consisting of reconnaissance geological mapping, soil, silt and rock sampling and geophysical surveys were completed in the early 1980's (Chapman *et al.*, 1982; Schindler, 1984). More recently two programs of diamond drilling were completed to test the known showings (Figure 6). The 1995 program tested the Orphan Boy and Ole Bull zones with 1347m of diamond drilling in 12 holes (Cooke, 1996). The following year (1996), the Orphan Boy, Aurun, Lund, Ole Bull and James zones were tested with 929 m of drilling in seventeen holes (Henneberry, 1997). Vein intersections from both programs returned spotty gold values and inconclusive results.

GEOLOGY

The Northern Selkirk Mountains comprises polydeformed Late Proterozoic to early Paleozoic metasediments and metavolcanic rocks of the Selkirk allochthon. These rocks accumulated along the western margin of ancestral North America and were deformed, metamorphosed and later displaced eastward during the Late Jurassic to Eocene (Brown *et al.*, 1986). In this area the Selkirk allochthon is intruded by two main suites of granitic rocks (Figure 5); the Middle Jurassic (ca. 180-165 Ma) Nelson Suite of granodiorite and quartz monzonite (*i.e.* Adamant and Pass Creek plutons) and the mid-Cretaceous (ca. 110-90 Ma) Bayonne Suite of quartz monzonite, diorite and two-mica granite (*i.e.* Goldstream and Long Creek). In addition, a less voluminous Late Cretaceous (ca. 70 Ma) suite of leucogranites, and an Early Mississippian (ca. 360 Ma) suite of orthogneiss have been recognized in the Clachnacudainn complex (Parrish, 1992) and the Downie Creek area (Logan and Friedman, 1997). The late Jurassic to Early Cretaceous zircon (149±11 Ma), and titanite (141±7 Ma) ages for the Bigmouth pluton (Marchildon *et al.*, 1998) are not common in southeastern British Columbia.

The strata north of the Goldstream River in the Groundhog basin is correlated with the Index Formation of the Lardeau Group (Logan and Colpron, 1995). It consists of a lower carbonaceous and calcareous dark

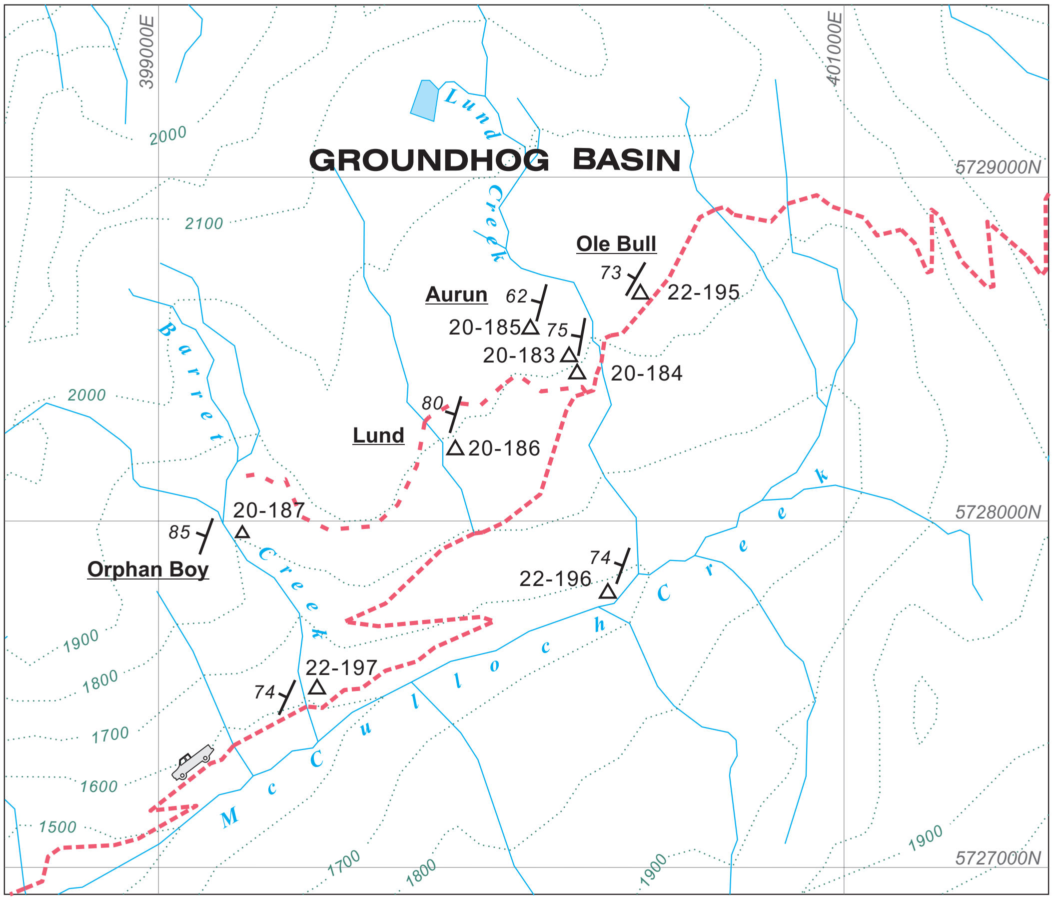

Figure 6. Location and vein orientation of auriferous quartz lode zones comprising Orphan Boy and Stanmack MINFILE showings in the Groundhog Basin. Sample locations correspond with Table 1. Small scale placer gold extraction is ongoing in McCulloch Creek.

phyllite and schist, a middle green member of chlorite schist, greenstone and phyllite and an upper member of micaceous quartzite and coarse quartz grits.

The Groundhog basin occupies the western flank of the Selkirk fan structure, an area dominated by southwest-verging folds and thrust faults (Wheeler, 1963,1965; Brown *et al.*, 1978; Price, 1986). Two generations of structures are recognized throughout the Goldstream area (Hoy, 1979; Logan and Colpron, 1995; Colpron *et al.*, 1995). The earlier generation of structures corresponds to northwest-trending, southwest-verging folds and thrust faults that define the map pattern. Regional relationships indicate a Middle Jurassic age for this generation of structures (Parrish and Wheeler, 1983; Brown *et al.*, 1992). The southwest-trending structures are deformed by younger, easterly-trending, gently plunging folds. These structures predate the emplacement of the mid-Cretaceous intrusive suite. North-trending fractures, normal faults and open warps are the youngest structures and are interpreted to be associated with Eocene crustal extension along the Columbia River fault.

Rocks of the Groundhog basin area contain mineral assemblages characteristic of greenschist facies metamorphism. This low-grade zone is bound to the south by contact metamorphic assemblages related to the Goldstream, Long Creek and Downie intrusive bodies. Assemblages of biotite-garnet±andalusite define this metamorphic culmination. Northeast of the Groundhog basin is a segment of the northwest-trending Windy Range metamorphic culmination. It extends for over 90 km between Mica Dam and Rogers Pass (Wheeler, 1965; Greenwood *et al.*, 1991; Read *et al.*, 1991). Regionally, the Windy Range culmination grades from biotite zone in the southwest, to sillimanite - potassium feldspar in the core of the culmination (Leatherbarrow, 1981). To the northeast, metamorphic grade decreases to kyanite-staurolite zone along the southwest flank of the Rocky Mountain Trench. These amphibolite facies rocks and migmatites follow the axis of the west-northwest-trending Selkirk fan, approximately 25 kilometres to the north (Figure 5).

The Groundhog basin rocks contain carbonate, chlorite, quartz, plagioclase assemblages characteristic of the chlorite zone of greenschist facies metamorphism and chlorite grade mineral assemblages define the dominant foliation. The west-northwest trend of the isograds is discordant with the more northerly trend of the regional structures north of the Goldstream River (Logan and Colpron, 1995). Porphyroblast growth in the Windy Range culmination appears to post-date the development of the dominant regional fabric. Synkinematic biotite-grade assemblages are present in the northern part of the basin and have been interpreted as contemporaneous with emplacement of the late Jurassic to Early Cretaceous Bigmouth granodiorite (Marchildon *et al.*, 1998).

GOLD-QUARTZ VEINS

Three separate quartz veining events are recognized for the area: a syn-metamorphic, likely Mid-Jurassic; a pre-mid-Cretaceous; and a young, gold- tungsten-mineralizing episode of either Late Cretaceous or Tertiary age. The first two events are widespread in the area while the latter is restricted to northeast-trending structures in the Groundhog Basin (Figure 7).

Synmetamorphic quartz veins parallel, and are folded by, the dominant foliation. The veins are bull quartz, grey to vitreous and rarely contain minor coarse cubic pyrite. Recrystallization during metamorphism exsolved the fluid inclusions to grain boundaries, and changed the milky white to grey coloured vein-quartz to a vitreous blue-grey colour (Figure 7a). East-trending, massive, white quartz and locally rusty-weathering quartz-iron carbonate veins (up to 0.5 m wide) parallel the attitude of late crenulation cleavage (Figure 7c). A third stage of auriferous ± galena and scheelite quartz veining corresponds with a period of northwest-southeast extension. These quartz and quartz-carbonate veins crosscut the early structures and are restricted to parallel northeast-trending structures (Figure 7b & d). The vein structures occur in parallel sets. At the Lund Creek showing three quartz veins are known and further north in area of the Orphan Boy Shaft, 5 parallel vein structures are contained within a 70 m wide zone. Weak alteration extends from 1 to 5 centimeters beyond the veins and includes, sulphidized, carbonatized and sericitized wallrock envelopes.

Analytical results for these various types of quartz veins from the Groundhog basin and surrounding areas are tabulated in Table 1. Gold, lead, tungsten and minor bismuth enrichment is present in quartz veins. A weak association of gold, lead and bismuth is apparent for samples of the Ole Bull-shaft, Lund, Aurun and Orphan Boy showings (Figure 6), but not from the two veins sampled north of the Ole Bull shaft (00JLO-22-195, 195-2). Mineralization consists of pyrite and lesser pyrrhotite, with minor galena and scheelite. In thin-section the east-trending veins exhibit substantial grain size reduction, variably strained quartz, and sericite filled fractures. The younger, northeast-trending auriferous veins consist of larger, weakly strained, interlocking quartz grains cut by narrow fractures filled with cubic pyrite, euhedral quartz and zoned dolomite crystals. A single grain of native gold associated with pyrite was recognized in one polished thin-section sample (JLO-22-195-2). Extending from the vein wall into the host rock is a zone of sericite alteration, which bleaches and overprints the chlorite-bearing greenschist-grade, micaceous quartzite and carbonaceous schists. Later-stage fracture-controlled carbonate (dolomite?) alteration is most prevalent in hanging-and footwall to the vein contacts. Southeast and structurally below the Groundhog veins in the French Creek area, another northeast-trending vein (JLO-22-202) is characterized by large strained quartz grains with numerous euhedral tourmaline crystals, no opaque minerals and low geochemical analyses (Table 1). An east-trending quartz-carbonate vein from this same general location (Figure 7c) also returned low geochemical analyses.

PROSPECTIVE AREAS - GROUNDHOG BASIN

There is a strong structural and paragenetic control to the different types of quartz veins in the Groundhog basin. The auriferous veins are restricted to northeast-striking, steep-dipping structures, commonly as sets of parallel veins ranging from 20 to 100 cm in width. These gold veins are not classical orogenic-gold deposits, generally associated in space and time with collisional tectonic regimes. Orogenic-gold deposits are characterised by their association with regional high-angle faults, vertical continuity, extensively developed wallrock alteration, and hydrothermal fluids sourced from metamorphic devolatillization at depth. The Groundhog basin veins post-date the Middle Jurassic syntectonic greenschist metamorphism, and probably any metamorphic fluids generated during development of the Cretaceous(?) Windy Range metamorphic culmination. The veins crosscut mid-Cretaceous or older structures and therefore any relation to magmatism is limited to mid-Cretaceous or younger intrusive suites.

The characteristics of the gold-quartz ± tungsten mineraliation in the Groundhog Basin are permissive for an intrusion-related gold-quartz system. The absence of any causative intrusive body would suggest that the veins are peripheral or distal-types of mineralization, and perhaps explains the weak correlation between Au:Bi and Au:Pb.

The restriction of gold mineralization to northeast-trending structures indicates a discrete strain and coincident hydrothermal event which to date is only recognized in the Groundhog Basin area. Therefore, this drainage basin with its significant gold placer production warrants further exploration for gold-rich veins. In the region mid- to Late Cretaceous intrusive bodies, such as the Goldstream Pluton, Long Creek or younger leucogranite are also likely the most prospective in the Groundhog area. Regional fault structures and reactive sulphidized, carbonaceous rocks are potential hosts for low-grade disseminated replacement gold mineralization.

Shuswap Region

In the area north of Shuswap Lake the Kootenay terrane is comprised of Neoproterozoic and younger amphibolite-grade sillimanite-bearing metamorphic rocks (Campbell, 1963; Okulitch, 1979; Read *et al.*, 1991) intruded by composite, deformed and plutonic rocks. Devono-Mississippian, Middle Jurassic, mid-Creta-

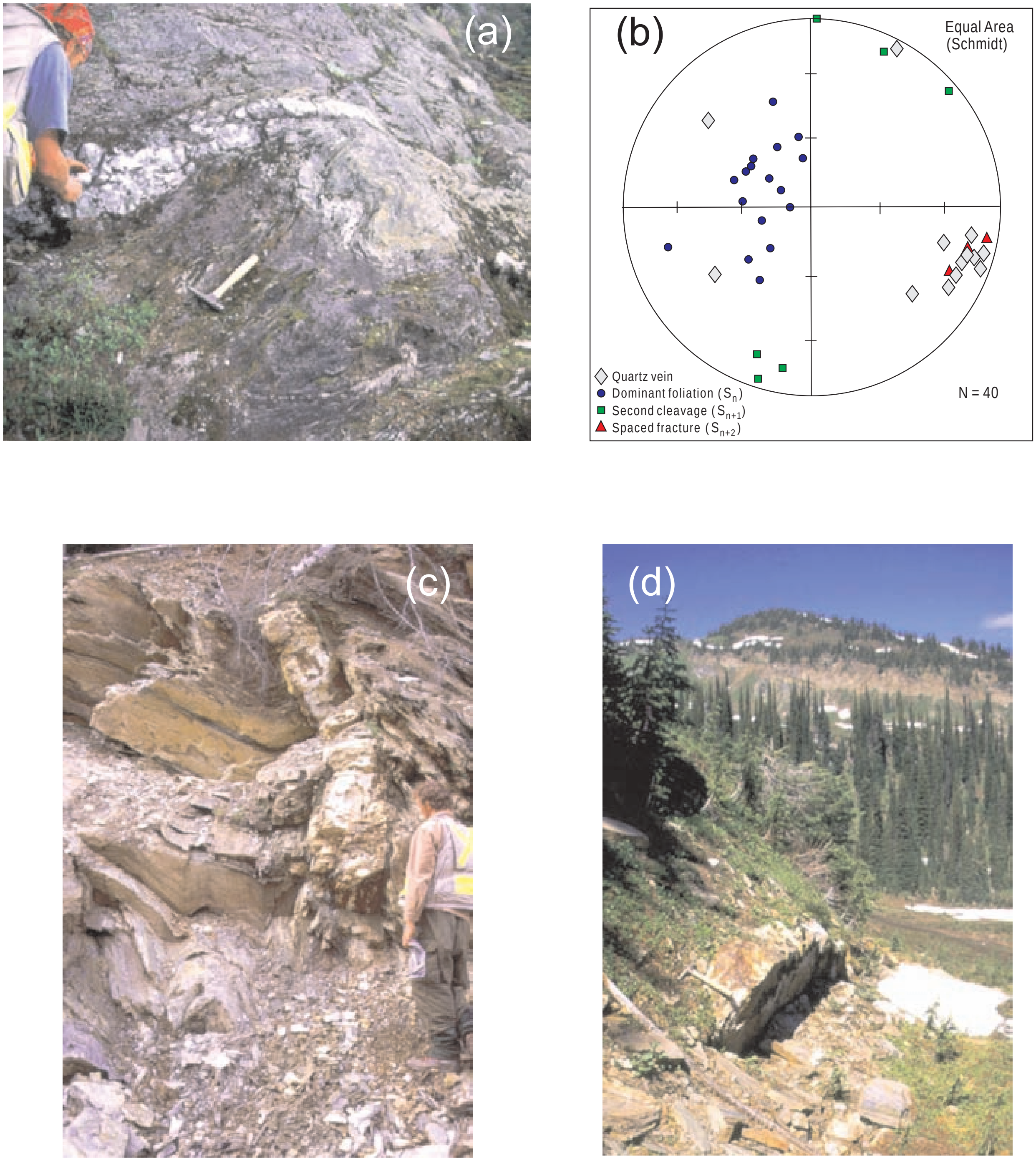

Figure 7. Three main quartz vein styles and morphologies found in the Groundhog Basin. Equal area plot of poles to; veins, dominant foliation (Sn), second cleavage (Sn+1) and late spaced fracture planes (Sn+2). Photos correspond to early synmetamorphic Sn parallel quartz veins (a), pre or syn mid-Cretaceous Sn+1 parallel veins (c) and northeast-trending late auriferous quartz veins (d).

ceous, late Cretaceous and Paleocene suites of magmatism are known from detailed studies elsewhere (Armstrong, 1988; Sevigny *et al.*, 1990; Scammell, 1993; Parrish, 1995), but isotopic dating and chemical classification of intrusions remains unresolved, and poses fundamental problems to the study of intrusive-related gold mineralizing systems in this high-grade terrane.

Baldy Batholith

GEOLOGY

Follow-up work from the 1999 season focused primarily in the northeast corner of the Baldy Batholith and the area south of the batholith between Adams and East Barriere lakes (Figure 8). The Baldy Batholith is a west-trending, mid- to Late Cretaceous post accretionary

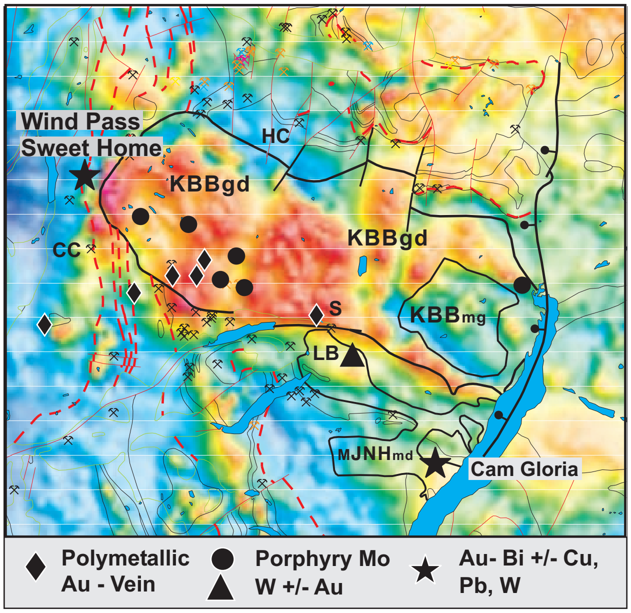

Figure 8. Aeromagnetic intensity survey map showing distribution and various styles of mineralization related to Cretaceous Baldy magmatism. The hornblende-biotite granite phase in the western 2/3rds of the batholith is distinct from the biotite-muscovite granite in the east and the hornblende quartz monzodiorite of the Honeymoon stock.

intrusive (Schiarizza and Preto, 1987; Calderwood *et al.*, 1990). It intrudes Proterozoic to mid-Paleozoic Kootenay terrane metasedimentary and metavolcanic rocks and postdates most of the penetrative deformation in the area. A variety of mineral deposits are related to its intrusion (Schiarizza and Preto, 1987, Logan, 2000). The intrusion is multiphase consisting (from oldest to youngest) of a K-spar megacrystic hornblende-biotite quartz monzonite, biotite monzogranite to granite and a biotite-muscovite granite (Logan, 2000). Molybdenum ± gold mineralized quartz veins, aplite and pegmatite bodies are concentrated in the northeastern corner of the batholith spatially associated with the youngest 2-mica granite phase.

Moss mat, traditional silt and heavy mineral separate-samples returned elevated to anomalous values of Au, Bi, W, and sulphate (in stream waters) from streams draining the northeast end of the Baldy Batholith (Lett, Jackaman and Englund, 2000). Follow-up mapping and sampling this year along logging roads in the area of Fisher and Gollen creeks recognized narrow, north and northeast-trending sulphide-bearing quartz veins and pegmatites. Three grab samples from two of these zones returned below detection gold values and very low Ag, As, Bi, Cu, Mo, Pb, Sb W, and Zn values (Table 2).

Last summer sampling in the Bendelin Creek area returned anomalous gold (6430 ppb), bismuth (562 ppm), and copper (900 ppm) values from grab sample 99JLO-2-18-2 (Logan and Mann, 2000). The pegmatitic segregation is hosted in leucocratic biotite, muscovite monzogranite of the Baldy Batholith. The irregular 2 to 2.5 m wide, northerly-trending pegmatite comprises coarsely intergrown muscovite, biotite, potassium feldspar, quartz and small pink garnets and a central core (1.8 m) of bullish grey quartz. Sericite alteration and molybdenum mineralization are concentrated along the margins of the pegmatite, adjacent to the central quartz core and monzogranite country rock. Chip sampling of the footwall (0.5 m), quartz core (1.8m) and hangingwall (1.2m) pegmatite zones returned slightly elevated molybdenum values in the latter and below detection gold values for all three samples (Table 2).

Similar molybdenum-only mineralization was located along the Adams Lake road at the eastern margin of the batholith where locally it is intruded by numerous aplite and pegmatite dikes. At this location, the potassium-feldspar megacrystic, biotite granite is silicified, weakly sericite-altered and cut by north-trending brittle faults.

Honeymoon Stock

South of the Baldy Batholith, between East Barriere and Adams lakes an irregular, east-trending granite body interfingers with Devono-Mississippian orthogneiss and Neoproterozoic to Paleozoic micaceous quartzites (Figure 8). Intrusive rocks include hornblende porphyry monzodiorite, biotite-hornblende-epidote quartz monzodiorite and biotite granodiorite. The southeastern-most apophysis (Honeymoon stock), hosts the gold-quartz Cam-Gloria vein and has an U-Pb titanite age of 161±7.8 Ma (personal communication J. Mortensen, 2000). The quartz monzodiorite is typically coarsely crystalline and equigranular with rare potassium feldspar megacrysts forming up to 5% of the rock. Dominant mineralogy includes andesine plagioclase, potassium feldspar, hornblende, biotite, quartz and epidote.

Continued mapping of the western and northern parts of this intrusive body indicate the majority are biotite-hornblende-epidote quartz monzodiorite, suggesting they be correlated with the Honeymoon stock and assigned a Middle Jurassic age. Coarse-grained gneissic units containing sillimanite-staurolite-biotite-hornblende assemblages, calcsilicate gneisses (Schriaizza and Preto, 1987) and rusty-weathering migmatites with felsic leucosomes, pegmatites and sugary-textured aplite dikes host the intrusions in this area. It is not known whether these metamorphic mineral assemblages represent contact or burial metamorphism.

An analogous structural and metamorphic setting is the Kootenay Arc south of Kootenay Lake (Archibald *et al.*, 1983), where late synkinematic Nelson suite rocks and their contact metamorphic aureoles are intruded and reset by mid-Cretaceous and younger metamorphism and plutonism.

MINERALIZATION

Cam-Gloria

The Cam-Gloria gold prospect (MINFILE 82M 266) is located three kilometres west of Honeymoon Bay, Adams Lake (Figure 8). The property was staked by Camille

TABLE 2
SELECTED GEOCHEMICAL ANALYSES, SHUSWAP AREA, BALDY, GOLDSTRIKE-BIZAR, AND GQ MINERAL OCCURRENCES

FIELD NUMBER	Au	Ag	As	Bi	Cu	Mo	Pb	Sb	W	Zn	DESCRIPTION
Baldy-Bendelin/Fisher Ck											
00JLO-1-3	7	-5	56	2.31	103	0.6	13	-0.1	0.4	84	garnet-diopside skarn
00JLO-3-14	-2	-5	23	0.29	<1	1.6	12.5	0.2	1.3	6	1.2 m chip FW-pegmatite
00JLO-3-14-2	-2	-5	8	0.34	1	0.6	1	-0.1	0.2	<2	1.5 m chip qtz core
00JLO-3-14-3	-2	-5	6	0.64	<1	**559**	18	0.3	1.8	8	0.5 m chip HW-pegmatite
00JLO-4-16-2	-2	-5	5	0.36	15	8.4	34.5	0.3	1.5	16	oxidized 5-10mm qtz veinlets
00JLO-4-21	-2	-5	1	0.18	3	3.8	26	-0.1	0.8	2	grab of pegmatite
00JLO-4-22	-2	-5	2	0.22	4	7	31.5	0.3	1.1	20	clay-altered leucogranite
00JLO-4-22-2	-2	-5	4	0.44	7	2	26	-0.1	1.3	20	pyritic quartz pegmatite
00JLO-4-27	-2	-5	3	5.47	<1	1.6	22	-0.1	1.8	12	grab of pegmatite
00JLO-5-47	-2	-5	<1	13.1	13	**1180**	22	-0.1	3.2	18	quartz vein w/ Mo
Windpass*											
GW-1	**2020**	1	10	58	532	3	2	<2	<10	48	Grab from dump
GW-2	**88590**	8	2	**1450**	1715	5	4	2	10	36	Grab from dump
GW-3	**30890**	16	40	**492**	4720	3	234	<2	10	44	1m channel, Compressor zone
GW-4	**2900**	0	<2	**86**	709	1	<2	<2	<10	16	grab, Fire Station trench
GW-5	**79410**	6	34	**2550**	3420	12	<2	<2	<10	52	chip, #3 Main adit
GW-6	**5900**	11	<2	**528**	6800	<1	<2	16	<10	64	grab, high grade dump
GW-7	**33870**	1	8	**992**	366	4	<2	<2	<10	10	Sweet Home dump
GW-8	**2180**	33	4	*	>10000	1	<2	<2	<10	502	7.5 m chip, #1 adit
GW-9	**13170**	1	<2	**508**	1275	1	<2	<2	10	10	3.5 m chip, #3 adit
Shuswap-GQ											
00JLO-15-144	-2	-5	7	0.05	18	0.6	3	-0.1	1.1	38	calcsilicate marble
00JLO-15-144-2	**115**	-5	7	7.73	**1445**	2.8	8	0.3	101	78	pyrrhotite-scapolite skarn
00JLO-16-151	-2	-5	<1	2.69	579	5	6	-0.1	**160.5**	108	pyrrhotite-scapolite skarn
00JLO-16-153	**854**	-5	5	**79.8**	**1005**	2	8	-0.1	**222**	102	pyrrhotite-scapolite skarn
00JLO-16-156	5	-5	4	1.17	7	0.2	9	0.2	2.9	88	carbonatite
00JLO-17-166	5	-5	5	0.12	2	0.4	60.5	-0.1	0.7	2	pegmatite, leucosome
Shuswap-Bizar											
00JLO-9-93	-2	-5	5	1.64	25	5.8	2.5	-0.1	0.2	4	grab 15 cm pyritic qtz vein
00JLO-10-95	2	-5	6	0.55	16	2	4	-0.1	0.3	6	qtz+muscovite vein, Sn //
00JLO-10-95-2	-2	-5	<1	0.29	11	0.8	7.5	-0.1	0.5	8	qtz+andalusite vein, X-cutting
00JLO-10-98	-2	-5	14	0.81	219	3.2	6	-0.1	0.9	8	grab 5 cm pyritic qtz vein
00JLO-10-99	-2	-5	5	0.05	3	1.4	3	-0.1	0.3	6	pegmatitc leucosome
00JLO-11-111	-2	-5	9	0.3	4	1	4	-0.1	0.3	<2	lensoidal bull quartz body
00JLO-13-133	-2	-5	10	0.82	<1	0.8	22.5	0.1	0.9	44	clay-altered leucogranite

Au, As and Sb by INA; other elements by total digestion-ICP
Au in ppb, rest in ppm
Sample locations *see* Figures 8, 9 and 10.
* Windpass samples from Jenks (1997)

Berubé in 1997 and optioned to Teck Corporation in early 1999. Teck carried out surface mapping, geophysical surveys and excavator trenching and drill tested the main vein. Seven holes totaling 835.9 metres were drilled, logged and sampled (Evans, 1999). No further work was undertaken and the property was returned to the owner.

The property was mapped and the vein and alteration system sampled in 1999 as part of our ongoing study to characterize intrusion-related gold deposits in British Columbia. For the results of this work the reader is referred to Logan (2000), Logan and Mann (2000) and references therein. In conjunction with the 1999 mapping, the stream sediment geochemical signature of the deposit was evaluated using multiple sampling media (Lett, Jackaman and Englund, 2000).

Gold mineralization at Cam Gloria occupies quartz veins, up to 7 meters thick, within multiple fault and shear zone structures hosted in potassium feldspar megacrystic quartz monzodiorite. The veins are enclosed by wide zones, in places up to 30 m of pervasive sericite alteration, which also contain elevated gold values. The wide alteration zone accompanying quartz veins and mineralization is not a well developed characteristic of intrusion-hosted deposits. Gold values are erratic in samples from trenches and diamond drill hole intersections of the vein and alteration, but do show good correlation with Bi, Pb and Ag (Evans, 1999). A weaker correlation with As, Cu, Zn, Te and W is evident. These correlation characteristics are similar to other intrusion-related deposits in Alaska and the Yukon (McCoy *et al.*, 1997).

U-Pb geochronology of quartz monzodiorite from the Honeymoon stock gives a preliminary Middle Jurassic date of 161.0±7.8 Ma from 2 concordant titanite fractions (personal communication, J. Mortensen, 1999). Pb-isotope analyses of vein sulphides give 207/206 and 208/206 ratios (personal communication, J. Gabites, 1999) which plot within a cluster of Cretaceous vein deposits from the Baldy and Revelstoke area (Logan, unpublished data), indicating the lead in the Cam-Gloria vein has a Cretaceous model age. Ar-Ar analysis on the sericite alteration envelope is ongoing (D. Archibald, Queens University) to help constrain the age and relationship of mineralization to the Jurassic and Cretaceous magmatic events in the Adams Lake area. Preliminary results indicate that mineralization is younger than the Middle Jurassic host stock and probably associated with the Mid-Cretaceous Baldy Batholith. Since the auriferous mineralization at Cam-Gloria is not related to the Honeymoon stock, it is interpreted as a peripheral (to the causative Baldy Batholith) intrusion-related, gold-quartz vein hosted in an older intrusion.

Windpass and Sweet Home

Other candidate "proximal/peripheral" intrusion-related gold-quartz veins related to the Baldy Batholith are the Windpass (MINFILE 82P-39) and Sweet Home (MINFILE 82P-40) mines (Figure 8). Both were important producers of gold prior to 1940 (Taylor, 1989). Total production between 1916 (discovery) and 1944 was 1071.7 kg of gold, 78 906 kg of copper and 53.5 kg of silver from 73 319 tonnes milled. Operating data indicate a millhead grade of 24 g/t gold (Smith, 1936).

Both the Windpass and Sweet Home are west-trending, north-dipping, shear-hosted quartz veins which cut a hornblende, pyroxene diorite sill and adjacent bedded cherts of the lower Fennell Formation approximately 1.5 km west of the Baldy Batholith (Schiarizza and Preto, 1987). Mineralization is restricted to that part of the shear zone hosted in the diorite and consists of, in apparent paragenetic sequence; magnetite, pyrrhotite, pyrite, cobaltite, chalcopyrite, gold, bismuthinite, bismuth and supergene native copper (Uglow and Osborne, 1926). Four grab samples from the Windpass dump, two from surface trenches and three chip samples, 2 from the #3 main adit and 1 from the # 1 Windpass adit (Table 2; Jenks, 1997) are plotted on Figure 11. Analyses show a strong Bi and Au correlation for mineralized samples. The presence of magnetite and chalcopyrite within the mineralizing system is not a common feature of deposits associated with reduced intrusions.

PROSPECTIVE AREAS - BALDY BATHOLITH

The area surrounding the mid-Cretaceous Baldy Batholith is prospective for intrusive-related peripheral deposits like the Windpass-Sweet Home (located approximately 1.5 km west) and the Cam-Gloria gold-quartz vein (located approximately 7.5 km south) of the main intrusive body. The former are hosted in west-striking moderately north-dipping fissure veins in Fennell Formation diorite, the latter in northeast-trending, steeply northwest-dipping fissure structures cutting Middle Jurassic monzodiorite. Copper, copper-molybdenum porphyry and base metal polymetallic vein showings are associated with the hornblende-biotite granite phase of the intrusion which comprises the western two-thirds of the batholith. This area may represent the upper?/mid-level of the intrusion, whereas the areas proximal to the margins or carapace (presently eroded) are more prospective to host late stage evolved fluids ± metals. The muscovite-biotite granite in the eastern one-third of the batholith is associated with abundant pegmatites, aplites and porphyry molybdenum mineralization. This style of mineralization characterizes the interior of the highly fractionated youngest phase of the batholith. The eastern end of the batholith is faulted off by the Adams Lake-North Thompson Fault, a west-side down listric normal post-Paleocene fault structure. Areas encompassing the known intrusive-related deposits extend from the mainly steeply-dipping contacts of the Baldy batholith at least as far as 7.5 km. This is a substantial amount of prospective ground remaining to be fully tested.

GQ

Several Au- Cu-W-Bi skarn occurrences were discovered northeast of Shuswap Lake in 1999 by Warner Gruenwald. The prospective nature of the area was recognized through silt sampling and the discoveries resulted from following up anomalous gold values. The showings (SW, SE and NE showings, Gruenwald, 1999) outcrop on new logging roads in Second Creek drainage (82M/02), a northwest-flowing tributary of the Anstey River. The GQ claims were staked in the fall to cover the area. The property was visited in 1999, and described by Cathro (Cathro and Lefebure, 2000). In July the author, together with M. Cathro, D. Lefebure and D. Marshal revisited the showings and spent 2 days sampling and mapping the sulphide occurrences.

GEOLOGY

The GQ property straddles the Monashee décollement, a major west-dipping contractional fault (Read and Brown, 1981), with large Late Cretaceous to Paleocene east-directed displacement (Parrish, 1995). West of the fault, in the hangingwall are Windermere-equivalent, amphibolite facies metamorphic rocks of the Selkirk allochthon (Figure 9). The Selkirk allochthon corresponds to the "paragneiss and pegmatite" map unit "E" of Wheeler (1965), which includes pelite and semi-pelite schist, quartzofeldspathic gneiss, impure marble, garnet-hornblende amphibolite and minor micaceous quartzite, at the GQ property. These metasedimentary rocks have been extensively intruded by numerous narrow lenses of granite and pegmatite. The mineralized showings are hosted in and adjacent to buff and rusty weathering impure marbles and calcsilicate horizons within a thick sequence of interlayered micaceous quartzites, pelite and semi-pelite and minor amphibolite.

The east side of the property is underlain by footwall rocks of the Monashee décollement, an Early Proterozoic crystalline basement of orthogneisses and an unconformably overlying sequence of paragneisses of uncertain age, termed the cover sequence (McMillan, 1973, Journeay, 1986). The rocks at GQ show wide zones of strong deformation related to shear strain within the Monashee décollement zone.

The western half of the property is underlain by a north-trending subalkalic, weakly peraluminous, biotite monzogranite intrusion. This is part of the large, 35 km^2 composite Anstey Pluton, which at its northern exposure, is a strongly sheared and metamorphosed tabular body, with a 92-94 Ma, crystallization age (U-Pb zircon and monazite age, Parrish, 1995). On the GQ property, the eastern contact is a 2-3 km wide zone of interlayered paragneiss and foliation parallel sills or crosscutting dikes of biotite monzonite, tourmaline ± garnet pegmatite and aplite bodies. The pegmatite and aplite show various relationships to the paragneiss and exhibit a variety of igneous textures including; coarse equigranular, crowded-potassium feldspar megacrystic, pegmatitic and gneissic varieties, all which can occur together at the outcrop scale. The relationships between textural phases are often gradational but crosscutting fine-grained dikes with chilled margins are present. Crosscutting, syn-tectonic foliated biotite-muscovite potassium feldspar pegmatite, coarse-grained tourmaline-bearing biotite leucogranite and aplite are the most common dikes located in the western part of the property. These vary from several centimetres up to ten's of metres wide and for the most part lie parallel with foliation of the gneisses. Where they cut the granite the contact is gradational and not always planar. Often there is no chilled margin, alteration envelope or any indication of non-equilibrium. Fine-grained, muscovite, garnet-bearing aplite dikes crosscut both the dominant foliation of the paragneisses and sills of biotite monzogranite. The youngest intrusive rocks are narrow 1 to 5m wide, dark green, aphanitic olivine basalt dikes. The dikes strike northerly and dip-steeply and probably occupy Tertiary or younger extensional structures.

The paragneiss and schist contain a north-northwest-trending moderate southwest-dipping bedding parallel foliation. Below the décollement, in Monashee complex rocks, a southwest-plunging crenulation cleavage is superposed on the dominant north-trending foliation. There are two areas in Third Creek where the paragneiss and pegmatite contain discrete ductile shear zones. Mylonite zones in monzogranite, shear bands in paragneiss, and leucosome-tails on rotated garnet-hornblende amphibolite boudins all show a tops to the northeast sense of shear related to strain within the Monashee décollement zone.

Pelitic rocks contain sillimanite-orthoclase±muscovite without kyanite suggests sillimanite-muscovite zone of amphibolite facies for the rocks hosting mineralization. The calcsilicate schist and marble contain calcite-diopside-quartz-tremolite and/or actinolite.

East of the décollement are interlayered semi-pelite, calcsilicate marble, stratabound carbonatite tuff, amphibolite augen and rare pegmatitic leucosomes. The pelite contain kyanite-muscovite-garnet-biotite ± sillimanite assemblages indicate upper amphibolite facies metamorphism (Journeay, 1986). Pods of coarse grained sillimanite and feldspar-quartz-biotite augen define a southwest-plunging stretching lineation. Carbonatite (pyroclastic-type) horizons were noted, and one was sampled east of the GQ showings, in footwall rocks within cover sequence rocks of the Monashee complex. The sample returned anomalous values for the rare earth elements: barium, cesium, lanthanum and niobium, which compare extremely well with the range of values for the Mount Grace carbonatite (Höy, 1987). The Cottonbelt and other Pb-Zn-Ag stratabound, Shuswap type deposits overlie bedded carbonatites in the Mount Grace area (Höy, 1987), suggesting that the eastern portion of the GQ property may share an equally high prospective nature to host these stratabound occurrences.

Mineralization

Mineralization in the Selkirk allochthon consists of narrow (10-40cm), auriferous sulphide skarns developed along the contact zones between leucocratic, siliceous aplitic to pegmatitic granite sills and calcsilicate marble or rusty pelitic schist. Sulphides of mainly pyrrhotite, minor pyrite and traces of chalcopyrite occur as disseminations and fracture-fillings of several percent to semi-massive pods comprising up to 20-30 percent of the rock. In the massive pods, sulphides are interstitial, forming a 'net-texture' to the subhedral and euhedral calcsilicate skarn assemblage of diopside, scapolite, garnet and quartz grains. The scapolite is approximately 25% marialite (Na end member) and 75% meionite (Ca end member) (personal communication, D. Marshall, 2000). In the majority of showings the sulphides are found in the intrusion or between it and the calcsilicate assemblage of the country rock, indicative of an endoskarn. A 3 m section across the 'middle sulphide occurrence' on the north side of Second Creek, consists of the following succession. Beginning at the hangingwall side of the sill and progressing westward is 7 cm of semi-massive net-textured pyrrhotite, scapolite, diopside skarn (sample JLO-16-151), gradational into 15 cm of garnet-diopside±pyrrhotite-skarned rusty schist. Beyond this is 1.5 meters of calcsilicate rock and then interlayered biotite schists and calcsilicate marbles. Pyrrhotite occupies high-angle, late stage crosscutting structures within the skarn zone. Cathro and Lefebure (2000) report anomalous values for Bi, Cu, Te , and W from grab samples from the SW showings.

Samples of the pegmatite, mineralization and calcsilicate marble show that enrichment of Au is limited to the narrow sulphide endoskarn. The only gold value from pegmatite is low (5 ppb Au). A sample of the calcsilicate located 4 m from the mineralization at the SW showing contains below detection Au values (Table 2). The enrichment of Au, Bi, and Cu, Au:Bi correlation and ratios, morphology and calcsilicate assemblage are similar to proximal tungsten-gold skarns developed adjacent to Tombstone intrusions at the Marn (Brown and Nesbitt, 1987) and Horn (Hart *et al.*, 2000) and in general to reduced gold-skarn mineralization (Meinert, 1998). Neither the timing of mineralization, nor the age or relationship of the causative pegmatites are known. If the pegmatites are related to the 'dated phase' of the Anstey Pluton, they are mid-Cretaceous, and predate the high-grade metamorphism and shearing (Scammell, 1993; Johnson, 1994) that occur between Late Cretaceous and Paleocene, at this structural level in the Selkirk allochthon (Parrish, 1995). Alternatively, the pegmatites may be anatectic leucosomes related to this younger period of crustal thickening and high heat flow. The mineralization indicated to date is limited to narrow and isolated gold-sulphide skarn zones which do not extend far into the calcsilicate or schist host.

Goldstrike-Bizar

The Goldstrike (Bizar) property (MINFILE 82M 267) is located 16 kilometres northeast of the village of Avola (Figure 10). Mineralization was discovered and staked by Leo Lindinger in 1998. The property was briefly visited in 1999 (Logan, 2000; Cathro and Lefebure, 2000). Five short holes drilled in October, 1999 by Cassidy Gold Corp, intersected narrow zones of quartz sulphide mineralization (Greunwald, 1999).

Mineralization at the Bizar showing consists of semi-concordant, and sheeted quartz-sulphide veinlets hosted by amphibolite grade micaceous quartzite and quartz-muscovite-biotite-garnet schist of the Shuswap complex. The style and characteristics of mineralization are similar to other intrusive-related proximal deposits in Alaska and the Yukon, in particular the high-grade Pogo deposit. Specifically these include; its structural morphology (shallow dipping, quartz sulphide layer), metamorphic grade of host rock, and high-grade gold assays correlative with high bismuth values. To assess the likelihood of these correlations the property was revisited in 2000 and four days were spent mapping the area surrounding the Bizar showing.

GEOLOGY

Mapping indicates the property is underlain by garnetiferous biotite-muscovite schist and micaceous quartzite with minor amphibolite and calcsilicate units. West of Tumtum Lake the metasediments consist of micaceous quartzite with interlayered biotite-muscovite-quartz schists and rusty, sericite-quartz-pyrite schist. Rare, thin amphibolite and orthoquartzite beds occur 2 km northwest of the lake. The pelitic rocks contain

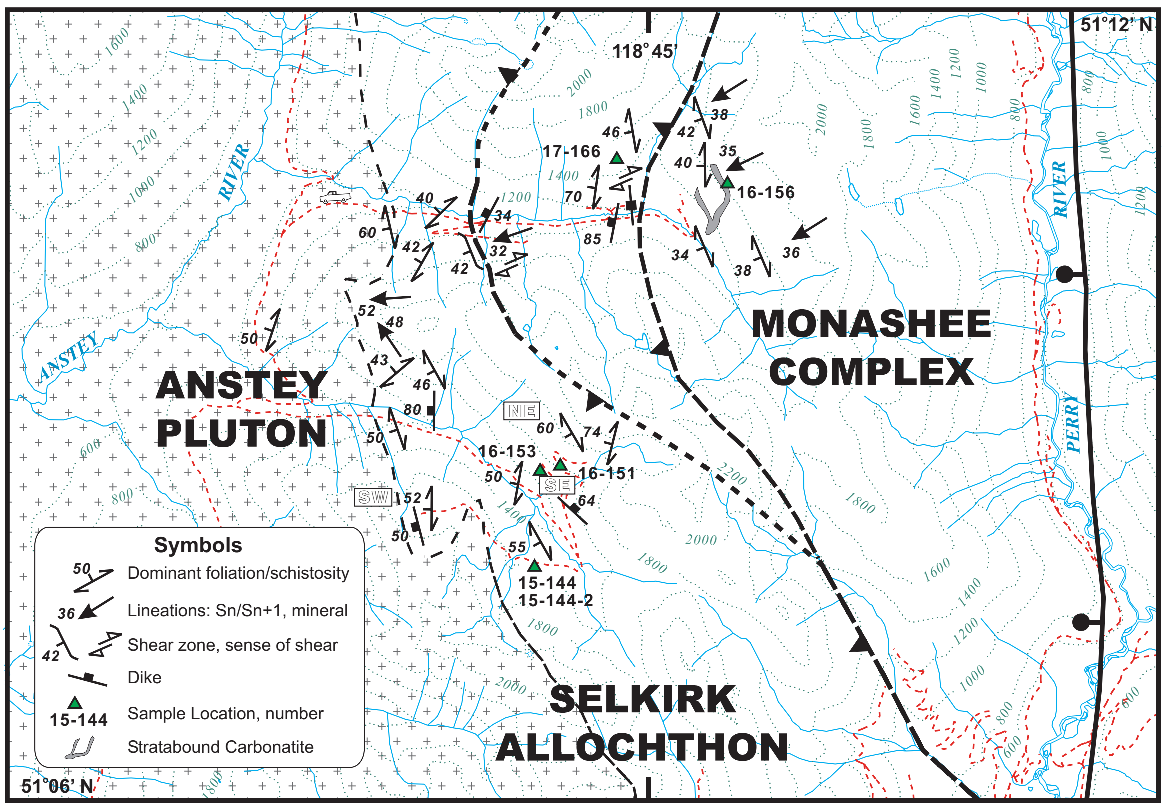

Figure 9. Geology of the Selkirk allochthon (SA) and the western edge of the Monashee Complex in the area between the Perry and Anstey rivers, modified from Höy and Brown (1981). A three-fold subdivision of the GQ property includes; leucogranites of the Anstey Pluton, a gneiss and pegmatite unit of the SA and paragneiss of the Monashee Complex. Shown are locations of the SW, SE and NE mineral showings, geochemical samples and the stratabound carbonatite locality.

biotite, muscovite, plagioclase and quartz ± garnet assemblages characteristic of the garnet zone of greenschist facies metamorphism. West from the lake, and up to the top of Groundhog Mountain the pelitic rocks contain staurolite, andalusite and chlorite, and the calcareous rocks contain garnet and hornblende in addition to the garnet zone assemblage minerals, indicating amphibolite facies metamorphism. Andalusite pseudomorphs up to 2 cm in length, commonly retrogressed to muscovite are developed along the foliation planes in pelitic layers close to the granodiorite contact on Groundhog Mountain. Thin sections show static garnet, biotite and amphibole porphyroblast overgrowth of an early dominant foliation. The contact assemblage minerals for the most part are retrograded; garnets have biotite and chlorite rims, andalusite is rimmed by sericite. The garnet-biotite-staurolite-andalusite assemblages most likely represent a contact aureole related to the large composite granitoid body which envelopes the western side of the property. The contact aureole and therefore the intrusion postdate the syntectonic development of the dominant regional fabric. Sparse mineral lineations within the aureole are similar to the younger, southeast-trending structures. This may constrain the second phase of folding to the time of pluton emplacement.

The metasedimentary rocks are intruded to the north, west and south by variably deformed, composite, hornblende, biotite and biotite-muscovite granitic bodies. Narrow leucosomes and peraluminous (andalusite-bearing) pegmatitic sills occur throughout the sequence, but are much more abundant farther north. Northwest of Tumtum Lake the intrusive body is a leucocratic, equigranular to sparse potassium feldspar megacrystic, biotite granodiorite. Marginal phases are foliated, lineated and contain more mafic minerals than the interior. The granodiorite contains abundant biotite-muscovite-quartz-potassium feldspar and garnet pegmatite dikes, sheeted quartz veins and aplite dikes. A second composite intrusive body consists of: an older foliated hornblende, biotite, epidote granodiorite; a potassium feldspar megacrystic, biotite granodiorite; and a younger equigranular biotite, muscovite granite phase. This body crops out west of Groundhog Mountain in fault contact with amphibolite facies micaceous quartzites. As much as 10 m from the fault the granodiorite is thoroughly fractured and pervasively chlorite altered. An isolated, small exposure of metamorphosed, gneissic feldspar metacrystic quartz monzodiorite is interlayered with micaceous quartzite and rusty metapelite 3 kilometres west of the south end of Tumtum Lake. On the modal quartz-alkali feldspar-plagioclase feldspar plot (LeMaitre, 1989), the few samples collected from all of these intrusion scatter across the granodiorite field. In addition they have major and trace element abundances similar to Devonian-Mississippian granodiorite orthogneisses and middle Jurassic quartz monzodiorite bodies in the Adams Lake area. In thin-section the foliated granodiorite samples contain plagioclase, potassium feldspar, biotite, hornblende, quartz and epidote with trace amounts of sphene, apatite and tourmaline. No isotopic age constraints are known for any of these intrusions.

The schists and quartzites contain a dominant north-northwest-trending dominant foliation defined by synmetamorphic biotite and muscovite. A younger phase of southeast-trending, steeply dipping crenulation cleavage and open folds deforms the north-trending structures. At the Bizar showing the stratabound massive sulphide horizon is tightly folded about these younger structures axis plunging 30° towards 140°Azimuth.

MINERALIZATION

Two main types of quartz bodies are present in the area. Bedding/foliation parallel, shallow-dipping quartz-biotite-feldspar ± sulphide layers and aplitic leucosomes; and steeper, north and northwest-trending quartz-muscovite-andalusite ± sulphide veins that crosscut bedding/foliation and generally parallel crenulation cleavage. The relatively younger, andalusite-bearing quartz veins vary in width from 1 to 20 cm depending primarily on the competency of the host. Where hosted in quartzite and micaceous quartzite the veins are narrow, but well defined and where the structure crosses into tightly crenulated mica schists they often pinch out. These veins tend to parallel southeast-trending structures. Andalusite indicates peraluminous magmatism, related to crustal thickening and anatectic melting which postdates the development of early structures and dominant foliation.

Lithogeochemical sampling of quartz veins, alteration and intrusive rocks was carried out in conjunction with mapping. Four individual veins ranging from 2-20 cm in width and containing minor pyrite and/or pyrrhotite were sampled across the property. All were steeply dipping, crosscut the dominant foliation and located distal from the main discovery zone (Logan, 2000; Cathro and Lefebure, 2000). A foliation parallel, 15 cm rusty weathering aplitic leucosome and a composite of sheeted quartz veinlets hosted in granite southwest of the Bizar showing were also sampled. Gold values for all samples were below detection and all of the other intrusion-related geochemical signature elements returned low values (Table 2).

The stratabound mineralization at the Bizar showing is concordant with dominant synmetamorphic foliation and has been deformed and metamorphosed together with the schists into southeasterly plunging folds (Logan, 2000). Conclusions from the 1999 drilling project indicate that mineralization is "stratigraphically controlled with quartz veins, veinlets and siliceous zones concordant with bedrock foliation" (Greunwald, 1999). The setting of the Bizar is similar to other Shuswap-type stratabound deposits of Pb-Zn-Ag±Cu (*i.e.* Cottonbelt, River Jordan, Ruddock Creek; Höy, 1996). With the exception of low silver values the enrichments of Au, Cu, Bi, As, Sb and Zn present at Bizar closely match the geochemical signature of the Shuswap-type deposits. Further prospecting and exploration is warranted on this property but a stratabound model, similar to the Broken

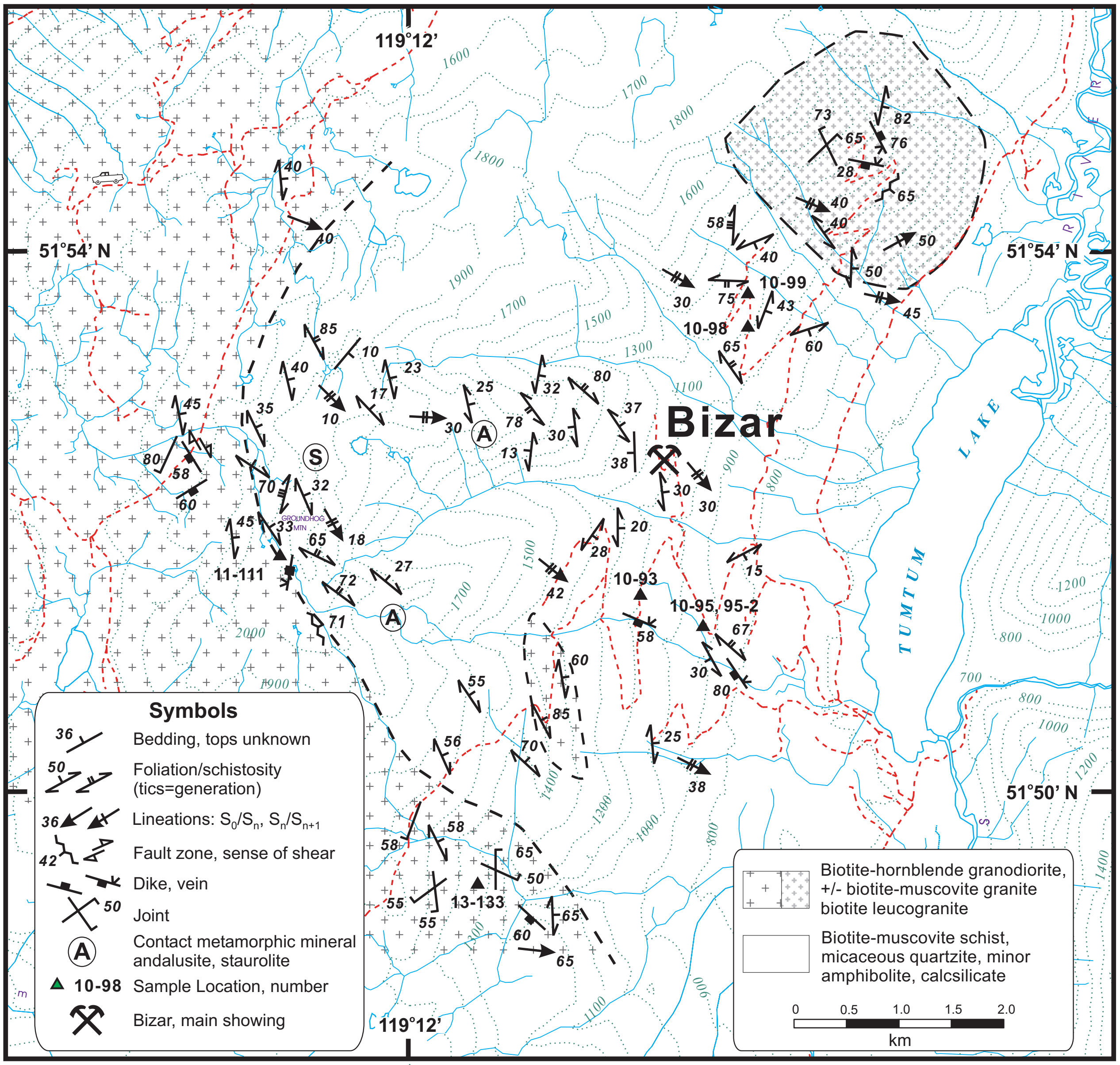

Figure 10. Geology of Tumtum Lake area showing the location of stratabound mineralization at the Bizar zone and the location of sampled quartz veins.

Hill/Shuswap-type is more applicable for evaluation of this area than an intrusion-related model.

DISCUSSION

One of the challenges for exploration for intrusive-related gold quartz veins, hosted by country rock is distinguishing them from other types of mesothermal quartz veins. In some cases there are diagnostic characteristics, such as direct association of gold mineralization and quartz veins with pegmatites or aplites, to show the genetic relationship to an intrusion. Otherwise, detailed studies of the fluids, paragenesis of mineral phases and/or dating of various geological events is required to prove the magmatic parentage of the fluids.

Since this data is frequently not available for mineral occurrences, it is more difficult to establish the genesis of auriferous quartz veins hosted by sedimentary, volcanic or unrelated intrusive rocks, or their metamorphic equivalents. As shown by the gold quartz veins in the Groundhog Basin, it is possible to use field characteristics to infer whether they are intrusive-related or belong to orogenic gold deposits. These characteristics include; vein structures that postdate the main (Middle Jurassic) orogenic event, narrow alteration envelopes, association of bismuth minerals with gold, and presence of tungsten minerals in the veins.

One area of research that may provide the exploration geologist with a quick and fairly reliable tool for distinguishing intrusion-related gold quartz veins is trace metal contents and ratios, particularly for gold and bismuth. In a recent paper Flanigan *et al.* (2000) show that bismuth, gold and arsenic values from intrusion-related deposits of Alaska and Yukon change systematically with respect to depth of emplacement or distance from the causative pluton. Average Bi:Au ratios range from 31:1 for deeper and more proximal deposits to 0.36:1 for shallower and more distal deposits. Bi vs Au correlations range from r=0.89 for deeper and/or more proximal deposits to r=0.12 for shallower and/or more distal deposits. The changes for As:Au are much less predictable that Bi:Au ratios. In addition, they suggest that correlation and ratios may be used predictively in less well known intrusive environments to direct exploration.

In British Columbia early results show some deposits exhibit very strong Bi to Au correlations. Statistical correlation values for Au and Bi from the highest to lowest are; .96 for Valparaiso (intrusion-hosted), .89 for the Windpass (proximal-peripheral vein) and .53 for Cam Gloria (peripheral vein). The higher correlation of Au and Bi has been linked to intrusion-hosted deposits and/or deeply emplaced deposits and to the initial precipitation of madonite (Au2Bi) Flanigan *et al.* (2000). Positive correlation of Bi and Au is also a well-known characteristic of reduced gold skarns. In particular, at the Crown Jewel gold skarn deposit in Washington, the presence of coarse-grained bismuthinite can be used to indicate ore-grade gold material (Meinert, 1998). The British Columbia deposits also indicate similar relationships between Bi:Au ratios from a limited data set of intrusion-related mineral occurrences (Figure 11). The majority of the data points fall above Bi:Au ratio of 10:1 (*i.e.* Bi concentrations are typical higher than gold by an order of magnitude). Average Bi:Au ratios are 36:1 for the Valparaiso samples, 32:1 for samples from the Windpass. The samples from Cam Gloria show a wide variability, with an average Bi:Au ratio of 269:1. The veins in the Groundhog Basin Basin and at the Ruth/Vermont and McMurdo past producers cannot be easily linked to specific intrusions. Vein samples from these areas have a negative correlation of Bi and Au and erratic Bi:Au ratios. The samples from Groundhog Basin show generally lower concentrations and a wide variability of Bi and Au values, possibly reflecting characteristics of a more distal intrusion-related system. If the values with below detection Au, and samples JLO22-195-2 (Au>Bi) and JLO22-187 (Au<Bi) are excluded from the calculation, the average Bi:Au ratio is 30:1.

The average Bi:Au ratio is 12:1 for the quartz-carbonate vein and replacement samples taken from the Ruth/Vermont and McMurdo base metal and gold past producers. Statistical correlation values for Au and Bi are -.11 for the Ruth/Vermont-McMurdo samples.

Low Rb and Nb abundances have been cited by McCoy (1999) as characteristics of gold mineralizing-intrusives of the plutonic-related deposit type. These are also characteristics of granites formed in volcanic arc settings Pearce *et al.* (1984). Bayonne suite intrusions from the southern Canadian Cordillera (Brandon and

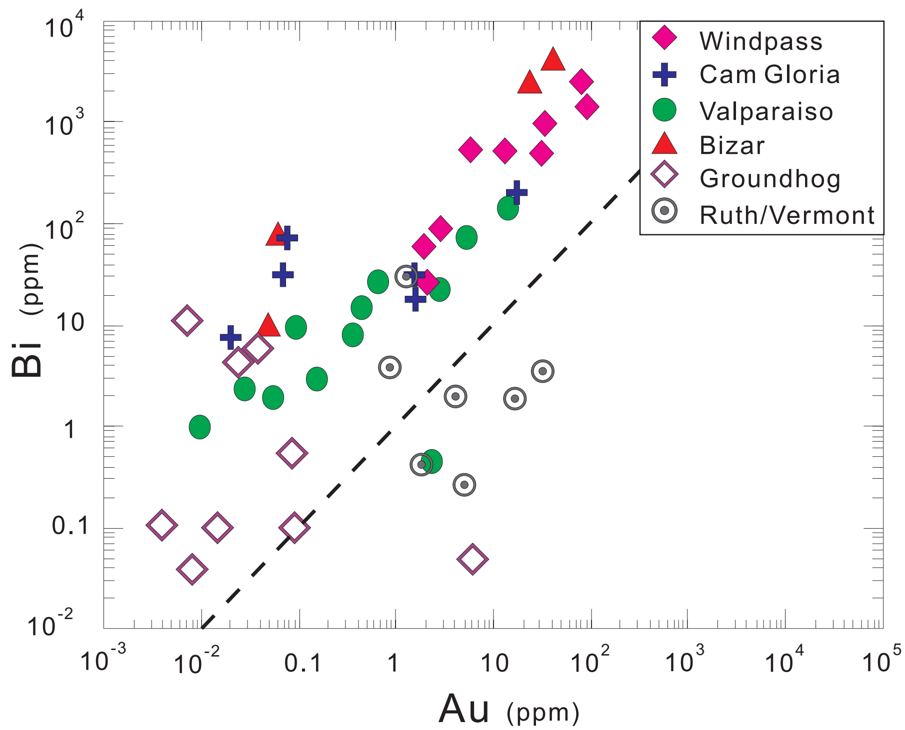

Figure 11. Bi vs. Au values for mineralized samples of intrusion-related quartz veins. Windpass samples from Jenks (1997); Bizar, Valparaiso and Cam Gloria samples from Logan (2000), Groundhog and Ruth/Vermont samples this study.

Lambert, 1993; this study) are shown in Figure 12 along with the field for mid-Cretaceous Tombstone suite intrusives (Murphy, 1997). The Bayonne suite intrusions overlap the volcanic-arc, syncollisional and within-plate fields, a non-diagnostic position shared by the Tombstone-Tungsten suite of Alaska and the Yukon (Lange *et al.*, 2000). The Middle Jurassic Honeymoon Bay stock plots in the volcanic-arc field, whereas the phases of the Baldy Batholith straddle the triple junction between VAG - syn-COLG and WPG (Logan *et al.*, 2000). Undated composite, deformed intrusive phases from the GQ and Bizar mineral occurrences (Figure 12b) plot in the volcanic-arc field but the relationships to gold-bismuth mineralization is equivocal. Unpublished data from the Goldstream pluton show the biotite granite phase overlaps the Tombstone field and hornblende quartzdiorites which plot in the WPG field (Figure 12a), while data for the Battle Range Batholith (Figure 12c), similar to the Bugaboo, Fry Creek and Horsethief Creek plutons from Brandon and Lambert (1993) have substantially higher Nb values and plot in the WPG field.

CONCLUSIONS

A key exploration approach for intrusion-related gold deposits is to explore in, and around, highly differentiated granitic intrusions, specifically those intruded in continental margin settings. In contrast with the metaluminous, subalkalic, reduced I-type Tombstone Suite, the Bayonne suite consists of mostly peraluminous, subalkalic hornblende-biotite granodiorite and highly fractionated 2-mica granites, aplites and pegmatites. These are emplaced into miogeoclinal rocks of ancestral North America and Kootenay terrane pericratonic rocks. This ancestral continental margin setting and mid-Cretaceous magmatic belt defines a W-Sn±Mo province which follows the Omineca belt south from Alaska to the Canadian-US border.

Intrusion-related gold-quartz vein occurrences are located in southern British Columbia associated with the Bayonne suite (ie. Valparaiso; intrusion-hosted mineralization, Sanca stock and at Cam-Gloria and Windpass, fissure veins peripheral to the Baldy Batholith). These occurrences have similar Au-W-Bi signatures and physical characteristics to the larger Alaska and Yukon deposits. More research is required to establish if the Bayonne suite plutons contain the metal and sulphur budget necessary to form economic intrusion-related mineralization.

ACKNOWLEDGMENTS

Marty Zaleski provided enthusiastic and capable field assistance for the work carried out in southern British Columbia. Dave Lefebure, Mike Cathro and Dan Marshall all provided stimulating geological discussions and insights during their field visit to the GQ property. Gerry Richard of Selkirk Mountain Helicopters is responsible for the safe and enjoyable flying around the Battle Range.

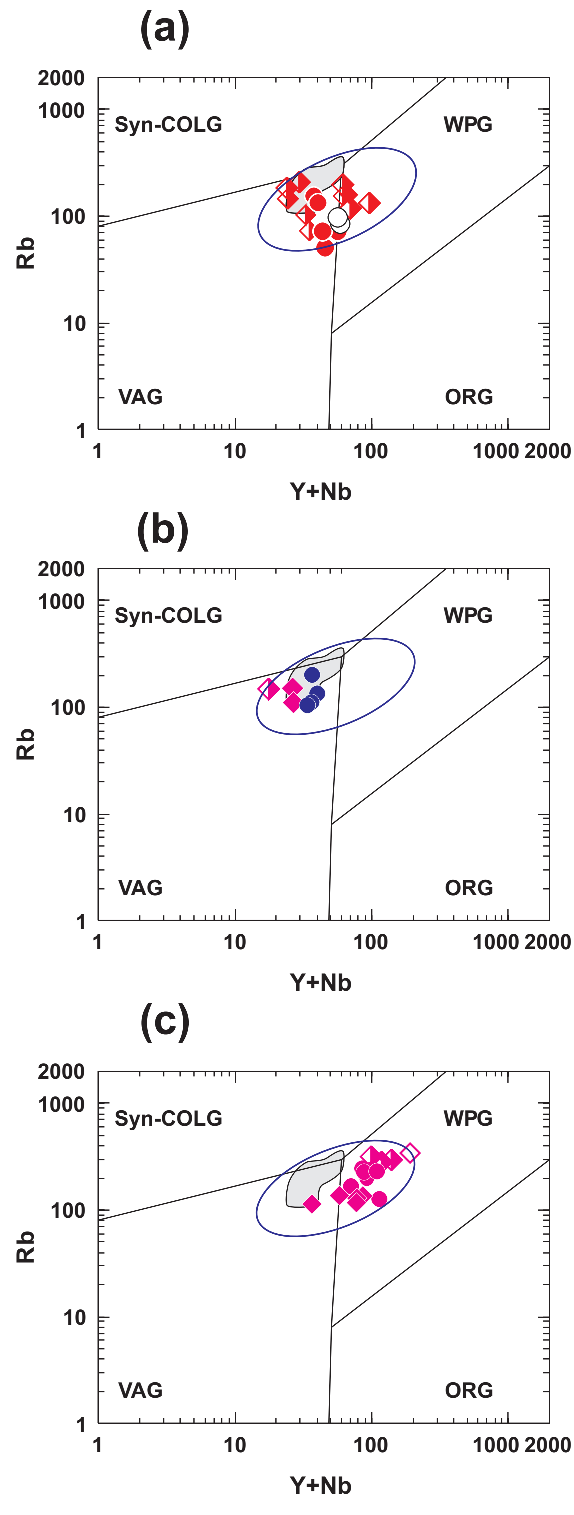

Figure 12. Rubidium vs. Yittrium + Niobium values for unaltered Cretaceous plutonic rocks of Southern British Columbia. Tectonic setting boundaries are from Pearce *et al.* (1984). The field for metaluminous Tombstone-tungsten suite plutons and dikes is shown (Murphy, 1997). 12a) Goldstream and Bigmouth samples, 12b) Anstey and unnamed Shuswap bodies in the vicinity of the Bizar-Goldstrike mineral occurrence, 12c) Battle Range Batholith samples, with symbols as in Figure 4 . Symbols for Goldstream Pluton are solid circle = hornblende diorite, diamonds = biotite granite; open circle = Bigmouth Pluton.

Dave Lefebure improved an earlier version of this manuscript and Verna Vilkos's help with the Figures is muchly appreciated. This study is part of a larger program investigating the potential for plutonic-related gold deposit in British Columbia.

REFERENCES

Armstrong, R. L., 1988, Mesozoic and Early Cenozoic Magmatic Evolution of the Canadian Cordillera: in Processes in Continental Lithospheric Deformation, ed., Clark, S. P., Jr., Burchfield, B. C. and Suppe, J., *Geological Society of America*, Special Paper 218, pages 55-91

Bobrowsky, P.T., Leboe, E.R., Dixon-Warren, A., Ledwon, A., MacDougall, D. and Sibbick, S.J. 1997, Till Geochemistry of the Adams Plateau-North Barriere Lake Area (82M/4 and 5: *B.C. Ministry of Employment and Investment*, Open File 1997-9, 262 pages.

Brandon, A.D. and Lambert, R.St.J. 1993, Geochemical characterization of mid-Cretaceous granitoids in the Kootenay Arc in the southern Canadian Cordillera: *Canadian Journal of Earth Sciences*, Volume 30, p. 1076-1090.

Brandon, A.D. and Smith, A.D. 1994) Mesozoic granitoid magmatism in southeast British Columbia: implications for the origin of granitoid belts in the North American Cordillera: *Journal of Geophysical Research*, Volume 99, p. 11,879-11,896.

Brown, R. L. and Carr, S. D. 1990, Lithospheric thickening and orogenic collapse within the Canadian Cordillera: *Australasian Institute of Mining and Metallurgy*, 1990 Pacific Rim Congress Proceedings, Volume II, p. 1-10.

Brown, R. L., Tippett, C. R. and Lane, L. S. 1978, Stratigraphy, Facies Change, and Correlations in the Northern Selkirk Mountains, Southern Canadian Cordillera: *Canadian Journal of Earth Sciences*, Volume 15, p. 1129-1140.

Calderwood, A.R., van der Hayden, P., and Armstrong, R.L., 1990, Geochronometry of the Thuya, Takomkane, Raft and Baldy batholiths, south-central British Columbia: *Geol. Assoc. Can. Mineral. Assoc. Can.* Ann. Meet. Programs with Abstr., 15, A19

Campbell, R.B. 1963, Adams Lake Map-area, British Columbia, *Geological Survey of Canada*, Map 48-1963, 1:250,000.

Carmichael, H. 1906, Big Bend District: in Minister of Mines Annual Report 1905, *B.C. Ministry of Energy, Mines and Petroleum Resources*, p. 149-150.

Cathro, M.S. 1998, Exploration and Development Highlights in South-Central British Columbia - 1997: *B.C. Ministry of Energy and Mines*, Exploration in British Columbia - 1997, p. 33-41.

Cathro, M. and Lefebure, D.V., 2000, Several new intrusive-related gold, bismuth and tungsten occurrences in Southern British Columbia: *British Columbia Ministry of Energy and Mines*, Geological Fieldwork 1999, p. 207-223.

Chapman, J., Dagenais, J., Philip, D. and Horne, E. 1982, Exploration Report, Groundhog Basin Project: *B.C. Ministry of Energy and Mines*, Assessment Report 10 393, 50 pages.

Colpron, M., Price, R.A. and Archibald, D.A. 1999, 40Ar/39Ar thermochronometric constraints on the tectonic evolution of the Clachnacudainn complex, southeastern British Columbia: *Canadian Journal of Earth Sciences*, Volume 36, p. 1989-2006.

Colpron, M., Logan, J. M., Gibson, G. and Wild, C. J. 1995, Geology and Mineral Occurrences of the Goldstream River Area, Northern Selkirk Mountains (NTS 82M/9 and Part of 10): *B. C. Ministry of Energy, Mines and Petroleum Resources*, Open File 1995-2, 1:50 000.

Cooke, D.L. 1996, Report on the 1996 Diamond Drill Program, Groundhog Basin Property: *unpublished report*, Orphan Boy Resources Inc. 9 pages.

Crowley, J.L. and Brown, R. L. 1994, Tectonic links between the Clachnacudainn terrane and implications for tectonic setting in the southern Omineca belt, Canadian Cordillea: *Tectonics*, v. 13, p. 1035-1051.

Evans,G. 1999, 1999 Geological & Geophysical & Geochemical & Diamond Drilling Report on the Cam Gloria Property: *B.C. Ministry of Energy and Mines*, Assessment Report 26 215, 21 pages.

Ghosh, D.K., 1995, Nd-Sr isotopic constraints on the interaction of the intermontane Superterrane with the western edge of North America in the Southern Canadian Cordillera: *Canadian Journal of Earth Sciences*, v. 32, p. 1740-1758.

Graf, C. 1986, Prospecting Assessment Report on the Cass 2, 3 claims Tungsten Prospect: *B.C. Ministry of Energy and Mines*, Assessment Report 14 749, 10 pages.

Greenwood, H.J., Woodsworth, G.J., Read, P.B., Ghent, E.D. and Evenchick, C.A. 1991, Metamorphism, Chapter 16: in Geology of the Cordilleran Orogen in Canada: H. Gabrielse, H., and C. J. Yorath, eds., *Geological Survey of Canada*, Geology of Canada, no. 4, p. 533-570 (also *Geological Society of America*, The geology of North America, v. G-2).

Gruenwald, W. 2000, Perry River Project: *B.C. Ministry of Energy and Mines*, Prospector's Assisstance Program Report, 11 pages.

Gruenwald, W. 1999, Geological, Geochemical and Diamond Drilling Report on the Goldstrike Property: *B.C. Ministry of Energy and Mines*, Assessment Report 26127, 9 pages.

Gunning, H. C. 1929, Geology and Mineral Deposits of the Big Bend Area, B.C.: *Geological Survey of Canada*, Summary Report 1928, Part A, pages 136-193.

Hart, C. J.R., Baker, T. and Burke, M. 2000, New Exploration Concepts for country-rock-hosted, intrusion-related gold systems: Tintina Gold Belt in Yukon: in The Tintina Gold Belt Concepts, Exploration and Discoveries,ed., J.L. Jambour, *British Columbia and Yukon Chamber of Mines*, Cordilleran Exploration Roundup 2000, Extended abstracts volume.

Henneberry, R.T. 1997, 1996 Exploration Program - Groundhog Basin Project: *B.C. Ministry of Energy and Mines*, Assessment Report 25 053, 28 pages.

Holland, S.S. 1950, Placer Gold Production of British Columbia: *B. C. Ministry of Energy, Mines and Petroleum Resources*, Bulletin 28, 89 pages.

Höy, T. 1996, Broken Hill-Type Pb-Zn-Ag±Cu: in Selected British Columbia Mineral Deposit Profiles, Volume 2, More Metallics, Lefebure, D.V. and Höy, T., Editors, *B.C. Ministry of Employment and Investment*, Open File 1996-13, pages 117-120.

Höy, T. 1987, Geology of the Cottonbelt Lead-Zinc-Magnetite layer, Carbonatites and Alkalic rocks in the Mount Grace Area, Frenchman Cap Dome, Southeastern British Columbia*: B. C. Ministry of Energy, Mines and Petroleum Resources*, Bulletin 80, 99 pages.

Höy, T. 1979, Geology of the Goldstream Area: *B. C. Ministry of Energy, Mines and Petroleum Resources*, Bulletin 71, 49 pages.

Höy, T. and Brown, R.L. 1981, Geology of the Eastern margin of Shuswap Complex, Frenchman Cap area, *B. C. Ministry of Energy, Mines and Petroleum Resources*, Preliminary Map 43.

Journeay, J.M. 1986, Stratigraphy, internal strain and thermotectonic evolution of northern Frenchman Cap dome: an exhumed duplex structure, Omineca hinterland, Southeast Canadian Cordillera. Ph.D. thesis, *Queen's University*, Kingston, Ont.

Johnson, B.J. 1994, Structure and tectonic setting of the Okanagan Valley fault system in the Shuswap Lake area, southern British Columbia: Ph.D. thesis, *Carleton University*, 266 pages.

Jung, A., 1986, Geochronometry and Geochemistry of the Thuya, Takomkane, Raft and Baldy batholiths, west of the Shuswap metamorphic complex, south-central British Columbia: Unpublished B.Sc. thesis, The *University of British Columbia*, Vancouver, British Columbia, 140 p.

Lang, J.R., Baker, T., Hart, C.J.R. and Mortensen, J.K. 2000, An exploration model for intrusion-related gold-systems: *SEG Newsletter*, no 40, p. 6-15.

Leatherbarrow, R.W. 1981, Metamorphism of pelitic rocks from the northern Selkirk Mountains, southeastern British Columbia: Ph.D. thesis, *Carleton University*, Ottawa, 218 pages.

Leech, G.B., Lowdon, J.A., Stockwell, C.H. and Wanless, R.K. 1963, Age Determinations and Geological Studies (Including Isotopic Ages-Report 4): *Geological Survey of Canada*, Paper 63-17, p. .

Lett, R.E., Bobrowsky, P., Cathro, M, and Yeow, A. 1998, Geochemical Pathfinders for Massive Sulphide Deposits in the Southern Kootenay Terrane: *B.C. Ministry of Employment and Investment*, Geological Fieldwork 1997, p. 15-19.

Lett, R.E. and Jackaman, W. 2000, Geochemical Exploration Techniques for Intrusive Hosted Gold Deposits in Southern B.C. (parts of 82M/4, 5, 6 and 82F/7): *in* Geological Fieldwork 1999*, B.C. Ministry of Energy and Mines*, Paper 2000-1.

Lefebure, D.V., Fournier, M.A. and Jackaman, W. 1999, Prospective areas in British Columbia for gold-tungsten-bismuth veins: *B. C. Ministry of Energy and Mines*, Open File 1999-3, 1:2 000 000 scale map with marginal notes and digital files.

Lefebure, D.V. and Cathro, M. 1999, Plutonic-related gold-quartz veins and their potential in British Columbia: in Short Course on Intrusion-Related Gold, *Kamloops Exploration Group*, p. 185-219.

Logan, J.M. 2000, Plutonic-Related Gold-Quartz Veins in Southern British Columbia: *British Columbia Ministry of Energy and Mines*, Geological Fieldwork 1999, p. 193-206.

Logan, J. M. and Colpron, M. 1995, Northern Selkirk Project - Geology of the Goldstream River Map Area (82M/9 and Parts of 82M/10): in Geological Fieldwork 1994, Grant, B. and Newell, J. M., Editors, *B. C. Ministry of Energy, Mines and Petroleum Resources*, Paper 1995-1, pages 215-241.

Logan, J.M. and Friedman, R.M. 1997, U-Pb ages from the Selkirk Allochthon, Seymour Arm map area, Southeast British Columbia (82M/8 and 9): *B.C. Ministry of Energy and Mines*, Geological Fieldwork 1996, p. 17-23.

Logan, J.M. and Mann, R.K. 2000, Geology and Mineralization in the Adams -East Barriere lakes area, South-central British Columbia, 82M/04: *B.C. Ministry of Energy and Mines*, Open File 2000-7.

Logan, J.M., Lefebure, D., and Cathro, M. 2000, Plutonic-Related Gold-Quartz Veins and their Potential in British Columbia in The Tintina Gold Belt Concepts, Exploration and Discoveries,ed., J.L. Jambour, *British Columbia and Yukon Chamber of Mines*, Cordilleran Exploration Roundup 2000, Extended abstracts volume.

Marchildon, N., Dipple, G.M. and Mortensen, J.K. 1998, New Metamorphic and Geochronological Constraints on the Tectonic evolution of the Northern Selkirk Mountains, SEBC: *Cordilleran Tectonics Workshop*, March 1998, Simon Fraser University, Lithoprobe Report No. 64, page 192.

Meinert, 1998, A Review of skarns that contain gold: *Mineralogical Association of Canada,* Short Course Series, v. 26, p. 359-414.

McCoy, D., Newberry, R.J., Layer, P., DiMarchi, J.J., Bakke, A., Masterman, J.S., and Minehane, D.L. 1997, Plutonic-related Gold Deposits of Interior Alaska: *Economic Geology*, Monograph 9, pages 191-241.

Monger, J.W.H. and Berg, H.C. 1984) Lithotectonic terrane map of western Canada and southeastern Alaska: in Lithotectonic Terrane Maps of the North American Cordillera, N.J. Siberling and D.L. Jones Editors, *United States Geological Survey*, Open File Report 84-523.

Monger, J.W.H., Price, R.A. and Tempelman-Kluit, D.J. 1982, Tectonic accretion and the origin of the two major metamorphic and plutonic welts in the Canadian Cordillera: *Geology*, Volume 10, pages 70-75.

McMillan, W.J. 1973, Petrology and Structure of the West Flank, Frenchman's Cap Dome, Near Revelstoke, British Columbia: *Geological Survey of Canada*, Paper 71-29, 88 pages.

Murphy, D.C., 1997, Geology of the McQuesten River Region, Northern McQuesten and Mayo map area, Yukon Territory (115P/14, 15, 16: 105M/13, 14, *Exploration and Geological Services Division*, Yukon, Indian and Northern Affairs Canada, Bulletin 6, 122 p.

Okulitch, A.V. 1979, Lithology, Stratigraphy, Structure and Mineral Occurrences of the Thompson-Shuswap-Okanagan area, British Columbia: *Geological Survey of Canada*, Open File 637.

Okulitch, A.V. 1984, The role of the Shuswap Metamorphic Complex in Cordilleran Tectonism, a review: *Canadian Journal of Earth Sciences*, Volume 16, pages1171-1193.

Parrish, R.R. 1995, Thermal Evolution of the Southeastern Canadian Cordillera: *Canadian Journal of Earth Sciences*, Volume 32, pages 1618-1642.

Parrish, R. R. 1992, Miscellaneous U-Pb Zircon Dates from Southeast British Columbia: in Radiogenic Age and Isotopic Studies: Report 5, *Geological Survey of Canada*, Paper 91-2, pages 143-153.

Parrish, R.R. and Wheeler, J.O. 1983, U-Pb zircon age of the Kuskanax batholith, southeastern British Columbia: *Canadian Journal of Earth Sciences*, 20: p. 1751-1756.

Parrish, , R.R., Carr, S.D. and Parkinson, D.L. 1988, Eocene extensional tectonics and geochronology of the southern Omineca Belt, British Columbia and Washington: *Tectonics*, Volume 7, pages 181-212.

Pearce, J.A., Harris, N.B.W. and Tindle, A.G. 1984, Trace element discrimination diagrams for the tectonic interpretation of granitic rocks: *Journal of Petrology*, Volume 25, pages 956-983.

Poulsen, K.H, Mortensen, J.K. and Murphy, D.C. 1997, Styles of intrusion-related gold mineralization in the Dawson-Mayo Area, Yukon Territory: in Current Research 1997-A, *Geological Survey of Canada*, pages 1-10.

Price, R. A. 1986, The Southeastern Canadian Cordillera: Thrust Faulting, Tectonic Wedging, and Delamination of the Lithosphere: *Journal of Structural Geology*, Volume 8, pages 239-254.

Price, R. A., Brown, R. L. and Tippett, C. R. 1979, The Selkirk Fan Structure of the Southeastern Canadian Cordillera: Discussion and Reply: *Geological Society of America*, Bulletin, Volume 90, pages 695-698.

Ray, G.E. and Webster, I.C.L. 1997, Skarns in British Columbia: *B.C. Ministry of Energy and Mines*, Bulletin 101, 131 pages.

Read, P. B. and Brown, R. L. 1981, Columbia River Fault Zone: Southeastern Margin of the Shuswap and Monashee Complexes, Southern British Columbia: *Canadian Journal of Earth Sciences*, Volume 18, pages 1127-1145.

Read, P. B. and Wheeler, J. O. 1976, Geology of Lardeau West-Half Map Area: *Geological Survey of Canada*, Open File 432, 1:125 000.

Read, P.B., Woodsworth, G.J., Greenwood, H.J., Ghent, E.D. and Evanchick, C.A. 1991, Metamorphic Map of the Canadian Cordillera, *Geological Survey of Canada*, Map 1714A, scale 1:2 000 000.

Scammell, R.J. 1993, Mid-Cretaceous to Tertiary thermotectonic history of former mid-crustal rocks, southern Omineca belt Canadian Cordillera. Ph.D. thesis, *Queen's University*, Kingston, Ont.

Schiarizza, P. and Preto, V.A. 1987, Geology of the Adams Plateau-Clearwater-Vavenby area: *B.C. Ministry of Energy, Mines and Petroleum Resources*, Paper 1987-2, 88 pages.

Schindler, J.N. 1984, Geological, Geochemical and Geophysical Report on the Groundhog Basin Joint Venture Property: *B.C. Ministry of Energy and Mines*, Assessment Report 11 860, 35 pages.

Sears, J. W. 1979, Tectonic Contrasts between the Infrastructure and Suprastructure of the Columbian Orogen, Albert Peak Area, Western Selkirk Mountains, British Columbia: unpublished Ph.D. thesis, *Queen's University*, 154 pages.

Sevigny, J.H., Parrish, R.R., Donelick, R.A., and Ghent, E.D. 1990, Northern Monashee Mountains, Omineca Crystalline Belt, British Columbia: Timing of metamorphism, anatexis and tectonic denudation: *Geology*, volume 18, pages 103-106.

Smith, A.J. 1936, Milling Operations at the Windpass Gold Mine, *The Miner.*

Smith, M. , Thompson, J.F.H., Bressler, J., Layer, P., Mortensen, J.K., Abe, I. and Takaoka, H. 1999, Geology of the Liese Zone, Pogo Property, East-Central Alaska: *SEG Newsletter*, No. 38, July 1999 pages 12-21.

Taylor, W.A. 1989, Windpass, Sweet Home (092P039, 49): *B.C. Ministry of Energy, Mines and Petroleum Resources*, Exploration in British Columbia 1988, pages B115-B121.

Thompson, J.F.H., Sillitoe, R.H., Baker, T., Lang, J.R. and Mortensen, J.K. 1999, Intrusion-related gold deposits associated with tungsten-tin provinces: *Mineralium Deposita*, Volume 34, Number 4, pages 323-334.

Uglow, W.L. and Osborne, F.F. 1926, A gold cobaltite-lodestone deposit, British Columbia, with Notes on the Occurrence of Cobaltite: *Economic Geology*, Volume XXI, No. 3, pages 285-293.

Westervelt, R.D. 1972, Geological Report on the Ice Claim Group, Albert Canyon-Revelstoke area*: B.C. Ministry of Energy and Mines*, Assessment Report 3 725, 7 pages.

Wheeler, J.O. 1965, Big Bend Map-Area, British Columbia, (82M East Half): *Geological Survey of Canada*, Paper 64-32, 37 pages.

Wheeler, J. O. 1963, Rogers Pass Map-area, British Columbia and Alberta (82N W Half): *Geological Survey of Canada*, Paper 62-32, 32 pages.

Wheeler J.O. and McFeely, P. 1991, Tectonic Assemblage Map of the Canadian Cordillera and adjacent parts of the United States of America: *Geological Survey of Canada*, Map 1712A, scale 1:2 000 000.

British Columbia Geological Survey
Geological Fieldwork 2000

The Mid-Cretaceous Rocky Ridge Formation - A New Target for Subaqueous Hot-Spring Deposits (Eskay Creek-Type) in Central British Columbia?

By D.G. MacIntyre

KEYWORDS: Skeena Arch, Skeena Group, Rocky Ridge Formation, volcanogenic massive sulphide potential, Eskay Creek potential, shallow marine, rhyolite domes, geochronology, lithogeochemistry, U/Pb age dating, Ar/Ar age dating.

INTRODUCTION

The Skeena Arch project was initiated in the 2000 field season as a follow up to work completed as part of the Nechako NATMAP project (MacIntyre and Struik, 1999). The main objective of this project is to define areas that have a high potential for the discovery of volcanogenic massive sulphide and/or subaqueous hot spring deposits (Eskay Creek type) along the trend of the Skeena Arch, in central British Columbia. In this area favourable host rocks for these deposit types occur in two separate geologic units - Lower to Middle Jurassic submarine volcanic rocks of the Hazelton Group and the mid-Cretaceous Rocky Ridge Formation of the Skeena Group. The latter represents a stratigraphic package whose potential was only identified during the recently completed Nechako NATMAP project.

In order to demonstrate the occurrence of favourable volcanic stratigraphy and associated vein and massive sulphide mineralization within the Rocky Ridge Formation, several key areas were visited and sampled in the 2000 field season. These include Nilkitkwa River, French Peak, Fort Babine, Fireweed, Suskwa River, Mt. Cronin, Beament , Rocky Ridge, Mt. Ney and Troitsa Lake (Figure 1). Samples for geochronology and litho geochemistry were collected at all of these sites.

GEOLOGIC SETTING

The study area is within the Stikine Terrane of the Intermontane geomorphological belt (Figure 1). The Stikine Terrane includes Carboniferous to Middle Jurassic arc volcanic and plutonic rocks. East of the study area, oceanic rocks of the Carboniferous to Early Jurassic Cache Creek Terrane are structurally imbricated with the Stikine Terrane. Remnants of Late Cretaceous to Early Eocene continental volcanic arc rocks cover the Stikine and Cache Creek terranes and their Late Jurassic to Late Cretaceous sedimentary overlap successions.

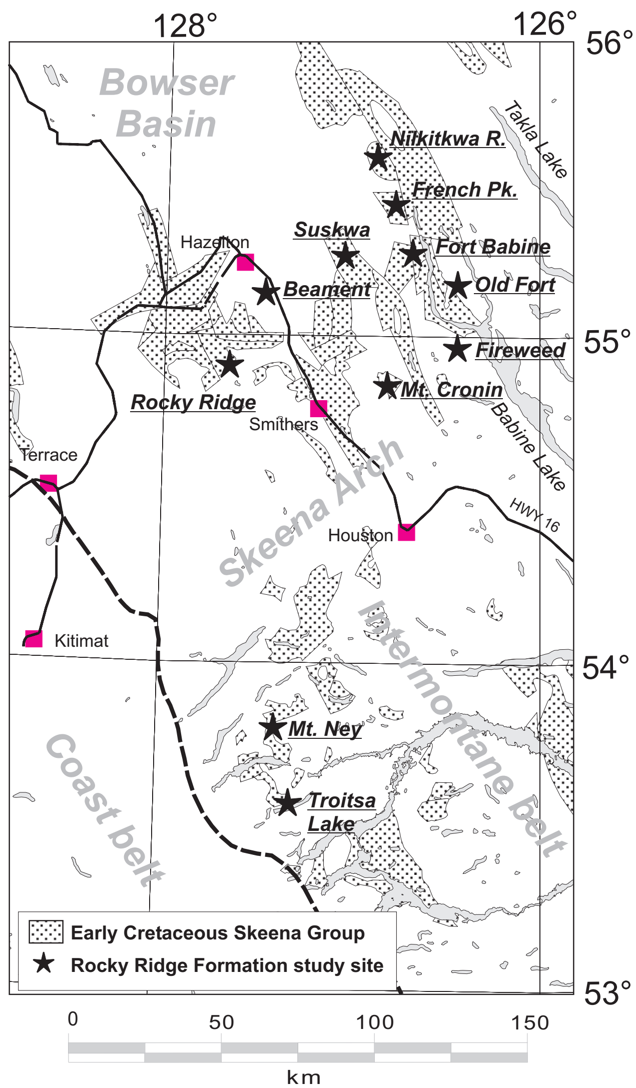

Figure 1. Map showing the areal extent of the Skeena Group (stippled pattern) in west central British Columbia relative to major tectonic elements. Stars mark sites where Rocky Ridge volcanic rocks of the Skeena Group were sampled as part of this study.

The best exposures of the Stikine Terrane occur along the Skeena Arch, a northeast trending uplift that forms the southern margin of the Bowser Basin. This uplift began to evolve in the early Jurassic as indicated by sedimentary and volcanic facies relationships in the area (MacIntyre *et al.*, in press). The core of the uplift exposes volcanic arc assemblages of the Early Permian Asitka, Late Triassic Takla and Early to Middle Jurassic Hazelton groups. Coeval plutonic rocks include the Late Triassic to Early Jurassic Topley and the newly recognized Early to Middle Jurassic Spike Peak intrusive suites (MacIntyre *et al.* 1998; in press). North of the Skeena Arch, the older volcanic arc rocks are onlapped by marine to non-marine sedimentary strata of the Late Jurassic Bowser Lake and Early Cretaceous Skeena groups; to the south the arch is covered by Tertiary volcanic rocks.

SKEENA GROUP STRATIGRAPHY

The Skeena Group is comprised of marine and non-marine sedimentary rocks that overlap Jurassic and older rocks along the southern margin of the Bowser Basin. Although the base of the Skeena Group is rarely seen, where it is exposed it is an angular unconformity with the underlying Hazelton or Bowser Lake group. The Skeena Group is unconformably overlain by continental volcanic arc rocks of the Late Cretaceous Kasalka and Early Eocene Ootsa Lake groups. In general the lower Skeena Group is fluvial to fluvial-deltaic mudstone, siltstone, and sandstone. Higher in the stratigraphy are the volcanic rocks of the Rocky Ridge Formation (Figure 2) as first recognized by Tipper and Richards (1976). Overlying these rocks, and in part interbedded with them, are chert-quartz bearing conglomerates, quartzo-feldspathic wackes and siltstones that were deposited in a fluvial-deltaic environment (Tipper and Ricahrds, 1976; Richards, 1980; 1990; Bassett 1991).

The main Skeena lithologies are dark grey shaly siltstone, greywacke, carbonaceous mudstone and chert-pebble conglomerate These sedimentary rocks were deposited in a fluviodeltaic, near-shore to shallow marine environment (Basset, 1991). Although fossils are rare, the Skeena Group appears to range from Hauterivian to late Albian or early Cenomanian in age. Paleocurrent measurements indicate north, west and southwest sediment transport with the source area located in the Omineca belt. Bassett and Kleinspehn (1996) suggest that this belt was the main axis of a mid-Cretaceous continental arc and that the Skeena Group is a forearc succession (Figure 3). The Skeena rocks were folded, uplifted and eroded during a mid to late Cretaceous contractional event related to evolution of the Skeena Fold Belt (Evenchick, 1999).

Richards (1990) subdivides Skeena Group rocks in the Hazelton map area (93M) into six formations or mappable units. These are, from oldest to youngest, the Kitsumkalum shale, Kitsuns Creek Formation, the Rocky Ridge Formation, the Hanawald conglomerate and the

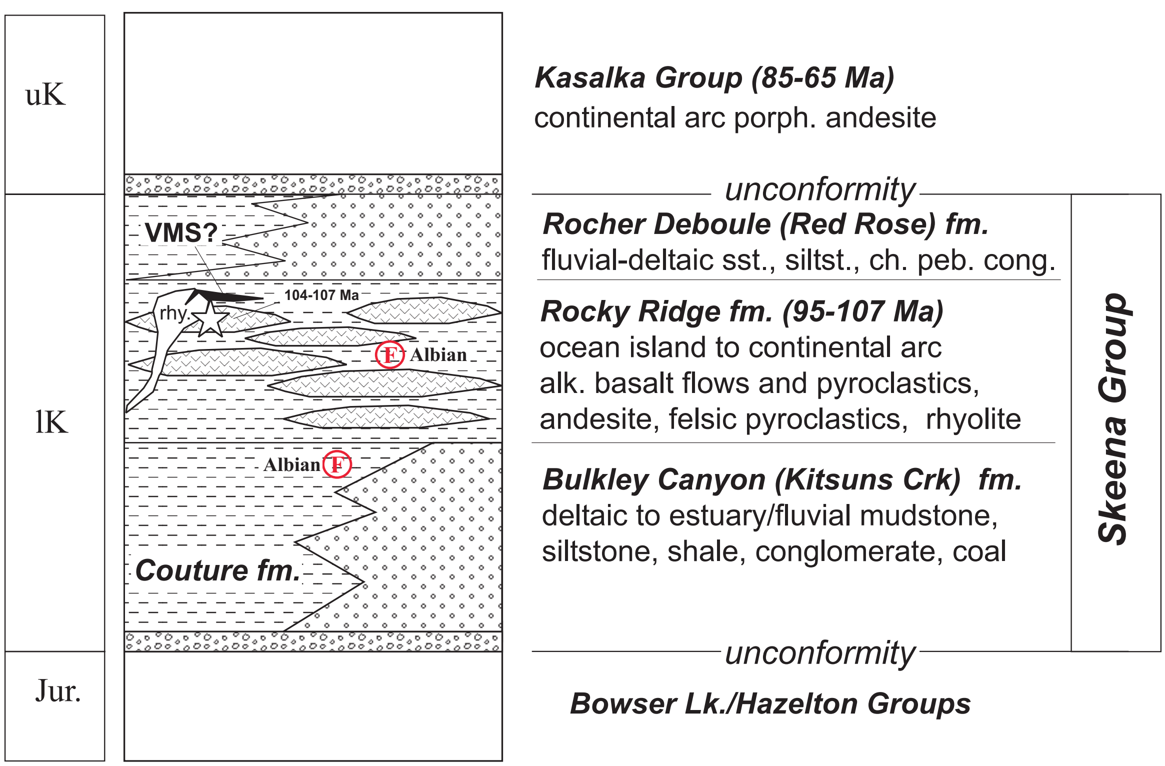

Figure 2. Schematic stratigraphy for the Skeena Group showing stratigraphic position of rhyolite domes and Rocky Ridge volcanic rocks discussed in this report.

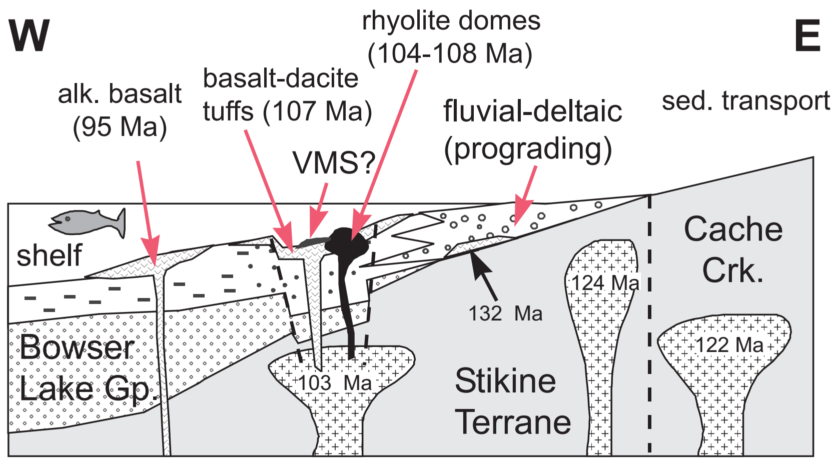

Figure 3. Schematic diagram illustrating the postulated depositional environment for the Skeena Group as suggested by Bassett and Kleinspehn (1996). Also shown are geochronologic controls determined during the Nechako Natmap project.

Red Rose Formation. In a recent paper, Bassett and Kleinspehn (1996) proposed a new stratigraphic nomenclature based on lithofacies. In their stratigraphy the lowest unit of the Skeena Group succession is the predominantly deltaic Bulkley Canyon Formation which includes, in the east, the fluvial Kitsuns Creek Member and to the west the subtidal, turbiditic Couture Formation. Locally these rocks are overlain by and in part interbedded with the volcanic arc rocks of the Rocky Ridge Formation, the main subject of this paper. The fluvial to deltaic Rocher Deboule Formation which would include the former Red Rose Formation and Hanawald conglomerate comprises the upper part of the Skeena Group succession. Table 1 compares this new stratigraphic nomenclature with that of Richards (1990).

Rocky Ridge Formation

The Rocky Ridge Formation is comprised of submarine alkali basalt flows, breccias, and lapilli tuffs that were erupted along the southern margin of the Bowser Basin (Bassett and Kleinspehn, 1996) as part of a primitive volcanic arc assemblage. Interbedded with the volcanic rocks are marine shales and siltstones that contain Early Albian to Early Cenomanian macrofossils. The thickness and lateral continuity of the Rocky Ridge Formation is variable. For example, at Rocky Ridge, the type locality, the volcanic succession is up to 1000 metres thick whereas in the next range to the west if is thin or absent. These variations probably reflect proximity to major eruptive centers.

One of the key results of the geochronologic dating completed as part of the Nechako NATMAP project was the recognition of mid-Cretaceous rhyolite domes in the Rocky Ridge succession (MacIntyre and Villeneuve, in press). The rhyolite domes occur as an arcuate belt of topographic highs north of Old Fort Mountain in the Babine Lake area (Figure 4). These domes may be the remnants of a submarine caldera complex (MacIntyre *et al.*, 1997; Tackaberry, 1998). Similar flow-banded rhyolites crop

TABLE 1
COMPARISON OF SKEENA GROUP STRATIGRAPHIC NOMENCLATURE

Richards (1990)	Bassett & Kleinspehn (1996)	Facies	Age Range
Red Rose Fm.	Rocher Deboule Fm.	fluvial, deltaic	Albian-Cenomanian
Hanawald conglomerate			
Rocky Ridge volcanics	Rocky Ridge Fm.	volcanic arc	
Kitsuns Creek Fm	Bulkley Canyon Fm.	deltaic	Hauterivian-Albian
	(Kitsuns Creek Mbr.)	fluvial, estuary	
Kitsumkalum shale	Couture Fm.	subtidal, turbiditic	

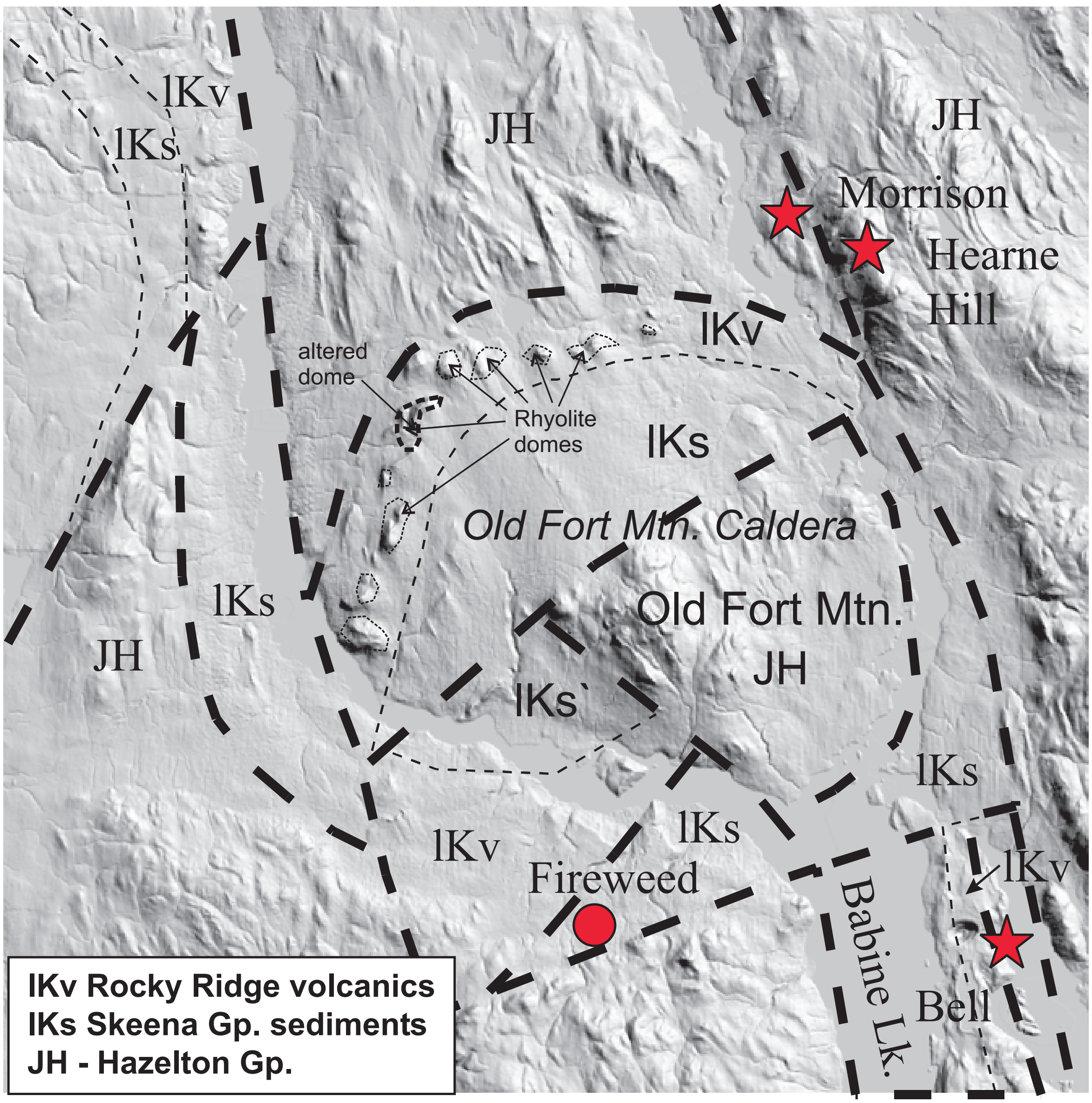

Figure 4. Shaded relief image derived from 20 metre digital elevation model data showing an arcuate belt of rhyolite domes north of Old Fort Mountain. The rhyolite domes are interpreted to be a ring dike structure bounding a resurgent caldera. Stars mark major Eocene age porphyry copper deposits; solid circles are massive sulphide prospects.

out in the vicinity of the Bell Mine on the Newman Peninsula. All of these rhyolites were previously mapped as part of the Eocene Babine intrusions (Richards, 1990), but are now mapped as Rocky Ridge Formation because they yield U/Pb and Ar/Ar isotopic ages between 104 and 108 Ma (MacIntyre and Villeneuve, in press). These ages suggest eruption of the domes occurred during Albian time. Marine sedimentary rocks that are intruded by the rhyolite domes contain Albian macrofossils suggesting the domes and sedimentary rocks are roughly coeval.

THE ESKAY CREEK DEPOSIT MODEL

The Eskay Creek property, which is located 80 km north of Stewart, includes several deposits of polymetallic sulphide and sulphosalt mineralization as both exhalative massive sulphides and discordant veins. These deposits are economically important because of their precious metal contents and polymetallic nature. As of December 31, 1998, Eskay Creek had proven and probable reserves of 1.9 Mt grading 60.2 g/t Au and 2652 g/t Ag, 3.2% Pb, 5.2% Zn and 0.7%Cu (Sherlock *et al.*, 1999).

The Eskay Creek deposit is classified as a subaqueous hot spring deposit (Alldrick, 1995), an important new class of mineral deposit that has only recently been recognized in modern geological environments (Hannington, 1999). This deposit type shares mineralogical, geochemical and other characteristics of both subaerial epithermal Au-Ag hot spring deposits and deeper water Kuroko and

Besshi type volcanogenic massive sulphide deposits. Many deposits appear to be associated with bimodal (basalt-rhyolite) submarine volcanic centers, including sea-flooded, breached calderas in an active volcanic arc setting.

Target Areas for Eskay Creek Type Deposits

The main focus of this study is to identify areas that may have potential for the discovery of Eskay Creek type shallow, subaqueous hot spring Au-Ag deposits along the trend of the Skeena Arch (Figure 1). A preliminary assessment of this area identified several areas with high potential for this type of deposit (Massey, 1999; Massey *et al.*, 1999) and four occurrences were classified as Eskay Creek type - French Peak, Fireweed, Mt. Cronin and the Knoll. The Fireweed, Mt. Cronin and Knoll properties all have massive Pb-Zn-Ag mineralization hosted in rhyolitic intrusions that are emplaced into marine sedimentary strata of the Lower Cretaceous Skeena Group. The rhyolitic intrusions were previously mapped as Eocene or Late Cretaceous but detailed mapping and isotopic age-dating of rhyolite domes in the Babine Lake area has shown that these rhyolites are part of the mid-Cretaceous Rocky Ridge Formation of the Skeena Group (MacIntyre and Villeneuve, in press) and are therefore coeval with surrounding sedimentary rocks.

Nilkitkwa River

Richards (1980, 1990) suggests rocks of the Rocky Ridge Formation underlie a series of ridges west of the Nilkitkwa River. This site was visited via helicopter and a grab sample was collected for Ar/Ar isotopic dating and lithogeochemistry. A brief examination of outcrops at the sample site suggests the volcanic succession is predominantly alkali basalt, typical of much of the Rocky Ridge Formaiton. No evidence for a felsic component to the volcanism was observed.

French Peak

Volcanic rocks on the east flank of French Peak have been mapped as part of the Late Cretaceous Kasalka Group (Richards, 1980, 1990). The stratigraphic succession is described as including subaerial and submarine dacite, andesite and rhyolite. These rocks were targeted for study because of the possibility that they may actually be Rocky Ridge Formation. The main exploration targets on the property are the UTE and Rio veins (Minfile 093M 015) both of which have been identified as having characteristics common to the Eskay Creek model (Massey, 1999). The UTE showing is a steep dipping, northeast-trending quartz-siderite vein system containing coarse argentiferous galena and tetrahedrite. Host rocks are sheared purple to orange weathering crystal-ash tuffs. The Rio vein is located 122 metres south and is comprised of massive, banded chalcopyrite, tetrahedrite, and pyrite hosted by andesitic to dacitic tuffs. The vein dips moderately to the northwest and appears to be conformable to bedding.

A total of 1.5 days was spent on the French Peak property. Based on examination of outcrop and core, it would appear that the host rocks for the UTE and Rio veins are not Late Cretaceous Kasaka Group or mid-Cretaceous Rocky Ridge Formation but rather the Lower to Middle Jurassic Saddle Hill Formation. This conclusion is supported by the occurrence of marine sedimentary rocks containing Middle Jurassic macrofossils within or overlying the volcanic succession (Robin Day, personal communication). The Saddle Hill Formation is the same age as host rocks for the Eskay Creek deposit and therefore, the French Peak area should be considered prospective for this type of deposit.

Fort Babine

An east trending, fault-bounded panel of Rocky Ridge volcanic rocks is sporadically exposed in clearcuts west of the northern tip of Babine Lake near Fort Babine (Figure 1). Mapping in this area in 1997 and 1998 suggests a number of rhyolite domes and rhyolite breccia bodies occur within a mixed mafic volcanic and marine sedimentary succession (Richards, 1980, 1990; MacIntyre, in press). Locally the sedimentary rocks contain Albian macrofossils. These rocks trend easterly and dip steeply to both the north and south. As part of the current study, one day was spent examining exposures of mafic flows in a borrow pit near the 4039 marker on the 4000 (Fort Babine) road. This site was also drilled for a regional paleomagnetic study being conducted by Randy Enkin of the Geological Survey of Canada. Although there are no known mineral occurrences associated with the Rocky Ridge volcanic rocks at this locality, the occurrence of a felsic component within the volcanic succession is considered evidence for a favourable environment for Eskay Creek type deposits.

Old Fort

An arcuate belt of resistant, rhyolite domes previously dated as mid-Cretaceous (MacIntyre and Villeneuve, in press) and interpreted to be a ring dike structure related to development of a submarine caldera crop out north of Old Fort Mountain in the Babine Lake area (Figure 4). These rhyolites are emplaced into mafic lapilli tuffs typical of the Rocky Ridge Formation. The volcanic succession is overlain and underlain by marine and non-marine clastic sedimentary rocks of the Skeena Group. Near the rhyolite domes, the sedimentary strata contain numerous angular clasts of rhyolite suggesting explosive volcanism accompanied emplacement of the domes (Photo 1a). One of these rhyolite domes has pervasive sericitic alteration accompanied by 1 to 2% finely disseminated pyrite (Figure 4). However, samples collected for assay in 1997 failed to detect anomalous metal concentrations in the rhyolite. Away from the domes, the area is heavily drift covered and has virtually no outcrop making exploration for massive sulphide lenses difficult.

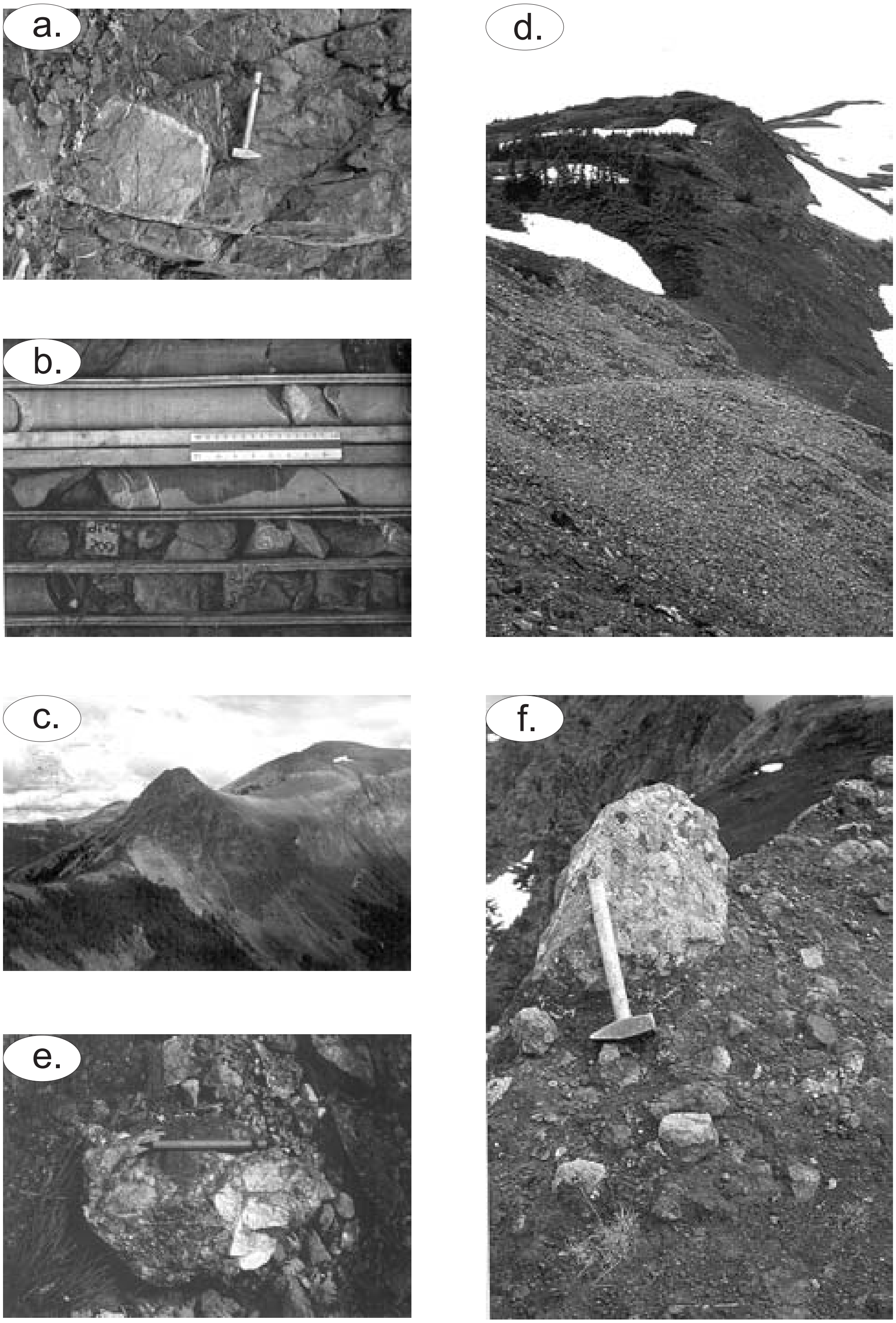

Photo 1. a. Large angular block of rhyolite in a tuffaceous siltstone. Photo taken in a borrow pit just north of a chain of rhyolite domes; b. Drill core from the Fireweed property showing rhyolite injected into graphitic mudstone. High grade Pb-Zn-Ag veins occur within the rhyolite; c. Prominent rhyolite dome intruding Skeena Group sedimentary rocks north of Mt. Cronin; d. Contact between rhyolite (light coloured talus) and siltstone at the Mt. Cronin property. Samples of rhyolite were collected near the contact for lithogeochemistry and U/Pb geochronology; e. Angular rhyolite clasts in Skeena Group conglomerate exposed in road cuts near Beament on Highway 16; f. Steeply dipping debris flow containing large, subangular to subrounded blocks of augite phyric basalt typical of the Rocky Ridge Formation. Photo taken on the crest of Rocky Ridge.

Fireweed

The Fireweed Ag-Pb-Zn-Cu-Au prospect (Minfile 093M 151) is located south of Old Fort Mountain (Figure 4), in a fault-bounded, poorly exposed, east-trending panel of Skeena Group clastic sedimentary rocks (Malott, 1988). This property has been classified as a subaqueous hot-spring deposit of the Eskay Creek type (Massey, 1999). Mineralization occurs as breccia zones and vein stockworks containing massive pyrite-pyrrhotite and lesser sphalerite, chalcopyrite and galena in both the sedimentary rocks and altered rhyolite dikes, as fine to coarse-grained interstitial pyrite, marcasite, sphalerite, galena and tetrahedrite in coarse sandstone and granule conglomerate beds and as conformable, fine-grained pyrite/pyrrhotite and sphalerite/galena bands in fine-grained carbonaceous, marine sedimentary rocks. Massive sulphide is spatially associated with both the breccia/stockwork zones and altered rhyolite (quartz latite) dikes. Porous sandstone beds contain quartz, ankerite, sericite, chlorite and kaolinite alteration minerals.

The Fireweed property was discovered in 1987 and drill tested in 1988, 1989 and 1990. Indicated reserves on the West zone are 584,500 tonnes grading 341.77 grams per tonne silver, 2.22 per cent zinc and 1.34 per cent lead (George Cross Newsletter No.66, 1989). In 1999 Mansfield Minerals Inc. completed an additional 1250 metres of diamond drilling in six holes. Numerous rhyolite dikes, lithologically identical to the rhyolite domes observed north of Old Fort Mountain, occur in the drill core and some of these host high grade sphalerite vein stockworks (Photo 1b).

Mt. Cronin

A number of rhyolite domes intrude Skeena Group sedimentary rocks in the vicinity of Mt. Cronin, in the Babine Range (Photo 1c). Two of these were sampled by helicopter during the current study - one on the northwest flank of the mountain and the other to the southwest. The latter hosts the Cronin past producing mine (Minfile 093L 127). From 1917 to 1974 sporadic production from this mine yielded 25,838 tonnes containing 8.17 million grams of silver, 8,772 grams of gold, 10,394 kilograms of copper, 1.37 million kilograms of lead and 1.52 million kilograms of zinc. Mineralization occurs as quartz veins and massive sulphide lenses containing high grade concentrations of argentiferous galena and sphalerite with minor pyrite and chalcopyrite. Boulangerite, freibergite and arsenopyrite have also been identified. The Cronin deposit was classified as a subaqueous hot-spring deposit by Massey (1999).

The rhyolite at the Cronin Mine (Photo 1d), which has at least two intrusive phases, is feldspar phyric and has pervasive sericite alteration. Mineralized quartz veins occur within the rhyolite and surrounding graphitic argillites and siltstones of the Skeena and Bowser Lake groups. These sedimentary rocks are strongly folded near the contact with the rhyolite. Some of this deformation is interpreted to be soft-sediment and related to emplacement of the rhyolite into weakly lithified strata. The rhyolite, which is lithologically identical to those in the Babine Lake area, has been mapped as Late Cretaceous or Tertiary in the past (Tipper and Richards, 1978) but may be coeval with surrounding mid-Cretaceous Skeena Group sedimentary rocks.

Suskwa (Knoll Property)

A resistant steep-sided rhyolite dome, approximately 600 metres long, 300 metres wide and 60 metres high, intrudes Skeena Group sedimentary strata within a fault-bounded, north-trending panel in the Harold Price Creek valley north of the Suskwa River (Figure 1). Rocks exposed on the knoll are massive to flow-banded, or spherulitic rhyolite, rhyolite breccia and volcaniclastic conglomerate with variable degrees of sericitic alteration (Wojdak *et al.*, 1999). The presence of rhyolite breccia suggests volcanism was locally explosive. The rocks intruded by the rhyolite are recessive and poorly exposed graphitic black mudstone and argillite of probable Albian age.

Dan Ethier discovered disseminations and veinlets of pyrite, sphalerite and galena in rhyolite breccia and lapilli tuff within and adjacent to the rhyolite dome, in 1983. He named the property the Knoll occurrence (Minfile 093M 100). Disseminated pyrite and manganese staining are also widespread in the rhyolite. The Knoll property has been classified as an epithermal massive sulphide (Wojdak *et al.*, 1999) and as a subaqueous hot-spring deposit (Massey, 1999).

Goldpac Investments Ltd. optioned the property in 1987 and drilled seven holes, totaling 978 metres (Figure 5). These were collared to test induced polarization anomalies. Mineralization intersected by these drill holes is mainly fracture-controlled pyrite, pyrrhotite and arsenopyrite with associated quartz and calcite. The best intersection was hole 88-3 with over 1 metre grading 0.51% Pb, 1.32% Zn, 9.58% As, 30 ppm Ag and 1610 ppb Au.

The rhyolite at the Knoll property is lithologically identical to the flow-banded rhyolite domes located north of Old Fort Mountain and dated as mid-Cretaceous. A similar age is inferred for the Knoll rhyolite.

Beament

A south-dipping section of feldspar phyric mafic volcanic rocks that overlie and are in part interbedded with quartzo-feldspathic wacke and chert-bearing heterolithic conglomerate is exposed in a 2 kilometre long road cut north of Beament station on Highway 16 (Figure 1). The volcanic rocks have been mapped as Late Cretaceous Kasalka Group (Richards 1980, 1990) but are lithologically identical to mid Cretaceous Rocky Ridge volcanic rocks elsewhere in the area. Sedimentary strata exposed at the north end of the road cut dip to the south and have been mapped as Lower Cretaceous Skeena Group. The contact with the overlying volcanic rocks appears to be conformable. Although no felsic component

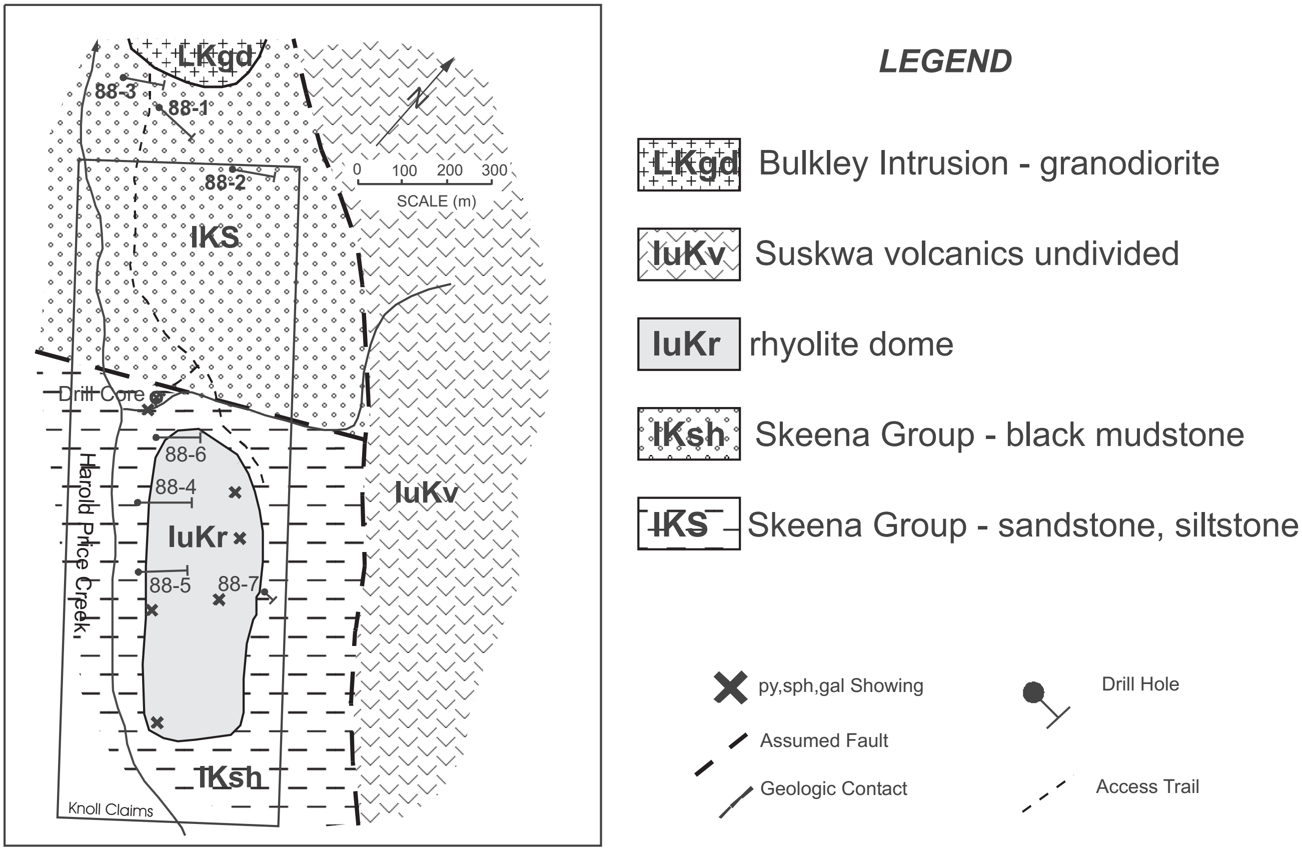

Figure 5. General geology and drill hole locations, Knoll property, Suskwa River area. Modified from Wojdak *et al.*, 1999.

was observed in the volcanic succession, coarse conglomerate beds underlying the volcanic rocks contain angular rhyolite clasts (Photo 1e) similar to those described in sedimentary rocks near rhyolite domes in the Babine Lake area (Photo 1a). This is indirect evidence for explosive rhyolite volcanism in the area prior to eruption of thick piles of mafic flows. This inferred bimodal volcanic style suggests rocks in the vicinity of Beament may have potential for subaqueous hot spring deposits associated with rhyolite eruptive centers.

Rocky Ridge

The type area for the Rocky Ridge Formation is at Rocky Ridge, a prominent, serrated, east-trending ridge at the southern limit of the Rocher Deboule Range (Figure 1). The ridge is underlain by a steeply-dipping, east-trending succession of feldspar phyric alkali basalt flows, lahar and volcanic conglomerate. Clasts in the lahar are subrounded to subangular, up to a metre in diameter and are compositionally the same as volcanic flows in the section (Photo 1f). No felsic clasts were observed in the lahar units. The coarse, poorly sorted nature of the lahars on Rocky Ridge suggests proximity to a major eruptive center with steep, unstable slopes, possibly a major collapse structure (Rocher Deboule caldera?).

A thick, poorly exposed section of Skeena Group sedimentary rocks underlies the broad valley south of Rocky Ridge. These sedimentary rocks are intruded by a large, elongate, east-trending rhyolite body that forms a prominent east-trending ridge. This rhyolite, which has previously been mapped as an Eocene Nanika intrusion (Tipper and Richards, 1976) is lithologically identical to mid-Cretaceous rhyolite intrusions in the Babine Lake area.

Mt. Ney

A thick succession of amygdaloidal, locally pillowed basaltic rocks underlies marine sedimentary rocks of the Skeena Group on the east flank of Mt. Ney (Figure 1) and elsewhere in the Tahtsa Lake area (Woodsworth, 1980; MacIntyre, 1985). These rocks, which were previously mapped as the Mt. Ney volcanics, are probably correlative with the Rocky Ridge Formation.

Troitsa Lake

A prominent, white weathering rhyolite dike crops out along the north shore of Troitsa Lake (Figure 1). This rhyolite appears to be emplaced into amygdaloidal flows of the Mt. Ney volcanics and sedimentary strata of the Skeena Group. The rhyolite has been interpreted as a ring dike bounding the Tahtsa Lake caldera (MacIntyre, 1985).

GEOCHRONOLOGY

U/Pb and $^{40}Ar/^{39}Ar$ isotopic dating in the Babine Lake area of central British Columbia documents a distinct magmatic event at 107-104 Ma (MacIntyre and Villeneuve, in press). This event involved emplacement of rhyolite domes into submarine volcanic rocks of the Rocky Ridge Formation. The volcanic rocks have yielded a U/Pb age of 107.9±0.2 Ma and an $^{40}Ar/^{39}Ar$ age of 104.8±1.2 Ma. Several samples of rhyolite were also dated but these did not give publishable ages. However, the data that was obtained is consistent with isotopic ages in the 104-108 Ma range (Mike Villeneuve, personal communication). The rhyolites, which were previously mapped as Eocene, are re-interpreted to be part of a previously unrecognized mid-Cretaceous cauldron subsidence complex (Figure 4).

Rhyolite at the Fireweed, Knoll, Mt. Cronin, Rocky Ridge and Troitsa Lake localities were sampled for U/Pb geochronology (Table 2). Mafic volcanic rocks of the Rocky Ridge Formation at the French Peak, Nilkitkwa River, Fort Babine, Rocky Ridge and Mt. Ney localities were also sampled for Ar/Ar geochronology (Table 2). All of the U/Pb and $^{40}Ar/^{39}Ar$ age determinations will be done at the GSC geochronology laboratory in Ottawa, Ontario, Canada under the supervision of Dr. Mike Villeneuve.

LITHOGEOCHEMISTRY

A total of 19 samples were collected for major oxide, trace and rare earth element analyses and most of these have also been submitted for isotopic age dating (Table 2). Seven of these samples are from suspected mid-Cretaceous rhyolite emplaced into Skeena Group sedimentary strata and seven samples are from mafic flows within the Rocky Ridge volcanic succession. For comparison pur-

TABLE 2
LITHOGEOCHEMICAL AND GEOCHRONOLOGICAL SAMPLES COLLECTED IN 2000

No.	Station	Map	Easting	Northing	Area	Unit	Lithology	Geochron	Comment
1	DMA00-001	93M3	602539	6116265	Rocky Ridge	Rocky Ridge	green aphyric basalt	Ar/Ar	from top of ridge
2	DMA00-002	93L13	594585	6093062	Rocky Ridge	Rocky Ridge	augite phyric basalt	Ar/Ar	from top of ridge
3	DMA00-003	93L13	594932	6093002	Rocky Ridge	Rocky Ridge	amygdaloidal basalt	Ar/Ar	from top of ridge
4	DMA00-007	93L15	640023	6088597	Mt. Cronin	Rhyolite dome	rhyolite	U/Pb	dome at Cronin Mine
5	DMA00-008	93L15	633729	6094767	Mt. Cronin	Kasalka	feldspar phyric andesite	U/Pb	north of Mt. Cronin
6	DMA00-009	93L15	628538	6088436	Mt. Cronin	Rhyolite dome	rhyolite	U/Pb	dome on ridge north of Lagopus Mtn.
7	DMA00-012	93M7	640334	6134053	French Peak	Saddle Hill	basalt	Ar/Ar	basalt at UTE vein
8	DMA00-015	93M7	649605	6128284	Fort Babine	Rocky Ridge	feldspar phyric andesite	Ar/Ar	quarry at km 39 on 4000 road
9	DMA00-016	93M7	649605	6128272	Fort Babine	Rocky Ridge	augite phyric basalt	Ar/Ar	quarry at km 39 on 4000 road
10	DMA00-017	93M7	618251	6125954	Sukwa River	Rhyolite dome	rhyolite	U/Pb	rhyolite dome on Knoll property
11	DMA00-018	93M7	618304	6125533	Sukwa River	Rhyolite dome	banded rhyolite		drill core from Knoll property
12	DMA00-020	93M7	637778	6138158	French Peak	Kasalka	feldspar phyric andesite		ridge E. of French Peak
13	DMA00-021	93M7	634262	6142600	French Peak	Kasalka	feldspar phyric andesite		ridge N. of French Peak
14	DMA00-022	93M7	633211	6154815	Nilkitkwa R.	Rocky Ridge	feldspar phyric andesite	Ar/Ar	ridge W. of Nilkitkwa River
15	DMA00-042	93E11	607034	5935011	Troitsa Lake	Rhyolite dome	rhyolite	U/Pb	dike along shores of Troitsa Lake
16	DMA00-043	93E11	612347	5943798	Swing Peak	Kasalka	feldspar phyric andesite	U/Pb	south slope of Swing Peak
17	DMA00-045	93E13	605138	5963620	Mt. Ney	Rocky Ridge	amygdaloidal basalt	Ar/Ar	volcanics south of Mt. Ney
18	DMA00-050	93L13	596691	6090754	Rocky Ridge	Rhyolite dome	rhyolite	U/Pb	large intrusion south of Rocky Ridge
19	DMA00-055	93M1	663294	6098762	Fireweed	Rhyolite dome	rhyolite	U/Pb	dike cutting Skeena seds (drill core)

N.B. Easting and Northing coordinates are in NAD83; all samples are in UTM zone 9

TABLE 3
MAJOR OXIDE AND TRACE ELEMENT ANALYSES

Element	Units	Limit	1	2	3	4	5	6	7	8	9
SiO2	%		51.63	47.74	48.04	76.5	62.54	74.01	44.93	49.47	48.59
TiO2	%		1.01	0.61	0.56	0.05	0.68	0.18	0.82	1.73	1.65
Al2O3	%		16.64	19.19	19.54	14.81	16.09	14.96	16.29	17.69	17.87
Fe2O3	%		8	9.63	7.98	0.95	5.5	1.32	11.48	8.93	9.14
MnO	%		0.17	0.15	0.18	0.01	0.03	0.07	0.2	0.18	0.18
MgO	%		3.39	3.5	2.53	0.14	2.25	0.15	8.38	5.28	5.19
CaO	%		5.8	10.27	8.18	0.03	3.17	0.38	7.36	5.96	7.51
Na2O	%		2.33	2.78	3.53	0.07	4.09	3.16	2.5	4.03	4.03
K2O	%		2.16	2.3	2.73	3.73	2.7	3.43	0.3	2.11	0.93
P2O5	%		0.38	0.43	0.62	0.01	0.31	0.01	0.07	0.51	0.47
Ba	%		0.03	0.16	0.23	0.06	0.13	0.12	0.05	0.16	0.03
LOI	%		8.3	2.57	5.32	2.81	2.34	1.96	7.36	3.73	3.95
SUM	%		99.84	99.33	99.44	99.17	99.83	99.75	99.74	99.78	99.54
Mo	ppm	0.01	0.32	0.77	0.97	0.03	1.05	0.39	0.06	0.21	1.13
Cu	ppm	0.01	1.82	29.2	23.75	24.3	24.27	0.69	52.45	37.95	36.59
Pb	ppm	0.01	1.79	10.15	17.37	1298.4	7.14	21.06	1.04	2.24	1.88
Zn	ppm	0.1	62.9	48.2	47	220.8	50.5	79.2	74.3	64.1	55.3
Ag	ppb	2	16	25	52	16468	68	62	74	30	49
Ni	ppm	0.1	6.1	8.3	0.9	0.9	36.5	0.7	102.6	39.2	39.8
Co	ppm	0.1	12.9	24	12.7	0.1	13.3	0.2	47.8	25.1	25.6
Mn	ppm	1	1344	738	1121	20	362	592	1233	828	795
Fe	%	0.01	4.63	5.11	4.03	0.27	2.69	0.51	5.7	4.95	4.54
As	ppm	0.1	< .1	< .1	0.2	794.7	4.5	0.4	42.5	< .1	< .1
U	ppm	0.1	0.2	1.6	2.7	1.3	1.2	1.7	< .1	0.3	0.3
Au	ppb	0.2	< .2	1.4	< .2	16.7	1	1.6	1.2	0.8	0.7
Th	ppm	0.1	1.6	5.6	10	2.2	2.8	13.7	< .1	0.7	0.8
Sr	ppm	0.5	70.8	460	673.9	1.8	67.5	43.1	70.1	55.3	73.8
Cd	ppm	0.01	0.01	0.03	0.09	3.02	0.05	0.36	0.05	0.04	0.05
Sb	ppm	0.02	0.18	0.11	0.13	5.35	0.23	0.27	0.66	0.03	0.07
Bi	ppm	0.02	0.02	0.03	< .02	0.07	0.03	0.02	0.18	< .02	< .02
V	ppm	2	67	179	110	< 2	81	< 2	147	65	86
Ca	%	0.01	3.5	3.95	3.43	0.01	0.87	0.25	2.87	1.35	1.28
P	%	0.001	0.159	0.178	0.252	0.001	0.122	0.015	0.035	0.23	0.197
La	ppm	0.5	18.8	16	27.5	1.7	15.8	24.6	1	16.3	14.6
Cr	ppm	0.5	9.2	26.5	10.3	46.7	104.4	27.4	138.7	53	51.1
Mg	%	0.01	1.94	0.95	0.57	0.01	1.33	0.02	3.98	2.67	2.39
Ba	ppm	0.5	49.6	214.1	219.5	80	145.8	120.2	386.7	82.9	37.9
Ti	%	0.001	0.001	0.133	0.145	0.001	0.052	< .001	0.075	0.448	0.303
B	ppm	1	5	4	13	8	6	14	6	8	8
Al	%	0.01	2.61	5.15	4.99	0.58	1.32	0.34	4.21	2.8	2.41
Na	%	0.001	0.017	0.403	0.685	0.009	0.115	0.026	0.204	0.159	0.29
K	%	0.01	0.24	0.13	0.4	0.44	0.12	0.23	0.07	0.06	0.03
W	ppm	0.2	< .2	0.3	0.5	< .2	< .2	< .2	< .2	< .2	< .2
Sc	ppm	0.1	4	2.5	0.9	0.3	5.1	0.5	9.8	4.2	3.2
Tl	ppm	0.02	0.13	< .02	0.05	0.16	0.02	0.05	0.11	< .02	< .02
S	%	0.01	0.05	< .01	< .01	0.07	< .01	< .01	0.1	0.01	0.01
Hg	ppb	5	< 5	< 5	< 5	112	10	9	< 5	< 5	< 5
Se	ppm	0.2	0.2	0.2	0.3	< .1	0.1	< .1	0.4	0.3	0.2
Te	ppm	0.02	< .02	0.04	0.05	< .02	< .02	< .02	0.02	< .02	< .02
Ga	ppm	0.02	9.5	9.6	8.9	1.6	6.2	0.7	12.2	11.9	6

TABLE 3
MAJOR OXIDE AND TRACE ELEMENT ANALYSES CONTINUED

Element	Units	Limit	10	11	12	13	14	15	16	17	18	19
SiO2	%		74.84	70.61	59.5	60.15	54.61	73.37	62.18	48.54	75.06	72.41
TiO2	%		0.1	0.11	0.51	0.43	0.56	0.1	0.54	0.89	0.05	0.17
Al2O3	%		11.94	13.82	16.61	17.12	18.01	14.52	16.17	16.55	14.47	13.35
Fe2O3	%		2	3.39	5.82	4.86	7.32	1.3	4.65	6.76	1.09	1.69
MnO	%		0.01	0.52	0.12	0.18	0.1	0.02	0.11	0.1	0.02	0.33
MgO	%		0.05	0.09	1.9	1.36	2.32	0.25	1.12	6.94	0.05	0.34
CaO	%		0.02	0.07	4.48	4.78	4.63	1.57	4.63	9.47	0.03	2.51
Na2O	%		0.15	0.12	5.05	4.23	5.25	2.89	3.76	2.48	2.78	0.46
K2O	%		7.78	6.86	1.24	2.5	3.27	3.6	2.21	0.28	3.85	2.93
P2O5	%		0.01	0.01	0.28	0.25	0.49	0.02	0.18	0.23	0.01	0.01
Ba	%		0.25	0.15	0.08	0.15	0.36	0.15	0.11	0.04	0.09	0.08
LOI	%		2.02	3.39	4.01	3.27	2.22	1.57	3.77	7.28	2.25	5.32
SUM	%		99.17	99.14	99.6	99.28	99.14	99.36	99.43	99.56	99.75	99.6
Mo	ppm	0.01	1.28	1.24	0.77	0.68	0.18	0.25	0.46	0.41	0.12	3.58
Cu	ppm	0.01	1.45	1.39	179.33	13.32	9.38	69.07	4.05	10.06	0.63	2.01
Pb	ppm	0.01	225.29	228.28	230.09	10.25	3.59	7.23	5.04	3.79	6.51	110.51
Zn	ppm	0.1	39.7	38.8	341.4	94.7	92.3	7.7	55.1	83.8	31.5	232.9
Ag	ppb	2	878	840	1301	49	30	350	20	16	14	155
Ni	ppm	0.1	1.8	1.6	211.6	1.9	1.6	1.2	6.2	201.9	1	1.1
Co	ppm	0.1	0.3	0.2	50.1	10.6	8.5	1	8.1	33.8	0.3	< .1
Mn	ppm	1	21	23	1604	1107	1205	87	867	835	199	2583
Fe	%	0.01	1.11	1.1	6.77	3.18	2.82	0.29	2.29	3.9	0.54	0.76
As	ppm	0.1	113.2	111	61.3	1.1	6.5	0.7	1	0.8	0.7	< .1
U	ppm	0.1	4.9	4.9	0.4	1	1.1	0.5	0.6	0.7	3.5	0.4
Au	ppb	0.2	0.3	2.8	29.8	< .2	< .2	2.3	0.8	0.6	< .2	0.4
Th	ppm	0.1	16.7	16.3	3.7	2.8	2.2	3.3	1	1.6	10	2.3
Sr	ppm	0.5	6.3	6.1	18	61.3	97.7	33.1	196.5	86.8	44	28.7
Cd	ppm	0.01	0.1	0.09	0.62	0.06	0.17	0.03	0.03	0.04	< .01	1.02
Sb	ppm	0.02	5.46	5.2	11.82	0.06	0.1	0.23	0.08	0.2	0.3	0.08
Bi	ppm	0.02	0.47	0.47	0.27	0.05	< .02	0.38	< .02	0.02	< .02	0.02
V	ppm	2	< 2	< 2	105	70	45	< 2	58	130	2	2
Ca	%	0.01	< .01	< .01	0.32	1.67	1.84	0.28	1.51	4.01	0.03	1.68
P	%	0.001	0.005	0.005	0.115	0.123	0.12	0.011	0.085	0.103	0.009	0.011
La	ppm	0.5	22.3	22	14.5	15.5	9.1	4.8	9.5	14	16.2	19.6
Cr	ppm	0.5	67.2	65.9	257.9	13.8	23.4	66.8	41.5	253.9	29.9	48.8
Mg	%	0.01	0.01	0.01	2.82	1.13	0.77	0.09	0.62	3.95	0.02	0.15
Ba	ppm	0.5	275.1	272.8	287	58.3	97.7	184.3	165.4	39.6	96.8	161.1
Ti	%	0.001	< .001	0.001	0.072	0.062	0.113	0.012	0.155	0.287	< .001	< .001
B	ppm	1	11	11	< 1	6	13	1	2	1	10	< 1
Al	%	0.01	0.31	0.3	2.76	1.4	2.06	0.9	1.63	3.07	0.63	0.75
Na	%	0.001	0.005	0.005	0.006	0.108	0.097	0.063	0.116	0.185	0.04	0.013
K	%	0.01	0.4	0.39	0.04	0.1	0.1	0.37	0.1	0.03	0.29	0.41
W	ppm	0.2	1.6	1.6	< .2	< .2	0.3	< .2	< .2	< .2	< .2	< .2
Sc	ppm	0.1	0.2	0.2	11.7	2.9	1.9	0.5	2.7	12.6	0.7	0.8
Tl	ppm	0.02	0.35	0.36	0.1	0.05	0.05	0.1	0.03	0.02	0.07	0.16
S	%	0.01	0.28	0.27	0.02	0.11	0.01	0.05	0.03	0.04	0.02	0.08
Hg	ppb	5	13	19	321	12	< 5	9	< 5	< 5	94	35
Se	ppm	0.2	< .1	< .1	0.8	< .1	0.1	< .1	< .1	0.1	< .1	< .1
Te	ppm	0.02	< .02	< .02	0.3	< .02	< .02	0.08	0.02	< .02	< .02	< .02
Ga	ppm	0.02	0.6	0.6	9.1	7.1	9.4	3	6.6	8.1	1.7	1.5

Note: *See* Table 2 for sample descriptions; major oxide analyses done by XRF at Cominco; trace element analyses by aqua regia digestion ICPMS at Acme Analytical Laboratories

TABLE 4
TRACE AND RARE EARTH ELEMENT ANALYSES

Element	Det. limit	1	2	3	4	5	6	7	8	9	10
Y	0.003	22.414	14.992	17.845	7.905	13.413	11.452	14.992	27.374	24.681	5.426
Zr	0.02	166.175	56.825	79.006	43.844	148.242	138.728	40.349	231.687	201.407	65.849
Nb	0.001	19.173	5.174	9.404	2.933	16.795	10.486	2.136	13.737	12.495	4.013
Ba	0.167	286.891	1516.915	2175.825	452.42	1219.38	972.947	418.986	1571.631	287.064	1856.938
La	0.003	20.699	16.57	27.153	1.902	22.861	23.917	1.904	15.793	14.555	24.775
Ce	0.002	43.271	30.894	48.29	3.912	41.663	41.266	5.533	39.053	35.415	33.068
Pr	0.001	5.402	3.665	5.569	0.526	4.768	4.33	0.912	5.292	4.751	2.666
Nd	0.002	22.313	15.154	22.042	2.282	18.165	15.083	4.861	22.91	20.726	7.738
Sm	0.006	4.931	3.573	4.851	0.833	3.605	2.582	1.737	5.412	4.979	1.152
Eu	0.002	1.427	1.153	1.523	0.185	1.025	0.568	0.747	1.943	1.815	0.256
Gd	0.004	4.444	3.419	4.354	1.028	3.026	1.99	2.382	5.655	5.154	0.701
Tb	0.002	0.684	0.487	0.61	0.192	0.433	0.303	0.408	0.853	0.782	0.103
Dy	0.007	4.441	2.954	3.567	1.283	2.58	1.917	2.745	5.248	4.795	0.672
Ho	0	0.931	0.599	0.723	0.264	0.52	0.405	0.598	1.091	0.993	0.166
Er	0.001	2.956	1.87	2.226	0.851	1.622	1.422	1.882	3.31	3.01	0.672
Tm	0	0.4	0.25	0.295	0.123	0.219	0.215	0.259	0.441	0.397	0.12
Yb	0.002	2.611	1.598	1.9	0.848	1.438	1.554	1.625	2.793	2.557	0.981
Lu	0.001	0.395	0.244	0.289	0.125	0.224	0.252	0.24	0.417	0.375	0.173
Hf	0.003	4.263	1.582	2.075	2.327	3.938	3.795	1.175	4.642	4.131	2.078
Ta	0.001	1.079	0.237	0.403	0.858	1.105	1.259	0.045	0.774	0.671	0.631
Th	0.01	4.919	6.002	10.131	2.376	9.083	14.039	0.175	1.167	1.1	25.876

Element	Det. limit	11	12	13	14	15	16	17	18	19
Y	0.003	9.803	13.986	14.995	20.091	7.765	8.473	19.414	9.646	16.76
Zr	0.02	80.152	127.288	140.022	162.9	78.382	99.886	145.146	41.206	164.118
Nb	0.001	15.292	13.816	20.728	21.032	8.064	5.982	7.603	18.683	16.667
Ba	0.167	1236.67	723.096	1400.019	3369.9	1349.38	1105.9	371.872	826.005	758.616
La	0.003	36.942	18.432	24.217	53.212	21.074	15.018	17.363	16.711	23.804
Ce	0.002	49.581	35.236	45.759	91.813	38.729	30.027	35.677	28.64	42.794
Pr	0.001	4.029	4.297	5.405	9.901	4.271	3.641	4.398	3.214	4.522
Nd	0.002	11.467	17.513	21.313	36.554	15.214	14.526	17.792	11.831	15.656
Sm	0.006	1.631	3.601	4.133	7.049	2.51	2.788	3.843	2.351	2.825
Eu	0.002	0.395	1.143	1.213	2.06	0.603	0.835	1.18	0.368	0.557
Gd	0.004	1.278	2.883	3.246	5.554	1.89	2.348	3.87	1.928	2.608
Tb	0.002	0.199	0.414	0.445	0.715	0.261	0.318	0.597	0.285	0.44
Dy	0.007	1.273	2.487	2.667	3.889	1.439	1.764	3.769	1.688	2.85
Ho	0	0.294	0.532	0.558	0.761	0.272	0.327	0.778	0.344	0.617
Er	0.001	1.107	1.706	1.79	2.218	0.837	0.955	2.363	1.111	2.094
Tm	0	0.193	0.237	0.252	0.294	0.123	0.128	0.323	0.166	0.315
Yb	0.002	1.528	1.631	1.685	1.878	0.846	0.811	2.133	1.15	2.231
Lu	0.001	0.272	0.254	0.27	0.281	0.126	0.12	0.309	0.17	0.335
Hf	0.003	2.633	3.371	3.701	3.987	2.495	2.653	3.451	1.89	4.149
Ta	0.001	1.091	0.791	1.213	1	0.589	0.323	0.415	1.645	1.303
Th	0.01	42.461	4.882	5.864	15.9	6.178	2.801	2.989	11.412	7.614

Note: *See* Table 2 for sample descriptions; all analyses done by peroxide fusion ICPMS at Memorial University of Newfoundland; values in ppm poses four samples were collected from the Late Cretaceous Kasalka Group and one sample was collected from the Early to Middle Jurassic Saddle Hill Formation at French Peak. Major oxides were determined by XRF at the Cominco laboratory and trace element determinations were done by aqua regia ICPMS at the Acme Analytical laboratory (Table 3). Additional trace and rare earth element analyses were done by peroxide fusion ICPMS at Memorial University, Newfoundland (Table 4). This data can be compared to the earlier study of Tackaberry (1998) who did detailed petrography and lithogeochemistry of the mid-Cretaceous rhyolite domes north of Old Fort Mountain.

Major oxide analyses indicate that the suspected mid-Cretaceous rhyolites have SiO_2 values ranging from 70.61 to 76.5 weight percent. By contrast interbedded Rocky Ridge basaltic flows contain between 47.74 to 54.61 weight percent SiO_2 and 0.56 to 0.89 weight percent TiO_2. Kasalka Group volcanics are more intermediate in composition with SiO_2 values ranging from 59.5 to 62.18 weight percent. A standard AFM ternary plot (Figure 6a) shows the bimodal, calc-alkaline nature of Rocky Ridge basalts and suspected coeval rhyolite domes. On an alkali-silica plot these samples range from alkaline to subalkaline in composition (Figure 6b) and plot in the rhyolite and sub-alkaline basalt to andesite fields of a Zr/TiO_2 versus SiO_2 diagram (Figure 6c). The major oxide compositions of Rocky Ridge basalts analyzed in this study are similar to those presented in Bassett and Kleinspehn (1996). Likewise, the rhyolite domes analyzed in this study have a similar composition to those analyzed by Tackaberry (1998) north of Old Fort Mountain (Figure 4).

Rhyolite that hosts Ag-Zn-Pb veins at the Cronin and Knoll properties appears to be strongly altered with nearly total removal of Na and Ca (samples 4, 10, 11, Table 3). Likewise, rhyolite dikes at the Fireweed property also appear to be depleted in Na but not Ca (sample 19, Table 3). Previous work by Tackaberry (1998) has also shown that one of the rhyolite domes north of Old Fort Mountain (Figure 4) is strongly quartz-sericite altered with very low Na and Ca concentrations. Interestingly, samples from adjacent domes in this chain do not show evidence of Na or Ca depletion, suggesting alteration intensity varies from dome to dome. Altered rhyolites can also have anomalous concentrations of Pb, Zn, Ag and As (Table 3).

A plot of K_2O versus Na_2O (Figure 6d) clearly distinguishes altered from unaltered rhyolite, with altered samples having very low Na_2O and relatively high K_2O values. K enrichment is interpreted to reflect the presence of sericitic alteration at the expense of Na-rich plagioclase feldspar.

Rare earth element concentrations for basalt and rhyolite were also determined as part of the current study. Chondrite normalized values are plotted in Figure 6e as are those previously determined by Tackaberry (1998). Both basalts and rhyolites, regardless of their degree of alteration, have light rare earth element enrichment whereas rhyolites are also moderately to strongly enriched in heavy rare earth elements relative to the basalts. A notable exception is the rhyolite from Cronin which has a much lower level of light rare earths compared to other rhyolites in this study. The significance of this difference is not known. All of the rhyolites, including the Cronin sample, have moderate to strong Eu depletion consistent with plagioclase fractionation (Tackaberry 1998). The rare earth patterns determined for Rocky Ridge basalts in this study are very similar to those presented in Bassett and Kleinspehn (1996) for compositionally similar rocks.

DISCUSSION

The focus of the current study was to demonstrate that rhyolite domes similar to those dated in the Babine Lake area occur elsewhere in the Rocky Ridge succession and that these represent local, felsic volcanic centers in a bimodal, submarine volcanic environment that is favourable for the formation of VMS and/or Eskay Creek type subaqueous hotspring deposits. Based on the presence of strong alteration in the host rhyolites as determined by lithogeochemical analyses and the presence of known mineral occurrences, the most favourable areas identified in this study are at the Fireweed, Cronin and Knoll properties (Table 5). Other, less well explored areas such as south of Rocky Ridge and at Troitsa Lake may also prove to be favourable. In all of these areas the rhyolite intrusions appear to be emplaced along ring structures related to the development of large submarine cauldron subsidence complexes. Isotopic dating of the rhyolitic intrusions will help constrain the timing of cauldron subsidence and thus demonstrate or repudiate correlation with Rocky Ridge volcanic rocks elsewhere in the study area.

Several polymetallic Ag-Au bearing mineral occurrences, including the Fireweed, Knoll and Cronin, appear to be spatially and temporally associated with rhyolite intrusions of probable mid-Cretaceous age. These properties have some of the characteristics of subaqueous hotspring deposits of the Eskay Creek type. If these deposits prove to be related to emplacement of rhyolite domes during bimodal Rocky Ridge volcanism then areas underlain by these rocks represent a new and exciting exploration target for this type of deposit in central British Columbia.

ACKNOWLEDGMENTS

The author wishes to thank Angelique Justason for excellent assistance in the field and Dave Lefebure, B.C. Geological Survey Branch for a critical review of an earlier manuscript. Karl Desjarlais of Highland Helicopters, Smithers provided excellent helicopter support for the project. The author also thanks Mike Villeneuve, Geological Survey of Canada, Ottawa for U/Pb and Ar/Ar age determinations completed during the Nechako Natmap project and Ray Lett, B.C. Geological Survey Branch for preparation and shipping of lithogeochemical samples.

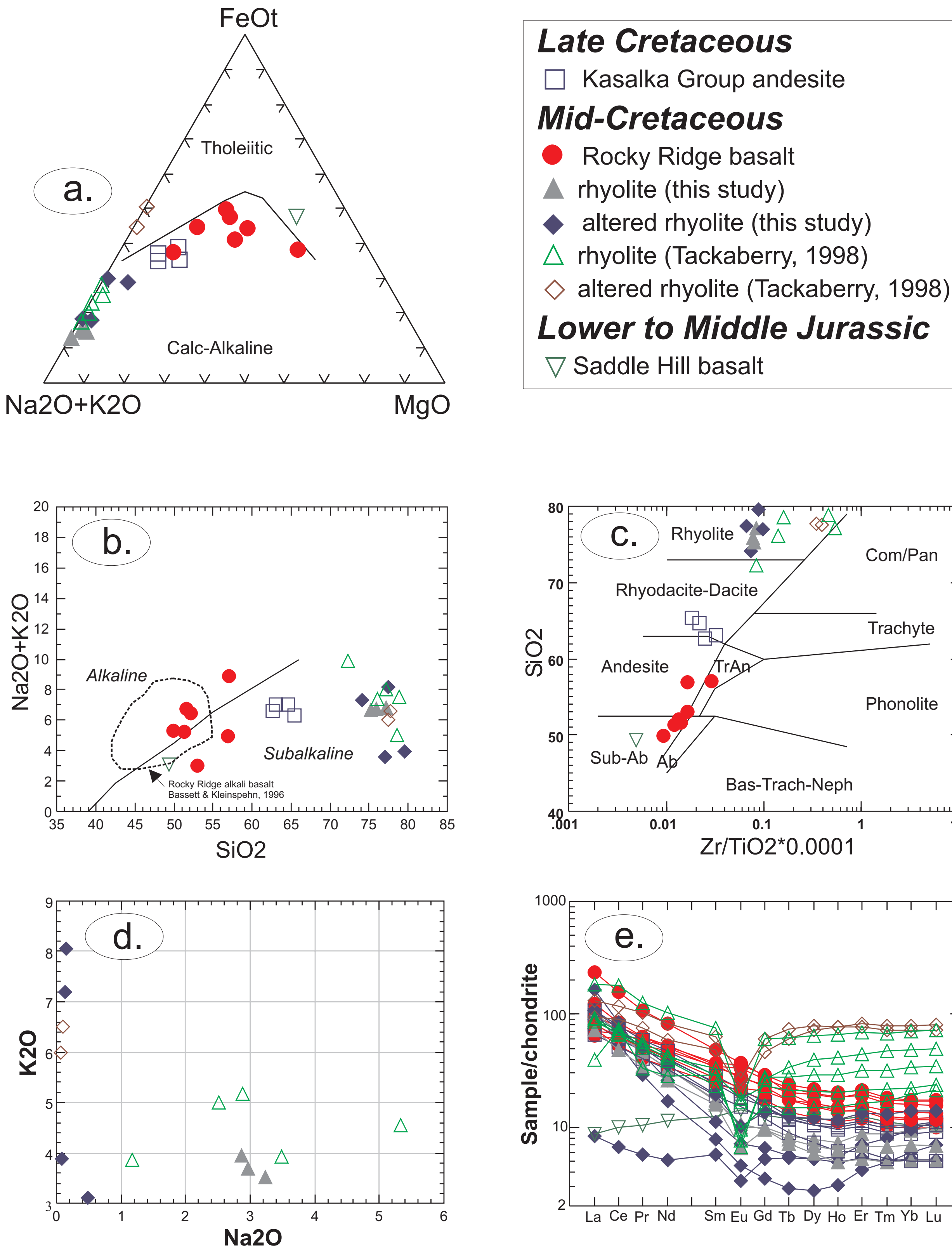

Figure 6. a. AFM ternary plot showing calc-alkaline nature of Rocky Ridge and Kasalka volcanic rocks; b. alkali-silica plot showing subalkaline to alkaline compositional trend; c. SiO2 versus Zr/TiO2 plot showing compositional range and classification of Rocky Ridge volcanic rocks and rhyolite domes; d. K20 versus Na2O plot showing Na depletion of altered rhyolite samples; e. plot of chondrite normalized rare earth element abundances for Rocky Ridge basalts and rhyolites.

TABLE 5
SUMMARY OF TARGET AREAS EXAMINED IN 2000

Rank	Area	Description	Mineralization	Alteration	Commodities	Exploration
1	Fireweed property (093M 151)	Rhyolite dikes intrude conglomerate, sandstone and siltstone of the Skeena Group; probable age of dikes is mid-Cretaceous; volcanics in area are probably part of Rocky Ridge formation	c.gr., massive py-po and lesser sph, gn, cpy in breccias zones; f.gr. py, marcasite, sph, gn and tetrahedrite as interstitial dissem. in coarse sediments; massive, f.gr. banded py, po, sph, gn in sediments; massive stockwork veins in rhyolite dikes	Rhyolite dikes are altered. Lithogeochemistry shows Na depletion but not Ca depletion. Strong Mn oxide staining in sedimentary rocks. Alteration minerals include quartz, ankerite, sericite, chlorite and kaolinite.	Zn, Pb, Cu, Ag; anomalous Au	Extensively drilled but still much untested ground
2	Suskwa R. Knoll property (093M 100)	Rhyolite dome intrudes graphitic black mudstone and argillite of the Skeena Group; rhyolite is probably mid-Cretaceous in age	Disseminations and veinlets of py, sph and gn in rhyolite breccia and lapilli tuff; fracture controlled py, pyrrhotite and arsenopyrite associated with quartz and calcite.	Rhyolite is extensively altered to sericite with disseminated pyrite and manganese staining; lithogeochemistry shows strong Na and Ca depletion in rhyolite.	Pb, Zn, As with anomalous Ag and Au	7 holes totaling 978 metres.
3	Mt. Cronin (093L 127)	Multi-phase rhyolite dome intrudes graphitic argillite, siltstone and conglomerate of the Skeena Group; rhyolite is probably mid-Cretaceous in age	Massive sulphide lenses and quartz vein stockworks containing argentiferous gn, sph, tetrahedrite, minor py and cpy; boulangerite, freibergite and arsenopyrite also present; mineralization occurs in rhyolite and to lesser extent surrounding sediments.	Rhyolite is extensively altered to sericite, calcite, zoisite and chlorite; lithogeochemistry indicates strong Na and Ca depletion near contact with sediments.	Ag, Pb, Zn, Au, Cu, Cadmium	Past producer; extensive underground workings
4	French Peak (093M 015)	Dacite, andesite and rhyolite of probable Lower to Middle Jurassic age cut by mineralized shear zones; near top of Saddle Hill stratigraphic succession.	quartz-siderite veins with tetrahedrite, argentiferous gn, cpy, sph and py in shear zones; banded cpy, tetrahedrite and pyrite in bedded rhyolite tuff	Carbonate and sericite alteration in rhyolitic rocks; manganese, clay and silica alteration associated with veins in shear zones; local strong K alteration in tuff.	Ag, Cu, Au, Pb, Zn; anomalous As, Sb	Developed prospect with open cuts, some drilling
5	Old Fort	Arcuate chain of rhyolite domes emplaced into graphitic tuffaceous sediments of the Skeena Gp.	non known	One rhyolite dome in chain has strong sericite-pyrite alteration; lithogeochemistry indicates strong Na and Ca depletion		No significant exploration
6	Fort Babine	Rhyolite domes and breccia bodies emplaced into mudstone and siltstone containing Albian fossils	non known	unknown		Some exploration in past
7	Rocky Ridge	Large rhyolite dike intrudes Skeena Group sedimentary rocks	non known	Lithogeochemistry at one site does not show evidence of alteration		No significant exploration
8	Beament	Angular rhyolite clasts in Skeena Group conglomerate	non known	some strong clay alteration associated with fault zones		Some exploration in past
9	Troitsa Lake	Large rhyolite dike along shores of Troitsa Lake; dike possibly mid-Cretaceous in age.	non known	Lithogeochemistry at one site does not show evidence of alteration		No significant exploration
10	Mt. Ney	Predominantly basalt. No felsic component observed	some interstitial gn and sph in conglomerate higher in section	Chlorite alteration of basalt		Some exploration in past
11	Nilkitkwa River	Predominantly basalt. No felsic component observed		Chlorite alteration of basalt		No significant exploration

REFERENCES

Alldrick, D.J. (1995): Subaqueous hot spring Au-Ag; *in* Selected British Columbia mineral deposit profiles, Volume 1 - metallics and coal, Lefebure, D.V. and Ray, G.E., Editors, *British Columbia Ministry of Employment and Investment*, Open File 1995-20, pages 55-58.

Bassett, K.N. (1991): Preliminary Results of the Sedimentology of the Skeena Group in West-central British Columbia; *in* Current Research, Part A*, Geological Survey of Canada*, Paper 91-1A, pages 131-141.

Bassett, K.N. and Kleinspehn, K.L, (1996): Mid-Cretaceous transtension in the Canadian Cordillera: evidence from the Rocky Ridge volcanics of the Skeena Group; *Tectonics*, Volume 15, pages 727-746.

Evenchick, C. A. (1999): Depositional and structural histories of the northern two-thirds of the Bowser Basin/Skeena Fold Belt, northern British Columbia: records of terrane interactions; *in* Terrane Paths 99, Circum-Pacific Terrane Conference, Abstracts and Program. C.A. Evenchick, G.J. Woodsworth, and R. Jongens, editors; *Geological Survey of Canada/Geological Association of Canada*, pages 30-32.

Hannington, M.D. (1999): Submarine epithermal deposits and the VMS-epithermal transition: a new exploration target; *in* Short Course Proceedings, *Prospectors and Developers Association of Canada*, Toronto, March 1999, pages 101-123.

MacIntyre, D.G. (1985): Geology and mineral deposits of the Tahtsa Lake District, west central British Columbia; *British Columbia Ministry of Energy, Mines and Petroleum Resources*, Bulletin 75.

MacIntyre, D.G. (2001): Geological compilation of the Babine Porphyry Copper district, *B.C. Ministry of Energy and Mines*, Open File Map 2001-3.

MacIntyre, D.G. and Struik, L.C. (1999): Nechako NATMAP Project, central British Columbia, 1998 Overview*; in* Geological Fieldwork 1998, *British Columbia Ministry of Energy and Mines*, Paper 1999-1, pages1-14.

MacIntyre, D.G. and Villeneuve, M.E. (in press): Geochronology and tectonic setting of mid-Cretaceous to Eocene magmatism, Babine porphyry copper district, central British Columbia; *Canadian Journal of Earth Sciences*, Volume 38.

MacIntyre, D.G., Villeneuve, M.E., and Schiarizza, P. (in press): Timing and tectonic setting of Stikine Terrane magmatism, Babine-Takla lakes area, central British Columbia. *Canadian Journal of Earth Sciences*, Volume 38.

Malott, M.L. (1988): Fireweed (093M151); B.C. *in* Exploration in British Columbia 1988, *B.C. Ministry of Energy, Mines and Petroleum Resources*, pages B127-131.

Massey, N.W.D. (1999): Volcanogenic Massive Sulphide Deposits in British Columbia; *B.C. Ministry of Energy and Mines*, Open File 1999-2.

Massey, N.W.D., Alldrick, D.J. and Lefebure, D.V.L. (1999): Potential for subaqueous hot-spring (Eskay Creek) deposits in British Columbia*; B.C. Ministry of Energy and Mines*, Open File 1999-14.

Richards, T.A. (1980): Geology of the Hazelton Map Area (93M); *Geological Survey of Canada*, Open File 720.

Richards, T.A. (1990): Geology of the Hazelton Map Area (93M); *Geological Survey of Canada*, Open File 2322.

Sherlock, R.L., Roth, T., Spooner, E.T.C. and Bray, C.J. (1999): Origin of the Eskay Creek precious metal-rich volcanogenic massive sulfide deposit: fluid inclusion and stable isotope evidence; *Economic Geology*, Volume 94, pages 803-824.

Tackaberry, D.M. (1998): Petrography, lithogeochemistry and VMS potential of Mid-Cretaceous Rocky Ridge volcanics, Babine Lake area, Central British Columbia, Unpublished honours B.Sc. thesis, *University of Victoria*.

Tipper, H.W. and Richards, T.A. (1976):. Geology of the Smithers Area; *Geological Survey of Canada*, Open File Map 351.

Wojdak, P.J., Ethier, D. and Hanson, D. (1999): Knoll (093M 100); *in* Exploration in B.C. 1999, *B.C. Ministry of Energy and Mines*

Woodsworth, J.G. (1980): Geology of the Whitesail Lake (93E) map-area, *Geological Survey of Canada*, Open file Map 708.

Age and Geologic History of the Ecstall Greenstone Belt, Northwest British Columbia

D.J. Alldrick[1], R.M. Friedman[2] and F.C. Childe[3]

INTRODUCTION

The Ecstall Greenstone Belt is 80 kilometres long and 3 to 20 kilometres wide, and lies midway between the northern port cities of Prince Rupert and Kitimat (Figure 1). A century of prospecting has located 37 sulphide mineral occurrences at surface, including 3 VMS deposits with combined reserves of 10 million tonnes (Alldrick, this volume). In response to continued interest and encouragement from the exploration industry, Ecstall has been the focus of many geological research programs, including four geochronological studies of intrusive, volcanic and sedimentary units (Gareau, 1991a; Childe, 1997; Gareau and Woodsworth, 2000; this report). This paper compiles all the results from these four studies and incorporates the dates into a geologic history for the belt.

GEOLOGIC SETTING

The Ecstall Greenstone Belt is a small segment of the Central Gneiss Complex, a 2000-kilometre-long anastomosing network of metamorphosed Proterozoic to Paleozoic volcanic, sedimentary and minor plutonic rocks (Wheeler and McFeely, 1991; Read *et al*., 1991). The Central Gneiss Complex is enclosed by Late Silurian to Eocene granitoid rocks of the Coast Plutonic Complex (Woodsworth *et al*., 1992). Together, these two complexes comprise the Coast Crystalline Belt.

[1] *British Columbia Ministry of Energy and Mines*
[2] *The University of British Columbia*
[3] *iMAP Interactive Mapping Solutions Inc.*

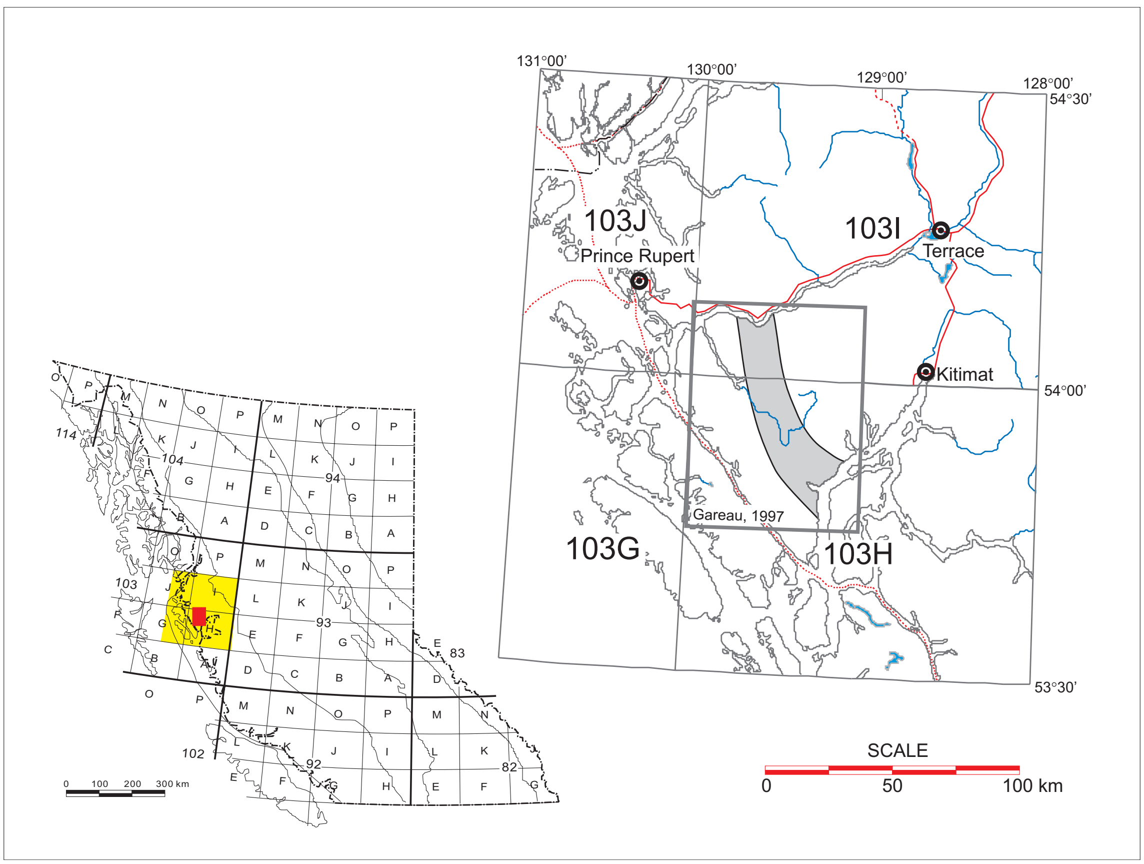

Figure 1. Location of the Ecstall belt in British Columbia. Box shows area of Gareau (1997) geology map.

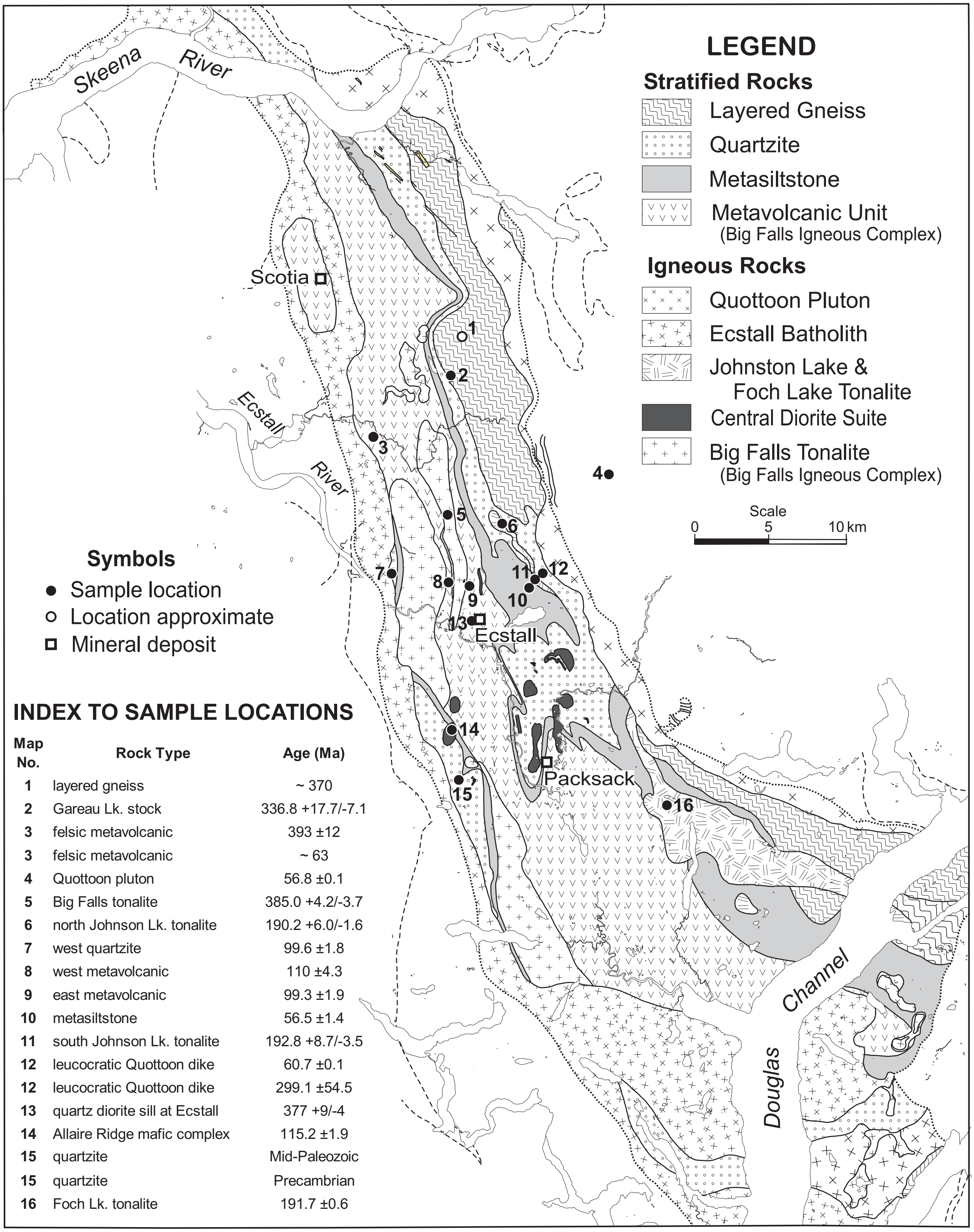

Figure 2. Simplified geology of the Ecstall belt (modified from Gareau, 1997) and geochronology sample sites (*see* Tables 1 and 2).

The Ecstall belt is a north-northwest trending, medium to high-grade metamorphic belt bounded by the elongate mid-Cretaceous Ecstall pluton on the west and the Paleocene Quottoon pluton on the east (Figure 2). Gareau (1991a) divided stratified rocks of the belt into four principal units: metavolcanic rocks, metasedimentary rocks, quartzite and layered gneiss. The metavolcanic unit consists of mafic to intermediate composition metavolcanic rocks, interlayered with lesser felsic metavolcanic and metasedimentary rocks. Within the belt, metavolcanic rocks have a gradational contact with the two large mid-Devonian plutons of the Big Falls tonalite (Figure 2). Gareau (1991a) suggests that the gradational zone between identifiable plutonic and volcanic rocks may mark a transition from cogenetic high-level intrusive to extrusive rocks, implying that the main volcanic sequence in the belt is also of mid-Devonian age. In addition to Paleozoic intrusions, two elongate plutonic bodies of Early Jurassic age, the Johnson Lake and the Foch Lake tonalites, intrude the eastern part of the belt (Figure 2).

GEOCHRONOLOGY STUDIES

Gareau (1991a, p.160-199) completed age determinations on a comprehensive suite of intrusive rocks from the Ecstall belt. Seven samples were dated using the U-Pb method to obtain ages of the protoliths of metamorphic rocks, to date magmatic episodes related to periods of tectonic activity, and to determine the ages of the two bounding plutons to the Ecstall belt. The latter would help to constrain the timing of regional metamorphism and deformation that affected Ecstall belt rocks. A suite of five hornblende K-Ar samples were collected to document the timing of cooling below the hornblende K-Ar closure temperature after the last regional metamorphic event, to evaluate the thermal effect of the bounding plutons, and to provide a minimum age for a mafic-ultramafic intrusive suite that could not be dated by U-Pb methods.

Childe (1997, p.222-238) dated a quartz diorite sill that crops out immediately west of the Ecstall volcanogenic massive sulphide deposit, to determine a minimum age for the syngenetic VMS mineralization.

Gareau and Woodsworth (2000, p.27-28) report preliminary results of U-Pb detrital zircon work on a sample of the extensive quartzite unit exposed along both margins of the Ecstall belt and a U-Pb date on zircon from the layered gneiss unit in the northeastern part of the belt.

This report presents two new U-Pb dates obtained from one rock sample; a protolith age for a felsic metavolcanic rock and an age for a metamorphic zircon separate from the same rock.

ANALYTICAL RESULTS

Analyses of 16 samples collected during these four geochronological studies have yielded 19 dates. These results are listed in geographical order (Table 1 and Figure 2) and in chronological order (Table 2). U-Pb analytical data are presented in Table 3 and Figure 3 shows the stan-

TABLE 1
INDEX TO SAMPLES LISTED NORTH TO SOUTH (*SEE* FIGURE 2).
(NOTE THAT 19 SEPARATE DATES HAVE BEEN DETERMINED FROM 16 SAMPLES)

Map N0.	Sample Number	Rock Type	Method	Mineral	Age (Ma)	Comment	Reference
1	G89-132-2	Layered Gneiss	U-Pb	zircon	**~ 370**	age of igneous protolith	G & W, 2000
2	G88-140-2	Gareau Lake stock	U-Pb	zircon	**336.8 +17.7 / -7.1**	age of quartz diorite stock	Gareau, 1991a
3	A99-5-6	felsic metavolcanic	U-Pb	zircon	**393 +/- 12**	age of felsic protolith	this report
3	A99-5-6	felsic metavolcanic	U-Pb	zircon	**~ 63**	metamorphic zircon	this report
4	G87-246-1	Quottoon pluton	U-Pb	zircon	**56.8 +/- 0.1**	age of tonalite pluton	Gareau, 1991a
5	G87-172-2	Big Falls tonalite	U-Pb	zircon	**385.0 +4.2 / -3.7**	age of tonalite protolith	Gareau, 1991a
6	G87-218-2	north Johnson Lake tonalite	U-Pb	zircon	**190.2 +6.0 / -1.6**	age of tonalite protolith	Gareau, 1991a
7	G88-67-2	west quartzite	K-Ar	hornblende	**99.6 +/- 1.8**	hornblende cooling age	Gareau, 1991a
8	G88-80-2	west metavolcanic	K-Ar	hornblende	**110 +/- 4.3**	hornblende cooling age	Gareau, 1991a
9	G88-73-2	east metavolcanic	K-Ar	hornblende	**99.3 +/- 1.9**	hornblende cooling age	Gareau, 1991a
10	G88-84-2	metasiltstone	K-Ar	hornblende	**56.5 +/- 1.4**	hornblende cooling age	Gareau, 1991a
11	G87-139-5	south Johnson Lake tonalite	U-Pb	zircon	**192.8 +8.7 / -3.5**	age of tonalite protolith	Gareau, 1991a
12	G87-140-2	leucocratic Quottoon dike	U-Pb	zircon	**60.7 +/- 0.1**	age of Quottoon dike	Gareau, 1991a
12	G87-140-2	leucocratic Quottoon dike	U-Pb	zircon	**299.1 +/- 54.5**	inherited zircon	Gareau, 1991a
13	EL-GC-01	quartz diorite sill at Ecstall VMS	U-Pb	zircon	**377 +9 / -4**	age of quartz diorite sill	Childe, 1997
14	G88-147-1	Allaire Ridge mafic complex	K-Ar	hornblende	**115.2 +/- 1.9**	hornblende cooling age	Gareau, 1991a
15	G89-98-6	quartzite	U-Pb	zircon	**Mid-Paleozoic**	detrital zircon	G & W, 2000
15	G89-98-6	quartzite	U-Pb	zircon	**Precambrian**	detrital zircon	G & W, 2000
16	G88-108-2	Foch Lake tonalite	U-Pb	zircon	**191.7 +/- 0.6**	age of tonalite protolith	Gareau, 1991a

TABLE 2
DATES FROM THE ECSTALL BELT IN CHRONOLOGICAL ORDER
(NOTE THAT 19 SEPARATE DATES HAVE BEEN DETERMINED FROM 16 SAMPLES)

Map No.	Rock Type	Age (Ma)	Comment
10	metasiltstone	56.5 ±1.4	hornblende cooling age
4	Quottoon pluton	56.8 ±0.1	age of tonalite pluton
12	leucocratic Quottoon dike	60.7 ±0.1	age of Quottoon dike
3	felsic metavolcanic	~ 63	metamorphic zircon
9	east metavolcanic	99.3 ±1.9	hornblende cooling age
7	west quartzite	99.6 ±1.8	hornblende cooling age
8	west metavolcanic	110 ±4.3	hornblende cooling age
14	Allaire Ridge mafic complex	115.2 ±1.9	hornblende cooling age
6	north Johnson Lk. tonalite	190.2 +6.0/-1.6	age of tonalite protolith
16	Foch Lk. tonalite	191.7 ±0.6	age of tonalite protolith
11	south Johnson Lk. tonalite	192.8 +8.7/-3.5	age of tonalite protolith
12	leucocratic Quottoon dike	299.1 ±54.5	inherited zircon
2	Gareau Lk. stock	336.8 +17.7/-7.1	age of quartz diorite stock
1	layered gneiss	~ 370	age of igneous protolith
15	quartzite	Mid-Paleozoic	detrital zircon
13	quartz diorite sill at Ecstall	377 +9/-4	age of quartz diorite sill
5	Big Falls tonalite	385.0 +4.2/-3.7	age of tonalite protolith
3	felsic metavolcanic	393 ±12	age of felsic protolith
15	quartzite	Precambrian	detrital zircon

dard Pb/U concordia plots. Results are discussed below in geochronological order, with reference to the schematic stratigraphy (Figure 4) and geologic history of the belt (Figure 5).

GEOLOGY AND GEOCHRONOLOGY

Regional stratigraphy was extensively discussed by Gareau (1991a,b,c and 1997). Stratigraphic tops, however, remain unclear (*e.g.* Figure 2 in Gareau, 1991a). Stratigraphic indicators identified by exploration geologists, such as pillow lavas (Hassard *et al.*, 1987, p.10), graded beds and accretionary lapilli (Schmidt, 1996, p.8) were too deformed to be interpreted reliably. The sense of stratigraphic `tops' used in this report is based on the conspicuous absence of the extensive Big Falls tonalite within the widespread metasedimentary units that are locally adjacent to the tonalite plutons (*e.g.* Gareau, 1997), and on the presence of abundant "granitoid" (tonalite) clasts within conglomeratic members of the metasiltstone unit (Gareau, 1991a; Figure 7b in Gareau and Woodsworth, 2000).

The oldest dates from Ecstall belt rocks are Precambrian and mid-Paleozoic ages obtained from detrital zircons in a sample of quartzite (metasandstone) collected along the southwestern edge of the Ecstall belt (sample location 15 on Figure 2 and Tables 1 and 2) (Gareau and Woodsworth, 2000). These detrital zircon ages suggest that the maximum possible age for deposition of this sandstone is mid-Paleozoic; however, the actual depositional age may be younger. As shown in Figures 4 and 5, these sedimentary rocks are now interpreted to have been deposited following the accumulation of the metavolcanic sequence.

At the base of the stratigraphic sequence is the metavolcanic unit which consists of mafic to intermediate to felsic metavolcanic rocks and derived metasedimentary rocks. The unit has been isoclinally folded (Gareau, 1991a, p.46), consequently apparent stratigraphic thicknesses, which range from 1 to 10 kilometres, are at least double their original value. A welded, felsic pyroclastic rock (sample number A99-5-6; location 3 on Figure 2 and Tables 1 and 2) was collected in the north-central part of the metavolcanic sequence, from a rockcut on a logging road along the south bank of Big Falls Creek. Felsic metavolcanic rocks from this same stratigraphic interval host the F-13 sulphide prospect on the north bank of Big Falls Creek, 220 metres to the north-northwest (Alldrick, this volume). Two populations of zircon were recovered from this sample: clear, colourless, gem-quality subrounded to stubby prismatic grains, interpreted as metamorphic in origin; and pale yellow, well-faceted, elongate prismatic grains, interpreted as igneous in origin. The results of four analysed fractions define a linear array on a concordia plot (Figure 3a). Clear rounded grains yield relatively young ages and euhedral elongate prismatic grains give older ages. A regression line through the data yields an upper intercept of 393 ± 12 Ma, interpreted as the best esti-

TABLE 3
U-Pb ANALYTICAL DATA FOR ROCKS FROM THE ECSTALL BELT

Fraction[1]	Wt	U[2]	Pb*[3]	^{206}Pb[4]/^{204}Pb	Pb[5]	^{208}Pb[6]	Isotopic ratios (1σ,%)[7]			Apparent ages (2σ,Ma)[7]		
	mg	ppm	ppm		pg	%	$^{206}Pb/^{238}U$	$^{207}Pb/^{235}U$	$^{207}Pb/^{206}Pb$	$^{206}Pb/^{238}U$	$^{207}Pb/^{235}U$	$^{207}Pb/^{206}Pb$
A99-5-6 felsic metavolcanic rock												
B m,4,p	0.030	443	12	3764	6.1	11.2	0.0275 (0.13)	0.1992 (0.19)	0.0525 (0.10)	175.0 (0.4)	184.5 (0.6)	307 (4.6)
C m,5,p,e	0.010	339	13	1511	5.3	10.1	0.0376 (0.13)	0.2781 (0.26)	0.0536 (0.18)	238.1 (0.6)	249.1 (1.1)	354 (8.3)
D m,4,sr	0.015	217	2.1	393	5.3	9.2	0.0099 (0.27)	0.0647 (1.5)	0.04761 (1.4)	63.3 (0.3)	63.7 (1.9)	80 (67/69)
E f,9,sr	0.015	315	5.5	774	6.8	9.3	0.0175 (0.18)	0.1213 (0.49)	0.05026 (0.42)	111.9 (0.4)	116.3 (1.1)	207 (20)
EL-GC-01 quartz diorite sill at Ecstall VMS property												
A c,40,p	0.315	393	22	20943	21	6.5	0.058 (0.25)	0.4331 (0.29)	0.05413 (0.10)	363.6 (1.8)	365.4 (1.8)	377 (4.4)
B c,35,p	0.236	474	26	27192	14	6.9	0.0559 (0.15)	0.4165 (0.21)	0.05406 (0.09)	350.5 (1.0)	353.5 (1.3)	374 (4.1)
C m,50,p	0.275	438	25	40696	11	6.7	0.0579 (0.63)	0.4315 (0.64)	0.05409 (0.10)	362.6 (4.4)	364.2 (3.9)	375 (4.4)
D f,90,p	0.072	511	29	18076	7.3	7.2	0.0573 (0.13)	0.4272 (0.20)	0.05408 (0.09)	359.1 (0.9)	361.2 (1.2)	374 (4.2)
E c,50,p	0.042	579	33	9146	10	6.5	0.0586 (0.11)	0.4371 (0.19)	0.05411 (0.10)	367.0 (0.8)	368.2 (1.2)	376 (4.3)
F c,30,p	0.091	430	24	5766	24	6.8	0.0566 (0.13)	0.4215 (0.21)	0.0540 (0.12)	354.7 (0.9)	357.1 (1.3)	373 (5.4)
G c,12,p	0.045	493	28	7931	10	6.6	0.0577 (0.21)	0.4304 (0.27)	0.05407 (0.11)	361.8 (1.5)	363.4 (1.6)	374 (4.7)
H m,40,p	0.054	484	27	8154	12	6.7	0.0576 (0.11)	0.4298 (0.20)	0.05409 (0.10)	361.2 (0.8)	363.0 (1.2)	375 (4.6)

Analytical techniques listed in Friedman et al., 2001 (in press).

[1] Zircon fractions air abraded except EL-GC-01, B. Grain size, intermediate dimension: cc=>250µm, c=<250µm and >134µm, m=<134µm and >104µm, f=<104µm and >74µm, ff <74µm; Grain size code followed by number of grains analysed. Grain character codes: b= broken, e=elongate, p=prismatic, sr=subrounded. Zircons nonmagnetic on Franz magnetic separator at field strength of 1.8A and sideslopes of 1°-2°. Front slope of 20°.

[2] U blank correction of 1pg ± 20%; U fractionation corrections were measured for each run with a double ^{233}U-^{235}U spike (about 0.004/amu).

[3]Radiogenic Pb

[4]Measured ratio corrected for spike and Pb fractionation of 0.0035 to 0.0042/amu ± 20% (Daly collector), which was determined by repeated analysis of NBS Pb 981 standard throughout the course of this study.

[5]Total common Pb in analysis based on blank isotopic composition.

[6]Radiogenic Pb

[7]Corrected for blank Pb (2-10 pg), U (1 pg) and common Pb concentrations based on Stacey Kramers model Pb at the age or the $^{207}Pb/^{206}Pb$ age of the rock.

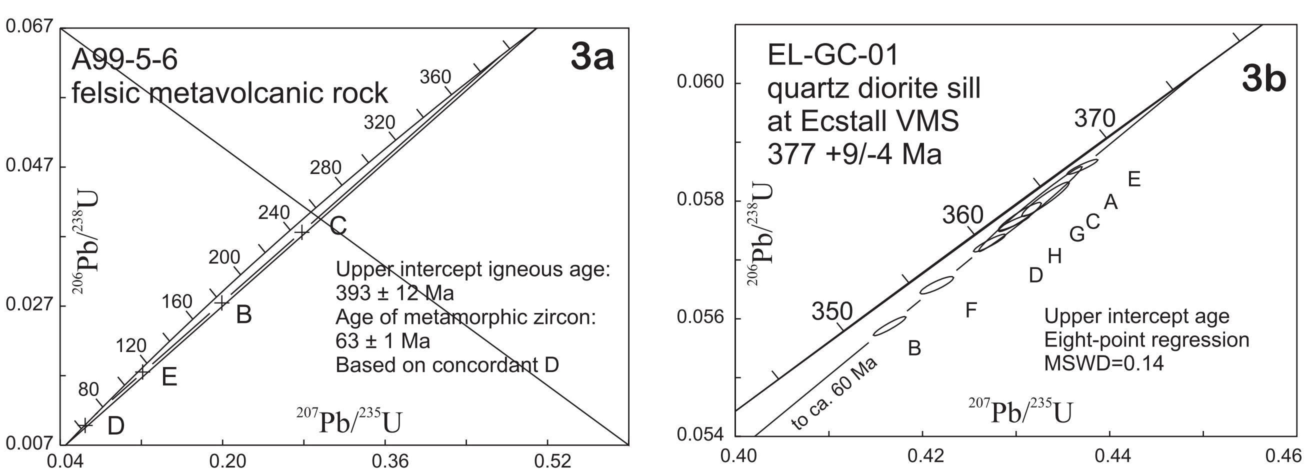

Figure 3. Concordia plots showing U-Pb zircon results for samples from the Ecstall belt: 3a. Sample A99-5-6, felsic metavolcanic rock; 3b. Sample EL-GC-01, quartz diorite sill from the Ecstall VMS property. Error ellipses are plotted at the 2σ level of uncertainty. Data on plot 5a are represented as crosses that do not reflect precision; see Table 3 for analytical precision. See text for detailed interpretations.

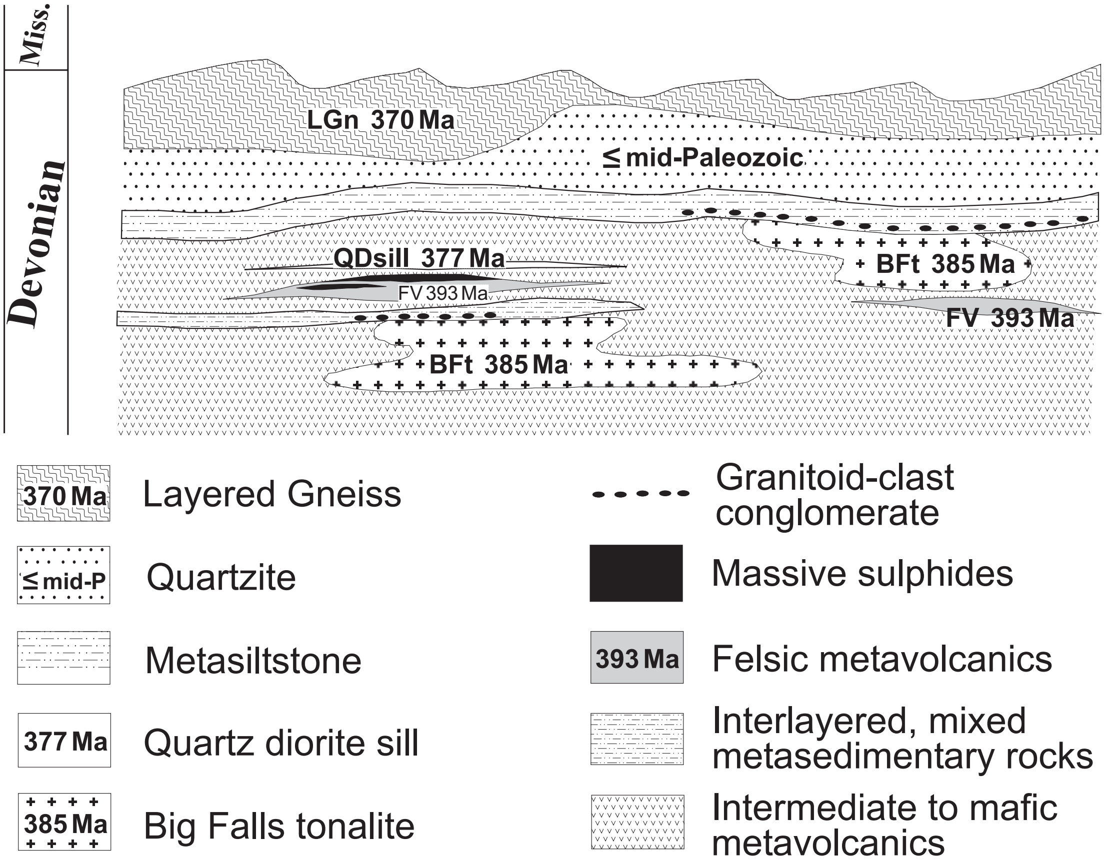

Figure 4. Schematic stratigraphy of the Ecstall belt.

mate for the igneous age of the sample. This U-Pb zircon age of 393 Ma confirms the mid-Devonian age attributed to the Ecstall belt volcanic sequence by Gareau (1991a,b). This sample also yielded fraction D (Figure 3a) which produced a concordant age of ~63 Ma that is interpreted as a good estimate for the crystallization age of metamorphic zircon in this rock.

Gareau (1997) mapped two large bodies of foliated intrusive rock, collectively named the Big Falls tonalite (location 5 on Figure 2 and Tables 1 and 2). These are enclosed mainly by the metavolcanic sequence of the Ecstall metamorphic belt, and locally by the overlying metasiltstone unit. A sample from the eastern lens of this rock produced a U-Pb zircon age of 385 ± 4 Ma, leading Gareau (1991a,b) to conclude that the tonalite bodies are coeval, subvolcanic intrusions that fed the overlying volcanic pile. Recent global research into the geologic setting of VMS deposits has stressed the importance of subvolcanic plutons of tonalite/trondhjemite composition as the heat source which generates VMS deposits at the overlying paleosurface (Galley, 1996; Large *et al.*, 1996).

Childe (1997) analysed a sample of foliated quartz diorite sill (location 13 on Figure 2 and Tables 1 and 2) that crops out just to the west of the North Lens of the Ecstall massive sulphide deposit (Alldrick, this volume; Schmidt, 1995). U-Pb analytical results for eight zircon fractions from sample EL-GC-01 define a linear array on a concordia plot (Figure 3b). A regression line through these data yield an upper intercept of 377 +9/-4 Ma, interpreted as the best estimate for the igneous age of the quartz diorite intrusion. This 377 Ma U-Pb zircon age provides a Late Devonian minimum age for the nearby, syngenetic sulphide deposit and its enclosing metavolcanic host rocks (Childe, 1997). The regression line also indicates a lower intercept age of 60 +107/-109 Ma, which likely records the age of Pb loss.

The U-Pb zircon age of 377 +9 / -4 Ma obtained from the quartz diorite sill at the Ecstall deposit is statistically similar to the 393 ± 12 Ma age for the metavolcanic rocks reported above. The age of this sill is also within error of the 385 +4.2 / -3.7 Ma age for the Big Falls tonalite. Taken together, these three U-Pb zircon results (locations 13, 3 and 5 on Figure 2) reveal a Middle Devonian intrusive-extrusive complex consisting of a suite of subvolcanic, synvolcanic stocks and sills; coeval, comagmatic volcanic rocks; and associated sedimentary rocks. This Middle Devonian volcanic rock succession hosts all three of the massive sulphide deposits and most of the smaller sulphide prospects of the Ecstall belt. These comagmatic rocks and their locally derived, intercalated sedimentary rocks are informally referred to as the Big Falls Igneous Complex to denote the rocks most important for the for-

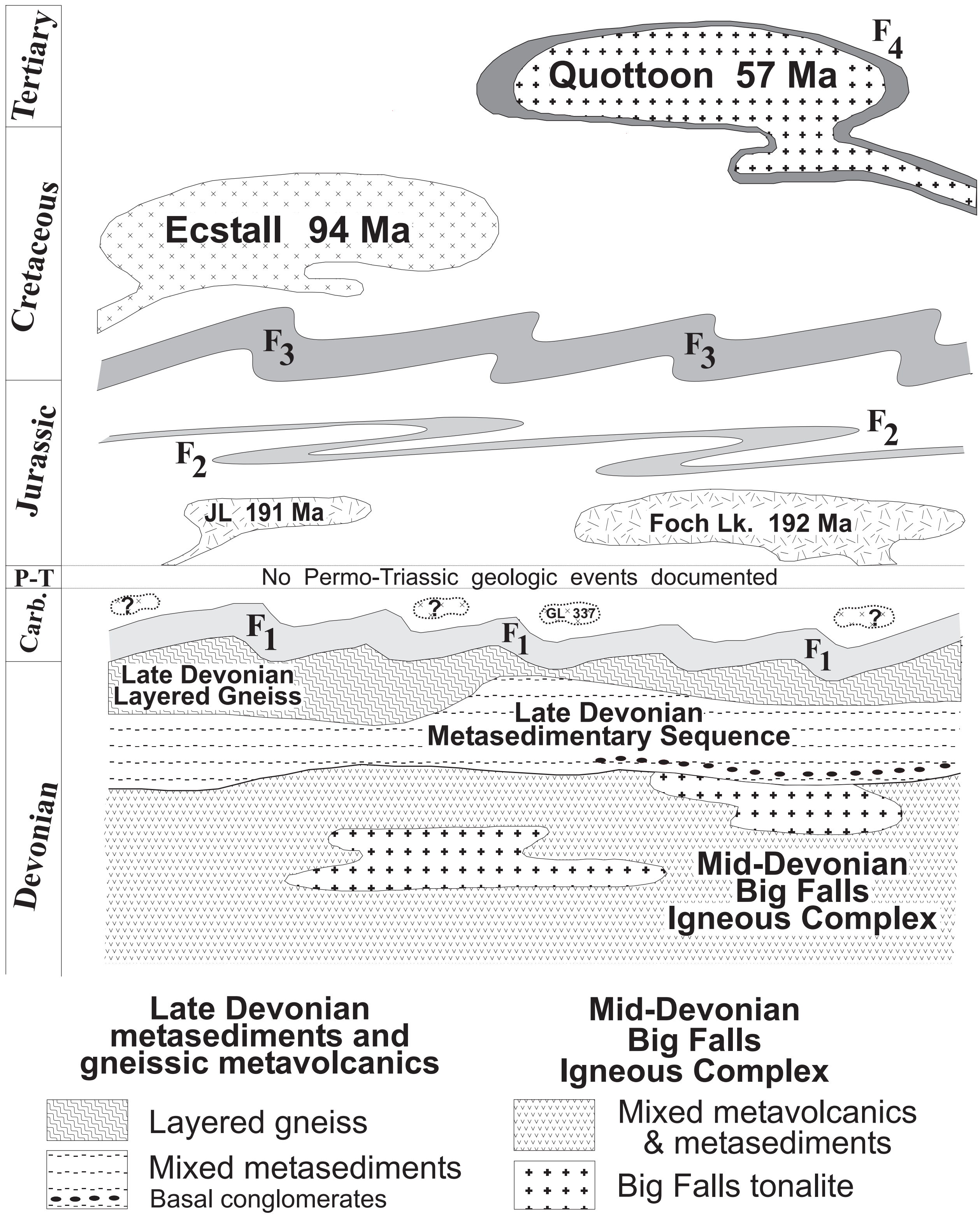

Figure 5. Schematic geologic history of the Ecstall belt. F-1, F-2, F-3 and F-4 are successive episodes of deformation. JL = Johnson Lake stock; GL = Gareau Lake stock (adapted from Gareau, 1991a,b,c and 1997).

mation and preservation of volcanogenic massive sulphide deposits within the belt.

The volcanic succession is overlain regionally by a unit of medium to dark grey to black metasiltstone that is locally pyritic. This is the “metasedimentary unit” of Gareau (1991a) and the “metaclastic unit” of Gareau and Woodsworth (2000). The hornblende-biotite-quartz-feldspar-epidote rock has a mafic mineral content ranging from 20% to 70% (Gareau, 1991a). Rare intervals that contain fine disseminated magnetite grains have been noted. Thickness of this unit ranges from 100 metres near the Packsack deposit to greater than 5 kilometres along Douglas Channel; much of this increase is due to structural thickening near the axis of a regional scale fold in the Douglas Channel-Hawkesbury Island area. Gareau (1991a) describes contacts between the metasiltstone unit and the metavolcanics ranging from gradational to sharp. This unit is significant in the regional stratigraphic construction because no dikes, sills or stocks correlated with the adjacent Big Falls Igneous Complex have been identified within the metasiltstone unit, although younger intrusive rocks are common. In contrast, the unit does incorporate repeated, extensive lenses of granitoid clast conglomerate (Gareau, 1991a). Clasts average 10 centimetres in diameter and typically make up 10% of the rock. Gareau (1991a) reports an exposure of conglomerate on the ridgecrest north of Johnston Lake that is 300 metres thick. Mafic mineral content of the granitoid clasts ranges from 20% to 70%, and K-feldspar is absent, indicating a compositional range from tonalite to quartz diorite. A K-Ar determination on hornblende from this metasiltstone unit yielded an age of 56.5 ±1.4 Ma. This young age was attributed to resetting by the nearby Late Paleocene Quottoon pluton (Gareau, 1991a). Gareau’s geological map (1997) shows one extra zircon sample site within this unit, at latitude 52º 47’ and longitude 129º 22’; this is a duplicated and mislocated plot of the Foch Lake orthogneiss sample.

The dark grey to black metasiltstone unit is overlain regionally by an extensive unit of quartzite (metasandstone). This white to light grey, well-laminated rock resembles thin-bedded sandstone, but the thin micaceous partings, rhythmically spaced at 5 to 10 centimetre intervals, are interpreted to result from metamorphic differentiation and do not reflect primary compositional variation. Minor associated lithologies include dark grey to black metapelite, black phyllite, dark grey metasiltstone and rare marble. Thickness of this unit ranges from 600 metres near Gareau Lake to more than 7 kilometres near the upper Ecstall River where the unit has been structurally thickened. Gareau (1991a) describes the contact between this unit and the metasiltstone unit as gradational over a 20 to 100 metre interval. Along the eastern margin of the Ecstall belt, this unit is in contact with a black and white layered gneiss. Gareau (1991a) describes the contact between these units as sharp to gradational over an interval of 500 metres. Like the subjacent metasiltsone unit, this quartzite unit is an important component in the regional stratigraphic construction because no dikes, sills or stocks correlated with the Big Falls Igneous Complex have been identified within it. A sample of this rock was collected to the south of the Allaire Ridge mafic intrusive complex, west-southwest of the Packsack deposit, for extraction of detrital zircons (location 15 on Figure 2 and Tables 1 and 2). Two zircon grains gave Precambrian and mid-Paleozoic U-Pb dates (Gareau and Woodsworth, 2000). The mid-Paleozoic date represents a maximum age for this extensive metasedimentary unit, and is consistent with the stratigraphic interpretation that this sedimentary unit overlies the Middle Devonian Big Falls Igneous Complex.

Along the eastern edge of the Ecstall belt, the quartzite unit is in contact with an extensive unit of black and white layered gneiss which is interpreted as a metavolcanic rock (Gareau, 1991a). The metamorphic grade here, upper amphibolite to granulite facies, is higher than the rest of the belt (Gareau, 1991a). The protolith to this gneiss might be a repeated fold limb of the metavolcanic sequence of the Big Falls Igneous Complex, or a different, younger, mafic volcanic rock. The unit is more homogeneous and more mafic than the Big Falls Igneous Complex (S. Gareau, personal communication, 2000). The regionally extensive metasiltstone rock unit has not been recognized anywhere along the contact between the quartzite and the layered gneiss units (Gareau, 1997), which suggests that the layered gneiss may be a different, younger volcanic unit, rather than a repetition of Big Falls Igneous Complex stratigraphy. Gareau and Woodsworth (2000) report a preliminary U-Pb zircon age of ~370 Ma (location 1 on Figure 2 and Tables 1 and 2) for a sample of this rock collected northeast of the Gareau Lake stock. All these lines of evidence support the interpretation that the mafic volcanic protolith for this rock is a younger volcanic package which stratigraphically overlies the quartzite unit.

The layered gneiss is the youngest (uppermost) stratigraphic unit preserved in the Ecstall metamorphic belt. The remaining 13 dates from the belt are from younger plutons that cross-cut the stratigraphy, from metamorphic zircons, or from zircon and hornblende that have undergone partial or complete thermal resetting during metamorphism.

Gareau (1991a, p.173-175) describes a small (<100 metres diameter) weakly foliated quartz diorite stock that intrudes the layered gneiss unit on a ridgecrest 2 kilometres southeast of Gareau Lake (location 2 on Figure 2 and Tables 1 and 2). The rock is composed of 75% plagioclase, 10% quartz, 5% biotite and 3% hornblende with accessory titanite, apatite, zircon and opaque minerals. The U-Pb zircon age for this rock is 336.8 + 17.7 / -7.1 Ma (Gareau, 1991a) although the data reasonably allow for an interpreted crystallization age as young as 320 Ma. This date is consistent with intrusion into the older layered gneiss unit and indicates a mid-Mississippian magmatic episode of quartz diorite composition.

Gareau (1991a, p.21-22) describes a series of Jurassic or Cretaceous mafic and ultramafic stocks intruded through the central Ecstall belt. These rocks crop out in three main areas: two stocks on Allaire Ridge, 10 kilometres south-southwest of Johnston Lake; several small stocks scattered all along on Prospect Ridge, immediately west and uphill of the Packsack VMS deposit; and a small body mapped on the peak of Red Gulch Mountain, 2.7 kilometres north-northeast of the north end of the Ecstall VMS deposit. These mafic rocks are dominantly diorites, but range in composition from quartz diorite through diorite and gabbro to hornblendite. Gareau sampled coarse-grained hornblendite from the Allaire Ridge intrusions for a K-Ar analysis on hornblende (location 14 on Figure 2 and Tables 1 and 2) and interpreted the 115 Ma K-Ar age as a reset date due to early to mid-Cretaceous regional metamorphism. The age of intrusion of all these rocks is unknown, although they must be younger than the quartzite host rock with a probable Late Devonian depositional age and older than the Early Cretaceous metamorphism. It is possible that these scattered clusters of weakly foliated mafic to ultramafic stocks are all comagmatic with the foliated Gareau Lake diorite stock, described above, in which case they would have a mid-Mississippian age of ~337 Ma (Figure 5).

Gareau's (1991a) U-Pb zircon analysis of a young (unfoliated) pegmatite dike gives an emplacement age of 61 Ma, but also contains a component of inherited zircon with a U-Pb age of 299.1 ± 54.5 Ma (location 12 on Figure 2 and Tables 1 and 2). This is interpreted as the average age of the inherited zircon in the grains analysed and indicates that the dike has incorporated some zircons from the enclosing Paleozoic host rocks (Gareau, 1991a).

An important discovery in Gareau's study was the identification of two large, elongate Early Jurassic intrusions emplaced along the eastern margin of the Ecstall belt. These plutons are both weakly to strongly foliated tonalite; one is medium-grained and equigranular and the other is plagioclase megacrystic. The northern, equigranular, Johnston Lake tonalite (location 6 and 11 on Figure 2 and Tables 1 and 2) yielded U-Pb zircon ages of 192.8 + 8.7 / -3.5 Ma and 190.2 + 6.0 / - 1.6 Ma from samples collected at the northern and southern ends of the pluton, respectively. The southern, coarsely porphyritic, Foch Lake tonalite (location 16 on Figure 2 and Tables 1 and 2) yielded a U-Pb zircon age of 191.7 ± 0.6 Ma. These plutons are coeval with igneous rocks within the Stikine terrane, and suggest Early Jurassic proximity of the Ecstall belt (Gareau and Woodsworth, 2000).

Gareau (1991a) collected a series of four samples across the central part of the Ecstall belt for K-Ar age determinations on hornblende (locations 7, 8, 9, 10 on Figure 2 and Tables 1 and 2). The results from west to east were 99.6 ± 1.8 Ma, 110 ± 4.3 Ma, 99.3 ± 1.9 Ma and 56.5 ± 1.4 Ma, Gareau (1991a). This pattern is attributed to resetting of the ages of the central samples by an Early Cretaceous metamorphic event, and to still younger thermal resetting of the westernmost and easternmost samples by the Ecstall (93.5 Ma) and Quottoon (56.8 Ma) plutons respectively. Together with the 115 Ma hornblendite K-Ar age (location 14 on Figure 2), these results support the interpretation that a major metamorphic event terminated in early to mid-Cretaceous time, Gareau (1991a).

Another metamorphic event affected Ecstall Belt rocks during the Paleocene, recorded by metamorphic zircon ages. Sample A99-5-6 (location 3 on Figure 2 and Tables 1 and 2) yielded fraction D (Figure 3a) which gave a concordant age of ~63 Ma that is interpreted as a good estimate for the crystallization age of metamorphic zircon in this rock. One other sample (location 10 on Figure 2 and Tables 1 and 2) shows the effect of Paleocene metamorphism. These ages coincide well with the two U-Pb zircon ages of 56.8 ± 0.1 Ma and 60.7 ± 0.1 Ma that Gareau (1991a) obtained from a sample from the centre of the Quottoon pluton and from a sample of a fresh pegmatite dike collected one kilometre west of the western edge of the Quottoon stock (locations 4 and 12 on Figure 2 and Tables 1 and 2).

GEOLOGIC HISTORY

The 19 dates reviewed in this report provide key constraints for deciphering the geologic history of this highly deformed, repeatedly metamorphosed region (Figure 5).

Mid-Devonian magmatism and volcanism generated the tonalitic stocks, dikes and sills, and a differentiated subaqueous volcanic succession with intercalated sedimentary rocks, collectively termed Big Falls Igneous Complex. Volcanism was followed in Late Devonian time by deposition of a thick sequence of fine-grained sediments with conglomeratic members, followed by an even thicker succession of well-sorted sandstone with minor siltstone members. These regionally extensive sedimentary blankets were overlain in latest Devonian time by another mafic volcanic sequence, now preserved as layered gneiss.

Alldrick and Gallagher (2000) concluded that regional deformation of the Ecstall belt rocks took place in early Mississippian time, following the deposition of the ~370 Ma protolith to the Layered Gneiss unit, but before intrusion of the 337 Ma, weakly foliated Gareau Lake stock.

The mid-Mississippian Gareau Lake diorite, a small stock cutting the Late Devonian Layered Gneiss unit, may be part of an extensive suite of scattered clusters of small, weakly foliated diorite stocks that are preserved throughout the central Ecstall belt.

Gareau and Woodsworth (2000) conclude that the first period of deformation and metamorphism still preserved in Ecstall Belt rocks occurred in the late Paleozoic (Pennsylvanian to Permian), after deposition of the early Mississippian layered gneiss and the intrusion of the mid-Mississippian Gareau Lake stock, but before the intrusion of the Early Jurassic Johnson Lake and Foch Lake plutons. Deformation and recrystallisation were significant and measurable, but Gareau and Woodsworth (op. cit.) consider that this was not the major metamorphic event in the history of the belt.

Two large, colinear, Early Jurassic tonalite plutons, the Johnston Lake and Foch Lake stocks, were intruded along the eastern margin of the belt, and indicate a possible connection with the Stikine Terrane by the Early Jurassic (Gareau and Woodsworth, 2000).

Two major, sequential, mid-Mesozoic (late Early Jurassic to late Early Cretaceous) metamorphic events left their imprint on the rocks of the Ecstall belt (Figure 6 in Alldrick and Gallagher, 2000; and Figure 4 in Gareau and Woodsworth, 2000).

Clusters of dates at mid-Cretaceous and Paleocene times record two metamorphic events associated with intrusion of the two bounding plutons of the Ecstall belt - the mid-Cretaceous Ecstall stock on the west and the Paleocene Quottoon stock on the east. Paleocene deformation only affected rocks along the eastern margin of the Ecstall belt, where they are in contact with the 57 Ma Quottoon pluton (Gareau, 1991a,b; Gareau and Woodsworth, 2000).

CONCLUSIONS

Compilation of results from four successive geochronological studies has helped to clarify the complex stratigraphic, intrusive, metamorphic and metallogenic histories of the Ecstall district. Ongoing research will focus on improving our understanding of the internal stratigraphy of the Big Falls Igneous Complex, the ages of the main metasedimentary rock units, the ages of granitoid clasts from conglomeratic units, the age(s) of the clusters of mafic intrusive stocks and the relative sequence and timing of the major metamorphic events.

ACKNOWLEDGMENTS

We thank Dr. Susie Gareau, who improved this report with a thorough review, and Mike Fournier, B.C. Geological Survey, who prepared our figures.

REFERENCES

Alldrick, D.J. and Gallagher, C.S. (2000): Geology and mineral potential of the Ecstall VMS belt (NTS 103H; 103 I); BC Ministry of Energy and Mines, Geological Fieldwork 1999, paper 2000-1, pages 249-265.

Alldrick, D.J. (2001): Geology and mineral deposits of the Ecstall greenstone belt (NTS 103H; 103 I); BC Ministry of Energy and Mines, Geological Fieldwork 2000, paper 2001-1, this volume.

Childe, F.C. (1997): Timing and tectonic setting of volcanogenic massive sulphide deposits in British Columbia: constraints from U-Pb geochronology, radiogenic isotopes, and geochemistry; unpublished Ph.D. thesis, The University of British Columbia, 298 pages.

Friedman, R.M., Diakow, L.J., Lane, R.A. and Mortensen, J.K. (2001): U-Pb age constraints on latest Cretaceous magmatism and associated mineralization in the Fawnie Range, Nechako Plateau, central British Columbia. Canadian Journal of Earth Sciences, in press.

Galley, A.G. (1996): Geochemical characteristics of subvolcanic intrusions associated with Precambrian massive sulfide deposits, *in* Wyman, D. A., editor, Trace Element Geochemistry of Volcanic Rocks: Applications for Massive Sulfide Exploration; Mineral Deposits Division, *Geological Association of Canad*a, pages 239-278.

Gareau, S.A. (1991a): Geology of the Scotia-Quaal metamorphic belt, Coast Plutonic Complex, British Columbia; unpublished Ph.D. thesis, Carleton University, 390 pages.

Gareau, S.A. (1991b): Geology of the Scotia-Quaal metamorphic belt, Coast Plutonic Complex, British Columbia; *Geological Survey of Canad*a, Open File Map 2337, scale 1:50 000, 4 sheets.

Gareau, S.A. (1991c): The Scotia-Quaal metamorphic belt: a distinct assemblage with pre-early Late Cretaceous deformational and metamorphic history, Coast Plutonic Complex, British Columbia; *Canadian Journal of Earth Sciences,* V.28, pages 870-880.

Gareau, S.A., compiler (1997): Geology, Scotia-Quaal metamorphic belt, Coast Plutonic Complex, British Columbia; *Geological Survey of Canad*a, Map 1868A, scale 1:100 000, 1 sheet.

Gareau, S.A. and Woodsworth, G.J. (2000): Yukon-Tanana terrane in the Scotia-Quaal belt, Coast Plutonic Complex, central-western British Columbia; *in* Tectonics of the Coast Mountains, southeastern Alaska and British Columbia, *Geological Society of America*, Special Paper 343, pages 23-43.

Hassard, F.R., Pattison J and Uher, L. (1987): Geological, geophysical and geochemical surveys and diamond drilling - Ecstall Project, January 1987, report for Falconbridge Limited, B.C. Ministry of Energy and mines Assessment report No. 15,756, 52p and 9 appendices.

Large, R.R., Doyle, M., Raymond, O., Cooke, D., Jones, A. and Heasman, L., 1996, Evaluation of the role of Cambrian granites in the genesis of world class VHMS deposits in Tasmania; *Ore Geology Review*s, v.10, pages 215-230.

Read, P.B., Woodsworth, G.J., Greenwood, H.J., Ghent, E.D. and Evenchick, C.A. (1991): Metamophic Map of the Canadian Cordillera; *Geological Survey of Canada*, Map 1714A, scale 1:2 000 000.

Schmidt, U. (1995): Report on the Geology and Geochemistry of the Ecstall Property; unpublished report for Atna Resources Ltd., Feb. 1995, 23p plus appendices plus 10 folded maps.

Schmidt, U. (1996): Report on Geology, Geophysics and Diamond Drilling of the Horsefly Property, Skeena Mining Division, NTS 103 H/14; unpublished report for Atna Resources Ltd., Feb. 27, 1996, 78 pages (16 pages plus appendices plus 1 property geology map at 1:2 000 scale).

Woodsworth, G.J., Anderson, R.G. and Armstrong, R.L. (1992): Plutonic Regimes; Chapter 15 *in* Geology of the Cordilleran Orogen in Canada, *Geological Survey of Canad*a, Geology of Canada, n.4, pages 491-531

Wheeler, J.O. and McFeely, P., compilers (1991): Tectonic Assemblage map of the Canadian Cordillera and adjacent parts of the United States of America; *Geological Survey of Canada*, Map No. 1712A, 2 sheets, scale 1:2 000 000.

British Columbia Geological Survey
Geological Fieldwork 2000

Geology and Mineral Deposits of the Ecstall Greenstone Belt, Northwest British Columbia (NTS 103 H/103 I)

By Dani J. Alldrick

KEYWORDS: Economic geology, mineral potential, geologic mapping, Central Gneiss Complex, Coast Plutonic Complex, Coast Crystalline Belt, Ecstall Metamorphic Belt, VMS, sulphide, metavolcanic, greenstone, Devonian, Ecstall, Scotia, Packsack, Prince Rupert.

INTRODUCTION

The Ecstall Greenstone Belt is part of the Central Gneiss Complex, a 2000 kilometre long anastomosing network of medium to high-grade metamorphic volcanic, sedimentary and minor plutonic rocks enclosed by younger granitoid rocks of the Coast Plutonic Complex. A century of prospecting has located 36 sulphide mineral occurrences at surface, including 3 deposits with combined reserves of 10 million tonnes. The high mineral potential of this belt has justified a new detailed mapping project, related mineral deposit studies, and a special regional geochemistry survey program (Alldrick and Gallagher, 2000; Jackaman *et al*., this volume). The second field season of this multi-year project focused on study of the local geologic setting of the major volcanogenic massive sulphide deposits of this mineral district, while documentation of the geology within the metavolcanic sequence continued. Companies with properties in the belt have contributed a wealth of detailed geological data to this ongoing project.

The Ecstall belt is 80 kilometres long, 3 to 20 kilometres wide, and extends from the Douglas Channel fiord north-northwesterly to the Skeena River (Figure 1).

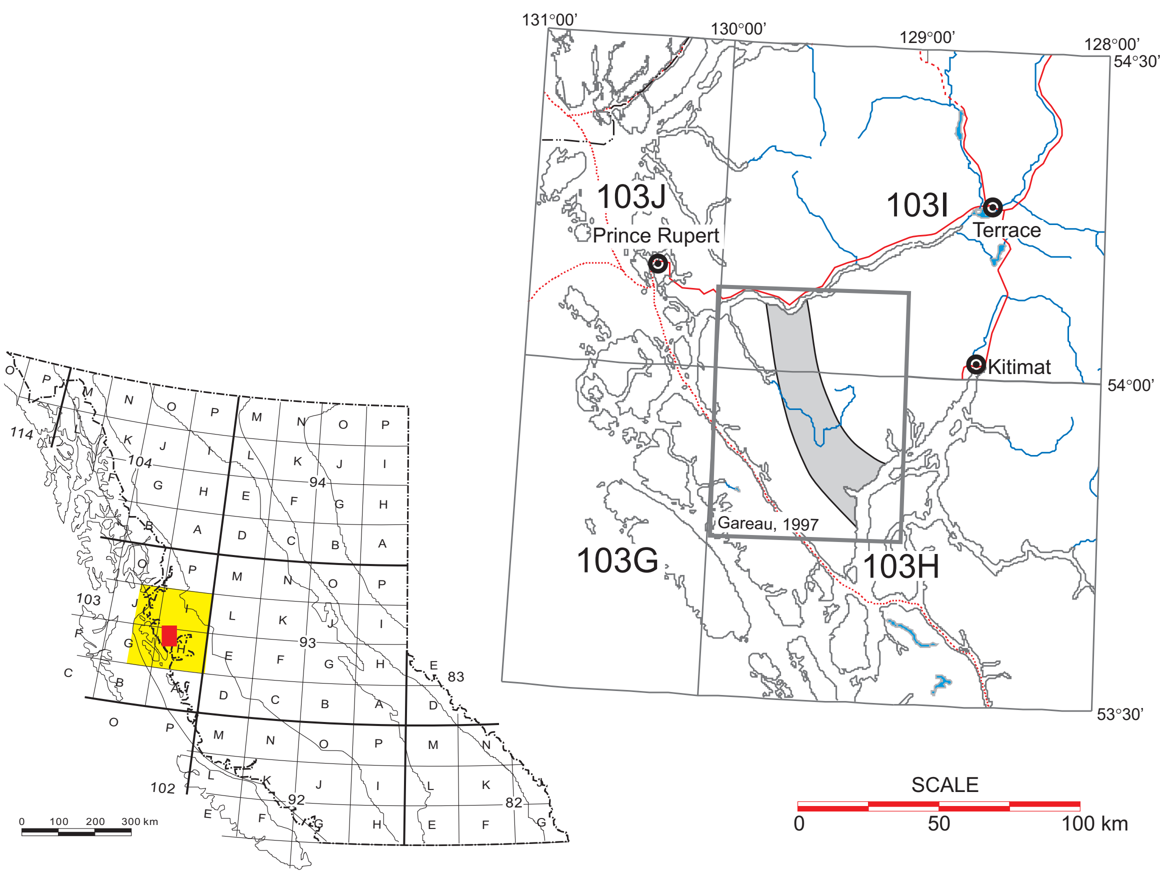

Figure 1. Location of the Ecstall belt in British Columbia.

Boasting admirable infrastructure, Ecstall lies midway between the northern port cities of Prince Rupert and Kitimat, and is close to tidewater, the Yellowhead Highway, the Skeena Railway line of VIA Rail and the national power grid (Table 1). Extensive logging road networks are established at the northern and southern ends of the belt (at the mouth of the Scotia River and at Kitkiata Inlet, respectively).

Elevation ranges from sea level to 1760 metres. Rounded ridgecrests are flanked by steep-walled glaciated valleys. Despite the precipitous terrain, it is possible to traverse the entire belt from north to south without exceeding 125 metres elevation by following a route of interconnecting valleys. Mining scenarios proposed since the 1940s have preferred haulage routes to the south to take advantage of the deep water shipping afforded by Douglas Channel (Mason, 1941b).

Rainfall is heavy; average annual precipitation at Prince Rupert is 244 centimetres (96 inches). The low elevation of the valley bottoms and their proximity to the coast leaves them free of snow through most of the year. Dense coastal rainforest covers all but the steepest slopes, where bedrock is exposed in cliffs or along avalanche tracks. Ridgecrests above 1100 metres elevation are free of trees and shrubs.

The name Ecstall comes from the Tsimshian dialect. Writers have recorded this name phonetically in English as: Eckstall, Ucstall, Oxtall, Hocsall, Hockstall, Huckstall, and Huxstall (Janet Mason, personal communication, 2000). The word means "tributary" or "something from the side", as in "secondary matter" or "side-issue". This label was clearly intended as a navigation aid, reminding Indians traveling up the broad estuary of the Skeena River that the equally wide mouth of the Ecstall estuary to the right-hand (south) side led to a relatively minor stream, navigable for just 56 kilometres before the first rapids were encountered.

PREVIOUS WORK

The Ecstall belt hosts 36 sulphide and 2 industrial mineral occurrences; only 21 of these are currently described in the MINFILE database. In 1890, the spectacularly exposed sulphide lenses of the Ecstall VMS deposit were discovered in Red Gulch Creek. A series of companies have investigated and developed this deposit throughout the last 100 years. Prospecting work during the 1930s and 1940s located 12 additional sulphide showings within 8 kilometres of the Ecstall deposit. Regional mapping and exploration programs conducted by Texas Gulf Sulphur Company Limited in 1957 and 1958, discovered the large Packsack (1957) and Scotia deposits (1958). For the past 20 years there has been continuous exploration work in the belt, carried out by many companies, resulting in the discovery of 21 more sulphide occurrences.

TABLE 1
KEY DISTANCES FOR DEPOSITS IN THE ECSTALL BELT

Deposit:	Scotia	Ecstall	Packsack
Elevation	758 m	182 m	242 m
Distance to:			
Ocean	27	24	18
Estuary / Tidewater	15	6	15
Hydro Powerline	10	19	29
Highway	15	39	49
Railway	15	39	49
Prince Rupert	49	72	82
Kitimat	67	60	59
Terrace	84	93	98

The first geology map of the Ecstall belt was the product of a corporate mapping program completed over a seven-year period (Holyk *et al.*, 1958) and remains unpublished. Seven geology maps relating to this area have been published by the Geological Survey of Canada over the last 35 years:

- Gareau (1991a and 1997) completed maps of the Ecstall Greenstone Belt at two scales
- Regional-scale maps have been produced by Hutchinson (1966 and 1979) and Roddick (1970b)
- Cordilleran-scale maps by Wheeler and McFeely (1991) and Read *et al.* (1991) yield important information about the regional setting of the Ecstall belt.

University research projects within the Ecstall belt have investigated a variety of geological features. Results are reported in theses by Padgham (1958), Money (1959), Turner (1961), Eldredge (1983), Krage (1984), Gareau (1991c) and Childe (1997). Research in adjacent rocks include studies by Kenah (1983), van der Heyden (1989), and Heah (1991). Geological studies continue under the supervision of M.L. Crawford at Bryn Mawr College, Pennsylvania and C. Davidson at Beloit College, Wisconsin.

New results from regional geological studies were published in Geological Society of America Special Paper 343 (Stowell and McClelland, 2000), including an important analysis of the regional stratigraphic correlation of the Ecstall stratigraphy by Gareau and Woodsworth (2000). Research by the Keck Geology Consortium, funded by the W.M. Keck Foundation, is scheduled for completion during the winter of 2000-2001 (*see* http://geology.beloit.edu/davidson/KeckBC/index.html).

Studies of VMS deposits in the North American cordillera have recently been completed by Newberry *et al.* (1997) and Massey (1999). Global studies of VMS deposits were reported in Barrie and Hannington (1999) and a new volume devoted to research on ore deposits in highly metamorphosed terranes has just been published (Spry, *et al.*, 2000).

Objectives of the current mapping program include: establish a detailed lithostratigraphic succession within the four large stratigraphic packages documented by Gareau (1997), study the relationships between this detailed lithostratigraphy and the mineral occurrences of the belt, trace out prospective strata, and investigate a possible coeval relationship between the intrusive Big Falls tonalite and the metavolcanic package. In the 2000 field season, a team of two mapped in the central part of the belt, investigating the Ecstall, Scotia and Packsack deposits, and some of the smaller prospects.

REGIONAL GEOLOGIC SETTING

The geologic setting of the Ecstall belt is shown in Figures 2 and 3. The Ecstall Greenstone Belt is part of the Central Gneiss Complex, an anastomosing network of high-grade metamorphic rocks enclosed by younger granitoid rocks of the Coast Plutonic Complex (Figure 2). Together these two complexes comprise the Coast Crystalline Belt or Coast Belt. The following summary is adapted from Greenwood *et al.*(1992), Woodsworth *et al.* (1992), Read *et al.* (1991) and Gareau (1991b,c).

Plutonic rocks of the Coast Plutonic Complex (CPC) make up more than 80% of the Coast Belt; the remainder is metavolcanic rocks, metasedimentary rocks and granitoid gneisses of the Central Gneiss Complex (CGC). Plutonic rocks of the CPC range in age from Late Silurian to Eocene (Woodsworth *et al.*, 1992). In general, the oldest plutons are exposed along the western edge of the CPC and the ages of plutons young progressively to the east. Rocks range in composition from granite to gabbro, but 70% of all plutonic rocks lie within the compositional range of tonalite-quartz diorite-diorite. Among the circum-Pacific plutonic terranes, the CPC is the largest, the most mafic, and the most deficient in K-feldspar.

Metamorphic rocks of the Central Gneiss Complex range in age from Proterozoic through Paleozoic and typically occur as screens or pendants surrounded or intruded by the plutonic rocks of the CPC (Figure 2). Evidence of Paleozoic regional metamorphism is preserved locally (e.g. Alldrick and Gallagher, 2000; Gareau and Woodsworth, 2000), but intense mid-Mesozoic and early Tertiary metamorphism, deformation and plutonism have obscured evidence of earlier events in many places. Most metamorphic effects can be attributed to regional metamorphism, but contact metamorphism from the adjacent plutons can also create a metamorphic overprint (e.g. Gareau, 1991a).

The Prince Rupert-Terrace corridor is the most extensively studied and best understood area of the Coast Crystalline Belt (Greenwood *et al.*, 1992; Stowell and McClelland, 2000). This is also the most deeply exhumed part of the Central Gneiss Complex; metamorphic grades range up to kyanite-amphibolite, sillimanite-amphibolite and granulite facies in different parts of this area (Read *et al.*, 1991). Within the Ecstall belt, Gareau (1991b,c) has documented a southwest to northeast progression from lower amphibolite facies to granulite facies, with most rocks falling within the kyanite-amphibolite (upper amphibolite) facies.

The mid-Devonian volcanic arc that evolved into the Ecstall Greenstone Belt likely developed in a similar setting as the extensive volcanosedimentary successions of the Yukon-Tanana terrane (Gareau and Woodsworth, 2000). The regional geologic history of the Ecstall belt is outlined in a separate report (Alldrick *et al.*, this volume) and summarized in Figure 4; Devonian volcanism, sedimentation and comagmatic intrusions are followed by three or four poorly-constrained phases of deformation and four well-dated plutonic episodes. The Jurassic to Eocene plutonic and metamorphic history of the Coast Crystalline Belt is consistent with a model of east-dipping subduction beneath a single, allochthonous Alexander-Wrangellia-Stikinia superterrane, emplaced against North America in Middle Jurassic time (van der Heyden, 1989)

GEOLOGY OF THE ECSTALL BELT

Summary

The Ecstall belt is a north-northwest trending, high-grade metamorphic belt bounded by the elongate mid-Cretaceous Ecstall pluton on the west and the Paleocene Quottoon on the east (Figure 3). Gareau (1991a) divided stratified rocks of the belt into four principal units: metavolcanic rocks, metasedimentary rocks, quartzite and layered gneiss. The metavolcanic unit consists of mafic and intermediate composition metavolcanic rocks, interlayered with lesser felsic metavolcanic and metasedimentary rocks. Metavolcanic rocks are intruded by two large, elongate, mid-Devonian plutons called the Big Falls tonalite. Recent geochronology studies (Alldrick *et al.*, this volume) confirm Gareau's (1991a) interpretation that the main metavolcanic sequence in the belt is also of mid-Devonian age. The metavolcanic package and its coeval subvolcanic stocks are overlain by a regionally extensive package of metasedimentary rocks, consisting of a lower metapelitic unit and an upper quartzite unit. These strata are overlain in turn along the eastern margin of the Ecstall belt by a mafic gneiss (Figures 3 and 4). The protolith for this black and white banded gneiss is interpreted as a mafic volcanic package of Late Devonian age.

The geologic history of the Ecstall Greenstone Belt (Figure 4) is outlined in Alldrick *et al.* (this volume). At least four plutonic events post-date the middle to upper Devonian stratigraphic succession. An extensive suite of small, weakly deformed diorite stocks are scattered throughout the central Ecstall belt. One stock has yielded an Early Mississippian age, which may indicate the age for all these plugs. In addition to Paleozoic intrusions, two elongate plutonic bodies of Early Jurassic age, the Johnston Lake and the Foch Lake tonalites, intrude the eastern part of the belt (Figure 3). The two bounding plutons, the mid-Cretaceous Ecstall on the west and the Paleocene Quottoon on the east, have associated dikes, sills and small stocks which cut the Ecstall belt rocks.

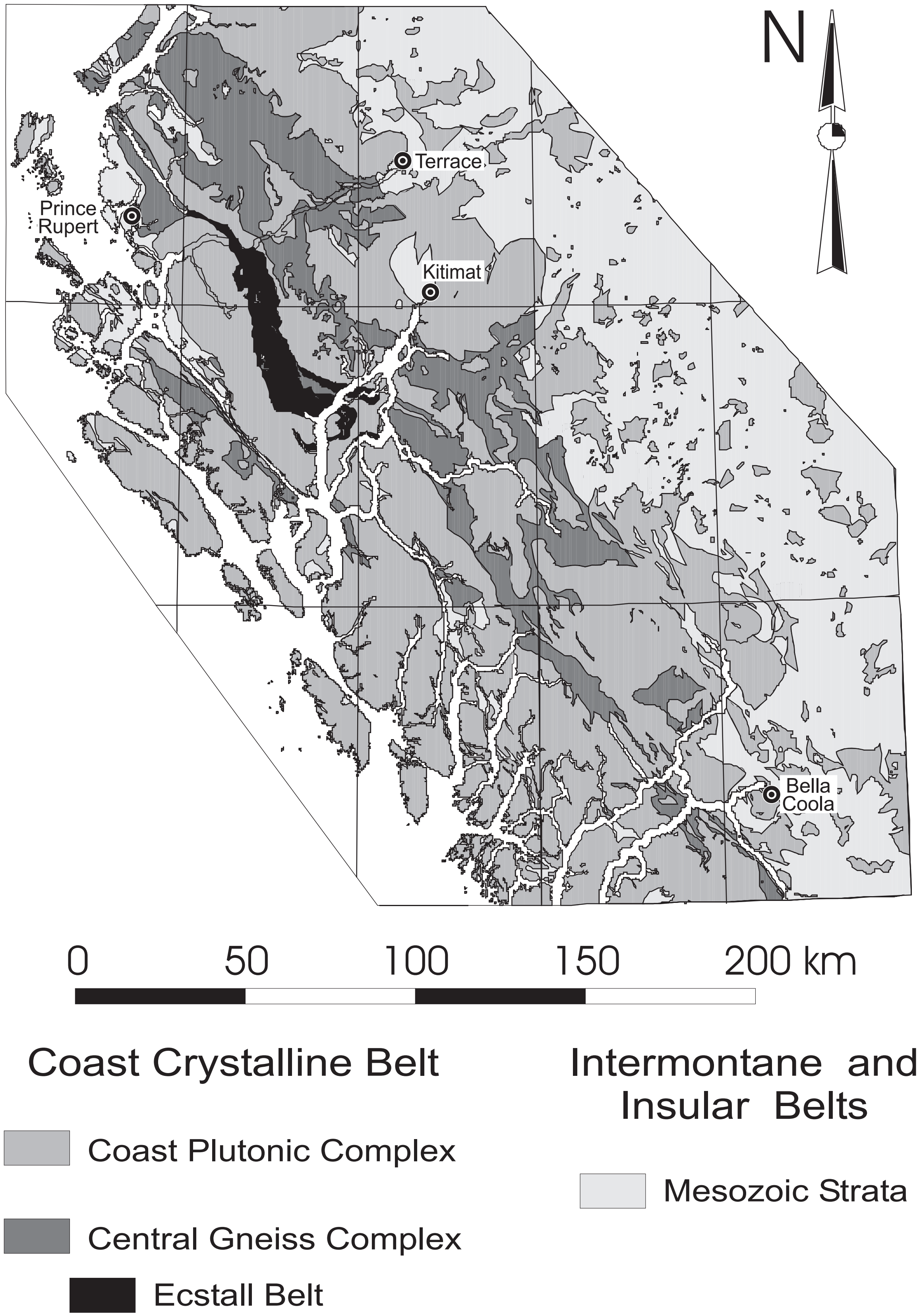

Figure 2. Geology of the mid-coast region of British Columbia, highlighting the location of the Ecstall metavolcanic belt within the Central Gneiss Complex and the Coast Plutonic Complex.

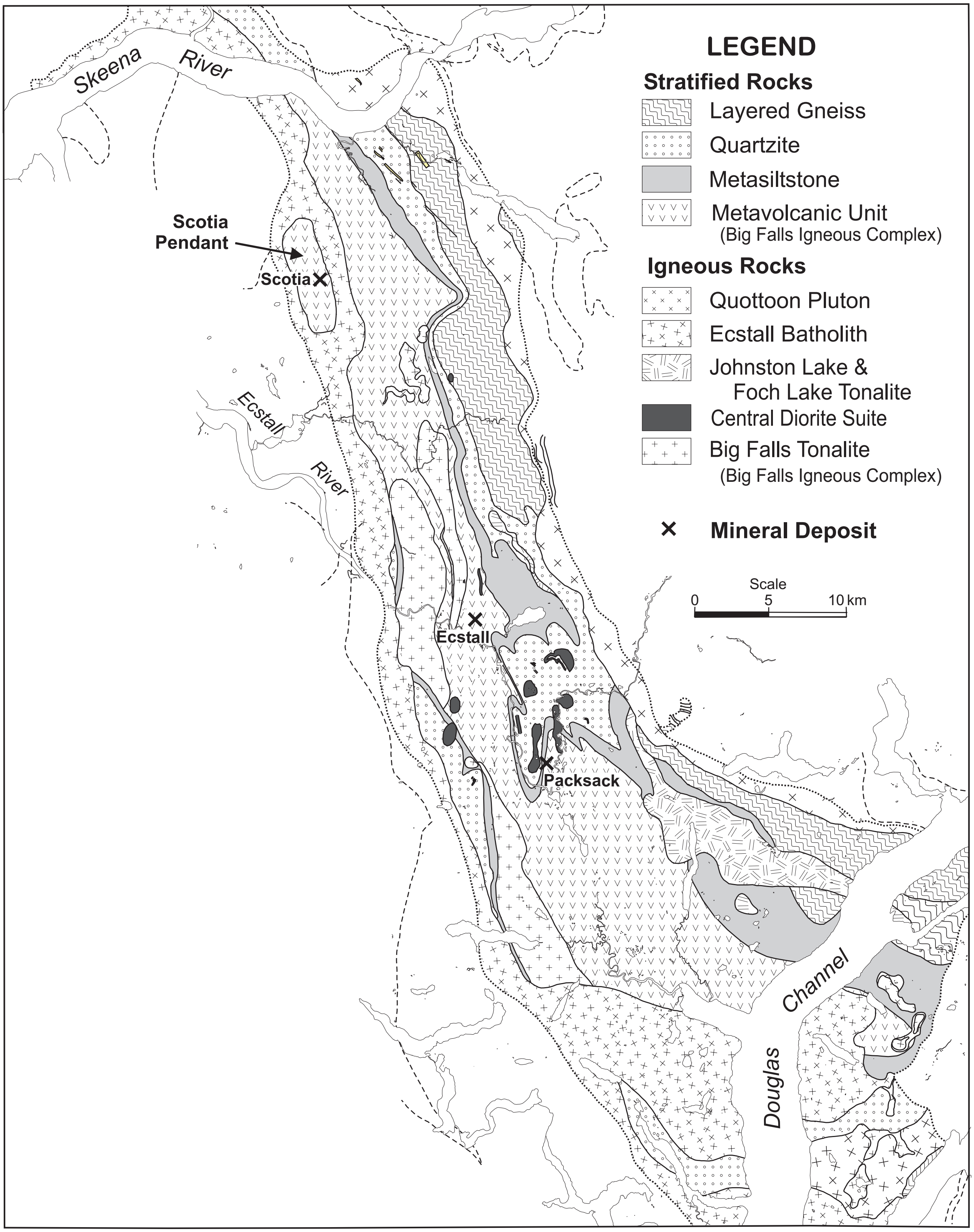

Figure 3. Simplified geology of the Ecstall belt (modified from Gareau, 1997) .

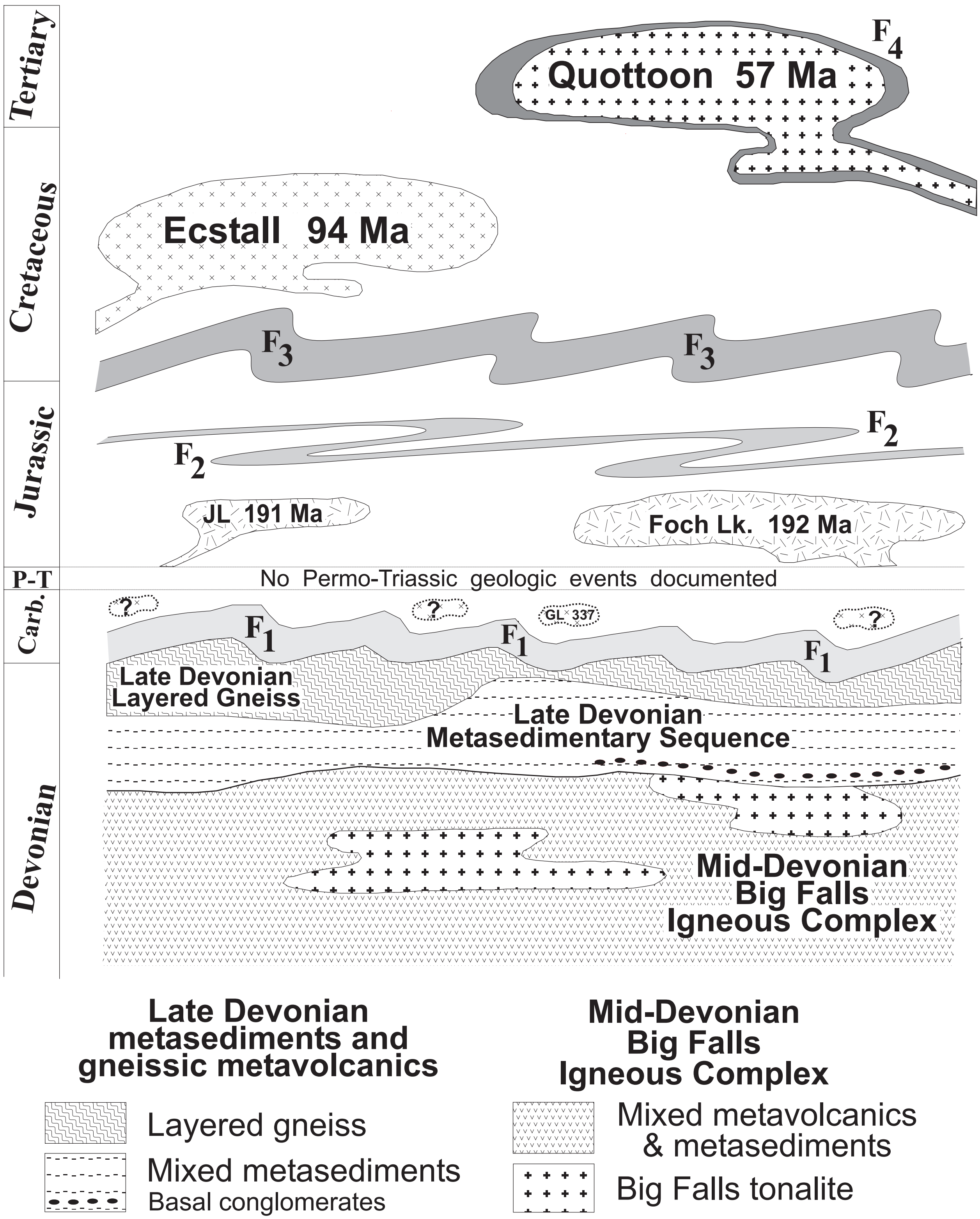

Figure 4. Schematic stratigraphy and geologic history of the Ecstall belt.

Stratified Rocks

The regional stratigraphic components have been well established by Gareau (1991a,b,c and 1997) and are reviewed in Gareau and Woodsworth (2000) and Alldrick *et al.*, (this volume), however, the sense of stratigraphic tops is not resolved. The sense of `tops' used in this report is based on 1. the conspicuous absence of the extensive Big Falls tonalite intrusion within the widespread and locally adjacent stratigraphic units of metasiltstone and quartzite (e.g. Gareau, 1997) which suggests that the intrusion pre-dates the sedimentary rocks, and on 2. the abundant "granitoid" (tonalite) clasts within conglomeratic members of the metasiltstone unit (Gareau, 1991a and Gareau and Woodsworth, 2000, Figure 7b).

UNIT 1 - METAVOLCANIC ROCKS (BIG FALLS IGNEOUS COMPLEX)

The base of the stratigraphic sequence is the metavolcanic unit which consists mafic to intermediate to felsic metavolcanic and derived metasedimentary rocks. The unit has been isoclinally folded (Gareau, 1991a, p.46), consequently apparent stratigraphic thicknesses, which range from 1 to 10 kilometres, are at least double their original value. This sequence is the largest unit defined by Gareau (1997), and extends the entire length of the belt, averaging four kilometres in thickness. Metavolcanic rocks are in gradational contact with the Big Falls tonalite (map unit A) and have sharp, but interlayered contacts with metasedimentary rock units. Metavolcanic rocks of the Ecstall belt host all but 3 of the 38 mineral occurrences (Figure 5).

The metavolcanic unit is heterogeneous. Biotite schist, hornblende-biotite schist and semi-schist comprise 70% of the unit. Interlayered with these lithologies are lenses of pyrite-quartz-sericite schist up to 100 metres thick, as well as amphibolite, quartzite, metasiltstone and calcareous muscovite-biotite schist layers. These smaller lenses may extend along strike for several kilometres.

Manojlovic and Fournier (1987) studied volcanic rock chemistry on the Scotia property. They concluded that most rocks are subalkalic, ranging in composition from basalt to rhyolite. The majority of mafic to intermediate rocks were tholeiitic, felsic rocks were dominantly calc-alkalic.

U-Pb zircon ages for a felsic metavolcanic member of this unit, for a quartz diorite sill at the Ecstall deposit, and for the Big Falls tonalite, are identical within error limits (Alldrick *et al.*, this volume). These contemporaneous rocks are components of a Middle Devonian age intrusive-extrusive complex consisting of a suite of subvolcanic, synvolcanic stocks and sills; coeval, comagmatic volcanic rocks; and associated sedimentary rocks. These comagmatic rocks and their locally derived, intercalated sedimentary rocks are informally referred to as the Big Falls Igneous Complex (Figure 4) to denote the rocks most important for the formation and preservation of volcanogenic massive sulphide deposits within the belt.

Unit 1a - Mafic Metavolcanics

Mafic metavolcanic rocks are preserved as strongly deformed pillow lavas and fragmental basalts, and as intensely foliated mafic schists or amphibolites. Subtle fragmental textures are preserved in some amphibolite outcrops. Hornblende-biotite schist is a black to greenish black recessive rock that is fissile and commonly highly weathered. It is the thickest of the metavolcanic units, averaging several hundred meters in thickness, and displays gradational boundaries with surrounding metavolcanic and metasedimentary lithologies. Also present within the mafic metavolcanics are lenses of resistant, homogeneous, black to rusty-coloured, garnet-hornblende amphibolite interlayered on a 5 to 20 metre scale.

Compositional layering is typically non-existent, or is very weak and defined by discontinuous millimetre-thick laminae. The rock contains more than 50% medium-grained biotite and 10% to 20% hornblende. Granular, fine to medium-grained plagioclase comprises up to 20% of the rock and is typically polygonal. Disseminated pyrite locally constitutes up to 5% of the rock and accessory skeletal garnet porphyroclasts are preserved. Euhedral titanite, that makes up to 10% of some thin sections, is a common mineral associated with sulphide grains. Titanite occurs as well defined layers, as radial masses cored by pyrite, or as interstitial clusters or individual grains. Epidote-hornblende knots or pods are common within this unit; when present these knots make up 5% to 15% of the rock. The schist locally displays discontinuous, orange, medium-grained, calcareous lenses that are highly recessive.

The abundance of hornblende and biotite and the lack of quartz is consistent with a mafic volcanic protolith. The lithologic heterogeneity observed in the unit suggests a highly dynamic depositional environment. Discontinuous carbonate lenses appear to be primary and are indicative of a subaqueous environment.

Unit 1b - Intermediate Metavolcanics

Gareau (1991a) concluded that hornblende-diopside-biotite-quartz-plagioclase semi-schist is the dominant lithology in the northern part of the Ecstall belt. Semi-schist is fine to medium-grained, granular, well indurated and weathers dark grey to black. This quartz-plagioclase rock has medium-grained biotite partings spaced 1 to 5 centimetres apart. Plagioclase and diopside microlithons have 5% to 10% interstitial biotite. Titanite occurs as euhedral interstitial grains making up less than 2% of the rock. Fine to medium-grained prismatic hornblende, ranging from 5% to 10% by volume, is concentrated along biotite parting surfaces.

The presence of biotite semi-schist members within the mafic metavolcanic schists marks a decrease in mafic minerals, and an increase in quartz from near zero to 10% to 20%. This mineral assemblage suggests that the protolith was a metamorphosed intermediate volcanic rock, or a volcaniclastic sedimentary rock.

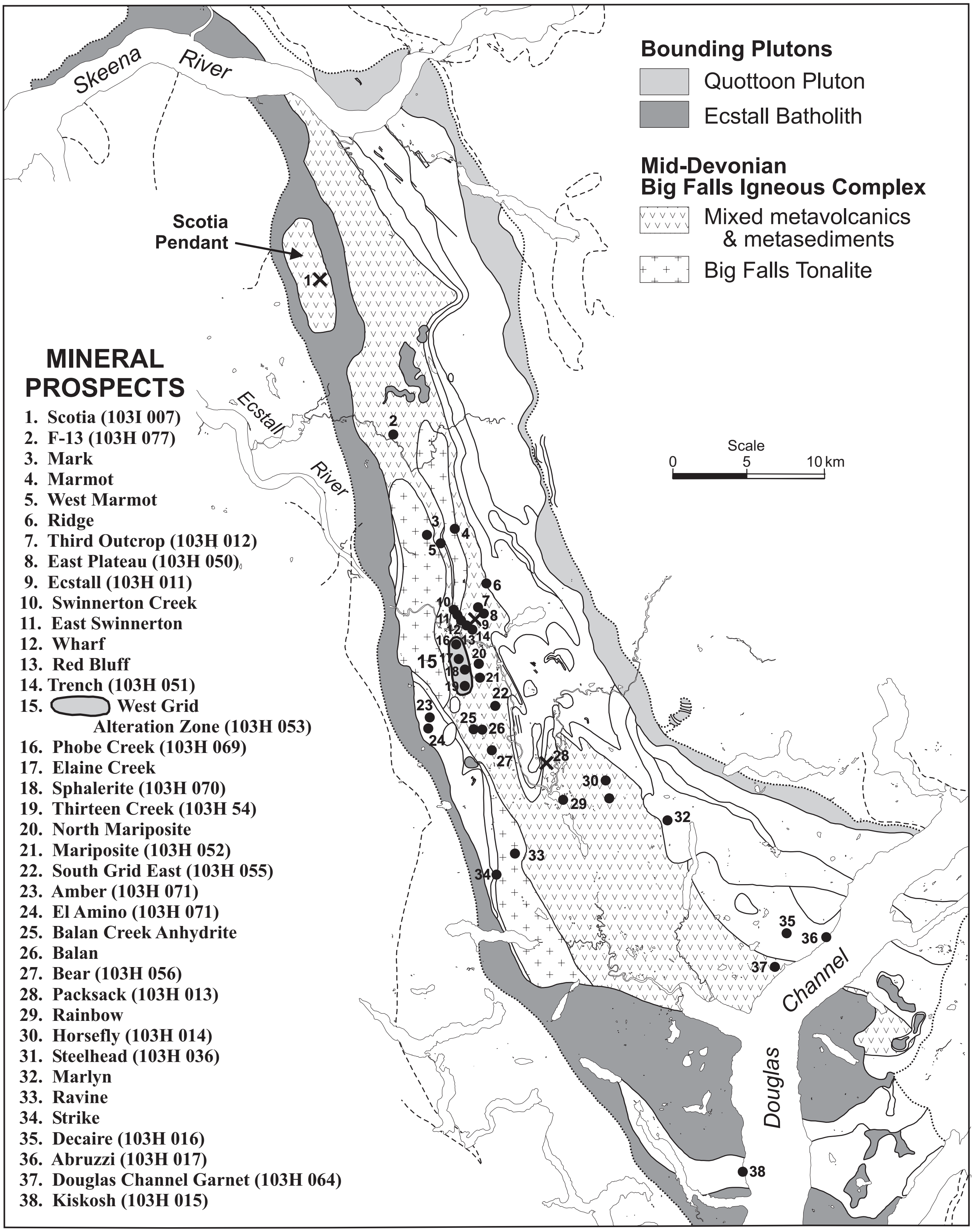

Figure 5. Mineral occurrences of the Ecstall belt (geology outlines modified from Gareau, 1997).

Unit 1c - Felsic Metavolcanics

These heterogeneous units are composed of pyritic quartz-sericite (muscovite) schist interlayered with 10 to 20 metre thick bands of muscovite-bearing quartzite and hornblende-biotite schist. Local thin units (1 to 5 metres) of thinly laminated (1 to 2 centimetres) quartz-rich rock that grades into the quartz-sericite schist are likely metamorphosed chert. Contacts with adjacent lithologies are typically sharp but may be gradational over half a metre to a metre.

Quartz-muscovite schist is a medium to coarse-grained rock with significant sulphides, containing on average 5% to 15% pyrite. These rocks also locally display relict clastic or fragmental volcanic textures. Primary compositional layering, on a 1 to 10 centimetre scale, is defined by alternating quartz and phyllosilicate layers. Pyrite seams or layers, up to 4 millimetres thick, are concordant with compositional layering and characterize the lithology. Subhedral garnet, with an average diameter of 5 millimetres, is commonly associated with the sulphides, as is biotite. Chlorite can be seen in handsample surrounding the garnet porphyroblasts. Quartz-rich metasediments associated with the felsic metavolcanic rocks are similar in composition to quartzites described below in Unit 2.

Pyritic quartz-sericite schists are interpreted as metamorphosed felsic volcanic flows, tuffs and fragmental rocks associated with subaqueous extrusion.

Unit 1d - Intercalated Metasedimentary Rocks

Minor metasedimentary members within the metavolcanic unit include metapelites, metasiltstones, granitoid-clast conglomerates, and rare chert or metaquartzite. South of Big Falls Creek, quartzite is interlayered with lenses of fine to very fine grained garnet-biotite-quartz schist. The gradational contact between the quartzite and schist is marked by quartz-rich rock with partings of medium-grained biotite and rare subhedral garnets ranging from 0.3 to 1.0 centimetres in diameter.

UNIT 2 - METASEDIMENTARY ROCKS

The Big Falls igneous complex is overlain by a regionally extensive package of metasedimentary rocks, consisting of a lower metasiltstone (metapelitic) unit and an upper quartzite unit.

Unit 2a - Metasiltstone

The volcanic succession is overlain regionally by a metasiltstone unit of medium to dark grey to black metapelite to metasiltstone to metaquartzite that is locally pyritic. This is the "metasedimentary unit" of Gareau (1991a) and the "metaclastic unit" of Gareau and Woodsworth (2000, p.27). The hornblende-biotite-quartz-feldspar-epidote rock has a mafic mineral content ranging from 20% to 70% (Gareau, 1991a). Rare intervals with fine disseminated magnetite grains have been noted. The thickness of this unit ranges from 100 metres near the Packsack deposit to over 5 kilometres along Douglas Channel; much of this increase is due to structural thickening near the axis of a regional scale fold in the Douglas Channel-Hawkesbury Island area. Gareau (1991a, p.10-13) describes contacts between the metasiltstone unit and the metavolcanics ranging from gradational to sharp.

This unit is significant in the regional stratigraphic construction because no dikes, sills or stocks correlated with the Big Falls magmatic complex have been identified within it, although younger intrusive rocks are common within this unit. Also, this unit includes repeated, extensive, granitoid clast conglomerate members (Gareau, 1991a). Clasts average 10 centimetres in diameter and typically make up 10% of the rock. Gareau (1991a) reports an exposure of conglomerate on the ridgecrest north of Johnston Lake that is 300 metres thick. Mafic mineral content of the granitoid clasts ranges from 20% to 70%, and K-feldspar is absent, indicating a tonalite composition.

Unit 2b - Quartzite

The black metapelite unit is overlain regionally by an extensive unit of quartzite (metasandstone). This white to light grey, well-laminated rock resembles thin-bedded sandstone, but the thin micaceous partings, rhythmic spaced at 5 to 10 centimetre intervals, are interpreted as a metamorphic effect. Minor associated lithologies include dark grey to black metapelite, black phyllite, dark grey metasiltstone and rare marble. Thickness of this unit ranges from 600 metres near Gareau Lake to more than 7 kilometres around the upper Ecstall River where the unit has been structurally thickened.

Gareau (1991a) describes the contact between this unit and the underlying metasiltstone unit as gradational over a 20 to 100 metre interval. Along the eastern margin of the Ecstall belt, the unit is in contact with a black and white layered gneiss, Gareau (1991a, p.14-15) describes the contact between these units as sharp to gradational over an interval of 500 metres.

Like the subjacent metasiltstone unit, this quartzite unit is an important component in the regional stratigraphic construction because no dikes, sills or stocks correlated with the Big Falls magmatic complex have been identified within it.

The quartzite unit consists predominantly of muscovite-bearing quartzite, but also includes minor units of metasiltsone. Quartzite contains greater than 95% quartz and is very well indurated, resistant, homogeneous, light to medium grey, and fine to very fine grained. The rock typically weathers light grey, but is rusty red when pyrite is present. The map unit is described as a "white to grey, locally pyritic quartzite, interlayered with lesser amounts of biotite-hornblende gneiss, fissile mica schist, black phyllite to meta-argillite, semi-pelite to pelite and marble… The unit locally contains lenses of matrix-supported conglomerate composed of stretched metatonalite and other granitoid cobbles with an aspect ratio of 10:2:1 or more. Finely laminated compositional layering is defined by light grey quartz-rich layers alternating with dark grey to black layers of quartz, biotite and graphite(?). Pyrite commonly occurs along partings as disseminations or semi-continuous laminae, not exceeding 5% of the rock." (Gareau, 1991a, p.14). The quartzite is a granoblastic rock; biotite is present in thin layers or partings less than 1 millimetre thick, or as minor interstitial grains. Accessory minerals are plagioclase, zoisite, cummingtonite, muscovite and carbonate. Gareau (1991a, p.14) concluded that these potassium and calcium-rich accessory minerals are consistent with a protolith of quartz arenite rather than chert.

UNIT 3 - LAYERED GNEISS

Gareau (1991a,b,c and 1997) defined a major stratigraphic unit of layered gneiss (Figure 3) along the eastern edge of the Ecstall belt, lying between the regionally extensive quartzites (map unit 2b) and the Quottoon pluton (map unit E). The metamorphic grade here is higher than the rest of the belt and lies within the upper amphibolite to granulite range (Gareau, 1991a).

The layered gneiss is interpreted as a metavolcanic rock (Gareau, 1991a). The protolith to this gneiss might be a repeated fold limb of the metavolcanic sequence of the Big Fall igneous complex (map unit 1), or a different, younger, mafic volcanic rock unit. Gareau and Woodsworth (2000) report a ~370 Ma U-Pb zircon age for this rock, which confirms that this unit is a younger volcanic package which stratigraphically overlies the quartzite unit (map unit 2b). The layered gneiss is the youngest (uppermost) stratigraphic unit preserved in the Ecstall Greenstone Belt (Alldrick *et al.*, this volume).

Intrusive Rocks

Five intrusive episodes are recorded in the rocks of the Ecstall belt (Figures 3 and 4). Two large, elongate, mid-Devonian plutons that are comagmatic with the host metavolcanic sequence and at least four plutonic suites post-date the mid to late Devonian stratigraphic succession. Small, weakly deformed diorite stocks are scattered throughout the central Ecstall belt. One stock has yielded an Early Mississippian age, which may indicate the age for all these plugs. In addition to Paleozoic intrusions, two elongate Early Jurassic plutons, the Johnston Lake and the Foch Lake tonalites, intrude the eastern part of the belt. Two bounding plutons, the mid-Cretaceous Ecstall on the west and the Paleocene Quottoon on the east, have associated dikes, sills and small stocks which cut the rocks of the Ecstall Greenstone Belt.

UNIT A - BIG FALLS TONALITE

Gareau (1997, *see* Figure 2) mapped out two large bodies of foliated tonalite, the Big Falls tonalite, which are enclosed mainly by the metavolcanic sequence of the Ecstall Greenstone Belt, and locally by the overlying metasiltstone unit. A sample from the eastern lens of this rock produced a U-Pb zircon age of 385 Ma, leading Gareau (1991a,b) to conclude that the tonalite bodies are coeval, synvolcanic, subvolcanic intrusions that fed the overlying volcanic pile. Recent global research into the geologic setting of VMS deposits has stressed the importance of subvolcanic plutons of tonalite/trondhjemite composition as the heat source which concentrates VMS deposits at the overlying paleosurface (Galley, 1996; Large *et al.*, 1996).

The Big Falls Tonalite is a Middle Devonian (385 Ma; Gareau, 1991a), foliated, medium to coarse-grained epidote-biotite-hornblende tonalite that crops out as two separate elongate plutons. The plutons have a maximum structural thickness of 3.5 kilometres. This homogeneous, resistant, light grey rock is in gradational contact with the surrounding metavolcanic unit. This contact zone is several hundred metres wide and characterized by decreasing grain size and increasing biotite content outward from the tonalite (Gareau, 1991a).

Textural variations range from weakly foliated to porphyroclastic to mylonitic. Gareau (1991a) reports gneissic zones tens of metres thick with 5 to 10 centimetre bands of alternating quartz-plagioclase and biotite-hornblende layers. Porphyroclastic tonalite consists of 0.5 to 1 centimetre diameter plagioclase porphyroclasts in a medium grey, fine to medium-grained matrix consisting of biotite, hornblende, quartz and plagioclase. Minor epidote pods and layers are common. Up to 2% garnet is locally present. A 20-metre-thick mylonite zone crops out south of Big Falls Creek. Within this zone, millimetre-scale plagioclase porphyroclasts are set in a very fine grained matrix.

The composition, homogeneity, and presence of clear, colourless, euhedral zircons led Gareau (1991a) to conclude that this is an intrusive rock. The gradational contacts, showing a progressive variation from medium to fine grain size, were interpreted as evidence of a large coeval subvolcanic pluton which fed the surrounding and overlying volcanic pile.

Childe (1997, p.225-228) analysed a sample of foliated quartz diorite sill that crops out just to the west of the North Lens of the Ecstall massive sulphide deposit (Alldrick *et al.*, this volume, and Schmidt, 1995). The U-Pb zircon age of 377 Ma provides a Late Devonian minimum age for the nearby, syngenetic sulphide deposit, and indicates that this sill is comagmatic with the two stocks of Big Falls tonalite.

UNIT B - THE CENTRAL DIORITE SUITE

An extensive suite of small, weakly deformed diorite stocks are scattered throughout the central Ecstall belt (Holyk *et al.*, 1958; Gareau, 1991c, 1997). One stock has yielded an Early Mississippian age, which may indicate the age for all these plugs. Gareau (1991a, p.21-22) describes a series of mafic and ultramafic stocks intruded through the central Ecstall belt, to which she ascribes a Jurassic or Cretaceous age. These rocks crop out in three main areas: as two stocks on Allaire Ridge, 10 kilometres south-southwest of Johnston Lake; as six small stocks scattered along Prospect Ridge, immediately west and uphill of the Packsack VMS deposit; and as a small body mapped on the peak of Red Gulch Mountain, 2.7 kilometres north-northeast of the Ecstall VMS deposit. These mafic rocks are dominantly diorites, but range in composition from quartz diorite to diorite to gabbro to hornblendite. The age of intrusion of all these rocks is unknown, although they must be younger that the quartzite host rock with a probable Late Devonian depositional age and older than the Early Cretaceous metamorphism. It is possible that these scattered clusters of weakly foliated mafic to ultramafic stocks are all comagmatic with the weakly foliated Gareau Lake diorite stock, described below, in which case they would have a mid-Mississippian age in the range of 337 Ma (Figure 4).

Unit B-1 - Gareau Lake Stock

Gareau (1991a, p.173-175) describes a small (<100 metres diameter) weakly foliated quartz diorite stock that intrudes the layered gneiss (map unit 3) on a ridgecrest 2 kilometres southeast of Gareau Lake. The rock is composed of 75% plagioclase, 10% quartz, 5% biotite and 3% hornblende with accessory titanite, apatite, zircon and opaque minerals. The U-Pb zircon age for this rock is 337 Ma (Gareau, 1991a). This date is consistent with intrusion into the 370 Ma layered gneiss host rock and indicates a mid-Mississippian magmatic episode of quartz diorite to diorite composition.

Unit B-2 - Allaire Ridge Mafic Complex

A large, irregular, mafic complex [JKum] is outlined on Gareau's map (1997) along the north-trending ridgecrest at the head of Allaire Creek, 5 kilometres to 9 kilometres south of the Ecstall deposit. Detailed mapping this season shows that this intrusion consists of two separate, but adjacent stocks that intrude metasedimentary rocks in the south and metavolcanic rocks in the north. The intrusive rock is resistant and underlies three prominent peaks along the ridgecrests. Two main phases are mapped: medium to coarse-grained diorite and very coarse grained hornblendite. At the 1242-metre peak at the northern edge of the northern stock, coarse-grained diorite is intruded in turn by tonalite of the Ecstall batholith, forming extensive intrusion breccias.

Diorite is medium to coarse-grained, and only weakly foliated. Massive hornblendite (hornblende gabbro) intrudes metasiltstone (map unit 2a) and quartzite (map unit 2b). The fresh rock is black and weathers rusty brown. Hornblendite is medium to very coarse grained, with hornblende (var. pargasite) crystals ranging up to 1.4 centimetres diameter. Metasediments within 1 to 2 metres of the intrusive contact are buckled, and screens of quartzite are incorporated near the margin of the intrusion. This intrusive phase was mapped across a 100 metre wide exposure along the ridgecrest, where it forms a prominent resistant spire. Gareau sampled this coarse-grained hornblendite for a K-Ar analysis, and interpreted the 115 Ma K-Ar age as a thermally reset date due to early to mid-Cretaceous regional metamorphism.

Unit B-3 - Prospect Ridge Diorite

West and uphill from the Packsack prospect, six small diorite stocks have been mapped along the crest and flanks of Prospect Ridge by Padgham (1958), Holyk *et al.* (1958), Delancey and Newell (1973), Maxwell and Bradish (1987b), Payne (1990c) and Gareau (1991c and 1997).

Unit B-4 - Red Gulch Mountain Diorite

Holyk *et al.* (1958) and Gareau (1997) show a small hornblende diorite stock at the peak of Red Gulch Mountain, 2.7 kilometres north-northeast of the North Lens of the Ecstall deposit. This resistant igneous rock underlies the prominent peak.

UNIT C - FOCH LAKE STOCK AND JOHNSTON LAKE STOCK

Gareau (1991a) identified two large, elongate Early Jurassic age intrusions emplaced along the eastern margin of the Ecstall belt. These plutons are both weakly to strongly foliated tonalite, but one is medium-grained and equigranular while the other is plagioclase megacrystic. The northern, equigranular Johnston Lake pluton yielded U-Pb zircon ages of 193 Ma and 190 Ma (Gareau, 1991a). The southern, coarsely porphyritic, Foch Lake stock yielded a U-Pb zircon age of 192 Ma (Gareau, 1991a). These plutons suggest that the Ecstall belt strata were associated with Stikine Terrane before the Early Jurassic time (Gareau and Woodsworth, 2000, p.39-40).

UNIT D - ECSTALL PLUTON

The Ecstall pluton is the largest of a series of magmatic-epidote-bearing plutons (Zen and Hammarstrom, 1984; Zen, 1985) in the western Cordillera called the Ecstall Suite (Woodsworth *et al.*, 1992, p.518-519). Regionally, the Ecstall suite includes diorite, tonalite and granodiorite phases (Gareau, 1991a). Along the western margin of the map area (Figure 3), the early Late Cretaceous Ecstall pluton is biotite-hornblende diorite to quartz diorite to tonalite. Age determinations span 98 Ma to 64 Ma, with the six most recent analyses averaging 93.5 Ma (unpublished data from van der Heyden, 1991, cited in Gareau, 1991a, p.161-164).

The rock is massive to moderately foliated, medium to coarse-grained, and weathers to a black and white, granular-textured surface. Foliation is defined by preferentially oriented biotite and hornblende. The rock is commonly equigranular, but locally displays plagioclase porphyroclasts. Hornblende-biotite-epidote tonalite ranges from light to medium grey on fresh surfaces. Grain size typically ranges from medium to coarse-grained equigranular, but local very coarse grained phases were noted. Foliation is generally more intense near the pluton margins. Primary layering (flow-banding or cumulate layering) was noted in one location. The pluton is highly sheared in places; mylonitic and pyritic shear zones were mapped this season. Cobble to boulder size mafic xenoliths are locally abundant. Screens of metasedimentary rock up to 40 metres wide are typically incorporated near the margins.

A distinctive feature of the Ecstall pluton is the presence of magmatic epidote, which increases in abundance from the margins to the centre of the intrusion. Within 200 metres of the contact, no epidote is apparent; epidote becomes progressively more abundant moving into the pluton, appearing first in fractures, then as fine interstitial grains, finally as equigranular coarse grains making up to 5% of the rock volume. Prominent crystals and aggregates of magmatic epidote comprise 5% of the rock and are associated with knots of biotite. Dark grey to black mafic schlieren are common and parallel the foliation within the rock. Medium-grained, euhedral, transparent titanite is also present. Contacts are sharp and discordant to the foliation. The eastern contact of the pluton is also discordant to the regional trend of map units. No chilled margin or contact metamorphic aureole was noted.

Along the southwest edge of the Ecstall Greenstone Belt, a porphyritic phase of the Ecstall pluton, crops out as a satellite pluton, roughly 1 kilometre in diameter, and consists of dark grey massive diorite(?) with an aphanitic groundmass and feldspar phenocrysts 3 to 4 millimetres across. Swarms of narrow pegmatite dikes concentrated along the western margin of the Ecstall belt are also likely components of the Ecstall magmatic episode.

UNIT E - QUOTTOON PLUTON

The Quottoon pluton intrudes along the eastern margin of the Ecstall Greenstone Belt (Figure 3). It is a long narrow body that extends north through southeastern Alaska, where it is called the "foliated tonalite sill" (Brew and Ford, 1978; Gehrels *et al.*, 1991a). The Quottoon Pluton is a medium to coarse-grained hornblende quartz diorite to tonalite and is intensely foliated close to its contact with the gneissic rocks of the Ecstall belt. Age determinations from this extensive pluton span Late Cretaceous (80 Ma) to mid-Eocene (43 Ma) time (van der Heyden, 1989, p.158-160), with Gareau's (1991a, p.184-185) age of 57 Ma determined for a sample site closest to the present study area. This pluton is the focus of ongoing studies by the Keck Geology Consortium.

Gareau (1991a, p.182-184) reported a U-Pb zircon age of 59 Ma for an unfoliated pegmatite dike near the eastern edge of the belt, which indicates that the extensive swarm of pegmatite dikes that intrudes the eastern margin of the Ecstall belt is a component of the Quottoon magmatic episode.

Structure

The stratigraphic sequence has been isoclinally folded (Gareau, 1991a, p.46). Strata are exposed as a mirror-image sequence along the two margins of the belt (Gareau, 1997), although the layered gneiss (map unit 3) is missing along the western limb of the fold. The two plutons of Big Falls tonalite are likely repetitions of the same subvolcanic pluton duplicated by folding.

Rocks of the central Ecstall belt are highly deformed and characterized by north-striking, steeply dipping to vertical foliation defined by near-parallel compositional layering and cleavage. Detailed analyses of the structure of this belt are presented in Gareau (1991a) and Alldrick and Gallagher (2000). Coaxial, map-scale, upright, F_1 and F_2 isoclinal folds and upright to inclined F_3 open folds are identified (Alldrick and Gallagher, 2000). Mineral lineations and stretching lineations are steeply northwest to southeast plunging. The relative timing of thermal and dynamic metamorphic events deduced from analysis of textures, mineralogy and cross-cutting plutons are illustrated in Figure 4 and discussed in Alldrick *et al*., (this volume).

Metamorphism

Two metamorphic episodes have been documented; a peak regional prograde metamorphic event (M_1) and a much later regional retrograde metamorphic event (M_2). Gareau (1991a) demonstrated that peak metamorphic grades varied from lower amphibolite facies in the southwest part of the belt to granulite facies in the northeast part of the belt. In the central part of the Ecstall Belt, biotite, muscovite, garnet and kyanite are consistent with upper amphibolite facies metamorphism. No gneiss units were noted in the central part of the Ecstall belt, in sharp contrast to extensive gneiss units mapped further to the north (Alldrick and Gallagher, 2000) and the layered gneiss (map unit 3) mapped to the east (Gareau, 1997). Rocks are generally moderately to highly deformed, but local areas of relatively undeformed rocks are preserved. A 400-metre-long unit of pillow lava and adjacent pillow breccia were mapped south of Thirteen Creek cirque; Hassard *et al.* (Figure 6 in 1987b) report a similar exposure of pillow lava in the canyon of Red Gulch Creek, 1050 metres upstream from the north end of the North Lens, and Schmidt (1996a) reports graded beds, accretionary lapilli and bomb sags in outcrops near the Steelhead prospect.

Gareau (1991a) attributed a series of mid-Cretaceous K-Ar dates on hornblende from metavolcanic rocks, and metasedimentary rocks to thermal resetting by an early to mid-Cretaceous regional-scale metamorphic event. Still younger thermal resetting of the westernmost and easternmost samples in the transect were caused by the thermal envelopes of the Ecstall (94 Ma) and Quottoon (57 Ma) plutons respectively. A Paleocene metamorphic event is attributed to emplacement of the Quottoon pluton, which created metamorphic zircons and titanites. The metamorphic ages coincide well with U-Pb zircon ages of 57 Ma and 61 Ma that Gareau (1991a) obtained from a samples of the Quottoon pluton and a related dike.

MINERAL DEPOSITS OF THE ECSTALL BELT

The 36 sulphide mineral prospects and 2 industrial mineral occurrences in the Ecstall Greenstone Belt (Figure 5) are described below, drawing extensively on information from files provided by Atna Resources Inc., Bishop Resources Ltd. and Ecstall Mining Corporation. Reserves for three deposits are summarised in Table 2.

1. Scotia (103I 007)

The Scotia deposit was discovered in 1958 by Texasgulf Ltd. geologists during a regional exploration program (Delancey, 1978). The property has been explored intermittently until 1999. The Scotia massive sulphide deposit lies within the Scotia pendant, a 3.5 kilometre by 7.5 kilometre roof pendant of metavolcanics and metasediments within the Ecstall batholith (Figure 3). The roof pendant is separated from the Ecstall Greenstone Belt by a 1.0 to 1.5 kilometre wide band of medium to coarse-grained Ecstall diorite, but the Scotia pendant is likely composed entirely of the same mid-Devonian metavolcanic unit that forms the basal metavolcanic sequence of the Ecstall belt.

The location of the Scotia deposit within a roof pendant of the Ecstall batholith has isolated the sulphide deposit and its host strata from the early to mid-Cretaceous and Paleogene deformation that affected rocks throughout the main part of the Ecstall belt. Scotia pendant rocks do not show the pronounced vertical mineral lineations, vertical fold axes and vertically stretched clasts that characterize the rest of the belt (Alldrick and Gallagher, 2000; Schmidt, 1995a; Gareau 1991a). Consequently the deposit has a form and attitude unlike any other sulphide occurrence in the region.

The deposit crops out in a southeast-facing cliff at 825 to 850 metres elevation. The Main Zone is a rod-like mass that trends 340º into the ridge, but plunges down at 9º toward 160º. At surface the deposit has a pod-like core of massive mineralization almost 10 metres in diameter. Bands, pods and stringers trending 20º up-dip to the east-northeast and 20º to 30º down-dip to the west-southwest (Birkeland *et al.*,1998). The up-dip extensions tend to pinch out abruptly or continue as thin but high-grade sphalerite sheets up to 30 cm thick that decrease in size and intensity to the east. The down-dip extensions to the west usually grade into increasingly iron sulphide-rich disseminated mineralization. Low-grade zinc mineralization has been intersected in these lenses more than 100 metres down-dip from the Main Zone.

TABLE 2
RESERVES FOR SULPHIDE DEPOSITS IN THE ECSTALL BELT

PROPERTY	SIZE (mT)	Cu %	Pb %	Zn %	Ag g/T	Au g/T
Scotia	1,240,000	0.1	0.4	3.8	13.0	0.25
Ecstall	6,878,539	0.65		2.45	17.0	0.5
Packsack	2,700,000	0.5	0.01	0.2	34.0	0.3
TOTAL	10,818,539	0.5	0.05	2.1	20.8	0.4

The deposit has been explored by prospecting and by geological, geochemical and geophysical programs over the last 41 years. Five drilling programs have been completed, totaling 4,340 metres in 42 holes. A geological resource of 1.34 million tonnes grading 3.8% Zn, 0.4% Pb, 13 g/t Ag and 250 ppb Au has been calculated by Lindinger (*in* Birkeland, Lindinger and Sinnot, 1998), which includes a drill-indicated and probable resource within the Main Zone of 232,000 tonnes grading 12.0% Zn, 1.2% Pb, 0.2% Cu, 23 g/t Ag and 550 ppb Au. The Scotia deposit remains open up-plunge to the north-northwest and down-dip to the west-southwest.

The Scotia deposit has higher zinc, lead and gold contents and lower copper content than the other deposits in the Ecstall belt (Ecstall and Packsack). The Scotia deposit is also furthest from the coeval, mid-Devonian Big Falls tonalite. These patterns are similar to the zoning patterns and intrusive relationships described for distal VMS deposits of the Mount Read VMS belt of western Tasmania by Large *et al.* (1996).

Host rocks are a highly metamorphosed volcanic sequence intruded by a series of diorite and pegmatite dikes. Volcanic rocks range in composition from tholeiitic basalt and andesite to calc-alkaline dacite to rhyolite (Manojlovic and Fournier, 1987). Metamorphism reached upper amphibolite facies and most rocks are preserved as gneissic units, schists or semi-schists. Protoliths are identified as basalt, andesite, dacite and rhyolite, plus minor siltstone, chert, chert breccia, "exhalite" and quartz porphyry units (Birkeland *et al.*, 1998). Fragmental textures can still be recognised in well-weathered outcrops of mafic volcanic rocks, now preserved as fine-grained amphibolite.

The Scotia deposit is the southwesternmost exposure of significant sulphides (> 2% pyrite) within the Scotia pendant. This season, several north-northwest striking horizons of pyritic quartz-sericite schist were mapped along the ridges to the north and east of the deposit. Some of these units have been previously sampled along the ridgecrests, but these prospective pyritic quartz-sericite schist units have not yet been investigated along the intervening slopes, valleys and creek drainages.

2. F-13 (103H 077)

The F-13 showing is exposed alongside a logging road on the north bank of Big Falls Creek. The roadcut transects a 300 metre thick section of rusty, weakly pyritic quartz-sericite schist that is interpreted as the metamorphic equivalent of a felsic tuff. Adjacent strata are hornblende-biotite-plagioclase schists that are interpreted as intermediate to mafic tuffs. Within the quartz-sericite schist unit, a 50-metre-thick strongly gossanous zone hosts increased (5% to 8%) disseminated pyrite, and four semi-massive and massive sulphide bands between 0.4 to 2.0 m thick. A 0.7-metre-thick band of semi-massive to massive sulphides is composed of granular pyrite with minor black sphalerite and trace chalcopyrite. A chip sample collected by the writer through this zone assayed 0.14% Cu, 166 ppm Zn and 17 ppb Au .

The exploration history of this prospect helps indicate the level of exploration coverage through the Ecstall belt. The showing as discovered on Friday, August 13, 1999 during follow-up of regional stream sediment and moss-mat survey anomalies. The prospect was located in an eight-year-old logging roadcut where it is exposed as a 50-metre-long highly gossanous band, now heavily overgrown by roadside brush. While this sequence of events demonstrates the effectiveness of stream sediment geochemistry, it also shows that logging roads in the area have not been routinely prospected.

3. Mark

The Mark prospect is 7 kilometres north-northwest of the Ecstall deposit. The showing crops out in a cirque at the head of an unnamed creek that drains northward into Big Falls Creek. This minor showing of pyritic quartz-sericite-chlorite schist is 50 metres thick and can be traced for 800 metres along strike (Graf, 1981c, p.19-20). Malachite was noted in all outcrops. The best assay values are 0.14% Cu, 0.01% Pb, 0.02% Zn, 0.06 opt Ag and 0.002 opt Au (Graf, 1981c).

4. Marmot

Marmot is exposed on a ridgecrest and on the adjacent south-facing slope, 7 kilometres north of the Ecstall deposit and along the linear trend of Red Gulch. In detail, the Marmot showing lines up along strike with the quartz-sericite schist horizon that hosts the Third Outcrop prospect (7).The Marmot prospect consists of rusty-weathering pyritic quartz-sericite schist; host rocks are chlorite schists (Graf, 1981c, p.20). Soil and stream sediment samples collected in the area of this occurrence are moderately anomalous in copper, lead and zinc. The best assay obtained for the showing was 0.006% Cu, 0.01% Pb, 0.02% Zn, 0.01 opt Ag and 0.002 opt Au (Graf, 1981c).

5. West Marmot

West Marmot crops out 2 kilometres southwest of the Marmot prospect, along the same high ridgecrest. No rock descriptions or assays are reported for this large rusty scree zone.

6. Ridge

The Northern Pyrites Limited prospecting map (Mason, 1937c) shows a short, narrow, north-northwest-trending gossanous alteration zone on the ridgecrest 500 metres east of the peak of Red Gulch Mountain.

7. Third Outcrop (103H 012)

This prospect lies 900 metres north-northeast of the northern end of the North Lens of the Ecstall deposit (9). The showing was discovered during the exploration program of 1919 (MacDonald, 1920, p.3) by searching for the source rocks of an iron-oxide cemented talus pile that had come to rest in Red Gulch Creek. The prospect crops out 60 metres east and uphill of Red Gulch Creek, exposed in a minor west-draining creek gully. A lens of massive pyrite, 30 metres long and 1.5 to 2.0 metres thick, is hosted in pyritic quartz-sericite schist (Hassard *et al.*, 1987b, p. 24-26 and Figure 6). A 1952 drill program completed 13 short holes; best assays obtained were 0.63% Cu and 2.3% Zn over 5.18 metres. The immediate hangingwall (east side) rock is a 30-centimetre-thick chert unit. The northward continuation of this zone crops out 150 metres to the north-northwest in Red Gulch Creek as a 10 centimetre-wide band of massive pyrite. The host pyritic quartz-sericite schist unit has been traced for another 1.4 kilometres to the north-northwest where it crops out as the Ridge prospect (6) along the crest of Red Gulch Ridge. The northward projection of this quartz-sericite schist horizon beyond Red Gulch Ridge coincides with the Marmot prospect (4).

8. East Plateau (103H 050)

This prospect crops out 930 metres northeast of the north end of the North Lens of the Ecstall deposit, at an elevation of 665 metres (Hassard *et al.*, 1987b, p.28 and Figure 6). Exposed in a west-southwest-draining creek, a one metre wide sericitic shear zone strikes sub-parallel to the Ecstall massive sulphide lenses and hosts 5% pyrite and trace disseminated sphalerite. A single grab sample assayed 0.184% Zn and 0.032% Cu (Hassard *et al.*, op. cit.). Host rocks to the pyrite-sericite schist are variable quartz-chlorite schists.

9. Ecstall (103H 011)

Seasoned gold prospector Charles Todd discovered the Ecstall massive sulphide deposit in 1890 (Flewin, 1924, p.209). His financial partner was J.N. MacKay, chief factor for the Hudson's Bay Company at Port Simpson. While no credit is given to local natives, Todd was the Indian Agent for northern British Columbia at the time of this discovery, and was likely guided to this remote, heavily overgrown site. One sample of Ecstall sulphides reached the Geological Survey of Canada laboratory in Ottawa in 1891 and is described by G.C. Hoffman (1892, p.67R) as:

"12. PYRITE. A crystalline, granular, massive, iron-pyrites, through which is disseminated a trifling amount of blende, occurs at the head of Eckstall Inlet, south of Port Essington, Skeena River, British Columbia, where it is said to constitute a vein fifteen feet wide, nearly vertical, running in a north-easterly direction from the shore and traceable for nearly a mile. It has been examined by Mr. Johnston and found to contain a trace of gold and 0.350 of an ounce of silver to the ton of 2,000 lbs., likewise a trace of copper and a little zinc, but no nickel or cobalt."

Todd decided not to stake the Ecstall showing, presumably reflecting his interest in gold prospects.

The Ecstall deposit remained open for 10 years and was finally staked for the first time in April, 1900 by prospector Henry Prevost for William Edgar Oliver of Victoria. The four initial claims, Bell-Helen, Bluestone, Red Bluff and Red Gulch were sold to John Bryden that same year (Flewin, 1901, p.788-789), and the claims were crown-granted in 1902. Table 3 summarizes the exploration history at the Ecstall deposit.

The geology at the Ecstall deposit has been described in reports by Schmidt (1995a), Hassard *et al.* (1987b), Douglas (1953), Bacon (1952), Holyk (1952a) and MacDonald (1918, 1927) and is illustrated in maps by Schmidt (Figure 4 in 1995a), Hassard *et al.* (Figure 6 in 1987b), Bacon (1952, p.A83) and Holyk (1952b,c).

The Ecstall deposit is best exposed in a spectacular outcrop in the floor of a narrow canyon (Figure 6). The floodwaters of Red Gulch Creek have exposed a continuous outcrop of faintly laminated, medium to coarse-grained pyrite over a 25 metre by 90 metre area on the east side of the creek, 1.5 kilometres upstream from the Ecstall River. This is the northernmost outcrop of the deposit which consists of two en echelon sulphide lenses, the North Lens and South Lens. These two lenses are exposed discontinuously for 570 metres along the banks of Red Gulch Creek. The two deposits strike north, dip 80º E and plunge 70º to the south. The North Lens is considerably larger and reaches a maximum width of 37 metres near its northern end. The North Lens has been completely delineated by drilling, but the South Lens remains open to the south and to depth at its southern end.

Both lenses are composed of medium to coarse-grained granular pyrite with trace to minor sphalerite and chalcopyrite, and rare galena and pyrrhotite. The sulphides are cemented by about 5% calcite-quartz-sericite gangue. This less resistant gangue material preferentially weathers out, freeing the sulphide grains. Consequently, outcrops of the Ecstall deposit massive sulphides have not formed major gossans; sections of the North Lens exposed along the creek are blanketed by bright pyrite sand banks and similar accumulations of pyrite sand have been built up by back eddies all the way down Red Gulch Creek.

The two massive sulphide lenses are enveloped by a one to two metre thick zone of quartz-muscovite/sericite schist. Schmidt (1995a, p.9) documented that footwall strata west of the South Lens and hangingwall strata east of the North Lens are mirror-image sequences consisting of quartz-muscovite schist, quartz-muscovite-biotite gneiss, quartz-chlorite schist and a unit of interlayered muscovite and chlorite schists. He concluded that the two main lenses of the Ecstall deposit lie in opposite limbs of a tightly-folded antiform. Douglas (1953a) noted that the lenses diverge at depth. The fold axis is near-horizontal and located above the present erosion surface. A distinctive sill-like body of foliated hornblende-quartz-feldspar quartz-diorite rock intrudes the hanging wall strata; Childe (1997, p.222-227) obtained a U-Pb age of 377 +9/-4 Ma from this rock, within analytical error of Gareau's U-Pb age of 385 +/- 4 Ma for the Big Falls tonalite, suggesting that the two foliated intrusions are comagmatic.

Base-metal sulphides show zonal distributions within the deposit. Sphalerite content increases in a narrow zone along the eastern (hangingwall) contact of the North Lens. Chalcopyrite is significantly enriched along the footwall of the North Lens. The upper section of the South Lens (that is, elevations greater than 35 metres below sea level) has copper grades 3 times greater than the deeper section of the lens, but zinc content is constant throughout (Table 4).

In plan, the outline of the North Lens resembles a tadpole; the northern end of the deposit is consistently the thickest part at all levels. In long section the North Lens has the outline of an heraldic shield. The maximum di-

TABLE 3
HISTORY OF EXPLORATION AND DEVELOPMENT AT THE ECSTALL DEPOSIT

Year	Work Done	Company	DDH	Surface		Underground	
			Holes	Length (ft)	Length (m)	Length (ft)	Length (m)
1901		BC Pyrites Co.	1	68	20.7		
1901	Bulk Sample	BC Pyrites Co.					
1916	Drilling	Hinman	3	734	223.7		
1918	Drilling	Granby	14	3,647	1,111.6		
1919	Drilling	Granby	17	6,446	1,964.7		
1923	Drilling	Granby	?	?	?		
1937-40	Drilling	TGS	40			5964	1,817.8
1952	Drilling	TGS	23	1,378	420.0	8880	2,706.6
1966	Bulk Sample	TGS					
TOTALS			98		3,740.8		4,524.5

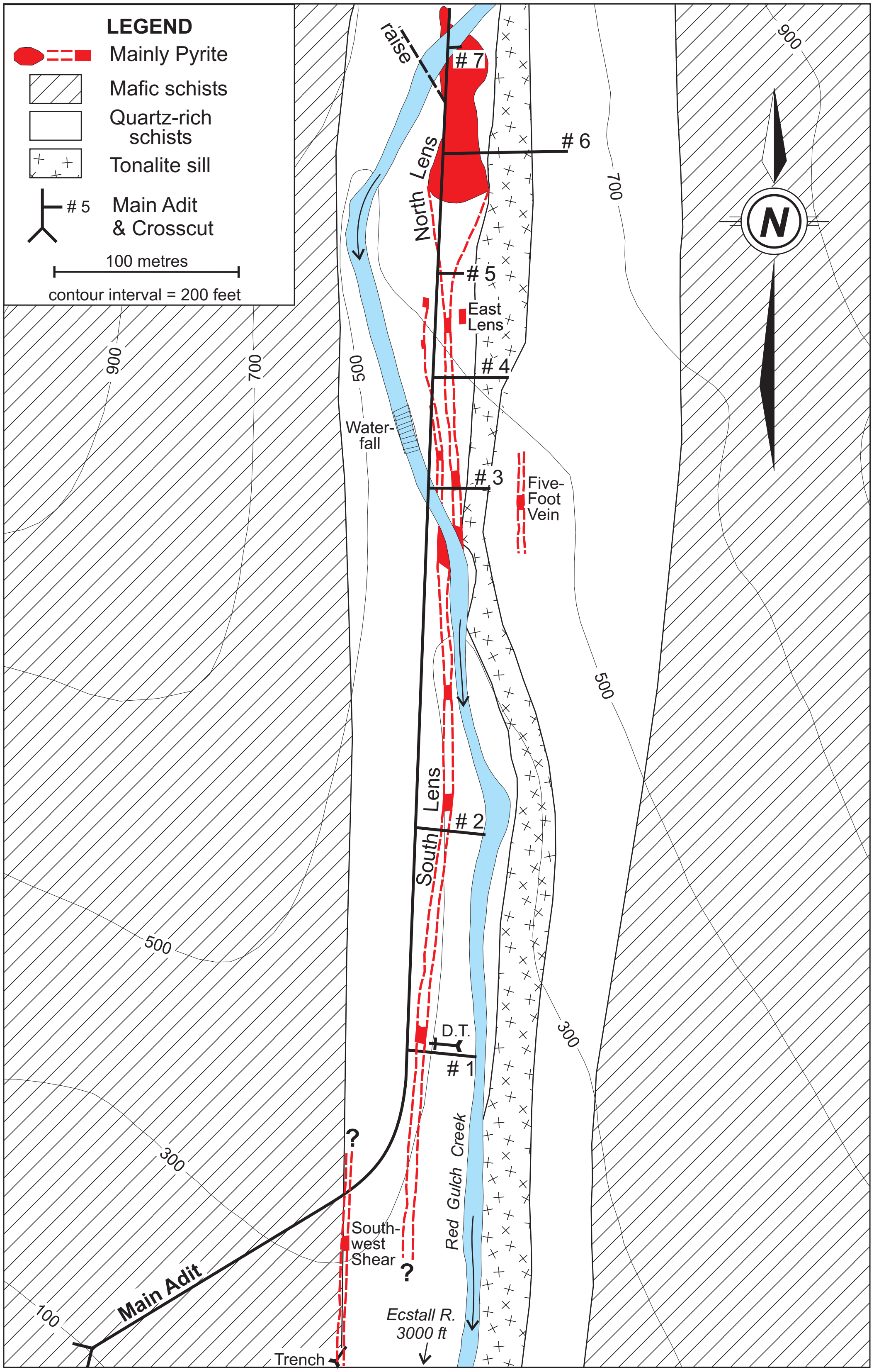

Figure 6. Geology of the Ecstall deposit (modified from Bacon, 1952).

TABLE 4
RESERVES AT THE ECSTALL DEPOSIT

Zone	Tons	Tonnes	% Cu	% Zn	% Pb	opt Ag	opt Au	Source
North Lens	3,400,000	3,084,140	0.80	2.00		0.5	0.015	Mason, 1961
North Lens	3,800,000	3,446,980	0.86	2.20	0.2	0.74	0.02	Gray, 1961
North Lens	3,030,000	2,748,513	0.80	2.00				Douglas, 1952
North Lens	3,240,000	2,939,004						Guernsey, 1936
North Lens	4,036,875	3,661,849	1.24			0.6	0.03	MacDonald, 1918
North Lens	3,843,475	3,486,416	0.86	2.20		0.74	0.02	MacDonald, 1920, 1927
North Lens Footwall	450,000	408,195	2.00			0.52	0.028	Gray, 1961
North Lens Footwall	339,100	307,598	1.91			0.5	0.028	Mason, 1940
North Lens Footwall	425,000	385,518	1.85			0.52	0.028	Mason, 1940
North Lens Footwall	623,200	565,305	1.89			0.8	0.03	MacDonald, 1920
North Lens Footwall	350,000	317,485	2.00			0.5	0.02	Peatfield, 1980
North Lens Footwall	412,500	374,179	2.79			1.2	0.05	MacDonald, 1918
South Lens	4,183,000	3,794,399	0.45	3.00		0.8	0.013	Mason, 1961
South Lens	4,756,000	4,314,168	0.44	2.95				Douglas, 1952
South Lens	3,900,000	3,537,690						Guernsey, 1936
South Lens	900,000	816,390	1.24			0.6	0.03	MacDonald, 1918
South Lens	1,000,000	907,100	0.50	2.90		0.6	0.01	MacDonald, 1920, 1927
Ecstall Deposit	4,843,475	4,393,516	0.79	2.30		0.71	0.02	MacDonald, 1920, 1927
Ecstall Deposit	7,140,000	6,476,694						Guernsey, 1936
Ecstall Deposit	7,786,000	7,062,681						Douglas, 1952
Ecstall Deposit	7,583,000	6,878,539	0.65	2.45				Mason, 1961
Ecstall Deposit	8,024,834	7,279,327	0.55	2.75		0.5	0.015	Tipple, 1958
Deposit: High Grade	4,883,000	4,429,369	0.85	2.20				Mason, 1940
Deposit: Lower Grade	2,700,000	2,449,170	0.30	2.90				Mason, 1940

mensions of this sulphide body are 333 metres long by 150 metres deep by 37 metres wide. The deposit has been drilled off, although potential still exists for separate lenses nearby. The western, footwall section of the North Lens includes a copper-rich zone of 385,000 tonnes grading 1.85% Cu, 18 g/t Ag and 1.0 g/t Au (Mason, 1940f and Table 4). A thin zinc-rich band has been identified along the eastern contact at the northern end of the lens. In 1940, five channel samples across the entire North Lens were collected from underground and analysed for 9 elements at the Texas Gulf Sulphur Company laboratory (Mason, 1940c); selenium analyses ranged from 40 ppm to 100 ppm. In the present study, four surface samples of North Lens sulphides were analysed for 39 elements; selenium concentrations ranged from 31 ppm to 108 ppm.

The South Lens is a thin sulphide slab. This lens thickens slightly below its surface exposure and the grade increases, then drops off again at depths below 35 metres below sea level. At its maximum, the South Lens measures 533.4 metres along strike and has a maximum thickness of 15.25 metres. It has been intersected in drilling at 293 metres below sea level, and no holes test the zone below this depth. In long section the South Lens resembles a parallelogram with one horizontal edge (along surface) and two roughly parallel edges plunging southward at 70 degrees. The South Lens remains open to depth at its southern end and to the south. The geological resource for the South Lens is 3.8 million tonnes at 0.44% Cu and 2.95% Zn (Douglas, 1952).

Two sulphide lenses lie just to the east and uphill of the North Lens. Both are small, but significant, because they indicate potential for additonal sulphide lenses to the east of the North Lens, perhaps stepped off in an en echelon pattern. Sixty-five metres north-northeast of the main waterfall in Red Gulch Creek, the East Lens crops out just 7 metres east of the North Lens, separated from it by a unit of black argillite (Figure 4 in Schmidt, 1995). Early geology maps depict the East Lens as one sulphide body, but Schmidt shows that the East Lens consists of two adjacent thin massive pyrite layers exposed in the canyon of a small creek that drains southwestward into Red Gulch Creek. The Five Foot Vein (Douglas, 1953, p.20-21) is another massive pyrite lens that lies east of the North Lens, 80 metres southeast of the main waterfall in Red Gulch Creek. It crops out at 160 metres elevation, in a small creek that drains into Red Gulch Creek at the southern end of the North Lens (Figure 4 in Schmidt, 1995a). A grab sample collected by Schmidt (sample US-E94-013 on Figure 5 in Schmidt, 1995a) assayed 1.38% Cu, 0.27% Zn, 54.5 g/t Ag and 280 ppb Au.

One massive sulphide lens has been identified on the west side of the deposit. The Southwest Shear (Douglas, 1953, p.21 and p.28) crops out uphill and to the west of the South Lens, 120 metres south-southwest of the portal of the Dunsmuir Tunnel, as a 25-centimetre-wide band of massive pyrite, hosted in quartz-sericite schist. Directly south, just north of the old mining camp and 140 metres east of the Main Adit portal, this horizon is exposed again in a large open cut near the base of the hill (Figure 6 in Hassard *et al.*, 1987b), where it is termed the Trench prospect (14). The sulphide layer is 10 centimetres wide in this location, again hosted in quartz-sericite schist, and a sample assayed 330 ppm Cu, 1200 ppm Zn, 46 ppm Pb, 4.5 ppm Ag and 70 ppb Au (Hassard *et al.*, 1987b, p.26). This same zone was intersected in the Main Adit, mid-way between the portal and the No. 1 crosscut, and was also intersected in underground drillholes 60 and 60a, drilled southward from the east end of the No.1

crosscut (Douglas, 1953). The Southwest Shear / Trench prospect is significant because it indicates good potential for a lens of massive sulphide mineralization en echelon to the southwest of the South Lens.

Further to the north and south of the Ecstall deposit, good potential for additional massive sulphide deposits along the Ecstall horizon is indicated by the Third Outcrop (7) and Marmot (4) prospects to the north, and by the North Mariposite (20) and Mariposite (21) prospects to the south.

The Ecstall deposit has been evaluated at different times as a possible source of pyrite (for sulphuric acid production), for copper and for zinc; consequently several reserve calculations have been completed (Table 4). The global resource for the deposit is 7,279,327 tonnes at 0.55% Cu, 2.75% Zn, 17 g/t Ag and 0.5 g/t Au (Tipple, 1958).

Nine diamond drill programs have been completed at the Ecstall deposit (Table 3). A total of 8265 metres of drilling have been completed in 98 surface and underground holes. The Ecstall deposit has been accessed from underground at five locations. In 1901, three short adits and a three-metre-deep shaft were completed (Flewin, 1902) . The Dunsmuir Tunnel, a 21-metre crosscut tunnel, was collared at 90 metres elevation, just below the southernmost outcrop of the South Lens. Track for a tramway was laid for 1006 metres from Dunsmuir tunnel to the wharf constructed on the north side of the Ecstall River. This adit allowed bulk sampling of the South Lens from two short (7 metres each) drifts blasted to the north and south of the main tunnel along the massive sulphide lens. During this same period, two short adits were collared at 145 and 155 metres elevation on the southern part of the North Lens, 20 metres east of the big waterfall in Red Gulch Creek (see Figure 4 in Schmidt, 1995a) and another short adit was collared into the base of the hillside at the campsite. The location of the 3-metre-deep shaft is unknown. The Main Adit system was developed between 1938 and 1940, collared at 37 metres elevation on the alluvial fan to the southwest of the deposit, west of the point where Red Gulch Creek emerges from its canyon. The underground workings total 1250 metres in length, consisting of a main drift (847 metres) along the footwall of the deposits, seven crosscuts (totaling 220 metres) off the main drift, one raise to surface (183 metres) at the north end of the drift, and three short exploration levels (drill stations) off this raise.

10. Swinnerton Creek

The Northern Pyrites Limited prospecting map (Mason, 1937c) shows a narrow, north-trending gossanous alteration zone 80 to 100 metres up the east bank of Swinnerton Creek, and 200 metres northeast of the mouth of Swinnerton Creek.

11. East Swinnerton

The Northern Pyrites Limited prospecting map (Mason, 1937c) shows a narrow, north-trending gossanous alteration zone 300 metres east of the mouth of Swinnerton Creek and parallel to and en echelon with the Swinnerton Creek showing (10).

12. Wharf

The Northern Pyrites Limited prospecting map (Mason, 1937c) shows a large, (300 metres wide, 650 metres long) gossanous alteration zone on the slopes just north of the Ecstall mine wharf (and one kilometre due west of the Ecstall North Lens). This zone trends east-northeast from a point 150 metres north of the Ecstall River to a point 800 metres from the river.

13. Red Bluff

The Northern Pyrites Limited prospecting map (Mason, 1937c) shows a short, narrow, north-trending gossanous alteration zone exposed in the east bank of Red Bluff Creek, 550 metres southwest of the large waterfall on Red Gulch Creek. This coincides exactly with the Red Bluff alteration zone mapped by Falconbridge (Figure 6 in Hassard *et al.*,1987b and p.26) and confirms the reliability of the earlier map. Falconbridge geologists describe the showing as a 10 centimetre wide band of massive pyrite in a 10 metre wide quartz-sericite schist unit, within a sequence of felsic to intermediate lapilli tuffs. A single sample (AB20730) of the massive sulphides assayed 2 ppm Cu, 51 ppm Zn and 40 ppb Au (Hassard *et al.*, op.cit.)

14. Trench (103H 051)

The Trench prospect crops out immediately southwest of the Ecstall South Lens (9). The showing is exposed by a large open cut near the base of the hill immediately north of the old mining camp, and 140 metres east of the Main Adit portal (Figure 6 in Hassard *et al.*, 1987b). In the exploration trench, quartz-sericite schist hosts a north-trending, 10 centimetre thick sulphide bed. A sample assayed 330 ppm Cu, 1200 ppm Zn, 46 ppm Pb, 4.5 ppm Ag and 70 ppb Au (Hassard *et al.*, 1987b, p.26).

This same thin massive sulphide bed crops out again uphill, directly to the north of this trench where it was termed the Southwest Shear (Douglas, 1953, p.21 and 28). This showing was investigated by a cluster of small prospecting pits to the west of the South Lens, 120 metres south-southwest of the portal of the Dunsmuir Tunnel, along the claim boundary between the Bluestone and the Red Gulch mineral claims. No assays are reported from these pits and outcrops. This same sulphide zone was intersected again in the Main Adit; mid-way between the portal and the No. 1 Crosscut is a 25 centimetre wide band of massive pyrite hosted in quartz-sericite schist (Douglas, 1953, Map Sheet 1). The Southwest Shear was also intersected in underground drillholes 60 and 60a, which were drilled southward from the east end of the

No.1 Crosscut (Douglas, 1953, p.21). The Trench / Southwest Shear prospect is significant because it indicates good potential for an en echelon lens of mineralization to the southwest of the South Lens.

15. West Grid Alteration Zone (103H 053)

The West Grid alteration zone encompasses a large area, including the whole of the basin of Thirteen Creek cirque, and extending as far north as Phobe Creek (Figure 5) (Figure 7 in Hassard *et al.*, 1987b and p.26-27). The entire West Grid area is also characterized by a broad alteration zone that extends from Phobe Creek to Thirteen Creek. Alteration consists of strong chloritization, sericitization and silicification over an area of 2.7 km^2 (Hassard *et al.*, 1987b, p. 21-22 and Figure 7). The alteration zone include four separate sulphide prospects: Phobe Creek (16), Elaine Creek (17), Sphalerite (18) and Thirteen Creek (19). Associated with the alteration is a unit of quartz-sericite schist up to 150 metres thick and characterized by chalcopyrite-malachite mineralization and anomalous copper-gold values up to 1.5% Cu and 310 ppb Au (Hassard *et al.*, 1987b). At Elaine Creek, the footwall (west side) chlorite schist is cut by numerous pyrite stringers which assay up to 0.87% Cu (Hassard *et al.*, 1987b). Several large boulders containing polymetallic sulphides have been identified scattered over the floor of the cirque, but the source of this float has not been located.

16. Phobe Creek (103H 069)

The Phobe Creek prospect was located during prospecting work in the early part of the century (Holyk *et al.*, 1958) This showing lies within the West Grid alteration zone (15) and is exposed along the banks of Phobe Creek at elevations ranging from 250 metres to 300 metres. Stringer and disseminated chalcopyrite occurrences are hosted in quartz-sericite-kyanite schist. This mineralization is similar in style and grade to the showings in Elaine Creek (17).

The disseminated chalcopyrite zone contains 5% disseminated chalcopyrite across a 6.5 metre wide band within the quartz-sericite-kyanite schist. A 7 metre composite chip sample across this mineralized band averaged 0.69% Cu, 66 ppm Zn, 2.22 ppm Ag and 251 ppb Au (Hassard *et al.*, 1987c, p.20-21 and Figure 7). The disseminated chalcopyrite zone is not well exposed and remains open along strike and to the west.

Stringers of chalcopyrite are scattered throughout the quartz-sericite-kyanite schist and adjacent mixed gneiss unit along Phobe Creek. Individual veinlets range from 1 to 3 centimetres wide and can be traced for a few metres. The best assays from grab samples are 6.56% Cu, 2041 ppm Zn, 19.1 ppm Ag, and 880 ppb Au (Hassard *et al.*, 1987c).

17. Elaine Creek

The Elaine Creek prospect lies within in the central area of the West Grid Alteration Zone (15) and consists of four separate showings well-exposed along the three main branches of Elaine Creek, and on the high ground mid-way between South Elaine Creek and Thirteen Creek. The Elaine Creek showings are very similar to the Phobe Creek (16) showings, and consist of chalcopyrite stringers and disseminated to blebby chalcopyrite, hosted by the quartz-sericite-kyanite schist unit (Hassard *et al.*, 1987c, p.19-20 and Figure 8). The numerous chalcopyrite veinlets are 1 to 3 centimetres wide and can be traced for a few metres. Grab samples from all four showings were averaged for each zone, and the best assays from these averaged samples ranged up to 3.04% Cu, 913 ppm Zn, 11.7 ppm Ag, and 1525 ppb Au (Hassard *et al.*, 1987c). The assays show a consistent pattern of increasing gold northward over the 800 metre distance between these showings.

18. Sphalerite (103H 070)

The Sphalerite showing lies within the West Grid Alteration Zone (15) and crops out at 465 metres elevation, 250 metres north of Thirteen Creek (Hassard *et al.*, 1987b, p.19 and Figure 8). A 4 centimetre thick layer of banded sphalerite is exposed in one small outcrop over a 2.2 metre strike length along the contact between quartz-chlorite-biotite schist and a marble unit. The immediate host rock is green, medium-grained calc-silicate rock. A grab sample assayed 6.0% Zn, 579 ppm Cu, 28 ppm Pb, 1.5 ppm Ag, 15 ppb Au and 746 ppm Cd (Hassard *et al.*, 1987b).

19. Thirteen Creek (103H 54)

The Thirteen Creek prospect lies within the West Grid Alteration Zone (15) and crops out on cliffs on the south side on the Thirteen Creek cirque at 640 metres elevation. The showing is a 30 centimetre wide chert bed which hosts pods of massive pyrite-chalcopyrite (Hassard *et al.*, 1987b, p.26 and Figure 7). The chert unit has been traced for 100 metres along strike. A grab sample assayed 8.05% Cu, 0.53% Zn, 350 g/t Ag and 2.4 g/t Au (Hassard *et al.*, 1987b).

20. North Mariposite

The North Mariposite prospect is the northward continuation of the Mariposite prospect (21) and hosts up to 50% pyrite in six separate units of bright green, pyritic, fuchsite-rich, quartz-sericite schist (Hassard *et al.*, 1987a, p.27-28 and Figures 7 and 8). One strongly pyritic sample, collected 1.2 kilometres north of Mariposite Lake, assayed 0.22% Zn. The quartz-sericite schist units of the Mariposite schist belt are exposed discontinuously for 3.5 kilometres between Allaire Creek and Thirteen Creek and are typically anomalous in zinc. In the area of the North Mariposite prospect, the formations display their thickest intervals, highest pyrite concentrations and best base metal grades.

21. Mariposite (103H 052)

The Mariposite showing trends south from Mariposite Lake, along Mariposite Creek to Allaire Creek, a distance of 1.75 kilometres. The prospect consists of a thick unit of bright green, pyritic quartz-mica semischist within a steeply dipping unit of charcoal to black, weakly pyritic metasiltsone. The thickness of individual units ranges up to 120 metres, and six separate units have been identified within the stratigraphic succession. Pyrite content of the quartz-mica schist typically ranges from 1% to 5%, but local concentrations up to 50% pyrite are exposed at the adjacent North Mariposite prospect (20). The bright green mica has been identified as the chromium-rich muscovite, fuchsite, by SEM-EDX analysis (McLeod, 1984a). This mica varies in abundance from 1% to 20% of the rock and averages 5%. Fuchsite is concentrated along foliation planes and is preferentially displayed along fracture surfaces. The probable protolith to this silica-rich schist has been identified as felsic tuff or a pyritic tuffaceous chert (exhalite).

The unit has been sampled in several shallow prospecting trenches. One drill hole, 86-MAR-1, completed by Falconbridge in 1986 at the Mariposite prospect intersected one unit of quartz-mica schist with a true thickness of 16 metres. Best assays from core samples are 290 ppm Cu, 1200 ppm Zn, 440 ppm Pb, 5.5 ppm Ag and 110 ppb Au (Hassard *et al.*, 1987a, p.27-28 and Figures 7 and 8). In comparison, drilling at the North Mariposite prospect intersected 6 intervals of quartz-sericite schist; however, the geologic setting differs at the Mariposite prospect where the western margin of the volcano-sedimentary succession is intruded by a large body of foliated diorite (variably mapped as amphibolite or pyroxenite).

22. South Grid East (103H 055)

The South Grid East quartz-sericite schist lies stratigraphically 350 metres east of the Mariposite quartz-sericite schist belt (20, 21 and 33), and crops out to the south of Allaire Creek. This unit is 20 to 90 metres thick, strikes 172º, dips 85ºE, and extends for 1.7 kilometres along strike from Allaire Creek to Balan Creek (Hassard *et al.*, 1987b, p.28 and Figure 8). Pyrite content ranges up to 30%. A grab sample assayed 0.12% Cu and 0.024% Zn (Hassard *et al.*, 1987b).

23. Amber (103H 071) and 24. El Amino (103H 071)

The El Amino (Frizzell) and the Amber prospects are hosted in metasedimentary rocks and are described in a separate report by Scott (this volume).

25. Balan Creek Anhydrite

The Falconbridge (1987c) geology map shows an anhydrite occurrence exposed at a bend of Balan Creek, 75 metres upstream from the Balan (26) showing.

26. Balan

The Falconbridge (1987c) geology map shows that the east-draining glacial valley of Balan Creek cuts through three horizons of pyritic quartz-sericite schist. These are 1. the Balan showing, 2. the continuation of the North Mariposite (20), Mariposite (21) and Ravine (33) prospects, and 3. the southern continuation of the South Grid East prospect (22).

27. Bear (103H 056)

The Bear prospect includes a series of parallel pyritic quartz-sericite schist horizons which lie along strike to the south of the South Grid East prospect (22). The felsic pyritic schist horizons range from a few centimetres to 25 metres thick and locally host massive to semi-massive sulphides (Maxwell and Bradish, 1987a, p.13). Country rocks are greywackes, well laminated siltstones, banded quartzite and argillite.

28. Packsack (103H 013)

The Packsack deposit crops out in five small exposures in two parallel east-draining creeks, at 230 metres elevation on the east slope of Prospect Ridge. The deposit was discovered by W. Padgham in September, 1957, as a single 4.5 metre wide massive sulphide band in Gunnysack Creek. Follow-up work revealed another four sulphide horizons distributed over a 25 metre interval along Packsack Creek, 150 metres to the south of Gunnysack Creek (Schmidt, 1996a,b).

The Packsack property has been repeatedly explored by prospecting and by geological, geochemical and geophysical programs over 40 years. The deposit was drilled in 1960 (11 holes) and again in 1990 (3 holes). Exploration trenches are conspicuous by their absence, but the sulphide deposit has been well-delineated by drill intersections and by EM surveys. Thirteen of the 14 drillholes intersected massive and semi-massive pyrite, and the deposit remains open to the north, south and at depth. Drilling has outlined two adjacent massive sulphide horizons, the Main and Hangingwall Zones, that range in true thickness from 2 to 8 metres. Both extend along strike for at least 500 metres. The geological resource at Packsack is 2.7 million tonnes at 0.5% Cu, 3.0% Zn, 0.01% Pb, 34 g/t Ag and 0.34 g/t Au (Graf, 1981c, p.23).

The sulphide lenses are hosted in pyritic quartz-sericite schist units that are interbedded with basaltic and andesitic tuffs and massive flows (Payne, 1990a). The pyritic quartz-sericite schists are interpreted and felsic ash tuffs and fragmental tuffs.

29. Rainbow

The Rainbow showing is located 250 metres east of Lower Ecstall Lake. The small outcrop knoll in this swampy area consists of north-trending, interlayered felsic and intermediate metavolcanics and two units of pyritic quartz-sericite schist. Noranda (1986c) evaluated the pyritic schist with two large east-trending exploration trenches. The highest assays obtained from 16 trench samples are 400 ppm Cu, 10 ppm Pb, 3100 ppm Zn and 1.8 ppm Ag (Noranda, 1986c). A sample of quartz vein exposed in the southwestern trench assayed 3.9 ppm Au.

30. Horsefly (103H 014)

The Horsefly prospect is located 4.5 km southeast of the Packsack deposit (28), high on the eastern slope above the upper reaches of the Ecstall River. The showing crops out at 685 metres elevation in three adjacent creeks over a distance of 100 metres, and the mineralized horizon is also exposed in a cliff-face 300 metres further to the south. Horsefly lies 1 kilometre north of, and along strike with, the Steelhead showing (31).

The prospect was discovered the Texas Gulf Sulphur Company Ltd. in 1960 during a regional exploration program following on from the discovery of the Packsack and Scotia deposits. Subsequently, the property was explored by a joint venture group in 1981, by Noranda Exploration in 1986, and by Atna Resources Ltd. in 1995. Five holes, totaling 652 metres, were drilled on the showing in October, 1995. The claims are owned by Ecstall Mining Corporation Ltd.

Local stratigraphy is a complex succession of mafic to intermediate to felsic volcaniclastic rocks and flows, and minor intercalated sedimentary units (Schmidt,1996a, p. 6-7). The showing consists of a 1 metre thick lens of massive pyrite with minor sphalerite, chalcopyrite and pyrrhotite hosted in a pyritic quartz-sericite schist unit that is 10 metres thick (Graf, 1981c, p.24). Siliceous argillite units adjacent to the host quartz-sericite schist are weakly pyritic and anomalous in zinc and lead. The best assay obtained from the discovery outcrops is 1.16% Cu, 0.13% Pb, 4.6% Zn, 39 g/t Ag and 0.5 g/t Au (Graf, 1981c). The drilling program outlined a blind, buried, 20 metre thick zone of disseminated and semi-massive sulphides, which is separate from the outcropping Horsefly prospect (Schmidt, 1996a, p.13). This zone is located 100 metres southeast of the Horsefly showing. It has been traced by drilling for 90 metres along strike and remains open in all directions. The best assay obtained from drill core was 2.75 metres of 1.69% copper; however, grades up to 5.6% copper, 1.65% Zn, 900 ppm Pb 30 ppm Ag and 860 ppb Au were obtained over narrower intervals of core (Schmidt, 1996a).

31. Steelhead (103H 036)

Located 1 kilometre south of the Horsefly (30) prospect, the Steelhead showing was discovered in 1986 during follow-up of Noranda Exploration's airborne EM survey. Investigation of the area around a series of strong ABEM anomalies outlined 3 pyritic quartz-sericite schist units hosting from 1% to 30% pyrite. In detail, these units consist of pyritic rhyolite, quartz-sericite schist and breccias (Schmidt, 1996a, p.8). Mineralization occurs as pods or patches of pyrite and pyrrhotite, with associated chalcopyrite and sphalerite. Some mineralization occurs in fragments within the breccias. As at the Horsefly prospect, the black siliceous argillite horizons in the Steelhead area are also mineralized with disseminated pyrite, pyrrhotite and rare chalcopyrite. Local geology consists of a succession of mafic to intermediate to felsic volcaniclastic rocks and flows, and minor intercalated sedimentary units (Schmidt, 1996a, p.6-7). Schmidt also reports (op. cit.) that fragmental rocks on the east side of the Steelhead grid have well-preserved primary textures - abundant lapilli and crystal fragments and rare bomb sags are evident. Numerous exposures of graded beds were also noted but textures were not clear enough to ascertain tops.

The best assays obtained from a series of grab samples were 1.65% Cu, 3.8% Zn, 5.8 g/t Ag and 120 ppb Au (Schmidt, 1996a). Three holes, totaling 424 metres, were drilled at Steelhead by Atna Resources Ltd. in September, 1995; the best intersection assayed 0.027% Cu, 1,276 ppm Pb, 362 ppm Zn, 13.8 ppm Ag and 24 ppb Au over 4.9 metres in an argillite unit hosting disseminated pyrrhotite and trace chalcopyrite (Schmidt, 1996a).

32. Marlyn

This showing lies 2.2 kilometres east of the Horsefly prospect (30), on the east-facing slope of Horsefly ridge. Rusty pyritic quartz-sericite schist assayed 0.005% Cu, 0.01% Pb, 0.05% Zn, 0.05 opt Ag and 0.002 opt Au (Graf, 1981c). Silt samples collected along the trend of this pyritic unit showed erratic, weakly anomalous copper and zinc values.

33. Ravine

A large semi-continuous gossanous zone trends north-northeast along this creek for 3.5 kilometres (Graf, 1981c). This marks the southern end of a prominent, narrow topographic depression that can be trace northward through exposures in Balan Creek to the Mariposite (21) and North Mariposite (20) zones.

34. Strike

This showing lies 6 kilometres west-southwest of Ecstall Lake. Two pyritic quartz-sericite schist units (up to 20 metres thick) and one pyritic argillite unit (50 metres thick) crop out in the area (Graf, 1981c, p.24-25). Only pyrite was noted in hand samples. The best assay from these exposures was 0.17% Cu, 0.27% Pb, 2.83% Zn, 1.13 opt Ag and 0.01 opt Au (Graf, 1981c). Stream sediment samples are moderately anomalous in copper and zinc over a distance of several thousand metres to the north of the showing.

35. Decaire (103H 016)

The Decaire lead-zinc prospect is located 1.5 kilometres north of Douglas Channel and 6 kilometres northeast of Kitkiata Inlet. The occurrence crops out on the easty side of the north fork of Koskeesh Creek at an elevation of 170 metres. This showing is a quartz vein which hosts minor cross-fractures of sphalerite, pyrite and minor galena. The quartz vein ranges from 2 to 4 metres wide over a 20 metre strike length, but the fracture-controlled sulphide mineralization is described as “very sparse” (Mandy, 1930, p.66). Two small prospecting pits were blasted in 1929. Early reports describe the quartz vein as hosted by silicified, foliated granite where the latter is cut by a lamprophyre dike; Gareau (1997) shows the occurrence within an area of extensive metasedimentary rocks.

36. Abruzzi (103H 017)

The Abruzzi showing is located along the north shore of Douglas Channel, 7.5 kilometres northeast of Kitkiata Inlet. This occurrence is hosted by a 10 metre wide zone of chlorite-altered mafic garnet-biotite-hornblende schist within a large lens of the mafic schist that is incorporated in granite (Mandy, 1929, p.70); Gareau (1997) shows this locality as an area of extensive metasedimentary rocks. The alteration zone, and the enclosing schist, strike 150º and dip 80º west. Mineralization consists of sparsely disseminated pyrrhotite and chalcopyrite, with local massive patches. Stringers of massive chalcopyrite, 0.5 to 4 centimetres wide are scattered across the chlorite-altered zone; the largest chalcopyrite vein is 23 centimetres wide and extends for 3 metres length. The mineralization has been explored along the shore by a shallow shaft and two open cuts, 10 metres apart. A 2.4-metre chip sample across the southern open cut assayed 1.4% Cu, 0.30 opt Ag and trace Au (Mandy, 1930, p.66).

37. Douglas Channel Garnet (103H 064)

Along this ridgecrest on the north side of Douglas Channel, biotite-garnet schists host up to 15% coarse garnet ranging up to 2.0 centimetres diameter.

38. Kiskosh (103H 015)

GSC map 278A (1933) plots a copper showing on the west shoreline of Douglas Channel, midway between Kiskosh Inlet and Kitkiata Inlet. This map also indicates that the showing is associated with schistose rocks, suggesting that the showing is likely hosted by the heterolithic “quartzite” unit of Gareau (1997). The most likely location for this showing is thus two kilometres north of the mouth of Kiskosh Inlet; that is, 2.5 kilometres south of the location shown on Gareau (1997).

EXPLORATION POTENTIAL

The three largest massive sulphide deposits in the belt (Table 2) are important indicators for the overall exploration potential in this belt. In the next two paragraphs, the size and grade of these 3 deposits are compared to typical grades and tonnages for this type of mineral deposit.

In a study of 878 volcanogenic massive sulphide deposits worldwide (Table 3 in Barrie and Hannington, 1997), the average size for VMS deposits associated with bimodal volcanic succession and hosted by felsic volcanic units is 5.2 million tonnes. The three deposits in the Ecstall belt are of this order of magnitude. Significantly, all three deposits crop out, and all have been eroded. Therefore the original VMS deposits at Scotia, Packsack and Ecstall must all have been substantially larger when deposited than they are today.

The grades of the Ecstall belt deposits should be carefully considered in assessing future exploration potential. A comprehensive tabulation (Table 2 in Leistel *et al.*, 1998) of the grades and tonnage of all the massive sulphide deposits in the Iberian Pyrite Belt shows that the median copper grade is 0.9% Cu, the median zinc grade is 2.0% Zn and the median deposit size is 2.75 million tonnes. These are similar to the average grade and size of the Ecstall Belt VMS deposits. The deposits of the Iberian Pyrite Belt have been in production for 5000 years. However, the richest deposit of the belt, the blind, deeply buried, Neves Corvo deposit, was discovered just 23 years ago, demonstrating the elusiveness - and the rewards - of high grade VMS orebodies within a volcanic belt characterized by lower grade deposits.

The 36 sulphide showings along the Ecstall Greenstone Belt (Figure 5) all crop out, suggesting that the potential for blind, buried deposits is high. The recent drill intersection of a blind, buried sulphide prospect adjacent to the Horsefly showing is proof of this potential.

DISCUSSION AND CONCLUSIONS

The Ecstall Greenstone Belt is a Middle to Late Devonian volcanosedimentary succession with a complex post-depositional history. The belt hosts 36 sulphide mineral prospects, primarily Kuroko-type polymetallic volcanogenic massive sulphide deposits. Deposits and prospects are hosted by felsic volcanic units within the differentiated mid-Devonian volcanosedimentary succession. Decades of industry mapping programs have traced out many favourable felsic units, as well as exhalative horizons and extensive stockwork-style mineralized zones.

Deposits are most abundant in the central section of the belt (Figure 5), but this may be an artifact of the concentration of prospecting efforts around the mining camp at the Ecstall deposit. Preliminary results of a new regional stream sediment geochemistry program (Jackaman *et al.*, this volume) suggest that base metal potential is evenly distributed along the 80 kilometre length of the belt.

The volcanic arc that evolved into the Ecstall Greenstone Belt developed close to a continental margin, similar to the setting envisaged for the extensive volcanosedimentary successions of the Yukon-Tanana and Nisling terranes.

ACKNOWLEDGMENTS

Fieldwork by geologist Brad Scott contributed to the success of the 2000 field season. Peter Delancey at Atna Resources Inc., Chris Graf at Ecstall Mining Corporation and Arne Birkeland of Arnex Resources Ltd. each arranged to share their comprehensive corporate files covering a century of exploration work in this region, and discussed ideas and areas deserving research. Mike Fournier, BCGS, prepared the figures with care.

BIBLIOGRAPHY

This list presents all reports and many maps relating to the geology and exploration history of the Ecstall Greenstone Belt. The list is available in three digital versions: 1. Standard reference list (below), 2. References sorted by property, 3. References sorted by type (reports, drill logs, maps, sections), which are available from the author or the ministry website.

Alldrick, D.J. and Gallagher, C.S. (2000): Geology and mineral potential of the Ecstall VMS belt (NTS 103H; 103 I); *B.C. Ministry of Energy and Mines*, Geological Fieldwork 1999, Paper 2000-1, p.249-265.

Alldrick, D.J. Friedman, R.M. and Childe, F.C. (2001): Age and geologic history of the Ecstall greenstone belt, northwest British Columbia; *B.C. Ministry of Energy and Mines*, Geological Fieldwork 2000, Paper 2001-1, this volume.

Atna Resources Ltd. (1995a): Geology of the Thirteen Creek Grid area; Figure 5a; Sheet 1, North sheet of 3 sheets, scale 1:2,000.

Atna Resources Ltd. (1995b): Geology of the Thirteen Creek Grid area; Figure 5b; Sheet 2, Central sheet of 3 sheets, scale 1:2,000.

Atna Resources Ltd. (1995c): Geology of the Thirteen Creek Grid area; Figure 5c; Sheet 3, South sheet of 3 sheets, scale 1:2,000.

Bacon, W.R. (1952): Ecstall (Sulgas Properties Ltd.) - Ecstall River; Annual Report of the Minister of Mines for 1952, p.A81-A84 and A87.

Bacon, W.R. (1957): Geology of Lower Jervis Inlet, British Columbia; British Columbia Department of Mines, Bulletin No. 39, 46p.

Bapty, H. (1966): Ecstall (Texas Gulf Sulphur Company) - Ecstall River; Annual Report of the Minister of Mines for 1966, p.54.

Barrie, C.T. and Hannington, M.D. (1999): Classification of volcanic-associated massive sulphide deposits based on host-rock composition; *in* Volcanic-associated massive sulphide deposits: processes and examples in modern and ancient settings, *Society of Economic Geologists*, Reviews in Economic Geology, v.8, p.1-11.

Barrie, C.T. and Hannington, M.D., editors (1999): Volcanic-associated massive sulphide deposits: processes and examples in modern and ancient settings; *Society of Economic Geologists*, Reviews in Economic Geology, v.8, 408p.

Birkeland A.O. (1994): Ecstall property exam; unpublished report for Inco Exploration Ltd., Feb. 1994, 12p. plus appendices

Birkeland, A.O. (1998): Scotia North claim block - Scotia River area; report for Bishop Resources Inc., 17p.

Birkeland, A.O. (1999): Rock and stream sediment geochemistry reconnaissance program on the Big, Scotia South and Ecstall North claim groups, south Scotia River area; report for Bishop Resources Inc., 44p., 4 appendixes.

Birkeland, A.O. Lindinger, L. and Sinnott, N. (1998): Diamond Drilling the Albere Zone, Scotia Prospect, Scotia River Area; report for Bishop Resources Inc., 45p. plus 3 appendixes, 6 tables, 51 figures - including 1 map, 8 long sections, 32 cross sections.

Bishop Resources Inc. (1997): Press Release; Dec. 5, 1997, 3p.

Bishop Resources Inc. (1998): Press Release in George Cross Newsletter; Jan. 12, 1998, 1p.

Boghossian, N.D. and Gehrels, G.E. (2000): Nd isotopic signature of metasedimentary pendants in the Coast Mountains between Prince Rupert and Bella Coola, British Columbia; *in* Tectonics of the Coast Mountains, southeastern Alaska and coastal British Columbia, *Geological Society of America*, Special Paper 343, p.77-87.

Brew, D.A. and Ford, A.B. (1978): Megalineament in southeastern Alaska marks southwest edge of Coast Range batholithic complex; Canadian Journal of Earth Sciences, v.15, p.1763-1772.

BCMEM AR (1939): Northern Pyrites Ltd. - Ecstall River; Annual Report of the Minister of Mines for 1939, p.A100.

BCMEM AR (1940): Northern Pyrites Ltd. - Ecstall River; Annual Report of the Minister of Mines for 1940, p.A86.

Childe, F.C. (1997): Timing and tectonic setting of volcanogenic massive sulphide deposits in British Columbia: constraints from U-Pb geochronology, radiogenic isotopes, and geochemistry; unpublished Ph.D. thesis, The University of British Columbia, 298p.

Clothier, G.A. (1918): Ecstall River - North-western District; Annual Report of the Minister of Mines for 1917, p.F45.

Clothier, G.A. (1919): North-western District; Annual Report of the Minister of Mines for 1918, p.K35.

Clothier, G.A. (1920): Ecstall River; Annual Report of the Minister of Mines for 1919, p.N42.

Clothier, G.A. (1921): Ecstall River; Annual Report of the Minister of Mines for 1920, p.N40.

Crawford, M.L. and Crawford, W.A. (1991): Magma emplacement in a convergent tectonic orogen, southern Revillagigedo Island, southeastern Alaska; *Canadian Journal of Earth Sciences*, v.28, p.929-938.

Crawford, M.L. and Hollister, L.S. (1982): Contrast of metamorphic and structural histories across the Work Channel lineament, Coast Plutonic Complex, British Columbia; *Journal of Geophysical Research*, v.87, p.3849-3860.

Crawford, M.L., Hollister, L.S. and Woodsworth, G.J. (1987): Crustal deformation and regional metamorphism across a terrane boundary, Coast Plutonic Complex, British Columbia; Tectonics, v.6, n.3, p.343-361.

Delancey, P.R. and Newell, J.M., (1973): Geological and Geochemical Report on the Packsack and Gunnysack claims; unpublished report for Texasgulf Inc., B.C. Ministry of Energy and Mines Assessment Report No. 4509, 12 p., 1 geology map at 1:6,000 scale.

Delancey, P.R. (1978): Report on the West Scotia Property; unpublished company report, Kidd Creek Mines Ltd.; 8p., 13 figures - including 1 geological map at 1:500 scale.

Delancey, P.R. (1981): Report on Diamond Drilling on the Albere 2 claim, (part of the Scotia property); report for Texasgulf Inc., BCMEM Assessment Report 9,302, 2p., 3 figures - including 1 map of drill hole locations at 1:500 scale.

Douglas, H. (1952): Estimate of ore reserves at the Ecstall mine, British Columbia; unpublished company report for Texas Gulf Sulphur Company, December, 1952, 44p.

Douglas, H. (1953): Geology of the Ecstall mine, Ecstall River, B.C.; unpublished company report for Texas Gulf Sulphur Company, Apr. 1953, 55p.

Drinkwater, J.L., Brew, D.A. and Ford, A.B. (1993): Chemical characteristics of major plutonic belts of the Coast Plutonic-Metamorphic Complex near Juneau, southeastern Alaska; *in* Geological Studies in Alaska by the U.S. Geological Survey, 1993, *United States Geological Survey*, p.161-172.

Dusel-Bacon, C., Brew, D.A. and Douglass, S.L. (1996): Metamorphic facies map of southeastern Alaska - distribution, facies and ages of regionally metamorphosed rocks; United States Geological Survey Professional Paper 1497-D, 42 p., 2 map sheets.

Ecstall Mining Corporation (1989): Prospectus.

Ecstall Mining Corporation (1998): Annual Report (10^{th} Anniversary); 14p.

Eldredge, R.A. (1983): A structural analysis of the West Scotia Property, British Columbia; unpublished B.Sc. thesis, Bryn Mawr College, Bryn Mawr, Pennsylvania, 89p., 2 maps.

Falconbridge Minerals Ltd., (1960): Simplified Diamond Drill Logs for Scotia drillholes S-1 to S-10.

Falconbridge Minerals Ltd., (1960): Drill Logs for Packsack Property: DDH-1 to DDH-11; July to August, 1960.

Falconbridge Ltd. (1987a): Geology of the Ecstall River Project area; Figure 6, Map No. 114-1-0150; North sheet, sheet 1 of 3 sheets, scale 1:5,000.

Falconbridge Ltd. (1987b): Geology of the Ecstall River Project area; Figure 7, Map No. 114-1-0151; Central sheet, sheet 2 of 3 sheets, scale 1:5,000.

Falconbridge Ltd. (1987c): Geology of the Ecstall River Project area; Figure 8, Map No. 114-1-0152; South sheet, sheet 3 of 3 sheets, scale 1:5,000.

Flewin, J. (1901): Bell-Helen, Bluestone, etc.; Annual Report of the Minister of Mines for 1900, p.788-789.

Flewin, J. (1902): Ecstall River - Bell-Helen, Bluestone, etc.; Annual Report of the Minister of Mines for 1901, p.991.

Flewin, J. (1903): Ecstall River - Bell-Helen Group; Annual Report of the Minister of Mines for 1902, p.H47 and p. H308.

Flewin, J. (1924): Hidden Creek - story of the Granby Company's mine at Anyox; Canadian Mining Journal, v.45, n.9, Feb.29, 1924, p.209-210.

Fraser, D.C. (1986): Dighem III Survey of the Ecstall River area, British Columbia; Noranda Exploration Company Ltd., September 9, 1986, 47p.

Galley, A.G. (1996): Geochemical characteristics of subvolcanic intrusions associated with Precambrian massive sulfide deposits, *in* Wyman, D. A., editor, Trace Element Geochemistry of Volcanic Rocks: Applications for Massive Sulfide Exploration; Mineral Deposits Division, *Geological Association of Canad*a, p.239-278.

Gareau, S.A. (1989): Metamorphism, deformation and geochronology of the Ecstall-Quaal rivers area, Coast Plutonic Complex, British Columbia; *Geological Survey of Canada*, Current Research, Part E, Paper 89-1E, p.155-162.

Gareau, S.A. (1991a): Geology of the Scotia-Quaal metamorphic belt, Coast Plutonic Complex, British Columbia; unpublished Ph.D. thesis, Carleton University, 390p.

Gareau, S.A. (1991b): Geology of the Scotia-Quaal metamorphic belt, Coast Plutonic Complex, British Columbia; *Geological Survey of Canad*a, Open File Map 2337, scale 1:50 000, 4 sheets.

Gareau, S.A. (1991c): The Scotia-Quaal metamorphic belt: a distinct assemblage with pre-early Late Cretaceous deformational and metamorphic history, Coast Plutonic Complex, British Columbia; *Canadian Journal of Earth Sciences,* v.28, p.870-880.

Gareau, S.A., compiler (1997): Geology, Scotia-Quaal metamorphic belt, Coast Plutonic Complex, *British Columbia; Geological Survey of Canad*a, Map 1868A, scale 1:100 000, 1 sheet.

Gareau, S.A. and Woodsworth, G.J. (2000): Yukon-Tanana terrane in the Scotia-Quaal belt, Coast Plutonic Complex, central-western British Columbia; *in* Tectonics of the Coast Mountains, southeastern Alaska and British Columbia, *Geological Society of America*, Special Paper 343, p.23-43.

Gasteiger, W.A. (1975): Report on a Geophysical Survey on the Packsack and Gunnysack claims, report for Texasgulf Inc., Sept. 1975, B.C. Ministry of Energy and Mines Assessment report No. 5,607, 12p.

Gasteiger, W.A. (1976): Report on Geophysical Work, Red Gulch area - Ecstall River Project, unpublished report for Texasgulf Canada Ltd., Jan. 1976, 5p.

Gasteiger, W.A. and Peatfield, G.R. (1975): Report on Geophysical Surveys and Supporting Work on the Red Gulch Group; unpublished report for Texasgulf Canada Ltd., BC Ministry of Energy and Mines Assessment Report No. 5,859, 16p.

Gehrels, G.E. and Boghossian, N.D. (2000): Reconnaissance geology and U-Pb geochronology of the west flank of the Coast Mountains between Bella Coola and Prince Rupert, coastal British Columbia; *in* Tectonics of the Coast Mountains, southeastern Alaska and coastal British Columbia, *Geological Society of America*, Special Paper 343, p.61-75.

Gehrels, G.E. and Kapp, P.A. (1998): Detrital zircon geochronology and regional correlation of metasedimentary rocks in the Coast Mountains, southeastern Alaska; *Canadian Journal of Earth Science*s, v.35, p.269-279.

Gehrels, G.E., McClelland, W.C., Samson, S.D., Jackson, J.L. and Patchett. P.J. (1991a): U-Pb geochronology of two pre-Tertiary plutons in the Coast Mountains batholith near Ketchikan, southeastern Alaska; *Canadian Journal of Earth Science*s, v.28, p.894-898.

Gehrels, G.E., McClelland, W.C., Samson, S.D. and Patchett, P.J. (1991b): U-Pb geochronology of Late Cretaceous and Early Tertiary plutons in the northern Coast Mountains batholith; *Canadian Journal of Earth Science*s, v.28, p.899-911.

Gehrels, G.E., McClelland, W.C. Samson, S.D. and Patchett, P.J. (1991c): U-Pb geochronology of detrital zircons from a continental margin assemblage in the northern Coast Mountains, southeastern Alaska; *Canadian Journal of Earth Science*s, v.28, p.1285-1300.

Graf, C.W. (1981a): Geology, Geochemistry and Geophysics of the Ecstall Claim Group, Ecstall 1-16.

Graf, C. (1981b): Ecstall River Massive Sulphide Project - Proposal for a Mineral Exploration Program; January, 1981, 7p.

Graf, C.W. (1981c): Ecstall River Joint Venture; unpublished report for Active Mineral Explorations Ltd., October 15, 1981, 34 pages plus 5 Appendices plus 24 map sheets.

Graf, C. (1986): Field notes from visit to Falconbridge's Mariposite Zone; August 12, 1986, 2p.

Graham, C. (1938): Northern Pyrites Ltd. - Ecstall River area; Annual Report of the Minister of Mines for 1938, p.B28.

Greenwood, H.J., Woodsworth, G.J., Read, P.B., Ghent, E.D. and Evenchick, C.A. (1992): Metamorphism; Chapter 16 *in* Geology of the Cordilleran Orogen in Canada, *Geological Survey of Canad*a, Geology of Canada, n.4, p.533-570.

Hallof, P.G. (1958): Supplementary report on the Electromagnetic detail in the Ecstall River area of British Columbia, McPhar Geophysics report, 6p.

Hassard, F.R. (1986): Geophysical Exploration on the Mariposite 1 and 2 claims; unpublished report for Falconbridge Limited, November, 1986, 21p.

Hassard, F.R.., Pattison, J. and Uher, L. (1987a): Geological and Geochemical Surveys and Diamond Drilling on the Mariposite property; unpublished report for Falconbridge Limited, January, 1987, 57p. plus drill logs.

Hassard, F.R., Pattison, J. and Uher, L. (1987b): Geological, Geophysical and Geochemical Surveys and Diamond Drilling - Ecstall Project, January 1987, report for Falconbridge Limited, B.C. Ministry of Energy and Mines Assessment Report No. 15,756, 52p. and 9 appendices.

Hassard, F.R., Manojlovic, P.M. and Fournier, J.D. (1987c): Geological, Geophysical and Geochemical Surveys - Ecstall Project (Red 1-6 and 10, Blue 1-4, Green 1, and Skinny Fr.); unpublished report for Falconbridge Ltd., December 1987, 3 volumes - 41p. plus 8 appendices.

Heah, T.S.T. (1990): Eastern margin of the Central Gneiss Complex in the Shames River area, Terrace, British Columbia; *in* Current Research, Part E, *Geological Survey of Canad*a, Paper 90-1E, p.159-169.

Heah, T.S.T. (1991): Mesozoic ductile shear and Paleogene extension along the eastern margin of the Central Gneiss Complex, Coast Belt, Shames River area, near Terrace, British Columbia; unpublished M.Sc. thesis, *University of British Columbi*a, 155p.

Hendrikson, G.A. (1987): Geophysical surveys on the Thirteen Creek Grid Area; unpublished report for Falconbridge Ltd., B.C. Ministry of Energy and Mines Assessment Report No. 16,600; 11p.

Hendrikson, G.A., (1987): Geophysical surveys - Scotia project, report for Kidd Creek Mines Ltd., BCMEM Assessment Report 16,795, 10p., 5 maps plus VLF sections.

Hendrickson, G.A. (1996): Geophysical report on the Steelhead and Horsefly prospects, northwest British Columbia, NTS 103 H/11 & H14, Delta Geoscience Ltd. for Atna Resources Ltd., Feb. 23, 1996, 13p.

Hilker, R. G., (1985): Scotia zinc property - 1984 exploration drill program; unpublished report for Andaurex Resources Ltd., BCMEM assessment Report 13,794, 38p.

Hill, C.T. (1953): Ecstall ore reserves; unpublished report for Texas Gulf Sulphur Company, March, 1953, 3p.

Hoffman, G.C. (1892): Chemical Contributions to the Geological Survey of Canada; Geological Survey of Canada, Annual Report, v. 5, part II, 1890-91, p.67R.

Hoffman, G.C. (1895): Chemical contributions to the Geological Survey of Canada; Geological Survey of Canada, Annual Report, v. 6, 1892-93, p.75R.

Holyk, W. (1952a): Geology of the Ecstall River mine area; unpublished company report for Texas Gulf Sulphur Company, 46p.

Holyk, W. (1952b): Geology of the Ecstall River mine area; unpublished map for Texas Gulf Sulphur Company, 1 sheet, scale 1:7920 (1 inch = 1/8 mile).

Holyk, W. (1952c): Geology of the Ecstall mine; unpublished map for Texas Gulf Sulphur Company, 1 sheet, scale 1:3000 (1 inch = 250 feet).

Holyk, W., Padgham, W., Money, P. and Read, P.B. (1958): Geological map of the Ecstall River Area; unpublished map for the Texas Gulf Sulphur Company, 1 sheet, scale 1:126,720 (1inch = 2 miles).

Hutchinson, W.W. (1970): Metamorphic framework and plutonic styles in the Prince Rupert region of the Central Coast Mountains, British Columbia; *Canadian Journal of Earth Science*s, v.7, p.376-405.

Hutchinson, W.W. (1979): Geology of the Prince Rupert-Skeena map area, British Columbia; Geological Survey of Canada, Map 1472A, scale 1:250 000.

Hutchinson, W.W. (1982): Geology of the Prince Rupert-Skeena map area, British Columbia; *Geological Survey of Canad*a, Memoir 394, 116p.

Jackaman, W., Lett, R. and Friske, P. (2001): B.C. Regional Geochemical Surveys: 2000 Field Programs; *B.C. Ministry of Energy and Mines*, Geological Fieldwork 2000, Paper 2001-1, this volume.

Kenah, C. (1983): Mechanism and Physical Conditions of Emplacement of the Quottoon Pluton, British Columbia; unpublished Ph.D. thesis, Princeton University, 184p., 2 maps.

Kenah, C. and Hollister, L.S. (1983): Anatexis in the Central Gneiss Complex, British Columbia; *in* Migmatites, Melting and Metamorphism, Proceedings of the Geochemical Group of the Mineralogical Society, p.142-162.

Krage, S.M. (1984): Metamorphic and fluid inclusion study of amphibolite grade rocks, West Scotia, British Columbia; unpublished M.A. thesis, *Bryn Mawr Colleg*e, Philadelphia, 98p.

Large, R.R., Doyle, M., Raymond, O., Cooke, D., Jones, A. and Heasman, L., 1996, Evaluation of the role of Cambrian granites in the genesis of world class VHMS deposits in Tasmania; *Ore Geology Review*s, v.10, p.215-230.

Ledoux and Company (1953): Spectrographic Analysis of Ecstall ore samples; unpublished assay report for the Texas Gulf Sulphur Company, Apr. 1953, 1p.

Leistel, J.M., Marcoux, E., Theiblemont, D., Quesada, C., Sanchez, A., Almodovear, G.R., Pascual, E. and Saez, R. (1998): The volcanic-hosted massive sulphide deposits of the Iberian Pyrite belt; Mineralium Deposita, v.33, n.1-2, p.2-30.

Lowrie (1952): Diamond drill logs and analysis for Ecstall Mine; unpublished report for Texas Gulf Sulphur Company, 79p

MacDonald, H.J.C. (1917): Report on a pyritic deposit on the Ecstall River, British Columbia; unpublished report for Granby Mines Ltd., August, 1917, 21p.

MacDonald, H.J.C. (1918): Progress report on the Ecstall Exploration; unpublished report for Granby Mines Ltd., December, 1918, 80p.

MacDonald, H.J.C. (1920): Final report on the Ecstall exploration; unpublished report for Granby Mines Ltd., March, 1920, 44p.

MacDonald, H.J.C. (1927): Ecstall: A mine of the future?; Engineering and Mining Journal, v.123, n.24, June 11, 1927, p.964-968.

Mandy, J.T. (1929): Ecstall River; Annual Report of the Minister of Mines for 1929, p.70.

Mandy, J.T. (1930): Ecstall River; Annual Report of the Minister of Mines for 1930, p.66.

Manojlovic, P.M. and Fournier, J.D. (1987): Geological and geophysical Surveys on the Scotia property; unpublished report for Kidd Creek Mines Ltd., 7p., 4 appendices, 6 maps.

Martyn, D. (1986): Airborne Electromagnetic / Magnetic survey on the Mariposite Property; unpublished report for Kidd Creek Mines Ltd. by Questor Surveys Ltd., 23p.

Martyn, D. (1986): Airborne electromagnetic / magnetic Survey - Ecstall River area; unpublished report for Kidd Creek Mines Ltd. by Questor Surveys Ltd., File No. 27H42, Feb. 1986, 23p.

Mason, E.E. (1937a): Tonnage Calculations of Granby Company confirmed; unpublished file note for Texas Gulf Sulphur Company Ltd., 1p.

Mason, E.E. (1937b): Map of the Ecstall River from Skeena River to Douglas Channel; unpublished map for Texas Gulf Sulphur Company, 1 sheet, scale 1 inch = 1 mile.

Mason, E.E. (1937c): Map of area adjoining Ecstall Pyrites property; unpublished map for Texas Gulf Sulphur Company, 1 sheet, Nov. 1937, scale 1 inch = 1/4 mile.

Mason, E.E. (1940a): Ecstall underground diamond drill holes: 1937-1940; unpublished drillhole sections for Texas Gulf Sulphur Company, 31p.

Mason, E.E. (1940b): Mine development work at the Ecstall mine; set of unpublished progress reports for the Texas Gulf Sulphur Company, 16p.

Mason, E.E. (1940c): Tonnage calculations at the Ecstall mine; unpublished report for the Texas Gulf Sulphur Company, 25p.

Mason, E.E. (1940d): Cross-sections of the Ecstall deposit; unpublished diagrams report for the Texas Gulf Sulphur Company, 16p.

Mason, E.E. (1940e): Assays for DDH 14 to DDH 40 plus #6 Crosscut; unpublished lab report for the Texas Gulf Sulphur Company, 16p.

Mason, E.E. (1940f): Northern Pyrites Ltd. 2% copper ore; unpublished report for the Texas Gulf Sulphur Company, 5p.

Mason, E.E. (1941a): Transportation on the Ecstall River and Tonnage Possibilities; unpublished report for the Texas Gulf Sulphur Company, March, 1941, 13p.

Mason, E.E. (1941b): Upper Section - Ecstall River; unpublished map of the Ecstall Pass route for Texas Gulf Sulphur Company, 1 sheet, Feb. 1941, scale 1 inch = 1/4 mile.

Mason, E.E. (1951a): Ecstall River Reconnaissance; unpublished file note for the Texas Gulf Sulphur Company, Sept. 1951, 5p.

Mason, E.E. (1951b): Ecstall River prospecting map; unpublished map for the Texas Gulf Sulphur Company, Sept. 1951, 1 sheet, scale 1 inch = 1 mile.

Mason, E.E. (1951c): Biogeochemical prospecting; unpublished file note for the Texas Gulf Sulphur Company, Oct. 1951, 3p

Mason, E.E. (1951d): Prospecting in the Ecstall mine area; unpublished file note for the Texas Gulf Sulphur Company, Nov. 1951, 3p.

Mason, E.E. (1961): Production Possibilities for the Ecstall Mine; unpublished company report for Texas Gulf Sulphur Company, Dolmage, Mason and Stewart Ltd., July, 1961, 30p. plus tables.

Massey, N.W.D. (1999): Volcanogenic massive sulphide deposits of British Columbia; *British Columbia Ministry of Energy and Mine*s, Geological Survey, Open File Map 1999-2, scale 1:2,000,000, 2 sheets.

Maxwell, G. and Mercer, W. (1986a): Petrographic Report on the Ecstall 8 claim (Horsefly Showing); unpublished report for Noranda Exploration Company Ltd., Feb. 1986, 20p.

Maxwell, G. and Mercer, W. (1986b): Geochemical and Petrographic report on the Ecstall Packsack group; unpublished report for Noranda Exploration Company Ltd., B.C. Ministry of Energy and Mines Assessment Report No. 15014, 17p.

Maxwell, G. and Bradish, L. (1986): Geological, Geophysical and Geochemical Report on the Horsefly Claim Group; unpublished report for Noranda Exploration Company Ltd., BCMEM Assessment Report 15,306; 31p.

Maxwell, G. and Bradish, L. (1987a): Report on Geology and Geophysics on the Graf Option; unpublished report for Noranda Exploration Company Ltd., January, 1987; 47p.

Maxwell, G. and Bradish, L. (1987b): Report on Geology and Geophysics in the Ecstall River area; unpublished report for Noranda Exploration Company Ltd., BCMEM Assessment Report 15,491; February, 1987; 55p.

McClelland, W.C., Anovitz, L.M. and Gehrels, G.E. (1991a): Thermobarometric constraints on the structural evolution of the Coast Mountains batholith, central southeastern Alaska; *Canadian Journal of Earth Science*s, v.28, p.912-928.

McClelland, W.C., Gehrels, G.E., Samson, S.D. and Patchett, P.J. (1991b): Protolith relations of the Gravina Belt and Yukon-Tanana terrane in central southeastern Alaska; *Journal of Geolog*y, v.100, p.107-123.

McLeod, J.W. (1984a): Microscopic descriptions of green mica samples; unpublished memo, Cominco Exploration Research Laboratory, 4p.

McLeod, J.W. (1984b): Report on West Scotia property; in Statement of Material Facts for Andaurex Resources Inc., Aug. 29, 1984.

McMullin, J.H. (1917): The British Columbia Pyrites Company Ltd., Skeena District - Coast District; Annual Report of the Minister of Mines for 1916, p.K50.

Meyers, R.E. and Moreton, E.P. (1982): Geological Mapping and Diamond Drilling on the Scotia and Albere mineral claims; report for Texasgulf Inc., BCMEM Assessment Report 10,332, 12p., 1 appendix, 2 maps, 4 sections.

Miyashiro, A. (1994): Metamorphic Petrology; Oxford University Press, New York, 404p.

Money, P.L. (1959): Geology of Hawkesbury Island, Skeena Mining Division, British Columbia; unpublished M.Sc. thesis, *University of British Columbi*a, 159p.

Money, D. P. (1989): Scotia Project Drill Data Review and Proposal for 1990 Field Program; report for Falconbridge Limited; 4p. 5 figures, 1 map, 3 level plans, 1 long section, 7 cross sections.

Newberry, R.J., Crafford, T.C., Newkirk, S.R., Young, L.E., Nelson, S.W. and Duke, N.A. (1997): Volcanogenic massive sulphide deposits of Alaska; *in* Mineral Deposits of Alaska, *Economic Geology Publishing Company,* Economic Geology Monograph number 8, p.120-150.

Noranda Exploration Company Ltd., (1986a): Geology of the Horsefly, Steelhead and Piranha Grids; Map 2; Scale 1:5,000.

Noranda Exploration Company Ltd., (1986b): Magnetometer Survey of the Horsefly, Steelhead and Piranha Grids; Map 4; Scale 1:5,000.

Noranda Exploration Company Ltd., (1986c): Geology of the Rainbow Grid; Map 5; Scale 1:5,000.

Noranda Exploration Company Ltd., (1986d): Magnetometer Survey of the Rainbow Grid; Map 7; Scale 1:5,000.

Padgham, W.A. (1957): Ecstall Geological Program; 11p., plus 2 maps.

Padgham, W.A. (1958): The Geology of the Ecstall-Quaal Rivers area, British Columbia; unpublished M.Sc. thesis, *University of British Columbi*a, 202p.

Payne, J.G. (1990a): Geology Report on the Packsack Property, Ecstall River Area; unpublished report for Cominco Limited, Sept. 1990, B.C. Ministry of Energy and Mines Assessment Report 20,422, 28p. plus drill logs.

Payne, J.G. (1990b): Figure 4 - Map of Packsack property geology; part of unpublished report for Cominco Limited, Sept. 1990, B.C. Ministry of Energy and Mines Assessment report 20,422, 1 sheet, scale 1:2,000.

Payne, J.G. (1990c): Figure 5 - Detailed Map of Packsack property geology; part of unpublished report for Cominco Limited, Sept. 1990, B.C. Ministry of Energy and Mines Assessment report 20,422, 1 sheet, scale 1:600.

Peatfield, G.R. (1988): Geological Report on the Ecstall Mineral Property, Ecstall River area, B.C.; unpublished report for Ecstall Mining Corporation, Nov. 1988, 19p.

Peatfield, G.R. (1995): Technical Report on the Atna Resources Ltd. Ecstall Area Mineral Properties; unpublished report for Atna Resources Ltd., Sept. 1995, 29p. plus appendices.

Pell, J. (1988): The Industrial Mineral Potential of kyanite and garnet in British Columbia; B.C. Ministry of Energy, Mines and Petroleum Resources, Geological Fieldwork - 1987, 421-424.

Read, P.B. (1958): A report on the Ecstall to Skeena River area within the Coast Range Septum; unpublished company report for Texas Gulf Sulphur Company Ltd., 22p.

Read, P.B., Woodsworth, G.J., Greenwood, H.J., Ghent, E.D. and Evenchick, C.A. (1991): Metamorphic Map of the Canadian Cordillera; *Geological Survey of Canada*, Map 1714A, scale 1:2000 000.

Renning, M. (1990): Assessment Report for the Amber-1 claim; BC Assessment Report 20,958, 18p.

Renning M. (1992): Assessment Report for the Amber-1 claim; BC Assessment Report 22,391, 12p.

Robinson, W.C. (1960): Scotia (Texas Gulf Sulphur Company) - Scotia River; Annual Report of the Minister of Mines for 1960, p.12.

Robinson, W.C. (1960): Packsack (Texas Gulf Sulphur Company) - Ecstall River; Annual Report of the Minister of Mines for 1960, p.12.

Roddick, J.A. (1970a): Douglas Channel - Hecate Strait map area, British Columbia; *Geological Survey of Canad*a, Paper 70-41, 56p.

Roddick, J.A. (1970b): Douglas Channel - Hecate Strait map area, British Columbia; *Geological Survey of Canad*a, Preliminary Map 23-1970, scale 1:250 000.

Rubin, C.M., Saleeby, J.B., Cowan, D.S., Brandon, M.T. and McGroder, M.F. (1990): Regionally extensive mid-Cretaceous west-vergent thrust system in the northwestern Cordillera: implications for continent-margin tectonism; *Geolog*y, v.18, p.276-280.

Runkle, D.E., (1979): Geology and Geochronology of the Coast Plutonic complex adjacent to Douglas, Sue and Laretta channels, British Columbia; unpublished M.Sc. thesis, University of British Columbia, 67p.

Samson, S.D., Patchett, P.J., McClelland, W.C. and Gehrels, G.E. (1991): Nd and Sr isotopic constraints on the petrogenesis of the west side of the northern Coast Mountains batholith, Alaskan and Canadian Cordillera; *Canadian Journal of Earth Science*s, v.28, p.939-946.

Schmidt, A.J. (1968): Summary Report for the Ecstall Geochemical Project; unpublished report for Texasgulf Inc., Nov. 1968.

Schmidt, U. (1995a): Report on the Geology and Geochemistry of the Ecstall Property; unpublished report for Atna Resources Ltd., Feb. 1995, 23p. plus appendices plus 10 folded maps.

Schmidt, U. (1995b): List of rock descriptions - 13 Creeks area; field notes for Atna Resources..

Schmidt, U. (1996a): Report on Geology, Geophysics and Diamond Drilling of the Horsefly Property, Skeena Mining Division, NTS 103 H/14; unpublished report for Atna Resources Ltd., Feb. 27, 1996, 78p. (16p. plus Appendices)

Schmidt, U. (1996b): Horsefly Property Geology Map; unpublished map for Atna Resources Ltd., Figure 12, Scale 1:2,000.

Scott, B. (2001): Geology of the Amber-El Amino area, northwest British Columbia (NTS 103 H); *B.C. Ministry of Energy and Mines*, Geological Fieldwork 2000, Paper 2001-1, this volume.

Shearer, J.T. (1988): Geological and geochemical report on the El Amino, Briton, Samson and Regal claims, Ecstall River area, Skeena Mining Division; report for Algonquin Minerals, BC Assessment Report 17,682, 26p.

Sheldrake, R.F. (1981): Report on a Helicopter Electromagnetic and Magnetometer Survey in the Ecstall River area; unpublished report for Welcome North Mines Ltd., BCMEM Assessment Report 10,007; 37p.

Sinnott, N. (1997): Geochemical and Prospecting Reconnaissance Program - Scotia River Area; unpublished report for Bishop Resources Inc., 81p., 2 maps.

Sisson, V.B. (1985): Contact metamorphism and fluid evolution associated with the intrusion of the Ponder Pluton, Coast Plutonic Complex, British Columbia, Canada; unpublished Ph.D. thesis, *Princeton Universit*y, New Jersey, 345p.

Smith, D. (1958): Ecstall (Ecstall Mining Company Limited) - Ecstall River; Annual Report of the Minister of Mines for 1958, Lode Metals section, p.7.

Smith, D. (1958): Packsack (Texas Gulf Sulphur Company) - Ecstall River; Annual Report of the Minister of Mines for 1958, Lode Metals section, p.9 and p.73.

Spry, P.G., Marshall, B. and Vokes, F.M., editors (2000): Metamorphosed and Metamorphogenic Ore Deposits, Society of Economic Geologists, Reviews in Economic Geology, v.11, 310p.

Stowell and McClelland, editors (2000): Tectonics of the Coast Mountains, southeastern Alaska and British Columbia, *Geological Society of America*, Special Paper 343, 289p.

Sutherland, D.B. and Davidson, S. (1958): Geophysical Report on the Packsack and Gunnysack claim groups; unpublished report for Texas Gulf Sulphur Co. Ltd. by McPhar Geophysics Ltd., BCMEM AR 214, 3p.

Sutter, J.F. and Crawford, M.L. (1985): Timing of metamorphism and uplift in the vicinity of Prince Rupert, British Columbia and Ketchikan, Alaska; in Geological Society of America, Cordilleran Section, Program with Abstracts, p.411.

Texasgulf Inc.; (1980): Diamond Drill Logs for holes S-11 to S-17.

Texasgulf Inc., (1981): Diamond Drill Logs for holes S-18 to S-21.

Tipple, F.E. (1958): Study and development of sulphide mines owned by Texas Gulf Sulphur Company with special reference to Ecstall and Copper King mines; unpublished file note for the Texas Gulf Sulphur Company Ltd., Aug. 1958, 4p.

Turner, S.G. (1961): Geology of a mineral deposit in the Skeena Mining District of northwestern British Columbia; unpublished B.Sc. thesis, The University of British Columbia, 111p., 2 maps.

van der Heyden, P. (1989): U-Pb and K-Ar geochronometry of the Coast Plutonic Complex, 53ºN to 54ºN, British Columbia, and implications for the Insular-Intermontane superterrane boundary; unpublished Ph.D. thesis, *University of British Columbi*a, 392p.

Vanderkamp, B.J. (1968): Ecstall Geochemical Orientation Project, unpublished report for Texasgulf Inc., Jan. 1968.

von Fersen, N. (1992): Summary of Ecstall Project; unpublished report for Kidd Creek Mines Ltd., January, 1992, 6p.

Wheeler, J.O. and McFeely, P., compilers (1991): Tectonic Assemblage map of the Canadian Cordillera and adjacent parts of the United States of America; Geological Survey of Canada, Map No. 1712A, 2 sheets, scale 1:2 000 000.

Wojdak, P. (1986): North Coast area; B.C. Ministry of Employment and Investment, Exploration in BC 1995, p.37.

Woodsworth, G.J., Anderson, R.G. and Armstrong, R.L. (1992): Plutonic Regimes; Chapter 15 *in* Geology of the Cordilleran Orogen in Canada, *Geological Survey of Canad*a, Geology of Canada, n.4, p.491-531.

Woodsworth, G.J., Crawford, M.L. and Hollister, L.S. (1983): Metamorphism and Structure of the Coast Plutonic Complex and adjacent belts, Prince Rupert and Terrace areas, British Columbia; *Geological Association of Canada Annual Meeting* - Victoria 1983, Field Trip Guidebook No.14, 62p.

Zen, E. and Hammarstrom, J.M. (1984): Magmatic epidote and its petrologic significance; Geology, v.12, p.515-518.

Zen, E. (1985): Implications of magmatic epidote-bearing plutons on crustal evolution in the accreted terranes of northwestern North America; *Geology,* v.13, p.266-269.

Geology of the Amber - El Amino Area, Ecstall Metamorphic Belt, British Columbia (NTS 103 H)

By Brad Scott

KEYWORDS: Economic geology, Geologic mapping, Amber, El Amino, Bent, Frizzell, Billy Goat, Central Gneiss Complex, Coast Plutonic Complex, Coast Crystalline Belt, Ecstall Metamorphic Belt.

INTRODUCTION

The Amber - El Amino area is located 75 kilometres southeast of Prince Rupert. Access to the area is by helicopter from Prince Rupert or Terrace (Figure 1). The El Amino showing (BC MINFILE 103H 071) is located on Sulphide Creek (Figure 2) which drains eastward into Hanna (El Amino) Creek. The Amber showing (BC MINFILE 103H 171) is located 700 metres north of the El Amino showing. Hanna Creek drains northwestward into Sparkling Creek, a tributary of the Ecstall River.

The Amber-El Amino area consists of a steep-sided, U-shaped glacial valley and rounded, undulating ridge-tops. The highest point along the ridgecrests is 1475 metres and elevation drops to 400 metres on the valley floor. The climate is wet and mild; vegetation ranges from dense, lush coastal rainforest in the valleys to alpine heather on the ridge tops. Proximity to the ocean results in high annual precipitation and a large accumulation of snow. In late August, much of the alpine areas were still covered with thick snow, and permanent snowfields cover parts of the ridgecrests.

The first reported prospecting in Hanna Creek was conducted by George Frizzell and J.B. Roerig of Prince Rupert sometime prior to 1950 (Mason, 1951, p.5, Holyk, 1952, p.29-31 and Douglas, 1953, p.21). Sulphide mineralization described in Frizzell's notes, and marked on a set of photographs, was later referred to as the "Frizzell outcrop". In 1952, some years after Frizzell's death, a prospecting party led by W. Holyk returned to the headwaters of Hanna Creek to relocate and resample the Frizzell outcrop, guided by the annotated photographs. From his notes and sketch map, reproduced in this report, it is clear that Holyk located the same mineralization now known as the El Amino prospect. The assay from Holyk's sample was disappointing, but one claim, the Billy Goat mineral claim, was staked and recorded at Prince Rupert.

The Amber- El Amino area was staked again in 1980 by US Borax as the Bent claims, after anomalous Mo and Pb values were obtained in a stream silt sample. Chalcopyrite-mineralized float was discovered in a follow-up prospecting visit (Shearer, 1988), but the company's primary target was porphyry Mo deposits and the Bent claims were allowed to lapse the following year.

In 1987, Algonquin Minerals staked the same area once more as the El Amino, Samson, Briton and Regal claims. The El Amino (Frizzell) showing was re-discovered during preliminary prospecting of the prominent rusty cliffs along a tributary on the west side of Hanna Creek. A follow-up soil sampling program was conducted in 1988, but these claims also lapsed.

In 1990, Darren Hayes staked the property as the Amber-1 claim and conducted a prospecting and silt sampling program (Renning, 1990). The Amber sulphide showing was discovered during a follow-up prospecting traverse in 1991 (Renning 1992).

This writer's work in the area during the 2000 field season included traverses along ridgecrests to the east, west and south of the Hanna Creek valley over a period of four days. Geological mapping of the Amber-El Amino area is part of a regional mapping program of the Ecstall greenstone belt for the Mid-Coast VMS Project (Alldrick and Gallagher, 2000). Samples were collected from representative lithological units and from strongly pyritic zones. The two prospects were not examined during these traverses, however the MINFILE location for the El Amino showing has been corrected and the deposit description updated, and the Amber showing has now been added to the MINFILE database.

REGIONAL GEOLOGIC SETTING

The Ecstall metamorphic belt is part of the Central Gneiss Complex which consists of Proterozoic(?) to Paleozoic metasedimentary and metavolcanic rocks (Alldrick and Gallagher, 2000 and Gareau, 1991). Regionally, these metamorphic rocks are bounded and intruded by late Silurian to Eocene plutons of the Coast Plutonic Complex.

Gareau (1997) produced a colour geological map of the Ecstall belt, which is interpreted as a Devonian volcanic arc, consisting of metasedimentary and metavolcanic rocks intruded by the comagmatic Big Falls orthogneiss (tonalite). The belt is bounded on the west by the Late Cretaceous Ecstall pluton, and on the east by the Late Paleocene to early Eocene Quotoon pluton.

Rocks of the Ecstall metamorphic belt have been deeply buried and metamorphosed to amphibolite facies.

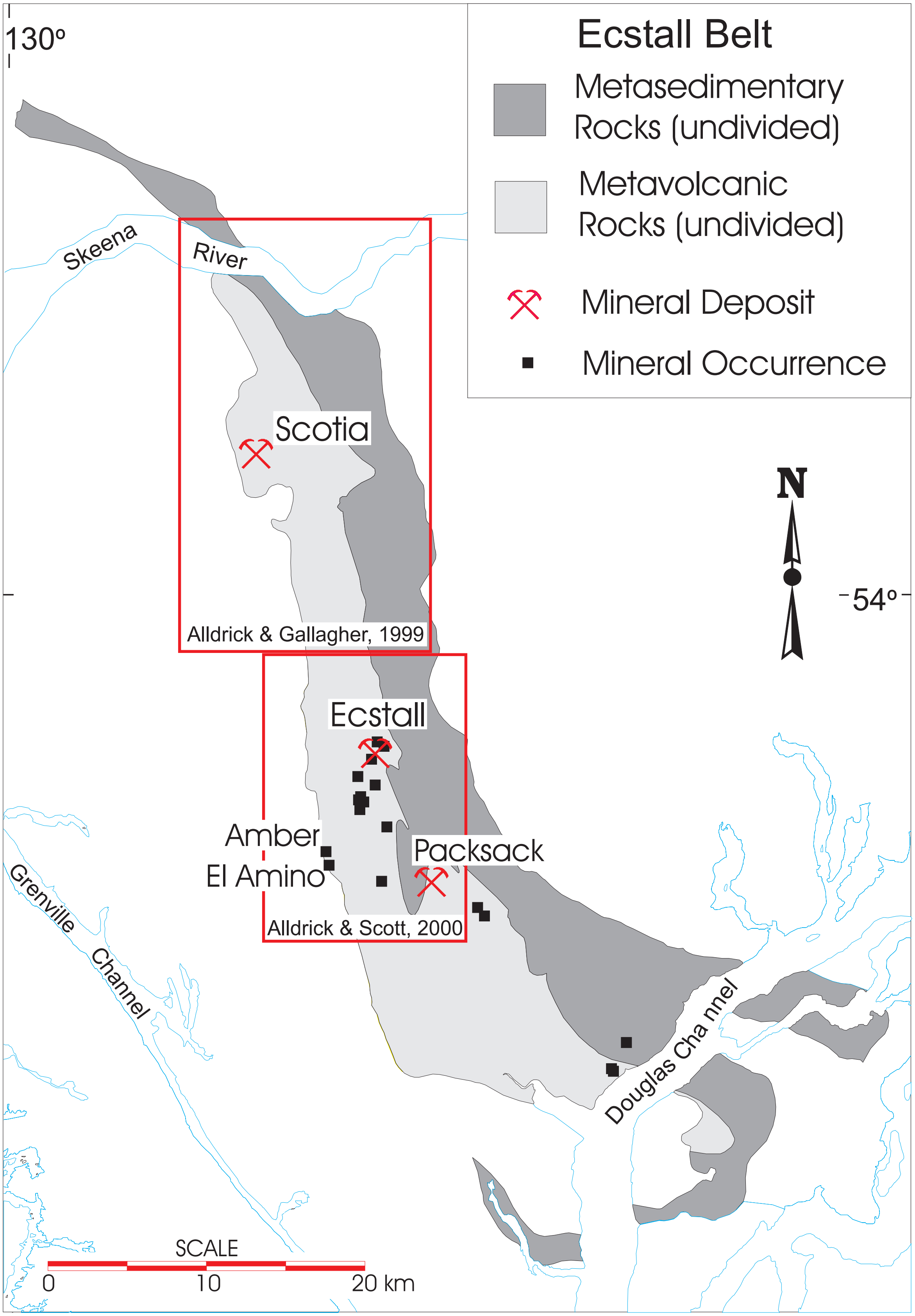

Figure 1. Simplified Geology and mineral prospects of the Ecstall Belt.

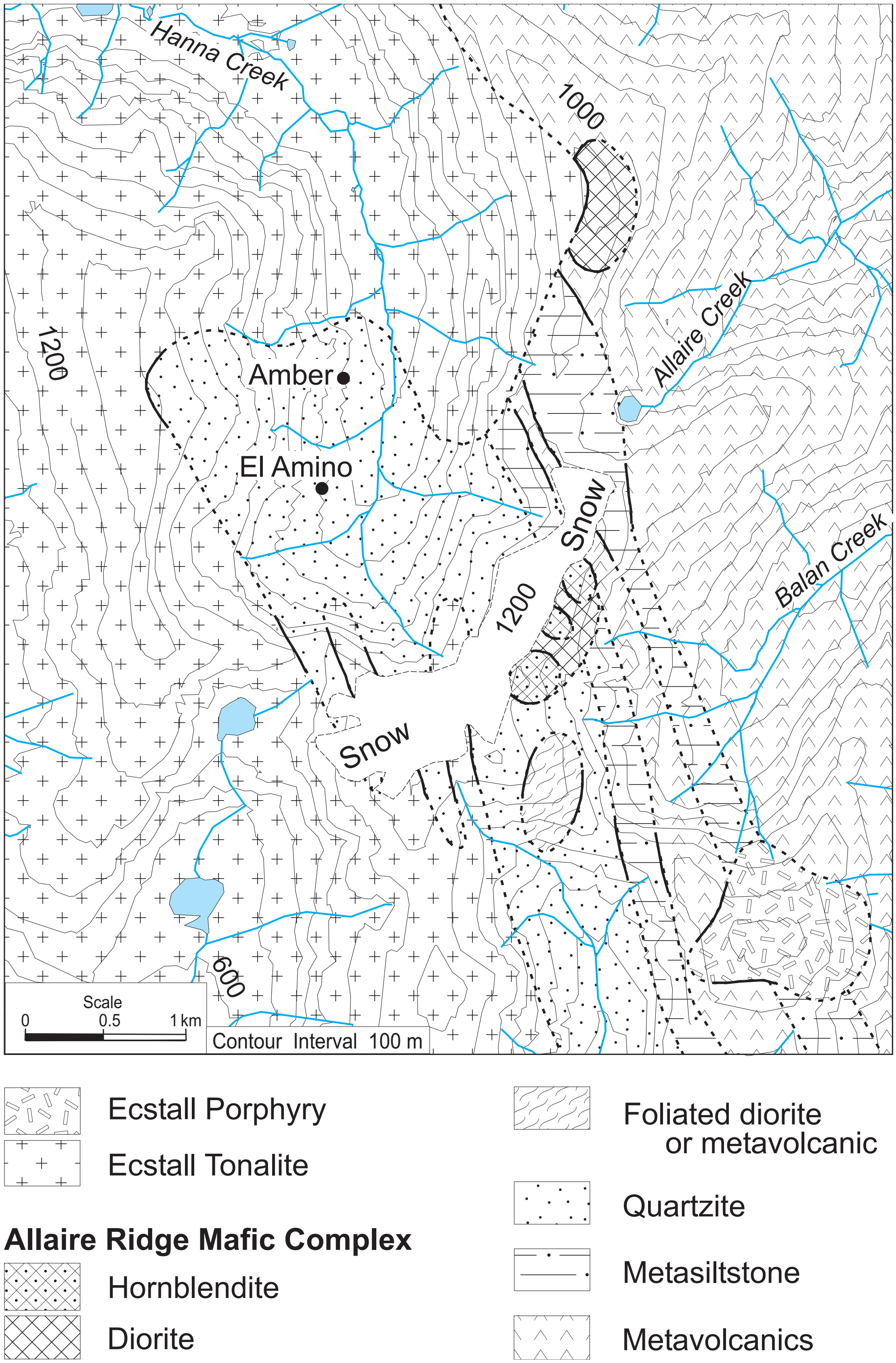

Figure 2. Geology of the Amber - El Amino area.

Regional retrograde metamorphism has been correlated with the intrusion of the Ecstall or Quotoon plutons.

GEOLOGY

The geology of the Amber-El Amino area is shown on Figure 2.

Stratified Rocks

Paleozoic metasedimentary rocks are interlayered siltstones and sandstones (arkose and quartzite). These are well-foliated and locally highly folded and contorted. Small, discontinuous carbonate lenses were noted in several outcrops and a 5 metre thick band of calc-silicate-altered metasedimentary rock was mapped at one location. A 10 metre thick fine-grained diorite sill intrudes the metasedimentary rocks at one site, and rare, narrow pegmatite dikes also cut these units.

Metasiltstone is dark grey to black fine-grained rock with granoblastic to schistose to hornfelsed texture. These rocks weather medium to dark grey to black, but pyritic exposures are rusty to buff weathering. Units are typically a few metres thick, finely laminated and interbedded with meta-arkose and/or quartzite, however they can form bands several metres thick. This rock is locally garnetiferous, with up to 10 percent fine to medium-grained (up to 8 mm diameter) red garnets.

Quartzite is typically coarsely laminated (tens of centimetres thick), with local exposures showing fine laminations. Quartzite is commonly interlayered with metasiltstone and meta-arkose, but may form monolithologic sections up to 40 metres thick. It forms a hard, pale grey, granoblastic rock, with widely spaced (5 to 10 cms) micaceous partings.

Meta-arkose is the least common metasedimentary rocks and does not form thick units. It consists of dark grey, arkosic, micaceous bands within metasiltstones and quartzites, and it typically grades into quartzite.

Metavolcanic rocks crop out in the southwest map area as foliated, contorted, greenish-grey to black, medium-grained, chlorite-altered mafic tuffs, which are locally epidote-rich.

Contacts between metasedimentary units and metavolcanic rocks and between different metasedimentary lithologies typically consist of wide zones of alternating interlayered bands. Contact relationships with intrusive rocks are complex. Metasedimentary rocks tend to be highly buckled near intrusive contacts. Within plutonic rocks, rafts of metasediments up to 40 metres thick appear for hundreds of metres into the pluton; small sills of the intrusive also occur interlayered within the metasedimentary rocks near the contact. The result is an overall `gradational' contact between a pluton and enclosing sediments.

Plutonic Rocks

Ecstall Tonalite

Regionally, the late Early Cretaceous Ecstall batholith includes diorite, tonalite and granodiorite phases (Gareau, 1991). In this study area, two distinct phases were noted: equigranular tonalite and porphyry. A distinctive feature of the Ecstall pluton is the presence of magmatic epidote, which increases in abundance from the margins to the centre of the intrusion. Within 200 metres of the contact, no epidote is apparent; it becomes progressively more abundant moving into the pluton, appearing first in fractures, then as fine interstitial grains, finally as equigranular coarse grains making up to 5% of the rock volume.

Equigranular hornblende-biotite-epidote tonalite ranges from light to medium grey on fresh surfaces, weathers medium to dark grey, and is locally rusty coloured. Grain size typically ranges from medium to coarse-grained equigranular, but local very coarse-grained phases were noted. The rock ranges from massive to moderately foliated, with the foliation defined by the alignment of mafic minerals. Foliation is generally more intense near the pluton margins. Primary layering (flow-banding or cumulate layering) was noted in one location. The pluton is highly sheared in places, mylonitic and pyritic shear zones were mapped in the northwest map area. Cobble to boulder size mafic xenoliths are locally abundant. Screens of metasedimentary rock up to 40 metres wide are typically incorporated near the margins. Narrow (50 to 100 cm wide) lamprophyre and pegmatite dikes cut the Ecstall pluton.

Ecstall porphyry is dark grey massive diorite(?) with an aphanitic groundmass and feldspar phenocrysts 3 to 4 millimetres across. Narrow lamprophyre dikes cut this unit and in one location the porphyry incorporates a 15-metre-thick screen of country rock composed of a calc-silicate unit and a thin metavolcanic interval.

Diorite

Fine-grained foliated diorite intrudes the metasedimentary rocks. The diorite crops out as a single large intrusion (400 metres wide) and as smaller sill-like layers in the metasediments. Near the margins of the main intrusion, 10 to 15-metre-thick screens of quartzite occur. In one outcrop, the diorite grades into black, moderately foliated, medium-grained, chlorite-altered amphibolite. This unit may be a phase of the mid-Devonian Big Falls tonalite.

Hornblendite

Coarse, massive hornblendite intrudes quartzite and mixed metasediments in the eastern map area. The fresh rock is black, and weathers rusty brown. The hornblendite is medium to very coarse-grained, with hornblende (var. pargasite) crystals ranging up to 1.4 centimetres in diameter. Metasediments within 1 to 2 metres of the intrusive contact are buckled, and screens of quartzite are incorporated near the margin of the intrusion.

STRUCTURE

Rocks in the Amber - El Amino area are dominantly northwest-trending and dip steeply. S_1 foliation is defined by the alignment of micas in metasedimentary and metavolcanic rocks, and by the alignment of mafic minerals in plutonic rocks.

S_0 is not well preserved, however two clear examples were found. In an outcrop of metasediments an S_0/S_1 intersection lineation was displayed, and cumulate layering was observed in one outcrop of Ecstall tonalite. Lineations, consisting of intersection lineations and minor fold axes, plunge steeply to the southeast. Together, these features suggest large-scale folding about an axis plunging 72º towards 150º.

MINERALIZATION

There are two MINFILE occurrences in the map area, the Amber and El Amino showings (Figure 2). Both showings consist of disseminated to massive sulphides hosted within the metasedimentary rock package. This contrasts with all other mineral occurrences in the Ecstall metamorphic belt, which are hosted within the metavolcanic rock sequence (Gareau, 1997 and Alldrick and Gallagher, 2000).

El Amino

Shearer (1988) describes this massive sulphide prospect that crops out in Sulphide Creek, a small tributary to Hanna Creek. The host rock sequence includes quartzite and limy siltstone, with minor calcareous sandstone. This succession is cut by pegmatite dikes. The sulphides are conformable and can be walked out for 30 metres then visually traced for another 30 metres up steep cliffs. The host rock metasediments are folded into a tight antiform; the sulphide layer ranges from 40 centimetres thickness in the west limb to 1.4 metres wide at the fold nose. Mineralization consists of pyrrhotite and chalcopyrite with minor sphalerite and galena.

Three styles of mineralization are present:

- Light green-grey granular rock with abundant disseminations and small lenses of pyrrhotite and 2-3 cm biotite knots with pyrrhotite and chalcopyrite rims. Gangue is mainly massive, non-foliated medium to coarse-grained calcite.
- Sulphides occur in rough layers, with massive pyrrhotite layers and pyrite nodules in some exposures. Gangue is fine grained and siliceous.
- Abundant chalcopyrite-bearing float boulders are found in the valley downslope. Grab samples from these boulders assay up to 4.46 % copper and 240 ppm silver, while the best assay obtained at the El Amino showing is 1.0% copper and 31 ppm silver. Shearer (1988) concludes that the likely source of the high-grade boulders is another sulphide horizon high up the cliffs.

The El Amino prospect described by Shearer is undoubtedly the Frizzell outcrop mentioned by Mason (1951, p.5), Holyk (1952, p.29-31) and Douglas (1953, p.20-21) and visited by Holyk 36 years earlier. Holyk's description and prospecting sketch map (Figure 3) are reproduced below:

"Massive sulphide deposits were found in the upper reaches of Hanna Creek. The deposits are located on the west side of Hanna Creek about 600 feet above the main valley floor and alongside an intermittent stream which flows into Hanna Creek at 1300 feet elevation. This position is approximately a half mile from the head of Hanna valley. The deposit occurs at a position corresponding with one of Frizzell's photographs and is believed to be the deposit reported by G. Frizzell, Prince Rupert B.C. to occur in the area.

The sulphide deposits occur as four separate lenticular bodies along a horizon of argillaceous quartzite and are replacements of this bed. …The largest body is 40 feet long, has a maximum true width of 3 feet at its mid portion, pinches out along strike at both ends, and is exposed along a dip slope (55º) distance for 10 to 15 feet. Three other lenticular bodies occur along strike of the quartzite horizon above the largest lens. They are 10 feet or less in length and have a true width of 1 foot or less. The four bodies are exposed along a slope distance of 200 feet."

The lenticular bodies are sulphide replacements of the quartzites and generally the sulphides form about 20-30% of the rock, but irregular plums of massive sulphide occur. Pyrrhotite is the dominant mineral. Sphalerite and chalcopyrite are locally abundant. A chip sample of the largest body assayed as follows: trace Au, 0.2 opt Ag, trace Pb, 0.6% Zn, 0.5% Cu, 35.6% Fe, 23.4% S.

Overburden conceals the mineralized horizon east of the sulphide outcrops down to Hanna Creek 600 feet be-

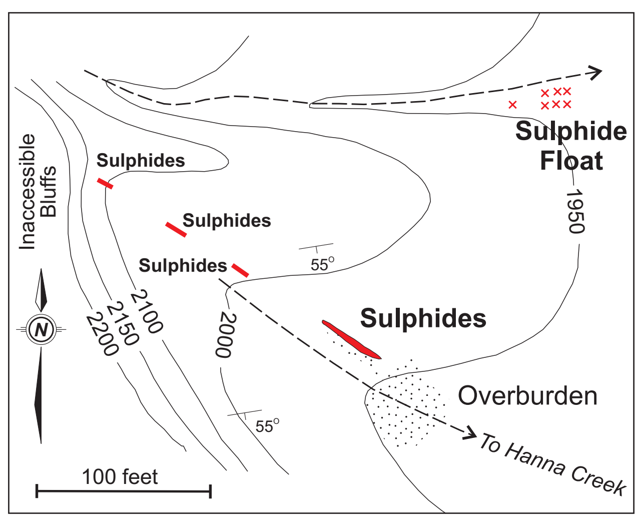

Figure 3. Sketch map of the Hanna Creek (El Amino) sulphide deposit (from Holyk, 1952).

low. The same horizon extends uphill to the west and occurs near the top of shear bluffs. This area is not accessible. Sulphide float was observed in a creek below these bluffs indicating that other lenses of sulphide might be present. The same horizon was investigated 1000 feet higher in elevation above the sulphide showing, but no mineralization was found.

Most of the rocks in the Hanna Creek area are granites with the exception of a quartzite wedge approximately 1000 feet wide in the upper reaches of the valley and in which the sulphides occur. The writer feels that the favourable area (non-granite) has been adequately prospected and that no major deposit in the area has been overlooked.

One claim, the "Billy Goat" mineral claim, was staked in this area and recorded at Prince Rupert B.C….The claim covers most of the area favourable to further sulphide occurrences."

Amber

At the Amber prospect, 700 metres north of the El Amino Prospect, massive sulphide mineralization is exposed along an east-draining creek (Renning, 1992). Sphalerite, chalcopyrite, pyrite and galena are hosted by dark quartzite. The showing is 60 centimetres wide and exposed for just 1.5 metres along strike before it is covered by overburden. No assay results are reported by Renning (1992), however analyses of soil and stream silt samples include 9 ppb gold, 1 ppm silver, 110 ppm copper, 186 ppm zinc and 1320 ppm barium.

DISCUSSION AND CONCLUSIONS

The Amber and El Amino deposits are significant because they are hosted by metasedimentary units, while all other prospects in the Ecstall Metamorphic Belt are hosted in the metavolcanic sequence. This indicates the potential for further discoveries within these largely unexplored units. The Amber-El Amino area has not been fully explored; steep valley walls hinder prospecting, and ropes and specialized climbing gear will be required to further investigate the mineral potential in the area of these two prospects (Shearer, 1988). Abundant chalcopyrite-rich float boulders along the valley floor of El Amino Creek (Shearer, 1998) and in the creek bed immediately north of Sulphide Creek (Figure 3 and Holyk, 1953), indicate the presence of additonal higher grade mineralization that has not been located in outcrop. All of the numerous tributary creeks should be sampled for stream sediment geochemistry.

REFERENCES

Alldrick, D.J. and Gallagher, C.S. (2000): Geology and mineral potential of the Ecstall VMS belt (NTS 103H; 103 I); BC Ministry of Energy and Mines, Geological Fieldwork 1999, Paper 2000-1, pages 249-265.

Douglas, H. (1953): Geology of the Ecstall mine, Ecstall River, B.C.; unpublished company report for Texas Gulf Sulphur Company Ltd., Apr. 1953, 36 p. plus attachments.

Gareau, S.A. (1991): The Scotia-Quaal metamorphic belt: a distinct assemblage with pre-early late Cretaceous deformational and metamorphic history, Coast Plutonic Complex, British Columbia; Canadian Journal of Earth Sciences, v. 28, pages 870-880.

Gareau, S.A., compiler (1997): Geology, Scotia-Quaal Metamorphic Belt, Coast Plutonic Complex, British Columbia; Geological Survey of Canada, Map 1868A, Scale 1:100 000, 1 sheet.

Holyk, W. (1952): Geology of the Ecstall River Mine area; unpublished company report for Texas Gulf Sulphur Company Ltd., 46p. plus attachments.

Mason, E.E. (1951): Ecstall River Reconnaissance; unpublished report for Texas Gulf Sulphur Company Ltd., Sept. 29, 1951, 5 pages.

Renning, M. (1990): Assessment Report for the Amber-1 claim; BC Assessment Report 20,958, 18 pages.

Renning M. (1992): Assessment Report for the Amber-1 claim; BC Assessment Report 22,391, 12 pages.

Shearer, J.T. (1988): Geological and geochemical report on the El Amino, Briton, Samson and Regal claims, Ecstall River area, Skeena Mining Division; report for Algonquin Minerals, BC Assessment Report 17,682, 26 pages.

Mineral Deposits of the Upper Kitsault River Area, British Columbia (103P/W)

By Robert H. Pinsent

KEYWORDS: Economic geology, Lower Jurassic, Hazelton Group, silver production, quartz-barite-carbonate-sulphide-oxide (Ag) deposits, quartz-sericite-chlorite-sulphide (Cu, Au) deposits, stockwork deposits, mesothermal, epithermal vein deposits, exhalative deposits, silver, lead, zinc, barium, strontium, copper, gold, Red Point, Homestake, Wolf, Torbrit, Northstar, Dolly Varden, Sault, Red Mountain, Eskay Creek.

INTRODUCTION

This report describes the mineral deposits of a portion of the northern Coast Mountains southeast of Stewart, British Columbia. It is based on public domain reports and visits to selected deposits; however, none of the underground workings were examined. The work was funded under the Provincial Government's Corporate Resource Inventory Initiative (CRII) as one part of the Ministry's contribution to the North Coast Land Resource Management Planning process. Other parts include a limited fluid inclusion study of upper Kitsault River rocks, geological mapping and stream sediment sampling programs in the Ecstall River area and stream sediment sampling around Porcher, Dundas and other off-shore islands. They will be reported on separately. In addition, the Ministry has scanned and released North Coast area assessment reports on its website (www.em.gov.bc.ca/geology).

The upper Kitsault River area hosts two past-producing silver mines, Dolly Varden (MINFILE 103P 188) and Torbrit (MINFILE 103P 191), and numerous other prospects that range in size from small showings to developed deposits. The latter include Northstar (MINFILE 103P 189) and Wolf (MINFILE 103P 198). There are four types of mineral deposits: 1) epigenetic copper-gold chlorite-pyrite vein stockwork deposits (*e.g.* Red Point (MINFILE 103P 196) and Homestake (MINFILE 103P 216)); (2) epigenetic silver-lead-zinc quartz-carbonate vein deposits (*e.g.* Wolf); (3) either epigenetic or syngenetic silver-lead-zinc-barium-strontium deposits (*e.g.* Torbrit, Northstar and Dolly Varden) and (4) syngenetic strontium-barium-lead-zinc-silver deposits (*e.g.* Sault (MINFILE 103P 233)). They are all hosted by lower Jurassic volcanic and sedimentary strata, near the top of the Hazelton volcanic arc sequence. There are conflicting opinions as to the origins of some of the deposits. In the absence of new data, this report makes no attempt to resolve the issues. It describes some of the more important occurrences and comments on possible similarities to precious-metal deposits at Red Mountain (MINFILE 103P 086) and Eskay Creek (MINFILE 104B 008).

PREVIOUS WORK

Most of the mineral deposits in the Stewart area were located in the late 1800s and early 1900s. Prospectors moved into the Kitsault River area, north of Alice Arm, in the early 1900s and staked the first discoveries in the upper Kitsault River area in 1913. The principal showings had been found by 1921, when the first phase of production at the Dolly Varden mine came to an end.

The showings in the Kitsault River area are referred to in Ministry of Mines Annual Reports and described in some detail by Hanson (1922, 1935) and Black (1951). Carter and Grove (1972) produced a 1:250 000-scale compilation map of the geology of the Kitsault River area in the early 1970s, and Grove (1986) discussed it in a bulletin on the geology and metallogeny of the "Stewart Complex", a term he applied to the volcanic and sedimentary rocks between the eastern margin of the Coast Plutonic Complex and the western margin of the Bowser Basin. He describes a broad regional zonation of mineral deposits within the Complex and notes the potential for silver deposits in the Alice Arm portion. The area was mapped at 1:50 000-scale by Alldrick *et al.* (1986) and described by Dawson and Alldrick (1986). Alldrick also discusses the stratigraphy of the area in a review of the distribution of volcanic centres in the Stewart Complex (Alldrick, 1989).

The mineral potential of the Stewart Complex has been recognized for over a century (Grove, 1986; Alldrick, 1993). However, over most of that period, precious-metal exploration was solely directed toward finding epigenetic vein deposits. In 1988, two discoveries added considerably to the range of deposit types explored for. The Eskay Creek deposit, a major gold-enriched, subaqueous hot-spring deposit, was discovered 100 km northwest of Stewart and the Red Mountain deposit, a major intrusion-related gold deposit, was found 20 kilometres east of Stewart. These discoveries lead to numerous exploration programs in the Stewart Complex in the late 1980s and early 1990s. Many of them are described in assessment reports filed with the Ministry and available on the Ministry's website.

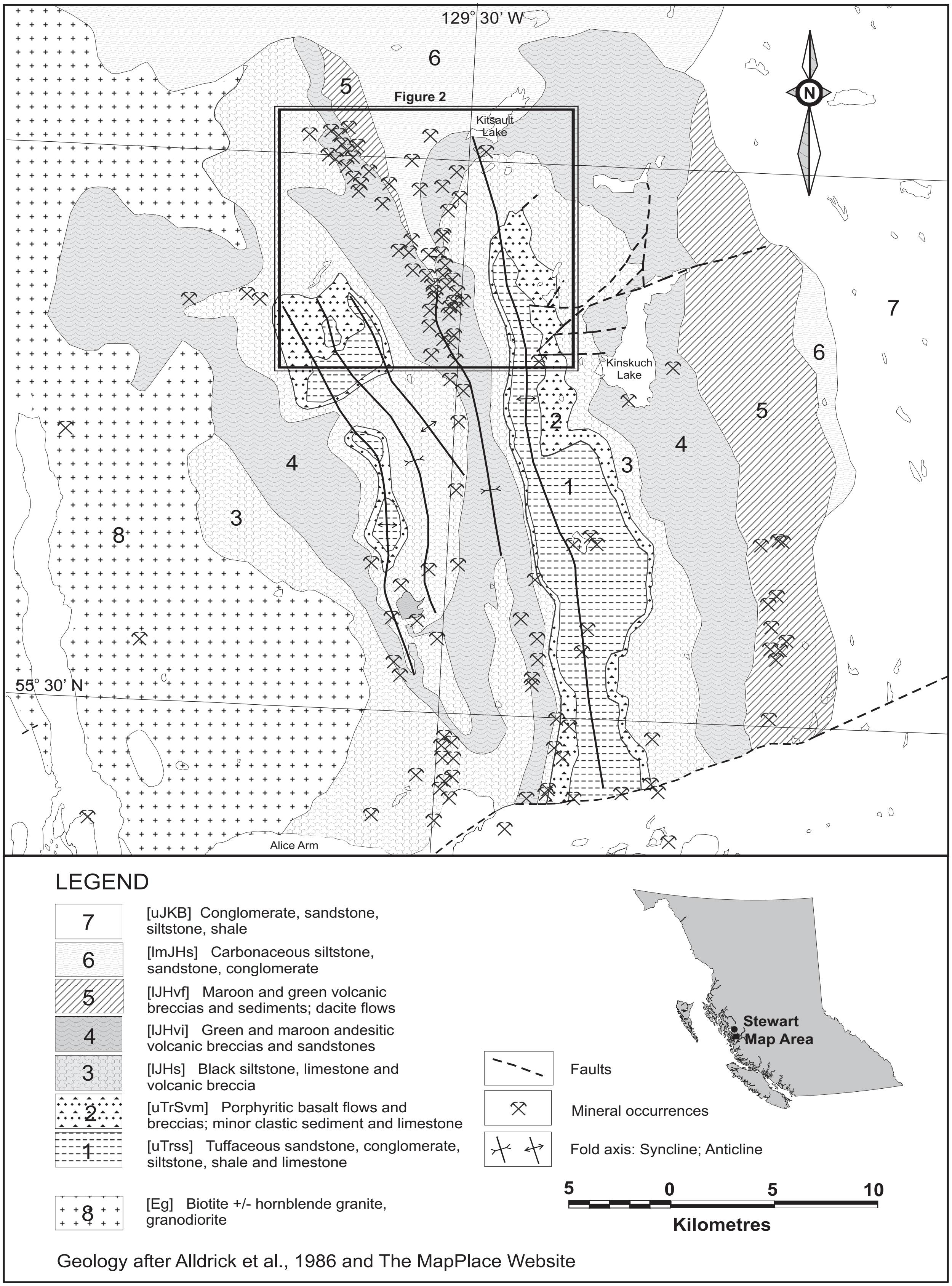

Figure 1. Generalized bedrock geology map of the Kitsault River area showing mineral occurrences and location of area studied.

Although there were no major government mapping programs in the Kitsault River area in the 1990s, several more modest programs helped to define the geology. Godwin *et al.* (1991) used plots of lead isotope values from galena samples from a broad area of northern British Columbia to differentiate between Jurassic and Tertiary-age mineralization. The same year, Greig (1991) mapped southeast of Kitsault Lake. In 1992, Mortensen and Kirkham (1992) obtained an approximate U-Pb zircon age for syngenetic mineralization near Kitsault Lake and, in 1994, Greig *et al.* (1994) mapped the geology of the Cambria Icefield area, including the uppermost part of the Kitsault River drainage. Most recently, Evenchick and Mustard (1996) studied the stratigraphy and structure of Bowser Lake Group sediments on the east side of the Stewart Complex. The geology of the Skeena-Nass area has been compiled by MacIntyre *et al.* (1994a) at 1:250 000-scale and it is this map that is available on the Ministry website.

GEOLOGY

The simplified geological maps of the Kitsault River area (Figures 1 and 2) are adapted from MacIntyre *et al.* (1994a). They are based on the work of Alldrick *et al.* (1986) who identified six stratigraphic units formed during two cycles of arc volcanism. From bottom to top, they include: 1) a thick flysch-siltstone layer (base unseen), topped by black limestone [uTrss]; (2) a mixed succession of locally-pillowed augite, feldspar and olivine porphyritic basalt flows, breccias and derived conglomerates [uTrSvm]; (3) mixed clastic sediment and volcanic breccia capped by a distinctive polymictic (chert or siltstone supported) conglomerate [lJHs]; (4) porphyritic andesitic pyroclastics (tuffs and breccias) and related flows and sills with 10-15% intercalated argillite, limestone and chert [lJHvi]; (5) alternating maroon and green volcanic breccias and conglomerates with discontinuous dacite flows and pyroclastics that are thought to be derived from discrete volcanic centres [lJHvf]; and, (6) black marine, fossiliferous shale, siltstone and wacke [lmJHs].

Units 1 [uTrss] and 2 [uTrSvm] are similar to upper Triassic Stuhini Group strata found elsewhere in northern British Columbia (MacIntryre *et al.*, 1994). Units 3 [lJHs], 4 [lJHvi] and 5 [lJHvf] are broadly correlatable with lower Jurassic rocks of the Hazelton Group, as defined by Grove (1986) in the Stewart area. Unit 3 is equivalent to the Unuk River Formation and Units 4 and 5 include rocks similar to those found in the overlying Betty Creek Formation. Unit 5 is discontinuous in the Kitsault River area and contains felsic rocks near its top that are equivalent in age and setting to Mount Dilworth Formation strata, as defined by Alldrick (1993). Unit 6 [lmJHs] resembles the Salmon River formation. It disconformably overlies older Hazelton Group strata (Dawson and Alldrick, 1986) and is, in turn, overlain by Bowser Lake Group sediments.

The strata are deformed into a series of relatively open, northwest trending, doubly plunging folds that limit the exposure of sub-Bowser Group strata in the Kitsault River area to a belt approximately 40 kilometres long and 25 kilometres wide (Alldrick *et al.*, 1986). The Kitsault River more or less follows the axis of the Kitsault River syncline, a major structure that has infolded volcanic and sedimentary rocks near the top of the Hazelton arc at both ends of the belt. The syncline is bounded by the Varden Glacier anticline to the west and the Mount McGuire anticline to the east (Figure 2). Fold configuration and topography affect the distribution of Units 4 and 5, which host most of the mineral showings in the area (Dawson and Alldrick, 1986).

Although there are relatively few faults mapped in the area, Greig *et al.* (1994) identified a high-angle, northeasterly dipping fault west of Homestake Ridge while mapping around the southern edge of the Cambria Icefield. There may be other unmapped structures of this type, formed during the shortening event that affected Bowser Lake Group and older rocks in the Cretaceous (Evenchick and Mustard, 1996).

Property-scale mapping by Campbell (1959) and Mitchell (1973) suggest that faulting has occurred episodically since the waning stages of arc volcanism. It includes a considerable amount of post-mineral faulting. Devlin and Godwin (1986) and Devlin (1987), show that the northern axis of the Kitsault River syncline has been disrupted by two sets of faults and Drown *et al.* (1990a,b) describe several northwesterly trending structures that splay off a major, northerly trending shear zone (Figure 3a,b).

Although the map area is bounded by rocks of the Coast Range Batholith to the west, there are relatively few intrusions mapped within it. Those present, are (1) subvolcanic intrusions emplaced during or shortly after Stuhini and Hazelton Group volcanism; (2) quartz monzonite intrusions of Eocene-age; and (3) a variety of Late Tertiary, cross-cutting dikes. The subvolcanic variety are relatively common in Unit 4 and are an important feature of the "Copper Belt", west of the headwaters of the Kitsault River (Black, 1951; Carter, 1970; Grove, 1986). Grieg *et al.*, (1994) mapped Goldslide intrusions in the area west of Homestake Ridge. They are similar to intrusions found at Red Mountain, on the north flank of the Cambria Icefield and are approximately contemporaneous with Hazelton volcanism. Greig *et al.* (1995) obtained a U-Pb age of 201.8 +/- 0.5 Ma from zircons from one of the intrusions near Red Mountain and a K-Ar age of 194 +/- 8 Ma from hornblende from a nearby Hazelton Group tuff breccia.

MINERALIZATION

There are numerous mineral occurrences in the Kitsault River area (Figure 1). Compositionally, they conform to three principal types: 1) Copper and gold-rich quartz-chlorite stockwork deposits; (2) silver-rich quartz-sulphate-carbonate deposits; and (3) molybde-

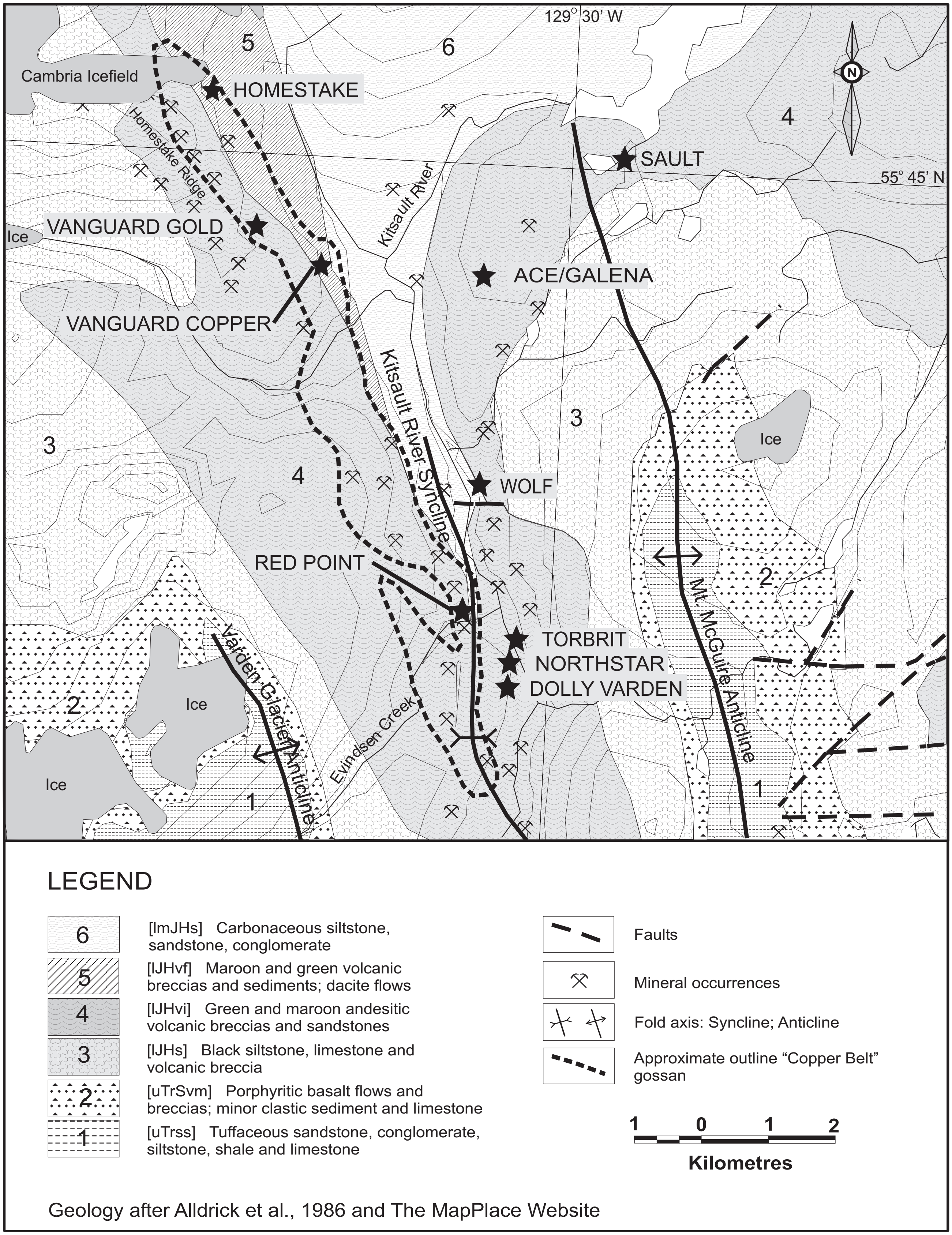

Figure 2. Generalized bedrock geology map of the upper Kitsault River area showing the location of the "Copper Belt" and mineral occurrences discussed in the report.

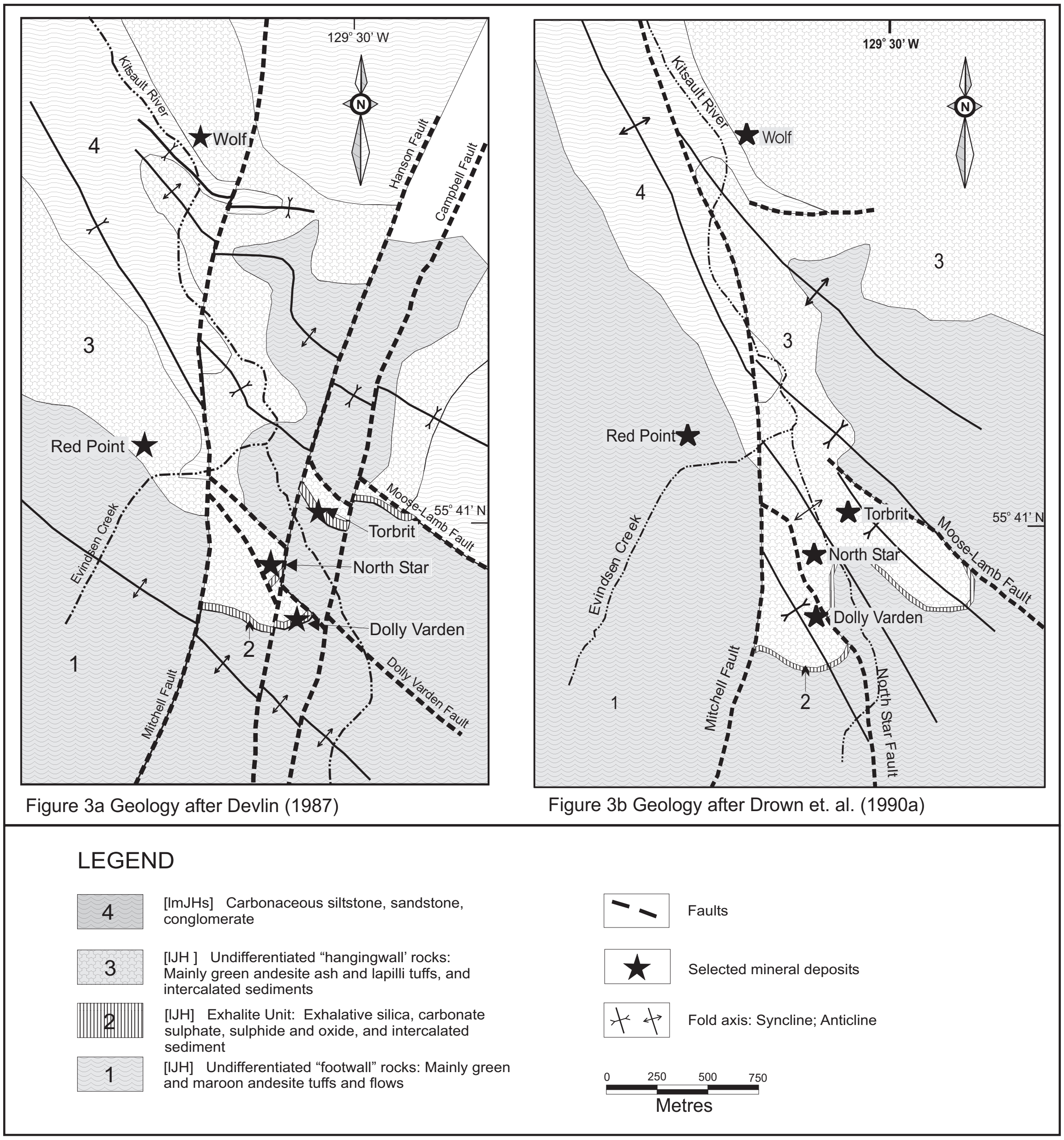

Figure 3a,b. Generalized bedrock geology maps of the upper Kitsault River area showing the structural and stratigraphic relationships inferred by Devlin (1987) and Drown *et al.* (1990a).

num-rich quartz stockwork deposits. The first two types are most abundant and are of particular importance in the upper Kitsault River area. They are considered to be Lower Jurassic in age and formed more or less contemporaneously with the Hazelton volcanic arc (Alldrick *et al.*, 1987; Godwin *et al.*, 1991). The third type is considerably younger; it is associated with a suite of Eocene-age (Alice Arm) quartz monzonite intrusions (Alldrick *et al.*, 1986).

The relationship between the gold-rich and silver-rich deposits in the upper Kitsault River area is uncertain. Although they are both hosted by Hazelton Group rocks below the Salmon River Formation disconformity, they have different styles of mineralization and they are found on different sides of the Kitsault River syncline. The Homestake, Red Point and related copper-gold deposits are in the "Copper Belt" (Black, 1951, Thompson and Michna, 1978), which is an extensive zone of dike injection and gossan development in Unit 4 and Unit 5 on the southwest side of the Kitsault River syncline. The Dolly Varden, Torbrit and related silver deposits occur with fewer dikes and considerably less gossan development in tuffs and breccias in Unit 4 on the northeast flank of the same structure.

The silver-rich, quartz-sulphate-carbonate deposits in the upper Kitsault River area (*e.g.* Dolly Varden and Torbrit) were historically considered to be structurally controlled (Black, 1951; Campbell, 1959; Mitchell, 1973; Thompson and Michna, 1978). However, more recently, Devlin and Godwin (1986) and Devlin (1987) have suggested that they may be exhalative in origin. Tupper and McCartney (1990) provide evidence that suggests that the nearby Sault deposit is stratiform; having formed through exhalation into a restricted marine basin near the top of the Hazelton volcanic arc.

Red Point (MINFILE 103P 196)

The Red Point Cu-Au-Ag prospect (latitude 55º 41' 28'' N, longitude 129º 31' 14'' W) is approximately 24 kilometres north of Alice Arm, on the north side of Evindsen Creek, west of its confluence with the Kitsault River (Figure 2). It is 1.5 kilometres northwest of the Torbrit portal and was linked to the Dolly Varden - Torbrit road by a trail. It is accessible now only by helicopter.

The area was explored by Granby Consolidated Mining, Smelting and Power Company in the early 1910s, and short adits were driven on several of the more attractive copper prospects in the area in the late 1920s. Dolly Varden Mines Limited acquired the area in 1961 and Dolly Varden Minerals Incorporated conducted geological, geochemical and geophysical exploration programs in 1986, locating a wide-spread, precious-metal, soil geochemical anomaly. Three years later, the company trenched and sampled the Red Point and several neighbouring showings and drilled 25 holes for an aggregate length of 2257 metres (Drown *et al.*, 1990b).

The volcanic rocks at the south end of the "Copper Belt" (Figure 2) are predominantly grey-green andesites and andesitic tuffs (Unit 4) that have a northwest strike consistent with their location on the western limb of the Kitsault River syncline (Alldrick *et al.*, 1986; Devlin, 1987; Drown *et. al.*, 1990b). The rocks are intruded by feldspar porphyry dikes ("Kitsault Intrusions") for a distance of approximately 15 kilometres, between the Cambria Icefield and the Kitsault River (Black,1951; Carter, 1970; Mitchell, 1973; Grove, 1986). However, these intrusions are not specifically mapped by Alldrick *et al.* (1986), Devlin (1987) or Drown *et al.* (1990b). They are included with the volcanic rocks.

The rocks are cut by numerous, steep, northwest-trending faults that predate and control much of the later alteration and mineralization, which occurred in stages. First, the rocks were deformed over a broad area and pervasively altered to sericite, quartz and pyrite. The more altered rocks along some of the major northwest-trending faults were then overprinted by potassium feldspar and re-deformed into extensive areas of "crackle-breccia". The brecciated rocks were later altered to chlorite and mineralized with pyrite. Other sulphides were deposited still later. Chalcopyrite, sphalerite and galena occur with chalcedony, quartz, carbonate and chlorite in veins and in the breccia cement (Drown *et al.*, 1990b). The rocks are cut by northeast-trending faults.

The Red Point and other prospects in the area are structurally controlled. They are northwest-trending "replacement zones" or quartz veins that locally contain appreciable amounts of copper, gold and silver. They are widespread and erratically distributed throughout the broad deformation and alteration zone. The rocks are pyritic and form highly gossanous outcrops.

Homestake (MINFILE 103P 216)

The Homestake Cu-Au-Ag prospect (latitude 55º 45' 32'' N, longitude 129º 35' 15'' W) is on Homestake Ridge, between the West Kitsault River and the Kitsault River, south of the Cambria Icefield (Figure 2). It is at the north end of the "Copper Belt", approximately 35 kilometres southeast of Stewart.

The property covers a prominent gossan that was located in the early 1900s and explored for copper and gold prior to the Second World War. Consolidated Homestake Mining and Development Company drove an adit on the Homestake claim in the 1920s and British Lion Mines Limited drove two more on the same structure in the 1930s. MINFILE reports that the latter extracted a small (7.9 tonnes) bulk sample with an average grade of 140 g/t gold, 203 g/t silver, 7.5% copper and 3.8% zinc.

Other prospects on the ridge, including Vanguard Gold (103P 091) and Vanguard Copper (103P 210) deposits were explored by Canex Aerial Explorations Limited in the 1960s. Newmont Exploration of Canada Limited consolidated ownership in the area in the late 1970s. The company interpreted some of the siliceous volcanic rocks as rhyolite and explored the area for volcanogenic massive sulphide deposits. In the mid 1980s, Cambria Resources Limited reinterpreted the accumulated data and changed the exploration focus back to epithermal vein-type deposits. Noranda Exploration Company Limited acquired the property in 1989. It conducted a substantial amount of grid work and drilled twelve holes, for an aggregate length of 1450 metres.

The geology of the area is described by Black (1951), Coombes (1986) and Chinn *et al.* (1990). The ridge is underlain by a northwest-trending package of andesitic agglomerates, flows and related tuffs and intercalated argillic sediments (Units 4 and 5). However, there has been extensive injection of dikes and sills of hornblende feldspar porphyry subparallel to the regional trend. As at Red Point, the intrusions are broadly coincident with the "Copper Belt" gossan. They pre- and post-date mineralization (Coombes, 1986).

The bedded strata and intrusive rocks are cut by northwest and east-trending brittle faults, fractures and breccia zones that have focused fluid flow. The rocks have been sequentially silicified, sericitized, chloritized, carbonatized and locally intensely pyritized. Some of the rocks have also been mineralized with chalcopyrite, sphalerite, galena and trace amounts of arsenopyrite and tetrahedrite. The economically more significant sulphides generally occur with quartz, calcite and lesser barite in vein and stringer stockworks and as pods and blebs in the matrix of the breccias.

Petrographic work suggests a minimum of three stages of vein development. Quartz veins containing pyrite, chalcopyrite and sphalerite are crosscut by carbonate veins and veinlets enriched in galena, arsenopyrite and tetrahedrite, and both of the above are overprinted by barite (Coombes, 1986). Rock and soil geochemical data also suggest multiple events. Copper is enriched with gold at Homestake; however, lead and zinc are more commonly found with silver near the Vanguard prospects. According to Chinn *et al.* (1990), the Vanguard area geochemical anomalies overlie altered volcanic rock on the west side of a major west-dipping fault. The age of the fault is uncertain; however, it marks the eastern contact of the volcanic unit in the area. The sedimentary rocks in the footwall of this fault are barren.

At Homestake, mineralization occurs in a quartz vein stockwork in a zone of intense silica-sericite-pyrite alteration in deformed, brecciated andesite and hornblende feldspar porphyry. The stockwork contains variable amounts of chalcopyrite, galena, sphalerite, pyrite and barite and it locally contains large pods and lenses of chalcopyrite. Higher-grade copper samples are locally strongly enriched in gold and mercury (Black, 1951; Chinn *et al.* 1990). The best copper and gold values at the Vanguard Copper prospect are from a pervasively chloritized, brecciated volcanic rock and the best silver values are from a quartz-carbonate vein (Chinn *et al.*, 1990). MINFILE reports that the Vanguard Copper deposit has an inventory of 11 800 tonnes grading 8.6% copper, 2.4 g/t gold and 141 g/t silver.

Wolf (MINFILE 103P 198)

The Wolf Pb-Zn-Ag property (latitude 55º 42' 27'' N, longitude 129º 31' 01'' W) is on the east side of the Kitsault River, approximately 25 kilometres upstream from Alice Arm and 6 kilometres southwest of Kitsault Lake (Figure 2 and 3 a,b). Prior to the mid-1980s, the property was accessed by the Dolly Varden - Torbrit mine road. It is accessible now by helicopter.

The Wolf deposit was located at the same time as the Dolly Varden and Torbrit deposits and saw considerable exploration in the early 1910s. By 1916, it was expected to supply lower-grade ore to a concentrator proposed for the nearby Dolly Varden mine (Muralt, 1985). In 1964, the Sunshine Mining Company optioned the property, drove an adit and crosscut and further developed the deposit (Carter, 1964). Dolly Varden Mines Limited continued the work, extended the drift and drilled the property four years later.

In 1980, Dolly Varden Minerals Inc. contracted Derry, Mitchener and Booth Limited to make an independent assessment of the reserves at the Wolf and nearby Northstar deposits. It also arranged for Wright Engineers Limited to determine the feasibility of mining the deposits at a rate of 275 tonnes per day, for six months of the year (Thompson and Pearson, 1981). The Company's Annual Report for 1971 shows that, at that time, the Wolf deposit had a resource of 485 324 tonnes grading 336 g/t silver, 0.59% lead and 0.12% zinc.

The geology of the area is described by Carter (1964) and Thiersch (1986). The deposit is composed of three north-northeasterly trending, near vertical, quartz-carbonate "replacement" zones in deformed andesitic tuffs and agglomerates near the apparent top of the Hazleton volcanic arc (Unit 4). The three zones are shear-hosted and may be fault off-set portions of a single occurrence (Thompson and Pearson, 1981). The shear-zone that hosts the mineralization is discordant to regional stratigraphy; however, it is not known whether it cuts through the disconformity below the Salmon River Formation strata (Unit 6) in the core of the Kitsault River syncline (Figure 2).

The zones are composed of quartz and carbonate with local concentrations of barite, jasper and sulphide. They are strongly internally brecciated and they appear to have formed in stages, as a result of intermittent movement on the controlling structure. Early-formed quartz was deposited with pyrite to create a vein with a variety of open space filling textures. This was later brecciated and cemented by a second generation of pyrite with sphalerite, galena and chalcopyrite. This was, in turn, brecciated and the sulphides present were recrystallized, giving the latest generation of pyrite a distinctive "framboidal" texture. The final stage was marked by the introduction of calcite with sphalerite and galena (Thiersch, 1986). The silver minerals were probably introduced relatively late in the deposit's development. Carter (1964) found that pyrite, galena, sphalerite, magnetite, hematite and silver-bearing minerals (pyrargyrite, tetrahedrite and native silver) are in small fractures in zones of fine-grained, crushed quartz, interstitial to larger quartz fragments.

Although inconclusive, sulphur and oxygen isotope studies carried out at the universities of Calgary and Alberta, suggest that the fluid that formed the Wolf deposit was of mixed origin. Sulphur isotope data suggest derivation from magmatic and sea water fluid sources, and oxygen isotope data suggest derivation from volcanic rocks and marine sediments (Thiersch, 1986). Devlin (1987) obtained similar results from samples from the nearby Torbrit mine and both authors conclude that the Wolf and neighbouring Dolly Varden and Torbrit deposits were formed by related hydrothermal systems.

Torbrit (MINFILE 103P 191)

The Torbrit Ag-Pb-Zn deposit (latitude 55º 41' 14'' N, longitude 129º 30' 21'' W) is on the east side of the Kitsault River, approximately 23 kilometres upstream from Alice Arm (Figure 2). In the 1920s, access was by trail or narrow-gauge railway from Alice Arm. In the mid-1940s, the railway was replaced by a road. Since the late 1980s, it has been accessible only by helicopter.

The Torbrit deposit was located and explored while the neighbouring Dolly Varden mine was in production. It was first developed in the mid to late-1920s, when a small tonnage of higher-grade ore was removed and processed through a small (45 tonnes per day) mill. The operation closed in 1930. Torbrit Silver Mines Limited bought the property in 1946 and subsequently built and operated a

350 tonnes per day, hydroelectric-powered mill, flotation concentrator and cyanidation plant. The mine produced 1 251 387 tonnes of ore yielding 579 996 kilograms of silver (80% in concentrate shipped to Trail and 20% as bullion), 3.5 kilograms of gold, 4 868 323 kilograms of lead and 283 037 kilograms of zinc between 1949 and 1959. MINFILE shows that it has a residual resource of 786 285 tonnes grading 311.90 g/t silver, 0.42% lead and 0.50% zinc.

The main deposit (Figures 2 and 3 a,b) is a crudely arcuate, northwest-plunging lens within an otherwise sub-economic sheeted "vein" in a moderately northwesterly dipping shear zone that cuts massive Hazelton volcanic rocks (Unit 4). The higher-grade, mineable zones are defined by assays and are conformable with the main vein. Early workers considered that the deposit formed through replacement of breccia along a tensional fault system (Black, 1951; Campbell, 1959; Mitchell, 1973). According to Campbell, the controlling breccia zone was likely deformed and folded prior to the introduction of the fluid that formed the "vein" and the economically significant portion formed where the shear was folded about a tight synformal axis. The mineralized lenses plunge to the northwest, parallel to the axis of this minor fold. Campbell (1959) notes the presence of horse-tail veins extending into the hangingwall of the deposit and an abundance of more or less altered country-rock fragments in its footwall.

Mitchell (1973) describes two stages to the mineralization. In the first, he suggests that breccia that formed along a major structure underwent mesothermal alteration; it was pervasively altered to quartz and carbonate and mineralized with pyrite. In the second, he suggests that the altered breccia was cross-cut by a series of high-angle faults and the original structure was reopened and mineralized during a later epithermal event. He concluded that the Torbrit, Northstar and Dolly Varden deposits were part of a single replacement vein deposit that was later disrupted by faulting.

The main vein at Tobrit is composed of barite, three varieties of silica (quartz, jasper and chalcedony) and carbonate. Where mineralized, it also contains small amounts of sulphide and oxide (magnetite, hematite, pyrite, sphalerite, galena, chalcopyrite, tetrahedrite, pyrargarite (ruby silver)) minerals and traces of native silver. The vein is compositionally banded and it is also colour-banded, commonly subparallel to deposit contacts and to the schistocity of the surrounding rock. Its gangue minerals contain vugs lined by quartz crystals with well-shaped terminations. In some localities, the deposit has a pronounced mottled appearance as different gangue mineral assemblages selectively replace country-rock fragments (Campbell, 1959).

Campbell (1959) analyzed crustiform barite samples from Torbrit by X-ray fluorescence and determined that they contained between 0.52 and 1.05% strontium. He also looked for systematic variation in Sr/Ba ratio in barite samples from throughout the mine, but did not find it. Barite Sr/Ba ratios are controlled both by temperature of formation and the Sr/Ba ratio of the coexisting fluid and Campbell concluded that both must have varied within the deposit during deposition. Campbell also used sphalerite composition data to obtain a preliminary temperature estimate (270º C) for the deposit. He concluded that the occurrence was intrusion-related and epigenetic in origin, possibly formed during deformation in the late Cretaceous to early Tertiary period.

In 1985, Devlin mapped parts of the upper Kitsault River valley at 1:5000 and 1:2000 scales to establish the stratigraphic and structural setting of the principal deposits and related showings (Figure 3a). He also studied the petrography and lithogeochemistry of the host rocks and determined whole-rock potassium-argon age dates. In addition, he studied the sulphur, oxygen, carbon and lead isotope contents of selected minerals. Based on the above studies, on the presence of sub-rounded ore fragments in tuffs found in the hanging wall of the deposit, and on the recognition of a stockwork vein system in the footwall of some of the deposits, Devlin concluded that the Torbrit, Northstar and Dolly Varden deposits were fault off-set segments of a single stratiform deposit (Devlin and Godwin, 1985; Devlin, 1987).

Devlin (1987) mapped a thick succession of shallow-water Hazelton Group volcanic and related volcano-sedimentary rocks under the fossiliferous sediments (Unit 6) exposed in the core of the northwest-plunging Kitsault River syncline. Within it, he identified a distinctive silica, carbonate, sulphate and sulphide-bearing horizon that he considered to be exhalative in origin. His mapping shows that the unit is underlain by a minimum 1200 metres of weakly-altered, green-maroon basaltic tuff; green-maroon porphyritic andesite; and green andesitic shard tuff (Unit 4). It also shows that it is overlain by approximately 1000 metres of pale grey basaltic to andesitic tuff; maroon basaltic to andesitic ash-lapilli tuff; dark green andesite tuff; grey-green porphyritic andesite; and pale green andesitic ash tuff (Units 4 and 5).

The exhalative unit can be traced for several kilometres along strike on the northeast side of the Kitsault River syncline. According to Devlin (1987), it hosts Dolly Varden, Northstar and Torbrit deposits and exhibits regional-scale zonation. He suggests that differences between the deposits are consistent with changing fluid chemistry, brought about by mixing of exhalative fluids and sea water, and differing depths of deposition. The horizon shows gradation from a silica-sulphide exhalite facies (Dolly Varden), through a carbonate-sulphate-sulphide exhalite facies (Northstar), to a sulphate-oxide-sulphide exhalite facies (Torbrit). The Dolly Varden deposit is inferred to have formed under less oxidizing, deeper water conditions than were found at Torbrit (Devlin and Godwin, 1986; Devlin, 1987).

Stable isotope data for selected samples from Wolf, Torbrit, Northstar and Dolly Varden indicate that the sulphur in the sulphide species may have originated from a source that was predominantly magmatic, and that found in the associated barite most likely came from oxygenated lower Jurassic seawater. The oxygen isotopes in barite, quartz and carbonate are compatible with a sedimentary marine origin and derivation from heated (ca. 245º C) sea water (Devlin, 1987).

Lead isotope ratios for galena crystals from the Wolf, Torbrit, Northstar, Dolly Varden and Red Point deposits cluster with those of other Early Jurassic deposits in the Stewart-Iskut area (Godwin *et al.*, 1991), suggesting that the mineralization is penecontemporaneous with the development of the Hazelton volcanic arc (Devlin, 1987). However, three volcanic rocks collected in the area gave whole-rock potassium-argon age dates (68.1 - 72.2 +/- 2.5 Ma.) suggesting a Late Cretaceous age of formation, inconsistent with the inferred age of the Hazelton volcanic arc. The samples are thought to have suffered argon loss during lower-greenschist facies metamorphism (Devlin, 1987).

Mapping around the Torbrit and other deposits shows considerable structural complexity in the Lower Jurassic Hazelton volcanic and sedimentary rocks on the east flank of the Kitsault River syncline (Alldrick *et al.*, 1986). According to Devlin (1986), rocks in the nose of the syncline are cut by near-vertical, northwest-trending structures that down-drop to the west. Later, near-vertical, north to northeast trending faults display moderate up and down motion (Figure 3a). Some of the post-mineral faults host late lamprophyre dikes. Drown *et al.* (1990a,b) also show that the silver deposits originally formed as a single occurrence; however, they suggest a different fault arrangement for splitting them up (Figure 3b).

Dolly Varden Minerals Inc. drilled a single hole under the Torbrit deposit in 1990, as part of a major exploration program for exhalative silver deposits associated with the known deposits in the area (Drown et. al., 1990a; McGuigan and Melnyk, 1991). The hole was collared to the northwest of the Torbrit glory hole and intersected 30 metres of "clastic" chalcedonic quartz, barite and minor sulphide. Analysis of core samples indicated anomalous concentrations of silver, copper, lead and zinc.

Northstar **(MINFILE 103P 189)**

The Northstar Ag-Pb-Zn deposit (latitude 55º 41' 06'' N, longitude 129º 30' 30'' W) is on the west side of the upper Kitsault River, approximately 23 kilometres north of Alice Arm (Figure 2). It is across the river from the Torbrit mine and can only be accessed by helicopter.

The deposit was located at approximately the same time as the Dolly Varden and three adits had been driven on it, and several high-grade bulk samples had been removed by the time the Dolly Varden mine closed in 1930. Torbrit Silver Mines Limited explored the deposit while its Torbrit mine was in operation but felt that the grade was too low to allow for production. Derry, Mitchener and Booth Limited resampled and redrilled the Northstar deposit in 1979/80 and identified a diluted reserve of 128 424 tonnes grading 401.4 g/t silver, using a 137 g/t silver cut-off (Thompson and Pearson, 1981). This reserve, along with comparable resource data for the Wolf deposit, was factored into a feasibility study that was then being conducted by Wright Engineers Limited.

Early workers (Black, 1951; Mitchell, 1973) described the Northstar deposit (Figure 2) as a high-grade lens in a replacement "vein" in Hazelton Group volcanic rocks (Unit 4). The vein strikes northeast and has a moderate to steep northwest dip. The deposit is cut by minor faults subparallel to its contacts and by lamprophyre dikes that have a similar strike but a more vertical dip.

Although it is less well documented than the Torbrit occurrence, the Northstar deposit is reported to be composed of barite, quartz and carbonate and to display similar banding and crustiform textures to those found across the river. The vein contains minor amounts of sulphide and sulphosalt minerals (pyrite, marcasite, galena, sphalerite, chalcopyrite, pyrargarite and argentite) and native silver. However, they are unevenly distributed and the mineable part is a tabular body within the plane of the vein. Devlin and Godwin (1986) and Devlin (1987) consider the Northstar deposit to be exhalative in origin and, based on the lack of oxide minerals, suggests that it may have formed in slightly deeper water, under slightly less oxidizing conditions than existed at Torbrit.

Dolly Varden Minerals Inc. applied Devlin's exhalative model to the Dolly Varden area and conducted major exploration programs in 1989 and 1990. It drilled the Northstar deposit down dip of the main adit and located the mineralized "exhalite" horizon below an andesitic debris flow unit. The "exhalite" unit is described as having a lower carbonate-rich (silica-calcite-barite) facies that is essentially barren and an upper sulphide and oxide-bearing facies that is weakly mineralized. The latter contains knots and patches of pyrite and trace amounts of chalcopyrite, honey-coloured sphalerite, galena and jasper. It is partially fragmental (Drown et. al., 1990a and McGuigan and Melnyk, 1991). Some of the holes drilled through the "exhalite" unit intersected substantial thicknesses of chlorite-calcite-pyrite alteration stockwork in its footwall. (Drown et al., 1990a).

Dolly Varden **(MINFILE 103P 188)**

The Dolly Varden Ag-Pb-Zn mine (latitude 55º 40' 55'' N, longitude 129º 30' 32'' W) is on the west side of the upper Kitsault River, approximately 22 kilometres upstream from Alice Arm (Figure 2). It was the first mine opened in the area and it triggered the development of much of the early infrastructure. It is accessible now by helicopter.

The original Crown-granted claim was located in 1910. By 1917, ore shoots at Dolly Varden were sufficiently well delineated that Dolly Varden Mines Company arranged for a contractor to build a narrow-gauge railway up the valley from Alice Arm. Unfortunately, the cost proved to be far higher than anticipated and the mining company was forced into bankruptcy. The contractor operated the mine between 1919 and 1921 and shipped high-grade "direct shipping" ore to smelters at Anyox and Tacoma (Muralt, 1985). Including intermittent production between 1935 and 1940, the mine produced 33 434 tonnes of ore containing 42 451 kilograms of silver. According to MINFILE, it has an inventory of 42 633 tonnes grading 754.1 g/t silver.

The Dolly Varden deposit was developed on five levels and several sublevels, and from three small glory holes. Early workers, including Black (1951), describe a single, arcuate, north-dipping replacement “vein” within a package of massive, altered and pyritic volcanic agglomerates and tuffs (Unit 4). The deposit is composed of quartz with lesser carbonate, barite and pyrite, and trace amounts of galena, sphalerite, chalcopyrite, tetrahedrite, pyrargarite and native silver. It is banded, ranges in colour from white through grey to black and it contains fragments of locally derived wallrock. The economic minerals are in relatively limited shoots within the vein. Sulphide contents are thought to increase with depth. Near surface, the shoots are strongly enriched in native silver and the glory hole stopes are reported to have yielded bonanza grades. Controls on the ore shoots are uncertain; however, Black (1951) notes their proximity to a major synclinal fold axis and Mitchell (1973) discusses the significance of cross-cutting structures.

Devlin and Godwin (1986) show that the deposit is bounded on the north by the Dolly Varden fault, an early northwest-trending structure and is cut by moderate to steep north to northeast-trending faults, some of which contain post-mineral lamprophyre dikes. To the west, the deposit terminates at the Mitchell Fault (Figure 3a). They also suggests that a major northwesterly trending fault (Hanson Fault) may have affected water depth during deposition. Devlin and Godwin (1986) divide the Dolly Varden deposit into western and eastern portions, based on mineralogical differences and suggests that the higher sulphide content found in the eastern portion may reflect exhalation in deeper water than was found further west or further north. However, Drown *et al.* (1990a) show no sign of the Hanson Fault (Figure 3b).

Dolly Varden Minerals Inc. traced the mineralized horizon in 1989 and drilled four holes in 1990 testing for the downdip extension of the mineralized zone. The holes intersected several zones of possible “exhalite” - a quartz-sulphide breccia composed of jasper, chalcedonic quartz and pyrite with trace amounts of economic sulphides. Two of the holes also encountered chlorite-calcite-pyrite stockwork alteration in the footwall of the deposit. The hostrock is similar to that found under the Northstar deposit (Drown *et al.*, 1990a; McGuigan and Melnyk, 1991).

Sault:Kit:Frog:Kitsault (MINFILE 103P 233)

The Sault property (latitude 55º 45’ 04’’ N, longitude 129º 29’ 24’’ W) includes several Zn-Pb-Ag-Sr-Ba prospects on the south shore of Kitsault Lake. It is at the head of the Kitsault River, approximately 30 kilometres upstream from Alice Arm (Figure 2). Access is by helicopter or float plane.

The showings were located in 1966 and explored intermittently until 1984. That year, Cominco Limited undertook a variety of geological, geochemical and geophysical surveys and drilled eight holes for a total length of 1269 metres (Tupper and McCartney, 1990). The property was acquired in 1988 by Oliver Gold Corporation (50%), Aber Resources Limited (25%) and Tanqueray Resources Limited (25%). The joint venture partners conducted regional and local exploration programs and the following year drilled a further five holes for an aggregate length totaling 998 metres (Tupper and McCartney, 1990). Lac Minerals Limited held the property in the mid-1990s (Sieb, 1995).

The Sault property (Figure 2) straddles the disconformity mapped at the top of the Hazelton volcanic arc. It is underlain by volcanic and sedimentary rocks (Units 4 and 5) and by fossiliferous sediments (Unit 6). The rocks are draped over the axis of the Mount McGuire anticline (Alldrick et. al., 1986) and the strata commonly display easterly to northeasterly strikes and relatively shallow dips towards the north or northwest. Greig (1991), mapping in an area under the disconformity to the southeast of Kitsault Lake, found a significant but volumetrically small amount of intermediate to felsic volcanic and associated clastic rocks on top of more abundant maroon and green andesitic pyroclastic rocks. The mineralized rocks near Kitsault Lake are underlain by feldspar-rich andesite to rhyolite tuff and lesser epiclastic material and overlain by andesitic to basaltic tuff, intercalated with minor flows and intermixed with epiclastic material.

The mineralization is in a carbonate unit interbedded with the volcanic rock, a short distance below the disconformity. The unit is up to 8 metres thick; however, rapid facies variation and block faulting have made it difficult to trace downdip. It includes a lower section of metalliferous carbonate diamictite, limestone and mudstone; a central volcaniclastic interval; and an upper sequence of laminated carbonate, sulphate and sulphide that contains a minor amount of tuff, chert and volcanic rock (Tupper and McCartney, 1990). The carbonate is crenulated and has micro-folds that plunge at a shallow angle to the north-northeast.

Tupper and McCartney (1990) refer to company reports by MacRobbie, written in 1988, that suggest that the mineralized carbonate deposits may be restricted to syn-sedimentary grabens that acted as traps for local accumulations of carbonate, sulphate and minor sulphide mineralization. The carbonate unit has been traced for approximately 5 kilometres along strike; however, it may extend further to the southwest. Mortensen and Kirkham (1992) report finding similar rocks including “1-2 cm thick conformable (?) layers of pale, fine-grained, sphalerite” in thinly laminated sedimentary rocks in drill core on the Ace/Galena (103P 208) Ag-Pb-Zn property, 2.5 kilometres southwest of the “Showing Lake” occurrence at Sault.

The Ace/Galena is otherwise described as being composed of silver-rich galena stringers in a bleached pyritic tuff in the footwall of a quartz-breccia vein that incorporates fine-grained fragments of country rock. The vein is controlled by a northeast-trending, moderate northwest-dipping fault that projects towards the Sault property (Carter, 1968).

Although the mineralized carbonate at Sault contains laminated to bedded and locally framboidal pyrite, fine-grained sphalerite and galena and locally well-bedded celestite, metal values are generally low. Drillhole K89-11 contained the best intersection reported in 1989. It assayed 1.3% zinc, 0.12% lead and 26.5 g/t silver over 4.95 metres (Tupper and McCartney, 1990). The sulphate at Sault was originally described as barite; however, Blackwell (1986) submitted samples for X-ray fluorescence analysis and found that they are highly enriched in strontium and contain only modest (0.1% to 0.5%) amounts of barium.

Mortensen and Kirkham (1992) analyzed zircons from a feldspar-phyric unit (probably a welded dacitic ash-flow tuff) 100 to 200 metres stratigraphically below the mineralized horizon and determined a U-Pb age of 193.5 +/- 0.4 Ma. This is an approximate age for the mineralization and for the cessation of volcanism in the upper Kitsault River area.

DISCUSSION

The subvolcanic, feldspar porphyry dike swarm that defines the "Copper Belt" on the western side of the Kitsault River syncline is an important control on mineralization in the upper Kitsault River area. Thompson and Michna (1987) suggest that the dikes are part of a "diorite to granodiorite intrusion" complex and show the mineralization is epigenetic and epithermal in origin. They describe four zones:1) copper and gold mineralization within and along the northeastern extremity of the "intrusion" (*e.g.* Homestake); (2) copper within the "intrusion" and copper-silver within volcanic rocks adjacent to the "intrusion" (*e.g.* Vanguard showings); (3) silver and silver-lead showings in volcanic rocks further away from the intrusion (*e.g.* Dolly Varden, Torbrit) and (4) more distal silver properties further east, including the Sault occurrence. The deposits are zoned from high-temperature in the west to low-temperature in the east.

The "Copper Belt" dikes are poorly differentiated but they are known to include Goldslide-type intrusions similar to those mapped at Red Mountain, 30 kilometres to the northwest (Greig *et al.*, 1994). Rhys *et al.* (1995) suggest that the Red Mountain gold deposit has "porphyry" affinities and speculate that the intense alteration found at Red Mountain may have been caused by fluids derived from a hornblende-biotite-quartz porphyry phase of the Goldslide intrusion suite. The fluids altered intrusive and volcanic rocks at Red Mountain to sericite-quartz-pyrite and chlorite-K-feldspar-sericite-titanite. They then formed tourmaline veins, altered the rocks to K-feldspar-pyrite-titanite-actinolite and deposited a semi-tabular body of gold-silver mineralization within an overprinted pyrite-pyrrhotite stockwork.

Some of the dikes in the "Copper Belt" are similarly intensely altered and mineralized and may have contributed the large volumes of porphyry-type fluid required to cause the extensive alteration and mineralization observed in the area. Others are described as being post mineral, constraining the time of alteration (Coombes, 1986). The Homestake and Red Point deposits in the "Copper Belt" appear to have been formed during a protracted period of alteration and mineralization. Early-formed copper-gold mineralization is overprinted by somewhat later-formed silver-lead-zinc mineralization and barite.

Although there are few coeval dikes mapped on the east side of the Kitsault River syncline, the Dolly Varden and Northstar deposits are partially underlain by a stockwork breccia that is described as being similar in appearance to rock found at Red Point and Homestake (McGuigan and Melnyk, 1991). The breccia is cemented by quartz, chlorite and pyrite with minor amounts of chalcopyrite and sphalerite. Drown *et al.* (1990a,b) note that similar rock is found in alteration zones underlying volcanogenic massive sulphide deposits and they suggest that the "Copper Belt" alteration zone may have formed in the footwall of the Dolly Varden - Torbrit exhalative horizon.

In an unpublished report, Mitchell (1973) suggests that the deposits in the upper Kitsault River area may be controlled by a ring structure that formed late in the development of the Hazelton volcanic arc. He suggests that the structure focused emplacement of the dike swarm on the west limb of the Kitsault River syncline and developed the breccia zone found on the east limb. The breccia was later silicified and carbonatized, re-brecciated near cross-faults and mineralized to created the ore-shoots found at Torbrit, Northstar and Dolly Varden. Mitchell (1973) suggests that the Wolf deposit formed along one of the cross-structures. It has had a prolonged history of mineralization and deformation, starting with deposition of quartz and pyrite (but without gold) and ending with precipitation of carbonate, sphalerite and galena, with silver

Devlin and Godwin (1986) and Devlin (1987) provide a different interpretation for the origin of the deposits. They suggest that the Torbrit, Northstar and Dolly Varden deposits are stratiform and exhalative and that differences between them may be attributable to formation under differing depths of water. Based on isotope studies, Devlin (1987) suggests that the deposits are lower Jurassic in age, formed during the development of the Hazelton volcanic arc and that the fluids that formed them may have included seawater. Thiersch (1986) found sufficient points of similarity between the sulphur and oxygen isotopes in the various minerals at Wolf and Torbrit to conclude that, whatever their origin, the deposits were probably formed by related hydrothermal systems.

The Eskay Creek Au-Ag-Cu-Zn subaqueous hot-spring deposit, 120 kilometres to the northwest, formed during the waning stages of volcanism in the Hazelton volcanic arc. It formed as a result of intra-arc rifting that occurred at an equivalent time to the transition between Unit 5 and Unit 6 in the Kitsault River area. According to Roth *et al.* (1999), the stratigraphic succession at Eskay Creek includes, from bottom to top, basal andesite, marine sedimentary rocks, intermediate to felsic volcaniclastic rocks, rhyolite flow domes, (mineralized) carbonaceous shales and basalts. Unit thickness and facies distribution at Eskay Creek suggest that the rhyolite domes were emplaced along active faults and breached the sea floor, partially filling an adjacent basin or trough with debris. The intrusions focused fluid flow which led to the creation of chimneys and mounds on the seafloor. These later collapsed to form barite and clastic sulphide-sulphosalt debris that was redeposited with argillaceous sediment on top of the volcaniclastic detritus in the basin.

The Sault prospects also formed in small basins formed through intra-arc rifting during the waning stages of Hazelton arc volcanism. They are locally thick-bedded exhalative deposits that are predominantly composed of carbonate and sulphate. They contain a small amount of sulphide but lack appreciable precious-metal content. The basins may have been simultaneously filled with clastic debris as the rocks show locally extreme thickness and facies variation. The metals present in the Sault exhalite (strontium, barium, silver, lead and zinc) deposit are similar to those found in the silver-rich deposits in the nearby upper Kitsault River valley and they may be genetically related.

SUMMARY AND CONCLUSIONS

Hazelton Group strata in the Alice Arm area are well mineralized and McIntyre *et al.*, (1994b) put the Alice Arm tract (JH26) in second place, after the Brucejack Lake (JH30) area, in their ranking of the metallic mineral potential of the Skeena - Nass area. The volcanic and sedimentary rocks in the Alice Arm area contain numerous mineral prospects and host two past producing silver mines near the head of the Kitsault River. The Dolly Varden and Torbrit mines produced 622 407 kilograms of silver between 1919 and 1959.

Based on published accounts, there are four, possibly related types of showings in the Upper Kitsault River area: These include: 1) epigenetic Cu-Au chlorite-pyrite vein deposits (*e.g.* Red Point, Homestake); (2) epigenetic Ag-Pb-Zn quartz-carbonate vein deposits (*e.g.* Wolf); (3) either epigenetic or syngenetic Ag-Pb-Zn-Ba deposits (*e.g.* Torbrit, Northstar, Dolly Varden); and (4) exhalative Sr-Ba-Pb-Zn-Ag deposits (*e.g.* Sault).

The deposits appear to be zoned outward from the Homestake occurrence in the "Copper Belt" as there is a rapid reduction in copper and gold and an increase in silver, lead and zinc in the occurrences found to the south and east. The deposits appear to have formed during two principal stages of mineralization. The copper and gold-rich deposits were formed during an early, sulphide-rich event coeval with the emplacement of dikes on the west side of the Kitsault River syncline. The silver-rich deposits formed during a later, relatively sulphide-poor event that overprinted the copper and gold deposits on the west side of the syncline and formed separate deposits on the east side. The fluids that formed the Dolly Varden and Torbrit deposits may have been cooler and more oxidized than those that formed the copper and gold-rich deposits. The strontium-rich deposits at Sault may be surface expressions of the second, silver-rich phase of mineralization.

Copper and gold-rich mineralization on the west side of the Kitsault River syncline is structurally controlled and related to the emplacement of subvolcanic dikes that may be emplaced along a ring structure. Volcanic, sedimentary and intrusive rocks are fractured and locally intensely altered to potassium feldspar, sericite and chlorite. The fractures contain abundant pyrite, lesser chalcopyrite and native gold. This style of mineralization has much in common with the Red Mountain Au-Ag deposit, which is hosted by similar rocks on the northern side of the Cambria Icefield.

There are few reported coeval dikes underlying the mineral deposits on the east side of the Kitsault River syncline and the controls on mineralization are less certain. Although there is some development of a chlorite-pyrite rich stockwork, similar to that found in the "Copper Belt", underneath the silver deposits at Dolly Varden and Northstar, the deposits themselves are low in sulphide content. They are composed of quartz, carbonate, barite, traces of pyrite, sphalerite, galena, chalcopyrite, tetrahedrite, pyrargarite and native silver.

The Dolly Varden, Torbrit and Northstar deposits may be epigenetic "replacement" deposits, as suggested by Campbell (1959), Mitchell (1973) and others, or exhalative, as proposed by Devlin and Godwin (1986) and Devlin (1987). In the absence of new data, or access to the old workings, this review is unable to resolve the issue. However, it seems likely that all the deposits are genetically related and formed at relatively shallow depth.

The Sault area prospect has a similar geochemical signature to those around Tobrit and may also be related. It appears to be exhalative in origin. The mineralization is in small basins that formed during the waning stages of Hazelton volcanism. The basins filled with clastic detritus, carbonate, sulphate and trace amounts of sulphide. The geologic setting appears to be similar to that of the Eskay Creek Au-Ag deposit.

The mineral deposits in the upper Kitsault River formed at a time of considerable tectonic instability during the waning stages of Hazelton arc volcanism. Subvolcanic intrusions appear to have provided magmatic fluid and heated sea-water brines. Brittle faults appear to have provided tensional sites for epigenetic mineralization and developed sea floor grabens for syngenetic deposits. The data show that there is considerable potential for several styles of precious-metal bearing mineralization in Hazelton Group strata in the Alice Arm area. In addition to silver-rich deposits similar to those previously found at Dolly Varden and Torbrit, there is excellent potential for gold and silver-rich deposits similar to those found at Red Mountain and Eskay Creek. This study reaffirms the high mineral potential of the area.

ACKNOWLEDGMENTS

The author gratefully acknowledges the contributions of numerous public and private sector geologists and others in the preparation of this report. In particular, he would like to thank Alex Burton, Fred Christensen and Steven Coombes for their insights into the geology and exploration history of the Kitsault River area; and Dani Alldrick, Gib McArthur, Garry Payie and Tom Schroeter for their comments on reviewing the article. Maggie Dittrick provided invaluable assistance in preparing the figures.

REFERENCES

Alldrick, D.J. (1989): Volcanic centres in the Stewart Complex (103P and 104A,B), *in* Geological Fieldwork 1988, *British Columbia Ministry of Energy, Mines and Petroleum Resources*, Paper 1989-1, pages 223-240.

Alldrick, D.J. (1993): Geology and metallogeny of the Stewart Mining Camp, northwestern British Columbia; *British Columbia Ministry of Energy, Mines and Petroleum Resources*, Bulletin 85, 105 pages.

Alldrick, D.J., Brown, D.A, Harakal, J.E., Mortensen, J.K. and R.L. Armstrong (1987): Geochronology of the Stewart mining camp (104B/1), *in* Geological Fieldwork 1986, *British Columbia Ministry of Energy, Mines and Petroleum Resources,* Paper 1987-1, pages 81-92.

Alldrick, D.J., Dawson, G.L., Bosher, J.A. and Webster, I.C.L. (1986): Geology of the Kitsault River area (NTS 103P). *British Columbia Ministry of Energy, Mines and Petroleum Resources*, Open File Map 1986-2, Scale 1:50 000.

Black, J.M. (1951): Geology and mineral occurrences of the upper Kitsault valley; *in British Columbia Ministry of Energy, Mines and Petroleum Resources* Ann. Rept. 1951, pages A76-A83.

Blackwell, J.D. (1986): The geology and geochemistry of the Sault 1, 3, 4, 5, 7 and 8 mineral claims, Skeena Mining Division; *British Columbia Ministry of Energy, Mines and Petroleum Resources*, Assessment Report # 15 364, 11 pages plus maps

Campbell, F.A. (1959): The geology of Torbrit silver mine; *Economic Geology*, Volume 54, pages 1461-1495.

Carter, N.C. (1964): Wolf (Dolly Varden Mines Limited) in Report of the Minister of Mines; *British Columbia Ministry of Mines and Petroleum Resources*, page 41-43.

Carter, N.C. (1968): Ace, Galena; *in* Report of Minister of Mines and Petroleum Resources, 1968; *British Columbia Ministry of Energy, Mines and Petroleum Resources*, pages 56-58.

Carter, N.C. (1970): Red Point, Copper Cliff, Dan Patch, Dana, Surprise, *in* Geology, Exploration and Mining, *British Columbia Ministry of Energy, Mines and Petroleum Resources*, pages 81-86.

Carter, N.C. and Grove E.W. (1972): Stewart, Anyox, Alice Arm and Terrace areas (103P/S1/2); *British Columbia Ministry of Energy, Mines and Petroleum Resources*, Preliminary Map 8, 1:250 000-scale.

Chinn, G., Baerg, R. and Wong, T. (1990): Report on the Homestake Property, Skeena Mining Division; *British Columbia Ministry of Energy, Mines and Petroleum Resources*, Assessment Report # 20 017, 28 pages plus maps.

Coombes, S.F. (1986) Assessment Report on the Cambria Group, Skeena Mining Division; *British Columbia Ministry of Energy, Mines and Petroleum Resources*, Assessment Report # 16 034, 29 pages plus maps

Dawson, G.L., and Alldrick, D.J. (1986): Geology and mineral deposits of the Kitsault valley (103P/11,12); *in* Geological Fieldwork 1985, *British Columbia Ministry of Energy, Mines and Petroleum Resources*, Paper 1986-1, pages 219-224.

Devlin, B.D. (1987): Geology and genesis of the Dolly Varden silver camp, Alice Arm area, northwestern British Columbia; Unpublished M.Sc. Thesis, *The University of British Columbia*, 131 pages plus maps.

Devlin, B.D. and Godwin, C.I. (1986): Geology of the Dolly Varden camp, Alice Arm area, (103P/11,12); *in* Geological Fieldwork 1985, *British Columbia Ministry of Energy, Mines and Petroleum Resources*, Paper 1986-1, pages 327-330.

Drown, T., McGuigan, P. and Melnyk, W. (1990a): 1989 North Star exploration program on the Dolly Varden property, Skeena Mining Division; *British Columbia Ministry of Energy, Mines and Petroleum Resources*, Assessment Report # 20 033, 34 pages plus maps.

Drown, T., McGuigan, P. and Melnyk, W. (1990b): 1989 Geological and diamond drilling report on the Dolly Varden property (Gold Belt), Skeena Mining Division; *British Columbia Ministry of Energy, Mines and Petroleum Resources*, Assessment Report # 20 041, 44 pages plus maps.

Evenchick, C.A. and Mustard, P.S. (1996): Bedrock geology of north-central and west-central Nass River map area, British Columbia; *in* Current Research 1996-A; *Geological Survey of Canada*, pages 45-55.

Godwin I.C. Pickering, A.D.R., Gabites, J.E. and Alldrick, D.J. (1991): Interpretation of galena lead isotopes from the Stewart-Iskut area (103 O, P; 104 A, B, G); *in* Geological Fieldwork 1990, *British Columbia Ministry of Energy, Mines and Petroleum Resources*, Paper 1991-1 pages 235-243.

Greig, C.J. (1991): Stratigraphic and structural relations along the west-central margin of the Bowser Basin, Oweegee and Kinskuch areas, northwestern British Columbia; *in* Current Research, Part A, *Geological Survey of Canada*, Paper 91-1A, pages 197-205.

Greig, C.J., Anderson, R.G., Daubeny, P.H., Bull, K.F. and Hinderman, T.K.(1994): Geology of the Cambria Icefield: regional setting for the Red Mountain gold deposit, northwestern British Columbia; *in* Current Research 1994-A; *Geological Survey of Canada*, pages 45-56.

Greig, C.J., McNicoll, V.J., Anderson, R.G., Daubeny, P.H., Harakal, J.E. and Runkle, D. (1995): New K-Ar and U-Pb dates for the Cambria Icefield area, northwestern British Columbia; *in* Current Research 1995-A; *Geological Survey of Canada*, pages 97-103.

Grove, E.W. (1986): Geology and mineral deposits of the Unuk-Salmon River-Anyox Area (103P); *British Columbia Ministry of Energy, Mines and Petroleum Resources*, Bulletin 63, 152 pages.

Hanson, G. (1922): Upper Kitsault valley, British Columbia; *in Geological Survey of Canada,* Summary Report, Part A. pages 7-21.

Hanson, G. (1935): Portland Canal area, British Columbia (103P/5,6,11,12); *Geological Survey of Canada*, Memoir 175, 179 pages, 1:253 440-scale.

MacIntyre, D.G., Ash, C.H. and Britton, J.M. (1994a): Geological compilation, Skeena-Nass area, west central British Columbia (NTS 93 E, L, M; 94D; 103 G, H, I, J, O, P; 104 A, B); *British Columbia Ministry of Energy, Mines and Petroleum Resources*, Open File 1994-14.

MacIntyre, D.G., Ash, C.H., Britton, J.M., Kilby, W. and Grunsky, E. (1994b): Mineral potential assessment of the Skeena -

Nass area (93E, L, M, 94 D, 103G, H, I, J, P, 104A, B); *in* Geological Fieldwork, 1994, *British Columbia Ministry of Energy, Mines and Petroleum Resources,* Paper 1995-1, pages 459-468.

McGuigan, P. and Melnyk, W. (1991): Diamond drill report on the Dolly Varden property, Skeena Mining Division; *British Columbia Ministry of Energy, Mines and Petroleum Resources*, Assessment Report # 20 900, 16 pages and maps.

Mitchell, M. A. (1973): Geology, Dolly Varden mine; unpublished report, *Dolly Varden Mines Limited,* 16 pages and figures.

Mortensen, J.K. and Kirkham, R.V.(1992): A U-Pb zircon age for host rocks of a syngenetic strontium (-zinc) occurrence in the Kitsault Lake area, west-central British Columbia; *in* Radiogenic Age and Isotope Studies: Report 5; *Geological Survey of Canada,* Paper 91-2, pages 181-185.

Muralt, D.E. (1985): Steel rails and silver dreams; Benchmark Publications Limited, Los Altos, 183 pages.

Rhys, D.A., Sieb, M., Frostad, S.R., Swanson, C.L., Prefontaine, M.A., Mortensen, J.K. and Smit, H.Q. (1995): Geology and setting of the Red Mountain gold-silver deposits, northwestern British Columbia; *in* Porphyry Deposits of the Northwestern Cordillera of North America, T.G. Schroeter, Editor, *Canadian Institute of Mining, Metallurgy and Petroleum*, Special Volume 46, pages 811-828.

Roth, T., Thompson, J.F.H. and Barrett, T.J. (1999): The precious metal-rich Eskay Creek deposit, northwestern British Columbia; *in* Volcanic-associated massive sulphide deposits: process and examples in modern and ancient settings, *Society of Economic Geologists, Inc*., Reviews in Economic Geology, Volume 8, pages 357-372.

Sieb, M. (1995): Baseline Environmental Studies on the Kitsault Claim Group, Skeena Mining Division; *British Columbia Ministry of Energy, Mines and Petroleum Resources*, Assessment Report # 23 819, 15 pages plus maps.

Thiersch, P. (1986): The geology of the Wolf silver prospect, upper Kitsault valley, British Columbia; Unpublished B.Sc. Thesis, *The University of British Columbia*, 45 pages.

Thompson I.S. and Michna, P.D. (1978): Geochemical and geological exploration of the claims, Crown grants and licenses held by Dolly Varden Resources Limited in the Kitsault River valley, Skeena Mining Division; *British Columbia Ministry of Energy, Mines and Petroleum Resources*, Assessment Report # 7098, 34 pages and maps.

Thompson I.S. and Pearson W.N. (1981): Ore reserves of the Northstar and Wolf deposits, held by Dolly Varden Minerals Inc., Kitsault Valley, Skeena Mining Divisions; *British Columbia Ministry of Energy, Mines and Petroleum Resources*, Assessment Report # 10 042, 8 pages plus appendices and maps.

Tupper, D.W. and McCartney, I.D. (1990): Geological geochemical and diamond drilling report on the Kits-Jade project, Skeena Mining Division; *British Columbia Ministry of Energy, Mines and Petroleum Resources*, Assessment Report # 20 167, 23 pages plus maps.

British Columbia Hydromagnesite-Magnesite Resources: Potential Flame Retardant Material

By George J. Simandl[1], Jana Simandl[2] and Alicia Debreceni[1]

INTRODUCTION

Hydromagnesite occurrences in British Columbia have been recognized since the beginning of the 19th century (Reinecke, 1920; Young, 1915). However, the known occurrences of hydromagnesite are too small to compete with the large sparry magnesite deposits in British Columbia (Grant, 1987; Simandl *et al.*, 1996 a,b and Simandl, 2000) as potential sources of raw materials for the production of industrial grade caustic, dead-burned and fused magnesia or magnesium metal.

This paper summarizes the information on British Columbia's hydromagnesite occurrences based on published data and 2 days of property examination in the 1997 field season. It also identifies a possible market for brucite and these hydrated carbonates as flame retardants. It is the first document that addresses the potential use of hydromagnesite raw material for flame retardants. Also highlighted are the difficulties in developing similar European hydromagnesite-huntite deposits over the last 20 years. Although much effort and focus has been put into the development of these deposits, they still only account for a very small portion of the flame retardant market.

In British Columbia, exploration and/or re-evaluation of known hydromagnesite occurrences may result in the discovery of deposits with a potential as a source of natural flame retardants. Rapid growth of the inorganic, natural flame retardant market or participation of the developer with the existing captive market are essential for the successful development of these resources.

FLAME RETARDANTS - BACKGROUND

Flame retardants are materials incorporated or applied to products (including plastics and textiles) to increase their resistance to fire. The current demand for flame retardant additives is driven largely by recent product liability concerns, more stringent flammability codes and intensified legislative pressures in Europe and North America. Currently there are at least three hundred and fifty substances that are used and listed as flame retardants according to the Danish Environmental Protection Agency. They can be divided into two fundamental categories: a) reactive retardants where molecules already contain flame retarding groups in their polymeric chain, and b) additive retardants which are essentially functional inorganic fillers.

In the mid 1990s, inorganic flame retardants had a share of about 70% of the consumption in the USA. Aluminium hydroxide (ATH), accounted for more than 50% of the total demand by volume (Kirschbaum, 1995). More recent data (Weber, 2000) indicates that flame retardant markets in the USA and Europe account for 344 800 and 339 900 tonnes, respectively (Figure 1). ATH still represents the lion's share of the total market. ATH is manufactured by digestion of bauxite in an alkaline media to produce a solution of sodium aluminate, from which it is crystallized.

Other commonly used flame retardants are magnesium hydroxide, antimony trioxide (Sb_2O_3), zinc compounds such as zinc borate and tin containing minerals such as zinc stannate and zinc hydroxystannate (Kirschbaum, 1995).

It is expected that major concerns about environmental issues will favor inorganic substances not containing any halogens or antimony compounds. Antimony by itself is ineffective, but it becomes very effective in combination with halogens.

The flame retardant efficiency of ATH, magnesium hydroxide ($Mg(OH)_2$), and similar materials like hydromagnesite and huntite is based largely on endothermic decomposition into an oxide and water. In addition to this, the released water vapor isolates flames and dilutes flammable gases. Chemical composition of these magnesium compounds is shown schematically in Figure 2.

Magnesium-based compounds are a rather new flame retardant in the market. Magnesium hydroxide has a higher temperature stability field (up to 340°C) than ATH (200°C). Therefore, ATH is only applicable to polymer systems compounded and processed at low temperatures such as PVC (polyvinyl chloride), EVA (ethylene vinyl acetate copolymer), PE (polyethylene), whereas, $Mg(OH)_2$ can be applied in polypropylene, nylons and thermoplastic polyesters such as PET (polyethylene terephthalate), PA 6 (polyamide) and PBT (polybutylene terephthalate) (Figure 3).

In addition to mined and processed brucite, $Mg(OH)_2$ can be obtained from brines or sea water processing, or

[1] *British Columbia Ministry of Energy and Mines*

[2] *McGill University, Montreal*

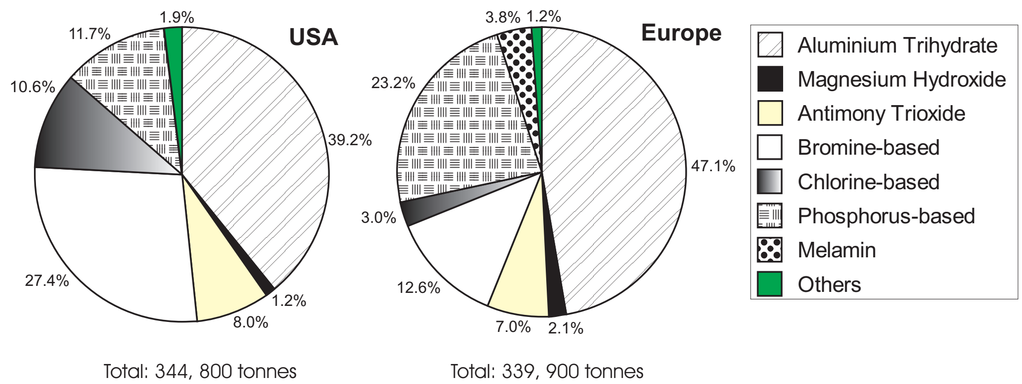

Figure 1. Flame retardant consumption in the USA and Europe for 1998 from Business Communications Co. Inc. Alusuisse Martinswerk GmbH. Figure modified from Weber (2000).

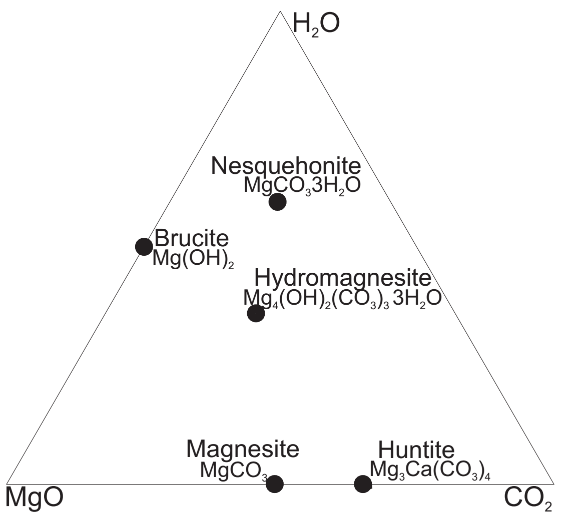

Figure 2. Ternary MgO - CO_2 - H_2O diagram showing chemical composition of magnesium compounds used as flame retardants (Molecular %).

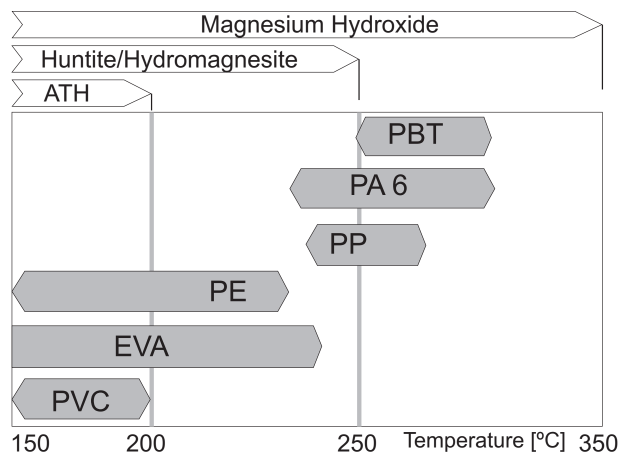

Figure 3. Decomposition/dehydration temperatures of ATH, huntite/hydromagnesite, $Mg(OH)_2$ and processing temperatures of selected polymers. Modified from Georgiades *et al.*,1995.

can be manufactured via specific synthetic routes from magnesite and other Mg-rich minerals such as serpentinite. The market for $Mg(OH)_2$ is estimated at 10 000 to 15 000 tonnes depending on the source of information and Figure 1 suggests that it is over 11 000 metric tonnes for Europe and the USA combined. The price for synthetic $Mg(OH)_2$ is estimated at 3000 to 4500 AU$ /tonne. (<http://www.minerals.csiro.au/public/work/stories/magnesit.htm>).

There is no published market data for natural hydromagnesite-huntite ore used as a flame retardant, but the market is much lower than that for $Mg(OH)_2$.

Mixtures of huntite-hydromagnesite were first seriously studied and examined in the ‘70s as part of a geological study of the magnesium carbonate minerals of the Serbia basin of Kozani (Georgiades *et al.*, 1996). These investigations were followed up by applied research on huntite-hydromagnesite for commercial scale production and exploitation. The relative volume/cost relations between the aluminium hydroxide, huntite-hydromagnesite and magnesium hydroxide at filling levels of 60%, 65% and 70% are shown in Figure 4. The diagram shows that,

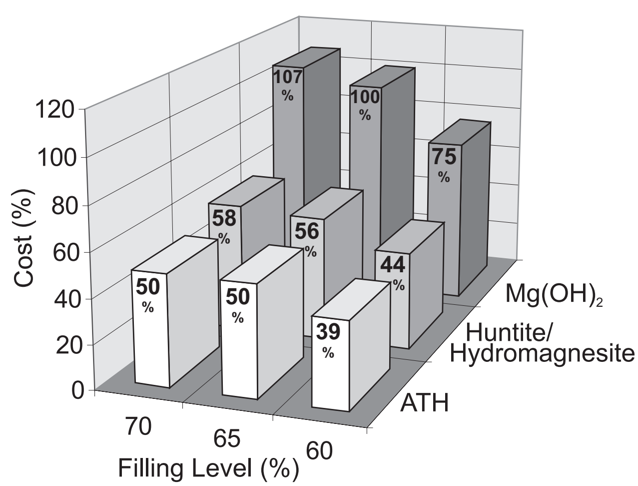

Figure 4. Volume-cost relations between ATH, huntite/hydromagnesite and $Mg(OH)_2$ filled products based on actual European prices. Modified from Georgiades *et al.*, 1995.

for example, at 60% filling of ATH, huntite-hydromagnesite and $M_g(OH)_2$ levels, the cost of the retardant accounts for 39%, 44% and 75% of the total product, respectively. Overall the market for ATH, $Mg(OH)_2$ and similar products such as huntite- hydromagnesite, is increasing as a result of their substitution for brominated flame retardants.

HYDROMAGNESITE ORE AND PRODUCT SPECIFICATIONS

There are a number of hydromagnesite ($Mg_4(OH)_2(CO_3)_3\,3H_2O$) and huntite ($Mg_3Ca(CO_3)_4$) occurrences worldwide. The major impurities in these deposits are magnesite, aragonite, calcite and dolomite. Only a few of these occurrences have material commercially exploited for their flame retarding properties.

The ore in the producing deposits from the Serbia basin of Kozani consists of a mixture of huntite-hydromagnesite with very low iron contents (Fe_2O_3<0.03%), high whiteness (~95% in comparison with chemically produced MgO) and total impurities (aragonite, calcite, magnesite, etc.) less than 8% (Georgiades *et al*., 1996).

An average mineralogical composition established by a combination of XRD and chemical analyses of current ores is as follows: huntite (46%), hydromagnesite (46%), magnesite (4%), aragonite (3%), calcite (1%). Typical chemical analysis of the ores consist of MgO (38.0%), CaO (9.5%), H_2O (9.1%), CO_2 (43.4%) and LOI (52.5%).

MINING AND PROCESSING

In the Serbia basin of Kozani, beds with known ratios of huntite/hydromagnesite are selectively mined and blended to obtain a marketable product of constant composition and quality. The primary processing consists of crushing to less than 10mm and drying to less than 1% moisture. Final processing consists of de-agglomeration and air classification to obtain desirable particle shape and particle size distribution. Depending on the final product, additional drying and surface treatment may be required (Georgiades *et al*., 1996).

CHARACTERISTIC PHYSICAL PROPERTIES

The typical end product has a huntite/hydromagnesite ratio of 1:1 and median diameter d_{50}=0.5-0.7 microns. The high huntite material has d_{50} 0.3-0.4 microns. The d_{97} of both products is below 5 microns (Sedigraph 5000D) and TAPPI brightness is over 95% (Georgiades *et al*., 1996). The stability of the product is intermediate between that of magnesium hydroxide and ATH (Figure 3).

HYDROMAGNESITE IN BRITISH COLUMBIA

The hydromagnesite occurrences in British Columbia were documented by Reinecke (1920); Cummings (1940) and reviewed by Grant (1987). In those studies the occurrences were considered chiefly as a potential source of magnesia and the flame retardant potential was not considered. The geological setting and sedimentation within Cariboo area playas and saline lakes is described by Renault and Long (1987, 1989) and Renault and Stead (1991). The last study suggests that hydromagnesite-magnesite in these environments are found: 1) as major constituents in carbonate playa basins where they precipitated subaqueously or in zones of shallow groundwater discharge; 2) in mudflats surrounding closed perennial lakes; 3) in marshy valley-bottoms and in saline mudflats of ephemeral lake complexes. In the last environment they occur in peripheral mudflats or near spring water discharges. The detailed genesis of hydromagnesite-magnesite accumulations in British Columbia is beyond the scope of the present study and the reader is invited to consult Renault and Stead (1990) and Calvo *et al.* (1995). Huntite was not reported in British Columbia deposits prior to the early 1990's (Renault, 1993), since most of the attempts to characterize hydromagnesite deposits in British Columbia predate the first description of huntite by Faust (1953).

All known British Columbia hydromagnesite occurrences reported in Minfile (http://www.em.gov.bc.ca/Mining/Geolsurv/Minfile/default.htm) are listed below and are located in Figure 5. Should the market for huntite-hydromagnesite increase, satellite photo interpretation, which was not available for early explorers, may become the best reconnaissance exploration tool.

61 Mile Creek (MINFILE 092P 078)

Hydromagnesite deposits are located within a swampy area in the headwaters of 61 Mile Creek and about 3 km east of Goose Lake, and approximately 15 km SE of Clinton. The deposits adjoin a small swampy lake (Cummings, 1940).

White hydromagnesite with a cauliflower-like surface texture covers about 1.1 hectares. The material has been test pitted to a depth of 30 cm but no data is available to indicate its total thickness (Cummings, 1940). Chemical analyses from Cummings (1940) are shown in Table 1, samples MC1, MC2 and MC3.

Barnhart Vale (MINFILE 092INE049)

A deposit of hydromagnesite occurs within a depression near the road to Campbell Range about 2 km north of the Campbell Range deposit and approximately 3.2 km east of the community of Barnhart Vale.

The depression is about 183 m long by 153 m wide and a second depression about 430 m to the east is also reported to contain hydromagnesite. Auger drilling indi-

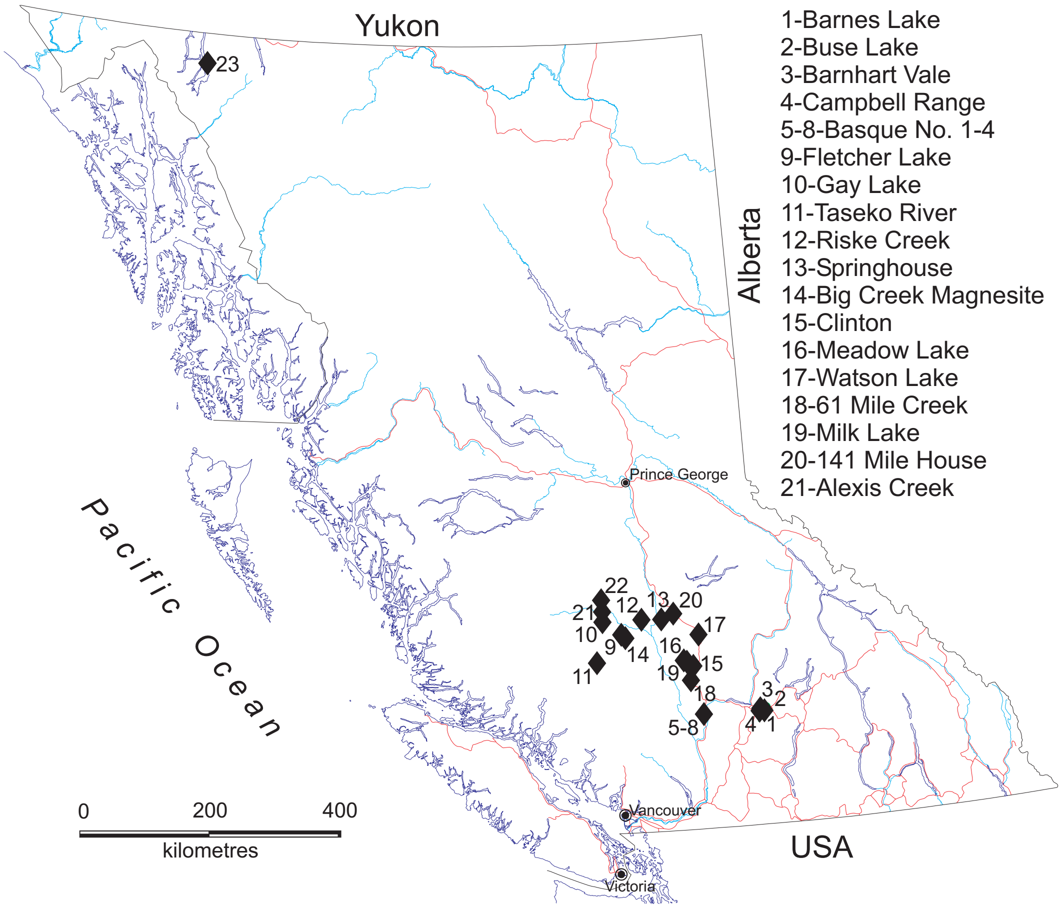

Figure 5. Hydromagnesite occurrences in British Columbia.

TABLE 1
CHEMICAL COMPOSITION OF SAMPLES FROM 61 MILE CREEK; BARNHART VALE, BUSE LAKE, CAMPBELL RANGE AND SPRINGHOUSE
[COMPILED FROM COCKFIELD (1948), CUMMINGS (1940)]

Sample No.	Deposit Thickness (m)	Sample Depth (cm)	MgO (%)	CaO (%)	Fe+Al (%)	MnO (%)	SiO_2 (%)	SO_3 (%)	Insol - ubles (%)	LOI (%)
MC1*	-	surface	38.00	1.60	1.70	-	9.80	-	-	48.90
MC2	-	surface	34.40	1.76	0.69	-	11.60	-	-	48.16
MC3	-	surface	32.75	3.32	0.67	-	12.40	-	-	47.74
BA1	1.83	-	27.44	5.71	3.58	0.05	-	-	23.28	nd
BU1	0.60	180	34.20	1.76	3.91	0.07	-	0.05	20.74	38.45
CA1	0.90	-	37.44	0.66	0.93	-	-	-	7.37	nd
CA2	0.90	-	41.00	nil	0.78		-	-	2.40	59.00
SP1	-	-	33.10	4.90	4.30	-	-	-	14.80	42.00

*MC - 61 Mile Creek; BA - Barnhart Vale; BU - Buse Lake; CA - Campbell Range; SP - Springhouse cated hydromagnesite to a depth of 1.83 m with about 15 cm of overburden (Cockfield, 1948). The chemical analysis from Cockfield (1948) is shown in Table 1, sample BA1. This sample has a relatively high content of insoluble (non-carbonate) minerals.

Buse Lake (MINFILE 092INE048)

The material lies in a depression which is about 430 m long and 60 to 125 m wide. Auger drilling indicated a hydromagnesite thickness of 30 to 76 cm which is overlain by 25 to 75 cm of drift material. The sample contains 77.9% hydromagnesite based on the MgO content (Cockfield, 1948; Cummings, 1940). The chemical analysis from Cockfield (1948) is shown in Table 1, sample BU1. The sample may have been contaminated by the overlying soil since it has a high content of insoluble (non-carbonate) minerals.

Campbell Range (MINFILE 092INE050)

About 550 tonnes of white hydromagnesite are reported in a small, 75 m diameter depression west of the Campbell Road about 19 km southeast of Kamloops. One auger hole indicated a thickness of about 90 cm of hydromagnesite while others intersected only sand and gravel (Cockfield, 1948; Cummings, 1940). Chemical analyses from Cockfield (1948) and Cummings (1940) are shown in Table 1, samples CA1 and CA2, respectively from the same drill hole.

Springhouse (MINFILE 092O 088)

The Springhouse hydromagnesite showing is probably older than other occurrences of the Chilcotin Plateau, where hydromagnesite is being formed in modern lakes, since it is covered in soil.

White, clay-like material is reported to underlie 10 to 30 cm of soil in scattered locations (Cockfield, 1948; Cummings, 1940). One occurrence close to the Williams Lake-springhouse Road, near Boitano Lake was sampled and the chemical analysis from Cummings (1940) is shown in Table 1, sample SP1.

141 MILE HOUSE (MINFILE 093A 156)

Hydromagnesite is deposited in an area over 30 m across and down-slope from a mineral spring near 141 Mile House and east of the railway tracks. The material contains freshwater shells and is predominantly calcium and magnesia and a small amount of alkalic carbonates (Reinecke, 1920). Samples 141A and 141B (Table 2) were collected 6 m and 30 m, respectively, downstream. However, the analysis of the two samples does not support the presence of hydromagnesite in the deposit. The CaO content of these samples is too high, while the H_2O content is too low.

Atlin (MINFILE 104N 079)

Hydromagnesite is located within topographic lows immediately east of Atlin. In addition to the two main bodies, a number of small, isolated patches of hydromagnesite occur along the lakeshore in the vicinity of Atlin (Grant, 1987 *see* also Figure 6).

Estimated resource is 107,037 tonnes grading 41% hydromagnesite; 83% of the resource would grade 41 to 42% MgO (Aitken, 1959).

The largest deposit is about 7.29 hectares with an average thickness of 81 cm and it has several smaller satellitic bodies.

Near the base of the deposit the hydromagnesite may be more porous and is cut by irregular vein-like, glassy hydromagnesite. The hydromagnesite is white, powdery and massive with no evidence of bedding or structure and its composition is homogeneous. The white surface color assumes a yellow tinge at a depth of about 30 cm below the surface. The tinge disappears with exposure to air. The material becomes quite plastic, like clay, when wet (Young, 1915).

Two holes drilled in the deposit were sampled and analyzed. Hole No. 1 indicated a hydromagnesite thickness of 66 cm and was sampled at depths of 8, 33 and 58 cm. Hole No. 2 indicated a thickness of 107 cm and was sampled at 10, 42 and 71 cm. Results of this sampling are presented in Table 2.

A second hydromagnesite deposit lies directly east of Atlin and southwest of the main deposit. It consists of three bodies within topographic depressions and is associated with larger areas of impure hydromagnesite. The first body covers about 1.82 hectares with an average thickness of about 1 m, but which varies from 0.3 to 1.5 m. Sample AT3 was collected at a depth of 53 cm near the center of the body. Sample AT4 was collected at a depth of 41 cm, about 30 m from sample AT3.

The second body underlies about 0.3 hectares with a thickness of 1 to 2.14 m. Near the northeast corner of this body the thickness is about 1.73 m and sample AT5 was collected from a depth of 46 cm. The material is partly granular and some-what clay-like with walnut sized, or smaller, pieces of hardened hydromagnesite. Sample AT6 is a surface sample where the thickness of the deposit is >1.8 m.

The third body is exposed over 0.4 hectares with a thickness of 0.3 to 1 m. Sample AT7 was collected about 10 cm above the base of the deposit at a depth of 51 cm. The material sampled is compact and traversed by thin micro-veinlets of hydromagnesite (Cummings, 1940; Fraser, 1904; Reinecke, 1920). Chemical analyses of all the above mentioned samples, from Young (1915), are shown in Table 2. One of these bodies was recently promoted by Stralak Resources as a potential source of magnesia.

TABLE 2
CHEMICAL COMPOSITION OF SAMPLES FROM 141 MILE HOUSE; ATLIN; BIG CREEK; CLINTON; MEADOW LAKE; RISKE CREEK AND WATSON LAKE

(NOTE: SAMPLES FROM THE ATLIN OCCURRENCE DATA ARE FROM HOLE 1 AND ATB FROM HOLE 2)

Sample No.	Deposit Thick-ness (m)	Sample Depth (cm)	MgO (%)	CaO (%)	SiO_2 (%)	Al_2O_3 (%)	Fe_2O_3 (%)	SO_3 (%)	Na_2O (%)	K_2O (%)	CO_2 (%)	H_2O (%)	H_2O +105
141A*	-	-	12.14	34.31	8.78	-	5.05	tr	0.10	0.58	36.84	3.10	-
141B**	-	-	5.00	43.32	5.22	-	1.45	tr	0.02	0.36	35.10	6.06	-
ATA1	0.66	8	41.13	2.04	1.86	0.67	0.82	-	-	-	35.98	18.02	-
ATA2	0.66	33	42.35	0.82	0.9	0.10	0.59	-	-	-	36.10	18.95	-
ATA3	0.66	58	42.19	0.68	0.54	0.17	0.82	-	-	-	36.17	19.05	-
ATB1	1.07	10	40.56	1.26	1.22	0.67	0.88	-	-	-	35.96	19.04	-
ATB2	1.07	42	41.93	1.5	1.96	0.14	1.17	-	-	-	36.04	17.66	-
ATB3	1.07	71	35.23	6.44	9.22	0.94	1.6	-	-	-	37.70	8.20	-
AT3	1	53	42.85	0.32	0.74	0.35	0.88	-	-	-	36.35	19.10	-
AT4	1	41	38.94	0.42	3.48	2.85	1.46	-	-	-	34.31	18.10	-
AT5	1.73	46	43.04	0.16	0.96	0.23	0.71	-	-	-	36.21	19.26	-
AT6	>1.83	surface	42.45	0.26	0.62	0.41	0.49	-	-	-	36.23	18.95	-
AT7	0.61	51	42.12	0.48	1.18	0.33	0.89	-	-	-	35.89	19.42	-
BI1***	-	-	43.19	4.10	-	0.60	1.00	0.04	0.64	-	36.47	11.00	-
CL1	1.45	0-61	41.60	0.22	2.30	0.63	0.13	0.36	-	-	35.88	18.65	17.53
ME1	0.2-0.81	0-38	41.38	1.32	4.00	1.36	0.40	-	-	-	37.67	13.60	12.12
ME2	0.9-1.25	38-130	35.68	6.38	11.33	2.88	0.46	-	-	-	36.63	6.44	4.15
ME3	-	130-168	20.34	25.55	7.60	-	0.24	-	-	-	-	-	-
ME4	0.2-0.81	0-99	36.63	2.86	13.10	1.34	0.30	-	-	-	35.64	9.58	7.00
ME5	0.9-1.25	99-153	24.32	20.12	10.32	1.35	0.49	-	-	-	38.64	4.38	2.93
ME6	0.7	0-30	20.14	9.20	36.78	1.54	2.47	-	-	-	20.24	10.32	6.80
ME7	-	composite	40.56	1.26	1.22	0.67	0.87	-	-	-	35.96	19.45	18.00
ME8	-	composite	38.80	0.80	7.40	2.50		-	-	-	38.70	11.50	11.50
RI1	75	0-66	41.14	0.10	1.22	0.48	0.19	0.08	-	-	37.70	19.06	17.78
RI2	composite	0-90	42.30	0.70	4.40	1.00		-	-	-	41.90	9.20	9.20
RI3	0.84	0-61	41.74	0.17	1.85	0.48	0.62	0.11	-	-	40.85	14.65	12.98
WA1	0.5-1.0	66	41.06	1.62	6.36	0.20	0.12	-	-	-	38.04	12.57	11.25
WA2	1	0-92	43.17	1.14	4.62	0.16	0.16	-	-	-	43.64	6.68	5.26
WA3	-	-	39.40	2.10	5.70	1.30		-	-	-	50.50	-	-
WA4	-	-	36.70	1.54	8.62	0.33	0.57	-	-	-	31.08	17.07	14.86

*141 - 141 Mile House; AT - Atlin; BI - Big Creek Magnesite; CL - Clinton; ME - Meadow Lake; RI - Riske Creek; WA - Watson Lake
**This sample also contained 4.01% carbonaceous matter
***This sample also contained 16% insolubles

Big Creek Magnesite (MINFILE 092O 089)

The Big Creek showing occurs about six km south of the Fletcher Lake showing (Minfile #092O 084). It contains about 500 tonnes of hydromagnesite (Cummings, 1940; Grant, 1987). Chemical analysis from Grant (1987) is shown in Table 2, sample BI1.

Clinton (MINFILE 092P 072)

The three pure hydromagnesite deposits occur about 1 km east of Clinton in the valley of Clinton Creek, within a larger area of impure hydromagnesite, covering a combined area of about 0.28 hectares. The material is 0.6 to 1.4 m thick and is underlain by a brown hydromagnesite to a depth of about 1.5 m. Sand and clay underlie the deposit (Reinecke, 1920).

Chemical analyses from Reinecke (1920) are shown in Table 2, sample CL1.

Meadow Lake (MINFILE 092P 074)

The area contains two main and a number of smaller areas of pure and impure hydromagnesite. The total area covered is about 20.4 hectares (Figure 7).

All occurrences have irregular outlines and a typical cauliflower-like surface which is raised 10 to 60 cm above the surrounding swamp. The impure hydromagnesite occurrences have a flat, cracked surface of dense, gray material. They occur east and west of Meadow Lake and the individual deposits vary widely in

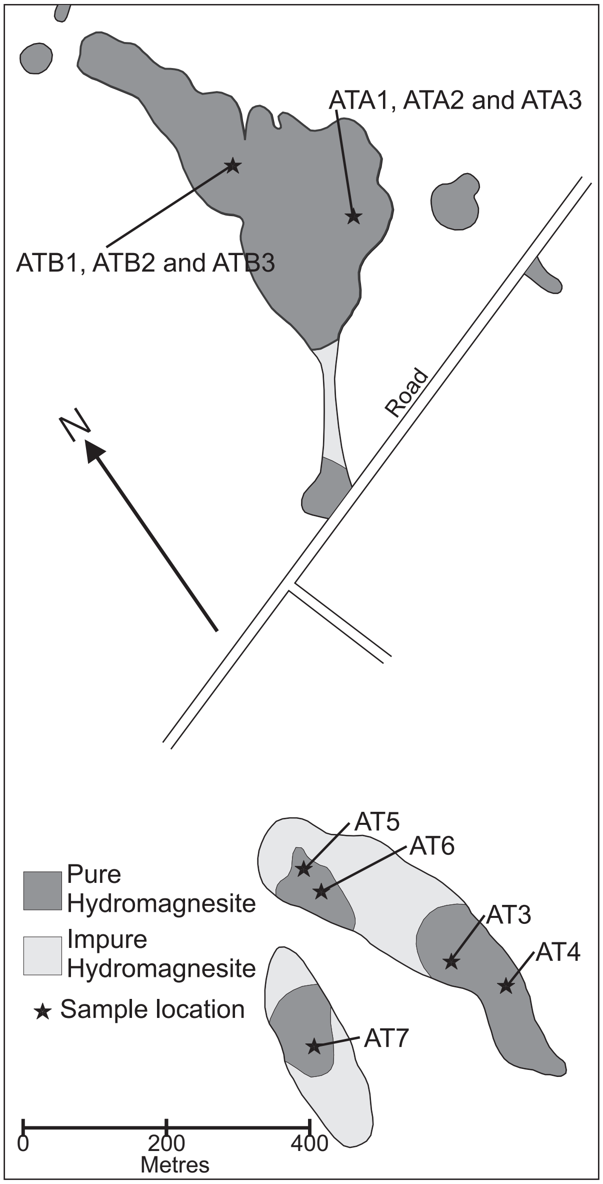

Figure 6. Atlin hydromagnesite deposit. Source: Young, 1915.

composition but generally contain elevated values of calcium and silica.

Area A, is about 1.5 km east of Meadow Lake. Drilling confirmed that the 11.87 hectares of white hydromagnesite has a thickness of 20 to 81 cm with an average of about 46 cm. Creamy yellow granular material underlies the white hydromagnesite in a layer which is in the order of 90 to 125 cm thick and is underlain in turn by impure hydromagnesite. Sample ME1 is of material from 0 to 38 cm depth within the white hydromagnesite at the center of the deposit. Sample ME2 is from 38 to 130 cm, below sample ME1, and consists of cream-colored hydromagnesite. Sample ME3 is cemented soil taken from 130 to 168 cm depth. Sample ME4 was collected near sample ME1 and is from 0 to 99 cm, but includes some yellow hydromagnesite. Sample ME5, taken below sample ME4 is from 99 to 153 cm and is entirely within yellow hydromagnesite (Grant, 1987).

Area B, the second largest occurrence, consists of white hydromagnesite covering about 5.85 hectares of swampy terrain, roughly 325 m southeast of Area A, the main deposit. In Area B, the hydromagnesite is 30 to 90 cm thick with an average thickness of 41 cm (Reinecke, 1920). Sample ME6 (Reinecke, 1920) represents a composite of white hydromagnesite from a number of the Meadow Lake occurrences. Sample ME8 is a similar composite, but is limited to white material from drill holes in areas A and B. Chemical analyses of the above-mentioned samples, from Reinecke (1920), are shown in Table 2.

Riske Creek (MINFILE 092O 087)

Deposits of hydromagnesite are contained within recent sediments that occur on low swampy terrain along the Riske Creek drainage, south of the Chilcotin Road.

The western deposit is estimated to cover 0.65 hectares. White hydromagnesite, 60 to 90 cm thick, grades downwards to a brown clayey soil at a depth of about one meter. Sample RI1 was collected from the eastern end of the deposit, as well as Sample RI3 which consisted of a composite from five drill holes throughout the deposit.

The eastern deposit is estimated to be about 0.84 hectares. It is white to cream hydromagnesite to about 84 cm depth and grades into brown clay at 1.27 m. Sample RI2 was collected from the center of this deposit (Cummings, 1940; Reinecke, 1920). Chemical analyses of these samples are shown in Table 2.

Watson Lake (MINFILE 092P 077)

Deposits of hydromagnesite are located in a swampy depression about 500 m to the southwest of Watson Lake and about 1.5 m above the lake level.

The larger area, is about 200 by 60 m along a northeast trend. It has a variable depth, to an underlying dark gray mud, up to about 2.16 m. The hydromagnesite has a white superficial layer which is 50 to 100 cm thick with an average of 58 cm. Underlying this layer is a 1.5 m thick, cream to brown Ca-rich hydromagnesite layer (Reinecke, 1920). Sample WA1 (Reinecke, 1920) is of 66 cm of white hydromagnesite and part of the layer of cream-colored hydromagnesite.

The second significant area is about 180 m southeast of the first. The white surface layer of hydromagnesite is about one meter thick. Sample WA2 is of white hydromagnesite collected from 0 to 92 cm from the surface. Sample WA3 (Cummings, 1940) is a composite sample of white hydromagnesite collected from seven drill holes representing all occurrences in this area. Sample WA4 (Reinecke, 1920) was collected from an isolated of hydromagnesite located about 1.5 km northeast of the main occurrence.

In total, the Watson Lake deposits cover approximately two hectares and contain slightly more than

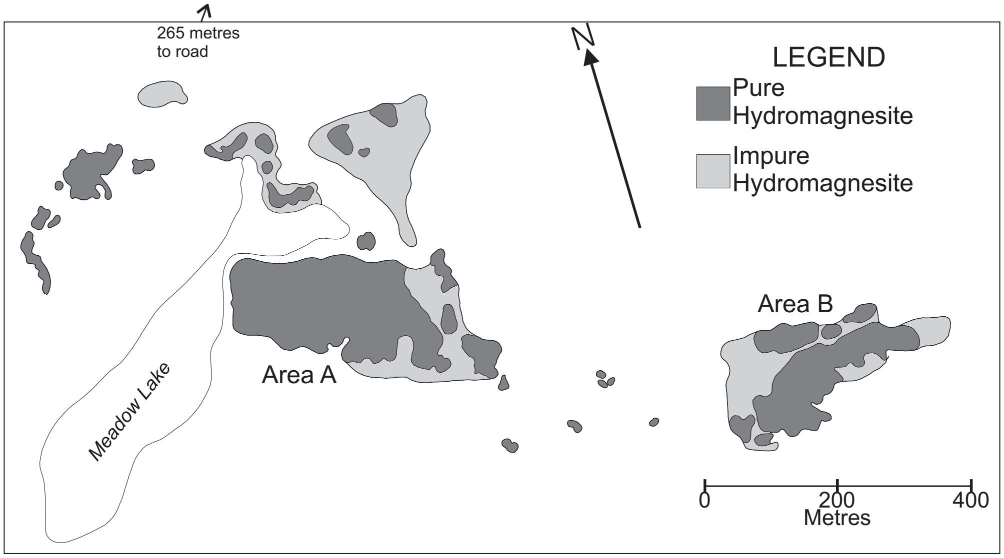

Figure 7. Meadow Lake hydromagnesite deposit. Source: Cummings, 1940.

20,000 tonnes of hydromagnesite (Cummings, 1940; Reinecke, 1920). Chemical analyses of the above samples, from Reinecke (1920), are shown in Table 2.

Alexis Creek (L.561) (MINFILE 093B 041)

The Alexis Creek showing may contain 900 tonnes of hydromagnesite resource. The showing is located 3 km west of the town of Alexis Creek along the Chilcotin River (Cummings, 1940). The chemical analysis from Cummings (1940) is shown in Table 3, sample AC1.

Alexis Lake (L.2833) (MINFILE 093B 056)

The Alexis Lake showing consists of about 1,800 tonnes of hydromagnesite. The deposit is likely to be a residual precipitate (Cummings, 1940). Chemical analysis from Cummings (1940) is shown in Table 3, sample AL1.

Barnes Lake (MINFILE 082LNW082)

Impure, gray hydromagnesite, up to 60 cm thick, and covered with about 30 cm of soil, underlies a couple of hectares near the north end of Barnes Lake about 43.5 km southeast of Kamloops near the Kamloops-Vernon Road (Grant, 1987). No data is available on the chemistry of the deposit.

Basque No. 1, 2, 3 and 4 (MINFILE 092INW043, 44, 45 and 46)

The Basque salt deposits consist primarily of four small basins or mud-filled ponds 2 km west of Highway 1 and 15 km south of the community of Ashcroft.

The Basque deposits consist primarily of mixed hydrous magnesium sulphate (epsomite or Epsom salt) and hydrous sodium magnesium sulphate (bloedite), as well as hydrous sodium sulphate (mirabilite or Glauber's salt). The top 1 m in all of the deposits is principally epsomite. Mirabilite generally occurs near the surface and the bloedite at depth. There are also small amounts of calcium sulphate, sodium bicarbonate and sodium chloride present. Potassium in detectable levels has been reported in the brines (Goudge, 1924; Grant, 1987).

Shallow, fresh-water ponds and small deposits of impure hydromagnesite and hydrous sodium sulphate (mirabilite) occur in small converging valleys close to and west of the Basque deposits.

Fletcher Lake (MINFILE 092O 084)

The Fletcher Lake hydromagnesite showing occurs within recent lacustrine sediments developed on glacial gravels and Tertiary volcanic rocks. The resource is estimated at 350 tonnes of hydromagnesite (Cummings, 1940). No data is available on the chemistry of the deposit.

TABLE 3
CHEMICAL COMPOSITION OF SAMPLES FROM ALEXIS CREEK AND ALEXIS LAKE COMPILED FROM CUMMINGS (1940)

Sample No.	$Mg(HCO_3)_2$ (%)	CaO (%)	Al_2O_3 + Fe_2O_3 (%)	Mn (%)	Insol - ubles (%)
AC1*	84.00	nil	0.20	-	13.00
AL1**	80.00	nil	1.20	tr	9.20

*AC - Alexis Creek

**AL - Alexis Lake

Gay Lake (MINFILE 092O 085)

Hydromagnesite of the Gay Lake showing is being deposited within recent lacustrine sediments within a playa developed on older glacial gravels and Tertiary volcanic rocks. Through evaporation of the water of Gay Lake during the summer, hydromagnesite is being concentrated in the clays of the lake bottom and around its margins (Grant, 1987). The deposit is estimated to contain about 100 tonnes of hydromagnesite (Cummings, 1940). No data is available on the chemistry of the deposit.

Milk Lake (MINFILE 092P 173)

A carbonate playa covers 300 m^2, 31 km north of Clinton and 19 km west-northwest of Seventy-mile House. It is underlain by a central mudflat forming a hard flat surface of pale gray mud, comprised mostly of hydromagnesite. A pit dug near the center of the playa encountered 80 cm of massive gray mud comprising magnesite and hydromagnesite underlain by cream-colored magnesite mud. The central mudflat is rimmed by a peripheral mudflat, a few meters to 20 m in width, containing a mixture of massive to crudely bedded siliciclastic detritus, precipitated magnesium carbonates (magnesite, hydromagnesite and dolomite) and organic matter.

The magnesite content increases downward at the expense of hydromagnesite. In two samples, hydromagnesite forms 25 to 30% of the total carbonate, 10 to 20 cm below the central playa surface. Dolomite occurs in the southern peripheral mudflats in association with magnesite, 40 to 80 cm below the surface. Four samples contained 1.2 to 5.4% acid insoluble matter comprised of clay, plagioclase silt, diatom debris and organic detritus (Campbell and Tipper, 1971; Renaut and Stead, 1989). No data is available on the chemistry of the deposit.

Taseko River (MINFILE 092O 086)

The Taseko River hydromagnesite occurrence is hosted by recent sediments deposited within an ephemeral lake system developed, possibly, as a result of meandering of the Taseko River. Hydromagnesite appears to be confined to lacustrine sediments in a small depression in the Taseko River valley (Grant, 1987). The showing is estimated to contain about 55 tonnes of hydromagnesite (Cummings, 1940). No data is available on the chemistry of the deposit.

SUMMARY

British Colombia has a large magnesite resource and quite a number of known hydromagnesite occurrences. While sparry magnesite deposits in British Columbia are relatively well documented, hydromagnesite deposits have received limited attention.

There is not sufficient information about thickness, mineralogy, continuity or the extent of the British Columbia hydromagnesite occurrences. The chemical analyses given in Tables 1, 2 and 3 were compiled from a variety of old sources. In many cases H_2O+ analyses, that are one of the essential factors in estimating hydromagnesite and huntite content, are not available. In most cases, the description of the analytical method is not given and no scanning electron or modern X-Ray diffraction data is available.

If the current trends in the application of flame retardants continue, the future market for hydromagnesite products may justify the reassessment of selected known occurrences and the possibity of exploration for new deposits. British Columbia hydromagnesite deposits do represent primary exploration targets for companies with a captive flame retardant market.

ACKNOWLEDGMENTS

Derek Brown of the British Columbia Geological Survey improved an earlier version of this manuscript.

REFERENCES

Aitken, J.D. (1959): Atlin Map-Area, British Columbia; *Geological Survey of Canada,* Memoir 307, page 79.

Anonymous (2000): Antimony trioxide; *Industrial Minerals No. 389*, page 17.

Anonymous (2000): Flame retardant markets await ignition; *Industrial Minerals No. 389, page 7.*

Baksa, G. and Sitkei, F. (2000): Changes in ATH use - A central and east European focus; *Industrial Minerals No. 394,* pages 79-85.

Calvo, J.P., Stamatakis, M.G., Magganas, A.C. (1995): Clastic Huntite in Upper Neogene Formations of the Kozani Basin, Macedonia, Northern Greece; *Journal of Sedimentary Research, Vol. A65, No. 4, October,* pages 627-632.

Campbell, R.B. and Tipper H.W. (1971): Geology of Bonaparte Lake Map-Area, British Columbia; *Geological Survey of Canada,* Memoir 363, pages 91, 92.

Cockfield, W.E. (1948): Geology & Mineral Deposits of the Nicola Map-Area, British Columbia; *Geological Survey of Canada,* Memoir 249, pages 145-148.

Cummings, J.M. (1940): Saline and Hydromagnesite Deposits of British Columbia; *B.C. Ministry of Energy, Mines and Petroleum Resources,* Bulletin 4, pages 29, 30, 40-55, 60-62, 101-129.

Duffell, S. and McTaggart, K.C. (1952): Ashcroft Map-Area, British Columbia; *Geological Survey of Canada,* Memoir 262, pages 94, 111-113.

Georgiades, G.N., Larsson, B.J. and Pust, C. (1996): Huntite-hydromagnesite Production & Applications; *12th Industrial Minerals International Congress,* pages 57-60.

Goudge, M.F. (1924): Magnesium Sulphate in British Columbia; *EMR Mines Branch,* Report No. 632, pages 62-75.

Grant, B. (1987): Magnesite, Brucite and Hydromagnesite Occurrences in British Columbia; *B.C. Ministry of Energy, Mines and Petroleum Resources,* Open File 1987-13, pages 54-67.

Kirschbaum, G.S. (1995): Flame Retardant Minerals - Markets and technology; *12th Industrial Minerals International Congress,* pages 53-56.

Reinecke, L. (1920): Mineral Deposits between Lillooet and Prince George, British Columbia; *Geological Survey of Canada,* Memoir 118, pages 3, 20-49.

Renault, R.W. (1993): Morphology, distribution, and preservation potential of microbial mats in the hydromagnesite-magnesite playas of the Cariboo Plateau, British Columbia, Canada; *Hydrobiologia, v. 267,* pages 75-98.

Renault, R.W. and Stead, D. (1990): Recent Magnesite-Hydromagnesite Sedimentation in Playa Basins of the Cariboo Plateau, British Columbia (92P); *B.C. Ministry of Energy, Mines and Petroleum Resources,* Geological Fieldwork 1990, Paper 1991-1, pages 279-288.

Simandl, G.J. (in print): Magnesite Deposits, British Columbia, Canada; Chemical Characteristics and Development Potential.

Simandl, G.J. and Hancock K.D. (1996): Magnesite in British Columbia, Canada: a neglected resource; *Minerals Industry International, Number 1030*, pages 33-44.

Simandl, G.J., Simandl, J., Hancock, K.D. and Duncan L.R. (1996): Magnesite deposits of British Columbia - Development potential; *Industrial Minerals, No. 343,* pages 125-135.

Weber, M. (2000): Mineral flame retardants - Overview & future trends; *Industrial Minerals, No. 389, pages 19-27.*

Young, G.A. (1915): Hydromagnesite Deposits of Atlin, British Columbia; *Geological Survey of Canada,* Summary Report 1915, pages 50-61.

Selenium in the Mist Mountain Formation of Southeast British Columbia

By Barry Ryan and Maggie Dittrick

KEYWORDS: Selenium, coal, Mist Mountain Formation.

INTRODUCTION

This study documents the distribution of Selenium (Se) in the Jurassic-Cretaceous Mist Mountain Formation of southeastern British Columbia and in various materials segregated by the five coal mines in the area. This study is preliminary and will be followed up by more detailed and focused studies.

The Mist Mountain Formation, which is part of the Kootenay Group (Table 1), outcrops extensively in the east Kootenays and varies in thickness from 25 to 665 metres (Gibsons, 1985). Typically 8% to 12% of the thickness of the formation is coal and in places this is distributed in over 30 seams. The rest of the formation is composed of non-marine siltstones, mudstones and sandstones. The formation is underlain by the Morrissey Formation, which is a sandstone unit that forms the footwall to most of the mining activity. This formation is underlain in turn by the Fernie Formation composed predominantly of marine shales. The Mist Mountain Formation is overlain by the Elk Formation, a non-marine sandy formation containing thin sapropelic coal seams.

TABLE 1
JURASSIC-CRETACEOUS STRATIGRAPHY OF THE KOOTENAY GROUP

LOWER CRETACEOUS	CADOMIN FORMATION		
JURASSIC AND CRETACEOUS	KOOTENAY GROUP	ELK FORMATION	
		MIST MOUNTAIN FORMATION coal seams	
		MORRISSEY FORMATION	MOOSE MOUNTAIN MEMBER
			WEARY RIDGE MEMBER
JURASSIC	FERNIE FORMATION	PASSAGE BEDS	

The Mist Mountain Formation outcrops in three distinct coalfields (Figure 1).

The Elk valley coalfield in the north hosts three coal mines, the Crowsnest coalfield hosts two and there are exploration properties but no mines in the southern-most Flathead coalfield. The formation is thinner in the Flathead coalfield and thicker in the other two coalfields, though there do not appear to be any consistent regional trends in thickness in the coalfields. The volume of the formation outcropping in each basin varies and is most in the Elk Valley and least in the Flathead coalfield. The Kootenay Formation, which is equivalent to the Mist Mountain Formation, outcrops to the east in Alberta where it is much thinner, though it still contains some coal seams.

Coal mining started in the east Kootenays in 1898 and over 460 million tonnes have been extracted up to 1999. Since 1970 about 400 million tonnes of coal have been mined from surface pits representing removal of over 2.5 billion cubic metres of rock.

This paper provides preliminary lithologic sections of the Mist Mountain from a number of areas illustrating the major lithologies including coal seams and indicating their Se content. In addition, samples of materials disturbed by mining were analyzed. These include coarse refuse, tailings material and material from settling ponds adjacent to waste rock dumps. The partitioning of Se in coal seams and rocks associated with the coal seams is investigated. The relationship of Se to sulphur (S) in these rocks gives some indications of how Se is bound and how easily it might be released into the environment.

BACKGROUND

Selenium is an unusual trace element in that there is a very narrow band of tolerance in all animals. There is, therefore, a heightened interest in Se levels in the environment and how these levels are effected by human ac-

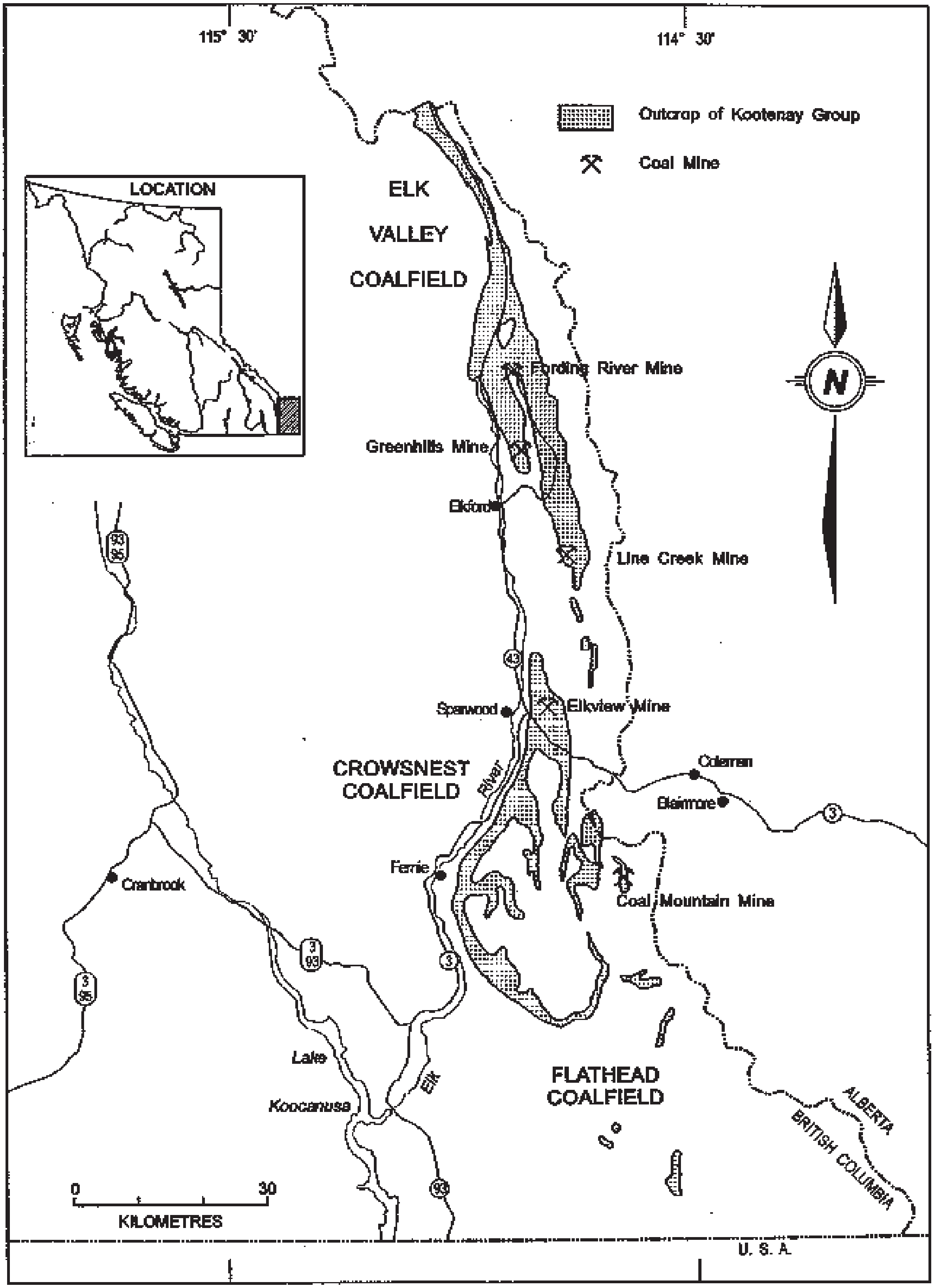

Figure 1. Elk Valley, Crowsnest and Flathead coalfields of southeast British Columbia.

tivity. It is considered to be a trace element of potential environmental concern (Harvey *et al.,* 1983) and a hazardous air pollutant (HAP) (Demir *et al.,* 1998). Cases of natural Se poisoning have been reported in China, but generally more problems result from Se deficiency in diets. In many areas soil is deficient in Se and available Se in vegetation is less than 0.05 ppm. Some countries such as New Zealand add Se to agricultural fertilizers to counter health problems in livestock resulting from Se deficiency in soil and vegetation. Salt licks often contain added Se for the same reason. If diets provide, on average, less than about 0.1 ppm, then Se deficiency problems occur that include impaired immunity, hepatic necrosis and cardiac functional changes (Keshan decease). If concentrations in soils are above about 4 ppm, then Se toxicity problems may occur. In farm animals these involve deformities, fertility problems and loss of muscle coordination referred to as the blind staggers. Chronic poisoning occurs in animals if they consistently ingest foods with average Se concentrations between 5 to 20 ppm daily.

In humans, it is recommended that the Se intake be between 100 and 250 mcg/day (therapeutic dose 350 - 400 mcg/day). This amount will usually be found in a normal diet, but not necessarily in what is sometimes referred to as the SAD diet (standard American diet). Foods especially rich in Se include meats, fish, whole grains, brewers yeast and mushrooms. Excess Se in humans may cause dental problems and very high levels reported in Hubei province in China caused hair loss, skin lesions and nerve damage (Zheng *et al.,* 1999).

Selenium is chemically similar to sulphur. It occurs in the ionic states, selenide (-2), elemental (0), selenite (+4), and selenate (+6). Selenium in Se bearing sulphides oxidizes readily to selenite and selenate. The latter is the most soluble and toxic form. In oxidizing conditions, selenate is usually reduced to selenite, which is easily removed from solution combined with $Fe(OH)_3$. In non oxidizing conditions Se is reduced to the elemental form, which is insoluble and generally non toxic.

World consumption of Se is probably in the range of 1000 to 2000 tonnes per year (1450 tonnes in 1989, Herring, 1990) . USA consumption in the 1990's has been between 500 and 600 tonnes. Uses for Se include, glass making (35%), agriculture and metallurgy (30%) chemical and pigments (20%) and electronics (15%). At present most of the Se is extracted as a by-product when smelting copper ore. In the future, the biggest resource of Se could well be world coal deposits. Se may be extracted from fly ash after coal combustion in power plants.

Average crustal abundance of Se is 0.05 - 0.1 ppm (Taylor 1964 and Turekian, and Wedephol, 1961), which is lower than its average concentration in the whole earth (6.1 ppm) because Se was easily volatilized from crustal rocks during crust formation. The value is usually calculated by dividing the Sulphur crustal average by a S/Se ratio. Selenium is concentrated in coal (average abundance about 2.15 ppm) and also in rocks rich in phosphate (Table 2).

In general Se concentrations in sedimentary rocks vary from less than 0.1 ppm in limestones and sandstones to an average of about 0.6 ppm in shales, which have a wide range of contents (<0.1-100 ppm) (Herring, 1990) (Table 2). Contents in marine or black shales tend to be higher than in other rock types and shales enriched in organic carbon (TOC) have higher concentrations because the micro organisms, responsible for the carbon, concentrate Se (Saiki *et al.,* 1993). Selenium is adsorbed onto clay minerals in shales as selenite under conditions of high pH and salinity. In sea water the S/Se ratio is very high (1.4×10^7) compared to about 2.5 to 3.5×10^3 in coal, because of adsorption of Se onto clays and the solubility of SO_4 in sea water. During diagenesis Se in clays may be incorporated into sulphides (pyrite) or remain as a trace element attached to the clay minerals.

Selenium is released as selenate (SeO_4^{-2}) during weathering when Se bearing sulphides oxidize or when clays are weathered. Once released, in alkaline environments, Se remains soluble as $CaSeO_4$ and is available to be taken up by plants. In humid conditions where soils are more acid it is either removed or converted to the less soluble selenite form.

Generally soils contain about 0.4 ppm Se. If the concentration is below 0.1 ppm they are considered to be deficient in Se and above 5 ppm enriched in Se. Soils in large areas of northeastern US and western parts of Washington and Oregon are considered to be Se deficient (Lag

TABLE 2
AVERAGE SE CONTENTS OF COMMON ROCK TYPES

	reference	Se range ppm	Se average	AREA
crustal average	G	0.05 - 0.1		
whole earth	G		6.1	
coal	D	<0.1ppm -5%	2.15	
sandstones	A	<0.1 - 1.7	0.1	
shale	A	<0.1 - 12	0.53	
cherts	A	<0.1 - 0.3	0.11	
limestones	A	<0.1 - 7.4	0.22	
sandstones	B	<0.1 - 1.5	0.22	Continental USA
siltstones	B	<0.1 - 0.79	0.21	
mudstones	D	0.4-0.6		
soil	F	0.14 - 4.32	0.45	Continental USA
Sandstones	D	0.05-0.08		
granites	D	0.01-0.05		
granodiorite	C	0.02 - 0.05		
mafic rocks	D	0.01-0.05		
ultramafic	D	0.02-0.05		
crude oil	D	0.01-1.4		
phosphate ore	E	0.7-7.0		

A	Connor and Shacklette, (1975)
B	Ebans and Shacklette (1982)
C	Kabata-Pendias and Pendias (1984)
D	Coleman *et al.* (1999)
E	Robbins and Carter, (1970)
F	Shacklette *et al.* (1974) and Shacklette and Boerngen (1984)
G	Herring (1990)
H	Taylor (1964), Turekian, and Wedephol, (1961)

and Agic, 1990), probably because of acid soil conditions. In dryer regions to the east (northwestern part of the great plains) Se contents are higher, possibly reflecting concentrations in the bedrock (Shacklette, 1974) or alkali soil conditions. Se can concentrate in the soil and in vegetation growing on the soil in semi-arid regions with impeded drainage. Crop plants in these areas may have toxic concentrations of Se (Gough *et al.,* 1979). Volcanic soils may have high Se contents depending on climate conditions.

Plants generally tolerate Se in amounts above the crustal average, though it is not clear what physiological role Se plays in plant growth. When available, in a soluble (oxidized) form, Se is readily absorbed by the plants, consequently the concentration in many plants reflects the concentration of the soluble component of total Se in the soil and is not particularly characteristic of the species. This means that Se concentrations in plants can vary year to year based on changes in climate, that effect soil conditions and solubility of Se (Erdman *et al*., 1990). Generally plant Se concentrations are less than that in soils except for mushrooms and other fungi, which are approximately 100 times better at extracting Se from soils than green plants and have contents that range from 0.1 to 16 ppm (Kabata-Pendias and Pendias, 1984). Some plants known as Se accumulators specifically concentrate Se and are toxic to animals; these plants often have a garlicky smell. When they decompose they release Se into the soil in a soluble form available to other species. Se concentrations in plants can range from 0 to 3% dry wt (Table 3).

Concentrations in cereals range 0 to 500 ppb and a general range for healthy leaves is 0.01 to 2 ppm. In plants, Se is concentrated in the growing points, seeds and roots. Concentrations in mature woody plants are probably less than those found in fast growing grasses. Generally Se concentrations in plants are less than concentrations in coal seams.

SELENIUM IN COAL

Selenium is enriched in coal compared to crustal average (0.05 to 0.1 ppm). Averages from different areas are hard to determine because of limited data and range of values; however Table 4 provides approximate numeric average data for a number of areas.

TABLE 3
AVERAGE SE CONTENTS IN SOME PLANTS

	Se concentrations in ppm range ppm	mean	reference
corn	0.01 - 0.5	0.055	A
soybean	0.04 - 1.25	0.11	A
cedar	0.01 - 0.04	0.023	A
oak	<0.01 - 0.04	0.026	A
pine	0.02 - 0.2	0.062	A
wheat	0.15 - 2.2	0.57	B
sage brush	0.01 - 7	0.16	B
grasses	0.013 -0.35	0.074	C

A= Connor *et al*. (1975)
B= Shacklette and Boerngen (1982)
C= Kabata-Pendias and Pendias (1984)

A more complete table can be found in Swaine (1990). The number of analyses available from each area varies, and some data may be reported for clean coal. As discussed later, because Se tends to concentrate in the ash in coal, concentrations in clean coal are substantially lower than those in raw coal. The average concentration in world coals (raw basis) is about 2.15 ppm.

Coleman *et al.* (1993) looked at the distribution of Se in U.S. coals and provided arithmetic and geometric averages for data from various regions of the U.S. The arithmetic averages are included in Table 4 because they are consistent with data from other countries. Coleman *et al*. (1993) obtained a geometric average for all coals in the U.S. of 1.7 ppm. Selenium concentrations are higher in coals from the eastern part of the continent irrespective of coal rank or age. Average Se concentration in the Rocky Mountain region, which is the southern extension of the Kootenay coal fields in southeast British Columbia, is 1.6 ppm compared to a combined average of data from previous publications and this study of 1.6 ppm for the Mist Mountain coals. In China the average Se concentration is 6.2 ppm (Ren *et al.,* 1999) and some coals are reported to have concentrations as high as 8.4% (Yang *et al.,* 1982). Older Carboniferous, Permian and Triassic coals in China have concentrations over 4 ppm and younger coals concentrations less than 2 ppm.

The detailed mineralogical associations and chemical forms of Se in coal are discussed subsequently using data collected in this study. Existing literature permits a general discussion of the association of Se with coal, mineral matter and pyrite. Generally authors attempt to outline an organic or non-organic affinity and look for correlations of Se with coal, ash, total, pyritic or organic sulphur. This does not necessarily reveal the source of the Se. Gluskoter *et al.* (1977) found that Se in coals from Illinois has an partial non-organic affinity and that there was no correlation of Se with organic sulphur. Consequently, Se may have a positive correlation with ash and to a lesser extent pyrite, which often tends to be associated with ash. Based on all the data in their paper, Se correlates with ash (r^2=0.4), uranium (r^2=0.38) and pyrite (r^2=0.29). A detailed look at four bench samples studied in their paper indicates that Se often concentrates in the upper part of seams and that this does not necessarily correlate with high ash concentrations (Figure 2).

Except for one bench, in which data are biased by a single sample containing a high pyrite concentration, Se tends not to correlate with pyritic or organic sulphur in the incremental bench samples. As with all the data in the paper, bench sample Se values correlate positively with ash and uranium. In fact the best overall correlation is with uranium despite the fact that uranium in contrast to Se has a clear organic affinity in coal seams.

The Se *versus* U correlation may result because both Se and U are removed from solution in the acid anaerobic conditions in coal swamps. The correlation does not appear to exist for marine influenced coals such as some Illi-

TABLE 4
AVERAGE SE CONTENTS FOR WORLD COALS

area	number of analyses	comments	value**	rank *	age	reference
Canada						
SE BC published+this study	208	raw	1.60	MV	Jura-Cretaceous	
BC Intermontane	59	raw	1.00	L, SB	Tertiary	Goodarzi and Van der Flier-Keller (1990)
BC Nanaimo coalfield	10	raw	0.60	HV	Cretaceous	Van der Flier-Keller and Dumais (1988)
BC	22	raw	0.91	HV	Cretaceous	Van der Flier-Keller and Dumais (1988)
Northeast BC	8	raw	1.5	MV	Cretaceous	Grieve and Goodarzi (1994)
Saskatchewan lignites			2.3,4.1	L	Tertiary	Beaton and Goodarzi (1989)
Nova Scotia	23	raw	1.90	MV	Pennsylvanian	Pilgrim and Zodrow (1990)
	452		0.8			Raask, (1985)
USA						
national average	86	raw	3.30		Variable	Pillar *et al.* (1969)
national average	101	raw	2.10	B		Raask (1985)
national average	799	raw	4.10	SB B		Raask (1985)
Eastern	4711	raw	4.20	HV to A	Pennsylvanian	Coleman *et al*. (1993)
Gulf	214	raw	5.60	L	Tertiary	Coleman *et al*. (1993)
Interior	705	raw	3.10	HV MV	Pennsylvanian	Coleman *et al*. (1993)
Northern Great Plains	1154	raw	0.99	SB	Cretaceous	Coleman *et al*. (1993)
Rocky Mountain	1615	raw	1.60	MV,HV	Jura Cretaceous	Coleman *et al*. (1993)
Alaska	258	raw	1.10	SB	Tertiary/Cretaceous	Coleman *et al*. (1993)
Pacific Coast	38	raw	1.90	L SB	Tertiary	Coleman *et al*. (1993)
Eastern Kentucky	22		4.29	MV	Pennsylvanian	Eble and Hower (1997)
Powder River			0.94	SB		Oman *et al*. (1988)
North Dakota	17		0.79	L	Tertiary	International Coal Reports, 1998 No. 463
Illinois			3.00	HV		International Coal Reports, 1998 No. 463
Appalachian			3.70	MV,HV		International Coal Reports, 1998 No. 463
England	24	raw	1.75	V	Carboniferous	Spears and Zheng (1999)
	23		2.70		Carboniferous	Raask, (1985)
	?		2.80	B	Carboniferous	Raask, (1985)
Indonesia	2	clean	0.17	HV	Tertiary	ACARP (1993)
Australia	?	raw	0.90	B	Permian	Swaine (1990)
Australia Bowen Basin	40	clean	0.44	B	Triassic-Jurassic	Riley and Dale (2000)
South Africa	6	clean	0.76	MV	Permian	ACARP (1993)
China	118	raw	6.22	V	variable	Ren *et al.* (1999)

rank* L=lignite SB=sub bituminous B=bituminous HV=high volatile bituminous
MV=medium-volatile bituminous LV=low-volatile bituminous LV=low-volatile bituminous A=Anthracite ** =Arithmetic mean V=variable

nois coals (Harvey *et al*., 1983) and coals from Nova Scotia (Pilgrim and Zodrow, 1990). These coals may have formed in more oxidizing environments in which U remained soluble. Boron concentrations are considered to indicate degree of salinity and therefore degree of marine influence. In the Coal Mountain mine data from Goodarzi (1987) both U and Se correlate negatively with B possibly indicating a preference for deposition in a non marine acid anaerobic environments.

They indicate an ash and pyrite association for Se with the pyrite connection being strongest. Finkelman (1994) considered Se to have a mixed association in coal with a significant organic component. Coleman *et al*. (1993) state that Se is associated with the organic fraction probably substituting for organic sulphur, though they did not always find a good correlation of Se with organic sulphur. Many other workers have found at least a partial association of Se with syngenetic pyrite (Clarke and Sloss, 1992). White *et al.,* (1989) found average concentrations of 97 and 64 ppm Se in pyrite and marcasite from UK coals. Higher concentrations have been found in pyrite and marcasite of higher temperature origin (up to 3% and 80 ppm respectively) (Wedepohl, 1978). Goodarzi and Swaine (1993) report finding trace amounts of clausthalite (PbSe) and ferroselite ($FeSe_2$) in coals. Harvey *et al*. (1983) found a mixed association of Se in coals from the Illinois basin. Data from their study can be used to estimate concentrations of Se in coal ash and pyrite. Sample Se concentrations were predicted using Se concentrations for the ash, coal and pyrite components of samples. The best fit (r^2=0.66) of predicted *versus* actual concentrations was obtained by assuming Se concentrations of 1 ppm in coal, 8 ppm in ash and 26 ppm in pyrite (Figure 3).

Obviously this solution is not unique but the analysis is consistent with lower concentrations in coal, moderate in ash and higher in pyrite, though not as high as found by White *et al*. (1989).

Few papers discuss the source of the Se in coal. Gluskoter *et al.* (1977) note the enrichment of Se in coal compared to average crustal abundance and attributed at least some of the Se to the original vegetation. However the amount of Se in coal often appears to be more than can be attributed to the vegetation from which the coal was derived. Most plant species average less than 1 ppm (Table 3) and even after increasing the Se concentration in coal, because of the loss of volatile matter during coalification, concentrations in coal still appear to be too high to be explained solely by concentrations in plants. It is also probable, that depending on conditions in the coal swamp, overlying vegetation may extract Se from the underlying rotting vegetation causing an upward migration of Se and consequently new vegetation may not be responsible for bringing additional Se into the coal swamp.

Some of the Se found in coal must be transported into the coal swamp either in solution or with detritus. In the Powder River coals, Se correlates positively with ash (r^2=0.62) and to a lesser extent with organic sulphur (r^2=0.4 in the south and 0.81 in the north) and pyritic sulphur (r^2=0.3) (Oman *et al*., 1988). The correlations with both organic sulphur and ash could imply that Se originated from Se rich Cretaceous formations to the south of the basin and was introduced into the coal swamp with detritus and in solution.

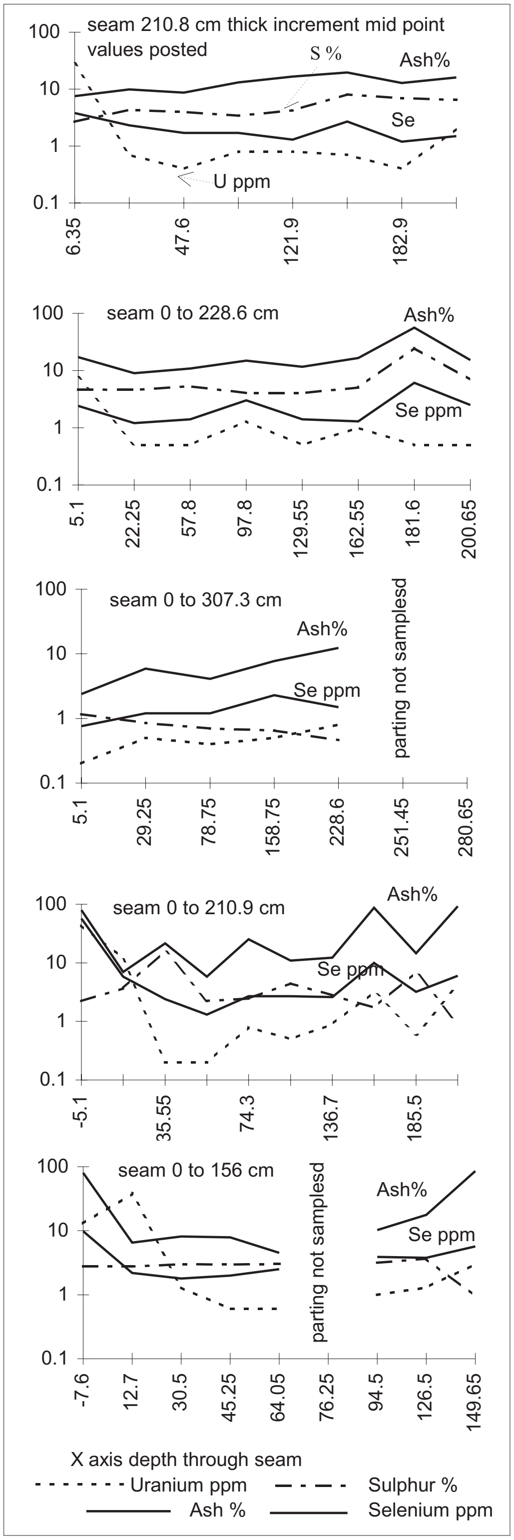

Figure 2. Se, U, S and ash in bench sample data from Gluskoter *et al*. (1977).

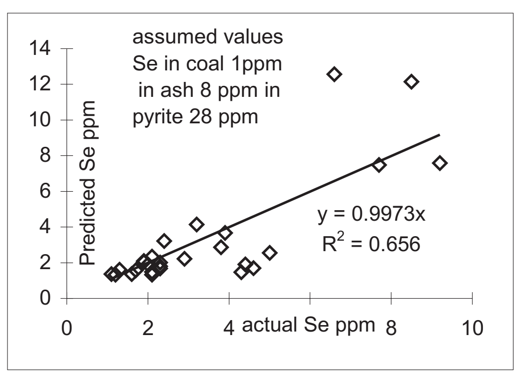

Figure 3. Predicted *versus* actual Se concentrations (analytical data from Harvey *et at*., 1983).

ANALYTICAL TECHNIQUES

Sample preparation for Se is important because it is very volatile and even with low temperature ashing of coal samples at less than 200°C, 10% to 30% of the Se may lost (Finkelman *et al*., 1990). Samples can be dissolved using wet chemical means in sealed containers or at low temperatures. Concentrations can be analyzed using atomic adsorption (AA) with hydride generation or a graphite furnace and using inductively coupled plasma mass spectroscopy (ICP-MS). Alternatively, samples can be analyzed using instrumental neutron activation analysis (INAA), which does not require any sample preparation other than crushing and pulverizing. INAA does take longer than techniques using AA or ICP-MS and Se analyses are effected by interference from tantalum, which can raise the detection limit. All these techniques have detection limits of 0.2 to 0.8 ppm. In this study INAA was used for determining Se concentrations, mainly because of concerns about Se volatility and chemical interferences.

The precision and accuracy of the data were checked by repeatedly analyzing one rock and one coal standard, by analyzing duplicates of samples and by obtaining duplicate analyses of some samples in a second laboratory also using INAA. The results of the various data checks (Table 5) indicate that in the range of 1 to 5 ppm, precision and accuracy are moderate, and there does not appear to be any systematic bias to the data.

Four analyses of the coal standard Lower Bakerstown CLB-1 provide an average result of 2.4 ppm compared to 2 ppm reported by the USGS. The value of 2 ppm is referred to as an information value based on analyses from less than 3 laboratories and the methods of analyses are not reported. Four analyses of a combined rock plus sulphide standard provide an average of 3.4 ppm compared to an average of 2.5 ppm obtained by wet chemical means. The latter value is low because of partial extraction of Se and loss of Se during acid digestion and heating. In general the analyses of standards and of duplicates indicate that the 1 sigma SD of the samples is probably less than 20%. There is no indication that the data is significantly biased and that the INAA is providing values that are too high or too low.

Some rock samples were analyzed for various metals including Se using ICP-MS. This technique uses an aqua regia digestion (samples heated to about 90°C) and provides ppm concentrations of a number of metals including Se. The acid digestion may only partially extract Se from silicates or organic material or may volatilize some, but in a cross plot with INAA results (Figure 4) there does not seem to be a bias.

In fact this analytical technique which is more sensitive for Se analyses than INAA provided a slightly higher averaged Se value of 3.4 compared to 2.7 for INAA. The ICP-MS technique was not used for coal samples because Se may not be completely extracted from organic samples using aqua regia.

TABLE 5
ANALYSES OF STANDARDS AND DUPLICATE ANALYSES, INSTRUMENTAL NEUTRON ACTIVATION ANALYSES

Sulphide rich rock standard					
sample 1	3.9	Se ppm			
2	3.7	Se ppm			
3	2.4	Se ppm			
4	3.6	Se ppm			
5	3.0	Se ppm			
Average	3.3	SD =	0.6	SD%=18.49	
USGS coal standard Coal, lower Bakerstown CLB-1					
medium-volatile bituminous coal					
information value for Se given as 2ppm					
i.e. less than 3 independent labs providing data					
analysis 1	1.6	ppm			
2	2.9	ppm			
3	2.7	ppm			
4	2.2	ppm			
Average	2.4	SD	0.6	SD% 24.69	
REPEAT ANALYSES AT LAB 1					
	Se ppm		diff	% diff	composition
sample 1	1.6	1.5	-0.1	-6.5	coal
2	5.3	5.2	-0.1	-1.9	coal
3	2.0	2.1	0.1	4.9	coal
4	2.6	3.8	1.2	37.5	sed
5	4.3	4.8	0.5	11.0	footwall
6	7.0	6.5	-0.5	-7.4	coal
DUPLICATE ANALASES LAB 1 AND LAB 2					
LABS	1	2	diff	% diff	composition
	Se ppm				
Sample 1	3.2	3.6	-0.4	-11.8	coal
2	2	2	0	0.0	coal
3	1.3	1.1	0.2	16.7	coal
4	2.5	2.6	-0.1	-3.9	mdst
5	2.2	2.8	-0.6	-24.0	mdst
6	3.6	3.3	0.3	8.7	rock stnd

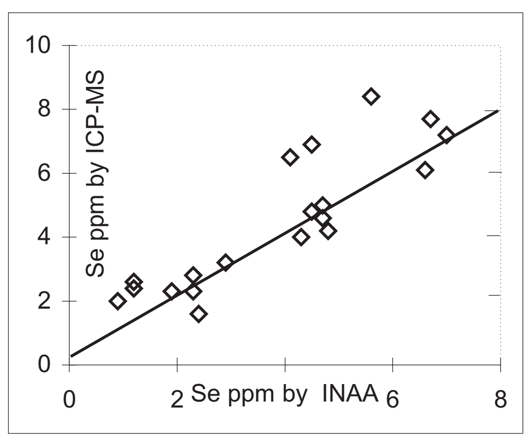

Figure 4. Cross plot of Se concentrations determined by INAA and ICP-MS.

In this study ash analyses were made on as-received samples. The small difference between as-received and air-dried results was not considered significant considering the cost saving and that the data are used only to outline the relationship between Se and ash. The ash analyses for samples that were analyzed for ash and oxides were made using a high temperature ashing technique that does not conform to the standard ASTM method but produces acceptable results (Figure 5).

EXISTING SELENIUM DATA FOR COALS IN BRITISH COLUMBIA

There is not a lot of data on Se in BC coals. Data for northeast BC (8 analyses) provides an average of 1.5 ppm for coal seams in the Jurassic-Cretaceous Gates Formation. Coal seams in the Cretaceous Telkwa deposit near Smithers in central BC have average Se contents of about 0.4 - 0.8 ppm with a lot of analyses below detection limit, which ranges from 0.2 to 0.8 ppm. Coal seams from the Upper Cretaceous Nanaimo and Comox coal basins average 0.6 ppm (10 analyses) and 0.91 ppm (22 analyses) respectively (Van der Keller and Dumais, 1998). The Tertiary Bowron Basin in the central part of the province has a higher average content of about 2.1 ppm and the Hat Creek Tertiary deposit a lower average of 1.1 ppm (Goodarzi and Van der Keller, 1988).

The Se content of coal seams in the Mist Mountain Formation has been studied by Goodarzi (1987, 1988 and 1993) who collected samples from the Fording River and Coal Mountain mines. Coal samples from a number of mines were analyzed by Grieve (personal communication, 1999). These data provide an average Se content in raw coals from the Mist Mountain Formation of 1.36 ppm. The average is biased by analyses of seams low in the section, which appear to have lower Se concentrations than seams higher in the section.

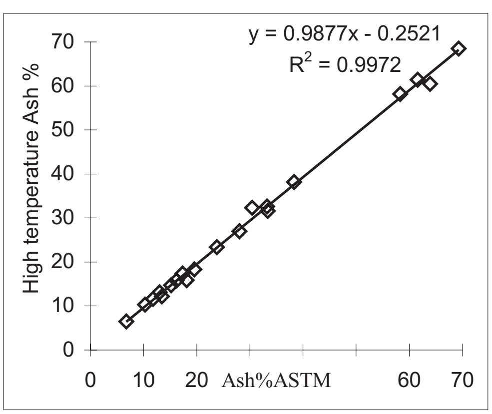

Figure 5. Cross plot of ash determined by ASTM and high temperature ashing methods.

EXISTING SELENIUM DATA FOR KOOTENAY GROUP ROCKS

Data on Se concentrations in rocks of the Kootenay group are not available. Analyses of water and sediments in areas adjacent to the coal mines were reported by McDonald and Strosher (1998) in a study of the potential effects of coal mining on Se concentrations in the Elk River basin. They documented a trend of increasing Se content over time in the Elk River measured at its mouth approximately 65 kilometres down river from the mines. They also documented increased concentrations of Se in tributary creeks draining areas of mining activity compared to concentrations in the Elk and Fording rivers up stream from the mines. Selenium contents of sediments range up to about 3 ppm except for the Michel Creek area where concentrations are lower. On average concentrations in sediments are higher in creeks draining mine areas (about 2 ppm) than in creeks above mining areas (less than 1ppm).

DATA

In this study approximately 375 samples were collected and over 400 Se analyses obtained. Samples were collected from the five coal mines in the east Kootenays identified by the letters A to E in this paper. Attempts were made to sample the complete exposed Mist Mountain section at each mine, however, because of mining activity this was not possible at all mines. At some mines, sections were sampled in more than one pit. Interburden rock was divided into simple rock units and sampled by collecting chips at approximately 1 to 3 metres intervals along high walls. Individual samples varied from 1 to 5 kilograms of rock or coal chips. Coal seams were sampled by channel sampling or by collecting chips. Hanging wall (HW) and foot wall (FW) material, adjacent to some seams, was sampled separately as were rock splits (partings) within some coal seams. All samples were analyzed for total Se. Some samples were also analyzed for total As using INAA; for major oxides using XRF and for metals using ICP-MS.

Coal samples were analyzed for ash and some for sulphur forms. Three coal seams were subjected to washability analysis. Incremental samples were collected across two seams to investigate the stratigraphic distribution of Se within seams.

Samples of wash plant reject material (coarse refuse > 0.15 mm and tails < 0.15 mm) were collected at each mine. At some mines the refuse material was screened into a number of size fractions. At one mine a sample of breaker reject was collected. More samples of this material were not collected because of the coarseness of the material and difficulty in getting a representative sample. At one wash plant samples of fine coal before and after the dryer were collected.

Rock and coal samples were crushed, split and then 100 to 200 grams pulverized to provide samples for INAA, XRF oxide and ICP-MS analyses. Splits of crushed material of samples containing coal were kept to be used for coal quality analyses. Some of these samples were floated in heavy liquids to provide separate coal and mudstone rich fractions, which were subjected to further analysis.

Before surface water from the mines is released into rivers, it is diverted through settling ponds, that collect fine sediment derived from waste dumps and other areas of the mine. Twenty nine sediment samples were collected from a number of settling ponds at each mine. Sediment samples were dried and minus 100 mesh material screened off and sent for oxide and Se analyses. Some sediment samples were also sent for total organic carbon (TOC) analysis.

SELENIUM STRATIGRAPHY IN THE MIST MOUNTAIN FORMATION

Based on sampling at the five mines 7 partial stratigraphic sections through the Mist Mountain Formation were established (Figures 6 to 10).

Sections were broken down into interburden rock and coal seams, which were generally sampled as single units, except in a few cases where partings 0.1 to 0.5 metre thick were sampled separately. Tonstein bands were identified in some seams and sampled separately. These are generally 0.01 to 0.05 metre thick brown kaolinite rich bands of volcanic origin. Interburden rock was subdivided into five units based on mudstone component (Table 6) ranging from carbonaceous mudstone to sandstone or siltstone.

Attempts were made to integrate units such that the minimum unit thickness was more than about 2 metres. Hanging wall (HW) and foot wall (FW) samples were collected for some seams, where there was an obvious gradation from coal seam to interburden lithology. These samples usually represented from 0.1 to 0.5 metre of mixed rock and coal and were not collected for all seams. A few samples were collected from the Fernie Formation, which underlies the Mist Mountain Formation and is exposed at some mines.

The Se concentrations and number of samples from each lithology are identified in Table 6 as composite averages and as averages for each mine. In each case two values are reported, the higher calculated assuming that values below detection limit are equivalent to the detection limit and the second calculated assuming that any value less than the detection limit is zero. The averages are weighted based on the thickness represented by each sample. Because coal and rock averages are calculated separately the thickness weighted averages are very close to mass weighted averages.

Individual lithologies are not identified on the sections (Figures 6 to 10) except for strip logs identifying location and thickness of coal seams. For all mines the lowest seam identified in the sections is the lowest seam mined and either rests on the Moose Mountain Member or is a few metres above it. Sections illustrate the approxi-

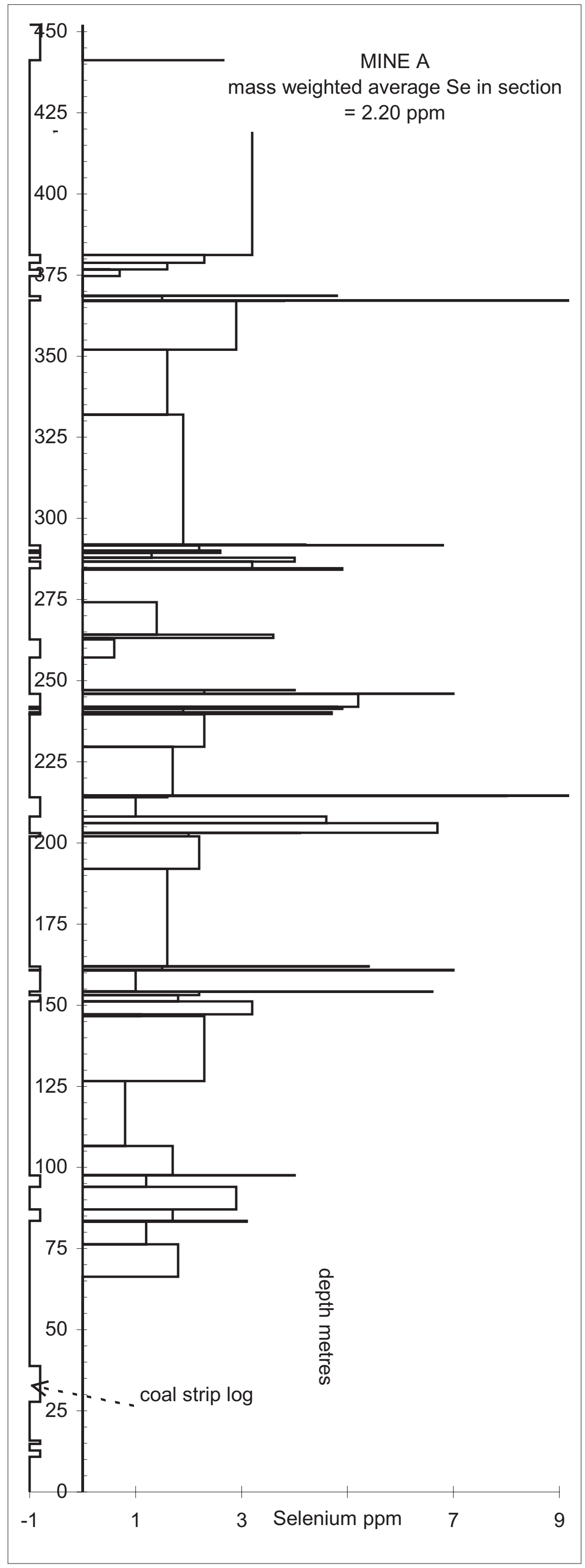

Figures 6 to 10. Stratigraphic sections at the 5 mines (A, B, C, D, and E) illustrating variation of Se content with depth. Locations of coal seams are indicated. Data below detection limit (0.2 to 0.8 ppm) are plotted as detection limit.

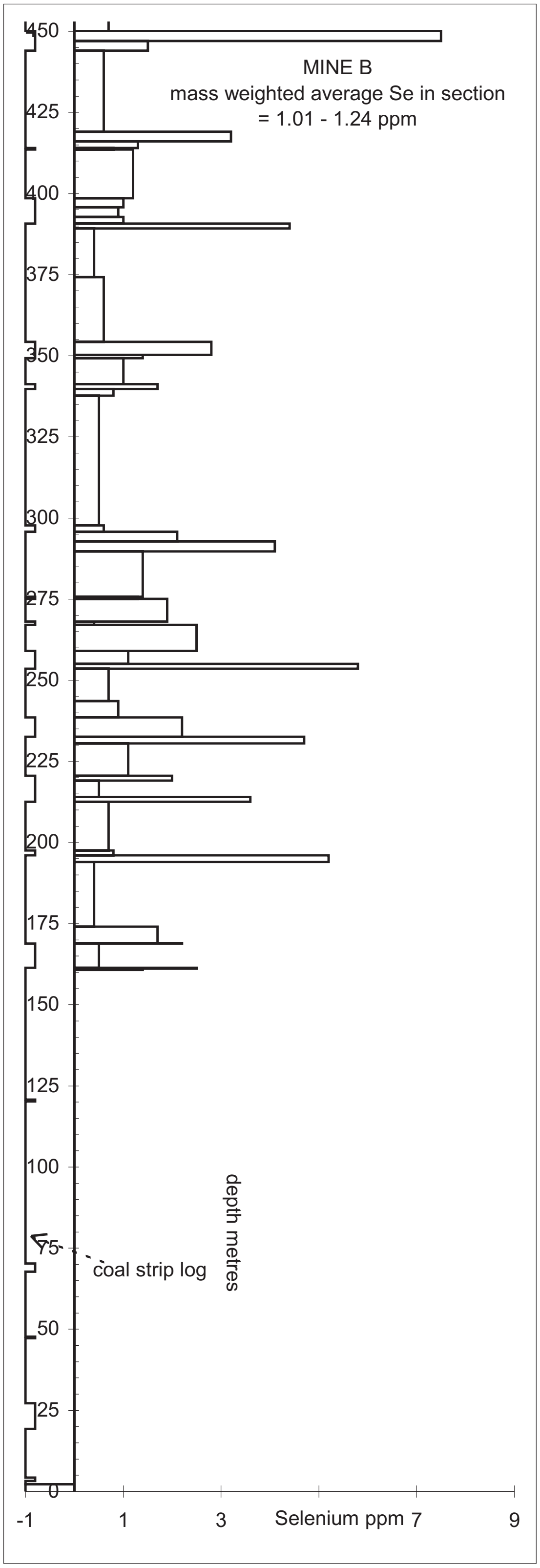

Figure 7

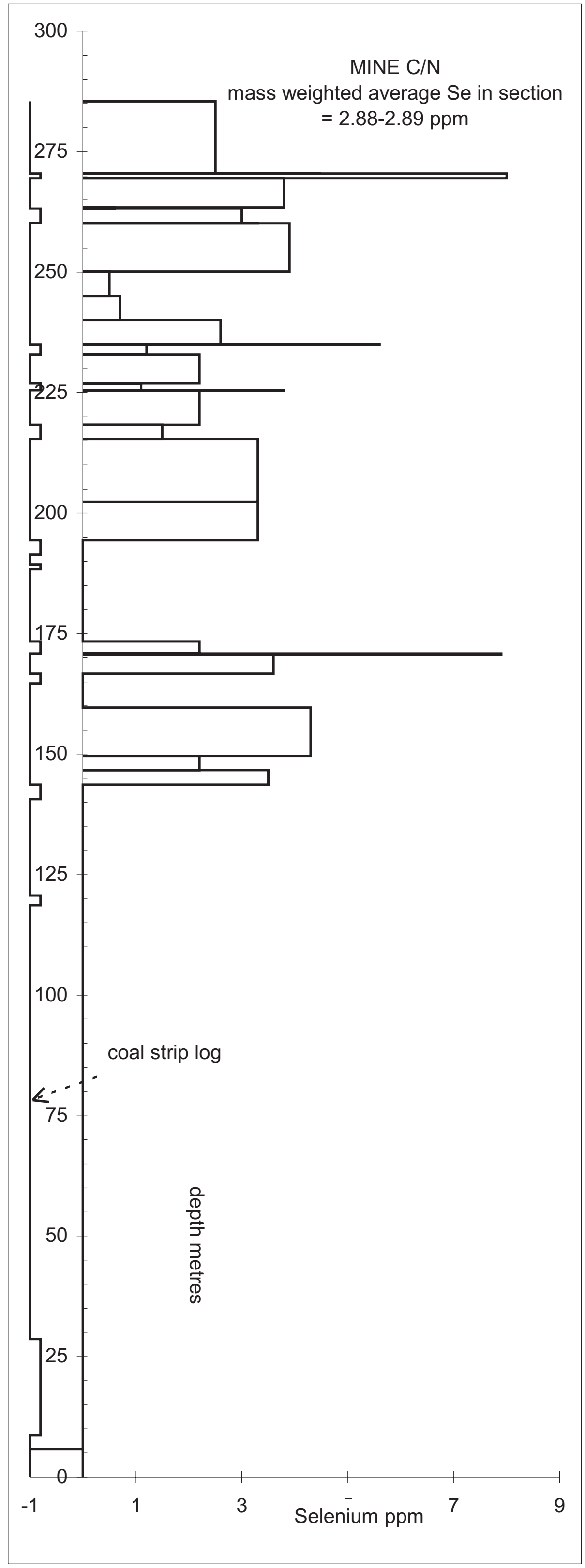

Figure 8a

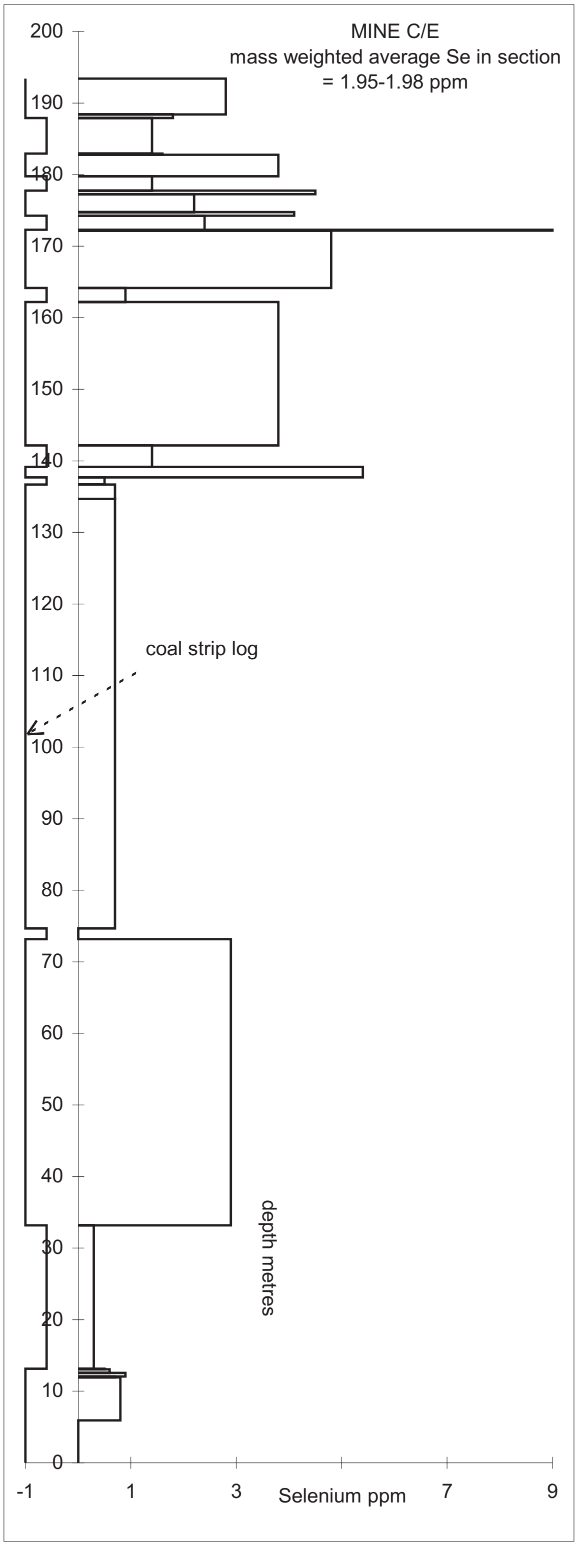

Figure 8b

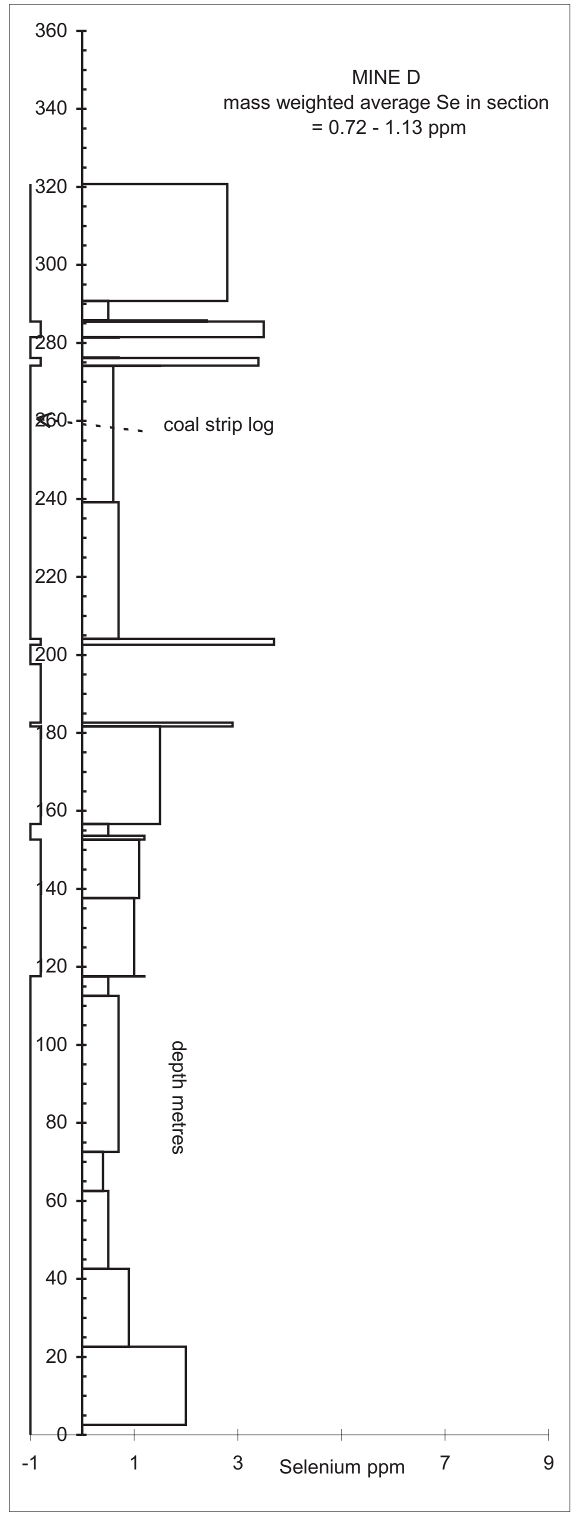

Figure 9

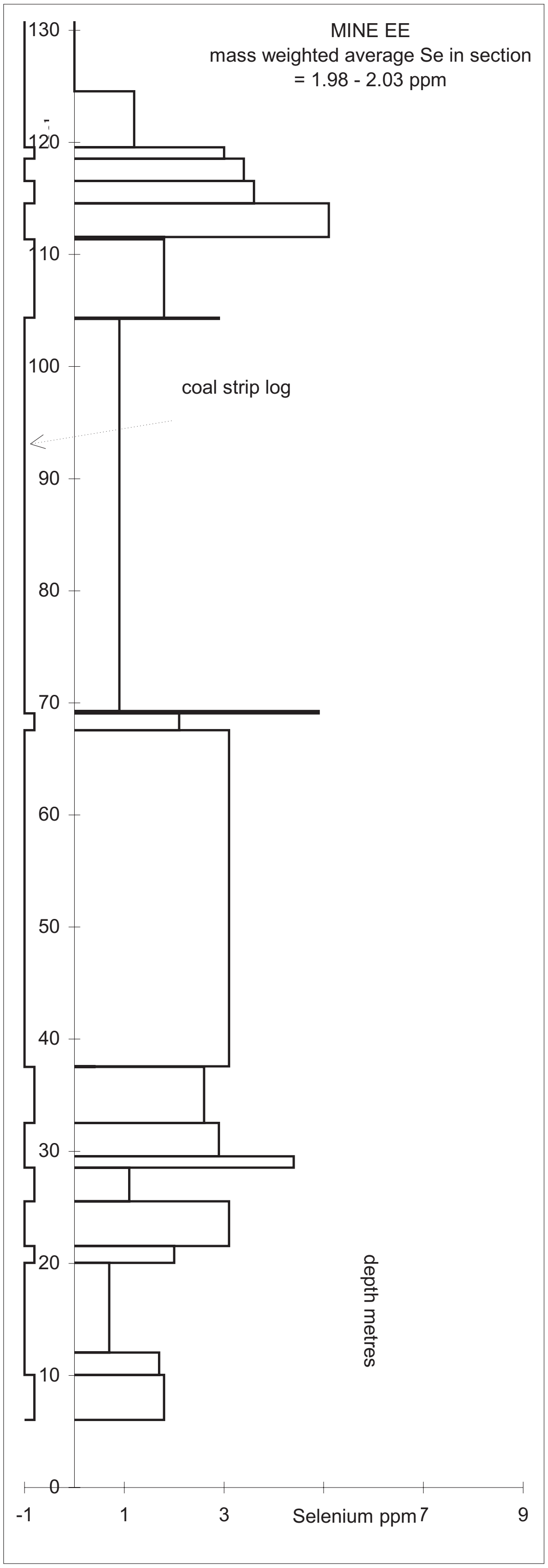

Figure 10a

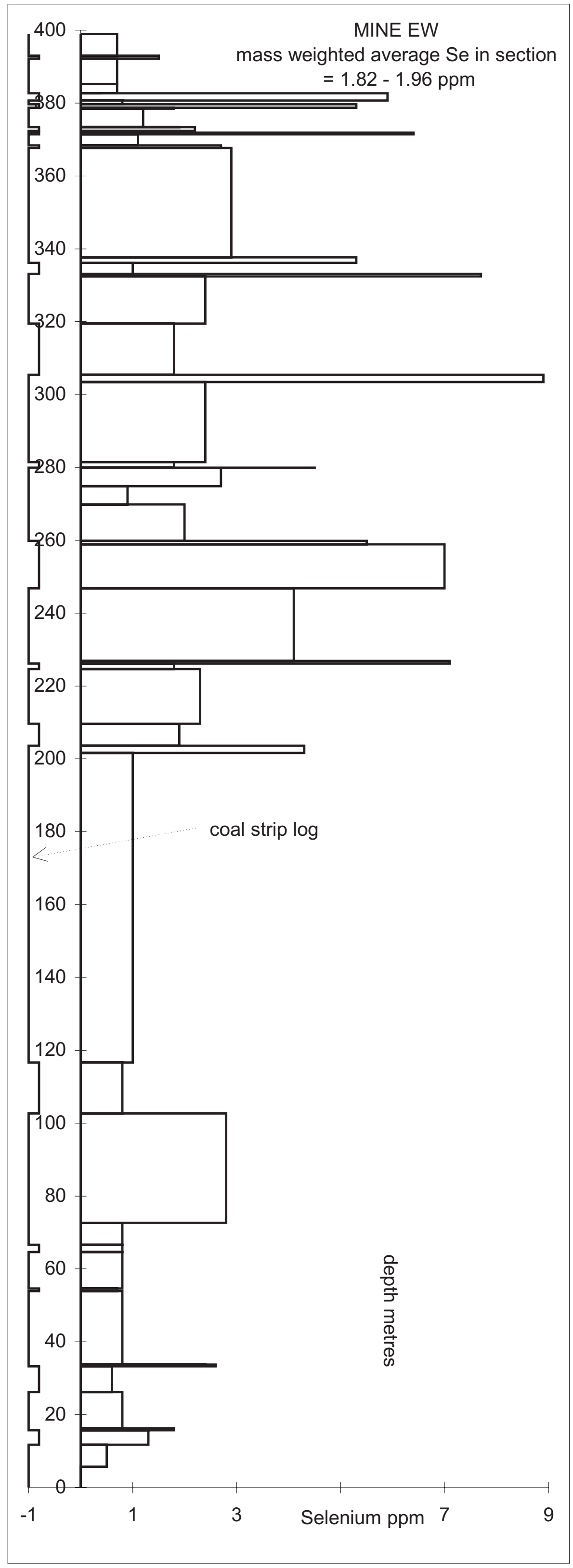

Figure 10b

TABLE 6
THICKNESS WEIGHTED AVERAGE SELENIUM CONCENTRATIONS BY MINE AND BY LITHOLOGY

	ALL MINES					MINE A			MINE B			MINE C			MINE D			MINE E		
	samples	Se high	Se low	samples	As	samples	Se high	Se low	samples	Se high	Se low	samples	Se high	Se low	samples	Se high	Se low	samples	Se high	Se low
coal seams	107	1.9	1.9	55	2.4	24	1.7	1.7	28	2.0	2.0	17	1.5	1.4	7	1.5	1.5	31	2.4	2.4
HW rock	21	4.2	4.2	8	3.7	10	4.2	4.2	1	2.2	2.2	4	2.8	2.8	2	1.8	1.6	4	5.6	5.6
FW rock	21	4.2	4.1	8	5.3	3	4.7	4.7	4	4.2	4.2	8	1.3	1.3	3	1.0	0.5	3	6.8	6.8
partings in coal seams	23	3.2	3.2	5	10.0	7	4.8	4.8	0			3	7.2	7.2	2	2.1	2.1	11	2.5	2.5
tonstein	3	1.8	1.8	0		1	1.6	1.6	0			0			0			2	2.1	2.1
mdst with coal stringers	20	3.2	3.2	2	2.7	3	3.1	3.1	7	2.9	2.9	3	3.9	3.9	0			7	3.1	3.1
mdst	24	2.8	1.9	4	4.6	7	2.5	2.5	4	1.5	0.9	9	2.3	2.3	0			4	1.2	1.2
silty mdst	26	2.0	1.9	2	9.3	4	1.8	1.8	8	1.1	0.9	8	2.9	2.9	0			6	2.4	2.4
muddy siltstone	33	2.0	1.9	4	7.4	4	3.0	3.0	7	0.9	0.9	14	2.1	2.1	4	1.2	0.8	4	2.5	2.5
siltstone/sandstone	27	1.1	0.9	4	12.9	5	1.5	1.5	5	0.6	0.0	7	1.8	1.8	2	0.5	0.0	8	0.9	0.7
refuse coarse and tails	23	2.8	2.8	7	3.6	7	3.2	3.2	4	2.7	2.7	4	1.6	1.6	4	1.8	1.8	4	2.9	2.9
breaker	1	2.1	2.1	1	4.7	0			0			1	2.1	2.1	0			0		
Fernie shale/siltstone passage beds	9	1.1	0.9	4	5.7	2	0.8	0.0	0			2	2.4	2.4	5	0.9	0.2	0		
sediments - 100 mesh fraction	29	3.1	3.0	13	5.4	8	2.4	2.4	6	5.7	5.7	5	2.1	2.1	3	0.9	0.5	7	3.3	3.3
pyrite	3	10.2	10.2	3	670	3	10.2	10.2	0			0			0			0		
clean coal	4	1.1	1.1																	
sample count	374			120		88			74			85			32			91		

note averages are weighted by unit thickness except for refuse, Fernie shale, sediments, pyrite and clean coal.
HW=hangingwall FW=footwall mdst=mudstone
Se high average calculated assuming data below detection limit=detection limit.
Se low average calculated assuming data below detection limit=0

mate thickness of rock and coal units and their Se contents. A Se content of zero indicates that the zone was not analyzed. In cases where Se concentrations were below the detection limit, the value plotted is the detection limit and consequently the sections tend to slightly over emphasize some Se concentrations. However the mass weighted average Se concentrations reported in Figures 6 to 10 are calculated in two ways similar to the data in Table 6. This provides a maximum and minimum estimate of the average Se concentration in the sections and in most cases there is not a lot of difference between the two values.

The Se concentration of rocks and coal in the sections at two of the mines average about 1 ppm and at the other mines 2 ppm to 3 ppm. Based on the number of samples and the thickesses of the sections these averages should no be considered as definitive. The sections clearly illustrate that Se concentrates in rocks adjacent to coal seams (HW and FW) and in some partings in the coal seams, but not necessarily in tonstein bands. In interburden rocks the Se content increases as the mudstone content of the units increases (Table 6). A lot of the analyses for the sand rich units were below detection limits, which vary from 0.2 ppm to 0.8 ppm depending on interferences from other elements. The Se concentrations in coal seams are generally less than in the HW and FW rocks. There is also a weak tendency for the Se concentrations in rocks to increase up section; this is probably related to the increased amount of mudstone in the upper part of the Mist Mountain section. There does not appear to be any major stratigraphic control of Se concentrations in seams, though there is a tendency for concentrations to be higher in the mid part of the section (Figure 11).

The concentration of Se in the Fernie Formation shale, which underlies the Mist Mountain Formation, ranges from below detection to 2.6 ppm, averaging about 1ppm, and is therefore not high based on the marine origin and mudstone composition of the formation.

The average Se concentrations for the lithologic subdivisions of the Mist Mountain Formation are generally higher than those reported in the literature for similar lithologies (Table 2). This is probably because of the amount of dispersed organic material in the section. However there are no major units that stand out as consistently having very high Se concentrations. No Se analyses were made of the overlying Elk Formation, which contains thin sapropelic coal seams. These seams may have high Se concentrations because of their high algae content.

As discussed later, the Se content of seams is influenced by ash content and seam petrography and therefore lateral consistency of Se concentrations in individual seams will probably depend on these variables. The Se content of seams from one mine were analyzed during this study and by Goodarzi (1988) and there is a tendency

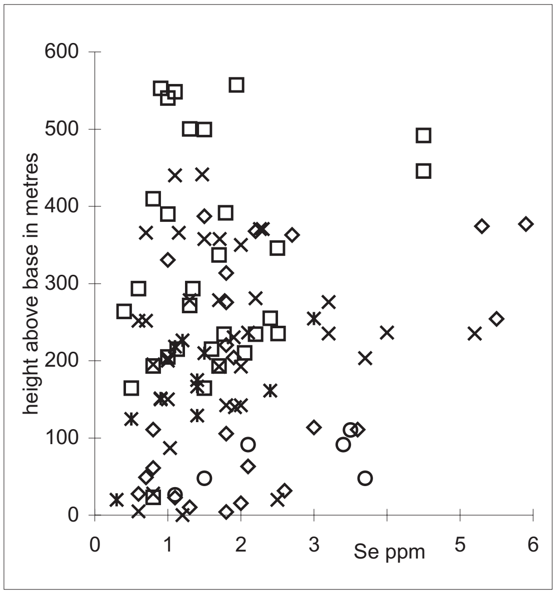

Figure 11. Se content in seams *versus* elevation above Moose Mountain Sandstone, data for all five mines; cross=mine A, square=mine B, star=mine C, circle=mine D, diamond = mine E.

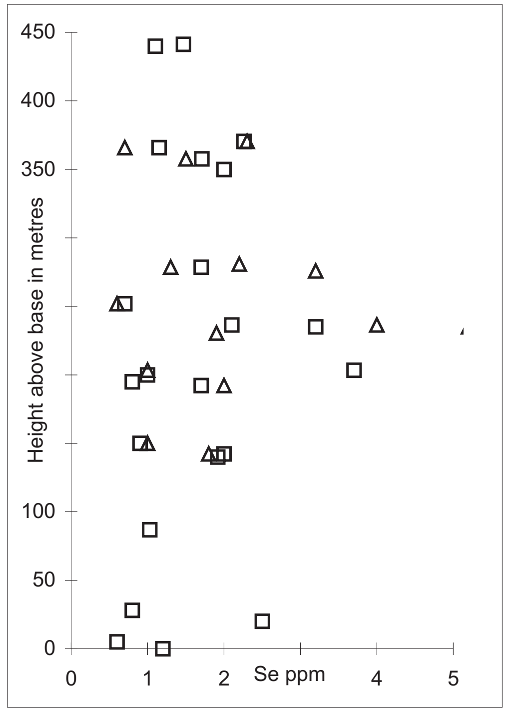

Figure 12. Comparison of Se contents for equivalent seams from this study and Goodarzi (1988); squares = Goodarzi (1988) data, triangles = this study.

for samples from the same seam to have similar Se concentrations (Figure 12).

The Se concentrates in HW and FW samples. However not all hanging wall and foot walls of seams were sampled so that these averages are not representative of the rock dilution that might be expected to be mined with the seams. In an attempt to get more representative averages, in cases where HW and FW material was not sampled, 0.5 metre of adjacent interburden was assigned to represent HW or FW and new averages calculated. Because Se tends to concentrate in rocks adjacent to seams, these second averages (contact rock Table 7) are probably lower than the averages that would have been obtained had all HW plus FW material been systematically sampled. The concentration of Se near seams is illustrated by 2 samples of FW material one representing 0.2 metres adjacent to the seam contained 2.5 ppm Se and another sample representing 0.4 metres also adjacent to the seam contained 1.4 ppm Se.

Sections totally representative of present mining operations were not sampled, however it is useful to calculate the average Se concentrations and the amount of Se in what is likely to be segregated as waste rock, run-of-mine coal and contact rock (Table 7).

Generally contact rock has the highest Se concentrations followed by raw coal and then interburden rock. Based on the 0.5 metre assignment to HW or FW (which is probably high) interburden rock accounts for over 80%, coal from 6% to 20% and contact rock 5% to 10% of the total Se in the section. The interburden material is transported to waste rock dumps. A lot of the contact material will after processing be segregated as coarse refuse and dumped somewhere on the mine site.

Refuse material is composed of contact material plus fine ash liberated from the coal. It should therefore be possible to estimate the average Se content of refuse material. The Se concentration of the contact material will be between that calculated in Table 7 and that calculated for HW+FW material in Table 6. The fine ash, which probably has Se concentrations in the range of 3.8 to 4.9 ppm based on ash *versus* Se plots (Figure 13), is extracted from the raw coal and ends up mainly as the tailings component of the refuse material.

Therefore average refuse material should have Se concentrations higher than the values for contact material in Table 7. Actually most of the refuse material has averages noticeably lower. A possible explanation is that some Se is lost easily and quickly from the fine ash and contact material during mining, crushing and washing.

SELENIUM IN COALS FROM THE MIST MOUNTAIN FORMATION

Coal samples from the Mist Mountain Formation, analyzed in this study, have average Se concentrations of about 1.9 ppm, (Table 6), when this data is combined with existing data for Mist Mountain coals the combined numeric average is about 1.6 ppm. This compares to a world average of 2.15 ppm (Coleman *et al.,* 1993). There are no

TABLE 7
AVERAGE SE CONCENTRATIONS AND PERCENTAGES OF MAJOR ROCK TYPES SEGREGATED BY MINING

		Mine A		Mine B		Mine C		Mine D		Mine E		Average	
	unit	ppm Se	% of total Se	ppm Se	% of total Se	ppm Se	% of total Se	ppm Se	total	ppm Se	% of total Se	ppm Se	% of total Se
section 1	coal	1.7	6.3	2.0	20.8	0.7	13.2	1.5	25.9	2.1	10.1	1.9	13.6
	contact	3.5	6.7	2.0	9.2	2.9	5.0	1.2	2.0	3.2	4.7	2.8	5.3
	interburden	2.2	87.0	1.0	70.0	2.2	81.7	1.1	72.0	1.3	85.2	1.8	81.1
section 2	coal					2.4	6.9			2.5	12.2		
	contact					3.1	3.9			3.4	5.4		
	interburden					2.9	89.2			1.8	82.5		
	refuse	3.2		2.7		1.6		1.8		2.9		2.4	

note mine C has sections CN and CE and mine E has sections EE and EW

major variations in the average Se content of coals from the 5 mines. At two mines incremental samples were taken though seams (Figure 14).

At one mine, Se and ash concentrations increase in the HW and FW parts of the seam (mine E) and the major control on Se concentrations is ash and not organic S. In the other seam from mine A, Se concentrations are high in the 2 partings and variable through the rest of the seam.

In Mist Mountain coals, which have low concentrations of pyrite, most of the Se is associated with ash rather than pyrite or coal. In general the Se *versus* ash correlations are moderate to poor. However in a number of plots (Figure 13) the Se concentrations in zero ash coal vary from 0.3 to 1.9 ppm and at 85% ash (100% mineral matter) from 1.8 to 9.1 ppm. The projected Se content of ash free coals in this study is higher for coals higher in the section than lower in the section (1.9 ppm compared to 0.4 ppm, Figure 13). This is probably because seams higher in the section tend to contain more vitrinite, which is host for more organic S and therefore probably more Se. The projected Se concentrations of 85% ash (4.9 and 3.8 ppm, Figure 13) are similar to the HW and FW material averages of about 4 ppm (Table 6). In coal seams, which average about 2 ppm Se (Table 6) and 23% ash, It appears that about half the Se is contained in the coal and half is associated with the ash. The Se concentration is reduced to the range 1 to 1.5 ppm in washed coals with about 10% ash (Table 6, Figure 13).

Selenium is similar to sulphur in terms of its chemical properties and one would expect an association of Se with pyrite or organic sulphur in the coal. In Mist Mountain coals the concentration of Se in pyrite appears to be low (about 10 ppm in massive pyrite, Table 6) and seams contain very little pyrite. Therefore Se in pyrite can not contribute much to the total Se concentration in samples. The concentration of Se in ash is higher than in ash-free coal, which makes it difficult to see if there is a relationship between Se and organic S in ash-free coal. To document a Se *versus* organic S relationship all the available samples for which Se, ash and organic S analyses were available were sorted based on ash content. Se *versus* organic S plots were then constructed for samples with limited ranges of ash contents (Figure 15).

In all cases Se correlates weakly with organic S though in higher ash ranges the Se/organic S ratio increases indicating introduction of Se but not organic S.

A number of washability experiments were performed to further investigate the relationship of Se to total, pyritic S, organic S and ash. The data (Figure 16) indicate a positive correlation of Se to ash in Mines A and D, with the pure ash (mineral matter) containing over 7 ppm and 2 ppm Se in ash from mines A and D. In mine C, Selenium concentrations do not increase systematically as ash increases, possibly because of changing maceral composition in the float fractions. Washability data confirms that Se concentrations are reduced in washed coal. Total S concentrations decrease as ash concentrations increase and the pyritic S component is small in all samples except for high ash samples from Mine C.

A maceral influence on Se contents in coal has been hinted at above. At present no data-bases of petrography and Se concentration on the same samples could be located. However average petrography does exist for seams from the various mines and when this is compared to the Se concentrations for the same numbered seams at each mine rough trends are apparent. Se concentrations tend to increase as the reactive maceral contents increase (Figure 17).

A probably explanation for this derives from the origin of inert macerals, which are formed by various degrees of charring of vegetation in the coal swamp (Lamberson *et al.,* 1996). This probably volatilizes some if not most of the Se from the vegetation before it forms inert coal macerals. Sulphur is less susceptible to volatilization and therefore inert macerals probably have lower Se/S ratios than reactive macerals. The Se and organic S are enriched in vitrinite macerals compared to the inert macerals (Demir and Harvey, 1991) and especially in the liptinite macerals, which are usually a minor constituent of coal. This explanation is supported by some washability data. It has been documented a number of

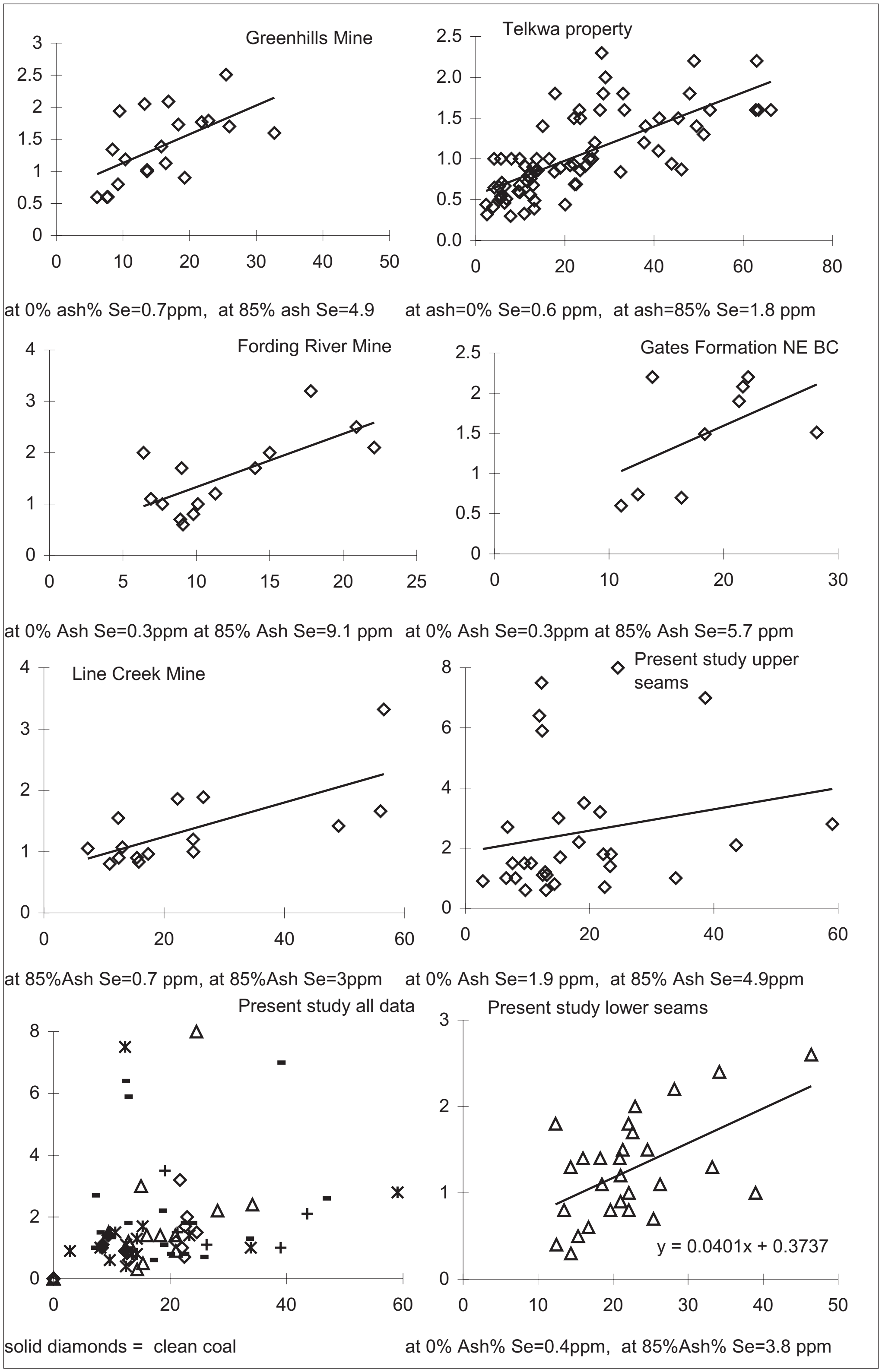

Figure 13. Ash *versus* Se plots for coal samples from a number of mines and properties data from this study, unpublished Geological Survey reports, Grieve and Goodarzi (1994) and Goodarzi (1988).

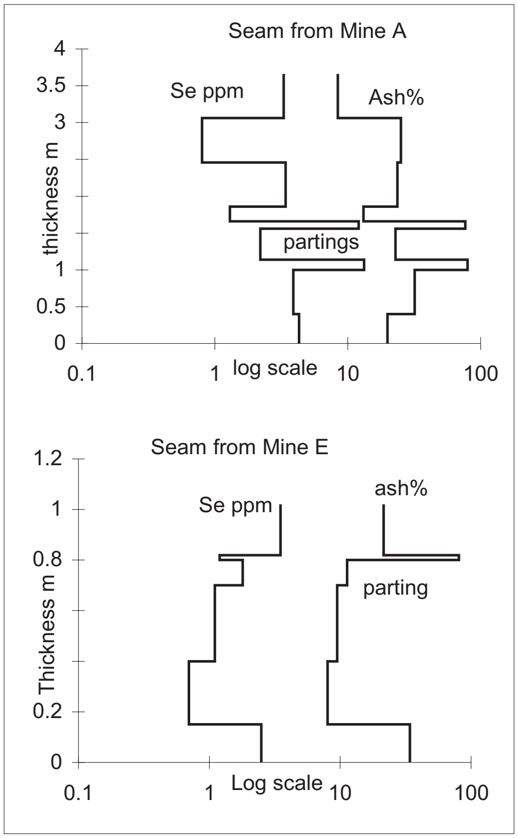

Figure 14. Se concentrations of incremental samples through 2 seams, Mines A and E.

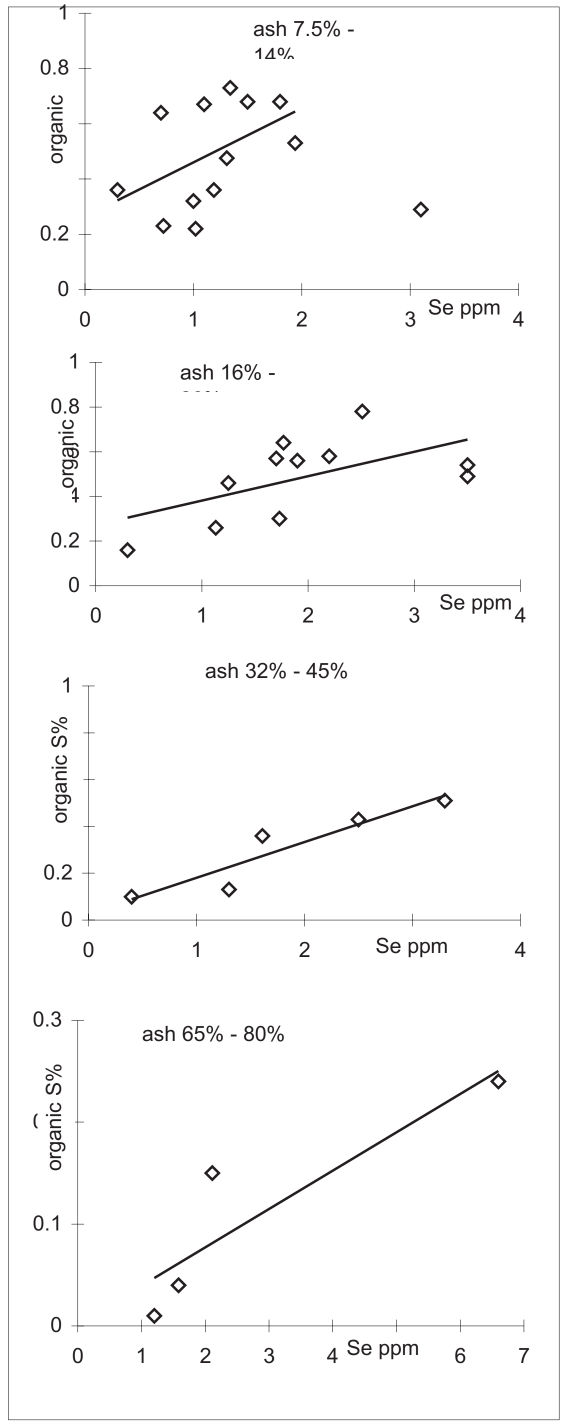

Figure 15. Se *versus* organic sulphur concentrations for all the data from this study, grouped in ash brackets.

times, that in float-sink data, reactive macerals (vitrinite) concentrate in the low SG fractions and inert macerals in the intermediate SG fractions (Ryan *et al*., 1999). This means that Se contents should decrease in intermediate SG fractions and the organic Se/S ratio decrease. These trends are seen in some of the data from Harvey *et al*. (1983) (Figure 18).

Selenium in coal seams in the Mist Mountain Formation comes from three major sources. A component that comes from the original vegetation and components introduced into the coal swamp either in solution or with detritus. The component from vegetation will be decreased by an amount based on the amount of charring by forest fires as indicated by the amount inert macerals in the coal. There should therefore be maceral control on the amount of vegetation derived Se. The externally sourced Se, which is introduced in solution, once in the swamp may bond with the detritus (ash) or substitute for S, which, based on the Eh pH environment, may form authogenic pyrite or organic S in the coal. The pyrite forms in low pH Eh swamp environments if excess S is available and may be associated with the ash or coal. The Se substituting for organic S is probably incorporated mainly into the rotting vegetation as Se^{-2} after reaction of H_2Se with the vegetation (Finkelman *et al.,* 1990). This material will evolve during coalification into the reactive macerals. The Se introduced with the detritus may be fixed in one of four ways; as elemental Se, as selinides, adsorbed onto clays as Se^{+4} or be bonded to iron hydroxides. Balistrieri and Chao (1987) have demonstrated that selinite is adsorbed by goethite. All of these ash associa-

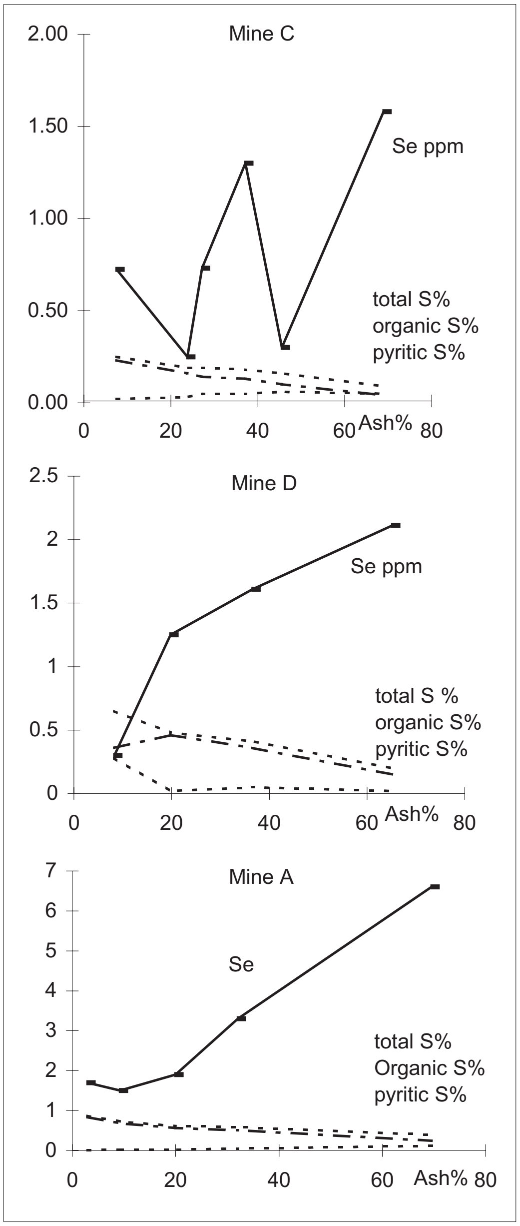

Figure 16. Se wash dta for coal samples from mines C, D and E.

tions with the exception of a pyrite association probably produce high Se/S ratios.

The Se that is introduced with the detritus probably remains fixed in the detritus. The fact that total Se tends to correlate with ash does not necessarily indicate that major source of Se is detritus because some Se introduced in solution may be added to the detritus. It appears that for Mist Mountain coals Se content will depend largely on ash content with an underlying maceral control, but correlations can not be expected to be good.

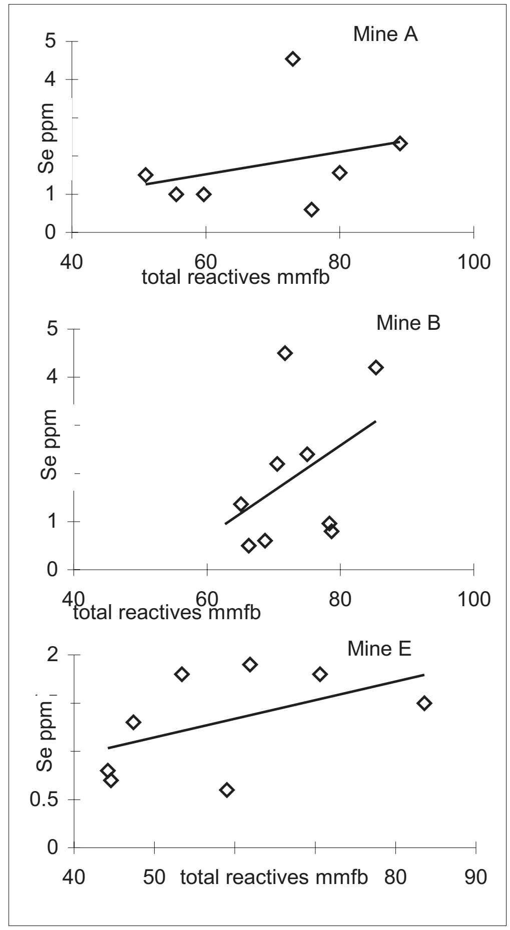

Figure 17. Average total reactives for seams from mines A, B and E *versus* Se content (mmfb, mineral matter free basis).

The Se that is volatilized by forest fires from the precursor of inert macerals is not lost to the system. Based on studies in power plants (Clarke and Sloss, 1992), Se is moderately to highly volatile during combustion but precipitates onto fine fly ash as the temperature falls. In a forest fire situation one can expect Se to condense onto fine ash particles that will be carried by the wind, eventually falling to earth possibly in rain drops. This Se may add to the Se already entering the coal swamp in solution or with fine detritus and consequently seams with high inert maceral contents may not always have lower Se contents, the Se may simply be redistributed with more occurring in the ash.

In order to investigate more closely the partitioning of Se between ash and coal in HW and FW samples, a number of samples were floated at 1.6 SG to produce low ash float and high ash sink samples (Table 8).

The Se and ash concentrations and yield were measured for the float and sink samples. The data confirm that Se is concentrated in the ash component of the HW and FW samples. In fact its concentration in coal ash and HW and FW material is greater than its concentration in

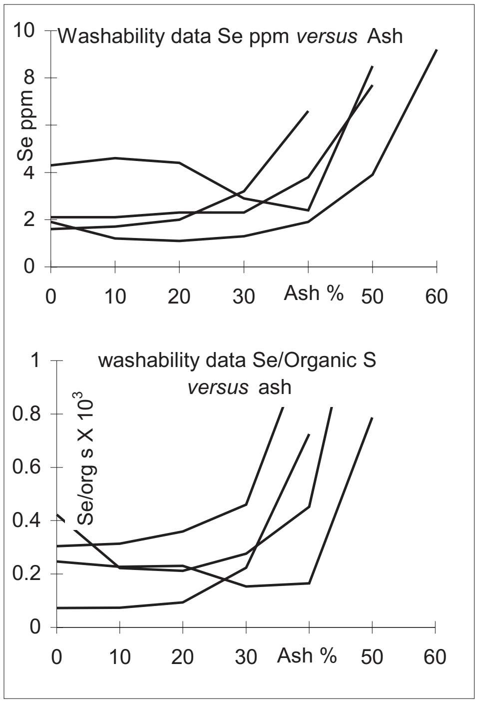

Figure 18. Se/organic S ratios *versus* ash for various SG splits, data from Harvey *et al*. (1983).

TABLE 8
FLOAT SINK DATA FOR HW AND FW SAMPLES

sample 99	raw ash %	raw Se M	sink wt > 1.6	sink ash %	sink Se M	float wt<1.6	float ash %	float Se M	Se lost C
A-12	69.8	8.00	99.4	70.1	5.80	0.6	25.9		
A-15	55.6	4.60	66.5	75.7	3.40	33.5	15.5	2.50	1.50
B-34	56.7	4.40	70.2	72.0	3.60	29.8	20.8	2.20	1.22
B-23	22.6	4.10	22.2	59.5	2.30	77.8	12.1	3.10	1.18
B-16	72.7	5.80	84.3	83.1	3.70	15.7	16.6	2.90	2.23
B-12	64.2	4.70	79.7	74.4	4.00	20.3	24.1		
E-17	58.5	5.30	70.6	76.1	4.40	29.4	16.1		
E-45	78.4	7.10	95.2	80.6	6.20	4.8	34.2		

M = measured C = calculated

mudstone. It also appears that the chlorine based heavy liquid used to separate the samples has leached Se from the samples and this is discussed later.

SEDIMENT SAMPLES

Twenty nine sediment samples were collected from settling ponds at the five mines. Samples of fine sediment were collected from as close to the inflow as possible. The quality of the samples varied considerably. At some sites samples were covered with algae and at others there was very little fine material. Samples were dried and the minus 100 mesh fraction recovered. Selenium and oxide analyses were performed on all sediment samples and total organic carbon (TOC) analyses on 14. The average Se content is 3 ppm but there is a wide spread of values and the average is influenced by 2 very high values. The Se concentrations of the sediment samples are in the range and a bit higher than that which would be expected based on the average values for mudstones and silty mudstones in the interburden (2-2.8 ppm). There is therefore no strong evidence that fine sediments washing out of the waste dumps are taking up or losing Se. McDonald and Strosher (1998) report finding no relationship between TOC and Se content in sediments. Despite a lot of the samples in this study having TOC values below detection limit (0.01%) there also appears to be no correlation of Se and TOC values (Table 9).

TABLE 9
TOTAL ORGANIC CARBON (TOC) AND SE DATA FOR SEDIMENT SETTLING POND SAMPLES

SAMPLE	TOC %	Se ppm	As ppm
A99-86	2.3	1.1	5.4
A99-92	<.01	5.4	
A99-93	1.76	4.4	
B99-70	0.11	12.8	
B99-71	<.01	7.8	
B99-73	<.01	2.4	
C99-90	<.01	3.8	
C99-94	1.69	1.7	6.6
D99-31	<.01	1.6	7.9
E99-77	<.01	1.4	5.8
E99-78	<.01	3	7
E99-79	<.01	1.7	
E99-81	4.91	1	3.8
E99-82	0.92	2.4	

Selenium does not correlate with Fe_2O_3 so there is no evidence of Se being taken up by iron hydroxides in the sediments (Table 10).

There is however a weak correlation with Mn indicating the possible presence of a secondary Mn mineral that is taking up Se.

SOURCE OF AND PARTITIONING OF SELENIUM IN COAL SWAMPS

A discussion of how Se is fixed in coal swamps requires a basic understanding of the geochemistry of a swamp environment. Bass-Becking *et al*. (1960) outlined fields on an Eh *versus* pH diagram of naturally occurring environments, shallow marine rocks and for coal formation (Figure 19).

Herring (1990) used a similar diagram to outlined fields of stability for the various Se ions and this information is included in Figure 19. Within the field of naturally occurring Eh and pH conditions Se can occur as Se^{-2}, Se^{0}, Se^{+4} and Se^{+6}. Selenium in a coal swamp environment is more likely to be fixed as a selinide (Se^{-2}) or elemental Se (Se^{0}), where as in a shallow water marine or terrestrial environment Se is more likely to be fixed as selinite

TABLE 10
CORRELATION FACTORS FOR SE *VERSUS* OXIDES FOR VARIOUS ROCK TYPES

	COAL	HW+FW	MUDSTONES	PARTINGS	REFUSE	SEDIMENTS
Samples	11	5	7	4	6	26
Ash%	**0.70**	0.36		-0.56	0.29	-0.08
SiO_2	**0.66**	**0.54**	-0.06	-0.21	0.28	-0.17
TiO_2	**0.70**	-0.10	0.00	-0.55	-0.49	0.04
Al_2O_3	**0.64**	-0.10	0.00	-0.55	-0.05	-0.01
Fe_2O_3	0.41	0.31	-0.33	0.21	**0.91**	-0.16
MnO	0.34	0.36	-0.56	0.02	0.43	**0.52**
MgO	**0.75**	0.06	-0.25	**0.77**	**0.76**	-0.30
CaO	**0.64**	0.07	-0.26	0.09	-0.52	0.20
Na_2O	0.44	-0.37		**0.82**	-0.67	-0.17
K_2O	**0.67**	-0.03	0.01	-0.60	**0.80**	0.08
P_2O_5	0.36	**0.61**	0.14	-0.10	**0.91**	0.10
Ba(4)	0.48	0.20	-0.02	-0.05	0.14	0.30

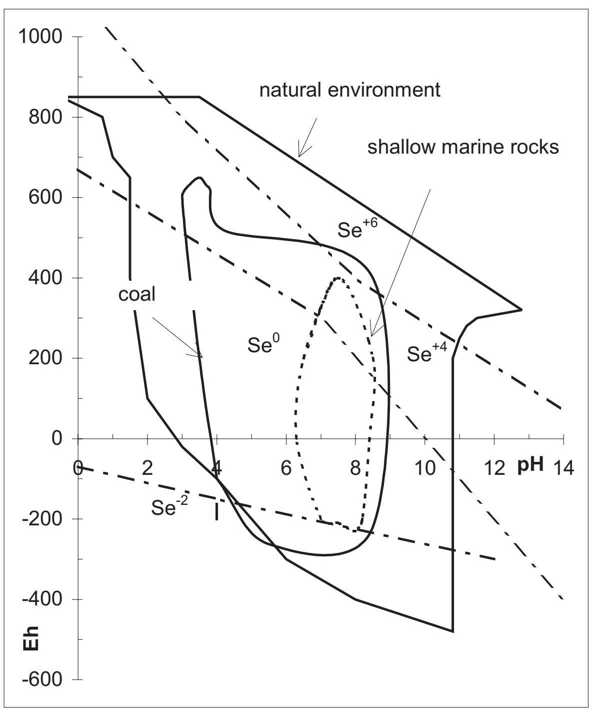

Figure 19. Viable Eh *versus* pH environments for coal, shallow marine rocks and selenium ions, data from Bass-Becking *et al*. (1960) and Herring (1990).

(Se^{+4}) or selenate (Se^{+6}). The shallow marine environment of Bass-Becking is probably similar to the shallow water terrestrial environment in which the interburden mudstones sampled in this study were deposited.

The partitioning of Se in coal seams in terms of source and present location has been discussed above. The concentration of Se in the fine detritus that enters the swamp, either water or air borne, is probably similar to the Se concentration of the mudstones i.e. in the 2 ppm range (Table 6). The Se concentration of the coal-ash and HW plus FW material is higher than that of mudstones averaging about 4 ppm with a wide range (Table 6 and Figure 13). The difference, 4 ppm minus 2 ppm times the ash content is probably a minimum estimate of the Se introduced into the coal swamp in solution in water. It is a minimum estimate because it does not take into account Se introduced in solution that is later fixed in the coal. For a coal seam with 25% ash and approximately 2 ppm Se, about half the Se is in the coal and half in the ash. Half of the Se in the ash was originally in solution and half was introduced with the detritus. The Se that was in solution and is now associated with the ash is more likely to form selinides or elemental Se in the seam, whereas the Se introduced with the detritus probably remains adsorbed onto the clays. Some of the Se introduced in solution will probably substitute for organic S in the reactive coal macerals to join the Se derived from the original vegetation. A small proportion of Se may be incorporated into pyrite.

Support for the suggestion that a substantial amount of the Se in coal seams was introduced in solution into the coal swamp comes from the correlation of Se with U seen in many East Kootenay coals (Figure 20).

The correlation probably indicates a common mode of introduction. Uranium like Se is soluble in alkaline high Eh environments and is probably introduced into the coal swamp in surface or ground water as complex alkali uranyl carbonates (Breger, 1974). It is insoluble once reduced in low pH-Eh coal swamp environments and will be extracted from water probably as uranyl-organic complexes (Swaine, 1990). Some Se is also introduced in this way being transported to the coal swamps in surface and ground waters with high pH and alkalinity that aid mobilization of Se. The Se *versus* U relationships vary between the different coal suites and for the mudstone and for HW+FW rock suites probably indicating a common mode of introduction but different host sites within the coal seams and rocks.

Selenium concentrations in surface water can range from below 1 ppb to 1 ppm depending on pH. Based on the low concentrations of Se in water and apparently moderately large proportion that it contributes to the 2 ppm Se in coal seams, a large volume of water is required to import the Se found in a coal seams. As an example, if the Se concentration of material in a coal swamp is to be increased by 1 ppm, by extracting Se from pore water with a concentration of 10 ppb, then there have to be 100 exchanges of pore water based on a 50% porosity. Obviously there has to be a continuous source of Se in ground and surface water. This implies moderate levels of Se in bed rocks in the region and a climate, which favours the ability of water to transport Se.

There is some evidence that a minor component of the Se in Mist Mountain coals may be contained in pyrite. Goodarzi (1987) studied samples of fresh and weathered coal. A plot of Se *versus* ash indicates that 3 of the 4

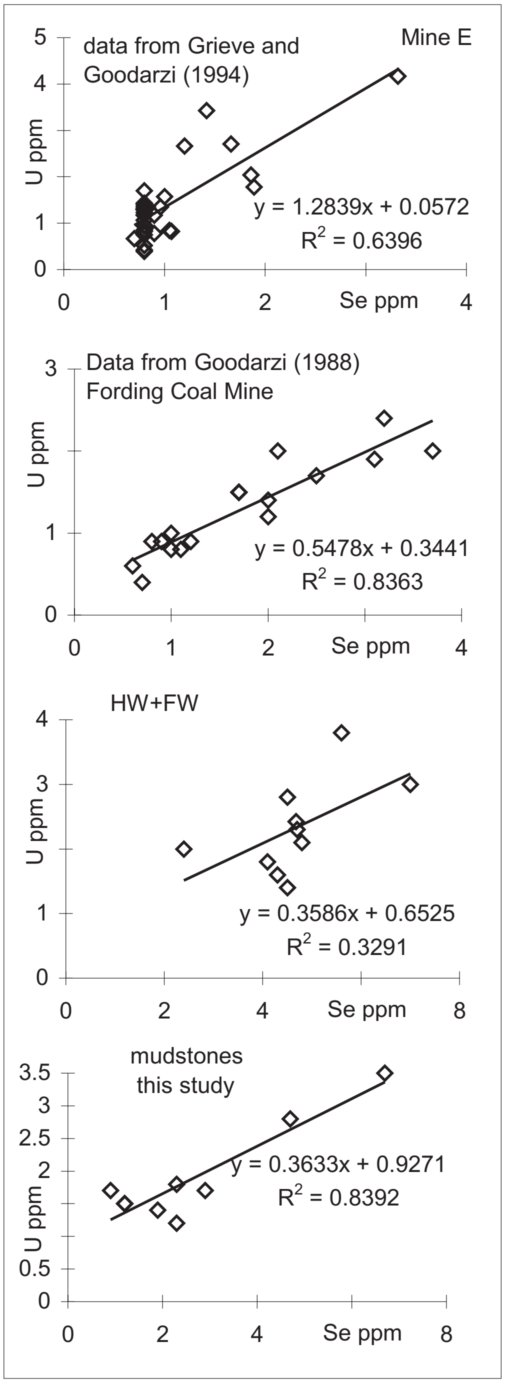

Figure 20. Se *versus* U concentrations in East Kootenay coals and rocks, data from this study, Grieve and Goodarzi (194) and Goodarzi (1988).

weathered samples may have lost Se and that the average amount of Se lost from all four samples is about 0.5 ppm. The Se/S ratio increases for the four weathered samples implying that S is more easily lost by weathering than the Se. This is consistent with the removal, from the weathered samples, of small quantities of pyrite, which have the lowest Se/S ratios of any phase in the sample (Table 6). Pyrite is susceptible to oxidation, which will release Se and S in soluble form. Mist Mountain coals generally contain low concentrations of pyrite and release of Se will depend on how easily it is removed from ash and coal.

DETAILED ASSOCIATION OF SELENIUM IN COAL AND ASSOCIATED SEDIMENTS

Four possible associations of Se in coal and associated sediments are considered these are:

- adsorption onto clay minerals in coal mineral matter and associated HW and FW mudstones. trace
- selinides such as clausthalite associated with the mineral matter.
- substitution for organic sulphur in reactive coal macerals.
- substitution for S in sulphides (mainly pyrite)

The Al_2O_3/SiO_2 ratio is a good indicator of clay content of a rock and therefore a correlation between Se contents with Al_2O_3/SiO_2 ratios may indicate that Se is adsorbed onto clays. Similarly a relationship between Se and trace metal contents may also indicate adsorption or an association with trace sulphides. These relationships can help in indicating how the Se is fixed in the various rock types, which include the coal and coal-ash fractions in coal seams; HW, FW and parting material and interburden lithologies.

Much of the Se in the coal fraction is probably substituting for organic S in the reactive macerals. As shown Se correlates with organic S and reactive coal macerals (Figures 15 and 17). The Se/S ratios for coal samples (Figure 21) are about 0.2 to 0.4 x 10^{-3} , which are much higher than the ratios for pyrite (about 0.02 x 10^{-3}) and probably characteristic of the ratio of Se/S in reactive macerals.

The coal probably formed in a low pH and Eh environment (Figure 19), which would also encourage the substitution of Se^{-2} for organic S in the coal fraction of the samples. Ren *et al.* (1999) suggest that high concentrations of chalcophile elements (including Se) are found in coals formed in low Eh environments favouring the growth of algae, which may contain high concentrations of S and Se.

In coal seams about half of the Se is associated with the ash. Total Se concentrations correlate with Cu, Zn and other metals but not Fe in the ash (Tables 9 and 10) indicating in part a common association of trace metals and Se, probably in the ash component of the samples. Coal samples generally have the high Al_2O_3/SiO_2 ratios, some samples approaching the ratio for kaolinite (0.847) (Figure 22) indicating that the included ash is almost exclusively clay.

There is a weak negative correlation of Se with the Al_2O_3/SiO_2 ratio, indicating that as more detritus with lower Al_2O_3/SiO_2 ratios is introduced the Se content increases. This combined with the trace metal association indicates that some of the Se associated with coal-ash may occur as trace selinides such as clausthalite (PbSe) or

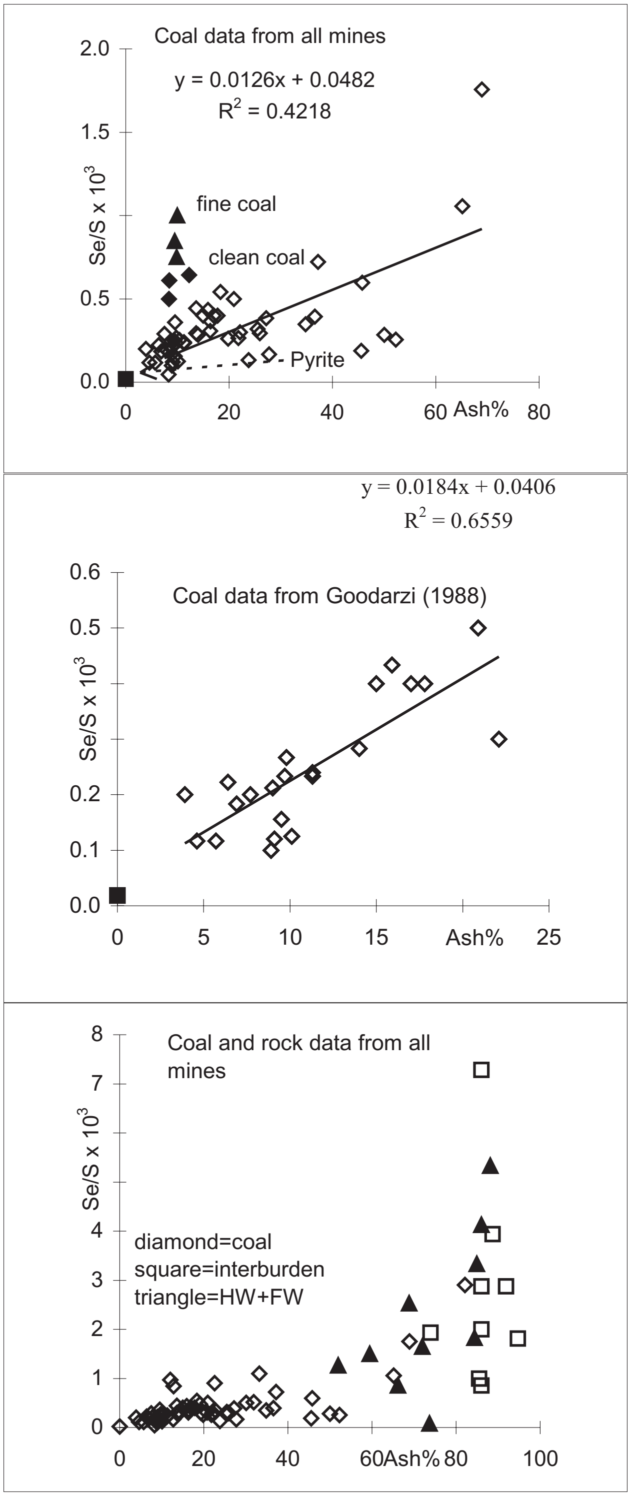

Figure 21. Se/S ratios *versus* ash contents for samples from this study.

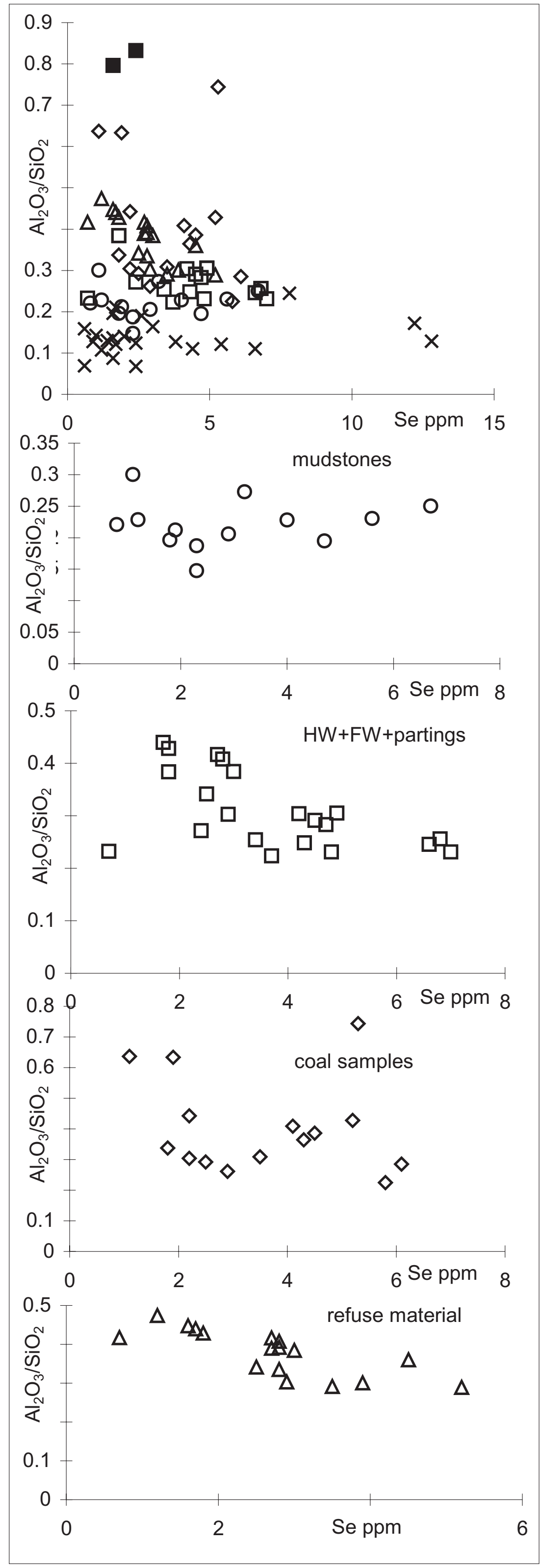

Figure 22. Plot of Al_2O_3/SiO_2 ratios *versus* Se contents of rocks; data from this study; cross = sediments, circle = mudstone, triangle = refuse, square = HW, FW & partings, diamond = coal, solid square = tonsteins.

ferrosilite ($FeSe_2$) or elemental selenium. Some Se is also probably adsorbed on clays because that was how it was introduced into the coal swamp. The lack of a good correlation between Al_2O_3/SiO_2 ratio and Se (Figure 22) indicates that in the coal ash, adsorption onto clays is not the major mode of occurrence. The Se/S ratio increases as the ash and Se contents increase indicating that Se is not associated with sulphides in the ash (Figure 21).

Mudrocks in the interburden probably formed in an environment characterized by higher Eh and pH values than the environment in which coal, coal-ash and HW+FW material were deposited (Figure 19). They were probably deposited in shallow marine or terrestrial environments in which Se would be stable as Se^{+4} or Se^{+6}. In these environments a higher proportion of the Se may be adsorbed onto clays such as montmorillonite or kaolinte and in fact based on limited number of mudstone samples, there is a tendency for the Se to increase as the Al_2O_3/SiO_2 ratio increases (Figure 22). Se in the mudstones has the strongest correlation with trace metals (Table 11), probably because these metals are also adsorbed onto clays.

It has been reported (Balistrieri and Chao, 1987; Hayes *et al.,* 1987) that selinite ions can be bonded directly onto goethite surfaces however in this study there is a negative correlation of Fe to Se in mudstones (Table 10). Based on limited data the average S contents of the mudstones is 0.08%.

The Se/S ratios for HW and FW material are generally higher than those for coal seams and they increase as ash contents increase (Figure 21) ruling out a sulphide association for the Se in this material. On a Al_2O_3/SiO_2 ratio *versus* Se plot (Figure 22) HW and FW material have lower Al_2O_3/SiO_2 ratios than coal ash and there is a negative correlation of Se with the Al_2O_3/SiO_2 ratio, indicating that not all the Se is associated with clay minerals.

TABLE 11
CORRELATION FACTORS FOR SE *VERSUS* TRACE METALS FOR VARIOUS ROCK TYPES

	HW+FW	mdst	Coal
No Samples	15	15	23
element	Se INAA	Se INAA	Se
Se ICP-MS	1	1	
Fe	0.43	-0.68	-0.03
Pb	0.58	0.93	
Cu	0.49	0.91	0.60
Zn	0.65	0.89	0.56
U	0.73	0.94	0.93
Co	0.40	0.60	0.37
Cr	-0.72	-0.65	0.70
Mn	-0.15	-0.76	-0.03
Ni	0.66	0.93	
Ag	0.48	0.93	
As	0.29	0.31	0.30
Au	-0.33	-0.38	
Hg	0.19	0.90	
Bi	0.55	0.79	
Mo	0.41	0.95	0.49

Coal data from Goodarzi (1988)

Also there is no correlation of $Fe_2O_3$with Se (Table 10) making an iron hydroxide association unlikely. It therefore appears that, in HW and FW material, a reasonable amount of the Se occurs in selinides or as elemental selenium The Se does correlate with a number of trace metals in HW and FW material (Table 11). The S content of the HW and FW material is 0.8% based on limited data.

Two tonsteins samples have high Al_2O_3/SiO_2 ratios but relatively low Se contents supporting the suggestion that adsorption of Se onto clays in the coal swamp environment is probably not the preferred mode of occurrence for Se in coal ash and HW and FW material.

The Se contents in sandstones and siltstones are generally low and often below detection limit. No trace metal or oxide data are available for these rocks. The higher As concentrations in these samples (Table 6) probably indicates the presence of trace amounts of arsenopyrite. There is a weak negative correlation of As to Se so it does not appear that arsenopyrite is the host for Se. The minus 100 mesh sediment samples have lower Al_2O_3/SiO_2 ratios than the mudstones and the ratios do not correlate with Se content (Figure 22).

In summary there is limited evidence to suggest that Se has four major modes of occurrence controlled by depositional environments. In the low pH-Eh environment of the coal swamp Se either substitutes for organic S in the reactive coal macerals or forms selinides or metallic Se associated with the coal ash. Some of the Se in this environment is introduced adsorbed on clays and probably remains adsorbed. The environment, in which HW, FW and parting material were deposited, may have been characterized by higher pH and Eh values than the environment in which coal was deposited, but there is still evidence that the Se occurs as selinides or metallic Se with probably some adsorbed onto the clays as Se^{+4}. Mudstones adjacent to coal seams probably formed in shallow water near shore or terrestrial environments characterized by neutral pH and high Eh values. In these rocks Se correlates with a number of trace metals (Table 11) and weakly with Al_2O_3/SiO_2 ratios and more of the Se may be adsorbed onto clays as Se^{+4} or Se^{+6} .

REMOVAL OF SELENIUM FROM COAL AND ASSOCIATED ROCKS

The ease with which Se may be removed from rocks during mining probably relates to the way it is bound in the rocks. Se substituting for organic S in coals is probably not easily removed. This Se accounts for about a third to half the Se in the coal and it is bound in the reactive macerals. An indication of this is the fact that the clean coal samples after crushing and washing do not indicate any loss of Se compared to the raw coal samples based on their ash content (Figure 13). The selinide and elemental Se components in the coal ash and HW plus FW material may be more easily removed. This might be indicated by the higher Se concentrations of HW and FW material compared to the concentrations for refuse material (Table 7). Also float sink data on HW and FW samples (Table 11) appear to indicate that the chlorine based heavy liquid used for the separation was removing Se from the high ash component. In every case the calculated Se content of the raw sample calculated using data from the float and sink samples is less than the measured Se content of the raw samples. In that the Se content of the float samples is similar to the average Se content of coals and the Se content of the sink samples is less than the average content of HW and FW samples, it appears that the Se is being removed from the ash component of the samples. In fact the amount of Se lost correlates with the ash content of the raw samples (Table 8) and at 30% ash is about 1 ppm increasing to about 2 ppm at 85% ash.

Se adsorbed onto clays in the mudstone units may be fairly immobile in the mine environment. Small grains of Se bearing sulphides in sandstones may oxidize easily if exposed, but the large fragment size of the rock after blasting will limit the number of grains exposed.

Se can be volatile if samples are heated. In coal wash plants, ash is removed using water based processes after which coal is partially dried. This can heat the fine coal to a high temperature for a short time. To see if Se is volatilized in the thermal dryer in the plant, fine coal samples before and after the dryer were analyzed for Se. The minus 100 mesh feed and dried coal both had Se concentrations in the range 1 to 1.4 ppm and there is no evidence of substantial amounts of Se being volatilized in the dryer (Figure 21).

Sometimes coal seams catch on fire probably ignited by lightning. The coal burns and bakes the surrounding rock producing clinker and rocks with various hues of orange and red. As an interesting aside samples of baked rock were analyzed for Se. The original material would probably have been HW or FW mudstone with Se concentrations in the 4 ppm range. The burnt rock had concentrations ranging from less than 0.4 ppm to 1 ppm indicating substantial volatilization of Se. The Se may be lost into the air or condense onto cooler rocks probably as a soluble compound.

ARSENIC IN COAL AND INTERBURDEN ROCKS

Arsenic was analyzed in a number of rock types. It is usually considered to be associated with sulphides in coal or rock. Its concentration is lowest in raw coal at 2.4 ppm. Swaine (1990) states that As ranges from 0.5 ppm to 80 ppm for most coals with averages of 1.5 ppm for Australian, 4 ppm for South African, 14 ppm for United States and 15 ppm for United Kingdom coals. The concentration increases in interburden rocks to a high of about 10 ppm in muddy siltstones and sandstones probably because of trace amounts of dispersed pyrite and arsenopyrite in the rocks. There is no trend of increasing As with increasing Se for any of the rock types (Figure 23).

CONCLUSIONS

Coals in the Mist Mountain Formation have world average levels of Se. Interburden rocks in the formation tend to have higher Se contents than rocks of similar lithology in other formations that do not contain coal. No lithologies were identified that consistently contained high concentrations of Se. Within the section, Se is concentrated in HW, FW and parting material associated with coal seams and the coal seams. Concentrations in interburden rocks are lower and depend on the mudstone content. In an average mining section, from 70% to 87% of the Se is in interburden rocks, 6% to 25% in coal and 4% to 7% in the material adjacent to the coal seams (contact material).

The low pH-Eh coal swamp environment is ideal for accumulating Se and much of the Se found in coal probably originates from outside the coal swamp and not from the original vegetation. This externally sourced Se enters the coal swamp in solution or adsorbed onto fine detritus. The coal swamp environment is a sink for Se. Se entering

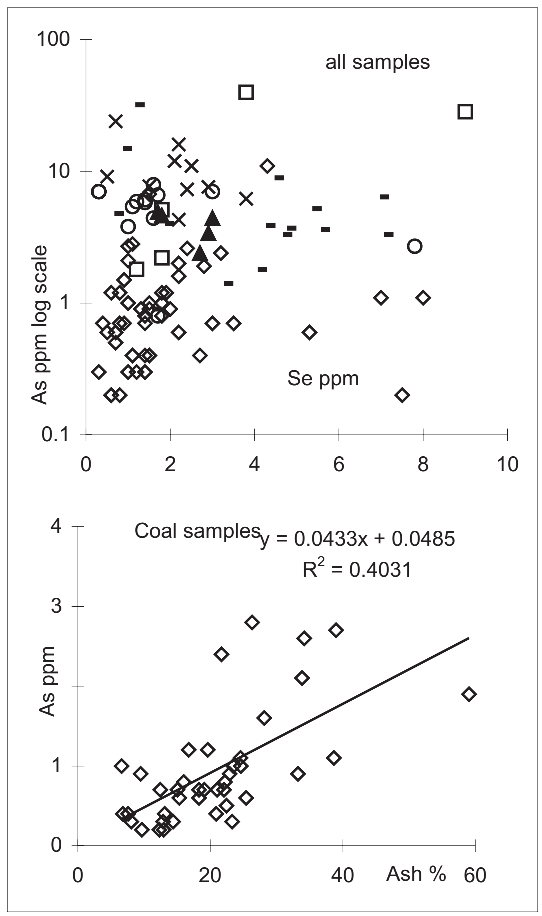

Figure 23. Plot of Se *versus* As for all rock types; data from this study; diamond=coal, dash= HW and FW, triangle = refuse, Square=partings, cross=interburden rocks, circle=sediment.

the coal swamp in solution substitutes for organic S in the reactive macerals in coal or forms selinides or metallic Se associated with the coal ash and HW and FW rock. About half of the Se in the coal is associated with the ash and about half of this may occur as selinides or as metallic Se. This Se may be easy to remove once the coal and associated rocks are brought to surface and crushed.

Compared to the coal swamp environment Se is not as concentrated in the higher Eh and pH environments associated with deposition of interburden mudstones. In these rocks the Se is probably adsorbed onto clay minerals as Se^{+4} and may be less easily removed than Se in coal, HW or FW rocks. Siltstones and sandstones have low Se concentrations and the Se is probably contained in small amounts of mudstone and pyrite. This Se could be easily released after oxidation of the sulphides, but the sulphide grains are contained in large blocks of rock which isolate them from the surface environment and consequently they either do not oxidize or they oxidize slowly.

ACKNOWLEDGMENTS

This study was a cooperative effort between the Ministry of Energy and Mines and all five coal mines in southeast British Columbia. It serves as an example of a proactive approach to studying issues of importance to coal mining in the province. Many people at the various mines helped with logistics and sample collection and it is not possible to acknowledge them all individually. However in no particular order the authors would like to thank some who helped with the actual sampling in the pits. Those individuals being Martin Zral, Scott Braithwaite, Brad Pisony, Mike Takkinen, Lyle Douglas, Jeff Schlender, Ed Heatherington, Dave Endicott, Sophie Van Eendenburg, Terry Cryderman, Dave Beranek, Billie O Brian and some that we have probably forgotten. The paper benefited from a very conscientious review by Nick Massey, however any mistakes and confusion are still credited to the author.

REFERENCES

ACARP (1993): Trace Elements in Coal; *Australian Coal Research,* Limited Issue Number 3 August 1996.

Balistrieri, L.S. and Chao, T.T. (1987): Selenium adsorption by Goethite; *Soil Science Society of America Journal*, Volume 51, pages 1145-1151.

Bass-Becking, L.G.M., Kaplan, L.R. and Moore, D. (1960): Limits of the natural environment in terms of pH and oxidation-reduction potentials; *Journal of Geology*, Volume 68, pages 243-283.

Beaton, A.P. and Goodarzi, F. (1989): The geochemistry and petrography of Lignites from southern Saskatchewan, Canada; *Journal of Coal Quality*, Volume 8, pages 110-117.

Breger, I.A. (1974): The Role of organic matter in the accumulation of uranium; in, Proceedings of Uranium Ore Deposits, Symposium Proceedings Athens Greece, International Atomic Agency, pages 99-124.

Clarke, L.B. and Sloss, L.S (1992): Trace elements emissions from coal combustion and gasification*; IEA Coal Research,* London, IEACR/49, pages 1-109.

Coleman, L., Bragg, L.J. and Finkelman, R.B. (1993): Distribution and mode of occurrence of Selenium in US Coals; *Environmental Geochemistry and Health,* Volume 15, pages 215-227.

Connor, J.J. and Shacklette, H.T. (1975): Background Geochemistry of some rocks, soils, plants and vegetables in the Conterminous United States; *United States Geological Survey*, Professional Paper 574-F.

Davidson, R.M. and Clarke, L.B. (1996): Trace elements in Coal; *IEA Coal Research,* London, IEA, Paper 21, pages 1-60.

Demir, I. and Harvey, R. (1991): Variation of organic sulphur in macerals of selected Illinois Basin Coals; *Organic Geochemistry*, 1991 Pergamon Press, Exiter, England, Volume 16, pages 525-533.

Demir, I. Ruch, R. Damberger, H.H, Harvey, R.D., Steele, J.D. and Ho, K.K. (1998): Environmentally critical elements in channel and cleaned samples of Illinois Coals; *Fuel*, Volume 77, pages 95-107.

Ebens, R.J. and Shacklette, H.T. (1982): Geochemistry of some rocks, mine spoils, stream sediments, soils, plants and waters in the Western Energy Region of the Conterminous United States; *United States Geological Survey,* Professional Paper 1237.

Eble, F.C. and Hower J.C. (1997): Coal quality trends and distribution of potentially hazardous trace elements in Eastern Kentucky Coals; *Fuel*, Volume 76, Number 8, pages 711-715.

Erdman, J.A., Severson, R.C., Crock, J.G., Harms, T.F. and Mayland, H.F. (1990): Selenium in soils and plants from native and irrigated lands at the Kendrick Reclamation Project Area, Wyoming; ; *U.S. Geological Survey,* Circular 1064, pages 91-105.

Finkelman, R.B. (1994): Modes of occurrence of potentially hazardous elements in Coal; levels of confidence; *Fuel Processing Technology*, Volume 39, pages 21-34.

Finkelman, R.B., Palmer, C.A., Krasnow, M.R., Aruscavage, P.J., Sellers, G.A. and Dulong, F.T. (1990): Combustion and leaching behaviour of elements in the Argonne Premium Coal samples; *Energy and Fuels*, Volume 4, pages 755-766.

Finkelman, R.B. (1993): Trace and minor elements in Coal; In*, Organic Geochemistry,* Engel M.H., Macho, S.A. (editors), Plenum, New York, pages 593-607.

Gibsons, D.W. (1985): Stratigraphy, sedimentology and depositional environments of the coal-bearing Jurassic-Cretaceous Kootenay Group, Alberta and British Columbia; *Geological Survey of Canada*, Bulletin 357.

Gluskoter, H.J., Ruch, R.R., Miller, W.G., Cahill, R.A., Dreher, B.G. and Kuhn, J.K. (1977): Trace elements in Coal: occurrence and distribution; *Illinois State Geological Survey*, Circular 499.

Goodarzi, F. (1987): Comparison of elemental distribution in fresh and weathered samples of selected Coals in the Jurassic-Cretaceous Kootenay Group, British Columbia, Canada; *Chemical Geology*, Volume 63, pages 21-28.

Goodarzi, H. (1987): Elemental concentrations in Canadian Coals 2. Byron Creek Collieries, British Columbia; *Fuel*, Volume 66, pages 250-254.

Goodarzi, F. (1988): Elemental distribution in coal seams at the Fording Coal Mine, British Columbia, Canada*; Chemical Geology*, Volume 68, pages 129-154.

Goodarzi, F. and Van der Flier-Keller, E. (1990): Variation of elements in the Southern Intermontane Coals of British Columbia, Canada; *Journal of Coal Quality,* pages 62-65.

Goodarzi, F. (1991): Geological factors controlling Coal quality in Western Canada; *Journal of Coal Quality*, Volume 10, pages 126-132.

Goodarzi, F. and Swaine, D.J. (1993): Chalcophile elements in Western Canadian Coals, *International Journal of Coal Geology*, Volume 24, pages 281-292.

Gough, P., Shackelette, H.T. and Case, A.A. (1979): Element concentrations toxic to plants, animals and man, *United States Geological Survey Bulletin,* Number 1466.

Grieve, D.A. and Goodarzi, F. (1994): Trace elements in coals of the East Kootenay and Peace River Coalfields, British Columbia; *Ministry of Energy, Mines and Petroleum Resources*, Open File 1994-15.

Harvey, R.D., Cahill, R.A., Chou, C.L. and Steele, D.J. (1983): Mineral matter and trace elements in the Herrin and Springfield Coals, Illinois Basin Coal Field; *Illinois Department of Energy,* ISGS Contract Report 1983-4.

Hayes, K.F., Roe, A.L., Brown, G.E., Hodgson, K.O., Leckie, J.O. and Parkes, G.A. (1987): *In situ* X-ray adsorption study of surface complexes: Selenium oxyanions on Alpha-FeOOH; *Science,* Volume 238, pages 783-786.

Herring, J.R. (1990): Se geochemistry -A Conspectus; in, *U.S. Geological Survey Circular*, Number 1064, pages 7-24.

International Coal Reports, 30 November 1998, Issue 463, page 26.

Kabata-Pendias, A. and Pendias, H. (1984): Trace elements in soils and plants; *CRC Press*, Boca Raton FL.

Lag, J. and Agric (1990): *Geomedicine*; CRC Press, Boston, page 218.

Lamberson, M.N., Bustin R.M., Kalkreuth W.D. and Pratt K.C. (1966): The formation of inertinite-rich peats in the Mid-Cretaceous Gates Formation: Implications for the interpretation of Mid-Albian history of paleaowildfire; *Palaeogeography, Palaeoclimatology, Palaeoecology*, Volume 120, pages 235-260..

McDonald, L.E. and Strosher, M.S. (1998): Selenium mobilization from surface coal mining in the Elk River Basin, British Columbia; A survey of water, sediment and biota; *British Columbia Ministry of Environment, Lands and Parks*, Pollution Prevention Branch, Cranbrook, BC.

Oman, C.L., Finkleman, R.B., Coleman, S.L. and Bragg, L.J. (1988): Se in coal from the Powder River Coal Basin,Wyoming and Montana; *U.S. Geological Survey,* Circular 1025.

Palmer, C.A. and Lyons, P.C. (1990): Chemistry and origin of minor and tace elements in selected vitrinite concentrations from bituminous and anthracitic coals*; International Journal of Coal Geology*, Volume 16, pages 189-192.

Pilgrim, D.B. and Zodrow, E. (1990): Trace element contents of coals and associated rocks of the Sydney Basin Nova Scotia; *Geological Survey of Canada*, Open File 2090.

Pillar, K.K.S., Thomas, C.C. Jr. and Kaminski, J. W. (1969): Neutron activation analysis of the Se content of fossil fuels*; Nuclear Applications and Technology*, Volume 7, Number 5, pages 478-483.

Raask, E. (1985): The mode of occurrence and concentration of Trace elements in coal; *Prog. Energy Combustion Science*, Volume 11, pages 97-118.

Ren, D., Zhao, F., Wang, Y. and Yang, S. (1999): Distributions of minor and trace elements in Chinese Coals; *International Journal of Coal Geology*, Volume 40, pages 109-118.

Robbins, .C.W. and Carter, D.L. (1970): Selenium concentrations in phosphorous fertilizer materials and associated uptake by plants; *Soil Science Society of America* ,Proceedings, Volume 34, pages 506-509.

Ryan, B.D., Leeder, R. Price, J.T. and Gransden, J.F. (1999): The effect of coal preparation on the quality of clean coal and coke; Geological Fieldwork 1998, *B.C. Ministry of Energy and Mines*, Paper 1999-1, pages 21-26.

Riley, K. and Dale, L (2000): Trace elements in the coals of the Bowen Basin: Good for Business; *Bowen Basin Symposium,* Rockhampton, Queensland, 2-24 October 2000, Pages 215-219.

Saiki, M.K., Jennings, M.R. and Brumbaugh, W.G. (1993): Boron, molybdenum and selenium in aquatic food chains from the Lower San Joaqui River and its tributaries, California; *Arch Env. Contam. Toxicol*, Volume 24, pages 307-319.

Shacklette, H.T., Boerngen, J.G. and Keith, J.R. (1974): Se, fluorine, and arsenic in surficial materials of the Conterminous United States; *U.S. Geological Survey,* Circular 692.

Spears, D.A. and Zheng, Y. (1999): Geochemistry and origin of elements in some UK coals; *International Journal of Coal Geology*, Volume 38, pages 161-179.

Swaine, D.J. (1990): Trace elements in coal; *Butterworth and Co*. London.

Taylor ,S.R. (1964): Abundance of chemical elements in the continental crust; a new Table; *Geochemica Cosmochimica Acta* , Volume 28, pages 1273-1285.

Turekian, K.K. and Wedephol, K.H. (1961): Distribution of elements in some major units of the Earth's Crust; *Geological Society of America Bulletin*, Volume 72, Number 2, pages 175-192.

Van der Keller-Flier, E. and Dumais, S. (1988): Inorganic matter content and specialized element potential of the Nanaimo and Comox Coalfields Vancouver Island (92G, F.K); *Ministry of Energy, Mines*, Geological Fieldwork 1987, Paper 1988-1, pages 435-439.

Valkovic, V. (1983): Trace elements in coal; *CRC Press Boca Raton*, Volume 1, page 210.

Wedepohl, K.H. (1978): Handbook of Geochemistry, Volume II, part 5, *Springer-Verlag*, Berlin.

White, R.N., Smith, J.V., Spears, D.A., Rivers, M.L. and Sutton, S.R. (1989): Analysis of Iron sulphides from UK coal by Synchrotron Radiation X ray Fluorescence. *Fuel,* Volume 68, pages 1480-1489.

Yang, G., Zhou, R., Sun, S., Wang, S. and Li, S. (1988): Endemic Se intoxication of men in China and Se levels of human body and environment; *Yingyang Xuebao,* Volume 4, pages 81-89.

Zheng, B., Ding, Z., Huang, R., Zhu, J., Yu, X., Wang, A., Zhhou, D., Mau, D. and Su, H. (1999): Issues of health and disease relating to Coal use in Southwestern China; *International Journal of Coal Geology*, Volume 40, pages 119-132.

Lithostratigraphy of the Comox and Trent River Formations in the Comox Coalfield, Vancouver Island (92F/7, 10, 11, 14)

By C. Gwyneth Cathyl-Bickford
Westwater Mining Ltd.

KEYWORDS: Stratigraphy, type sections, Comox Formation, Trent River Formation, Nanaimo Group, coal geology, building stone, natural gas.

INTRODUCTION

This report is part of an ongoing study, begun in 1987, to establish the distribution, sedimentology and resource stratigraphy of the Vancouver Island coalfields. Knowledge of the extent and quality of the coal deposits and associated natural gas resources is essential to land-use planning along the increasingly-urbanised western shores of Georgia Strait.

Results of this study have included five fieldwork papers (Bickford and Kenyon, 1988; Kenyon and Bickford, 1989, Bickford, *et al*., 1989 and 1990; Cathyl-Bickford, 1992), one stand-alone paper (Kenyon, Bickford and Hoffman, 1991) and a set of fourteen maps (Cathyl-Bickford and Hoffman, 1998). In the course of this work, 21 stratigraphic sections were measured, and four of the sections were published (in Kenyon, *et al*., 1991). Although new lithostratigraphic units were introduced and used in some of these publications as well as Mustard (1994), no type-sections have yet been described for the new rock-units and their definitions have therefore remained incomplete by modern standards.

In this year's field programme, additional stratigraphic sections have been measured, allowing the formal proposal of type-sections for six of the members within the coal-measures and overlying marine strata of the Comox sub-basin. Four measured stratigraphic sections are presented in this report, in the expectation that they will prove useful to exploration geologists working in the Comox sub-basin, as well as providing a much-needed lithostratigraphic context for amateur and professional paleontological collectors.

LOCATION AND ACCESS

The study area covers the east-central coastal plain of Vancouver Island, extending southeastward from Headquarters Creek (in 92F/14) to Cougarsmith Creek (in 92F/7). A dense network of public and private roads affords access to the area, with the exception of the river and stream canyons which must be traversed on foot. Some of the smaller streams are choked with logging debris, requiring an exhausting combination of wading, swimming and burrowing between wet logs and clumps of devils-club. Rivers and streams within the study area are subject to winter and spring freshets, and are best accessed for geological purposes during their seasonal low flows in August and September. Fieldwork is virtually impossible during January and February, owing to torrential rains relieved only by occasional heavy wet snows. Outside of the canyons, slopes are gentle to moderate, and much of the study area is blanketed by unconsolidated glacial, glaciofluvial and glaciomarine sediments. Courtenay and Comox are the major population centres in the study area.

Fieldwork

In contrast to previous years' programmes, only a modest amount of geological mapping was undertaken in 2000, mainly along the newly-constructed subgrade of the Vancouver Island Highway. Geological stations were located by reference to construction stakes along the highway, and positions marked on grading plans provided by the Ministry of Transportation and Highways. Outside of the area covered by the highway plans, forest cover maps provided by Weyerhaeuser Canada were used for station-keeping alongside logging roads and within cutblocks. Orthophotos provided by the Regional District of Comox-Strathcona were used to select and locate sites for outcrop sections along the stream and river canyons.

Geological Setting

The study area comprises the central third of the Comox sub-basin of the Late Cretaceous Georgia Basin. Coal measures occur within the non-marine portions of the Comox Formation (Bickford and Kenyon, 1988). The Comox Formation dips gently to moderately eastward, and is overlain by the Cretaceous marine rocks of the Trent River Formation, and unconsolidated Pleistocene sediments. Sills and laccoliths of probable Tertiary age cut the Comox Formation between Puntledge and Browns Rivers, northwest of Courtenay. Economic basement within the study area is formed by Triassic volcanic and volcaniclastic rocks of the Karmutsen Formation.

STRATIGRAPHY

Cretaceous rocks of the study area have been the target of considerable mapping, drilling and mining for more than 125 years (Richardson, 1878; McKenzie, 1922), and the basics of their lithostratigraphy have been established since 1911 (Clapp, 1912). Nevertheless, type and reference sections of the rocks have not been formalised beyond preliminary studies in the 1960's and 1970's (Muller and Jeletzky, 1970; Muller and Atchison, 1971; Atchison, 1968), and the depiction of section locations on regional geological maps (Cathyl-Bickford and Hoffman, 1998).

Type sections and surface reference sections for most of the members of the Comox and Trent River formations are proposed below. Measured sections accompanying this paper are designated as No.5 through No.8, following the previously-published sections No.1 through No.4 (Kenyon *et al.,* 1991). Only the basal portion of the Trent River Formation has been included in the present discussion, since its poorly-exposed upper portion requires further study before its subdivision can be confidently and fully documented.

Comox Formation

The Comox Formation was introduced by Clapp (1912) for a dominantly sandy succession of coals and clastic sedimentary rocks exposed in the vicinity of the Comox coal mines, southwest of Comox Harbour. Clapp did not report a detailed section of the formation, and he did not specify its type locality beyond the most general terms. Bickford and Kenyon (1988) proposed three subdivisions of the formation within the Comox sub-basin: the basal Benson conglomerate, overlying Cumberland coal measures, and uppermost Dunsmuir sandstone, but specified type sections for none of them. In the present study, sections have been measured of the coal-bearing Cumberland and Dunsmuir members. The basal, dominantly-conglomeratic Benson Member has not been studied in detail owing to its lack of significant coal beds, and the general inaccessibility of its outcrops.

Cumberland Member

The Cumberland Member is named for the Cumberland coal-mining district (Bickford and Kenyon, 1988). Its proposed type-section is in the western part of the middle canyon of Browns River [*see* GeoFile 2001-1 (www.em.gov.bc.ca/mining/geolsurv/publications/catalog/cat_geof), measured section No.5], where it is 73.1 metres thick, exclusive of a dacite sill 0.75 metres thick. The type-section may be reached by walking westward along the canyon floor from the Duncan Bay Main logging road, or by descending the north wall of the canyon from the western end of the mostly-overgrown Browns River Main logging road.

The Cumberland Member interfingers with the underlying Benson Member (where present); in most of the basin, the Benson is absent and the Cumberland unconformably overlies the Karmutsen Formation. The sub-Comox unconformity is irregular in detail, marked by considerable local relief (McKenzie, 1922; Graham, 1924; Muller and Atchison, 1971). Paleoscarps up to 10 metres high are visible in some outcrops. In a few localities, such as in the middle canyon of the Tsable River near the old mine pumphouse, the Karmutsen paleosurface is mantled by a few metres of grey volcaniclastic sandstones and possible tuffs, which may be of older Cretaceous age.

The Cumberland Member is abruptly (and locally erosionally) overlain by the Dunsmuir Member of the Comox Formation. Channel-filling sandstone, and blankets of siltstone, variably-carbonaceous mudstone and coal are the dominant lithologies of the Cumberland Member. The Comox No.2 coal bed and its associated splits, the Comox No.2 Rider and Comox No.2A, form the best stratigraphic markers within the Cumberland Member. The Cumberland ranges in thickness from 0.2 to 160.4 metres, with a median thickness of 65 metres.

The Cumberland thickens to the southeast, and thins to the north and west of its type locality. Thickness of the Cumberland is controlled mainly by basement paleotopography, and to a lesser extent by erosion of its uppermost beds; geophysical correlations of coal beds suggest that up to 20 metres of the uppermost Cumberland (including the Comox No.2 Rider coal bed) is locally absent due to the sub-Dunsmuir disconformity. Probable depositional environments of the Cumberland include meandering streams, alluvial plains and mires within a low-energy deltaic system.

The Cumberland contains numerous well-preserved plant fossils, mainly in the immediate roofs and floors of coal beds; these indicate a general Late Cretaceous, possibly Santonian, age. Outside of the Quinsam coalfield, where abundant shell fossils are presented in Cumberland siltstones (as reported by Kenyon, Bickford and Hoffman, 1991), the Cumberland Member does not appear to contain body fossils other than occasional fish, one of which is on display in the Cumberland Museum.

Dunsmuir Member

The Dunsmuir Member is named for the Dunsmuir coal mines at Cumberland (Bickford and Kenyon, 1988). Its proposed type-section is located in the eastern part of the middle canyon of Browns River (*see* GeoFile 2001-1, measured section No.5), where it is 115.27 metres thick. The proposed type-section of the Dunsmuir Member is accessible on foot from the west end of a dirt road which follows the south bank of Browns River westward from TimberWest's Duncan Bay Main logging road.

The Dunsmuir Member is abruptly (and locally erosionally) overlain by the Cougarsmith or Puntledge members of the Trent River Formation. Blankets of medium- to coarse-grained sandstone and lenses of siltstone, mudstone and coal are the dominant lithologies of the Dunsmuir Member. Oil shale forms a minor but distinctive part of the Dunsmuir, mostly as a series of lenses in between the Comox No.1 and Comox No.1 Rider coal beds; some of the oil shales are relatively highly radioactive, producing spectacular responses on gamma-ray logs. The Dunsmuir ranges in thickness from 11.5 to 356 metres, with a median thickness of 107.8 metres. The Dunsmuir thickens to the northeast, and thins to the south and west. Figure 1 shows details of the Dunsmuir's thickness variation southwest of Courtenay, where logs of numerous boreholes are in the public domain (CX-series borehole records in Kenyon, 1987).

Thickness of the Dunsmuir appears to be mainly controlled by gradual southwestward thinning of its constituent sandstone beds, and to a lesser extent by erosion of its uppermost beds.

Probable depositional environments of the Dunsmuir include tidal inlets, submerged lobate tidal deltas above wave base, sheltered back-barrier lagoons and barrier bars or barrier islands, within a high-energy, southwestward-prograding deltaic system. The Dunsmuir contains locally-abundant plant fossils, mainly in the immediate roofs of coal beds; these indicate a general Late Cretaceous, possibly Santonian or Campanian, age (Bell, 1957). The Dunsmuir also locally contains non-diagnostic thick-shelled pelecypod fossils within its sandstones, and possible vertebrate trackways in the immediate roof of the Comox No.1 coal bed.

Trent River Formation

The Trent River Formation was introduced by Clapp (1912) for a thick unit of shales overlying the Comox Formation, southwest of Comox Harbour. Clapp did not report a detailed section of the formation, and he did not specify its type locality. McKenzie (1922) produced a graphic section of the formation, probably based on borehole records from the north side of the Tsable River; he recognised a fairly persistent sandstone band near the base of the formation, but otherwise did not attempt its subdivision.

Bickford and Kenyon (1988), Cathyl-Bickford (1992) and England (1989, 1990) proposed nine subdivisions of the Trent River Formation within the Comox sub-basin: the basal Cougarsmith shale, overlying Cowie sandstone, Puntledge shale, Browns sandstone, Tsable conglomerate, Royston shale, Oyster River coal-measures, Baynes Sound sandstone, and uppermost Willow Point shale, but specified type-sections for none of them.

In the present study, sections have been measured of the basal four units: the Cougarsmith, Cowie, Puntledge and Browns members. The Oyster River Member is not interpreted to be present within the study area, being recognised only within the coastal lowland between Oyster River and the city of Campbell River. The Tsable,

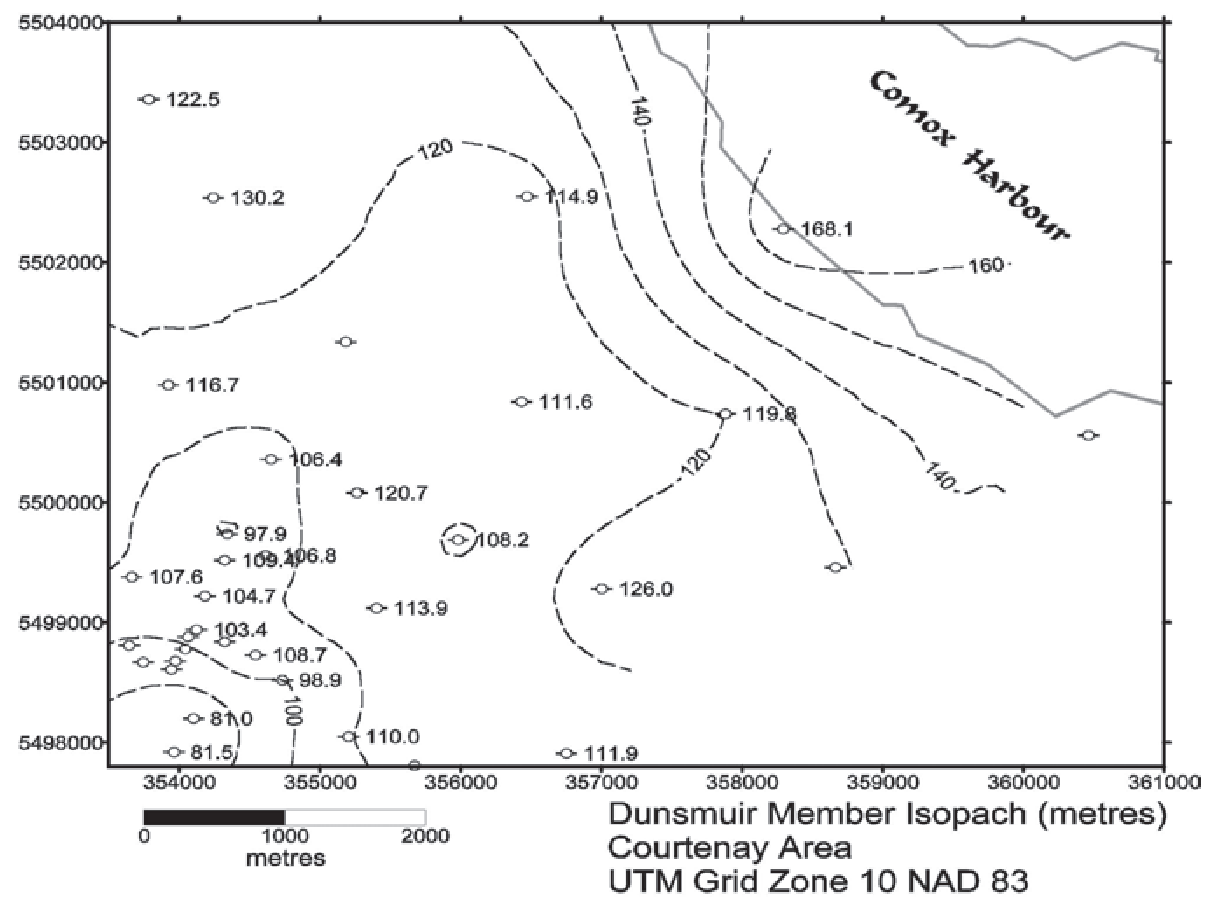

Figure 1. Dunsmuir Member isopach map.

Royston, Baynes Sound and Willow Point members were not studied in detail, owing to their structural and stratigraphic complexity; resolution of their stratigraphic relationships and thickness trends may have to await future deep drilling into their largely drift-covered outcrop belts.

Cougarsmith Member

The Cougarsmith Member was introduced by Cathyl-Bickford (1992) for a thin but laterally-persistent unit of mudstones and siltstones immediately overlying the Comox Formation, first noted in outcrop along Cougarsmith Creek south of Tsable River. Its proposed type-section is located in the lower canyon of the creek [Appendix 2 (*see* GeoFile 2001-1), measured section No.8), where it is 20.15 metres thick. This locality is accessible on foot by descending the north wall of the canyon, starting from the southwestern corner of a gravel pit on the south side of Weyerhaeuser's TR-33 logging road. The Cougarsmith Member is incompletely exposed in its type locality, and an additional reference section in the middle canyon of Browns River is hereby proposed [Appendix 1 (*see* GeoFile 2001-1), measured section No.5].

The Cougarsmith Member is abruptly overlain by the Cowie Member of the Trent River Formation. Blankets of dark grey to brownish-grey siltstone and mudstone form the bulk of the Cougarsmith Member, accompanied by thin lenticular interbeds of fine-grained sandstone. The Cougarsmith ranges in thickness from 0.6 to 36 metres, with a median thickness of 8.7 metres. The Cougarsmith thickens to the northeast, and thins to the northwest, west and south. Figure 2 shows details of the Cougarsmith's thickness variation southwest of Courtenay.

Probable depositional environments of the Cougarsmith Member include sheltered lagoons and bays, lying seaward (southwestward) of the Dunsmuir delta-front and landward (northeastward) of offshore bars. The Cougarsmith contains a sparse fauna of thin-shelled bivalves, none of which have thus far been determinable as to age.

Cowie Member

The Cowie Member was introduced by Cathyl-Bickford (1992) for a laterally-persistent unit of thick-bedded to massive sandstones overlying the Cougarsmith shales near Cowie Creek, south of Tsable River. Its proposed type-section is located in the lower canyon of Cougarsmith Creek [Appendix 2 (*see* GeoFile 2001-1), measured section No.8], where it is 11.20 metres thick. This locality is accessible on foot by descending the north wall of the canyon, starting from the southwestern

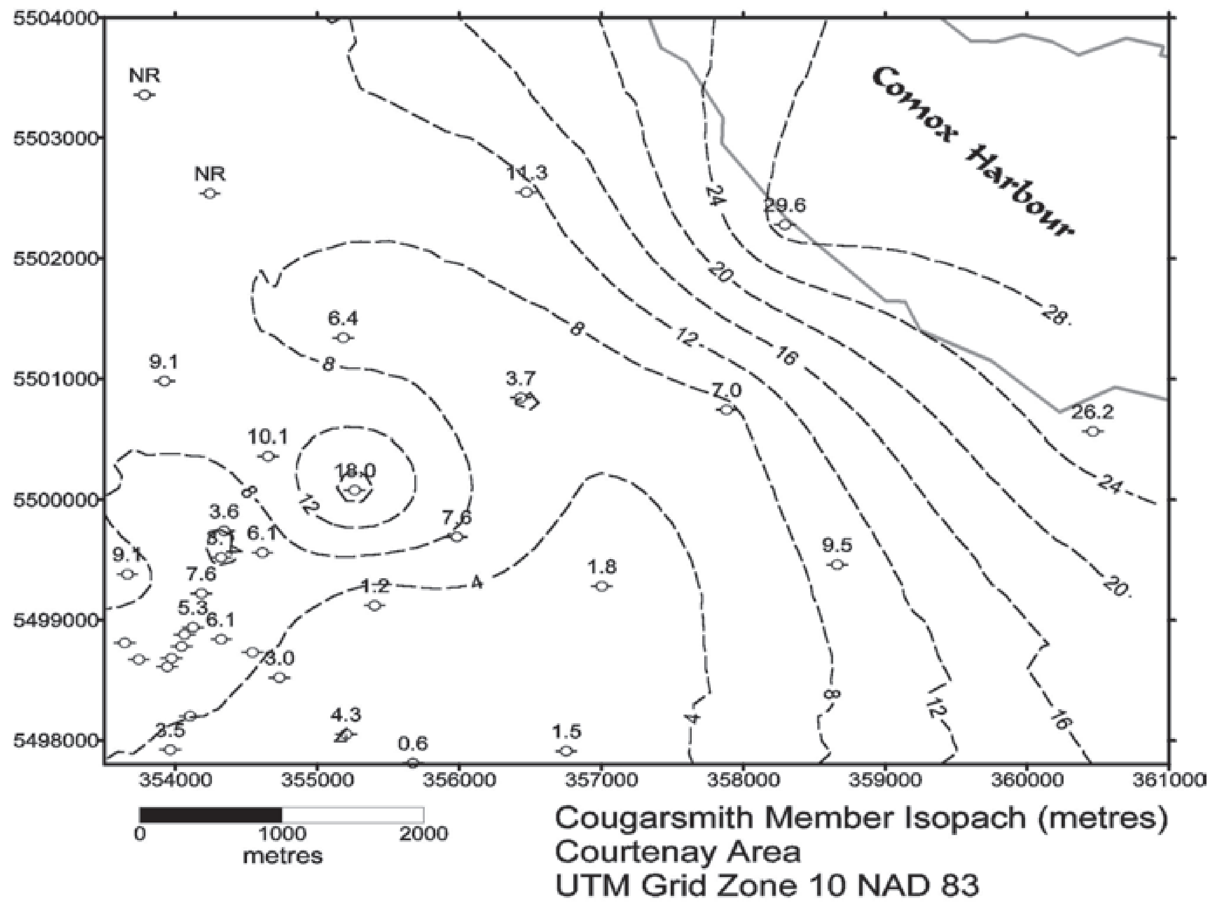

Figure 2. Cougarsmith Member isopach map.

corner of a gravel pit on the south side of Weyerhaeuser's TR-26 logging road. Additional sections of the Cowie Member are exposed on Tsable River downstream from the old Baynes Sound Mine, on Trent River upstream of the former site of the Van Logging bridge, on Puntledge River downstream from Nymph Falls [9.26 metres thick -Appendix 3 (*see* Geofile 2001-1), measured section No.6] and on Browns River upstream from the Inland Island Highway bridge [2.24 metres thick - Appendix 1 (*see* GeoFile 2001-1), measured section No.5]. Sandstones, probably correlative to the Cowie Member, are also exposed in road cuts on the west side of the Inland Island Highway, between the Duncan Bay Main logging road overpass and the Dove Creek bridge.

The Cowie Member is overlain by the Puntledge Member of the Trent River Formation. In most outcrops this is an abrupt contact, but borehole records suggest that the Cowie/Puntledge contact is interfingering or intertonguing in some parts of the study area, particularly north of Dove Creek. Fine to coarse-grained sandstone forms the bulk of the Cowie Member, but thin to medium interbeds of dark grey to black, moderately to intensely bioturbated siltstone are also locally present. The Cowie ranges in thickness from 0.5 to 24.4 metres, with a median thickness of 5.8 metres. Figure 3 shows details of the Cowie's thickness variation southwest of Courtenay.

The Cowie Member is absent altogether in approximately 20% of the boreholes between Courtenay and Tsable River; this absence may be due to lateral pinch-out of the sandstones, or to postdepositional erosion. Where the Cowie Member is absent, and there is no other obvious lithological break near the base of the Trent River Formation, the Puntledge Member is mapped as directly overlying the Dunsmuir Member.

Probable depositional environments of the Cowie Member include barrier islands or submerged and emergent offshore bars (Cathyl-Bickford, 1992), with a slight tendency to southeastward elongation . The Cowie Member locally contains heavy-mineral bands and *Thalassinoides* and *Ophiomorpha* burrows, suggestive of deposition in a high-energy setting. Abundant pelecypod fossils are present in the Cowie sandstone at Browns River (in bed 193 of measured section No.8), but these fossils are not yet known to have been collected or identified.

Puntledge Member

The Puntledge Member was introduced by Bickford *et al*. (1990) for a thick unit of dark grey to black mudstones and siltstones overlying the Dunsmuir sandstones near Puntledge River. No formal type-section was established at that time. As originally envisaged, the

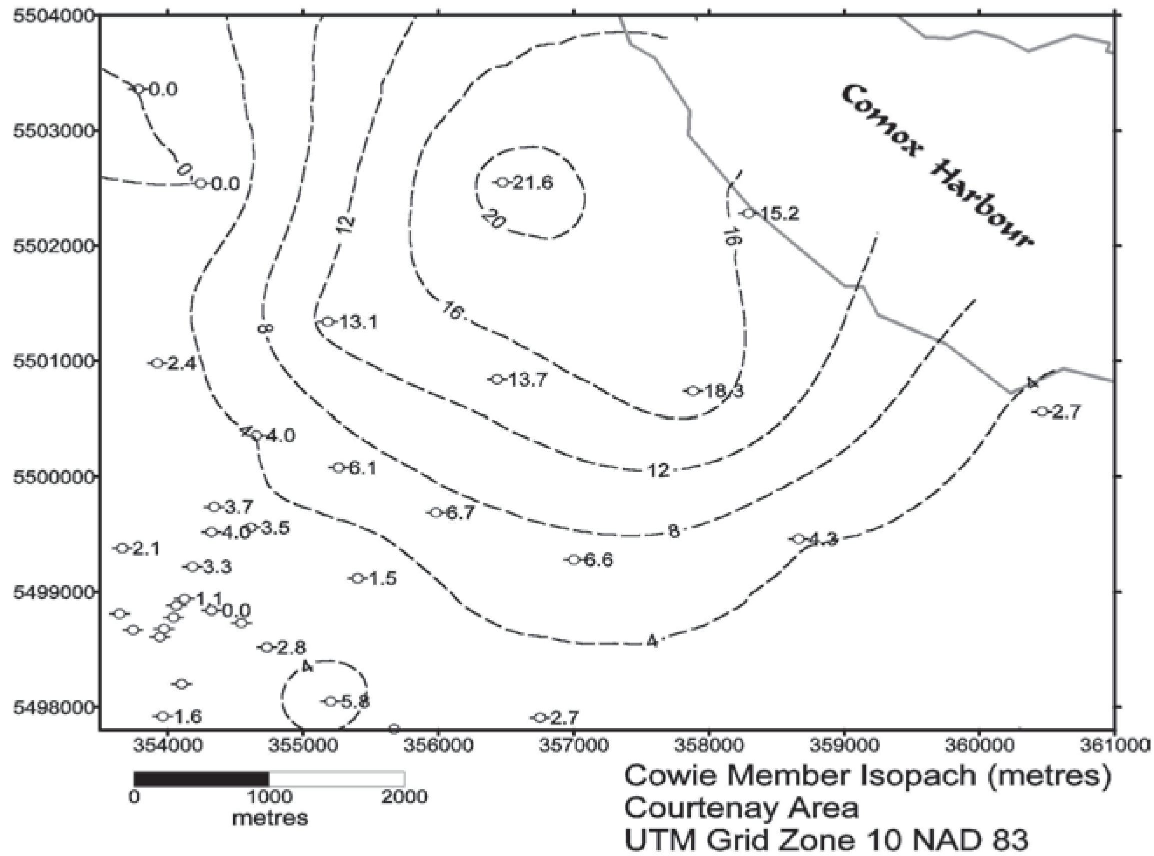

Figure 3. Cowie Member isopach map.

Puntledge Member included all beds between the Browns and Dunsmuir sandstones, but following the recognition of the Cougarsmith and Cowie members the Puntledge Member was implicitly redefined to consist solely of the mudstones, siltstones and minor sandstones overlying the Cowie Member (Cathyl-Bickford, 1992, Table 4-4-1). The proposed type-section of the Puntledge Member, as currently understood, is located along the course of Puntledge River, extending downstream from the prominent point formed by the Cowie sandstones to the overhanging ledge formed by the Browns sandstones on the south bank of the river east of Stotan Falls[139.42 metres thick - Appendix 4 (*see* GeoFile 2001-1), measured section No.7]. This section is accessible on foot from a dirt road which follows the north side of the steel-pipe penstock serving B.C. Hydro's Puntledge Generating Station. A partial reference section of the Puntledge Member, with more complete exposure of its basal 20 metres, is located along the north bank of Browns River, beneath and upstream of the Inland Island Highway bridge[Appendix 1 (*see* GeoFile 2001-1), measured section No.5].

The Puntledge Member is abruptly or locally erosionally overlain by the sandstones of the Browns Member, or by the conglomerates of the younger Tsable Member. This contact is readily recognised on lithological and geophysical logs of boreholes, and constitutes a useful marker for subsurface mapping. The Puntledge Member consists of thin to medium, generally fining-upwards interbeds of siltstone, very fine to fine-grained sandstone and mudstone; in outcrop the Puntledge presents a distinctively ribbed appearance owing to the relative erosional resistance of its sandstone bands. Subsurface lithological logs generally describe the Puntledge as consisting of thick, monotonous beds of shale or 'sandy shale'; this contrast in scale of lithological variation between outcrops and borehole records may be an artefact of the lower level of interest given by coal geologists to non-coal-bearing strata.

A distinctive feature of the Puntledge Member in outcrop, most notably along Puntledge River near Stotan Falls, is the occurrence of hard, erosionally resistant 'biscuit bands' of silty glauconitic sandstone, which weather into light-coloured, polygonally jointed layers. Some of the biscuit bands are intensely bioturbated, and they may represent hardgrounds formed at the sea floor during periods of reduced terrigenous clastic sediment influx, perhaps maximum flooding surfaces (as defined by Walker, 1992). These biscuit bands may eventually be of some value in regional correlations, as similar beds are known in outcrop from the Puntledge Member along Englishman River, southwest of the town of Parksville.

The Puntledge Member ranges in thickness from 1.8 to 128.3 metres, with a median thickness of 73 metres. The wide variation in thickness is due at least in part to post-depositional erosion of the Puntledge Member. Boreholes situated between Royston and Maple Lake indicate considerable erosional relief at the sub-Tsable disconformity, and in nearly all cases where the Puntledge Member is directly overlain by the Tsable Member, the Puntledge is less than 39 metres thick.

Possible depositional environments of the Puntledge Member include delta-front bays and deeper prodeltaic slopes. The Puntledge contains a rich vertebrate and invertebrate fauna, including plesiosaurs, ammonites, inoceramid and other bivalves, and corals (Trask, 1997), referred to the *Polyptychoceras vancouverense* zone of the Santonian by Ludvigsen and Trask (1991).

Browns Member

The Browns Member was introduced by Bickford *et al.,* (1990) for ledge-forming sandstones exposed in the beds of the Browns, Puntledge and Tsable Rivers. No type-section was originally suggested, and the outcrop trace of the Browns Member was at first poorly defined. Further mapping since 1990 has allowed a better definition of the Browns outcrop (Cathyl-Bickford and Hoffman, 1998), and a type-section is now proposed along the lower canyon of the Browns River, between a waterfall and rapids lying upstream of B.C. Hydro's transmission-lines [8.99 metres thick - Appendix 3 (*see* GeoFile 2001-1), measured section No.6]. The type-section of the Browns Member is accessible on foot by wading upstream from the southeast end of the powerline access road which runs between Piercy Road and the river. An additional reference section, 4.57 metres thick, is situated on the south bank of Puntledge River, downstream from Stotan Falls (see measured section No.7 for details). The Browns Member is either absent or represented only by sandy siltstone at Trent River (Trask, 1997).

In the northern part of the study area, north of the Courtenay Parkway, the Browns Member is overlain by the silty shales of the Royston Member. The contact is locally abrupt, but more often marked by a zone of interbedded sandstone, siltstone and shale. In such areas, the contact is arbitrarily drawn as the upward limit of the beds where sandstone comprises at least 50 percent of the section. South of the Comox Parkway, the Browns Member is locally erosionally overlain, or altogether truncated by, the conglomerates of the Tsable Member. The southward limits of the zone of sub-Tsable erosion are not well-defined owing to poor bedrock exposure and wide drill spacing; further study or exploration may disclose more than one belt of Tsable channel-fills.

The Browns Member consists mainly of mixed granitic-basaltic sandstone and siltstone which is moderately to intensely bioturbated (Bickford *et al.,* 1990). The Browns Member ranges in thickness from 0.6 to 50 metres, with a median thickness of 28.7 metres within the study area. The Browns thickens to the north and southeast of its type locality; its northward thickening appears to be at the expense of the underlying Puntledge Member, and its southeastward thickening appears to be part of a general wedging-up as it approaches the zone of channelling associated with the thicker sections of the Tsable Member. The Browns Member of the Courtenay area may have been deposited on a shallow to moderately-deep marine shelf, perhaps by current-driven redistribution of coarse-grained proximal turbidite sediments. At its type locality, the Browns Member contains a rich fauna of ammonites, referred to the basal part of the *Eupachydiscus perplicatus* zone of the early Campanian (Ludvigsen and Trask, 1991; Trask, 1997).

ECONOMIC GEOLOGY

Coal is the most abundant known mineral resource within the Cretaceous rocks of the study area. All known coal beds are contained within the Cumberland and Dunsmuir members of the Comox Formation. The Cumberland Member has been extensively drilled during the course of 130 years of coal exploration; to date, at least 250 boreholes have intersected the member within the study area, and it contains at least 94 million tonnes of coal resources of immediate interest (Gardner, 1999). The Dunsmuir Member has also been extensively drilled in search of coal. Approximately 110 boreholes have intersected substantially complete sections of the Dunsmuir, the bulk of these boreholes are in the Tsable River area or between Cumberland and Royston area of the Comox coalfield. Resources of immediate interest are probably confined to the Comox No.1 coal bed, near the base of the member.

The coals of the Comox Formation are known to be gassy within the study area (Cathyl-Bickford, 1991; Ryan, 2000), and several shows of gas have been reported from coal exploration boreholes in the Cumberland and Tsable River areas (CX-series and TR-series boreholes, collected by Kenyon, 1987). Unlicensed gas production for agricultural or domestic use has been taken from at least two of these old boreholes. Coal beds and sandstones within the Comox Formation (Dawson *et al.,* 2000), and sandstones of the Cowie Member (Cathyl-Bickford, 1992) could serve as reservoirs for natural gas. Being surrounded by organic-rich shale, the Cowie Member may be of particular interest as a hydrocarbon reservoir, provided that a viable migration pathway has extended into it. Critical risks in all conceptual gas plays would include timing of gas generation relative to formation of structural traps (England *et al*., 1989), lack of assured reservoir quality (Gordy, 1988; Hannigan *et al.*, 1998) and the possible existence of internal barriers between porous sand bodies.

Stone for building construction has been quarried from a locality near the old Number Five Mine at Cumberland, and used in the construction of the Cumberland Post Office in 1907-1909 (Barr, 1997). The stratigraphic position of this sandstone is unknown, but it is most likely either in the uppermost Dunsmuir Member or in the Cowie Member. Cowie sandstones have also been quarried for riprap and drain-rock from outcrops along the Inland Island Highway north of Browns River. The potential of the Dunsmuir, Cowie and Browns sandstones for building stones has not been studied in detail, but of the three units, the Dunsmuir sandstone may be the most accessible for quarrying near Cumberland since it forms prominent ledges and bluffs to the west and south of the village, and it appears to be relatively free from joints.

Refractory clays associated with the seatearths beneath the Comox No.3A and No.4 coal beds have been produced on a limited scale for pottery- and tile-making, basically as a co-product of underground coal mining in the Number Four Mine of Comox Colliery. Although these rocks were described by the miners as ‘fireclays’, they are unlikely to be true fireclays owing to their generally high content of organic matter.

Shales and siltstones of the Trent River Formation have been quarried on a small scale near Trent River and Bloedel Creek, for production of road-surfacing material. Their performance in this use appears to have been adequate, as demonstrated by the stability of logging roads built from these rocks.

FURTHER WORK

Although lithostratigraphic fieldwork in outcrop sections of the Comox Formation is now essentially complete, most of the results remain unpublished. An open-file report documenting the surface and subsurface lithostratigraphy and coal content of the Comox Formation is in preparation, for anticipated release in the spring or summer of 2001. The Trent River Formation requires further fieldwork, notably in its sparsely drilled and poorly exposed upper portion. Although all major outcrop areas have been mapped for their structure and for stratigraphic contacts, sections of the Trent River have been completed only in the canyons of the Oyster River and Puntledge River. In the summer of 2001, stratigraphic sections of the upper Trent River Formation will be measured along the lower canyons of the Trent and Tsable rivers, and attempts will be made to tie known vertebrate and invertebrate fossil localities into measured sections within these structurally complex areas.

Subsurface correlation studies of the Comox coals are complete in the Cumberland, Royston and Tsable River areas, except for the most recent boreholes at Tsable River, whose geophysical logs are not yet available for examination. Surface and subsurface sections throughout the Comox sub-basin will be tied together by examination of geophysical logs of boreholes which have been drilled ‘behind the outcrop’ near Trent River and Dove Creek. Results of these further studies will be published as open file reports.

ACKNOWLEDGEMENTS

Barbara Lemky, curator of the Cumberland Museum and Archives, provided workspace in the museum office, a welcome refuge on rainy mornings. Bryan Kern, geotechnical design co-ordinator for the Vancouver Island Highway Project, provided records of boreholes and test-pits which were excavated during design and construction of the northern portion of the highway. Joanna Plecke, student planner for the Comox-Strathcona Regional District, provided copies of orthophotos of the study area. Ana Leigh, Cindy Bickford and Susan Jane Davidson provided warm and comfortable lodgings during fieldwork. John Eden, area engineer for Weyerhaeuser Canada's Northwest Bay Operations, provided base maps and gate keys necessary for access to the canyons of Tsable River and Cougarsmith Creeks. Special thanks are due to Barry Ryan, Gordon Bell, Stephen Gardner and Neil Swift for discussion of stratigraphic and sedimentological problems of the Comox and Trent River formations, Barry Ryan and Nick Massey for editorial assistance, and to Suzanne Twelker, Mike Trask, Pat Trask and James Haggart for discussions of the paleontology of the study area.

REFERENCES

Atchison, M. (1968): Stratigraphy and depositional environments of the Comox Formation (Upper Cretaceous), Vancouver Island, British Columbia; unpublished Ph.D. thesis, *Northwestern University*, Evanston, Illinois.

Barr, J.N. (1997): Cumberland heritage: a selected history of people, buildings, institutions & sites, 1888-1950; *Corporation of the Village of Cumberland*, 258 pages.

Bell, W.A. (1957): Flora of the Upper Cretaceous Nanaimo Group of Vancouver Island, British Columbia; *Geological Survey of Canada*, Memoir 293.

Bickford, C.G.C., Hoffman, G. and Kenyon, C. (1989): Coal measures geology of the Quinsam area (92F); *B.C. Ministry of Energy and Mines*, Geological Fieldwork, 1988, Paper 1989-1, pages 559-563.

Bickford, C.G.C., Hoffman, G. and Kenyon, C. (1990): Geological investigations in the coal measures of the Oyster River, Mount Washington and Cumberland areas, Vancouver Island (92F/10, 11, 14); *B.C. Ministry of Energy and Mines*, Geological Fieldwork, 1989, Paper 1990-1, pages 431-437.

Bickford, C.G.C. and Kenyon, C. (1988): Coalfield geology of eastern Vancouver Island (92F); *B.C. Ministry of Energy and Mines*, Geological Fieldwork, 1987, Paper 1988-1, pages 441-450.

Cathyl-Bickford, C.G. (1991): Coal geology and coalbed methane potential of Comox and Nanaimo coalfields; *Rocky Mountain Association of Geologists*, *in* Coalbed Methane of Western North America; pages 155-162.

Cathyl-Bickford, C.G. (1992): Geology and energy resource potential of the Tsable River and Denman Island (92F/10, 11); *B.C. Ministry of Energy and Mines*, Geological Fieldwork, 1991, Paper 1992-1, pages 419-426.

Cathyl-Bickford, C.G. and Hoffman, G.L. (1998): Geological maps of the Nanaimo and Comox coalfields; *B.C. Ministry of Energy and Mines*, Open File Report 1998-7, 14 maps.

Clapp, C.H. (1912): Note on the geology of the Comox and Suquash coal fields; *Geological Survey of Canada,* Summary Report, 1911, pages 105-117.

Dawson, F.M., Marchioni, D.L., Anderson, T.C. and McDougall, W.J. (2000): An assessment of coalbed methane exploration projects in Canada; *Geological Survey of Canada*, Bulletin 549.

England, T.D.J. (1989): Lithostratigraphy of the Nanaimo Group, Georgia Basin, southwestern British Columbia; *Geological Survey of Canada*, *in* Current Research, Part E, Paper 1989-1E, pages 197-206.

England, T.D.J. (1990): Late Cretaceous to Paleogene evolution of the Georgia Basin, southwestern British Columbia; *Memorial University of Newfoundland*, unpublished Ph.D. thesis.

England, T.D.J., Piggott, N. and Douglas, T.R. (1989): Hydrocarbon charge control on the prospectivity of the Georgia Basin, Vancouver Island, British Columbia; *Canadian Society of Petroleum Geologists*, Programs and Abstracts, page 36.

Gardner, S.L. (1999): Coal resources and coal mining on Vancouver Island; *B.C. Ministry of Energy and Mines*, Open File 1999-8.

Gordy, P.L. (1988): Evaluation of the hydrocarbon potential of the Georgia depression; *B.C. Ministry of Energy and Mines*, Petroleum Geology Branch, Geological Report 88-03.

Graham, C. (1924): The problems of the Vancouver Island coal industry; *Canadian Institute of Mining and Metallurgy*, Transactions, volume XXVII, pages 456 to 477.

Hannigan, P.K., Dietrich, J.R., Lee, P.J. and Osadetz, K.G. (1998): Petroleum resource potential of sedimentary basins on the Pacific margin of Canada; *Geological Survey of Canada*, Open File 3629.

Kenyon, C. (1987): Records of coal exploration boreholes in Comox sub-basin; *B.C. Ministry of Energy and Mines*, Coal Assessment Report No. 694.

Kenyon, C. and Bickford, C.G.C. (1989): Vitrinite reflectance study of Nanaimo Group coals of Vancouver Island (92F); *B.C. Ministry of Energy and Mines*, Geological Fieldwork, 1988, Paper 1989-1, pages 543-552.

Kenyon, C., Bickford, C.G.C. and Hoffman, G.L. (1991): Quinsam and Chute Creek coal deposits (NTS 92F/13, 14); *B.C. Ministry of Energy and Mines*, Paper 1991-3.

Ludvigsen, R. and Trask, M. (1991): Upper Cretaceous biostratigraphy of the Browns and Puntledge Rivers, east-central Vancouver Island; unpublished paper presented at *1st Canadian Paleontology Conference*, Vancouver.

McKenzie, J.D. (1922): The coal measures of Cumberland and vicinity, Vancouver Island, British Columbia; *Canadian Institute of Mining and Metallurgy*, Transactions, volume XXV, pages 382-411.

Muller, J.E. and Atchison, M.E. (1971): Geology, history and potential of Vancouver Island coal deposits; *Geological Survey of Canada*, Paper 70-53.

Muller, J.E. and Jeletzky, J.A. (1970): Geology of the Upper Cretaceous Nanaimo Group, Vancouver Island and Gulf Islands, British Columbia; *Geological Survey of Canada*, Paper 69-25.

Mustard, P.S. (1994): The Upper Cretaceous Nanaimo Group, Georgia Basin; *in* Monger, J.W.H. (ed.)Geology and geological hazards of the Vancouver region, southwestern British Columbia; *Geological Survey of Canada*, Bulletin 481, pages 27-95.

Richardson, J. (1878): Coal fields of Nanaimo, Comox, Cowichan, Burrard Inlet and Sooke, British Columbia; *Geological Survey of Canada*, Report of Progress 1876-1877, Part 7, pages 307-318.

Ryan, B. (2000): Coalbed gas potential in British Columbia; unpublished paper for *Canadian Coalbed Methane Forum*, Calgary, Alberta.

Trask, M. (1997): Biostratigraphic studies of the Upper Cretaceous Trent River Formation, Vancouver Island, British Columbia; unpublished monograph, *Courtenay and District Museum*.

Walker, R.G. (1992): Facies, facies models and modern stratigraphic concepts; *Geological Association of Canada*, in Facies models: response to sea level change, Geotext 1, pages 1-14.

Leonardite-Type Material at Red Lake Diatomite Deposit, Kamloops Area, British Columbia

By George J. Simandl[1], Jana Simandl[2] and Peter B. Aylen[3]

KEYWORDS: Industrial mineral, leonardite, humate, humic acid, oxidized lignite, agriculture.

INTRODUCTION

"Leonardite" and "humate" are loosely used terms covering a variety of naturally occurring lithologies with high humic acid content, including weathered (oxidized) lignite, sub-bituminous coal and a variety of carbonaceous rocks such as mudstones, shales and claystones (Kohanowski, 1957 and 1970; Hoffman *et al.*, 1993). These raw materials are used mainly as soil conditioners, however they also have use in wood stains, drilling fluid additives and as binder in iron pelletizing (Broughton, 1972a and Hoffman *et al.,* 1993). To our knowledge, this is the first publication describing leonardite in British Columbia, therefore in addition to describing the deposit, this paper also provides background information about leonardite, humic acids and the methodology used in this study.

BACKGROUND

Humic substances are formed from the chemical and biological degradation of plant and animal residues, and from microbial activity. Based on their solubility in alkali and acids, humic substances are partitioned into three main fractions: humic acid, fulvic acid and humin. Humic acid is soluble in dilute alkali but is coagulated by acidification of the alkaline extract. The fraction which remains in solution when the alkaline extract is acidified (i.e. soluble in both dilute alkali and dilute acid), is termed fulvic acid. Humin is the fraction which cannot be extracted by either dilute base nor by dilute acid (Martin, 1997).

Carbon is the major element in humic and fulvic acids. Typical elemental analysis of humic acid is presented in Table 1.

Given the diversity of synthesis and degradation, the humic acid structure is loosely defined as a mixture of complex macromolecules having polymeric phenolic structures consisting of aromatic rings joined by alkyl chains of various lengths (Merck Index, 1996). The degree of aromaticity of humic acid has been estimated at 70% on the basis of oxidative degradation products. Several purely hypothetical structural models have been proposed in response to observed chemical and physical behaviour. The humic acid structure is presumed to contain voids of various dimensions that could trap and bind other organics.

The determination of relative molecular mass, size and shape depends on polydispersity, charge effects, aggregation properties and hydration properties. Consequently, the reported values of humic acid molecular mass range from 200 to 10 000. The values are a strong function of pH (Filella, Parthasarathy, and Buffle, 1995).

TABLE 1
COMPOSITION OF SOIL HUMIC ACID (BUFFLE, 1988)

Elemental composition	(%)
Carbon	53.8-58.7
Hydrogen	3.2-6.2
Nitrogen	0.8-5.5
Sulfur	0.1-1.5
Oxygen	32.7-38.3
Functional group content	(meq/g)
Total acidity	5.6-8.9
#NAME?	1.5-5.7
Phenolic OH	2.1-5.7
Alcoholic OH	0.2-4.9
> C=O Quinones	.4-2.6
> C=O Ketones	0.3-1.7
-O-CH3	0.0-0.8
Structural Composition	(%)
aromaticity	69
%H: Aromatic	16-43
%C: Aromatic	21-35
	10-30
fraction of total OH (%)	
aliphatic COOH	9
aromatic COOH	20
phenolic OH	14

[1]*British Columbia Ministry of Energy and Mines*
[2]*McGill University*
[3]*Western Industrial Clay Products Ltd.*

Humic acids promote the decomposition of rocks and minerals in soil, increasing the acidity of alkaline soils which liberates nutrients that then become available to plants. For this reason the majority of leonardite products are used as soil conditioners in agriculture and in tailings rehabilitation (Cooley *et al.*, 1970; Hoffman and Austin, 1993).

Materials with high humic acid content may be further processed for use as water-soluble wood stains, drilling fluid additives (Odenbaugh and Ellman, 1967, Roybal *et al.*, 1986), binders in iron ore pellets and lignite briquettes.

The biggest growth potential for humic acid-based products is in soil conditioning and agricultural applications. Although humic acid or similar materials can be derived by controlled oxidation of coal, such products are considered synthetic and therefore, are not used in organic growing operations. Leonardite and humates on the other hand, are considered to be natural products. Because of its industrial and soil conditioning applications, leonardite is typically considered an industrial mineral (Gulliov, 1991; Hamilton, 1991 and Hoffman and Austin, 1993). In most cases the energy value of leonardite and humate is too low to be considered as a fuel.

In North America, known, potentially economical deposits are reported in Arkansas, Florida, Louisiana, New York, North Dakota (Dove, 1926), Michigan, Minnesota, Texas and Wyoming (Burdick, 1965). Deposits in Wyoming, New Mexico (Shomaker and Hiss, 1974; Siemers and Wadell, 1975a, b and 1977, Roybal and Barker, 1986), North Dakota, Alberta and Saskatchewan (Figure 1) have received the most attention (Broughton, 1972a, Carter, 1982; Hoffman *et al.*, 1993; Hamilton, 1991 and Guliov, 1991).

Raw humate or leonardite should contain a sufficient concentration of humic acid to be of economic interest. New Mexico's agricultural humate typically contains 12 to 18% humic acid. The material should also have low Hg, As, Se, Cd, Ba, Pb, Zn and radionucleide content (Hoffman *et al.*, 1993). The materials used for drilling fluid applications typically contain over 65% humic acid (Hoffman *et al.*, 1993).

The Red Lake deposit is currently mined for diatomite-bearing rocks and the ore is shipped for processing to the Western Industrial Clay Products plant in Kamloops. At the plant, the ore is processed and blended with other materials to produce a variety of industrial absorbents and pet litter products.

Depending on the average humic acid content of the Upper Carbon-rich unit (*Muc*) currently exposed in the floor of the operation (Photo 1), the Red Lake deposit could become a significant producer of humic acid-bearing material marketable as leonardite or humate.

LOCATION AND REGIONAL SETTING

The Red Lake diatomite mine (092INE081), originally operated by D.E.M. Resource Processors Ltd., belongs to Western Industrial Clay Products. It is located approximately 40 km northwest of Kamloops (Figure 2).

1- Red Lake, BC; 2- Battle River, Alta;
3- Sheerness, Alta; 4- Estevan, Sask;
5- North Dakota; 6- Glenrock, Wyoming;
7- San Juan area, New Mexico

Figure 1. Leonardite-type deposits in North America.

The deposit is accessible by a combination of paved and gravel roads. Mining is seasonal due to the relatively high elevation of the deposit (1300 m above sea level), which results in unpredictable road conditions in the winter.

Tertiary Basins are indicated by shaded areas. The deposit is interpreted to lie near the base of the Miocene Deadman River Formation. The andesite or basalt flow basement that underlies the deposit is believed to belong to the Eocene Kamloops Group (Read, 1995).

DEPOSIT GEOLOGY

The presence of diatomite in the Red Lake area was known since 1928 (Eardley-Wilmot, 1928 and Cockfield, 1948). The geology of the deposit was described recently by Read (1995). The general form and geology of the deposits can be conveniently summarised by north-south and east-west sections (Figure 3a and 3b).

These sections indicate that the lithologies at the mine site include Grey Andesite, Basal Carbon-rich unit (*Mbc*), Basal Diatomaceous Earth (*Mbd*), Upper Carbon-rich unit (*Muc*) , Upper Diatomaceous Earth (*Mde*)

Photo 1. View of the Red Lake mining operation. Upper carbon-rich unit (*Muc*) containing leonardite is exposed within the bench in the central portion of the photo.

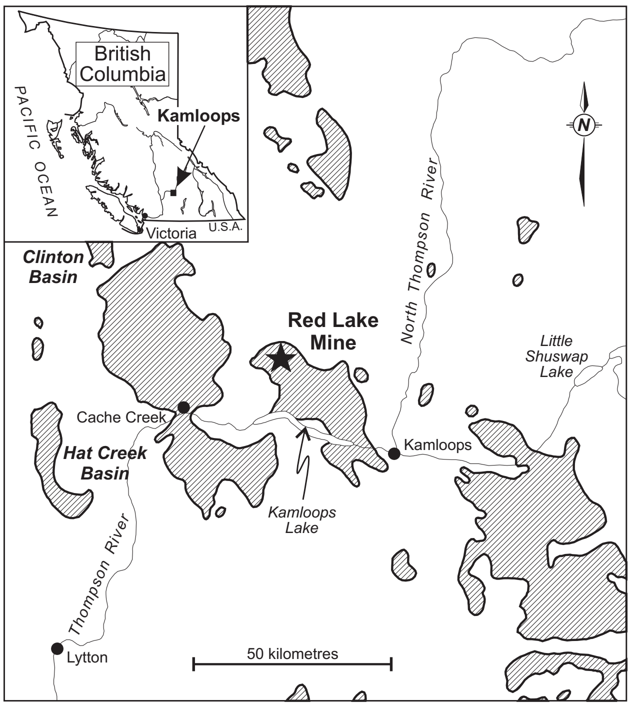

Figure 2. Geological setting of the Red Lake deposit, British Columbia, Canada. Tertiary basins are indicated by shaded areas.

and overburden (*Qs*). These units are described in stratigraphic order (from oldest to youngest) below.

Grey Andesite (possibly basalt) is the oldest unit that outcrops in the mine area. It is a grey, locally purplish, in places vesicular or amygdaloidal. This andesite forms the basin that holds the diatomite deposit and it probably belongs to the Eocene Kamloops Group (Read, 1995). It consists essentially of plagioclase laths (50-70%), measuring less than 0.5 mm, set in a glassy matrix. Altered feromagnesian minerals form less than 7% of the rock. The materials observed to fill vesicles are calcium carbonate, zeolite (probably analcime), celadonite, hematite and amorphous silica.

Medium grey, vesicular breccia consisting of angular clasts ranging from a few millimetres to a few centimetres (rarely 20 centimetres) was described by (Read, 1995), however it is not shown on the cross sections of the deposit. Read (1995) interprets it as sedimentary in origin.

Basal Carbon-rich unit (Mbc) forms lenses up to 2 m in thickness (Figure 3a and 3b). This layer was not exposed at the time of our visit and therefore not studied or sampled.

Basal Diatomaceous Earth (Mbd) is a brown diatomite layer overlaying the lower organic-rich horizon. It may locally reach over 5 m in thickness. This layer is relatively porous, soft and relatively ductile. In places, one can drive a geological pick into it without breaking it. Because of its water content, this rock appears denser than the diatomite-bearing rock from the *Upper Diatomaceous Earth unit.* It has a massive appearance and consists mainly of clay (probably montmorillonite) and diatoms.

Upper Carbon-rich unit (Muc) is described as carbonaceous shale, coal-like material and black wood fragments (Read, 1995). The unit is over 2 metres thick locally and it separates the previously described brown Basal Diatomaceous Earth from the Upper Diatomaceous Earth unit. This organic-rich layer was exposed in the floor of the mine at the time of our visit and nine samples were collected from it. The upper 15 centimetres is particularly rich in light-weight woody fragments. The unit also contains crumbly, sand-like diatomite-bearing lenses or layers.

Upper Diatomaceous Earth (Mde) unit is mostly beige to pale grey in colour, but it may also be brownish. It locally reaches up to 7 m in thickness (Figure 3). It is commonly laminated or massive, but in many places blocky. Centimetre-scale parting is a dominant texture. This highly absorbent, light-weight unit (density 0.61 g/cm^3) consists of montmorillonitic clay, and contains 20 to 35% of diatomite skeletons. This rock has provided, up to now, the bulk of the raw material for the Western Industrial Clay Products plant.

Overburden (Qs) consists mainly of unconsolidated glacial and alluvial deposits, however, it may consist locally of material that was relocated during mining.

GEOCHEMISTRY OF THE UPPER CARBON-RICH UNIT

Nine representative samples were selected and described in the field. All samples came from the Upper carbon-rich unit (*Muc*). These samples weighed 3 to 5 kilograms each.

All samples were split; one half was kept for further studies and the other was sent to Loring Laboratories in Calgary for sample preparation and chemical analyses.

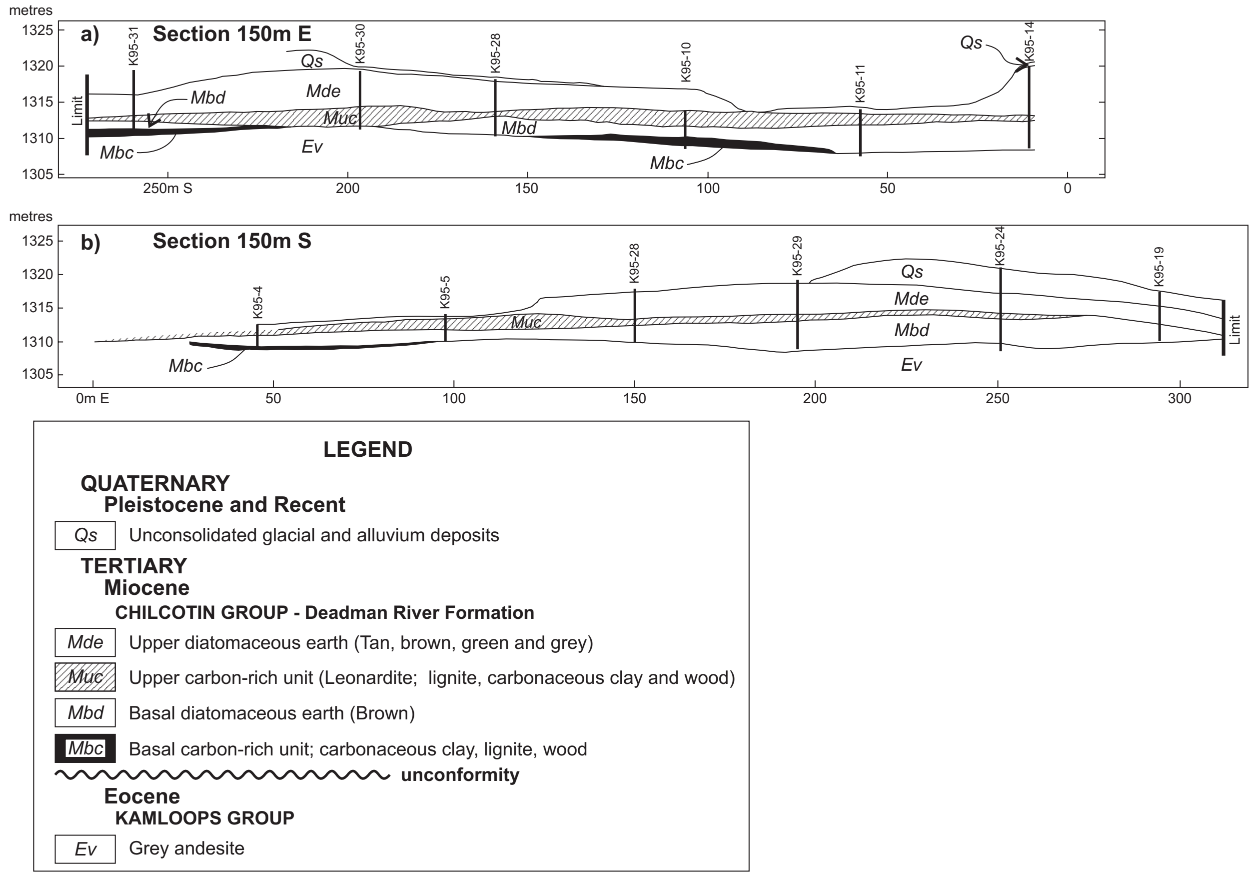

Figure 3. North-south (a) and east-west (b) sections of the Red Lake deposit (modified from Read (1995).

Analytical Procedure

The sample preparation and analytical methods are described below.

Sample preparation: All samples were weighed, partially dried to bring the moisture near equilibrium with the atmosphere, crushed and split using a riffle. A representative sample was obtained and crushed to -60 mesh and mixed again. The detailed methodology is described under ASTM Designation D 2013 - 86.

Humic acid determination (colorimetric method): A 0.5 g sample was extracted with 50 ml of 0.5 N NaOH solution for 10 minutes. Two ml of the filtered solution was transferred to a 100 ml flask and brought to bulk volume. The absorbency was read on the Bausch and Lomb Spectronic 20 spectrometer and compared to the standard carried with the analysis.

Humic acid determination (chemical precipitate method): A 2 g sample was extracted with 50 ml of 0.5 N NaOH solution for 1.5 hours and centrifuged. The supernatant liquid was transferred to another weighed bottle and acidified to pH < 1 and centrifuged again. The solid was dried and weighed as humic acid solid.

Major elements analysis: 0.2 g of coal ash was fused with lithium metaborate, dissolved in 5% HNO_3 and analysed using the Thermo Jarrell Ash Model IRIS high resolution ICP unit. Consequently the results are reported on an "in ash" basis.

Trace elements analysis: 1 g of coal was ashed and then transferred to a Teflon beaker and digested using HF, HNO_3 and HCl until near dryness. The sample was then boiled with 20% HCl and transferred to a 100 ml flask and made up to a final volume of 100 ml. The sample was analyzed by the Thermo Jarrell Ash Model IRIS high resolution ICP unit.

Ultimate analysis: This analysis involves the determination of the water (H_2O), carbon (C), hydrogen (H), nitrogen (N), sulphur (S) and ash content. The value of oxygen is not measured, but determined by difference. The standard method for ultimate analysis of coal and coke as described under ASTM Standard Designation D 3176 - 84 was used.

Broughton (1972b) describes a low-angle X-ray scattering method for identification of leonardite. There was no time to test this method and to compare the results with above described methods used to determine humic acid content, but this analytical procedure may be a worthwhile as an exploration tool.

TABLE 2
HUMIC ACID CONTENT OF THE UPPER CARBON-RICH UNIT (*MUC*) DETERMINED USING COLORIMETRIC AND CHEMICAL PRECIPITATION METHODS

SAMPLE ID	BASIS	% Humic Acid Colorimetric	% Humic Acid Chemical ppt
RED-00-7	A.D.	5	-
RED-00-15	A.D.	12	-
RED-00-16	A.D.	52	75.0
RED-00-17	A.D.	43	45.2
RED-00-19	A.D.	9	5.8
RED-00-20	A.D.	47	48.8
RED-00-22	A.D.	22	7.0
RED-00-23	A.D.	13	3.7
RED-00-24	A.D.	20	13.8

Results of Analyses

The results of the humic acid determination using both the colorimetric and chemical precipitate methods are shown in Table 2.

Nine samples were analysed using the former and only seven using the latter method, as a cost saving measure. Both types of determinations were done on air dried samples. The same seven samples as used above were also analysed for major (Table 3) and trace elements (Table 4). Table 5 shows the results of the ultimate analysis. For every sample H_2O, C, H, N, ash , S and oxygen content are reported as A.R. (as received), A.D. (air dried) and Dry (oven dried).

DISCUSSION OF THE DATA

The Red Lake diatomite deposit contains the Upper carbon-rich unit (*Muc*) which is the first documented occurrence of humic acid-rich material, that can be described as leonardite or humate, in British Columbia. The correlation coefficient (r) method described by Harrell (1987) was used to compare the results of the colorimetric and chemical precipitate methods. In this correlation r varies from -1 to 1. These values correspond to either perfect negative or positive correlation, respectively. If r = 0, it means that there is no correlation at all. In our case, r = 0.96, indicating excellent correlation.

Figure 4 indicates that the low-cost colorimetric method is probably sufficient for exploration purposes, and suggests that the chemical precipitate method should be used where precision is required. The line with 45º slope on Figure 4., originating at the intersection of X and Y axis, is shown for reference purpose only. If the two, humic acid determination methods that we used gave identical results, all the data would plot directly on this line.

The samples from this study indicate extreme variations in humic acid concentrations perpendicular to the strike and possibly along strike. Such variation indicates that a much broader systematic sampling is required to obtain a representative humic acid content of the *Upper Carbon-rich unit* at the mine site. It also suggests that careful blending would be needed to obtain and maintain a consistent humic acid content if leonardite material from Red Lake were to be mined and marketed as a soil conditioner.

Trace element data, reported on "total rock" basis (not in ash), indicate that silver (Ag), arsenic (As), gold (Au), berylium (Be), bismuth (Bi), cadmium (Cd) and selenium (Se) are below the detection limit. Other elements are present in trace, but detectable quantities including Ba (< 291 ppm), Co (< 96 ppm), Cr (< 19 ppm), Cu (< 32 ppm), La (< 119 ppm), Mn (< 187 ppm), Mo (< 44 ppm), Ni (< 107 ppm), P (< 0.087 %), Pb (< 47 ppm), Sb (< 16 ppm), Sr (< 86 ppm), Th (< 5 ppm), U (< 5 ppm), V (< 270 ppm), W (< 23 ppm), Zn (< 74 ppm). Boron levels (19 to 547 ppm) most likely reflect the original playa-type environment. The concentrations of ash from these samples (Table 4) indicate that there are no anomalous levels of trace elements including As, Se, base metals and

TABLE 3
MAJOR ELEMENTS ANALYSIS OF ASH DERIVED FROM THE UPPER CARBON-RICH UNIT (*MUC*), RED LAKE DEPOSIT (WHOLE ROCK ICP ANALYSIS)

Sample No.	Al_2O_3 (%)	Ba (ppm)	CaO (%)	Cr (ppm)	Fe_2O_3 (%)	K_2O (%)	MgO (%)	MnO (%)	Na_2O (%)	Ni (ppm)	P_2O_5 (%)	SO_3 (%)	SiO_2 (%)	Sr (ppm)	TiO_2 (%)	V_2O_5 (%)	Undet. (%)
RED-00-16	19.97	555	3.10	110	28.14	0.20	1.15	0.01	0.17	467	0.209	0.92	41.32	138	0.55	0.09	3.92
RED-00-17	15.31	621	1.67	38	26.43	0.45	0.83	0.02	0.56	92	0.535	0.33	48.87	137	0.99	0.13	3.27
RED-00-19	5.13	79	0.72	29	1.62	0.14	0.56	0.01	0.06	67	0.013	0.30	87.80	36	0.13	0.03	3.34
RED-00-20	14.75	283	13.64	79	10.88	0.23	6.34	0.16	0.13	401	0.093	3.03	45.09	393	0.32	0.07	5.16
RED-00-22	17.26	210	1.23	34	3.17	0.20	0.94	0.02	0.12	32	0.031	0.30	69.09	64	0.57	0.04	6.96
RED-00-23	19.25	163	1.26	61	4.56	0.18	1.08	0.02	0.15	353	0.046	0.48	67.40	65	0.64	0.04	4.76
RED-00-24	22.95	241	4.30	85	9.16	0.22	3.54	0.07	0.21	175	0.100	1.74	48.84	142	1.05	0.09	7.55

Whole rock analysis expressed on an "in ash" basis.
0.2 g Coal ash fused with lithium metaborate, and dissolved in 5% HNO_3.

TABLE 4
TRACE ELEMENTS ANALYSIS FROM THE UPPER CARBON-RICH UNIT (*MUC*), RED LAKE DEPOSIT (32 ELEMENT ICP ANALYSIS)

Sample Name	Ag (ppm)	Al (%)	As (ppm)	Au (ppm)	B (ppm)	Ba (ppm)	Be (ppm)	Bi (ppm)	Ca (%)	Cd (ppm)	Co (ppm)	Cr (ppm)	Cu (ppm)	Fe (%)	K (%)	La (ppm)
RED-00-16	<0.5	2.57	<5	<5	64	148	<5	<5	0.44	<5	96	19	15	4.17	0.03	119
RED-00-17	<0.5	3.99	<5	<5	123	291	<5	<5	0.50	<5	76	12	22	7.41	0.19	50
RED-00-19	<0.5	2.42	<5	<5	80	53	<5	<5	0.42	<5	35	<5	20	0.85	0.08	16
RED-00-20	<0.5	1.52	<5	<5	19	67	<5	<5	1.54	<5	29	12	12	1.43	0.04	35
RED-00-22	<0.5	7.62	<5	<5	547	185	<5	<5	0.71	<5	18	19	77	1.83	0.19	42
RED-00-23	<0.5	8.28	<5	<5	470	120	<5	<5	0.70	<5	29	19	32	2.68	0.16	42
RED-00-24	<0.5	2.03	<5	<5	145	48	<5	<5	0.41	<5	25	<5	19	0.96	0.04	24

Sample Name	Mg (%)	Mn (ppm)	Mo (ppm)	Na (%)	Ni (ppm)	P (%)	Pb (ppm)	Sb (ppm)	Sr (ppm)	Th (ppm)	Ti (%)	U (ppm)	V (ppm)	W (ppm)	Zn (ppm)	Se (ppm)
RED-00-16	0.16	7	22	0.04	82	0.020	21	6	35	<5	0.08	<5	65	23	74	<5
RED-00-17	0.23	52	44	0.33	107	0.087	24	13	64	<5	0.25	<5	270	14	60	<5
RED-00-19	0.26	45	7	0.05	44	0.007	17	7	31	<5	0.06	<5	27	10	71	<5
RED-00-20	0.67	187	<5	0.03	101	0.009	14	<5	86	<5	0.04	<5	70	6	33	<5
RED-00-22	0.48	94	<5	0.23	32	0.016	47	16	54	<5	0.31	<5	89	8	52	<5
RED-00-23	0.53	95	<5	0.24	41	0.021	47	13	52	<5	0.34	<5	77	6	67	<5
RED-00-24	0.32	74	<5	0.05	38	0.008	18	<5	29	<5	0.11	<5	68	9	49	<5

Results expressed on an "in coal" basis.
1g of coal was ashed, and the ash was then totally dissolved using HF and aqua regia and taken to a final volume of 100 ml.

TABLE 5
ULTIMATE ANALYSIS OF UPPER CARBON-RICH UNIT (*MUC*) RED LAKE DEPOSIT (A.R. - AS RECEIVED, A.D. - AIR DRIED)

SAMPLE ID	BASIS	H2O (%)	C (%)	H (%)	N (%)	ASH	S (%)	O (%)
RED-00-16	A.R.	67.56	14.08	0.97	0.44	8.60	0.17	8.17
	A.D.	10.98	38.65	2.67	1.20	23.60	0.47	22.43
	Dry	-	43.42	3.00	1.35	26.51	0.53	25.20
RED-00-17	A.R.	30.23	21.56	1.52	0.77	33.99	0.38	11.55
	A.D.	8.18	28.37	2.00	1.01	44.74	0.50	15.20
	Dry	-	30.90	2.18	1.10	48.73	0.54	16.55
RED-00-19	A.R.	53.31	4.80	0.85	0.38	37.81	0.22	2.64
	A.D.	4.2	9.85	1.74	0.77	77.57	0.45	5.42
	Dry	-	10.28	1.82	0.80	80.97	0.47	5.65
RED-00-20	A.R.	42.01	28.49	2.27	0.76	11.60	0.81	14.07
	A.D.	8.19	45.11	3.59	1.20	18.36	1.28	22.27
	Dry	-	49.13	3.91	1.31	20.00	1.39	24.26
RED-00-22	A.R.	39.78	6.09	0.65	0.48	47.70	0.21	5.09
	A.D.	3.97	9.71	1.04	0.77	76.06	0.33	8.12
	Dry	-	10.11	1.08	0.80	79.20	0.34	8.46
RED-00-23	A.R.	33.25	6.67	1.03	0.20	52.79	0.30	5.75
	A.D.	4.36	9.56	1.48	0.29	75.64	0.43	8.24
	Dry	-	10.00	1.54	0.30	79.09	0.45	8.62
RED-00-24	A.R.	33.25	34.24	3.07	0.01	12.58	0.71	16.15
	A.D.	5.73	48.36	4.33	0.01	17.76	1.00	22.81
	Dry	-	51.30	4.60	0.01	18.84	1.06	24.19

Note: Hydrogen and Oxygen do not include H and O from sample moisture. Value of oxygen by difference.

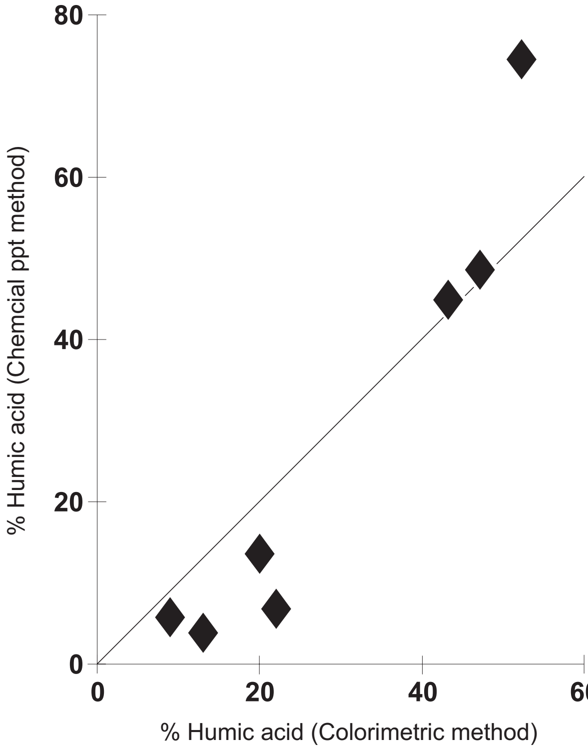

Figure 4. Relationship between humic acid determination results using the chemical precipitate and colorimetric methods.

radionucleids that would limit the use of this material in agricultural and horticultural applications.

The ultimate analysis also provided useful information. It indicates that within the pit, water may represent 30 to over 67% and ash 8.6 to over 50% of the unprocessed raw material from the Upper Carbon-rich unit (*Muc*). Sulphur content varies from 0.17 to 0.71%, nitrogen from 0.01 to 0.77% and oxygen from 2.64 to 16.15% on an as received basis. Upon drying the proportions of all of these constituents, except water, will increase substantially.

Major element analyses (Table 3) shows that SiO_2 (41 to over 80%), Fe_2O_3 (1.62 to 28.14%) and Al_2O_3 are the major constituents in the ash. High SiO_2 content was expected because the host is diatomite-bearing. High Al_2O_3 is due to clay content. There appears to be no relationship between Fe_2O_3 and SO_3 confirming the absence of sulphides previously established by visual observation and fully expected in the highly oxidized environment

SUMMARY

Organic material from the Red Lake diatomite mine can be described as leonardite or humate. This preliminary study is not based on systematic sampling, and indicates extreme fluctuations in humic acid content within the organic-rich layer. We can not speculate on the average humic acid content of the *Upper Carbon-rich unit* (*Muc*) exposed at the Red Lake mine. No high levels of trace elements that would preclude the use of the material as a soil conditioner were detected. In summary, our data suggests that the *Upper Carbon-rich unit* currently exposed in the floor of the open pit has potential as a soil conditioner or at the very least, as a material for tailing rehabilitation. The *Lower Carbon-rich* unit was not sampled but it is possible that it may also have high humic acid content.

ACKNOWLEDGEMENTS

Thanks are in order to Brian Grant, Garry Payie and Alicia Debreceni, of British Columbia Ministry of Energy and Mines, for improving an earlier version of this manuscript. Amy Boulton assisted with the fieldwork and Mike Fournier drafted the figures. Western Industrial Clay Products permitted and facilitated our access to the property. All the chemical analyses were made by Loring Laboratories Ltd. in Calgary, Alberta.

REFERENCES AND BIBLIOGRAPHY

Broughton, P.L. (1972a): Humic acid complexes from naturally oxidized lignite: their genesis, chemistry and utilization; *in Eighth Forum on the Geology of Industrial Minerals,* Iowa City, Iowa, April 12-14, 1972, p. 135-157.

Broughton, P.L. (1972b): Identification of leonardite, a naturally oxidized lignite, by low-angle X-ray scattering method; *Journal of Sedimentary Petrology 42,* p. 356-358.

Buffle, J. (1988): Complexation Reactions in Aquatic Systems. An Analytical Approach; Ellis Horwood series in analytical Chemistry; Ellis Horwood, UK, 692 pages.

Burdick, E.M. (1965): Commercial Humates for Agriculture and the Fertilizer Industry; *Economic Botany,* Vol. 19*,* p. 152-159.

Carter, J. (1982): Leonardite, Sheerness, Alberta; *Dresser Industries,* internal report, 23p.

Cockfield, W.E. (1948): Geology and Mineral Deposits of Nicola Map-Area, B.C; *Canada Department of Mines and Resources*, Memoir 249, 164p.

Cooley, A.M., Douglas, G., Rasmussen, W.H., Rasmussen, J.J. and Theis, J. (1970): Leonardite in fertilizer; *in* Elder, J.L. and Kube, W.R., compilers, *Technology and Uses of Lignite, Proceedings: Bureau of Mines - University of North Dakota Symposium,* Grand Forks, N. Dakota, May 1-2, 1969. U.S. Bureau of Mines, Information Circular 8471, p. 157-164.

Dove, L. 1926. Dakalite; *University of North Dakota, D*epartment Bulletin, v. 11, no. 1*,* p. 33-37.

Eardley-Wilmot, V.L. (1928): Diatomite; Mines Branch, *Department of Mines*, Canada; No.691, p-44-45.

Filella, M., Parthasarathy, N. and Buffle, J. (1995): Humic and Fulvic Compounds, *in:* Encyclopedia of Analytical Science, Alan Townshend ed., Vol. 4., *Academic Press*, Harcourt Brace & Co. Publishers, p. 2017-2027.

Guliov, P. (1991): Overview of Industrial Minerals in Saskatchewan; Proceedings, 27th Forum on the Geology of Industrial Minerals, Industrial Minerals of Alberta and British Columbia, Canada, Z.D. Hora, *et al.*, eds., Information Series 115, *Alberta Geological Survey,* p. 19-36.

Hamilton, W.N. (1991): Industrial Minerals in Alberta; Proceedings, 27th Forum on the Geology of Industrial Minerals, Industrial Minerals of Alberta and British Columbia, Canada, Z.D. Hora, *et al.*, eds., Information Series 115, *Alberta Geological Survey*, p. 19-36.

Harrell, J.A. (1987): The Analysis of Bivariate Association; *in* W.B. Size, editor, Use and Abuse of Statistical Methods in the Earth Sciences; International Association or Mathematical Geology; Studies in Mathematical Geology No.1, *Oxford University Press*, p. 142-165.

Hoffman, G.K. and Austin, G.S. (1993): Agricultural materials: soil additives; in D.D. Carr, senior editor, Industrial Rocks and Minerals, 6th Edition, *Society of Mining*, Metallurgy and Exploration, Littleton, Colorado.

Hoffman, G.L., Nikols, D.J., Stuhec, S. and Wilson, R.A. (1993): Evaluation of Leonardite (Humalite) Resources of Alberta; *Energy, Mines and Resources Canada,* Alberta Research Council*,* Open File Report 1993-18, 45p.

Kohanowski, N.N. (1957): On the origin of leonardite; *North Dakota Academy of Science,* Proceedings, 11, p. 60-64.

Kohanowski, N.N. (1970): Leonardite in North Dakota; *North Dakota Quarterly 3,* p. 36-42.

McKenzie, R.C. (1970): Agricultural use of coal-derived humic acids; *M.Sc. thesis, University of Alberta,* Edmonton, Alberta, 86 p.

Merck Index (1996): 12th edition, Susan Budavari ed. Merck & Co., Whitehouse Station NJ. USA, page 812.

Martin, J. P. (1997): Humus; McGraw-Hill Encyclopedia of Science & Technology, Vol. 8, 8th edition, pages 620-624.

Odenbaugh, M.L. and Ellman, R.C. (1967): Leonardite and other materials as drilling fluid dispersants and viscosity control agents; *U.S. Bureau of Mines,* Report of Investigation 7043, 22 p.

Read, P.B. (1995): Geology and Ore Reserves, Red Lake Open Pit, Kamloops Mining Division (92I/15w/2); Assessment Report #25358, *British Columbia Ministry of Energy and Mines*, 42 p.

Roybal, G.H. and Barker, J.M. (1986): Geology and production of humate and weathered coal in New Mexico; *American Institute of Mining, Metallurgical and Petroleum Engineers,* Transactions 280, p. 2105-2111.

Senn, T.L. and Kingman, A.R. (1973): A review of humus and humic acids; *South Carolina Agricultural Experimental Research Series*, No. 145*,* 18 p.

Shomaker, J.W. and Hiss, W.L. (1974): Humate Mining in Northwestern New Mexico; *New Mexico Geological Society, 2*5th Field Conference, p. 333-336.

Siemers, C.T. and Wadell, J.S. (1975): IV. Humate and Associated Deposits of the Lower Part of the Menefee Formation (Stop 2), Field Trip to Central New Mexico, *AAPG-SEPM*, Rocky Mountain Section Meeting, Alburquerque, June 1-4, p. 39-46.

Siemers, C.T. and Wadell, J.S. (1975): Humate deposits in New Mexico; *American Association of Petroleum Geologists,* Bulletin 59, p. 923.

Siemers, C.T. and Wadell, J.S. (1977): Humate deposits of the Menefee Formation (Upper Cretaceous), Northwestern New Mexico; *New Mexico Geological Society,* Supplement to the 28th Field Conference, 22p.

BC Regional Geochemical Survey: 2000 Field Programs

By Wayne Jackaman[1], Ray Lett[1] and Peter Friske[2]

KEYWORDS: Applied geochemistry, mineral exploration, drainage sediments and waters, orientation studies, Regional Geochemical Surveys.

INTRODUCTION

The Exploration Services and Information Section of the British Columbia Geological Survey Branch is responsible for administering the Regional Geochemical Survey (RGS) program and providing complementary research and orientation studies designed to promote the effective use of exploration geochemistry. Results are used by industry to pinpoint exploration opportunities and by government for resource management, land-use planning and environmental assessments. The section's activities during the 2000 field season are summarized in this paper (Figure 1).

Regional Geochemical Survey Program (RGS)

The British Columbia Ministry of Energy, Mines and Petroleum Resources (MEMPR) has been involved in reconnaissance-scale stream sediment and water surveys since 1976. This joint federal-provincial initiative was originally referred to as the Uranium Reconnaissance Program (URP). In 1978 the provincial program was renamed the Regional Geochemical Survey (RGS) and in 1987 the Province began to independently administer surveys conducted in British Columbia. As part of Canada's National Geochemical Reconnaissance (NGR) program, the RGS program continues to maintain sample collection, preparation and analytical standards established by the Geological Survey of Canada.

Archive Release

Since 1975, over 45,000 drainage sediment and water samples have been collected and analyzed by the RGS Program. Starting in 1991, the RGS Archive program has upgraded the database with previously unavailable analytical information. Sediment samples saved from surveys conducted from 1976 to 1985 have been re-analysed by instrumental neutron activation analysis (INAA) for gold and several other metals not included as part of the original data releases. To date, the RGS Archive Program has compiled and published new data for over 21,000 samples covering 18-1:250 000 NTS map sheets.

In June of this year, new INAA data plus original field and analytical results for 2,727 sediment samples collected from surveys conducted in the late 1970's in the Atlin (NTS 104N), Jennings River (NTS 104O) and McDame (NTS 104P) map sheets were published (Jackaman, 2000). The data clearly highlighted existing mining camps and identified many other precious and base metal anomalies (Figure 2). RGS archive data for the Quesnel (NTS 93B) 1:250 000 survey area are scheduled for release in the summer of 2001 (Jackaman, in preparation).

Dease Lake RGS

In cooperation with the Geological Survey of Canada (GSC), a new reconnaissance-scale stream sediment and water survey was completed in the Dease Lake (NTS 104J) map sheet. Truck and helicopter supported sam-

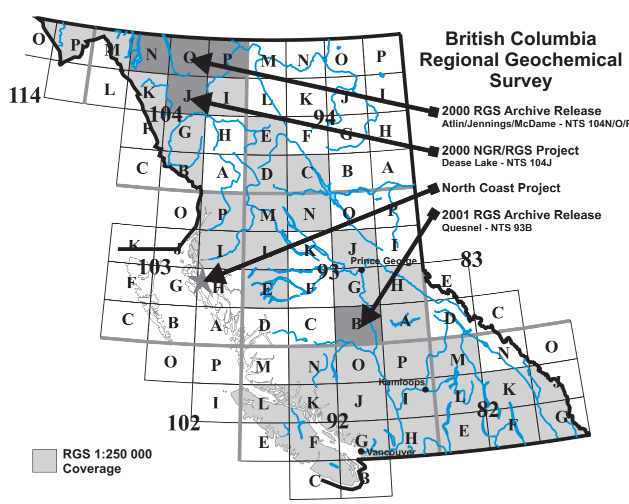

Figure 1. Location map of RGS and related projects.

[1] *British Columbia Ministry of Energy and Mines*

[2] *Geological Survey of Canada*

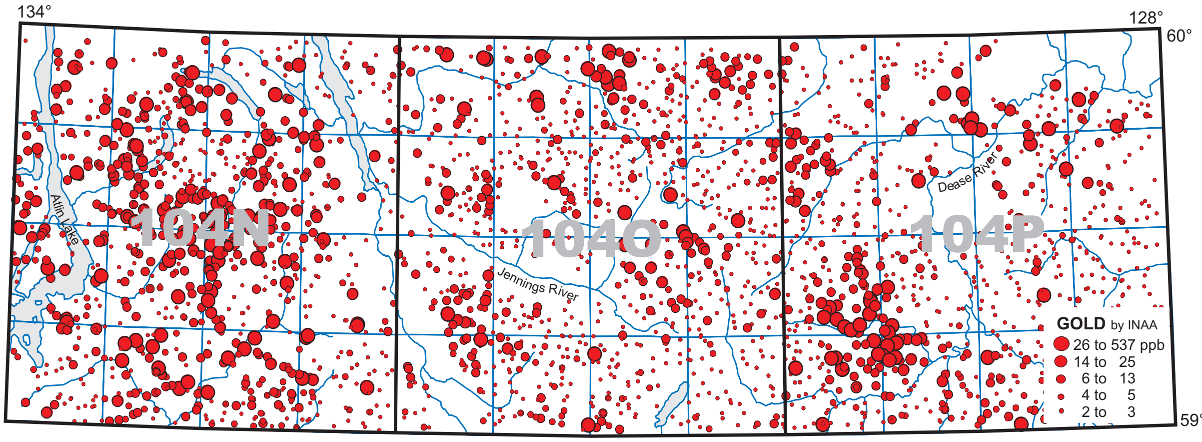

Figure 2. Distribution of gold in NTS 104N/O/P.

pling was conducted during July and August, 2000. A total of 963 stream sediment and water samples were collected from 908 sites at an average density of 1 site every 13 square kilometres.

Recognized for its mineral potential, the central and northern parts of the map sheet are underlain by the oceanic, ophiolitic Cache Creek terrane and are bounded by Mesozoic rocks to the north (Quesnellia Terrane) and south (Stikinia Terrane). The map sheet covers a relatively under-explored frontier area with a strong mineral exploration community based on placer activities, and nearby mines such as Golden Bear (MINFILE 104K 01W). In addition, there are numerous adjacent developed prospects such as Kutcho Creek (MINFILE 104I 60), Gnat Pass (MINFILE 104I 01)and Red Chris (MINFILE 104H 05). The potential for further mineral discoveries includes porphyry Cu-Mo-Au, VMS, Au (vein and intrusion related) and PGE occurrences.

In contrast to previous RGS programs, which routinely used atomic absorption spectroscopy (AAS) as the standard analytical technique for a variety of metals including zinc, copper, lead, nickel, cobalt, silver, manganese and molybdenum, this year's sediment samples are being analyzed by aqua-regia inductively coupled plasma-mass spectroscopy (ICP-MS) and instrumental neutron activation analysis (INAA). Table 1 lists the elements and associated detection limits. Water samples are being analyzed for pH, uranium and fluoride. Trace metal analysis by ICP-MS will also be run on additional 125 millilitre water samples collected from 213 sites. Quality analytical results are ensured by monitoring analytical variation with sample duplicates and control reference standards.

This survey is being funded in part by the Geological Survey of Canada Targeted Geoscience Initiative (TGI) and the B.C. Geological Survey Branch. Results are expected to be published in 2001.

North Coast Drainage Sediment and Water Survey

Drainage sediment and water samples were collected from several locations in the North Coast during the summer field season (Figure 3). In the Ecstall River area (NTS 103H/I), sediment and water samples were collected from 229 sites covering an area approximately 2000 square kilometres. Samples were also collected from 71 sites on Porcher Island, Dundas Island and along the Inside Passage (NTS 103G/H/J). These surveyed areas contain mineral deposit environments favourable for the discovery of massive sulphides along the Ecstall/Scotia belt, gold bearing quartz veins on Porcher Island, and VMS on Dundas Island.

These surveys are designed to provide baseline regional geochemical data that can be used in the evaluation of the mineral potential of the target areas. Funded under

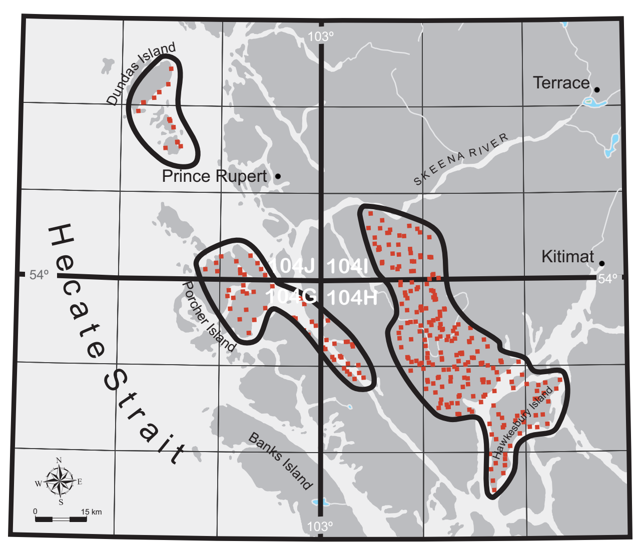

Figure 3. Location map of North Coast surveys.

TABLE 1
RGS ANALYTICAL SUITE OF ELEMENTS

Element		Method	D.L.	Units
Aluminium	Al	ICP	0.01	%
Antimony	Sb	INA/ICP	0.1/0.02	ppm
Arsenic	As	INA/ICP	0.5/0.1	ppm
Barium	Ba	INA/ICP	50/0.5	ppm
Bismuth	Bi	ICP	0.02	ppm
Boron	B	ICP	1	ppm
Bromine	Br	INA	0.5	ppm
Cadmium	Cd	ICP	0.01	ppm
Calcium	Ca	INA/ICP	1.0/0.01	%
Cerium	Ce	INA	3	ppm
Cesium	Cs	INA	1	ppm
Chromium	Cr	INA/ICP	5.0/0.5	ppm
Cobalt	Co	INA/ICP	1.0/0.1	ppm
Copper	Cu	ICP	0.1	ppm
Fluorine	Fe	ICP	10	ppm
Gallium	Ga	ICP	0.2	ppm
Gold	Au	INA/ICP	2/0.2	ppb
Hafnium	Hf	INA	1	ppm
Iron	Fe	INA/ICP	0.02/0.01	%
Lanthanum	La	INA/ICP	0.5/0.5	ppm
Lead	Pb	ICP	0.01	ppm
Lutetium	Lu	INA	0.05	ppm
Magnesium	Mg	ICP	0.01	%
Manganese	Mn	ICP	1	ppm
Mercury	Hg	INA/ICP	10/5	ppm
Molybdenum	Mo	INA/ICP	1.0/0.01	ppm
Neodymium	Nd	INA	5	ppm
Nickel	Ni	INA/ICP	20/0.1	ppm
Phosphorus	P	ICP	0.001	%
Potassium	K	ICP	0.01	%
Rubidium	Rb	INA	15	ppm
Samarium	Sm	INA	0.1	ppm
Scandium	Sc	INA/ICP	0.1/0.1	ppm
Selenium	Se	INA/ICP	3/0.1	ppm
Silver	Ag	INA/ICP	5/2	ppb
Sodium	Na	INA/ICP	0.01/0.001	%
Strontium	Sr	ICP	0.5	ppm
Sulphur	S	ICP	0.02	%
Tantalum	Ta	INA	0.5	ppm
Tellurium	Te	ICP	0.02	ppm
Terbium	Tb	INA	0.5	ppm
Thallium	Tl	ICP	0.02	ppm
Thorium	Th	INA/ICP	0.2/0.1	ppm
Titanium	Ti	ICP	0.001	%
Tungsten	W	INA/ICP	1/0.2	ppm
Uranium	U	INA/ICP	0.5/0.1	ppm
Vanadium	V	ICP	2	ppm
Ytterbium	Yb	INA	0.2	ppm
Zinc	Zn	INA/ICP	50/0.1	ppm

the Provincial government's Corporate Resource Inventory Initiative (CRII), these surveys are part of the Ministry of Energy and Mines' contribution to the North Coast Land Resource Planning process. Although this survey did not cover a complete map sheet the sampling and analyses were carried out to RGS standards and the data will be incorporated into the provincial RGS database as well as surveys of adjacent areas. Results are expected to be published in 2001.

REFERENCES

Jackaman, W. (in preparation): British Columbia Regional Geochemical Survey - Quesnel (93B), *B.C. Ministry of Energy and Mines*, BC RGS 54.

Jackaman, W. (2000): British Columbia Regional Geochemical Survey - Atlin (104N), *B.C. Ministry of Energy and Mines*, BC RGS 51.

Jackaman, W. (2000): British Columbia Regional Geochemical Survey - Jennings River (104O), *B.C. Ministry of Energy and Mines*, BC RGS 52.

Jackaman, W. (2000): British Columbia Regional Geochemical Survey - McDame (104P), *B.C. Ministry of Energy and Mines*, BC RGS 53.

Barkerville Project: Regional Till Geochemistry (93H/4, 5) and Orientation (93A/14) Studies

Ahren Bichler[1] and Peter T. Bobrowsky[2]

KEYWORDS: Till geochemistry, orientation studies, Barkerville Terrane, Slide Mountain Terrane, Cariboo Terrane, Quesnel Terrane, surficial geology, Quaternary, ice-flow, glaciation, mineral exploration, drift prospecting, Ancient Pacific Margin, Ace, VMS, NATMAP.

INTRODUCTION

During the 2000 field season, both regional and detailed till sampling surveys were conducted in the Cariboo region of central British Columbia (Figure 1). These surveys complement the longer term objectives of the NATMAP Ancient Pacific Margin (APM) project (see Nelson, 2000) and provide continuity to the surficial till geochemistry work initiated by Dixon-Warren and Hickin (2000) in 1999 as part of the APM project team. The regional till survey discussed here, represents work in the first of a multi-year, integrated exploration program, hereafter called the Barkerville Project. The Barkerville Project follows a series of previous integrated or focused multi-year Geological Survey Branch initiatives completed throughout the province in areas of high mineral potential (e.g. Northern Vancouver Island 1991-1994; Kerr *et al*., 1992; Bobrowsky and Sibbick, 1996; Nechako/Fraser Plateaus 1991-1995; Levson and Giles, 1997; Eagle Bay 1996-1998; Bobrowsky *et al*., 1997; Dixon-Warren *et al*., 1997; Paulen *et al*., 1998, 1999). In contrast, the Ace Project is a detailed till orientation study, also located in the Cariboo region, that complements previous orientation and property-scale surveys completed in the province which aim to model site specific behaviour of elements in different types of media (*e.g*. Cook and Pass, 2000).

The Barkerville Project is centred primarily over rocks of the Barkerville and Slide Mountain terranes (Figure 2). This first year of work evaluated till geochemistry in the southern half of NTS map sheet 93H/05 (Stony Lake) and the northern half of 93H/04 (Wells), located directly north of the town of Wells (Figure 1). The study covers an area of approximately 1000 square kilometers. A number of factors provide the impetus for this project area: 1) the high mineral potential of the terranes for lode

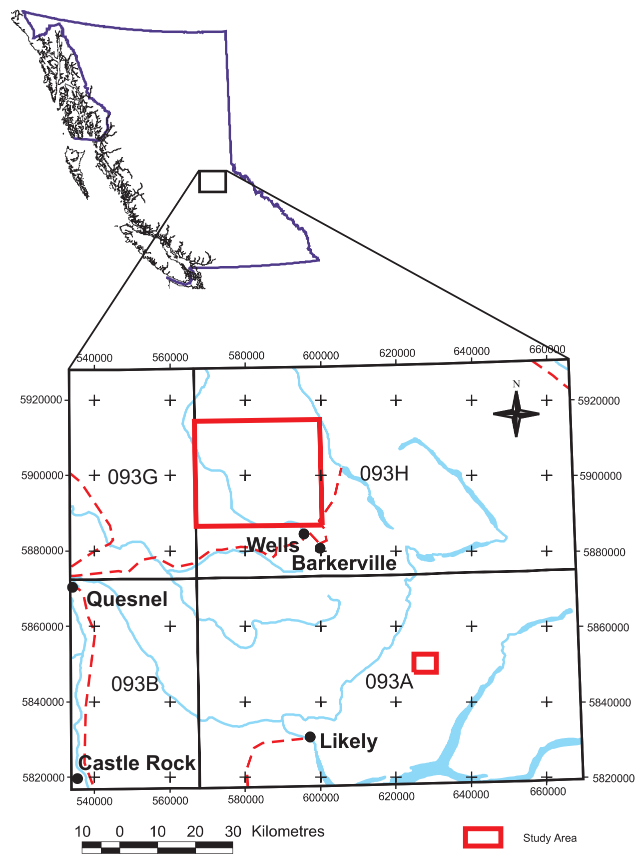

Figure 1. Location of study area for both the Barkerville (large square) and Ace (small square) Projects in the Cariboo region of British Columbia.

gold mineralization and placers; 2) the previous successful industry record for locating new showings using till geochemistry farther south in Eagle Bay rocks (also Barkerville Terrane); and, 3) the increasing industry exploration activity and the need for this type of data in the Cariboo region. In the past, placer and lode gold deposits supported the local mining industry in the region, but with the more recent realization of VMS potential, exciting new mineral prospects including the Lottie, Frank Creek and the Bonanza Ledge Zone have come to light. The primary purpose of the multi-year survey is to provide reconnaissance level till geochemistry data and re-

[1] *University of Victoria*

[2] *British Columbia Ministry of Energy and Mines*

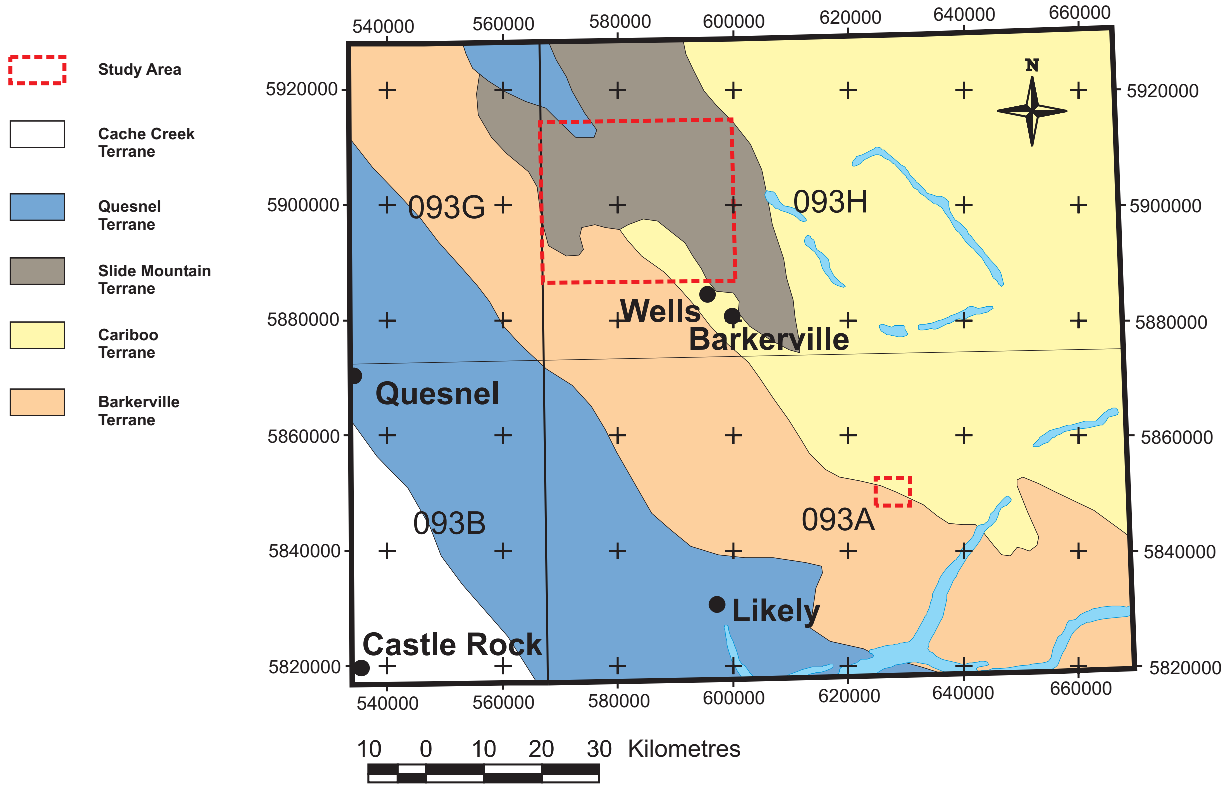

Figure 2. Generalized bedrock geology map showing the distribution of terranes in the vicinity of the Barkerville and Ace Project areas.

gional ice flow pattern information to industry clients as an incentive for further exploration.

The Ace Project is located within NTS map sheet 93A/14 (Caribou Lake) (Figure 1) and covers approximately 30 square kilometers on claims owned by Barker Minerals Ltd. This particular area has been shown to contain abundant mineralized type float thought to be the source of anomalous magnetic and soil survey results (personal communication, Louis Doyle 2000). Speculation thus far suggests that the float and soil data are possibly linked to massive sulphides and gold-quartz veining (MINFILE 093A 142 Ace) located to the northwest. The purpose of this orientation study is to evaluate and model the pattern and behaviour of geochemical dispersion in the vicinity of the anomalous zone. Multi-year, related bedrock mapping and mineral deposit studies are also currently being conducted by other staff in the GSB (*see* Ferri 2001; Ray *et al*., 2001; both in this volume).

The thick cover of surficial sediments in both study areas has hampered the use of more traditional geochemical exploration techniques making both ideal locations for the implementation of a till geochemistry program. The following objectives provide the direction for the Cariboo region projects:

- To further stimulate exploration and economic activity in the Cariboo Mining Division.
- To generate a regional pattern of till geochemistry data to define new anomalies and assist in the discovery of new mineralization.
- To assist the exploration community by demonstrating the use of till geochemistry as a more effective exploration tool in areas of thick overburden compared to conventional geochemical surveys.
- To map ice flow indicators and discern both regional and local ice flow patterns to aid drift prospecting.
- To document the dispersal of pathfinder elements down-ice from known sources of mineralization.
- To further expand the use of drift prospecting as both a reconnaissance and property-scale exploration technique.

This paper summarizes the surficial geology work that was conducted during the 2000 field season and provides background information for industry to use in concert with the final till geochemistry data. Analytical results from the till geochemical sampling program are pending and will be released separately as a GSB Open File.

PHYSIOGRAPHY, CLIMATE AND VEGETATION

Both studies occur within the Interior Plateau physiographic region. The Interior Plateau, in turn, is divided into seven subdivisions, two of which, the Fraser Plateau and the Quesnel Highlands intersect the two project studies. The Ace Project is found entirely within the Quesnel Highlands.

The Quesnel Highlands are situated on the eastern boundary of the Interior Plateau and lie to the west of the Cariboo Mountains (Photo 1). They are bounded to the north and west by the Fraser Plateau and to the south by the Shuswap Highlands. The highlands were once plateaus of moderate relief and have since been dissected, leaving upland regions that rise from approximately 1600 metres asl in the west to 2100 metres asl in the east (Photo 2) (Holland, 1976). The distinction between the Fraser Plateau and the Quesnel Highlands is an arbitrary one, as there is no visible boundary that can be discerned (Holland, 1976). The eastward rise of the dissected Fraser Plateau continues within the Quesnel Highlands.

The highest peak in the Barkerville study area is Two Sisters Mountain, rising to about 2100 metres asl. The lowest elevation is approximately 980 metres asl, in the Willow River Valley. Throughout, the landscape shows abundant evidence of previous glaciations and post-glacial erosion. In contrast, sampling at the Ace Project was concentrated on a glaciated northeast-facing valley slope that rises from 900 to 1920 metres asl.

Both study areas occur mainly within the Sub-Boreal Spruce(SBS) Zone, with minor parts in the Engelmann Spruce-Subalpine Fir (ESSF) Zone. Extending from the valley bottoms up to 1300 metres, the SBS zone is dominated by white spruce and sub-alpine fir with Douglas fir, lodgepole pine and aspen also common (Meidinger and Pojar, 1991). Luvisolic, podzolic and brunisolic soils are typical. Above 1300 metres the Engelmann Spruce-Subalpine Fir Zone is encountered and is dominated by these two species. The climate in the region is characterized by seasonal extremes. Severe snowy winters contrast to relatively warm, moist and short summers with a moderate annual rainfall (Meidinger and Pojar, 1991).

BEDROCK GEOLOGY

The regional bedrock geology of the Cariboo region has been described by Holland (1954), Sutherland Brown (1957, 1963), Tipper (1959, 1961), Campbell *et al*. (1973), Campbell (1978), Struik (1986, 1988), Bloodgood (1989), Panteleyev and Hancock (1989) and more recently Ferri *et al*. (1997), Ferri and Höy (1998a; 1998b) and Ferri (2001; this volume).

Both project areas lie on the western edge of the Omineca tectonic belt, where it abuts the Intermontane Belt. Within the regional project area, there are four terrane units represented: the Cariboo, Slide Mountain, Barkerville and Quesnel terranes. The detailed project area occurs over the Cariboo and Barkerville terranes.

Rocks of the Slide Mountain Terrane underlie the majority of the Barkerville Project area, (~75 per cent),

Photo 1. View from Two Sisters Mountain to the east of the Cariboo Mountains. During the peak of the Fraser Glaciation, thick ice would have advanced westwards from this region overriding the Quesnel Highlands.

Photo 2. View northeast from Slide Mountain showing typical relief in the Quesnel Highlands.

and are found in the eastern and northern portions of the region (Figure 2). Slide Mountain rocks are Mississippian to Permian in age and are characterized by oceanic marginal basin volcanic and sedimentary rocks. The dominant rock types are basalts and chert pelite sequences with some intruded diorite, gabbro and ultramafic rocks. The Slide Mountain Terrane is internally imbricated by small thrust faults, but as a whole, the terrane is thrust on top of the Cariboo and Barkerville terranes along the Pundata Thrust Fault (Struik, 1986, 1988).

The Barkerville Terrane makes up the next largest portion of the study area, comprising some 15 per cent of the area (Figure 2). The terrane is Precambrian to Palaeozoic in age and is an assemblage of pericratonic marine clastic and volcanic rocks, as well as their metamorphic equivalents. Typical rocks of this terrane consist of siliceous argillite, chert and quartzite. In this area, the Barkerville Terrane is generally considered to be the most metamorphosed of the four terranes represented. The Barkerville Terrane is recognized as the northern extension of the Kootenay Terrane found in south-central British Columbia (Struik, 1986, 1988). The northwest trending Pleasant Valley Fault separates the Barkerville and Cariboo terranes.

The remainder of the regional study area is underlain by rocks of the Cariboo and Quesnel terranes and comprise some 10 per cent of the area (9 per cent and 1 per cent; respectively). Cariboo rocks are Precambrian to Permo-Triassic in age, whereas the younger Quesnel Terrane is upper Triassic to lower Jurassic. Rocks of the Cariboo Terrane are found in the south-central portion of the study area and are characterized by clastic sedimentary rocks of an ancient passive continental margin typified by siltstone, sandstone, chert and shale. This differs markedly from the rocks of the Quesnel Terrane, to the north-west (Figure 2), which are related to a volcanic arc origin; primarily andesite, dacite, rhyolite, shale and siltstone.

As previously noted, only the Barkerville and the Cariboo terranes are found within the Ace project area where they are relatively equally distributed. At this location, rocks of the Cariboo Terrane can be found to the northeast, whereas Barkerville rocks occur to the southwest.

MINERAL EXPLORATION

Historically, the Cariboo Mining Division has been a "hotspot" for placer mining and continues to be so today. Within the Barkerville regional study, there are 185 placer claims (Figure 3; Table 1) as of June 2000. Similarly, a total of 181 mineral claims were registered, accounting for ~21 per cent of the area investigated in this project (Figure 3).

Both mineral occurrences (MINFILE) and assessment report (ARIS) sites are shown on Figure 4. As of this report, there are a total of 21 mineral occurrences that fall within the current Barkerville Project boundaries (Table 2), six of which are mineral showings. Table 2 shows the distribution of mineral occurrences based on the highest ranked mineral commodity; gold being the most common represented in 19 sites. Notable gold occurrences within the Barkerville Terrane include Mosquito Creek, Island Mountain, Cariboo Gold Quartz, Cariboo Hudson as well as the Snowshoe and Midas veins (Struik, 1986, 1988). Similarly, silver, tungsten, lead, zinc and copper have also been documented in this region. Proportionately, the Slide Mountain Terrane has been less successful in the past, yielding only one minor copper occurrence (Struik, 1986, 1988).

Of the 57 assessment reports filed within the Barkerville Project area, 11 were completed in the 1990s, whereas the majority (44) were completed in the 1980's (Table 3). Previous to 1980, only two assessment reports were filed in this area. During 2000, the region has experienced a revival in exploration with major projects from companies such as Hudson Bay Mining and Smelting Co. and International Wayside Ltd.

QUATERNARY HISTORY

The Cariboo region contains abundant evidence resulting from at least two episodes of glaciation during the Pleistocene: the penultimate glaciation and the Fraser Glaciation. During these two events, glaciers generally flowed eastward from the Coast Mountains and westward

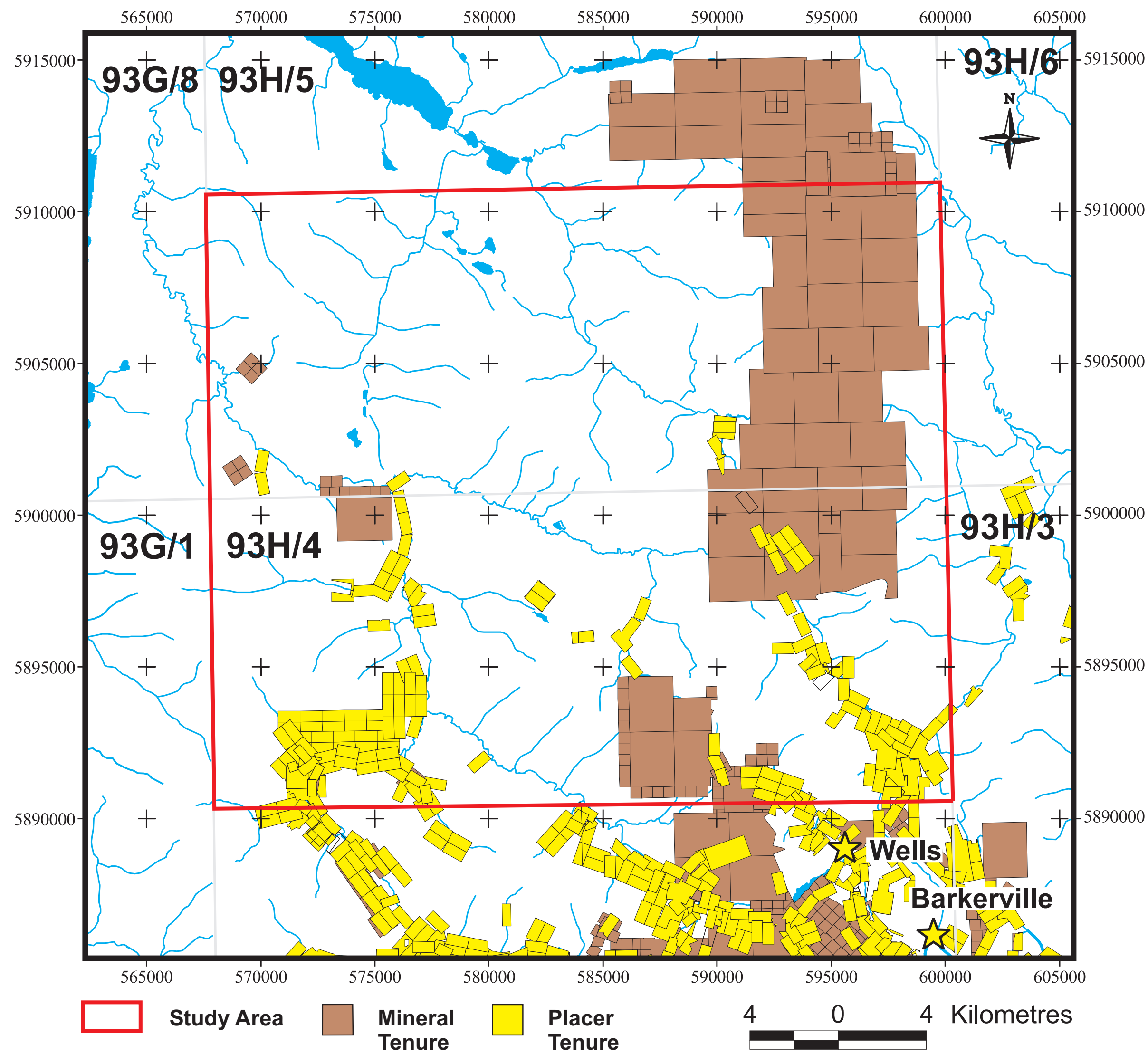

Figure 3. Distribution of mineral and placer claims within the Barkerville study area (summer of 2000 data).

TABLE 1
NUMBER OF MINERAL OCCURRENCES, ASSESSMENT REPORTS AND MINERAL AND PLACER CLAIMS FOR THE BARKERVILLE PROJECT AREA

	Count
Minfile	21
ARIS	57
Claims (Mineral)	181
Claims (Placer)	185

TABLE 2
MINERAL OCCURRENCES FOR THE BARKERVILLE PROJECT AREA, BASED ON THEIR HIGHEST RANKED MINERAL COMMODITY

Commodity	No. of Occurrences
Gold	19
Lead	6
Silver	3
Zinc	4

from the Cariboo Mountains to coalesce over the Interior Plateau (Tipper, 1971; Fulton, 1991).

Tertiary deposits consisting of broad, stable, gravel fluvial deposits are exposed primarily in deeply incised river valleys (Levson and Giles, 1993). Such deposits are often gold bearing and have been a major focus of activity for the placer industry in the area.

Overlying the Tertiary fluvial deposits are younger glaciofluvial and glacial sediments. Most deposits of this age consist of massive and stratified silt, sand and gravel occasionally intercalated with till. Though very rare, the oldest till deposits are from the penultimate glaciation, and are likely pre-Late Wisconsinan in age (Clague, 1988; Levson and Giles, 1993). Such deposits are described as units of diamicton separated by thin sand and gravel beds (Clague, 1988; Clague, 1991). The presence of striated and faceted stones, the texture, and the fabric of the diamictons suggest that in most cases, these are in fact

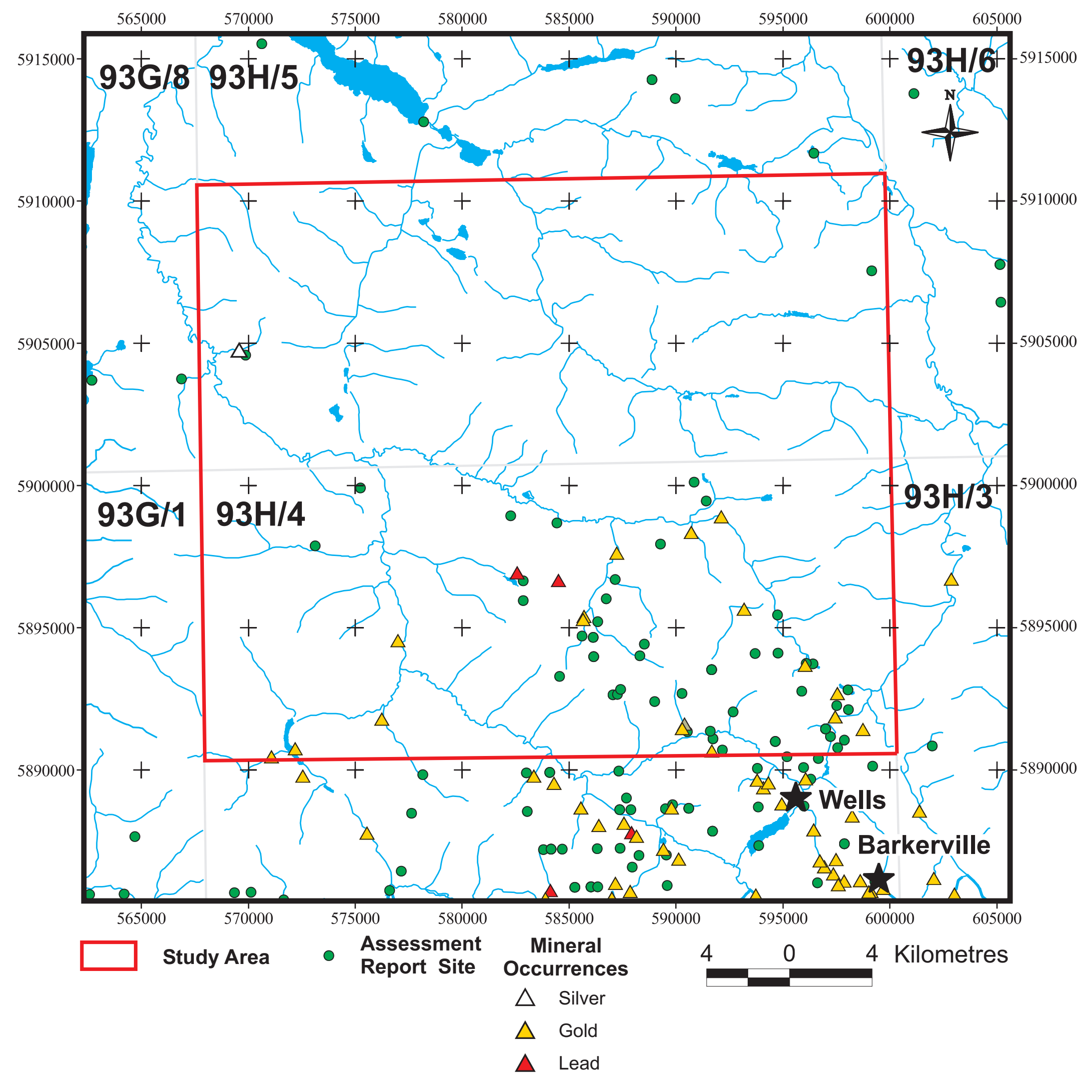

Figure 4. Distribution of exploration assessment report sites and mineral occurrences within the Barkerville study area.

TABLE 3
ASSESSMENT REPORTS WITHIN THE BARKERVILLE PROJECT AREA
(REPORTS ARE GROUPED ACCORDING TO THE YEAR IN WHICH THEY WERE FILED)

Year	Count
1990-1999	11
1980-1989	44
1970-1979	1
<1970	1

tills. No concrete dates have been assigned to this older till unit as they are beyond the limits of radiocarbon dating.

Once the glaciers of the penultimate glaciation had receded, the region remained ice-free from about 51,000 to 40,000 years ago (Clague *et al*., 1990). During this time interval, valleys were incised by ancestral rivers to levels similar to present (Clague, 1991). Following this erosional phase, the deposition of thick units of fluvial and lacustrine sediments directly preceded the Fraser Glaciation.

Evidence for the last glacial advance, the Fraser Glaciation (Late Wisconsinan), is much more pronounced. Glaciers advancing from the Cariboo Mountains, in the east, deposited thick layers of glacial, glaciofluvial and glaciolacustrine sediments over the landscape. This last event contributed most of the landforms presently observed, including U-shaped valleys, terraces, eskers, drumlins, roche moutonnées and whale backs throughout the region.

METHODS

The 2000 field season was divided into two separate field camps. The first, based out of the Barker Minerals Ltd. field camp in the township of Likely, provided access to the Ace Project to the east, where a property-scale till geochemistry orientation program was conducted. The second camp, based out of the Hudson Bay Mining and Smelting Co. field camp in Wells, provided access for the regional till geochemistry sampling program to the north.

Within the regional study area, road coverage is extensive and is serviced by a good network of major logging roads. Active logging in several of the valleys has resulted in regular road maintenance, thereby leaving the roads in relatively good condition. Secondary roads vary in their condition, ranging from excellent to unusable. Some areas proved to be inaccessible except by foot. Most of the fieldwork was conducted using 4-wheel drive vehicles. In extreme cases, where roads were impassable with 4-wheel drive vehicles, all-terrain vehicles were used.

In the vicinity of the Ace project, road access is generally less favourable, but given the objectives of the orientation study and its small area, road coverage proved adequate. Here, the bulk of the sampling was conducted on main access roads that are in relatively good condition and can be driven using a 2 or 4-wheel drive vehicles.

Prior to field work, maps of the study area were compiled using GIS software. Data collected were based on digital TRIM II maps as reference. Information on road access was obtained from Ministry of Forests and West Timber Fraser Ltd., and geological data were provided by Hudson Bay Mining and Smelting Co. (for the Barkerville Project) and from Barker Minerals Ltd. (for the Ace Project). Vertical aerial photographs of the region were also assembled to assist in both navigation and landform interpretation.

For each field station, including geological stops where no till samples were collected, the following data were collected for the site: UTM location; general geomorphology; terrain polygon unit; average slope; orientation of streamlined landforms, striations and grooves; description of bedrock; elevations of post-glacial deposits; and active geological processes.

For the regional till survey, bulk sediment samples for geochemical analysis were collected throughout the study area to generate a sampling density of approximately one sample per 2-3 square kilometres. Sampling was directed, where possible, towards unweathered, C-horizon basal till. This preferred media represents a first derivative product of glacial deposition (as per Shilts, 1993). Basal till was sampled at maximum depth, utilizing natural exposures and hand excavations (Photo 3). Where basal till was unobtainable, ablation till and colluviated till were collected.

At each till sample site, the following information was recorded: type of exposure (gully, road cut, etc.); depth to sample from surface; total thickness of exposure; stratigraphy and thickness of units within exposure; internal structures; clast percentage, angularity, and size; clast lithology; matrix or clast supported diamicton; matrix texture and colour; consolidation; and geologic interpretation (whether the material being sampled was a basal till, ablation till or colluviated till).

Sampling during the Ace Project varied slightly from the above-described method. In this case, a higher sampling density was used over most of the area, with horizontal sampling intervals every 150 to 200 metres along the main roads. At each sampling station, a small back-hoe excavator was used to create a trench approximately one meter wide and several metres deep (Photo 4). Within each trench, a B-horizon, BC-horizon and a C-horizon sample was collected. The sedimentology and stratigraphy of each sampling trench was described.

Once collected, labeled and recorded, samples were shipped to Bondar Clegg Laboratories in North Vancouver for sample preparation. Samples were first air dried and then split and sieved to <63 m. The unsieved split sample, along with the pulps and <63 m samples were then returned to the GSB. The <63 m fraction was then split, with one part subjected to aqua regia digestion and analysed for 30 elements by ICP (inductively coupled plasma emission spectroscopy) and for major oxides by

Photo 3. Hand excavated till pit in the Barkerville Project area, exposing basal till at a road cut.

Photo 4. Till trench excavated using a small back-hoe alongside a road as part of the Ace Project. Trenches were up to a metre wide and up to three metres deep, thereby allowing for samples to be collected from various depths in the sediment profile.

$LiBO_2$ fusion – ICP (11 oxides, loss on ignition and 7 minor elements). The other portion was submitted for INA (thermal neutron activation analysis) for 35 elements.

RESULTS

A total of 368 bulk sediment samples were collected during the regional till geochemistry Barkerville Project, including 42 duplicate samples for quality control. This results in 326 unique sample sites within the full 1:50,000 area, thus yielding a sampling density of ~1 sample per 2.86 km^2 (Figure 5). Table 4 shows the distribution of sample media types collected. Of the 326 samples, 290 represent basal till and account for 89 per cent of the suite, 30 samples (9 per cent) were colluviated till and six samples (2 per cent) were ablation till. Although not as reliable, the 36 non-basal till samples, are still useful for the regional exploration program, but require additional effort in their interpretation. More importantly, was the occurrence of mineralized float at a number of locations scattered over the project area. Although geochemical data have yet to be generated, it is anticipated that exceptional values of several key indicator elements will correspond to the mineralization observed in exposures.

Figure 6 shows the distribution of till samples for the Ace Project. A total of 202 samples were collected in this case, including 22 duplicates. Table 5 summarizes the distribution of sample types, as well as the average depth for each within the suite of 180 non-duplicate samples. At each of the 54 sampling stations, trenches were excavated and samples collected with increasing depth: one sample was taken from the B-soil horizon; one deep within the C-horizon; and one sample in between, either as a shallow C or a BC-horizon. At stations where interval samples were not collected, only C-horizon till samples were ob-

TABLE 4
SAMPLE MEDIUM DISTRIBUTION FOR BARKERVILLE PROJECT

Till Type	No. of Samples	Per cent
Ablation	6	2
Basal	290	89
Colluviated	30	9
Total	326	100

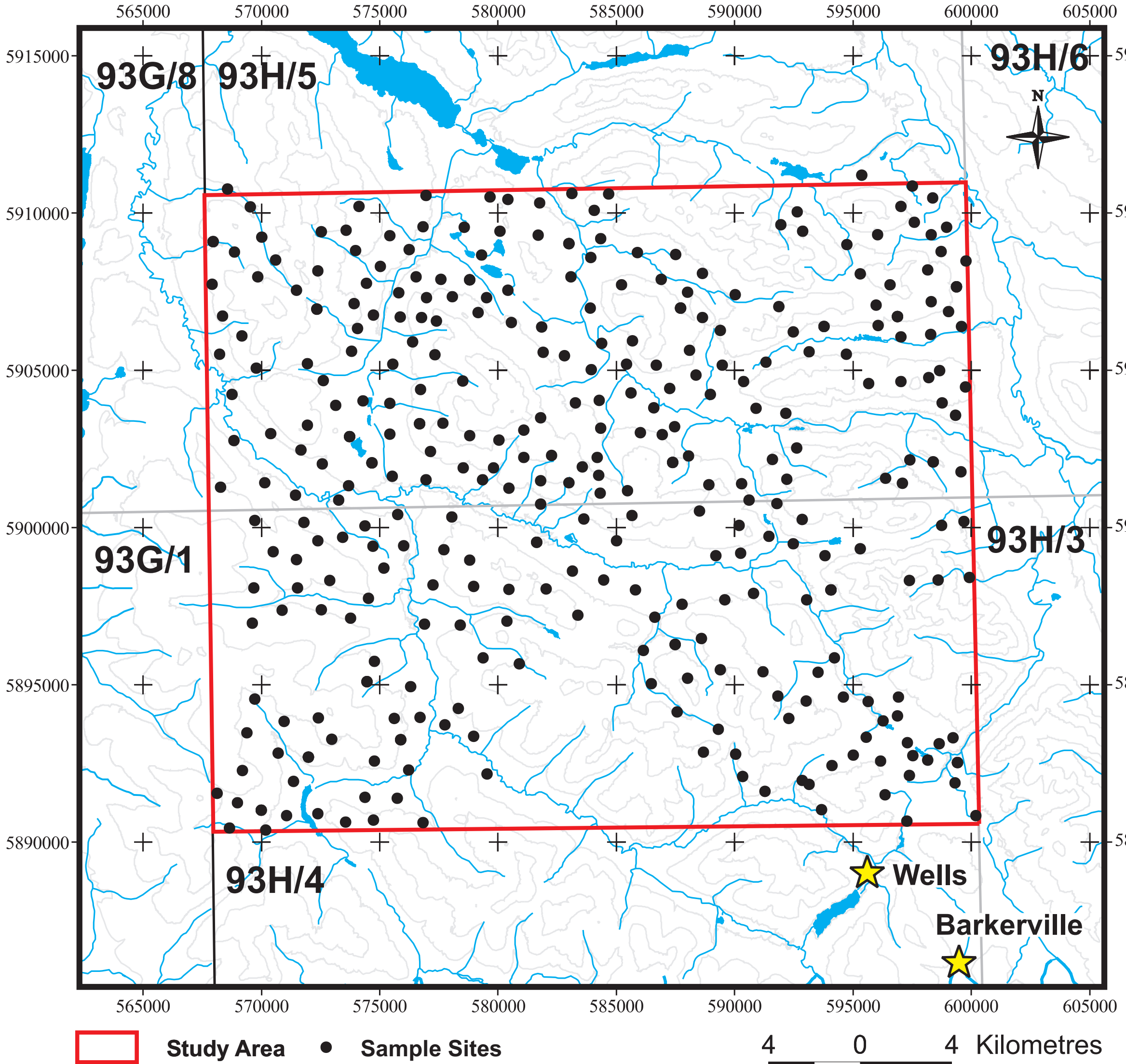

Figure 5. Till geochemistry sample distribution within the Barkerville Project area. There are 326 sample sites that yield a sampling density of approximately one sample per 2.86 square kilometres.

tained. All geochemical samples are currently being analyzed and the final results will appear in a separate publication.

During the regional till survey, a number of ice flow directional indicator features were also encountered and studied (Figure 7). This involved mainly small scale and intermediate scale erosional forms. Most ice flow evidence was derived from the measurement of striations and rat tails, although grooves and gouges also figured prominently (Photos 5 and 6). Minor directional data were collected in the field from roche moutonnées, whale backs, rock drumlins and crag and tail features. All of the evidence compiled thus far comes from the northern half of the regional study area (93H/5 south half). Documented ice flow direction is quite variable, ranging through most cardinal directions. One unique pattern is the unequivocal evidence for flow toward the east in the centre part of the map sheet. A number of sites confirm this ice flow direction. This pattern alone is remarkable given the close proximity of the study area to the mountains located farther east. In this area, one would expect that westward flowing ice from the Cariboo Mountains would have over-shadowed any eastward flowing interior ice. The full appreciation and interpretation of the multiple ice flow directions have yet to be reconciled, however, the implications are significant. Back calculation of ice flow direction is usually a simple up-ice effort. Here, cross-cutting striations over such a broad area will require site specific interpretations when tracing anomalous geochemical results.

A variety of different surficial sediment types were observed in the Barkerville Project area. Till (basal till and less commonly ablation till), colluvial, fluvial, glaciofluvial, glaciolacustrine, organic and anthropogenic sediments are common. In general, fluvial, glaciofluvial and glaciolacustrine sediments are

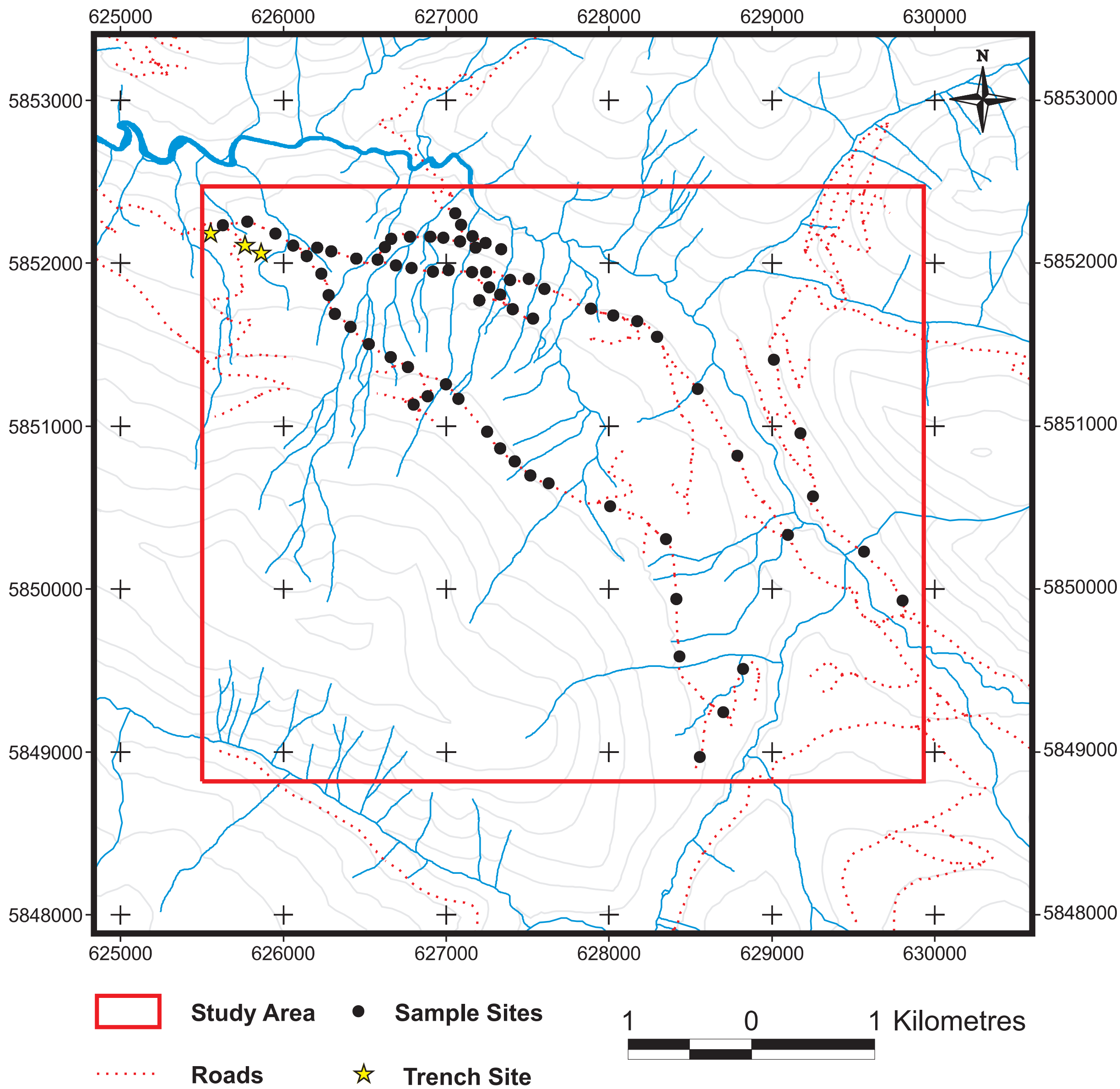

Figure 6. Till geochemistry sample distribution within the Ace Project area. Samples were collected from back-hoe trenches located along roads in an up-ice direction to the mineralized exploration trenches (indicated by stars on the map).

TABLE 5
SAMPLE MEDIUM DISTRIBUTION AND CORRESPONDING AVERAGE SAMPLE DEPTH

Sample Medium	No. of Samples	Per cent	Average Depth (m)
B Soil	55	31	0.27
B-C Soil	26	14	0.64
C Till	99	55	1.38
Total	180	100	

found in the bottom of valleys to elevations of about 1050 metres above sea level. Underlying these sediments at depth, deposits of till and other materials are occasionally present. Above this elevation, ground moraine dominates except where slopes are steep in which case colluvium occurs. Sediments disturbed or derived by anthropogenic activities are found in and around communities, along roads and, in particular, within surface workings such as placer mines. Organic deposits occur locally in all types of terrain.

Basal till deposits are characterized as being very poorly-sorted, matrix-supported diamictons (Photo 7). They occur throughout the study area as variably thick veneers (<1 metre) to blankets (>8 metres) that are primarily massive, although some minor stratification was ob-

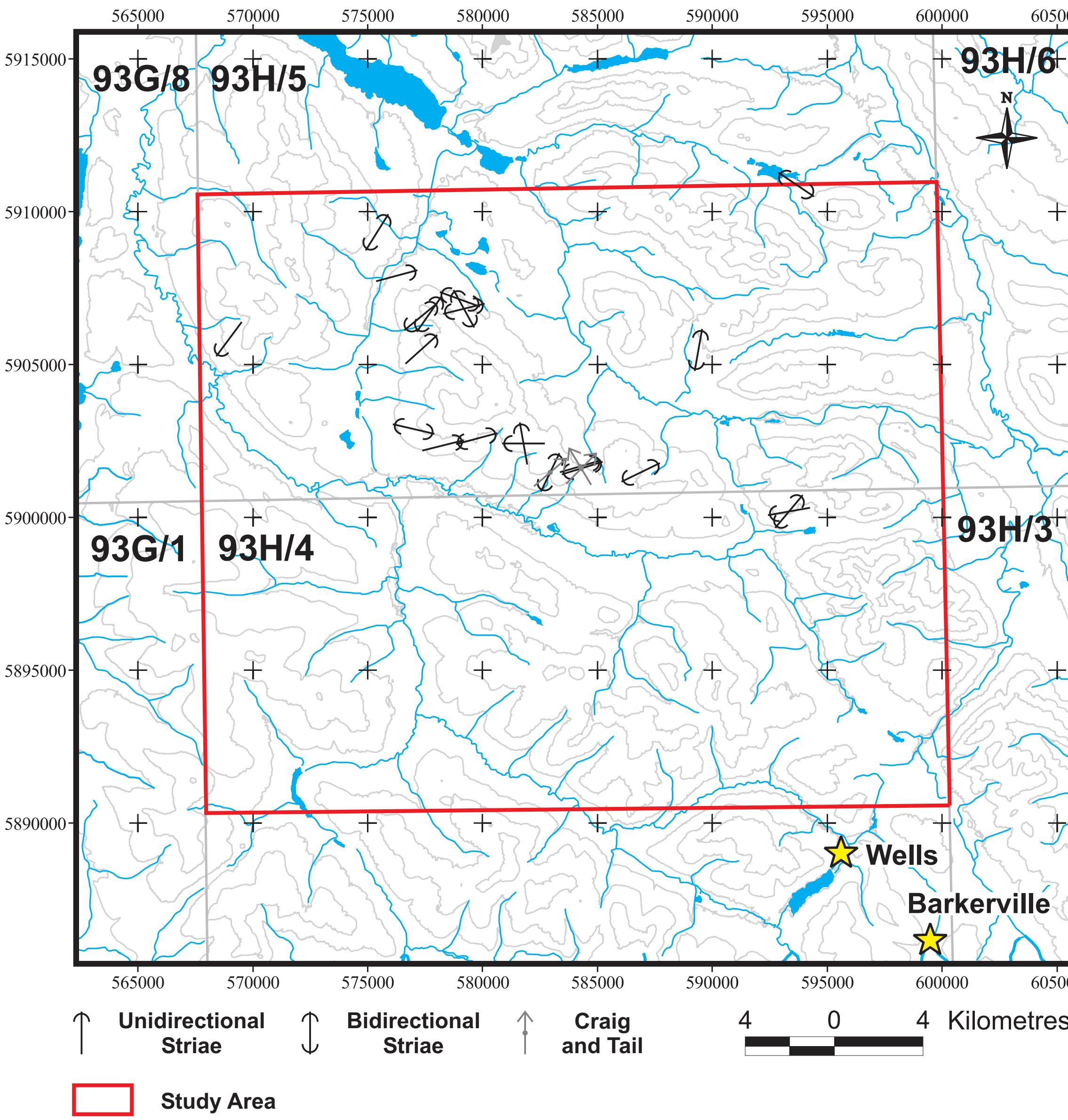

Figure 7. Ice flow map for the Barkerville study area.

served. The tills are moderately to highly consolidated and cohesive. The matrix is generally an olive grey or olive brown colour and has a clayey-silt to silty-sand texture. Clast percentages within the basal till range from 5 to 45 per cent averaging 26 per cent. Clast size ranges from granular to >2 metres with an average of about 1.7 centimetres. The clasts in till are primarily subrounded to subangular in shape and often have faceted and/or striated surfaces.

Deposits of ablation till are massive to crudely-stratified diamictons often occurring as veneers overlying deposits of basal till or bedrock. Such deposits are generally less consolidated compared to a typical basal till accumulation (moderately compact and cohesive). The matrix is also sandier than that of a basal till. The ablation tills sampled have a range of clast percentage from 20 to 70 per cent; averaging 39 per cent. Clast size ranges from granular to ~60 centimetres with a mean of about 4.0 centimetres. The shape of clasts ranges from very angular to subrounded and shows less faceting and striations than those found in a basal till.

As noted earlier, other sediment types were also observed in the two study areas, and their characteristics were noted. However, given that they play no role in our till geochemistry survey, we do not describe their attributes and distribution in this paper.

SUMMARY

During the 2000 field season, two drift prospecting projects were successfully completed in the Cariboo

Photo 5. Striated and grooved bedrock surface found in the north-western part of the Barkerville study area. Ice is interpreted to have flowed from the southwest towards the northeast at this site.

Photo 6. Bullet-shaped boulder found within basal till. The photo was taken from a perspective of looking obliquely down onto the boulder. Ice flow is interpreted as coming out of the page towards the viewer.

Mining Division. The first was a regional study that focused on collecting bulk till samples for geochemical analysis over the Barkerville and Slide Mountain terranes in the vicinity of Wells. This project covered half of two 1:50,000 NTS map sheets with a total of 326 sampling sites. The second project was a detailed orientation program, conducted within an area of known mineral potential near Likely. As part of this latter project, 180 samples were collected from 70 sampling sites. All samples are currently in the process of being analyzed and their results will be published separately at a later date.

The most important implications of the till geochemistry work accomplished to date include:

- the significant mineral potential of the region has been confirmed through our work;
- basal till is a common surficial deposit type in the region and is ideally suited for geochemical drift prospecting;
- evidence for multiple ice flow directions requires additional work for resolution to a satisfactory level that industry can use;
- mineralized float was encountered in a number of locations in the study region;
- significant areas of high mineral potential remain unstaked.

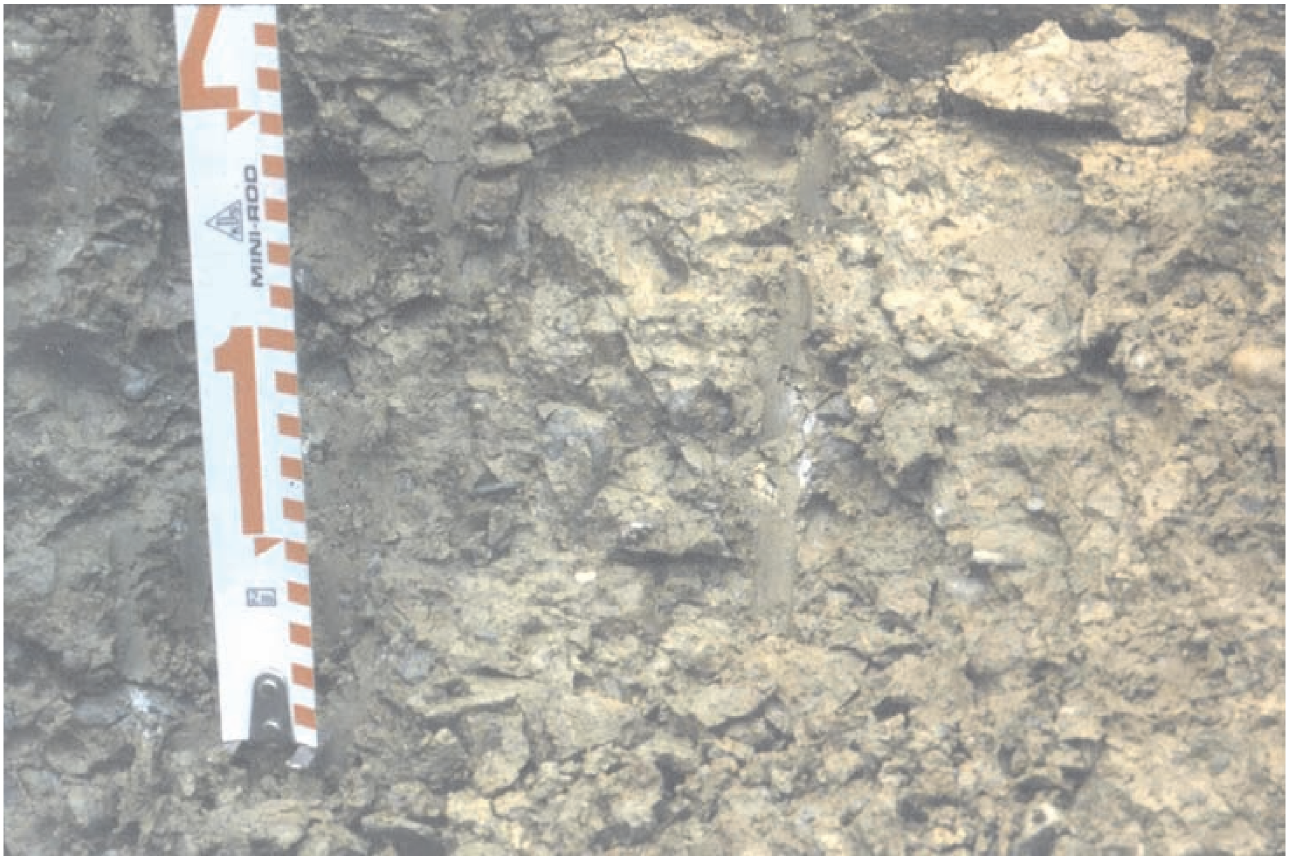

Photo 7. Example of a poorly sorted, basal lodgement till that contains ~15% clasts and has a fine sand, silty matrix. Note the strongly fissile texture.

ACKNOWLEDGMENTS

This work was completed as part of the British Columbia Geological Survey Branch, Barkerville and Ace Projects. We are grateful to Hudson Bay Mining and Smelting Co. and Barker Minerals Ltd., in particular Messers. Jerry Bidwell and Louis Doyle, respectively, for their hospitality and invaluable understanding into the local geology as well as their willingness to share information. We extend our thanks to the Ministry of Forests and West Fraser Timber, in particular Al Hunter, for supplying digital data for map compilation. Our thanks are also extended to the many prospectors, who were very informative and cooperative. Thanks also to students Beth Brooks, Adrian Hickin, Gloria Lopez and Roger Paulen of the GSB for assisting throughout the project above and beyond their obligations. Thanks to Ray Lett for managing till sample preparation and analysis. Gerry Ray and Fil Ferri advised us on bedrock geology. And finally thanks are also due to Ray Lett and David Lloyd for their logistic and equipment support throughout the field season. We appreciate the effort of Gib McArthur for editing an earlier version of this paper.

REFERENCES

Bloodgood, M.A. (1989): Geology of the Quesnel Terrane in the Spanish Lake Area, central British Columbia, 93A/11; *in* Geological Fieldwork 1987, *B.C. Ministry of Energy, Mines and Petroleum Resources*, Paper 1988-1, pages 139-145.

Bobrowsky, P.T. and Sibbick, S.J. (1996): Till Geochemistry of Northern Vancouver Island Area (92L/5, 6W, 11W, 12); *B.C. Ministry of Employment and Investment*, B.C. Geological Survey Branch, Open File 1996-7.

Bobrowsky, P.T., Leboe, E.R., Dixon-Warren, A. and Ledwon, A. (1997): Eagle Bay Project: Till geochemistry of the Adams Plateau (82M/4) and North Barriere Lake (82M/5) map areas; *in* Geological Fieldwork 1996, D.V. Lefebure, W.J. McMillan and G. McArthur, Editors; *B.C. Ministry of Employment and Investment*, Paper 1997-1, pages 413-421.

Campbell, R.B. (1978): Quesnel Lake 93A Map Area; *Geological Survey of Canada*, Open File 574.

Campbell, R.B., Mountjoy, E.W. and Young, F.G. (1973): Geology of the McBride map area, British Columbia; *Geological Survey of Canada*, Paper 72-35, 104 pages.

Clague, J.J. (1988): Quaternary stratigraphy and history, Quesnel, British Columbia; *Geographie physique et Quaternaire*, Volume 42, pages 279-288.

Clague, J.J. (1991): Quaternary stratigraphy and history of Quesnel and Cariboo river valleys, British Columbia: implications for placer gold exploration; *in* Current Research, Part A, *Geological Survey of Canada*, Paper 91-1A, pages 1-5.

Clague, J.J., Hebda, R.J. and Mathewes, R.W. (1990): Stratigraphy and paleoecology of Pleistocene interstadial sediments, central British Columbia; *Quaternary Research*, Volume 34, pages 208-228.

Cook, S.J. and Pass, H.E. (2000): Ancient Pacific Margin Part V: Preliminary results of geochemical studies for VMS deposits in the Big Salmon Complex, Northern British Columbia (104N/9, 16; 104O/11, 12, 13, 14); *in* Geological Fieldwork 1999*; B.C. Ministry of Energy and Mines*, Paper 2000-1, pages 71-105.

Dixon-Warren, A., Bobrowsky, P.T., Leboe, E.R. and Ledwon, A. (1997): Eagle Bay Project: Surficial geology of the Adams Plateau (82M/4) and North Barriere Lake (82M/5) map areas; *in* Geological Fieldwork 1996, D.V. Lefebure, W.J. McMillan and G. McArthur, Editors; *B.C. Ministry of Employment and Investment*, Paper 1997-1, pages 405-411.

Dixon-Warren, A. and Hickin, A. (2000): Ancient Pacific Margin NATMAP Part IV: Surficial mapping and till geochemistry in the Swift River Area, Northwestern British Columbia; *in* Geological Fieldwork 1999, *B.C. Ministry of Energy and Mines*, Paper 2000-1, pages 47-69.

Ferri, F. (2001): Geological setting of the Frank Creek massive sulphide occurrence near Cariboo Lake, east-central British Columbia (93A/11, 14); *in* Geological Fieldwork 2000, *B.C. Ministry of Energy and Mines*, this volume.

Ferri, F., Höy, T. and Friedman, R.M. (1997): Description, U-Pb age and tectonic setting of the Quesnel Lake Gneiss, east-central British Columbia; *in* Geological Fieldwork 1996, D.V. Lefebure, W.J. McMillan and G. McArthur, Editors; *B.C. Ministry of Employment and Investment*, Paper 1997-1, pages 69-80.

Ferri, F. and Höy, T. (1998a): Zn-Pb deposits in the Cariboo Subterrane, central British Columbia (93A/ NW); *in* Geological Fieldwork 1997, D.V. Lefebure and W.J. McMillan, Editors; *B.C. Ministry of Employment and Investment*, Paper 1998-1, pages 14.1-14.9.

Ferri, F. and Höy, T. (1998b): Stratabound base metal deposits of the Barkerville Subterrane, central British Columbia (093A/ NW); *in* Geological Fieldwork 1997, D.V. Lefebure and W.J. McMillan, Editors; *B.C. Ministry of Employment and Investment*, Paper 1998-1, pages 13.1-13.12.

Fulton, R.J. (1991): A conceptual model for growth and decay of the Cordilleran ice sheet; *Geographie physique et Quaternaire*, Volume 45, no. 3, pages 281-286.

Holland, S.S. (1954): Geology of the Yanks Peak-Roundtop Mountain area, Cariboo District, British Columbia; *B.C. Ministry of Energy, Mines and Petroleum Resources*, Bulletin 34, 102 pages.

Holland, S.S. (1976): Landforms of British Columbia, a physiographic outline; *B.C. Ministry of Energy, Mines and Petroleum Resources*, Bulletin 48.

Kerr, D.E., Sibbick, S.J. and Jackaman, W. (1992): Till geochemistry of the Quatsino map area (92L/12); *B.C. Ministry of Energy, Mines and Petroleum Resources*, Open File 1992-21.

Levson, V.M. and Giles, T.R. (1993): Geology of tertiary and quaternary gold-bearing placers in the Cariboo region, British Columbia (93A,B,G,H); *B.C. Ministry of Employment and Investment*, Bulletin 89, 202 pages.

Levson, V.M and Giles, T.R. (1997): Quaternary geology and till geochemistry studies in the Nechako and Fraser Plateaus, Central British Columbia (NTS 93 C/1,8,9,10; F/2,3,7; L/16; M/1); *in* Interior Plateau Geoscience Project: Summary of Geological, Geochemical and Geophysical Studies, L.J. Diakow and J.M. Newell, Editors, *B.C. Ministry of Employment and Investment*, Paper 1997-2, pages 123-146.

Meidinger, D. and Pojar, J. (1991): Ecosystems of British Columbia; *B.C. Ministry of Forests*, Special Report Series, no. 6.

Nelson, J. (2000): Ancient Pacific Margin Part I: BCGS contributions and collaborative activities with GSC and Yukon geology program; *in* Geological Fieldwork 1999; *B.C. Ministry of Energy and Mines*, pages 15-18.

Panteleyev, A. and Hancock, K. (1989): Quesnel mineral belt: Summary of the geology of the Beaver Creek- Horsefly River map area; *in* Geological Fieldwork 1988, *B.C. Ministry of Energy, Mines and Petroleum Resources*, Paper 1989-1, pages 159-165.

Paulen, R.C., Bobrowsky, P.T., Little, E.C., Prebble, A.C. and Ledwon, A. (1998): Surficial deposits in the Louis Creek and Chu Chua Creek Area; *in* Geological Fieldwork 1997, D.V. Lefebure and W.J. McMillan, Editors, *B.C. Ministry of Employment and Investment*, Paper 1998-1, pages 16.1-16.12.

Paulen, R.C., Bobrowsky, P.T., Lett, R.E., Bichler, A.J. and Wingerter, C. (1999): Till Geochemistry in the Kootenay, Slide Mountain and Quesnel Terranes; *in* Geological Fieldwork 1998, *B.C. Ministry of Employment and Investment*, Paper 1999-1, pages 307-319.

Ray, G.E., Webster, I., Lane, B., Rhys, D., Ross, K., Hall, R. and Dunne, K.P.E. (2001): Variable geochemistry of the gold mineralization in the Wells-Barkerville Camp; *in* Geological Fieldwork 2000; *B.C. Ministry of Energy and Mines*, this volume.

Shilts, W.W. (1993): Geological Survey of Canada's contributions to understanding the composition of glacial sediments; *Canadian Journal of Earth Sciences*, Volume 30, pages 333-353.

Struik, L.C. (1986): Imbricated terranes of the Cariboo Gold Belt with correlations and implications for tectonics in southeastern British Columbia; *Canadian Journal of Earth Sciences*, Volume 23, pages 1047-1061.

Struik, L.C. (1988): Structural geology of the Cariboo Gold Mining District, east-central British Columbia; *Geological Survey of Canada*, Memoir 421, 100 pages and four 1:50 000 maps.

Sutherland Brown, A. (1957): Geology of the Antler Creek area, Cariboo District, British Columbia; *B.C. Ministry of Energy, Mines and Petroleum Resources*, Bulletin 38, 105 pages.

Sutherland Brown, A. (1963): Geology of the Cariboo River area, British Columbia; *B.C. Ministry of Energy, Mines and Petroleum Resources*, Bulletin 47, pages 60.

Tipper, H.W. (1959): Geology, Quesnel, Cariboo District, British Columbia; *Geological Survey of Canada*, Map 12-1959, 1:250 000.

Tipper, H.W. (1961): Geology, Prince George, British Columbia; *Geological Survey of Canada*, Map 49-1960, 1:250 000.

Tipper, H.W. (1971): Multiple glaciations in central British Columbia; *Canadian Journal of Earth Sciences*, Volume 8, pages 743-752.

Quaternary Geology and Till Geochemistry of the Huckleberry Mine Area

By Travis Ferbey[1] and Victor M. Levson[2]

KEYWORDS: Till geochemistry, ice flow history, drift prospecting, Quaternary stratigraphy, dispersal train, basal till, copper-molybdenum porphyry, surficial geology, exploration geochemistry.

INTRODUCTION

This paper summarizes Quaternary geology and till geochemistry studies conducted as part of a detailed case study on the Huckleberry Mine area. The study was initiated as a follow up to previous research conducted in the Nechako Plateau on the Late Wisconsinan glacial history of west-central British Columbia; specifically, studies that have confirmed the westward flow of ice from the interior of British Columbia towards the Pacific Ocean (Levson *et al*., 1998; Stumpf *et al*., 2000). Building on the deposit scale study of the Nak porphyry copper prospect (MINFILE No. 093M 010) (Levson *et al*., 1997), this paper also investigates the three-dimensional geometry of dispersal plumes in till. The purpose of this study is to:

- Build on the current ice-flow model of west-central British Columbia for the Late Wisconsinan through the identification and interpretation of small and intermediate scale erosional and streamlined forms, and dispersal trains and/or plumes in till; and
- Model dispersal of mineralization in till by investigating the two and three-dimensional geometry of dispersal plumes using selected clast lithologies and trace element geochemistry.

The results of this case study will be significant to the exploration community working in west-central British Columbia, as results will provide guidance on how to interpret till geochemical data and efficiently identify the bedrock source of anomalous till samples. As well, these results will suggest strategies on design and implementation of till geochemistry programs in areas with similar physical and geological characteristics and glacial histories. On a larger scale, this work is significant as it may be useful in developing and revising conceptual models of glacial dispersal and geochemical exploration.

[1]*University of Victoria*

[2]*British Columbia Ministry of Energy and Mines*

LOCATION AND PHYSICAL SETTING

Detailed stratigraphic, sedimentologic, and geochemical studies were conducted at Huckleberry Mine (MINFILE No. 093E 037), a producing porphyry copper-molybdenum open pit mine (north half of NTS 93E/11), while glacial history and ice flow studies extended into the surrounding area (NTS 93E/10-11, 93E/14-16) (Figure 1). This area was chosen for this 3-dimensional till study because a large number of overburden drill samples had been collected by Huckleberry Mines Ltd. (HBL) on the property and the type and distribution of mineralization in bedrock at Huckleberry Mine is well understood. In addition, the area has an extensive and thick mantle of Quaternary sediments and good access.

The Huckleberry Mine area falls within the transition zone between the Nechako Plateau, to the east, and the Coast Mountains, to the west (Figure 1). This area, the Tahtsa Ranges, is a belt of mountains 16-24 kilometres wide, with the highest peak being 2431 metres; the remaining peaks typically ranging from 2100 to 2250 metres. The Tahtsa Ranges are divided into east-west trending ranges by major valleys that are occupied by large lakes (*e.g. Tahtsa, Troitsa, and Whitesail Lakes). These lakes are prominent features of the Tahtsa Ranges, and they occur at a relatively high elevations (784 to 930 metres) therefore reducing the overall relief of the area (Holland, 1976). Valley bottoms and mountain flanks are forested and have thick sequences of Quaternary sediments with little bedrock exposure, while upper slopes and peaks extend into subalpine and alpine environments.*

Huckleberry Mine is located on the north side of Tahtsa Reach, approximately 130 kilometres due south of Smithers, or approximately 120 kilometres southwest of Houston, via Forest Service and private mine roads. The minesite is located in a poorly drained, boggy, arcuate shaped valley (averaging 1015 metres elevation), adjacent to the southern flank of Huckleberry Mountain (1526 metres) (Photo 1). Huckleberry Mine is a porphyry copper-molybdenum open pit mine, with minor recoverable amounts of gold and silver, and has a production rate of 21,000 tonnes/day ore. The mine has 185 direct employees and operates year round. Huckleberry Mine began production in 1997 with an estimated mine life of 11 years (Huckleberry, 2000).

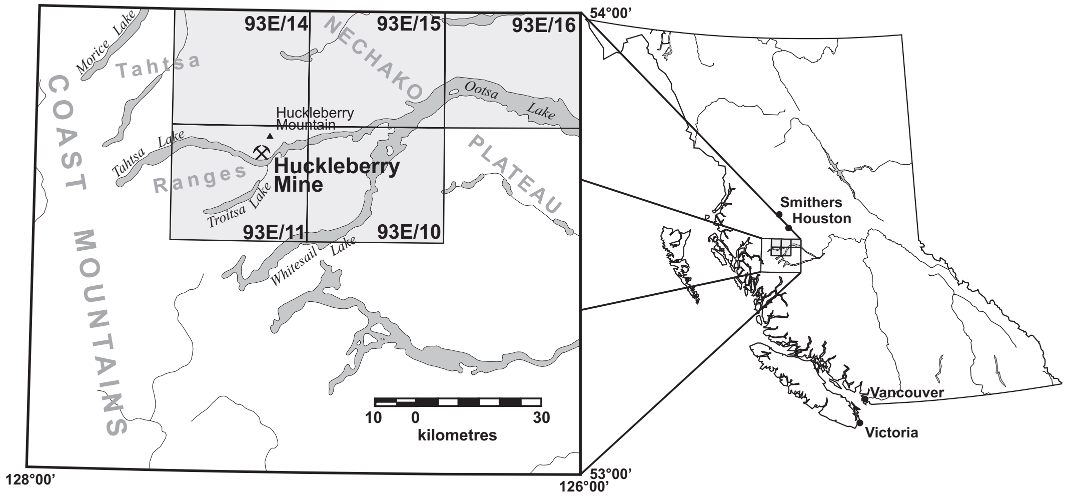

Figure 1. Study area location map.

Photo 1. Looking northeast towards Huckleberry Mine, Tahtsa Reach in foreground (photo courtesy of David Mate).

BEDROCK GEOLOGY

The study area lies just east of the Coast Crystalline Belt within the Intermontane Tectonic Belt (MacIntyre, 1985; Jackson and Illerbrun, 1995). It is underlain mainly by Early to Middle Jurassic Hazelton Group volcanic and sedimentary rocks, which are unconformably overlain by Bowser Lake sedimentary rocks of the Middle to Late Jurassic, and Early Cretaceous Skeena Group turbidites and basalt flows. These rocks are in turn unconformably overlain by Late Cretaceous Kasalka Group volcanics. Many small to medium, Late Cretaceous to Early Tertiary stocks have intruded these Jurassic and Cretaceous rocks (MacIntyre, 1985; Jackson and Illerbrun, 1995).

Underlying the Huckleberry Mine property are hornfelsed, fragmental, andesitic rocks of the Lower Jurassic Telkwa Formation, of the Hazelton Group (MacIntyre, 1985; Jackson and Illerbrun, 1995). These volcanic rocks have been intruded by two porphyritic hornblende-biotite-feldspar granodiorite stocks of the Late Cretaceous Bulkley Intrusions. Although there is copper and molybdenum mineralization within both stocks, nearly all ore mined is from the adjacent hornfelsed volcanic rocks (S. Blower, pers. comm., 2000). The Main Zone (15.6 million tonnes at 0.519% Cu) extends east from the most westerly stock into the adjacent hornfelsed volcanic rocks, while the East Zone (46.2 million tonnes at 0.488% Cu) is peripheral to the most easterly stock, within the adjacent hornfelsed volcanic rocks (Huckleberry, 2000). Mineralization is controlled both structurally and by the contact of the stocks themselves (Jackson and Illerbrun, 1995; S. Blower, pers. comm., 2000).

QUATERNARY GEOLOGY

The surficial geology of the study area was mapped by the British Columbia Ministry of Environment, Lands, and Parks (1976) at a scale of 1:50,000, while a more detailed 1:10,000 scale map of the Huckleberry Mine property was produced by New Canamin Resources (1993). In both cases, these maps are limited to the delineation and interpretation of surficial sediments only; identification and interpretation of landforms was not included. Other Quaternary geological studies have been conducted by Tipper (1994), Levson *et al.* (1998, 1999), Mate and Levson (1999), and Stumpf *et al*. (2000), but are limited to areas immediately adjacent to NTS 93E.

Surficial Geology

Detailed stratigraphic and sedimentologic studies were conducted at 12 exposures on the Huckleberry Mine property to better understand the glacial history of the area. Most Quaternary exposures studied were the result of mining and related activities (i.e. road cuts, borrow pits; see Photo 2), but also included natural gully exposures. Exposures ranged from a few to tens of metres high, with a maximum height of 27 metres, and a few to hundreds of metres long, with a maximum length of 250 metres.

The dominant surficial unit found in the study area is a massive diamict, 2.5 to 12 metres thick. It's character varies laterally and vertically, but it typically is a matrix-supported, sandy-silt, light brown to light gray, diamict. Locally the diamict is dark grey and clay-rich. It has moderately well developed vertical jointing and exhibits good sub-horizontal fissility and high density. Modal clast size is medium to large pebble, but ranges from granule up to large cobble. Clast shape is sub-angular to sub-rounded, with locally higher concentrations of angular to sub-angular clasts. Matrix percent is typically 60-80%, and striated clasts are common. Mineralized andesite and granodiorite clasts are common immediately adjacent to, and west of, the Main and East Zones; as are pyrite and chalcopyrite grains within the diamict matrix. Iron and manganese oxidation occurs mainly on joint planes, but near the surface (in the upper 1-2 metres) the entire diamict matrix is commonly oxidized. Where there is oxidation in the matrix, extreme weathering of clasts (in particular granitic lithologies) is common. Lower contacts are typically clear to diffuse, and sub-horizontal to weakly undulating. These characteristics are consistent with those of a subglacially derived diamict (Dreimanis, 1989), and this unit is therefore interpreted as a basal till (Photo 3).

In most sections, this basal till overlies polished, grooved, and striated bedrock, but locally can overlie clast-supported, matrix-filled, rounded, small to large pebble gravels, commonly with cross-bedded, fine to coarse-grained sand lenses, ranging from a few centimetres to a few metres wide, and a few centimetres to tens of centimetres high. These gravel units are up to 3 metres thick, and have sharp, trough-shaped lower contacts. They are interpreted as being glaciofluvial in origin. Basal till also locally overlies laminated silts and clays, and thinly bedded, fine to medium-grained sands, that contain numerous, small to medium pebble dropstones and deformed sedimentary structures. These silts and clays are commonly interbedded with massive, matrix supported, sandy diamict lenses, 2 to 3 metres in length, and up to 1 metre high. Lenses have sharp, small scale (5 to 30 centimetres long, 0.5 to 1 centimetre high) undulatory to trough shaped lower contacts. Silt and clay units are up to 3 metres thick, and have sharp, planar to sub-horizontal lower contacts. They are interpreted as glaciolacustrine (possibly subglacial) sediments, with interbedded subaqueous debris flow deposits. They are

Photo 2. West Borrow Pit where till was excavated for use in tailings dam construction. This Pit was one of the 12 exposures studied on the Huckleberry Mine property. Note the trucks in foreground for scale.

Photo 3. Basal till, the dominant surficial unit found in the study area, overlying mineralized volcanics within the Main Zone. The till is overconsolidated and stands vertical in excavation.

only observed in exposures in the vicinity of the East Zone.

Glacial units are typically capped on steep valley slopes by angular to subangular, medium pebble to large cobble, colluvial deposits up to 1metre thick. In valley bottom settings they commonly grade upwards into organic soils. The depth of Holocene soil development on well drained soils varies from a few tens of centimetres to about 1 metre.

Quaternary geological studies within NTS 93E, have not yet produced any sub-till radiocarbon dates. However, 100 kilometres east of the Huckleberry Mine area, on Cheslaslie Arm, organic rich sediments that underlie till have produced dates that range from approximately 27 000 to >45 000 years B.P. (Levson and Giles, 1997; Levson *et al*., 1998). As well, nonglacial sediments under till that have yielded finite radiocarbon dates occur in a number of other localities farther east in the Nechako Plateau (Plouffe and Jetté, 1997; Plouffe and Levson, 2001) and to the north in the Babine Lake area, approximately 200 kilometres north of the Huckleberry Mine area at the Bell Mine (Harington *et al.*, 1974; Levson, 2001a). The Quaternary sediments of the Huckleberry Mine area are believed to be correlative with those found in areas adjacent to NTS 93E, which overlie these dated lacustrine and organic rich deposits. The Quaternary sediments of the Huckleberry Mine area are therefore interpreted as being Late Wisconsinan to Holocene in age.

Ice Flow Indicators

Ice flow data were observed and recorded at over 130 ice flow stations. Most striated outcrops were observed in valley bottom settings along roads and shorelines along Tahtsa Reach, Tahtsa Lake and Ootsa Lake. Data were also collected at elevations over 1500 metres at six mountain peaks. Various small scale (grooves, striae, rat tails) and intermediate scale (roches moutonnées, crag and tails, flutes, and drumlins) streamlined forms, were studied to better understand the ice flow history of the Huckleberry Mine area. The distribution of selected clast lithologies in till were also investigated for this reason.

Data collected at each ice flow station included: general site description (topographic position, aspect, slope); orientation and dimensions of form; and relative degree of preservation of forms. Particular attention was given to: stoss (up-ice) and lee (down-ice) face relationships, the media the form was created and preserved in, and cross-cutting and/or superimposition relationships with other forms. These observations are important not only when interpreting ice flow direction, but in determining the timing and magnitude of multiple ice flow events. As most of these sites are in human-disturbed areas, correct identification of linear forms was important (i.e. natural or human-made). To supplement this data, air photo interpretation was ongoing while in the field.

In addition to this, fabric measurements and pebble counts were taken in undisturbed till, at Huckleberry Mine. For fabric measurements, clast shape, a-axis trend and plunge, and the presence and orientation of striae on clasts relative to a-axis orientation, were recorded. In the case of pebble counts, clasts were first categorized based on lithology and then described in terms of roundness and presence of mineralization. Stratigraphic and sedimentologic descriptions were completed at each of the fabric and pebble count sites, with particular attention given to site location relative to the Main and East Zones.

TILL GEOCHEMISTRY

To date, no till geochemistry programs have been conducted in the Huckleberry Mine area, however various other geochemical programs were completed by exploration companies. The Len Claims, now the Huckleberry Mine property, were staked in 1962 by Kennco Explorations (Western) Ltd., as a result of follow up work on anomalous stream sediment samples collected in 1960 (Jackson and Illerbrun, 1995). Shortly after staking, Hornbrook (1970) conducted a biogeochemical and geochemical prospecting program on these claims, as part of a comparative study on the effectiveness of biogeochemical surveys for detecting buried mineral deposits. Since then, three soil geochemistry surveys have been conducted on the Huckleberry Mine property as a part of advanced exploration programs (Stevenson, 1970; Bradish *et al.*, 1989; Myers and Roney, 1990). On a regional scale, the British Columbia Ministry of Energy and Mines and the Geological Survey of Canada conducted a Regional Geochemical Survey (RGS) of NTS 93E (RGS, BC RGS 16/GSC Open File 1360, 1987).

The objectives of this detailed till geochemistry program are to identify anomalous copper values in till, and to determine the relationship between these values at the surface and in profile, and their bedrock source(s). As well, by investigating changes in copper concentration in till with increasing vertical and horizontal distance from known mineralization, direction of ice flow can be determined, and geochemical values in till for a given distance from known mineralization can be modelled. The likelihood of meeting these objectives is enhanced because the trend of ice flow is known to be valley-parallel, the type and distribution of mineralization in bedrock is well understood, and the depth of till in many places is known or can be inferred.

Sample Media

Basal till, a first derivative of bedrock (Shilts, 1993), is transported in a relatively linear fashion parallel to ice flow direction, down ice of it's bedrock source. Mineral anomalies in basal till tend to be relatively large, and the contrast between anomalous and background geochemical values can be clear. Geochemical patterns found in basal till produce a regional signature, whereas residual soils and colluvium reflect more local geochemical variations (Levson, 2001b). Likewise, second or third derivative sediments, such as glaciofluvial or glaciolacustrine sediments, typically have much more complex transport histories than basal till. These characteristics of basal till make it an effective tool for tracing anomalous geochemical values back to their bedrock sources, and is one reason why basal till (previously described in the Surficial Geology section of this paper) was chosen as the sample media for this study.

While conducting a till geochemistry program, the proper identification of sample media is imperative, not only to ensure consistency between sample sites but also to ensure that the origin and mode of transportation and deposition of the sampled sediments is understood when interpreting geochemical results (Levson, 2001b). At each sample site, sedimentological data such as: type of sediment and thickness; primary and secondary structures; density; matrix percent, texture, and colour; clast mode, shape, and presence of striae, were collected. These data were collected in order to ensure the proper identification of basal till from other sediment types such as colluvium, debris flows, and glaciolacustrine diamicts. As well, at each sample site, notes were made on: type of exposure sampled; terrain map unit; sample site geomorphology (*e.g.* topographic position, aspect, slope, drainage); stratigraphy; and the type and thickness of soil horizons present. These data were collected to assess which surficial processes, if any, could have physically or geochemically altered the sediments sampled. Again, this information can be critical when interpreting geochemical data.

At each sample site, clasts found in till were examined in detail. Data such as, clast lithology, shape (i.e. rounded, sub-rounded, sub-angular, or angular), size, presence of striae, and presence of mineralization, were recorded. From these data, inferences on clast provenance can be made, as well as interpretation of ice flow direction.

Sample Types

During the course of the 2000 field season 452 samples of surficial sediments were collected on the Huckleberry Mine property: 205 of basal till from Becker Hammer boreholes; 71 from till, soil, and peat profiles; and 176 routine surface samples of basal till. Sample sites were selected to optimize spatial coverage of the study area, taking into account ice flow direction and location of ore bodies. Limitations on sample site selection were due mainly to the absence of appropriate sample media, but were also a result of human disturbance (*e.g. tailings pond location, re-working of surficial sediments by heavy machinery, road beds, etc.). Becker Hammer drill site locations were selected by HBL with no input as a result of this program.*

From 1998-2000, HBL carried out a Becker Hammer drill program as part of on-site geotechnical investigations for appropriate tailings dam construction material. Basal till samples were collected at depth which enabled HBL to evaluate the quality and quantity of basal till available. Quaternary sediments were sampled at depths up to 29 metres with a Becker Hammer drill rig which hydraulically pounds a hollow drill stem into the substrate. Cohesive sediments, like basal till, come up the drill stem in consolidated balls 10-15 centimetres in diameter; samples were taken and logged every 1.3 metres (4 feet). Sample splits of these consolidated balls were taken from every sample interval where till was recovered in sufficient quantity and quality. Much emphasis was put on sample preparation, which included describing the characteristics of each sample, scraping the outside surfaces of the samples to remove other sediments, and examining sample splits for possible reconstitution as the original sample was brought up the drill stem. As part of this study, 19 of the boreholes were sampled throughout their length, and 28 were sampled at or near the surface (Figure 2, lower half).

To supplement these borehole samples, profile sampling was conducted in basal tills, peats, and soils, at 13 sites on the Huckleberry Mine property (Figure 2, lower half). At each of these sites, detailed stratigraphic descriptions were completed followed by sampling of each stratigraphic unit identified. These profiles ranged in depth from 1 to 9.5 metres. Borehole and profile samples will be used to investigate horizontal and vertical geochemical dispersal in basal till.

Routine surface samples also were taken mainly along roadcuts on the Huckleberry Mine property, but included other artificial sites (trenches, soil and borrow pits) and natural sites (wave-cut banks on lake shorelines and gullies). Average sample depth was about 200 centimetres below surface, but ranged from 50 to 850 cm. To test dispersal direction, and change in copper values in till with distance from known mineralization, valley-parallel, east/west sample transects were run along roadcuts north and south of the Main and East Zone pits. Sample spacing varied from approximately 100 metres on the northern transect to approximately 500 metres on the southern transect. In addition, samples were taken (sample spacing of 250 to 500 m) up to 4 kilometres west of the Main Zone, and up to 2 kilometres east of the East Zone, to again test for dispersal direction and changes in copper values in till with distance from these known sources of mineralization (Figure 2, upper half).

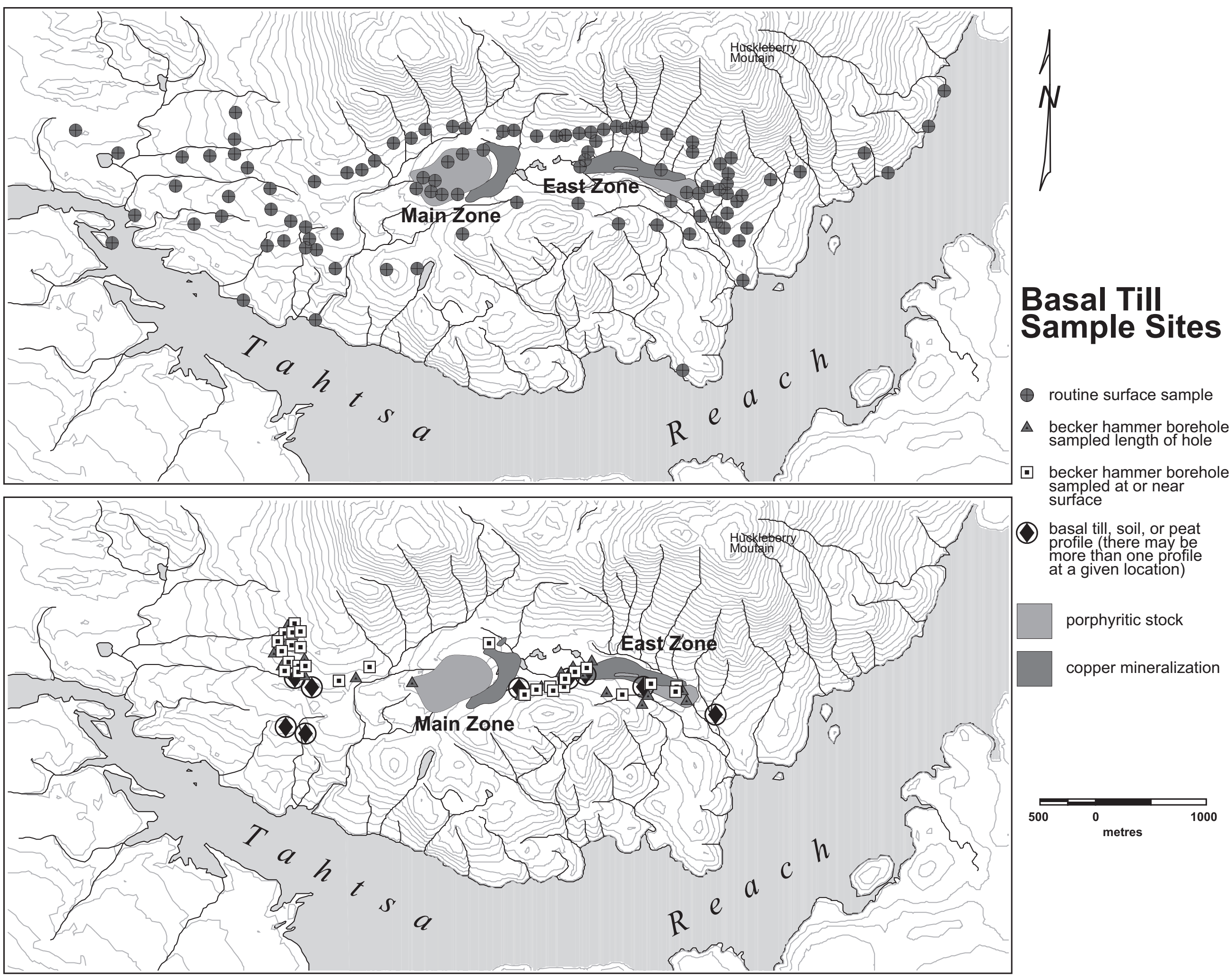

Figure 2. Upper: routine surface sample locations; Lower: Becker Hammer borehole sample, and basal till, peat, and soil profile locations.

Laboratory Methods

Samples collected for this study, ranging from 2 to 5 kilograms, were air dried, split and sieved to –230 mesh (<62.5 mm). This fraction was analyzed for a total of 52 elements by instrumental neutron activation (INA) at Activation Laboratories Ltd. in Ancaster, Ontario and by inductively coupled plasma mass spectrometry (ICP-MS) at Acme Analytical Laboratories Ltd. in Vancouver, British Columbia. Half of each sample split was archived for grain size or other follow-up analyses.

In each block of 20 samples submitted for analyses, 17 are routine field samples. The remaining 3 samples are quality control measures, utilized in both the sample collection and sample analysis components of the study, to differentiate true geochemical trends from those that reflect random and systematic sampling or analytical errors. Quality control measures include the use of field duplicates, analytical duplicates, and control standards.

ICE FLOW HISTORY OF THE HUCKLEBERRY MINE AREA

The Huckleberry Mine area has a complex glacial history. Preliminary results suggest there are two dominant ice flow directions in the region, 236º-265º and 40º-91º (Figure 3). The results also suggest that ice flow direction, and the preservation of ice flow indicators, have been effected at least in part by topography and/or elevation. In addition, air photo interpretation alone locally yields different results than field studies. For example in the region east of the Huckleberry Mine, the orientation of intermediate to large scale erosional and streamlined landforms suggests a dominant ice flow direction of east to northeast during the last glacial maximum. However, field investigations of these landforms and small scale features suggest a more complex ice flow history with an earlier westerly flow event followed by the east to northeast event.

At relatively high elevation sites (>1500 metres), west to southwest flow is clearly indicated in well preserved landforms such as roche moutonnée, striae, and rat tails, and is the only direction preserved here (Photo 4). At these sites there is no evidence of topographic control as these features are observed with orientations that cross mountain tops and do not conform to the trend of the adjacent valleys. At lower elevations, in valley bottoms and along lake shores in particular, the preserved record of ice flow direction is much more complicated. Along the shores of Tahtsa Reach and Tahtsa and Ootsa lakes for example, ice flow was topographically controlled and appears to have flowed parallel to the valleys, regardless of the regional ice flow direction. At these lower elevation sites it is common to find west to southwest and east to northeast ice flow indicators on opposite sides of the same outcrop (Photo 5). It is also common to find evidence of one flow direction superimposed on a landform which indicates flow in the opposite direction.

Based on the relative degree of landform preservation, and the magnitude of these opposing ice flow events inferred from cross-cutting and/or superimposition relationships, the west to southwest event appears to be earlier and of a larger magnitude than the east to northeast

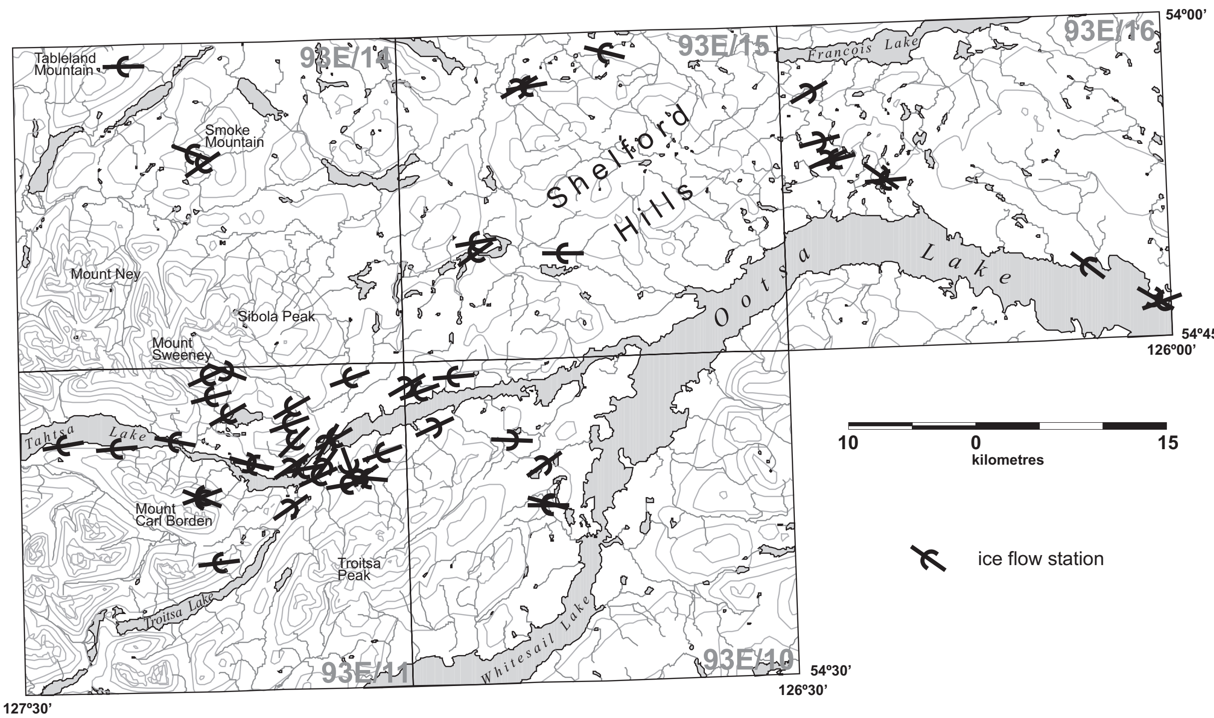

Figure 3. Ice flow stations with inferred ice flow direction. Ice flow data are generalized to improve clarity.

Photo 4. Roche moutonnée on Smoke Mountain (1707 metres asl) showing evidence of southwest ice flow (in photo, ice flow direction is from left to right).

event. In other words, in the Huckleberry Mine area west to southwest flow dominated during the Fraser Glaciation maximum and was followed in some low elevation areas by a weaker, possibly shorter lived, east to northeast ice flow event. These results are in general agreement with those discussed by Levson *et al*. (1998, 1999), and Stumpf *et al.* (2000), and indicate the presence of an ice dome in central British Columbia during the Fraser Glaciation maximum. With the development of this ice dome, ice that once flowed east from the Coast Mountains, controlled by the Tahtsa and Ootsa Lake valleys, now flowed west to southwest back through these valleys and over neighbouring mountain peaks producing the observed west to southwest ice flow indicators. Towards the end of the Late Wisconsinan this divide locally shifted west, back towards the Coast Mountains, and as the ice sheet began to thin, ice flow resumed natural drainage patterns producing the east to northeast ice flow indicators observed in air photos and in the field. Evidence of early ice flow eastward out of the Coast Mountains was probably obliterated in many areas by the westward flow event; of the 136 ice flow stations visited, only a few provided good evidence of an earlier eastward ice flow event although in many case it is difficult to differentiate early and late easterly flow indicators.

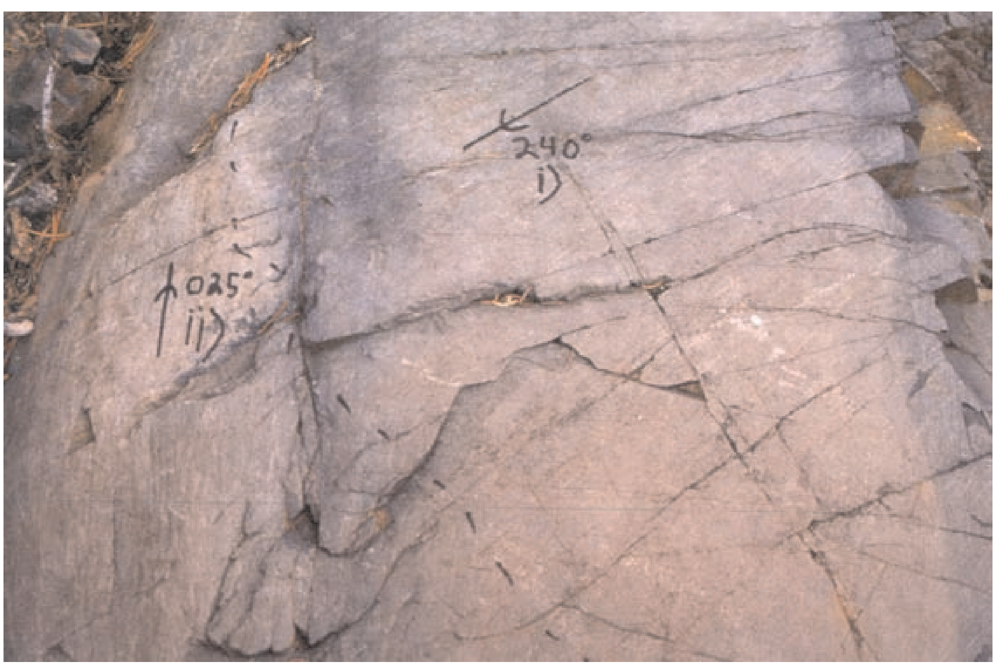

Photo 5. Typical striated outcrop observed at lower elevation sites (Tahtsa Reach) , with evidence of two ice flow events (i) earlier southwest ice flow; (ii) later northeast ice flow.

GEOCHEMICAL CHARACTERISTICS OF THE HUCKLEBERRY MINE AREA TILLS - PRELIMINARY RESULTS

At the time of writing, geochemical analyses had been completed on only 18 of the 205 Becker Hammer borehole samples collected. These 18 samples closely follow an east-west transect through the Main and East Zones (Figure 4), but were taken at various depths below surface (Table 1); two samples were taken from boreholes OB98-11, OB99-26, and OB99-36 at different depths. Figure 5 shows how copper concentrations of these 18 samples vary relative to depth below surface and distance from known mineralization. As well, at the time of writing, geochemical analyses had been completed for 48 of the 176 routine surface basal till samples collected. Copper concentrations at these sample sites are plotted in Figure 6 as a graduated symbol map and they are shown relative to the two primary zones of known copper mineralization in bedrock. Routine surface sample sites north and south of the Main and East Zones, and east of the East Zone, were collected in the early stages of this study to determine the local signature of the orebodies and to test for westerly dispersal of mineralization. The sites west of the Main Zone were sampled in the later stages of this study to investigate the probable source of a high copper value encountered in the till in that area in the early part of the study.

The median copper concentration of the 66 samples analyzed to date is 181 ppm, with a minimum value of 43 ppm and a maximum of 8924 ppm. Only 13 had copper concentrations of less than 100 ppm. In general, copper concentrations below 100 ppm are found at distances greater than about 1 kilometre from known mineralization or they occur at sites off the trend of the valley that hosts the Huckleberry porphyry system (Figure 6). The highest copper concentration in till in the area (8924 ppm) occurs at the west end of the Main Zone where the sample was taken 30 centimetres above mineralized volcanics. The bedrock at this site had a 0.5 to 1.0 centimetre thick amorphous precipitate of an unknown chemical composition suggesting that the anomalously high copper content in the till at this site is a result of groundwater transport of copper in solution. Similarly, high copper in till (446 ppm) at a site directly downslope (southeast) of the East Zone may be the result of hydromorphic dispersion. Strong iron staining of surface till and pronounced groundwater seepage observed this site provides good evidence for the movement of metals in solution in that area. Aside from this site, most other surface tills in the vicinity of the East Zone have copper contents less than the area median and values drop quickly to levels as low as 63 ppm directly southeast of the East Zone. In contrast, copper concentrations at most sites west of both the East and Main zones exceed the median and several exceed the 70th percentile (245 ppm) for surface tills in the area (Fig-

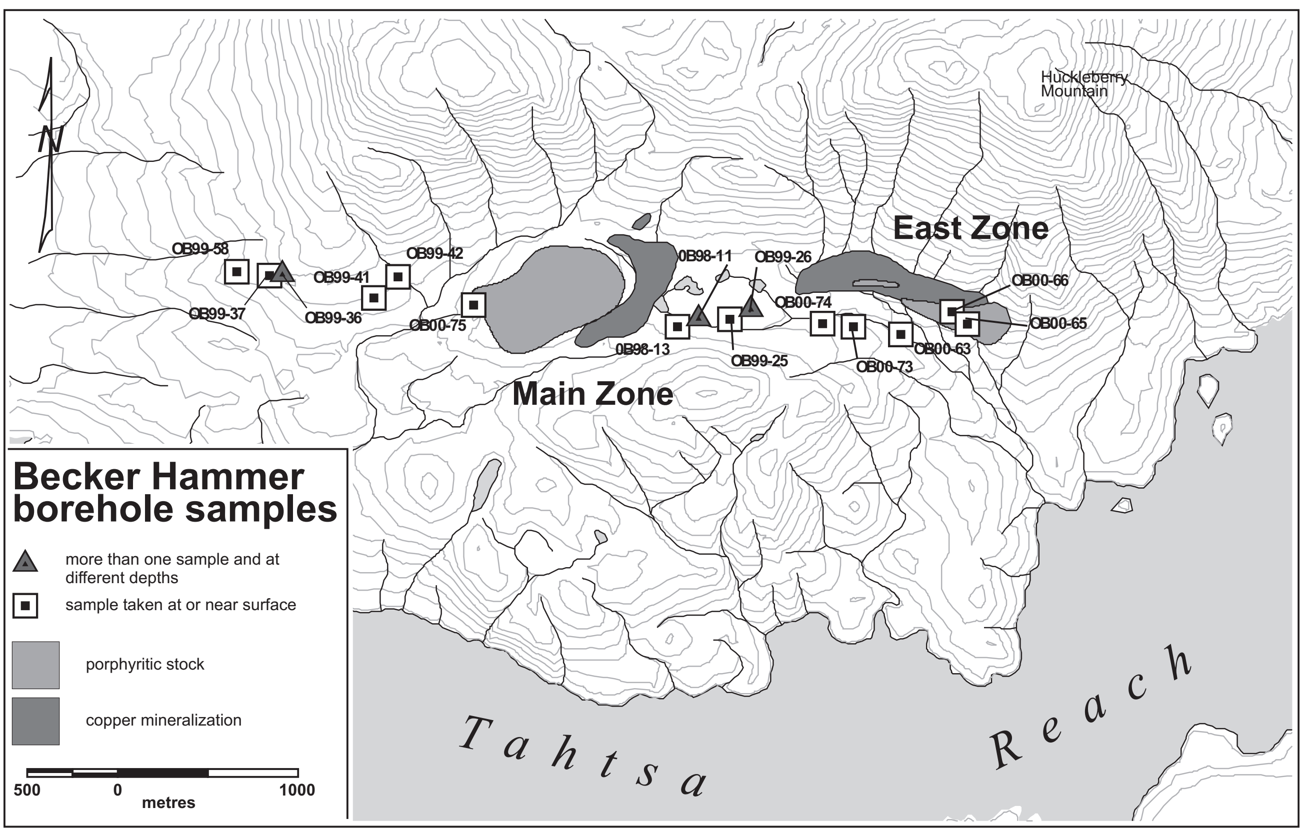

Figure 4. Location of the 18 Becker Hammer borehole samples analysed to date.

TABLE 1
SUMMARY TABLE OF BECKER HAMMER BOREHOLE SAMPLES ANALYZED TO DATE

Becker Hammer Borehole ID	Depth to Bedrock (m)	Sample Interval Below Surface (m)	Copper (ppm)
0B98-11	14.4	8.0 - 9.3	144
0B98-11	14.4	13.3 - 14.7	424
0B98-13	10.2	8.0 - 9.3	230
OB99-25	17.1	8.0 - 9.3	133
OB99-26	19.8	9.3 - 10.7	295
OB99-26	19.8	16.7 - 18.0	634
OB99-36	11.0	2.7 - 4.0	44
OB99-36	11.0	4.0 - 5.3	43
OB99-37	18.9	2.7 - 4.0	85
OB99-41	11.3	2.0 - 2.7	550
OB99-42	11.3	5.3 - 6.7	57
OB99-58	>19.2	2.7 - 4.0	135
OB00-63	6.9	4.0 - 5.3	451
OB00-65	14.7	6.7 - 8.0	180
OB00-66	6.9	4.0 - 5.3	180
OB00-73	26.4	4.0 - 5.3	478
OB00-74	26.7	3.3 - 4.7	908
OB00-75	14.0	8.0 - 9.3	257

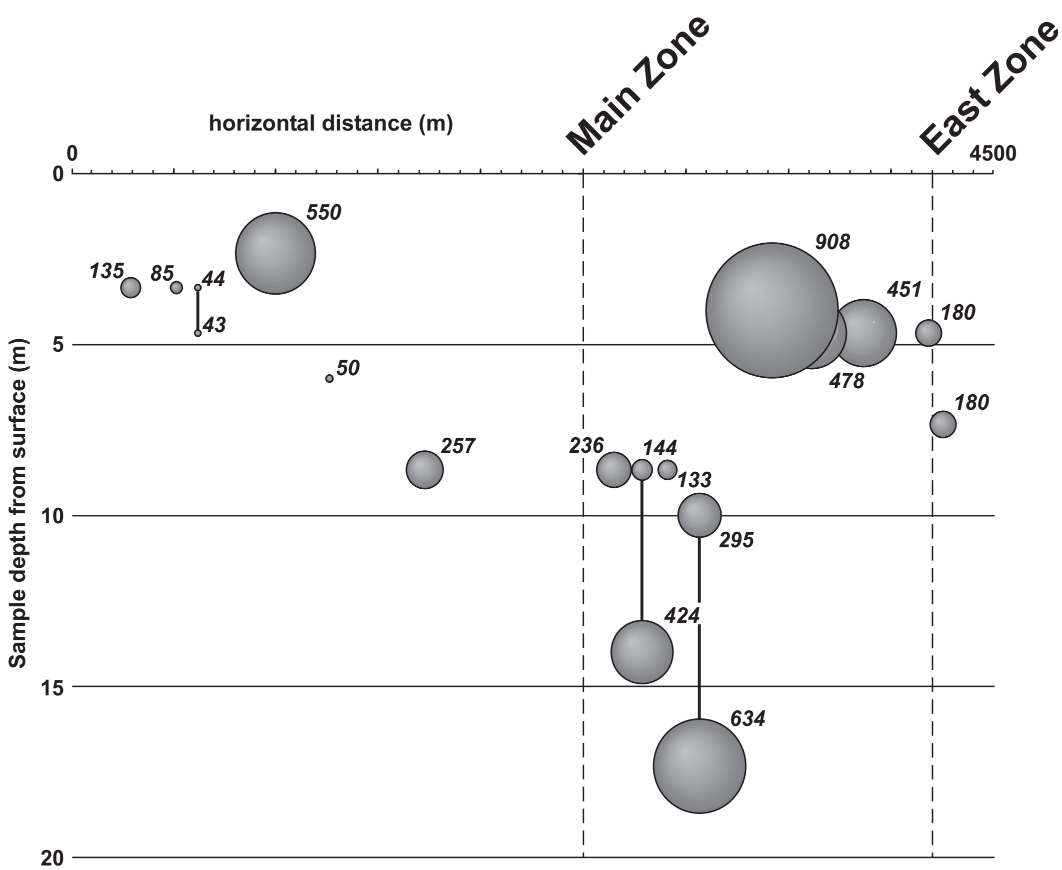

Figure 5. Becker Hammer borehole samples analysed to date, plotted with depth and distance from known mineralization (i.e. Main and East Zones). Diameter of data point is proportional to copper concentration; labels are actual copper values (ppm). Samples from the same borehole are connected with a solid line.

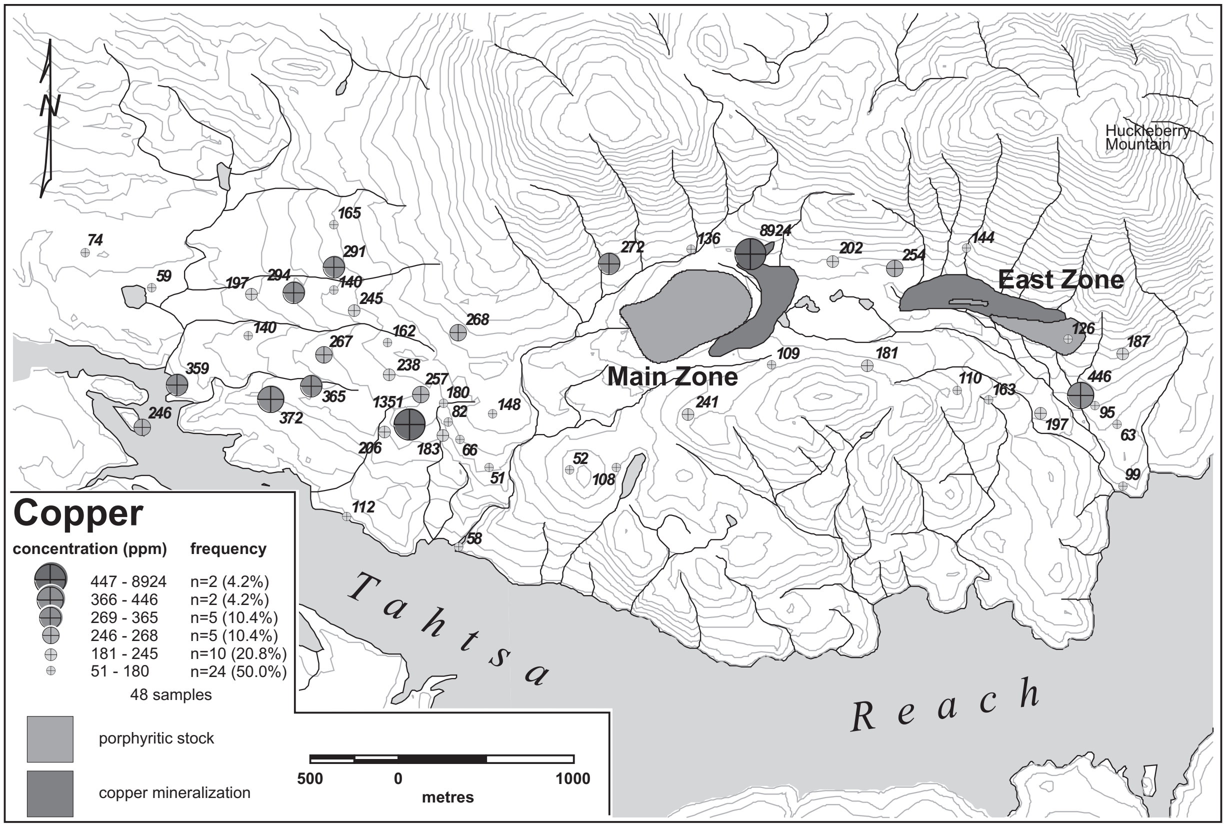

Figure 6. Gradational symbol map of routine surface samples analyzed to date. Samples are labelled with actual copper values (ppm).

ure 6). These data are suggestive of westerly dispersal and in general support the evidence from ice flow indicators indicating a strong westerly flow event in the region. However, generally low concentrations of copper in tills from bore holes in the western part of the Huckleberry Mine property (Figure 4 and Table 1; *e.g.* 43, 44, 50, and 85 ppm) may reflect early easterly transport of till from non-mineralized areas to west. Preliminary results of stratigraphic and lithologic analysis of tills, well exposed in borrow pits in this area, support this interpretation.

Indications of Undiscovered Mineralization

The copper content of surface tills close to the East and Main zones is relatively low in comparison with an area on the west side of the property about 2 to 3 kilometres west of the Main Zone (Figure 6). Five sites in this area exceed the 80th percentile (268 ppm) and the second highest copper content encountered in till to date in the region (1351 ppm) occurs at a sixth site in this same area. The latter site occurs at the crest of a till ridge and it is therefore unlikely that the high copper there is a result of hydromorphic dispersion. Also, several clasts with chalcopyrite mineralization were observed in the till at this site, one yielding an assay of 0.62% Cu. Two samples taken along a bush traverse to the west of this site also yielded high copper values (365 and 372 ppm; Figure 6) and mineralized erratics. In contrast, several surface till samples located to the east of this site yielded copper concentrations near or below the area median.

These data are suggestive of a west-trending dispersal plume with an apex at or around the 1351 ppm copper sample site. Copper values decrease from 372 to 246 ppm to the west of this site over a distance of 1.5 kilometres. To the east, copper values abruptly drop from 183 to 66 ppm copper, over a distance of 250 metres. Although it is possible that these data could represent dispersal from the Main Zone, a number of factors suggest that there may be an undiscovered bedrock source for the mineralization near the high copper till site. These factors include: the relatively long distance of the anomalous tills from the Main Zone (about 2 kilometres); the high concentration of copper (1351 ppm) in till at the one site; and the sharp decrease in copper to the east of that site. It is also possible that the source of the copper in the tills could be mineralized volcanics located under the tailings pond (approximately 750 metres to the east). However, a more optimistic target occurs directly north of the till site with the 1351 ppm copper, in a low swampy area that is geomorphologically similar to the poorly drained areas that originally obscured much of the Main and East zones. Further work is required to determine the location, extent and grade of the bedrock source for the high copper in tills on the west side of the property.

Comparison of Huckleberry Tills with Other Areas

The median copper concentration of till in the Huckleberry area (181 ppm) is considerably higher than median values obtained in detailed studies around copper porphyry deposits at the Nak property (66 ppm, Levson *et al*., 1997) and the Bell Mine (MINFILE No. 093M 001) (63 ppm, Stumpf *et al*., 1997) and could be attributable to differences in the lithology of the host rocks or the type of mineralization. At the Bell Mine, for example, mineralization is hosted mainly in a biotite-feldspar porphyry whereas at Huckleberry mineralization is mainly within the country rocks (andesites).

In contrast with findings at the Nak property where copper concentrations in most holes varied little with depth (generally less than 50 ppm, Levson *et al*., 1997), there is significant variance in copper concentrations with depth at Huckleberry Mine. This is clearly illustrated between the Main and East zones in Figure 5 where elevated values of 180-908 ppm found at 2 to 5 metres depth and 424 to 634 ppm at 14 to 17 metres depth, are separated by relatively low values of 133-295 ppm from 7 to 10 metres depth. As well, Figure 5 illustrates that in the borehole samples copper concentrations generally decrease away from known mineralization with the lowest concentrations generally occurring farthest west. This pattern however, is observed with a data set of only 18 samples and interpretations should be viewed with caution. Of particular interest, are two sites at the east end of the East Zone (sites OB00-65 and OB00-66, Figure 4). These samples were taken between 4 and 8 metres depth and both have relatively low copper concentrations of 180 ppm (Table 1). Since these sites lie to the east of copper mineralization in both the East and Main zones, it seems unlikely that the till there was deposited by ice flowing to the east. Westerly flow is also supported by the high copper content in till at sites OB00-63, OB00-73 and OB00-74, to the west of these two sites (Figures 4 and 5).

The geochemical results and interpretations presented here are preliminary. More geochemical analyses are needed before dispersal plumes, and their two and three-dimensional geometry, can be thoroughly investigated, and before the potential effects of a change in ice flow direction from west/southwest to east/northeast in the Huckleberry Mine area can be determined.

SUMMARY

Preliminary analyses of ice flow data indicate that glaciers early in the Fraser Glaciation, sourced in high elevation areas in the Coast Mountains, flowed easterly through the Huckleberry Mine area into the Nechako Plateau, but west to southwest ice flow dominated in the region during the glacial maximum. This latter event was regionally significant as there is clear evidence of west to southwest ice flow across mountain peaks above elevations of 1500 metres in the Huckleberry region, and across high mountain ranges elsewhere in the western part of the Nechako Plateau. The source of ice for this event was an ice dome(s) east of the study area in central British Columbia, which formed a migrating ice divide(s). Towards the end of the Late Wisconsinan this divide locally shifted west back towards the Coast Mountains, probably as the ice sheet that covered west-central British Columbia began to thin. As a result, in some areas such as in the region east of the Huckleberry mine, ice flow directions reversed and glaciers again flowed east and northeast from the Tahtsa Ranges out into the Nechako Plateau.

Geochemical analyses conducted to date in the Huckleberry mine area show significant variance both laterally and in vertical profile, in elemental concentrations of basal tills. Preliminary results indicate that copper concentrations in basal till decrease with increasing distance from known mineralization and are consistent with westerly dispersal in most cases. This relationship is observed in both bore hole samples and in routine surface samples although there are some indications of early easterly dispersal in the region. Also of interest is an area of anomalous copper (>80th percentile) in surface till samples on the west end of the Huckleberry Mine property. Copper concentrations there gradually decrease west of a site with the second highest copper value (1351 ppm) in till encountered in the study area to date. Copper concentrations in till east of this site, closer to the Main Zone, are relatively low suggesting the presence of a westerly directed dispersal plume. Although the source of mineralization for this dispersal plume could be mineralized volcanics under the tailings pond (approximately 750 metres east), or possibly even the Main Zone further (~2 kilometres) to the east, the data is suggestive of an as yet unidentified source closer to the till anomaly.

The results and interpretations presented here are preliminary. Further analyses on striae data, fabric measurements, and pebble counts are required to refine the ice flow model presented for the Huckleberry Mine property. More geochemical analyses are also needed before dispersal plumes, and their two and three-dimensional geometry, can be thoroughly investigated, and before the effects of a shifting ice divide in the Huckleberry Mine area on geochemical dispersal in till, can be fully determined.

ACKNOWLEDGEMENTS

The authors would like to thank to Huckleberry Mines Ltd. for providing access to the Huckleberry Mine site and the volumes of historical and recent data collected on it (including the Becker Hammer borehole samples), and for providing board and lodging during the 2000 field season. Special thanks to Steve Blower (Mine Geologist, Huckleberry Mine Ltd.) for his interest in this project and insights on the local bedrock geology. Tansy O'Connor-Parsons and Joanne Doyle assisted with data collection during the 2000 field season. As well, special thanks are extended to Don MacIntyre for insights on the regional bedrock geology and for providing helicopter time. Ray Lett is gratefully acknowledged for the timely preparation of samples for geochemical analyses and for his assistance with analytical and quality control procedures on those analyses. Thanks are extended to David Mate for his assistance and ideas offered during the 2000 field season.

REFERENCES

Bradish, L., Myers, D.E. and Roney, C. (1989): Geological, geochemical and geophysical report on the Huckleberry Property, NTS 093E/11E, Omineca Mining Division; submitted by Noranda Exploration Company Ltd., *British Columbia Ministry of Energy and Mines*, AR19087, 217 pages.

British Columbia Ministry of Environment, Lands, and Parks (1976): Landforms 93E/10, 11, 14, 15, 16; Department of Lands and Forests, Air Division, Survey and Mapping Branch, 1:50 000 scale maps.

Dreimanis, A. (1989): Tills: their genetic terminology and classification; *in* Genetic Classification of Glacigenic Deposits; Goldthwait, R.P. and Matsch, C.L., Editors, *A.A. Balkema*, Rotterdam, pages 17-83.

Harington, C.R., Tipper, H.W. and Mott, R.J. (1974): Mammoth from Babine Lake, British Columbia; *Canadian Journal of Earth Sciences*, Volume 11, pages 285-303.

Holland, S.S. (1976): Landforms of British Columbia: a physiographic outline; *British Columbia Ministry of Energy and Mines*, *and Petroleum Resources, Bulletin 48, 138 pages.*

Hornbrook, E.H.W. (1970): Biogeochemical prospecting for copper in west-central British Columbia; *Geological Survey of Canada*, Paper 69-49, 39 pages.

Huckleberry Mines Ltd. (2000): Facts Sheet; 1 page, unpublished.

Jackson, A. and Illerbrun, K. (1995): Huckleberry porphyry copper deposit, Tahtsa Lake District, west-central British Columbia; *in* Porphyry Deposits of the Northwestern Cordillera of North America, Schroeter, T.G., Editor, *Canadian Institute of Mining, Metallurgy, and Petroleum*, Special Volume 46, pages 313-321.

Levson, V.M. (2001a): Quaternary geology of the Babine Porphyry Copper District: implications for geochemical exploration; *Canadian Journal of Earth Science*s, Volume 38, in press.

Levson, V.M. (2001b): Regional till geochemical surveys in the Canadian Cordillera: sample media, methods, and anomaly evaluation; *in* Drift Exploration in Glaciated Terrain, *Geological Society,* Special Publication, in press.

Levson, V.M. and Giles, T.R. (1997): Quaternary geology and till geochemistry studies in the Nechako and Fraser Plateaus, central British Columbia (NTS 93C/1, 8, 9, 10; F/2, 3, 7; L/16; M/1); *in* Interior Plateau Geoscience Project: Summary of Geological, Geochemical, and Geophysical Studies, Diakow, L.J. and Newell, J.M., Editors, *Geological Society of Canada*, Open File 3448, and British Columbia Ministry of Employment and Investment, Paper 1997-2, pages 121-145.

Levson, V.M., Meldrum, D.G., Cook, S.J., Stumpf, A.J., O'Brien, E.K., Churchill, C., Coneys, A.M. and Broster, B.E. (1997): Till geochemical studies in the Babine Porphyry Belt: regional surveys and deposit scale studies (NTS 93L/16, M/1, M/2, M/7, M/8); *in* Geological Fieldwork 1996, *British Columbia Ministry of Employment and Investment*, Paper 1997-1, pages 457-466.

Levson, V.M., Stumpf, A.J. and Stuart, A.J. (1998): Quaternary geology and ice-flow studies in the Smithers and Hazelton map areas (93L and M): implications for drift prospecting; *in* Geological Fieldwork 1997, *British Columbia Ministry of Employment and Investment,* Paper 1998-1, pages 15-23.

Levson, V. M., Mate, D.J. and Stuart, A.J. (1999): Quaternary geology and drift prospecting studies in the north central Nechako Plateau (93F and K); *in* Geological Fieldwork 1998, *British Columbia Ministry of Energy and Mines*, Paper 1999-1, pages 15-24.

MacIntyre, D.G. (1985): Geology and mineral deposits of the Tahtsa Lake District, west-central British Columbia; *British Columbia Ministry of Energy, Mines and Petroleum Resources*, Bulletin 75, 82 pages.

Mate, D.J. and Levson, V.M. (1999): Quaternary Geology of the Marilla map sheet (NTS 93F/12); *in* Geological Fieldwork 1998, *British Columbia Ministry of Energy and Mines*, Paper 1999-1, pages 25-32.

Myers, D.E. and Roney, C. (1990): Geological and geochemical report on the Huckleberry Property, NTS 093E/11E, Omineca Mining Division; submitted by Noranda Exploration Company Ltd.,*British Columbia Ministry of Energy and Mines*, AR19764, 46 pages.

New Canamin Resources Ltd. (1993): Surficial geology, Huckleberry Mountain; drafted by McElhanney Resources Ltd, 1:10 000 scale.

Plouffe, A. and Jetté, H. (1997): Middle Wisconsinan sediments and paleoecology of central British Columbia: sites at Necoslie and Nautley Rivers; *Canadian Journal of Earth Sciences*, Volume 34, pages 200-208.

Plouffe, A. and Levson, V.M. (2001): Quaternary geology of the north half of the Nechako map area (NTS 93F); *Canadian Journal of Earth Sciences*, Volume 38, in press.

RGS 093E, Johnson, W.M., Hornbrook, E.H.W., and Friske, P.W.B. (1987): Whitesail Lake, British Columbia (NTS 93E); *British Columbia Ministry of Energy, Mines, and Petroleum Resources*, BC RGS 16, Geological Survey of Canada, Open File 1360.

Shilts, W. (1993): Geological Survey of Canada's contributions to understanding the composition of glacial sediments; *Canadian Journal of Earth Sciences*, Volume 30, pages 333-353.

Stevenson, R.W. (1970): Report on soil geochemical survey Len No. 3 Group (Len Mineral Claims No. 15-18, 29-32, 35-38, 42FR, 45-58FR, 84 FR), NTS 093E/11E, Omineca Mining Division; submitted by Kenneco Explorations (Canada) Ltd., *British Columbia Ministry of Energy and Mines*, AR02691, 10 pages.

Stumpf, A.J., Broster, B.E. and Levson, V.M. (1997): Evaluating the use of till geochemistry to define buried mineral targets: a case study from the Bell Mine Property (NTS 93 L/16, 93 M/1), west-central British Columbia; in Geological Fieldwork 1996, *British Columbia Geological Survey*, Paper 1997-1, pages 439-456.

Stumpf, A.J., Broster, B.E. and Levson, V.M. (2000): Multi-phase flow of the Late Wisconsinan Cordilleran ice sheet in western Canada; *Geological Society of America*, Bulletin, Volume 112 (12), in press.

Tipper, H.W. (1994): Preliminary interpretations of glacial and geomorphic features of Smithers map area (93L), *British Columbia; Geological Survey of Canada*, Open File 2837, 7 pages.

Sea-To-Sky Aggregate Potential Mapping Project

By Adrian S. Hickin, Elizabeth D. Brooks and Peter T. Bobrowsky

KEYWORDS: *A*ggregate, aggregate potential mapping, sand and gravel, Whistler, Squamish, Pemberton, Sea-To-Sky, inventory, database.

INTRODUCTION

The Sea-to-Sky region, north of Vancouver, British Columbia, is currently experiencing competing land use options which range from the development of scarce, but economically important aggregate resources to complete conservation and preservation of the natural resources. However, with the continued urban growth of communities such as the Villages of Whistler and Pemberton and the City of Squamish, coupled with a potentially successful bid for the 2010 Winter Olympics, pressure on the existing local aggregate reserves will eventually reach a critical stage. To address these concerns, the Ministry of Energy and Mines with funding assistance from the Corporate Resource Inventory Initiative (CRII), British Columbia Assets and Lands (BCAL), and Ministry of Transportation and Highways (MOTH), initiated a joint project to assess, at a reconnaissance level, the aggregate potential of the Sea-to-Sky corridor.

The Sea-to-Sky Aggregate Potential Map Project has four main objectives:

(1) Locate, compile and review all existing and readily available geological and geotechnical information housed within government, academia, and industry.

(2) Through fieldwork, identify and accurately record (using GPS and UTM grid references) the location of currently and previously active sand, gravel, and crushed stone aggregate extraction operations.

(3) Generate a Level III Aggregate Potential Map at a scale of 1:50,000 using surficial landform polygons as a base-map according to a methodology which most closely approximates provincial standards for this procedure (Bobrowsky *et al*., 1996a).

(4) Create a multi-layered comprehensive digital map and interactive database in a GIS format (ARCVIEW) that is readily accessible via the Internet to government, industry, and the public.

The Sea-to-Sky project is a regional reconnaissance study or "first approximation" which does not consider in detail the inherent properties of the material within a deposit. As defined elsewhere, the objective here is to generate Level III quality maps which provide, in a qualitative sense, the aggregate potential of distinct landforms (polygons) (*see* Table 1). The procedure adopted here places the reliability of the interpretations above Level IV and V maps, but below Level I and II maps. It is, therefore, the responsibility of the map user to not exceed the intended use of the product. Quality of aggregate, volume and grade estimates, for instance, require additional detailed study to that provided here.

The purpose of this paper is to provide a brief record of the activities undertaken thus far. Completion of the project and release of the data is anticipated for early 2001.

PREVIOUS AGGREGATE POTENTIAL STUDIES

In the last several years, the British Columbia Geological Survey Branch (GSB) has produced a number of Aggregate Resource Potential Maps. The current project follows the objectives and methodology established in the previous efforts. To date the following aggregate potential maps have been completed: Prince George region (Bobrowsky *et al*., 1996b); Okanagan region (Bobrowsky *et al.*, 1998) and Nanaimo Regional District (Massey *et al.*, 1998) (Figure 1) .

The Prince George pilot project consisted of five, 1:50 000 NTS map sheets (93G/10, 14, 15, 16 and 93H/2) in the shape of a cross centered over Prince George in north-central British Columbia. A digital map was produced from the exercise, which provided a means of evaluating the efficiency of the methods developed during the

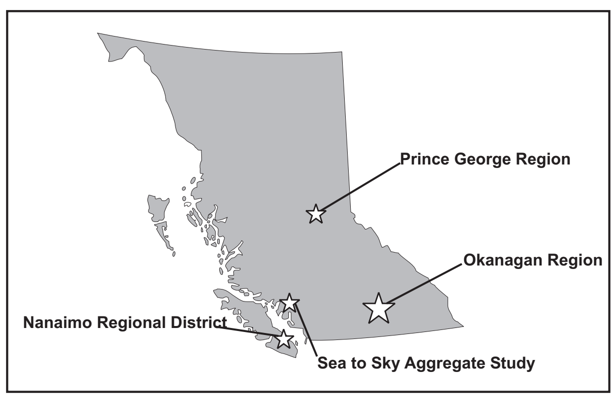

Figure 1. Locations of British Columbia Geological Survey Branch (GSB) aggregate potential mapping projects.

TABLE 1
SUMMARY OF DATA RELIABILITY, COST AND SUITABILITY OF LEVEL I TO LEVEL V AGGREGATE POTENTIAL MAPS IN BRITISH COLUMBIA

	I	II	III	IV	V
Map scales	1:100 to 1:10,000	1:10,000 to 1:50,000	1:50,000 to 1:100,000	1:100,000 to 1:250,000	1:250,000 to 1:500,000
Surficial (landform) data	yes	yes	yes	yes	yes
Field verification of polygons	yes	minimal	no	no	no
Air photo interpretation	new, detailed	new and pre-existing	as required	minimal	none
Water well data	yes	yes	yes	no	no
Use of existing geotech. data	yes	yes	minimal	no	no
Drilling and/or trenching	yes	minimal	no	no	no
New laboratory tests	yes	minimal	no	no	no
Literature research	detailed studies included	detailed studies included	regional studies	basic to regional studies	minimal
Verification of agg. pit locations	yes	yes	yes	minimal	no
Geo. mapping of agg. pits	yes	yes	yes	minimal	no
Product reliability	very high	high	moderate	low	very low
Avg. cost / map sheet	$50,000 +	$20,000 to $50,000	$10,000 to $25,000	$5,000 to $15,000	$1,000 to $10,000
Suitability of maps	site construction purposes	city planning to municipal planning	municipal to regional planning	broad regional planning	provincial planning

1995 Aggregate Forum (Bobrowsky *et al*., 1996a). Later, aggregate mapping for the Okanagan area included sixteen NTS 1:50,000 map sheets (82L/W and 82E/W) in the interior of British Columbia. The general area covers a rectangular section from Osoyoos on the Canada-US border, north to Salmon Arm. More recently, the Nanaimo Regional District study covered 9 NTS 1:50 000 map sheets (parts of 92C, B, F and G) on southeastern Vancouver Island. This last study area corresponds to the coastal section south of Duncan north to Qualicum Beach.

Dixon-Warren initiated aggregate potential mapping work on the Sea-to-Sky project in March, 2000, with the completion of NTS map sheets 92G/11 and 14,. Subsequent funding has extended the boundaries north defining the current Sea-to-Sky project.

AGGREGATE

Aggregate is defined as naturally occurring, hard construction material, such as sand, gravel, crushed stone or slag, which can be mixed with cementing material to form concrete and asphalt or can be used alone in road building, railroad ballast or other construction or manufacturing activities (Edwards *et al*., 1985). Aggregate is an essential commodity in urban and suburban areas and despite its relatively low unit value, it has become a major contributor to the economy.

Globally, the aggregate sector has experienced increasing pressure to manage this resource properly as accelerated urbanization has markedly increased consumption near large urban centers. Municipal expansion, alternate land uses, land sterilization, and public concern are some of the factors which have limited the availability of many traditional aggregate sources. Such factors, including the elevated cost of the product due to increased transportation distances, has created considerable concern about the aggregate industry's ability to supply aggregates to meet future demand. Initiatives such as the Sea-to-Sky Aggregate Potential Map Project provide the first step for ensuring the sustainable development of aggregate resources. The methodology used here provides a means for land planners to manage land areas which may be vital to continued development and maintenance of municipalities and their infrastructure.

Natural aggregate, such as sand and gravel, are the product of unique geological processes (Langer and Glanzman 1993). This generally restricts the location for potential aggregate deposits to those areas where specific environments of deposition either exist or existed. Understanding such processes and environments, has enabled aggregate geologists to predict those landforms which are most likely to contain aggregate.

LOCATION

The study area is located in southwestern British Columbia north of the Vancouver. The area is best described as a 10 kilometre wide corridor along the major transportation routes, delimited in the south by Daisy Lake and in the north by the head of the Lillooet River Valley near Salal Creek. Specifically, the corridor extends from Daisy Lake north to the town of Pemberton, and includes Callaghan Creek and Rutherford Creek. At Pemberton the corridor divides to encompass the Upper Lillooet River Valley as well as Birkenhead Lake and D'Arcy on the southern end of Anderson Lake. In total, the area examined here covers portions of NTS (1:50 000) map sheets 92J/2, 92J/3, 92J/6, 92J/7, 92J/8, 92J/9, 92J/10, 92J/11, 92J/12 (Figure 2). The communities of Whistler, Pemberton, Mt Currie, and D'Arcy all fall within the study boundaries.

PHYSIOGRAPHY

The study area is on the west coast of British Columbia some 40 kilometres north of Squamish (at the head of Howe Sound). This area is part of the "Coast Mountain" morpho-geological belt (summarized in Gabrielse *et al.*, 1991) with terrain typified by high, rugged mountains and deep glaciated valleys. The study area includes three biogeoclimatic zones, the Coastal Western Hemlock, the Mountain Hemlock, and the Alpine Tundra zones, each differentiated by elevation (Meidinger and Pojar, 1991). At lower elevations (sea-level to 900m), parts of the Coastal Western Hemlock zone predominate. This zone typically has cool summers and mild winters. The subalpine occurs within in the Mountain Hemlock zone, between 900 to 1800 metres asl. In this zone, climate is characterized by short, cool summers and long cool wet winters, with heavy snow cover for several months. The very high peaks occupy a relatively small portion of the study area and fall within the Alpine Tundra zone generally above 2250 metres asl. This zone is typically cold, windy, and snowy with short frost free periods.

GLACIAL HISTORY

Most unconsolidated deposits present in British Columbia owe their existence to the processes of glaciation and deglaciation. During the past few million years, the entire province has experienced a number of glacial and non-glacial cycles, the most recent of which (the Wisconsinan ca. 25,000 to 10,000 years BP) has had the greatest impact on aggregate accumulation and distribution.

As climate began to deteriorate some 25,000 years ago, ice previously restricted to the high alpine started to gradually expand. Valley glaciers advanced, eventually over topping inter-valley ridges and coalescing to form small mountain ice sheets (Davis and Mathews, 1944). Eventually glaciers spread across the interior plateaus and coastal lowland, covering most of the province and parts of the continental shelf, finally producing the Cordilleran Ice Sheet (Clague, 1986).

Minimal effort has been directed toward resolving the chronology of Quaternary events in the study area, but deglaciation can be inferred from work completed nearby at the head of Howe Sound and the Mamquam River Valley (Friele and Clague, personal communication, 2000). Apparently, glaciers had retreated from the Mamquam River Valley leaving it ice free and forested by about 14,000 yr BP. Deformed glaciolacustrine and diamicton deposits overlying unmodified glaciolacustrine sediments provide evidence for a glacial readvance about 13,500 yr. BP. A dated submerged end moraine at Porteau Cove marks the maximum extent of the readvance and further indicates that ice began to recede shortly after 12,800 yr BP. Ice continued to retreat up the Squamish River Valley as far as the confluence of the Cheakamus River by 11,800 yr BP. It is likely that the main trunk glaciers in the Cheakamus, Pemberton, and Birkenhead Valleys continued to decay throughout the Holocene by retreating into the high alpine, where remnant ice bodies persist today.

BEDROCK GEOLOGY

The rocks in this area can generally be divided into stratified and intrusive rocks and range in age from Upper Triassic to Recent. A number of faults and shear zones have locally stressed many of these rocks, as both brittle and ductile deformation can be observed at a number of outcrops.

Four groups are represented within the stratified division and include the Garibaldi, Gambier, Tyaughton, and Cadwallader groups (Journeay and Monger, 1994). The Garibaldi Group consists of Recent basalt to rhyodacite flows and pyroclastics, with minor sandstone, shale and conglomerate. The Gambier Group is Lower Cretaceous andesitic to dacitic tuff, breccia agglomerate, and andecite with argillite, conglomerate, lesser marble, greenstone and phyllite. A small sliver of the Upper Triassic Tyaughton Group occurs in the northeast and consists of shale, siltstone, sandstone, conglomerate and limestone. The Cadwallader Group includes the Hurley, Pioneer and possibly the Noel formations. This Upper Triassic group includes argillite, phyllite, sandstone, limestone, siltstone, conglomerate chert and mudstone, in addition to pillowed and massive tuff, with andesitic to basaltic flows and pyroclastics.

The intrusive rocks predominate in the area and are part of the Jurassic and/or Cretaceous Coast Plutonic Complex. These rocks include quartz monzanite, granodiorite, quartz diorite and dioritic complexes containing quartz diorite, amphibolite, greenstone and dike swarms.

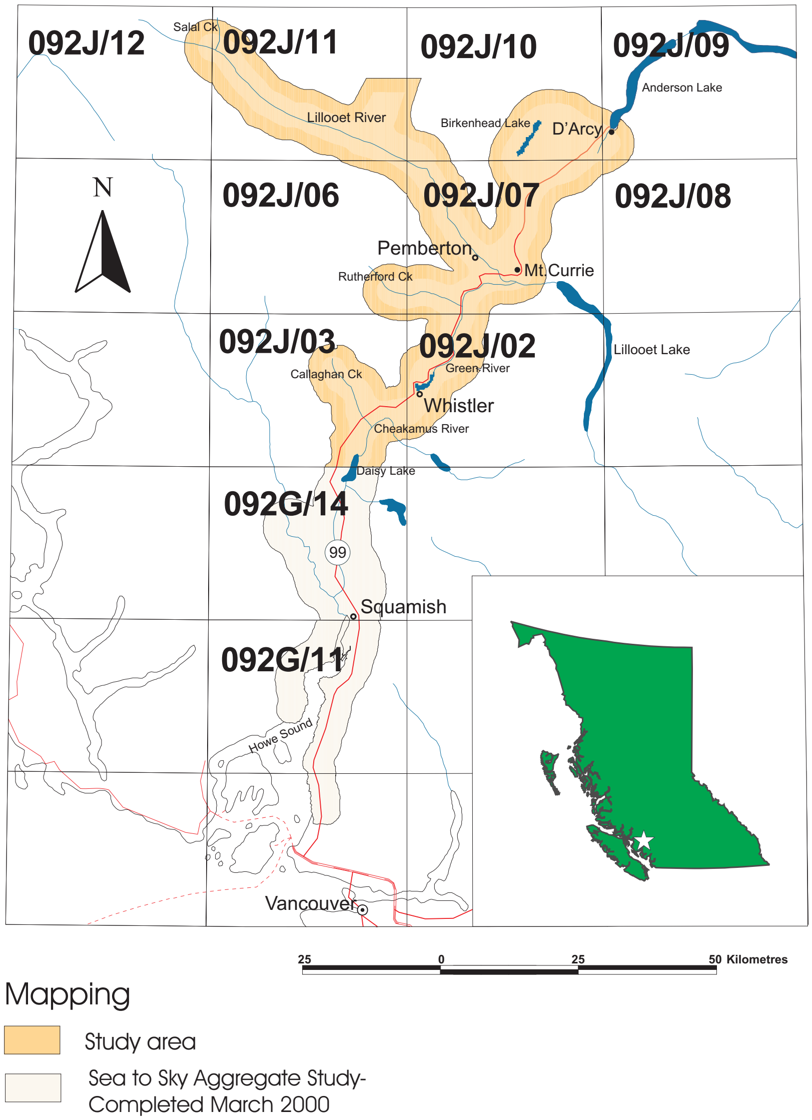

Figure 2. Sea-to-Sky Aggregate Potential Map Project is located directly north of the City of Vancouver and includes the communities of Whistler, Pemberton, D'Arcy, and Mt. Currie.

METHODOLOGY

The methodology for this study follows procedures and provincial standards established elsewhere (Bobrowsky *et al*., 1996a). The process consists of three parts and can be summarized as follows:

(1) data acquisition and compilation;

(2) fieldwork;

(3) polygon ranking.

Data from a number of sources must be located, compiled and evaluated to produce an integrated interpretive product. Information such as geotechnical reports, surficial and bedrock geology, water-well logs, drill reports, and consulting reports all contribute to better evaluating the surficial polygon data. Sources of this information include government, crown corporations, municipalities, and industry.

The following layers of data were compiled for this study:

- surficial material (primary and secondary)
- texture of surficial material (primary and secondary)
- landform expression (primary and secondary)
- quality and thickness of aggregate
- polygon area
- bedrock
- presence/absence of aggregate operations
- overburden thickness

The basemap was prepared from airphoto interpretation of surficial landforms, materials, and textures by J.M. Ryder & Associates Terrain Analysis Inc. following Howes and Kenk (1997) Terrain Classification System for British Columbia. This information was then digitized and the polygonal data then analyzed on a polygon-by-polygon basis for aggregate potential.

Fieldwork consisted of locating all active and inactive aggregate extraction operations including commercial pits as well as highway and logging (mainlines only) borrow pits (Figure 3). The pit descriptions include locations (verified and recorded using a hand held GPS unit), elevation, type of exposure, rough pit dimensions, number of sedimentary units present, clast size range, roundness range, sorting, estimate of size fraction percentages, estimate of clast lithology, bedding, imbrication, surficial material, texture, surface expression, and interpretation.

Once all available information is compiled, polygon attributes are assessed and assigned a numeric value (Table 2). Those attributes which are considered more relevant to aggregate potential (*e.g.* surficial material) are assigned a weighting factor to reflect the greater importance of this attribute. Individual values for the various layers of data are then incorporated into an algorithm that provides an overall value or ranking, for each polygon. Although the algorithms used change between the various studies primarily as a function of the available data, the concept and methodology has remained unchanged.

Those polygons, which are considered "undesirable" (ice, water, etc.), are identified and removed from the analysis. The frequency distribution of the final rank scores for the polygons is then evaluated and the distribution is divided into categories corresponding to primary, secondary, or tertiary aggregate potential.

Figure 3. Typical borrow pit used to facilitate logging road construction. Pits are generally small (~2000m^3) and exploit local material to reduce transportation distance (forest service road south of Birkenhead Lake).

RESULTS

The study encompasses an area of 2020 square kilometres (excluding work completed previously on NTS map sheets 92G/11 and 14), within which a total of 1467 surficial landform polygons were mapped (terrain mapping completed on contract with J. Ryder and Associates) (Figure 4). As noted earlier, such terrain polygons form the basis for categorizing aggregate potential. Polygon area ranges in size from 1.2 to 2225 hectares, which fur-

TABLE 2
EXAMPLE OF VALUES USED TO DETERMINE RANK FOR VARIOUS PARAMETERS. ATTRIBUTES ARE LISTED ON THE LEFT SIDE, AND THE PARAMETERS UNDER THE NUMERIC RANK VALUE
(THE PARAMETERS THAT ARE CONSIDERED MORE RELEVANT TO AGGREGATE POTENTIAL WILL RECEIVE A HIGHER RANK)

Ranking	5	4	3	2	1	0
Landform	Glaciofluvial	Fluvial	Ablation Till, Colluvium	Eolian, Moraine	Lacustrine Organic, Bedrock	Water
Texture	Gravel	Sandy Gravel	Boulders, Sandy Gravel, Silt	Silt, Clay, Sand, Gravel	Silt, Clay, Sand	Unknown
Area	>679 ha	398-679 ha	239-398 ha	132-239 ha	<132 ha	all water
Pit	N/A	N/A	N/A	N/A	Present	Absent
Overburden (from water wells)	0-3 ft (0-1 m)	4-6 ft (1-2 m)	7-16 ft (2-5 m)	17-33 ft (5-10 m)	>33 ft (>10 m)	Unknown
Thickness of gravel (from water wells)	>87 ft (>27 m)	56-87 ft (17-27 m)	34-55 ft (10-17 m)	16-33 ft (5-10 m)	0-15 ft (0-5 m)	Unknown
Volume (Pit)	>1 000 000 m^3	1 000 000 - 500 000 m^3	500 000 - 50 000 m^3	50 000 - 5 000 m^3	5 000 - 0 m^3	Unknown

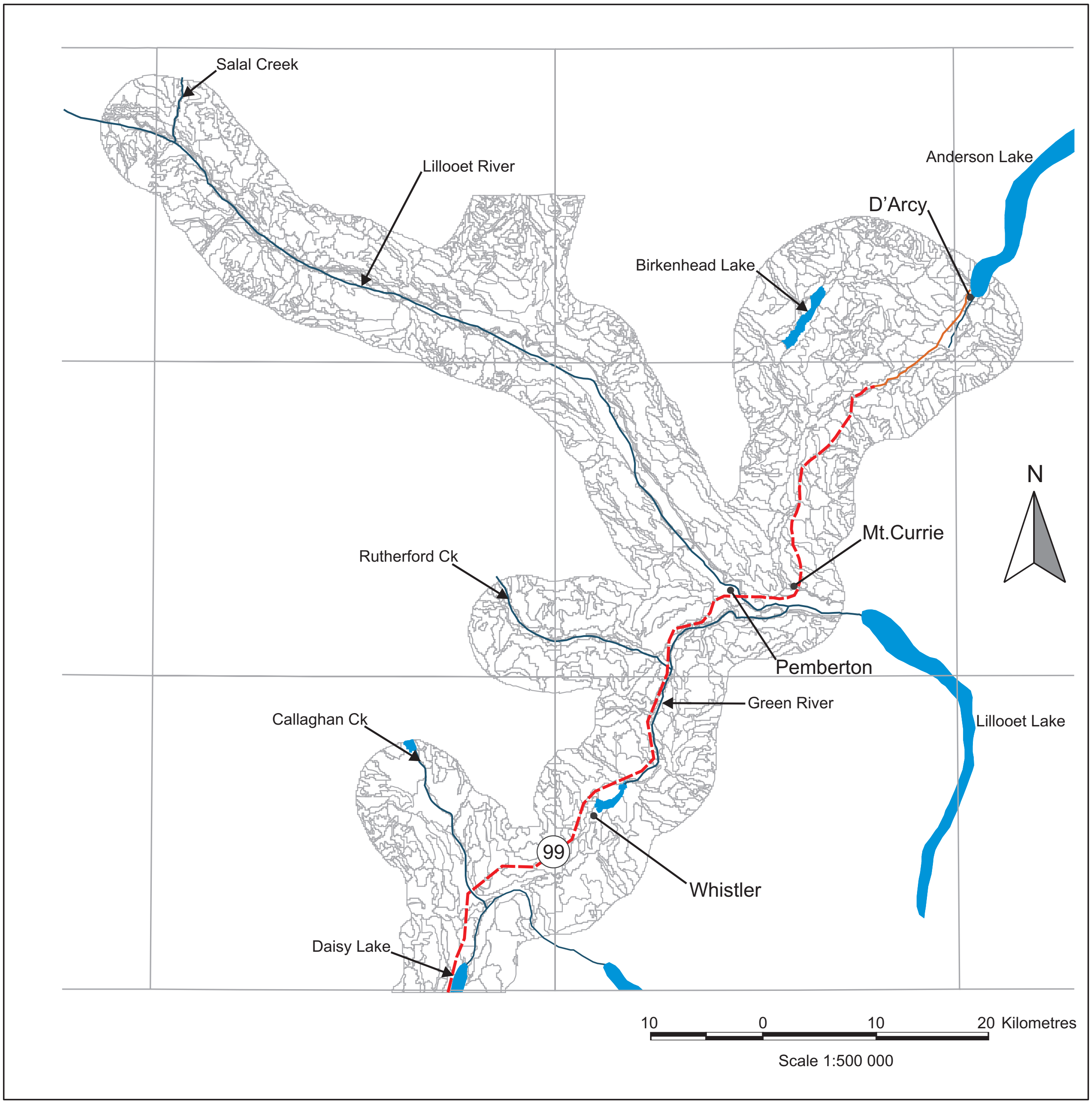

Figure 4. Polygon map produced for the Sea-to-Sky Aggregate Potential Map Project. Polygons delineate landforms of similar surficial material determined through airphoto interpretation.

ther defines the upper and lower theoretical limits for "area" as used in the aggregate algorithm. Similarly, 89 water-well records were obtained and described for the study (Figure 5). Well depths range from 8 to 145 metres, and are disproportionately distributed over the region, most occurring in valley bottoms and near transportation corridors. In addition to the water well information, 163 test pits and geotechnical drill holes were located from consultant or Ministry of Transportation and Highways reports (Figure 6). Test pits and drill holes ranged in depth from 1 to 37 metres. A further 56 drill logs were reviewed from the Ministry of Energy and Mines mineral assessment reports (ARIS). This information provided limited sedimentological data, though did provided a rough estimate of depth to bedrock. Finally, the distribution of active and inactive aggregate operations described in detail is shown in Figure 7. A total of 83 pits were visited of which 39, 32, and 12 were borrow, commercial, and miscellaneous operations, respectively.

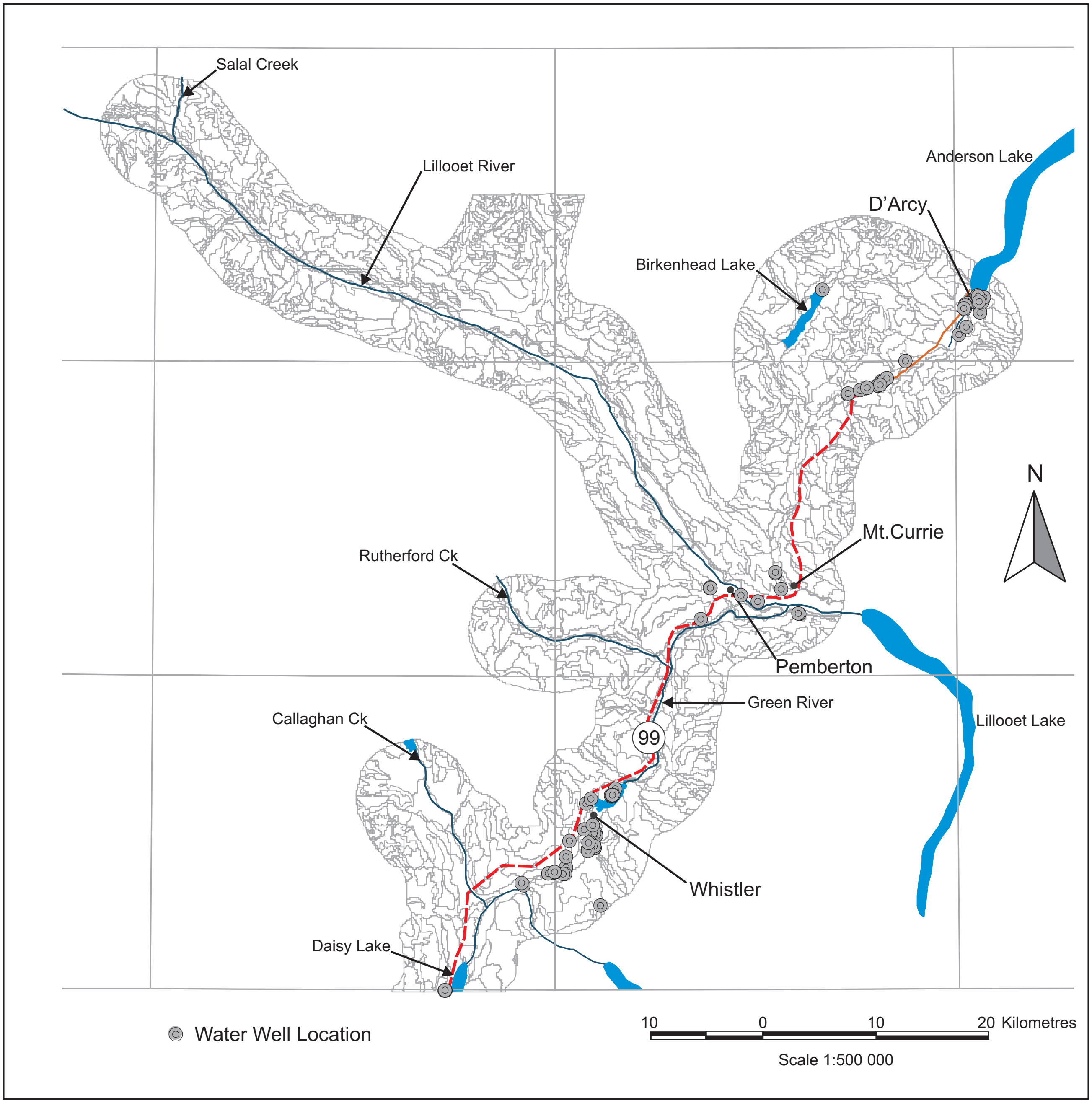

Figure 5. Water-well locations used to determine sedimentology and depth of overburden. Wells are generally concentrated around the communities of Whistler, Pemberton Mt. Currie and D'Arcy.

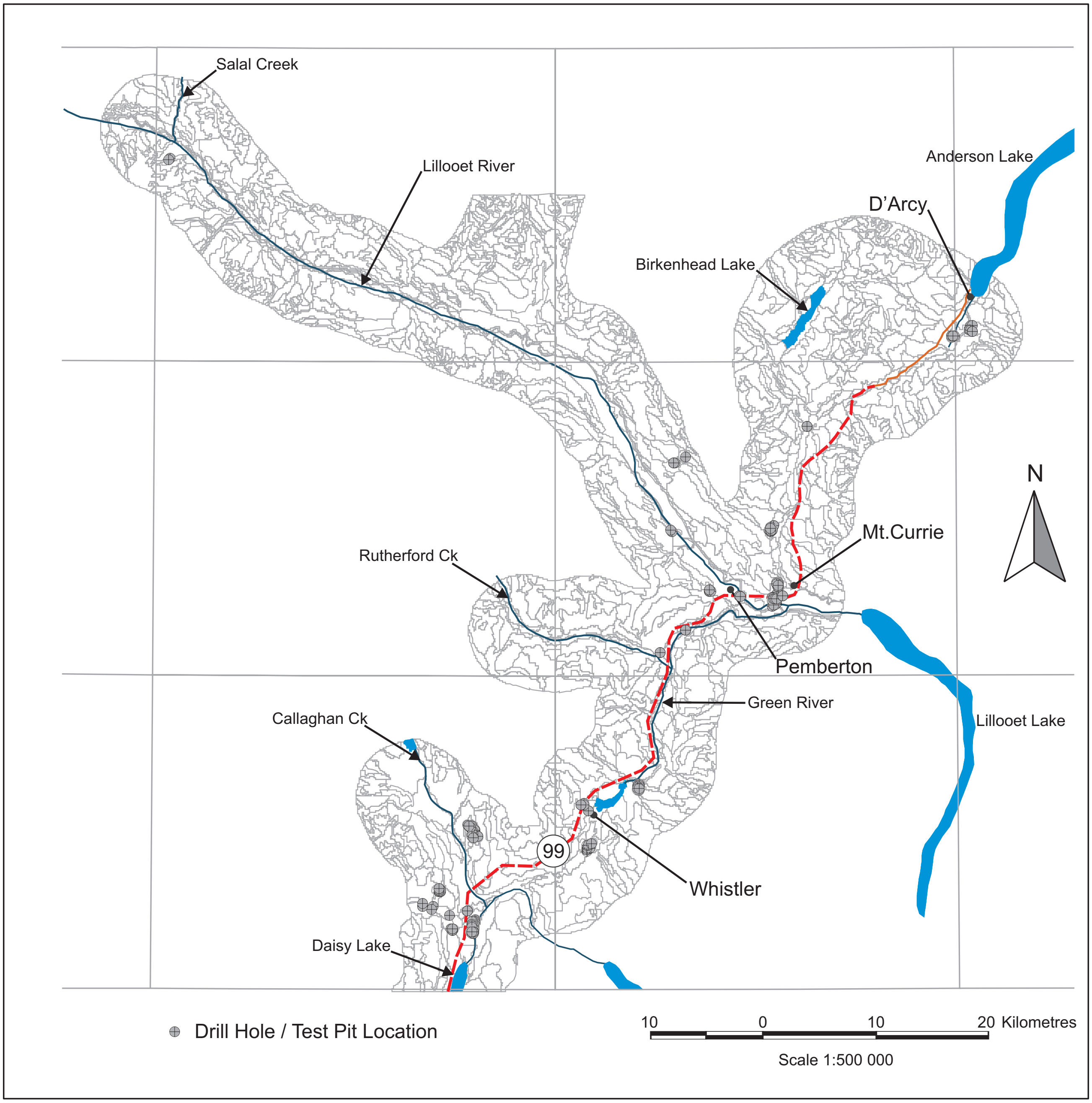

Figure 6. Drill hole and test pit locations from mineral assessment (ARIS), consultant, and MoTH reports. ARIS reports contain the results of mineral exploration programs and only provide minimal information on surficial sediments. The MOTH reports describe shallow test pits used to determine the suitability of sediments for aggregate. Consultant reports contain the most detail, although the distribution is restricted to a limited number of sites.

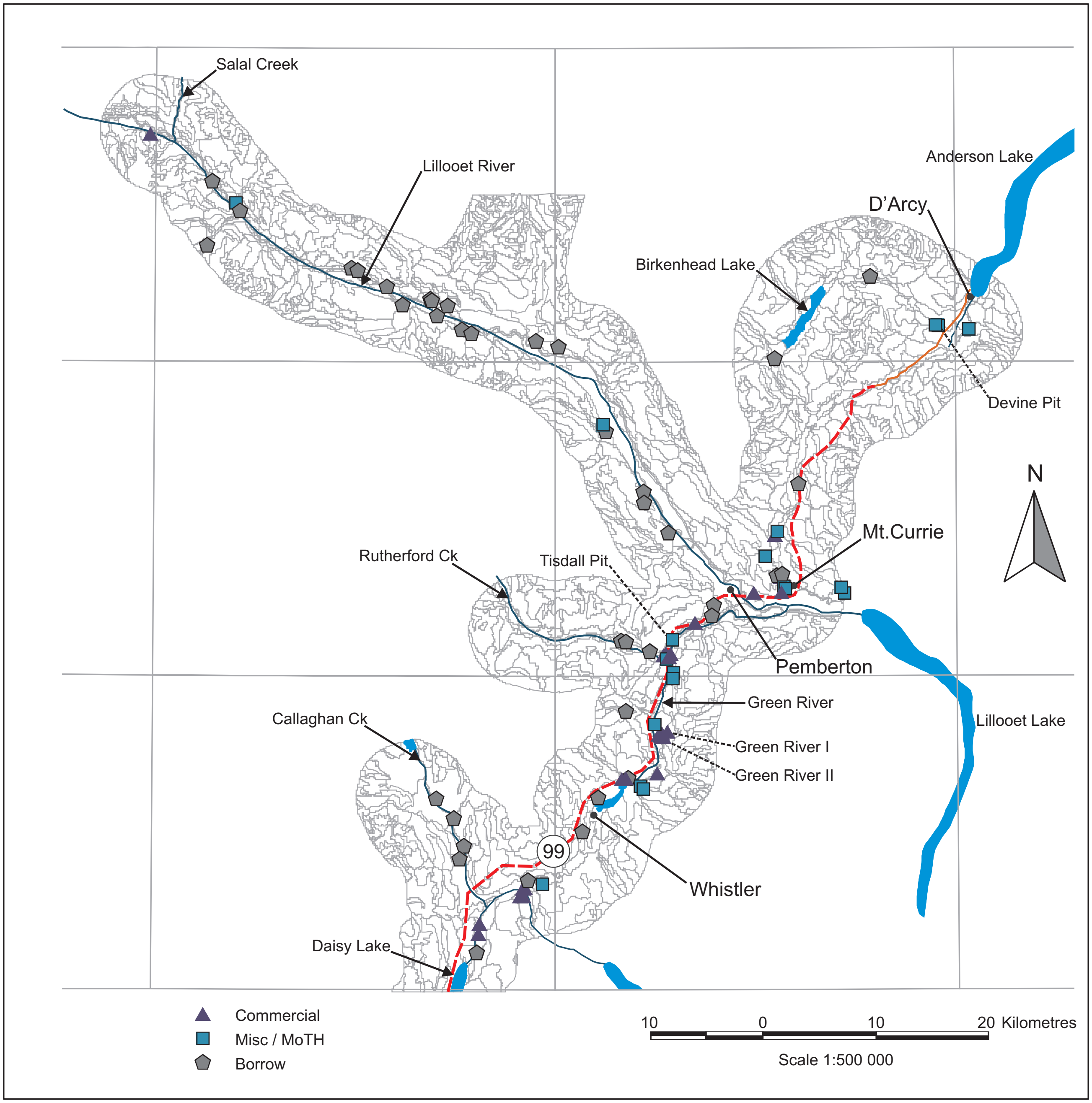

Figure 7. Active and inactive aggregate extraction operations including commercial, borrow, and other miscellaneous pits. Most commercial operations occur along Highway 99 as it is the major transportation route in the area. Borrow pits are more common on the logging roads, though MoTH have established some local borrow pits along the highway.

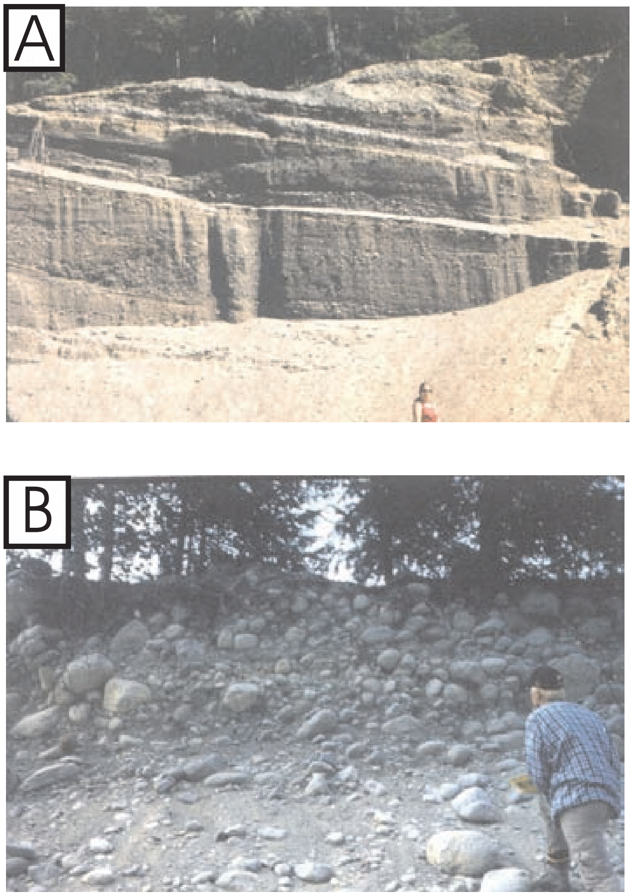

Photo 1. Examples of glaciofluvial deposits in the study area. “A” is from Devine Pit south of D’Arcy and consists of coarse sand and gravel beds dipping to the east. “B” is from the Tisdall Pit, north of Rutherford creek on Highway 99. Clasts range in size from sand to boulders and generally coarsen upwards (*see* Figure 7 for location).

Photo 2. Active mining of the colluvium along Lillooet Forest Service Road, in the upper Lillooet River Valley. Material here is being used to armor river banks (rip-rap) along reaches where erosion threatens the logging road. Other locations provide aggregate for road base and diking material.

As stated earlier, aggregate resources are restricted to specific locations where favorable geologic processes have deposited material. In this area, the dominant processes include fluvial, colluvial and glacial environments.

In general, the majority of active extraction operations in the study area are exploiting glaciofluvial and post-glacial fluvial deposits in the valley bottoms. During fieldwork, stranded glaciofluvial deposits were noted in terraces at elevations as high as 836 metres along some of the tributary valleys, however, for the most part, the larger deposits are commonly found in the major valley bottoms (average elevation: 200-600m). Typically the sediment is medium sand to large boulders, moderate to poorly-sorted, massive to moderately well-stratified (Figure 8). The dominant landforms are poorly to moderately-developed terraces, and fluvial and glaciofluvial floodplains and fans. One of the larger operations (Green River I and Green River II) (Figure 7) is currently working a combination of glaciofluvial, fluvial and lacustrine (well-sorted sand) material.

Many of the valleys contain over-steepened valley walls resulting from glacial scouring and erosion. Consequently, active colluvial processes such as rockslides, rockfalls, and debris flow activity are present. Along the base of the valley walls, some operations are removing this material for rip-rap and gravel, particularly for the construction of forest logging roads (Photo 2). Such deposits can generally be described as sand to very large boulders, moderately to poorly-sorted, massive to weakly-stratified, and very angular to subangular. Evidence for debris flow activity occurs on most steep mountain streams, and fresh debris flow scars are commonly visible.

Till is a sediment deposited directly from ice with very little, or no reworking by other processes. It is well known that the study area was glaciated during the Pleistocene and many of the landforms and bedrock features are the result of glacial activity. It is likely that much of the area was at one time covered with till, however significant portions of this material have subsequently been modified or eroded during the post-glacial period. A large portion of the till in the valley bottoms has been eroded by glacial melt waters and then buried by glaciofluvial and fluvial material. The occasional remnant, or isolated deposit of till is exposed particularly on eroded slopes or where road excavation has stripped overlying material. Despite relatively limited quantities, we observed a few operations developing sand-rich primary till as an aggregate source, but more commonly modified till (washed or colluviated till) seems to be preferred.

Table 3 summarizes the distribution of pits by the primary surficial material of the polygon in which the pits are located. An estimate of the area for the commercial operations ranges from 1800 to 53 240 square metres. Borrow pits are generally much smaller, ranging in areas from 136 to 3750 square metres. Material is generally moderate to poorly sorted and requires processing (*i.e.*

TABLE 3
SUMMARY OF PIT DISTRIBUTION BY THE PRIMARY SURFICIAL MATERIALOF THE POLYGON IN WHICH THE PIT IS LOCATED

	Commercial	Borrow	Misc.	Total
Colluvium	1	18	1	**20**
Fluvial	12	7	6	**25**
Glaciofluvial	9	3	2	**14**
Moraine	6	6	2	**14**
Rock	3	3	1	**7**
Undiff.	0	2	0	**2**
Volcanic	1	0	0	**1**
Total	**32**	**39**	**12**	**83**

washing, sorting, and/or crushing) before the aggregate becomes an acceptable product.

CONCLUSIONS

Most active aggregate extraction in the study area is exploiting fluvial and glaciofluvial deposits, though some operations are mining colluvium and to a lesser extent, till. Most operation occur along the major transportation routes in the valley bottoms where material is thickest and access easiest. Future operations are likely to follow this trend as existing infrastructure and shorter hauling distances dictate the economics of aggregate extraction.

ACKNOWLEDGEMENT

As this project integrated information from many different sources, it is difficult to acknowledge all the individuals that contributed to this study. Information was provided by BC Agriculture and Land Reserve, BC Hydro, BC Rail, Capilano Highway Services, Howe Sound School District, Ministry of Transportation and Highways, Pemberton Dyking District, Resort Municipality of Whistler, Squamish Forest District, Thurber Consultants, and Western Forest Products. The project was jointly funded by the Corporate Resource Inventory Initiative (CRII), British Columbia Assets and Lands (BCAL), Ministry of Transportation and Highways (MoTH), and Ministry of Energy and Mines.

REFERENCES

Bobrowsky, P.T., Massey, N.W.D., and Matysek, P.F. (1996a): Aggregate Forum, developing an inventory that works for you! Report proceedings March 30-31, 1995; *B.C. Ministry of Energy Mines and Petroleum Resources*, Information Circular 1996-6.

Bobrowsky, P.T., Massey, N.W.D., and Matheson, A. (1996b): Aggregate resource potential of the Prince George area; *B.C. Ministry of Energy, Mines and Petroleum Resources*, Open-File 1996-24, 5 maps, scale 1:50 000.

Bobrowsky, P.T., Massey, N.W.D., and Matheson, A. (1998): Aggregate resource potential map of the Okanagan area (NTS 82E (west) and 82L (west)); *B.C. Ministry of Energy and Mines*, Open-File 1998-5, 16 maps, scale 1:50 000.

Clague, J.J. (1986): The Quaternary stratigraphic Record of British Columbia-Evidence for Episodic sedimentation and erosion controlled by Glaciation; *Canadian Journal of Earth Sciences,* volume 23, pages 885-894.

Davis, N.F.G. and Mathews, W.H. (1944): Four Phases of Glaciation with illustrations from southwestern British Columbia; *Journal of Geology*, volume 52, pages 403-413.

Dixon-Warren, A.B., and Brooks, E.D. and Bobrowsky, P.T. (2000); Aggregate resource potential of the Sea-to-Sky Highway Area (NTS 92G11 and 14); *B.C. Ministry of Energy and Mines*, digital data, Open File 2000-30.

Edwards, W.A.D., Hudson, R.B., Scafe, D.W. (1985): Aggregate Resources of the Edmonton/Lloydminster Region; Alberta Research Council, Natural Resource Div., *Alberta Geological Survey,* Bulletin No. 47.

Gabrielse, H., Monger, J.W.H., Wheeler, J.O., Yorath, C.J. (1991): Part A. Morphogeological belts, tectonic assemblages, and terranes; *in* Chapter 2 of Geology of the Cordilleran Orogen in Canada, H. Gabrielse and C.J. Yorath (ed.); *Geological Survey of Canada*, Geology of Canada, no.4, p.15-28 (also *in* Geological Society of America, The Geology of North America, v. G-2).

Howes, D.E. and Kenk, E. (1997): Terrain classification system for British Columbia (revised edition); *B.C. Ministry of Environment, Lands and Parks,* Survey and Resource Mapping Branch, MOE Manual 10.

Journeay, J.M. and Monger, J.W.H. (1994): Geology and crustal structure of the south coast and Intermontane Belts, southern Canadian Cordillera, British Columbia; *Geological Survey of Canada,* Open File 2940, scale 1:500 000.

Langer, W.H. and Glanzman, V.M. (1993): Natural aggregate building America's future; Public Issue in Earth Science, *US Geological Survey*, Circular 1110.

Massey, N.W.D., Matheson, A., and Bobrowsky, P.T. (1998): Aggregate resource potential of the Nanaimo area (parts of NTS 92B/12, 92B/13, 92C/9, 92C/16, 92F/1, 92F/2, 92F/7, 92F/8, 92G/1); *B.C. Ministry of Energy and Mines*, Open File 1998-12, 9 maps, scale 1:50 000.

Meidinger, D. and Pojar, J. (1991): Ecosystems of British Columbia; *B.C. Ministry of Forests*, Special Report Series, no. 6.